CHEMOPROTEOMIC METHODS TO EVALUATE CYSTEINE OXIDATION IN THE MITOCHONDRIA

Eleni A. Kisty

A dissertation

submitted to the Faculty

of the department of Chemistry

in partial fulfillment

of the requirements for the degree of

Doctor of Philosophy

Boston College
Morissey College of Arts and Sciences
Graduate School

June 2022

© Copyright 2022 Eleni A. Kisty

Chemoproteomic Methods to Evaluate Cysteine Oxidation in the Mitochondria

Eleni A. Kisty

Advisor: Eranthie Weerapana, Ph.D.

Reactive oxygen species (ROS) modulate protein function through cysteine oxidation. Identifying protein targets of ROS can provide insight into uncharacterized ROS-regulated pathways especially within ROS generating organelles such as the mitochondria. There are several known examples of mitochondrial cysteine targets that alter protein and pathway activity resulting in pathological effects. Several chemoproteomic workflows, including ABPP and OxICAT, can be used to identify sites of cysteine oxidation. However, determining ROS targets localized within subcellular regions and ROS hotspots remains challenging with existing workflows. Here, we present combined cysteine-monitoring chemoproteomic platforms (isoTOP-ABPP and OxICAT) with mitochondrial enrichment (organelle isolation and proximity labeling) to monitor cysteine oxidation events within the mitochondria. First, we profile redox-sensitive cysteines under exogenous and endogenous peroxide in isolated mitochondria using isoTOP-ABPP and OxICAT. Next, we introduce PL-OxICAT which combines enzymatic proximity labeling (PL) (TurboID/APEX) and OxICAT to monitor localized cysteine oxidation events within subcellular compartments such as the mitochondrial matrix and intermembrane space as well as ROS hotspots. Together, these platforms further hone our ability to monitor cysteine oxidation events within specific subcellular locations and ROS hotspots and provide a deeper understanding of the protein targets of endogenous and exogenous ROS.

Acknowledgments

First, I would like to my express my deepest gratitude to my advisor, Eranthie Weerapana. Thank you for your invaluable advice, encouragement, support, and patience. I will always be extremely appreciative of the opportunity to grow under your mentorship. Under your guidance, I was able to advance as a scientist and expand my curiosity for scientific discovery.

I would also like to take this opportunity to thank my committee members, Abhishek Chatterjee and Huiqing Zhou, as well as the other members of the chemistry department at Boston College for their scientific enthusiasm and creativity. Your ability to challenge my understanding throughout graduate school has pushed me to a higher scientific and professional level. Thanks to each member of the department for their collaboration and kindness. Additionally, I would like to thank my undergraduate research advisor, Dr. Lindsay Comstock-Ferguson and graduate student advisor, Natalia Bremner-Jordan. Joining the Comstock lab as a sophomore cemented my interest in chemical biology research. Both of you made the lab fun and exciting while providing a space to build my confidence as a female in science.

To all the Weerapana lab members past (Shalise, Lisa, Kyle, Masahiro, Rebecca, Tyler, Jenny, Ari, Aaron) and current (Dan, Julia, Ben, Qianni, Sarah C, Angela, Sarah M, Avinash, and Madison), thank you for cultivating a lively, scientific culture. I'm appreciative for all the support and collaboration throughout my time in the lab. My original attraction to Boston College was the positive and fun Weerapana lab members I met. Additionally, many thanks goes to my former

undergraduate student, Emma. It was lovely to work together and I am grateful for the opportunity to learn as a scientific mentor.

To the Merkert staff, thank you for taking care of the necessary behind-the-scenes administrative work for us to pursue our dreams. A special thanks to Stephen and Tim in the business office, who were so patient and always on top of everything related to ordering. The work that you do daily to keep the department and science running is incredible. You really made my lab ordering responsibilities as easy as it could have been. Additionally, thank you to Marek for your support and kindness since the beginning of graduate school. I always enjoyed our conversations and learning more about mass spectrometry.

To the friends far and near who supported me through it all, understanding when I was constantly unavailable but still including me anyways, thank you! I have so much gratitude towards the many exceptional people who have kept me grounded throughout this journey. Special thanks to Shalise and Tom for being the best BLS and BLB-in-law and always helping me navigate each step. I have had the most wonderful memories, and I am so thankful to be surrounded by many incredible role models and humans (and dogs).

To my family, thank you for always believing in. I'm beyond grateful for your support and generosity over the past six years. Special thanks to my parents for accompanying me on many bike-commuting phone calls and providing an encouraging environment to pursue my academic goals. I'm truly grateful for all that you do! Tyler and Lilo, thank you for being the best little family. Lilo, thanks for the ankle bites herding me towards success. Between the thesis writing, snuggles, and encouraging smoochies, I'm very lucky to have you as a dogter. Thank you for your attentive listening during all my practice presentations and

only interrupting with the most necessary suggestions. Tyler, I'm beyond appreciative of your companionship. We both know that I wouldn't be in this position today without you, and I am forever grateful for your support and guidance. Thanks for being there by my side through the ups and downs and always finding ways to make me laugh. Additionally, thank you for instilling in me some of your midwestern traits to soften my high-strung Bostonian personality. I can't wait to go on more fun adventures together.

Table of Contents

List of Tables ..... **x**

List of Figures ..... **xiv**

List of Abbreviations ..... **xxv**

Chapter 1 - Mitochondrial Reactive Oxygen Species and Cysteine Redox Signaling **1**

Mitochondrial topography. 2

Mitochondrial ROS production. 7

Antioxidant defenses against elevated mtROS. 10

Oxidative cysteine modifications. 13

Cysteine redox signaling in disease. 18

Apoptotic signaling and mtROS. 19

MtROS in neurodegeneration. 21

MtROS and diabetes and cardiopathy. 22

Therapeutics targeting mitochondria and mtROS. 24

Chemoproteomic approaches in evaluating global cysteine oxidation events. 25

Small molecules for labeling of specific cysteine oxoforms in the mitochondria. 27

Conclusion 28

Chapter 2 - Identifying Redox-Sensitive Cysteine Residues in the Mitochondria **49**

Introduction 50

Results and Discussion 53

Enrichment of mitochondrial cysteines by organelle isolation. 53

Unique Cysteine Sensitivity to Oxidation. 57
Heightened cysteine reactivity response on known redox-sensitive proteins. 63
Distinct effects of cysteine oxidation in mitochondrial pathways. 66
Electron transport inhibition results in mitochondrial cysteine oxidation.... 68
Quantification of mitochondrial redox environment under normal and oxidizing metabolic states. 74
Evaluation of functional sites of cysteine oxidation. 79
PPA2. 80
Evaluation of redox-sensitive cysteines in mammalian cells. 82
RARS2. 83
NLRX1 and MAVS. 85
OGDH. 89
Conclusion 93
Experimental Procedures 95
Chapter 3 - Combining Redox Proteomics and Proximity Labeling with TurboID to Monitor Localized Cysteine Oxidation 126
Introduction 127
Results and discussion 134
Targeting TurboID to mitochondrial sub-compartments. 134
PL-OxICAT with TurboID enables quantification of cysteine oxidation events within the mitochondrial matrix and IMS. 138
Conclusion 149
Experimental Procedures 150

Chapter 4 - Combining Redox Proteomics and Proximity Labeling with APEX to Monitor Localized Cysteine Oxidation in ROS Hotspots..... 167

Introduction 168

Results and Discussion..... 173

PL-OxICAT with APEX enables quantification of cysteine oxidation events within ROS hotspots. 173

PL-OxICAT with APEX identifies cysteine oxidation events induced by macrophage differentiation. 186

Conclusion 194

Experimental Procedures..... 196

Chapter 5 - Integrated Phenotypic Screening and Target Identification of Fully Functionalized Electrophilic and Photo-reactive Small-Molecule Library 216

Introduction 217

Results and Discussion..... 220

FFSMP library development and molecular diversity. 220

Electrophilic FFSMP scaffold diversity leads to variety in protein labeling. 222

Evaluation of FFSMP breast cancer cell cytotoxicity. 228

Target deconvolution of cytotoxic probes. 230

PJDU-112 is a potent inhibitor of PDIA1. 233

Conclusion 240

Experimental Procedures..... 242

Appendix I..... 260

Appendix II 444

List of Tables

Chapter 2.

Table 2-1. Panther gene ontology (GO) overrepresentation analysis for the top 10 enriched biological processes in mitochondrial sample compared to whole cell.

Chapter 3.

Table 3-1. Antibodies used with sources, catalog number and use.

Table 3-2. Vectors and descriptions including features, promoters, and uses for this study.

Chapter 4.

Table 4-1. Antibodies used with sources, catalog number and use.

Table 4-2. Vectors and descriptions including features, promoters, and uses for this study.

Appendix I.

Table 2A-1. List of proteins identified in HEK293T and Whole-Cell (WC) and pure isolated mitochondria (Mito) samples containing at least 4 spectral counts. Corresponding GO cellular compartments.

Table 2A-2. Panther GO Biological Processes enrichment analysis for proteins identified in whole-cell lysates. Data filtered for processes enriched > 5-fold.

Table 2A-3. Panther GO Biological Processes enrichment analysis for proteins identified in Mito-P lysates. Data filtered for processes enriched > 5-fold.

Table 2A-4. List of average L:H ratios for mitochondrial cysteines containing peptides identified in Mito-P lysates treated with 1 mM, 2.5 mM, 5 mM and 10 mM peroxide using isoTOP-ABPP. Cysteines identified from Mito-P lysates treated with peroxide were alkylated by IA-H and control mito-P lysates were alkylated by IA-L. Data was filtered for mitochondrial peptides with ratio values in 2 out of 3 replicates.

Table 2A-5. List of average L:H ratios for mitochondrial cysteine containing peptides identified in Mito-P from cells treated with DMSO or AMA. Data was filtered for mitochondrial peptides with ratio values in 2 out of 3 replicates, with a coefficient of variance <50%. Cysteines identified in Mito-

P from DMSO- or AMA-treated cells were alkylated by IA-L or IA-H, respectively.

Table 2A-6. List of average percent oxidation values for mitochondrial cysteine containing peptides identified in Mito-P from cells treated with DMSO or AMA alkylated by IA-L and IA-H. Data was filtered for mitochondrial peptides with ratio values in 2 out of 3 replicates, with a standard deviation < 20%.

Table 2A-7. List of ReDiMe ratios and spectral counts for proteins identified by FLAG immunoprecipitation of overexpressing RARS2-FLAG cell lysates with (light) and without 10 mM peroxide (heavy).

Table 2A-8. List of ReDiMe ratios and spectral counts for proteins identified by FLAG immunoprecipitation of overexpressing NLRX1WT-FLAG (light) and NLRX1C331S-FLAG (heavy).

Table 2A-9. List of ReDiMe ratios and spectral counts for proteins identified by FLAG immunoprecipitation of overexpressing MAVSWT-FLAG (light) and MAVSC283S-FLAG (heavy).

Table 2A-10. List of ReDiMe ratios and spectral counts for proteins identified by FLAG immunoprecipitation of overexpressing OGDHWT-FLAG (light) and OGDHC395S-FLAG (heavy).

Table 3A-1. List of all proteins identified in matrix-TID, IMS-TID, and cyto-TID MS analyses. Mitochondrial localization is denoted by "mito", and is derived from uniprot subcellular localization, MitoCarta2.0, and previous studies (mito-APEX, IMS-APEX, and IMSGold+). Protein identifications for matrix-TID and IMS-TID are the average of 3 replicates. Protein identifications for cyto-TID are the average for 2 replicates.

Table 3A-2. Gene ontology (GOrilla) analysis for enrichment of biological processes for proteins identified in matrix-TID analysis.

Table 3A-3. Gene ontology (GOrilla) analysis for enrichment of biological processes for proteins identified in IMS-TID analysis.

Table 3A-4. Gene ontology (GOrilla) analysis for enrichment of biological processes for proteins identified in cyto-TID analysis.

Table 3A-5. Sum of all cysteine-containing peptides identified in matrix-TID, IMS-TID, and cyto-TID analyses. Mitochondrial localization is denoted by "mito", and is derived from uniprot subcellular localization, MitoCarta2.0, and previous studies (mito-APEX, IMS-APEX, and IMSGold+). Peptide identifications for matrix-TID and IMS-TID are the sum of 3 replicates. Protein identifications for cyto-TID are the sum of 2 replicates.

Table 3A-6. Average percent oxidation for mitochondria localized cysteines from matrix-TID analysis. Data was filtered for peptides with ratio values in 2 out of 3 replicates, with a standard deviation <30%.

Table 3A-7. Average percent oxidation for mitochondria localized cysteines from IMS-TID analysis. Data was filtered for peptides with ratio values in 2 out of 3 replicates, with a standard deviation <30%.

Table 3A-8. Average percent oxidation for mitochondria localized cysteines from cyto-TID analysis. Data was filtered for peptides with ratio values in 2 out of 3 replicates, with a standard deviation <30%.

Table 4A-1. List of all proteins identified in matrix-APEX analysis. Mitochondrial localization is denoted by "mito", and is derived from uniprot subcellular localization, MitoCarta2.0, and previous studies (mito-APEX, IMS-APEX, and IMSGold+). "DMSO" denotes DMSO treatment for 45 min. "AMA" denotes 100 μM Antimycin A treatment for 45 min. "H2O2" denotes 1 mM H2O2 treatment for 1 min. Protein identifications are the average of 3 replicates for each treatment.

Table 4A-2. Gene ontology (GOrilla) analysis for enrichment of biological processes for proteins identified in matrix-APEX analysis.

Table 4A-3. List of all cysteine-containing peptides identified in matrix-APEX analyses. Mitochondrial localization is denoted by "mito", and is derived from uniprot subcellular localization, MitoCarta2.0, and previous studies (mito-APEX, IMS-APEX, and IMSGold+). "DMSO" denotes DMSO treatment for 45 min. "AMA" denotes 100 μM Antimycin A treatment for 45 min. "H2O2" denotes 1 mM H2O2 treatment for 1 min. Peptide identifications are the average of 3 replicates for each treatment.

Table 4A-4. Average percent oxidation for mitochondria localized cysteines from AMA-treated matrix-APEX analysis. Data was filtered for peptides with ratio values in 2 out of 3 replicates, with a standard deviation <30%.

Table 4A-5. Average percent oxidation for mitochondria localized cysteines from 100 μM peroxide-treated matrix-APEX analysis. Data was filtered for peptides with ratio values in 2 out of 3 replicates, with a standard deviation <30%.

Table 4A-6. Average percent oxidation for mitochondria localized cysteines from 1 mM H_2O_2-treated matrix-APEX analysis. Data was filtered for peptides with ratio values in 2 out of 3 replicates, with a standard deviation <30%.

Table 4A-7. List of all proteins identified in cyto-APEX analysis. "LPS" denotes 1 μg/mL LPS. "none" denotes no treatment. Protein identifications are the average of 4 replicates (2 technical replicates from 2 biological replicates).

Table 4A-8. Gene ontology (GOrilla) analysis for enrichment of biological processes for proteins identified in cyto-APEX analysis.

Table 4A-9. List of all cysteine-containing peptides identified in cyto-APEX analyses. "LPS" denotes 1 μg/mL LPS. "none" denotes no treatment. Peptide identifications are the average of 4 replicates (2 technical replicates from 2 biological replicates).

Table 4A-10. Average percent oxidation for cysteines from cyto-APEX analysis. Data was filtered for peptides with ratio values in 2 out of 4 replicates, with a standard deviation <30%.

Table 5A-1. List of proteins enriched in cells treated with either DMSO or 500 nM PJDU-112, PJDU-156, and PDJU-229. Data is filtered for > 20 spectral counts.

Table 5A-2. List of spectral counts and L:H ratios of ReDiMe labeled proteins enriched in cells treated with either 500 nM PJDU-112 (heavy) or 500 nM VPDU-229 (light).

Appendix II. Supplemental Figures

Supplemental Figure 2-1. L:H ratios plotted for 10 mM peroxide treated Mito-P isoTOP-ABPP sample. Cysteines are plotted for proteins belonging to mitochondrial biological pathways and categories including the (A) citric acid cycle, (B) innate immunity, (C) transport, (D) urea cycle, (E) fatty acid oxidation, (F) redox regulation, (G) Fe-S biogenesis, (H) apoptosis, (I) tRNA ligases, (J) mitochondrial (mt)-ribosomal subunits, (K) electron transport chain, (L) transcription and translation.

List of Figures

Chapter 1.

Figure 1-1. Mitochondrial multicompartmental structure with annotations of general biochemical pathways including the electron transport chain, citric acid cycle, mitochondrial DNA gene expression, β-oxidation (BO) of fatty acids (FA) and apoptotic signaling through cytochrome c release.

Figure 1-2. Mitochondrial intermembrane space (IMS) protein import through MIA40/ERV1 disulfide bond relay. After IMS targeting sequence recognition by outer membrane translocase (TOMM), a series of redox reactions starting with structural disulfide bond introduction to imported peptide with $Cx_{3/9}C$ motifs by ERV1 and electron transfer to MIA40, cytochrome c and complex IV of the ETC and finally ending with the reduction of oxygen to water. Reactive oxygen species (ROS) are a byproduct of electron leakage by MIA40 to oxygen.

Figure 1-3. ROS formation through subsequent reductions spontaneously or by antioxidant defense enzymes including superoxide dismutase (SOD), glutathione peroxidase (GPX), catalase (CAT), peroxiredoxin (PRX).

Figure 1-4. Thiol oxidative modifications in the presence of different ROS levels. Arrows depict the reversibility of each modification.

Figure 1-5. Aerobic respiration sites of major superoxide production (ETC complex I and complex III) and known redox thiol sensors of metabolism on ETC complexes and TCA enzymes. Complexes illustrated represent corresponding PDB files.

Figure 1-6. Cellular consequences centered on mtROS abundance. Pathologically relevant ROS-related signaling found in the "sweet spot" of slight oxidative stress. When levels exceed antioxidants, macromolecular injury and cell death is observed.

Figure 1-7. Assortment of diseases impacted by mitochondrial redox signaling and oxidative stress.

Figure 1-8. Chemoproteomic methods of quantifying cysteine oxidation. (A) Schematic of IsoTOP-ABPP where reactive thiols are alkylated by either a light cysteine alkylating reagent or heavy cysteine alkylating reagent in treated (H_2O_2) and untreated sample (H_2O). The sample is combined after click chemistry with a cleavable biotin azide tag and trypsinized after streptavidin enrichment. Cysteine reactivity is quantified in MS^1 abundance of the isotopically labeled cysteine containing peptides. MS^2 reports on peptide identification. (B) Schematic of OxICAT platform where in a single sample, cysteine oxidation is reported. Reduced cysteines are alkylated by

a light cysteine alkylating reagent. After reduction, previously oxidized cysteines are alkylated by a heavy cysteine alkylating reagent. MS analysis of MS^1 chromatogram indicates the abundance of isotopically alkylated peptides and can be converted to percent oxidation values.

Chapter 2.

Figure 2-1. Whole mitochondrial isolation by differential centrifugation used to enrich for mitochondrial cysteines.

Figure 2-2. Western blot analysis of isolated fractionation steps and subcellular compartments from mitochondrial enrichment by differential centrifugation using organelle markers including Histone H3 (nuclear), Calreticulin (endoplasmic reticulum), GAPDH (cytosol), and ATPIF1 (mitochondria).

Figure 2-3. (A) Total annotated mitochondrial proteins and peptides identified from whole cell (blue) or isolated mitochondria (red). (B) Percentage of total spectral counts belonging to proteins with specified Uniprot sub-cellular localizations in a whole cell (blue) and isolated mitochondria (red) samples. Annotated compartments include cell membrane (CM), cytoskeleton (Cyto. Skel.), endosome (Endo.), endoplasmic reticulum (ER), golgi apparatus (Golgi), lysosome (Lyso.), mitochondria (Mito.), nucleus (Nuc.), peroxisome (Perox.), and secreted (Sec.).

Figure 2-4. Workflow for evaluating peroxide-dependent changes in cysteine reactivity in isolated mitochondria lysates using IsoTOP-ABPP. Labeling of thiols from control or peroxide treated samples with IA-L or IA-H, respectively, appending cleavable biotin-azide tags, enrichment of labeled cysteine containing proteins, trypsin digestion, and isolation of labeled cysteine-containing peptides for quantitative MS to identify and quantify cysteine reactivity changes due to oxidation.

Figure 2-5. (A) Isotopically coded alkylating reagents, light (IA-L, ^{12}C) and heavy (IA-H, ^{13}C) iodoacetamide alkyne. (B) Structure of cleavable diazo biotin azide tag.

Figure 2-6. Violin plot annotating median ratios of mitochondrial cysteine reactivity with increasing concentrations of peroxide (1 mM, 2.5 mM, 5 mM and 10 mM H_2O_2).

Figure 2-7. (A) Plotted average L:H ratios (log_2L:H) of mitochondrial cysteines with increasing peroxide. (B) Extracted ion chromatograms of cysteines from Figure 2-7A alkylated by IA-L (red) or IA-H (blue) in the control and peroxide treated samples, respectively. Displayed chromatograms are representative of a single replicate.

Figure 2-8. L:H ratio plot (log_2L:H) of mitochondrial cysteine-containing peptides identified with 10 mM peroxide treatments by IsoTOP-ABPP with annotations of redox-sensitive proteins (red). Inlet highlights cysteine-containing peptides with the highest changes in L:H ratios. Annotated redox-sensitive parent proteins denoted (X).

Figure 2-9. MS extracted ion chromatogram for identified cysteines of GRPEL2. Blue peaks signify cysteine labeling in 10 mM peroxide treated sample and red peaks are the untreated control cysteine labeling abundances. Displayed chromatograms are representative of a single replicate.

Figure 2-10. Average L:H ratios for cysteines identified on proteins belonging to mitochondrial bioenergetic pathways including the citric acid cycle (blue), urea cycle (red), and electron transport chain (green) in 10 mM peroxide IsoTOP-ABPP dataset. High peroxide sensitivity (L:H ratio of 5) is denoted as a gray line.

Figure 2-11. Depiction of ETC inhibition of complex III by Antimycin A (AMA). Concurrent electron leakage and superoxide production located in mitochondrial matrix and IMS.

Figure 2-12. Immunofluorescence imaging of HeLa cells treated with increasing concentrations of Antimycin A (AMA). Mitochondrial superoxide is staining with MitoSOX (red) and nucleus stained with DAPI (blue).

Figure 2-13. Workflow quantification of changes in cysteine reactivity in mitochondria isolated from whole cells treated with DMSO (control) or Antimycin A (AMA) using IsoTOP-ABPP.

Figure 2-14. L:H ratio plot (log_2L:H) of mitochondrial cysteine-containing peptides identified after AMA treatments by IsoTOP-ABPP with annotations of redox-sensitive proteins (red). Inlet highlights cysteine-containing peptides with the highest changes in L:H ratios.

Figure 2-15. Workflow OxICAT in isolated mitochondria treated with from DMSO control-treated cells or AMA-treated cells. Platform includes differential alkylation of reduced and oxidized cysteine thiols with IA-L or IA-H followed by incorporation of cleavable biotin-azide tag for labeled cysteine-containing protein enrichment, trypsin digestion, labeled cysteine-containing peptide capture. L:H ratios directly correspond to percent oxidation values of cysteines.

Figure 2-16. Percent oxidation values for DMSO-treated, control mitochondria. Uniprot annotations of cysteine residues that partake in disulfide bonding (blue), metal binding (red) and *s*-palmitoylation (green). Percent oxidation is directly calculated from L:H and H:L ratios.

Figure 2-17. Plot of overlapping percent oxidation values from mitochondria from cells treated with DMSO (control) or AMA. Colored regions demonstrate cysteines with > 15% change in percent oxidation.

Figure 2-18. (A) Michaelis-Menten kinetic plot of PPA2 wild-type (blue) and PPA2 C161S (red) pyrophosphatase activity, n=3 (B) Time and concentration dependent effects of hydrogen peroxide as measured by percent inhibition in PPA2 WT and PPA2 C161S by hydrogen peroxide, n=3.

Figure 2-19. Western blot analysis analysis of HEK 293T lysates expressing follow up proteins (RARS2, MAVSWT/C283S, OGDHWT/C395S, and NLRX1WT/C331S). Overexpressed proteins were visualized using an anti-FLAG. Anti-GAPDH and panceau staining was used as a loading control.

Figure 2-20. Depiction of RARS2 protein with bars representing all cysteines. The cysteine identified from our proteomic studies (C11) is in dark green. Chromatogram traces corresponding to ratios from each study are show with red lines as the IA-L labeled (light) and blue lines as the treatment (IA-H labeled).

Figure 2-21. (A) Log_2 L:H ratio plot of immunoprecipitated proteins on anti-FLAG resin from lysates overexpressing RARS2-FLAG treated with 10 mM peroxide (heavy) against the untreated control (light), n=3. (B) Average Log_2 L:H ratio from immunoprecipitation plotted against the average protein spectral matches (PSMs), n=9.

Figure 2-22. Illustration of NLRX1 protein with all cysteines in light red and those identified by our MS studies in dark red. Traces corresponding to chromatograms of cysteine-containing peptides are shown with red (IA-L) and blue (IA-H) labeling.

Figure 2-23. Illustration of MAVS protein with all cysteines in light purple and those identified by our MS studies in dark purple. Traces corresponding to chromatograms of cysteine-containing peptides are shown with red (IA-L) and blue (IA-H) labeling.

Figure 2-24. (A) Log_2 L:H ratio plot of immunoprecipitated proteins on anti-FLAG resin from lysates overexpressing NLRX1-FLAG (light) and NLRX1C331S-FLAG (heavy), n=3. (B) Average Log_2 L:H ratio from immunoprecipitation plotted against the average protein spectral matches (PSMs), n=9.

Figure 2-25. (A) Log_2 L:H ratio plot of immunoprecipitated proteins on anti-FLAG resin from lysates overexpressing MAVS-FLAG (light) and MAVSC283S-FLAG (heavy), n=3. (B) Average Log_2 L:H ratio from immunoprecipitation plotted against the average protein spectral matches (PSMs), n=9.

Figure 2-26. Illustration of OGDH protein with all cysteines in light blue and those identified by our MS studies in dark blue. Traces corresponding to chromatograms of cysteine-containing peptides are shown with red (IA-L) and blue (IA-H) labeling.

Figure 2-27. CETSA assay with HEK 293T lysates overexpressing wild-type (WT) OGDH and OGDHC395S stability in the presence or absence of 10 mM peroxide. Thermal degradation was performed at temperatures ranging from 40 to 70 C for 5 minutes before samples were spun down with precipitants removed. Western blotting was completed against FLAG tags on overexpressed proteins.

Figure 2-28. (A) Immunoprecipitation and western blot analysis of HEK 293T lysates overexpressing OGDH-FLAG and OGDHC395S-FLAG in the presence or absence of 10 mM peroxide. Blotting was conducted against DLST, DLD, native OGDH, and overexpressed OGDH (FLAG) presence. (B) Bar graph depicting DLST signal quantification normalized to FLAG signal from western blot in A.

Figure 2-29. (A) Log_2 L:H ratio plot of immunoprecipitated proteins on anti-FLAG resin from lysates overexpressing OGDH-FLAG (light) and OGDHC395S-FLAG (heavy), n=3. (B) Average Log_2 L:H ratio from immunoprecipitation plotted against the average protein spectral matches (PSMs), n=9.

Chapter 3.

Figure 3-1. Mechanism of TurboID labeling proximal proteins with (A) biotin activation and (B) lysine SN2 reaction.

Figure 3-2. Schematic demonstrating the use of a matrix-TID, IMS-TID and matrix-APEX construct to selectively biotinylate proteins localized within the mitochondrial matrix, IMS and ROS hotspots, respectively.

Figure 3-3. Workflow for PL-OxICAT includes differential alkylation of reduced and oxidized thiols with isotopically light and heavy species, enrichment of biotinylated proteins, trypsin digestion, and quantitative MS analysis to identify and quantify cysteine oxidation.

Figure 3-4. Immunofluorescence imaging of HEK 293T cells expressing no-TID, matrix-TID, IMS-TID, and cyto-TID. TID expression was monitored using anti-HA AlexaFluor488 (green), mitochondria were stained with Mitotracker Red CMXROS (red), and the nucleus was stained with DAPI (blue).

Figure 3-5. Western blot analysis of HEK 293T lysates expressing no-TID, matrix-TID, and cyto-TID. Cells were treated with 500 μM biotin for increasing incubation times, and biotinylated proteins were visualized

using strep-HRP. Expression of TID constructs was confirmed using anti-HA, and anti-GAPDH was used as a loading control. The asterisk denotes biotinylation of the TID construct.

Figure 3-6. Western blot analysis of HEK 293T lysates expressing no-TID, matrix-TID, and cyto-TID. Cells were treated with various biotin concentrations, and biotinylated proteins were visualized using strep-HRP. Expression of TID constructs was confirmed using anti-HA, and anti-GAPDH was used as a loading control. The asterisk denotes biotinylation of the TID construct.

Figure 3-7. Western blot analysis of HEK 293T cells expressing IMS-TID. Cells were treated with 500 μm biotin for 1 hour and biotinylated proteins were visualized using strep-HRP. IMS-TID expression was confirmed using anti-HA, and anti-GAPDH was used as a loading control.

Figure 3-8. (A) Quantitative analysis of total spectral counts for proteins labeled by TurboID localized to cytosol, matrix and IMS with mitochondrial annotations (red). Spectral counts plotted for proteins labeled by (B) Cytosolic-TurboID and PDK1-TurboID and (C) Cytosolic-TurboID and IMS-TurboID with mitochondrial annotations (red). Proteins with greater or equal to 4 spectral counts and identified in 2 replicates were included.

Figure 3-9. Venn diagrams comparing mitochondrial proteins identified using matrix-TID (blue) to previous reports using mitochondrial differential centrifugation in (Bak, *et al*., 2017) (red).

Figure 3-10. (A) Venn diagrams comparing mitochondrial proteins identified using IMS-TID (blue) to previous reports using mitochondrial differential centrifugation in (Bak, *et al*., 2017) (red). (B) Venn diagrams comparing IMS proteins identified using IMS-TID (blue) to previous reports of IMS proteins identified using mitochondrial differential centrifugation in (Bak, *et al*., 2017) (red).

Figure 3-11. Venn diagrams comparing mitochondrial proteins identified using (A) matrix-TID (blue) to previous reports using mito-APEX (red) or (B) IMS-TID (blue) to previous reports using IMS-APEX (red).

Figure 3-12. Panther[46] gene ontology (GO) analysis of most enriched processes for (A) Cyto-TID, (B) matrix-TID and (C) IMS-TID recovered proteins determined by GOrilla ranked evaluation with redundant terms removed.

Figure 3-13. Percent oxidation values for mitochondrial cysteines identified in the matrix-TID sample.

Figure 3-14. Percent oxidation values for mitochondrial cysteines identified in the IMS-TID sample. IMS localized proteins annotated in red.

Figure 3-15. Percent oxidation values for mitochondrial cysteines identified in the cyto-TID sample.

Chapter 4.

Figure 4-1. Radical mechanism of APEX proximity-dependent labeling with activation of biotin phenol to biotin phenoxy radical with resolution and covalent modification on adjacent tyrosine residue.

Figure 4-2. Workflow for PL-OxICAT includes differential alkylation of reduced and oxidized thiols with isotopically light and heavy species, enrichment of biotinylated proteins, trypsin digestion, and quantitative MS analysis to identify and quantify cysteine oxidation.

Figure 4-3. Schematic of matrix-APEX activation in endogenous ETC-inhibitor derived ROS hotspot in the mitochondrial matrix.

Figure 4-4. Confirmation of intracellularly-guided APEX2 expression in HEK293T cells. Immunofluorescence imaging of wild-type (WT), cytosolic (V5-APEX2), and mitochondrial matrix (PDK1-APEX2) expressing HEK293T cells. Fusion proteins contain V5 epitope tags for visualization (green, AlexaFluor488). APEX2 expression was overlayed with nuclear DAPI stain (blue) and mitochondria stain by MitotrackerCMXRedROS (red).

Figure 4-5. Expression and activity of PDK1 (P) and Cytosolic (C) APEX2 with increasing peroxide treatment. Western blotting of HEK293T cells overexpressing PDK1-V5-APEX2 and Cytosolic V5-APEX2 subjected to increasing concentrations of H2O2 for 1 min followed by quenching with 3 washes of quenching buffer (QB) and 3 washes of DPBS. Protein expression was visualized by anti-V5 blotting. Strep-HRP blotting allowed for investigation of APEX2 substrate biotin labeling.

Figure 4-6. Western blot analysis of HEK 293T lysates expressing matrix-APEX. Cells were treated with DMSO (-) or 500 μM biotin-phenol (+) for 45 min followed by the addition of ETC inhibitors, AMA (100 μM) and Oligo (10 μM), or additional DMSO (-) for a supplementary 45 min. Biotinylated proteins were visualized using strep-HRP. Expression of APEX was confirmed using anti-V5, and Ponceau staining used to normalize protein loading.

Figure 4-7. Quantification of total (blue) and mitochondrial (red) proteins and spectral counts identified in DMSO and AMA treated matrix-APEX cells.

Figure 4-8. Venn diagram showing overlap between proteins identified in matrix-TID (blue) and matrix-APEX (red) datasets.

Figure 4-9. Percent oxidation values for mitochondrial cysteines identified in the matrix-APEX sample under AMA treatment.

Figure 4-10. Heat map comparing the percent oxidation for 164 cysteines identified in both matrix-APEX and matrix-TID samples (Chapter 3).

Figure 4-11. (A) Venn diagram showing overlap between proteins identified in matrix-APEX cells treated with hydrogen peroxide (blue) and AMA (red). (B) Heat map comparing the percent oxidation for cysteines identified in both matrix-APEX activated by AMA and peroxide.

Figure 4-12. Percent oxidation values for mitochondrial cysteines identified in the matrix-APEX sample during treatments with DMSO, AMA, and peroxide (100 μM for 45 min or 1 mM for 1 min).

Figure 4-13. Schematic of cyto-APEX activation in cytosolic ROS hotspot in Raw 264.7 cells. Endogenous ROS is generated by NOX activation under cytokine-receptor binding.

Figure 4-14. Immunofluorescence imaging of Raw 264.7 cells expressing cyto-APEX. APEX expression was monitored using anti-V5 (green), mitochondria were stained with Mitotracker Red CMXROS (red), and the nucleus was stained with DAPI (blue).

Figure 4-15. Western blot analysis of Raw 264.7 lysates expressing cyto-APEX. Cells were treated with 1 μg/mL LPS and 10 ng/mL IFNγ treatment for 20 hours prior to a 2.5 hour treatment with 500 μM biotin-phenol (+) or DMSO (-). Biotinylated proteins were visualized using strep-HRP. Expression of APEX was confirmed using anti-V5, and Ponceau staining used to normalize protein loading.

Figure 4-16. Quantification of total (blue) and cytosolic (red) proteins and spectral counts identified in DMSO and LPS treated cyto-APEX Raw 264.7 cells.

Figure 4-17. Quantification of total (blue) and cytosolic (red) proteins and spectral counts identified in DMSO and LPS treated cyto-APEX Raw 264.7 cells.

Figure 4-18. Enzymes within the glycolytic pathway with corresponding values for percent oxidation for identified cysteines.

Chapter 5.

Figure 5-1. Illustration of FFSMP design with three consistent elements including a protein binding appendage for selectivity, a protein reactive group (either electrophilic or photo-reactive) for covalent modification, and enrichment handle for click chemistry (alkyne).

Figure 5-2. Structures of the 49 FFSMP library members with great scaffold appendage and protein reactivity diversity.

Figure 5-3. Molecular shape diversity assessment by principle moment of inertia plot. The molecular shape diversity of 49 IMCR-based FFSMPs (red dots), which includes each enantiomer of racemic FFSMPs, in comparison with reference sets of 40 top-selling brand-name drugs (green squares) and 60 diverse natural products (filled blue triangles).

Figure 5-4. Photo-reactive FFSMP library member labeling in MCF10CA1a lysates. Lysates were incubated with either 10 or 20 μM probe for 30 min followed with irradiation with UV light for 1 hr. (A) Click chemistry was performed to append TAMRA-N_3 for fluorescent visualization. (B) Normalized protein concentration was confirmed by Coomassie protein staining.

Figure 5-5. Evaluation of FFSMPs of electrophilic diversities with consistent core scaffold in MCF10CA1a cells. (A) FFMSP library member structures shown with electrophilic war heads in red with similar skeletal backbones in black. (B) Whole MCF10CA1a cells were incubated with probes for 3 hr followed by lysate preparation and click chemistry with TAMRA-azide to visualize labeling through fluorescent imaging Coomassie staining confirms protein normalized concentration.

Figure 5-6. Assessment of FFSMPs with scaffold appendage diversity but electrophilic similarity. (A) Library members with sulfonyl fluoride electrophile on different core structural backbones (B) Whole MCF10CA1a cells were incubated with probes for 3 hr followed by lysate preparation and click chemistry with TAMRA-azide to visualize labeling through fluorescent imaging Coomassie staining confirms protein normalized concentration.

Figure 5-7. 17 Library members containing electrophilic protein reactive groups. Probes are separated by functional electrophilic moieties with sulfonyl fluorides in turquoise, cholornitrobenzenes in green, acrylamide in purple and choloracetamides in blue.

Figure 5-8. Biological characterization of the electrophilic FFSMP library members in MCF10CA1a cells. (A) Cell proliferation screen of the seventeen electrophilic FFSMP library members, grouped by electrophile (sulfonyl fluoride (SF), chloronitrobenzene (CNB), acrylamide (A), and chloroacetamide (CA), upon incubation with MCF10CA1a cells at 50 μM concentrations for 24 and 48 hours. Cell viability is assessed by MTT reagent relative to a DMSO control. (B) Cell proliferation screen of nine electrophilic FFSMP library members upon incubation with MCF10CA1a cells at 25 μM concentrations for 24 and 48 hours. Cell viability is assessed by MTT reagent relative to a DMSO control.

Figure 5-9. In-gel fluorescence assay of proteins covalently modified by each of five electrophilic FFSMPs upon treatment of live cells with 10 μM of compound for 24 hours.

Figure 5-10. Average enriched spectral counts plotted for (A) PJDU-216 and (B) PJDU-156 normalized against spectral counts present in DMSO control samples. Proteins with similar masses to banding patterns found in Figure 5-9A are annotated (n=2).

Figure 5-11. Concentration-dependent cell proliferation data for PJDU-112 upon treatment of MCF10CA1a cells at 24 and 48 hours with 0.5 – 75 μM concentrations. EC_{50} was determined to be 22 μM.

Figure 5-12. Workflow for quantitative proteomic analysis to identify protein targets of PDJU-112 and VPDU-229. MCF10CA1a cells were treated with 500 nM PDJU-112 or VPDU-229 for 1 hr, and probe-modified proteins enriched on streptavidin beads after cell lysis and CuAAC with biotin-azide. Peptides resulting from on-bead trypsin digestion were isotopically labeled by reductive dimethylation (ReDiMe) with light (VPDU-229) and heavy (PDJU-112) formaldehyde. The isotopically tagged peptides were analyzed by LC/LC-MS/MS to afford peptide identification and quantification in the form of heavy:light (H:L) isotopic ratios (Table 5A-2).

Figure 5-13. Ratio plot of proteins enriched for by PJDU-112 and VPDU-229. H:L ratios for proteins identified in two biological replicates of PDJU-112:VPDU-229 treated samples. Inset displays average spectral counts for those proteins displaying H:L ratios of ~20.

Figure 5-14. Visualization of spectral counts in PJDU-112 enrichment and H:L ratios for proteins identified in two biological replicates of PDJU-112:VPDU-229 treated samples.

Figure 5-15. Evaluation of PDIA1-FFSMP engagement in SKOV3PDIA1 KO cell line (A) In-gel fluorescence demonstrating PJDU-112, KSC-34, VPDU-229 (500 nM for 1 hour) labeling in SKOV-3 wild-type (WT) and PDIA1 knock-out (KO) cells. (B) Coomassie total protein staining to confirm consistent concentrations.

Figure 5-16. In-gel fluorescence displaying PJDU-112 (500 nM for 1 hour) labeling in PDIA1 wild-type (WT) and active-site cysteine mutant (C53A and C397A) expressing HEK293T cells. FFSMP PJDU-112 labeling was compared to KSC-34, a characterized PDIA1 covalent inhibitor. Labeling of endogenous PDIA1 (*) and overexpressed PDIA1 (#) is observed. Over-expression of PDIA1 was confirmed by anti-myc western blot.

Figure 5-17. Evaluation of PJDU-112 and KSC-34 inhibition of PDIA1 (A) Insulin reductase assay to monitor PDIA1 activity upon treatment with DMSO and PJDU-112 (n=3) (B) PDIA1 activity upon treatment of KSC-34

and PJDU-112 (5 μM; 30 minutes). Statistical significance emphasized by asterisks.

List of Abbreviations

Standard 3-letter and 1-letter codes are used for the 20 natural amino acids.

ACE	angiotensin converting enzyme
ACO2	aconitate hydratase 2
AD	Alzheimer's disease
ADP	adenosine diphosphate
AKR1B1	aldose reductase
AKT	RAC-alpha serine/threonine-protein kinase
ALS	Amyotrophic Lateral Sclerosis
AMA	Antimycin A
AMP	adenosine monophosphate
ANT	adenine nucleotide translocase
APEX	engineered ascorbate peroxidase for PL
APEX2	second generation APEX
ATIPIF1	ATPase inhibitor
ATP	adenosine triphosphate
azo-tag	cleavable diazo biotin azide tag
BCKDH	branched-chain keto-acid dehydrogenase
BCL-2	apoptosis regulator Bcl-2
bioGEE	biotinylated glutathione ethyl ester
bioGSH	biotinylated GSH
bioGSSG	biotinylated GSSG
BioID	proximity-dependent biotin identification
CAT	catalase
CETSA	cellular thermal shift assay
co-IP	co-immunoprecipitation
COX	cytochrome c oxidase
COX6B1	cytochrome c oxidase subunit 6B1
CuAAC	copper(I)-assisted azide-alkyne cycloaddition
cyto-APEX	APEX localized to the cytosol
cyto-TID	TurboID localized to the cytosol
DAB	denaturing alkylation buffer
DAPI	4',6-diamidino-2-phenylindole
DARS2	mitochondrial aspartate tRNA ligase

DCXR	L-xylulose reductase
DHX15	putative pre-mRNA splicing factor
DiaAlk	diazine alkyne
DLD	dihydrolipoamide dehydrogenase
DLST	dihydrolipoyl succinyltransferase
DMSO	dimethyl sulfoxide
DOD	dihydroorotate dehydrogenase
EC50	half maximal effective concentration
ECL	enhanced chemiluminescence
ER	endoplasmic reticulum
ERK	extracellular signal-regulated protein kinase
ERV1	Mitochondrial FAD-linked sulfhydryl oxidase
ETC	electron transport chain
ETF:QO	electron transfer flavoprotein:ubiquinol oxidoreductase
FA	fatty acid
FBS	fetal bovine serum
FFSMPs	fully functionalized small-molecule probes
FMN	flavin mononuceotide
GAPDH	glycerol-3-phosphate dehydrogenase
GO	gene ontology analysis
GPX	glutathione peroxidase
GR	glutathione reductase
GRPEL2	GrpE protein homolog 2
GSH	reduced glutathione
GSNO	*s*-nitrosoglutathione
GSSG	oxidized glutathione
GSTO1	glutathione s-transferase 1
H-Ras	GTPase Hras
HD	Huntington's disease
HNRNF	heterogeneous nuclear ribonucleoprotein F
HRP	horseradish peroxidase
IA	iodoacetamide
IA-H	IA-alkyne heavy
IA-L	IA-alkyne light
ICAT	isotope-coded affinity tags
IDH	isocitrate dehydrogenase
IFNγ	interferon gamma

IKK	inhibitor of NF-κβ kinase subunit beta
IMCR	Isocyanide-based Multi-Component Reaction
IMM	inner mitochondrial membrane
IMS	intermembrane space
IMS-TID	TurboID localized to the mitochondrial IMS
IsoTOP-ABPP	isotopic tandem orthogonal proteolysis – activity-based protein profiling
KO	knockout
L:H Ratio	L:H Ratio
LACTB	lactamase beta
LC	liquid chromatography
LPS	lipopolysaccharide
MAPK	mitogen activated protein kinase
matrix-APEX	APEX localized to the mitochondrial matrix
matrix-TID	TurboID localized to the mitochondrial matrix
MAVS	mitochondrial antiviral signaling protein
MFN2	mitofusin 2
mGPDH	mitochondrial glycerol-3-phosphate dehydrogenase
MIA40	Mitochondrial intermembrane space import and assembly protein 40
Mito-C	crude isolated mitochondria
Mito-P	pure isolated mitochondria
MitoCarta	mammalian mitochondrial gene inventory
MitoSOX	mitochondrial superoxide sensor
MRPL39	mitochondrial ribosomal protein L39
MS	mass spectrometry
MT-ND3	ND3 subunit of complex I
mtDNA	mitochondrial Deoxyribonucleic acid
mtRNS	mitochondrial RNS
mtROS	mitochondrial ROS
MTS	mitochondrial targeting sequence
MYD88	Myeloid differentiation primary response protein
NADH	nicotinamide adenine dinucleotide
NADPH	nicotinamide adenine dinucleotide phosphate
NDUFA8	NADH dehydrogenase 1 alpha subcomplex subunit
NEM	n-ethylmaleimide

NEMO	NF-κβ essential modulator
NF-κβ	Nuclear Factor NF-κβ
NIK	mitogen-activated protein kinase kinase kinase 14
NLRX1	NLR family member X1
NOS2	inducible nitric oxide synthase
NOTCH2	NOX-promoting inflammatory messenger
NOX	NADPH oxidase
NT5DC2	5'-nucleotidase domain-containing protein 2
OGDH	2-oxoglutarate dehydrogenase
OGDHL	2-oxoglutarate dehydrogenase-like (isoform)
Oligo	oligomycin
OMM	outer mitochondrial membrane
OxICAT	oxidative isotope-coded affinity tags
OXPHOS	oxidative phosphorylation
oxPTM	oxidative PTM
PAM	presequence translocase-associated motor for mitochondrial protein import
PCR	polymerase chain reaction
PD	Parkinson's disease
PDH	pyruvate Ddhydrogenase
PDIA1	protein disulfide isomerase 1
PDK1	pyruvate dehydrogenase kinase 1
PL	proximity labeling
PMI	principal moment-of-intertia
PPA2	mitochondrial inorganic pyrophosphatase 2
PPP2CB	serine/threonine-protein phosphatase 2A
PRX	peroxiredoxin
PSMA6	Proteasome subunit alpha type-6
PTMs	post translational modifications
PTPRC	receptor-type tyrosine-protein phosphatase C
RARS2	mitochondrial arginine aminoacyl transferase
ReDiMe	isotopic reductive dimethylation
RNS	reactive nitrogen species
ROS	reactive oxygen species
S100A2	S100A2 protein
SD	standard deviation
SDHA	succinate dehydrogenase A

SDS	sodium dodecyl sulfate
SEM	standard error of the mean
SICyLIA	stable isotope cysteine labeling with iodoacetamide
SILAC	stable isotope labeling by amino acids in cell culture
SN2	nucleophilic substitution reaction
SOD	superoxide dismutase
SRX	sulfiredoxin
T1D	type I diabetes
T2D	type II diabetes
TAMRA-N_3	tetramethylrhodamine-azide
TBS-T	tris buffered saline with tween 20
TCA	trichloroacetic acid
TCA cycle	tricarboxylic acid cycle
TCEP	tris(2-carboxyethyl)phosphine
TEAB	triethylammonium bicarbonate
TIMM	mitochondrial import inner membrane translocase
TLR	toll-like receptor
TNFα	tumor necrosis factor alpha
TOMM	mitochondrial import outer membrane translocase
TPP^+	triphenyl phosphine
TRX	thioredoxin
TRXR	thioredoxin reductase
TUBA8	tubulin
TurboID	second generation BioID
UCP	uncoupling protein
UniProt	universal protein resource
UPR	unfolded protein response
VDAC	voltage-dependent ion channel
WC	whole-cell
WT	wild-type
βO	beta oxidation

Chapter 1

Mitochondrial Reactive Oxygen Species and Cysteine Redox Signaling

Mitochondrial topography.

Mitochondria date back to the early stages of eukaryotic evolution emerging from the prokaryotic engulfment of an alpha-proteobacterium.[1] This endosymbiotic event explains the unique structure of the organelle. Two distinct membranes, the outer (OMM) and inner (IMM) mitochondrial membranes, together, construct the organelle's functionally diverse sub-compartments, the intermembrane space (IMS) and matrix, each having their own specific role in ATP production and energetic renewal (Figure 1-1).[2] The proteomic composition of the IMS and matrix compartments greatly vary with numerous barriers to entry. Besides from electron transport chain (ETC) enzymes (Complex I, III, IV, V)[3], most mitochondrial proteins are encoded by the nucleus and translated by ribosomes in the cytosol. The recognition of positively charged and amphipathic α-helices on N-terminal mitochondrial targeting sequence (MTS) by translocases on the outer membrane (TOMMs) and inner membrane (TIMMs) is required for mitochondrial protein entry.[4, 5]

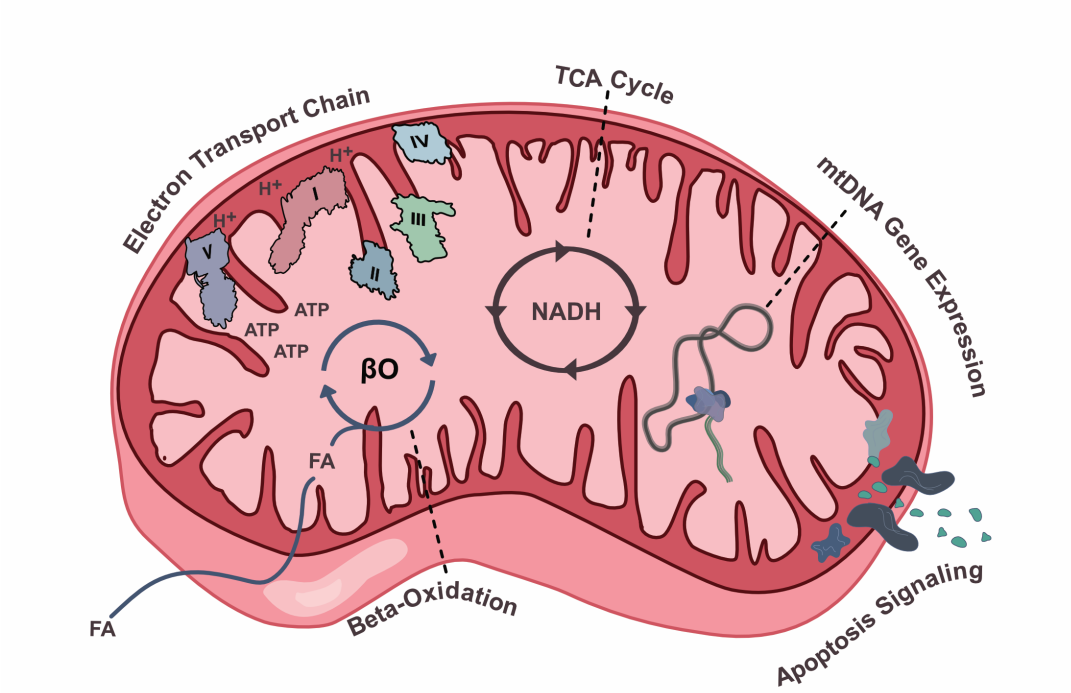


Figure 1-1. Mitochondrial multicompartmental structure with annotations of general biochemical pathways including the electron transport chain, citric acid cycle, mitochondrial DNA gene expression, β-oxidation (BO) of fatty acids (FA) and apoptotic signaling through cytochrome c release.

The IMS proteome consists of a variety of enzymes, metal ion and polypeptide binders, as well as, several apoptotic factors, B-cell lymphoma 2 (BCL-2) family members.[6] A mixture of IMS import techniques is known depending on the size and personalities of the pre-protein, including import through TOMM recognition and pre-sequence cleavage upon admission. Many larger proteins contain bipartite pre-sequences with combinations of mitochondrial targeting and hydrophobic sorting domains. The TIM23 complex drives these precursor proteins' import into the IMM where the hydrophobic portions are proteolytically

cleaved giving soluble, matured protein forms in the IMS.[7] For the small Tim proteins, ranging from between 7 to 16 kDa, the evolutionary conservation of C-terminal cysteine residue patterns, CX_3C and CX_9C, allows for disulfide bridge formation with MIA40/ERV1 complexes permitting proper folding upon IMS import.[8] With the folding of nascent IMS proteins, there are a series of oxidation-reduction (redox) events with electron transfers progressing from the newly formed disulfide bond of the imported protein to MIA40 and ERV1's FAD cofactor to cytochrome *c* heme and cytochrome *c* oxidase (COX) Cu-heme of the ETC, and finally to oxygen producing water (Figure 1-2).[9] This "disulfide relay" is crucial for IMS redox state sensing and the dictation of mitochondrial proliferation.[10] Due to the oxidizing environment of the IMS (-255 mV), there is a higher density of disulfide bonds in the IMS compared to the matrix (-296 mV), and cytosol (-300 mV) which are the most reducing cellular environments.[11]

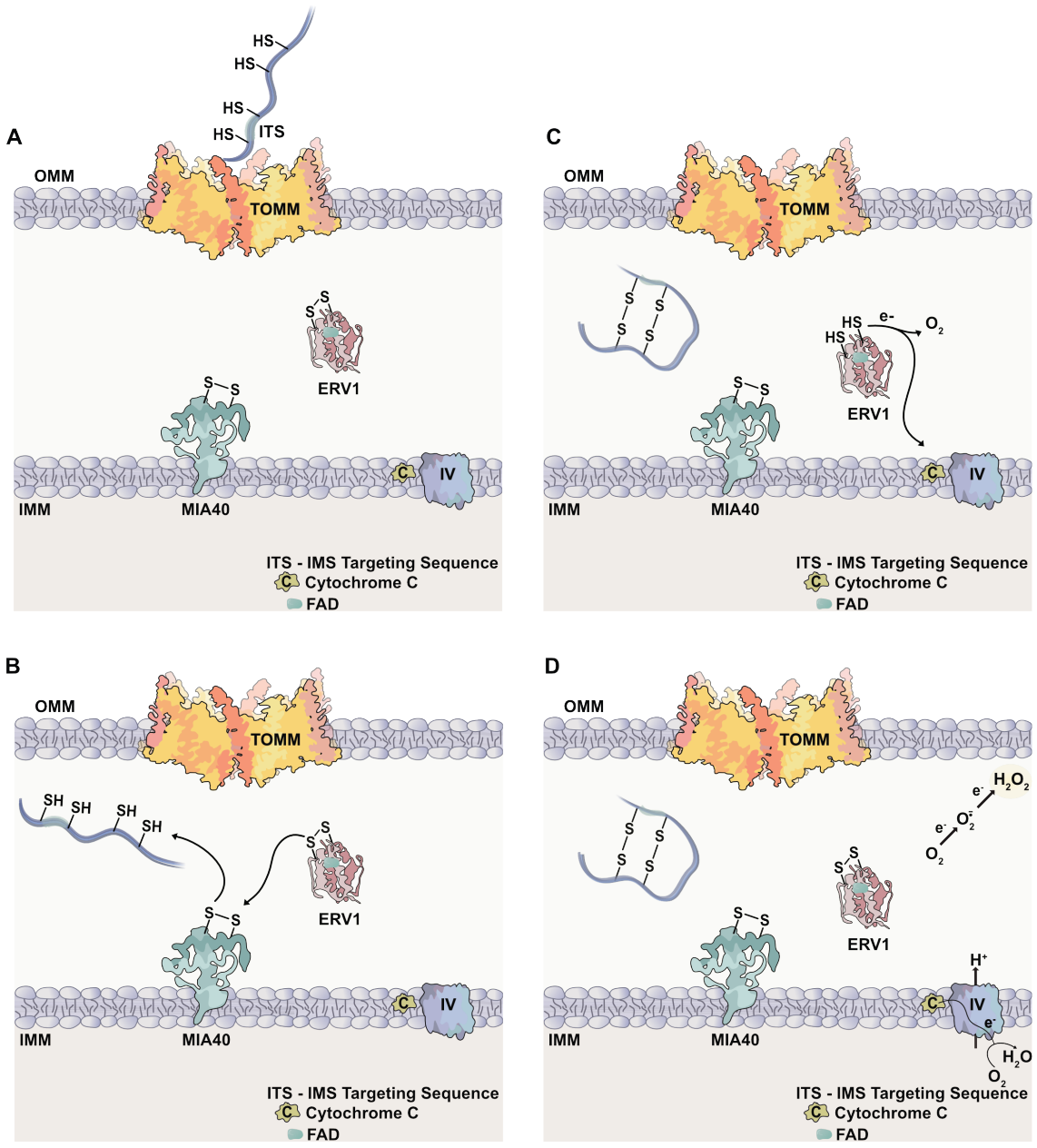


Figure 1-2. Mitochondrial intermembrane space (IMS) protein import through MIA40/ERV1 disulfide bond relay. After IMS targeting sequence recognition by outer membrane translocase (TOMM), a series of redox reactions starting with structural disulfide bond introduction to imported peptide with $Cx_{3/9}C$ motifs by ERV1 and electron transfer to MIA40, cytochrome c and complex IV of the ETC

and finally ending with the reduction of oxygen to water. Reactive oxygen species (ROS) are a byproduct of electron leakage by MIA40 to oxygen.

The innermost region of the mitochondria, the matrix, is home to not only nuclear-encoded proteins such as calcium transporters[12,13] and tricarboxylic acid (TCA) cycle enzymes[14], but also proteins exclusively encoded by the mitochondrial genome (mtDNA) including proteins necessary for mtDNA transcription and translation of the ETC complexes.[15,16] 40% of the mitochondrial-targeted cytosolically-translated proteome incorporate specific N-terminal matrix-MTSs that are required for entry through TIMM complexes and cleaved by mitochondrial processing peptidases resulting in a matured protein. In the matrix, there is a higher density of thiols compared to the IMS due to its highly reducing environment and the high concentration of glutathione.[11]

In addition to variations in protein import and composition, the intramitochondrial compartments have equally different molecular import and composition. The IMS liberally exchanges with the cytosol through large OMM residing voltage-dependent anion channel (VDAC) pores allowing for the unrestricted transmission of ions, small molecules, and metabolites into the IMS. Contrasting the liberal passage of molecules through the OMM, import into the matrix is extremely restrictive due to the high impermeability of the IMM. Therefore, the IMM is impervious to most molecules unless they are recognized and actively imported into the matrix by specialized transporters.[17] The formation of a shallow pH gradient, 7.2-7.4 pH in the IMS and 7.8-8 pH in the matrix[18] results from the varying diffusibility of the mitochondrial membranes and is necessary for aerobic respiration and oxidative phosphorylation (OXPHOS).

Mitochondrial ROS production.

Since their nascency, mitochondria have been the primary energy producers for cellular function with OXPHOS supplying about 90% of total cellular ATP.[19] The folded cristea of the IMM increases surface area by compacting numerous complexes of the ETC and, therefore, enhancing the efficiency of OXPHOS and energy production. [20] Since early eukaryotic evolution, the mitochondrion has been involved in intracellular and extracellular redox-signaling as it regulates and reports on stressors, as well as, overall cell health. [21] ROS and nitrogen species (RNS) are readily generated through enzymatic and non-enzymatic means with the partial reduction of oxygen to form these highly reactive species. The major endogenous mtROS originate from the spontaneous formation of a superoxide anion radical, $O_2^{\bullet-}$. Due to its high reactivity, instability, and membrane impervious nature, $O_2^{\bullet-}$ is rapidly converted to hydrogen peroxide (H_2O_2) by superoxide dismutase (SOD) or spontaneously.[22] The further reduction of H_2O_2 by the Fenton reaction with iron cations gives rise to highly damaging hydroxyl radicals ($^{\bullet}OH$).[23] Moreover, RNS in the primary form of nitric oxide radicals ($^{\bullet}NO$), are produced by nitric oxide synthase (NOS) conversion of *L*-arginine to citrulline. Similarly to the mtROS derivatives, $^{\bullet}NO$ can couple with $O_2^{\bullet-}$ evolving into peroxynitrite ($ONOO^-$) which can undergo a series of couplings with $^{\bullet}NO$ yielding two $^{\bullet}NO_2$ species or N_2O_3.[24] The ROS and RNS, H_2O_2 and N_2O_3, are the primary oxidative signaling molecules due to their lipid solubility, membrane diffusibility, and longer half-lives, 1 ms and 2 s, respectively.[25] These species are secondary derivatives of cellular respiration and are critical for the homeostasis of

energy production along with signaling fluctuations in metabolism or environmental stimuli.[26]

The majority of ROS and RNS are produced by components of aerobic respiration, specifically electron transport by enzymes of the ETC and the TCA cycle.[27] Previously, it was considered that under normal levels of aerobic respiration, ~2% of electrons are leaked from the ETC and react with O_2 in the mitochondria producing mtROS and mtRNS. [28,29] More recent developments conclude that under normal conditions, 0.1%-0.5% of respiratory oxygen may undergo conversions to $O_2^{\bullet-}$.[30] The flow of electrons in the ETC begins as NADH, originating from the TCA cycle, is oxidized by complex I of the ETC where electrons are shuttled from a proximal flavin cofactor to a series of 8 [Fe-S] clusters until they are stored in a reduced quinol pool in the IMM.[31] Oxidation of the quinone:quinol pool from the acquisition of electrons by complex III results in multiple electron exchanges by a multifaceted Q-cycle before advancing electron flow to cytochrome c.[32] A reduction relay from cytochrome c to complex IV guides the electron to the final acceptor, O_2, producing H_2O. Synchronized with the ETC electron relay, complexes I, III, and IV actively pump positively charged hydrogen ions into the IMS producing a proton gradient and consequent membrane potential. Proton relocation from the IMS into the matrix is necessary for complex V phosphorylation of ADP to ATP and matrix protein import.

Complex I and complex III of the ETC are the major generators of superoxide as electrons are leaked through their electron transfer sites.[33] More exclusively, complex I is considered to be the highest producer of mtROS where superoxide is generated at two sites, the flavin mononuceotide (FMN)-bound

proximal end, responsible for initiation of the ETC relay, and the terminal transfer site, both liberating electrons into the matrix.[31] Likewise, complex III is responsible for a significant migration of electrons into the matrix and IMS released from its quinone reduction sites of the Q-cycle.[34, 35]

Besides from complex I and complex III, there are a variety of other sites of mtROS generation in the mitochondria depending on the metabolic state of the cell. Additionally, generous concentrations of mtROS can be supplied under conditions of heightened membrane potential.[36,37] For instance, under these conditions, additional enzymes interacting with the quinol pool release various levels of superoxide originating from the FMN-binding sites through the opposing electron flux established by complex I and reversal of the reduction relay by reducing NAD^+ to NADH.[32,38] MtROS can be released into the matrix by complex II[32], dihydroorotate dehydrogenase (DOD)[38], and electron transfer flavoprotein:ubiquinol oxidoreductase (ETF:QO).[32,38] Furthermore, in the IMS there are several potential ROS producing sites such as mitochondrial glycerol-3-phosphate dehydrogenase (mGPDH), known to be a significant mtROS generator[32] and protein import pathways.[39] During IMS protein import, the MIA40/ERV1 disulfide-bond relay can also result in single electron reduction of oxygen if electrons escape into the IMS before resolving with COX forming water.[39]

Oxidoreductases and flavoprotein complexes occupying the TCA cycle are known to produce lower levels of mtROS, however, this can surpass ETC-derived mtROS during high concentrations of electron transferring molecules (NADH) and substrates, as a result of hypoxic conditions.[40] Under impaired metabolic circumstances, leading transgressors include oxoglutarate dehydrogenase

(OGDH)[41], branched-chain keto-acid dehydrogenase (BCKDH), and pyruvate dehydrogenase (PDH).[26,40,42] Studies have shown small molecules that inhibit the ETC such as at complex I (rotenone[27,43]) and at complex III (Antimycin A, AMA[44]) greatly increase mtROS production. However, under conventional conditions there is generally a low, basal level of mtROS found in isolated mitochondria.[33, 45] These low levels of mtROS are critical for maintenance of metabolic homeostasis and healthy redox signaling pathways.[2]

Antioxidant defenses against elevated mtROS.

Due to the toxic nature of high concentrations of cellular mtROS and mtRNS, tight regulation comes from an abundance of antioxidant including mtROS/RNS scavenger enzymes and molecules (Figure 1-3). SOD is essential for the conversion of $O_2^{\bullet-}$ (half-life 10^{-9}s) to the more stable H_2O_2 (half-life 1 ms) which can diffuse through the membrane, covering distances of over 5 μm and spanning regions outside of the mitochondria.[22] $O_2^{\bullet-}$ is 5 to 10-fold higher in the mitochondria than in the cytosol.[46] Since $O_2^{\bullet-}$ is uniquely contained between the mitochondrial sub-compartments and membranes, as it is not lipid-soluble, there exist three isoforms of SOD residing in different regions of the cell exist including, Cu/Zn-SOD (SOD1) in the IMS, cytosol, and nucleus, Mn-SOD (SOD2) in the mitochondrial matrix, and Ni-SOD (SOD3) in the extracellular environment.[47] $O_2^{\bullet-}$ in the mitochondrial matrix is converted to H_2O_2 by SOD2 before further reduction by glutathione peroxidase (GPX) to water. However, in the IMS, $O_2^{\bullet-}$ has two potential fates. It can be reduced either by SOD1 or by cytochrome c. Cytochrome c has been shown to act as a superoxide-scavenger primarily to complex III-

derived mtROS, due to its proximal location within the ETC and heme groups.[48] In combatting oxidative stress and maintaining $O_2^{\bullet-}$ in low picomolar levels, SODs are expressed in the mitochondria at high concentrations (10 μM) and have rapid dismutasion rates (10^9 M^{-1} S^{-1}) compared to spontaneous dismutasion (10^5 M^{-1} S^{-1}).[49]

Hydrogen peroxide in high concentrations is also lethal to cells, and therefore, neutralizing enzymes, including glutathione peroxidase (GPX), catalase (CAT), and peroxiredoxin (PRX3, PRX5), are necessary second lines of the antioxidant defense system. Intracellular H_2O_2 is degraded into water predominantly by CAT, PRX, and GPX by different mechanisms.[50] Originally discovered in peroxisomes and recently found in mitochondria, CAT is the least specific enzyme responsible for the basic reaction of free H_2O_2 conversion to H_2O.[51] On the other hand, PRX3 and PRX5 protect the matrix from H_2O_2-mediated oxidative damage by reducing 90% of total H_2O_2. Isoform-substrate preferences reveal PRX3 as the most efficient (2-fold) at diminishing free H_2O_2, while PRX5 favors the reduction of organic-hydroperoxides. Interestingly, PRXs make up over 1% of total cellular proteins alluding to their importance in redox homeostasis and oxidative stress management.[52] Both PRX isoforms are active in a homodimer and use two reactive cysteines for catalysis through a redox-active disulfide bond. The redox-sensing peroxidatic cysteine binds H_2O_2, forming sulfenic acid (-SOH), before the resolving cysteine reacts to form an intermolecular disulfide bond resulting in the production of water.[52] To regenerate the free thiol dimer, reduced thioredoxin (TRX) becomes oxidized which is then itself reduced by thioredoxin reductase (TRXR) and NADPH.[53] Similarly, two isoforms of GPX exist in the mitochondria catalyzing the displacement of hydroperoxides from specific

substrates utilizing oxidizing two equivalents of reduced glutathione (GSH) to oxidized glutathione (GSSG). GPX1 is specialized to remove peroxides of the matrix while, phospholipid hydroperoxide glutathione peroxidase (GPX4) reduces fatty acid hydroperoxides throughout the cell.[54,55]

Non-enzymatic removal of mtROS is accomplished with the aid of antioxidant small molecules such as GSH and ascorbate. As the most abundant small molecule thiol, GSH is synthesized exclusively in the cytosol and imported through porins and TOMM into the IMS.[56] To be translocated into the matrix, GSH needs assistance from dicarboxylate and 2-oxoglutarate carriers in order to for active transportation across the IMM.[57,58] Scavenging for reactive species and proteins, GSH is converted to GSSG. Conversion back to the reduced form occurs by glutathione reductase (GR).[59] Concentrations of GSH in the mitochondria (10-14 mM) are similar to the cytosol, however, the ratios of GSH:GSSG vary by organelle sublocation providing differences in redox environments.[60] The cytosol being the most reducing compartment, ~3000:1 GSH:GSSG, followed by the matrix with higher oxidative stress species, ~900:1 GSH:GSSG, and the more oxidizing disulfide-bond concentrated IMS ~250:1 GSH:GSSG.[11, 61]

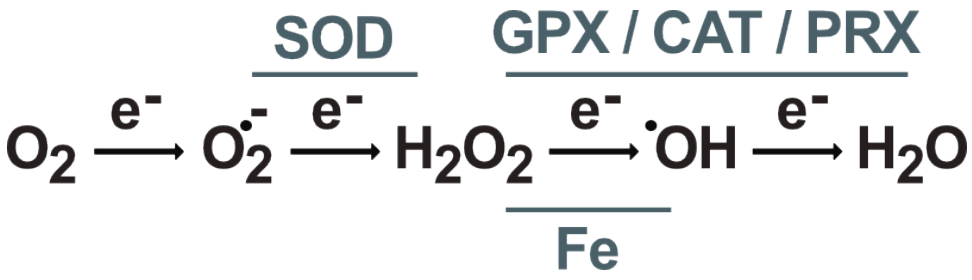


Figure 1-3. ROS formation through subsequent reductions spontaneously or by antioxidant defense enzymes including superoxide dismutase (SOD), glutathione peroxidase (GPX), catalase (CAT), peroxiredoxin (PRX).

Oxidative cysteine modifications.

MtROS are essential for cellular signaling through reversible post-translational modifications (PTMs) on proteins. Due to their characteristic electron density and physiological pKa ranging from as low as 3.5 to as high as 12, thiol groups on amino acids are inherently highly reactive nucleophiles and, therefore, are exceedingly susceptible to oxidation.[62] These mtROS can regularly react with cysteine thiols resulting in stable post-translational alterations such as oxidation to sulfenic acid (-SOH), sulfinic acid (-SO_2H), sulfonic acid (-SO_3H), *S*-nitrosation (-SNO), and *S*-glutathionylation (-SSG) which are imperative for downstream signaling events connected to innate cell function and redox homeostasis (Figure 1-4).[63] With increasing concentrations of ROS, oxidative-PTMs become more irreversible, switching from transient signaling events to macromolecular damage. Notably, of the most stable modifications, -SO_2H can only be physiologically reversed by the antioxidant enzyme sulfiredoxin (SRX) while -SO_3H formation is complete irreversible damage occurring under high oxidative pressure.

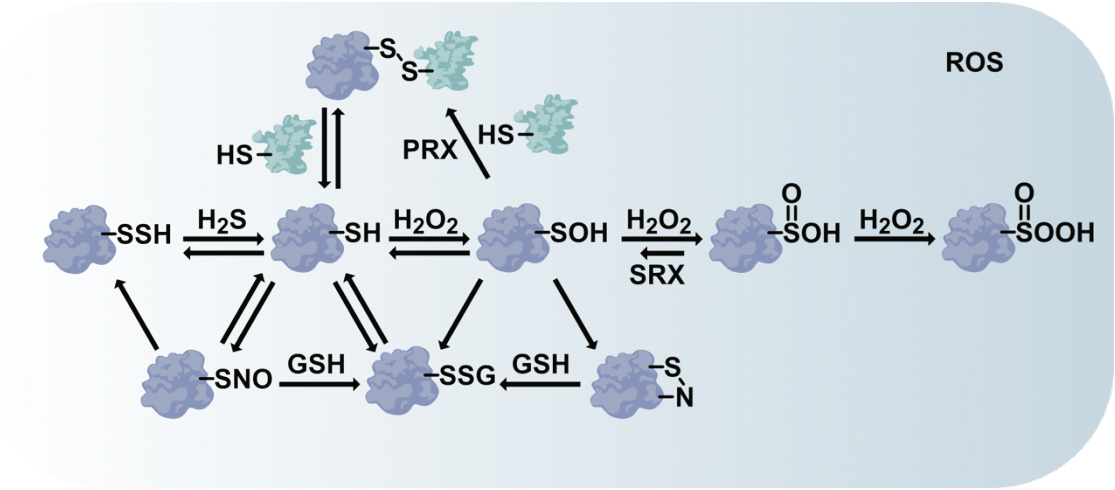


Figure 1-4. Thiol oxidative modifications in the presence of different ROS levels. Arrows depict the reversibility of each modification.

Known mitochondrial targets of mtROS include ETC complexes, TCA enzymes such as aconitase (ACO2) and isocitrate dehydrogenase (IDH), and uncoupling proteins (UCP). These proteins are distinguished to operate under "redox thiol switches" as their enzymatic activity can be modulated by mtROS-induced cysteine oxidation (Figure 1-5).[64] Multiple oxidative-PTMs of complex I have been highly characterized. Cysteine oxidation can occur on both subunits of complex I including the hydrophobic arm of the 51kDa FMN cofactor binding unit and proximal to the 75kDa unit which is major ROS source of complex I. Most notably, C531 and C704 are shown to be reversibly *s*-glutathionylated at low oxidant levels protecting the enzyme from potentially more severe oxidation.[65] Cysteine modifications in these locations lead to conformational changes of complex I blocking NADH electron transfer to FMN, ultimately, inactivating the enzyme and decreasing overall ROS production.[66] GRX-mediated deglutathionylation leads to reactivation of the ETC complex. Interestingly, •NO reversibly modified C39 on complex I and is a protective mechanism to deactivate the enzyme in ischemic and low NADH circumstances with *s*-nitrosylation of the C39 adjacent to a ubiquitination site.[67] Additional cysteine oxidation of ETC enzymes is recognized and, although less conclusive, most alterations are thought to be preventative against further oxidative injury. Accompanying high oxidative stress, complex II undergoes cysteine *s*-glutathionylation at C90 on SDHA as well as tyrosine nitration.[68-70] In addition, *s*-glutathionylation increases electron flow and decreases superoxide production as a defense mechanism against mtROS while deglutathionylation of complex II reveals increased IMM potential.[68, 71]

Also situated in the IMM, UCPs (UCP1 and UCP2 found in brown adipose tissue, heart, and skeletal tissue, and UCP3 found in a wide variety of tissues) are distinctively regulated by cysteine oxidation during oxidative stress conditions.[72] While protons are purposefully sent from the IMS to the matrix in a coupled manner and shuttled by ATP-synthase to generate ATP, OXPHOS is never a completely efficient system. Protons can leak through the phospholipid bilayer resulting in decreases in the electron-generated proton motive (Δp) force and release of heat. Escape of protons can occur by two processes. Basal proton leakage occurs with increases in fatty-acyl composition of IMM and adenine nucleotide translocase (ANT), while, inducible proton escape through the IMM is controlled by UCPs by uncoupling the ETC proton gradient and opposing OXPHOS.[73,74] UCPs and ANT buffer mtROS through a complex pathway including activation by IMM lipids oxidized by $O_2^{\bullet-}$ and 4-hydroxy-2-nonenal (HNE) lipid peroxidation, as well as deactivation by reversible glutathionylation of conserved matrix membrane spanning cysteine residues such as C25 and C259 in UCP3. Notably, in high levels of mtROS, glutathionylation can be reversed resulting in increased respiration.[73,74] As multifaceted metabolic attenuators, UCPs are able to sway metabolism towards fatty-acid breakdown instead of glucose breakdown. This metabolic control is crucial in pathologies such as type I and II diabetes (T1D and T2D) and obesity. When UCPs are activated, there is disruption of glucose sensing in the brain and pancreas due to the secretion of glucose-stimulated insulin. Additionally, UCP activity and the increase in fatty acids are linked to heart failure.[65] Discrepancies in UCP OXPHOS switching and proton leakage lead

to resting metabolic rate variations correlated to metabolic diseases such as obesity and, conversely, extreme weight loss.[73-75]

With its operations proportionally dysregulated by the matrix redox environment and H_2O_2, ACO2 is a critical TCA cycle enzyme with pronounced mtROS sensitivity. Crucial for catalysis, a [4Fe-4S] cluster is held by 3 cysteine residues, C385, C448, C451 and a water molecule designating one Fe center as labile.[76] Typically, citrate is bound by the unstable Fe lacking a thiolate that serves as a Lewis acid to promote the conversion to isocitrate. The single unligated Fe in ACO2 has unique sensitivity to $O_2^{\bullet-}$ inactivation as the cluster is easily destabilized with oxidation of this metal-binding center to produce H_2O_2 and free Fe^{2+}. Under strained circumstances, not only is catalysis abolished, but the peroxide and iron products consequently associate through further reductions in a Fenton reaction giving highly toxic $^{\bullet}OH$.[76]

TCA cycle enzyme and ROS generator OGDH is highly vulnerable to cysteine oxidation as 37 cysteine residues reside in the full complex.[77, 78] The several thiols, located in E2 and E3 subunits cycle between oxidation states and mixed disulfide bonds necessary for catalysis and may be frequently glutathionylated to protect the enzyme from irreversible oxidative damage.[77] H_2O_2 production by OGDH is uniformly stimulated by NADH:NAD^+ concentrations. The production of mtROS by OGDH is suggested to be a key regulator of the ETC and the TCA cycle as oxidation of NADH and electron transfer are impaired under oxidative conditions. At high micromolar concentrations of rotenone-induced production of H_2O_2, the conversion of α-ketoglutarate to succinyl-CoA and CO_2 is inhibited by the glutathionylation of covalently bound lipoic acid.[69, 70] Depending upon H_2O_2

consumption and reduced states of GSH, GRX can cleave glutathione modifications on OGDH rendering the enzyme active. Since OGDH is the rate-limiting step of the TCA cycle, the enzyme's inhibition by mtROS is correlated with decreased NADH levels and the halting of ETC and OXPHOS.[78-80] However, ACO2 is more sensitive to mtROS, and its inhibition is linked to H_2O_2 generated by OGDH.[81] Therefore, oxidative PTMs on OGDH, as well as OGDH-derived ROS, are considered to alter OGDH function and regulate TCA cycle activity.[79]

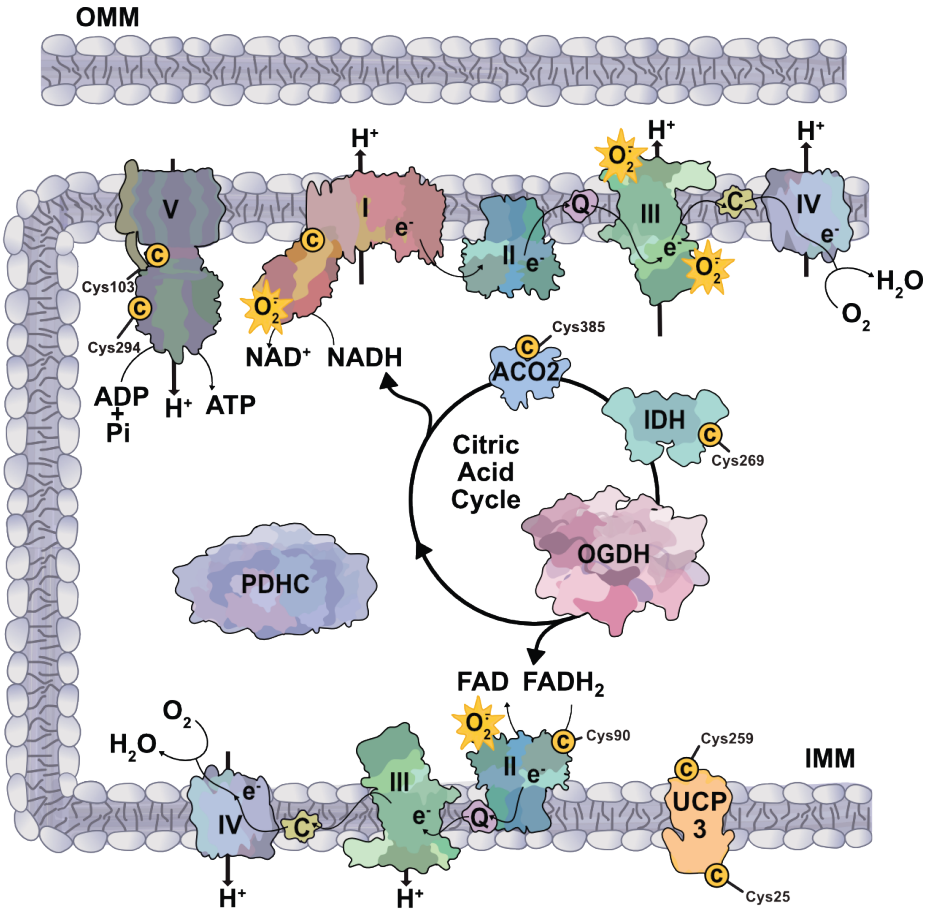


Figure 1-5. Aerobic respiration sites of major superoxide production (ETC complex I and complex III) and known redox thiol sensors of metabolism on ETC complexes and TCA enzymes. Complexes illustrated represent corresponding PDB files.

Cysteine redox signaling in disease.

Synonymous to the phosphorylation of kinases, mtROS is crucial for deciding downstream cellular functions. A low and essential level of mtROS is crucial for mitochondrial signaling for adaptations to stress, metabolism, aerobic respiration, cellular proliferation, and differentiation.[2] When high concentrations of mtROS overpower antioxidant defenses, senescence[82] and apoptosis[83] may be prompted through irreversibly and directly damaging cellular building blocks including nucleotides[84], lipids[85], and amino acids[86] (Figure 1-6). Consequently, mitochondrial dysfunction and the subsequent overall oxidative damage, originating from high levels of mtROS and mtRNS, are shown to drive aging and the pathogenesis of several diseases neurodegeneration[87] and ischemia-reperfusion injury[88] to diabetes[89] and cancer[90] (Figure 1-7).

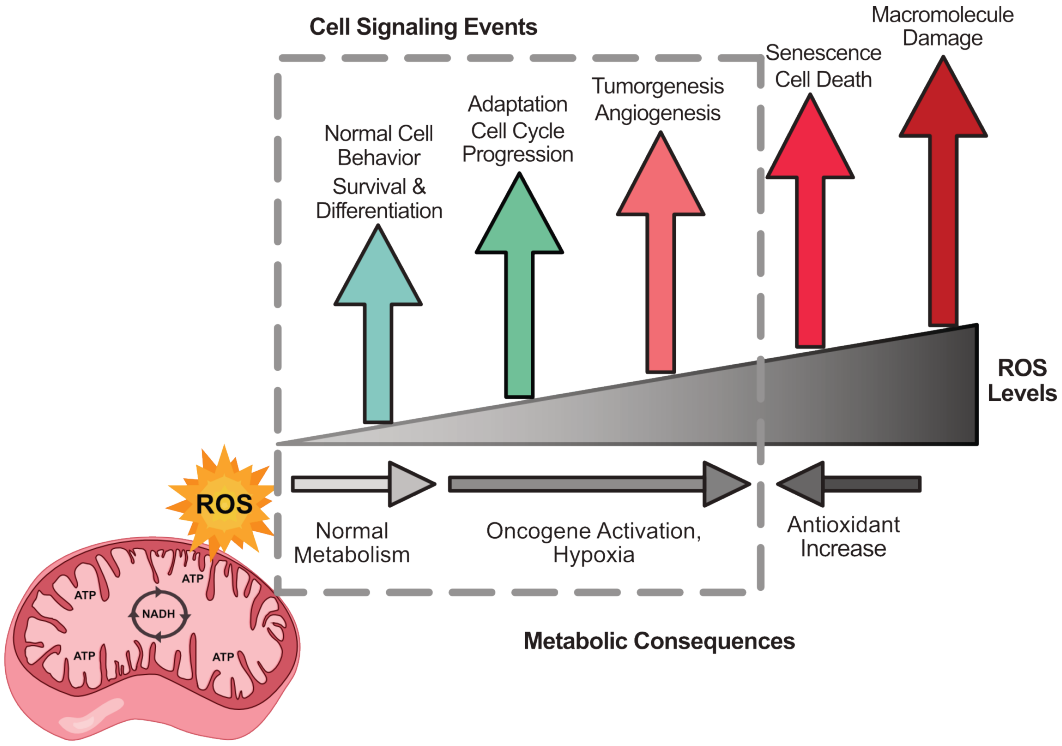


Figure 1-6. Cellular consequences centered on mtROS abundance. Pathologically relevant ROS-related signaling found in the "sweet spot" of slight oxidative stress.

When levels exceed antioxidants, macromolecular injury and cell death is observed.

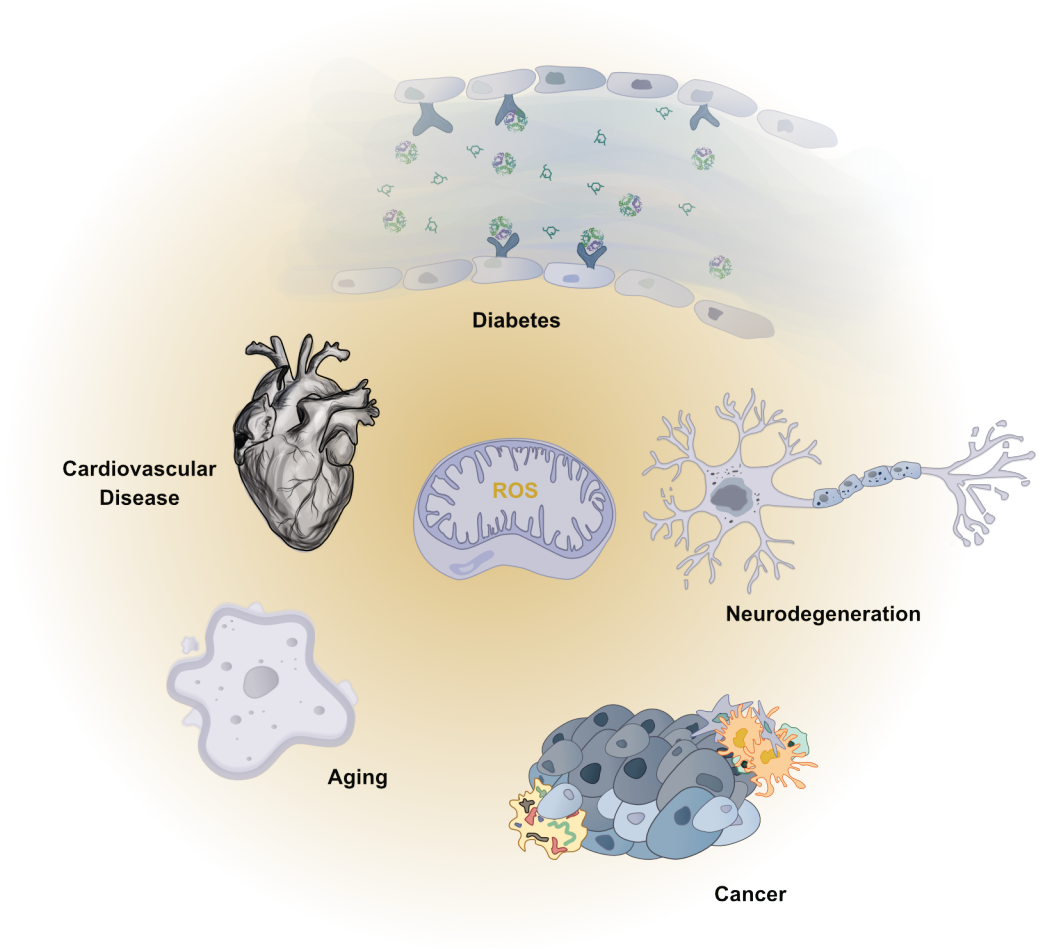


Figure 1-7. Assortment of diseases impacted by mitochondrial redox signaling and oxidative stress.

Apoptotic signaling and mtROS.

Among its many roles in energy production, mitochondria are the principal determinators of cell death. MtROS-induced apoptosis begins in the mitochondria with cytochrome c release. Anti-apoptotic protein BCL-2 resides in the IMS and is responsible for the induction of apoptosis. BCL-2 inhibits apoptotic regulators

BAX/BAK OMM pore establishment through heterodimer formations.[91] The effectiveness of apoptotic inhibition is lost with oxidation or mutations on conserved BCL-2 cysteine residues, C158 and C229.[92,93] In addition to BCL-2 influence, mtROS oxidation of cardiolipin in the IMM obstructs cytochrome c insertion to the membrane and, therefore, cytochrome c is liberated to the IMS where it acts as a cofactor for apoptosome assembly and caspase activation for apoptotic cell death.[94-96]

MtROS in cancer.

With evasion of apoptosis as a trademark of cancer, there are countless ways in which mtROS, and more specifically cysteine oxidation, is necessary for metastasis and cancer drug resistance. For instance, in non-tumorigenic cells, glycolysis and oxidative metabolism are highly regulated events, however, tumorigenic cells accelerate metabolic mechanisms supporting survival and hyperproliferation. Accompanied by hypermetabolism are high quantities of mtROS/mtRNS which are beneficial to tumorigenesis as these reactive species can oxidize cysteines and activate pathways such as mitogen activated protein kinases MAPK/ERK and NF-KB to promote oncogenic, growth factor, and cell cycle stimulation.[86] With pathogenic amounts of mtROS, C118 on GTPase Ras is known to become oxidized halting GDP binding and stabilizing the active GTP-bound enzyme while initiating the cascade of AKT and ERK1/2MAPK kinase pathways which ultimately results in tumorgenesis.[97-99] Additionally, NF-KB is a redox-regulated sensor for oxidative stress. At low concentrations of H_2O_2, NF-KB releases from its inhibitory proteins (IKK, NEMO, and NIK) and translocates to the nucleus to activate oncogenic transcription. While mtROS is highly

concentrated in the mitochondria, its ability to transverse membranes can lead to pervasive signaling in a variety of intracellular spaces including the cytosol pathways and cross-talk engaging organelles such as the endoplasmic reticulum and nucleus.[100-101]

MtROS encourage cell proliferation in the low oxygen (hypoxic) environments created in tumors by stabilizing hypoxia inducible factor (HIFα) and stimulating dimerization. HIFα translocates to the nucleus where it behaves as a transcription factor initiating expression of hypoxia-adaptation genes protecting tumors.[90] Moreover, commonly referred to as the Warburg Effect, cancer cells rely on glycolysis and the heightened uptake of glucose to avoid apoptotic signaling keeping the cells in a "sweet spot" of mtROS to increase proliferation and cancer cell survival without extending into mtROS levels toxic to cells and activating cell death pathways (Figure 1-6).[102] These cancer-initiated metabolic shifts are also the result of direct oxidation and perturbation of the TCA cycle and ETC enzymes.[103] Interestingly, due to the relationship between increased oxidative stress and cancer progression, the monitoring of mtROS levels may indicate the effectiveness of chemotherapeutic treatments.[104]

MtROS in neurodegeneration.

Furthermore, an imbalance of oxidants and antioxidants in mitochondria is a prominent feature in many neurodegenerative diseases such as Alzheimer's (AD), Parkinson's (PD), and Huntington's disease (HD)[105] as mtROS can trigger direct oxidative damage to proteins as well as mtDNA, leading to mutations. For instance, mutations to SOD1, resulting in increased levels of available superoxide,

are characteristically found amongst 10% of PD and amyotrophic lateral sclerosis (ALS) patients.[106, 107] Moreover, links between AD and higher concentrations mtROS in the brain were found. Patients with abnormally abundant levels of Fe tend to have increased rates of AD maturity and severity due to increases in mtROS, specifically •OH. These species are produced by Fe-dependent Fenton reactions which oxidize the brain.[108] Moreover, general mechanisms of cell senescence and aging correlate to radically-formed crosslinking, point mutations, and deletions of mtDNA and, ultimately, lead to mitochondrial dysfunction.[109-111] In AD, HD, and PD disease models including SOD2 knockout mice models, higher levels of mtROS is observed with decreases in OGDH complex activity suggesting the role of mtROS-induced dysregulation of metabolism.[108, 112, 113] In patients with AD, reduced activity of the OGDH complex has been reported in 57% of brain tissue which has similarly been shown in other neurodegenerative pathologies.[114] Similarly in HD, a reduction in glucose metabolism alongside diminished OGDH complex catalysis points towards decreased activities of many TCA enzymes including PDH complex.[112]

MtROS and diabetes and cardiopathy.

Mitochondrial dysfunction and mtROS are centralized themes in diabetic and cardio pathologies.[115] With oxidative stress stemming from and contributing to nutritional insufficiencies, both types of diabetes (T1D and T2D) demonstrate elevated ROS concentrations as extensive contributors to disease progression, however in different ways. Genetic mutations in T1D can lead to insulin deficiencies and hyperglycemia caused by pancreatic B-cell mtROS-related injury,

mitochondrial dysfunction, and death. In addition to universal increases in B-cell mtROS, elevated levels of ROS in T-cells and macrophages increase activation and inflammatory cytokine release targeting B-cells for elimination perpetuating a cycle of ROS-promoted B-cell injury and hyperglycemia.[116] On the other hand, T2D is also characterized by hyperglycemia led mtROS, however, this process is typically accelerated by the inability of the pancreas to yield enough insulin to meet the demand of glucose ingestion and is not influenced by immune system recognition and targeting of B-cells as in T1D. Interestingly, hyperglycemia appears to be the driving force behind mitochondrial oxidative stress due to metabolic stress. The challenge of processing abnormally high glucose concentrations leaves the mitochondria exhausted with loss of basic biochemical functions and the inability for metabolic maintenance.[89,115,117,118]

The pathophysiological progression and disease states of diabetes are intertwined with mtROS signaling and mitochondrial injury resulting in multiple cardiovascular complications including microvascular (neuropathy) and macrovascular (coronary heart disease and stroke).[119] With cardiac tissue abundant with and reliant on mitochondria for operation, it is unsurprising that any perturbation to mitochondrial function may contribute significantly to vascular pathology.[119] MtROS pools present significant modifications to many different mitochondrial systems from IMM potential, electron transport, and [Fe-S] cluster generation to mitochondrial polymerase activity and DNA stability all of which can result in overall mitochondrial dysfunction and signaling for apoptosis or necrosis.[120]

Therapeutics targeting mitochondria and mtROS.

Because mtROS are integral to numerous pathologies, there has been increased attention focused on the pursuit of therapeutics to ameliorate the negative effects of oxidative stress. Antioxidant-based drugs could allow for overcoming multiple challenges of small-molecule inhibitors and cytotoxic-based chemotherapeutics such as drug resistance and toxicity.[121] Over the past decade, ROS-targeting cancer and cardiovascular therapeutics have been introduced to clinical trials with several gaining FDA approval. Because pathological mtROS signaling in cancer lies in an intermediate range, higher than can be regulated by natural antioxidant concentrations, but, lower than cell death signal induction, large increases or decreases of mtROS could be viable therapeutic strategies.[122,123] For instance, Vitamin C and Vitamin E have been studied for years in clinical trials aimed at antioxidant ROS-decreasing therapies while, antibacterial repurposed drugs, such as doxycycline, have revealed promising cancer cell targeting through pathways of ROS induction.[121] However, the efficacy of each antioxidant molecule appears to be influenced strongly by cancer type.[124]

There is overlap in the exploration of ROS-altering therapies for combatting cancer and cardiovascular disease including ROS-seeking Vitamin C and Vitamin E treatments.[125] Furthermore, in mouse cardiovascular disease models, encouraging results of a significant restoration of cardiac operations were demonstrated with mtROS scavenger treatments including N-acetyl cysteine[126] and MitoTEMPO.[127] In addition, a small-molecule peptide mimetic, Elamipretide, initially showed cardiolipin and general mitochondrial protection from ROS, however, phase 3 clinical trials were not met.[128] Although promising, more efforts are needed to translate the positive effects of ROS scavengers in mice to human

trials including the complexities in drug targeting to the mitochondria, dosing and timing of treatments, and improving safety and efficacy.[119]

Chemoproteomic approaches in evaluating global cysteine oxidation events.

Chemoproteomic platforms such as isotopic tandem orthogonal proteolysis activity-based protein profiling (isoTOP-ABPP) have previously been used by Bak *et al*. to quantitatively profile mitochondria functional cysteines through the labeling of isolated mitochondria with cysteine-reactive iodoacetamide alkyne probe followed by heavy and light isotopically labeled cleavable biotin-azide tags (Figure 1-8A).[129,130] The identification of highly reactive cysteines sets the groundwork for further assessment of cysteine redox signaling. The isoTOP-ABPP platform was applied to map cysteines sensitive to *s*-nitrosation modifications revealing several cysteines on VDAC family members with decreased reactivity upon GSNO treatment.[130] The development of isotopically coded iodoacetamide alkyne probes allowed for expansion of IsoTOP-ABPP platforms to quantify of cysteine reactivity in the endoplasmic reticulum.[131,132] The IsoTOP-ABPP platform is highly amenable to profile reactivity changes of cysteines in various intracellular compartments and can report on a multitude of properties from reactivity and oxidation to cysteine targeted-fragment ligandability[133,134] and [Fe-S] cluster investigation.[135]

Although fluctuations in cysteine reactivity revealed by IsoTOP-ABPP can be proportional to changes in oxidation states, other methods can directly survey oxidation-specific cysteine changes. OxICAT (isotopically coded affinity tags) is a chemoproteomic platform based upon the use of cysteine-specific ICAT reagents to directly profile reversible cysteine oxidation states by trapping reduced thiols

with a light-ICAT reagent followed by a reduction with TCEP allowing for the labeling of newly reduced thiols with heavy-ICAT reagent (Figure 1-8B).[136] Light to heavy (L:H) ratios can quantitatively report if residues are fully oxidized, partially reduced, or fully reduced and provide key information on the changes in redox states of various organelles. Previous groups have used the OxICAT platform to identify trends in purified yeast revealing multiple cysteine sites sensitive to oxidation by hydrogen peroxide and disulfide bond monitoring in endoplasmic reticulum under thapsigargin-induced unfolded protein response/ER-stress.[132] Yet, OxICAT and IsoTOP-ABPP applications have not been extended to evaluation of cysteine oxidation in mammalian cell mitochondria conditions of oxidative stress.

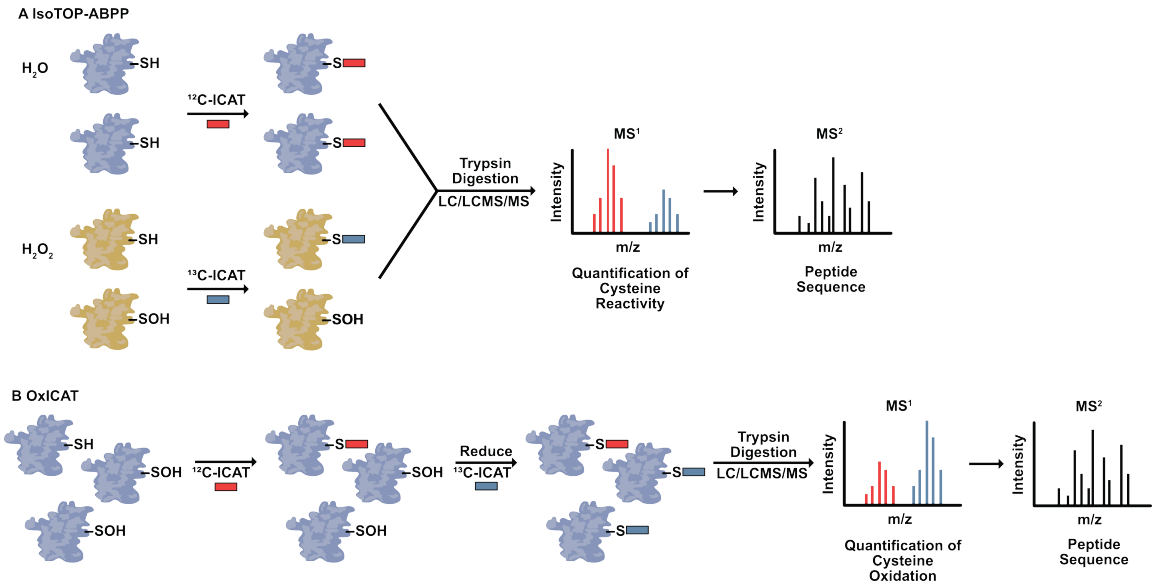


Figure 1-8. Chemoproteomic methods of quantifying cysteine oxidation. (A) Schematic of IsoTOP-ABPP where reactive thiols are alkylated by either a light cysteine alkylating reagent or heavy cysteine alkylating reagent in treated (H_2O_2) and untreated sample (H_2O). The sample is combined after click chemistry with a cleavable biotin azide tag and trypsinized after streptavidin enrichment. Cysteine

reactivity is quantified in MS^1 abundance of the isotopically labeled cysteine containing peptides. MS^2 reports on peptide identification. (B) Schematic of OxICAT platform where in a single sample, cysteine oxidation is reported. Reduced cysteines are alkylated by a light cysteine alkylating reagent. After reduction, previously oxidized cysteines are alkylated by a heavy cysteine alkylating reagent. MS analysis of MS^1 chromatogram indicates the abundance of isotopically alkylated peptides and can be converted to percent oxidation values.

Small molecules for labeling of specific cysteine oxoforms in the mitochondria.

Although redox-monitoring platforms such as OxICAT, ICAT, and IsoTOP-ABPP allow for broad, comprehensive profiling of cystiene oxPTMs, these methods are unable to distinguish between unique cysteine modifications. Recently, small-molecule probes have been an attractive strategy in profiling specific cysteine oxoforms. For example, the investigation of *s*-glutathionylation events has been streamlined through the use of biotinylated (cell impermeable, bioGSH,[137] and cell permeable, bioGEE)[137,138] and clickable GSH probes.[139] Furthermore, the Carroll lab has pioneered the development of clickable sulfinic acid-targeting diazene (DiaAlk) probes[140] and sulfenic acid-targeting dimedone[141] and Wittig probes[142] providing significant impact in efforts to identify specific ox-PTMs on cysteines in *C. elegans*[140] and yeast systems.[143] Although, the use of positively-charged, mitochondrial-targeting moieties such as rhodamine and triphenylphosphine (TPP^+) are attractive strategies for mitochondrial cysteine enrichment without additional organelle isolation steps, chemically-directed mitochondrial molecular probes limit analysis to the matrix-facing IMM and matrix proteomes.[144] To that end, work from the Hamachi lab demonstrates

successful mitochondrial matrix targeting, tetraethyl-rhodamide chloroacetamide probes.[145] However, recognize only a small fraction (290 cysteines on 196 mitochondrial proteins) of the ~1500 total proteins encoded for mitochondrial localization. In addition, the Carroll lab has appended TPP^+ to Wittig probes for mitochondrial matrix sulfenic acid examination which effectively identified 2,063 sulfenylated cysteines, however without the anticipated mitochondrial specificity.[142] The multiplicity of chemoproteomic advancements sets the groundwork for future investigation of cysteine oxidation and reactivity specifically within mammalian mitochondria during conditions of heightened ROS analogous to pathologies.

Conclusion

Mitochondria are the principal sites of intracellular ROS production. The generation of mtROS fuels redox signaling facilitated through cysteine oxidation events. Although mitochondrial redox signaling is widely recognized and there are several known instances of "thiol switches"[64] (UCP1[75], complex V[146], complex I,[147] ACO2[78]), it is likely that many more of these types of regulatory cysteine oxidation sites may exist. Here, we describe chemoproteomic methods in unraveling cysteine oxidation events that may be responsible for altered enzymatic functions and contributing to pathological cellular states. In this dissertation, we describe methods of chemoproteomics (IsoTOP-ABPP and OxICAT) and mitochondrial enrichment (organelle isolation and proximity labeling) to assess changes in mitochondrial cysteine oxidation in different metabolic states. Through IsoTOP-ABPP, a comprehensive analysis of redox-sensitive cysteines is reported in mitochondria subjected to exogenous ROS (H_2O_2

treatments), as well as endogenous mtROS generated as an effect of ETC inhibition by AMA. Furthermore, using an innovative combinatorial technique of enzymatic proximity labeling (PL) coupled to reversible cysteine oxidation profiling by OxICAT (PL-OxICAT), we streamline and localize our efforts of evaluating cysteine oxidation to the intracellular sub-compartments including the IMS, matrix, and cytosol. Increased resolution of oxidatively-modified cysteines in "ROS hotspots" was determined with the direction of APEX to areas of the cell known to have high ROS. APEX was activated by endogenous ROS from ETC inhibition in HEK 293T as well as during cytokine-based differentiation activation in Raw 264.7 cell lines. Together, this work demonstrates the ability for innovative chemoproteomic platform development to assess pathologically relevant sites of cysteine oxidation.

REFERENCES

(1) Lane, N.; Martin, W. The energetics of genome complexity. *Nature* **2010**, *467* (7318), 929-934.

(2) Sena, L. A.; Chandel, N. S. Physiological Roles of Mitochondrial Reactive Oxygen Species. *Mol. Cell* **2012**, *48* (2), 158-167.

(3) Wallace, D. C.; Brown, M. D.; Lott, M. T. Mitochondrial DNA variation in human evolution and disease. *Gene* **1999**, *238* (1), 211-230.

(4) Pfanner, N.; Geissler, A. Versatility of the mitochondrial protein import machinery. *Nat. Rev. Mol. Cell Biol.* **2001**, *2* (5), 339-349.

(5) Abe, Y.; Shodai, T.; Muto, T.; Mihara, K.; Torii, H.; Nishikawa, S.; Endo, T.; Kohda, D. Structural basis of presequence recognition by the mitochondrial protein import receptor Tom20. *Cell* **2000**, *100* (5), 551-560.

(6) Wang, C. X.; Youle, R. J. The Role of Mitochondria in Apoptosis. *Annu. Rev. Genet.* **2009**, *43*, 95-118.

(7) Chacinska, A.; Lind, M.; Frazier, A. E.; Dudek, J.; Meisinger, C.; Geissler, A.; Sickmann, A.; Meyer, H. E.; Truscott, K. N.; Guiard, B.; et al. Mitochondrial presequence translocase: Switching between TOM tethering and motor recruitment involves Tim21 and Tim17. *Cell* **2005**, *120* (6), 817-829.

(8) Wrobel, L.; Sokol, A. M.; Chojnacka, M.; Chacinska, A. The presence of disulfide bonds reveals an evolutionarily conserved mechanism involved in mitochondrial protein translocase assembly. *Sci. Rep.-Uk* **2016**, *6*.

(9) Riemer, J.; Bulleid, N.; Herrmann, J. M. Disulfide Formation in the ER and Mitochondria: Two Solutions to a Common Process. *Science* **2009**, *324* (5932), 1284-1287.

(10) Mesecke, N.; Terziyska, N.; Kozany, C.; Baumann, F.; Neupert, W.; Hell, K.; Herrmann, J. M. A disulfide relay system in the intermembrane space of mitochondria that mediates protein import. *Cell* **2005**, *121* (7), 1059-1069.

(11) Hu, J. J.; Dong, L. X.; Outten, C. E. The Redox Environment in the Mitochondrial Intermembrane Space Is Maintained Separately from the Cytosol and Matrix. *J. Biol. Chem.* **2008**, *283* (43), 29126-29134.

(12) Kamer, K. J.; Mootha, V. K. The molecular era of the mitochondrial calcium uniporter. *Nat. Rev. Mol. Cell Biol.* **2015**, *16* (9), 545-553.

(13) Xing, Y.; Wang, M.; Wang, J.; Nie, Z.; Wu, G.; Yang, X.; Shen, Y. Dimerization of MICU Proteins Controls Ca(2+) Influx through the Mitochondrial Ca(2+) Uniporter. *Cell Rep.* **2019**, *26* (5), 1203-1212 e1204.

(14) Cavalcanti, J. H.; Esteves-Ferreira, A. A.; Quinhones, C. G.; Pereira-Lima, I. A.; Nunes-Nesi, A.; Fernie, A. R.; Araujo, W. L. Evolution and functional implications of the tricarboxylic acid cycle as revealed by phylogenetic analysis. *Genome Biol. Evol.* **2014**, *6* (10), 2830-2848.

(15) Meisinger, C.; Sickmann, A.; Pfanner, N. The mitochondrial proteome: from inventory to function. *Cell* **2008**, *134* (1), 22-24.

(16) Richter-Dennerlein, R.; Oeljeklaus, S.; Lorenzi, I.; Ronsor, C.; Bareth, B.; Schendzielorz, A. B.; Wang, C.; Warscheid, B.; Rehling, P.; Dennerlein, S. Mitochondrial Protein Synthesis Adapts to Influx of Nuclear-Encoded Protein. *Cell* **2016**, *167* (2), 471-483 e410.

(17) Zorov, D. B.; Juhaszova, M.; Yaniv, Y.; Nuss, H. B.; Wang, S.; Sollott, S. J. Regulation and pharmacology of the mitochondrial permeability transition pore. *Cardiovasc. Res.* **2009**, *83* (2), 213-225.

(18) Llopis, J.; McCaffery, J. M.; Miyawaki, A.; Farquhar, M. G.; Tsien, R. Y. Measurement of cytosolic, mitochondrial, and Golgi pH in single living cells with green fluorescent proteins. *Proc. Natl. Acad. Sci.* **1998**, *95* (12), 6803-6808.

(19) Griffiths, E. J.; Rutter, G. A. Mitochondrial calcium as a key regulator of mitochondrial ATP production in mammalian cells. *Biochim. Biophys. Acta. Bioenerg.* **2009**, *1787* (11), 1324-1333.

(20) Cogliati, S.; Enriquez, J. A.; Scorrano, L. Mitochondrial Cristae: Where Beauty Meets Functionality. *Trends Biochem Sci* **2016**, *41* (3), 261-273. DOI: 10.1016/j.tibs.2016.01.001.

(21) Friedman, J. R.; Nunnari, J. Mitochondrial form and function. *Nature* **2014**, *505* (7483), 335-343.

(22) Giorgio, M.; Trinei, M.; Migliaccio, E.; Pelicci, P. G. Hydrogen peroxide: a metabolic by-product or a common mediator of ageing signals? *Nat. Rev. Mol. Cell Biol.* **2007**, *8* (9), 722a-728.

(23) Brand, M. D. Mitochondrial generation of superoxide and hydrogen peroxide as the source of mitochondrial redox signaling. *Free Radic. Biol. Med.* **2016**, *100*, 14-31.

(24) Forstermann, U.; Sessa, W. C. Nitric oxide synthases: regulation and function. *Eur. Heart J.* **2012**, *33* (7), 829.

(25) D'Autreaux, B.; Toledano, M. B. ROS as signalling molecules: mechanisms that generate specificity in ROS homeostasis. *Nat. Rev. Mol. Cell Biol.* **2007**, *8* (10), 813-824.

(26) Murphy, M. P. How mitochondria produce reactive oxygen species. *Biochem J.* **2009**, *417*, 1-13.

(27) Indo, H. P.; Davidson, M.; Yen, H. C.; Suenaga, S.; Tomita, K.; Nishii, T.; Higuchi, M.; Koga, Y.; Ozawa, T.; Majima, H. J. Evidence of ROS generation by mitochondria in cells with impaired electron transport chain and mitochondrial DNA damage. *Mitochondrion* **2007**, *7* (1-2), 106-118.

(28) Balaban, R. S.; Nemoto, S.; Finkel, T. Mitochondria, oxidants, and aging. *Cell* **2005**, *120* (4), 483-495.

(29) Chance, B.; Schoener, B.; Oshino, R.; Itshak, F.; Nakase, Y. Oxidation-Reduction Ratio Studies of Mitochondria in Freeze-Trapped Samples - Nadh and Flavoprotein Fluorescence Signals. *J. Biol. Chem.***1979**, *254* (11), 4764-4771.

(30) Bayne, A. C. V.; Mockett, R. J.; Orr, W. C.; Sohal, R. S. Enhanced catabolism of mitochondrial superoxide/hydrogen peroxide and aging in transgenic Drosophila. *Biochem. J.* **2005**, *391*, 277-284.

(31) Baradaran, R.; Berrisford, J. M.; Minhas, G. S.; Sazanov, L. A. Crystal structure of the entire respiratory complex I. *Nature* **2013**, *494* (7438), 443-448.

(32) Quinlan, C. L.; Orr, A. L.; Perevoshchikova, I. V.; Treberg, J. R.; Ackrell, B. A.; Brand, M. D. Mitochondrial Complex II Can Generate Reactive Oxygen Species at High Rates in Both the Forward and Reverse Reactions. *J. Biol. Chem.* **2012**, *287* (32), 27255-27264.

(33) Quinlan, C. L.; Perevoshchikova, I. V.; Hey-Mogensen, M.; Orr, A. L.; Brand, M. D. Sites of reactive oxygen species generation by mitochondria oxidizing different substrates. *Redox Biol.* **2013**, *1* (1), 304-312.

(34) Chen, Q.; Vazquez, E. J.; Moghaddas, S.; Hoppel, C. L.; Lesnefsky, E. J. Production of reactive oxygen species by mitochondria - Central role of complex III. *J. Biol. Chem.* **2003**, *278* (38), 36027-36031.

(35) Guzy, R. D.; Schumacker, P. T. Oxygen sensing by mitochondria at complex III: the paradox of increased reactive oxygen species during hypoxia. *Exp. Physiol.* **2006**, *91* (5), 807-819.

(36) Lambert, A. J.; Brand, M. D. Superoxide production by NADH: ubiquinone oxidoreductase (complex I) depends on the pH gradient across the mitochondrial inner membrane. *Biochem. J.* **2004**, *382*, 511-517.

(37) Lambert, A. J.; Brand, M. D. Inhibitors of the quinone-binding site allow rapid superoxide production from mitochondrial NADH : ubiquinone oxidoreductase (complex I). *J. Biol. Chem.* **2004**, *279* (38), 39414-39420.

(38) Hey-Mogensen, M.; Goncalves, R. L.; Orr, A. L.; Brand, M. D. Production of superoxide/H2O2 by dihydroorotate dehydrogenase in rat skeletal muscle mitochondria. *Free Radic. Biol. Med.* **2014**, *72*, 149-155.

(39) Edwards, R.; Eaglesfield, R.; Tokatlidis, K. The mitochondrial intermembrane space: the most constricted mitochondrial sub-compartment with the largest variety of protein import pathways. *Open Biol.* **2021**, *11* (3), 210002.

(40) Quinlan, C. L.; Goncalves, R. L. S.; Hey-Mogensen, M.; Yadava, N.; Bunik, V. I.; Brand, M. D. The 2-Oxoacid Dehydrogenase Complexes in Mitochondria Can Produce Superoxide/Hydrogen Peroxide at Much Higher Rates Than Complex I. *J. Biol. Chem.* **2014**, *289* (12), 8312-8325.

(41) Tretter, L.; Adam-Vizi, V. Alpha-ketoglutarate dehydrogenase: a target and generator of oxidative stress. *Philos. Trans. R. Soc. Lond. B. Biol. Sci.* **2005**, *360* (1464), 2335-2345.

(42) Bak, D. W.; Weerapana, E. Cysteine-mediated redox signalling in the mitochondria. *Mol. Biosyst.* **2015**, *11* (3), 678-697.

(43) Li, N.; Ragheb, K.; Lawler, G.; Sturgis, J.; Rajwa, B.; Melendez, J. A.; Robinson, J. P. Mitochondrial complex I inhibitor rotenone induces apoptosis through enhancing mitochondrial reactive oxygen species production. *J. Biol. Chem.* **2003**, *278* (10), 8516-8525.

(44) Vonjagow, G.; Engel, W. D. Complete Inhibition of Electron-Transfer from Ubiquinol to Cytochrome-B by the Combined Action of Antimycin and Myxothiazol. *FEBS Lett.* **1981**, *136* (1), 19-24.

(45) Quinlan, C. L.; Treberg, J. R.; Perevoshchikova, I. V.; Orr, A. L.; Brand, M. D. Native rates and sites of mitochondrial ROS production. *J. Neurosci. Res.* **2013**, *91* (8), 1085-1085.

(46) Cadenas, E.; Davies, K. J. A. Mitochondrial free radical generation, oxidative stress, and aging. *Free Radic. Biol. Med.* **2000**, *29* (3-4), 222-230.

(47) Fukai, T.; Ushio-Fukai, M. Superoxide Dismutases: Role in Redox Signaling, Vascular Function, and Diseases. *Antioxid. Redox Signal.* **2011**, *15* (6), 1583-1606.

(48) Goldsteins, G.; Keksa-Goldsteine, V.; Ahtoniemi, T.; Jaronen, M.; Arens, E.; Akerman, K.; Chan, P. H.; Koistinaho, J. Deleterious role of superoxide dismutase in the mitochondrial intermembrane space. *J. Biol. Chem.* **2008**, *283* (13), 8446-8452.

(49) Fridovich, I. Superoxide Radical - an Endogenous Toxicant. *Annu. Rev. Pharmacol.* **1983**, *23*, 239-257.

(50) Ighodaro, O. M.; Akinloye, O. A. First line defence antioxidants-superoxide dismutase (SOD), catalase (CAT) and glutathione peroxidase (GPX): Their fundamental role in the entire antioxidant defence grid. *Alexandria J. Med.* **2018**, *54* (4), 287-293.

(51) Salvi, M.; Battaglia, V.; Brunati, A. M.; La Rocca, N.; Tibaldi, E.; Pietrangeli, P.; Marcocci, L.; Mondovi, B.; Rossi, C. A.; Toninello, A. Catalase takes part in rat liver mitochondria oxidative stress Defense. *J. Biol.Chem.* **2007**, *282* (33), 24407-24415.

(52) Cox, A. G.; Winterbourn, C. C.; Hampton, M. B. Mitochondrial peroxiredoxin involvement in antioxidant defence and redox signalling. *Biochem. J.* **2010**, *425*, 313-325.

(53) Chang, T. S.; Cho, C. S.; Park, S.; Yu, S. Q.; Kang, S. W.; Rhee, S. G. Peroxiredoxin III, a mitochondrion-specific peroxidase, regulates apoptotic signaling by mitochondria. *J. Biol. Chem.* **2004**, *279* (40), 41975-41984.

(54) de Haan, J. B.; Bladier, C.; Griffiths, P.; Kelner, M.; O'Shea, R. D.; Cheung, N. S.; Bronson, R. T.; Silvestro, M. J.; Wild, S.; Zheng, S. S.; et al. Mice with a homozygous null mutation for the most abundant glutathione peroxidase, Gpx1, show increased susceptibility to the oxidative stress-inducing agents paraquat and hydrogen peroxide. *J. Biol. Chem.* **1998**, *273* (35), 22528-22536.

(55) Imai, H.; Nakagawa, Y. Biological significance of phospholipid hydroperoxide glutathione peroxidase (PHGPx, GPx4) in mammalian cells. *Free Radic. Biol. Med.* **2003**, *34* (2), 145-169.

(56) Kojer, K.; Bien, M.; Gangel, H.; Morgan, B.; Dick, T. P.; Riemer, J. Glutathione redox potential in the mitochondrial intermembrane space is linked to the cytosol and impacts the Mia40 redox state. *EMBO. J.* **2012**, *31* (14), 3169-3182.

(57) Chen, Z. F.; Putt, D. A.; Lash, L. H. Enrichment and functional reconstitution of glutathione transport activity from rabbit kidney mitochondria: Further evidence for the role of the dicarboxylate and 2-oxoglutarate carriers in mitochondrial glutathione transport. *Arch. Biochem. Biophys.* **2000**, *373* (1), 193-202.

(58) Chen, Z. F.; Lash, L. H. Evidence for mitochondrial uptake of glutathione by dicarboxylate and 2-oxoglutarate carriers. *J. Pharmacol. Exp. Ther.* **1998**, *285* (2), 608-618.

(59) Dickinson, D. A.; Forman, H. J. Glutathione in defense and signaling - Lessons from a small thiol. *Cell Signaling, Transcription, and Translation as Therapeutic Targets* **2002**, *973*, 488-504.

(60) Mari, M.; Morales, A.; Colell, A.; Garcia-Ruiz, C.; Fernandez-Checa, J. C. Mitochondrial Glutathione, a Key Survival Antioxidant. *Antioxid. Redox Signal.* **2009**, *11* (11), 2685-2700.

(61) Oyewole, A. O.; Birch-Machin, M. A. Mitochondria-targeted antioxidants. *FASEB J* **2015**, *29* (12), 4766-4771.

(62) McBean, G. J.; Aslan, M.; Griffiths, H. R.; Torrao, R. C. Thiol redox homeostasis in neurodegenerative disease. *Redox Biol.* **2015**, *5*, 186-194.

(63) Belcastro, E.; Gaucher, C.; Corti, A.; Leroy, P.; Lartaud, I.; Pompella, A. Regulation of protein function by S-nitrosation and S-glutathionylation: processes and targets in cardiovascular pathophysiology. *Biol Chem* **2017**, *398* (12), 1267-1293. DOI: 10.1515/hsz-2017-0150.

(64) Groitl, B.; Jakob, U. Thiol-based redox switches. *Biochim. Biophys. Acta.* **2014**, *1844* (8), 1335-1343.

(65) Mailloux, R. J.; Ayre, D. C.; Christian, S. L. Induction of mitochondrial reactive oxygen species production by GSH mediated S-glutathionylation of 2-oxoglutarate dehydrogenase. *Redox Biol.* **2016**, *8*, 285-297.

(66) Taylor, E. R.; Hurrell, F.; Shannon, R. J.; Lin, T. K.; Hirst, J.; Murphy, M. P. Reversible glutathionylation of complex I increases mitochondrial superoxide formation. *J. Biol. Chem.* **2003**, *278* (22), 19603-19610.

(67) Bharath, M. M. S. Post-Translational Oxidative Modifications of Mitochondrial Complex I (NADH: Ubiquinone Oxidoreductase): Implications for Pathogenesis and Therapeutics in Human Diseases. *J. Alzheimer's Dis.* **2017**, *60*, S69-S86.

(68) Chen, Y. R.; Chen, C. L.; Pfeiffer, D. R.; Zweier, J. L. Mitochondrial complex II in the post-ischemic heart: oxidative injury and the role of protein S-glutathionylation. *J. Biol. Chem.* **2007**, *282* (45), 32640-32654.

(69) Mailloux, R. J.; Willmore, W. G. S-glutathionylation reactions in mitochondrial function and disease. *Front. Cell Dev. Biol.* **2014**, *2*.

(70) Mailloux, R. J.; Craig Ayre, D.; Christian, S. L. Induction of mitochondrial reactive oxygen species production by GSH mediated S-glutathionylation of 2-oxoglutarate dehydrogenase. *Redox Biol.* **2016**, *8*, 285-297.

(71) Zhang, L.; Kang, P. T.; Chen, C. L.; Green, K. B.; Chen, Y. R. Oxidative modifications of mitochondria complex II. *Methods Mol. Biol.* **2013**, *1005*, 143-156.

(72) Boss, O.; Samec, S.; Paoloni-Giacobino, A.; Rossier, C.; Dulloo, A.; Seydoux, J.; Muzzin, P.; Giacobino, J. P. Uncoupling protein-3: a new member of the mitochondrial carrier family with tissue-specific expression. *FEBS Lett.* **1997**, *408* (1), 39-42.

(73) Mailloux, R. J.; Seifert, E. L.; Bouillaud, F.; Aguer, C.; Collins, S.; Harper, M. E. Glutathionylation Acts as a Control Switch for Uncoupling Proteins UCP2 and UCP3. *J. Ciol. Chem.* **2011**, *286* (24), 21865-21875.

(74) Akhmedov, A. T.; Rybin, V.; Marin-Garcia, J. Mitochondrial oxidative metabolism and uncoupling proteins in the failing heart. *Heart Fail. Rev.* **2015**, *20* (2), 227-249.

(75) Mailloux, R. J.; Harper, M. E. Mitochondrial proticity and ROS signaling: lessons from the uncoupling proteins. *Trends Endocrinol. Metab.* **2012**, *23* (9), 451-458.

(76) Cantu, D.; Schaack, J.; Patel, M. Oxidative Inactivation of Mitochondrial Aconitase Results in Iron and H2O2-Mediated Neurotoxicity in Rat Primary Mesencephalic Cultures. *Plos One* **2009**, *4* (9).

(77) Starkov, A. A. An update on the role of mitochondrial alpha-ketoglutarate dehydrogenase in oxidative stress. *Mol. Cell Neurosci.* **2013**, *55*, 13-16.

(78) McLain, A. L.; Szweda, P. A.; Szweda, L. I. alpha-Ketoglutarate dehydrogenase: A mitochondrial redox sensor. *Free Radical Res.* **2011**, *45* (1), 29-36.

(79) Tretter, L.; Adam-Vizi, V. Inhibition of Krebs cycle enzymes by hydrogen peroxide: A key role of alpha-ketoglutarate dehydrogenase in limiting NADH production under oxidative stress. *J. Neurosci.* **2000**, *20* (24), 8972-8979.

(80) Nulton-Persson, A. C.; Starke, D. W.; Mieyal, J. J.; Szweda, L. I. Reversible inactivation of alpha-ketoglutarate dehydrogenase in response to alterations in the mitochondrial glutathione status. *Biochem.* **2003**, *42* (14), 4235-4242.

(81) Tretter, L.; Adam-Vizi, V. Generation of reactive oxygen species in the reaction catalyzed by alpha-ketoglutarate dehydrogenase. *J. Neurosci.* **2004**, *24* (36), 7771-7778.

(82) Song, Y. S.; Lee, B. Y.; Hwang, E. S. Dinstinct ROS and biochemical profiles in cells undergoing DNA damage-induced senescence and apoptosis. *Mech. Ageing Dev.* **2005**, *126* (5), 580-590.

(83) Simon, H. U.; Haj-Yehia, A.; Levi-Schaffer, F. Role of reactive oxygen species (ROS) in apoptosis induction. *Apoptosis* **2000**, *5* (5), 415-418.

(84) Hernansanz-Agustin, P.; Ramos, E.; Navarro, E.; Parada, E.; Sanchez-Lopez, N.; Pelaez-Aguado, L.; Cabrera-Garcia, J. D.; Tello, D.; Buendia, I.; Marina,

A.; et al. yy Mitochondrial complex I deactivation is related to superoxide production in acute hypoxia. *Redox Biol.* **2017**, *12*, 1040-1051.

(85) Xiao, M.; Zhong, H.; Xia, L.; Tao, Y.; Yin, H. Pathophysiology of mitochondrial lipid oxidation: Role of 4-hydroxynonenal (4-HNE) and other bioactive lipids in mitochondria. *Free Radic. Biol. Med.* **2017**, *111*, 316-327.

(86) Cai, Z.; Yan, L. J. Protein Oxidative Modifications: Beneficial Roles in Disease and Health. *J. Biochem. Pharmacol. Res.* **2013**, *1* (1), 15-26.

(87) Lin, M. T.; Beal, M. F. Mitochondrial dysfunction and oxidative stress in neurodegenerative diseases. *Nature* **2006**, *443* (7113), 787-795.

(88) Chouchani, E. T.; Pell, V. R.; James, A. M.; Work, L. M.; Saeb-Parsy, K.; Frezza, C.; Krieg, T.; Murphy, M. P. A Unifying Mechanism for Mitochondrial Superoxide Production during Ischemia-Reperfusion Injury. *Cell Metab.* **2016**, *23* (2), 254-263.

(89) Victor, V. M.; Rocha, M.; Herance, R.; Hernandez-Mijares, A. Oxidative Stress and Mitochondrial Dysfunction in Type 2 Diabetes. *Curr. Pharm. Design* **2011**, *17* (36), 3947-3958.

(90) Diebold, L.; Chandel, N. S. Mitochondrial ROS regulation of proliferating cells. *Free Radic. Biol. Med.* **2016**, *100*, 86-93.

(91) Adams, J. M.; Cory, S. Bcl-2-regulated apoptosis: mechanism and therapeutic potential. *Curr. Opin. Immunol.* **2007**, *19* (5), 488-496.

(92) Luanpitpong, S.; Chanvorachote, P.; Stehlik, C.; Tse, W.; Callery, P. S.; Wang, L.; Rojanasakul, Y. Regulation of apoptosis by Bcl-2 cysteine oxidation in human lung epithelial cells. *Mol. Biol. Cell* **2013**, *24* (6), 858-869.

(93) Maser, R. S.; Antoku, K.; Scully, W. J., Jr.; Cho, R. L.; Johnson, D. E. Analysis of the role of conserved cysteine residues in the bcl-2 oncoprotein. *Biochem. Biophys. Res. Commun.* **2000**, *277* (1), 171-178.

(94) Sastre, J.; Pallardo, F. V.; Vina, J. Mitochondrial oxidative stress plays a key role in aging and apoptosis. *IUBMB Life* **2000**, *49* (5), 427-435.

(95) Ott, M.; Gogvadze, V.; Orrenius, S.; Zhivotovsky, B. Mitochondria, oxidative stress and cell death. *Apoptosis* **2007**, *12* (5), 913-922.

(96) Ott, M.; Zhivotovsky, B.; Orrenius, S. Role of cardiolipin in cytochrome c release from mitochondria. *Cell Death Differ.* **2007**, *14* (7), 1243-1247.

(97) Messina, S.; De Simone, G.; Ascenzi, P. Cysteine-based regulation of redox-sensitive Ras small GTPases. *Redox Biol.* **2019**, *26*, 101282.

(98) Hobbs, G. A.; Bonini, M. G.; Gunawardena, H. P.; Chen, X.; Campbell, S. L. Glutathiolated Ras: characterization and implications for Ras activation. *Free Radic. Biol. Med.* **2013**, *57*, 221-229.

(99) Batista, W. L.; Ogata, F. T.; Curcio, M. F.; Miguel, R. B.; Arai, R. J.; Matsuo, A. L.; Moraes, M. S.; Stern, A.; Monteiro, H. P. S-nitrosoglutathione and endothelial nitric oxide synthase-derived nitric oxide regulate compartmentalized ras S-nitrosylation and stimulate cell proliferation. *Antioxid. Redox Signal.* **2013**, *18* (3), 221-238.

(100) Chandel, N. S. Evolution of Mitochondria as Signaling Organelles. *Cell Metab.* **2015**, *22* (2), 204-206.

(101) Gomes, A. P.; Price, N. L.; Ling, A. J.; Moslehi, J. J.; Montgomery, M. K.; Rajman, L.; White, J. P.; Teodoro, J. S.; Wrann, C. D.; Hubbard, B. P. Declining NAD+ induces a pseudohypoxic state disrupting nuclear-mitochondrial communication during aging. *Cell* **2013**, *155* (7), 1624-1638.

(102) Liberti, M. V.; Locasale, J. W. The Warburg Effect: How Does it Benefit Cancer Cells? *Trends Biochem. Sci.* **2016**, *41* (3), 211-218.

(103) Quijano, C.; Trujillo, M.; Castro, L.; Trostchansky, A. Interplay between oxidant species and energy metabolism. *Redox Biol.* **2016**, *8*, 28-42.

(104) Zaidieh, T.; Smith, J. R.; Ball, K. E.; An, Q. ROS as a novel indicator to predict anticancer drug efficacy. *BMC Cancer* **2019**, *19* (1).

(105) Manoharan, S.; Guillemin, G. J.; Abiramasundari, R. S.; Essa, M. M.; Akbar, M.; Akbar, M. D. The Role of Reactive Oxygen Species in the Pathogenesis of Alzheimer's Disease, Parkinson's Disease, and Huntington's Disease: A Mini Review. *Oxid. Med. Cell Longev.* **2016**.

(106) Valentine, J. S.; Hart, P. J. Misfolded CuZnSOD and amyotrophic lateral sclerosis. *Proc. Natl. Acad. Sci. USA* **2003**, *100* (7), 3617-3622.

(107) Jin, H.; Kanthasamy, A.; Ghosh, A.; Anantharam, V.; Kalyanaraman, B.; Kanthasamy, A. G. Mitochondria-targeted antioxidants for treatment of Parkinson's disease: Preclinical and clinical outcomes. *Biochim Biophys Acta Mol Basis Dis.* **2014**, *1842* (8), 1282-1294.

(108) Casadesus, G.; Smith, M. A.; Zhu, X.; Aliev, G.; Cash, A. D.; Honda, K.; Petersen, R. B.; Perry, G. Alzheimer disease: evidence for a central pathogenic role of iron-mediated reactive oxygen species. *J. Alzheimer's Dis.* **2004**, *6* (2), 165-169.

(109) Kujoth, G. C.; Hiona, A.; Pugh, T. D.; Someya, S.; Panzer, K.; Wohlgemuth, S. E.; Hofer, T.; Seo, A. Y.; Sullivan, R.; Jobling, W. A.; et al. Mitochondrial DNA mutations, oxidative stress, and apoptosis in mammalian aging. *Science* **2005**, *309* (5733), 481-484.

(110) Kudryavtseva, A. V.; Krasnov, G. S.; Dmitriev, A. A.; Alekseev, B. Y.; Kardymon, O. L.; Sadritdinova, A. F.; Fedorova, M. S.; Pokrovsky, A. V.; Melnikova, N. V.; Kaprin, A. D.; et al. Mitochondrial dysfunction and oxidative stress in aging and cancer. *Oncotarget* **2016**, *7* (29), 44879-44905.

(111) Nunnari, J.; Suomalainen, A. Mitochondria: in sickness and in health. *Cell* **2012**, *148* (6), 1145-1159.

(112) Naseri, N. N.; Xu, H.; Bonica, J.; Vonsattel, J. P. G.; Cortes, E. P.; Park, L. C.; Arjomand, J.; Gibson, G. E. Abnormalities in the Tricarboxylic Acid Cycle in Huntington Disease and in a Huntington Disease Mouse Model. *J. Neuropath. Exp. Neur.* **2015**, *74* (6), 527-537.

(113) Gibson, G. E.; Kingsbury, A. E.; Xu, H.; Lindsay, J. G.; Daniel, S.; Foster, O. J. F.; Lees, A. J.; Blass, J. P. Deficits in a tricarboxylic acid cycle enzyme in brains from patients with Parkinson's disease. *Neurochem. Int.* **2003**, *43* (2), 129-135.

(114) Gibson, G. E.; Sheu, K. F. R.; Blass, J. P.; Baker, A.; Carlson, K. C.; Harding, B.; Perrino, P. Reduced Activities of Thiamine-Dependent Enzymes in the Brains and Peripheral-Tissues of Patients with Alzheimers-Disease. *Arch. Neurol-Chicago* **1988**, *45* (8), 836-840.

(115) Kaludercic, N.; Di Lisa, F. Mitochondrial ROS Formation in the Pathogenesis of Diabetic Cardiomyopathy. *Front. Cardiovasc. Med.* **2020**, *7*, 12.

(116) Chen, J.; Stimpson, S. E.; Fernandez-Bueno, G. A.; Mathews, C. E. Mitochondrial Reactive Oxygen Species and Type 1 Diabetes. *Antioxid. Redox Signal.* **2018**, *29* (14), 1361-1372.

(117) Teodoro, J. S.; Nunes, S.; Rolo, A. P.; Reis, F.; Palmeira, C. M. Therapeutic options targeting oxidative stress, mitochondrial dysfunction and

inflammation to hinder the progression of vascular complications of diabetes. *Front. Phys.* **2019**, 1857.

(118) Kaneto, H.; Katakami, N.; Matsuhisa, M.; Matsuoka, T. Role of Reactive Oxygen Species in the Progression of Type 2 Diabetes and Atherosclerosis. *Mediat. Inflamm.* **2010**, *2010*.

(119) Peoples, J. N.; Saraf, A.; Ghazal, N.; Pham, T. T.; Kwong, J. Q. Mitochondrial dysfunction and oxidative stress in heart disease. *Experimental & molecular medicine* **2019**, *51* (12), 1-13.

(120) Chistiakov, D. A.; Shkurat, T. P.; Melnichenko, A. A.; Grechko, A. V.; Orekhov, A. N. The role of mitochondrial dysfunction in cardiovascular disease: a brief review. *Ann. Med.* **2018**, *50* (2), 121-127.

(121) Tong, F.; Ye, Y.; Chen, B.; Gao, J.; Liu, L.; Ou, J.; van Hest, J. C.; Liu, S.; Peng, F.; Tu, Y. Bone-targeting prodrug mesoporous silica-based nanoreactor with reactive oxygen species burst for enhanced chemotherapy. *CS Appl. Mater. Interfaces* **2020**, *12* (31), 34630-34642.

(122) Perillo, B.; Di Donato, M.; Pezone, A.; Di Zazzo, E.; Giovannelli, P.; Galasso, G.; Castoria, G.; Migliaccio, A. ROS in cancer therapy: the bright side of the moon. *Exp. Mol. Med* **2020**, *52* (2), 192-203.

(123) Zhang, L.; Li, J. H.; Zong, L.; Chen, X.; Chen, K.; Jiang, Z. D.; Nan, L. G.; Li, X. Q.; Li, W.; Shan, T.; et al. Reactive Oxygen Species and Targeted Therapy for Pancreatic Cancer. *Oxid. Med. Cell Longev.* **2016**, *2016*.

(124) Wang, J.; Sun, D.; Huang, L.; Wang, S.; Jin, Y. Targeting Reactive Oxygen Species Capacity of Tumor Cells with Repurposed Drug as an Anticancer Therapy. *Oxi.d Med. Cell. Longev.* **2021**, *2021*.

(125) Ye, Y.; Li, J.; Yuan, Z. Effect of antioxidant vitamin supplementation on cardiovascular outcomes: a meta-analysis of randomized controlled trials. *PLOS One* **2013**, *8* (2), e56803.

(126) Yesilbursa, D.; Serdar, A.; Senturk, T.; Serdar, Z.; Sağ, S.; Cordan, J. Effect of N-acetylcysteine on oxidative stress and ventricular function in patients with myocardial infarction. *Heart Vessels* **2006**, *21* (1), 33-37.

(127) Hoshino, A.; Okawa, Y.; Ariyoshi, M.; Kaimoto, S.; Uchihashi, M.; Fukai, K.; Iwai-Kanai, E.; Matoba, S. Oxidative post-translational modifications develop LONP1 dysfunction in pressure overload heart failure. *Circ. Heart Fail.* **2014**, *7* (3), 500-509.

(128) Karaa, A.; Haas, R.; Goldstein, A.; Vockley, J.; Weaver, W. D.; Cohen, B. H. Randomized dose-escalation trial of elamipretide in adults with primary mitochondrial myopathy. *Neurology* **2018**, *90* (14), e1212-e1221.

(129) Weerapana, E.; Wang, C.; Simon, G. M.; Richter, F.; Khare, S.; Dillon, M. B. D.; Bachovchin, D. A.; Mowen, K.; Baker, D.; Cravatt, B. F. Quantitative reactivity profiling predicts functional cysteines in proteomes. *Nature* **2010**, *468* (7325), 790-U779.

(130) Bak, D. W.; Pizzagalli, M. D.; Weerapana, E. Identifying Functional Cysteine Residues in the Mitochondria. *ACS Chem. Biol.* **2017**, *12* (4), 947-957.

(131) Abo, M.; Li, C.; Weerapana, E. Isotopically-Labeled Iodoacetamide-Alkyne Probes for Quantitative Cysteine-Reactivity Profiling. *Mol. Pharm.* **2018**, *15* (3), 743-749.

(132) Bechtel, T. J.; Li, C.; Kisty, E. A.; Maurais, A. J.; Weerapana, E. Profiling Cysteine Reactivity and Oxidation in the Endoplasmic Reticulum. *ACS Chem. Biol.* **2020**, *15* (2), 543-553.

(133) Roberts, A. M.; Miyamoto, D. K.; Huffman, T. R.; Bateman, L. A.; Ives, A. N.; Akopian, D.; Heslin, M. J.; Contreras, C. M.; Rape, M.; Skibola, C. F. Chemoproteomic screening of covalent ligands reveals UBA5 as a novel pancreatic cancer target. *ACS Chem. Biol.* **2017**, *12* (4), 899-904.

(134) Bateman, L.; Nguyen, T.; Roberts, A.; Miyamoto, D.; Ku, W.-M.; Huffman, T.; Petri, Y.; Heslin, M.; Contreras, C.; Skibola, C. Chemoproteomics-enabled covalent ligand screen reveals a cysteine hotspot in reticulon 4 that impairs ER morphology and cancer pathogenicity. *Chem. Commun.* **2017**, *53* (53), 7234-7237.

(135) Backus, K. M.; Correia, B. E.; Lum, K. M.; Forli, S.; Horning, B. D.; Gonzalez-Paez, G. E.; Chatterjee, S.; Lanning, B. R.; Teijaro, J. R.; Olson, A. J.; et al. Proteome-wide covalent ligand discovery in native biological systems. *Nature* **2016**, *534* (7608), 570.

(136) Leichert, L. I.; Gehrke, F.; Gudiseva, H. V.; Blackwell, T.; Ilbert, M.; Walker, A. K.; Strahler, J. R.; Andrews, P. C.; Jakob, U. Quantifying changes in the thiol redox proteome upon oxidative stress in vivo. *Proc. Natl. Acad. Sci. USA* **2008**, *105* (24), 8197-8202.

(137) Brennan, J. P.; Miller, J. I.; Fuller, W.; Wait, R.; Begum, S.; Dunn, M. J.; Eaton, P. The utility of N, N-biotinyl glutathione disulfide in the study of protein S-glutathiolation. *Mol. Cell Proteomics* **2006**, *5* (2), 215-225.

(138) Sullivan, D. M.; Wehr, N. B.; Fergusson, M. M.; Levine, R. L.; Finkel, T. Identification of oxidant-sensitive proteins: TNF-α induces protein glutathiolation. *Biochemistry-US* **2000**, *39* (36), 11121-11128.

(139) Samarasinghe, K. T.; Godage, D. N. M.; Zhou, Y.; Ndombera, F. T.; Weerapana, E.; Ahn, Y.-H. A clickable glutathione approach for

identification of protein glutathionylation in response to glucose metabolism. *Mol. Biosyst.* **2016**, *12* (8), 2471-2480.

(140) Akter, S.; Fu, L.; Jung, Y.; Conte, M. L.; Lawson, J. R.; Lowther, W. T.; Sun, R.; Liu, K.; Yang, J.; Carroll, K. S. Chemical proteomics reveals new targets of cysteine sulfinic acid reductase. *Nat. Chem. Biol.* **2018**, *14* (11), 995-1004.

(141) Paulsen, C. E.; Carroll, K. S. Cysteine-mediated redox signaling: chemistry, biology, and tools for discovery. *Chem. Rev.* **2013**, *113* (7), 4633-4679.

(142) Shi, Y.; Fu, L.; Yang, J.; Carroll, K. S. Wittig reagents for chemoselective sulfenic acid ligation enables global site stoichiometry analysis and redox-controlled mitochondrial targeting. *Nat. Chem.* **2021**, *13* (11), 1140-1150.

(143) Meng, J.; Fu, L.; Liu, K.; Tian, C.; Wu, Z.; Jung, Y.; Ferreira, R. B.; Carroll, K. S.; Blackwell, T. K.; Yang, J. Global profiling of distinct cysteine redox forms reveals wide-ranging redox regulation in C. elegans. *Nat. Commun.* **2021**, *12* (1), 1415.

(144) Zielonka, J.; Joseph, J.; Sikora, A.; Hardy, M.; Ouari, O.; Vasquez-Vivar, J.; Cheng, G.; Lopez, M.; Kalyanaraman, B. Mitochondria-targeted triphenylphosphonium-based compounds: syntheses, mechanisms of action, and therapeutic and diagnostic applications. *Chem. Rev.* **2017**, *117* (15), 10043-10120.

(145) Yasueda, Y.; Tamura, T.; Fujisawa, A.; Kuwata, K.; Tsukiji, S.; Kiyonaka, S.; Hamachi, I. A Set of Organelle-Localizable Reactive Molecules for Mitochondrial Chemical Proteomics in Living Cells and Brain Tissues. *J. Am. Chem. Soc.* **2016**, *138* (24), 7592-7602.

(146) Wang, S. B.; Murray, C. I.; Chung, H. S.; Van Eyk, J. E. Redox regulation of mitochondrial ATP synthase. *Trends Cardiovasc. Med.* **2013**, *23* (1), 14-18.

(147) Chouchani, E. T.; Methner, C.; Nadtochiy, S. M.; Logan, A.; Pell, V. R.; Ding, S.; James, A. M.; Cocheme, H. M.; Reinhold, J.; Lilley, K. S.; et al. Cardioprotection by S-nitrosation of a cysteine switch on mitochondrial complex I. *Nat. Med.* **2013**, *19* (6), 753-759.

Chapter 2

Identifying Redox-Sensitive Cysteine Residues in the Mitochondria

Introduction

Mitochondria are renowned hubs of homeostatic redox signaling. As the primary site of reactive oxygen species (ROS) production, mitochondria are suggested to have emerged from prokaryotic engulfment of an alpha-proteobacterium evolving eukaryotes with highly specialized redox signaling pathways.[1] This endosymbiotic event is responsible for the unique double membraned mitochondrial structure. The outer (OMM) and inner (IMM) mitochondrial membranes separate two diverse sub-compartments, the intermembrane space (IMS) and matrix, each having their own specific proteome and biochemical roles for metabolic regulation and energetic renewal.[2] The inner most compartment, the matrix, houses the bioenergetic machinery essential for ATP production and resource recycling.[3] The IMS, on the other hand, is critical for cytosolic protein import and folding and apoptotic signaling.[4-7] In addition to aerobic respiration pathways, oxidative phosphorylation (OXPHOS) and the tricarboxylic acid (TCA) cycle, mitochondria are responsible for several complementary biological mechanisms including beta oxidation of fatty acids, mitochondrial-specific DNA transcription and translation, and iron sulfur cluster biogenesis. With whole cell reliance on these vital cellular processes, mitochondria are known to cross-talk between a variety or cellular components, such as the endoplasmic reticulum and nucleus.[8]

A series of oxidation and reduction reactions drive the flow of electrons from the TCA cycle to the electron transport chain (ETC). Before reaching the final electron acceptor, oxygen, single electrons may prematurely leak from these bioenergetic pathways resulting in the formation of superoxide and further alterations to a variety of ROS (H_2O_2, $^{\cdot}OH$, N_2O_3). The delicate balance of

metabolism, antioxidant concentrations, and mtROS flux influence redox signaling in the mitochondria.[9] Because of their nucleophilicity and microenvironment pKa flexibility, cysteines can adopt reversible (-SOH, -SO_2H, -SSG, -SNO, -SSR) and irreversible (-SO_3H) oxidative post-translational modifications (oxPTMs).[10]

The transient nature of many of the cysteine oxPTMs governs their role in cellular redox signaling through directly impacting protein structure, enzymatic activity, complex formation, localization, and degradation[11-15]. To-date, there are several characterized functional sites of cysteine oxidation by mtROS, or "thiol switches"[16], including C385 on aconitate hydratase (ACO2) which regulates the TCA cycle[17,18], C39 on ND3 subunit of complex I (MT-ND3) which tunes ETC electron flux[19,20], and C253 on uncoupling protein 1 (UCP1) which is responsible for disrupting the IMM proton gradient[21,22]. Each "thiol switch" showcases the ability for cysteine oxPTMs to fine-tune elegant metabolic processes, a necessary feed-back mechanism for maintaining cell homeostasis. However, the resulting mitochondrial cysteine-mediated redox signaling has wide reaching implications beyond regulation of routine metabolic pathways including determination of cell health. High levels of mtROS command a variety of pathologies including cancer[23], diabetes[24,25], neurodegeneration[26], and cardiac disease.[27] Therefore, understanding cysteine oxidation and sensitivities to ROS may contribute to gained comprehension of pathological pathways and potential therapeutic targets.

Due to the importance of understanding mitochondrial cysteine oxidation, there has been great interest in profiling the mitochondrial proteome and assessing cysteine reactivity. Because the mitochondria make up only 6% of the human protein-coding genome[18,29], it is difficult to obtain complete coverage of

mitochondrial proteins in whole cell lysate analysis where the highest proteomic abundance is contributed by the nucleus and cytosol. Organelle enrichment[30], targeted probes[31,32], and proximity labeling through mitochondrial-directed enzymes (BioID[33,34], APEX[35-37]) and small molecules[38] have been successful strategies at magnifying mitochondrial proteomic coverage. Although advances in proximity labeling have reduced labor and time intensive aspects of intracellular enrichment, whole mitochondrial isolation provides the advantage of global surveillance for all mitochondrial sub-compartments while also maintaining respiratory function, redox signaling and protein complexes. Additionally, several appealing chemo-proteomic techniques have been exploited to study mitochondrial cysteine reactivity and oxidation using organelle isolation. Previous work from our lab mapped highly reactive cysteines and changes in cysteine reactivity upon treatment with *s*-nitrosating reagent (GSNO) using mitochondrial isolation and isoTOP-ABPP with iodoacetamide alkyne and isotopically coded biotin-azide conjugation.[39] In complementation, oxidative isotopically coded affinity tags (OxICAT[40] and SICyLIA[41]) has allowed for robust profiling of cysteine oxidation events in isolated organelles and cells including disulfide bond formation in the endoplasmic reticulum[42] and ROS-sensitive sites in yeast[43], bacteria[40] and drosophila.[44] Furthermore, current innovations in chemoproteomic cysteine oxidation studies have relied on numerous probes surveying individual cysteine oxidation modifications including probes targeting sulfenic[31,45] and sulfinic acids[46], that have been applied to *C. elegans*[47] and yeast[48] model systems and directed to the mitochondrial matrix through the appendage of triphenyl-phosphine. Yet, to-date there have been limited effort towards

generating a comprehensive analysis of mitochondrial redox-sensitive cysteines in pathologically relevant oxidative stress conditions and mammalian cell models.

With the combination of organelle isolation and quantitative mass spectrometry (MS) proteomics (IsoTOP-ABPP and OxICAT), we aim to develop a complete report of mitochondrial cysteines annotating varying degrees of sensitivities to exogenous ROS (H_2O_2) and endogenous ROS by ETC inhibitor, Antimycin A (AMA). We demonstrate the ability of both IsoTOP-ABPP and OxICAT platforms to represent an encompassing snapshot of cysteine oxidation changes during levels of mitochondrial oxidative stress analogous to a variety of ROS-driven pathological states. Together, our work uncovers a comprehensive representation of cysteines sensitive to oxidation in the mitochondria expanding the knowledge of cysteine-mediated redox signaling networks.

Results and Discussion

Enrichment of mitochondrial cysteines by organelle isolation.

To analyze perturbations in mitochondrial cysteine oxidation and reactivity, we sought to first increase coverage of the mitochondrial proteome through established methods of differential centrifugation[30,39] (Figure 2-1). Multiple centrifugation rounds were used to fractionate HEK 293T cells affording a crude mitochondrial sample (Mito-C). The Mito-C fraction was further purified by an isopycnic gradient to a pure mitochondrial sample (Mito-P), removing residual cytosolic and nuclear contamination (Figure 2-1). By western blot, pure mitochondrial enrichment was confirmed (Figure 2-2). However, the ER marker, calreticulin, was still present in the Mito-P sample most likely due to the inability

of differential centrifugation to remove well characterized ER-mitochondrial contact sites.

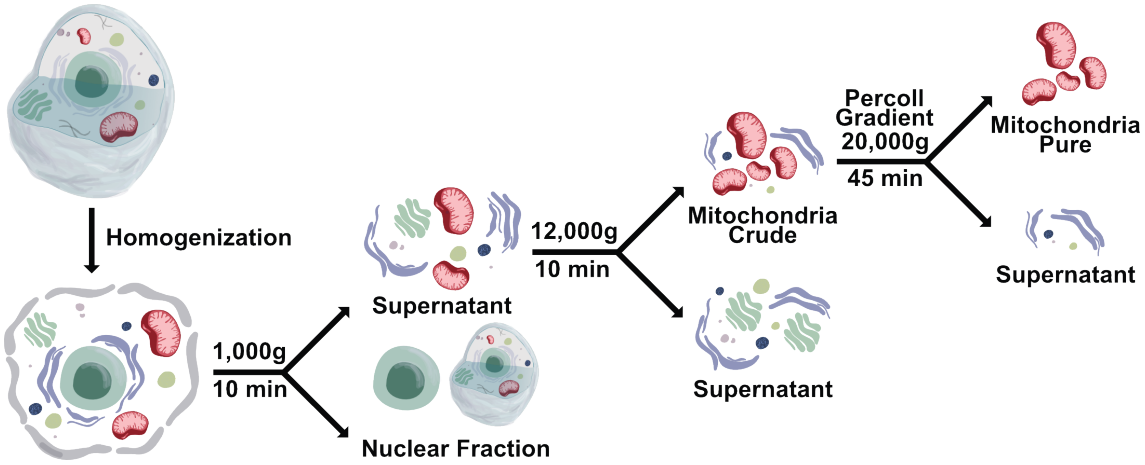


Figure 2-1. Whole mitochondrial isolation by differential centrifugation used to enrich for mitochondrial cysteines.

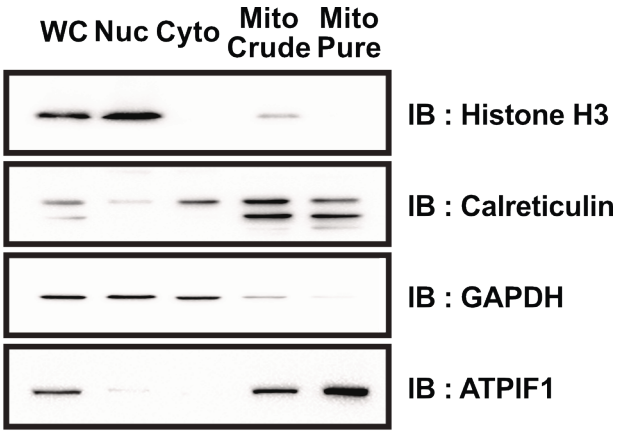


Figure 2-2. Western blot analysis of isolated fractionation steps and subcellular compartments from mitochondrial enrichment by differential centrifugation using organelle markers including Histone H3 (nuclear), Calreticulin (endoplasmic reticulum), GAPDH (cytosol), and ATPIF1 (mitochondria).

MS analysis of cysteine-containing peptides in trypsin-digested lysates from isolated Mito-P samples and whole cell samples were compared. In the Mito-P sample, mitochondrial coverage was determined to be similar to previous fractionation reports[39] with a total of 1370 cysteine-containing peptides and 398 proteins identified and characterized to localize to the mitochondria by Uniprot[49] and MitoCarta2.0.[50] Furthermore, compared to whole cell lysate coverage which identified 278 peptides residing on 172 mitochondrial proteins, mitochondrial isolation allowed for a ~3-fold increase in mitochondrial proteins and ~5-fold increase in mitochondrial peptides (Figure 2-3A, Table 2A-1). Additionally, the majority of spectral counts (57%) in the Mito-P sample originate from mitochondria annotated proteins whereas only 11% of whole cell spectral counts accounted for mitochondrial proteins (Figure 2-3B, Table 2A-1). Furthermore, the majority of spectral counts (25%) in the whole cell sample originate from nuclear annotated proteins (Figure 2-3B, Table 2A-1). Gene ontology (GO) analysis of the Mito-P sample revealed robust enrichment for common mitochondrial processes such as mitochondrial protein translation, mitochondrial gene expression, and the TCA cycle, none of which overlapped with the enriched biological processes in the whole cell sample (Table 2-1, Table 2A-2 and Table 2A-3). Together, our data confirms differential centrifugation as a valuable method for mitochondrial proteomic isolation.

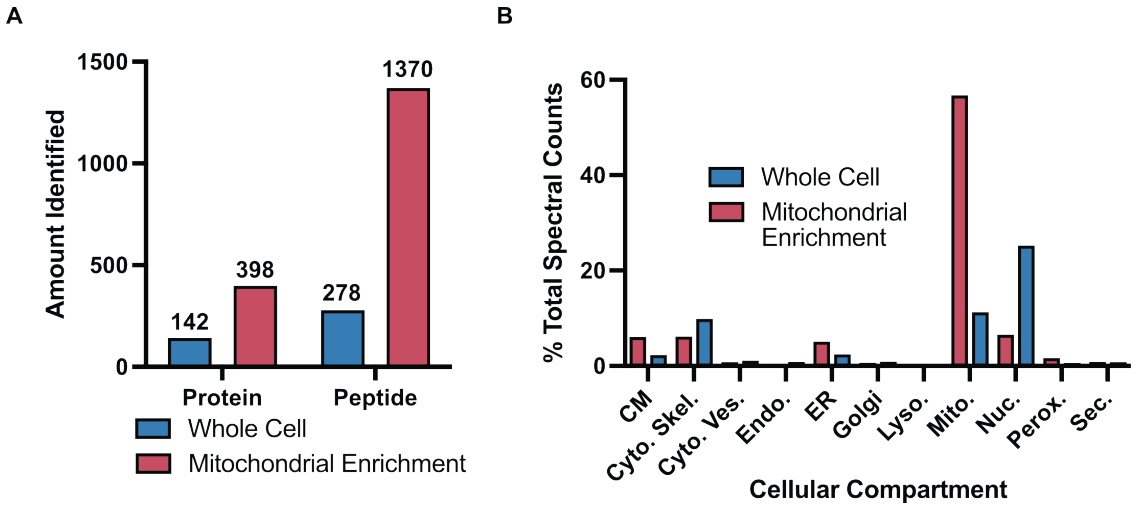


Figure 2-3. (A) Total annotated mitochondrial proteins and peptides identified from whole cell (blue) or isolated mitochondria (red). (B) Percentage of total spectral counts belonging to proteins with specified Uniprot sub-cellular localizations in a whole cell (blue) and isolated mitochondria (red) samples. Annotated compartments include cell membrane (CM), cytoskeleton (Cyto. Skel.), endosome (Endo.), endoplasmic reticulum (ER), golgi apparatus (Golgi), lysosome (Lyso.), mitochondria (Mito.), nucleus (Nuc.), peroxisome (Perox.), and secreted (Sec.).

Table 2-1. Panther gene ontology (GO) overrepresentation analysis for the top 10 enriched biological processes in mitochondrial sample compared to whole cell.

Gene Ontology Biological Process Complete	Fold Enrichment
tRNA Aminoacylation for Mitochondrial Protein Translation	15.84
Branched-chain Amino Acid Catabolic Process	12.93
Branched-chain Amino Acid Metabolic Process	12.07
Tricarboxylic Acid Cycle	11.71
Mitochondrial Translation	10.43
Mitochondrial Gene Expression	10.08
Mitochondrial RNA Metabolic Process	9.95
Mitochondrial Translational Elongation	9.67
Mitochondrial Fusion	9.58
Mitochondrial Translational Termination	9.56

Unique Cysteine Sensitivity to Oxidation.

Upon confirming mitochondrial enrichment, we sought to better understand the individual redox sensitivities of mitochondrial cysteines. Mitochondrial cysteine reactivity changes from exogenous ROS (H_2O_2) were profiled using isoTOP-ABPP (Figure 2-4).[51,52] IsoTOP-ABPP reports on cysteine reactivity through thiol labeling with isotopically coded iodoacetamide alkyne probes, IA-L (light) and IA-H (heavy) (Figure 2-5). Mito-P lysates from HEK 293T cells were treated with varying concentrations of peroxide for 20 minutes before cysteine thiols were alkylated by IA-H. Concurrently, untreated control Mito-P lysates were incubated with IA-L, capturing the cysteine thiols under basal conditions. When cysteines become oxidized by peroxide treatments, there would be a resulting loss of IA-H labeling of that cysteine relative to the IA-L labeling of cysteines in the control sample. Through copper-assisted azide-alkyne cycloaddition (CuAAC), a cleavable diazo biotin azide tag (azo-tag, Figure 2-5)

was appended to IA-labeled cysteines. Peroxide treated and untreated samples were mixed at a 1:1 ratio and proteins containing the modified cysteine residues were enriched on streptavidin resin. Following an on-bead trypsin digestion, alkylated cysteine-containing peptides were subsequently eluted off the beads with sodium dithionite and analyzed by LC/LC-MS/MS. Cysteine reactivity changes were reported as light to heavy (L:H) ratios. Upon peroxide treatment, a L:H ratio > 1 corresponded to decreases in cysteine reactivity, representative of oxidation modifications, whereas a L:H ratio < 1 indicated increases in cysteine reactivity. A L:H ratio < 1 equivalent to 1 indicated no change in cysteine reactivity in the presence of peroxide.

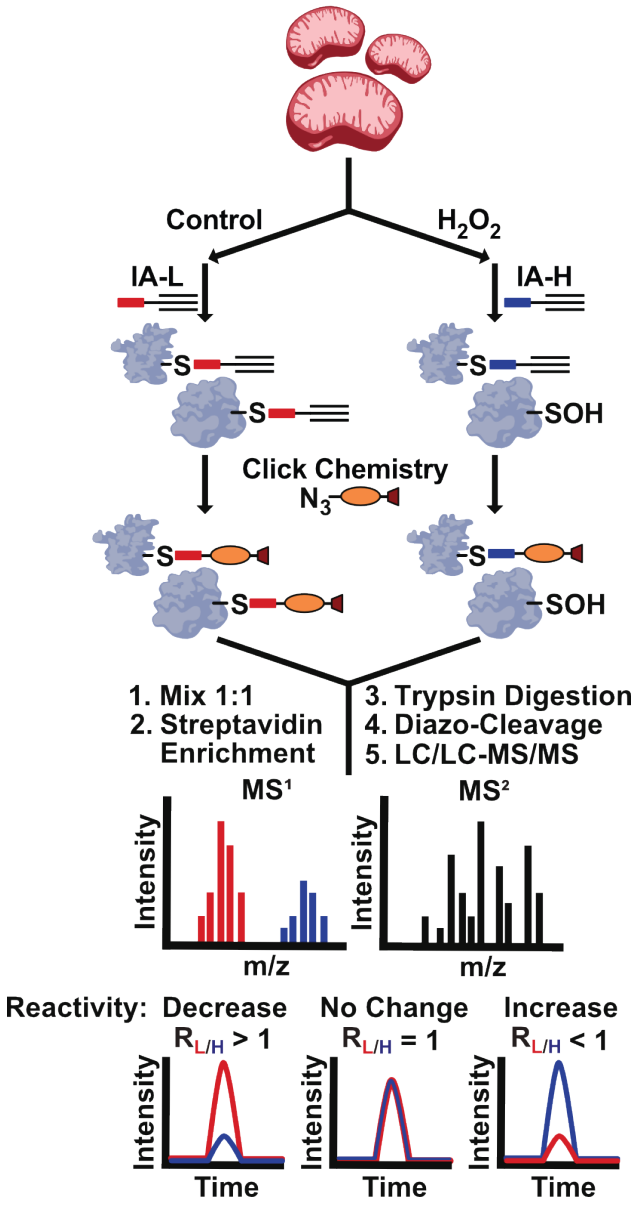


Figure 2-4. Workflow for evaluating peroxide-dependent changes in cysteine reactivity in isolated mitochondria lysates using IsoTOP-ABPP. Labeling of thiols from control or peroxide treated samples with IA-L or IA-H, respectively, appending cleavable biotin-azide tags, enrichment of labeled cysteine containing proteins, trypsin digestion, and isolation of labeled cysteine-containing peptides for quantitative MS to identify and quantify cysteine reactivity changes due to oxidation.

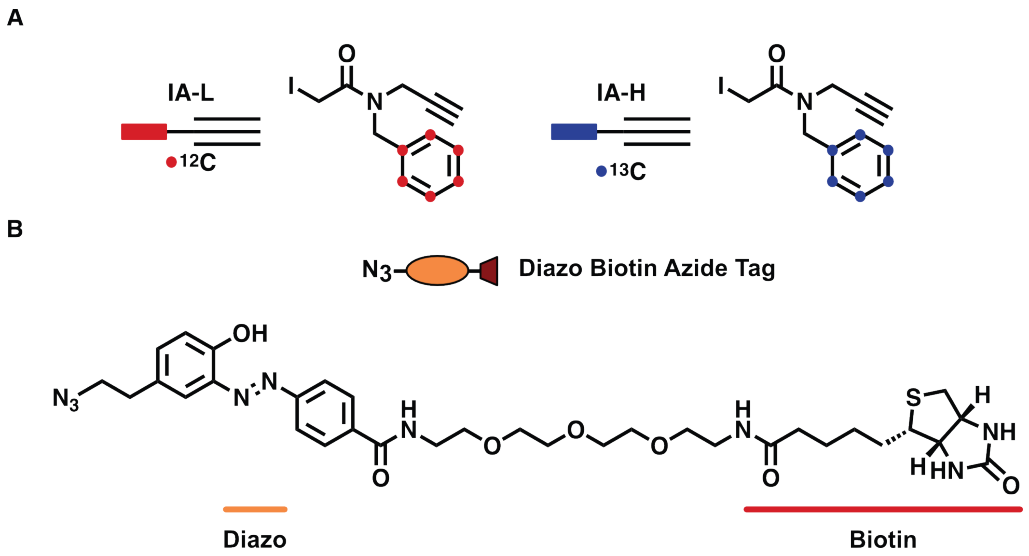


Figure 2-5. (A) Isotopically coded alkylating reagents, light (IA-L, ^{12}C) and heavy (IA-H, ^{13}C) iodoacetamide alkyne. (B) Structure of cleavable diazo biotin azide tag.

Across all peroxide treated samples analyzed by IsoTOP-ABPP, we enriched for an average of 3719 cysteine-containing peptides on 1197 proteins (Table 2A-4). Of these, an average of 1971 (53%) cysteine-containing peptides were identified on 467 (39%) proteins known to be localized to the mitochondria further demonstrating clear enrichment for the mitochondrial proteome using methods of differential centrifugation (Table 2A-4). Because the cysteine-containing peptides were subjected to IsoTOP-ABPP workflow, we filtered the identified cysteine-containing peptides for those that were annotated as residing on mitochondrial parent proteins and gave statistically significant L:H ratios in both replicates for each peroxide concentration, respectively. On average, our datasets gave 789 ratios for cysteines identified on 427 mitochondrial proteins (Table 2A-4).

The extent of cysteine oxidation in each sample appeared in a peroxide concentration-dependent manner evident by the increasing median L:H ratios with increasing peroxide addition (Figure 2-6, Table 2A-4). Notably, 1 mM peroxide treatment led to minor changes in cysteine modifications (median L:H ratio of 1.09) as compared to the 10 mM peroxide treatments which demonstrated large-scale cysteine oxidation effects (median L:H ratio of 2.34) (Table 2A-4). Treatments of 2.5 mM and 5 mM peroxide gave median L:H ratio of 1.29 and 1.66, respectively (Table 2A-4). Although peroxide impacted overall mitochondrial cysteine reactivity, many unique variations in redox sensitivities were detected on individual peptides with ~22% of thiols remaining unaffected by oxidation at any concentration of peroxide with L:H ratio ~1 including C536 on succinate dehydrogenase A (SDHA), (Figure 2-7A, Table 2A-4). Conversely, concentration-dependent decreases in reactivity were observed on numerous cysteine-containing peptides such as C348 on Mitofusin 2 (MFN2), an OMM protein central to mitochondrial network remodeling and inter-organelle contact (Figure 2-7A, Table 2A-5). The redox sensitivity of C348 on MFN2 followed a linear trend in L:H ratios proportional to the increasing peroxide molarities (Figure 2-7A, Table 2A-4). Due to the reliance of basic mitochondrial functions and health on mitochondrial morphology, MFN2 dysfunction and oxidative stress have been correlated with overlapping events of mitochondrial and cellular injury including mitophagy, unfolded protein response, metabolism maintenance and membrane potential, in addition to the pathogenesis of several diseases from neurodegeneration and cardiomyopathy to cancer.[53] Interestingly, C684 on MFN2 has been identified as a redox sensor prompting dimerization with MFN2 and homolog MFN1, through disulfide bond formation and stimulating mitochondrial

fusion.[54] MFN1 and MFN2 respectively contain 4 and 5 highly conserved, yet uncharacterized, cysteines and notably, C348 on MFN2 is located prior to a HR1 (heptad repeating coiled-coil) domain in similarly positioned to C684 preceding the HR2 domain supporting potential similar redox-inducible function of the two cysteines.[55] Furthermore, although some cysteines identified in peroxide studies displayed intense sensitivity to peroxide treatments, many of the cysteine-containing peptides, including C126 on matrix-residing GrpE protein homolog 2 (GRPEL2) and C590 on mitochondrially-localized aspartate tRNA ligase (DARS2), depicted intermediate sensitives to peroxide emphasizing the singularity of cysteine susceptibility to oxidation (Figure 2-7A, Table 2A-4). Trends in cysteine redox sensitivity was further visualized by the extracted ion chromatograms for each L-IA and H-IA labeled cysteine-containing peptide. Variations in the abundance of each isotopically-labeled cysteine directly corresponds to the L:H ratios assigned (Figure 2-7B).

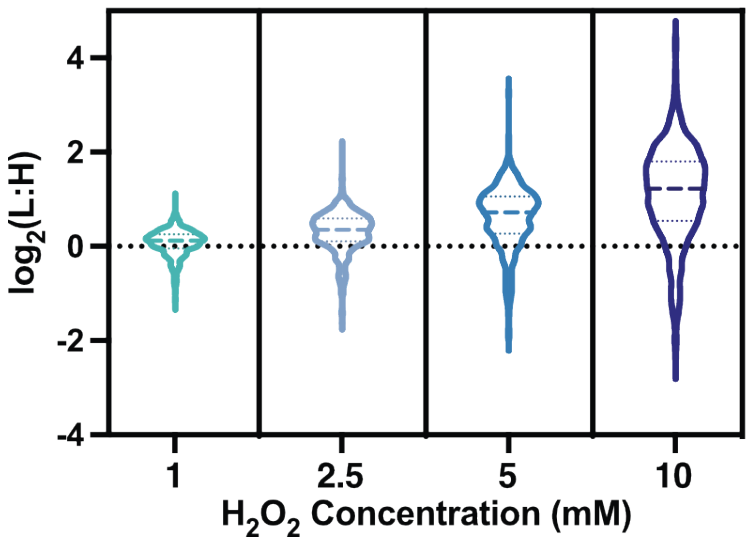


Figure 2-6. Violin plot annotating median ratios of mitochondrial cysteine

reactivity with increasing concentrations of peroxide (1 mM, 2.5 mM, 5 mM and 10 mM H_2O_2).

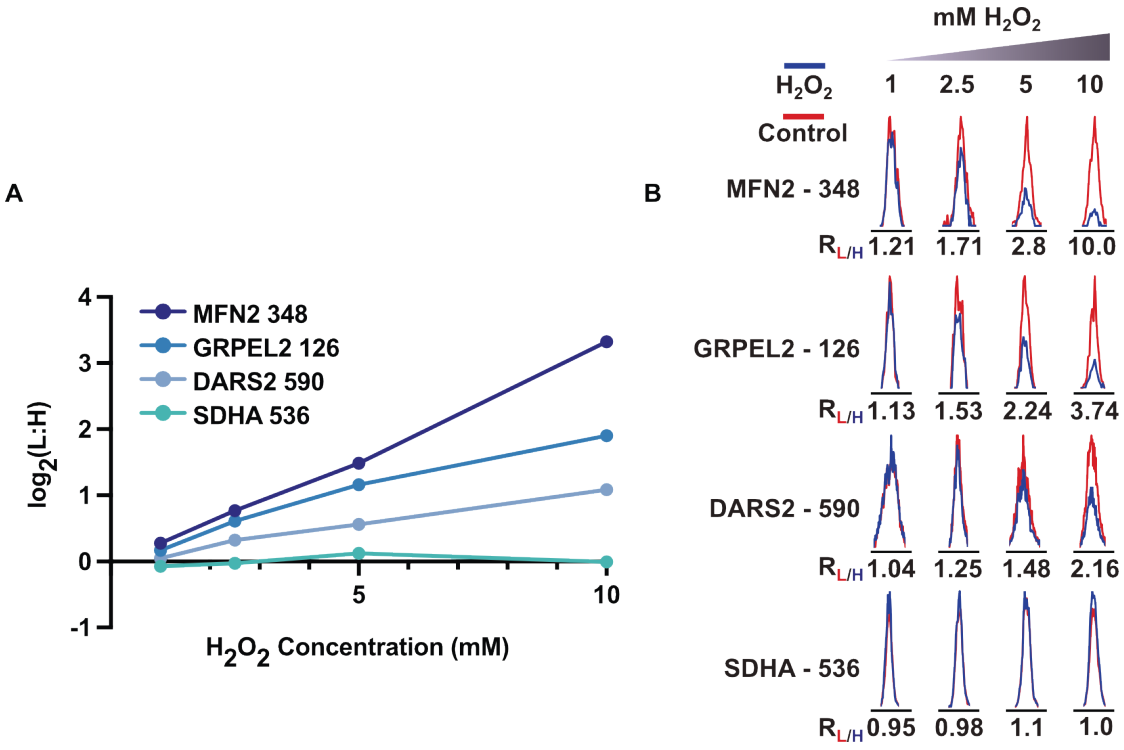
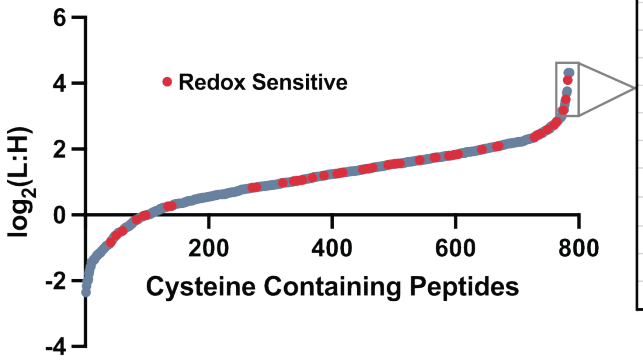


Figure 2-7. (A) Plotted average L:H ratios (log_2L:H) of mitochondrial cysteines with increasing peroxide. (B) Extracted ion chromatograms of cysteines from Figure 2-7A alkylated by IA-L (red) or IA-H (blue) in the control and peroxide treated samples, respectively. Displayed chromatograms are representative of a single replicate.

Heightened cysteine reactivity response on known redox-sensitive proteins.

As evident by the highest median ratio (2.34), the greatest changes in mitochondrial cysteine reactivity were observed in Mito-P lysates exposed to 10 mM peroxide (Figure 2-8, Table 2A-4). Out of the 785 statistically significant ratios

for mitochondrial cysteine-containing peptides identified, 58% (454) of cysteines revealed a 2-fold decrease in reactivity including 8% (65) of cysteines at higher than 5-fold decrease in reactivity. Moreover, previously documented redox-sensitive proteins and thiol switches were identified and corresponded to high L:H ratios such as C385 on ACO2 (L:H ratio of 13.26), as well as C395 on 2-oxoglutarate dehydrogenase (OGDH, L:H ratio of 17.31) (Figure 2-8, Table 2A-4). Both proteins, ACO2 and OGDH, are known to attenuate the TCA cycle through oxidation-mediated inhibition.[56,57] Moreover, OGDH catalyzes the rate-limiting step of the TCA cycle and is the highest generator of mtROS outside of the ETC. Furthermore, OGDH is known to be self-regulated through cysteine modifications such as glutathionylation.[58,59] Precise sites of cysteine oxidation that result in OGDH functional alteration remain uncharacterized, however, C395 on OGDH has previously been shown to undergo *s*-nitrosylation in a biotin-switch study in cardiac mitochondria[59] which presents C395 as a plausible redox thiol switch.



Protein	Cysteine	$R_{L/H}$	Redox Sensitive
LRPPRC	500	20.00	
CCT7	29	20.00	
POLG	647	20.00	
OGDH	395	17.31	X
PPA2	161	13.58	
NLRX1	331	14.27	
ACO2	385	13.26	X
AASS	240	13.00	
NLRX1	735	11.34	
QRSL1	88	12.11	
MFN2	348	10.02	X
PTCD1	744	9.62	
CCDC58	74	11.21	
FASTKD5	670	7.99	
MTHFD1L	302	7.74	

Figure 2-8. L:H ratio plot (log_2L:H) of mitochondrial cysteine-containing peptides identified with 10 mM peroxide treatments by IsoTOP-ABPP with annotations of

redox-sensitive proteins (red). Inlet highlights cysteine-containing peptides with the highest changes in L:H ratios. Annotated redox-sensitive parent proteins denoted (X).

Complimentary to the unique sensitivities of cysteines to variations in oxidant concentrations, our analysis of 10 mM peroxide treatment to mitochondrial lysate suggests that cysteine reactivity changes are cysteine specific and not protein dependent. For instance, of the 6 total cysteines residing on GRPEL2, an essential component in the PAM complex required for matrix translocation of transit peptide-containing proteins through the IMM, we identified 3 reactive cysteines displaying unique responses to oxidation (Figure 2-9, Table 2A-4). In the presence of ROS, reactivity of C110 is preserved (L:H ratio of 1.10), while C87 and C127 develop ~6-fold and ~3-fold decreases in reactivity with L:H ratios of 6.14 and 3.74, respectively. Moreover, the unique traits in cysteine redox sensitivities supports that C87 as a known redox thiol switch involved in a intermolecular dimer of GRPEL2 found to protect against proteolysis during conditions of mitochondrial oxidative stress.[60] As a regulator of redox homeostasis and mitochondrial protein folding and import, GRPEL2 has emerged as a prospective therapeutic target for cancer with studies in a GRPEL2 knock-down glioblastoma model exhibiting decreased cell proliferation and mtROS.[61] The impact of cysteine oxidation on GREPL2 function mitochondrial matrix protein

import highlights the selective and functional nature of cysteine oxidation events and the ability of mtROS to regulate diverse components of mitochondrial biology.

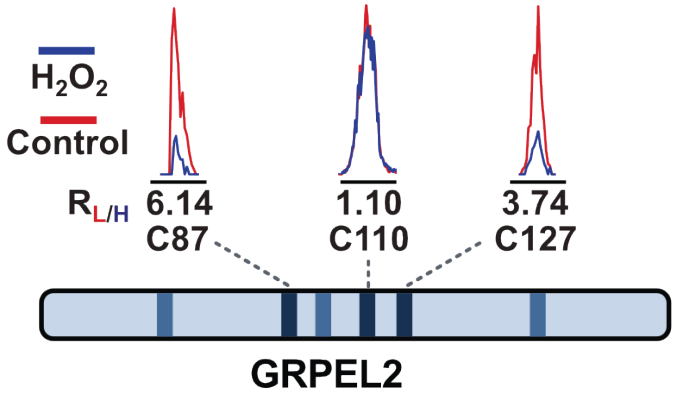


Figure 2-9. MS extracted ion chromatogram for identified cysteines of GRPEL2. Blue peaks signify cysteine labeling in 10 mM peroxide treated sample and red peaks are the untreated control cysteine labeling abundances. Displayed chromatograms are representative of a single replicate.

Distinct effects of cysteine oxidation in mitochondrial pathways.

The most well characterized redox thiol switches are known to reside within ROS-regulated pathways.[16] Therefore, we were curious if trends in cysteine redox sensitivities may be exclusive to individual mitochondrial pathways. To address this question, identified cysteine-containing peptides were sorted into 12 well-established biochemical classifications; TCA cycle, innate immunity, transport, urea cycle, fatty acid oxidation, redox regulation, Fe-S biogenesis, apoptosis, tRNA-ligases, mitochondrial (mt) ribosomal subunits, ETC, and mitochondrially transcription and translation (Supplemental Figure 2A-1, Table 2A-4. Variations in cysteines with high sensitivity to oxidation indicated by

elevated L:H ratios were detected in different mitochondrial pathways. Although most metabolic pathways represent some sensitivities to oxidation, proteins identified to belong to the TCA cycle had the greatest number of cysteines (4) above 5-fold change in reactivity amongst the metabolic processes (Figure 2-10, Table 2A-4). Cysteines that highlight the TCA cycle oxidation sensitivity include those on redox-regulated enzymes such as C385 on ACO2[18], a characterized thiol switch, and C395 on OGDH[62], a previously recognized site of *s*-nitrosation in cardiac mitochondrial study. Additionally, across all pathways considered, innate immunity and mitochondrial transcription and translation contain the largest abundance of highly redox-sensitive cysteines with 5 and 14 cysteines above 5-fold change, respectively. Trends in oxidation sensitive cysteines with on proteins central to mitochondrial translation support recent literature indicating mtROS regulation of mitochondrial ribosome and aminoacyl tRNA complex formation.[43,63] These data highlight the diverse array of mitochondrial biological processes with redox-sensitive cysteines and the potential for cysteine oxidation to regulate mitochondria biology through redox signaling.

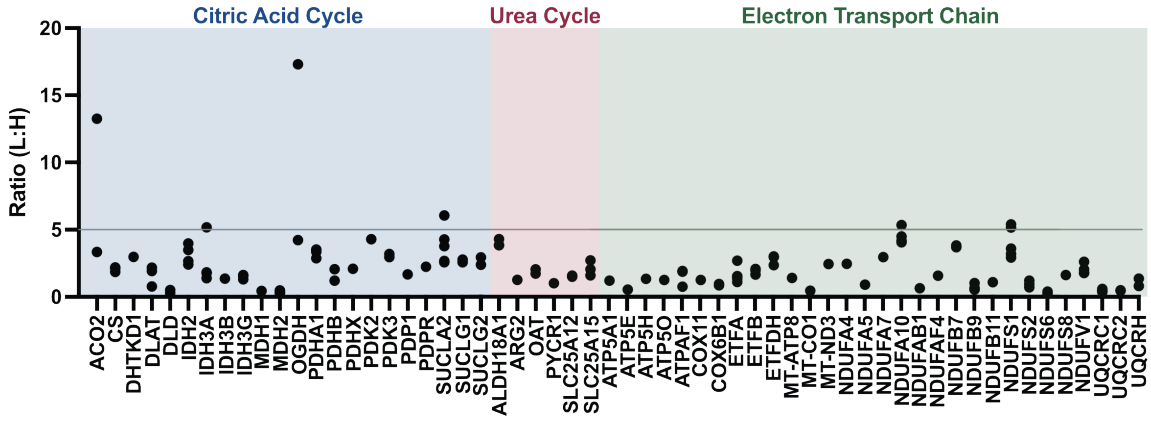


Figure 2-10. Average L:H ratios for cysteines identified on proteins belonging to mitochondrial bioenergetic pathways including the citric acid cycle (blue), urea

cycle (red), and electron transport chain (green) in 10 mM peroxide IsoTOP-ABPP dataset. High peroxide sensitivity (L:H ratio of 5) is denoted as a gray line.

Electron transport inhibition results in mitochondrial cysteine oxidation.

Cysteine-mediated redox signaling and elevated ROS are known to be central components in a variety of pathologies.[15,64] Therefore, we set out to adapt our IsoTOP-ABPP platform to assess changes in cysteine reactivity and oxidation in the presence of endogenous mitochondrial oxidative stress. Antimycin A (AMA), a well-characterized complex III inhibitor, was chosen to induce the release of physiologically and pathologically relevant levels of endogenous mtROS (Figure 2-11). AMA binds to the Q_i-site of cytochrome c reductase, inhibiting the reduction of ubiquinol to ubiquinone and thus halting the ETC.[65] Disruption of electron flow leads to the termination of the proton-gradient and OXPHOS as well as the dual-sided release of mtROS into the matrix and IMS resulting in modifications of reactive mitochondrial cysteines. Prior to proteomic studies, immunofluorescence imaging using mitoSOX, a mitochondrial superoxide stain, allowed for confirmation of AMA as a tool for providing increased mtROS production without inducing cell death (Figure 2-12).

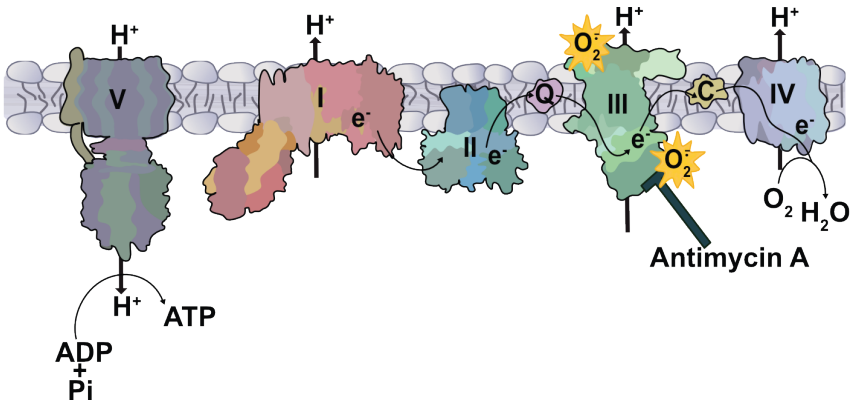


Figure 2-11. Depiction of ETC inhibition of complex III by Antimycin A (AMA). Concurrent electron leakage and superoxide production located in mitochondrial matrix and IMS.

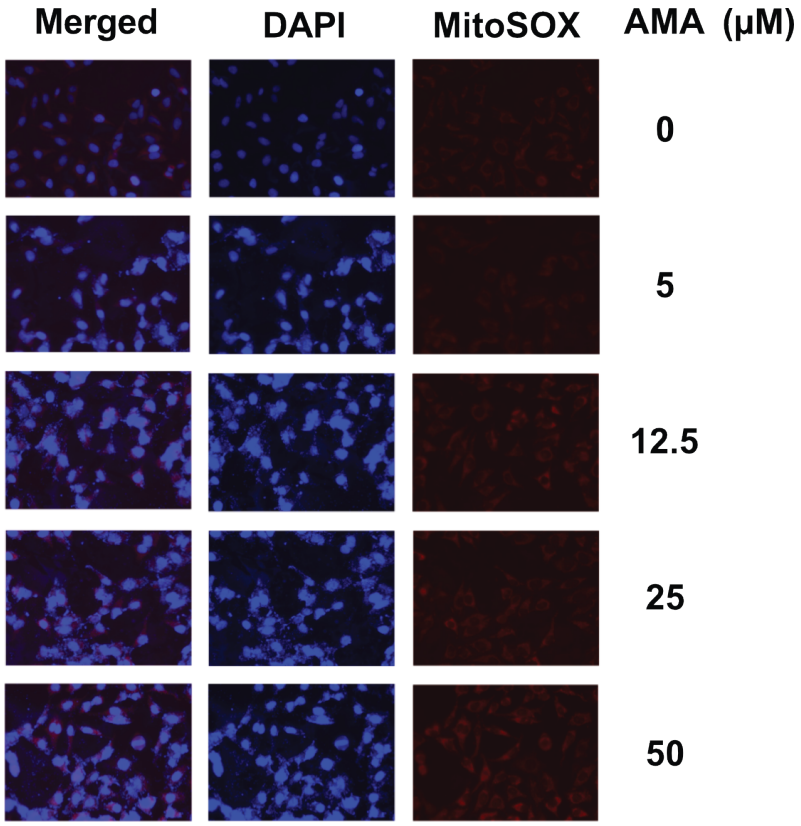


Figure 2-12. Immunofluorescence imaging of HeLa cells treated with increasing concentrations of Antimycin A (AMA). Mitochondrial superoxide is staining with MitoSOX (red) and nucleus stained with DAPI (blue).

To investigate cysteine oxidation in conditions of mitochondrial oxidative stress, cells were incubated with either AMA or DMSO (control) for 1 hour prior to fractionation and Mito-P isolation. Intact Mito-P from AMA treated cells were labeled with IA-H, while Mito-P from the control cells were labeled with IA-L. After lysis, the isoTOP-ABPP workflow was followed, as previously described, to achieve quantitative, chemoproteomic analysis of cysteine reactivity by LC/LC-MS/MS (Figure 2-13, Table 2A-5). The resulting MS analysis identified 1358 proteins, of which 490 (36%) were localized to the mitochondria. A total of 3582 cysteines were identified, of which 1752 cysteines were identified on 529 mitochondrial proteins. Of the 1752 mitochondrial cysteine-containing peptides identified in the dataset, 1109 were assigned L:H ratios. Filtering these hits for those cysteines for which L:H ratios were determined across at least two replicates with statistical significance (coefficient of variance < 50%), ratios were generated for 828 cysteines on 432 mitochondrial proteins (Figure 2-14, Table 2A-5). As expected, the majority of cysteines (96% under 2-fold change) were not affected by endogenous ROS generated by AMA. However, 31 cysteines (4%) were identified with greater than 2-fold decreases in reactivity (Table 2A-5).

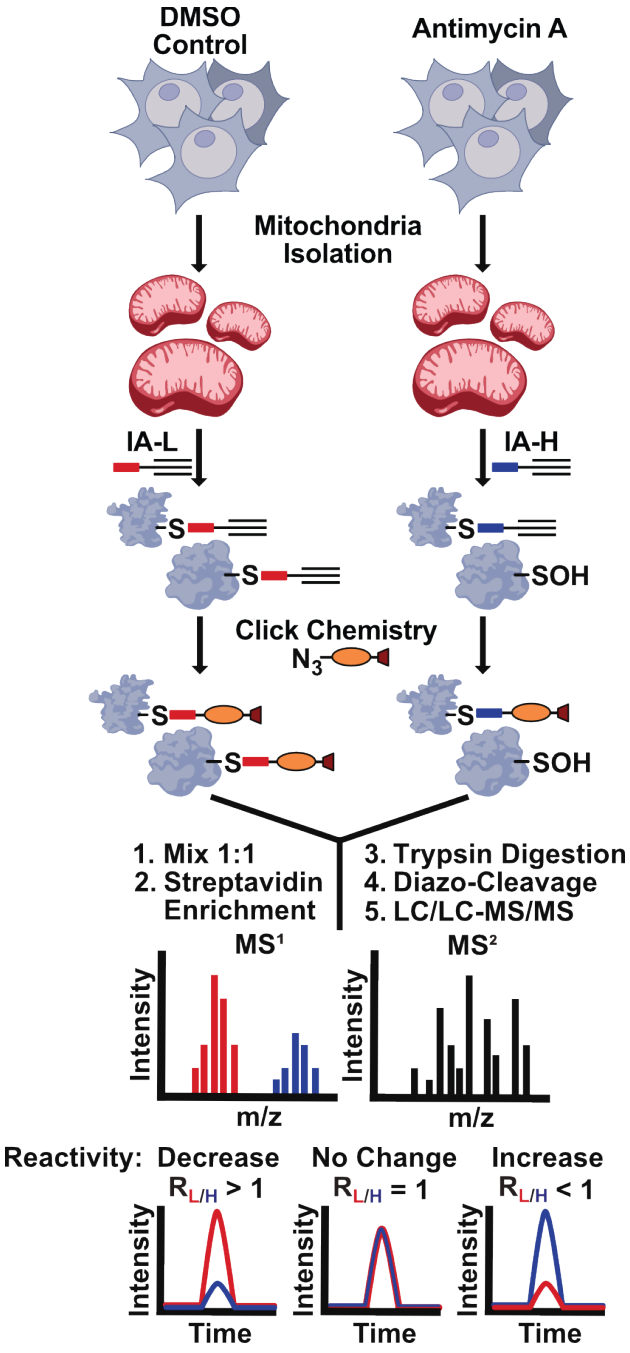
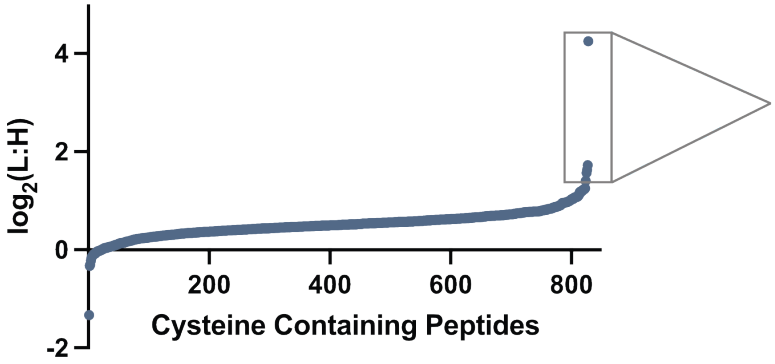


Figure 2-13. Workflow quantification of changes in cysteine reactivity in mitochondria isolated from whole cells treated with DMSO (control) or Antimycin A (AMA) using IsoTOP-ABPP.



Protein	Cysteine	$R_{L/H}$
MRPL39	146	19.06
HMGCL	307	3.46
SPTLC2	204	3.12
CLIC4	35	2.99
PDSS2	365	2.65
CCT7	364	2.41
NDUFS1	75	2.38
NLRX1	331	2.35
ALDH9A1	96	2.35
FASN	212	2.34

Figure 2-14. L:H ratio plot (log_2L:H) of mitochondrial cysteine-containing peptides identified after AMA treatments by IsoTOP-ABPP with annotations of redox-sensitive proteins (red). Inlet highlights cysteine-containing peptides with the highest changes in L:H ratios.

Compared to 10 mM peroxide exposure, AMA-induced mtROS resulted in sweeping increases in L:H ratios and overall decreases in cysteine reactivity, however, in a more subtle manner as expected with endogenous ROS levels involved in redox signaling. To that end, global decreases in cysteine reactivity from endogenous mtROS gave a median L:H ratio of 1.42 compared to more heightened changes in cysteine reactivity in the 10 mM peroxide treatment (median L:H ratio of 2.34) (Table 2A-5). Interestingly, C146 on mitochondrial ribosomal protein L39 (MRPL39) exhibited the highest L:H ratio value of 19.06 out of the entire AMA-treated dataset. C146 on MRPL39 was the only cysteine with a 5-fold decrease in reactivity under AMA-induced mtROS. Although, cysteine oxidation on MRPL39 has not been studied, proximal cysteines on adjacent MRPs have appeared to be sensitive to oxidative stress and disulfide bonding warranting further investigation.[66] Furthermore, in mitochondrial yeast OxICAT studies[43],

numerous proteins involved in mitochondrial translation demonstrated high oxidation in the presence of peroxide including a previously characterized redox-regulated MRP (MRPL32) indicating the potential for the MRP family to be regulated by mtROS.[43,67] Cysteine oxidation on MRPL39 upon ETC inhibition by AMA, supports the hypothesis of redox-mediated attenuation of mitochondrial protein synthesis previously suggested.[43] Additionally, MRPL39 has abnormal expression in gastric cancer which may be associated with tumor suppression suggesting a link between mitochondrial translation, mtROS, and cancer.[68]

Additionally, when comparing to 10 mM peroxide treatment and AMA-induced mtROS, some cysteines showed stark decreases in reactivity with both studies. For instance, C331 on NLR family member X1 (NLRX1) displayed an average L:H ratio of 14.27 with exogenous 10 mM peroxide and average L:H ratio of 2.35 with AMA-induced endogenous mtROS (Table 2A-). NLRX1 is involved in antiviral signaling and injury prevention by enhancing the immune response through promotion of ROS signaling of NFKB and JUNK pathways.[69] Although, NRLX1 is known to provoke redox signaling and contains multiple reactive cysteines shown to be redox sensitive by our exogenous and endogenous mtROS treatments, specific cysteine oxidation events have not previously been studied. Notably, NLRX1 is a negative regulator of mitochondrial antiviral signaling protein (MAVS) which also presents cysteine redox sensitivity, however trending in an opposing pattern with increased reactivity upon AMA ETC inhibition (C283, L:H ratio of 0.40) (Table 2A-5). MAVS is confirmed to undergo ROS-dependent oligomerization, interferon regulatory factor and NFKB innate immune activation and RIG-I signaling centered around potential disulfide bonding of C79 (not identified in this study) located in the N-terminal CARD-domain.[70]

Quantification of mitochondrial redox environment under normal and oxidizing metabolic states.

Complementing the isoTOP-ABPP platform to survey changes to mitochondrial cysteine reactivity, a more direct method for analyzing dynamic changes to cysteine oxidation through isotope coded affinity tags (OxICAT)[39] was employed. OxICAT can indicate the degree of cysteine oxidation by initially alkylating free thiols with IA-L followed by a reduction of reversibly oxidized thiols and subsequent labeling of newly reduced thiols with IA-H within the same sample (Figure 2-15). Incorporating OxICAT into our mitochondrial cysteine oxidation studies was a beneficial strategy as it allowed direct quantification of cysteine oxidation events on all cysteines, compared to exclusively studying changes in reactivity on most reactive cysteines using isoTOP-ABPP. However, by profiling all cysteines, there is a loss in lower abundant cysteines which are sometimes less present in the more reactive population. Nevertheless, both methods are necessary in discerning overall cysteine changes during oxidative stress. The OxICAT method was applied to Mito-P isolated from AMA or DMSO (control) treated whole cells, respectively.

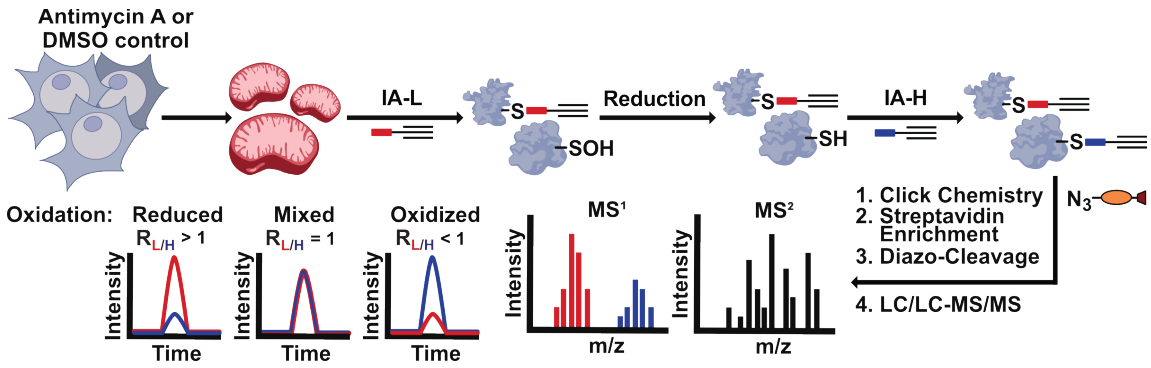


Figure 2-15. Workflow OxICAT in isolated mitochondria treated with from DMSO control-treated cells or AMA-treated cells. Platform includes differential alkylation of reduced and oxidized cysteine thiols with IA-L or IA-H followed by incorporation of cleavable biotin-azide tag for labeled cysteine-containing protein enrichment, trypsin digestion, labeled cysteine-containing peptide capture. L:H ratios directly correspond to percent oxidation values of cysteines.

Our OxICAT platform resulted in the enrichment of a total of 2181 cysteine-containing peptides from 885 parent proteins in Mito-P samples from the control cells and 2560 cysteine-containing peptides from 918 parent proteins in Mito-P samples from the AMA-treated cells. Of these, 52% of peptides in each sample were found on annotated mitochondrial proteins with 1140 cysteine-containing peptides from 378 proteins localized to the mitochondria in Mito-P samples from the control cells and 1342 cysteine-containing peptides from 378 proteins localized to the mitochondria in Mito-P samples from the AMA-treated cells. A total of 1208 and 1210 L:H ratios of peptides on 677 and 799 proteins containing isotopically coded cysteines labeled by either IA-L or IA-H were obtained for both the control and AMA-treated samples, respectively. For both samples, 55% of ratios came from peptides on mitochondrial localized proteins with 667 L:H from 346

mitochondrial proteins in the control sample and 777 L:H ratios from 405 mitochondrial proteins in the AMA-treated sample. The mitochondrial 667 and 777 L:H ratios were further filtered for those found in at least 2 out of 3 replicates and statistical significance (< 30% standard error of the mean, SEM) (Table 2A-10).

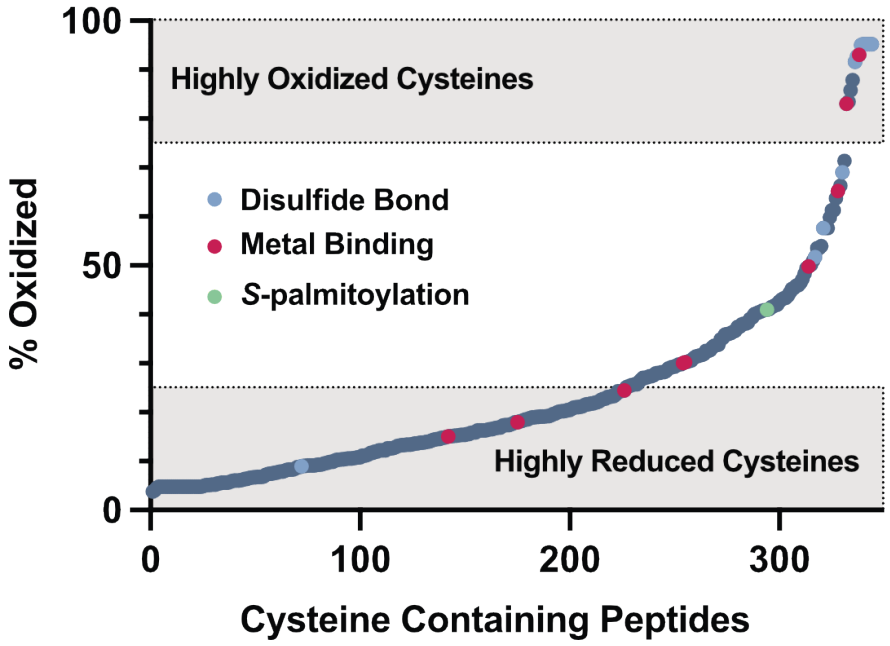


Figure 2-16. Percent oxidation values for DMSO-treated, control mitochondria. Uniprot annotations of cysteine residues that partake in disulfide bonding (blue), metal binding (red) and *s*-palmitoylation (green). Percent oxidation is directly calculated from L:H and H:L ratios.

The overlapping 344 statistically significant mitochondrial L:H ratios from both the AMA-treated and control Mito-P samples were converted into corresponding percent oxidation values. As anticipated, the mitochondrial proteome from the control cell population was representative of the reducing

redox environment of mitochondria under normal conditions with most cysteines in a highly reduced state (74% of cysteines below 30% oxidized, 254 out of 344 total cysteines identified) (Figure 2-16, Table 2A-6). Of the small subset of cysteines over 50% oxidized (8.4%, 29 of 344 total cysteines identified), several were annotated as disulfide (11 cysteines) and metal binding (3 cysteines). Of all cysteines annotated partaking in disulfide bonds, many of them correspond to high percent oxidation values including C50 on mitochondrial import inner membrane translocase subunit TIM13 (TIMM13) at 95% oxidized. C50 on TIMM13 is predicted to partake in an intramolecular disulfide bond with C65 (not identified). Additionally, our OxICAT dataset identifies C80 the active site of on dihydrolipoamide dehydrogenase (DLD) as highly oxidized (95%). C80 on DLD is known to form a catalytically redox-active disulfide bond with C85 (not identified). Several disulfide-bonding cysteines, C30, C54, and C65 on cytochrome c oxidase subunit 6B1 (COX6B1) were each identified at 95% oxidized (Table 2A-6).

When comparing the L:H ratios of the 344 cysteines identified in both Mito-P OxICAT samples, a modest change in cysteine oxidation is observed following AMA-induced oxidative stress (Figure 2-17, Table 2A-6). A similar percentage of cysteines (66% and 75%) are highly reduced in both samples. However, our datasets identify several cysteines with increased oxidation upon induction of mtROS by ETC inhibition. The peroxidatic cysteine, C100, on peroxiredoxin 5 (PRDX5) displayed one of the more profound changes with 58% oxidation in the control sample compared to 94% in the AMA-treated sample. PRDX5 is an antioxidant enzyme critical in mediating peroxide concentrations as well as protecting the cell from irreversible oxidative damage under high levels of oxidative stress.[71] C100 is known to become sulfenylated and form a redox-active

disulfide bond bridge with C204.[72,73] Interestingly, the resolving cysteine of PRDX5, C204, is also identified in both samples with 92% oxidation indicating PRDX5's response to mtROS production by ETC inhibition. Additionally, C110 on NADH dehydrogenase 1 alpha subcomplex subunit (NDUFA8), a complex I subunit, is an annotated disulfide bond and was found to have increasing oxidation upon AMA treatments (95% oxidized) compared to the control treatment (70% oxidized). NDUFA8 contains four CX_9C motifs that may undergo disulfide exchanges reliant on the redox conditions of the IMS.[74,75] Furthermore, it has been suggested that NDUFA8 may participate in electron leakage at complex I.[76]

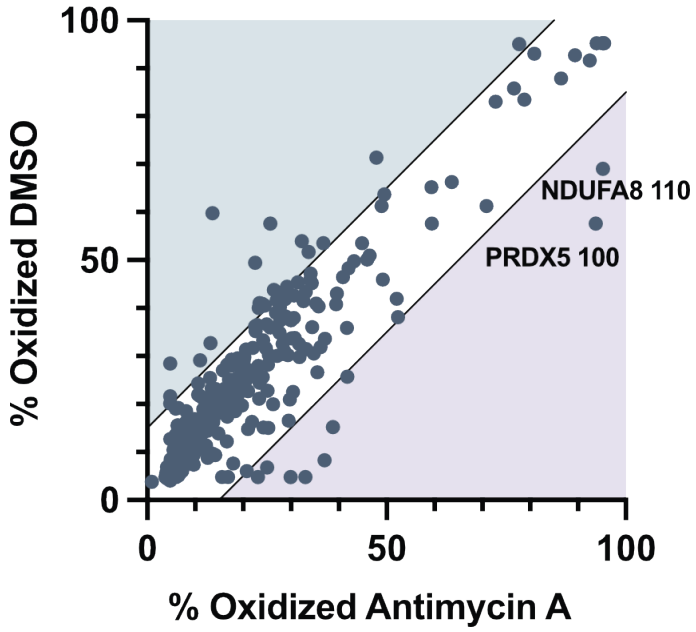


Figure 2-17. Plot of overlapping percent oxidation values from mitochondria from cells treated with DMSO (control) or AMA. Colored regions demonstrate cysteines with > 15% change in percent oxidation.

A decreased amount of cysteine oxidation events was observed using the OxICAT plaform compared to IsoTOP-ABPP. Due to the loss in some of the lower abundant, yet highly redox-sensitive cysteine-containing peptides, other considerable changes to cysteine oxidation may have gone undetected. Furthermore, the OxICAT platform only allows observation of reversible cysteine modifications (sulfenic acids and disulfide bonds). Therefore, if cysteines undergo irreversible oxidation, this method is unable to quantify percent oxidation of the cysteines. Although both platforms offered analysis of cysteine oxPTMs, the OxICAT method provided distinct insight on trends in mitochondrial cysteine oxidation with little overlap between cysteines identified with IsoTOP-ABPP. Each method recognizes unique populations of cysteines due to the concentrations of iodoacetamide used. With OxICAT using 100-fold higher alkylating reagent (10 mM IA) and incorporating reversibly oxidized thiol reduction, all cysteines in a sample will be labeled and therefore, the most highly abundant species will be favored in the MS analysis. Whereas investigation of cysteine oxidation using IsoTOP-ABPP profiles the most reactive, but potentially less abundant cysteines. By isolating a subset of highly reactive cysteines, inherently, there will be enhanced coverage of those peptides by MS analysis.

Evaluation of functional sites of cysteine oxidation.

To evaluate if cysteine oxidation sites observed result in perturbation to protein function, mitochondrial cysteines with high sensitivity to exogenous and endogenous ROS, by peroxide and AMA-derived mtROS, respectively, were considered as potential thiol switch sites. Specifically, proteins with cysteines what have not been previously characterized as functional oxidation sites were elected

for follow-up evaluations including C161 and C171 on mitochondrial inorganic pyrophosphatase 2 (PPA2), C11 on mitochondrial arginine aminoacyl transferase (RARS2), C395 on OGDH, C331 on NLRX1, and C283 on MAVS.

PPA2.

Initial investigation was completed for cysteines with amplified ROS sensitivities (C161 and C171) on PPA2. PPA2 is an essential mitochondrial enzyme that is critical for ATP production and thought to control membrane potential. Furthermore, deficiencies in PPA2 are strongly associated with cardiac sudden death.[77] C161 and C171 reside on the sample tryptic cysteine-containing peptide and therefore, an undistinguishable change in reactivity was observed for both cysteines with both position labeled by IA-L and IA-H. L:H ratios of 13.58 with exogenous 10 mM peroxide treatment (Table 2A-4) and 2.06 with endogenous mtROS produced by AMA treatment (Table 2A-5) were observed. To evaluate the relationship between cysteine oxidation and PPA2 activity, *in vitro* activity assays on recombinantly expressed PPA2 were completed. (32-304)PPA2 was recombinantly expressed with removal of mitochondrial localization sequence for solubility. (32-304)PPA2 single (C161S and C171S) and double (C161S/C171S) mutants were generated. However, due to the C171S mutation insolubility and low yielding protein expression, only (32-304)PPA2C161S was examined. Although crystal structures of PPA2 are yet to be resolved, disruptions to PPA2 structure with the C171S mutation may also suggest the importance of this cysteine in the stability and function of the protein.

Activity of PPA2 was monitored through observation of the conversion of pyrophosphate (PPi) to *ortho*-phosphate (Pi) using a phosphate activity assay with

ammonium-molybdate and malachite green.[78] We delineated previously unreported k_{cat} and k_m values for human PPA2 (444.5 s^{-1} and 10.18 μM, respectively) which present similar values to its cytosolic homologs in *S. cerevisiae* and *E. coli*.[79,80] Furthermore, (32-304)PPA2C161S displayed similar kinetics with k_{cat} of 524.8 s^{-1} and k_m of 7.692 μM (Figure 2-18A). Hydrogen peroxide treatments strongly correlate to inhibition of both PPA2 WT and C161S mutant with inhibition of 73.15% and 56.6%, respectively (Figure 2-18B) emphasizing the ability of mtROS to modulate PPA2 activity. However, this data also suggests that oxidation of C161 is not solely responsible for decreased PPA2 activity under oxidizing conditions. If C161S was a thiol switch, we would expect to see no change in activity of the PPA2 C161S mutant under oxidizing conditions. Our data corresponds to an opposing trend where C161S is more sensitive to peroxide than WT PPA2.

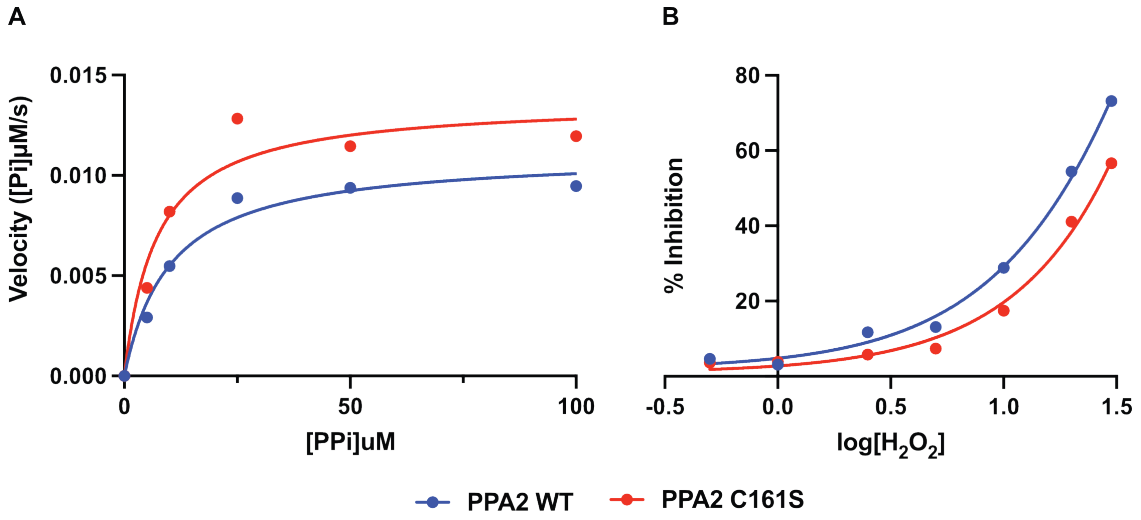


Figure 2-18. (A) Michaelis-Menten kinetic plot of PPA2 wild-type (blue) and PPA2 C161S (red) pyrophosphatase activity, n=3 (B) Time and concentration dependent effects of hydrogen peroxide as measured by percent inhibition in PPA2 WT and PPA2 C161S by hydrogen peroxide, n=3

In efforts to further understand which cysteines (C161S and C171S) on PPA2 are becoming oxidized in the presence of ROS, the OxICAT platform was adapted and used on purified wild-type (32-304)PPA2 and (32-304)PPA2C161S. Unfortunately, spectra gave unclear indication of a particular cysteine that is susceptible to oxidation. Both cysteines appear to have a mix of labeling by IA-L and IA-H under oxidizing conditions. Due to the difficulties in determining reactivity and sensitivity of C161 and C171 individually, we were unable to determine the strength of peroxide alterations to protein function.

Evaluation of redox-sensitive cysteines in mammalian cells.

Mammalian cell expression and immunoprecipitation of wild-type and cysteine mutants gave insights on complex formation and protein-protein interactions reliant on cysteine redox states for OGDH, RARS2, NLRX1, and MAVS. Each follow up was chosen not only by their distinctive changes in reactivity in the presence of exogenous peroxide and/or AMA-induced endogenous oxidative stress, but also, their recognized roles in important mitochondrial complex formations. To explore changes in their interaction network, follow ups and cysteine mutants were overexpressed with incorporation of a C-terminal FLAG-epitope tag for immunoprecipitation. Overexpression of cysteine mutants were only successful for MAVSC283S, OGDH385S and NLRX1C331S (slightly) (Figure 2-19).

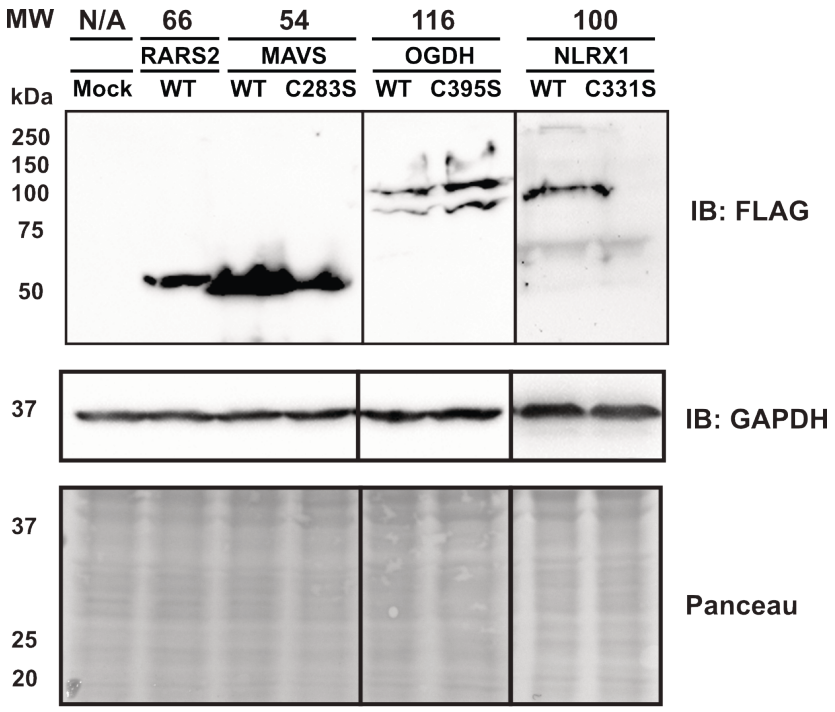


Figure 2-19. Western blot analysis analysis of HEK 293T lysates expressing follow up proteins (RARS2, MAVSWT/C283S, OGDHWT/C395S, and NLRX1WT/C331S). Overexpressed proteins were visualized using an anti-FLAG. Anti-GAPDH and panceau staining was used as a loading control.

RARS2.

A recent study by Xiao *et al.*, analyzing reversible cysteine oxidation in a whole mouse model[63], encouraged our efforts toward investigating the effects of cysteine oxidation on the formation and assembly of the aminoacyl transferase complex in the mitochondria. Xiao *et al.* found that the tRNA multi-synthase complex is highly redox sensitive. In the presence of reducing agent (DTT), pulldown of cytosolic aminoacyl-transferase RARS demonstrated association of many supplementary aminoacyl transferases.[63] Due to the evidence that RARS and the aminoacyl tRNA synthase complex formation redox dependent, it was

hypothesized that the mitochondrial arginine aminoacyl-transferase, RARS2, may operate in the same redox-dependent manner. From our cysteine reactivity studies, C11 on RARS2 was determined to have 3.20 -fold decrease in reactivity upon peroxide treatment making it a promising candidate for potential redox sensing capabilities (Figure 2-20, Table 2A-4).

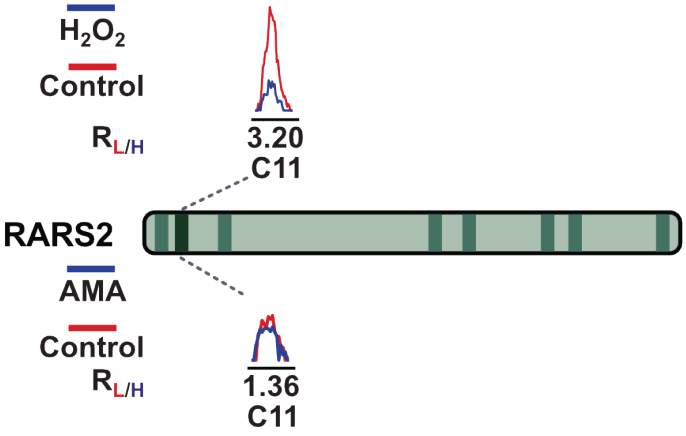


Figure 2-20. Depiction of RARS2 protein with bars representing all cysteines. The cysteine identified from our proteomic studies (C11) is in dark green. Chromatogram traces corresponding to ratios from each study are show with red lines as the IA-L labeled (light) and blue lines as the treatment (IA-H labeled).

To examine the effects of ROS on the ability for RARS2 to mediate tRNA synthetase complex formation, immunoprecipitation using anti-FLAG resin was performed on HEK 293T cells overexpressing RARS2 with a C-terminal FLAG tag following incubation with 10 mM peroxide for 20 min (Figure 2-21A, Table 2A-7). Interacting proteins were enriched and quantified by mass spectrometry. Unfortunately, although mitochondrial ribosomal subunits were strongly enriched, other aminoacyl transferases were not. Furthermore, no significant

changes were uncovered, as the largest enrichment changes corresponded with the lowest abundant proteins in the sample (Figure 2-21B). Further work is required to determine the effects of oxidation on complex formation. Comparison of oxidized and fully reduced sample (with the addition of a reducing agent such as DTT) may provide greater insight on the extent of redox regulation of the mitochondrial translational process. Given the mitochondrial matrix is a more oxidizing environment (900:1 GSH:GSSG) than the cytosol (3000:1 GSH:GSSG), it is possible that RARS2 and the tRNA aminoacyl synthetase complex may have different sensitivities to oxidation compared to its cytosolic counterpart. [81]

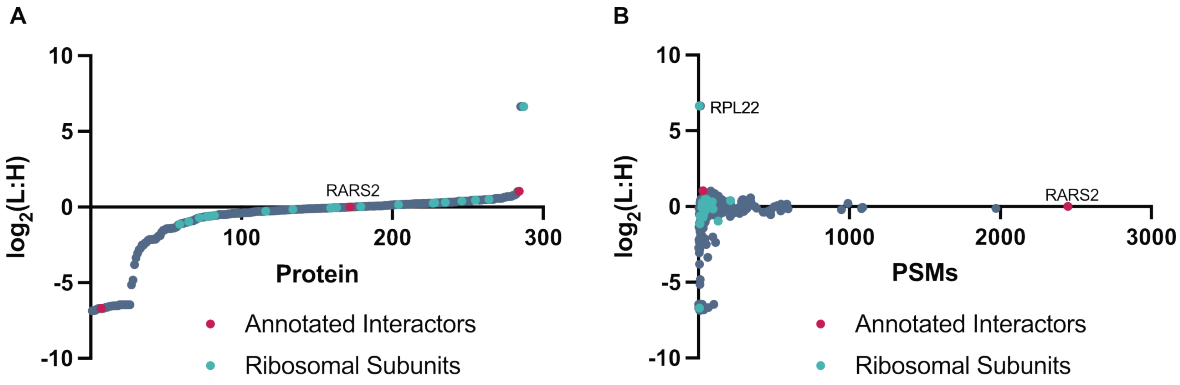


Figure 2-21. (A) Log_2 L:H ratio plot of immunoprecipitated proteins on anti-FLAG resin from lysates overexpressing RARS2-FLAG treated with 10 mM peroxide (heavy) against the untreated control (light), n=3. (B) Average Log_2 L:H ratio from immunoprecipitation plotted against the average protein spectral matches (PSMs), n=9.

NLRX1 and MAVS.

Several proteins identified with cysteines sensitive to oxidation, within both the exogenous and endogenous ROS treatments, resided on proteins

involved in innate immunity including, NLRX1 and MAVS (Table 2A-4 and Table 2A-5). Both proteins are known to be integral to innate immune signaling and have unique responsibilities and a variety of interacting partners including interactions with each other.[69,70] NLRX1 is a member of the immune regulatory NLR family which is comprised of pattern recognition receptors (PRRs) essential for the cellular distinction between foreign and familiar entities. In addition to NLRX1 being the negative regulator of MAVS, NLRX1 has shown to play a nuanced role in immune signaling as it has found to be implicated in both the upregulation and downregulation of ROS production by OXPHOS.[82] Furthermore, the many reactive cysteines identified to be sensitive to oxidation on NLRX1 make it a candidate for redox thiol sensing (Figure 2-22). Particularly, in our studies, C331 on NLRX1 has shown high levels of oxidation upon both endogenous (AMA) and exogenous (H_2O_2) ROS treatments with L:H ratios of 14.27 and 2.35 in each treatment, respectively (Table 2A-4 and Table 2A-5).

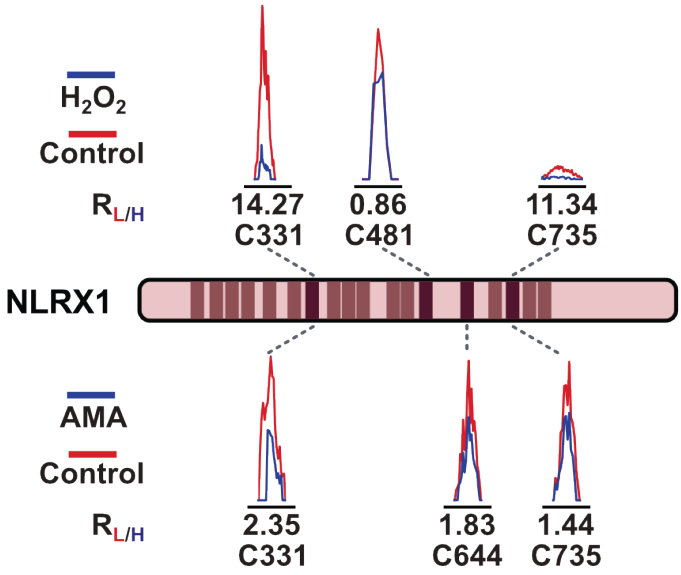


Figure 2-22. Illustration of NLRX1 protein with all cysteines in light red and those identified by our MS studies in dark red. Traces corresponding to chromatograms

of cysteine-containing peptides are shown with red (IA-L) and blue (IA-H) labeling.

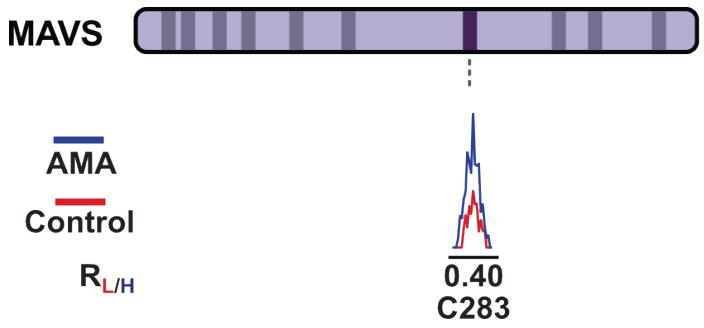


Figure 2-23. Illustration of MAVS protein with all cysteines in light purple and those identified by our MS studies in dark purple. Traces corresponding to chromatograms of cysteine-containing peptides are shown with red (IA-L) and blue (IA-H) labeling.

Additionally, MAVS, which associates and binds to NLRX1 to prevent oligomerization and immune signal pathway activation, displayed a unique increase in reactivity upon the induction of oxidative stress by AMA.[69,83] C283 on MAVS showed 2.5 increase in reactivity (L:H ratio of 0.40) with AMA-derived mtROS which was an exceptional result from our studies (Figure 2-23, Table 2A-5). To analyze the potential importance of cysteines on protein-protein interactions of immune regulatory proteins, HEK 293T cells were overexpressed with wild-type or C331S NLRX1 or wild-type or C283S MAVS with C-terminal FLAG tags, respectively. Interestingly, through immunoprecipitation analysis, NLRX1 showed increased protein associations with the C331S mutation reflecting it's known response and role as a signaler for immune system function triggered by ROS (Figure 2-24, Table 2A-8).[82] Several proteasome proteins are identified in the

sample including PSMA6 a potential interactor of NLRX1 (Figure 2-24, Table 2A-8). However, this shift in protein association occurred on each of the interacting proteins identified and therefore may be a result of challenges of normalization since there was much lower NLRX1C331S expression compared to wild-type NLRX1.

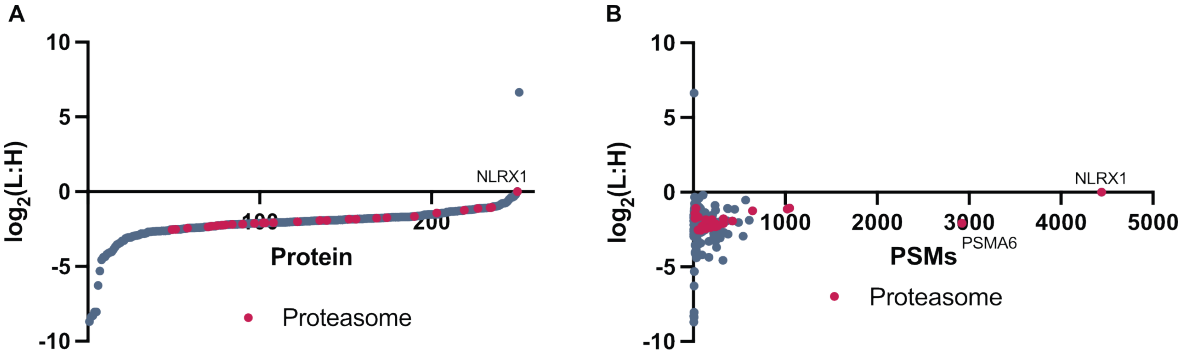


Figure 2-24. (A) Log_2 L:H ratio plot of immunoprecipitated proteins on anti-FLAG resin from lysates overexpressing NLRX1-FLAG (light) and NLRX1C331S-FLAG (heavy), n=3. (B) Average Log_2 L:H ratio from immunoprecipitation plotted against the average protein spectral matches (PSMs), n=9.

Similar analysis was completed to understand the role of C283 on MAVS protein complex formation. Wild-type and C283S MAVS expressed at comparably high amounts and therefore, analysis of cysteine-dependent changes of MAVS protein-interactors was completed. Similar to NLRX1 and RARS2, immunoprecipitation was employed for both wild-type and C283S MAVS. Notably, although many proteasome members and known interactors were identified, NLRX1 and MAVS did not appear in each corresponding samples (Figure 2-25, Table 2A-8 and Table 2A-9). Additionally, both NLRX1 peroxide

sensitivity and MAVS redox-cysteine mutants did not result in significant alterations to protein associations.

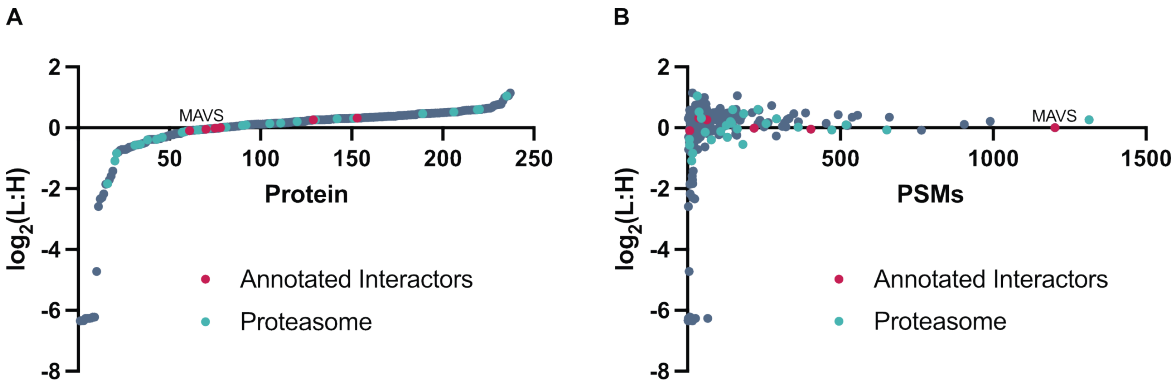


Figure 2-25. (A) Log_2 L:H ratio plot of immunoprecipitated proteins on anti-FLAG resin from lysates overexpressing MAVS-FLAG (light) and MAVSC283S-FLAG (heavy), n=3. (B) Average Log_2 L:H ratio from immunoprecipitation plotted against the average protein spectral matches (PSMs), n=9.

OGDH.

OGDH is the central regulating step of the TCA cycle.[84] The well-established accounts of production of and regulation by mtROS present OGDH as a probable participant in cysteine-mediated redox signaling and homeostasis of TCA cycle activity. Furthermore, our data demonstrates that C395 is highly sensitive to exogenous ROS (L:H ratio of 17.31) at levels consistent with known redox switch, C385 on ACO2 (L:H ratio of 13.26). Additionally, OGDH is a cysteine-rich protein with 21 cysteines total. We identify several other cysteines (C283 and C487) with sensitivities to peroxide treatment as well (Figure 2-26). However, C395 displayed the highest changes in the presence of ROS.

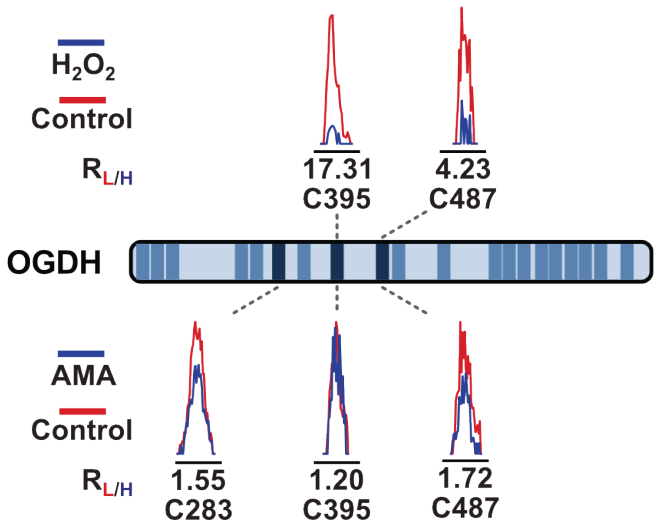


Figure 2-26. Illustration of OGDH protein with all cysteines in light blue and those identified by our MS studies in dark blue. Traces corresponding to chromatograms of cysteine-containing peptides are shown with red (IA-L) and blue (IA-H) labeling.

To evaluate C395 on OGDH as a thiol sensor, wild-type and cysteine mutant (C395S) were stably overexpressed with C-terminal FLAG tags in HEK 293T cells using lentiviral transduction. Lysates were subjected to peroxide treatments and analyzed for changes in OGDH multimeric complex formation including specifically interactions between other OGDH and isoform OGDHL, as well as subunits dihydrolipoyl succinyltransferase (DLST) and DLD. Thermal shift assay (CETSA) analysis revealed slight destabilization of wild-type OGDH but not the cysteine mutant (C395S) under peroxide treatments. Moreover, the OGDH C395S stability remains uniform in the presence of oxidants which may be due to the cysteine mutation protecting the protein from oxidative damage (Figure 2-27).

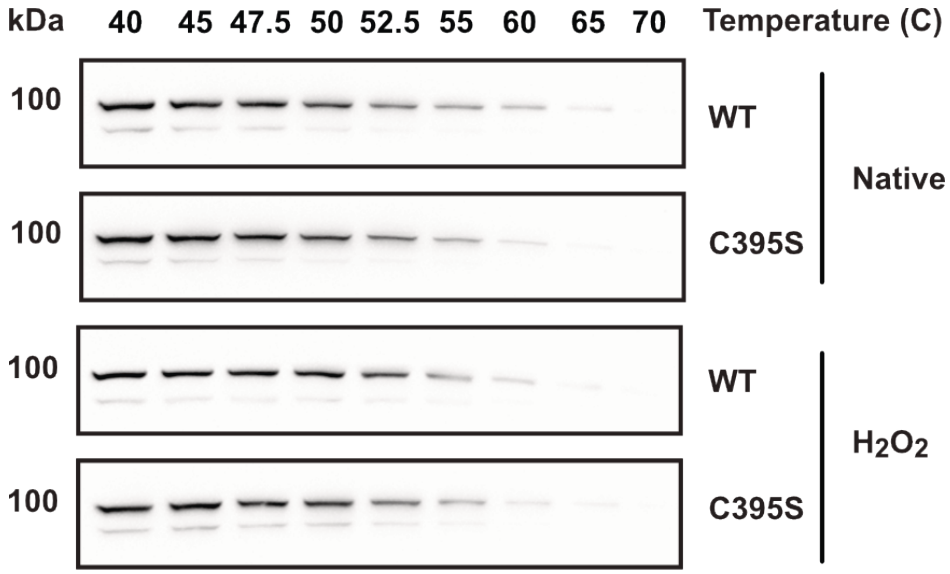


Figure 2-27. CETSA assay with HEK 293T lysates overexpressing wild-type (WT) OGDH and OGDHC395S stability in the presence or absence of 10 mM peroxide. Thermal degradation was performed at temperatures ranging from 40 to 70 C for 5 minutes before samples were spun down with precipitants removed. Western blotting was completed against FLAG tags on overexpressed proteins.

To further investigate complex stability, immunoprecipitation and western blotting were performed on lysates from cells overexpressing wild-type and C395S OGDH after incubation with or without peroxide. The required OGDH complex subunits were blotted for including OGDH, DLST, and DLD in addition to blotting against the incorporated FLAG epitope tag used to visualize of OGDH and ODGHC395S overexpression (Figure 2-28A). Notably, a slight decline in DLST association (30%) was observed in the peroxide treated of wild-type OGDH sample. This event was unique to oxidant treatments and not perceived with other

subunits or in the C395S mutant OGDH (Figure 2-28B). Interestingly, the brain isoform of OGDH (OGDHL) does not containing C395. Moreover, it is known that OGDH expression and activity in brain tissue is linked to neurodegenerative disorders.[85,86] Therefore, we hypothesize that the absence of this redox-sensitive cysteine (C395) on OGDHL may be an evolutionary protective mechanism against oxidative damage in the brain.[87,88]

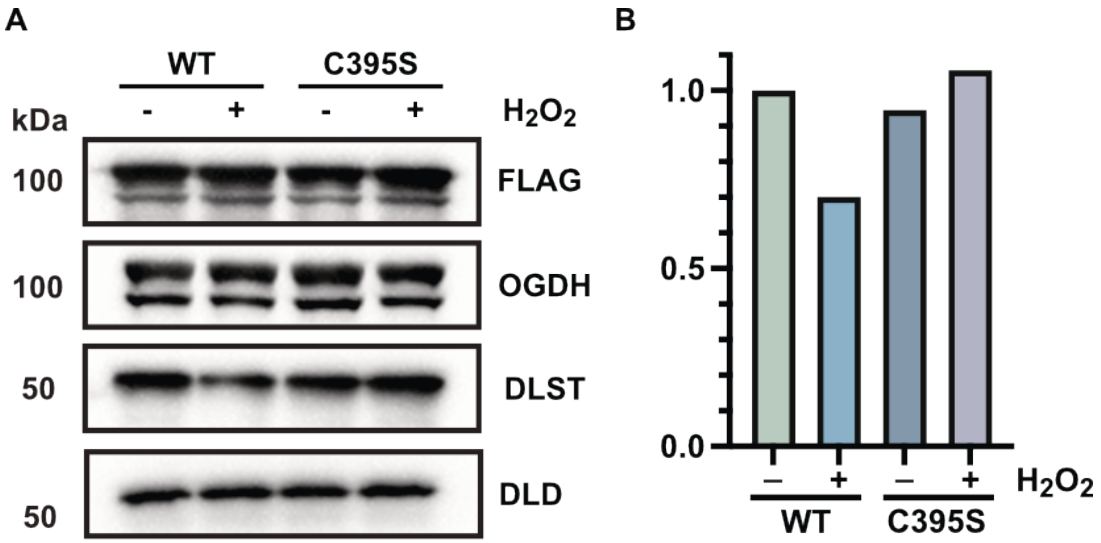


Figure 2-28. (A) Immunoprecipitation and western blot analysis of HEK 293T lysates overexpressing OGDH-FLAG and OGDHC395S-FLAG in the presence or absence of 10 mM peroxide. Blotting was conducted against DLST, DLD, native OGDH, and overexpressed OGDH (FLAG) presence. (B) Bar graph depicting DLST signal quantification normalized to FLAG signal from western blot in A.

In an effort to quantify the loss in OGDH complex association, immunoprecipitation coupled was coupled to MS analysis to analyze changes protein-protein interactors between wild-type and C395S OGDH. DLD and DLST

subunits were identified as having high spectral counts, however, no change between wild-type and C395S OGDH interactions were observed (Figure 2-29A, Figure 2-29B and Table 2A-10). Future work is needed to evaluate C395S as a potential thiol switch. The use of TMT multiplexing may be helpful in comparing the changes in protein-protein interactions in the presence or absence of peroxide in cells overexpressing wild-type and C395S OGDH by MS. Additionally, activity assays should also be considered to identify the role of C395 on OGDH activity. Furthermore, since several other cysteines (C283 and C487) were identified to be redox sensitive, there is potential for regulatory cysteine oxidation events to be dependent upon multiple cysteine modifications (Figure 2-30, Table 2A-10).

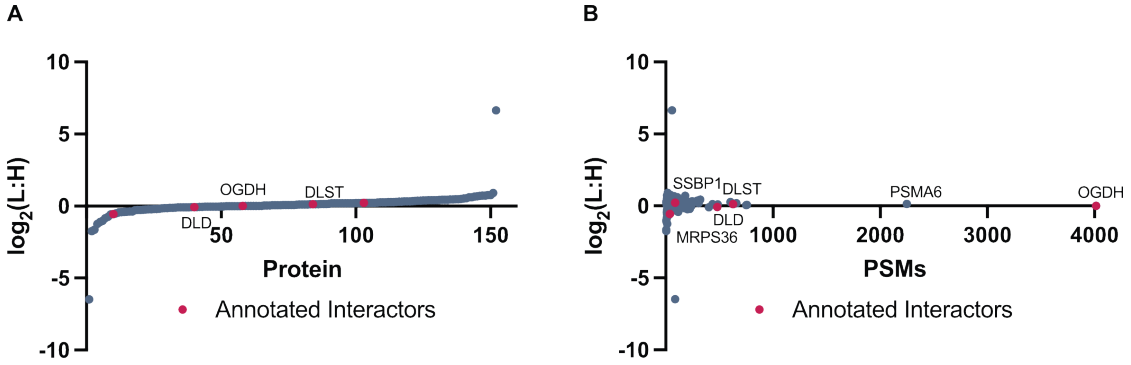


Figure 2-29. (A) Log_2 L:H ratio plot of immunoprecipitated proteins on anti-FLAG resin from lysates overexpressing OGDH-FLAG (light) and OGDHC395S-FLAG (heavy), n=3. (B) Average Log_2 L:H ratio from immunoprecipitation plotted against the average protein spectral matches (PSMs), n=9.

Conclusion

Mitochondria are intricate organelles central to a variety of cell functions including aerobic respiration to cell health determination. Many of these

mitochondrial processes are governed by redox signaling through oxidative cysteine modifications. As notorious signaling hubs, there is continued interest in deciphering functional sites of cysteine oxidation that may promote down-stream pathological events. Here, we propose the combination of chemoproteomic methods (IsoTOP-ABPP and OxICAT) and organelle isolation to generate a comprehensive map of redox-sensitive cysteines in the mitochondria. Together, global proteomic analysis to delineate mitochondrial cysteine oxidation events lead to evaluation of over 2000 cysteine residues in over 550 mitochondrial proteins using IsoTOP-ABPP and OxICAT technologies combined. Collectively, each complementary chemoproteomic platform offered an in-depth analysis mitochondrial cysteines redox sensitivity under basal and oxidative stress conditions. Although OxICAT investigates the most abundant cysteines in a sample, the ability to characterize reversible oxidation events in cellular states of elevated ROS is useful for identifying transient cysteine redox signaling networks. The chemoproteomic platforms proposed with isolated mitochondria combined with IsoTOP-ABPP and OxICAT methods should be considered for other applications such as evaluating cysteine oxidation in different disease models to expand the knowledge of pathology-specific cysteine-mediated redox signaling. Moreover, future investigation into highly redox-sensitive cysteines should be considered to evaluate the potential functions and impact of cysteine oxidation on protein and whole pathway regulation. Together, these findings set the groundwork for unraveling how mtROS-implicated pathologies harness oxidative stress mechanisms for progression. Additionally, the foundational understanding of cysteine-mediated redox signaling and identification of cysteine oxidation sites

are essential in the pursuit of ligand-able therapeutic targets which can have wide-reaching impact on the mtROS-mediated pathological landscape.

Experimental Procedures

Materials.

Chemicals were obtained from commercial sources, Sigma-Aldrich and Fisher Scientific, without further purification, unless otherwise noted. HEK 293T cells were obtained from ATCC (number). Phosphate buffered saline (PBS), DMEM, Trypsin EDTA, and Antibiotic-Antimycotic (Anti-Anti) were purchased from Fisher Scientific. Fetal bovine serum (FBS) was acquired from Biotechne. All protein concentrations were determined by the DC Protein Assay kid from Bio-Rad. IA-light and IA-heavy were synthesized in-house according to Abo, M. *et al.*[51] Diazo-biotin azide was purchased from Click Chemistry Tools. Anti-GAPDH (14C10), Anti-ATPIF1 (D6P1Q), Anti-Histone-H3 (D1H2), Anti-CALR (D3E6), Anti-DYKDDDK (FLAG) antibodies were purchased from Cell Signaling Technology.

Methods.

Mammalian cell culture.

HEK 293T cells were maintained at 37 °C under an atmosphere of 5% CO_2 in DMEM medium (Corning) supplemented with 10% FBS (Biotechne) and 1% Anti-Anti (25 μg/mL Amphotecerin B, 10, 000 units/mL penicillin, 10,000 μg/mL streptomycin, Gibco). Cells were harvested by scraping and pelleted 600g and

washed with PBS. To collect cell lysates, pellets were resuspended in PBS and lysed by ultrasonic tip sonicator (Cole Parmer). Soluble lysate fractions were obtained after separation by spinning at 45,000 rpm for 45 minutes at 4 °C and pelleted insoluble fractions were discarded. Protein concentrations were determined by DC Protein Assay kit (Bio-Rad).

Isolation of mitochondria.

HEK 293T pellets were washed 3 times with mitochondrial isolation buffer (10 mM Tris-MOPS, 1 mM EDTA/Tris, 200 mM Sucrose, pH 7.4, IBC). Following the general protocol of differential centrifugation and isopycnic separation by *Frezza, C. et al*.[30], crude mitochondria (Mito-C) were obtained. The HEK 293T cell pellet was resuspended in 10 times the volume of IBC and homogenized by a motor driven teflon homogenizer (Wheaton) at 1000 rpm with 30 strokes over the course of 15 min in a prechilled glass potter. After ever 10 strokes, the homogenate was briefly incubated on ice. The homogenate was centrifuged at 600 g for 10 min at 4 °C. The supernatant was collected and centrifugated twice more at 600 g for 10 min at 4 °C discarding the pellet after each spin. The supernatant was centrifuged further at 12,500g for 10 min at 4 °C. The supernatant was collected as the cytosolic fraction (Cyto). The pellet was washed in 2 times the volumes of IBC and pelleted at 12,500 g for 10 min at 4 °C. The pellet obtained at this point is considered crude mitochondria (Mito-C). To obtain pure mitochondria (Mito-P), further fractionation of Mito-C using a percoll density gradient made of 0.5 mL 80%, 1 mL 52%, and 1 mL 26% percoll with Mito-C layered on top in a 3 mL ultracentrifuge tube. The isotonic percoll solutions were prepared by 4 parts of 100% percoll (23% colloidal suspension) and 1 part 5X IBC to make 80% percoll

solutions. The 52% and 26% solutions were made generated by dilution of 80% percoll with 1X IBC. The gradient was centrifuged at 20,000 rpm for 45 min (Thermo Sorvall MX 120 ultracentrifuge). Mitochondria was removed from the interface of the 52% and 26% layers. The mitochondria was then diluted to 2 mL with IBC and centrifuged at 12,500g for 10 min at 4 °C The pellet was collected and washed in 2 additional steps in IBC affording pure mitochondria (Mito-p). For cysteine reactivity studies, the mito-p pellet was washed 3 additional times in DPBS and either labeled with cysteine alkylating reagents as whole mitochondria or lysed using an ultrasonic tip sonicator (Cole Parmer). Concentrations of isolated mito-p were determined through DC Protein Assay kit (Bio-Rad). For intact mitochondrial labeling, protein concentration was calculated, and mitochondrial samples were normalized to 1 mg/mL prior to alkylation.

Western blot detection of GAPDH, CALR, Histone H3 and ATPIF1.

25 μg of whole cell (WC), cytosolic (Cyto), crude mitochondrial (mito-c) and pure mitochondrial (mito-p) lysate fractions were separated on a 12.5% SDS-PAGE gel and transferred on to a nitrocellulose membrane at 75V for 100 min. Membranes were washed 3 times with TBST for 5 min and blocked for 1 hr at 25 °C in 5% Milk:TBSTBlocked membranes were washed 3 times with TBST and incubated with either rabbit anti-GAPDH (1:1000, TBST and 5% bovine serum albumin (BSA)), rabbit anti-Histone H3 (1:1000, TBST and 5% milk)), rabbit anti-CALR (1:1000, TBST and 5% milk)), rabbit anti-ATPIF1 (1:1000, TBST and 5% bovine serum albumin (BSA)) primary antibodies overnight at 4 °C. Membranes were then washed 3 times with TBST for 5 mins and incubated with secondary anti-Rabbit IgG HRP conjugate (1:2000) in TBST:Milk for 2 hr at 25 °C. Membranes

were washed 3 times with TBST and the blot was imaged by addition of ECL western blotting reagents.

Antimycin A HEK 293T Treatments.

Confluent HEK 293T cells were incubated with either 100 μM Antimycin A in DMSO or an equivalent volume of DMSO for a total of 1 hr at 37 °C. Cells were then washed 3 times with DPBS. Cells were harvested by scraping and pelleted by centrifugation at 600g for 5 min at 4 °C. Cells were washed further with IBC for mitochondrial isolation preparation described above.

MS sample preparation.

MS Sample Preparation: isoTOP-ABPP to study mitochondrial cysteine sensitivity

Cysteine reactivity studies were adapted from Weerapana, E. *et al*.[52], Bak, D. *et al*.[39] and Abo, M. *et al*.[51] Intact mito-p and lysates were alkylated with 100 μM IA-light or and 100 μM IA-light for 1 hr at 25 °C. A cleavable diazobenzene biotin-azide tag was appended to samples by CuAAC. 100 μM diazo biotin-azide (Click Chemistry Tools), 1 mM TCEP, 100 μM TBTA (17X stock in 4:1 t-BuOH:DMSO) and 1 mM copper (II) sulfate was added and the reaction was incubated for 1 hr at 25 °C. IA-heavy treated and IA-light control lysates were combined 1:1 and proteins were pelleted at 6,500g for 4 min at 4 °C. Protein were resuspended in 500 μL of cold methanol by tip sonication and centrifuged at 6,500g for 4 min. Proteins were washed for a second time with cold methanol and pelleted before being solubilized in 1.2% SDS/PBS solution by tip sonication and incubated for 5 min at 85 °C. SDS concentrations were diluted to 0.2% SDS by the addition of 5 mL DPBS

and samples were incubated with 100 μL streptavidin resin overnight at 4 °C and then a 2 hr 25 °C, rotating.

The resin and bound proteins were washed with 1- mL 0.2% SDS/DPBS for 10 mins followed by 3 quick washes with 5 mL DPBS and 3 quick washes with 5 mL water. Each wash was followed by centrifugation at 1400g for 3 mins to pellet the resin. Next, the resin was resuspended in 500 μL of 6 M urea/DPBS and incubated with 10 mM DTT at 65 °C for 20 min. After reduction, the resin incubated with 20 mM iodoacetamide for 30 min at 25 °C. The resin was diluted to 2 M urea and centrifuged at 1,400 g for 3 min before being resuspended in 200 μL of 2 M urea/DPBS, 1 mM $CaCl_2$, and 2 μg of sequencing grade trypsin (Promega) and incubated overnight at 37 °C.

The digested sample and resin were washed 3 times with 500 μL DPBS and 3 times with 500 μL water removing unbound peptides. Washed resin was resuspended in 50 μL of 50 mM sodium dithionite in PBS and rotated for 1hr at 25 °C. After centrifugation at 1,400 g for 3 min, the supernatant was collected, and the beads were incubated with twice more with 75 μL of 50 mM sodium dithionite for 1 hr at 25 °C with supernatant collected. The resin was washed two times with 75 μL water and the supernatant was collected and combined with the previously gathered fractions. To the sample (total volume 350 μL), 17.5 μL of formic acid was added and the samples were stored at -20 °C pending mass spectrometry analysis.

For cysteine reactivity studies comparing cysteine sensitivities with different hydrogen peroxide concentrations, 0.5 mg of isolated Mito-P lysates in 500 μL were pretreated with either 1 μL of 5 M, 2.5 M,1.25 M, 0.5 M H_2O_2 stocks (for 10 mM, 5 mM, 2.5 mM, 1 mM final H_2O_2 concentrations) or water on ice, in the dark for 20 minutes. H_2O_2 treated lysates were alkylated with 100 μM IA-heavy

and water controls were alkylated with 100 μM IA-light for 1 hr at 25 °C. Treated, IA-heavy and control, IA-light samples underwent CuAAC with diazo biotin-azide and were combined 1:1. Further enrichment and preparation was performed as described above.

For cysteine reactivity studies monitoring sensitivity by mtROS generated from electron transport chain inhibitor, Antimycin A, 0.5 mg of intact mito-p samples in 500 μL were alkylated either 100 μM IA-Light (control) or 100 μM IA-Heavy (treated) for 1 hr at 25 °C. Mitochondria were then lysed, CuAAC with diazo biotin-azide was performed, and samples were mixed 1:1. MS preparation then followed the aforementioned details.

MS Sample Preparation: OxICAT mass spectrometry and cysteine oxidation analysis

Direct cysteine oxidation monitoring in isolated mitochondria was adapted from protocols by Topf, U. *et al*.[43] and Abo, M. *et al*.[51] Isolated Mito-P (4 mg) from HEK 293T cells, treated with either 100 μM Antimycin A or DMSO, were resuspended in 500 μL denaturing alkylation buffer (DAB) (6 M urea, 200 mM Tris-HCl, 10 mM EDTA, 0.5 % SDS, pH 8.5) containing 10 mM IA-light and lysed using an ultrasonic tip sonicator. Cysteines were labeled for 2 hours at 37 °C shaking. After alkylation, insoluble debris was pelleted by centrifugation at 16,000 g for 1 min at 4 °C. Supernatants were diluted 3-fold with water and proteins were precipitated by 5 sample volumes of ice-cold acetone for 2 hr at -20 °C. After precipitation, proteins were pelleted through centrifugation at 4500 g for 30 min at 4 °C. Pellets were washed once with 500 μL ice-cold acetone and centrifuged at 4500 g for 10 min at 4 °C and allowed to air dry. Pellets were resolubilized in DAB and protein concentrations were determined using the DC Assay Kit. 200 μg of

protein was resuspended to a final volume of 80 μL for each replicate. 25 mM TCEP was added and the samples were incubated at 37 °C for 5 min. After initial incubation, samples were diluted with 120 μL DAB and 10 mM IA-Heavy and briefly sonicated to clarify. Labeling occurred over 2 hr at 37 °C. Following incubation, samples were diluted 3-fold with water and proteins were precipitated in 5 total volumes of ice-cold acetone overnight at -20 °C. After precipitation, proteins were pelleted by centrifugation 4500 g for 30 min at 4 °C, washed with ice-cold acetone and centrifuged in the same conditions for 10 min. Air-dried samples were resolubilized in 500 μL DPBS by ultrasonic tip sonicator.

A cleavable diazo-benzene biotin-azide was appended by conventional methods of CuAAC. 500 μM diazo biotin-azide, 5 mM TCEP, 500 μM TBTA (17X stock in 4:1 t-BuOH:DMSO) and 5 mM copper (II) sulfate was added and the reaction was incubated for 1 hr at 25 °C. Proteins were then pelleted through centrifugation at 6,500 g for 4 min at 4 °C. Sample pellets were resuspended in 500 μL of ice-cold methanol by tip sonication and centrifuged at 6500 g for 4 min at 4 °C. After a second time with methanol wash and centrifugation, protein pellets were resuspended in 1 mL of 1.2% SDS/DPBS by tip sonication and incubation at 85 °C for 5 min. With addition of 5 mL DPBS, SDS concentrations were lowered to 0.2% SDS and 100 μL streptavidin agarose resin was added. Samples rotated overnight at 4 °C and then SDS was resolubilized for 2 hr at 25 °C before resin being washed with 5mL of 0.2% SDS/DPBS, 3 times with 5 mL DPBS and 3 times with 5 mL water. After each wash, resin was pelleted by centrifugation at 1400g for 3 min. Following the washes, resin was resuspended in 500 μL 6 M urea/DPBS and incubated for 30 min at 25 °C. Resin were centrifuged for 3 min and

resuspended in 200 μL of 2M urea/DPBS, 1 mM $CaCl_2$, and 2 μg of sequencing-grade trypsin. Samples were digested overnight at 37 °C with shaking.

After on-bead trypsin digestion, resin and bound peptides were pelleted at 1400 g for 3 min and the supernatant containing unbound peptides was discarded. Following 3 washes with 500 μL DPBS and 3 washes with 500 μL water, resin was resuspended in 50 μL of 50 mM sodium dithionite in DPBS and rotated for 1hr at 25 °C. Resin was pelleted by centrifugation at 1400g for 3 min and the supernatant was collected. Supernatant was collected from two additional cleavages with 75 μL of 50 mM sodium dithionite for 1 hr each at 25 °C . The resin was then washed twice with 75 μL of water and supernatant was collected and combined with the rest of the sample for a total volume of 350 μL. 17.5 μL of formic acid was added and samples were stored at -20 °C for future mass spectrometry analysis.

MS proteomics.

Mass spectrometry data for cysteine reactivity and OxICAT studies were performed using a Thermo Fisher LTQ Orbitrap Discovery mass spectrometer coupled to an Agilent 1200 series HPLC. Using a high-pressure injection cell (Next Advance), labeled peptides were loaded onto 250 μm fused silica desalting column (Agilent) packed with 4 cm of Aqua C18 reverse phase resin (Phenomenex). Peptides were eluted on to a 100 μm fused silical biphasic column with a 5 μm tip, packed with 10 cm of C18 resin followed by 4 cm of Partisphere strong cation exchange resin (SCX, Whatman) by means of multidimensional LC/LC-MS/MS protocol (MudPIT)[52] of 5 runs with gradients from 0% to 100% Buffer B (20% water, 80% ACN, 0.1% formic acid) in Buffer A (95% water, 5% ACN, 0.1% formic acid). The flow rate of buffer through the column was 0.25 μL/min and the spray voltage

was 2.75 kV. One full MS scan (FTMS) was followed by 8 data dependent sans (ITMS) of the n^{th} most intense ions with dynamic exclusion enabled for each run.

MS proteomic analysis.

The tandem MS data was searched using the SEQUEST algorithm[89] against a concatenated target/decoy non-redundant variant of the human UniProt database. A static modification (+57.02146 m/z) on cysteine for the iodoacetamide alkylation was included in the search. SEQUEST output files were filtered by DTASelect 2.0[90] with applied -trypstat and -modstat options and peptides and a false discovery rate of 5%. Searched peptides were also required to be fully tryptic (-y 2) and have a found modification (-m 0), delta-CN score greater than 0.06 (-d 0.06), and a single peptide per locus (-p 1). Light to heavy (L:H) ratios were quantified using the cimage quantification package. Functional annotations of cysteines within each study's data set are described below. Datasets were evaluated against UniProtKB for residue specific information including function, conservation, position number using a Python program described in Bak, D. *et al.*[39]

MS data analysis: isoTOP-ABPP to study mitochondrial cysteine sensitivity to peroxide

In addition to static modifications on cysteine, MS data was searched for dynamic modifications for IA-light with the diazo biotin-azide cleaved adduct (306.14806 m/z) and IA-heavy with the diazo biotin-azide cleaved adduct (312.16819 m/z). Two replicates of each peroxide concentration (1, 2.5, 5, 10 mM H_2O_2). Average ratios were calculated for peptides with ratios present in both replicates and values exhibiting > 2-fold changes and coeffience of variance > 50% were removed. Data

was filtered by mitochondrial localization through comparison with Uniprot[49] and MitoCarta3.0[91] databases.

MS data analysis:: isoTOP-ABPP to study mitochondrial cysteine sensitivity to peroxide

For isoTOP-ABPP studies with samples from Antimycin A/DMSO treated cells, dymanic modifications of IA-light with the diazo biotin-azide cleaved adduct (306.14806 m/z) and IA-heavy with the diazo biotin-azide cleaved adduct (312.16819 m/z) were searched in addition to the static cysteine modification. L:H ratios were required to be in two out of 3 replicates. Average ratios were filtered >2 fold change were filtered by a coeffience of variance cut off of 50%. Peptides from only mitochondria-annotated proteins were included.

MS Data Analysis: OxICAT

For OxICAT samples, differential modifications of IA-light with the diazo biotin-azide cleaved adduct (306.14806 m/z) and IA-heavy with the diazo biotin-azide cleaved adduct (312.16819 m/z). L:H and H:L ratios were quantified from three replicates for each sample type (from DMSO control or Antimycin A treated cells). Data was filtered to include only mitochondrial proteins and peptides that appeared in two out of three replicates. L:H and H:L ratios were converted to % oxidation values by using the equations: 1-(L:H/(L:H+1)) or H:L/(H:L+1). Average % oxidation values were determined for each peptide and those with standard deviation of the mean >30% were removed. Statistically significant peptides that were present in both the DMSO and Antimycin A samples were included in the final data set.

Statistical analysis of overrepresented GO biological processes using PANTHER.

Protein ID lists from whole cell cysteine reactivity data from Weerapana, E. *et al.*[52] and mito-p cysteine reactivity data from 1 mM peroxide studies were analyzed by Panther 16.0 overrepresentation tests (http:/pantherdb.org)[92]. PANTHER determines an "expected" value for the number of protein IDs that are predicted to be in an input dataset for each functional category (GO biological process complete) based on the percentage of protein IDs for each category within the reference dataset (complete human genome). Overrepresentation is expressed as a ratio of the observed over the expected number of protein IDs is annotated for each biological process. A Fisher's exact test with a Bonferroni correction determined the statistical significance of overrepresentation of each biological process (P-value < 0.05).

Cloning.

Follow up protein gene pcDNA 3.1(+) with a C-terminal DYKDDDDK (FLAG) tag was purchased from Origene. Cysteine mutants were generated through site directed mutagenesis for the following NLRX1 (C331S), OGDH (C395S), RARS2, and MAVS (C283S). pcDNA3.1(+) PPA2 (gene) was purchased from Genscript. PPA2 was cloned into pET23a vector with a 6X HIS tag. Site-directed mutagenesis was used to generate PPA2 cysteine to serine mutants (C161S, C171S, and double mutant C161S/C171S).

PPA2 protein expression.

The PPA2 pET vectors with ampicillin (AMP) resistance were transformed into BL21DE3 cells and recombinantly expressed with 1 mM IPTG induction at 0.6 OD_{600} under 100 μg/mL AMP. BL21 cells were amplified for 16 hr at 27 C. Bacterial cell pellets were harvested, washed and lysed in phosphate free buffer (10X solution 30mM NaCl, 30mM Tris pH 7.4). PPA2 proteins were purified on nickel resin with washes at 10 mM imidazole and elutions in a gradient of 250 mM to 500 mM imidazole in phosphate free buffer (pH 7.4). Purified proteins were desalted using PD10 columns and stored at 4C for a maximum of 2 weeks. Bio-Rad DC protein concentration assay was used to determine the milligrams of protein recovered.

Inorganic ortho-phosphate activity assay with malachite green detection.

PPA2 activity was evaluated through monitoring the formation of ortho-phosphate (Pi) using a malachite green (MLG) assay adapted from Feng *et al.*[93] and Shatton *et al.*[78] and completed in 96 well plate. A concentration curve of Pi using anhydrous K_2HPO_4 was completed for concentrations 0, 1.56, 3.13, 6.25, 12.5, and 25 μM. All PPA2 peroxide pre-treatments and phosphatase reactions were incubated in eppendorf tubes with a total volume of 500 μL containing 50 μL of 25 nM PPA2, 10 μL of pyrophosphate decahydrate (PPi), 40 μL H_2O, and 400 μL of stock reaction buffer (0.05M in histidine and 5 mM Mg^{2+}, pH 7.2) at 25 °C. 25 nM PPA2 in each reaction with varying concentrations of pyrophosphate (PPi) added (0, 1, 5, 10, 25, 50, 100 nM PPi) for the PPA2 activity assays and 25 nM PPA2 and 50 nM PPi were used for the inhibition assays with H_2O_2 pre-treatments . After reaction was completed, 50uL aliquots were transferred to reaction buffer in 96

well plates and quenched with 5 μL of acidic buffer (2.4 M $HClO_4$) for 5 min and followed by (10 μL 50.0 mM ammonium molybdate in 3.4 M sulfuric acid) incubated for 10 min with subsequent addition of 15 μL malachite green buffer (1.0 mM MLG, 0.16% PVA, 6.0 mM sulfuric acid). Color was developed for 30 min, RT, dark and absorbance was monitored through plate reader at 660 nm against a PPi blank.

K_{cat} was calculated from linear regression analysis performed for each pre-PPi concentration and time point to determine the rates of the reactions (5 slopes, 5 different PPi concentrations). For each concentration, the Rate of Activity vs concentration was plotted. Non-linear fit michaelis menton kinetics gave K_{cat}, Km, and V_{max} values for both PPA2WT and PPA2C161S. The dose-response curve showing percent inhibition was calculated using a simple linear regression extracted from the activity vs time (slopes of each H_2O_2-pretreatment) extracted. The velocity ([Pi]/s) was normalized to the untreated sample giving a percentage of inhibition that was plotted.

Transient mammalian protein overexpression.

Transient transfections were conducted in HEK 293T cells at 90% confluency in 10 cm plates. To 180 μL of serum free DMEM, 8.8 μg of DNA and 45.76 μL of PEI Max (1mg/mL) were added and the solutions were incubated for 15 min. 40 μL of 500 mM sodium butyrate was added to 10 mL of complete DMEM media and DNA-PEI complex solutions were added dropwise to the plates. After 24 hr, media was removed and fresh DMEM complete was added to the cells. Cells were harvested and lysed after a total of 48 hr post-transfection.

Stable mammalian protein overexpression.

Stable expression of OGDHWT and OGDHC395S was completed using lentiviral transduction. Lentivirus was produced in HEK 293T cells, under passage 10, grown in DMEM and 10% heat inactivated fetal bovine serum (HIS) in 10 cm plates. At 80% confluency, cells were transfected with 2 μg vsv-g, 2 μg psPAX2, 2 μg respective pLenti plasmid and 24 μL of Lipofectamine 2000 (Invitrogen). After 24 hr, media was replaced by 5 mL DMEM with 10% HIS. At 48 hr, the media was collected and filtered through a 0.45 μm filter and mixed with 5 mL DMEM-HIS and 10 μg/mL polybrene. Virus was added to the target cell lines at 20% confluency and infected for 48 hr. Growth for 7 days in 2 μg/mL puromycin allowed for selection of stable protein overexpression in HEK 293T cells.

Immunoprecipitation.

Plates of transfected HEK 293T cells overexpressing follow up proteins were gently washed 3 times with cold DPBS followed by lysis with 1 mL Thermo Scientific Pierce lysis buffer (CN #8788) and 0.5 μL universal nuclease with plate rotations for 1 min followed by incubation on ice for 5 min. Lysates were transferred to Eppendorf tubes and membrane and unlysed fractions were pelleted by centrifugation at 16,000g for 20 min. While lysates were purified, 50 μL of Thermo Scientific Pierce Anti-DYKDDDDK magnetic agarose resin (CN# A36797) were equilibrated at RT and washed 3 times with lysis buffer. Purified lysates were added to the equilibrated magnetic resin and rotated at RT for 30 min. Flow through was removed and resin was washed gently twice with 500 μL DPBS followed by one wash of 500 μL water. Proteins were eluted in different ways depending on their final analysis. Samples undergoing peroxide treatments were

incubated with 10 mM H_2O_2 for 20 minutes before resin incubations were completed.

Western blot on immunoprecipitated OGDH samples.

After immunoprecipitation of anti-FLAG resin, resin was boiled for 5 min at 95C in 100 μL 2X protein loading buffer. Western blot was completed as described above with anti-FLAG antibody to visualize OGDH (WT and C395S)-FLAG expression and interactor DLST1, DLD, and OGDH pulldown. Panceau and anti-GAPDH antibody allowed for confirmation of protein normalization. Western blots confirming overexpressed proteins were completed using anti-FLAG antibodies.

CETSA assays.

HEK 293T lysates overexpressing OGDHWT and OGDHC395S were treated for 20 min in with 10 mM peroxide on ice in the dark. Thermal degradation was performed at temperatures ranging from 40 to 70 °C for 5 min. Samples were incubated on ice for 10 min and spun down with precipitating proteins removed. The soluble fractions were analyzed by western blotting using an anti-FLAG antibody to visualize OGDHWT and OGDHC395S expression.

ReDiMe MS analysis of immunoprecipitated proteins.

Immunoprecipitated proteins were removed from the anti-FLAG resin by resuspension in 30 μL of 8M urea in 100 mM triethylamine buffer (TEAB) and boiling at 95 C. Supernatant was removed and beads were washed twice more with 35 μL 100 mM ammonium bicarbonate (100 μL final sample volume). After

reduction with 1.5 μL of 1 M DTT at 65 °C for 15 min, thiol alkylation with 2.5 μL of 500 mM iodoacetamide was completed in the dark for 30 min. Samples were diluted with 120 μL 100 mM TEAB and vortexed rapidly. An overnight digestion using 4 μL of trypsin (0.5 μg/uL in 100 mM TEAB) and 2.5 μL of 100 mM $CaCl_2$ at 37 C with shaking afforded tryptic peptides. After 16 hr, standard reductive dimethylation (redime) procedure was completed in the dark. Peroxide treated or lysates of cysteine mutant follow-up proteins were labeled with 4 μL of 20% "heavy" formaldehyde ($DC_{13}DO$) while control or lysates overexpressing wild-type follow-up proteins were labeled with 4 μL of 20% "light" formaldehyde ($HC_{12}HO$). After formaldehyde addition, proteome samples were vortexed and 20 μL of 0.6 M light sodium cyanoborohydride or heavy sodium cyanoborodeuteride was added. Samples were vortexed and incubated for 2 hr without light exposure. Corresponding light and heavy samples were combined and desalted and analyzed by MudPIT.

Immunoprecipitation of FLAG-tagged proteins and ReDiMe MS preparation.

HEK 293T cells were transfected with 10 μg follow-up (WT or cysteine mutant) pcDNA, 52 μL polyethylene (PEI), and 2mM sodium butyrate in SF DMEM. After 48 hr, each plate of cells were lysed with Pierce IP lysis buffer for mammalian cells (Thermo Scientific) and 0.5 μL universal nuclease inhibitor. Following clarification at 16,000g for 30 min at 25 °C, sample was incubated on 50 μL Pierce anti-DYKDDDDK magnetic agarose resin (Thermo Scientific) pre-equilibrated with binding buffer. Resin was washed twice with 500 μL DPBS and once with 500 μL water. Washed resin was boiled at 95 °C in 30 μL of 8M Urea/100 mM TEAB and supernatant was collected. Resin was washed two additional times with 35 μL

TEAB and the supernatant was collected and combined with previous fractions. 1.5 μL of 1 M DTT was added and the samples incubated for 15 min at 65 °C. After reduction, 2.5 μL of 500 mM iodoacetamide was added and the samples were incubate for 30 min at 25 °C. Subsequent dilution of the sample with 120 μL of TEAB and 2.5 μL of 100mM $CaCl_2$ and 2 μg of sequence-grade modified trypsin was added. Samples were digested overnight at 37 °C with shaking.

Samples were dimethylated through reductive dimethylation (ReDiMe). Wild-type-enriched peptides were dimethylated with 'light' formaldehyde, (16 μL, 4%, CH_2O), and sodium cyanoborohydride, (16 μL, 0.6 M stock, $NaBH_3CN$), while mutant enriched peptides were dimethylated with 'heavy' formaldehyde, (16 μL, 4% stock, $^{13}CD_2O$), and sodium cyanoborodeuteride (16 μL, 0.6M stock, $NaBD_3CN$) for 2 hr at 25 °C. After the reactions were quenched with 4 μL 30% NH4OH for 10 min on ice, WT-enriched 'light' and corresponding mutant-enriched 'heavy' dimethylated peptides were combined 1:1. Formic acid was added to the sample (final concentration of 5%). Samples were desalted on Sep Pak 1 C18 columns (50 mg, Waters) and dried overnight by SpeedVac (ThermoFisher). Peptides were resuspended in 100 μL MS grade water and .1% formic acid and stored at -20 °C until mass spectrometry analysis.

MS data analysis: Immunoprecipitated ReDiMe labeled samples.

Samples were subjected to MS analysis as described above with static modifications of +28.0313 (light) and +34.06312 (heavy) methylation on lysine and N-terminal amines of the peptide in addition to the static IA modifications on cysteine (+57.02146 m/z). Similar searches to identify proteins was conducted using SEQUEST[89] and DTASelect2.0.[90] Files were filtered –trypstat for unique

proteins. Protein ratios were normalized by the ratios of the proteins used in the immunoprecipitation experiment (example OGDH in the OGDHWT and OGDHC395S immunoprecipitation samples). Final datasets included proteins identified in 2 out of 3 runs with standard deviation less than 20%.

References

(1) Lane, N.; Martin, W. The Energetics of Genome Complexity. *Nature* **2010**, *467* (7318), 929–934.

(2) Friedman, J. R.; Nunnari, J. Mitochondrial Form and Function. *Nature* **2014**, *505* (7483), 335–343.

(3) Spinelli, J. B.; Haigis, M. C. The Multifaceted Contributions of Mitochondria to Cellular Metabolism. *Nat. Cell. Biol.* **2018**, *20* (7), 745–754.

(4) Riemer, J.; Bulleid, N.; Herrmann, J. M. Disulfide Formation in the ER and Mitochondria: Two Solutions to a Common Process. *Science* **2009**.

(5) Hell, K. The Erv1–Mia40 Disulfide Relay System in the Intermembrane Space of Mitochondria. *Biochim. Biophys. Acta Mol. Cell Res.* **2008**, *1783* (4), 601–609.

(6) Redza-Dutordoir, M.; Averill-Bates, D. A. Activation of Apoptosis Signalling Pathways by Reactive Oxygen Species. *Biochim. Biophys. Acta Mol. Cell Res.* **2016**, *1863* (12), 2977–2992.

(7) Wang, C.; Youle, R. J. The Role of Mitochondria in Apoptosis. *Annu. Rev. Genet.* **2009**, *43*, 95–118.

(8) Lackner, L. L. The Expanding and Unexpected Functions of Mitochondria Contact Sites. *Trends Cell Biol.* **2019**, *29* (7), 580–590.

(9) Ott, M.; Gogvadze, V.; Orrenius, S.; Zhivotovsky, B. Mitochondria, Oxidative Stress and Cell Death. *Apoptosis* **2007**, *12* (5), 913–922.

(10) Paulsen, C. E.; Carroll, K. S. Cysteine-Mediated Redox Signaling: Chemistry, Biology, and Tools for Discovery. *Chem. Rev.* **2013**, *113* (7), 4633–4679.

(11) Bechtel, T. J.; Weerapana, E. From Structure to Redox: The Diverse Functional Roles of Disulfides and Implications in Disease. *Proteomics* **2017**, *17* (6), 10.1002/pmic.201600391.

(12) Morgan, M. J.; Liu, Z. Crosstalk of Reactive Oxygen Species and NF-KB Signaling. *Cell Res.* **2011**, *21* (1), 103–115.

(13) Canet-Avilés, R. M.; Wilson, M. A.; Miller, D. W.; Ahmad, R.; McLendon, C.; Bandyopadhyay, S.; Baptista, M. J.; Ringe, D.; Petsko, G. A.; Cookson, M. R. The Parkinson's Disease Protein DJ-1 Is Neuroprotective Due to Cysteine-Sulfinic Acid-Driven Mitochondrial Localization. *Proc. Natl. Acad. Sci.* **2004**, *101* (24), 9103–9108.

(14) Aiken, C. T.; Kaake, R. M.; Wang, X.; Huang, L. Oxidative Stress-Mediated Regulation of Proteasome Complexes. *Mol. Cell. Proteomics* **2011**, *10* (5), R110.006924.

(15) Sena, L. A.; Chandel, N. S. Physiological Roles of Mitochondrial Reactive Oxygen Species. *Mol. Cell* **2012**, *48* (2), 158–167.

(16) Groitl, B.; Jakob, U. Thiol-Based Redox Switches. *Biochim. Biophys. Acta Proteins Proteom.* **2014**, *1844* (8), 1335–1343.

(17) Cantu, D.; Schaack, J.; Patel, M. Oxidative Inactivation of Mitochondrial Aconitase Results in Iron and H2O2-Mediated Neurotoxicity in Rat Primary Mesencephalic Cultures. *PLoS ONE* **2009**, *4* (9), e7095.

(18) Lushchak, O. V.; Piroddi, M.; Galli, F.; Lushchak, V. I. Aconitase Post-Translational Modification as a Key in Linkage between Krebs Cycle, Iron Homeostasis, Redox Signaling, and Metabolism of Reactive Oxygen Species. *Redox Rep.* **2013**, *19* (1), 8–15.

(19) Chouchani, E. T.; Methner, C.; Nadtochiy, S. M.; Logan, A.; Pell, V. R.; Ding, S.; James, A. M.; Cochemé, H. M.; Reinhold, J.; Lilley, K. S.; Partridge, L.; Fearnley, I. M.; Robinson, A. J.; Hartley, R. C.; Smith, R. A. J.; Krieg, T.; Brookes, P. S.; Murphy, M. P. Cardioprotection by S-Nitrosation of a Cysteine Switch on Mitochondrial Complex I. *Nat. Med.* **2013**, *19* (6), 753–759.

(20) Burger, N.; James, A. M.; Mulvey, J. F.; Hoogewijs, K.; Ding, S.; Fearnley, I. M.; Loureiro-López, M.; Norman, A. A. I.; Arndt, S.; Mottahedin, A.; Sauchanka, O.; Hartley, R. C.; Krieg, T.; Murphy, M. P. ND3 Cys39 in Complex I Is Exposed during Mitochondrial Respiration. *Cell Chem. Biol.* **2021**.

(21) Chouchani, E. T.; Kazak, L.; Jedrychowski, M. P.; Lu, G. Z.; Erickson, B. K.; Szpyt, J.; Pierce, K. A.; Laznik-Bogoslavski, D.; Vetrivelan, R.; Clish, C. B.; Robinson, A. J.; Gygi, S. P.; Spiegelman, B. M. Mitochondrial ROS Regulate Thermogenic Energy Expenditure and Sulfenylation of UCP1. *Nature* **2016**, *532* (7597), 112–116.

(22) Ježek, P.; Jabůrek, M.; Porter, R. K. Uncoupling Mechanism and Redox Regulation of Mitochondrial Uncoupling Protein 1 (UCP1). *Biochim. Biophys. Acta - Bioenerg.* **2019**, *1860* (3), 259–269.

(23) Sullivan, L. B.; Chandel, N. S. Mitochondrial Reactive Oxygen Species and Cancer. *Cancer Meta.b* **2014**, *2* (1), 17.

(24) Chen, J.; Stimpson, S. E.; Fernandez-Bueno, G. A.; Mathews, C. E. Mitochondrial Reactive Oxygen Species and Type 1 Diabetes. *Antioxidants & Redox Signaling* **2018**, *29* (14), 1361–1372.

(25) Kaludercic, N.; Di Lisa, F. Mitochondrial ROS Formation in the Pathogenesis of Diabetic Cardiomyopathy. *Front. Cardiovasc. Med.* **2020**, *7*.

(26) Lin, M. T.; Beal, M. F. Mitochondrial Dysfunction and Oxidative Stress in Neurodegenerative Diseases. *Nature* **2006**, *443* (7113), 787–795.

(27) Moris, D.; Spartalis, M.; Spartalis, E.; Karachaliou, G.-S.; Karaolanis, G. I.; Tsourouflis, G.; Tsilimigras, D. I.; Tzatzaki, E.; Theocharis, S. The Role of Reactive Oxygen Species in the Pathophysiology of Cardiovascular Diseases and the Clinical Significance of Myocardial Redox. *Ann. Transl. Med.* **2017**, *5* (16), 326.

(28) Thul, P. J.; Åkesson, L.; Wiking, M.; Mahdessian, D.; Geladaki, A.; Ait Blal, H.; Alm, T.; Asplund, A.; Björk, L.; Breckels, L. M.; Bäckström, A.; Danielsson, F.; Fagerberg, L.; Fall, J.; Gatto, L.; Gnann, C.; Hober, S.; Hjelmare, M.; Johansson, F.; Lee, S.; Lindskog, C.; Mulder, J.; Mulvey, C. M.; Nilsson, P.; Oksvold, P.; Rockberg, J.; Schutten, R.; Schwenk, J. M.; Sivertsson, Å.; Sjöstedt, E.; Skogs, M.; Stadler, C.; Sullivan, D. P.; Tegel, H.; Winsnes, C.; Zhang, C.; Zwahlen, M.; Mardinoglu, A.; Pontén, F.; von Feilitzen, K.; Lilley, K. S.; Uhlén, M.; Lundberg, E. A Subcellular Map of the Human Proteome. *Science* **2017**, *356* (6340), eaal3321.

(29) *The Human Protein Atlas*. https://www.proteinatlas.org/ (accessed 2022-02-09).

(30) Frezza, C.; Cipolat, S.; Scorrano, L. Organelle Isolation: Functional Mitochondria from Mouse Liver, Muscle and Cultured Filroblasts. *Nat. Protoc.* **2007**, *2* (2), 287–295.

(31) Shi, Y.; Fu, L.; Yang, J.; Carroll, K. S. Wittig Reagents for Chemoselective Sulfenic Acid Ligation Enables Global Site Stoichiometry Analysis and Redox-Controlled Mitochondrial Targeting. *Nat. Chem.* **2021**, *13* (11), 1140–1150.

(32) Yasueda, Y.; Tamura, T.; Fujisawa, A.; Kuwata, K.; Tsukiji, S.; Kiyonaka, S.; Hamachi, I. A Set of Organelle-Localizable Reactive Molecules for Mitochondrial Chemical Proteomics in Living Cells and Brain Tissues. *J. Am. Chem. Soc.* **2016**, *138* (24), 7592–7602.

(33) Roux, K. J.; Kim, D. I.; Raida, M.; Burke, B. A Promiscuous Biotin Ligase Fusion Protein Identifies Proximal and Interacting Proteins in Mammalian Cells. *J. Cell Biol.* **2012**, *196* (6), 801–810.

(34) Branon, T. C.; Bosch, J. A.; Sanchez, A. D.; Udeshi, N. D.; Svinkina, T.; Carr, S. A.; Feldman, J. L.; Perrimon, N.; Ting, A. Y. Efficient Proximity Labeling in Living Cells and Organisms with TurboID. *Nat. Biotechnol.* **2018**, *36* (9), 880–887.

(35) Hung, V.; Udeshi, N. D.; Lam, S. S.; Loh, K. H.; Cox, K. J.; Pedram, K.; Carr, S. A.; Ting, A. Y. Spatially Resolved Proteomic Mapping in Living Cells with the Engineered Peroxidase APEX2. *Nat. Protoc.* **2016**, *11* (3), 456–475.

(36) Hung, V.; Zou, P.; Rhee, H.-W.; Udeshi, N. D.; Cracan, V.; Svinkina, T.; Carr, S. A.; Mootha, V. K.; Ting, A. Y. Proteomic Mapping of the Human Mitochondrial Intermembrane Space in Live Cells via Ratiometric APEX Tagging. *Mol. Cell* **2014**, *55* (2), 332–341.

(37) Rhee, H.-W.; Zou, P.; Udeshi, N. D.; Martell, J. D.; Mootha, V. K.; Carr, S. A.; Ting, A. Y. Proteomic Mapping of Mitochondria in Living Cells via Spatially Restricted Enzymatic Tagging. *Science* **2013**, *339* (6125), 1328–1331.

(38) Wang, H.; Zhang, Y.; Zeng, K.; Qiang, J.; Cao, Y.; Li, Y.; Fang, Y.; Zhang, Y.; Chen, Y. Selective Mitochondrial Protein Labeling Enabled by Biocompatible Photocatalytic Reactions inside Live Cells. *JACS Au* **2021**, *1* (7), 1066–1075.

(39) Bak, D. W.; Pizzagalli, M. D.; Weerapana, E. Identifying Functional Cysteine Residues in the Mitochondria. *ACS Chem. Biol.* **2017**, *12* (4), 947–957.

(40) Leichert, L. I.; Gehrke, F.; Gudiseva, H. V.; Blackwell, T.; Ilbert, M.; Walker, A. K.; Strahler, J. R.; Andrews, P. C.; Jakob, U. Quantifying Changes in the Thiol Redox Proteome upon Oxidative Stress in Vivo. *Proc. Natl. Acad. Sci.* **2008**, *105* (24), 8197–8202.

(41) van der Reest, J.; Lilla, S.; Zheng, L.; Zanivan, S.; Gottlieb, E. Proteome-Wide Analysis of Cysteine Oxidation Reveals Metabolic Sensitivity to Redox Stress. *Nat. Commun.* **2018**, *9* (1), 1581.

(42) Bechtel, T. J.; Li, C.; Kisty, E. A.; Maurais, A. J.; Weerapana, E. Profiling Cysteine Reactivity and Oxidation in the Endoplasmic Reticulum. *ACS Chem. Biol.* **2020**, *15* (2), 543–553.

(43) Topf, U.; Suppanz, I.; Samluk, L.; Wrobel, L.; Böser, A.; Sakowska, P.; Knapp, B.; Pietrzyk, M. K.; Chacinska, A.; Warscheid, B. Quantitative Proteomics Identifies Redox Switches for Global Translation Modulation by Mitochondrially Produced Reactive Oxygen Species. *Nat. Commun.* **2018**, *9* (1), 324.

(44) Menger, K. E.; James, A. M.; Cochemé, H. M.; Harbour, M. E.; Chouchani, E. T.; Ding, S.; Fearnley, I. M.; Partridge, L.; Murphy, M. P. Fasting, but Not Aging, Dramatically Alters the Redox Status of Cysteine Residues on Proteins in Drosophila Melanogaster. *Cell Rep.* **2015**, *11* (12), 1856–1865.

(45) Alcock, L. J.; Oliveira, B. L.; Deery, M. J.; Pukala, T. L.; Perkins, M. V.; Bernardes, G. J. L.; Chalker, J. M. Norbornene Probes for the Detection of Cysteine Sulfenic Acid in Cells. *ACS Chem. Biol.* **2019**, *14* (4), 594–598.

(46) Akter, S.; Fu, L.; Jung, Y.; Conte, M. L.; Lawson, J. R.; Lowther, W. T.; Sun, R.; Liu, K.; Yang, J.; Carroll, K. S. Chemical Proteomics Reveals New Targets of Cysteine Sulfinic Acid Reductase. *Nat. Chem. Biol.* **2018**, *14* (11), 995–1004.

(47) Meng, J.; Fu, L.; Liu, K.; Tian, C.; Wu, Z.; Jung, Y.; Ferreira, R. B.; Carroll, K. S.; Blackwell, T. K.; Yang, J. Global Profiling of Distinct Cysteine Redox Forms Reveals Wide-Ranging Redox Regulation in C. Elegans. *Nat. Commun.* **2021**, *12* (1), 1415.

(48) Paulsen, C. E.; Carroll, K. S. Chemical Dissection of an Essential Redox Switch in Yeast. *Chem. Biol.* **2009**, *16* (2), 217–225.

(49) The UniProt Consortium. UniProt: The Universal Protein Knowledgebase in 2021. *Nucleic Acids Res.* **2021**, *49* (D1), D480–D489.

(50) Calvo, S. E.; Clauser, K. R.; Mootha, V. K. MitoCarta2.0: An Updated Inventory of Mammalian Mitochondrial Proteins. *Nucleic Acids Re.s* **2016**, *44* (Database issue), D1251–D1257.

(51) Abo, M.; Li, C.; Weerapana, E. Isotopically-Labeled Iodoacetamide-Alkyne Probes for Quantitative Cysteine-Reactivity Profiling. *Mol. Pharm.* **2017**, *15* (3), 743–749.

(52) Weerapana, E.; Wang, C.; Simon, G. M.; Richter, F.; Khare, S.; Dillon, M. B. D.; Bachovchin, D. A.; Mowen, K.; Baker, D.; Cravatt, B. F. Quantitative Reactivity Profiling Predicts Functional Cysteines in Proteomes. *Nature* **2010**, *468* (7325), 790–795.

(53) Filadi, R.; Pendin, D.; Pizzo, P. Mitofusin 2: From Functions to Disease. *Cell Death Dis.* **2018**, *9* (3), 1–13.

(54) Thaher, O.; Wolf, C.; Dey, P. N.; Pouya, A.; Wüllner, V.; Tenzer, S.; Methner, A. The Thiol Switch C684 in Mitofusin-2 Mediates Redox-Induced Alterations of Mitochondrial Shape and Respiration. *Neurochem. Int.* **2018**, *117*, 167–173.

(55) Wolf, C.; López del Amo, V.; Arndt, S.; Bueno, D.; Tenzer, S.; Hanschmann, E.-M.; Berndt, C.; Methner, A. Redox Modifications of Proteins of the Mitochondrial Fusion and Fission Machinery. *Cells* **2020**, *9* (4), 815.

(56) Lushchak, O. V.; Piroddi, M.; Galli, F.; Lushchak, V. I. Aconitase Post-Translational Modification as a Key in Linkage between Krebs Cycle, Iron Homeostasis, Redox Signaling, and Metabolism of Reactive Oxygen Species. *Redox Rep.* **2014**, *19* (1), 8–15.

(57) McLain, A. L.; Szweda, P. A.; Szweda, L. I. Alpha-Ketoglutarate Dehydrogenase: A Mitochondrial Redox Sensor. *Free Radical Res* **2011**, *45* (1), 29–36.

(58) Mailloux, R. J.; Craig Ayre, D.; Christian, S. L. Induction of Mitochondrial Reactive Oxygen Species Production by GSH Mediated S-Glutathionylation of 2-Oxoglutarate Dehydrogenase. *Redox Biol.* **2016**, *8*, 285–297.

(59) Murray, C. I.; Kane, L. A.; Uhrigshardt, H.; Wang, S.-B.; Van Eyk, J. E. Site-Mapping of In Vitro S-Nitrosation in Cardiac Mitochondria: Implications for Cardioprotection. *Mol. Cell Proteomics* **2011**, *10* (3), M110.004721.

(60) Konovalova, S.; Liu, X.; Manjunath, P.; Baral, S.; Neupane, N.; Hilander, T.; Yang, Y.; Balboa, D.; Terzioglu, M.; Euro, L.; Varjosalo, M.; Tyynismaa, H. Redox Regulation of GRPEL2 Nucleotide Exchange Factor for Mitochondrial HSP70 Chaperone. *Redox Biol.* **2018**, *19*, 37–45.

(61) Tang, C.; Li, Y.; Chou, C.; Huang, L.; Huang, S.; Hueng, D.; Tsai, C.; Chen, Y. GRPEL2 Knockdown Exerts Redox Regulation in Glioblastoma. *Int. J. Mol. Sci*. **2021**, 22(23), 12705

(62) Mclain, A. L.; Szweda, P. A.; Szweda, L. I. α-Ketoglutarate Dehydrogenase: A Mitochondrial Redox Sensor. *Free Radic Re.s* **2011**, *45* (1), 29–36.

(63) Xiao, H.; Jedrychowski, M. P.; Schweppe, D. K.; Huttlin, E. L.; Yu, Q.; Heppner, D. E.; Li, J.; Long, J.; Mills, E. L.; Szpyt, J.; He, Z.; Du, G.; Garrity, R.; Reddy, A.; Vaites, L. P.; Paulo, J. A.; Zhang, T.; Gray, N. S.; Gygi, S. P.; Chouchani, E. T. A Quantitative Tissue-Specific Landscape of Protein Redox Regulation during Aging. *Cell* **2020**, *180* (5), 968-983.e24.

(64) Bak, D. W.; Weerapana, E. Cysteine-Mediated Redox Signalling in the Mitochondria. *Mol. BioSyst.* **2015**, *11* (3), 678–697.

(65) Quinlan, C. L.; Gerencser, A. A.; Treberg, J. R.; Brand, M. D. The Mechanism of Superoxide Production by the Antimycin-Inhibited Mitochondrial Q-Cycle. *J. Biol. Chem.* **2011**, *286* (36), 31361–31372.

(66) De Silva, D.; Tu, Y.-T.; Amunts, A.; Fontanesi, F.; Barrientos, A. Mitochondrial Ribosome Assembly in Health and Disease. *Cell Cycle* **2015**, *14* (14), 2226–2250.

(67) Bonn, F.; Tatsuta, T.; Petrungaro, C.; Riemer, J.; Langer, T. Presequence-Dependent Folding Ensures MrpL32 Processing by the m-AAA Protease in Mitochondria. *EMBO J* **2011**, *30* (13), 2545–2556.

(68) Yu, M. J.; Zhao, N.; Shen, H.; Wang, H. Long Noncoding RNA MRPL39 Inhibits Gastric Cancer Proliferation and Progression by Directly Targeting MiR-130. *Genet. Test Mol. Biomarkers* **2018**, *22* (11), 656–663.

(69) Nagai-Singer, M. A.; Morrison, H. A.; Allen, I. C. NLRX1 Is a Multifaceted and Enigmatic Regulator of Immune System Function. *Front. Immun.* **2019**, *10*.

(70) Buskiewicz, I. A.; Montgomery, T.; Yasewicz, E. C.; Huber, S. A.; Murphy, M. P.; Hartley, R. C.; Kelly, R.; Crow, M. K.; Perl, A.; Budd, R. C.; Koenig, A. Reactive Oxygen Species Induce Virus-Independent MAVS Oligomerization in Systemic Lupus Erythematosus. *Sci. Signal.* **2016**, *9* (456), ra115.

(71) De Simoni, S.; Linard, D.; Hermans, E.; Knoops, B.; Goemaere, J. Mitochondrial Peroxiredoxin-5 as Potential Modulator of Mitochondria-ER Crosstalk in MPP+-Induced Cell Death. *J. Neurochem.* **2013**, *125* (3), 473–485.

(72) Seo, M. S.; Kang, S. W.; Kim, K.; Baines, I. C.; Lee, T. H.; Rhee, S. G. Identification of a New Type of Mammalian Peroxiredoxin That Forms an Intramolecular Disulfide as a Reaction Intermediate. *J. Biol. Chem.* **2000**, *275* (27), 20346–20354.

(73) Smeets, A.; Marchand, C.; Linard, D.; Knoops, B.; Declercq, J.-P. The Crystal Structures of Oxidized Forms of Human Peroxiredoxin 5 with an Intramolecular Disulfide Bond Confirm the Proposed Enzymatic Mechanism for Atypical 2-Cys Peroxiredoxins. *Arch. Biochem. Biophys.* **2008**, *477* (1), 98–104.

(74) Szklarczyk, R.; Wanschers, B. F. J.; Nabuurs, S. B.; Nouws, J.; Nijtmans, L. G.; Huynen, M. A. NDUFB7 and NDUFA8 Are Located at the Intermembrane Surface of Complex I. *FEBS Lett.* **2011**, *585* (5), 737–743.

(75) Fischer, M.; Horn, S.; Belkacemi, A.; Kojer, K.; Petrungaro, C.; Habich, M.; Ali, M.; Küttner, V.; Bien, M.; Kauff, F.; Dengjel, J.; Herrmann, J. M.; Riemer, J. Protein Import and Oxidative Folding in the Mitochondrial Intermembrane Space of Intact Mammalian Cells. *Mol. Biol. Cell* **2013**, *24* (14), 2160–2170.

(76) Meston, D.; Bi, W.; Rietschel, T.; van Ham, M.; Leichert, L. I.; Jänsch, L. Identification of MtROS-Sensitive Processes in Activated CD4 T Cells. *Biorxiv* **2020**.

(77) Kennedy, H.; Haack, T. B.; Hartill, V.; Mataković, L.; Baumgartner, E. R.; Potter, H.; Mackay, R.; Alston, C. L.; O'Sullivan, S.; McFarland, R.; Connolly, G.; Gannon, C.; King, R.; Mead, S.; Crozier, I.; Chan, W.; Florkowski, C. M.; Sage, M.; Höfken, T.; Alhaddad, B.; Kremer, L. S.; Kopajtich, R.; Feichtinger, R. G.; Sperl, W.; Rodenburg, R. J.; Minet, J. C.; Dobbie, A.; Strom, T. M.; Meitinger, T.; George, P. M.; Johnson, C. A.; Taylor, R. W.; Prokisch, H.; Doudney, K.; Mayr, J. A. Sudden Cardiac Death Due to Deficiency of the Mitochondrial Inorganic Pyrophosphatase PPA2. *Am. J. Hum. Genet.* **2016**, *99* (3), 674–682.

(78) Shatton, J. B.; Shah, H.; Williams, A.; Morris, H. P.; Weinhouse, S. Activities and Properties of Inorganic Pyrophosphate in Normal Tissues and Hepatic Tumors of the Rat. *Cancer Res.* **1981**, *41* (5), 1866–1872.

(79) Avaeva, S.; Ignatov, P.; Kurilova, S.; Nazarova, T.; Rodina, E.; Vorobyeva, N.; Oganessyan, V.; Harutyunyan, E. Escherichia Coli Inorganic

Pyrophosphatase : Site-Directed Mutagenesis of the Metal Binding Sites. *FEBS Letters* **1996**, *399* (1–2), 99–102.

(80) Owen A. Moe; Butler, L. G. Yeast Inorganic Pyrophosphatase. *J. Biol. Chem.* **1972**, *247* (22), 7315–7319.

(81) Hu, J.; Dong, L.; Outten, C. E. The Redox Environment in the Mitochondrial Intermembrane Space Is Maintained Separately from the Cytosol and Matrix. *J. Biol. Chem.* **2008**, *283* (43), 29126–29134.

(82) Moore, C. B.; Bergstralh, D. T.; Duncan, J. A.; Lei, Y.; Morrison, T. E.; Zimmermann, A. G.; Accavitti-Loper, M. A.; Madden, V. J.; Sun, L.; Ye, Z.; Lich, J. D.; Heise, M. T.; Chen, Z.; Ting, J. P.-Y. NLRX1 Is a Regulator of Mitochondrial Antiviral Immunity. *Nature* **2008**, *451* (7178), 573–577.

(83) Qin, Y.; Xue, B.; Liu, C.; Wang, X.; Tian, R.; Xie, Q.; Guo, M.; Li, G.; Yang, D.; Zhu, H. NLRX1 Mediates MAVS Degradation To Attenuate the Hepatitis C Virus-Induced Innate Immune Response through PCBP2. *J. Virol.* **2017**, *91* (23), e01264-17.

(84) Tretter, L.; Adam-Vizi, V. Inhibition of Krebs Cycle Enzymes by Hydrogen Peroxide: A Key Role of Alpha-Ketoglutarate Dehydrogenase in Limiting NADH Production under Oxidative Stress. *J. Neurosci.* **2000**, *20* (24), 8972–8979.

(85) Chen, H.; Denton, T. T.; Xu, H.; Calingasan, N.; Beal, M. F.; Gibson, G. E. Reductions in the Mitochondrial Enzyme α-Ketoglutarate Dehydrogenase Complex in Neurodegenerative Disease - Beneficial or Detrimental? *J. Neurochem.* **2016**, *139* (5), 823–838.

(86) Artiukhov, A. V.; Graf, A. V.; Kazantsev, A. V.; Boyko, A. I.; Aleshin, V. A.; Ksenofontov, A. L.; Bunik, V. I. Increasing Inhibition of the Rat Brain 2-Oxoglutarate Dehydrogenase Decreases Glutathione Redox State, Elevating Anxiety and Perturbing Stress Adaptation. *Pharmaceuticals* **2022**, *15* (2), 182.

(87) Bunik, V.; Kaehne, T.; Degtyarev, D.; Shcherbakova, T.; Reiser, G. Novel Isoenzyme of 2-Oxoglutarate Dehydrogenase Is Identified in Brain, but Not in Heart. *FEBS J.* **2008**, *275* (20), 4990–5006.

(88) Yoon, W. H.; Sandoval, H.; Nagarkar-Jaiswal, S.; Jaiswal, M.; Yamamoto, S.; Haelterman, N. A.; Putluri, N.; Putluri, V.; Sreekumar, A.; Tos, T.; Aksoy, A.; Donti, T.; Graham, B. H.; Ohno, M.; Nishi, E.; Hunter, J.; Muzny, D. M.; Carmichael, J.; Shen, J.; Arboleda, V. A.; Nelson, S. F.; Wangler, M. F.; Karaca, E.; Lupski, J. R.; Bellen, H. J. Loss of Nardilysin, a Mitochondrial Co-Chaperone for α-Ketoglutarate Dehydrogenase, Promotes MTORC1 Activation and Neurodegeneration. *Neuro.n* **2017**, *93* (1), 115–131.

(89) Eng, J. K.; McCormack, A. L.; Yates, J. R. An Approach to Correlate Tandem Mass Spectral Data of Peptides with Amino Acid Sequences in a Protein Database. *J. Am. Soc. Mass. Spectrom.* **1994**, *5* (11), 976–989.

(90) Tabb, D. L.; McDonald, W. H.; Yates, J. R. DTASelect and Contrast: Tools for Assembling and Comparing Protein Identifications from Shotgun Proteomics. *J. Proteome Re.s* **2002**, *1* (1), 21–26.

(91) Rath, S.; Sharma, R.; Gupta, R.; Ast, T.; Chan, C.; Durham, T. J.; Goodman, R. P.; Grabarek, Z.; Haas, M. E.; Hung, W. H. W.; Joshi, P. R.; Jourdain, A. A.; Kim, S. H.; Kotrys, A. V.; Lam, S. S.; McCoy, J. G.; Meisel, J. D.; Miranda, M.; Panda, A.; Patgiri, A.; Rogers, R.; Sadre, S.; Shah, H.; Skinner, O. S.; To, T.-L.; Walker, M. A.; Wang, H.; Ward, P. S.; Wengrod, J.; Yuan, C.-C.; Calvo, S.

E.; Mootha, V. K. MitoCarta3.0: An Updated Mitochondrial Proteome Now with Sub-Organelle Localization and Pathway Annotations. *Nucleic Acids Res.* **2021**, *49* (D1), D1541–D1547.

(92) Mi, H.; Ebert, D.; Muruganujan, A.; Mills, C.; Albou, L.-P.; Mushayamaha, T.; Thomas, P. D. PANTHER Version 16: A Revised Family Classification, Tree-Based Classification Tool, Enhancer Regions and Extensive API. *Nucleic Acids Res.* **2021**, *49* (D1), D394–D403.

(93) Feng, J.; Chen, Y.; Pu, J.; Yang, X.; Zhang, C.; Zhu, S.; Zhao, Y.; Yuan, Y.; Yuan, H.; Liao, F. An Improved Malachite Green Assay of Phosphate: Mechanism and Application. *Anal. Biochem.* **2011**, *409* (1), 144–149.

Chapter 3

Combining Redox Proteomics and Proximity Labeling with TurboID to Monitor Localized Cysteine Oxidation

Introduction

Reactive oxygen species (ROS), such as hydrogen peroxide and hydroxyl radicals, are critical sub-cellular messengers that regulate cell homeostasis, differentiation, and death.[1-6] Dysregulation of cellular ROS levels contribute to numerous pathologies such as inflammation, cancer, neurodegeneration, type-II diabetes, and cardiovascular disease.[7-12] The mechanisms by which ROS impact cellular function are multifaceted, but ROS-induced protein oxidation is an immediate and direct result of elevated ROS levels. Protein oxidation primarily occurs on cysteine residues, resulting in the generation of both reversible and irreversible cysteine oxidative posttranslational modifications. Notably, due to the high reactivity of ROS and the concentration of antioxidants throughout the cell, ROS have limited diffusion from the site of production. Therefore, characteristic differences in redox environments and cysteine oxidation levels are sustained in unique subcellular compartments.

Mitochondria are organelles with multiple sub-compartments, including the matrix and intermembrane space (IMS). Since these compartments are separated by an impermeable membrane, the matrix and IMS maintain unique proteomic and redox environments. Specifically, the IMS is a significantly more oxidizing environment (-255 mV or 250:1 GSH:GSSG) compared to the thiol-rich matrix (-296 mV or 900:1 GSH:GSSG).[13] It is therefore important to determine the sites and varying degrees of oxidation on proteins localized within these separate mitochondrial sub-compartments. The majority of mitochondrial ROS is generated in the electron transport chain (ETC). Specifically, the flavin-cofactor binding and terminal electron-transfer sites of complex I and quinone-exchanging sites of complex III routinely leak electrons leading to localized ROS production.[14-

[16] It is therefore important to determine the sites and varying degrees of oxidation on proteins localized within these separate mitochondrial sub-compartments. Identifying cysteine oxidation events within specific subcellular compartments is key to understanding the localized and divergent effects of cellular ROS.

Numerous chemical tools and proteomic technologies exist to identify sites of cysteine oxidation and have been critical to furthering our understanding of the role of ROS-mediated cellular signaling. For example, specific cysteine oxoforms, such as sulfenic[17,18] and sulfinic acid[19,20], can be directly monitored using chemical probes that selectively react with these chemotypes. Additionally, reversible cysteine oxidation events can be more generally interrogated using differential labeling techniques, such as oxidative isotope-coded affinity tags (OxICAT).[21] Briefly, a typical OxICAT workflow begins by tagging all reduced thiols in a sample with an isotopically 'light' variant of a cysteine capping agent, such as N-ethyl maleimide (NEM). Reversibly oxidized cysteines are then reduced and subsequently capped with an isotopically "heavy" variant. Quantitative mass-spectrometry analysis affords light:heavy ratios that represent the oxidation percentage for all identified cysteine-containing peptides. These and other workflows have been broadly applied to identify sites of cysteine oxidation in numerous cell and tissue samples.[22-27] However, the coverage of low-abundant proteins in subcellular compartments, such as the mitochondria, have been limited due to the presence of highly abundant cysteine-containing cytosolic proteins that suppress low-abundant signals during MS analysis.

To provide deeper coverage of mitochondrial proteins, differential centrifugation methods can be used to fractionate and isolate mitochondria prior to implementing OxICAT-type workflows. For example, cysteine oxidation in

yeast mitochondria was monitored under basal and oxidative stress conditions using mitochondrial fractionation and OxICAT, resulting in the discovery that the function of components of the translational machinery is attenuated by ROS.[28] Additionally, mitochondrial fractionation and cysteine-reactivity profiling upon treatment with nitrosative stress identified several cysteine targets of nitrosation, including members of the outer mitochondrial membrane localized VDAC family.[29] However, differential centrifugation for mitochondrial isolation is time and labor intensive, and contamination from co-eluting organelles such as the endoplasmic reticulum (ER) is common. As an alternative to mitochondrial fractionation, cysteine-targeted chemical probes can be specifically localized to the mitochondria using positively charged triphenylphosphine (TPP) and rhodamine groups. For example, a TPP-based sulfenic-acid probe was applied to identify mitochondrial cysteines sensitive to sulfenylation upon treatment with exogenous ROS.[30] Additionally, a rhodamine-based chloroacetamide probe was used to monitor cysteine-reactivity changes of 290 cysteines on 196 mitochondrial-annotated proteins after paraquat-initiated ROS generation.[31] These mitochondria-specific redox-proteomic analyses have deepened our understanding of targets of ROS within the mitochondria. However, opportunities remain to probe deeper into mitochondrial cysteine oxidation by further localizing our redox proteomic analysis to specific mitochondrial compartments and ROS hotspots.

Proximity labeling (PL) methods led by promiscuous enzymes (APEX[32] and BioID[33]) and small-molecule catalysts[34,35] have become powerful strategies in accessing defined regions of the cell, with notable temporal and spatial resolution, including mitochondrial sub-compartments.[36,37] PL allows for the generation of reactive tags that typically biotinylate proximal protein residues. PL methods

allow for innovative, alternative strategies to investigate protein-protein interactions. Traditionally, protein-protein interaction assessments were conducted using classical methods of co-immunoprecipitation (co-IP). The co-IP strategy not only requires cell lysis that can disrupt transient protein-protein contacts but also relies upon highly specific antibodies for protein enrichments. To that end, differential centrifugation was previously considered the sole method for organelle proteomic isolation. However, the time-intensive multiple fractionation steps are often prone to contamination by the cytosol and similarly dense organelles. To overcome these challenges, the use of an *E. coli* biotin ligase (BirA) discovered by Roux, *et al*. enabled the first-generation enzymatic proximity labeling with a single amino acid mutation R118G of the ligase active site (BirA* or BioID) enabling promiscuous biotin-tagging of the subcellar proteome in live cells.[33] BioID can be directed to a subcellular region through conjugation with a protein of known localization. Upon incubation with biotin, the ligase converts biotin to an activated form, biotinyl-AMP, resulting in biotin labeling of lysine residues on proteins proximal to BioID (Figure 3-1). Subsequent affinity purification of biotinylated proteins on streptavidin resin allows for capturing of labeled proteins and identification through MS analysis or western blotting furthering a clever, streamlined approach for protein-interaction and subcellular enrichment.

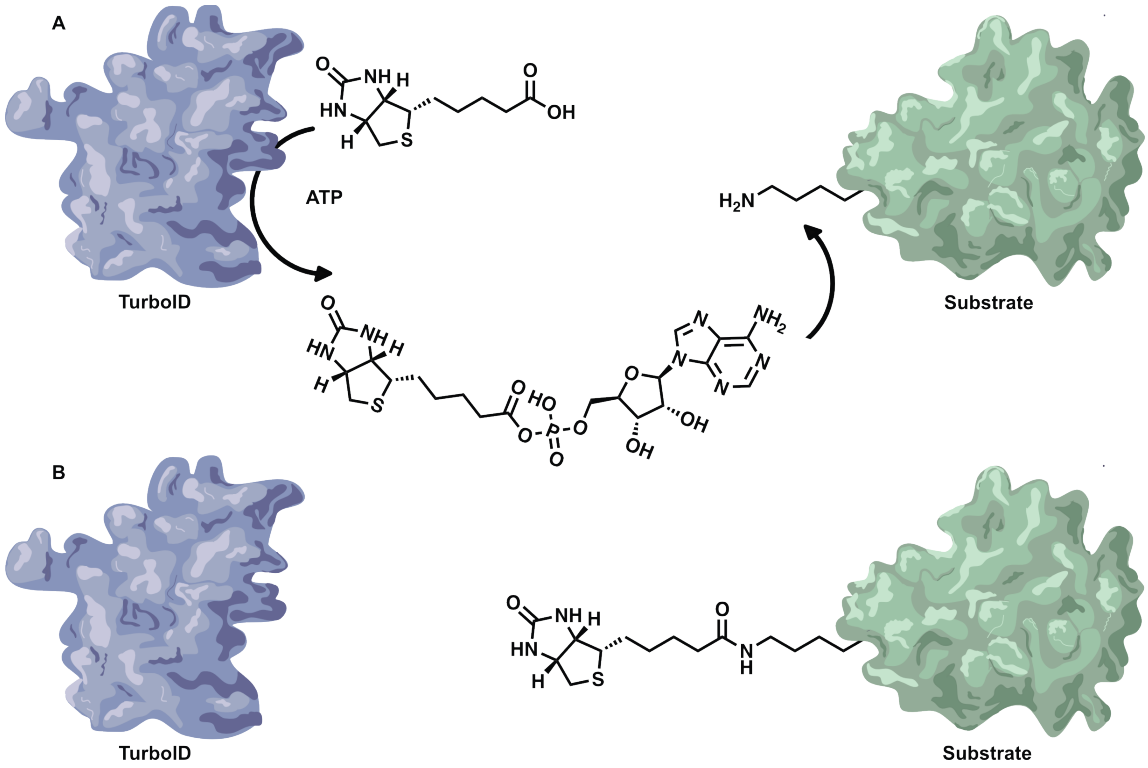


Figure 3-1. Mechanism of TurboID labeling proximal proteins with (A) biotin activation and (B) lysine SN2 reaction.

Although BioID pioneered the PL field, optimization was necessary due to low catalytic activity and biotin incubation times of 18 hr resulting in poor labeling efficiency.[33] The low temporal resolution decreased the utilization of BioID for monitoring dynamic protein-protein engagements or proteomic localization changes. With 15 optimized amino acid substitutions, most significantly the introduction of R118S to BioID's active site, the Ting lab established the second generation BioID (TurboID) with 23-fold improvement of efficiency and temporal resolution with complete labeling in 10 minute to 1 hour of biotin incubation.[38] Since then, TurboID has been expanded into multiple generations including miniTurbo[38], a smaller and more amenable but less effective clone, and Split-

TurboID[39], reliant on the engagement of two TurboID halves for high spatial resolution by contact-dependent based PL. Additionally, TurboID platforms have been harnessed in strategies to map out signaling networks and interactomes in plants and mammalian cells.[39,40]

As both biotin ligase PL performance relies on the *in situ* enzymatic generation of reactive biotin-AMP intermediate, which can diffuse as far as ~10 nm, allows for enzyme identification of tightly and loosely associated interactors within the same region with most the intense tagging at the site of biotin-AMP production.[41] Therefore, with such an expansive labeling radius, minute changes in molecular engagements may be lost and therefore, co-IP may still be ultimately preferred for verifying strong protein-protein interactors. Moreover, the wide-tagging radius makes PL with TurboID well-suited for intracellular enrichment. With guiding to multiple organelle regions, including the mitochondrial matrix, the Ting group has confirmed the ability of TurboID to localize proteomic coverage to subcellular compartments.[38]

Here we combine PL methods with an OxICAT workflow to specifically identify cysteine oxidation events within localized subcellular regions. Specifically, we show that coupling TurboID with OxICAT enables monitoring cysteine oxidation events within the mitochondrial matrix and IMS, providing previously unprecedented resolution to subcellular redox proteomic workflows (Figure 3-2 and Figure 3-3). Together, the PL-OxICAT platform further expands the toolkit for redox proteomics by allowing for localized evaluation of cysteine oxidation within very specific cellular regions.

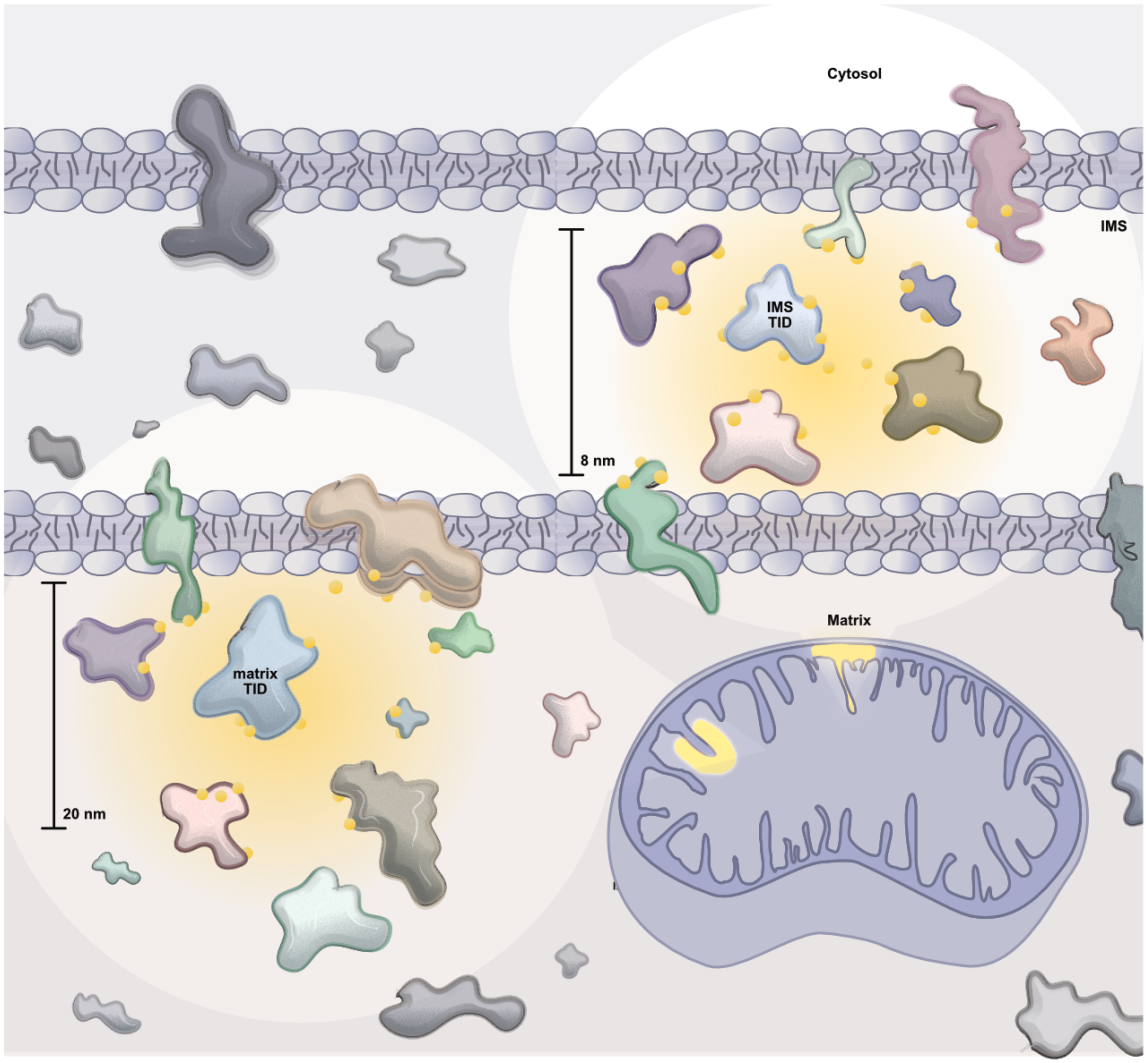


Figure 3-2. Schematic demonstrating the use of a matrix-TID, IMS-TID and matrix-APEX construct to selectively biotinylate proteins localized within the mitochondrial matrix, IMS and ROS hotspots, respectively.

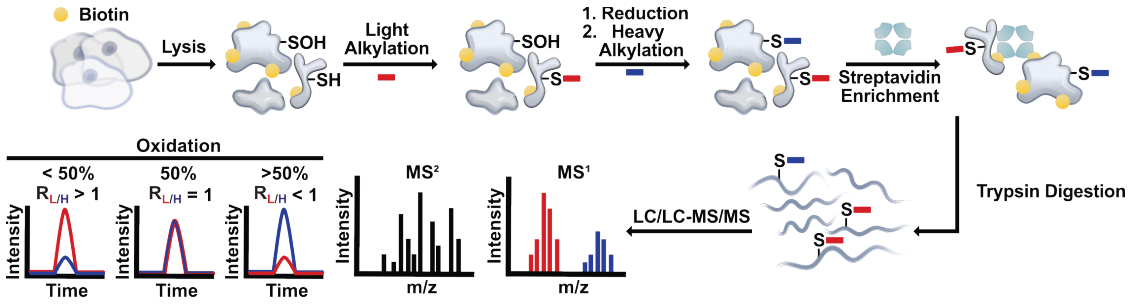


Figure 3-3. Workflow for PL-OxICAT includes differential alkylation of reduced and oxidized thiols with isotopically light and heavy species, enrichment of biotinylated proteins, trypsin digestion, and quantitative MS analysis to identify and quantify cysteine oxidation.

Results and discussion

Targeting TurboID to mitochondrial sub-compartments.

To implement the PL-OxICAT platform to monitor cysteine oxidation in the mitochondrial matrix and IMS, we generated TurboID fusions to a known matrix and IMS protein leader sequence, respectively (**Figure 3-3**).[36,42] For matrix localization, TurboID was fused to pyruvate dehydrogenase kinase 1 (PDK1), a matrix-residing kinase, to generate matrix-TID.[43] Localization to the IMS was achieved through a LACTB leader sequence to generate IMS-TID. The LACTB leader sequence was previously used for APEX studies of the IMS proteome.[36] Additionally, a cytosol-localized TurboID construct, cyto-TID, was also generated as cytosolic biotinylation control. All of the TurboID constructs contained the desired localization sequence at the N-terminus and an HA tag on the C-terminus. HEK 293T cells with stable expression of the TurboID constructs were generated using lentiviral transduction. Proper cellular localization of each TurboID fusion

was confirmed by confocal fluorescence microscopy (**Figure 3-4**). Both matrix-TID and IMS-TID expression profiles co-localized with the MitoTracker stain. In contrast, cyto-TID displayed no mitochondrial localization, instead displaying the expected widespread distribution across the cytosol.

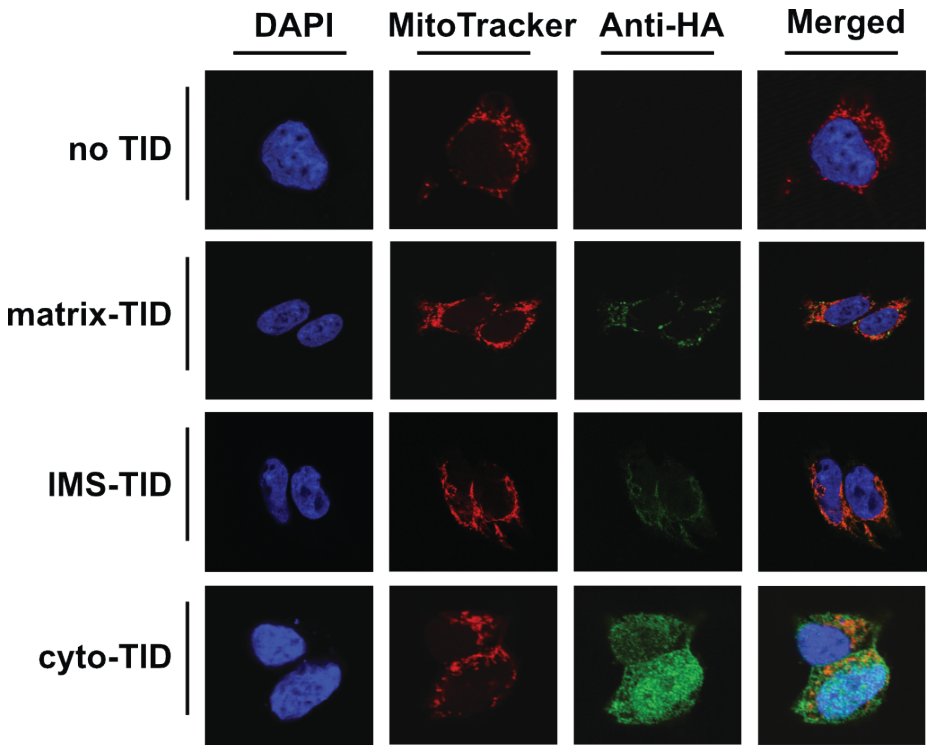


Figure 3-4. Immunofluorescence imaging of HEK 293T cells expressing no-TID, matrix-TID, IMS-TID, and cyto-TID. TID expression was monitored using anti-HA AlexaFluor488 (green), mitochondria were stained with Mitotracker Red CMXROS (red), and the nucleus was stained with DAPI (blue).

Upon confirming the desired mitochondrial localization, the biotinylation efficiency of matrix-TID and cyto-TID was determined upon varying biotin incubation times (Figure 3-5) and biotin concentrations (Figure 3-6). Maximal

biotinylation was achieved using 500 μM biotin for 1 hr. As expected, the levels of biotinylation for cyto-TID was significantly higher than that observed for matrix-TID, likely due to the higher concentration and larger diversity of proteins in the cytosol relative to the mitochondria. These optimized biotinylation conditions were also applied to IMS-TID, demonstrating successful biotinylation with this TID construct (Figure 3-7). Furthermore, each localized TID chimera shared in characteristic organelle labeling patterns previously reported.[42]

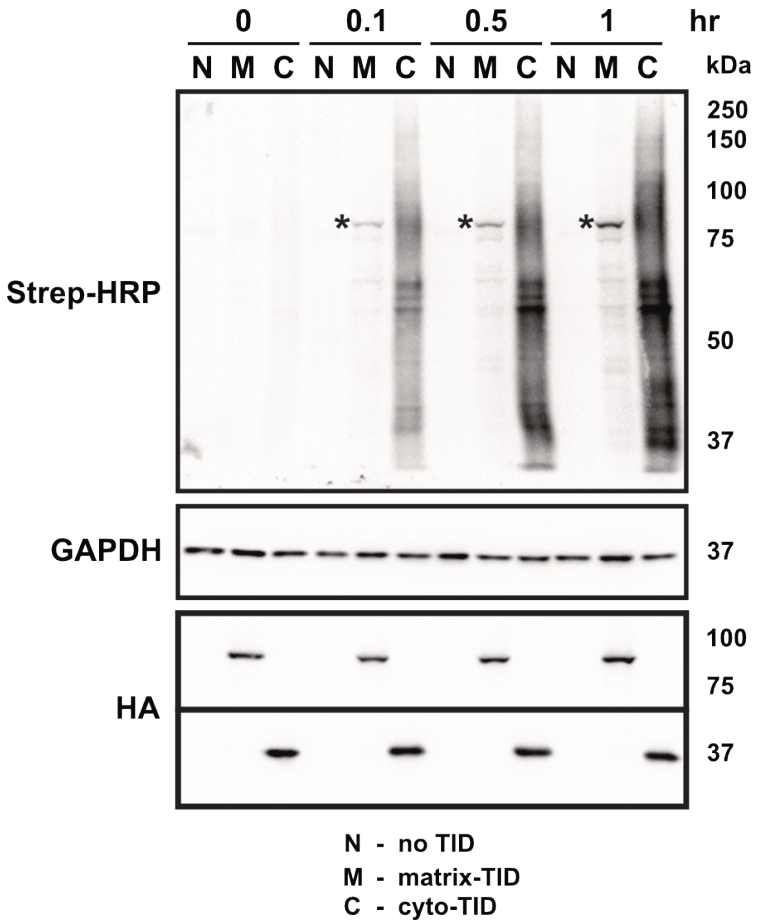


Figure 3-5. Western blot analysis of HEK 293T lysates expressing no-TID, matrix-TID, and cyto-TID. Cells were treated with 500 μM biotin for increasing incubation times, and biotinylated proteins were visualized using strep-HRP. Expression of

TID constructs was confirmed using anti-HA, and anti-GAPDH was used as a loading control. The asterisk denotes biotinylation of the TID construct.

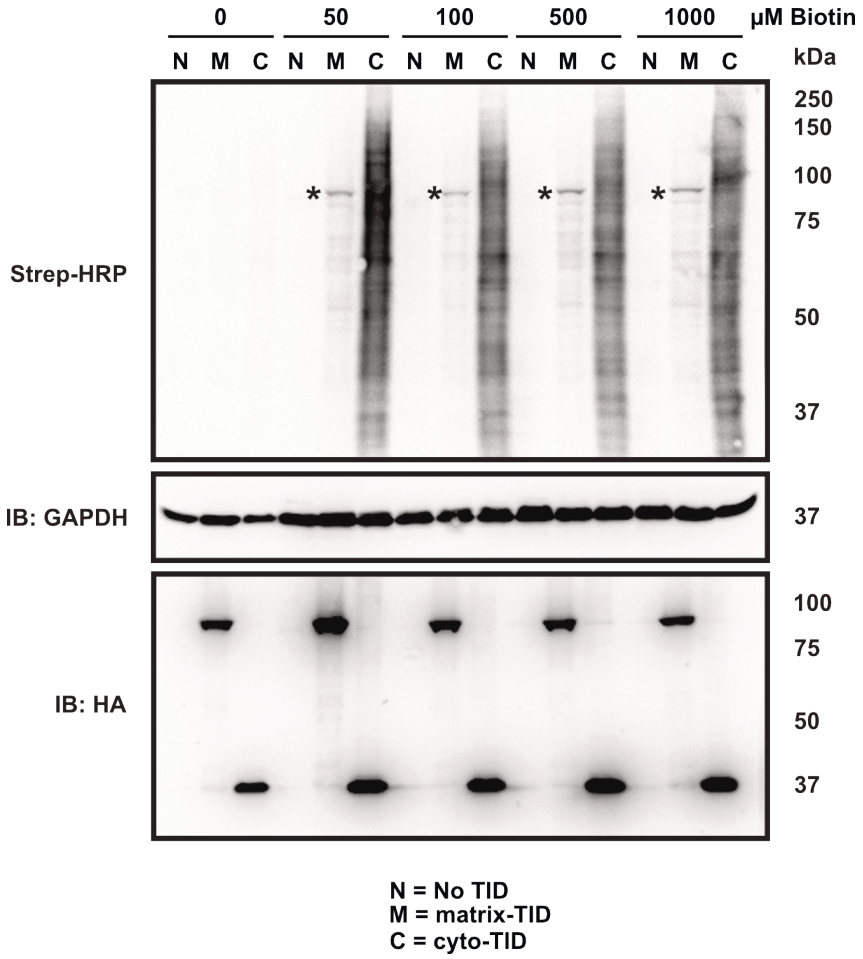


Figure 3-6. Western blot analysis of HEK 293T lysates expressing no-TID, matrix-TID, and cyto-TID. Cells were treated with various biotin concentrations, and biotinylated proteins were visualized using strep-HRP. Expression of TID constructs was confirmed using anti-HA, and anti-GAPDH was used as a loading control. The asterisk denotes biotinylation of the TID construct.

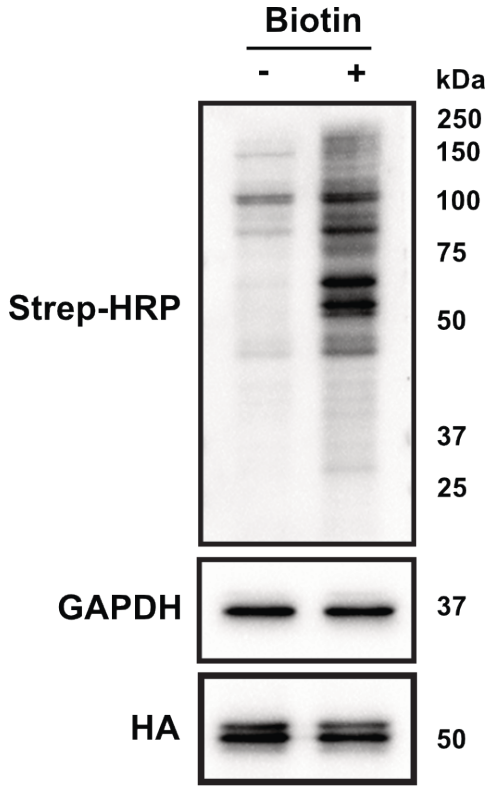


Figure 3-7. Western blot analysis of HEK 293T cells expressing IMS-TID. Cells were treated with 500 μm biotin for 1 hour and biotinylated proteins were visualized using strep-HRP. IMS-TID expression was confirmed using anti-HA, and anti-GAPDH was used as a loading control.

PL-OxICAT with TurboID enables quantification of cysteine oxidation events within the mitochondrial matrix and IMS.

Upon confirming mitochondrial localization and successful protein biotinylation by the three TurboID constructs, we then devised a workflow to combine PL, which enriches proteins proximal to the expressed TurboID construct, with OxICAT, which quantifies the level of cysteine oxidation (Figure 3-3). Cells expressing cyto-TID, matrix-TID and IMS-TID were incubated with 500

μM biotin for 1 hr to biotinylate proteins within the desired subcellular regions. After cell lysis, all reduced cysteine thiols were capped with isotopically light NEM or iodoacetamide-alkyne (IA-light).[25] Reversibly oxidized cysteine thiols were then reduced using tris(2-carboxyethyl)phosphine (TCEP) and subsequently reacted with isotopically heavy NEM or IA-heavy. The biotinylated proteins generated by each of the Turbo-ID constructs were then enriched on streptavidin resin and subjected to an on-bead trypsin digestion. The resulting tryptic peptides were analyzed by LC/LC-MS/MS to generate corresponding peptide and protein identifications. For each cysteine-containing peptide that was identified, the abundance of the isotopically light versus heavy species could be quantified in the form of a light:heavy ratio. These light:heavy ratio values can be used to determine the percentage of oxidation for each identified cysteine residue within the sample.

We first focused our attention on the protein identifications obtained from the MS analyses to assess the subcellular localization of proteins enriched through biotinylation by each of the three TurboID constructs. Protein identifications from the cyto-TID, matrix-TID, and IMS-TID samples (Table 3A-1) were compared to mitochondrial annotations reported by Uniprot[44] and MitoCarta2.0[45] and previous matrix and IMS proteins identified using APEX PL.[37,36] The Matrix-TID sample generated 1180 protein identifications of which 450 (38%) are annotated as mitochondria localized. Similarly, 1980 proteins were identified in the IMS-TID analysis, of which 456 (23%) are mitochondria localized. In contrast, the cyto-TID sample generated 1765 total proteins, but only 126 (7%) are annotated as localized to the mitochondria (Figure 3-8A, Table 3A-1). The difference was even more pronounced when comparing peptide spectral counts across the three samples, where 75% and 36% of the matrix-TID and IMS-TID counts originated from

mitochondrial proteins compared to 6% in the cyto-TID sample (Figure 3-8A, Table 3A-1). A higher fraction of the proteins identified in the IMS-TID sample compared to the matrix-TID sample (62% versus 77%) were not mitochondria localized. This is likely due to diffusion of the biotin-AMP intermediate through the outer mitochondrial membrane, which is known to be significantly more permeable than the inner mitochondrial membrane.[36] Direct comparison of matrix-TID and IMS-TID samples to the cyto-TID sample clearly demonstrates that mitochondrial proteins were identified with higher average spectral counts in the matrix-TID and IMS-TID samples, compared to cyto-TID (Figure 3-8B,C, Table3A-1).

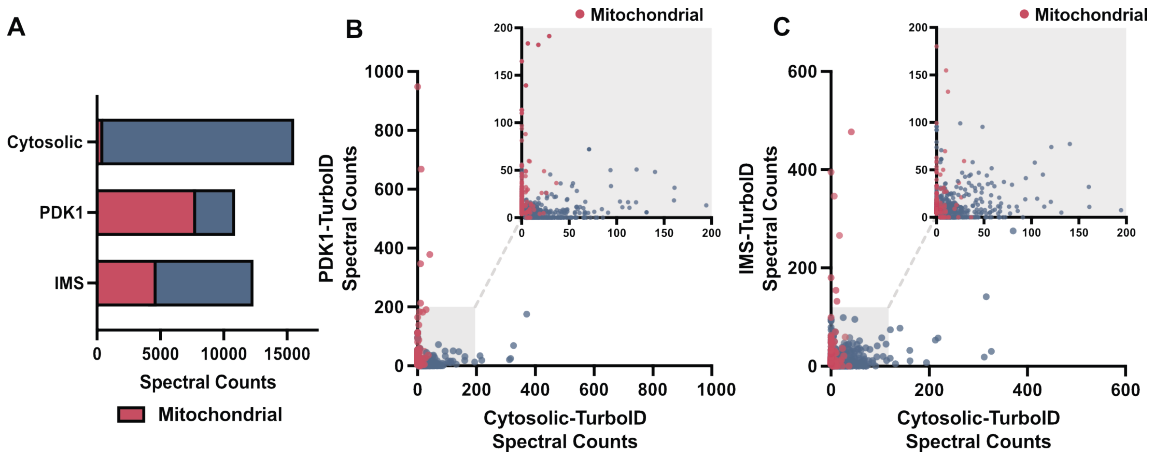


Figure 3-8. (A) Quantitative analysis of total spectral counts for proteins labeled by TurboID localized to cytosol, matrix and IMS with mitochondrial annotations (red). Spectral counts plotted for proteins labeled by (B) Cytosolic-TurboID and PDK1-TurboID and (C) Cytosolic-TurboID and IMS-TurboID with mitochondrial annotations (red). Proteins with greater or equal to 4 spectral counts and identified in 2 replicates were included.

Compared to a previous dataset generated using differential centrifugation to fractionate mitochondria[29], we see a larger number of mitochondrial proteins identified using the TurboID enrichment method (Figure 3-9 and Figure 3-10A, Table 3A-1). This was particularly noticeable for proteins localized within the IMS, where the low abundance of IMS proteins relative to matrix proteins results in reduced identification in whole-mitochondria proteomic analyses (Figure 3-10B, Table 3A-1). This improved coverage is noteworthy because the TurboID enrichment is significantly less labor-intensive and requires reduced cell input compared to the differential centrifugation method. Together, these data serve to confirm that the use of matrix-TID and IMS-TID constructs enable enrichment of proteins annotated to be localized to the mitochondria.

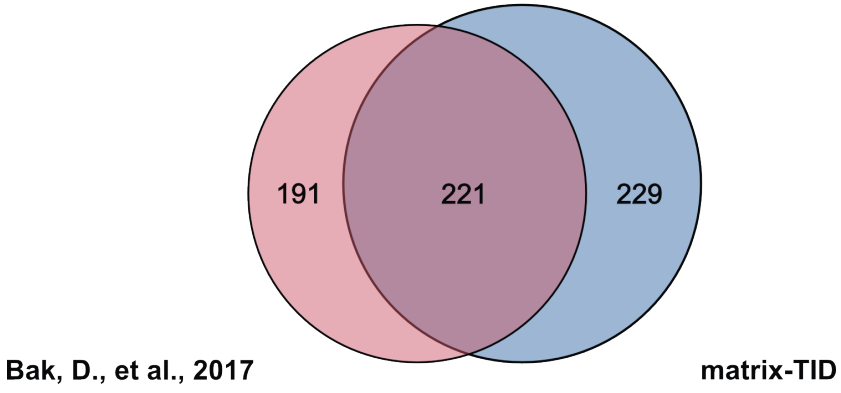


Figure 3-9. Venn diagrams comparing mitochondrial proteins identified using matrix-TID (blue) to previous reports using mitochondrial differential centrifugation in (Bak, *et al.*, 2017) (red).

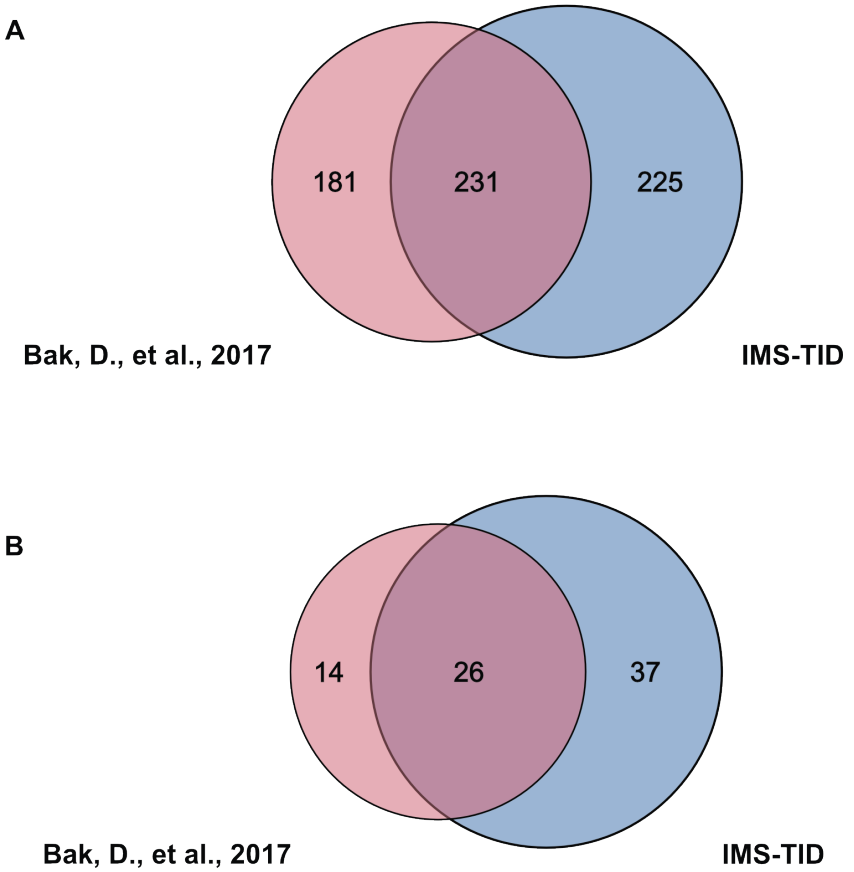


Figure 3-10. (A) Venn diagrams comparing mitochondrial proteins identified using IMS-TID (blue) to previous reports using mitochondrial differential centrifugation in (Bak, *et al.*, 2017) (red). (B) Venn diagrams comparing IMS proteins identified using IMS-TID (blue) to previous reports of IMS proteins identified using mitochondrial differential centrifugation in (Bak, *et al.*, 2017) (red).

The 450 annotated mitochondrial proteins identified in the matrix-TID analysis were compared to previous studies that used TurboID and APEX constructs containing a matrix-targeting signal sequence.[38,37] These previous TurboID and APEX studies identified 205 and 589 mitochondrial proteins, respectively. Our matrix-TID data identified 375 (64%) of the mitochondrial

proteins identified previously using matrix-targeted APEX (Figure 3-11A). Similarly, the 456 mitochondrial proteins identified in the IMS-TID analysis were compared to a previous study that used an IMS-targeted APEX construct. This prior APEX study identified 136 putative IMS proteins, and 63 (46%) of these were also identified in our IMS-TID analysis (Figure 3-11B). Together, these comparisons to previous mitochondria-targeting PL studies show that our constructs are similarly enriching the desired subset of mitochondrial proteins. To further confirm enrichment of the desired mitochondrial compartments, we performed gene ontology (GO) analysis of the proteins identified in the matrix-TID, IMS-TID and cyto-TID datasets. Our matrix-TID data revealed enrichment of known mitochondrial processes including carboxylic acid catabolism and mitochondrial RNA metabolism (Table 3A-2). Similarly, the IMS-TID data show enrichment of mitochondrial protein transport, ATP transmembrane transport, and protein refolding (Table 3A-3). In contrast, GO analysis of the cyto-TID dataset showed no enrichment of known mitochondrial processes (Figure 3-12, Table 3A-4).

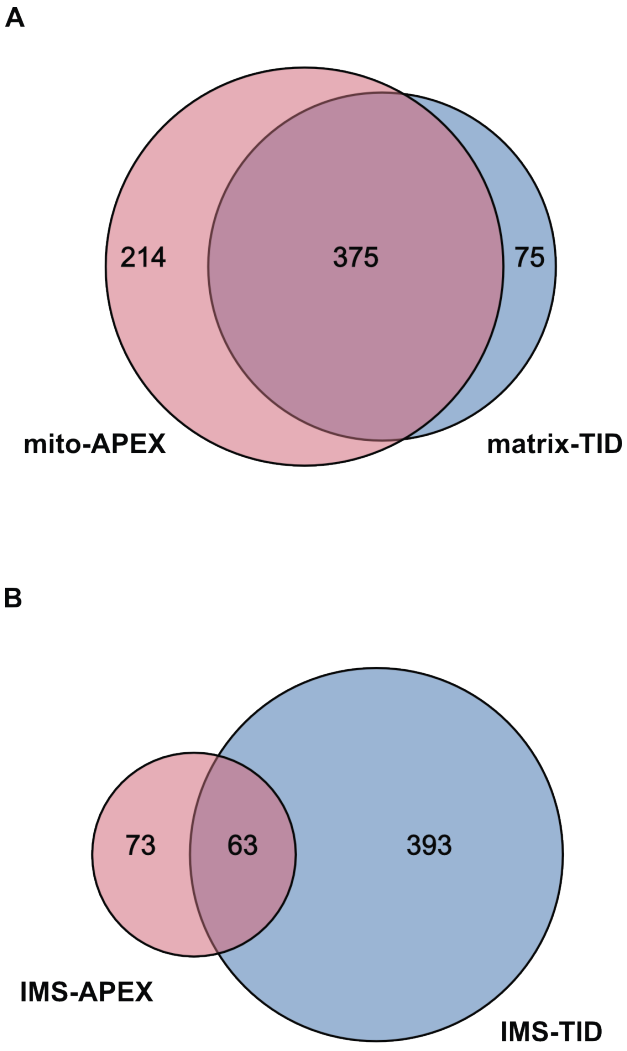


Figure 3-11. Venn diagrams comparing mitochondrial proteins identified using (A) matrix-TID (blue) to previous reports using mito-APEX (red) or (B) IMS-TID (blue) to previous reports using IMS-APEX (red).

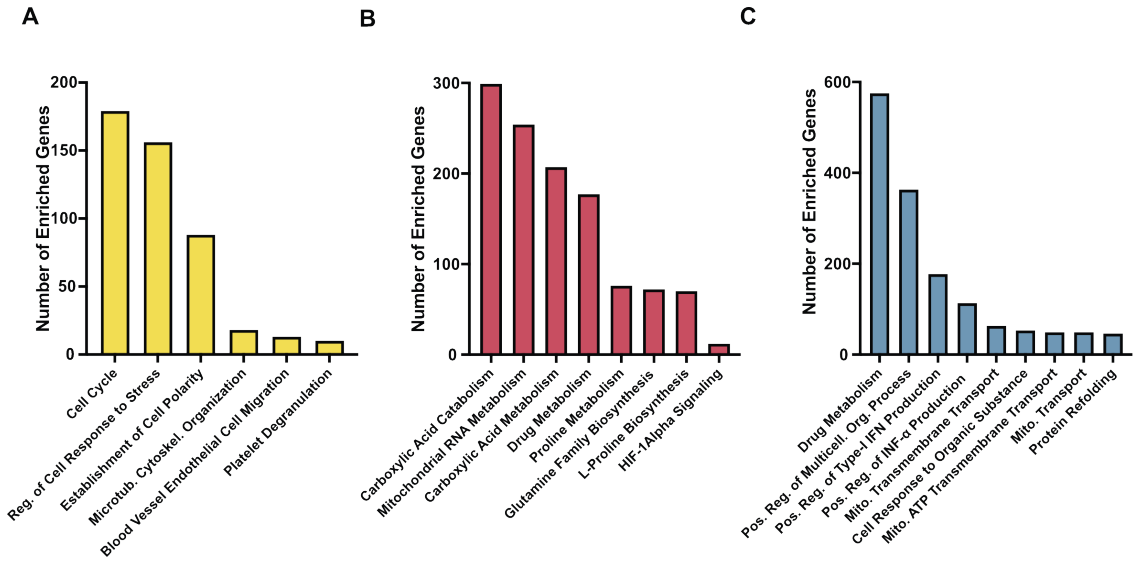


Figure 3-12. Panther[46] gene ontology (GO) analysis of most enriched processes for (A) Cyto-TID, (B) matrix-TID and (C) IMS-TID recovered proteins determined by GOrilla ranked evaluation with redundant terms removed.

Upon confirming that MS analysis of the matrix-TID and IMS-TID samples identified proteins with known localization within these two compartments, we then focused on the individual cysteine-containing peptides that were identified. The matrix-TID data identified 1710 cysteine peptides, with 885 residing on annotated mitochondrial proteins (Table 3A-5). Since the samples were processed using the OxICAT workflow, all reduced cysteine thiols were labeled with a light cysteine-capping reagent, whereas all reversibly oxidized cysteines were labeled with the corresponding isotopically heavy reagent. Therefore, light:heavy ratios can be obtained for each cysteine-containing peptide, which can then be used to calculate the percent oxidation of that cysteine residue. We filtered the identified mitochondrial cysteine peptides for those that afforded light:heavy ratios in two of three replicates, resulting in 277 cysteines for which corresponding percent

oxidation values were obtained with high confidence (Figure 3-13, Table 3A-6). Given the highly reducing environment of the mitochondrial matrix, the majority (96%) of these cysteines were found in a highly reduced state (less than 20% oxidation). There were 10 cysteines with greater than 20% oxidation, and of these, only one cysteine (C48 from NT5DC2) was found to be highly oxidized at 95%. The IMS-TID sample generated 2151 cysteine-containing peptides, of which 613 were derived from mitochondrial proteins. High confidence percent oxidation values were determined for a total of 196 cysteines (Figure 3-14, Table 3A-7). Similar to the matrix-TID data, the majority (96%) were highly reduced with less than 20% oxidation. There were 9 cysteines with greater than 20% oxidation, and of these 6 cysteines were found to be greater than 50% oxidized. The cysteines that were highly oxidized included several that are annotated to participate in mitochondrial disulfide-bond formation. For example, C65 and C30 in the cytochrome c oxidase subunit 6B1 (COX6B1), a subunit of ETC complex IV, were found to be 79% and 82% oxidized, respectively. These cysteines are located within signature CX_9C and $CX_{10}C$ motifs, which have been shown to form intramolecular disulfide bonds on the IMS face of this inner membrane protein.[47-49] Additionally, C36 in the NADH dehydrogenase 1 alpha subcomplex subunit 8, NDUFA8, was found to be 56% oxidized. This cysteine is annotated to form an intramolecular disulfide bond with C46, within a CX_9C motif.[50] Lastly, from the corresponding cyto-TID data, percent oxidation was calculated for 580 cysteines, of which 30 are annotated as mitochondrial and 275 as cytoplasmic (Figure 3-15, Table 3A-8). Of the cytoplasmic cysteines identified, the majority (95%) were determined to be less than 20% reduced, reflecting the reducing environment of the cytosol. Together, these data demonstrate the ability of PL-OxICAT quantify the percent oxidation

of matrix and IMS-localized cysteines under basal cellular conditions, setting the stage for monitoring changes in oxidation state of these cysteines in cellular models of oxidative stress.

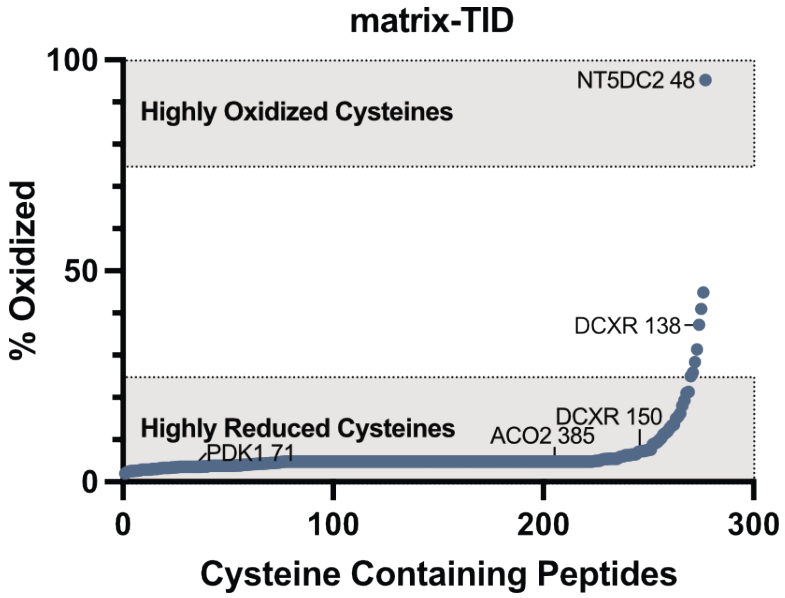


Figure 3-13. Percent oxidation values for mitochondrial cysteines identified in the matrix-TID sample.

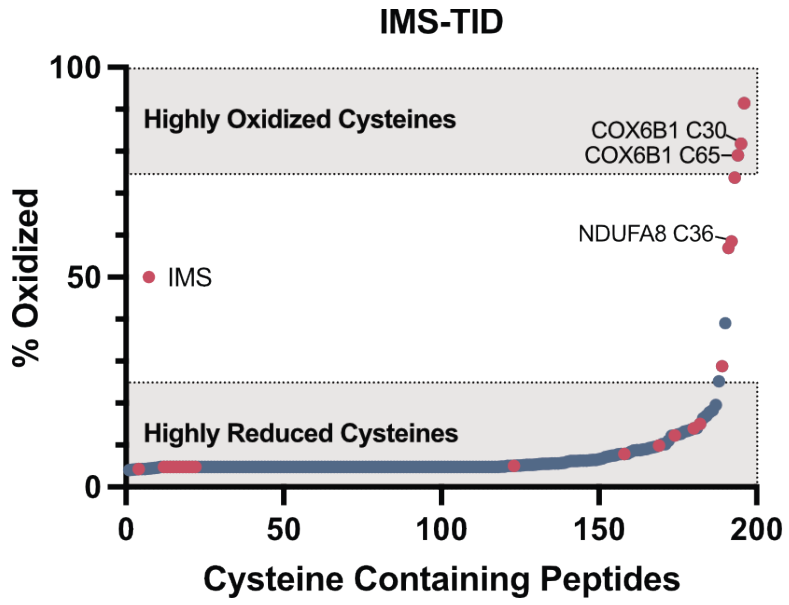


Figure 3-14. Percent oxidation values for mitochondrial cysteines identified in the IMS-TID sample. IMS localized proteins annotated in red.

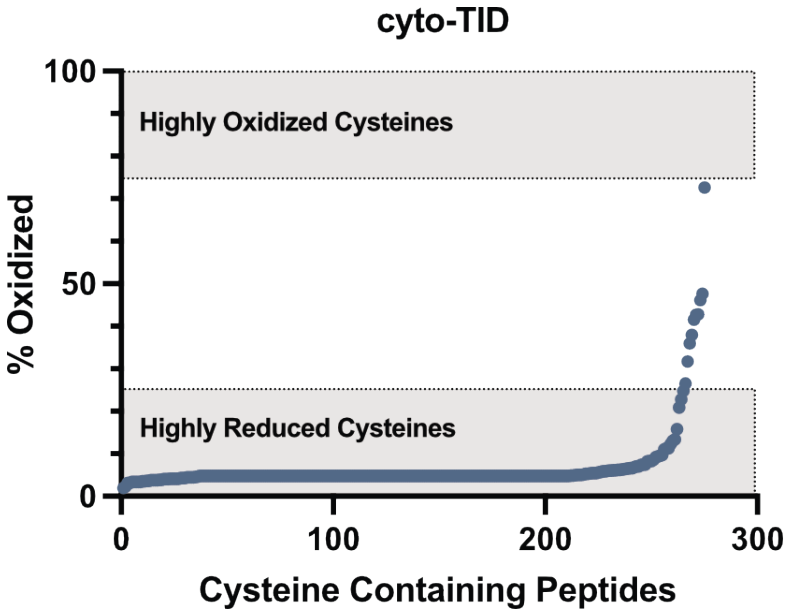


Figure 3-15. Percent oxidation values for mitochondrial cysteines identified in the cyto-TID sample.

Conclusion

Proximity labeling methods such as BioID and TurboID, have proved to be an enabling technology for identifying proteins localized to a particular subcellular localization. Here, we couple these elegant PL techniques with an established redox-proteomic workflow, termed OxICAT, to allow for interrogation of localized cysteine oxidation events. Specifically, we couple TurboID proximity labeling within specific mitochondrial compartments with OxICAT to quantify cysteine oxidation within these localized regions. The implementation of this PL-OxICAT platform in the mitochondrial matrix and IMS enables the identification of cysteines within these compartments and the quantitation of the percent oxidation of these cysteines under basal cellular conditions. Importantly, analysis of whole-cell lysates typically results in poor coverage of cysteines within the matrix and IMS, and therefore selectively enriching for these subcellular proteomes with TurboID serves to increase coverage. We anticipate that future studies that utilize PL-OxICAT in different cellular locations will allow for selectively monitoring changes in cysteine oxidation within these compartments.

We demonstrate the use of these PL-OxICAT workflows to quantify cysteine oxidation in three different systems; (1) the mitochondrial matrix; (2) the IMS; and (3) the cytosol. One limitation of this platform is inherent to proximity labeling itself, where biotinylation is not strictly confined to the cellular location of interest, likely due to diffusion of some of the reactive biotin intermediates further than anticipated from the site of generation. Minimization of these non-specifically biotinylated proteins would serve to enhance the coverage of cysteine residues within the desired protein subset. Additionally, the number of cysteines

for which percent oxidation is calculated can potentially be improved by further fractionation of the peptide samples prior to MS analysis. These studies set the foundation for localized monitoring of cysteine oxidation, and we anticipate that the methods can be further honed with improved fractionation and MS advancements to provide further insight into the role of cysteine oxidation in (patho)physiological processes.

Experimental Procedures

Materials.

All materials were purchased from Fisher Scientific or Sigma-Aldrich unless otherwise specified. Antibodies were purchased from Cell Signaling Technology and listed in Table 3-1.

Table 3-1. Antibodies used with sources, catalog number and use.

Antibody	SOURCE	IDENTIFIER	USE
HA-Tag (C29F4) Rabbit mAb (1:1000)	Cell Signaling Technology	Cat# 3724	Western Blot
HA-Tag (6E2) Mouse mAb (1:500)	Cell Signaling Technology	Cat# 2367	Immunofluorescence
GAPDH (14C10) Rabbit mAb (1:1000)	Cell Signaling Technology	Cat# 2118	Western Blot
Streptavidin-HRP (1:200mg)	Sigma-Aldrich	Cat# OR03L	Western Blot
Anti-mouse IgG (H+L), F(ab')2 Fragment (Alexa Fluor® 488 Conjugate) (1:500)	Cell Signaling Technology	Cat# 4408	Immunofluorescence
Anti-rabbit IgG, HRP-linked Antibody (1:2000)	Cell Signaling Technology	Cat# 7074	Western Blot
ProLong® Gold Antifade Reagent with DAPI	Cell SignalingTechnology	Cat# 8961	Immunofluorescence

Cell culture.

HEK 293T cells were obtained from the ATCC, cultured at 37°C under 5% CO_2 in DMEM/high glucose with L-glutamine, sodium pyruvate (Cytiva) and supplemented with 10% fetal bovine serum (Bio-techne), 100 units/mL of penicillin, 100 μg/mL streptomycin, 0.25 μg/mL Amphotericin B (Gibco) and grown until a maximum passage of 25.

Cloning of TurboID and APEX2 plasmids.

Traditional cloning methods of PCR gene amplification, restriction enzyme digestion, ligation, and gateway cloning allowed for generation of pLenti TurboID (matrix-TID, IMS-TID, and cyto-TID) plasmids. For all plasmids, initial parent pDONR221 vectors containing MCS-TurboID-HA were generated from PCR amplification of V5-TurboID-NES_pCDNA3 (addgene 107169) with attb1/attb2 sites for gateway cloning into pDONR221 vectors. For the pLenti matrix-TurboID plasmid, full length PDK1 (NM_002610) was PCR amplified with a N-terminal kozak sequence and inserted into pDONR221 MCS-TurboID-HA vector using restriction enzyme digestion and ligation followed by gateway cloning into a pLenti vector. For pLenti IMS-TID, Gibson assembly was used to PCR amplify a codon optimized LACTB leader sequence dsDNA fragment (Genewiz) with overhanging sequences for Gibson assembly into the pDONR221 MCS-TurboID-HA vector followed by gateway cloning into pLenti destination vector. All plasmids incorporated an N-terminal kozak sequence for mammalian translation. Mammalian protein expression was driven through CMV promoters in all pLenti plasmids (Table 3-2).

Table 3-2. Vectors and descriptions including features, promoters, and uses for this study

Vector	Features	Promoter	Use
pLenti-cyto-TurboID-HA	attb-MCS-kozak-TurboID-HA-stop-attb	CMV/SV40	Used to generate Lentivirus for transduction into HEK293T cells for cytosolic TurboID expression (cyto-TID)
pLenti matrix-TurboID-HA	attb-NotI-kozak-PDK1-EcoRI-TurboID-HA-stop-attb	CMV/SV40	Insertion of full length PDK1. Used to generate Lentivirus for transduction into HEK293T cells for PDK1-TurboID expression (matrix-TID)
pLenti IMS-TurboID-HA	attb2-kozak-LACTB (1-68) - TurboID-HA-stop-attb2	CMV/SV40	Incorporation of mammalian cell codon optimized LACTB leader sequence(1-68): MYRLLSSVTARAAATAGPAWD GGRRGAHRRPGLPVLGLGWAG GLGLGLGLALGAKLVVGLRGA VPIQS (Polianskyte et al., 2009) (Hung et al., 2014). Used to generate Lentivirus for transduction into HEK293T cells for LACTB-TurboID expression (IMS-TID).
pDONR221 TurboID-HA	attL1-MCS-TurboID-HA-stop-attL2	M13	Intermediate TurboID plasmid used for incorporation of PDK1 (matrix) and LACTB leader sequence (IMS) and generation of pLenti vectors

Generation of stable matrix-TID-HA, IMS-TID-HA, and cyto-TID-HA HEK 293T cells.

Lentivirus was produced in HEK 293T cells, under passage 10, grown in DMEM and 10% heat inactivated fetal bovine serum (HIS) in 10 cm plates. At 80% confluency, cells were transfected with 2 μg vsv-g, 2 μg psPAX2, 2 μg respective pLenti plasmid and 24 μL of Lipofectamine 2000 (Invitrogen). After 24 hr, media was replaced by 5 mL DMEM with 10% HIS. At 48 hr, the media was collected and filtered through a 0.45 μm filter and mixed with 5 mL DMEM-HIS and 10 μg/mL

polybrene. Virus was added to the target cell lines at 20% confluency and infected for 48 hr. Growth for 7 days in 2 μg/mL puromycin allowed for selection of stable protein overexpression in HEK 293T cells.

TurboID activation.

HEK 293T cells overexpressing matrix-TID, IMS-TID, and cyto-TID were plated on 10 cm dishes and grown to full confluency. Treatments with either increasing concentrations (0, 10, 100, 500, 1000 μM) of biotin in DMSO for 1hr or 500 μM biotin in DMSO for a variety of incubation times (0.1, 0.2, 0.5, 1 hr) were quenched by washing 3 times with cold DPBS (Corning). For MS preparations, cells were treated with 500 μM biotin for 1 hr at 37°C. Reactions were quenched 3 washes with cold DPBS.

Lysate preparation.

Cells were harvested by scraping and washed with DPBS (Corning). Cell pellets were resuspended in DPBS and lysed by ultrasonic tip sonication (Cole Parmer). Soluble lysate fractions were obtained after separation by centrifugation at 45,000 rpm for 45 min at 4°C pelleted insoluble fractions were discarded for matrix-TID and cyto-TID HEK 293T cell lysates. For IMS-TID HEK cell lysates, whole cell lysates were enriched by centrifugation at 4,500g for 10 min at 4°C with supernatant collected. To determine protein concentrations, DC Protein Assay kit (Bio-Rad) was performed.

Immunoblotting.

All samples were separated by 12.5% SDS-PAGE gels and transferred to nitrocellulose membranes by electrophoresis at 75 volts for 140 min. Membranes were washed with tris-buffered saline with 1% Tween:20 (TBS-T) 3 times for 5 min followed by staining with Ponceau S (2 min in 0.1% w/v Ponceau S in 5% acetic acid/water) and imaged on a ChemiDoc MP imaging system (BioRad, Hercules, CA). After 3 washes with TBS-T, membranes were blocked with 5% (w/v) non-fat dry milk in TBS-T at room temperature for 1 hr. Following 3 additional washes with TBS-T, membranes were incubated with respective primary antibodies overnight at 4°C. Following removal and additional 3 washes with TBS-T, the membranes were coated with secondary HRP-conjugated antibodies for 1 hr at room temperature. For biotin blots, membranes were blocked in 5% milk overnight at 4°C and after washes, was incubated with 200 ng/mL streptavidin-HRP in TBS-T for 1 hr. After final washes with TBS-T, membranes were developed with HRP-super signal chemiluminescence reagents (Thermo Fisher) and visualized as described above.

Immunohistochemistry and immunofluorescence

For fluorescence microscopy imaging, cells were grown on 35 mm glass bottom dishes (MatTek) that were treated with 1 mg/mL poly-D-lysine (Sigma-Aldrich) incubated for 5 min at 37°C and washed 3 times with DPBS. Without exposure to light, cells were treated with 50 nM MitoTracker Red CMXRos (Invitrogen) in RPMI medium without phenol red (Gibco) for 45 min at 37°C. Cells were washed with 3 times with DPBS for 5 min and fixed with 4% formaldehyde (Thermo Fisher Pierce) in DPBS for 15 min at room temperature. After additional

washes with DPBS for 5 min 3 times, cells were blocked with blocking buffer of 5% normal goat serum (Cell Signaling Technology) and 0.3% Triton X-100 in DPBS for 1 hr at room temperature. After washing 3 times with DPBS, cells were incubated with primary antibodies diluted in 1% BSA and 0.3% Triton X-100 in DPBS overnight at 4°C. Cells were washed 3 times with DPBS and incubated with secondary antibodies conjugated to AlexaFluor488 for 2 hr at room temperature. After the final 3 washes with DPBS for 5 min, Prolong Gold Antifade Reagent with DAPI (Cell Signaling Technology) was applied and the samples were cured overnight at room temperature. A coverslip was added and sealed with clear nail polish before imaging with a Leica TCS SP5 scanning confocal microscope.

Proximity labeling PL-OxICAT MS preparation.

OxICAT sample preparations were adapted from Bechtel, *et al*. [22] and Topf, *et al*. [28]. 4 mg total protein for matrix-TID and IMS-TID and 2 mg total protein for cyto-TID cell lysates were precipitated by TCA at -80°C for 1 hr or overnight. Samples were pelleted at 15,000 rpm for 10 min and resuspended in 500 μL acetone. After centrifugation at 5,000 rpm for 10 min, sample pellets were resuspended and solubilized in 250 μL denaturing-alkylation buffer (DAB) (6 M Urea, 200 mM Tris-HCl, 10 mM EDTA and 0.5% SDS, pH 8.5) containing 10 mM Light-NEM (5 μL of 500 mM Light-NEM, Sigma-Aldrich). Reduced cysteines were alkylated in the dark at 37°C for 2 hr with shaking. Samples were centrifuged at 21,000 g for 1 min to pellet any precipitant and supernatant was collected and diluted 3-fold with water to lower the urea content. Proteins were precipitated with 5-fold volume of ice-cold acetone and incubated at -20°C for 2 hr or overnight. After precipitation, samples were pelleted at 4500 g for 30 min, 4°C. Pellets were

washed with 500 μL acetone and centrifuged at 4500 g for 10 min. Samples were solubilized in 160 μL DAB and cysteines were reduced with 8 μL of 50 mM tris(2-carboxyethyl)phosphine (TCEP, 2.5 mM final concentration). Samples were agitated at 37°C for 5 min. After reduction, 240 μL DAB was added to dilute TCEP and newly reduced cysteines were labeled by the addition of 10 mM heavy-NEM (8 μL of 500 mM D5-NEM, Cambridge Isotope Laboratories) incubate 2 hr at 37°C in the dark. After the final alkylation, samples were diluted 3-fold with water and 5-fold total volume of acetone was added and proteins precipitated at -20°C for 2 hr or overnight. Proteins were pelleted by centrifugation at 4500 g for 30 min at 4°C and washed with 500 μL acetone. Following centrifugation at 4500 g for 10 min, labeled-protein pellets were resuspended in 1 mL 1.2% (w/v) SDS/PBS using sonication. Solubilized samples were diluted to 0.2% SDS with the addition of 5mL PBS containing 100 μL of washed streptavidin agarose resin (Thermo Scientific) and rotated overnight at 4°C. SDS solutions were resolubilized at room temperature for 2.5 hr and the resin was incubated with 0.2% SDS/PBS for 10 min followed by 3 washes with PBS and 3 washes with water (5 mL each). Resin was pelleted by centrifugation (1400 g for 3 min) and supernatant removed between each wash step. After the final wash step, resin was resuspended in 200 μL of 2 M Urea and 1 mM $CaCl_2$. 2 μg of trypsin (Promega) was added, and the samples digested overnight at 37°C with agitation. The supernatant was collected, and resin was washed 3 times with 50 μL water and combined generating a total sample volume of 350 μL. Trypsin digestion was quenched by the addition of 17.5 μL formic acid (5% final concentration). For matrix-TID and cyto-TID, cysteines were isotopically labeled by light-IA and heavy-IA (made in house) [25].

MS proteomics.

Peptide analysis was achieved by Multidimensional Protein Identification Technology (MudPIT) on an LTQ Orbitrap Discovery mass spectrometer (Thermo Fisher) with sample separation coupled to an Agilent 1200 series HPLC (Agilent Technologies). Peptides were loaded onto a self-packed reverse phase C18 resin 250 μm fused-silica capillary column. 5 Gradients of 100% Buffer B in Buffer A (Buffer A: 95% water, 5% acetonitrile, 0.1% formic acid; Buffer B: 20% water, 80% acetonitrile, 0.1% formic acid) with 5 salt pushes, eluted peptides onto a biphasic 100 μm fused-silica capillary column with a 5 μm tip packed with 10 cm of C18 resin and 4 cm of Partisphere strong cation exchange resin (SCX, Whatman). Instrumentation operated at a flow rate of ~0.25 μL/min buffer through the column and spray voltage of 2.75 kV. One full MS scan (400 – 1800 MW) was followed by 7 data dependent scans of the n^{th} most intense ions with dynamic exclusion enabled.

MS proteomic analysis.

Mass spectrometry data in all samples were searched using a SEQUEST algorithm[51] against a concatenated target/decoy non-redundant variant of *Homo sapien* and *Mus musculus* FASTA databases containing UniProt descriptions[44], respectively. Dynamic modifications on cysteine were included to survey the alkylation by either light-NEM (+125.04766) and heavy-NEM (+130.07906) or light-IA (+185.08406) and heavy-IA (+191.10419). Proteins were identified in matched MS^2 spectra, packaged, and filtered using DTASelect2.0.[52] Spectra were sorted with options for -trypstat applied for analyzing tryptic protein enrichment and -modstat applied for specific analysis of labeled cysteine-containing peptides

and were restricted to a 5% maximum false discovery rate. For analysis of proximity-labeling enrichment, protein spectral counts were pooled by an in-house Python program with additional annotations for localization and function.[22]

OxICAT specific MS analysis.

Furthermore, all identified cysteine-containing peptides were delimited to having full tryptic cleavage (-y 2), required at least one peptide per locus (-p 1) and a delta-CN score greater than 0.06 (-d 0.06). Cysteine residue position, function, species conservation, domain, and subcellular localizations were annotated by an in-house Python program. Characterized mitochondrial localization was determined by UniProt[44] and MitoCarta2.0[45] specifications. Heavy:light (H:L) and light:heavy (L:H) ratios were resolved using cimage quantification package.[53] L:H and H:L ratios were converted to percent oxidation values by the following equations: 1-(L:H/(L:H+1)) and H:L/(H:L+1). All considered peptides were presented in at least 2 replicates. Average percent oxidation values were calculated for each peptide and standard deviations >30% were removed from the final compilation of labeled-peptides analyses.

Statistical analysis of overrepresented gene ontology (GO) process using PANTHER, GOrilla, and ReviGO.

Panther overrepresentation gene ontology tests (http://pantherdb.org)[46] were performed on all TurboID-enriched protein datasets. Enriched processes were determined by GOrilla using a ranked gene ontology (GO) analysis and FDR corrected for multiple testing using Benjamini and Hochberg and Fisher methods. Enrichment (E) was defined in terms of the number of intersecting genes (b) over

the number of top genes in the target set (n) divided by the total number of genes correlated to a unique GO term (B) over the total number of genes analyzed (N) (E = (b/n) / (B/N). Enriched terms were sorted by the number of top genes (n) and redundant terms were manually removed after analysis by ReviGO.[54]

References

(1) Sies, H.; Jones, D. P. Reactive Oxygen Species (ROS) as Pleiotropic Physiological Signalling Agents. *Nat. Rev. Mol. Cell Biol.* **2020**, *21* (7), 363–383.

(2) Sun, Y.; Lu, Y.; Saredy, J.; Wang, X.; Drummer IV, C.; Shao, Y.; Saaoud, F.; Xu, K.; Liu, M.; Yang, W. Y.; Jiang, X.; Wang, H.; Yang, X. ROS Systems Are a New Integrated Network for Sensing Homeostasis and Alarming Stresses in Organelle Metabolic Processes. *Redox Biol.* **2020**, *37*, 101696.

(3) Dickinson, B. C.; Chang, C. J. Chemistry and Biology of Reactive Oxygen Species in Signaling or Stress Responses. *Nat. Chem. Biol.* **2011**, *7* (8), 504–511.

(4) Del Prete, A.; Zaccagnino, P.; Di Paola, M.; Saltarella, M.; Oliveros Celis, C.; Nico, B.; Santoro, G.; Lorusso, M. Role of Mitochondria and Reactive Oxygen Species in Dendritic Cell Differentiation and Functions. *Free Radic. Biol. Med.* **2008**, *44* (7), 1443–1451.

(5) Redza-Dutordoir, M.; Averill-Bates, D. A. Activation of Apoptosis Signalling Pathways by Reactive Oxygen Species. *Biochim. Biophys. Acta Mol. Cell Res.* **2016**, *1863* (12), 2977–2992.

(6) Dixon, S. J.; Stockwell, B. R. The Role of Iron and Reactive Oxygen Species in Cell Death. *Nat. Chem. Biol.* **2014**, *10* (1), 9–17.

(7) Checa, J.; Aran, J. M. Reactive Oxygen Species: Drivers of Physiological and Pathological Processes. *J Inflamm Res* **2020**, *13*, 1057–1073.

(8) Liou, G.-Y.; Storz, P. Reactive Oxygen Species in Cancer. *Free Radic Res.* **2010**, *44* (5), 10.3109/10715761003667554.

(9) Sullivan, L. B.; Chandel, N. S. Mitochondrial Reactive Oxygen Species and Cancer. *Cancer Metab.* **2014**, *2* (1), 17.

(10) Lin, M. T.; Beal, M. F. Mitochondrial Dysfunction and Oxidative Stress in Neurodegenerative Diseases. *Nature* **2006**, *443* (7113), 787–795.

(11) Victor, V. M.; Rocha, M.; Herance, R.; Hernandez-Mijares, A. Oxidative Stress and Mitochondrial Dysfunction in Type 2 Diabetes. *Curr Pharm Design* **2011**, *17* (36), 3947–3958.

(12) Akhmedov, A. T.; Rybin, V.; Marín-García, J. Mitochondrial Oxidative Metabolism and Uncoupling Proteins in the Failing Heart. *Heart Fail. Rev.* **2015**, *20* (2), 227–249.

(13) Hu, J.; Dong, L.; Outten, C. E. The Redox Environment in the Mitochondrial Intermembrane Space Is Maintained Separately from the Cytosol and Matrix. *J. Biol. Chem.* **2008**, *283* (43), 29126–29134.

(14) Kussmaul, L.; Hirst, J. The Mechanism of Superoxide Production by NADH:Ubiquinone Oxidoreductase (Complex I) from Bovine Heart Mitochondria. *Proc. Natl. Acad. Sci.* **2006**, *103* (20), 7607–7612.

(15) Lambert, A. J.; Brand, M. D. Inhibitors of the Quinone-Binding Site Allow Rapid Superoxide Production from Mitochondrial NADH:Ubiquinone Oxidoreductase (Complex I). *J. Biol. Chem.* **2004**, *279* (38), 39414–39420.

(16) Turrens, J. F.; Alexandre, A.; Lehninger, A. L. Ubisemiquinone Is the Electron Donor for Superoxide Formation by Complex III of Heart Mitochondria. *Arch. Biochem. Biophys.* **1985**, *237* (2), 408–414.

(17) Yang, J.; Gupta, V.; Carroll, K. S.; Liebler, D. C. Site-Specific Mapping and Quantification of Protein S-Sulphenylation in Cells. *Nat Commun* **2014**, *5* (1), 4776.

(18) Shi, Y.; Fu, L.; Yang, J.; Carroll, K. S. Wittig Reagents for Chemoselective Sulfenic Acid Ligation Enables Global Site Stoichiometry Analysis and Redox-Controlled Mitochondrial Targeting. *Nat. Chem.* **2021**, *13* (11), 1140–1150.

(19) Akter, S.; Fu, L.; Jung, Y.; Conte, M. L.; Lawson, J. R.; Lowther, W. T.; Sun, R.; Liu, K.; Yang, J.; Carroll, K. S. Chemical Proteomics Reveals New Targets of Cysteine Sulfinic Acid Reductase. *Nat. Chem. Biol.* **2018**, *14* (11), 995–1004.

(20) Meng, J.; Fu, L.; Liu, K.; Tian, C.; Wu, Z.; Jung, Y.; Ferreira, R. B.; Carroll, K. S.; Blackwell, T. K.; Yang, J. Global Profiling of Distinct Cysteine Redox Forms Reveals Wide-Ranging Redox Regulation in C. Elegans. *Nat. Commun.* **2021**, *12* (1), 1415.

(21) Leichert, L. I.; Gehrke, F.; Gudiseva, H. V.; Blackwell, T.; Ilbert, M.; Walker, A. K.; Strahler, J. R.; Andrews, P. C.; Jakob, U. Quantifying Changes in the Thiol Redox Proteome upon Oxidative Stress in Vivo. *Proc. Natl. Acad. Sci.* **2008**, *105* (24), 8197–8202.

(22) Bechtel, T. J.; Li, C.; Kisty, E. A.; Maurais, A. J.; Weerapana, E. Profiling Cysteine Reactivity and Oxidation in the Endoplasmic Reticulum. *ACS Chem. Biol.* **2020**, *15* (2), 543–553.

(23) Shakir, S.; Vinh, J.; Chiappetta, G. Quantitative Analysis of the Cysteine Redoxome by Iodoacetyl Tandem Mass Tags. *Anal Bioanal Chem* **2017**, *409* (15), 3821–3830.

(24) Brandes, N.; Reichmann, D.; Tienson, H.; Leichert, L. I.; Jakob, U. Using Quantitative Redox Proteomics to Dissect the Yeast Redoxome. *J. Biol. Chem.* **2011**, *286* (48), 41893–41903.

(25) Abo, M.; Li, C.; Weerapana, E. Isotopically-Labeled Iodoacetamide-Alkyne Probes for Quantitative Cysteine-Reactivity Profiling. *Mol. Pharm.* **2017**, *15* (3), 743–749.

(26) Xiao, H.; Jedrychowski, M. P.; Schweppe, D. K.; Huttlin, E. L.; Yu, Q.; Heppner, D. E.; Li, J.; Long, J.; Mills, E. L.; Szpyt, J.; He, Z.; Du, G.; Garrity, R.; Reddy, A.; Vaites, L. P.; Paulo, J. A.; Zhang, T.; Gray, N. S.; Gygi, S. P.; Chouchani, E. T. A Quantitative Tissue-Specific Landscape of Protein Redox Regulation during Aging. *Cell* **2020**, *180* (5), 968-983.e24.

(27) van der Reest, J.; Lilla, S.; Zheng, L.; Zanivan, S.; Gottlieb, E. Proteome-Wide Analysis of Cysteine Oxidation Reveals Metabolic Sensitivity to Redox Stress. *Nat. Commun.* **2018**, *9* (1), 1581.

(28) Topf, U.; Suppanz, I.; Samluk, L.; Wrobel, L.; Böser, A.; Sakowska, P.; Knapp, B.; Pietrzyk, M. K.; Chacinska, A.; Warscheid, B. Quantitative Proteomics Identifies Redox Switches for Global Translation Modulation by Mitochondrially Produced Reactive Oxygen Species. *Nat. Commun.* **2018**, *9* (1), 324.

(29) Bak, D. W.; Pizzagalli, M. D.; Weerapana, E. Identifying Functional Cysteine Residues in the Mitochondria. *ACS Chem. Biol.* **2017**, *12* (4), 947–957.

(30) Shi, Y.; Fu, L.; Yang, J.; Carroll, K. S. Wittig Reagents for Chemoselective Sulfenic Acid Ligation Enables Global Site Stoichiometry Analysis and Redox-Controlled Mitochondrial Targeting. *Nat. Chem.* **2021**, *13* (11), 1140–1150.

(31) Yasueda, Y.; Tamura, T.; Fujisawa, A.; Kuwata, K.; Tsukiji, S.; Kiyonaka, S.; Hamachi, I. A Set of Organelle-Localizable Reactive Molecules for Mitochondrial Chemical Proteomics in Living Cells and Brain Tissues. *J. Am. Chem. Soc.* **2016**, *138* (24), 7592–7602.

(32) Lam, S. S.; Martell, J. D.; Kamer, K. J.; Deerinck, T. J.; Ellisman, M. H.; Mootha, V. K.; Ting, A. Y. Directed Evolution of APEX2 for Electron Microscopy and Proximity Labeling. *Nat. Methods* **2015**, *12* (1), 51–54.

(33) Roux, K. J.; Kim, D. I.; Raida, M.; Burke, B. A Promiscuous Biotin Ligase Fusion Protein Identifies Proximal and Interacting Proteins in Mammalian Cells. *J. Cell Biol.* **2012**, *196* (6), 801–810.

(34) Geri, J. B.; Oakley, J. V.; Reyes-Robles, T.; Wang, T.; McCarver, S. J.; White, C. H.; Rodriguez-Rivera, F. P.; Parker, D. L.; Hett, E. C.; Fadeyi, O. O.; Oslund, R. C.; MacMillan, D. W. C. Microenvironment Mapping via Dexter Energy Transfer on Immune Cells. *Science* **2020**, *367* (6482), 1091–1097.

(35) Wang, H.; Zhang, Y.; Zeng, K.; Qiang, J.; Cao, Y.; Li, Y.; Fang, Y.; Zhang, Y.; Chen, Y. Selective Mitochondrial Protein Labeling Enabled by Biocompatible Photocatalytic Reactions inside Live Cells. *JACS Au* **2021**, *1* (7), 1066–1075.

(36) Hung, V.; Zou, P.; Rhee, H.-W.; Udeshi, N. D.; Cracan, V.; Svinkina, T.; Carr, S. A.; Mootha, V. K.; Ting, A. Y. Proteomic Mapping of the Human

Mitochondrial Intermembrane Space in Live Cells via Ratiometric APEX Taggving. *Mol. Cell* **2014**, *55* (2), 332–341.

(37) Rhee, H.-W.; Zou, P.; Udeshi, N. D.; Martell, J. D.; Mootha, V. K.; Carr, S. A.; Ting, A. Y. Proteomic Mapping of Mitochondria in Living Cells via Spatially Restricted Enzymatic Tagging. *Science* **2013**, *339* (6125), 1328–1331.

(38) Branon, T. C.; Bosch, J. A.; Sanchez, A. D.; Udeshi, N. D.; Svinkina, T.; Carr, S. A.; Feldman, J. L.; Perrimon, N.; Ting, A. Y. Efficient Proximity Labeling in Living Cells and Organisms with TurboID. *Nat. Biotechnol.* **2018**, *36* (9), 880–887.

(39) Cho, K. F.; Branon, T. C.; Rajeev, S.; Svinkina, T.; Udeshi, N. D.; Thoudam, T.; Kwak, C.; Rhee, H.-W.; Lee, I.-K.; Carr, S. A.; Ting, A. Y. Split-TurboID Enables Contact-Dependent Proximity Labeling in Cells. *Proc. Natl. Acad. Sci.* **2020**, *117* (22), 12143–12154.

(40) Zhang, Y.; Li, Y.; Yang, X.; Wen, Z.; Nagalakshmi, U.; Dinesh-Kumar, S. P. TurboID-Based Proximity Labeling for In Planta Identification of Protein-Protein Interaction Networks. *J. Vis. Exp.* **2020**, No. 159, 10.3791/60728.

(41) Kim, D. I.; Kc, B.; Zhu, W.; Motamedchaboki, K.; Doye, V.; Roux, K. J. Probing Nuclear Pore Complex Architecture with Proximity-Dependent Biotinylation. *PNAS* **2014**, *111* (24), E2453–E2461.

(42) Lee, S.-Y.; Kang, M.-G.; Park, J.-S.; Lee, G.; Ting, A. Y.; Rhee, H.-W. APEX Fingerprinting Reveals the Subcellular Localization of Proteins of Interest. *Cell Rep.* **2016**, *15* (8), 1837–1847.

(43) Zimmer, A. D.; Walbrecq, G.; Kozar, I.; Behrmann, I.; Haan, C. Phosphorylation of the Pyruvate Dehydrogenase Complex Precedes HIF-1-Mediated Effects and Pyruvate Dehydrogenase Kinase 1 Upregulation

during the First Hours of Hypoxic Treatment in Hepatocellular Carcinoma Cells. *Hypoxia (Auckl)* **2016**, *4*, 135–145.

(44) The UniProt Consortium. UniProt: The Universal Protein Knowledgebase in 2021. *Nucleic Acids Res.* **2021**, *49* (D1), D480–D489.

(45) Calvo, S. E.; Clauser, K. R.; Mootha, V. K. MitoCarta2.0: An Updated Inventory of Mammalian Mitochondrial Proteins. *Nucleic Acids Res.* **2016**, *44* (Database issue), D1251–D1257.

(46) Mi, H.; Ebert, D.; Muruganujan, A.; Mills, C.; Albou, L.-P.; Mushayamaha, T.; Thomas, P. D. PANTHER Version 16: A Revised Family Classification, Tree-Based Classification Tool, Enhancer Regions and Extensive API. *Nucleic Acids Res.* **2021**, *49* (D1), D394–D403.

(47) Zong, S.; Wu, M.; Gu, J.; Liu, T.; Guo, R.; Yang, M. Structure of the Intact 14-Subunit Human Cytochrome C Oxidase. *Cell Res* **2018**, *28* (10), 1026–1034.

(48) Taanman, J. W.; Schrage, C.; Ponne, N.; Bolhuis, P.; de Vries, H.; Agsteribbe, E. Nucleotide Sequence of CDNA Encoding Subunit VIb of Human Cytochrome c Oxidase. *Nucleic Acids Res.* **1989**, *17* (4), 1766.

(49) Massa, V.; Fernandez-Vizarra, E.; Alshahwan, S.; Bakhsh, E.; Goffrini, P.; Ferrero, I.; Mereghetti, P.; D'Adamo, P.; Gasparini, P.; Zeviani, M. Severe Infantile Encephalomyopathy Caused by a Mutation in COX6B1, a Nucleus-Encoded Subunit of Cytochrome C Oxidase. *Am. J. Hum. Genet.* **2008**, *82* (6), 1281–1289.

(50) Stroud, D. A.; Surgenor, E. E.; Formosa, L. E.; Reljic, B.; Frazier, A. E.; Dibley, M. G.; Osellame, L. D.; Stait, T.; Beilharz, T. H.; Thorburn, D. R.; Salim, A.; Ryan, M. T. Accessory Subunits Are Integral for Assembly and Function of Human Mitochondrial Complex I. *Nature* **2016**, *538* (7623), 123–126.

(51) Eng, J. K.; McCormack, A. L.; Yates, J. R. An Approach to Correlate Tandem Mass Spectral Data of Peptides with Amino Acid Sequences in a Protein Database. *J. Am. Soc. Mass Spectrom.* **1994**, *5* (11), 976–989.

(52) Tabb, D. L.; McDonald, W. H.; Yates, J. R. DTASelect and Contrast: Tools for Assembling and Comparing Protein Identifications from Shotgun Proteomics. *J. Proteome Res.* **2002**, *1* (1), 21–26.

(53) Weerapana, E.; Wang, C.; Simon, G. M.; Richter, F.; Khare, S.; Dillon, M. B. D.; Bachovchin, D. A.; Mowen, K.; Baker, D.; Cravatt, B. F. Quantitative Reactivity Profiling Predicts Functional Cysteines in Proteomes. *Nature* **2010**, *468* (7325), 790–795.

(54) Supek, F.; Bošnjak, M.; Škunca, N.; Šmuc, T. REVIGO Summarizes and Visualizes Long Lists of Gene Ontology Terms. *PLOS ONE* **2011**, *6* (7), e21800.

Chapter 4

Combining Redox Proteomics and Proximity Labeling with APEX to Monitor Localized Cysteine Oxidation in ROS Hotspots

Introduction

Reactive oxygen species (ROS) are essential signaling molecules that regulate a variety of physiological processes.[1] However, imbalances in redox homeostasis can result in numerous pathologies from neurodegeneration[2] and cancer[3] to diabetes[4] and cardiopathy.[5] ROS-mediated signaling relies upon reversible oxidative posttranslational modifications (oxPTMs) on cysteine thiols including sulfenylation (SOH), *s*-nitrosation (SNO), *s*-glutathionylation (GSH) and disulfide bond formation.[6] The transient nature of many of the cysteine ox-PTMs governs their amenability to participate in cellular signaling pathways through directly impacting protein structure, enzymatic activity, complex formation, localization, and degradation.[7-11] Importantly, due to the high reactivity of ROS and the ubiquitous presence of subcellular antioxidants, the diffusion distance of ROS from the site of generation is limited. As a result, different subcellular regions maintain unique redox environments and varying levels of oxidized cysteine residues. Additionally, even within subcellular compartments, the distribution of ROS is non-uniform, whereby regions of elevated ROS, termed ROS hotspots, exist. Cysteine oxidation is amplified within these ROS hotspots relative to other regions of the cell. Identifying cysteine oxidation events within specific subcellular ROS hotspots is key to understanding the localized and divergent effects of cellular ROS as well as may provide insight into uncharacterized ROS-regulated pathways.

The majority of ROS is generated in the mitochondria by the electron transport chain (ETC). Specifically, the flavin-cofactor binding and terminal electron transfer sites of complex I[12-14] and quinone exchanging sites of complex III[15] each routinely leak electrons leading to localized ROS production. As a result,

proteins in immediate proximity to these complexes are likely exposed to higher levels of ROS and are thereby oxidized to a higher extent. It is therefore important to directly monitor the extent of cysteine oxidation within mitochondrial ROS hotspots, as it would inform on proteins whose function is most significantly impact by the ETC-generated ROS. Although mitochondria are the cornerstone ROS producers, other regions including the cytosol and extracellular space are known to be involved in highly sensitive, pathway-triggering ROS bursts critical for cell-type differentiation[16,17], immune system activation[18], and wound healing.[19]

Unlike in the mitochondria, cytosolic ROS generating enzymes are typically plasma membrane bound and responsive to ligand-receptor binding at the cell surface. For example, NADPH oxidase (NOX) is the primary generator of cytosolic and extracellular peroxide.[20] NOX can undergo secondary activation through multiple initiation events including EGF-receptor binding or cytokine recognition such as tumor necrosis factor alpha (TNFα)[21], interferon gamma (IFNγ) or lipopolysaccharide (LPS) by toll-like receptors (TLRs) on macrophage.[22] Although activation events are favorable to specific cell types and lead to a variety of signaling cascades from proliferation to differentiation, each prompting of NOX results in a concentrated extracellular superoxide release which is converted to H_2O_2 by SOD3 and re-enters the cytosol via aquaporin pores on the cell surface.[23,24] Identifying ROS targets within ROS hotspots is invaluable in determining the role of cysteine oxidation within (patho)physiological states. Specifically, accessing unique intracellular sites of cysteine oxidation may offer ligandable therapeutic targets in mediating disease progression.

Recent advances in enzymatic proximity labeling (PL) have allowed for robust, regional proteomic acquisition bypassing organelle isolation. At the

forefront of enzymatic PL efforts emerged a cytosolic, plant ascorbate peroxidase (first-generation APEX[25] and second-generation APEX2[26]) engineered by the Ting lab as a promiscuous peroxidase able to convert phenol to a phenoxy radical. The flexibility in the parent phenol compound structure provides applications from electron microscopy imaging with diaminobenzidine-phenol to proteomic interactome mapping with biotin-phenol.[26,27] The core heme-iron center of APEX is responsible for the unique peroxide-dependent mechanism of action in which peroxide is chelated by Fe^{II} which is subsequently oxidized to Fe^{III}, while providing a single electron transfer to the phenol. These phenoxy radical species label surrounding electron-rich amino acids (i.e. tyrosine) providing proximal protein tagging, Figure 4-1.

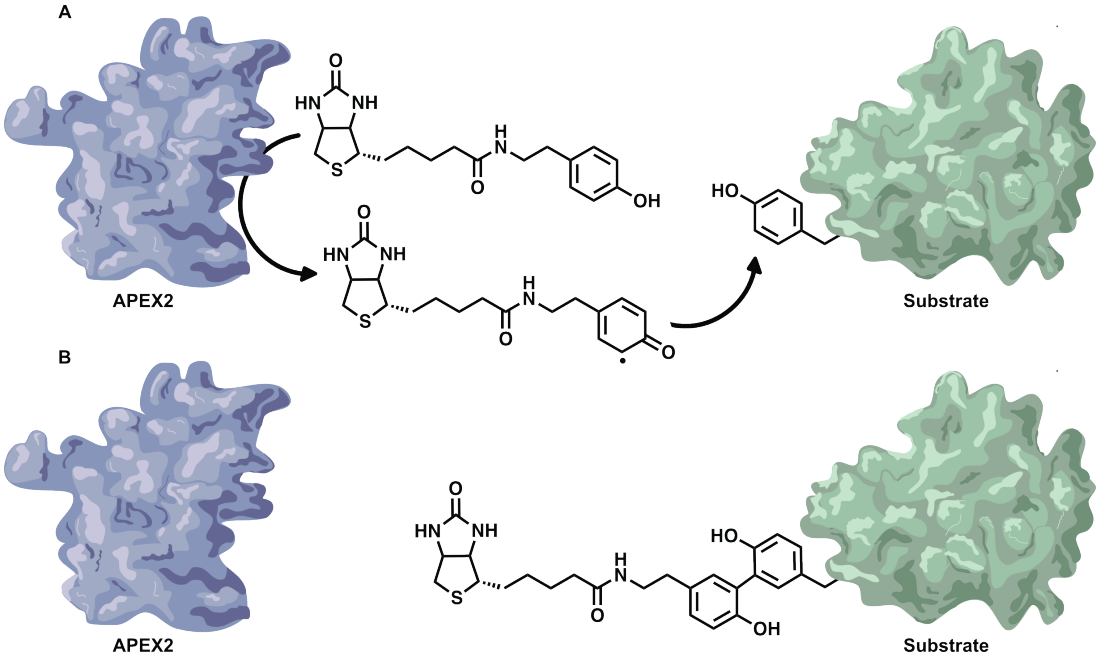


Figure 4-1. Radical mechanism of APEX proximity-dependent labeling with activation of biotin phenol to biotin phenoxy radical with resolution and covalent modification on adjacent tyrosine residue.

Driven by a radical mechanism, APEX's robust labeling capabilities (<1 minute) deliver instant protein interactome and localization snapshots that can be leveraged for both spatial and temporal sensitive experiments. Furthermore, the APEX PL-platform improves comprehension of mitochondrial protein composition through chimeric pre-sequence guiding to the matrix[28] and IMS.[27] Unlike other PL methods using biotin ligases (BirA*)[29], the reliance on peroxide for catalysis makes APEX an attractive strategy for infiltrating ROS hotspots within the subcompartments of cells with high ROS levels. With this work, we adapt the PL-OxICAT platform (Figure 4-2), incorporating proximal peroxide-dependent biotinylation by APEX, to specifically monitor cysteine oxidation events within

localized subcellular ROS hotspots. Here, we exclude the exogenous ROS addition that is required for APEX PL studies, and instead generate intracellular ROS by activating known ROS-generating systems, such as the ETC and NADPH oxidases.[30] The resulting endogenous ROS will activate proximity labeling by APEX only in regions where ROS levels are elevated, thereby enabling redox proteomics studies on proteins localized within ROS hotspots. This study further expands the toolkit for redox proteomics by allowing for localized evaluation of cysteine oxidation within very specific intracellular regions. Together, we aim to improve regio-selectivity in mapping cysteine disposition and precision in identifying redox-sensitive cysteines providing insight on therapeutically relevant oxidation signaling.

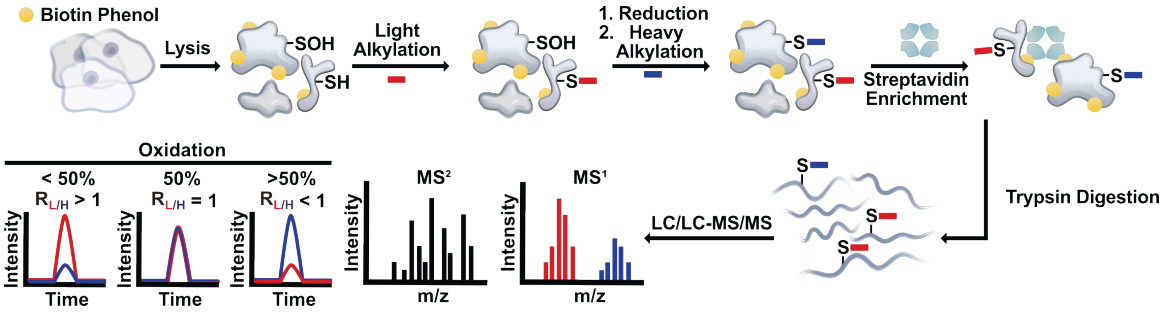


Figure 4-2. Workflow for PL-OxICAT includes differential alkylation of reduced and oxidized thiols with isotopically light and heavy species, enrichment of biotinylated proteins, trypsin digestion, and quantitative MS analysis to identify and quantify cysteine oxidation.

Results and Discussion

PL-OxICAT with APEX enables quantification of cysteine oxidation events within ROS hotspots.

Upon demonstrating the utility of PL-OxICAT with TurboID to enrich and quantify cysteine oxidation within specific subcellular compartments (Chapter 3), we sought to develop a complementary technology that would allow us to selectively monitor oxidation of proteins localized within ROS hotspots. ROS hotspots are regions of high levels of ROS that typically surround the source of ROS generation. Here we shifted our focus to the PL method APEX, which is a peroxidase that upon treatment with exogenous hydrogen peroxide activates biotin-phenol to biotinylate proteins within spatially confined cellular locations. We hypothesized that we could substitute the exogenous hydrogen peroxide with endogenously produced hydrogen peroxide to activate APEX and biotinylate proteins proximal to the source of ROS. Since ROS levels are elevated within ROS hotspots, we sought to determine if these endogenous ROS levels were sufficiently high to activate APEX selectively within these localized ROS hotspots. We first focused on ROS hotspots within the mitochondria, where ROS is known to be produced by components of the ETC. [31,32] Treatment of cells with the ETC inhibitors, Antimycin A (AMA), a complex III Q-cycle inhibitor[33], and Oligomycin (Oligo), an ATP-synthase proton translocation inhibitor[34], are known to increase ROS levels in the mitochondrial matrix[35-37]. Since activation of APEX by endogenous ROS has not previously been demonstrated, we initially focused on localizing APEX to the mitochondrial matrix to determine if ETC inhibition would sufficiently increase hydrogen peroxide levels to induce APEX activation and subsequent biotinylation of mitochondrial proteins (Figure 4-3).

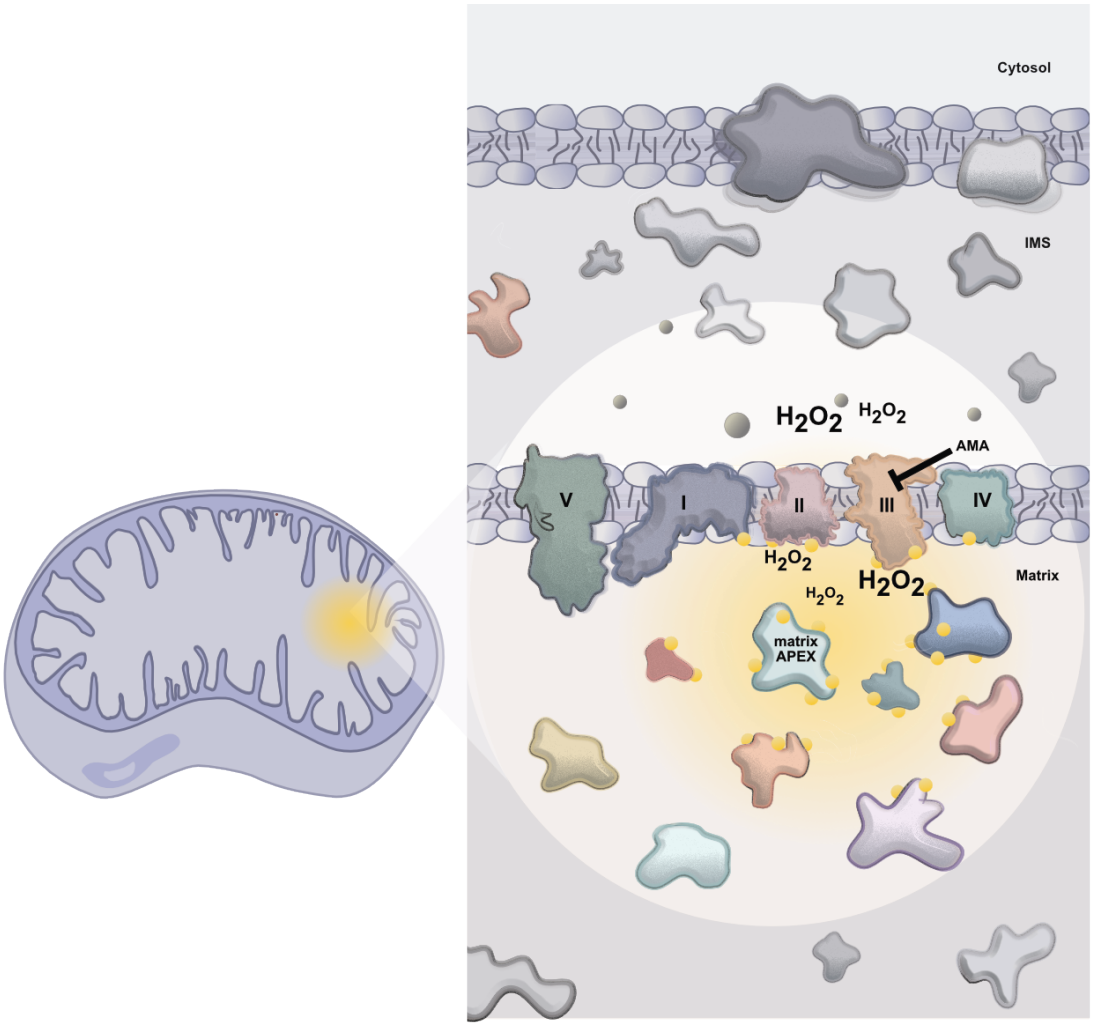


Figure 4-3. Schematic of matrix-APEX activation in endogenous ETC-inhibitor derived ROS hotspot in the mitochondrial matrix.

To localize APEX to the mitochondrial matrix, we generated a construct whereby APEX2 was fused to the C-terminus of PDK1 to produce a PDK1-V5-APEX2 protein, termed matrix-APEX. A cytosol localized construct (cyto-APEX) was also generated as a control that would express APEX only within the cytosol. HEK 293T cells stably expressing both matrix-APEX and cyto-APEX were

generated using lentiviral transduction. Immunofluorescence imaging using an anti-V5 antibody confirmed expression and mitochondrial localization of matrix-APEX (Figure 4-4). In contrast, cyto-APEX was shown to be expressed only within the cytosol (Figure 4-4). We then confirmed that both APEX constructs were functional by evaluating biotinylation upon treatment with biotin-phenol and exogenous hydrogen peroxide. Matrix-APEX and cyto-APEX expressing cells pre-treated with biotin-phenol were treated for 1 min with increasing concentrations of hydrogen peroxide, prior to cell lysis and evaluation of biotinylation using western blot analysis (Figure 4-5). The level of biotinylation increased with peroxide concentration for both constructs, confirming that the APEX constructs were functionally active. Notably, the pattern of biotinylated bands was significantly different between cyto-APEX and matrix-APEX, serving as further confirmation that these APEX constructs were expressed in different subcellular locations. Importantly, standard APEX experiments are performed using 1 mM hydrogen peroxide treatment[40], however, we observed detectable levels of biotinylation at concentrations as low as 100 μM. The observation that APEX-mediated biotinylation can occur at lower and more physiologically relevant hydrogen peroxide concentrations, known to be in the pico to micromolar range[38,39], supported the potential of using endogenous ROS sources for APEX activation.

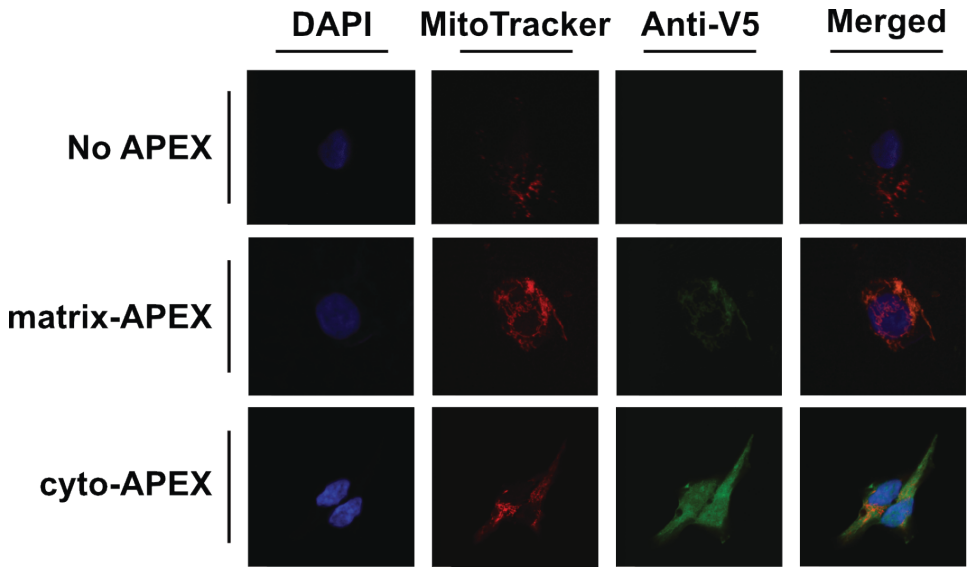


Figure 4-4. Confirmation of intracellularly-guided APEX2 expression in HEK293T cells. Immunofluorescence imaging of wild-type (WT), cytosolic (V5-APEX2), and mitochondrial matrix (PDK1-APEX2) expressing HEK293T cells. Fusion proteins contain V5 epitope tags for visualization (green, AlexaFluor488). APEX2 expression was overlayed with nuclear DAPI stain (blue) and mitochondria stain by MitotrackerCMXRedROS (red).

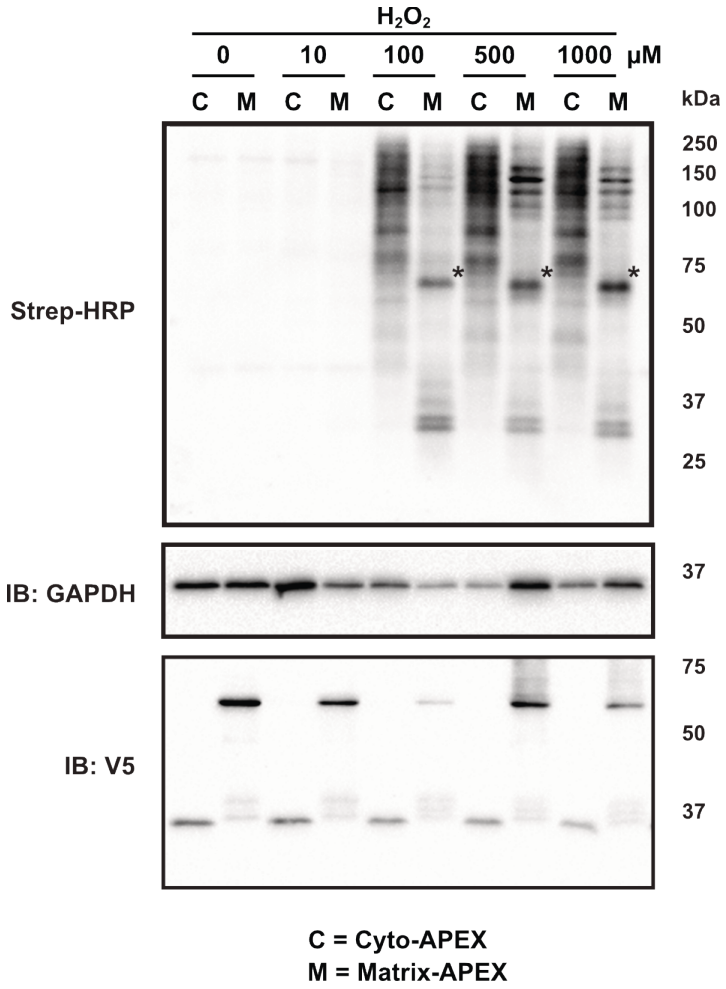


Figure 4-5. Expression and activity of PDK1 (P) and Cytosolic (C) APEX2 with increasing peroxide treatment. Western blotting of HEK293T cells overexpressing PDK1-V5-APEX2 and Cytosolic V5-APEX2 subjected to increasing concentrations of H2O2 for 1 min followed by quenching with 3 washes of quenching buffer (QB) and 3 washes of DPBS. Protein expression was visualized by anti-V5 blotting. Strep-HRP blotting allowed for investigation of APEX2 substrate biotin labeling.

Upon confirming activation of matrix-APEX with exogenous hydrogen peroxide, we next evaluated the effectiveness of endogenous ROS as an APEX activator. Matrix-APEX expressing cells were treated with biotin-phenol prior to inducing ROS generation. To induce ROS generation in the mitochondria, we treated cells with the ETC inhibitors, AMA and Oligo, and monitored protein biotinylation using western blot analysis. The concentrations of ETC inhibitors used (100 μM AMA and 10 μM Oligo) were optimized for maximal ROS generation without the induction of cell death. AMA treatment led to a significant increase in protein biotinylation, whereas Oligo treatment showed negligible levels of biotinylation (**Figure 4-6**). This is expected as AMA is a more direct inducer of ROS compared to Oligo and is known to have a markedly reduced level of ROS generation.[35,36,40] Given that Oligo alone did not produce detectable biotinylation, the combined treatment with both AMA and Oligo did not increase biotinylation levels relative to AMA alone. These studies confirm that the endogenous ROS generated by AMA-mediated inhibition of Complex III is sufficient to generate detectable levels of protein biotinylation through activation of matrix-localized APEX.

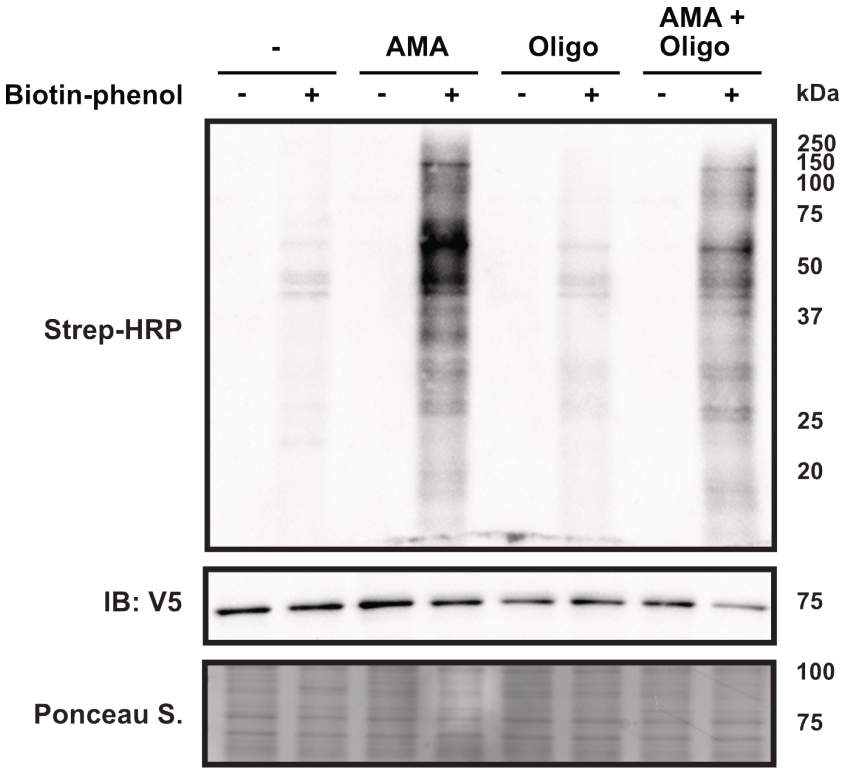


Figure 4-6. Western blot analysis of HEK 293T lysates expressing matrix-APEX. Cells were treated with DMSO (-) or 500 μM biotin-phenol (+) for 45 min followed by the addition of ETC inhibitors, AMA (100 μM) and Oligo (10 μM), or additional DMSO (-) for a supplementary 45 min. Biotinylated proteins were visualized using strep-HRP. Expression of APEX was confirmed using anti-V5, and Ponceau staining used to normalize protein loading.

We then proceeded to use the PL-OxICAT platform to identify biotinylated proteins and quantify the percentage of cysteine oxidation within ROS hotspots resulting from AMA treatment. Briefly, cells pre-treated with biotin-phenol were then treated with AMA and subjected to the OxICAT workflow described previously (Figure 4-2). The resulting MS analysis identified 1322 proteins, of

which 389 (29%) were localized to the mitochondria (Figure 4-7, Table 4A-1). MS analysis of the corresponding control sample that was not treated with AMA generated significantly fewer protein identifications, since APEX is likely minimally activated without a significant influx of hydrogen peroxide (Figure 4-7). GO analysis confirmed enrichment of mitochondria-localized pathways, including oxidation-reduction processes (Table 4A-2). Comparing the total proteins identified in the matrix-APEX data to our matrix-TID data showed 961 proteins shared across these two PL methods, with 310 overlapping mitochondrial proteins (Figure 4-8). These data confirm that matrix-APEX is localized to the mitochondria and activation by endogenous ROS produced by AMA treatment results in selective biotinylation of mitochondrial proteins.

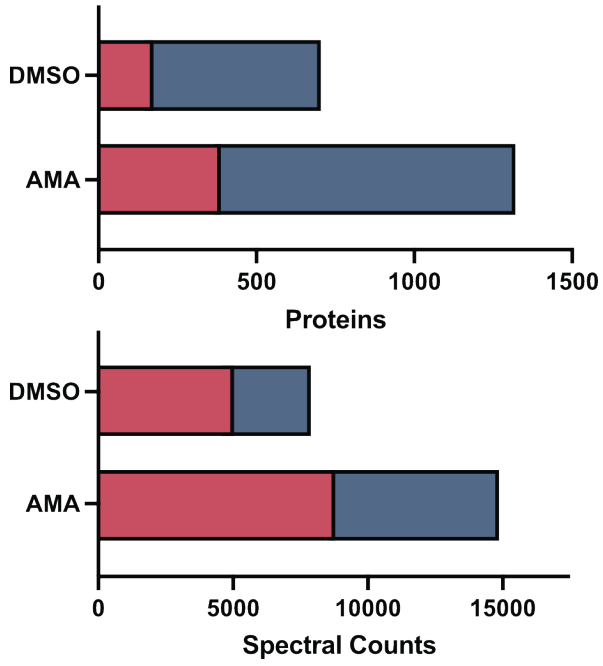


Figure 4-7. Quantification of total (blue) and mitochondrial (red) proteins and spectral counts identified in DMSO and AMA treated matrix-APEX cells.

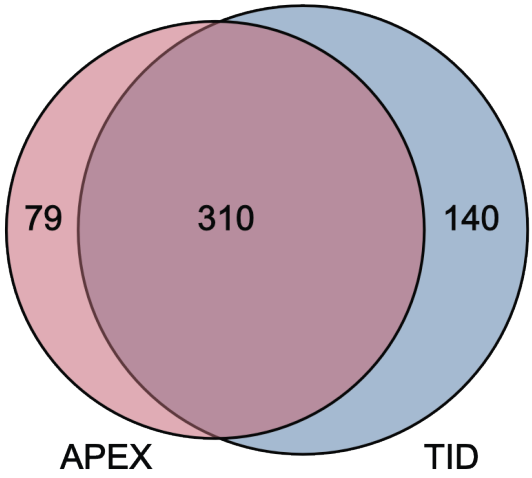


Figure 4-8. Venn diagram showing overlap between proteins identified in matrix-TID (blue) and matrix-APEX (red) datasets.

We then focused on cysteine-containing peptides identified within the matrix-APEX dataset. A total of 2200 cysteines were identified, of which 883 were cysteines that resided on 271 mitochondrial proteins (Table 4A-3). Filtering these hits for those cysteines for which light:heavy ratios were determined across at least two replicates, generated percent oxidation values for 427 cysteines (Figure 4-9, Table 4A-4). The majority of identified cysteines (75%) were found to be highly reduced (<20% oxidation), with 4% of cysteines (16) found to be in a highly oxidized (>50% oxidized) state. Within this subset of highly oxidized cysteines were several well-characterized sites of cysteine oxidation. For example, oxidation of C385 in aconitase 2 (ACO2) is known to inhibit enzymatic activity through loss of a critical [4Fe-4S] cofactor. [41,42] Additionally, C47, the peroxidatic cysteine of peroxiredoxin 6 (PRDX6), is known to form a sulfenic acid in the presence of ROS.[43]

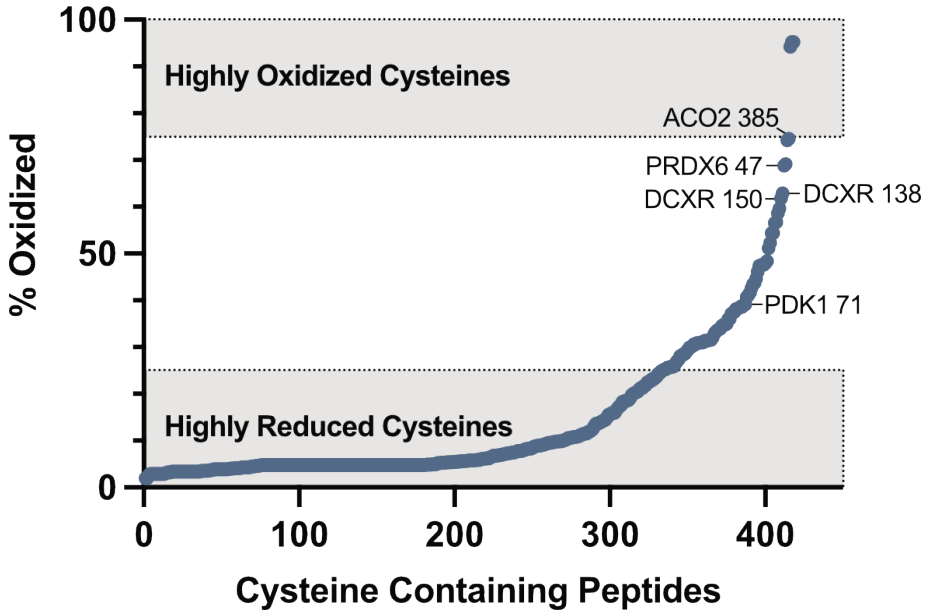


Figure 4-9. Percent oxidation values for mitochondrial cysteines identified in the matrix-APEX sample under AMA treatment.

The cysteine oxidation events determined in the matrix-APEX sample were compared to the matrix-TID sample. There were 164 cysteines for which percent oxidation values were obtained in both samples, and comparison of percent oxidation values for these cysteines show an overall increased degree of oxidation in the matrix-APEX relative to the matrix-TID (Figure 4-10). For example, within this overlapping subset of cysteines, the matrix-APEX sample contained 36 cysteines that were >20% oxidized, compared to 3 cysteines in the matrix-TID sample. These values thereby confirm that the percentage of oxidation of cysteines within ROS hotspots is generally higher than across the entire mitochondrial matrix. For example, C385 of ACO2 is ~5% oxidized under resting conditions (matrix-TID), and the degree of oxidation increases to 74% within ROS hotspots

(matrix-APEX). Similarly, C138 and C150 on *L*-xylulose reductase (DCXR) is known to form a disulfide bond in the presence of ROS, and disulfide-bond formation restricts catalytic activity.[44,45] These cysteines show 60% and 59% oxidation within ROS hotspots, but only 37% and 7% oxidation under resting conditions. Interestingly, conserved and highly reactive C71 on PDK1 also shows increased oxidation from 4% to 38%.[46]

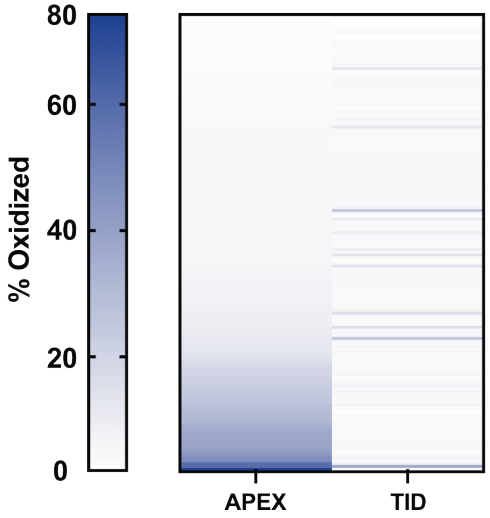


Figure 4-10. Heat map comparing the percent oxidation for 164 cysteines identified in both matrix-APEX and matrix-TID samples (Chapter 3).

We then compared the biotinylation profile and percent oxidation for mitochondrial cysteines upon induction of endogenous versus exogenous ROS. Matrix-APEX cells were treated with 1 mM hydrogen peroxide for 1 min to generate global cellular ROS. We then compared the cysteine oxidation profiles upon exogenous hydrogen peroxide treatment to endogenous ROS generation via AMA treatment. There was 86% and 56% overlap in the mitochondrial proteins

and cysteines identified across these two datasets (Figure 4-11A). Within the subset of 206 cysteines with calculated percent oxidation values that overlapped, we observed an overall increase in oxidation in the AMA-treated sample, relative to the hydrogen peroxide-treated sample (Figure 4-11B, Table 4A-5), again indicating that cysteine oxidation events are magnified within ROS hotspots.

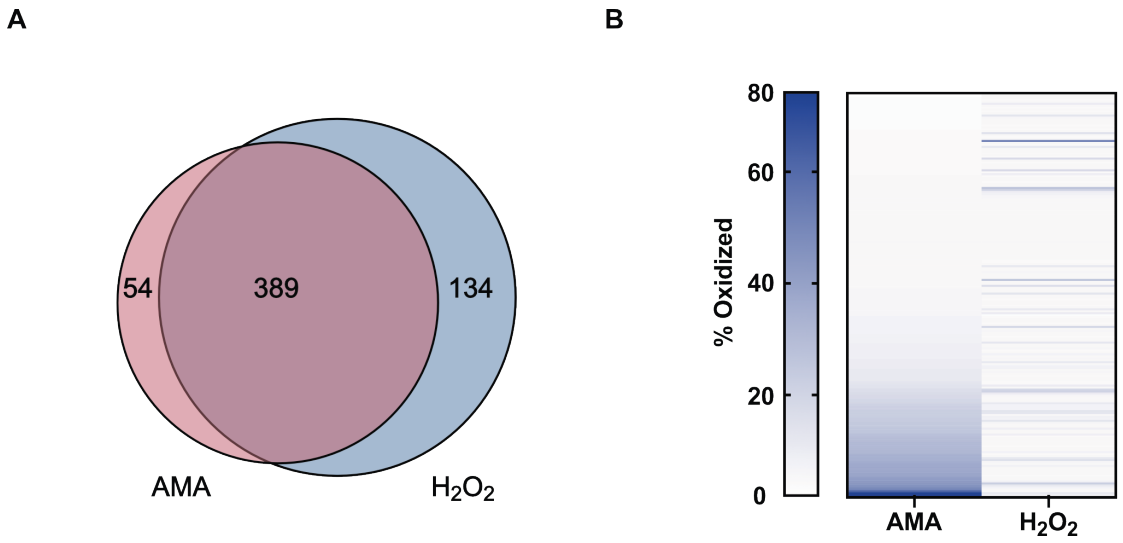


Figure 4-11. (A) Venn diagram showing overlap between proteins identified in matrix-APEX cells treated with hydrogen peroxide (blue) and AMA (red). (B) Heat map comparing the percent oxidation for cysteines identified in both matrix-APEX activated by AMA and peroxide.

To determine if cysteine oxidation observed using AMA treatments was specific to cysteines in mitochondrial ROS hotspots generated by ETC inhibition, matrix-APEX cells were treated with 100 μM H_2O_2 for the same amount of time (45 min). Similar to 1 mM H_2O_2 APEX activation, no significant enrichment in oxidized cysteines was observed. Compared to matrix-APEX activation through AMA-

induced ROS which gave a total of 81 mitochondrial cysteines (20%) above 25% oxidized with 15 cysteines (3.7%) greater than 50% oxidized, a smaller number of mitochondrial cysteines (11 out of 485 total cysteines, 2.3%) were identified to be over 25% oxidized with only 1 cysteine (0.2%) above 50% oxidized with 100 μM H_2O_2 treatments (Figure 4-12, Table 4A-6). Comparatively, 1 mM H_2O_2 treatments gave 13 mitochondrial cysteines (2.2%) greater than 25% oxidized and only 5 cysteines (0.85%) greater than 50% oxidized (Figure 4-12, Table 4A-5). Interestingly, similar trends in cysteine oxidation were observed for our DMSO control and peroxide treated matrix-APEX samples (Figure 4-12). As mitochondria produce basal levels of ROS during ordinary metabolic function, we identified % oxidation on a small subset of cysteines within the mitochondria without auxiliary endogenous or exogenous ROS. Of the L:H ratios calculated for 130 mitochondrial cysteines identified in the DMSO treated sample, as expected a minority of cysteines (11) were greater than 25% oxidized with 6 cysteines greater than 50% oxidized. These data support our hypothesis that matrix-APEX activation by endogenous mtROS (through AMA treatments) allows for exclusive resolution of cysteine oxidation events in areas of high ROS concentrations, presumably closest to the site of production in the matrix.

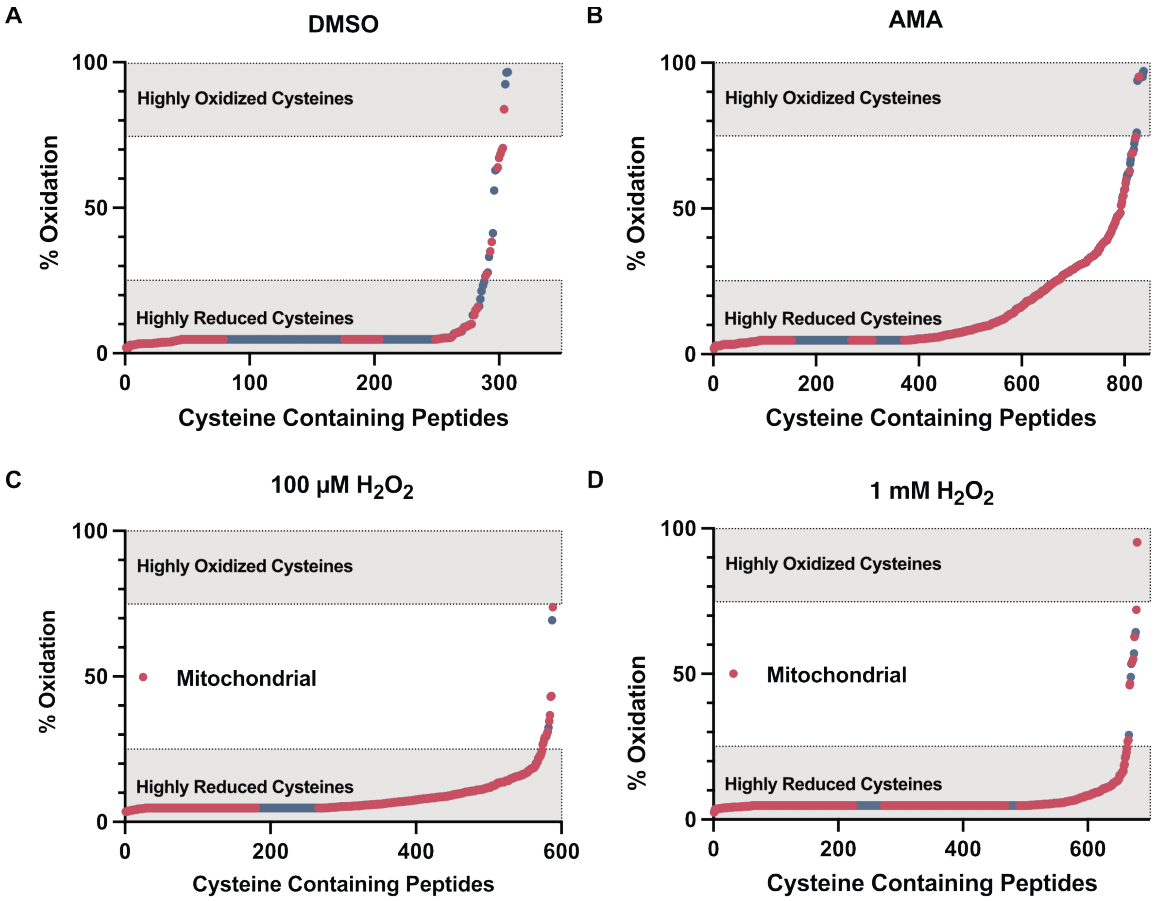


Figure 4-12. Percent oxidation values for mitochondrial cysteines identified in the matrix-APEX sample during treatments with DMSO, AMA, and peroxide (100 μM for 45 min or 1 mM for 1 min).

PL-OxICAT with APEX identifies cysteine oxidation events induced by macrophage differentiation.

To demonstrate the generality of PL-OxICAT with APEX to other ROS hotspots outside of the mitochondria, we induced endogenous ROS through activation of NADPH oxidase (NOX) in Raw 264.7 mouse macrophages (Figure 4-13). [1,47,48] It is known that cytokine treatment results in NOX activation and generation of cellular hydrogen peroxide that subsequently regulates a

transcriptional program essential for macrophage differentiation.[20,24,49] The ROS generated by NOX is released extracellularly but is known to diffuse into the cytosol to generate intracellular ROS hotspots proximal to the plasma membrane. We therefore generated a Raw 264.7 cell line that stably expressed cyto-APEX. Cytosolic localization was confirmed by immunofluorescence (**Figure 4-14**). Macrophage activation was initiated by treatment with interferon-γ (IFNγ) and lipopolysaccharides (LPS).[50] Previous studies reported that peroxide concentrations reach a maximum after 20 hours of IFNγ/LPS treatment.[51] Based on these reports, the cyto-APEX Raw 264.7 cell line was treated with cytokines for 20 hours, prior to addition of biotin-phenol. Protein biotinylation was monitored by western blot, and observable biotinylation signal was detected upon LPS treatment, confirming that NOX-generated ROS levels are sufficiently high to activate APEX. Minimal biotinylation was observed for IFNγ treatment and therefore all subsequent experiments used LPS for APEX activation (Figure 4-15).

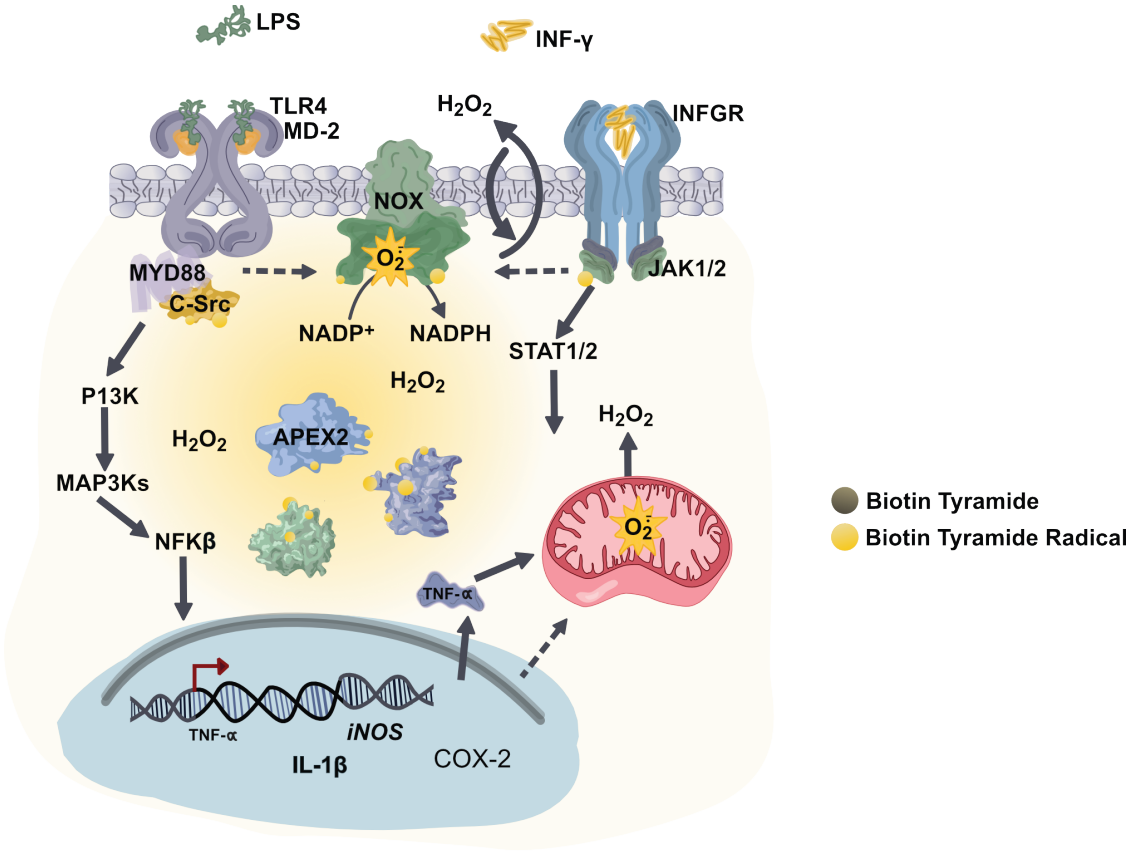


Figure 4-13. Schematic of cyto-APEX activation in cytosolic ROS hotspot in Raw 264.7 cells. Endogenous ROS is generated by NOX activation under cytokine-receptor binding.

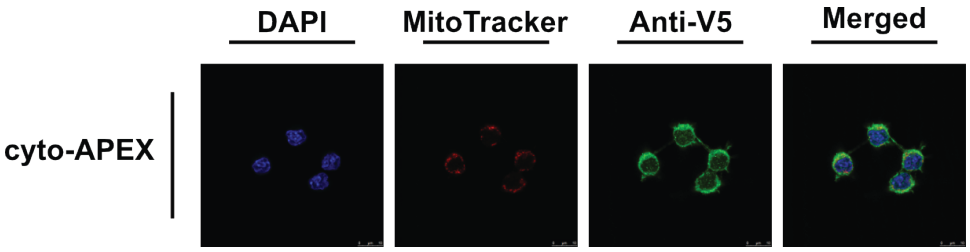


Figure 4-14. Immunofluorescence imaging of Raw 264.7 cells expressing cyto-APEX. APEX expression was monitored using anti-V5 (green), mitochondria were

stained with Mitotracker Red CMXROS (red), and the nucleus was stained with DAPI (blue).

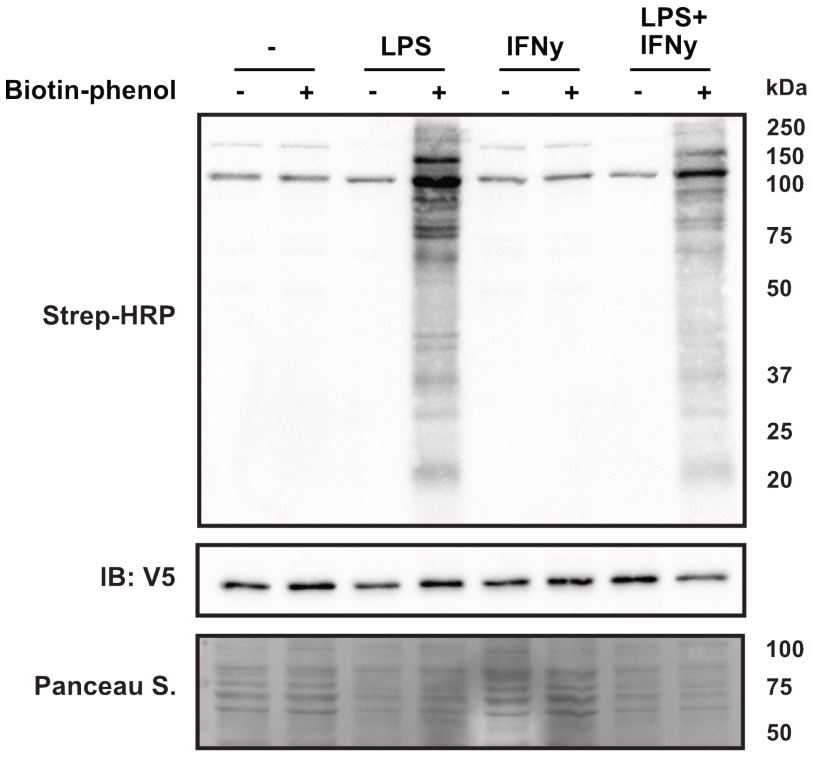


Figure 4-15. Western blot analysis of Raw 264.7 lysates expressing cyto-APEX. Cells were treated with 1 μg/mL LPS and 10 ng/mL IFNγ treatment for 20 hours prior to a 2.5 hour treatment with 500 μM biotin-phenol (+) or DMSO (-). Biotinylated proteins were visualized using strep-HRP. Expression of APEX was confirmed using anti-V5, and Ponceau staining used to normalize protein loading.

We then proceeded to perform the PL-OxICAT analysis, where cyto-APEX Raw 264.7 cells were treated with and without LPS for 20 hours, followed by biotin-phenol addition. Cell lysates were subjected to the OxICAT workflow as described previously. MS analysis identified 1627 proteins in the LPS-treated sample, compared to 376 proteins in the absence of LPS (Figure 4-16, Table 4A-7).

This increase in biotinylated proteins upon LPS treatment is expected since the increased ROS levels lead to APEX activation and enhanced biotinylation relative to the untreated sample. The majority of identified proteins (66%) were annotated as cytosolic proteins, confirming the cytosolic localization of cyto-APEX. Interestingly, 423 plasma membrane proteins were identified to be biotinylated with the cyto-APEX construct, which is expected since NOX is membrane localized, and the highest levels of ROS are likely to be localized proximal to the cell membrane (Figure 4-16, Table 4A-7). Furthermore, GO analysis of the proteins identified in the cyto-APEX Raw 264.7 cells revealed enrichment for cytosolic and differentiation-related processes including regulation of type-I interferon production, cytoplasmic translation initiation, and glycolysis (Table 4A-8).

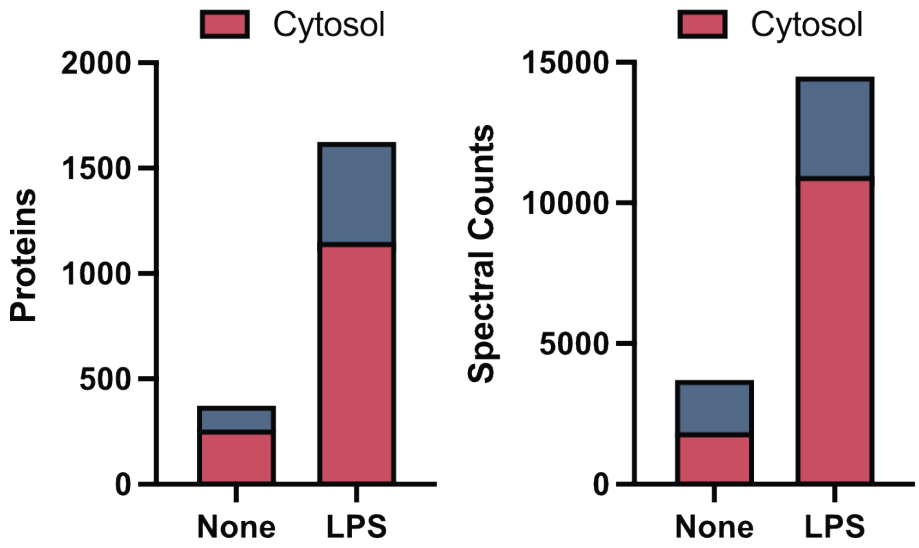


Figure 4-16. Quantification of total (blue) and cytosolic (red) proteins and spectral counts identified in DMSO and LPS treated cyto-APEX Raw 264.7 cells.

The PL-OxICAT analysis of cyto-APEX in the presence of LPS identified 1777 cysteine-containing peptides (Table 4A-9). Of these, light:heavy ratios and corresponding percent oxidation values were calculated for 599 cysteines (Figure 4-17, Table 4A-10). Of these cysteines, 499 were >50% oxidized. Examples of highly oxidized cysteines include C480 and C482 of the NOX-promoting inflammatory messenger (NOTCH2) were 95% oxidized.[52,53] These cysteines are annotated as extracellular disulfides.[54] Additionally, four cysteines, C33, C857, C938 and C629, on inducible nitric oxide synthase (NOS2) were identified to be 68-87% oxidized. NOS2 expression is known to be induced by NOX activation and LPS stimulation.[55, 21] Furthermore, we identify high oxidation (94%) of an extracellular disulfide-bonded cysteine, C353 on toll-like receptor 2 (TRL2) which is known to mediate innate immunity and inflammatory responses to bacterial lipopeptides by activating MYD88 resulting in cytokine release through nuclear factor- κB (NF-κB) and mitogen activating protein kinase (MAPK).[56,57] Identification of these previously characterized oxidized cysteines on proteins known to localize with NOX, where ROS levels are highest, serve to confirm the ability of our PL-OxICAT strategy to enrich proteins within ROS hotspots.

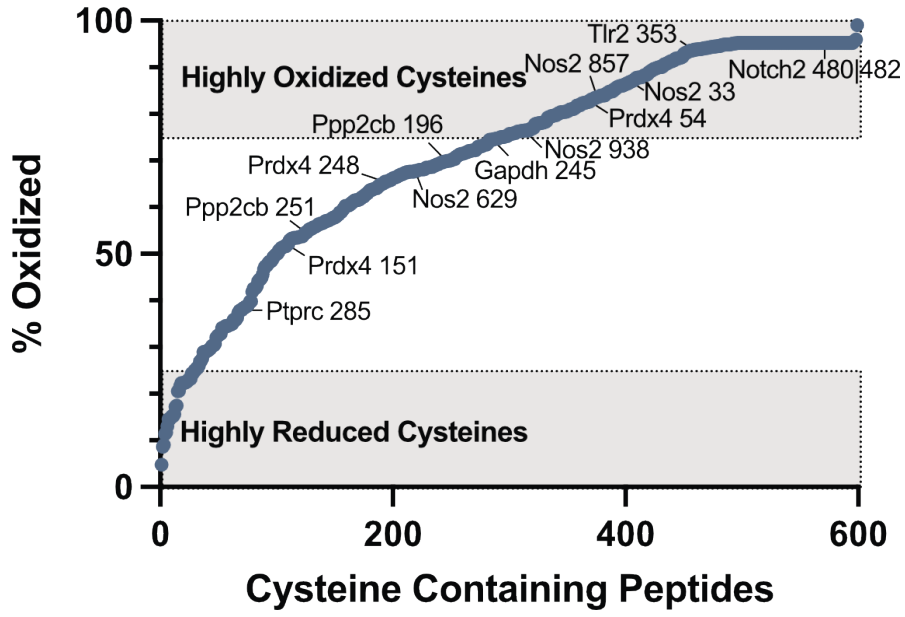


Figure 4-17. Quantification of total (blue) and cytosolic (red) proteins and spectral counts identified in DMSO and LPS treated cyto-APEX Raw 264.7 cells.

Interestingly, multiple cysteines were identified to be oxidized on the detoxifying enzyme peroxiredoxin 4 (PRDX4), including the resolving cysteine, C248 (65% oxidized). Additionally, non-catalytic cysteines C54 and C151 on PRDX4 were also identified to be 83% and 52% oxidized, respectively. These cysteines are implicated in oligomerization and activation of PRDX4 under oxidizing conditions.[58] PRDX4 is known to mediate redox signaling events in the cytosol upon LPS stimulation of macrophages, and our data demonstrates the presence and increased oxidation of PRDX4 within ROS hotspots generated during pro-inflammatory signaling.[59-61] Additionally, we identified oxidized cysteines on several proteins involved in glycolysis (Figure 4-18). This was notable because many glycolytic enzymes have previously been identified as targets of

oxidation.[62-64] For example, we identified C245 on glyceraldehyde 3-phosphate dehydrogenase (GAPDH) to be 74% oxidized. This cysteine is known to be a site of *S*-nitrosation and sulfinylation in human GAPDH.[65] Lastly, several phosphatases and kinases involved in regulating the cell cycle and cellular differentiation were identified to be oxidized. For example, C285 on receptor-type tyrosine-protein phosphatase C (PTPRC), a central receptor in T-cell activation upon cytokine engagement, was identified to be 38% oxidized.[66] Additionally, C196 and C251 on serine/threonine-protein phosphatase 2A (PPP2CB), a modulator of a variety of kinases including ERK1/2 MAPK signaling cascades, was found to be 70% and 54% oxidized, respectively.[67,68] Together, our data demonstrate that cysteines on a diverse array of proteins involved in redox regulation, metabolism, and phosphorylation, are localized and oxidized within ROS hotspots during immune-cell activation.

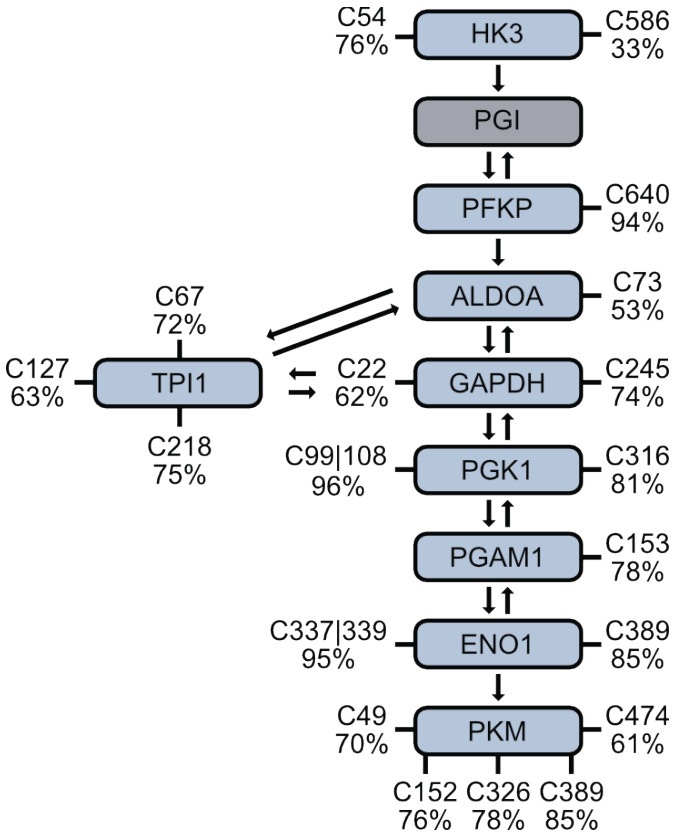


Figure 4-18. Enzymes within the glycolytic pathway with corresponding values for percent oxidation for identified cysteines.

Conclusion

ROS are known to be generated endogenously during (patho)physiological processes and can oxidize cysteine residues to modulate protein function. Due to the high reactivity of ROS, and the presence of a vast array of antioxidant enzymes, endogenous ROS are often highly spatially and temporally localized. It is well known that ROS, such as hydrogen peroxide, do not diffuse far from the site of generation, resulting in the presence of regions of high ROS, termed ROS hotspots, within the cell. These ROS hotspots are localized proximal to ROS generating systems, such as the ETC and NOX, and proteins confined within these ROS

hotspots are exposed to high ROS and therefore subject to significant oxidation. Typical redox-proteomic workflows that use whole-cell lysates only report on the percent oxidation of a particular protein averaged across the entirety of the cell. Therefore, elevated levels of oxidation within these ROS hotspots are often overlooked. These high levels of oxidation could contribute to localized modulation of protein function, resulting in the activation or inhibition of cellular signaling pathways in the vicinity of the ROS source. It is therefore important to incorporate spatial restraints into redox-proteomic pathways that monitor cysteine oxidation.

To specifically interrogate cysteine oxidation within ROS hotspots, we adapted the APEX PL method, which typically requires exogenous hydrogen peroxide treatment to activate the peroxidase for localized protein biotinylation. We hypothesized that the high peroxide concentrations found within ROS hotspots could substitute for the exogenous hydrogen peroxide treatment, resulting in APEX activation only in regions of high peroxide within the cell. We demonstrate that generation of endogenous ROS through ETC inhibition, or NOX stimulation, results in APEX activation, demonstrating that the levels of ROS within these ROS hotspots is sufficient to induce biotinylation of proximal proteins. Moreover, we coupled PL by APEX with OxICAT, a chemoproteomic platform that allows for quantifying the percent oxidation of individual cysteine residues within spatially restricted cellular regions. The implementation of PL-OXICAT using APEX allows for the selective monitoring of cysteine oxidation within ROS hotspots. Collectively these findings show the versatility of the PL-OxICAT platform in examining functional intracellular cysteine oxidation events. We anticipate that PL-OxICAT method can be further expanded upon with

improved proteomic resolution and MS innovations to advance our understanding of the role of cysteine oxidation in (patho)physiological states.

Experimental Procedures

Materials.

All materials were purchased from Fisher Scientific or Sigma-Aldrich unless otherwise specified. Antibodies were purchased from Cell Signaling Technology (Table 4-1).

Table 4-1. Antibodies used with sources, catalog number and use.

Antibody	SOURCE	IDENTIFIER	USE
V5-Tag (D3H8Q) Rabbit mAb (1:1000) (1:500)	Cell Signaling Technology	Cat# 13202	Western Blot/ Immunofluorescence in Raw264.7
V5-Tag (E9H8O) Mouse mAb (1:500)	Cell Signaling Technology	Cat# 80076	Immunofluorescence
GAPDH (14C10) Rabbit mAb (1:1000)	Cell Signaling Technology	Cat# 2118	Western Blot
Streptavidin-HRP (1:200mg)	Sigma-Aldrich	Cat# OR03L	Western Blot
Anti-rabbit IgG, HRP-linked Antibody (1:2000)	Cell Signaling Technology	Cat# 7074	Western Blot
Anti-mouse IgG (H+L), F(ab')2 Fragment (Alexa Fluor® 488 Conjugate) (1:500)	Cell Signaling Technology	Cat# 4408	Immunofluorescence
Anti-rabbit IgG (H+L), F(ab')2 Fragment (Alexa Fluor® 488 Conjugate) (1:500)	Cell Signaling Technology	Cat# 4412	Immunofluorescence (Raw 264.7)
ProLong® Gold Antifade Reagent with DAPI	Cell SignalingTechnology	Cat# 8961	Immunofluorescence

Methods.

Cell culture.

HEK 293T and Raw 264.7 cells were obtained from the ATCC, cultured at 37°C under 5% CO_2 in DMEM/high glucose with L-glutamine, sodium pyruvate (Cytiva) and supplemented with 10% fetal bovine serum (Bio-techne), 100 units/mL of penicillin, 100 μg/mL streptomycin, 0.25 μg/mL Amphotericin B (Gibco) and grown until a maximum passage of 25.

Cloning of APEX2 plasmids.

Traditional cloning methods of PCR gene amplification, restriction enzyme digestion, ligation, and gateway cloning allowed for generation of pLenti APEX2 (matri-APEX and cyto-APEX). A parent MCS-V5-APEX2 pDONR221 vector was generated from PCR amplification of V5-APEX2 region of mito-V5-APEX2 (addgene 72480) with additional attb1/attb2 sites for gateway cloning into pDONR221 vectors. For pLenti matrix-APEX plasmids, full length PDK1 (NM_002610) with N-terminal kozak sequence was PCR amplified and inserted into pDONR221 MCS-V5-APEX2 vector using restriction enzyme digestion and ligation followed by gateway cloning into a pLenti vector. For cyto-APEX, a kozak sequence was inserted into the pDONR221 V5-APEX2 vector by site-directed mutagenesis kit. Mammalian protein expression was driven through CMV promoters in all pLenti plasmids. (Table 4-1).

Table 4-1. Vectors, features, promoters, and usage for study.

Vector	Features	Promoter	Use
pLenti cyto-V5-APEX2	attb1-MCS-kozak-V5-APEX2-stop-attb2	CMV/SV40	Used to generate Lentivirus for transduction into HEK293T and Raw264.7 cells for cytosolic APEX2 expression (cyto-APEX)
pLenti matrix-V5-APEX2	attb1-MCS-NotI-kozak-PDK1-V5-APEX2-stop-EcoRI-attb2	CMV/SV40	Insertion of full length PDK1. Used to generate Lentivirus for transduction into HEK293T cells for PDK1-TurboID APEX2 (matrix-APEX).
pDONR221 V5-APEX2	attL1-MCS-V5-APEX2-stop-attL2	M13	Intermediate APEX2 plasmid used for incorporation of PDK1 (matrix) and generation of pLenti vectors

Generation of stable matrix-V5-APEX2 and cyto-V5-APEX2 HEK 293T cells and cyto-V5-APEX2 Raw 264.7 cells.

Lentivirus was produced in HEK 293T cells, under passage 10, grown in DMEM and 10% heat inactivated fetal bovine serum (HIS) in 10 cm plates. At 80% confluency, cells were transfected with 2 μg vsv-g, 2 μg psPAX2, 2 μg respective pLenti plasmid and 24 μL of Lipofectamine 2000 (Invitrogen). After 24 hr, media was replaced by 5 mL DMEM with 10% HIS. At 48 hr, the media was collected and filtered through a 0.45 μm filter and mixed with 5 mL DMEM-HIS and 10 μg/mL polybrene. Virus was added to the target cell lines at 20% confluency and infected for 48 hr. Growth for 7 days in 2 μg/mL puromycin allowed for selection of stable protein overexpression in HEK 293T cells. The cyto-v5-APEX2 expressing Raw 264.7 cell line was grown for 7 days in 10 μg/mL puromycin and continuously passaged in 4 μg/mL puromycin to maintain APEX overexpressed populations.

APEX activation by peroxide.

For HEK 293T and Raw 264.7 cells overexpressing APEX chimeras, activation was evaluated through incubation with 500 μM biotin-phenol (Sigma-Aldrich) for 30 min at 37°C followed by removal of media and treatments with various increasing concentrations of H_2O_2 in DPBS for 1 min. Biotinylation was quenched by washing 3 times with quenching buffer (10 mM sodium azide, 10 mM sodium ascorbate and 5 mM Trolox) and 3 times with cold DPBS.

APEX activation by endogenous cellular ROS.

Matrix-APEX HEK 293T cells were treated with biotin-phenol for 45 min at 37°C. 100 μM Antimycin A/DMSO, 10 μM Oligomycin/DMSO, and DMSO control were added to the cells, respectively, and the treatment was conducted at 37°C for 45 min. APEX labeling was quenched by washes with quenching buffer as described above.

Cyto-APEX Raw 264.7 cells were incubated with 1 μg/mL LPS, 10 ng/mL IFNγ or no treatment, respectively, for 20 hr. Subsequently, 500 μM biotin-phenol was added for an additional 2.5 hr. Reactions were quenched by the same conditions described above.

Lysate Preparation.

Cells were harvested by scraping and washed with DPBS (Corning). Cell pellets were resuspended in DPBS and lysed by ultrasonic tip sonication (Cole Parmer). Soluble lysate fractions were obtained after separation by centrifugation at 45,000 rpm for 45 min at 4°C pelleted insoluble fractions were discarded for matrix-APEX HEK 293T cell lysates. For cyto-APEX Raw 264.7 cell lysates, whole

cell lysates were enriched by centrifugation at 4,500g for 10 min at 4°C with supernatant collected. To determine protein concentrations, DC Protein Assay kit (Bio-Rad) was performed.

Immunoblotting.

All samples were separated by 12.5% SDS-PAGE gels and transferred to nitrocellulose membranes by electrophoresis at 75 volts for 140 min. Membranes were washed with tris-buffered saline with 1% Tween:20 (TBS-T) 3 times for 5 min followed by staining with Ponceau S (2 min in 0.1% w/v Ponceau S in 5% acetic acid/water) and imaged on a ChemiDoc MP imaging system (BioRad, Hercules, CA). After 3 washes with TBS-T, membranes were blocked with 5% (w/v) non-fat dry milk in TBS-T at room temperature for 1 hr. Following 3 additional washes with TBS-T, membranes were incubated with respective primary antibodies overnight at 4°C. Following removal and additional 3 washes with TBS-T, the membranes were coated with secondary HRP-conjugated antibodies for 1 hr at room temperature. For biotin blots, membranes were blocked in 5% milk overnight at 4°C and after washes, was incubated with 200 ng/mL streptavidin-HRP in TBS-T for 1 hr. After final washes with TBS-T, membranes were developed with HRP-super signal chemiluminescence reagents (Thermo Fisher) and visualized as described above.

Immunohistochemistry and immunofluorescence.

For fluorescence microscopy imaging, cells were grown on 35 mm glass bottom dishes (MatTek) that were treated with 1 mg/mL poly-D-lysine (Sigma-Aldrich) incubated for 5 min at 37°C and washed 3 times with DPBS. Without

exposure to light, cells were treated with 50 nM MitoTracker Red CMXRos (Invitrogen) in RPMI medium without phenol red (Gibco) for 45 min at 37°C. Cells were washed with 3 times with DPBS for 5 min and fixed with 4% formaldehyde (Thermo Fisher Pierce) in DPBS for 15 min at room temperature. After additional washes with DPBS for 5 min 3 times, cells were blocked with blocking buffer of 5% normal goat serum (Cell Signaling Technology) and 0.3% Triton X-100 in DPBS for 1 hr at room temperature. After washing 3 times with DPBS, cells were incubated with primary antibodies diluted in 1% BSA and 0.3% Triton X-100 in DPBS overnight at 4°C. Cells were washed 3 times with DPBS and incubated with secondary antibodies conjugated to AlexaFluor488 for 2 hr at room temperature. After the final 3 washes with DPBS for 5 min, Prolong Gold Antifade Reagent with DAPI (Cell Signaling Technology) was applied and the samples were cured overnight at room temperature. A coverslip was added and sealed with clear nail polish before imaging with a Leica TCS SP5 scanning confocal microscope.

Proximity labeling PL-OxICAT MS preparation.

OxICAT sample preparations were adapted from Bechtel, *et al.*[69] and Topf, *et al.*[70] 2 mg total protein for cell lysates were precipitated by TCA at -80°C for 1 hr or overnight. Samples were pelleted at 15,000 rpm for 10 min and resuspended in 500 μL acetone. After centrifugation at 5,000 rpm for 10 min, sample pellets were resuspended and solubilized in 250 μL denaturing-alkylation buffer (DAB) (6 M Urea, 200 mM Tris-HCl, 10 mM EDTA and 0.5% SDS, pH 8.5) containing 10 mM Light-NEM (5 μL of 500 mM Light-NEM, Sigma-Aldrich). Reduced cysteines were alkylated in the dark at 37°C for 2 hr with shaking. Samples were centrifuged at 21,000 g for 1 min to pellet any precipitant and supernatant was collected and

diluted 3-fold with water to lower the urea content. Proteins were precipitated with 5-fold volume of ice-cold acetone and incubated at -20°C for 2 hr or overnight. After precipitation, samples were pelleted at 4500 g for 30 min, 4°C. Pellets were washed with 500 μL acetone and centrifuged at 4500 g for 10 min. Samples were solubilized in 160 μL DAB and cysteines were reduced with 8 μL of 50 mM tris(2-carboxyethyl)phosphine (TCEP, 2.5 mM final concentration). Samples were agitated at 37°C for 5 min. After reduction, 240 μL DAB was added to dilute TCEP and newly reduced cysteines were labeled by the addition of 10 mM heavy-NEM (8 μL of 500 mM D5-NEM, Cambridge Isotope Laboratories) incubate 2 hr at 37°C in the dark. After the final alkylation, samples were diluted 3-fold with water and 5-fold total volume of acetone was added and proteins precipitated at -20°C for 2 hr or overnight. Proteins were pelleted by centrifugation at 4500 g for 30 min at 4°C and washed with 500 μL acetone. Following centrifugation at 4500 g for 10 min, labeled-protein pellets were resuspended in 1 mL 1.2% (w/v) SDS/PBS using sonication. Solubilized samples were diluted to 0.2% SDS with the addition of 5 mL PBS containing 100 μL of washed streptavidin agarose resin (Thermo Scientific) and rotated overnight at 4°C. SDS solutions were resolubilized at room temperature for 2.5 hr and the resin was incubated with 0.2% SDS/PBS for 10 min followed by 3 washes with PBS and 3 washes with water (5 mL each). Resin was pelleted by centrifugation (1400 g for 3 min) and supernatant removed between each wash step. After the final wash step, resin was resuspended in 200 μL of 2 M Urea and 1 mM $CaCl_2$. 2 μg of trypsin (Promega) was added, and the samples digested overnight at 37°C with agitation. The supernatant was collected, and resin was washed 3 times with 50 μL water and combined generating a total

sample volume of 350 μL. Trypsin digestion was quenched by the addition of 17.5 μL formic acid (5% final concentration).

MS proteomics.

Peptide analysis was achieved by Multidimensional Protein Identification Technology (MudPIT) on an LTQ Orbitrap Discovery mass spectrometer (Thermo Fisher) with sample separation coupled to an Agilent 1200 series HPLC (Agilent Technologies). Peptides were loaded onto a self-packed reverse phase C18 resin 250 μm fused-silica capillary column. 5 Gradients of 100% Buffer B in Buffer A (Buffer A: 95% water, 5% acetonitrile, 0.1% formic acid; Buffer B: 20% water, 80% acetonitrile, 0.1% formic acid) with 5 salt pushes, eluted peptides onto a biphasic 100 μm fused-silica capillary column with a 5 μm tip packed with 10 cm of C18 resin and 4 cm of Partisphere strong cation exchange resin (SCX, Whatman). Instrumentation operated at a flow rate of ~0.25 μL/min buffer through the column and spray voltage of 2.75 kV. One full MS scan (400 – 1800 MW) was followed by 7 data dependent scans of the n^{th} most intense ions with dynamic exclusion enabled.

MS proteomic analysis.

Mass spectrometry data in all samples were searched using a SEQUEST algorithm[71] against a concatenated target/decoy non-redundant variant of *Homo sapien* and *Mus musculus* FASTA databases containing UniProt descriptions[72], respectively. Dynamic modifications on cysteine were included to survey the alkylation by either light-NEM (+125.04766) and heavy-NEM (+130.07906). Proteins were identified in matched MS^2 spectra, packaged, and filtered using

DTASelect2.0.[73] Spectra were sorted with options for -trypstat applied for analyzing tryptic protein enrichment and -modstat applied for specific analysis of labeled cysteine-containing peptides and were restricted to a 5% maximum false discovery rate. For analysis of proximity-labeling enrichment, protein spectral counts were pooled by an in-house Python program with additional annotations for localization and function.[69]

OxICAT specific MS analysis.

Furthermore, all identified cysteine-containing peptides were delimited to having full tryptic cleavage (-y 2), required at least one peptide per locus (-p 1) and a delta-CN score greater than 0.06 (-d 0.06). Cysteine residue position, function, species conservation, domain, and subcellular localizations were annotated by an in-house Python program. Characterized mitochondrial localization was determined by UniProt[72] and MitoCarta2.0[74] specifications. Heavy:light (H:L) and light:heavy (L:H) ratios were resolved using cimage quantification package.[75] L:H and H:L ratios were converted to percent oxidation values by the following equations: 1-(L:H/(L:H+1)) and H:L/(H:L+1). All considered peptides were presented in at least 2 replicates. Average percent oxidation values were calculated for each peptide and standard deviations >30% were removed from the final compilation of labeled-peptides analyses.

Statistical analysis of overrepresented gene ontology (GO) process using PANTHER, GOrilla, and ReviGO.

Panther overrepresentation gene ontology tests (http://pantherdb.org)[76] were performed on APEX-enriched protein datasets. Enriched processes were determined by GOrilla using a ranked gene ontology (GO) analysis and FDR corrected for multiple testing using Benjamini and Hochberg and Fisher methods. Enrichment (E) was defined in terms of the number of intersecting genes (b) over the number of top genes in the target set (n) divided by the total number of genes correlated to a unique GO term (B) over the total number of genes analyzed (N) (E = (b/n) / (B/N). Enriched terms were sorted by the number of top genes (n) and redundant terms were manually removed after analysis by ReviGO[77] for all datasets except for matrix-APEX.

References

(1) Sun, Y.; Lu, Y.; Saredy, J.; Wang, X.; Drummer IV, C.; Shao, Y.; Saaoud, F.; Xu, K.; Liu, M.; Yang, W. Y.; Jiang, X.; Wang, H.; Yang, X. ROS Systems Are a New Integrated Network for Sensing Homeostasis and Alarming Stresses in Organelle Metabolic Processes. *Redox Biol.* **2020**, *37*, 101696.

(2) Lin, M. T.; Beal, M. F. Mitochondrial Dysfunction and Oxidative Stress in Neurodegenerative Diseases. *Nature* **2006**, *443* (7113), 787–795.

(3) Liou, G.-Y.; Storz, P. Reactive Oxygen Species in Cancer. *Free Radic Res* **2010**, *44* (5), 10.3109/10715761003667554.

(4) Chen, J.; Stimpson, S. E.; Fernandez-Bueno, G. A.; Mathews, C. E. Mitochondrial Reactive Oxygen Species and Type 1 Diabetes. *Antioxid. Redox Signal.* **2018**, *29* (14), 1361–1372.

(5) Moris, D.; Spartalis, M.; Spartalis, E.; Karachaliou, G.-S.; Karaolanis, G. I.; Tsourouflis, G.; Tsilimigras, D. I.; Tzatzaki, E.; Theocharis, S. The Role of Reactive Oxygen Species in the Pathophysiology of Cardiovascular Diseases and the Clinical Significance of Myocardial Redox. *Ann. Transl. Med.* **2017**, *5* (16), 326.

(6) Paulsen, C. E.; Carroll, K. S. Cysteine-Mediated Redox Signaling: Chemistry, Biology, and Tools for Discovery. *Chem. Rev.* **2013**, *113* (7), 4633–4679.

(7) Bechtel, T. J.; Weerapana, E. From Structure to Redox: The Diverse Functional Roles of Disulfides and Implications in Disease. *Proteomics* **2017**, *17* (6), 10.1002/pmic.201600391

(8) Morgan, M. J.; Liu, Z. Crosstalk of Reactive Oxygen Species and NF-KB Signaling. *Cell Res.* **2011**, *21* (1), 103–115.

(9) Canet-Avilés, R. M.; Wilson, M. A.; Miller, D. W.; Ahmad, R.; McLendon, C.; Bandyopadhyay, S.; Baptista, M. J.; Ringe, D.; Petsko, G. A.; Cookson, M. R. The Parkinson's Disease Protein DJ-1 Is Neuroprotective Due to Cysteine-Sulfinic Acid-Driven Mitochondrial Localization. *Proc. Natl. Acad. Sci.* **2004**, *101* (24), 9103–9108.

(10) Aiken, C. T.; Kaake, R. M.; Wang, X.; Huang, L. Oxidative Stress-Mediated Regulation of Proteasome Complexes. *Mol. Cell Proteomics* **2011**, *10* (5), R110.006924.

(11) Sena, L. A.; Chandel, N. S. Physiological Roles of Mitochondrial Reactive Oxygen Species. *Mol. Cell* **2012**, *48* (2), 158–167.

(12) Kussmaul, L.; Hirst, J. The Mechanism of Superoxide Production by NADH:Ubiquinone Oxidoreductase (Complex I) from Bovine Heart Mitochondria. *Proc. Natl. Acad. Sci.* **2006**, *103* (20), 7607–7612.

(13) Lambert, A. J.; Brand, M. D. Superoxide Production by NADH:Ubiquinone Oxidoreductase (Complex I) Depends on the PH Gradient across the Mitochondrial Inner Membrane. *Biochem. J.* **2004**, *382* (Pt 2), 511–517.

(14) Lambert, A. J.; Brand, M. D. Inhibitors of the Quinone-Binding Site Allow Rapid Superoxide Production from Mitochondrial NADH:Ubiquinone Oxidoreductase (Complex I). *J. Biol. Chem.* **2004**, *279* (38), 39414–39420.

(15) Turrens, J. F.; Alexandre, A.; Lehninger, A. L. Ubisemiquinone Is the Electron Donor for Superoxide Formation by Complex III of Heart Mitochondria. *Arch. Biochem. Biophys.* **1985**, *237* (2), 408–414.

(16) Del Prete, A.; Zaccagnino, P.; Di Paola, M.; Saltarella, M.; Oliveros Celis, C.; Nico, B.; Santoro, G.; Lorusso, M. Role of Mitochondria and Reactive Oxygen Species in Dendritic Cell Differentiation and Functions. *Free Radic. Biol. Med.* **2008**, *44* (7), 1443–1451.

(17) Ji, A.-R.; Ku, S.-Y.; Cho, M. S.; Kim, Y. Y.; Kim, Y. J.; Oh, S. K.; Kim, S. H.; Moon, S. Y.; Choi, Y. M. Reactive Oxygen Species Enhance Differentiation of Human Embryonic Stem Cells into Mesendodermal Lineage. *Exp. Mol. Med.* **2010**, *42* (3), 175–186.

(18) Williams, M. S.; Kwon, J. T Cell Receptor Stimulation, Reactive Oxygen Species, and Cell Signaling. *Free Radic. Biol. Med.* **2004**, *37* (8), 1144–1151.

(19) Dunnill, C.; Patton, T.; Brennan, J.; Barrett, J.; Dryden, M.; Cooke, J.; Leaper, D.; Georgopoulos, N. T. Reactive Oxygen Species (ROS) and Wound

Healing: The Functional Role of ROS and Emerging ROS-modulating Technologies for Augmentation of the Healing Process. *Int. Wound J.* **2015**, *14* (1), 89–96.

(20) Lambeth, J. D. NOX Enzymes and the Biology of Reactive Oxygen. *Nat. Rev. Immunol.* **2004**, *4* (3), 181–189.

(21) Salim, T.; Sershen, C. L.; May, E. E. Investigating the Role of TNF-α and IFN-γ Activation on the Dynamics of INOS Gene Expression in LPS Stimulated Macrophages. *PLoS ONE* **2016**, *11* (6), e0153289.

(22) Eog Ji, G.; Young Park, S.; Shyan Wong, S.; Pestka, J. J. Modulation of Nitric Oxide, Hydrogen Peroxide and Cytokine Production in a Clonal Macrophage Model by the Trichothecene Vomitoxin (Deoxynivalenol). *Toxicology* **1998**, *125* (2), 203–214.

(23) Lennicke, C.; Rahn, J.; Lichtenfels, R.; Wessjohann, L. A.; Seliger, B. Hydrogen Peroxide – Production, Fate and Role in Redox Signaling of Tumor Cells. *Cell Commun. Signal.* **2015**, *13* (1), 39.

(24) Bedard, K.; Krause, K.-H. The NOX Family of ROS-Generating NADPH Oxidases: Physiology and Pathophysiology. *Physiol. Rev.* **2007**, *87* (1), 245–313.

(25) Martell, J. D.; Deerinck, T. J.; Sancak, Y.; Poulos, T. L.; Mootha, V. K.; Sosinsky, G. E.; Ellisman, M. H.; Ting, A. Y. Engineered Ascorbate Peroxidase as a Genetically Encoded Reporter for Electron Microscopy. *Nat. Biotechnol.* **2012**, *30* (11), 1143–1148.

(26) Lam, S. S.; Martell, J. D.; Kamer, K. J.; Deerinck, T. J.; Ellisman, M. H.; Mootha, V. K.; Ting, A. Y. Directed Evolution of APEX2 for Electron Microscopy and Proximity Labeling. *Nat. Methods* **2015**, *12* (1), 51–54.

(27) Hung, V.; Udeshi, N. D.; Lam, S. S.; Loh, K. H.; Cox, K. J.; Pedram, K.; Carr, S. A.; Ting, A. Y. Spatially Resolved Proteomic Mapping in Living Cells with the Engineered Peroxidase APEX2. *Nat. Protoc.* **2016**, *11* (3), 456–475.

(28) Rhee, H.-W.; Zou, P.; Udeshi, N. D.; Martell, J. D.; Mootha, V. K.; Carr, S. A.; Ting, A. Y. Proteomic Mapping of Mitochondria in Living Cells via Spatially Restricted Enzymatic Tagging. *Science* **2013**, *339* (6125), 1328–1331.

(29) Roux, K. J.; Kim, D. I.; Raida, M.; Burke, B. A Promiscuous Biotin Ligase Fusion Protein Identifies Proximal and Interacting Proteins in Mammalian Cells. *J. Cell Biol.* **2012**, *196* (6), 801–810.

(30) Magnani, F.; Mattevi, A. Structure and Mechanisms of ROS Generation by NADPH Oxidases. *Curr. Opin. Struct. Biol.* **2019**, *59*, 91–97.

(31) Bak, D. W.; Weerapana, E. Cysteine-Mediated Redox Signalling in the Mitochondria. *Mol. BioSyst.* **2015**, *11* (3), 678–697.

(32) Scialò, F.; Fernández-Ayala, D. J.; Sanz, A. Role of Mitochondrial Reverse Electron Transport in ROS Signaling: Potential Roles in Health and Disease. *Front. Physiol.* **2017**, *8*, 428.

(33) Quinlan, C. L.; Gerencser, A. A.; Treberg, J. R.; Brand, M. D. The Mechanism of Superoxide Production by the Antimycin-Inhibited Mitochondrial Q-Cycle. *J. Biol. Chem.* **2011**, *286* (36), 31361–31372.

(34) Symersky, J.; Osowski, D.; Walters, D. E.; Mueller, D. M. Oligomycin Frames a Common Drug-Binding Site in the ATP Synthase. *Proc. Natl. Acad. Sci.* **2012**, *109* (35), 13961–13965.

(35) Sipos, I.; Tretter, L.; Adam-Vizi, V. The Production of Reactive Oxygen Species in Intact Isolated Nerve Terminals Is Independent of the Mitochondrial Membrane Potential. *Neurochem. Res.* **2003**, *28* (10), 1575–1581.

(36) St-Pierre, J.; Buckingham, J. A.; Roebuck, S. J.; Brand, M. D. Topology of Superoxide Production from Different Sites in the Mitochondrial Electron Transport Chain. *J. Biol. Chem.* **2002**, *277* (47), 44784–44790.

(37) Chen, Y.-R.; Zweier, J. L. Cardiac Mitochondria and Reactive Oxygen Species Generation. *Circ. Res.* **2014**, *114* (3), 524–537.

(38) Sies, H.; Jones, D. P. Reactive Oxygen Species (ROS) as Pleiotropic Physiological Signalling Agents. *Nat Rev Mol Cell Biol* **2020**, *21* (7), 363–383.

(39) Stone, J. R.; Yang, S. Hydrogen Peroxide: A Signaling Messenger. *Antioxid. Redox Signal.* **2006**, *8* (3–4), 243–270.

(40) Santamaría, G.; Martínez-Diez, M.; Fabregat, I.; Cuezva, J. M. Efficient Execution of Cell Death in Non-Glycolytic Cells Requires the Generation of ROS Controlled by the Activity of Mitochondrial H + -ATP Synthase. *Carcinogenesis* **2006**, *27* (5), 925–935.

(41) Castro, L.; Tórtora, V.; Mansilla, S.; Radi, R. Aconitases: Non-Redox Iron–Sulfur Proteins Sensitive to Reactive Species. *Acc. Chem. Res.* **2019**, *52* (9), 2609–2619.

(42) Cantu, D.; Schaack, J.; Patel, M. Oxidative Inactivation of Mitochondrial Aconitase Results in Iron and H2O2-Mediated Neurotoxicity in Rat Primary Mesencephalic Cultures. *PLoS ONE* **2009**, *4* (9), e7095.

(43) Kang, S. W.; Baines, I. C.; Rhee, S. G. Characterization of a Mammalian Peroxiredoxin That Contains One Conserved Cysteine. *J. Biol. Chem.* **1998**, *273* (11), 6303–6311.

(47) Yang, S.; Jan, Y.-H.; Mishin, V.; Heck, D. E.; Laskin, D. L.; Laskin, J. D. Diacetyl/ L -Xylulose Reductase Mediates Chemical Redox Cycling in Lung Epithelial Cells. *Chem. Res. Toxicol.* **2017**, *30* (7), 1406–1418.

(45) Zhao, H.-T.; Endo, S.; Ishikura, S.; Chung, R.; Hogg, P. J.; Hara, A.; El-Kabbani, O. Structure/Function Analysis of a Critical Disulfide Bond in the Active Site of l-Xylulose Reductase. *Cell. Mol. Life Sci.* **2009**, *66* (9), 1570–1579.

(46) Bak, D. W.; Pizzagalli, M. D.; Weerapana, E. Identifying Functional Cysteine Residues in the Mitochondria. *ACS Chem. Biol.* **2017**, *12* (4), 947–957.

(47) Di, A.; Gao, X.-P.; Qian, F.; Kawamura, T.; Han, J.; Hecquet, C.; Ye, R. D.; Vogel, S. M.; Malik, A. B. The Redox-Sensitive Cation Channel TRPM2 Modulates Phagocyte ROS Production and Inflammation. *Nat. Immunol.* **2012**, *13* (1), 29–34.

(48) Furman, D.; Campisi, J.; Verdin, E.; Carrera-Bastos, P.; Targ, S.; Franceschi, C.; Ferrucci, L.; Gilroy, D. W.; Fasano, A.; Miller, G. W.; Miller, A. H.; Mantovani, A.; Weyand, C. M.; Barzilai, N.; Goronzy, J. J.; Rando, T. A.; Effros, R. B.; Lucia, A.; Kleinstreuer, N.; Slavich, G. M. Chronic Inflammation in the Etiology of Disease across the Life Span. *Nat. Med.* **2019**, *25* (12), 1822–1832.

(49) Nakao, N.; Kurokawa, T.; Nonami, T.; Tumurkhuu, G.; Koide, N.; Yokochi, T. Hydrogen Peroxide Induces the Production of Tumor Necrosis Factor-α in RAW 264.7 Macrophage Cells via Activation of P38 and Stress-Activated Protein Kinase. *Innate Immun.* **2008**, *14* (3), 190–196.

(50) Lorsbach, R. B.; Murphy, W. J.; Lowenstein, C. J.; Snyder, S. H.; Russell, S. W. Expression of the Nitric Oxide Synthase Gene in Mouse Macrophages Activated for Tumor Cell Killing. Molecular Basis for the Synergy between

Interferon-Gamma and Lipopolysaccharide. *J. Biol. Chem.* **1993**, *268* (3), 1908–1913.

(51) Eog Ji, G.; Young Park, S.; Shyan Wong, S.; Pestka, J. J. Modulation of Nitric Oxide, Hydrogen Peroxide and Cytokine Production in a Clonal Macrophage Model by the Trichothecene Vomitoxin (Deoxynivalenol). *Toxicology* **1998**, *125* (2), 203–214.

(52) Kang, X.; Wei, X.; Wang, X.; Jiang, L.; Niu, C.; Zhang, J.; Chen, S.; Meng, D. Nox2 Contributes to the Arterial Endothelial Specification of Mouse Induced Pluripotent Stem Cells by Upregulating Notch Signaling. *Sci. Rep.* **2016**, *6* (1), 33737.

(53) Satpathy, A. T.; Briseño, C. G.; Lee, J. S.; Ng, D.; Manieri, N. A.; Kc, W.; Wu, X.; Thomas, S. R.; Lee, W.-L.; Turkoz, M.; McDonald, K. G.; Meredith, M. M.; Song, C.; Guidos, C. J.; Newberry, R. D.; Ouyang, W.; Murphy, T. L.; Stappenbeck, T. S.; Gommerman, J. L.; Nussenzweig, M. C.; Colonna, M.; Kopan, R.; Murphy, K. M. Notch2-Dependent Classical Dendritic Cells Orchestrate Intestinal Immunity to Attaching-and-Effacing Bacterial Pathogens. *Nat. Immunol* .**2013**, *14* (9), 937–948.

(54) Gordon, W. R.; Vardar-Ulu, D.; Histen, G.; Sanchez-Irizarry, C.; Aster, J. C.; Blacklow, S. C. Structural Basis for Autoinhibition of Notch. *Nat Struct Mol Biol* **2007**, *14* (4), 295–300.

(55) Lee, J. A.; Song, H. Y.; Ju, S. M.; Lee, S. J.; Kwon, H.-J.; Eum, W. S.; Jang, S. H.; Choi, S. Y.; Park, J. Differential Regulation of Inducible Nitric Oxide Synthase and Cyclooxygenase-2 Expression by Superoxide Dismutase in Lipopolysaccharide Stimulated RAW 264.7 Cells. *Exp. Mol. Med.* **2009**, *41* (9), 629.

(56) Akira, S.; Hoshino, K.; Kaisho, T. The Role of Toll-like Receptors and MyD88 in Innate Immune Responses. *J. Endotoxin Res.* **2000**, *6* (5), 383–387.

(57) Chen, S.-T.; Li, J.-Y.; Zhang, Y.; Gao, X.; Cai, H. Recombinant MPT83 Derived from *Mycobacterium Tuberculosis* Induces Cytokine Production and Upregulates the Function of Mouse Macrophages through TLR2. *J.I.* **2012**, *188* (2), 668–677.

(58) Elko, E. A.; Manuel, A. M.; White, S.; Zito, E.; Vliet, A. van der; Anathy, V.; Janssen-Heininger, Y. M. W. Oxidation of Peroxiredoxin-4 Induces Oligomerization and Promotes Interaction with Proteins Governing Protein Folding and Endoplasmic Reticulum Stress. *J. Biol. Chem.* **2021**, *296*.

(59) Lipinski, S.; Pfeuffer, S.; Arnold, P.; Treitz, C.; Aden, K.; Ebsen, H.; Falk-Paulsen, M.; Gisch, N.; Fazio, A.; Kuiper, J.; Luzius, A.; Billmann-Born, S.; Schreiber, S.; Nuñez, G.; Beer, H.; Strowig, T.; Lamkanfi, M.; Tholey, A.; Rosenstiel, P. Prdx4 Limits Caspase-1 Activation and Restricts Inflammasome-mediated Signaling by Extracellular Vesicles. *EMBO J.* **2019**, *38* (20), e101266.

(60) Schulte, J. Peroxiredoxin 4: A Multifunctional Biomarker Worthy of Further Exploration. *BMC Medicine* **2011**, *9* (1), 137.

(61) Hoebe, K.; Georgel, P.; Rutschmann, S.; Du, X.; Mudd, S.; Crozat, K.; Sovath, S.; Shamel, L.; Hartung, T.; Zähringer, U.; Beutler, B. CD36 Is a Sensor of Diacylglycerides. *Nature* **2005**, *433* (7025), 523–527.

(62) Jia, J.; Arif, A.; Willard, B.; Smith, J. D.; Stuehr, D. J.; Hazen, S. L.; Fox, P. L. Protection of Extraribosomal RPL13a by GAPDH and Dysregulation by S-Nitrosylation. *Mol. Cell* **2012**, *47* (4), 656–663.

(63) López-Grueso, M.; González-Ojeda, R.; Requejo-Aguilar, R.; McDonagh, B.; Fuentes-Almagro, C.; Muntané, J.; Bárcena, J. A.; Padilla, C. Thioredoxin and Glutaredoxin Regulate Metabolism through Different Multiplex Thiol Switches. *Redox Biol.* **2019**, *21*, 101049.

(64) van der Reest, J.; Lilla, S.; Zheng, L.; Zanivan, S.; Gottlieb, E. Proteome-Wide Analysis of Cysteine Oxidation Reveals Metabolic Sensitivity to Redox Stress. *Nat. Commun.* **2018**, *9* (1), 1581.

(65) Akter, S.; Fu, L.; Jung, Y.; Conte, M. L.; Lawson, J. R.; Lowther, W. T.; Sun, R.; Liu, K.; Yang, J.; Carroll, K. S. Chemical Proteomics Reveals New Targets of Cysteine Sulfinic Acid Reductase. *Nat. Chem. Biol.* **2018**, *14* (11), 995–1004.

(66) Al Barashdi, M. A.; Ali, A.; McMullin, M. F.; Mills, K. Protein Tyrosine Phosphatase Receptor Type C (PTPRC or CD45). *J. Clin. Pathol.* **2021**, *74* (9), 548–552.

(67) Raman, M.; Chen, W.; Cobb, M. H. Differential Regulation and Properties of MAPKs. *Oncogene* **2007**, *26* (22), 3100–3112.

(68) Dougherty, M. K.; Müller, J.; Ritt, D. A.; Zhou, M.; Zhou, X. Z.; Copeland, T. D.; Conrads, T. P.; Veenstra, T. D.; Lu, K. P.; Morrison, D. K. Regulation of Raf-1 by Direct Feedback Phosphorylation. *Mol. Cell* **2005**, *17* (2), 215–224.

(69) Bechtel, T. J.; Li, C.; Kisty, E. A.; Maurais, A. J.; Weerapana, E. Profiling Cysteine Reactivity and Oxidation in the Endoplasmic Reticulum. *ACS Chem. Biol.* **2020**, *15* (2), 543–553.

(70) Topf, U.; Suppanz, I.; Samluk, L.; Wrobel, L.; Böser, A.; Sakowska, P.; Knapp, B.; Pietrzyk, M. K.; Chacinska, A.; Warscheid, B. Quantitative Proteomics Identifies Redox Switches for Global Translation Modulation by

Mitochondrially Produced Reactive Oxygen Species. *Nat. Commun.* **2018**, *9* (1), 324.

(71) Eng, J. K.; McCormack, A. L.; Yates, J. R. An Approach to Correlate Tandem Mass Spectral Data of Peptides with Amino Acid Sequences in a Protein Database. *J. Am. Soc. Mass Spectrom.* **1994**, *5* (11), 976–989.

(72) The UniProt Consortium. UniProt: The Universal Protein Knowledgebase in 2021. *Nucleic Acids Res.* **2021**, *49* (D1), D480–D489.

(73) Tabb, D. L.; McDonald, W. H.; Yates, J. R. DTASelect and Contrast: Tools for Assembling and Comparing Protein Identifications from Shotgun Proteomics. *J. Proteome Res.* **2002**, *1* (1), 21–26.

(74) Calvo, S. E.; Clauser, K. R.; Mootha, V. K. MitoCarta2.0: An Updated Inventory of Mammalian Mitochondrial Proteins. *Nucleic Acids Res.* **2016**, *44* (Database issue), D1251–D1257.

(75) Weerapana, E.; Wang, C.; Simon, G. M.; Richter, F.; Khare, S.; Dillon, M. B. D.; Bachovchin, D. A.; Mowen, K.; Baker, D.; Cravatt, B. F. Quantitative Reactivity Profiling Predicts Functional Cysteines in Proteomes. *Nature* **2010**, *468* (7325), 790–795.

(76) Mi, H.; Ebert, D.; Muruganujan, A.; Mills, C.; Albou, L.-P.; Mushayamaha, T.; Thomas, P. D. PANTHER Version 16: A Revised Family Classification, Tree-Based Classification Tool, Enhancer Regions and Extensive API. *Nucleic Acids Res.* **2021**, *49* (D1), D394–D403.

(77) Supek, F.; Bošnjak, M.; Škunca, N.; Šmuc, T. REVIGO Summarizes and Visualizes Long Lists of Gene Ontology Terms. *PLOS ONE* **2011**, *6* (7), e21800.

Chapter 5

Integrated Phenotypic Screening and Target Identification of Fully Functionalized Electrophilic and Photo-reactive Small-Molecule Library

This work was done in collaboration with the Lapsinky lab at Duquesne University, Pittsburg, PA.

Introduction

Despite many pathologies having clear genetic influence over disease phenotypes, most of the human proteome remains uncharacterized and deemed "undruggable".[1] As one of the major challenges in chemical biology is identifying small-molecule modulators for all proteins within the proteome, the scarcity of chemical probes for selective protein modification has stalled progress towards advances in understanding much of the biological space as well as innovation of new therapeutics.[2] Improvement in the efficiency and structural diversity of small-molecule probes is essential to the expansion of the variety and number of ligandable proteins for drug discovery.[3,4]

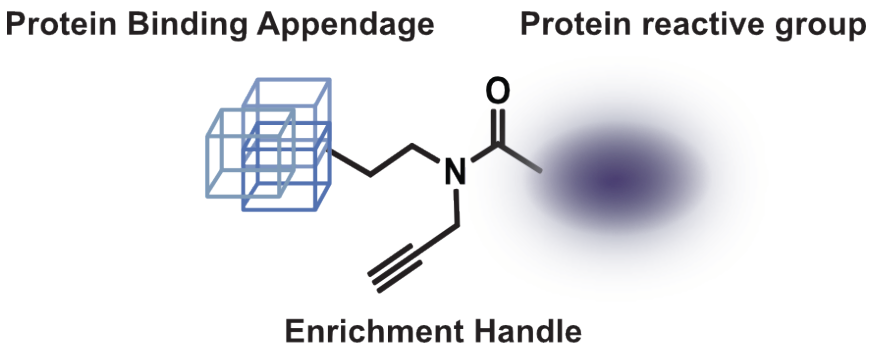


Figure 5-1. Illustration of FFSMP design with three consistent elements including a protein binding appendage for selectivity, a protein reactive group (either electrophilic or photo-reactive) for covalent modification, and enrichment handle for click chemistry (alkyne).

Classical methods of drug discovery involve streamlined phenotypic screening of large small-molecule libraries scouting for applications against a

drug-targeted landscape using fully functionalized small-molecule probes (FFMSPs).[5-,15] FFSMPs contain three characteristic features including: (1) a protein-binding motif containing one or more structural diversity elements increasing interaction specificity, (2) an electrophilic or photoreactive handle to facilitate irreversible covalent bond formation between the probe and target protein, and (3) a terminal alkyne for reporter tag conjugation through click chemistry to visualize, enrich, and identify protein-linked proteins (Figure 5-1). Throughout the past couple of decades, FFSMP libraries have dominated phenotypic screening campaigns and have enabled discovery of a variety of bioactive chemical probes helping to increase comprehension of their corresponding protein target functions and mechanisms of action in disease.[16,17] Furthermore, libraries of increased structural diversity are crucial in driving success of novel small-molecule interactions with previously unligandable proteins broadening the druggable space.[18,19] Conventional FFSMP libraries involve peripheral structural complexity and chemical diversity around a single chemical scaffold. Although intermediate structure allows for synthetic simplicity, this design strategy limits discovery of new protein targets as the lack of molecular diversity governs a small, biased sampling of chemical space. Moreover, full scaffold diversity, rather than appendage diversity, is critical for reaching a multiplicity of three-dimensional molecular shapes allowing for robust sampling of potential protein-interactions.[20] Together with incorporations of a vast array of electrophilic and photoreactive groups makes for robust sampling of a wide-range of potential protein-interactions.

To overcome the challenges in narrow probe designs, our collaborators the Lapinsky lab at Duquesne University developed an appendage and scaffold-

diverse FFSMP of 49 library members using Isocyanide-based Multi-Component Reactions (IMCRs). A general three-step IMCR-Boc deprotection-arming synthetic sequence was started with a minimalist bifunctional isocyanide linker derived from previous reports by the Yao group.[21,22] This well-known set of minimalist linkers contain a photoreactive aliphatic diazirine functional group for target protein capture, a terminal alkyne click chemistry handle, and either a carboxylic acid, 1˚ aliphatic iodide, or 1˚ aliphatic amine for attachment to a small-molecule of interest. However, instead of attaching of the minimalist linkers via heteroatom-alkylation or -acylation to produce FFSMPs, we employed the isocyanide functional group within **1** in several different IMCRs involving a wide variety of commercially available carboxylic acids, 1˚ amines, aldehydes, and ketones.[18] The resulting structurally diverse FFSMPs incorporated different privileged structures[23,24] to direct the FFSMP to sample biologically relevant chemical space. Additionally, Topliss moieties, which are structural entities that allow for facile substitution of an aromatic ring or an aliphatic side chain substituent for improved biological activity, were also incorporated.[25,26] Chemoproteomic drug discovery strategies including phenotypic screening-target identification workflows were employed to evaluate the FFSMP library engagement in MCF10CA1a, breast cancer proteomic space. We find that overall diversification of both structure and electrophilic or photoreactive protein capturing motifs are responsible for an assortment of protein reactivity profiles of library members.

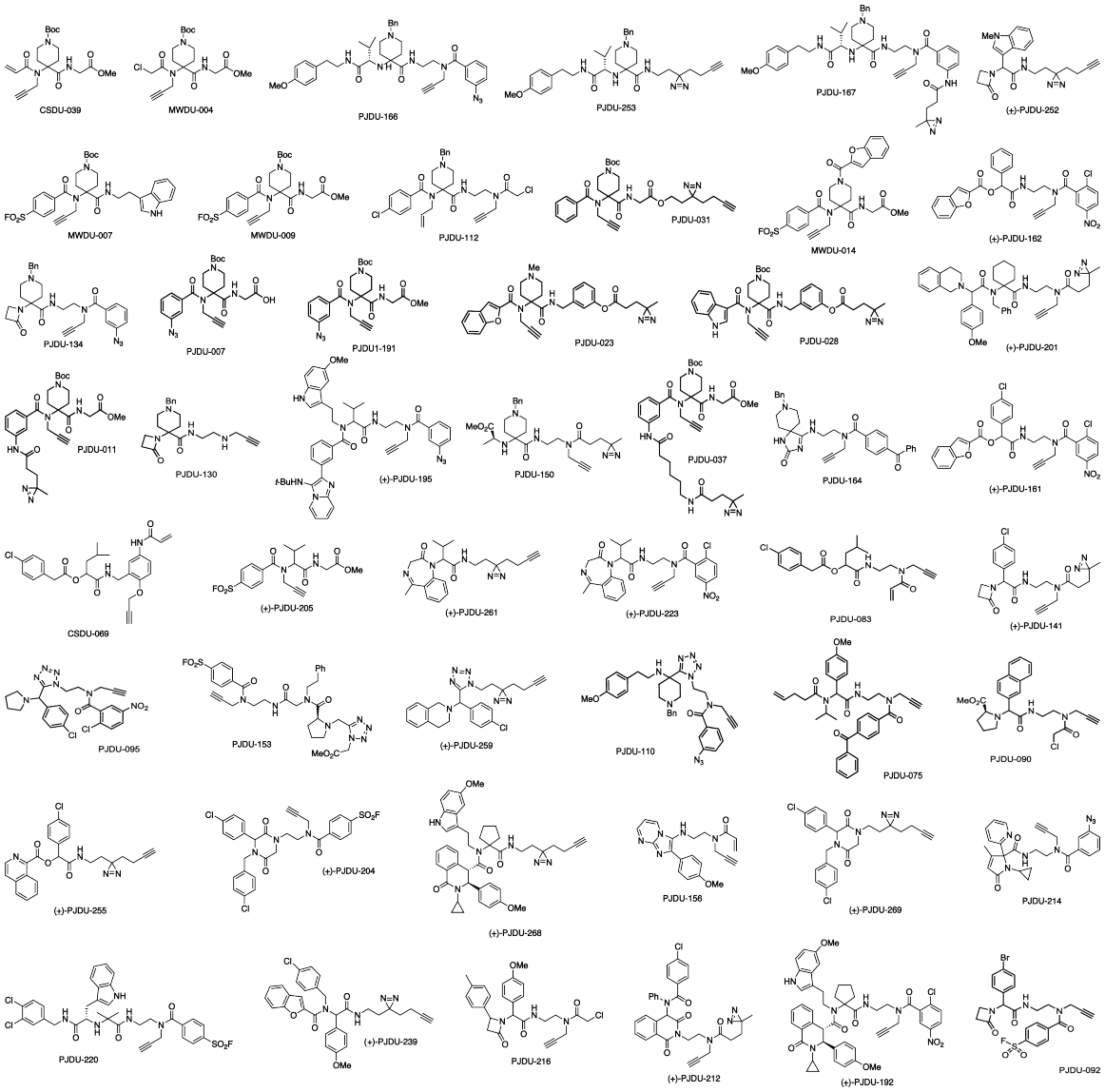


Figure 5-2. Structures of the 49 FFSMP library members with great scaffold appendage and protein reactivity diversity.

Results and Discussion

FFSMP library development and molecular diversity.

The 49 member FFSMP library was synthesized incorporating a wide-range of base scaffolds and protein reactive groups (Figure 5-2). The original library design was constructed with the desire of having similarity in molecular-shape

diversity to bioactive natural products. The Nolan lab at Duquesne University contributed structural configuration analysis of the synthesized compounds. The 3 dimensional-shape diversity of the library was analyzed comparing set of FFSMPs to two references collections including one of a set of 60 diverse natural products as well as another set of 40 top-selling brand-name drugs. Based on the lowest-energy conformation of all compounds, normalized ratios of principal moment-of-inertia (PMI) were calculated and plotted.[20] The PMI plot visualized the 3-dimensional shape diversity of each collections in terms of "molecular-shape space" spanned by three basic shapes including "spherical', "rod-like", and "disc-like" (Figure 5-3). With unique and complex structures, the natural product drug space typically possesses significantly higher 3-dimensional space diversity with an emphasis on "spherical" characteristics. In contrast, the reference of standard drug molecules displays primarily "rod-like" structures with diversified "disc-like" characteristics. As intended, the FFSMP library analyzed controlled a very high molecular-shape diversity with some similarity to the natural product compilation.

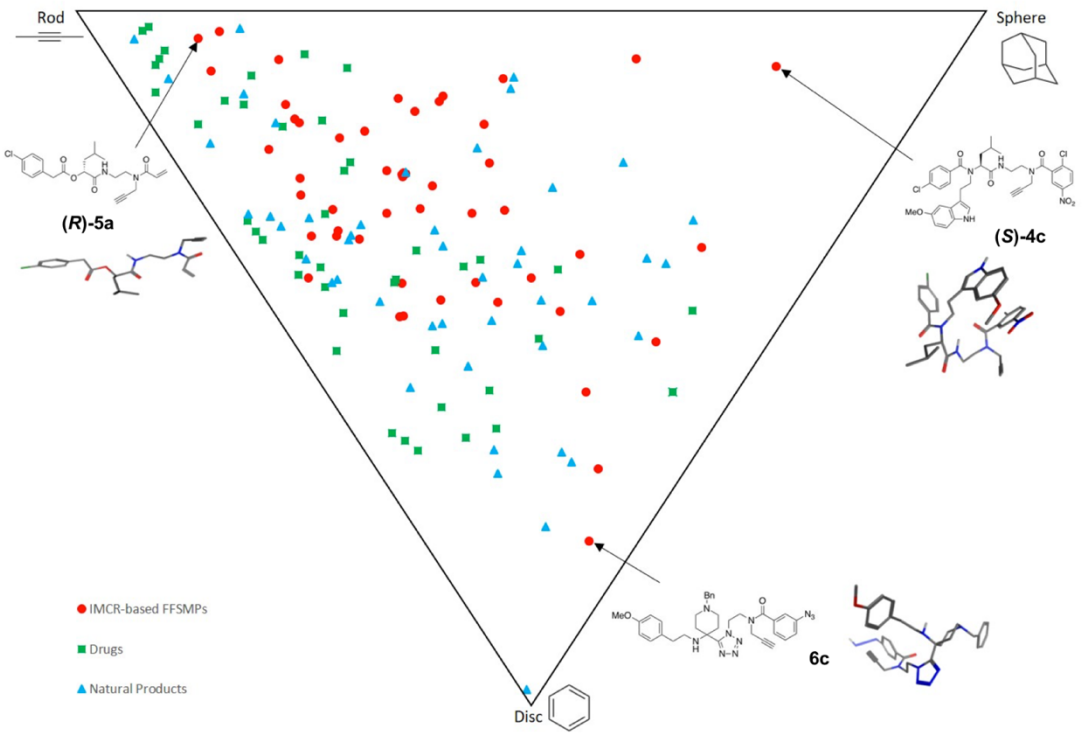


Figure 5-3. Molecular shape diversity assessment by principle moment of inertia plot. The molecular shape diversity of 49 IMCR-based FFSMPs (red dots), which includes each enantiomer of racemic FFSMPs, in comparison with reference sets of 40 top-selling brand-name drugs (green squares) and 60 diverse natural products (filled blue triangles).

Electrophilic FFSMP scaffold diversity leads to variety in protein labeling.

To evaluate the bioactivity and potential of our FFSMPs to covalently modify protein targets directly in living cells, the electrophilic members of the FFSMP library were evaluated in a phenotypic screen for antiproliferative activity against MCF10CA1a breast cancer cells. MCF10CA1a cells are derived from the normal human mammary epithelial cell line, MCF-10A.[27] Expression of constitutively active H-Ras resulted in MCF-10AT cells that are pre-malignant.

Further selection for tumor-forming capacity upon in vivo passaging generated the highly aggressive MCF-10CA1a cell line.[28] Although the FFSMP library included a diverse array of both electrophilic and photo-reactivity moieties, due to the decreased labeling specificities and potency of the photo-affinity probes, continued focus on compounds with diverse electrophilic protein modifying moieties, Figure 5-4. Although there is benefit of photoaffinity labeling being less reliant of specific amino acids due to the promiscuity of highly reactive photo-activated species, there is a lower frequency of photo-affinity probe covalent modifications between target proteins.[29,30,31] The photoreactive probes were evaluated in whole cells, however, no significant labeling was found compared to lysate labeling. Alternative conditions with should be considered for future evaluation.

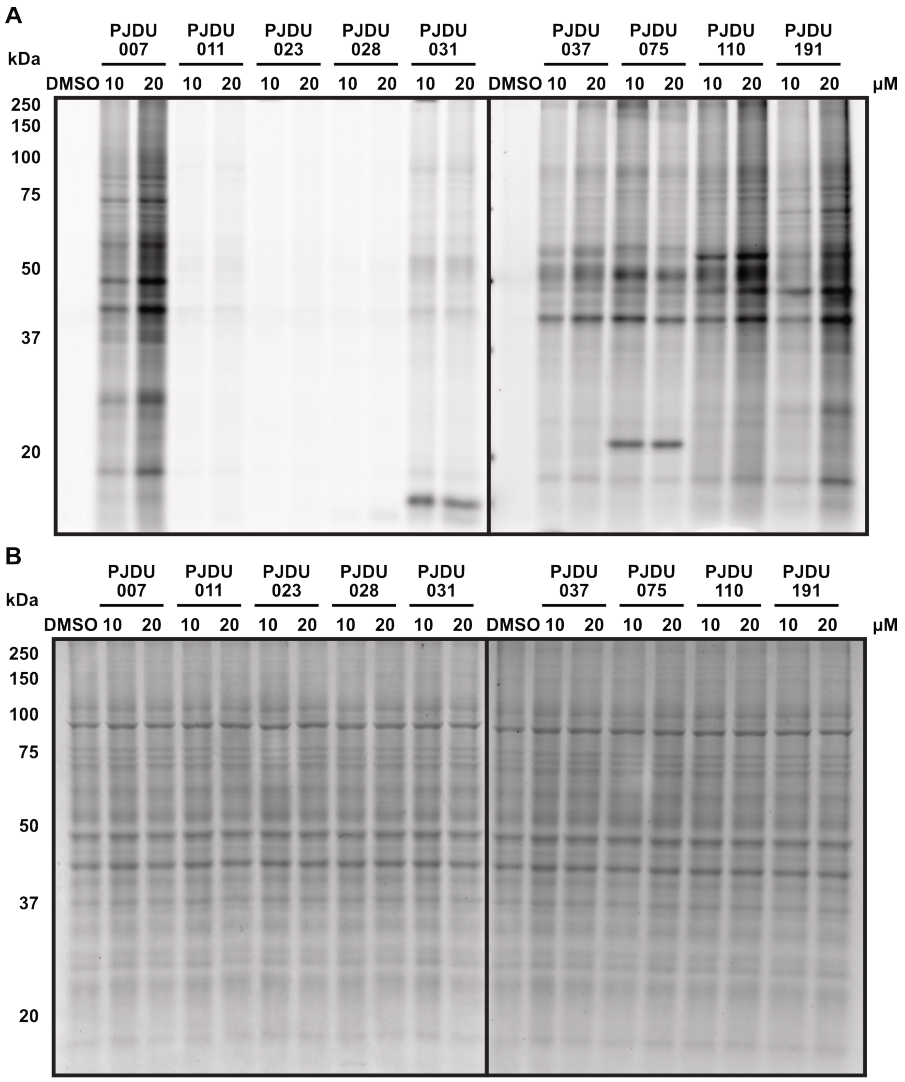


Figure 5-4. Photo-reactive FFSMP library member labeling in MCF10CA1a lysates. Lysates were incubated with either 10 or 20 μM probe for 30 min followed with irradiation with UV light for 1 hr. (A) Click chemistry was performed to append TAMRA-N_3 for fluorescent visualization. (B) Normalized protein concentration was confirmed by Coomassie protein staining.

To determine if the nature of the electrophile affects the subset of proteins targeted by the probe, protein labeling by four probes with identical scaffolds, but

different electrophiles (MWDU-004, MWDU-009, CSDU-039 and VPDU-231) were evaluated (Figure 5-5A). MCF10CA1a, a highly proliferative breast cancer cell line from the MCF10a progression series, was used to screen library members. Briefly, cells were treated with each probe at 10 μM concentrations for 24 hr. Cells were harvested, lysed, and lysates subjected to copper (I)-catalyzed azide-alkyne cycloaddition (CuAAC) to append a fluorophore (tetramethylrhodamine-azide; TAMRA-N_3) to probe-labeled proteins. In-gel fluorescence after gel electrophoresis was used to determine the pattern of protein labeling by each of these probes. MWDU-004, a chloroacetamide, exhibited the greatest reactivity, with two intense protein targets around 50 kDa. Interestingly, CSDU-039 containing an acrylamide, demonstrated a similar protein labeling pattern with reduced reactivity, confirming the lower reactivity of the acrylamide relative to the chloroacetamide. MWDU-009 and VPDU-231, bearing sulfonyl fluoride and chloronitrobenzene electrophiles, showed minimal protein reactivity, likely due to the reduced reactivity of these electrophiles (Figure 5-5B).

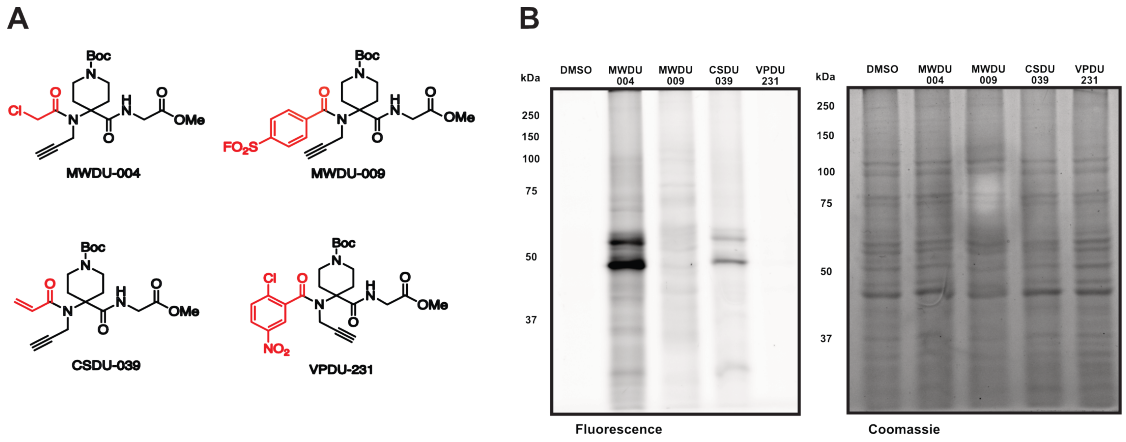


Figure 5-5. Evaluation of FFSMPs of electrophilic diversities with consistent core scaffold in MCF10CA1a cells. (A) FFMSP library member structures shown with electrophilic war heads in red with similar skeletal backbones in black. (B) Whole MCF10CA1a cells were incubated with probes for 3 hours followed by lysate preparation and click chemistry with TAMRA-azide to visualize labeling through fluorescent imaging Coomassie staining confirms protein normalized concentration.

In a similar vein, to determine the effects of appendage diversity on protein targeting, four sulfonyl fluoride-containing library members with varying appendages (MWDU-007, MWDU-009, MWDU-014, and MWDU-019; Figure 5-6A) were evaluated. Cells were treated with at 10 μM concentrations for 1hr. In-gel fluorescence data demonstrated distinct protein labeling patterns for each of the four probes (Figure 5-6B), suggesting that the appendage serves to direct these probes toward distinct subsets of the proteome. Together, these initial screens accentuate the modularity of the fully functionalized probe library, whereby

potency and target diversity can be achieved by varying the electrophile and the appendages on the probes.

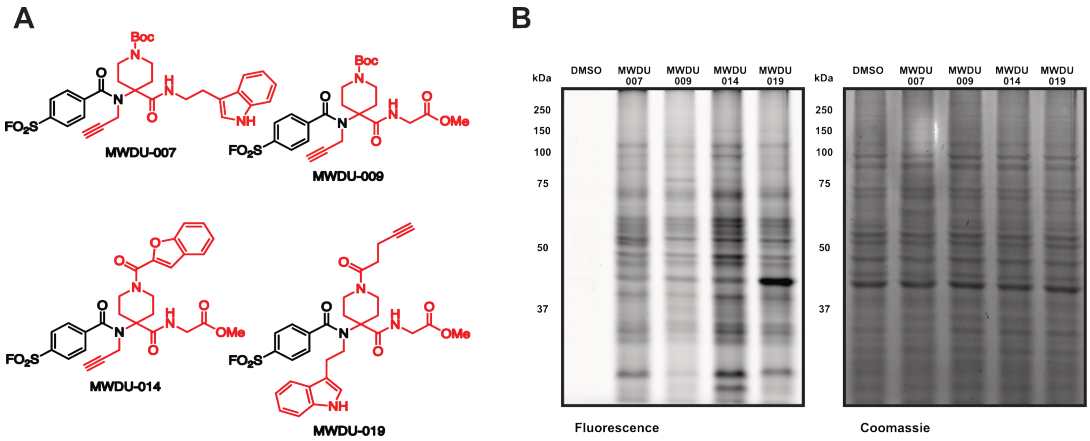


Figure 5-6. Assessment of FFSMPs with scaffold appendage diversity but electrophilic similarity. (A) Library members with sulfonyl fluoride electrophile on different core structural backbones (B) Whole MCF10CA1a cells were incubated with probes for 3 hours followed by lysate preparation and click chemistry with TAMRA-azide to visualize labeling through fluorescent imaging Coomassie staining confirms protein normalized concentration.

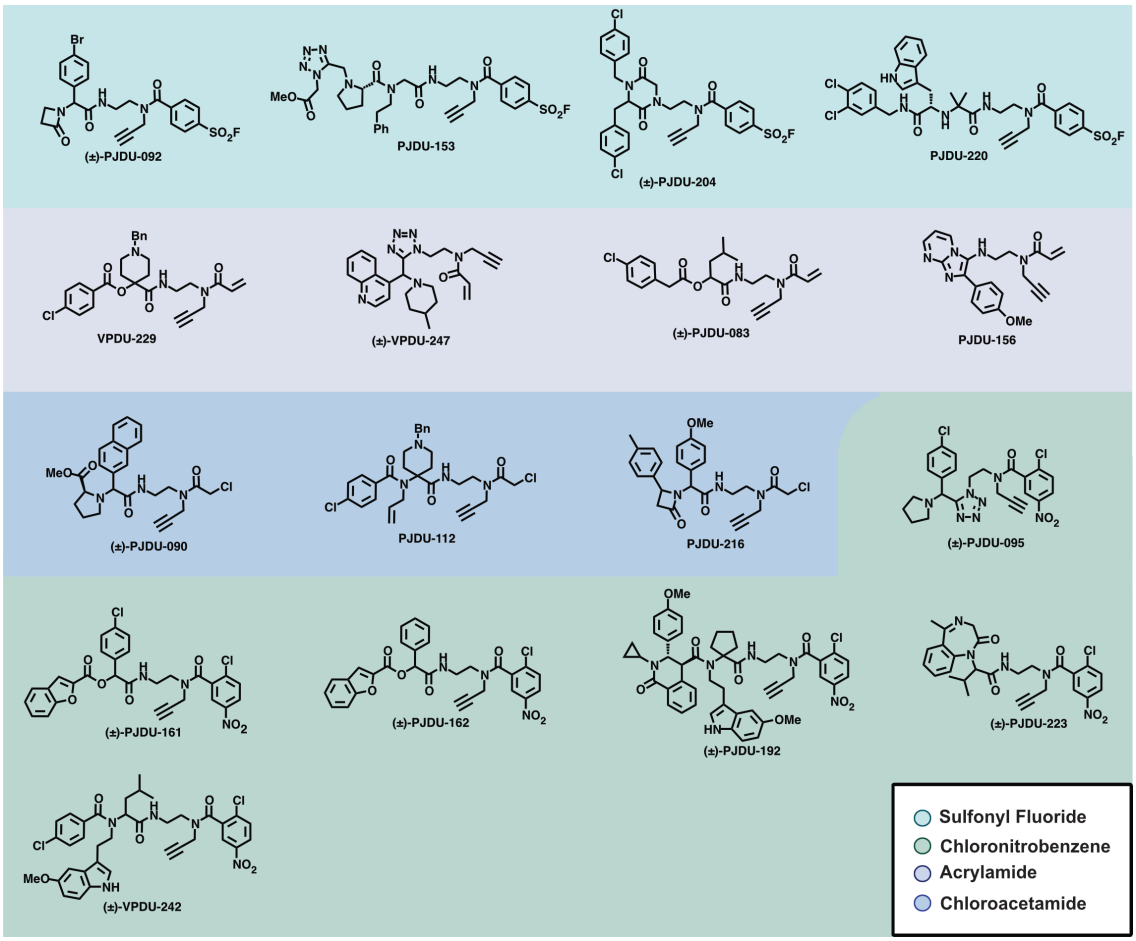


Figure 5-7. 17 Library members containing electrophilic protein reactive groups. Probes are separated by functional electrophilic moieties with sulfonyl fluorides in turquoise, cholornitrobenzenes in green, acrylamide in purple and choloracetamides in blue.

Evaluation of FFSMP breast cancer cell cytotoxicity.

To evaluate the bioactivity and potential of our electrophilic FFSMPs (Figure 5-7) to covalently modify protein targets directly in living cells, the electrophilic members of the FFSMP library were evaluated in a phenotypic screen for antiproliferative activity against MCF10CA1a breast cancer cells. Electrophilic

phenotypic screening was performed at 50 μM FFSMP concentrations at both 24- and 48-hour treatments, revealing several compounds with potent antiproliferative activity at this concentration (Figure 5-8A). Of the four different electrophilic groups tested during this work, the chloronitrobenzyl electrophile displayed the least number of antiproliferative compounds, likely reflecting on the low reactivity of this electrophile relative to the aryl sulfonyl fluoride, chloroacetamide, and acrylamide protein-reactive functional groups. From this primary screen, 8 members that exhibited greater than 50% decrease in cell proliferation at 48 hours were selected for a secondary proliferation screen at 25 μM concentration (Figure 5-8B).

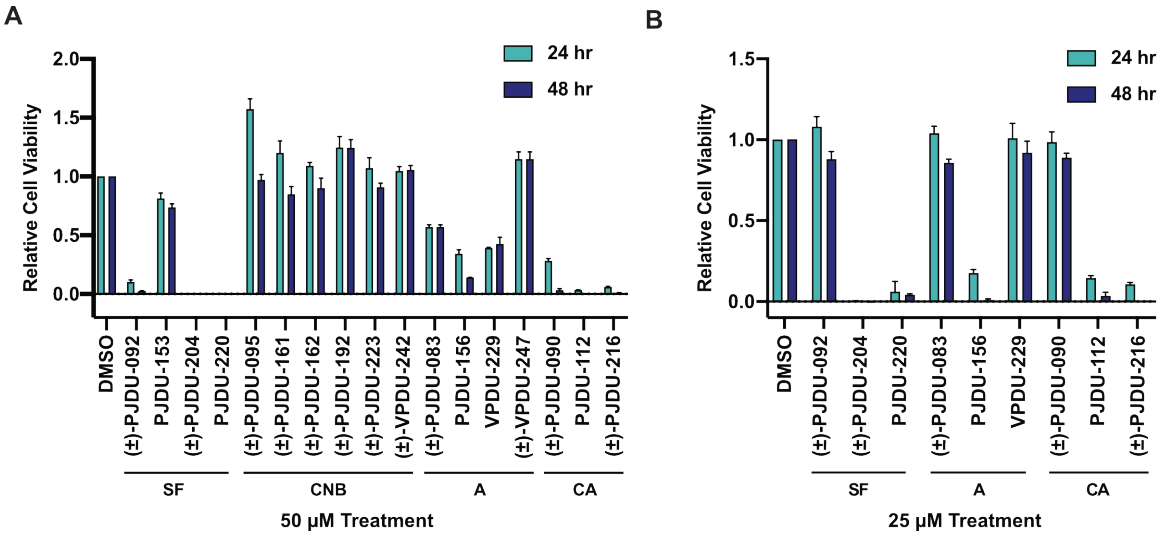


Figure 5-8. Biological characterization of the electrophilic FFSMP library members in MCF10CA1a cells. (A) Cell proliferation screen of the seventeen electrophilic FFSMP library members, grouped by electrophile (sulfonyl fluoride (SF), chloronitrobenzene (CNB), acrylamide (A), and chloroacetamide (CA), upon incubation with MCF10CA1a cells at 50 μM concentrations for 24 and 48 hours.

Cell viability is assessed by MTT reagent relative to a DMSO control. (B) Cell proliferation screen of nine electrophilic FFSMP library members upon incubation with MCF10CA1a cells at 25 μM concentrations for 24 and 48 hours. Cell viability is assessed by MTT reagent relative to a DMSO control.

Target deconvolution of cytotoxic probes.

The four most potent FFSMPs from this secondary screen (PJDU-112, (±)-PJDU-204, PJDU-216, and PJDU-220) were selected for further characterization. To visualize the general protein-labeling promiscuity of these FFSMPs, protein targets of each of these probes were visualized using in-gel fluorescence. Briefly, cells treated with each of the FFSMPs were lysed, and a fluorophore appended to probe-labeled proteins using copper (I)-catalyzed azide-alkyne cycloaddition (CuAAC).[32] Probe-labeled proteins within the cell lysate were then visualized upon gel electrophoresis and in-gel fluorescence imaging. In-gel fluorescence studies displayed a similar protein labeling pattern for two of the four probes (PJDU-112 and (±)-PJDU-216), with dominant labeling of protein bands around ~50 kD (Figure 5-9). Surprisingly, the two sulfonyl fluoride probes, (±)-PJDU-204 and PJDU-220, displayed minimal protein labeling by in-gel fluorescence, despite the potent antiproliferative activity observed.

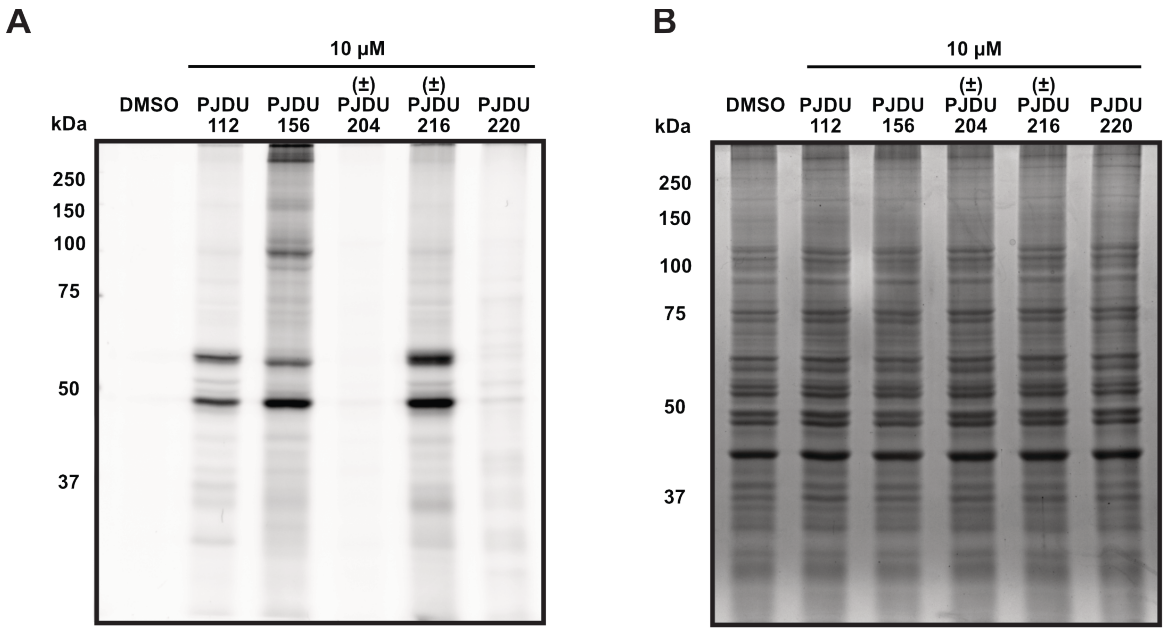


Figure 5-9. In-gel fluorescence assay of proteins covalently modified by each of five electrophilic FFSMPs upon treatment of live cells with 10 μM of compound for 24 hours.

Next, efforts were focused to better understand the apparent phenotypic response and labeling patterns of electrophilic FFSMPs with high cytotoxicity and biological activity. Initial target identification experiments were completed using FFSMPs, PJDU-156 and PJDU-216, which have similar properties to that of PJDU-112. MCF10CA1a cells were treated with 10 μM of probe for 3 hr before harvesting, lysing and click chemistry to append a biotin-azide tag. A shortened incubation time has shown to help improve selectivity and reduce some off target effects. After streptavidin enrichment and on-bead trypsin digest, we were afforded with peptides corresponding to the probe-modified proteins which were analyzed by mass spectrometry. Average spectral count enrichment was normalized against DMSO control samples and several proteins with corresponding molecular

weights to gel banding were annotated. Our data suggest several targets for both probes with highest target-engagement between PJDU-216 and protein disulfide isomerase 1 (P4HB:PDIA1) at 57 kD, thioredoxin reductase 1 (TXNRD1:TR1) at 70.7 kD, and glutathione s-transferase 1 (GSTO1) at 27.6 kD (Figure 5-10A, Table 5A-1). PJDU-156 appears to interact with and label more proteins than the other cytotoxic FFSMPs. Proteins with highest identification and labeling by PJDU-156 were angiotensin converting enzyme (ACE) at 149.7 kD, aldose reductase (AKR1B1) at 35.9 kD, and S100A2 protein (S100A2) at 11 kD (Figure 5-10B, Table 5A-1). Furthermore, intensive banding by PJDU-156 at 90.9 kD and 45.7 kD corresponds to labeling of a putative pre-mRNA splicing factor (DHX15) and heterogeneous nuclear ribonucleoprotein F (HNRNF), respectively. Interestingly, a similar band appears around 50 kD for both PJDU-156 and PJDU-216, this appears to be a modification of tubulin (TUBA8) present in both probe's populations of enriched proteins. No additional analysis was completed on PJDU-216 and PJDU-156 as the selectivity and cytotoxic responses were not as potent compared to PJDU-112 treatments in MCF10CA1a cells.

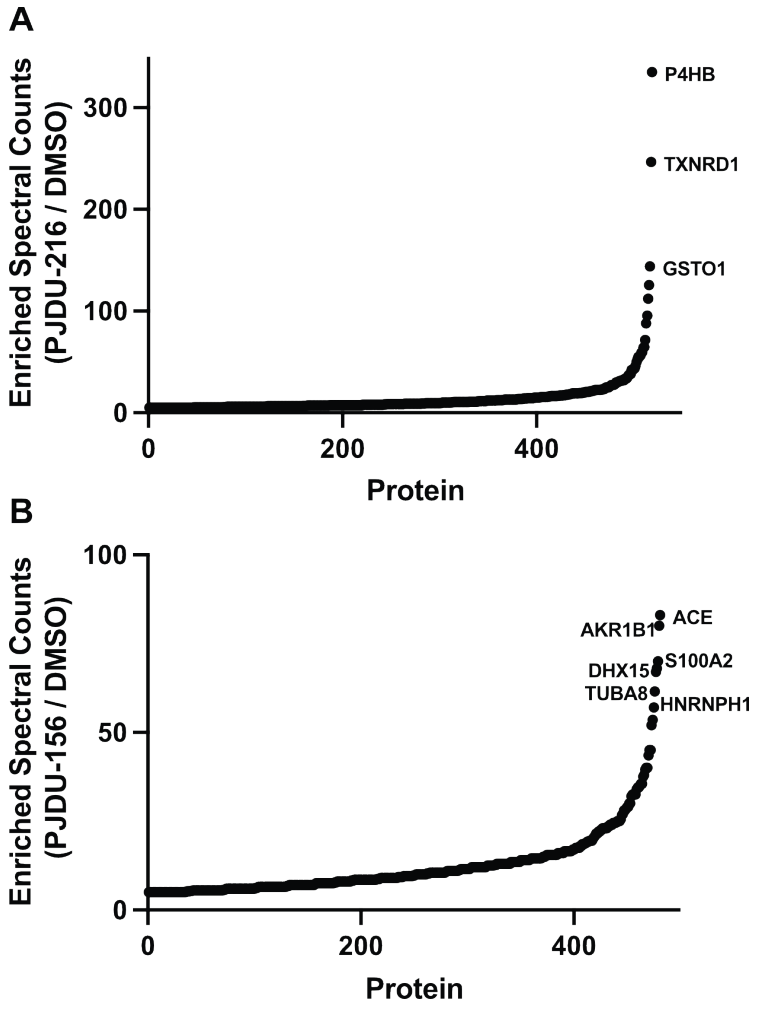


Figure 5-10. Average enriched spectral counts plotted for (A) PJDU-216 and (B) PJDU-156 normalized against spectral counts present in DMSO control samples. Proteins with similar masses to banding patterns found in Figure 5-9A are annotated (n=2).

PJDU-112 is a potent inhibitor of PDIA1.

For further drug target characterization, we focused on PJDU-112 due to its potent antiproliferative activity and selective targeting of two distinct protein bands at ~50 kD, with reduced labeling of other protein bands relative to PJDU-

216. Concentration-dependent analysis of the effects of PJDU-112 on cell proliferation demonstrated an EC50 value of ~22 μM (Figure 5-11).

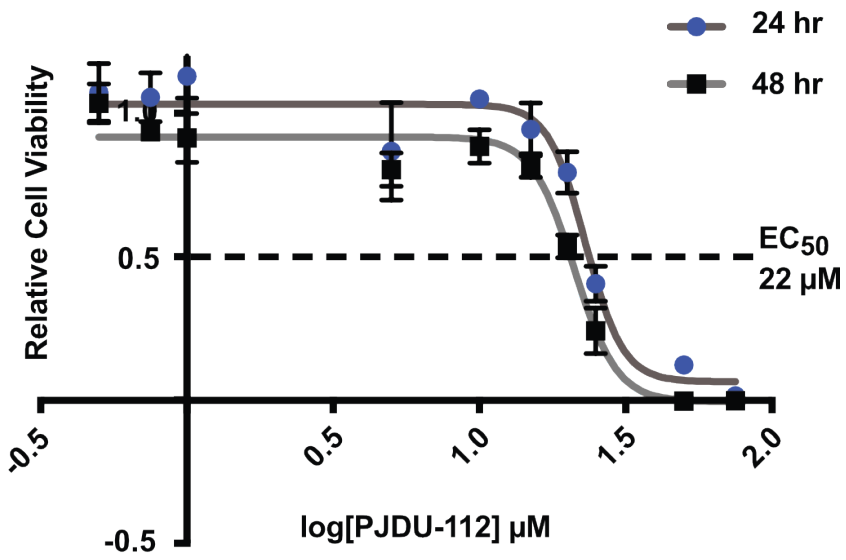


Figure 5-11. Concentration-dependent cell proliferation data for PJDU-112 upon treatment of MCF10CA1a cells at 24 and 48 hours with 0.5 – 75 μM concentrations. EC_{50} was determined to be 22 μM.

To determine the bioactive protein targets of PJDU-112, quantitative mass-spectrometry experiments were pursued to identify proteins selectively modified by PJDU-112, relative to the structurally similar, yet biological inert analog, VPDU-229, bearing an acrylamide electrophile. Briefly, cells were treated with PJDU-112 or VPDU-229 at 500 nM concentrations for 1 hour. Cells were then lysed, and probe-labeled proteins appended to biotin using CuAAC with biotin-azide. Biotinylated proteins were then enriched on streptavidin resin and subjected to on-bead trypsin digestion. To enable quantitative comparisons of the protein targets of PJDU-112 and VPDU-229, peptide mixtures were subjected to reductive

dimethylation (ReDiMe)[33] with heavy (PJDU-112) or light (VPDU-229) formaldehyde. The resulting peptide mixtures were analyzed by tandem mass spectrometry (LC-LC/MS-MS) to identify and quantify the abundance of each labeled protein in PJDU-112- and VPDU-229-treated samples (Figure 5-12).

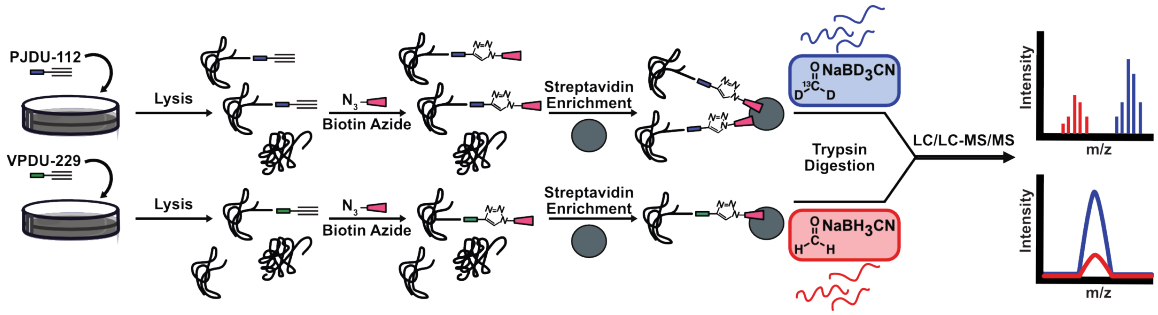
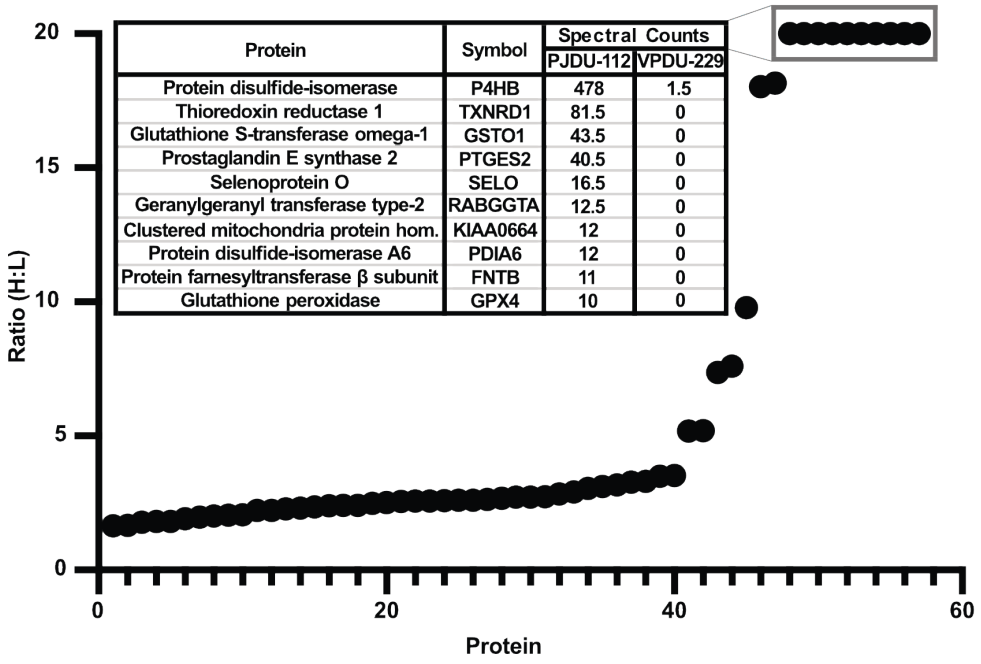


Figure 5-12. Workflow for quantitative proteomic analysis to identify protein targets of PDJU-112 and VPDU-229. MCF10CA1a cells were treated with 500 nM PDJU-112 or VPDU-229 for 1 hr, and probe-modified proteins enriched on streptavidin beads after cell lysis and CuAAC with biotin-azide. Peptides resulting from on-bead trypsin digestion were isotopically labeled by reductive dimethylation (ReDiMe) with light (VPDU-229) and heavy (PDJU-112) formaldehyde. The isotopically tagged peptides were analyzed by LC/LC-MS/MS to afford peptide identification and quantification in the form of heavy:light (H:L) isotopic ratios (Table 5A-2).

Protein targets selective for PJDU-112 are expected to display high heavy:light (H:L) ratios. Several proteins were identified with H:L ratio values of 20, indicating that they were only labeled by PJDU-112 and not by VPDU-229 (Figure 5-13, Figure 5-14). These included proteins well-characterized to contain highly reactive cysteine or selenocysteine residues, including protein disulfide

isomerase 1 (PDI),[34] thioredoxin reductase 1 (TXNRD1),[35] and glutathione S-transferase omega 1 (GSTO1).[36] Notably, protein targets overlap slightly with those identified in PJDU-156 and PJDU-216, however, PJDU-112 has heightening selectivity as evident by spectral count enrichments. Of these protein targets, the protein disulfide isomerase PDIA1 was the most significantly enriched according to spectral counts in the PJDU-112 sample, relative to VPDU-229 (Table 5A-2).



Protein	Symbol	Spectral Counts	
		PJDU-112	VPDU-229
Protein disulfide-isomerase	P4HB	478	1.5
Thioredoxin reductase 1	TXNRD1	81.5	0
Glutathione S-transferase omega-1	GSTO1	43.5	0
Prostaglandin E synthase 2	PTGES2	40.5	0
Selenoprotein O	SELO	16.5	0
Geranylgeranyl transferase type-2	RABGGTA	12.5	0
Clustered mitochondria protein hom.	KIAA0664	12	0
Protein disulfide-isomerase A6	PDIA6	12	0
Protein farnesyltransferase β subunit	FNTB	11	0
Glutathione peroxidase	GPX4	10	0

Figure 5-13. Ratio plot of proteins enriched for by PJDU-112 and VPDU-229. H:L ratios for proteins identified in two biological replicates of PDJU-112:VPDU-229 treated samples. Inset displays average spectral counts for those proteins displaying H:L ratios of ~20.

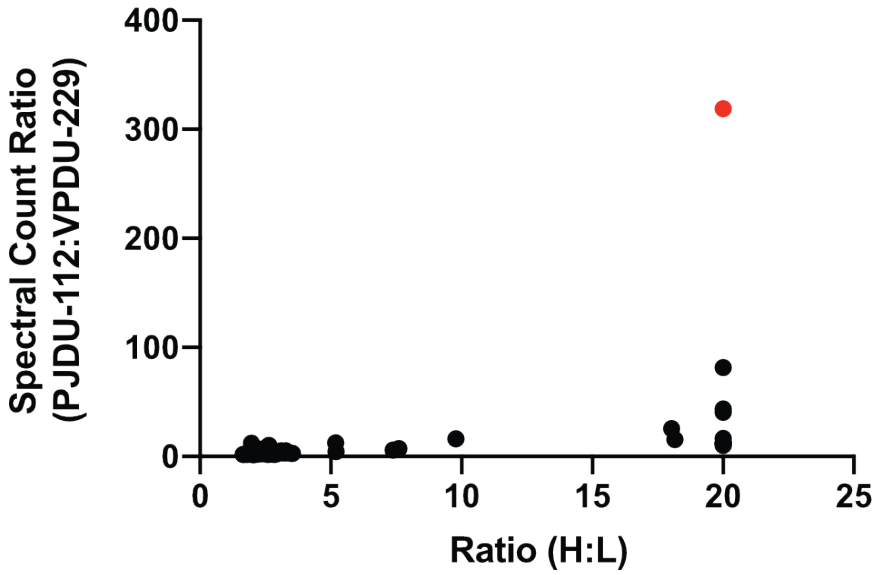


Figure 5-14. Visualization of spectral counts in PJDU-112 enrichment and H:L ratios for proteins identified in two biological replicates of PDJU-112:VPDU-229 treated samples.

PDIA1 is an oxidoreductase primarily localized to the endoplasmic reticulum that facilitates disulfide-bond formation, reduction, and isomerization within nascent proteins. PDIA1 contains two active-site domains, classified as a and a', each of which contain two highly reactive cysteines within a CGHC motif.[34,37] The two N-terminal cysteines (C53 and C397) within each CGHC motif are known to be highly reactive.[64] To confirm PDIA1 as a target of FFSMP PJDU-112, protein labeling by PJDU-112 in a SKOV-3 cell line deficient in PDIA1 was evaluated. The labeling of the ~50 kD band present in the parental SKOV-3 was abolished in the PDIA1 deficient cells, confirming PDIA1 as the predominant target of FFSMP PJDU-112 (Figure 5-15).

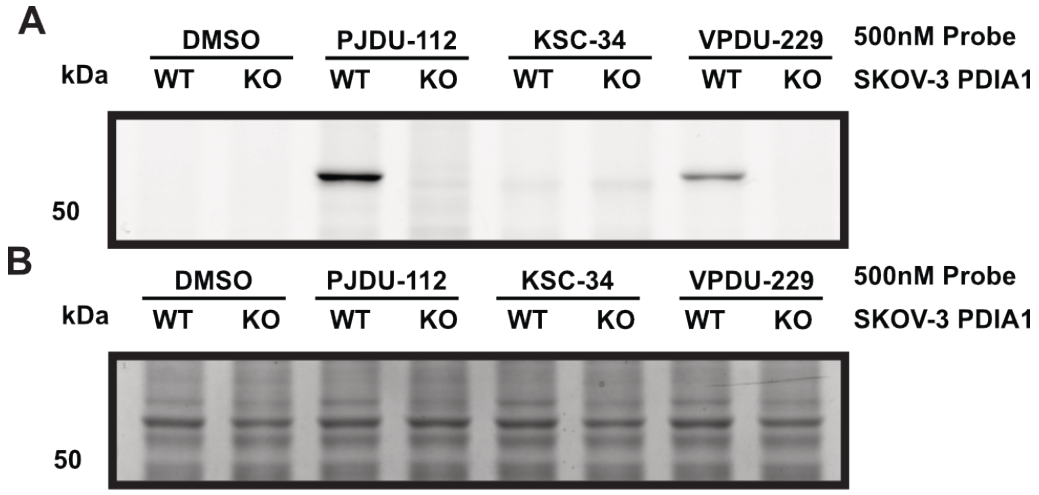


Figure 5-15. Evaluation of PDIA1-FFSMP engagement in SKOV3PDIA1 KO cell line (A) In-gel fluorescence demonstrating PJDU-112, KSC-34, VPDU-229 (500 nM for 1 hour) labeling in SKOV-3 wild-type (WT) and PDIA1 knock-out (KO) cells. (B) Coomassie total protein staining to confirm consistent concentrations.

To determine the cysteine that is targeted by FFSMP PJDU-112, wild-type PDIA1 and cysteine mutants (C53A and C397A) were overexpressed in HEK293T cells, and protein labeling by PJDU-112 was evaluated. No labeling was observed for the C53A mutant, confirming that labeling was selectively occurring at the N-terminal cysteine of the CGHC motif in the 'a' domain of PDIA1 (Figure 5-16). This is similar to the activity of a previously reported a-site inhibitor of PDIA1, KSC-34.[38]

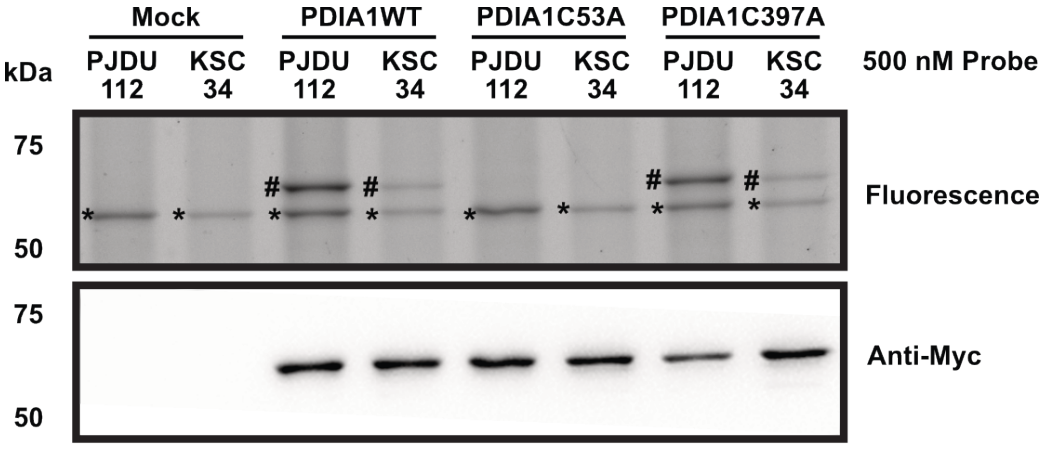


Figure 5-16. In-gel fluorescence displaying PJDU-112 (500 nM for 1 hour) labeling in PDIA1 wild-type (WT) and active-site cysteine mutant (C53A and C397A) expressing HEK293T cells. FFSMP PJDU-112 labeling was compared to KSC-34, a characterized PDIA1 covalent inhibitor. Labeling of endogenous PDIA1 (*) and overexpressed PDIA1 (#) is observed. Over-expression of PDIA1 was confirmed by anti-myc western blot.

Lastly, the effects of FFSMP PJDU-112 on PDIA1 activity in vitro was evaluated using an assay that monitors the aggregation of insulin induced by PDIA1-mediated reduction of disulfide bonds on insulin.[39] FFSMP PJDU-112 was shown to inhibit PDIA1 at low μM concentrations (Figure 5-17A). Furthermore, FFSMP PJDU-112 inhibition was shown to be more potent than KSC-34 (Figure 5-17B).[38] Together, these data confirm that FFSMP PJDU-112 covalently modifies C53 of PDIA1, resulting in inhibition of PDIA1 activity, which likely contributes to the antiproliferative phenotype observed for FFSMP PJDU-112.

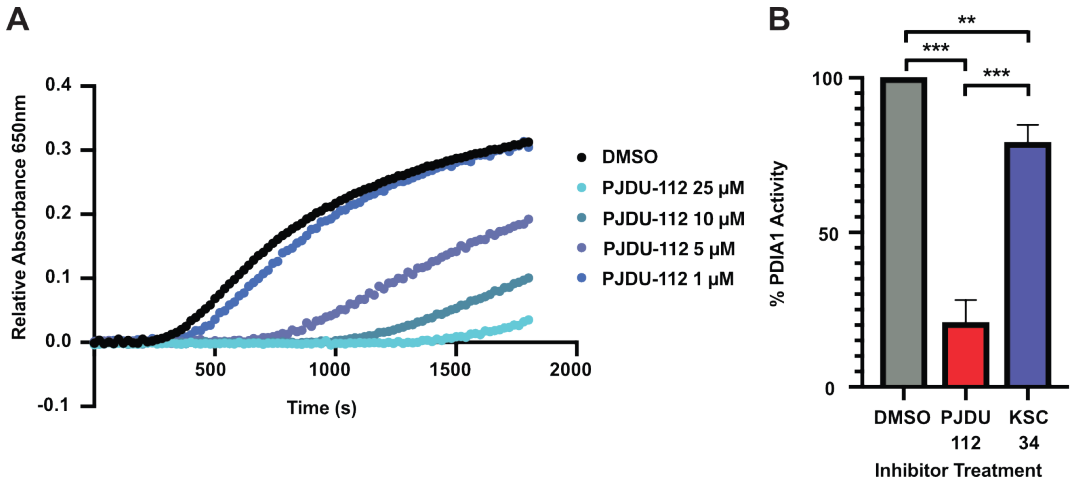


Figure 5-17. Evaluation of PJDU-112 and KSC-34 inhibition of PDIA1 (A) Insulin reductase assay to monitor PDIA1 activity upon treatment with DMSO and PJDU-112 (n=3) (B) PDIA1 activity upon treatment of KSC-34 and PJDU-112 (5 μM; 30 minutes). Statistical significance emphasized by asterisks.

Conclusion

Here, we demonstrate that the minimalist bifunctional isocyanide is a valuable building block for producing FFSMPs with considerable appendage-, scaffold-, and PRFG-diversity for integrated phenotypic screening-target identification campaigns. 49 FFSMPs were generated with containing electrophilic protein reactive groups (chloronitrobenzyl, aryl sulfonyl fluoride, chloroacetamide, and acrylamide) and containing photoreactive groups (benzophenone, aryl azide, and aliphatic diazirine). Computational chemistry assessment of the overall 3-D shape diversity of this FFSMP library revealed comparable sampling of molecular-shape space versus a set of sixty diverse natural products. FFMSP library were screened against MCF10ACA1a progressive breast cancer cells. With a decrease in efficiency and selectivity of

photoaffinity probes, attention was focused on the 17 electrophilic library members. Protein binding and electrophilic reactivity diversity were confirmed to be crucial for unique proteomic engagement and targeting efficiency. Subsequent phenotypic screening of the electrophilic FFSMP library members led to the identification of four compounds (PJDU-112, PJDU-156, PJDU-204, PJDU-216, and PJDU-220) possessing appreciable antiproliferative activity against MCF10CA1a breast cancer cells. In turn, chemoproteomic target identification methods were employed to discern protein disulfide isomerase A1 (PDIA1) as a major protein target most likely associated with the antiproliferative activity of one of the FFSMPs, U-4CR-derived[22] chloroacetamide PJDU-112.

Combining the three elements necessary for a diverse-FFMSP library, reactive warhead, protein docking ligand and bio-orthogonal reporter tags, require involved synthetic efforts. Modular approaches such as MCR enable facile generation of interchangeable structural motifs, and application of "library from library" approaches to further amplify library diversity. Although the tandem synthetic platform outlined offers simplified access to expansive functional combinations, limitations arise from accessibility of building blocks such as bifunctional isocyanides, which are less commonly available than other MCR inputs.[20] With a more widely accessible collection of reactive monomers comes opportunities to further diversify FFMSP libraries. In the future, a second generation FFMSP library could be achieved through Topliss optimization.[25] Such approaches would be useful to further improve upon the micromolar potency of PJDU-112 and selectivity towards PDIA1, as well as unearth ligands for previously intractable protein targets.

Experimental Procedures

Materials.

Chemicals were obtained from commercial sources, Sigma-Aldrich and Fisher Scientific, without further purification, unless otherwise noted. Phosphate buffered saline, PBS, was purchased from Fisher Scientific.

Methods.

Mammalian cell culture.

MCF10CA1a and MCF10A cell lines were maintained under 37°C and 5% CO_2 in DMEM:F12 media (Invitrogen) supplemented with 5% horse serum (Invitrogen), 25 μg/mL of Amphotericin B, 10,000 units/mL of penicillin, and 10,000 μg/mL streptomycin (1%, Anti-Anti, Gibco), 10 μg/mL insulin (from bovine pancreas, Sigma-Aldrich), 0.5 mg/mL hydrocortisone (Sigma-Aldrich), 20 ng/mL epidermal growth factor (EGF, Sigma-Aldrich), 100 ng/mL cholera toxin (Sigma-Aldrich). SKOV-3 wild-type (American Type Culture Collection) and SKOV-3 PDIA1 CRISPR-Cas9 knockout (generated in house) lines were maintained under the same conditions in RPMI media (Corning) supplemented with 10% FBS and 1% Anti-Anti. HEK293T cells were grown under the same conditions in DMEM media supplemented with 10% FBS, and 1% Anti-Anti.

Following various treatments, cells were harvested and washed with PBS. To collect cell lysates, pellets were resuspended in PBS and lysed by ultrasonic tip sonicator (Cole Parmer). Soluble lysate fractions were obtained after separation by spinning at 45,000 rpm for 45 minutes at 4°C and pelleted insoluble fractions were

discarded. To determine protein concentrations, DC Protein Assay kit (Bio-Rad) was performed.

MTT cell viability assay.

MCF10CA1a cells were seeded maximizing the log phase growth (1,000 cells / well) to each well of a 96-well plate in 100 μL DMEM:F12 complete media. After 24hours, 50 μM or 25 μM compound or DMSO in 100 μL fresh media was added with a no cell control with DMSO and media. Cells were grown for an additional 24 or 48hours, after which, each well was aspirated. 110 μL of MTT (0.45 mg/ml) in dye-free RPMI-1640 (Fisher Scientific) and cells were incubated for 4hr. 100 μL 10% SDS solution in 0.01% aqueous HCl was added to each well. The solution was covered and left at room temperature overnight and absorption was measured at 570 nm with SpectraMax M5 plate reader (Molecular Devices). Relative viability was determined by subtracting background and normalizing to DMSO treated control cells. Averaging three replicates gave reported relative cell viability values with error bars of stand error of the mean.

Photoreactive library member MCF10CA1a lysate labeling and fluorescence gel analysis.

MCF10CA1 cells were harvest, lysed and samples were normalized to 1.5 mg mL^{-1} protein concentrations. Lysates were treated with 10 and 20 μM concentrations of photo-reactive probes for 30 min followed by irradiation with UV light for 1 hr. Probe labeled proteins were functionalized with a fluorophore (tetramethylrhodamine-azide; TAMRA-N_3, Click Chemistry Tools) by CuAAC.[32] Cycloaddition of fluorescence reporter tag to the small molecule probes occurred

by incubating samples with TAMRA-N_3 (25 μM, 100x stock in DMSO), TCEP (1 mM, 50x stock in water), TBTA (100 μM, 17x stock in *t*-BuOH:DMSO 4:1), and copper (II) sulfate (1 mM, 50x stock in water) at room temperature for one hour, vortexing every 15 minutes. Reactions were quenched by the addition of equivalent volume of reducing SDS-loading dye (2x concentrated). Proteome solutions were then separated on 10% SDS-PAGE gel at 100 volts for ~ 2.5 hours and rhodamine fluorescence was visualized on a ChemiDoc MP imaging system (BioRad, Hercules, CA). Gels were then coomassie stained for one hour and destained overnight, following a standard procedure, and visualized on the imager.

Electrophilic library member *in situ* labeling and fluorescence gel analysis.

MCF10CA1a and SKOV-3 WT and PDIA1 CRISPR-Cas9 KO cells were grown to 100% confluency and treated with probe in the respective fresh media for one hour at 37°C and 5% CO_2. Cells were harvested and soluble fraction was collected, as described. Probe labeled proteins were functionalized with a fluorophore (tetramethylrhodamine-azide; TAMRA-N_3, Click Chemistry Tools) by CuAAC. Cycloaddition of fluorescence reporter tag to the small molecule probes occurred by incubating samples with TAMRA-N_3 (25 μM, 100x stock in DMSO), TCEP (1 mM, 50x stock in water), TBTA (100 μM, 17x stock in *t*-BuOH:DMSO 4:1), and copper (II) sulfate (1 mM, 50x stock in water) at room temperature for one hour, vortexing every 15 minutes. Reactions were quenched by the addition of equivalent volume of reducing SDS-loading dye (2x concentrated). Proteome solutions were then separated on 10% SDS-PAGE gel at 100 volts for ~ 2.5 hours and rhodamine fluorescence was visualized on a

ChemiDoc MP imaging system (BioRad, Hercules, CA). Gels were then coomassie stained for one hour and destained overnight, following a standard procedure, and visualized on the imager.

Transient protein expression.

HEK293T cells were grown on 10 cm plates to 60% confluency at 37 °C under 5% CO_2 in DMEM media supplemented with 10% fetal bovine serum (FBS, Atlanta Biologicals), and 1% Anti-Anti. Serum free (sf) DMEM media (1.5 mL) was combined with either lipofectamine 2000 (40 μL) or 8.8 μg pcDNA3.1(+)-myc mammalian expression vectors with either PDIA1 wild-type (WT), cysteine 53 alanine (C53A) or cysteine 397 alanine (C397A) mutants. Lipofectamine 2000 and pcDNA containing sf DMEM were mixed (3 mL total volume) and incubated for 7 minutes before the dropwise addition to each HEK293T plate. Plates were incubated for 24 hours at 37 °C under 5% CO_2. Cell lysates were prepared followed by conjugation to TAMRA-N_3 and fluorescent gel analysis, as previously described.

Western blot analysis.

SDS-PAGE gels were transferred to nitrocellulose membranes by electrophoresis at 75 volts for 140 min. Membranes were washed with tris-buffered saline with 1% Tween 20 (TBS-T) 3 times for 5 minutes followed by blocking with 5% (w/v) non-fat dry milk in TBS-T at room temperature for 1 hour. Following additional washes with TBS-T, membranes were incubated with primary anti-myc tag rabbit antibody (Cell Signaling, 1:1000) overnight at 4°C. Following removal and additional 3 washes with TBS-T, the membrane was incubated with secondary

anti-rabbit-HRP conjugated antibody for 2 hours at room temperature. After final washes with TBS-T, membranes were developed with HRP-super signal chemiluminescence reagents and imaged on the same imager described above.

MS preparation and analysis of PJDU-216 and PJDU-156.

MCF10CA1a cells were grown to 100% confluency in 20 cm tissue culture plates and treated with 500 nM PJDU-156 or PJDU-216, respectively. Cells were incubated at 37 °C under at 5% CO_2 for 1 hour before being harvested. Soluble labeled lysates were prepared as described previously. Probe-labeled MCF10CA1a lysates in PBS (500 μL, 2 mg mL^{-1}) underwent CuAAC with biotin-azide (200 μM, 100x stock in DMSO), TCEP (1 mM, 50x stock in water), TBTA (100 μM, 17x stock in t-BuOH:DMSO 4:1), and copper (II) sulfate (1 mM, 50x stock in water). The reaction proceeded at room temperature for 1 hour with vortexing every 15 minutes. Samples were centrifuged (5 min, 4500 g, 4 °C) pelleting the precipitated proteins. Protein pellets were resuspended in ice cold MeOH by tip sonication followed by spun and a second MeOH wash. The pellets were solubilized in 1.2% (w/v) SDS in PBS by sonication and heating (5 minutes at 80 °C). Copper was then pelleted by spinning of the solubilized probe-labeled proteomes at 6500 g for 5 min. The supernatant was diluted with 5 mL PBS giving a final concentration of 0.2% SDS. 100 μL streptavidin agarose resin (Thermo Scientific) was added to the samples, incubating overnight at 4 °C. Solutions were resolublized at room temperature for 2.5 hour and the beads were washed with 0.2% SDS/PBS (5 mL) for 10 minutes followed by PBS (3 x 5 mL), and water (3 x 5 mL). Between washes, beads were pelleted by spinning in a centrifuge (1400 g for 3 minutes).

After the final wash, the beads were resuspended in 6 M Urea/PBS (500 μL) and 10 mM DTT (20x stock in water) and incubated at 65 °C for 20 minutes. Iodoacetamide (10 mM, 50x stock in water) was then added and the samples reacted in the dark at room temperature for 30 minutes. Next, beads were diluted with 950 μL PBS, pelleted (1400 g for 3 min) and washed twice with 500 uL PBS. Subsequent resuspension in 200 μL of 2 M Urea/PBS buffer, 1 mM $CaCl_2$ (100x stock in water), and 2 μg trypsin in PBS (Promega, Madison, WI) allowed for on-bead trypsin digestions to proceed overnight at 37 °C with shaking. Supernatants were collected and placed in new tubes and samples were washed 3 x with 50 uL water.

LC/LC-MS/MS analysis was performed by Multidimensional Protein Identification Technology (MudPIT)[40,41] on an LTQ Orbitrap Discovery mass spectrometer (Thermo Fisher) with separation coupled to an Agilent 1200 series HPLC (Agilent Technologies). Tryptic peptides were pressure loaded onto a 250 μm fused silica desalting column packed with 4 cm of Aqua C18 reversed phase resin (Phenomenex). Peptides were then eluted onto a biphasic 100 μm fused silica column with a 5 μm tip, packed with 10 cm of C18 and 4 cm of Partisphere strong cation exchange resin (SCX, Whatman). Gradients 5-100% Buffer B in Buffer A (Buffer A: 95% water, 5% acetonitrile, 0.1% formic acid; Buffer B: 20% water, 80% acetonitrile, 0.1% formic acid), eluted peptides from the desalting columns displacing them on to the biphasic column. Before transfer to the mass spectrometer, peptides were further separated by elutions from the SCX to the C18 resin using four salt pushes.[39] Flow rates of buffer through the column was set to ~0.25 μL/min with spray voltage of 2.75 kV. One full MS scan (400 – 1800 MW)

was followed by 8 data dependent scans of the 8th most intense ions with dynamic exclusion enabled.

Two biological replicates of both PJDU-216 and PJDU-156 enriched peptides enriched from MCF10CA1a proteomic labeling were subjected to tandem mass spectrometric analysis described. The generated tandem MS data was searched using the SEQUEST[42] algorithm against the human UniProt database. Peptides reported were required to be tryptic with a static modification of +57.0215 on cysteine to account for alkylation of cysteine residues with iodoacetamide. For spectral count analysis, the SEQUEST output files were then filtered using DTASelect 2.0[43] to produce a curation of proteins identified with a false-discovery rate of less than 5%. Plotted proteins were filtered to include only samples with an average of 5 spectral counts or greater and spectral counts are representative of the average spectral counts of enriched proteins over those enriched in the DMSO (background) sample (Table 5A-2).

MS preparation and analysis of PJDU-112 and VPDU-229.

MCF10CA1a cells were grown to 100% confluency in 20 cm tissue culture plates and treated with 500 nM PJDU-112 or VPDU-229. Cells were incubated at 37 °C under at 5% CO_2 for 1 hour before being harvested. Soluble labeled lysates were prepared as described previously. Probe-labeled MCF10CA1a lysates in PBS (500 μL, 2 mg mL^{-1}) underwent CuAAC with biotin-azide (200 μM, 100x stock in DMSO), TCEP (1 mM, 50x stock in water), TBTA (100 μM, 17x stock in t-BuOH:DMSO 4:1), and copper (II) sulfate (1 mM, 50x stock in water). The reaction proceeded at room temperature for 1 hour with vortexing every 15 minutes.

Samples were centrifuged (5 min, 4500 g, 4 °C) pelleting the precipitated proteins. Protein pellets were resuspended in ice cold MeOH by tip sonication followed by spun and a second MeOH wash. The pellets were solubilized in 1.2% (w/v) SDS in PBS by sonication and heating (5 minutes at 80 °C). Copper was then pelleted by spinning of the solubilized probe-labeled proteomes at 6500 g for 5 min. The supernatant was diluted with 5 mL PBS giving a final concentration of 0.2% SDS. 100 μL streptavidin agarose resin (Thermo Scientific) was added to the samples, incubating overnight at 4 °C. Solutions were resolublized at room temperature for 2.5 hour and the beads were washed with 0.2% SDS/PBS (5 mL) for 10 minutes followed by PBS (3 x 5 mL), and water (3 x 5 mL). Between washes, beads were pelleted by spinning in a centrifuge (1400 g for 3 minutes).

After the final wash, the beads were resuspended in 6 M Urea/PBS (500 μL) and 10 mM DTT (20x stock in water), and incubated at 65 °C for 20 minutes. Iodoacetamide (10 mM, 50x stock in water) was then added and the samples reacted in the dark at room temperature for 30 minutes. Next, beads were diluted with 950 μL PBS, pelleted (1400 g for 3 min) and washed in 100 mM TEAB buffer. Subsequent resuspension in 200 μL of 2 M Urea in 100 mM triethyl ammonium bicarbonate (TEAB) buffer, 1 mM $CaCl_2$ (100x stock in water), and 2 μg trypsin in PBS (Promega, Madison, WI) allowed for on-bead trypsin digestions to proceed overnight at 37 °C with shaking. Supernatants were collected and placed in new tubes for reductive dimethylation (ReDiMe) labeling. PJDU-112-enriched peptides were dimethylated with 'heavy' formaldehyde, (16 μL, 4% stock, $^{13}CD_2O$), and sodium cyanoborodeuteride (16 μL, 0.6M stock, $NaBD_3CN$), while, VPDU-229-enriched peptides were dimethylated with 'light' formaldehyde, (16 μL, 4%, CH_2O), and sodium cyanoborohydride, (16 μL, 0.6 M stock, $NaBH_3CN$) for 2 hours

at room temperature. After the reactions were quenched with 3 μL 30% NH_4OH for 10 minutes at 0°C, PJDU-112 enriched heavy dimethylated peptides and VPDU-229-enriched light dimethylated peptides were combined (1:1 ratio). Formic acid (Thermo Fisher Scientific) was added to each sample for a final concentration of 5%. Samples were desalted on sepPak 1 cc C18 columns (50 mg, Waters) and dried overnight by speed vac. Peptide samples were resuspended in 95% water, 5% acetonitrile, 0.1% formic acid and the samples were stored at -20 °C until mass spectrometry analysis.

LC/LC-MS/MS analysis was performed by Multidimensional Protein Identification Technology (MudPIT)[40,41] on an LTQ Orbitrap Discovery mass spectrometer (Thermo Fisher) with separation coupled to an Agilent 1200 series HPLC (Agilent Technologies). ReDiMe labeled tryptic peptides were pressure loaded onto a 250 μm fused silica desalting column packed with 4 cm of Aqua C18 reversed phase resin (Phenomenex). Peptides were then eluted onto a biphasic 100 μm fused silica column with a 5 μm tip, packed with 10 cm of C18 and 4 cm of Partisphere strong cation exchange resin (SCX, Whatman). Gradients 5-100% Buffer B in Buffer A (Buffer A: 95% water, 5% acetonitrile, 0.1% formic acid; Buffer B: 20% water, 80% acetonitrile, 0.1% formic acid), eluted peptides from the desalting columns displacing them on to the biphasic column. Before transfer to the mass spectrometer, peptides were further separated by elutions from the SCX to the C18 resin using four salt pushes.[2] Flow rates of buffer through the column was set to ~0.25 μL/min with spray voltage of 2.75 kV. One full MS scan (400 – 1800 MW) was followed by 8 data dependent scans of the 8^{th} most intense ions with dynamic exclusion enabled.

Two biological replicates of combined PJDU-112 enriched heavy dimethylated peptides and VPDU-229-enriched light dimethylated peptides from MCF10CA1a proteome were subjected to tandem mass spectrometric analysis described. The generated tandem MS data was searched using the SEQUEST[42] algorithm against the human UniProt database. Peptides reported were required to be tryptic whilst also containing the differential modifications on lysine or the N-terminus of +36.07567 for 'heavy' dimethylation of PJDU-112 given peptides and +28.0313 for 'light' dimethylation of VPDU-229 given peptides. Each search included a static modification of +57.0215 on cysteine to account for alkylation of cysteine residues with iodoacetamide. For spectral count analysis, the SEQUEST output files were then filtered using DTASelect 2.0[43] to produce a curation of proteins identified with a false-discovery rate of less than 5%. The presented proteins were filtered to include only samples with an average of 10 spectral counts or greater in two PJDU-112 samples. For these proteins surpassing the provided criteria, the change in spectral counts between PJDU-112 treated proteome and VPDU-229 treated proteome was calculated. For quantitative analysis of heavy:light (H:L) ratios, fold enrichment of proteins labeled by PJDU-112 compared to VPDU-229, was calculated through cimage quantification package.[44] Spectral counts and H:L ratios are presented in sorted mass spectrometry data, (Table 5A-2).

Recombinant expression of PDIA1.

pET23a C-terminal His_6 tag-fused PDIA1 WT was transformed in *Escherichia coli* BL21 cells grown in Luria-Bertani broth with 100 μg/mL ampicillin at 37°C to A_{600} = 0.8. Expression was induced by 0.6 mM isopropyl β-D-1-

thiogalactopyranoside (IPTG) and incubated overnight at 27 °C. Cells were pelleted by centrifugation, lysed open by tip sonication in PBS, and soluble fraction collected. PDIA1 WT was isolated by Ni-NTA column and purified by PD10 size exclusion column.

Protein disulfide isomerase reductase assay.

Preparation of the insulin turbidity[39] PDI activity assay began with 25 μL aliquots of 5 μM PDIA1 in PBS incubated with inhibitors, PJDU-112, KSC-34, or DMSO (0.5 μL of 50x) with final concentrations ranging from 1 μM to 25 μM for 30 minutes. Upon brief mixing, 10 μL of the solutions were added to 70 μL of freshly prepared assay buffer (100 mM K_2HPO_4, 2 mM EDTA, pH 7.0) in one well of a 96 well plate. 10 μL of bovine insulin solubilized in 0.1 N HCl (10x, 1.6 mM, Sigma-Aldrich) was also added to each reaction and the samples were shaken on the plate reader. Assay reactions were initiated by the addition of 10 μL dithiothreitol (DTT, 10x, 10 mM). Included was a control sample without PDIA1 containing DTT. Absorbances were read at 650 nm every 25 seconds for 30 minutes with plate shaking between each read. Assay final concentrations for each well included 0.5 μM PDIA1 WT, 0.16 mM bovine insulin, and 1 mM DTT. Background absorbances (from the sample without PDIA1) were subtracted for each sample at each time point read. Absorbance vs time plots were generated and the linear slopes from each plot were illustrating the decline in PDIA1 activity upon inhibitor treatments.

References

(1) Oprea, T. I.; Bologa, C. G.; Brunak, S.; Campbell, A.; Gan, G. N.; Gaulton, A.; Gomez, S. M.; Guha, R.; Hersey, A.; Holmes, J.; Jadhav, A.; Jensen, L. J.; Johnson, G. L.; Karlson, A.; Leach, A. R.; Ma'ayan, A.; Malovannaya, A.; Mani, S.; Mathias, S. L.; McManus, M. T.; Meehan, T. F.; von Mering, C.; Muthas, D.; Nguyen, D.-T.; Overington, J. P.; Papadatos, G.; Qin, J.; Reich, C.; Roth, B. L.; Schürer, S. C.; Simeonov, A.; Sklar, L. A.; Southall, N.; Tomita, S.; Tudose, I.; Ursu, O.; Vidović, D.; Waller, A.; Westergaard, D.; Yang, J. J.; Zahoránszky-Köhalmi, G. Unexplored Therapeutic Opportunities in the Human Genome. *Nat. Rev. Drug Discov.* **2018**, *17* (5), 317–332.

(2) Antolin, A. A.; Tym, J. E.; Komianou, A.; Collins, I.; Workman, P.; Al-Lazikani, B. Objective, Quantitative, Data-Driven Assessment of Chemical Probes. *Cell Chem. Biol.* **2018**, *25* (2), 194-205.e5.

(3) Arrowsmith, C. H.; Audia, J. E.; Austin, C.; Baell, J.; Bennett, J.; Blagg, J.; Bountra, C.; Brennan, P. E.; Brown, P. J.; Bunnage, M. E.; Buser-Doepner, C.; Campbell, R. M.; Carter, A. J.; Cohen, P.; Copeland, R. A.; Cravatt, B.; Dahlin, J. L.; Dhanak, D.; Edwards, A. M.; Frederiksen, M.; Frye, S. V.; Gray, N.; Grimshaw, C. E.; Hepworth, D.; Howe, T.; Huber, K. V. M.; Jin, J.; Knapp, S.; Kotz, J. D.; Kruger, R. G.; Lowe, D.; Mader, M. M.; Marsden, B.; Mueller-Fahrnow, A.; Müller, S.; O'Hagan, R. C.; Overington, J. P.; Owen, D. R.; Rosenberg, S. H.; Ross, R.; Roth, B.; Schapira, M.; Schreiber, S. L.; Shoichet, B.; Sundström, M.; Superti-Furga, G.; Taunton, J.; Toledo-Sherman, L.; Walpole, C.; Walters, M. A.; Willson, T. M.; Workman, P.; Young, R. N.; Zuercher, W. J. The Promise and Peril of Chemical Probes. *Nat. Chem. Biol.* **2015**, *11* (8), 536–541.

(4) Schreiber, S. L.; Kotz, J. D.; Li, M.; Aubé, J.; Austin, C. P.; Reed, J. C.; Rosen, H.; White, E. L.; Sklar, L. A.; Lindsley, C. W.; Alexander, B. R.; Bittker, J. A.; Clemons, P. A.; de Souza, A.; Foley, M. A.; Palmer, M.; Shamji, A. F.; Wawer, M. J.; McManus, O.; Wu, M.; Zou, B.; Yu, H.; Golden, J. E.; Schoenen, F. J.; Simeonov, A.; Jadhav, A.; Jackson, M. R.; Pinkerton, A. B.; Chung, T. D. Y.; Griffin, P. R.; Cravatt, B. F.; Hodder, P. S.; Roush, W. R.; Roberts, E.; Chung, D.-H.; Jonsson, C. B.; Noah, J. W.; Severson, W. E.; Ananthan, S.; Edwards, B.; Oprea, T. I.; Conn, P. J.; Hopkins, C. R.; Wood, M. R.; Stauffer, S. R.; Emmitte, K. A.; Brady, L. S.; Driscoll, J.; Li, I. Y.; Loomis, C. R.; Margolis, R. N.; Michelotti, E.; Perry, M. E.; Pillai, A.; Yao, Y. Advancing Biological Understanding and Therapeutics Discovery with Small-Molecule Probes. *Cell* **2015**, *161* (6), 1252–1265.

(5) Cisar, J. S.; Cravatt, B. F. Fully Functionalized Small-Molecule Probes for Integrated Phenotypic Screening and Target Identification. *J. Am. Chem. Soc.* **2012**, *134* (25), 10385–10388.

(6) Banerjee, R.; Pace, N. J.; Brown, D. R.; Weerapana, E. 1,3,5-Triazine as a Modular Scaffold for Covalent Inhibitors with Streamlined Target Identification. *J. Am. Chem. Soc.* **2013**, *135* (7), 2497–2500.

(7) Couvertier, S. M.; Weerapana, E. Cysteine-Reactive Chemical Probes Based on a Modular 4-Aminopiperidine Scaffold. *Med. Chem. Commun.* **2014**, *5* (3), 358–362.

(8) Kambe, T.; Correia, B. E.; Niphakis, M. J.; Cravatt, B. F. Mapping the Protein Interaction Landscape for Fully Functionalized Small-Molecule Probes in Human Cells. *J. Am. Chem. Soc.* **2014**, *136* (30), 10777–10782.

(9) Parker, C. G.; Galmozzi, A.; Wang, Y.; Correia, B. E.; Sasaki, K.; Joslyn, C. M.; Kim, A. S.; Cavallaro, C. L.; Lawrence, R. M.; Johnson, S. R.; Narvaiza, I.; Saez, E.; Cravatt, B. F. Ligand and Target Discovery by Fragment-Based Screening in Human Cells. *Cell* **2017**, *168* (3), 527-541.e29.

(10) Backus, K. M.; Correia, B. E.; Lum, K. M.; Forli, S.; Horning, B. D.; Gonzalez-Paez, G. E.; Chatterjee, S.; Lanning, B. R.; Teijaro, J. R.; Olson, A. J.; Wolan, D. W.; Cravatt, B. F. Proteome-Wide Covalent Ligand Discovery in Native Biological Systems. *Nature* **2016**, *534* (7608), 570–574.

(11) Galmozzi, A.; Parker, C. G.; Kok, B. P.; Cravatt, B. F.; Saez, E. Discovery of Modulators of Adipocyte Physiology Using Fully Functionalized Fragments. *Methods Mol. Biol.* **2018**, *1787*, 115–127.

(12) Liu, W.; Zhang, Z.; Zhang, Z.-M.; Hao, P.; Ding, K.; Li, Z. Integrated Phenotypic Screening and Activity-Based Protein Profiling to Reveal Potential Therapy Targets of Pancreatic Cancer. *Chem. Commun.* **2019**, *55* (11), 1596–1599.

(13) Conway, L. P.; Jadhav, A. M.; Homan, R. A.; Li, W.; Rubiano, J. S.; Hawkins, R.; Lawrence, R. M.; Parker, C. G. Evaluation of Fully-Functionalized Diazirine Tags for Chemical Proteomic Applications. *Chem. Sci.* **2021**, *12* (22), 7839–7847.

(14) Wang, Y.; Dix, M. M.; Bianco, G.; Remsberg, J. R.; Lee, H.-Y.; Kalocsay, M.; Gygi, S. P.; Forli, S.; Vite, G.; Lawrence, R. M.; Parker, C. G.; Cravatt, B. F. Expedited Mapping of the Ligandable Proteome Using Fully Functionalized Enantiomeric Probe Pairs. *Nat. Chem.* **2019**, *11* (12), 1113–1123.

(15) West, A. V.; Muncipinto, G.; Wu, H.-Y.; Huang, A. C.; Labenski, M. T.; Jones, L. H.; Woo, C. M. Labeling Preferences of Diazirines with Protein Biomolecules. *J. Am. Chem. Soc.* **2021**, *143* (17), 6691–6700.

(16) Moellering, R. E.; Cravatt, B. F. How Chemoproteomics Can Enable Drug Discovery and Development. *Chem. Biol.* **2012**, *19* (1), 11–22.

(17) Jones, L. H.; Neubert, H. Clinical Chemoproteomics—Opportunities and Obstacles. *Sci. Transl. Med.* **2017**, *9* (386), eaaf7951.

(18) Deng, Z. L.; Du, C. X.; Li, X.; Hu, B.; Kuang, Z. K.; Wang, R.; Peng, S. Y.; Zhang, H. Y.; Kong, D. X. Exploring the Biologically Relevant Chemical Space for Drug Discovery. *J. Chem. Inf. Model.* **2013**, *53* (11), 2820–2828.

(19) Oeljeklaus, J.; Kaschani, F.; Kaiser, M. Streamlining Chemical Probe Discovery: Libraries of "Fully Functionalized" Small Molecules for Phenotypic Screening. *Angew. Chem. Int. Edit.* **2013**, *52* (5), 1368–1370.

(20) Sauer, W. H. B.; Schwarz, M. K. Molecular Shape Diversity of Combinatorial Libraries: A Prerequisite for Broad Bioactivity. *J. Chem. Inf. Comput. Sci.* **2003**, *43* (3), 987–1003.

(21) Li, Z.; Hao, P.; Li, L.; Tan, C. Y. J.; Cheng, X.; Chen, G. Y. J.; Sze, S. K.; Shen, H.-M.; Yao, S. Q. Design and Synthesis of Minimalist Terminal Alkyne-Containing Diazirine Photo-Crosslinkers and Their Incorporation into Kinase Inhibitors for Cell- and Tissue-Based Proteome Profiling. *Angew. Chem. Int. Edit.* **2013**, *52* (33), 8551–8556.

(22) Jackson, P.; Lapinsky, D. J. Appendage and Scaffold Diverse Fully Functionalized Small-Molecule Probes via a Minimalist Terminal Alkyne-Aliphatic Diazirine Isocyanide. *J. Org. Chem.* **2018**, *83* (18), 11245–11253.

(23) Duarte, C. D.; Barreiro, E. J.; Fraga, C. A. M. Privileged Structures: A Useful Concept for the Rational Design of New Lead Drug Candidates. *Mini. Rev. Med. Chem.* **2007**, *7* (11), 1108–1119.

(24) Welsch, M. E.; Snyder, S. A.; Stockwell, B. R. Privileged Scaffolds for Library Design and Drug Discovery. *Curr. Opin. Chem. Biol.* **2010**, *14* (3), 347–361.

(25) Topliss, J. G. Utilization of Operational Schemes for Analog Synthesis in Drug Design. *J. Med. Chem.* **1972**, *15* (10), 1006–1011.

(26) Richter, L. Topliss Batchwise Schemes Reviewed in the Era of Open Data Reveal Significant Differences between Enzymes and Membrane Receptors. *J. Chem. Inf. Model.* **2017**, *57* (10), 2575–2583.

(27) Soule, H.; Maloney, T.; Wolman, S.; Peterson, W.; Brenz, R.; McGrath, C.; Russo, J.; Pauley, R.; Jones, R.; Brooks, S. Isolation and Characterization of a Spontaneously Immortalized Human Breast Epithelial Cell Line, MCF-10. *Cancer Res.* **1990**, *50* (18), 6075–6078.

(28) Imbalzano, K. M.; Tatarkova, I.; Imbalzano, A. N.; Nickerson, J. A. Increasingly Transformed MCF-10A Cells Have a Progressively Tumor-like Phenotype in Three-Dimensional Basement Membrane Culture. *Cancer Cell Int.* **2009**, *9*, 7.

(29) Narayanan, A.; Jones, L. H. Sulfonyl Fluorides as Privileged Warheads in Chemical Biology. *Chem. Sci.* **2015**, *6* (5), 2650–2659.

(30) Shiraiwa, K.; Cheng, R.; Nonaka, H.; Tamura, T.; Hamachi, I. Chemical Tools for Endogenous Protein Labeling and Profiling. *Cell Chem. Biol.* **2020**, *27* (8), 970–985.

(31) Sumranjit, J.; Chung, S. J. Recent Advances in Target Characterization and Identification by Photoaffinity Probes. *Molecules* **2013**, *18* (9), 10425–10451.

(32) Rostovtsev, V. V.; Green, L. G.; Fokin, V. V.; Sharpless, K. B. A Stepwise Huisgen Cycloaddition Process: Copper(I)-Catalyzed Regioselective "Ligation" of Azides and Terminal Alkynes. *Angew. Chem. Int. Edit.* **2002**, *41* (14), 2596.

(33) Boersema, P. J.; Raijmakers, R.; Lemeer, S.; Mohammed, S.; Heck, A. J. R. Multiplex Peptide Stable Isotope Dimethyl Labeling for Quantitative Proteomics. *Nat. Protoc.* **2009**, *4* (4), 484–494.

(34) Kozlov, G.; Määttänen, P.; Thomas, D. Y.; Gehring, K. A Structural Overview of the PDI Family of Proteins. *FEBS J.* **2010**, *277* (19), 3924–3936.

(35) Zhong, L.; Arnér, E. S. J.; Holmgren, A. Structure and Mechanism of Mammalian Thioredoxin Reductase: The Active Site Is a Redox-Active Selenolthiol/Selenenylsulfide Formed from the Conserved Cysteine-Selenocysteine Sequence. *Proc. Natl. Acad. Sci.* **2000**, *97* (11), 5854–5859.

(36) Menon, D.; Board, P. G. A Role for Glutathione Transferase Omega 1 (GSTO1-1) in the Glutathionylation Cycle. *J. Biol. Chem.* **2013**, *288* (36), 25769–25779.

(37) Xu, S. L.; Sankar, S.; Neamati, N. Protein Disulfide Isomerase: A Promising Target for Cancer Therapy. *Drug Discov. Today* **2014**, *19* (3), 222–240.

(38) Cole, K. S.; Grandjean, J. M. D.; Chen, K.; Witt, C. H.; O'Day, J.; Shoulders, M. D.; Wiseman, R. L.; Weerapana, E. Characterization of an A-Site Selective Protein Disulfide Isomerase A1 Inhibitor. *Biochemistry-US* **2018**, *57* (13), 2035–2043.

(39) Holmgren, A. Thioredoxin Catalyzes the Reduction of Insulin Disulfides by Dithiothreitol and Dihydrolipoamide. *J. Biol. Chem.* **1979**, *254* (19), 9627–9632.

(40) Delahunty, C. M.; Yates, J. R. MudPIT: Multidimensional Protein Identification Technology. *Biotechniques* **2007**, *43* (5), 563-567

(41) Weerapana, E.; Speers, A. E.; Cravatt, B. F. Tandem Orthogonal Proteolysis-Activity-Based Protein Profiling (TOP-ABPP)—a General Method for Mapping Sites of Probe Modification in Proteomes. *Nat. Protoc.* **2007**, *2* (6), 1414–1425.

(42) Eng, J. K.; McCormack, A. L.; Yates, J. R. An Approach to Correlate Tandem Mass Spectral Data of Peptides with Amino Acid Sequences in a Protein Database. *J. Am. Soc. Mass Spectrom.* **1994**, *5* (11), 976–989.

(43) Tabb, D. L.; McDonald, W. H.; Yates, J. R. DTASelect and Contrast: Tools for Assembling and Comparing Protein Identifications from Shotgun Proteomics. *J Proteome Res.* **2002**, *1* (1), 21–26.

(44) Weerapana, E.; Wang, C.; Simon, G. M.; Richter, F.; Khare, S.; Dillon, M. B. D.; Bachovchin, D. A.; Mowen, K.; Baker, D.; Cravatt, B. F. Quantitative Reactivity Profiling Predicts Functional Cysteines in Proteomes. *Nature* **2010**, *468* (7325), 790–795.

Appendix I

Mass Spectrometry and GO Analysis Tables

Table 2A-1. List of proteins identified in HEK293T and Whole-Cell (WC) and pure isolated mitochondria (Mito) samples containing at least 4 spectral counts. Corresponding GO cellular compartments.

UniProt ID	Protein Description	Mito	WC	GO Cellular Component
P10809	HSPD1 60 kDa heat shock protein, mitochondrial	171	50	cytosol;endosome;extracellular region or secreted;mitochondrion;plasma membrane;early endosome;extracellular exosome;extracellular space;mitochondrial inner membrane;mitochondrial matrix;clathrin-coated pit;cell surface;coated vesicle;cytoplasm;lipopolysaccharide receptor complex;membrane;protein-containing complex;secretory granule
P60709	ACTB Actin, cytoplasmic 1	161	23	cytoskeleton;cytosol;extracellular region or secreted;nucleus;plasma membrane;actin cytoskeleton;actin filament;postsynaptic actin cytoskeleton;blood microparticle;extracellular exosome;extracellular space;nua4 histone acetyltransferase complex;nucleoplasm;adherens junction;apical junction complex;axon;cell-cell junction;chromatin;cytoplasm;cytoplasmic ribonucleoprotein granule;dense body;focal adhesion;glutamatergic synapse;lamellipodium;membrane;presynapse;protein-containing complex;ribonucleoprotein complex;synapse;tight junction;vesicle
P45880	VDAC2 Voltage-dependent anion-selective channel protein 2	118	6	mitochondrion;nucleus;mitochondrial membrane;mitochondrial nucleoid;mitochondrial outer membrane;acrosomal vesicle;membrane;membrane raft;pore complex;synaptic vesicle
Q9Y277	VDAC3 Voltage-dependent anion-selective channel protein 3	107	1	extracellular region or secreted;mitochondrion;nucleus;extracellular exosome;mitochondrial outer membrane;membrane;pore complex
O94826	TOMM70A Mitochondrial import receptor subunit TOM70	93	0	extracellular region or secreted;mitochondrion;extracellular exosome;mitochondrial outer membrane;mitochondrial outer membrane translocase complex;integral component of membrane;membrane
P30084	ECHS1 Enoyl-CoA hydratase, mitochondrial	77	20	mitochondrion;mitochondrial matrix
P12236	SLC25A6 ADP/ATP translocase 3	77	0	mitochondrion;nucleus;mitochondrial inner membrane;tim23 mitochondrial import inner membrane translocase complex;integral component of membrane;membrane
P12235	SLC25A4 ADP/ATP translocase 1	76	0	mitochondrion;plasma membrane;integral component of mitochondrial membrane;mitochondrial inner membrane;mitochondrial permeability transition pore complex;integral component of plasma membrane;membrane
P49411	TUFM Elongation factor Tu, mitochondrial	62	3	extracellular region or secreted;mitochondrion;extracellular exosome;mitochondrial nucleoid;membrane;synapse
P05141	SLC25A5 ADP/ATP translocase 2	62	0	cytoskeleton;mitochondrion;nucleus;plasma membrane;mmxd complex;mitochondrial inner membrane;mitochondrial nucleoid;mitochondrial permeability transition pore complex;integral component of plasma membrane;membrane;membrane raft
Q9UJZ1	STOML2 Stomatin-like protein 2	56	0	cytoskeleton;mitochondrion;plasma membrane;mitochondrial inner membrane;mitochondrial intermembrane space;extrinsic component of plasma membrane;membrane raft
P42704	LRPPRC Leucine-rich PPR motif-containing protein, mitochondrial	39	4	cytoskeleton;mitochondrion;nucleus;microtubule;mitochondrial nucleoid;condensed nuclear chromosome;nuclear inner membrane;nuclear outer membrane;nucleoplasm;membrane;perinuclear region of cytoplasm;ribonucleoprotein complex
P38646	HSPA9 Stress-70 protein, mitochondrial	35	2	extracellular region or secreted;mitochondrion;nucleus;extracellular exosome;mib complex;mitochondrial matrix;mitochondrial nucleoid;sam complex;nucleolus;cytoplasm;focal adhesion
P24752	ACAT1 Acetyl-CoA acetyltransferase, mitochondrial	28	25	extracellular region or secreted;mitochondrion;extracellular exosome;mitochondrial matrix
B4DLN1	SLC25A10 cDNA FLJ60124, highly similar to Mitochondrial dicarboxylate carrier	26	0	mitochondrion;nucleus;mitochondrial membrane;nucleoplasm;integral component of membrane;ribosome
O95299	NDUFA10 NADH dehydrogenase	25	0	mitochondrion;mitochondrial inner membrane;mitochondrial matrix;mitochondrial respiratory chain complex i;cytoplasm
P40939	HADHA Trifunctional enzyme subunit alpha, mitochondrial	25	0	mitochondrion;mitochondrial fatty acid beta-oxidation multienzyme complex;mitochondrial inner membrane;mitochondrial nucleoid
Q99714	HSD17B10 3-hydroxyacyl-CoA dehydrogenase type-2	23	9	mitochondrion;plasma membrane;mitochondrial matrix;mitochondrial nucleoid;mitochondrial ribonuclease p complex;cytoplasm
P32322	PYCR1 Pyrroline-5-carboxylate reductase 1, mitochondrial	22	4	mitochondrion;mitochondrial matrix
O75431	MTX2 Metaxin-2	22	0	mitochondrion;nucleus;mib complex;mitochondrial outer membrane;sam complex;nucleolus;cytoplasm
P34897	SHMT2 Serine hydroxymethyltransferase, mitochondrial	21	6	cytoskeleton;cytosol;extracellular region or secreted;mitochondrion;nucleus;microtubule cytoskeleton;extracellular exosome;mitochondrial inner membrane;mitochondrial intermembrane space;mitochondrial matrix;mitochondrial nucleoid;brisc complex;cytoplasm
P21796	VDAC1 Voltage-dependent anion-selective channel protein 1	21	1	extracellular region or secreted;mitochondrion;nucleus;plasma membrane;extracellular exosome;mitochondrial membrane;mitochondrial nucleoid;mitochondrial outer membrane;mitochondrial permeability transition pore complex;membrane;membrane raft;pore complex;synaptic vesicle
P31930	UQCRC1 Cytochrome b-c1 complex subunit 1, mitochondrial	21	1	mitochondrion;mitochondrial inner membrane;mitochondrial respirasome;mitochondrial respiratory chain complex iii
Q07021	C1QBP Complement component 1 Q subcomponent-binding protein, mitochondrial	20	2	cytosol;extracellular region or secreted;mitochondrion;nucleus;plasma membrane;extracellular space;mitochondrial matrix;nucleolus;cell surface;cytoplasm;gaba-ergic synapse;glutamatergic synapse;membrane;presynaptic active zone
O75947	ATP5H ATP synthase subunit d, mitochondrial	19	1	mitochondrion;mitochondrial inner membrane;mitochondrial proton-transporting atp synthase complex;mitochondrial proton-transporting atp synthase, stator stalk
P19367	HK1 Hexokinase-1	19	1	cytosol;mitochondrion;mitochondrial outer membrane;membrane raft
Q92552	MRPS27 28S ribosomal protein S27, mitochondrial	19	0	mitochondrion;nucleus;mitochondrial inner membrane;mitochondrial small ribosomal subunit;nucleolus;cytoplasm

Q96EY7	PTCD3 Pentatricopeptide repeat-containing protein 3, mitochondrial	19	0	cytosol;mitochondrion;nucleus;plasma membrane;mitochondrial inner membrane;nucleoplasm;ribosome
Q9Y4W6	AFG3L2 AFG3-like protein 2	19	0	mitochondrion;m-aaa complex;mitochondrial inner membrane
O60313	OPA1 Dynamin-like 120 kDa protein, mitochondrial	18	0	cytosol;mitochondrion;nucleus;extrinsic component of mitochondrial inner membrane;mitochondrial crista;mitochondrial inner membrane;mitochondrial intermembrane space;mitochondrial membrane;mitochondrial outer membrane;nucleoplasm;axon cytoplasm;cytoplasm;dendrite;integral component of membrane;membrane
O95563	MPC2 Mitochondrial pyruvate carrier 2	18	0	mitochondrion;nucleus;integral component of mitochondrial inner membrane
P13639	EEF2 Elongation factor 2	17	33	cytosol;extracellular region or secreted;nucleus;plasma membrane;extracellular exosome;extracellular region;aggresome;cytoplasm;ficolin-1-rich granule lumen;membrane;membrane raft;polysomal ribosome;ribonucleoprotein complex;secretory granule lumen;synapse
Q12931	TRAP1 Heat shock protein 75 kDa, mitochondrial	17	10	mitochondrion;nucleus;mitochondrial inner membrane;mitochondrial intermembrane space;mitochondrial matrix;nucleoplasm;membrane
P40926	MDH2 Malate dehydrogenase, mitochondrial	17	4	extracellular region or secreted;mitochondrion;nucleus;extracellular exosome;mitochondrial matrix;cytoplasm;membrane
P28331	NDUFS1 NADH-ubiquinone oxidoreductase 75 kDa subunit, mitochondrial	17	0	mitochondrion;mitochondrial intermembrane space;mitochondrial matrix;mitochondrial respiratory chain complex i
P49821	NDUFV1 NADH dehydrogenase	17	0	cytosol;mitochondrion;mitochondrial inner membrane;mitochondrial respiratory chain complex i
Q96EL3	MRPL53 39S ribosomal protein L53, mitochondrial	17	0	mitochondrion;mitochondrial inner membrane;mitochondrial large ribosomal subunit
P46782	RPS5 40S ribosomal protein S5	16	19	cytosol;extracellular region or secreted;nucleus;cytosolic small ribosomal subunit;extracellular exosome;nucleoplasm;focal adhesion;membrane;ribonucleoprotein complex;ribosome
O75521	ECI2 Enoyl-CoA delta isomerase 2, mitochondrial	16	6	cytosol;mitochondrion;peroxisome;peroxisomal matrix;intracellular membrane-bounded organelle;membrane
P43897	TSFM Elongation factor Ts, mitochondrial	16	2	mitochondrion;nucleus;mitochondrial matrix;nucleoplasm
O00483	NDUFA4 NADH dehydrogenase	16	0	mitochondrion;mitochondrial inner membrane;mitochondrial respiratory chain complex i;mitochondrial respiratory chain complex iv;integral component of membrane
P05023	ATP1A1 Sodium/potassium-transporting ATPase subunit alpha-1	16	0	endoplasmic reticulum;endosome;extracellular region or secreted;golgi apparatus;plasma membrane;extracellular exosome;extracellular vesicle;apical plasma membrane;basolateral plasma membrane;caveola;lateral plasma membrane;photoreceptor inner segment membrane;sarcolemma;sodium:potassium-exchanging atpase complex;t-tubule;integral component of membrane;intercalated disc;melanosome;membrane;membrane raft;organelle membrane;postsynaptic density;protein-containing complex;sperm flagellum
P14618	PKM Pyruvate kinase isozymes M1/M2	15	15	cytosol;endoplasmic reticulum;extracellular region or secreted;mitochondrion;nucleus;rough endoplasmic reticulum;extracellular exosome;extracellular region;extracellular vesicle;cilium;collagen-containing extracellular matrix;cytoplasm;ficolin-1-rich granule lumen;pyruvate kinase complex;secretory granule lumen;vesicle
P27635	RPL10 60S ribosomal protein L10	15	5	cytosol;endoplasmic reticulum;nucleus;cytosolic large ribosomal subunit;membrane;protein-containing complex
P63010	AP2B1 AP-2 complex subunit beta	15	2	cytosol;endosome;lysosome;plasma membrane;endolysosome membrane;ap-2 adaptor complex;clathrin adaptor complex;clathrin-coated endocytic vesicle;clathrin-coated endocytic vesicle membrane;endocytic vesicle membrane;glutamatergic synapse;membrane;postsynapse;presynapse
P62879	GNB2 Guanine nucleotide-binding protein G(I)/G(S)/G(T) subunit beta-2	15	1	cytosol;extracellular region or secreted;lysosome;plasma membrane;extracellular exosome;extracellular space;lysosomal membrane;heterotrimeric g-protein complex;cell body;cytoplasm;focal adhesion;membrane;perinuclear region of cytoplasm;vesicle
P08574	CYC1 Cytochrome c1, heme protein, mitochondrial	15	0	mitochondrion;nucleus;mitochondrial inner membrane;mitochondrial respiratory chain complex iii;integral component of membrane;membrane
P31040	SDHA Succinate dehydrogenase	15	0	mitochondrion;nucleus;mitochondrial inner membrane;mitochondrial respiratory chain complex ii, succinate dehydrogenase complex (ubiquinone);nucleolus
Q9HAV7	GRPEL1 GrpE protein homolog 1, mitochondrial	14	6	mitochondrion;nucleus;mitochondrial matrix;pam complex, tim23 associated import motor;nucleoplasm
O00217	NDUFS8 NADH dehydrogenase	14	1	mitochondrion;mitochondrial matrix;mitochondrial respiratory chain complex i
P61224	RAP1B Ras-related protein Rap-1b	14	0	cytosol;extracellular region or secreted;lysosome;plasma membrane;extracellular exosome;azurophil granule membrane;cell-cell junction;lipid droplet;membrane
Q9BVA1	TUBB2B Tubulin beta-2B chain	13	22	cytoskeleton;nucleus;microtubule;microtubule cytoskeleton;cytoplasm;schaffer collateral - ca1 synapse
P48735	IDH2 Isocitrate dehydrogenase	13	4	cytosol;extracellular region or secreted;mitochondrion;peroxisome;extracellular exosome;mitochondrial matrix
Q6PI48	DARS2 Aspartate--tRNA ligase, mitochondrial	13	3	mitochondrion;nucleus;mitochondrial matrix;nucleoplasm
P13804	ETFA Electron transfer flavoprotein subunit alpha, mitochondrial	13	1	mitochondrion;mitochondrial matrix
P62873	GNB1 Guanine nucleotide-binding protein G(I)/G(S)/G(T) subunit beta-1	13	1	cytosol;extracellular region or secreted;lysosome;plasma membrane;extracellular exosome;extracellular vesicle;lysosomal membrane;heterotrimeric g-protein complex;photoreceptor outer segment membrane;cell body;cytoplasm;dendrite;membrane;photoreceptor disc membrane;photoreceptor inner segment;synapse
P07437	TUBB Tubulin beta chain	13	0	cytoskeleton;cytosol;extracellular region or secreted;lysosome;nucleus;microtubule;extracellular exosome;extracellular region;azurophil granule lumen;nuclear envelope lumen;cell body;cytoplasm;cytoplasmic ribonucleoprotein granule;membrane raft;protein-containing complex
P53701	HCCS Cytochrome c-type heme lyase	13	0	mitochondrion;mitochondrial inner membrane;membrane
P68371	TUBB4B Tubulin beta-4B chain	13	0	cytoskeleton;cytosol;extracellular region or secreted;lysosome;nucleus;microtubule;extracellular exosome;extracellular region;extracellular vesicle;azurophil granule lumen;cytoplasm
Q16891	IMMT Mitochondrial inner membrane protein	13	0	mitochondrion;mib complex;micos complex;mitochondrial inner membrane;mitochondrial intermembrane space;sam complex;membrane

P05388	RPLP0 60S acidic ribosomal protein P0	12	5	cytosol;endoplasmic reticulum;extracellular region or secreted;nucleus;cytosolic large ribosomal subunit;extracellular exosome;cytoplasm;cytoplasmic ribonucleoprotein granule;dendrite;focal adhesion;membrane;postsynapse;postsynaptic density;ribonucleoprotein complex
P38117	ETFB Electron transfer flavoprotein subunit beta	12	4	mitochondrion;mitochondrial matrix
P09543	CNP 2',3'-cyclic-nucleotide 3'-phosphodiesterase	12	1	cytoskeleton;extracellular region or secreted;mitochondrion;plasma membrane;microtubule;extracellular exosome;extracellular space;mitochondrial inner membrane;mitochondrial outer membrane;cytoplasm;melanosome;membrane;microvillus;myelin sheath abaxonal region;myelin sheath adaxonal region;perinuclear region of cytoplasm;pseudopodium;synapse
Q00325	SLC25A3 Phosphate carrier protein, mitochondrial	12	1	extracellular region or secreted;mitochondrion;plasma membrane;extracellular exosome;integral component of mitochondrial inner membrane;mitochondrial inner membrane;integral component of plasma membrane;membrane
O96008	TOMM40 Mitochondrial import receptor subunit TOM40 homolog	12	0	cytosol;mitochondrion;integral component of mitochondrial outer membrane;mitochondrial inner membrane;mitochondrial outer membrane;mitochondrial outer membrane translocase complex;integral component of membrane;mitochondria-associated endoplasmic reticulum membrane;pore complex
P10620	MGST1 Microsomal glutathione S-transferase 1	12	0	endoplasmic reticulum;lysosome;mitochondrion;nucleus;peroxisome;plasma membrane;endoplasmic reticulum membrane;azurophil granule membrane;mitochondrial outer membrane;peroxisomal membrane;apical part of cell;integral component of membrane
Q9BYD6	MRPL1 39S ribosomal protein L1, mitochondrial	12	0	cytosol;mitochondrion;cytosolic large ribosomal subunit;mitochondrial inner membrane
Q9BZE1	MRPL37 39S ribosomal protein L37, mitochondrial	12	0	mitochondrion;mitochondrial inner membrane;mitochondrial large ribosomal subunit;mitochondrial ribosome
Q9Y4P3	TBL2 Transducin beta-like protein 2	12	0	endoplasmic reticulum;integral component of endoplasmic reticulum membrane
P68366	TUBA4A Tubulin alpha-4A chain	11	57	cytoskeleton;cytosol;extracellular region or secreted;microtubule;microtubule cytoskeleton;extracellular exosome;extracellular region;cytoplasm
P14625	HSP90B1 Endoplasmin	11	5	cytosol;endoplasmic reticulum;extracellular region or secreted;nucleus;endoplasmic reticulum lumen;endoplasmic reticulum membrane;sarcoplasmic reticulum lumen;extracellular exosome;extracellular region;collagen-containing extracellular matrix;endocytic vesicle lumen;focal adhesion;melanosome;membrane;midbody;perinuclear region of cytoplasm;protein-containing complex
Q7L0Y3	TRMT10C Mitochondrial ribonuclease P protein 1	11	2	mitochondrion;nucleus;mitochondrial matrix;mitochondrial nucleoid;mitochondrial ribonuclease p complex;nucleoplasm
I3L0E3	MRPS17 28S ribosomal protein S17, mitochondrial	11	1	mitochondrion;mitochondrial small ribosomal subunit
P00367	GLUD1 Glutamate dehydrogenase 1, mitochondrial	11	1	endoplasmic reticulum;mitochondrion;mitochondrial matrix;cytoplasm
P46777	RPL5 60S ribosomal protein L5	11	1	cytosol;endoplasmic reticulum;extracellular region or secreted;nucleus;cytosolic large ribosomal subunit;extracellular exosome;nucleolus;nucleoplasm;cytoplasm;focal adhesion;membrane;protein-containing complex;ribonucleoprotein complex
P08754	GNAI3 Guanine nucleotide-binding protein G(k) subunit alpha	11	0	cytoskeleton;extracellular region or secreted;golgi apparatus;lysosome;plasma membrane;centrosome;extracellular exosome;lysosomal membrane;heterotrimeric g-protein complex;cytoplasm;membrane;membrane raft;midbody;zymogen granule
P21912	SDHB Succinate dehydrogenase	11	0	mitochondrion;nucleus;plasma membrane;mitochondrial inner membrane;mitochondrial membrane;mitochondrial respiratory chain complex ii, succinate dehydrogenase complex (ubiquinone);nucleoplasm
P82933	MRPS9 28S ribosomal protein S9, mitochondrial	11	0	mitochondrion;nucleus;mitochondrial inner membrane;mitochondrial small ribosomal subunit;nucleolus;small ribosomal subunit
Q9H845	ACAD9 Acyl-CoA dehydrogenase family member 9, mitochondrial	11	0	mitochondrion;nucleus;mitochondrial inner membrane;mitochondrial membrane;dendrite
Q9H9J2	MRPL44 39S ribosomal protein L44, mitochondrial	11	0	mitochondrion;nucleus;plasma membrane;mitochondrial inner membrane;mitochondrial large ribosomal subunit;nuclear body;nucleoplasm
Q9NVH1	DNAJC11 DnaJ homolog subfamily C member 11	11	0	mitochondrion;nucleus;mib complex;mitochondrial outer membrane;sam complex;nuclear speck;nucleoplasm
Q9UHQ9	CYB5R1 NADH-cytochrome b5 reductase 1	11	0	endoplasmic reticulum;extracellular region or secreted;mitochondrion;plasma membrane;endoplasmic reticulum membrane;extracellular exosome;integral component of membrane;membrane;platelet alpha granule membrane
P08107	HSPA1B Heat shock 70 kDa protein 1A/1B	10	30	no_annotated_location
P61586	RHOA Transforming protein RhoA	10	3	cytoskeleton;cytosol;endoplasmic reticulum;endosome;extracellular region or secreted;plasma membrane;endoplasmic reticulum membrane;extracellular exosome;cleavage furrow;extrinsic component of cytoplasmic side of plasma membrane;apical junction complex;cell cortex;cell junction;cell periphery;cell projection;cytoplasmic vesicle;dendritic spine;ficolin-1-rich granule membrane;focal adhesion;glutamatergic synapse;intracellular membrane-bounded organelle;lamellipodium;midbody;postsynapse;secretory granule membrane;vesicle
P27797	CALR Calreticulin	10	2	cytosol;endoplasmic reticulum;extracellular region or secreted;golgi apparatus;nucleus;plasma membrane;endoplasmic reticulum lumen;endoplasmic reticulum membrane;endoplasmic reticulum quality control compartment;integral component of lumenal side of endoplasmic reticulum membrane;mhc class i peptide loading complex;sarcoplasmic reticulum lumen;smooth endoplasmic reticulum;extracellular exosome;extracellular region;extracellular space;nuclear envelope;external side of plasma membrane;acrosomal vesicle;cell surface;collagen-containing extracellular matrix;cortical granule;cytoplasm;endocytic vesicle lumen;endoplasmic reticulum-golgi intermediate compartment membrane;focal adhesion;membrane;perinuclear region of cytoplasm;phagocytic vesicle membrane;polysome
O14654	IRS4 Insulin receptor substrate 4	10	1	cytosol;plasma membrane
P04899	GNAI2 Guanine nucleotide-binding protein G(i) subunit alpha-2	10	1	cytoskeleton;cytosol;extracellular region or secreted;nucleus;plasma membrane;centrosome;extracellular exosome;extracellular vesicle;nucleoplasm;heterotrimeric g-protein complex;cell body;cytoplasm;dendrite;membrane;membrane raft;midbody;synapse

Q96DV4	MRPL38 39S ribosomal protein L38, mitochondrial	10	1	mitochondrion;mitochondrial inner membrane;mitochondrial large ribosomal subunit
Q99798	ACO2 Aconitate hydratase, mitochondrial	10	1	cytosol;mitochondrion;mitochondrial matrix
O75746	SLC25A12 Calcium-binding mitochondrial carrier protein Aralar1	10	0	mitochondrion;mitochondrial inner membrane;integral component of membrane
P04181	OAT Ornithine aminotransferase, mitochondrial	10	0	mitochondrion;nucleus;mitochondrial matrix;nucleoplasm;cytoplasm
P55084	HADHB Trifunctional enzyme subunit beta, mitochondrial	10	0	endoplasmic reticulum;mitochondrion;mitochondrial envelope;mitochondrial inner membrane;mitochondrial nucleoid;mitochondrial outer membrane
P63096	GNAI1 Guanine nucleotide-binding protein G(i) subunit alpha-1	10	0	cytoskeleton;extracellular region or secreted;lysosome;nucleus;plasma membrane;centrosome;extracellular exosome;lysosomal membrane;heterotrimeric g-protein complex;cell cortex region;cytoplasm;membrane raft;midbody
Q53H12	AGK Acylglycerol kinase, mitochondrial	10	0	cytosol;mitochondrion;integral component of mitochondrial inner membrane;mitochondrial inner membrane;mitochondrial intermembrane space;mitochondrial membrane;mitochondrial outer membrane;tim22 mitochondrial import inner membrane insertion complex;cytoplasm;intracellular membrane-bounded organelle;membrane
Q7Z7H8	MRPL10 39S ribosomal protein L10, mitochondrial	10	0	mitochondrion;nucleus;mitochondrial inner membrane;mitochondrial large ribosomal subunit;nucleoplasm;large ribosomal subunit;ribonucleoprotein complex
Q86UT6	NLRX1 NLR family member X1	10	0	mitochondrion;plasma membrane;mitochondrial outer membrane;cell junction
Q9NSE4	IARS2 Isoleucine--tRNA ligase, mitochondrial	10	0	mitochondrion;mitochondrial matrix
Q9UJS0	SLC25A13 Calcium-binding mitochondrial carrier protein Aralar2	10	0	mitochondrion;plasma membrane;mitochondrial inner membrane;integral component of plasma membrane
P00505	GOT2 Aspartate aminotransferase, mitochondrial	9	7	extracellular region or secreted;mitochondrion;plasma membrane;extracellular exosome;mitochondrial inner membrane;mitochondrial matrix;t-tubule;cell surface;perikaryon;protein-containing complex
P78527	PRKDC DNA-dependent protein kinase catalytic subunit	9	5	cytosol;nucleus;dna-dependent protein kinase-dna ligase 4 complex;nucleolus;nucleoplasm;chromosome, telomeric region;membrane;nonhomologous end joining complex;protein-containing complex;protein-dna complex;small-subunit processome;transcription regulator complex
Q4VCS5	AMOT Angiomotin	9	3	cytoskeleton;cytosol;nucleus;plasma membrane;actin filament;stress fiber;nucleoplasm;external side of plasma membrane;bicellular tight junction;cell junction;cell surface;cytoplasm;cytoplasmic vesicle;endocytic vesicle;integral component of membrane;lamellipodium;ruffle
P50213	IDH3A Isocitrate dehydrogenase	9	2	mitochondrion;nucleus;mitochondrial matrix
P51553	IDH3G Isocitrate dehydrogenase	9	2	mitochondrion;nucleus;mitochondrial matrix;nucleolus
P51659	HSD17B4 Peroxisomal multifunctional enzyme type 2	9	1	cytosol;peroxisome;peroxisomal matrix;peroxisomal membrane;membrane
O60716	CTNND1 Catenin delta-1	9	0	cytosol;extracellular region or secreted;nucleus;plasma membrane;extracellular exosome;catenin complex;adherens junction;cell-cell junction;cytoplasm;dendritic spine;glutamatergic synapse;growth cone;hippocampal mossy fiber to ca3 synapse;lamellipodium;midbody;postsynaptic density, intracellular component;presynaptic active zone cytoplasmic component;schaffer collateral - ca1 synapse;zonula adherens
O95202	LETM1 LETM1 and EF-hand domain-containing protein 1, mitochondrial	9	0	mitochondrion;mitochondrial inner membrane;integral component of membrane
P03928	MT-ATP8 ATP synthase protein 8	9	0	mitochondrion;mitochondrial inner membrane;mitochondrial proton-transporting atp synthase complex;mitochondrial proton-transporting atp synthase complex, coupling factor f(o);integral component of membrane
Q02218	OGDH 2-oxoglutarate dehydrogenase, mitochondrial	9	0	mitochondrion;nucleus;mitochondrial matrix;mitochondrial membrane;oxoglutarate dehydrogenase complex
Q8NBU5	ATAD1 ATPase family AAA domain-containing protein 1	9	0	cytosol;mitochondrion;peroxisome;plasma membrane;mitochondrial outer membrane;peroxisomal membrane;postsynaptic membrane;glutamatergic synapse;integral component of membrane;membrane
Q9Y512	SAMM50 Sorting and assembly machinery component 50 homolog	9	0	extracellular region or secreted;mitochondrion;extracellular exosome;mib complex;mitochondrial outer membrane;sam complex;integral component of membrane
Q71U36	TUBA1A Tubulin alpha-1A chain	8	53	cytoskeleton;cytosol;endosome;extracellular region or secreted;nucleus;cytoplasmic microtubule;microtubule;microtubule cytoskeleton;recycling endosome;extracellular exosome;cytoplasm;cytoplasmic ribonucleoprotein granule;membrane raft;myelin sheath;neuromuscular junction
Q00610	CLTC Clathrin heavy chain 1	8	8	cytoskeleton;cytosol;endosome;extracellular region or secreted;golgi apparatus;lysosome;plasma membrane;mitotic spindle;mitotic spindle microtubule;spindle;endolysosome membrane;extracellular exosome;extracellular vesicle;clathrin coat of trans-golgi network vesicle;trans-golgi network membrane;clathrin coat of coated pit;clathrin coat;clathrin complex;clathrin-coated endocytic vesicle;clathrin-coated endocytic vesicle membrane;clathrin-coated vesicle;focal adhesion;melanosome;membrane;protein-containing complex
P28838	LAP3 Cytosol aminopeptidase	8	7	cytosol;extracellular region or secreted;golgi apparatus;nucleus;extracellular exosome;trans-golgi network;nucleoplasm;focal adhesion;midbody
P54886	ALDH18A1 Delta-1-pyrroline-5-carboxylate synthase	8	3	mitochondrion;mitochondrial inner membrane
O00410	IPO5 Importin-5	8	2	nucleus;nuclear pore;nucleolus;cytoplasm;membrane
P22695	UQCRC2 Cytochrome b-c1 complex subunit 2, mitochondrial	8	2	mitochondrion;nucleus;mitochondrial inner membrane;mitochondrial respiratory chain complex iii;mitochondrial respiratory chain complex iv;nucleoplasm
P82912	MRPS11 28S ribosomal protein S11, mitochondrial	8	2	cytosol;mitochondrion;cytosolic small ribosomal subunit;mitochondrial inner membrane;mitochondrial small ribosomal subunit
Q9BSH4	TACO1 Translational activator of cytochrome c oxidase 1	8	2	mitochondrion
P35579	MYH9 Myosin-9	8	1	cytoskeleton;cytosol;extracellular region or secreted;nucleus;plasma membrane;actin cytoskeleton;actomyosin;actomyosin contractile ring;myosin ii complex;spindle;stress fiber;extracellular exosome;cleavage furrow;cytoplasmic side of plasma membrane;immunological synapse;adherens junction;brush border;cell leading edge;cytoplasm;focal

				adhesion;membrane;myosin ii filament;neuromuscular junction;protein-containing complex;ruffle;uropod
Q6YN16	HSDL2 Hydroxysteroid dehydrogenase-like protein 2	8	1	mitochondrion;peroxisome;membrane
Q9Y5M8	SRPRB Signal recognition particle receptor subunit beta	8	1	cytoskeleton;endoplasmic reticulum;cytoplasmic microtubule;endoplasmic reticulum membrane;signal recognition particle receptor complex;cytoplasm;integral component of membrane;membrane
O14874	BCKDK	8	0	mitochondrion;mitochondrial alpha-ketoglutarate dehydrogenase complex;mitochondrial matrix
O60488	ACSL4 Long-chain-fatty-acid--CoA ligase 4	8	0	endoplasmic reticulum;extracellular region or secreted;mitochondrion;peroxisome;plasma membrane;endoplasmic reticulum membrane;extracellular exosome;mitochondrial outer membrane;peroxisomal membrane;cytoplasm;integral component of membrane;lipid droplet;membrane;mitochondria-associated endoplasmic reticulum membrane;neuronal cell body
P04843	RPN1 Dolichyl-diphosphooligosaccharide--protein glycosyltransferase subunit 1	8	0	cytosol;endoplasmic reticulum;endoplasmic reticulum membrane;oligosaccharyltransferase complex;rough endoplasmic reticulum;integral component of membrane;melanosome;membrane
P10515	DLAT Dihydrolipoyllysine-residue acetyltransferase component of pyruvate dehydrogenase complex, mitochondrial	8	0	mitochondrion;mitochondrial matrix;mitochondrial pyruvate dehydrogenase complex;intracellular membrane-bounded organelle;pyruvate dehydrogenase complex
P11177	PDHB Pyruvate dehydrogenase E1 component subunit beta, mitochondrial	8	0	mitochondrion;nucleus;mitochondrial matrix;mitochondrial pyruvate dehydrogenase complex;nucleoplasm;pyruvate dehydrogenase complex
P16615	ATP2A2 Sarcoplasmic/endoplasmic reticulum calcium ATPase 2	8	0	endoplasmic reticulum;plasma membrane;endoplasmic reticulum membrane;longitudinal sarcoplasmic reticulum;sarcoplasmic reticulum;sarcoplasmic reticulum membrane;extrinsic component of cytoplasmic side of plasma membrane;integral component of plasma membrane;apical ectoplasmic specialization;calcium ion-transporting atpase complex;membrane;perinuclear region of cytoplasm;plasma membrane bounded cell projection;platelet dense tubular network membrane;protein-containing complex;ribbon synapse;vesicle membrane
P22033	MUT Methylmalonyl-CoA mutase, mitochondrial	8	0	mitochondrion;mitochondrial matrix;cytoplasm
Q53GQ0	HSD17B12 Estradiol 17-beta-dehydrogenase 12	8	0	endoplasmic reticulum;endoplasmic reticulum membrane;fatty acid elongase complex;extracellular matrix;integral component of membrane
Q7L2E3	DHX30 Putative ATP-dependent RNA helicase DHX30	8	0	cytosol;mitochondrion;mitochondrial nucleoid;cytoplasm;ribonucleoprotein granule
Q96RP9	GFM1 Elongation factor G, mitochondrial	8	0	mitochondrion;mitochondrial matrix
Q9BPX6	MICU1 Calcium uptake protein 1, mitochondrial	8	0	mitochondrion;integral component of mitochondrial membrane;mitochondrial inner membrane;mitochondrial intermembrane space;uniplex complex;calcium channel complex;intracellular anatomical structure
Q9Y3E5	PTRH2 Peptidyl-tRNA hydrolase 2, mitochondrial	8	0	cytosol;mitochondrion;membrane
Q9Y6C9	MTCH2 Mitochondrial carrier homolog 2	8	0	mitochondrion;nucleus;mitochondrial inner membrane;integral component of membrane;membrane
P04406	GAPDH Glyceraldehyde-3-phosphate dehydrogenase	7	22	cytoskeleton;cytosol;extracellular region or secreted;nucleus;plasma membrane;microtubule cytoskeleton;extracellular exosome;nuclear membrane;cytoplasm;gait complex;intracellular membrane-bounded organelle;lipid droplet;membrane;perinuclear region of cytoplasm;ribonucleoprotein complex;vesicle
P12532	CKMT1B Creatine kinase U-type, mitochondrial	7	8	mitochondrion;mitochondrial inner membrane
P17540	CKMT2 Creatine kinase S-type, mitochondrial	7	8	mitochondrion;mitochondrial inner membrane
Q15366	PCBP2 Poly(rC)-binding protein 2	7	7	cytosol;extracellular region or secreted;nucleus;extracellular exosome;nucleoplasm;cytoplasm;focal adhesion;membrane;postsynaptic density
P36551	CPOX Coproporphyrinogen-III oxidase, mitochondrial	7	5	cytosol;mitochondrion;mitochondrial intermembrane space;cytoplasm
Q9H2U2	PPA2 Inorganic pyrophosphatase 2, mitochondrial	7	4	cytosol;mitochondrion;mitochondrial matrix
O75439	PMPCB Mitochondrial-processing peptidase subunit beta	7	3	mitochondrion;mitochondrial inner membrane;mitochondrial processing peptidase complex
P23378	GLDC Glycine dehydrogenase	7	3	mitochondrion;nucleus;plasma membrane;mitochondrial matrix;nucleoplasm;glycine cleavage complex
Q14697	GANAB Neutral alpha-glucosidase AB	7	3	endoplasmic reticulum;extracellular region or secreted;golgi apparatus;endoplasmic reticulum lumen;glucosidase ii complex;extracellular exosome;intracellular membrane-bounded organelle;melanosome;membrane
P36578	RPL4 60S ribosomal protein L4	7	1	cytosol;endoplasmic reticulum;extracellular region or secreted;nucleus;cytosolic large ribosomal subunit;rough endoplasmic reticulum;extracellular exosome;nucleolus;cytoplasm;focal adhesion;membrane;ribonucleoprotein complex
Q7Z2W9	MRPL21 39S ribosomal protein L21, mitochondrial	7	1	mitochondrion;mitochondrial inner membrane;mitochondrial large ribosomal subunit
Q9UDR5	AASS Alpha-aminoadipic semialdehyde synthase, mitochondrial	7	1	cytosol;mitochondrion;nucleus;mitochondrial matrix;cytoplasm;intracellular membrane-bounded organelle
Q9UL25	RAB21 Ras-related protein Rab-21	7	1	cytosol;endoplasmic reticulum;endosome;extracellular region or secreted;golgi apparatus;plasma membrane;endoplasmic reticulum membrane;cytoplasmic side of early endosome membrane;early endosome;early endosome membrane;extracellular exosome;golgi cisterna membrane;trans-golgi network;cleavage furrow;cytoplasmic side of plasma membrane;axon cytoplasm;cytoplasmic vesicle membrane;endomembrane system;focal adhesion;synapse;vesicle membrane
O14880	MGST3 Microsomal glutathione S-transferase 3	7	0	endoplasmic reticulum;nucleus;endoplasmic reticulum membrane;nuclear envelope;integral component of membrane;intracellular membrane-bounded organelle;membrane
P09874	PARP1 Poly	7	0	mitochondrion;nucleus;nuclear body;nuclear envelope;nucleolus;nucleoplasm;chromosome, telomeric region;membrane;protein-containing complex;protein-dna complex;site of dna damage;site of double-strand break;transcription regulator complex
P53007	SLC25A1 Tricarboxylate transport protein, mitochondrial	7	0	extracellular region or secreted;mitochondrion;nucleus;extracellular exosome;mitochondrial inner membrane;integral component of membrane
P63092	GNAS Guanine nucleotide-binding protein G(s) subunit alpha isoforms short	7	0	cytosol;extracellular region or secreted;golgi apparatus;plasma membrane;extracellular exosome;trans-golgi network

				membrane;heterotrimeric g-protein complex;cytoplasm;intrinsic component of membrane;membrane
Q16698	DECR1 2,4-dienoyl-CoA reductase, mitochondrial	7	0	cytosol;mitochondrion;nucleus;mitochondrial matrix;nucleoplasm;catalytic complex
Q5JRX3	PITRM1 Presequence protease, mitochondrial	7	0	mitochondrion;mitochondrial matrix
Q5JWF2	GNAS Guanine nucleotide-binding protein G(s) subunit alpha isoforms XLas	7	0	cytosol;extracellular region or secreted;plasma membrane;extracellular exosome;apical plasma membrane;heterotrimeric g-protein complex;dendrite;membrane
Q8IWA4	MFN1 Mitofusin-1	7	0	mitochondrion;integral component of mitochondrial outer membrane;intrinsic component of mitochondrial outer membrane;mitochondrial outer membrane;outer mitochondrial membrane protein complex;integral component of membrane
Q969Z0	TBRG4 Protein TBRG4	7	0	mitochondrion;mitochondrial matrix
Q96ER9	CCDC51 Coiled-coil domain-containing protein 51	7	0	mitochondrion;integral component of mitochondrial inner membrane;mitochondrial atp-gated potassium channel complex
Q9BPW8	NIPSNAP1 Protein NipSnap homolog 1	7	0	mitochondrion;plasma membrane;synaptic membrane
Q9UBQ7	GRHPR Glyoxylate reductase/hydroxypyruvate reductase	7	0	cytosol;extracellular region or secreted;peroxisome;extracellular exosome;peroxisomal matrix;catalytic complex;cytoplasm
Q9Y619	SLC25A15 Mitochondrial ornithine transporter 1	7	0	mitochondrion;mitochondrial inner membrane;integral component of membrane
P22234	PAICS Multifunctional protein ADE2	6	9	cytosol;extracellular region or secreted;extracellular exosome;cytoplasm;membrane
P22307	SCP2 Non-specific lipid-transfer protein	6	7	cytosol;endoplasmic reticulum;mitochondrion;nucleus;peroxisome;nucleoplasm;peroxisomal matrix;cytoplasm;intracellular membrane-bounded organelle;membrane;protein-containing complex
P06733	ENO1 Alpha-enolase	6	5	cytosol;extracellular region or secreted;nucleus;plasma membrane;phosphopyruvate hydratase complex;extracellular exosome;extracellular space;cell cortex region;cell surface;cytoplasm;m band;membrane
P09104	ENO2 Gamma-enolase	6	5	cytosol;extracellular region or secreted;plasma membrane;phosphopyruvate hydratase complex;extracellular exosome;extracellular space;membrane;perikaryon;photoreceptor inner segment
P63244	GNB2L1 Guanine nucleotide-binding protein subunit beta-2-like 1	6	5	cytosol;extracellular region or secreted;mitochondrion;nucleus;plasma membrane;extracellular exosome;nucleoplasm;phagocytic cup;cytoplasm;dendrite;ire1-rack1-pp2a complex;midbody;neuronal cell body;perikaryon;perinuclear region of cytoplasm;small ribosomal subunit
A6NE09	RPSAP58 Protein RPSAP58	6	2	no_annotated_location
P30101	PDIA3 Protein disulfide-isomerase A3	6	2	endoplasmic reticulum;endosome;extracellular region or secreted;nucleus;endoplasmic reticulum lumen;mhc class i peptide loading complex;recycling endosome membrane;extracellular exosome;extracellular space;cell surface;focal adhesion;melanosome;phagocytic vesicle
Q12849	GRSF1 G-rich sequence factor 1	6	2	mitochondrion;nucleus;mitochondrial nucleoid;nucleoplasm;cytoplasm;ribonucleoprotein complex;ribonucleoprotein granule
P23284	PPIB Peptidyl-prolyl cis-trans isomerase B	6	1	endoplasmic reticulum;extracellular region or secreted;nucleus;endoplasmic reticulum lumen;extracellular exosome;nucleoplasm;cytoplasm;focal adhesion;intracellular membrane-bounded organelle;melanosome;membrane;perinuclear region of cytoplasm;protein-containing complex
P30050	RPL12 60S ribosomal protein L12	6	1	cytosol;extracellular region or secreted;cytosolic large ribosomal subunit;extracellular exosome;focal adhesion;large ribosomal subunit;membrane;postsynaptic density
Q9NP72	RAB18 Ras-related protein Rab-18	6	1	cytosol;endoplasmic reticulum;golgi apparatus;plasma membrane;endoplasmic reticulum membrane;endoplasmic reticulum tubular network;apical plasma membrane;endomembrane system;lipid droplet;secretory granule membrane
O75306	NDUFS2 NADH dehydrogenase	6	0	mitochondrion;nucleus;mitochondrial matrix;mitochondrial respiratory chain complex i;nucleoplasm
O94925	GLS Glutaminase kidney isoform, mitochondrial	6	0	cytosol;mitochondrion;mitochondrial matrix;synapse
P07355	ANXA2 Annexin A2	6	0	endosome;extracellular region or secreted;lysosome;nucleus;plasma membrane;late endosome membrane;extracellular exosome;extracellular region;extracellular space;azurophil granule lumen;lysosomal membrane;basolateral plasma membrane;adherens junction;anxa2-p11 complex;basement membrane;cell surface;collagen-containing extracellular matrix;cytoplasm;lipid droplet;melanosome;membrane;midbody;pcsk9-anxa2 complex;vesicle
P11182	DBT Lipoamide acyltransferase component of branched-chain alpha-keto acid dehydrogenase complex, mitochondrial	6	0	cytoskeleton;cytosol;mitochondrion;microtubule cytoskeleton;mitochondrial alpha-ketoglutarate dehydrogenase complex;mitochondrial matrix;mitochondrial nucleoid;cytoplasm
P13929	ENO3 Beta-enolase	6	0	cytosol;extracellular region or secreted;plasma membrane;phosphopyruvate hydratase complex;extracellular exosome;extracellular space;membrane
P23786	CPT2 Carnitine O-palmitoyltransferase 2, mitochondrial	6	0	mitochondrion;nucleus;mitochondrial inner membrane;nucleolus;nucleoplasm
P25705	ATP5A1 ATP synthase subunit alpha, mitochondrial	6	0	extracellular region or secreted;mitochondrion;plasma membrane;extracellular exosome;mitochondrial inner membrane;mitochondrial matrix;mitochondrial proton-transporting atp synthase complex;membrane;proton-transporting atp synthase complex;proton-transporting atp synthase complex, catalytic core f(1)
P36776	LONP1 Lon protease homolog, mitochondrial	6	0	cytosol;mitochondrion;nucleus;mitochondrial matrix;mitochondrial nucleoid;nucleoplasm;membrane
P49189	ALDH9A1 4-trimethylaminobutyraldehyde dehydrogenase	6	0	cytosol;extracellular region or secreted;extracellular exosome;cytoplasm
P62834	RAP1A Ras-related protein Rap-1A	6	0	cytosol;endosome;extracellular region or secreted;plasma membrane;early endosome;endosome membrane;late endosome;extracellular exosome;cell junction;cytoplasm;glutamatergic synapse;guanyl-nucleotide exchange factor complex;neuron projection;perinuclear region of cytoplasm;phagocytic vesicle;specific granule membrane
Q15119	PDK2	6	0	cytosol;mitochondrion;nucleus;mitochondrial matrix;mitochondrial pyruvate dehydrogenase complex;nucleoplasm
Q15120	PDK3	6	0	mitochondrion;nucleus;mitochondrial matrix;nucleolus

Q5TC12	ATPAF1 ATP synthase mitochondrial F1 complex assembly factor 1	6	0	mitochondrion
Q6NUQ4	TMEM214 Transmembrane protein 214	6	0	cytoskeleton;cytosol;endoplasmic reticulum;golgi apparatus;cytoplasmic microtubule;endoplasmic reticulum membrane;integral component of membrane
Q86VU5	COMTD1 Catechol O-methyltransferase domain-containing protein 1	6	0	integral component of membrane
Q96CS3	FAF2 FAS-associated factor 2	6	0	endoplasmic reticulum;extracellular region or secreted;lysosome;vcp-npl4-ufd1 aaa atpase complex;extracellular region;azurophil granule lumen;lipid droplet
Q9BRT2	MNF1 Mitochondrial nucleoid factor 1	6	0	mitochondrion;nucleus;mitochondrial inner membrane;mitochondrial intermembrane space;mitochondrial matrix;mitochondrial nucleoid;nuclear body
Q9HAV0	GNB4 Guanine nucleotide-binding protein subunit beta-4	6	0	cytosol;extracellular region or secreted;lysosome;plasma membrane;extracellular exosome;lysosomal membrane;heterotrimeric g-protein complex;cytoplasm
Q9P2R7	SUCLA2 Succinyl-CoA ligase	6	0	extracellular region or secreted;mitochondrion;extracellular exosome;mitochondrial matrix;succinate-coa ligase complex
P37802	TAGLN2 Transgelin-2	5	23	cytosol;extracellular region or secreted;extracellular exosome;extracellular region;vesicle
Q99832	CCT7 T-complex protein 1 subunit eta	5	9	cytoskeleton;cytosol;extracellular region or secreted;microtubule;chaperonin-containing t-complex;extracellular exosome;cell body;cytoplasm
P49419	ALDH7A1 Alpha-aminoadipic semialdehyde dehydrogenase	5	8	cytosol;extracellular region or secreted;mitochondrion;nucleus;extracellular exosome;mitochondrial matrix
P25398	RPS12 40S ribosomal protein S12	5	6	cytosol;golgi apparatus;nucleus;cytosolic small ribosomal subunit;nucleoplasm;intracellular membrane-bounded organelle;membrane
P49368	CCT3 T-complex protein 1 subunit gamma	5	6	cytoskeleton;cytosol;extracellular region or secreted;microtubule;chaperonin-containing t-complex;extracellular exosome;cell body;zona pellucida receptor complex
Q7Z4W1	DCXR L-xylulose reductase	5	6	cytoskeleton;extracellular region or secreted;nucleus;plasma membrane;cytoplasmic microtubule;extracellular exosome;brush border;microvillus
O14561	NDUFAB1 Acyl carrier protein, mitochondrial	5	5	mitochondrion;nucleus;mitochondrial inner membrane;mitochondrial matrix;mitochondrial membrane;mitochondrial respiratory chain complex i;nucleoplasm
P42765	ACAA2 3-ketoacyl-CoA thiolase, mitochondrial	5	5	mitochondrion;mitochondrial matrix
P61247	RPS3A 40S ribosomal protein S3a	5	5	cytosol;endoplasmic reticulum;extracellular region or secreted;nucleus;cytosolic small ribosomal subunit;extracellular exosome;nucleolus;nucleoplasm;cytoplasm;focal adhesion;ribonucleoprotein complex
P07858	CTSB Cathepsin B	5	3	endosome;extracellular region or secreted;lysosome;plasma membrane;endolysosome lumen;extracellular exosome;extracellular region;extracellular space;apical plasma membrane;collagen-containing extracellular matrix;ficolin-1-rich granule lumen;intracellular anatomical structure;melanosome;perinuclear region of cytoplasm
P09110	ACAA1 3-ketoacyl-CoA thiolase, peroxisomal	5	3	cytosol;extracellular region or secreted;peroxisome;extracellular region;peroxisomal matrix;membrane;specific granule lumen
P15924	DSP Desmoplakin	5	3	cytoskeleton;extracellular region or secreted;nucleus;plasma membrane;intermediate filament;extracellular exosome;basolateral plasma membrane;cornified envelope;cytoplasm;desmosome;fascia adherens;ficolin-1-rich granule membrane;intercalated disc;membrane
Q8N1F7	NUP93 Nuclear pore complex protein Nup93	5	3	cytosol;nucleus;nuclear envelope;nuclear membrane;nuclear periphery;nuclear pore;host cell;membrane
F5H5P2	Uncharacterized protein	5	2	no_annotated_location
P12694	BCKDHA 2-oxoisovalerate dehydrogenase subunit alpha, mitochondrial	5	2	mitochondrion;mitochondrial alpha-ketoglutarate dehydrogenase complex;mitochondrial matrix
P21953	BCKDHB 2-oxoisovalerate dehydrogenase subunit beta, mitochondrial	5	2	mitochondrion;nucleus;mitochondrial alpha-ketoglutarate dehydrogenase complex;mitochondrial matrix;nucleolus
O75390	CS Citrate synthase, mitochondrial	5	1	extracellular region or secreted;mitochondrion;nucleus;extracellular exosome;mitochondrial matrix
P48047	ATP5O ATP synthase subunit O, mitochondrial	5	1	mitochondrion;nucleus;plasma membrane;mitochondrial inner membrane;mitochondrial proton-transporting atp synthase complex;mitochondrial proton-transporting atp synthase, stator stalk;proton-transporting atp synthase complex, catalytic core f(1)
P51149	RAB7A Ras-related protein Rab-7a	5	1	cytosol;endosome;extracellular region or secreted;lysosome;plasma membrane;endosome membrane;late endosome;late endosome membrane;extracellular exosome;extrinsic component of lysosome membrane;lysosomal membrane;autophagosome membrane;lipid droplet;melanosome membrane;phagocytic vesicle;phagocytic vesicle membrane;secretory granule membrane
P52948	NUP98 Nuclear pore complex protein Nup98-Nup96	5	1	cytosol;nucleus;nuclear body;nuclear envelope;nuclear inclusion body;nuclear membrane;nuclear periphery;nuclear pore;nuclear pore nuclear basket;nuclear pore outer ring;nucleoplasm;host cell;intracellular membrane-bounded organelle;ribonucleoprotein complex
Q02543	RPL18A 60S ribosomal protein L18a	5	1	cytosol;cytosolic large ribosomal subunit;membrane;polysomal ribosome
Q13011	ECH1 Delta(3,5)-Delta(2,4)-dienoyl-CoA isomerase, mitochondrial	5	1	cytosol;extracellular region or secreted;mitochondrion;peroxisome;extracellular exosome;peroxisomal matrix;membrane
Q15390	MTFR1 Mitochondrial fission regulator 1	5	1	cytosol;mitochondrion;plasma membrane
Q16822	PCK2 Phosphoenolpyruvate carboxykinase	5	1	cytosol;mitochondrion;mitochondrial matrix
Q3SY69	ALDH1L2 Mitochondrial 10-formyltetrahydrofolate dehydrogenase	5	1	extracellular region or secreted;mitochondrion;nucleus;extracellular exosome;mitochondrial matrix;nucleoplasm
Q6P087	RPUSD3 RNA pseudouridylate synthase domain-containing protein 3	5	1	mitochondrion;mitochondrial matrix;ribonucleoprotein granule
Q96AG4	LRRC59 Leucine-rich repeat-containing protein 59	5	1	endoplasmic reticulum;mitochondrion;nucleus;endoplasmic reticulum membrane;mitochondrial nucleoid;nuclear envelope;integral component of membrane;membrane
Q9BXW7	CECR5 Cat eye syndrome critical region protein 5	5	1	mitochondrion
Q9HCC0	MCCC2 Methylcrotonoyl-CoA carboxylase beta chain, mitochondrial	5	1	cytosol;mitochondrion;3-methylcrotonyl-coa carboxylase complex, mitochondrial;mitochondrial matrix;methylcrotonoyl-coa carboxylase complex

Q9NVS2	MRPS18A 28S ribosomal protein S18a, mitochondrial	5	1	mitochondrion;mitochondrial inner membrane;mitochondrial large ribosomal subunit;mitochondrial small ribosomal subunit
Q9NYK5	MRPL39 39S ribosomal protein L39, mitochondrial	5	1	mitochondrion;mitochondrial inner membrane;mitochondrial large ribosomal subunit;mitochondrial ribosome
O00186	STXBP3 Syntaxin-binding protein 3	5	0	cytosol;extracellular region or secreted;plasma membrane;extracellular exosome;apical plasma membrane;basolateral plasma membrane;phagocytic vesicle;platelet alpha granule;presynapse;secretory granule;specific granule;tertiary granule
O00411	POLRMT DNA-directed RNA polymerase, mitochondrial	5	0	mitochondrion;mitochondrial dna-directed rna polymerase complex;mitochondrial matrix;mitochondrial nucleoid;protein-containing complex
O15228	GNPAT Dihydroxyacetone phosphate acyltransferase	5	0	cytosol;mitochondrion;peroxisome;mitochondrial membrane;peroxisomal matrix;peroxisomal membrane;membrane
O75380	NDUFS6 NADH dehydrogenase	5	0	mitochondrion;mitochondrial inner membrane;mitochondrial respiratory chain complex i
O75394	MRPL33 39S ribosomal protein L33, mitochondrial	5	0	mitochondrion;mitochondrial inner membrane;mitochondrial large ribosomal subunit
O95831	AIFM1 Apoptosis-inducing factor 1, mitochondrial	5	0	cytosol;mitochondrion;nucleus;mitochondrial inner membrane;mitochondrial intermembrane space;perinuclear region of cytoplasm
P05091	ALDH2 Aldehyde dehydrogenase, mitochondrial	5	0	extracellular region or secreted;mitochondrion;extracellular exosome;mitochondrial matrix
P05165	PCCA Propionyl-CoA carboxylase alpha chain, mitochondrial	5	0	cytosol;mitochondrion;mitochondrial matrix
P18031	PTPN1 Tyrosine-protein phosphatase non-receptor type 1	5	0	cytosol;endoplasmic reticulum;endosome;mitochondrion;cytoplasmic side of endoplasmic reticulum membrane;early endosome;sorting endosome;mitochondrial crista;mitochondrial matrix;protein-containing complex
P35221	CTNNA1 Catenin alpha-1	5	0	cytoskeleton;cytosol;plasma membrane;actin cytoskeleton;catenin complex;flotillin complex;acrosomal vesicle;cell junction;cell-cell junction;focal adhesion;intercalated disc;intracellular membrane-bounded organelle;lamellipodium;zonula adherens
P35222	CTNNB1 Catenin beta-1	5	0	cytoskeleton;cytosol;extracellular region or secreted;nucleus;plasma membrane;centrosome;spindle pole;extracellular exosome;beta-catenin-tcf complex;beta-catenin-tcf7l2 complex;nucleoplasm;basolateral plasma membrane;catenin complex;lateral plasma membrane;adherens junction;beta-catenin destruction complex;cell cortex;cell junction;cell periphery;cell projection;cell-cell junction;cytoplasm;euchromatin;focal adhesion;membrane;perinuclear region of cytoplasm;protein-containing complex;protein-dna complex;synapse;transcription regulator complex;wnt signalosome
P49406	MRPL19 39S ribosomal protein L19, mitochondrial	5	0	mitochondrion;nucleus;mitochondrial inner membrane;mitochondrial large ribosomal subunit;nuclear membrane
Q10713	PMPCA Mitochondrial-processing peptidase subunit alpha	5	0	extracellular region or secreted;mitochondrion;extracellular space;mitochondrial inner membrane;mitochondrial matrix
Q15286	RAB35 Ras-related protein Rab-35	5	0	cytosol;endosome;extracellular region or secreted;plasma membrane;endosome membrane;recycling endosome membrane;extracellular exosome;intercellular bridge;cell projection membrane;clathrin-coated pit;anchored component of synaptic vesicle membrane;clathrin-coated endocytic vesicle;clathrin-coated endocytic vesicle membrane;melanosome
Q16134	ETFDH Electron transfer flavoprotein-ubiquinone oxidoreductase, mitochondrial	5	0	mitochondrion;integral component of mitochondrial inner membrane;mitochondrial matrix;mitochondrial membrane
Q16762	TST Thiosulfate sulfurtransferase	5	0	extracellular region or secreted;mitochondrion;extracellular space;mitochondrial matrix
Q5T653	MRPL2 39S ribosomal protein L2, mitochondrial	5	0	mitochondrion;nucleus;mitochondrial inner membrane;mitochondrial large ribosomal subunit;nucleoplasm
Q7KZF4	SND1 Staphylococcal nuclease domain-containing protein 1	5	0	cytosol;extracellular region or secreted;nucleus;extracellular exosome;cytoplasm;dense body;melanosome;membrane;risc complex
Q8TAE8	GADD45GIP1 Growth arrest and DNA damage-inducible proteins-interacting protein 1	5	0	mitochondrion;nucleus;mitochondrial matrix;nucleoplasm;ribosome
Q8WVM0	TFB1M Dimethyladenosine transferase 1, mitochondrial	5	0	mitochondrion;mitochondrial matrix;mitochondrial nucleoid
Q92667	AKAP1 A-kinase anchor protein 1, mitochondrial	5	0	cytosol;mitochondrion;mitochondrial outer membrane;integral component of membrane;membrane
Q96A33	CCDC47 Coiled-coil domain-containing protein 47	5	0	endoplasmic reticulum;rough endoplasmic reticulum membrane;integral component of membrane;membrane
Q96BW9	TAMM41 Mitochondrial translocator assembly and maintenance protein 41 homolog	5	0	mitochondrion;extrinsic component of mitochondrial inner membrane;mitochondrial inner membrane;extrinsic component of membrane
Q96TA2	YME1L1 ATP-dependent zinc metalloprotease YME1L1	5	0	mitochondrion;nucleus;mitochondrial inner membrane;nuclear body;integral component of membrane;membrane
Q99536	VAT1 Synaptic vesicle membrane protein VAT-1 homolog	5	0	extracellular region or secreted;lysosome;mitochondrion;extracellular exosome;extracellular region;azurophil granule lumen;mitochondrial outer membrane;integral component of membrane
Q9BRJ2	MRPL45 39S ribosomal protein L45, mitochondrial	5	0	mitochondrion;mitochondrial inner membrane;mitochondrial large ribosomal subunit
Q9H078	CLPB Caseinolytic peptidase B protein homolog	5	0	mitochondrion;mitochondrial intermembrane space;cytoplasm
Q9H4I3	TRABD TraB domain-containing protein	5	0	no_annotated_location
Q9H936	SLC25A22 Mitochondrial glutamate carrier 1	5	0	mitochondrion;mitochondrial inner membrane;integral component of membrane
Q9NX14	NDUFB11 NADH dehydrogenase	5	0	mitochondrion;mitochondrial inner membrane;mitochondrial respiratory chain complex i;integral component of membrane
Q9NX63	CHCHD3 Coiled-coil-helix-coiled-coil-helix domain-containing protein 3, mitochondrial	5	0	extracellular region or secreted;mitochondrion;nucleus;extracellular exosome;mib complex;micos complex;mitochondrial inner membrane;sam complex
Q9UGP8	SEC63 Translocation protein SEC63 homolog	5	0	endoplasmic reticulum;sec62/sec63 complex;integral component of membrane;membrane
Q9UH62	ARMCX3 Armadillo repeat-containing X-linked protein 3	5	0	cytosol;mitochondrion;nucleus;integral component of mitochondrial outer membrane;axon cytoplasm
Q9Y2W6	TDRKH Tudor and KH domain-containing protein	5	0	mitochondrion;pi-body;pip-body
Q96HE7	ERO1L ERO1-like protein alpha	4	19	endoplasmic reticulum;endoplasmic reticulum lumen;endoplasmic reticulum membrane;dendrite;intracellular membrane-bounded organelle;membrane

Q15365	PCBP1 Poly(rC)-binding protein 1	4	12	cytosol;extracellular region or secreted;nucleus;extracellular exosome;nuclear speck;nucleoplasm;cytoplasm;cytoplasmic ribonucleoprotein granule;membrane
O14950	MYL12B Myosin regulatory light chain 12B	4	10	cytoskeleton;cytosol;extracellular region or secreted;myosin complex;extracellular exosome;cell cortex region
P00558	PGK1 Phosphoglycerate kinase 1	4	9	cytosol;extracellular region or secreted;extracellular exosome;extracellular space;membrane;membrane raft
P23396	RPS3 40S ribosomal protein S3	4	5	cytoskeleton;cytosol;endoplasmic reticulum;extracellular region or secreted;mitochondrion;nucleus;plasma membrane;mitotic spindle;cytosolic small ribosomal subunit;extracellular exosome;mitochondrial inner membrane;mitochondrial matrix;nf-kappab complex;nucleolus;nucleoplasm;ruffle membrane;cytoplasm;focal adhesion;membrane;polysome;postsynaptic density;ribonucleoprotein complex;ribosome
P62241	RPS8 40S ribosomal protein S8	4	5	cytosol;endoplasmic reticulum;extracellular region or secreted;nucleus;cytosolic small ribosomal subunit;extracellular exosome;nucleoplasm;focal adhesion;membrane;ribonucleoprotein complex
P62280	RPS11 40S ribosomal protein S11	4	5	cytosol;extracellular region or secreted;nucleus;cytosolic small ribosomal subunit;extracellular exosome;nucleolus;nucleoplasm;cytoplasm;focal adhesion;membrane;ribosome
Q86YH6	PDSS2 Decaprenyl-diphosphate synthase subunit 2	4	5	cytosol;mitochondrion;mitochondrial matrix;transferase complex
Q9ULV4	CORO1C Coronin-1C	4	5	cytoskeleton;endosome;plasma membrane;actin cytoskeleton;endosome membrane;flotillin complex;lateral plasma membrane;ruffle membrane;sarcolemma;cell cortex;focal adhesion;lamellipodium;sarcomere;synapse
Q5U5X0	LYRM7 LYR motif-containing protein 7	4	4	mitochondrion;mitochondrial matrix;mitochondrial membrane
Q86SX6	GLRX5 Glutaredoxin-related protein 5, mitochondrial	4	4	mitochondrion;nucleus;mitochondrial matrix;dendrite;neuronal cell body
O43837	IDH3B Isocitrate dehydrogenase	4	3	mitochondrion;nucleus;mitochondrial matrix
P21333	FLNA Filamin-A	4	3	cytoskeleton;cytosol;extracellular region or secreted;golgi apparatus;nucleus;plasma membrane;actin cytoskeleton;actin filament;actin filament bundle;cortical cytoskeleton;extracellular exosome;extracellular region;trans-golgi network;myb complex;nucleolus;apical dendrite;axonal growth cone;brush border;cell-cell junction;cytoplasm;dendritic shaft;focal adhesion;glutamatergic synapse;membrane;perikaryon;perinuclear region of cytoplasm;postsynapse;z disc
Q00839	HNRNPU Heterogeneous nuclear ribonucleoprotein U	4	3	cytoskeleton;nucleus;centrosome;mitotic spindle;mitotic spindle microtubule;mitotic spindle midzone;spindle pole;catalytic step 2 spliceosome;nuclear chromosome;nuclear matrix;nuclear speck;nucleoplasm;telomerase holoenzyme complex;cell surface;condensed chromosome kinetochore;crd-mediated mrna stability complex;cytoplasmic ribonucleoprotein granule;dendrite cytoplasm;inactive sex chromosome;kinetochore;membrane;midbody;protein-containing complex;ribonucleoprotein complex
Q01518	CAP1 Adenylyl cyclase-associated protein 1	4	3	cytoskeleton;extracellular region or secreted;lysosome;plasma membrane;cortical actin cytoskeleton;extracellular exosome;extracellular region;azurophil granule lumen;cytoplasm;focal adhesion
O75879	PET112 Glutamyl-tRNA(Gln) amidotransferase subunit B, mitochondrial	4	2	mitochondrion;glutamyl-trna(gln) amidotransferase complex
P17844	DDX5 Probable ATP-dependent RNA helicase DDX5	4	2	cytosol;extracellular region or secreted;nucleus;extracellular exosome;catalytic step 2 spliceosome;nucleolus;nucleoplasm;cytoplasm;membrane;ribonucleoprotein complex
Q16643	DBN1 Drebrin	4	2	cytoskeleton;cytosol;plasma membrane;actin cytoskeleton;actomyosin;cortical actin cytoskeleton;cortical cytoskeleton;postsynaptic cytosol;postsynaptic membrane;cytoplasm;dendrite;gap junction;glutamatergic synapse;growth cone;lamellipodium;postsynaptic density;site of polarized growth
Q92947	GCDH Glutaryl-CoA dehydrogenase, mitochondrial	4	2	mitochondrion;mitochondrial matrix
Q96AY3	FKBP10 Peptidyl-prolyl cis-trans isomerase FKBP10	4	2	endoplasmic reticulum;mitochondrion;endoplasmic reticulum lumen;mitochondrial intermembrane space;membrane
P37268	FDFT1 Squalene synthase	4	1	endoplasmic reticulum;endoplasmic reticulum membrane;integral component of membrane
P39023	RPL3 60S ribosomal protein L3	4	1	cytosol;extracellular region or secreted;nucleus;cytosolic large ribosomal subunit;extracellular exosome;nucleolus;cytoplasm;focal adhesion;protein-containing complex;synapse
P60763	RAC3 Ras-related C3 botulinum toxin substrate 3	4	1	cytoskeleton;cytosol;extracellular region or secreted;plasma membrane;filamentous actin;extracellular exosome;cell cortex;cell periphery;cell projection;cytoplasmic vesicle;endomembrane system;growth cone;intracellular membrane-bounded organelle;lamellipodium;neuron projection;neuronal cell body;perinuclear region of cytoplasm;synapse
P60866	RPS20 40S ribosomal protein S20	4	1	cytosol;extracellular region or secreted;nucleus;cytosolic small ribosomal subunit;extracellular exosome;nucleoplasm;membrane;small ribosomal subunit
P63000	RAC1 Ras-related C3 botulinum toxin substrate 1	4	1	cytoskeleton;cytosol;endoplasmic reticulum;endosome;extracellular region or secreted;golgi apparatus;plasma membrane;endoplasmic reticulum membrane;recycling endosome membrane;extracellular exosome;golgi membrane;trans-golgi network;extrinsic component of cytoplasmic side of plasma membrane;ruffle membrane;cell cortex;cell projection;cytoplasm;cytoplasmic ribonucleoprotein granule;cytoplasmic vesicle;dendritic spine;ficolin-1-rich granule membrane;focal adhesion;glutamatergic synapse;intracellular membrane-bounded organelle;lamellipodium;melanosome;membrane;postsynapse;secretory granule membrane
P78368	CSNK1G2 Casein kinase I isoform gamma-2	4	1	cytosol;nucleus;plasma membrane;cell cortex;cytoplasm;membrane
Q01082	SPTBN1 Spectrin beta chain, non-erythrocytic 1	4	1	cytoskeleton;cytosol;extracellular region or secreted;nucleus;plasma membrane;spectrin;spectrin-associated cytoskeleton;extracellular exosome;nucleolus;axolemma;cytoplasm;m band
Q15005	SPCS2 Signal peptidase complex subunit 2	4	1	endoplasmic reticulum;endoplasmic reticulum membrane;signal peptidase complex;integral component of membrane
Q9BQ69	MACROD1 O-acetyl-ADP-ribose deacetylase MACROD1	4	1	nucleus;nucleoplasm

Q9H0R6	QRSL1 Glutamyl-tRNA(Gln) amidotransferase subunit A, mitochondrial	4	1	mitochondrion;glutamyl-trna(gln) amidotransferase complex
Q9NVH0	EXD2 Exonuclease 3'-5' domain-containing protein 2	4	1	cytoskeleton;mitochondrion;nucleus;intermediate filament cytoskeleton;mitochondrial matrix;mitochondrial outer membrane;cytoplasm;integral component of membrane;site of dna damage
A1L0T0	ILVBL Acetolactate synthase-like protein	4	0	endoplasmic reticulum;endoplasmic reticulum membrane;acetolactate synthase complex;integral component of membrane;membrane
E7EVK2	MTG1 Mitochondrial GTPase 1	4	0	mitochondrion;mitochondrial inner membrane
E9PI62	MTG1 Mitochondrial GTPase 1	4	0	no_annotated_location
G3V325	PTCD1 Pentatricopeptide repeat-containing protein 1	4	0	no_annotated_location
O15091	KIAA0391 Mitochondrial ribonuclease P protein 3	4	0	mitochondrion;nucleus;mitochondrial matrix;mitochondrial ribonuclease p complex;nucleoplasm
O43772	SLC25A20 Mitochondrial carnitine/acylcarnitine carrier protein	4	0	cytosol;mitochondrion;mitochondrial inner membrane;integral component of membrane
O60264	SMARCA5 SWI/SNF-related matrix-associated actin-dependent regulator of chromatin subfamily A member 5	4	0	cytosol;nucleus;chromatin silencing complex;fibrillar center;nucleoplasm;nurf complex;rsf complex;condensed chromosome;intracellular membrane-bounded organelle
P16278	GLB1 Beta-galactosidase	4	0	extracellular region or secreted;golgi apparatus;lysosome;extracellular exosome;extracellular region;azurophil granule lumen;lysosomal lumen;cytoplasm;ficolin-1-rich granule lumen;intracellular membrane-bounded organelle;perinuclear region of cytoplasm;vacuole
P21964	COMT Catechol O-methyltransferase	4	0	cytosol;extracellular region or secreted;plasma membrane;extracellular exosome;axon;dendrite;integral component of membrane;intracellular membrane-bounded organelle;membrane
P27824	CANX Calnexin	4	0	endoplasmic reticulum;extracellular region or secreted;endoplasmic reticulum lumen;endoplasmic reticulum membrane;integral component of lumenal side of endoplasmic reticulum membrane;extracellular exosome;melanosome;membrane;mitochondria-associated endoplasmic reticulum membrane;presynapse
P30040	ERP29 Endoplasmic reticulum resident protein 29	4	0	endoplasmic reticulum;endoplasmic reticulum lumen;smooth endoplasmic reticulum;cell surface;melanosome;membrane;transport vesicle
P33121	ACSL1 Long-chain-fatty-acid--CoA ligase 1	4	0	endoplasmic reticulum;mitochondrion;peroxisome;plasma membrane;endoplasmic reticulum membrane;mitochondrial outer membrane;peroxisomal membrane;integral component of membrane;membrane
P43304	GPD2 Glycerol-3-phosphate dehydrogenase, mitochondrial	4	0	mitochondrion;mitochondrial inner membrane;glycerol-3-phosphate dehydrogenase complex
P50914	RPL14 60S ribosomal protein L14	4	0	cytosol;extracellular region or secreted;cytosolic large ribosomal subunit;extracellular exosome;membrane;postsynaptic density
P52272	HNRNPM Heterogeneous nuclear ribonucleoprotein M	4	0	extracellular region or secreted;nucleus;extracellular exosome;catalytic step 2 spliceosome;nuclear matrix;nucleolus;nucleoplasm;paraspeckles;post-mrna release spliceosomal complex;spliceosomal complex;collagen-containing extracellular matrix;cytoplasm;membrane;ribonucleoprotein complex
P53597	SUCLG1 Succinyl-CoA ligase	4	0	mitochondrion;mitochondrial matrix;succinate-coa ligase complex (adp-forming)
P54819	AK2 Adenylate kinase 2, mitochondrial	4	0	extracellular region or secreted;mitochondrion;extracellular exosome;mitochondrial intermembrane space;cytoplasm;sperm mitochondrial sheath
P61026	RAB10 Ras-related protein Rab-10	4	0	cytoskeleton;cytosol;endoplasmic reticulum;endosome;extracellular region or secreted;golgi apparatus;plasma membrane;endoplasmic reticulum membrane;endoplasmic reticulum tubular network;recycling endosome;recycling endosome membrane;extracellular exosome;golgi membrane;trans-golgi network;adherens junction;cilium;cytoplasmic vesicle membrane;exocytic vesicle;focal adhesion;insulin-responsive compartment;perinuclear region of cytoplasm;phagocytic vesicle membrane;secretory granule membrane;synaptic vesicle
P62424	RPL7A 60S ribosomal protein L7a	4	0	cytosol;nucleus;cytosolic large ribosomal subunit;nucleolus;cytoplasm;focal adhesion;membrane;polysomal ribosome;synapse
P82663	MRPS25 28S ribosomal protein S25, mitochondrial	4	0	mitochondrion;mitochondrial inner membrane;ribosome
Q16718	NDUFA5 NADH dehydrogenase	4	0	mitochondrion;mitochondrial inner membrane;mitochondrial respiratory chain complex i
Q5VT66	MARC1 MOSC domain-containing protein 1, mitochondrial	4	0	mitochondrion;mitochondrial outer membrane;integral component of membrane;nitric-oxide synthase complex
Q6NUK1	SLC25A24 Calcium-binding mitochondrial carrier protein SCaMC-1	4	0	mitochondrion;mitochondrial inner membrane;integral component of membrane
Q6P2I3	FAHD2B Fumarylacetoacetate hydrolase domain-containing protein 2B	4	0	no_annotated_location
Q8IXI1	RHOT2 Mitochondrial Rho GTPase 2	4	0	cytosol;mitochondrion;integral component of mitochondrial outer membrane;mitochondrial outer membrane;membrane
Q969Z3	MARC2 MOSC domain-containing protein 2, mitochondrial	4	0	mitochondrion;peroxisome;mitochondrial outer membrane
Q96CQ1	SLC25A36 Solute carrier family 25 member 36	4	0	mitochondrion;mitochondrial inner membrane;integral component of membrane
Q96I51	WBSCR16 Williams-Beuren syndrome chromosomal region 16 protein	4	0	mitochondrion;mitochondrial inner membrane;mitochondrial membrane
Q96KR6	FAM210B Protein FAM210B	4	0	mitochondrion;mitochondrial outer membrane;integral component of membrane;intrinsic component of membrane
Q99595	TIMM17A Mitochondrial import inner membrane translocase subunit Tim17-A	4	0	mitochondrion;nucleus;integral component of mitochondrial inner membrane;mitochondrial inner membrane;tim23 mitochondrial import inner membrane translocase complex;nucleoplasm
Q9BYC8	MRPL32 39S ribosomal protein L32, mitochondrial	4	0	mitochondrion;mitochondrial inner membrane;mitochondrial large ribosomal subunit;mitochondrial ribosome
Q9H0U6	MRPL18 39S ribosomal protein L18, mitochondrial	4	0	extracellular region or secreted;mitochondrion;extracellular space;mitochondrial inner membrane;mitochondrial large ribosomal subunit;mitochondrial ribosome
Q9H5Q4	TFB2M Dimethyladenosine transferase 2, mitochondrial	4	0	mitochondrion;mitochondrial matrix;mitochondrial nucleoid
Q9HCU5	PREB Prolactin regulatory element-binding protein	4	0	endoplasmic reticulum;nucleus;endoplasmic reticulum exit site;endoplasmic reticulum membrane;integral component of endoplasmic reticulum membrane;membrane
Q9NVV4	MTPAP Poly(A) RNA polymerase, mitochondrial	4	0	mitochondrion;nucleus;nucleoplasm;cytoplasm;intracellular membrane-bounded organelle

Q9NZJ7	MTCH1 Mitochondrial carrier homolog 1	4	0	mitochondrion;mitochondrial inner membrane;integral component of membrane;membrane
Q9P032	NDUFAF4 NADH dehydrogenase	4	0	mitochondrion;mitochondrial inner membrane;mitochondrial membrane
Q9P0M9	MRPL27 39S ribosomal protein L27, mitochondrial	4	0	mitochondrion;mitochondrial inner membrane;mitochondrial large ribosomal subunit
Q9UGM6	WARS2 Tryptophan--tRNA ligase, mitochondrial	4	0	mitochondrion;nucleus;plasma membrane;mitochondrial matrix;nucleoplasm
Q9Y2R9	MRPS7 28S ribosomal protein S7, mitochondrial	4	0	mitochondrion;mitochondrial inner membrane;mitochondrial small ribosomal subunit;ribosome
Q9Y673	ALG5 Dolichyl-phosphate beta-glucosyltransferase	4	0	endoplasmic reticulum;endoplasmic reticulum membrane;integral component of membrane;membrane
P68104	EEF1A1 Elongation factor 1-alpha 1	3	41	cytoskeleton;cytosol;extracellular region or secreted;lysosome;nucleus;plasma membrane;cortical actin cytoskeleton;extracellular exosome;extracellular region;extracellular space;cytoplasmic side of lysosomal membrane;nucleolus;ruffle membrane;cytoplasm;eukaryotic translation elongation factor 1 complex;ficolin-1-rich granule lumen;membrane;secretory granule lumen
P23528	CFL1 Cofilin-1	3	38	cytoskeleton;cytosol;extracellular region or secreted;nucleus;plasma membrane;actin cytoskeleton;extracellular exosome;extracellular space;nuclear matrix;lamellipodium membrane;ruffle membrane;cytoplasm;focal adhesion;lamellipodium;membrane;vesicle
O00244	ATOX1 Copper transport protein ATOX1	0	33	cytosol
P49458	SRP9 Signal recognition particle 9 kDa protein	1	28	cytosol;endoplasmic reticulum;signal recognition particle receptor complex;signal recognition particle, endoplasmic reticulum targeting
Q13526	PIN1 Peptidyl-prolyl cis-trans isomerase NIMA-interacting 1	0	27	cytoskeleton;cytosol;mitochondrion;nucleus;ciliary basal body;postsynaptic cytosol;nuclear speck;nucleoplasm;cytoplasm;glutamatergic synapse;midbody;neuron projection
P12277	CKB Creatine kinase B-type	3	26	cytosol;extracellular region or secreted;nucleus;extracellular exosome;extracellular space;dendrite;neuronal cell body
P17987	TCP1 T-complex protein 1 subunit alpha	3	25	cytoskeleton;cytosol;extracellular region or secreted;golgi apparatus;centrosome;microtubule;pericentriolar material;chaperonin-containing t-complex;extracellular exosome;acrosomal vesicle;cell body;heterochromatin;zona pellucida receptor complex
P27348	YWHAQ 14-3-3 protein theta	2	23	cytosol;extracellular region or secreted;mitochondrion;extracellular exosome;cytoplasm;focal adhesion;membrane;protein-containing complex;synapse
Q6S8J3	POTEE POTE ankyrin domain family member E	0	23	extracellular region or secreted;blood microparticle;extracellular exosome;extracellular space
Q99873	PRMT1 Protein arginine N-methyltransferase 1	0	22	cytosol;nucleus;nucleoplasm;cytoplasm;methylosome
Q15185	PTGES3 Prostaglandin E synthase 3	2	21	cytosol;nucleus;nucleoplasm;telomerase holoenzyme complex;chaperone complex;chromosome, telomeric region;protein-containing complex
P13797	PLS3 Plastin-3	1	20	cytoskeleton;cytosol;plasma membrane;actin filament;actin filament bundle;cytoplasm
P26599	PTBP1 Polypyrimidine tract-binding protein 1	0	19	extracellular region or secreted;nucleus;extracellular exosome;nucleolus;nucleoplasm;membrane
P26641	EEF1G Elongation factor 1-gamma	2	17	cytosol;extracellular region or secreted;nucleus;extracellular exosome;cytoplasm;membrane
Q9Y696	CLIC4 Chloride intracellular channel protein 4	1	16	cytoskeleton;cytosol;extracellular region or secreted;mitochondrion;nucleus;plasma membrane;actin cytoskeleton;centrosome;extracellular exosome;nuclear matrix;apical part of cell;cell surface;cell-cell junction;chloride channel complex;cytoplasm;cytoplasmic vesicle membrane;microvillus;midbody;perinuclear region of cytoplasm
P14174	MIF Macrophage migration inhibitory factor	3	14	cytosol;extracellular region or secreted;nucleus;plasma membrane;extracellular exosome;extracellular region;extracellular space;nucleoplasm;cell surface;cytoplasm;ficolin-1-rich granule lumen;secretory granule lumen;vesicle
Q9Y3F4	STRAP Serine-threonine kinase receptor-associated protein	0	14	cytosol;nucleus;cytoplasm;smn complex;smn-sm protein complex
P62258	YWHAE 14-3-3 protein epsilon	2	13	cytoskeleton;cytosol;extracellular region or secreted;mitochondrion;nucleus;kinesin complex;extracellular exosome;central region of growth cone;cytoplasm;focal adhesion;glutamatergic synapse;melanosome;membrane
P63104	YWHAZ 14-3-3 protein zeta/delta	1	13	cytosol;extracellular region or secreted;mitochondrion;nucleus;blood microparticle;extracellular exosome;extracellular space;nucleoplasm;cytoplasm;focal adhesion;glutamatergic synapse;melanosome;vesicle
Q9NQ88	TIGAR Fructose-2,6-bisphosphatase TIGAR	0	13	cytosol;mitochondrion;nucleus;mitochondrial outer membrane;cytoplasm
P25789	PSMA4 Proteasome subunit alpha type-4	2	12	cytosol;extracellular region or secreted;nucleus;extracellular exosome;nucleoplasm;cytoplasm;intracellular membrane-bounded organelle;p-body;proteasome complex;proteasome core complex;proteasome core complex, alpha-subunit complex
P49327	FASN Fatty acid synthase	0	12	cytosol;extracellular region or secreted;golgi apparatus;plasma membrane;extracellular exosome;glycogen granule;melanosome;membrane
P22061	PCMT1 Protein-L-isoaspartate(D-aspartate) O-methyltransferase	3	11	cytosol;extracellular region or secreted;extracellular exosome;extracellular vesicle;cytoplasm
P54136	RARS Arginine--tRNA ligase, cytoplasmic	2	11	cytosol;extracellular region or secreted;nucleus;extracellular exosome;nucleoplasm;aminoacyl-trna synthetase multienzyme complex;cytoplasm;membrane
P60981	DSTN Destrin	2	11	cytoskeleton;extracellular region or secreted;actin cytoskeleton;cortical actin cytoskeleton;extracellular exosome;cytoplasm
P00492	HPRT1 Hypoxanthine-guanine phosphoribosyltransferase	1	11	cytosol;extracellular region or secreted;extracellular exosome;cytoplasm
P08238	HSP90AB1 Heat shock protein HSP 90-beta	3	10	cytosol;extracellular region or secreted;lysosome;mitochondrion;nucleus;plasma membrane;extracellular exosome;extracellular region;lysosomal membrane;nucleoplasm;apical plasma membrane;basolateral plasma membrane;brush border membrane;sperm head plasma membrane;aryl hydrocarbon receptor complex;axonal growth cone;cell surface;cytoplasm;dendritic growth cone;ficolin-1-rich granule lumen;hsp90-cdc37 chaperone complex;inclusion body;melanosome;membrane;neuronal cell body;ooplasm;perinuclear region of cytoplasm;protein-containing complex;secretory granule lumen

P60174	TPI1 Triosephosphate isomerase	2	10	cytosol;extracellular region or secreted;nucleus;extracellular exosome;extracellular space
P62937	PPIA Peptidyl-prolyl cis-trans isomerase A	1	10	cytosol;extracellular region or secreted;nucleus;extracellular exosome;extracellular region;extracellular space;cytoplasm;ficolin-1-rich granule lumen;focal adhesion;intracellular membrane-bounded organelle;membrane;protein-containing complex;secretory granule lumen;vesicle
P50990	CCT8 T-complex protein 1 subunit theta	3	9	cytoskeleton;cytosol;extracellular region or secreted;lysosome;nucleus;centrosome;intermediate filament cytoskeleton;microtubule;chaperonin-containing t-complex;extracellular exosome;extracellular region;azurophil granule lumen;nucleoplasm;cell body;cilium;cytoplasm;ficolin-1-rich granule lumen;secretory granule lumen;zona pellucida receptor complex
P62826	RAN GTP-binding nuclear protein Ran	3	9	cytoskeleton;cytosol;endosome;extracellular region or secreted;nucleus;centriole;recycling endosome;extracellular exosome;nuclear envelope;nuclear pore;nucleolus;nucleoplasm;cytoplasm;host cell;melanosome;membrane;midbody;protein-containing complex;rna nuclear export complex
O14980	XPO1 Exportin-1	2	9	cytosol;nucleus;cajal body;nuclear envelope;nuclear membrane;nucleolus;nucleoplasm;annulate lamellae;cytoplasm;host cell;intracellular membrane-bounded organelle;kinetochore;membrane;protein-containing complex;ribonucleoprotein complex
Q99439	CNN2 Calponin-2	2	9	cytoskeleton;extracellular region or secreted;stress fiber;extracellular region;cell-cell junction;focal adhesion;membrane;specific granule lumen;tertiary granule lumen
P30153	PPP2R1A Serine/threonine-protein phosphatase 2A 65 kDa regulatory subunit A alpha isoform	1	9	cytoskeleton;cytosol;extracellular region or secreted;mitochondrion;nucleus;plasma membrane;microtubule cytoskeleton;extracellular exosome;lateral plasma membrane;chromosome, centromeric region;cytoplasm;dendrite;membrane;protein phosphatase type 2a complex;protein serine/threonine phosphatase complex
P61289	PSME3 Proteasome activator complex subunit 3	1	9	cytosol;nucleus;nucleoplasm;cytoplasm;membrane;proteasome activator complex;proteasome complex
Q16576	RBBP7 Histone-binding protein RBBP7	1	9	cytosol;nucleus;esc/e(z) complex;nucleoplasm;nurd complex
Q9BRA2	TXNDC17 Thioredoxin domain-containing protein 17	0	9	cytosol;extracellular region or secreted;extracellular exosome
Q9NVG8	TBC1D13 TBC1 domain family member 13	0	9	cytosol;membrane
Q9UNH7	SNX6 Sorting nexin-6	0	9	cytosol;endosome;nucleus;early endosome membrane;tubular endosome;cytoplasm;retromer complex;retromer, tubulation complex
P09936	UCHL1 Ubiquitin carboxyl-terminal hydrolase isozyme L1	1	8	cytosol;endoplasmic reticulum;nucleus;endoplasmic reticulum membrane;nucleoplasm;cytoplasm
O00299	CLIC1 Chloride intracellular channel protein 1	0	8	extracellular region or secreted;mitochondrion;nucleus;plasma membrane;blood microparticle;extracellular exosome;extracellular space;nuclear envelope;nuclear membrane;brush border;chloride channel complex;cytoplasm;membrane;perinuclear region of cytoplasm;vesicle
P52564	MAP2K6 Dual specificity mitogen-activated protein kinase kinase 6	0	8	cytoskeleton;cytosol;nucleus;nucleoplasm
Q9BV86	NTMT1 N-terminal Xaa-Pro-Lys N-methyltransferase 1	0	8	cytosol;nucleus;nucleoplasm;cytoplasm
P62829	RPL23 60S ribosomal protein L23	3	7	cytosol;extracellular region or secreted;nucleus;cytosolic large ribosomal subunit;extracellular exosome;nucleolus;nucleoplasm;cytoplasm;focal adhesion;membrane;postsynaptic density;protein-containing complex;ribosome
Q9UBB4	ATXN10 Ataxin-10	3	7	cytosol;extracellular region or secreted;plasma membrane;extracellular space;cytoplasm;dendrite;membrane;neuronal cell body;perinuclear region of cytoplasm
O43175	PHGDH D-3-phosphoglycerate dehydrogenase	2	7	cytosol;extracellular region or secreted;extracellular exosome
P50991	CCT4 T-complex protein 1 subunit delta	2	7	cytoskeleton;cytosol;extracellular region or secreted;nucleus;centrosome;microtubule;chaperonin-containing t-complex;extracellular exosome;nucleoplasm;cell body;cell projection;melanosome;zona pellucida receptor complex
P60891	PRPS1 Ribose-phosphate pyrophosphokinase 1	2	7	cytosol;cytoplasm;ribose phosphate diphosphokinase complex
Q15417	CNN3 Calponin-3	2	7	cytoskeleton;cytosol;actin cytoskeleton;adherens junction;dendritic spine;focal adhesion;neuronal cell body;postsynaptic density
P06280	GLA Alpha-galactosidase A	1	7	extracellular region or secreted;golgi apparatus;lysosome;extracellular exosome;extracellular region;azurophil granule lumen;lysosomal lumen;cytoplasm
P31943	HNRNPH1 Heterogeneous nuclear ribonucleoprotein H	1	7	cytosol;nucleus;catalytic step 2 spliceosome;nucleoplasm;membrane;ribonucleoprotein complex
P04632	CAPNS1 Calpain small subunit 1	0	7	cytosol;extracellular region or secreted;plasma membrane;extracellular exosome;membrane
P07741	APRT Adenine phosphoribosyltransferase	0	7	cytosol;extracellular region or secreted;nucleus;extracellular exosome;extracellular region;nucleoplasm;cytoplasm;secretory granule lumen
P23921	RRM1 Ribonucleoside-diphosphate reductase large subunit	0	7	cytosol;nucleus;ribonucleoside-diphosphate reductase complex;nuclear envelope;cell projection;neuronal cell body
P39687	ANP32A Acidic leucine-rich nuclear phosphoprotein 32 family member A	0	7	endoplasmic reticulum;nucleus;nucleoplasm;cytoplasm;perinuclear region of cytoplasm
P55795	HNRNPH2 Heterogeneous nuclear ribonucleoprotein H2	0	7	cytosol;nucleus;nucleoplasm;membrane;postsynaptic density;ribonucleoprotein complex
Q13642	FHL1 Four and a half LIM domains protein 1	0	7	cytosol;nucleus;plasma membrane;cytoplasm;focal adhesion
Q9BUF5	TUBB6 Tubulin beta-6 chain	0	7	cytoskeleton;extracellular region or secreted;nucleus;microtubule;extracellular exosome;cytoplasm
P00338	LDHA L-lactate dehydrogenase A chain	2	6	cytosol;extracellular region or secreted;nucleus;extracellular exosome;membrane
P63167	DYNLL1 Dynein light chain 1, cytoplasmic	2	6	cytoskeleton;cytosol;mitochondrion;nucleus;plasma membrane;centrosome;cytoplasmic dynein complex;dynein complex;microtubule;mitotic spindle;axon cytoplasm;ciliary tip;cilium;cytoplasm;ficolin-1-rich granule membrane;kinetochore;membrane;tertiary granule membrane
Q9NRW3	APOBEC3C Probable DNA dC- dU-editing enzyme APOBEC-3C	2	6	nucleus;cytoplasm;p-body

Q13561	DCTN2 Dynactin subunit 2	1	6	cytoskeleton;cytosol;extracellular region or secreted;centrosome;dynactin complex;dynein complex;microtubule;extracellular exosome;cytoplasm;growth cone;kinetochore;membrane;vesicle
Q96P16	RPRD1A Regulation of nuclear pre-mRNA domain-containing protein 1A	1	6	nucleus;nucleoplasm;rna polymerase ii, holoenzyme
H3BQZ7	Uncharacterized protein	0	6	nucleus
P13489	RNH1 Ribonuclease inhibitor	0	6	cytosol;extracellular region or secreted;nucleus;angiogenin-pri complex;extracellular exosome;nucleoplasm
P18669	PGAM1 Phosphoglycerate mutase 1	0	6	cytosol;extracellular region or secreted;extracellular exosome;extracellular region;cytoplasm;ficolin-1-rich granule lumen;membrane;secretory granule lumen
P28072	PSMB6 Proteasome subunit beta type-6	0	6	cytosol;extracellular region or secreted;nucleus;extracellular exosome;nucleoplasm;cytoplasm;proteasome complex;proteasome core complex;proteasome core complex, beta-subunit complex
P38606	ATP6V1A V-type proton ATPase catalytic subunit A	0	6	cytosol;extracellular region or secreted;lysosome;nucleus;plasma membrane;extracellular exosome;lysosomal membrane;nucleoplasm;apical plasma membrane;intracellular membrane-bounded organelle;microvillus;proton-transporting two-sector atpase complex;proton-transporting v-type atpase, v1 domain;vacuolar membrane
P53611	RABGGTB Geranylgeranyl transferase type-2 subunit beta	0	6	cytosol;plasma membrane;rab-protein geranylgeranyltransferase complex
Q06124	PTPN11 Tyrosine-protein phosphatase non-receptor type 11	0	6	cytosol;mitochondrion;nucleus;nucleoplasm;cytoplasm;protein-containing complex
Q08J23	NSUN2 tRNA (cytosine(34)-C(5))-methyltransferase	0	6	cytoskeleton;extracellular region or secreted;mitochondrion;nucleus;spindle;extracellular exosome;nucleolus;nucleoplasm;chromatoid body;cytoplasm
Q13200	PSMD2 26S proteasome non-ATPase regulatory subunit 2	0	6	cytosol;extracellular region or secreted;nucleus;extracellular exosome;extracellular region;nucleoplasm;ficolin-1-rich granule lumen;membrane;proteasome accessory complex;proteasome complex;proteasome regulatory particle;proteasome regulatory particle, base subcomplex;proteasome storage granule;secretory granule lumen
Q15019	SEPT2 Septin-2	0	6	cytoskeleton;extracellular region or secreted;nucleus;plasma membrane;actin cytoskeleton;axoneme;microtubule cytoskeleton;septin complex;septin ring;spindle;extracellular exosome;intercellular bridge;nucleoplasm;ciliary membrane;cleavage furrow;cell division site;condensed chromosome kinetochore;cytoplasm;exocyst;midbody;non-motile cilium;perinuclear region of cytoplasm;photoreceptor connecting cilium;sperm annulus;synaptic vesicle
Q1KMD3	HNRNPUL2 Heterogeneous nuclear ribonucleoprotein U-like protein 2	0	6	nucleus;nucleoplasm;membrane
Q9Y508	RNF114 RING finger protein 114	0	6	cytosol;nucleus;plasma membrane
Q9Y617	PSAT1 Phosphoserine aminotransferase	0	6	cytosol;extracellular region or secreted;extracellular exosome;cytoplasm
Q04637	EIF4G1 Eukaryotic translation initiation factor 4 gamma 1	3	5	cytosol;nucleus;cytoplasm;cytoplasmic stress granule;eukaryotic translation initiation factor 4f complex;membrane;polysome
P07814	EPRS Bifunctional glutamate/proline--tRNA ligase	2	5	cytosol;plasma membrane;aminoacyl-trna synthetase multienzyme complex;cytoplasm;gait complex;membrane;ribonucleoprotein complex
P36873	PPP1CC Serine/threonine-protein phosphatase PP1-gamma catalytic subunit	2	5	cytoskeleton;cytosol;mitochondrion;nucleus;plasma membrane;mitochondrial outer membrane;nuclear speck;nucleolus;cleavage furrow;condensed chromosome kinetochore;cytoplasm;dendritic spine;focal adhesion;glutamatergic synapse;midbody;presynapse;protein phosphatase type 1 complex;protein-containing complex;ptw/pp1 phosphatase complex
P62136	PPP1CA Serine/threonine-protein phosphatase PP1-alpha catalytic subunit	2	5	cytosol;extracellular region or secreted;nucleus;plasma membrane;extracellular exosome;nucleolus;nucleoplasm;adherens junction;cytoplasm;dendritic spine;glutamatergic synapse;glycogen granule;perikaryon;presynapse;protein phosphatase type 1 complex;ptw/pp1 phosphatase complex
P62140	PPP1CB Serine/threonine-protein phosphatase PP1-beta catalytic subunit	2	5	cytosol;extracellular region or secreted;nucleus;plasma membrane;extracellular exosome;nucleolus;nucleoplasm;cytoplasm;focal adhesion;glycogen granule;protein phosphatase type 1 complex;ptw/pp1 phosphatase complex
O75348	ATP6V1G1 V-type proton ATPase subunit G 1	1	5	cytosol;extracellular region or secreted;lysosome;plasma membrane;extracellular exosome;lysosomal membrane;vacuolar proton-transporting v-type atpase complex
O95373	IPO7 Importin-7	1	5	cytosol;nucleus;nuclear envelope;nuclear pore;nucleoplasm;membrane
P04075	ALDOA Fructose-bisphosphate aldolase A	1	5	cytoskeleton;cytosol;extracellular region or secreted;nucleus;actin cytoskeleton;extracellular exosome;extracellular region;extracellular space;ficolin-1-rich granule lumen;i band;m band;membrane;platelet alpha granule lumen;secretory granule lumen;sperm head;tertiary granule lumen
P07900	HSP90AA1 Heat shock protein HSP 90-alpha	1	5	cytosol;extracellular region or secreted;lysosome;mitochondrion;nucleus;plasma membrane;extracellular exosome;extracellular region;lysosomal lumen;nucleoplasm;axonal growth cone;cytoplasm;dendritic growth cone;endocytic vesicle lumen;ficolin-1-rich granule lumen;melanosome;membrane;myelin sheath;neuronal cell body;perinuclear region of cytoplasm;protein-containing complex;secretory granule lumen
P09972	ALDOC Fructose-bisphosphate aldolase C	1	5	cytoskeleton;cytosol;extracellular region or secreted;extracellular exosome;extracellular region;ficolin-1-rich granule lumen;secretory granule lumen;tertiary granule lumen
P10599	TXN Thioredoxin	1	5	cytosol;extracellular region or secreted;nucleus;extracellular exosome;extracellular region;nucleoplasm;cytoplasm
P30041	PRDX6 Peroxiredoxin-6	1	5	cytosol;extracellular region or secreted;lysosome;mitochondrion;nucleus;extracellular exosome;extracellular region;extracellular space;azurophil granule lumen;cytoplasm;membrane;perinuclear region of cytoplasm
P35611	ADD1 Alpha-adducin	1	5	cytoskeleton;cytosol;nucleus;plasma membrane;f-actin capping protein complex;nuclear body;nucleoplasm;adherens junction;cytoplasm;focal adhesion;postsynaptic density
P41091	EIF2S3 Eukaryotic translation initiation factor 2 subunit 3	1	5	cytosol;extracellular region or secreted;extracellular exosome;cytoplasm;eukaryotic translation initiation factor 2 complex
P83731	RPL24 60S ribosomal protein L24	1	5	cytosol;endoplasmic reticulum;extracellular region or secreted;cytosolic large ribosomal subunit;extracellular exosome;cytoplasm;membrane;polysomal ribosome;synapse
A6NDG6	PGP Phosphoglycolate phosphatase	0	5	cytoplasm
O75369	FLNB Filamin-B	0	5	cytoskeleton;cytosol;extracellular region or secreted;nucleus;plasma membrane;actin cytoskeleton;extracellular exosome;cell cortex;cytoplasm;focal

				adhesion;integral component of membrane;neuron projection;neuronal cell body;z disc
O75663	TIPRL TIP41-like protein	0	5	cytosol
O95757	HSPA4L Heat shock 70 kDa protein 4L	0	5	cytosol;nucleus;cytoplasm
O95801	TTC4 Tetratricopeptide repeat protein 4	0	5	nucleus;nucleoplasm;cytoplasm
P21266	GSTM3 Glutathione S-transferase Mu 3	0	5	cytosol;extracellular region or secreted;nucleus;extracellular exosome;intercellular bridge;cytoplasm;sperm fibrous sheath
P30086	PEBP1 Phosphatidylethanolamine-binding protein 1	0	5	cytosol;extracellular region or secreted;nucleus;extracellular exosome
P40222	TXLNA Alpha-taxilin	0	5	cytosol;extracellular region or secreted;extracellular region;cytoplasm;membrane
P47756	CAPZB F-actin-capping protein subunit beta	0	5	cytoskeleton;cytosol;extracellular region or secreted;actin cytoskeleton;f-actin capping protein complex;extracellular exosome;sarcomere;wash complex
P49321	NASP Nuclear autoantigenic sperm protein	0	5	nucleus;nucleoplasm;chromatin;cytoplasm;protein-containing complex
P49591	SARS Serine--tRNA ligase, cytoplasmic	0	5	cytosol;extracellular region or secreted;nucleus;extracellular exosome;cytoplasm
P52597	HNRNPF Heterogeneous nuclear ribonucleoprotein F	0	5	cytosol;nucleus;plasma membrane;catalytic step 2 spliceosome;nucleoplasm;membrane;ribonucleoprotein complex
P53041	PPP5C Serine/threonine-protein phosphatase 5	0	5	cytosol;nucleus;plasma membrane;nucleoplasm;chaperone complex;intracellular membrane-bounded organelle;perikaryon;protein-containing complex;proximal dendrite
P84090	ERH Enhancer of rudimentary homolog	0	5	nucleus;methylosome;midbody
Q06203	PPAT Amidophosphoribosyltransferase	0	5	cytosol
Q12888	TP53BP1 Tumor suppressor p53-binding protein 1	0	5	nucleus;nuclear body;nucleoplasm;chromosome, telomeric region;condensed chromosome kinetochore;cytoplasm;dna repair complex;replication fork;site of double-strand break
Q15369	TCEB1 Transcription elongation factor B polypeptide 1	0	5	cytosol;nucleus;elongin complex;nucleoplasm;cul2-ring ubiquitin ligase complex;vcb complex
Q16527	CSRP2 Cysteine and glycine-rich protein 2	0	5	nucleus;cytoplasm;focal adhesion;z disc
Q5TFE4	NT5DC1 5'-nucleotidase domain-containing protein 1	0	5	no_annotated_location
Q6FI81	CIAPIN1 Anamorsin	0	5	mitochondrion;nucleus;mitochondrial intermembrane space;nucleolus;nucleoplasm;cytoplasm
Q86VP6	CAND1 Cullin-associated NEDD8-dissociated protein 1	0	5	cytosol;extracellular region or secreted;golgi apparatus;nucleus;extracellular exosome;extracellular region;nucleoplasm;cullin-ring ubiquitin ligase complex;cytoplasm;ficolin-1-rich granule lumen;membrane;secretory granule lumen;ubiquitin ligase complex
Q96CD2	PPCDC Phosphopantothenoylcysteine decarboxylase	0	5	cytosol;phosphopantothenoylcysteine decarboxylase complex
Q9C0B1	FTO Alpha-ketoglutarate-dependent dioxygenase FTO	0	5	cytosol;nucleus;plasma membrane;nuclear speck;nucleoplasm;cytoplasm;intracellular membrane-bounded organelle
Q9H0C8	ILKAP Integrin-linked kinase-associated serine/threonine phosphatase 2C	0	5	cytosol;nucleus;nucleoplasm
Q9NPH2	ISYNA1 Inositol-3-phosphate synthase 1	0	5	cytosol;cytoplasm
Q9NTK5	OLA1 Obg-like ATPase 1	0	5	cytoskeleton;cytosol;extracellular region or secreted;nucleus;centrosome;extracellular exosome;extracellular region;nucleolus;cytoplasm;membrane;platelet alpha granule lumen
Q9NYL2	MLTK Mitogen-activated protein kinase kinase kinase MLT	0	5	cytosol;nucleus;cytoplasm
P09622	DLD Dihydrolipoyl dehydrogenase, mitochondrial	3	4	mitochondrion;nucleus;mitochondrial matrix;acrosomal matrix;motile cilium;oxoglutarate dehydrogenase complex;pyruvate dehydrogenase complex
P30044	PRDX5 Peroxiredoxin-5, mitochondrial	3	4	cytosol;extracellular region or secreted;mitochondrion;nucleus;peroxisome;extracellular exosome;extracellular space;mitochondrial matrix;peroxisomal matrix;cytoplasm;cytoplasmic vesicle;intracellular membrane-bounded organelle;perinuclear region of cytoplasm
P61158	ACTR3 Actin-related protein 3	3	4	cytoskeleton;cytosol;extracellular region or secreted;nucleus;actin cytoskeleton;arp2/3 protein complex;extracellular exosome;brush border;cell-cell junction;cytoplasm;focal adhesion;lamellipodium;membrane;site of double-strand break
P61978	HNRNPK Heterogeneous nuclear ribonucleoprotein K	3	4	cytoskeleton;extracellular region or secreted;nucleus;podosome;extracellular exosome;catalytic step 2 spliceosome;nucleoplasm;cell projection;chromatin;cytoplasm;cytoplasmic stress granule;focal adhesion;membrane
Q9HB71	CACYBP Calcyclin-binding protein	3	4	cytosol;extracellular region or secreted;nucleus;extracellular exosome;nuclear envelope lumen;nucleoplasm;beta-catenin destruction complex;cell body;neuron projection;scf ubiquitin ligase complex
P14868	DARS Aspartate--tRNA ligase, cytoplasmic	2	4	cytosol;extracellular region or secreted;extracellular exosome;aminoacyl-trna synthetase multienzyme complex;cytoplasm;membrane;synapse
P53634	CTSC Dipeptidyl peptidase 1	2	4	cytoskeleton;endoplasmic reticulum;extracellular region or secreted;golgi apparatus;lysosome;nucleus;centrosome;endoplasmic reticulum lumen;extracellular exosome;extracellular region;extracellular space;azurophil granule lumen;nucleoplasm;collagen-containing extracellular matrix;copii-coated er to golgi transport vesicle;endoplasmic reticulum-golgi intermediate compartment membrane;intracellular membrane-bounded organelle;membrane
Q99567	NUP88 Nuclear pore complex protein Nup88	2	4	cytosol;nucleus;nuclear pore;nucleoplasm;host cell
O43765	SGTA Small glutamine-rich tetratricopeptide repeat-containing protein alpha	1	4	cytosol;nucleus;trc complex;cytoplasm;membrane
O95861	BPNT1 3'(2'),5'-bisphosphate nucleotidase 1	1	4	cytosol
P00390	GSR Glutathione reductase, mitochondrial	1	4	cytosol;extracellular region or secreted;mitochondrion;plasma membrane;extracellular exosome;mitochondrial matrix;external side of plasma membrane
P31153	MAT2A S-adenosylmethionine synthase isoform type-2	1	4	cytosol;methionine adenosyltransferase complex
P53396	ACLY ATP-citrate synthase	1	4	cytosol;extracellular region or secreted;lysosome;nucleus;plasma membrane;extracellular exosome;extracellular region;azurophil granule lumen;nucleoplasm;ficolin-1-rich granule lumen;membrane

P55072	VCP Transitional endoplasmic reticulum ATPase	1	4	cytosol;endoplasmic reticulum;extracellular region or secreted;lysosome;nucleus;derlin-1 retrotranslocation complex;endoplasmic reticulum membrane;vcp-npl4-ufd1 aaa atpase complex;extracellular exosome;extracellular region;azurophil granule lumen;nucleoplasm;atpase complex;cytoplasm;cytoplasmic stress granule;ficolin-1-rich granule lumen;glutamatergic synapse;intracellular membrane-bounded organelle;lipid droplet;perinuclear region of cytoplasm;proteasome complex;protein-containing complex;secretory granule lumen;site of double-strand break;vcp-nsfl1c complex
P55769	NHP2L1 NHP2-like protein 1	1	4	nucleus;dense fibrillar component;nucleolus;nucleoplasm;precatalytic spliceosome;u2-type precatalytic spliceosome;u4/u6 x u5 tri-snrnp complex;u4atac snrnp;box c/d rnp complex;protein-containing complex;small-subunit processome
P60660	MYL6 Myosin light polypeptide 6	1	4	cytoskeleton;cytosol;extracellular region or secreted;myosin complex;unconventional myosin complex;extracellular exosome;brush border;membrane;vesicle
P62266	RPS23 40S ribosomal protein S23	1	4	cytosol;endoplasmic reticulum;nucleus;cytosolic small ribosomal subunit;rough endoplasmic reticulum;nucleoplasm;membrane;polysomal ribosome;ribosome
Q13148	TARDBP TAR DNA-binding protein 43	1	4	nucleus;interchromatin granule;nuclear speck;nucleoplasm;perichromatin fibrils;cytoplasmic stress granule
Q14204	DYNC1H1 Cytoplasmic dynein 1 heavy chain 1	1	4	cytoskeleton;cytosol;extracellular region or secreted;lysosome;centrosome;cytoplasmic dynein complex;cytoplasmic microtubule;dynein complex;microtubule;extracellular exosome;extracellular region;azurophil granule lumen;axon cytoplasm;cell cortex;membrane
Q6IS14	EIF5AL1 Eukaryotic translation initiation factor 5A-1-like	1	4	endoplasmic reticulum;nucleus;endoplasmic reticulum membrane;nuclear pore
Q99497	PARK7 Protein DJ-1	1	4	cytosol;endoplasmic reticulum;extracellular region or secreted;mitochondrion;nucleus;plasma membrane;extracellular exosome;mitochondrial intermembrane space;mitochondrial matrix;nucleoplasm;pml body;adherens junction;axon;cell body;chromatin;cytoplasm;membrane raft;perinuclear region of cytoplasm;presynapse
Q9GZV4	EIF5A2 Eukaryotic translation initiation factor 5A-2	1	4	cytosol;endoplasmic reticulum;nucleus;endoplasmic reticulum membrane;nuclear pore;intracellular membrane-bounded organelle
Q9Y5Y2	NUBP2 Cytosolic Fe-S cluster assembly factor NUBP2	1	4	cytoskeleton;cytosol;nucleus;centriole;spindle pole centrosome;cilium
B4DPH6	LIMS3L cDNA, FLJ79109, highly similar to Particularly interesting newCys-His protein	0	4	cytoplasm
O14733	MAP2K7 Dual specificity mitogen-activated protein kinase kinase 7	0	4	cytosol;nucleus;cytoplasm
O15355	PPM1G Protein phosphatase 1G	0	4	nucleus;nucleoplasm;cytoplasm;membrane
O43776	NARS Asparagine--tRNA ligase, cytoplasmic	0	4	cytosol;extracellular region or secreted;extracellular exosome;cytoplasm
O60701	UGDH UDP-glucose 6-dehydrogenase	0	4	cytosol;extracellular region or secreted;nucleus;extracellular exosome;nucleoplasm
O75179	ANKRD17 Ankyrin repeat domain-containing protein 17	0	4	nucleus;nuclear membrane;nucleoplasm;chromatin;cytoplasm;membrane
O75934	BCAS2 Pre-mRNA-splicing factor SPF27	0	4	cytoskeleton;nucleus;centrosome;catalytic step 2 spliceosome;nuclear speck;nucleolus;nucleoplasm;spliceosomal complex;u2-type catalytic step 2 spliceosome;prp19 complex
P09211	GSTP1 Glutathione S-transferase P	0	4	cytosol;extracellular region or secreted;mitochondrion;nucleus;plasma membrane;extracellular exosome;extracellular region;extracellular space;cytoplasm;ficolin-1-rich granule lumen;secretory granule lumen;traf2-gstp1 complex;vesicle
P12955	PEPD Xaa-Pro dipeptidase	0	4	extracellular region or secreted;extracellular exosome
P14866	HNRNPL Heterogeneous nuclear ribonucleoprotein L	0	4	extracellular region or secreted;nucleus;extracellular exosome;nucleoplasm;cytoplasm;membrane;ribonucleoprotein complex;ribonucleoprotein granule
P30626	SRI Sorcin	0	4	cytosol;endoplasmic reticulum;extracellular region or secreted;mitochondrion;nucleus;plasma membrane;endoplasmic reticulum membrane;sarcoplasmic reticulum;sarcoplasmic reticulum membrane;smooth endoplasmic reticulum;extracellular exosome;nucleoplasm;t-tubule;axon terminus;cytoplasm;dendritic spine neck;membrane;z disc
P31939	ATIC Bifunctional purine biosynthesis protein PURH	0	4	cytosol;extracellular region or secreted;plasma membrane;extracellular exosome;membrane
P31948	STIP1 Stress-induced-phosphoprotein 1	0	4	cytosol;golgi apparatus;nucleus;chaperone complex;protein-containing complex
P35754	GLRX Glutaredoxin-1	0	4	cytosol;extracellular region or secreted;nucleus;extracellular exosome
P45985	MAP2K4 Dual specificity mitogen-activated protein kinase kinase 4	0	4	cytosol;nucleus;axon;dendrite cytoplasm;perikaryon
P48059	LIMS1 LIM and senescent cell antigen-like-containing domain protein 1	0	4	cytosol;plasma membrane;cell-cell junction;cytoplasm;focal adhesion;perinuclear region of cytoplasm;protein-containing complex
P53384	NUBP1 Cytosolic Fe-S cluster assembly factor NUBP1	0	4	cytoskeleton;cytosol;nucleus;plasma membrane;centriole;cilium
P55060	CSE1L Exportin-2	0	4	cytosol;extracellular region or secreted;nucleus;extracellular exosome;nuclear envelope;nucleoplasm;cytoplasm;membrane
P60900	PSMA6 Proteasome subunit alpha type-6	0	4	cytosol;extracellular region or secreted;nucleus;extracellular exosome;nuclear matrix;nucleoplasm;cytoplasm;myofibril;p-body;polysome;proteasome complex;proteasome core complex;proteasome core complex, alpha-subunit complex;sarcomere
Q14151	SAFB2 Scaffold attachment factor B2	0	4	extracellular region or secreted;nucleus;extracellular exosome;nuclear body;nucleoplasm;cytoplasm;intracellular membrane-bounded organelle
Q14203	DCTN1 Dynactin subunit 1	0	4	cytoskeleton;cytosol;extracellular region or secreted;nucleus;centriole;centrosome;dynein complex;microtubule;microtubule associated complex;microtubule cytoskeleton;microtubule plus-end;mitotic spindle;spindle;spindle pole;intercellular bridge;nuclear envelope;axon;cell cortex;cell cortex region;centriolar subdistal appendage;cytoplasm;kinetochore;membrane;neuron projection;neuronal cell body
Q15424	SAFB Scaffold attachment factor B1	0	4	nucleus;nucleoplasm;midbody
Q6QNY0	BLOC1S3 Biogenesis of lysosome-related organelles complex 1 subunit 3	0	4	cytosol;bloc-1 complex;axon cytoplasm;transport vesicle

Q7RTV0	PHF5A PHD finger-like domain-containing protein 5A	0	4	nucleus;nuclear matrix;nuclear speck;nucleoplasm;precatalytic spliceosome;u12-type spliceosomal complex;u2 snrnp;u2-type precatalytic spliceosome
Q86X76	NIT1 Nitrilase homolog 1	0	4	mitochondrion;nucleus;cytoplasm
Q8IWZ3	ANKHD1 Ankyrin repeat and KH domain-containing protein 1	0	4	cytoplasm
Q92973	TNPO1 Transportin-1	0	4	cytosol;extracellular region or secreted;nucleus;extracellular exosome;cilium;cytoplasm
Q96CP2	FLYWCH2 FLYWCH family member 2	0	4	no_annotated_location
Q96FW1	OTUB1 Ubiquitin thioesterase OTUB1	0	4	cytosol;extracellular region or secreted;nucleus;extracellular exosome;nucleoplasm
Q96GM5	SMARCD1 SWI/SNF-related matrix-associated actin-dependent regulator of chromatin subfamily D member 1	0	4	nucleus;nbaf complex;npbaf complex;nucleoplasm;swi/snf complex;intracellular membrane-bounded organelle
Q9BV38	WDR18 WD repeat-containing protein 18	0	4	nucleus;nuclear pre-replicative complex;nucleolus;nucleoplasm;cytoplasm;rix1 complex
Q9BY32	ITPA Inosine triphosphate pyrophosphatase	0	4	cytosol;nucleus;nucleoplasm;cytoplasm;intracellular membrane-bounded organelle
Q9C0C9	UBE2O Ubiquitin-conjugating enzyme E2 O	0	4	cytosol;nucleus;nuclear body;nucleoplasm;cytoplasm
Q9H773	DCTPP1 dCTP pyrophosphatase 1	0	4	cytosol;mitochondrion;nucleus
Q9ULC4	MCTS1 Malignant T-cell-amplified sequence 1	0	4	cytosol;plasma membrane
Q9Y314	NOSIP Nitric oxide synthase-interacting protein	0	4	cytosol;golgi apparatus;nucleus;golgi membrane;nucleoplasm;cytoplasm

Table 2A-2. Panther GO Biological Processes enrichment analysis for proteins identified in whole-cell lysates. Data filtered for processes enriched > 5-fold.

Analysis Type: PANTHER Overrepresentation Test (Released 20210224)
Annotation Version and Release Date: GO Ontology database DOI: 10.5281/zenodo.4495804 Released 2021-02-01
Reference List: Homo sapiens (all genes in database)
Test Type: FISHER
Correction: BONFERRONI
Bonferroni count: 9036

		Protein Number			
GO biological process complete	**REFLIST**	**Observed**	**Expected**	**Fold Enrichment**	**P-value**
purine nucleobase biosynthetic process (GO:0009113)	10	10	0.68	14.77	9.4E-04
purine ribonucleoside monophosphate biosynthetic process (GO:0009168)	21	14	1.42	9.85	9.4E-05
positive regulation of telomerase RNA localization to Cajal body (GO:1904874)	15	10	1.02	9.85	1.2E-02
purine nucleoside monophosphate biosynthetic process (GO:0009127)	23	15	1.56	9.64	3.5E-05
nucleobase biosynthetic process (GO:0046112)	19	12	1.29	9.33	1.7E-03
purine nucleobase metabolic process (GO:0006144)	19	12	1.29	9.33	1.7E-03
regulation of telomerase RNA localization to Cajal body (GO:1904872)	18	10	1.22	8.21	4.2E-02
ribonucleoside monophosphate biosynthetic process (GO:0009156)	35	18	2.37	7.6	1.7E-05
tRNA aminoacylation (GO:0043039)	49	25	3.32	7.54	1.4E-08
amino acid activation (GO:0043038)	50	25	3.38	7.39	2.0E-08
tRNA aminoacylation for protein translation (GO:0006418)	46	23	3.11	7.39	1.5E-07
nucleoside monophosphate biosynthetic process (GO:0009124)	44	21	2.98	7.05	2.2E-06
S phase (GO:0051320)	65	30	4.4	6.82	6.5E-10
mitotic S phase (GO:0000084)	65	30	4.4	6.82	6.5E-10
nucleobase metabolic process (GO:0009112)	35	16	2.37	6.75	4.9E-04
NADH regeneration (GO:0006735)	27	12	1.83	6.57	2.9E-02
glucose catabolic process to pyruvate (GO:0061718)	27	12	1.83	6.57	2.9E-02
canonical glycolysis (GO:0061621)	27	12	1.83	6.57	2.9E-02
glycolytic process through glucose-6-phosphate (GO:0061620)	28	12	1.9	6.33	3.8E-02
glycolytic process through fructose-6-phosphate (GO:0061615)	28	12	1.9	6.33	3.8E-02
NADH metabolic process (GO:0006734)	40	17	2.71	6.28	4.4E-04
nucleoside biosynthetic process (GO:0009163)	38	16	2.57	6.22	1.2E-03
glucose catabolic process (GO:0006007)	31	13	2.1	6.2	1.9E-02
mitotic interphase (GO:0051329)	79	33	5.35	6.17	3.5E-10
interphase (GO:0051325)	79	33	5.35	6.17	3.5E-10
pre-replicative complex assembly (GO:0036388)	65	27	4.4	6.14	8.0E-08
intracellular transport of virus (GO:0075733)	54	22	3.66	6.02	9.0E-06
purine ribonucleoside monophosphate metabolic process (GO:0009167)	40	16	2.71	5.91	2.1E-03
purine nucleoside monophosphate metabolic process (GO:0009126)	43	17	2.91	5.84	1.0E-03
glycolytic process (GO:0006096)	41	16	2.78	5.77	2.7E-03
tRNA-containing ribonucleoprotein complex export from nucleus (GO:0071431)	34	13	2.3	5.65	4.2E-02
tRNA export from nucleus (GO:0006409)	34	13	2.3	5.65	4.2E-02

ATP generation from ADP (GO:0006757)	42	16	2.84	5.63	3.6E-03
glycosyl compound biosynthetic process (GO:1901659)	42	16	2.84	5.63	3.6E-03
positive regulation of telomere maintenance via telomere lengthening (GO:1904358)	37	14	2.5	5.59	2.0E-02
positive regulation of telomere maintenance (GO:0032206)	51	19	3.45	5.5	3.9E-04
multi-organism localization (GO:1902579)	63	23	4.26	5.39	2.1E-05
multi-organism transport (GO:0044766)	63	23	4.26	5.39	2.1E-05
transport of virus (GO:0046794)	61	22	4.13	5.33	5.6E-05
regulation of transcription from RNA polymerase II promoter in response to hypoxia (GO:0061418)	78	28	5.28	5.3	5.4E-07
anaphase-promoting complex-dependent catabolic process (GO:0031145)	87	31	5.89	5.26	6.0E-08
regulation of cellular response to heat (GO:1900034)	79	28	5.35	5.24	6.8E-07
ribonucleoside monophosphate metabolic process (GO:0009161)	57	20	3.86	5.18	3.9E-04
anaphase (GO:0051322)	157	55	10.63	5.18	8.1E-16
mitotic anaphase (GO:0000090)	157	55	10.63	5.18	8.1E-16
M phase (GO:0000279)	160	56	10.83	5.17	3.9E-16
mitotic M phase (GO:0000087)	160	56	10.83	5.17	3.9E-16
translational initiation (GO:0006413)	143	50	9.68	5.17	4.1E-14
DNA replication initiation (GO:0006270)	43	15	2.91	5.15	2.0E-02
cellular modified amino acid biosynthetic process (GO:0042398)	43	15	2.91	5.15	2.0E-02
viral transcription (GO:0019083)	116	40	7.85	5.09	1.3E-10
NAD metabolic process (GO:0019674)	47	16	3.18	5.03	1.2E-02
monosaccharide biosynthetic process (GO:0046364)	53	18	3.59	5.02	2.7E-03
regulation of cellular amino acid metabolic process (GO:0006521)	65	22	4.4	5	1.4E-04

Table 2A-3. Panther GO Biological Processes enrichment analysis for proteins identified in Mito-P lysates. Data filtered for processes enriched > 5-fold.

Analysis Type: PANTHER Overrepresentation Test (Released 20210224)

Annotation Version and Release Date: GO Ontology database DOI: 10.5281/zenodo.4495804 Released 2021-02-01

Test Type: FISHER

Correction: BONFERRONI

		Protein Number			
GO biological process complete	**REFLIST**	**Observed**	**Expected**	**Fold Enrichment**	**P-value**
tRNA aminoacylation for mitochondrial protein translation (GO:0070127)	8	7	0.44	15.84	4.25E-02
branched-chain amino acid catabolic process (GO:0009083)	21	15	1.16	12.93	9.92E-07
branched-chain amino acid metabolic process (GO:0009081)	24	16	1.33	12.07	4.97E-07
tricarboxylic acid cycle (GO:0006099)	34	22	1.88	11.71	1.89E-10
mitochondrial translation (GO:0032543)	111	64	6.13	10.43	3.27E-33
mitochondrial gene expression (GO:0140053)	140	78	7.74	10.08	2.51E-40
mitochondrial RNA metabolic process (GO:0000959)	40	22	2.21	9.95	2.24E-09
mitochondrial translational elongation (GO:0070125)	88	47	4.86	9.67	1.48E-22
mitochondrial fusion (GO:0008053)	17	9	0.94	9.58	3.60E-02
mitochondrial translational termination (GO:0070126)	89	47	4.92	9.56	2.15E-22
cristae formation (GO:0042407)	31	16	1.71	9.34	8.40E-06
translational termination (GO:0006415)	97	49	5.36	9.14	8.52E-23
regulation of mitochondrial translation (GO:0070129)	26	13	1.44	9.05	4.26E-04
fatty acid beta-oxidation (GO:0006635)	59	29	3.26	8.9	3.48E-12
viral transcription (GO:0019083)	116	56	6.41	8.74	1.16E-25
mitochondrial calcium ion transmembrane transport (GO:0006851)	25	12	1.38	8.69	1.98E-03
SRP-dependent cotranslational protein targeting to membrane (GO:0006614)	96	45	5.3	8.48	1.10E-19
inner mitochondrial membrane organization (GO:0007007)	52	24	2.87	8.35	3.54E-09
NADH metabolic process (GO:0006734)	40	18	2.21	8.14	4.24E-06
cotranslational protein targeting to membrane (GO:0006613)	101	45	5.58	8.06	5.59E-19
regulation of mitochondrial gene expression (GO:0062125)	30	13	1.66	7.84	1.58E-03
protein targeting to ER (GO:0045047)	111	48	6.13	7.83	5.59E-20
mitochondrial transmembrane transport (GO:1990542)	105	45	5.8	7.76	1.93E-18
tRNA aminoacylation (GO:0043039)	49	21	2.71	7.76	3.13E-07
establishment of protein localization to endoplasmic reticulum (GO:0072599)	115	49	6.35	7.71	3.15E-20

translational elongation (GO:0006414)	125	53	6.91	7.67	5.10E-22
fatty acid catabolic process (GO:0009062)	90	38	4.97	7.64	5.45E-15
amino acid activation (GO:0043038)	50	21	2.76	7.6	4.22E-07
tRNA aminoacylation for protein translation (GO:0006418)	46	19	2.54	7.48	4.42E-06
tRNA-containing ribonucleoprotein complex export from nucleus (GO:0071431)	34	14	1.88	7.45	8.79E-04
tRNA export from nucleus (GO:0006409)	34	14	1.88	7.45	8.79E-04
protein targeting to mitochondrion (GO:0006626)	56	23	3.09	7.43	7.29E-08
NADH dehydrogenase complex assembly (GO:0010257)	66	27	3.65	7.4	1.21E-09
mitochondrial respiratory chain complex I assembly (GO:0032981)	66	27	3.65	7.4	1.21E-09
NADH regeneration (GO:0006735)	27	11	1.49	7.37	2.27E-02
glucose catabolic process to pyruvate (GO:0061718)	27	11	1.49	7.37	2.27E-02
canonical glycolysis (GO:0061621)	27	11	1.49	7.37	2.27E-02
pyruvate metabolic process (GO:0006090)	69	28	3.81	7.34	5.01E-10
glycolytic process through glucose-6-phosphate (GO:0061620)	28	11	1.55	7.11	3.02E-02
glycolytic process through fructose-6-phosphate (GO:0061615)	28	11	1.55	7.11	3.02E-02
aerobic respiration (GO:0009060)	77	30	4.25	7.05	1.51E-10
mitochondrial electron transport, NADH to ubiquinone (GO:0006120)	49	19	2.71	7.02	1.03E-05
gluconeogenesis (GO:0006094)	44	17	2.43	6.99	8.08E-05
cellular protein complex disassembly (GO:0043624)	138	53	7.63	6.95	2.14E-20
hexose biosynthetic process (GO:0019319)	47	18	2.6	6.93	3.31E-05
fatty acid oxidation (GO:0019395)	84	32	4.64	6.89	3.35E-11
tRNA transport (GO:0051031)	37	14	2.04	6.85	2.03E-03
viral gene expression (GO:0019080)	172	65	9.5	6.84	2.56E-25
translational initiation (GO:0006413)	143	54	7.9	6.83	1.50E-20
purine ribonucleoside triphosphate metabolic process (GO:0009205)	61	23	3.37	6.82	2.94E-07
nucleotide transport (GO:0006862)	32	12	1.77	6.79	1.61E-02
nuclear-transcribed mRNA catabolic process, nonsense-mediated decay (GO:0000184)	120	45	6.63	6.79	1.39E-16
interleukin-12-mediated signaling pathway (GO:0035722)	46	17	2.54	6.69	1.38E-04
cellular respiration (GO:0045333)	157	58	8.68	6.69	6.99E-22
ncRNA export from nucleus (GO:0097064)	38	14	2.1	6.67	2.65E-03
translation (GO:0006412)	384	141	21.22	6.65	9.20E-58
lipid oxidation (GO:0034440)	88	32	4.86	6.58	9.64E-11
purine ribonucleoside triphosphate biosynthetic process (GO:0009206)	47	17	2.6	6.55	1.79E-04
ATP biosynthetic process (GO:0006754)	36	13	1.99	6.54	8.45E-03
protein localization to endoplasmic reticulum (GO:0070972)	142	51	7.85	6.5	1.81E-18
monosaccharide biosynthetic process (GO:0046364)	53	19	2.93	6.49	2.98E-05
purine nucleoside triphosphate metabolic process (GO:0009144)	67	24	3.7	6.48	2.63E-07
cellular response to interleukin-12 (GO:0071349)	48	17	2.65	6.41	2.30E-04
purine nucleoside triphosphate biosynthetic process (GO:0009145)	48	17	2.65	6.41	2.30E-04
protein localization to mitochondrion (GO:0070585)	82	29	4.53	6.4	3.02E-09
ribonucleoside triphosphate metabolic process (GO:0009199)	68	24	3.76	6.39	3.39E-07
guanosine-containing compound metabolic process (GO:1901068)	40	14	2.21	6.33	4.40E-03
peptide biosynthetic process (GO:0043043)	409	142	22.6	6.28	1.02E-55
response to interleukin-12 (GO:0070671)	49	17	2.71	6.28	2.95E-04
glycolytic process (GO:0006096)	41	14	2.27	6.18	5.63E-03
ribonucleoside triphosphate biosynthetic process (GO:0009201)	53	18	2.93	6.15	1.53E-04
monocarboxylic acid catabolic process (GO:0072329)	115	39	6.35	6.14	8.12E-13
mitochondrial respiratory chain complex assembly (GO:0033108)	101	34	5.58	6.09	9.12E-11
mitochondrial transport (GO:0006839)	229	77	12.65	6.09	9.42E-28
acyl-CoA biosynthetic process (GO:0071616)	45	15	2.49	6.03	2.90E-03
intracellular transport of virus (GO:0075733)	54	18	2.98	6.03	1.94E-04
thioester biosynthetic process (GO:0035384)	45	15	2.49	6.03	2.90E-03
establishment of protein localization to mitochondrion (GO:0072655)	75	25	4.14	6.03	3.65E-07
ATP generation from ADP (GO:0006757)	42	14	2.32	6.03	7.14E-03
nucleoside diphosphate phosphorylation (GO:0006165)	60	20	3.32	6.03	3.23E-05
ribosome assembly (GO:0042255)	64	21	3.54	5.94	1.66E-05
nucleotide phosphorylation (GO:0046939)	61	20	3.37	5.93	4.08E-05
cellular modified amino acid biosynthetic process (GO:0042398)	43	14	2.38	5.89	9.01E-03
mitochondrial membrane organization (GO:0007006)	140	45	7.74	5.82	1.90E-14
dicarboxylic acid metabolic process (GO:0043648)	94	30	5.19	5.78	1.04E-08
NAD metabolic process (GO:0019674)	47	15	2.6	5.78	4.59E-03
multi-organism localization (GO:1902579)	63	20	3.48	5.75	6.43E-05
multi-organism transport (GO:0044766)	63	20	3.48	5.75	6.43E-05
amide biosynthetic process (GO:0043604)	528	166	29.18	5.69	6.54E-61
transport of virus (GO:0046794)	61	19	3.37	5.64	1.97E-04
cytoplasmic translation (GO:0002181)	75	23	4.14	5.55	8.47E-06
ADP metabolic process (GO:0046031)	49	15	2.71	5.54	7.13E-03
respiratory electron transport chain (GO:0022904)	108	33	5.97	5.53	2.15E-09
protein targeting to membrane (GO:0006612)	183	55	10.11	5.44	4.09E-17
nucleoside triphosphate metabolic process (GO:0009141)	91	27	5.03	5.37	5.58E-07
energy derivation by oxidation of organic compounds (GO:0015980)	227	67	12.54	5.34	4.42E-21
nuclear membrane organization (GO:0071763)	58	17	3.2	5.3	2.23E-03
nucleoside triphosphate biosynthetic process (GO:0009142)	65	19	3.59	5.29	4.59E-04
oxidative phosphorylation (GO:0006119)	120	35	6.63	5.28	1.27E-09
organic acid catabolic process (GO:0016054)	240	69	13.26	5.2	3.05E-21
peptide metabolic process (GO:0006518)	537	154	29.67	5.19	1.07E-51
carboxylic acid catabolic process (GO:0046395)	224	63	12.38	5.09	9.97E-19
mitochondrial ATP synthesis coupled electron transport (GO:0042775)	89	25	4.92	5.08	7.39E-06
regulation of cellular response to heat (GO:1900034)	79	22	4.37	5.04	8.65E-05

acyl-CoA metabolic process (GO:0006637)	97	27	5.36	5.04	1.86E-06
thioester metabolic process (GO:0035383)	97	27	5.36	5.04	1.86E-06
ATP synthesis coupled electron transport (GO:0042773)	90	25	4.97	5.03	8.98E-06
ATP metabolic process (GO:0046034)	206	57	11.38	5.01	2.12E-16

Table 2A-4. List of average L:H ratios for mitochondrial cysteines containing peptides identified in Mito-P lysates treated with 1 mM, 2.5 mM, 5 mM and 10 mM peroxide using isoTOP-ABPP. Cysteines identified from Mito-P lysates treated with peroxide were alkylated by IA-H and control mito-P lysates were alkylated by IA-L. Data was filtered for mitochondrial peptides with ratio values in 2 out of 3 replicates.

UniProt ID	Protein Description	Peptide Sequence	Residue	1mM H2O2	2.5mM H2O2	5 mM H2O2	10mmM H2O2
A3KMH1	VWA8 von Willebrand factor A domain-containing protein	K.LGHILVVDEADKAPTNVTC*ILK.T	858	1.43			
A3KMH1	VWA8 von Willebrand factor A domain-containing protein	R.LLSQPC*ASDR.F	416	1.17	1.66	2.67	5.65
A3KMH1	VWA8 von Willebrand factor A domain-containing protein	R.AGTAFYIDQC*AVR.A	162				5.35
A4D1E9	GTPBP10 GTP-binding protein 10	K.GKDC*EIPVPVGISVTDENGK.I	88	1.105	1.23	1.7	3.615
A6NJ78	METTL15 Probable methyltransferase-like protein 15	K.AGVQPGTFDGVLMDLGC*SSMQLDTPER.G	172	1.11	1.335		
B4DLN1	SLC25A10 cDNA FLJ60124, highly similar to Mitochondrial dic	R.C*EALAGAPLDNAPK.E	45				1.815
B4DLN1	SLC25A10 cDNA FLJ60124, highly similar to Mitochondrial dic	K.GEYQGVFHC*AVETAK.L	395	1.055	1.105	1.285	1.53
B4DLN1	SLC25A10 cDNA FLJ60124, highly similar to Mitochondrial dic	R.GALVTVGQLSC*YDQAK.Q	336	1.02	1.075	1.2	1.44
B4DLN1	SLC25A10 cDNA FLJ60124, highly similar to Mitochondrial dic	R.TDGILALYSGLSASLC*R.Q	224	0.995	1.04	1.21	1.34
E7ERL9	VARS2 Valine--tRNA ligase, mitochondrial	K.GGEIC*EQLR.A	Bad ID	1.465	1.97	3.495	7.42
E7ERL9	VARS2 Valine--tRNA ligase, mitochondrial	R.LALAAQEC*ER.G	Bad ID	3.49	2.03	3.06	4.905
E7EVK2	MTG1 Mitochondrial GTPase 1	K.LVDC*IIEVHDAR.I	51	0.98	0.99	1.61	
E7EVK2	MTG1 Mitochondrial GTPase 1	K.NVIFTNC*VK.D	113	1.195	1.865	2.61	5.1
E7EVK2	MTG1 Mitochondrial GTPase 1	R.FGYVQHYGLGSAC*DNVER.V	211	1.47	1.51	2.55	4.57
G3V325	PTCD1 Pentatricopeptide repeat-containing protein 1	R.NTPYWYFLQC*K.H	192	1.01	1.48	1.77	
G3V325	PTCD1 Pentatricopeptide repeat-containing protein 1	R.TKPQGDQDTGKEADDGC*ALGGR.-	744	1.29	1.69	3.18	9.615
G3V325	PTCD1 Pentatricopeptide repeat-containing protein 1	R.LQPMESNYTVLIGGC*GR.V	232				7.55
G3V325	PTCD1 Pentatricopeptide repeat-containing protein 1	R.DC*GLGDPQVASELLLKPR.E	381	1.23	1.625	2.03	4.855
G3V325	PTCD1 Pentatricopeptide repeat-containing protein 1	R.MC*LDVFK.E	315	1.255	1.67	0.63	3.96
I3L0E3	MRPS17 28S ribosomal protein S17, mitochondrial	K.TYFAHDALQQC*TVGDIVLLR.A	153	1.09	1.34	1.79	3.06
I3L0E3	MRPS17 28S ribosomal protein S17, mitochondrial	K.VIDPVTGKPC*AGTTYLESPLSSETTQLSK.N	195	1.11	1.295	1.725	2.86
O00142	TK2 Thymidine kinase 2, mitochondrial	R.TNPETC*YQR.L	189			0.7	
O00154	ACOT7 Cytosolic acyl coenzyme A thioester hydrolase	R.HC*NSQNGER.C	92	0.695	0.885	1.11	1.245
O00154	ACOT7 Cytosolic acyl coenzyme A thioester hydrolase	R.LC*EFGR.Q	11				0.79
O00217	NDUFS8 NADH dehydrogenase	K.LC*EAIC*PAQAITIEAEPR.A	117	0.795		20	3.45
O00217	NDUFS8 NADH dehydrogenase	K.LC*EAICPAQAITIEAEPR.A	117	1.04	1.195	1.245	1.63
O00330	PDHX Pyruvate dehydrogenase protein X component, mitoch	K.STVPHAYATADC*DLGAVLK.V	307	1.05	1.25	1.415	2.09
O00411	POLRMT DNA-directed RNA polymerase, mitochondrial	R.VC*VVSVEKPTLPSK.E	413	1.11	1.86	2.54	
O00411	POLRMT DNA-directed RNA polymerase, mitochondrial	K.DAGLTPDLLSYAAALQC*MGR.Q	305			4.17	
O00411	POLRMT DNA-directed RNA polymerase, mitochondrial	K.TLQC*LFEK.Q	398	1.24			

O00411	POLRMT DNA-directed RNA polymerase, mitochondrial	R.C*LEQMSQEGLK.L	319	1.48	2.03	3.45	20
O00411	POLRMT DNA-directed RNA polymerase, mitochondrial	R.LPEC*GSGDGSLQPPR.K	94	1.195	1.865	4.03	4.8
O00429	DNM1L Dynamin-1-like protein	R.IIQHC*SNYSTQELLR.F	446				5.05
O00429	DNM1L Dynamin-1-like protein	R.C*VELVHEEMQR.I	431		0.86	2.9	0.48
O00483	NDUFA4 NADH dehydrogenase	R.LALFNPDVC*WDR.N	44	1.13	1.285	1.62	2.45
O00571	DDX3X ATP-dependent RNA helicase DDX3X	R.WC*DKSDEDDWSKPLPPSER.L	128	1.04			
O00571	DDX3X ATP-dependent RNA helicase DDX3X	K.RDLMAC*AQTGSGK.T	223	1.22	2.71	3.16	3.8
O14561	NDUFAB1 Acyl carrier protein, mitochondrial	K.LMC*PQEIVDYIADKK.D	140	0.785	0.715	0.665	0.635
O14874	BCKDK	K.LTDFPPIKDQADEAQYC*QLVR.Q	152	1.095	1.21	1.305	1.715
O14880	MGST3 Microsomal glutathione S-transferase 3	K.SGLGSGPKC*CH.-	150	0.925			
O14880	MGST3 Microsomal glutathione S-transferase 3	K.VEYPIMYSTDPENGHIFNC*IQR.A	56	0.8	0.815	0.875	1.005
O15091	KIAA0391 Mitochondrial ribonuclease P protein 3	K.TIESIQLSPEEYEC*LK.G	367	1.42	2.05	3.46	
O15091	KIAA0391 Mitochondrial ribonuclease P protein 3	R.DHKAC*LPDAK.T	507	1.31	1.6	2.25	6.135
O15091	KIAA0391 Mitochondrial ribonuclease P protein 3	R.C*SCEVPTK.W	568	1.37	1.755	1.865	4.51
O15091	KIAA0391 Mitochondrial ribonuclease P protein 3	K.SGQC*SGCGK.T	348	1.06	1.64	2.15	4.005
O15235	MRPS12 28S ribosomal protein S12, mitochondrial	K.YDC*GHVQK.K	132	1.09	1.245	1.8	3.185
O15235	MRPS12 28S ribosomal protein S12, mitochondrial	K.GVVLC*TFTR.K	64	0.98			1.84
O15270	SPTLC2 Serine palmitoyltransferase 2	R.FC*LSAAHTK.E	511	0.89	1.29	1.62	
O15270	SPTLC2 Serine palmitoyltransferase 2	R.ANGC*VANGEVR.N	19		1.56	2.265	4.4
O15270	SPTLC2 Serine palmitoyltransferase 2	R.NTGSC*QEAAAK.V	188	1.12	1.33	1.62	2.415
O15270	SPTLC2 Serine palmitoyltransferase 2	K.VLEEYGAGVC*STR.Q	204	0.895	2.15	1.995	2.155
O15382	BCAT2 Branched-chain-amino-acid aminotransferase, mitoch	R.EVFGSGTAC*QVCPVHR.I	342	0.94	1.05	1.295	1.315
O43169	CYB5B Cytochrome b5 type B	K.DPSKNDTC*K.S	115	1.345	1.095	1.98	2.635
O43464	HTRA2 Serine protease HTRA2, mitochondrial	R.AC*LTSGTPGPR.A	71	1.48			
O43678	NDUFA2 NADH dehydrogenase	K.ANPDLPILIREC*SDVQPK.L	58	1.08	1.16		
O43772	SLC25A20 Mitochondrial carnitine/acylcarnitine carrier prot	R.AFPANAAC*FLGFEVAMK.F	283	0.99	1.08	1.14	
O43772	SLC25A20 Mitochondrial carnitine/acylcarnitine carrier prot	R.LQTQPPSLPGQPPMYSGTFDC*FR.K	58	1.12	1.15		
O43772	SLC25A20 Mitochondrial carnitine/acylcarnitine carrier prot	K.YTGTLDC*AK.K	155	1.005	1.115	1.3	1.6
O43772	SLC25A20 Mitochondrial carnitine/acylcarnitine carrier prot	K.C*LLQIQASSGESK.Y	136	0.97	1.155	1.205	1.28
O43837	IDH3B Isocitrate dehydrogenase	K.LGDGLFLQC*C*EEVAELYPK.I	232	0.89	0.97	1.205	1.46
O43837	IDH3B Isocitrate dehydrogenase	K.LGDGLFLQC*CEEVAELYPK.I	232	0.875	1.005	1.165	1.355
O43920	NDUFS5 NADH dehydrogenase	K.IEYDDFVEC*LLR.Q	66		1.01	1.2	1.4
O60313	OPA1 Dynamin-like 120 kDa protein, mitochondrial	K.NRTQEQC*VHNETK.N	786	1.155	1.855	2.93	7.17
O60313	OPA1 Dynamin-like 120 kDa protein, mitochondrial	K.C*NEEHPAYLASDEITTVR.K	801	1.235	1.695	2.905	6.035
O60313	OPA1 Dynamin-like 120 kDa protein, mitochondrial	R.NLSLAVSDC*FWK.M	551				3.78
O60313	OPA1 Dynamin-like 120 kDa protein, mitochondrial	K.TALNHC*NLCR.R	853	1.055	1.285	1.79	2.96
O60313	OPA1 Dynamin-like 120 kDa protein, mitochondrial	K.EGC*TVSPETISLNVK.G	375	1.155	1.475	1.85	2.71
O60313	OPA1 Dynamin-like 120 kDa protein, mitochondrial	K.AYMQNPNAIILC*IQDGSVDAER.S	435	1.025	1.18	1.6	2.095
O60488	ACSL4 Long-chain-fatty-acid--CoA ligase 4	K.NC*PLIDNICAFAK.S	595	1.49	2.09		
O60488	ACSL4 Long-chain-fatty-acid--CoA ligase 4	K.GDC*TVLKPTLMAAVPEIMDR.I	363	1.355	2.12	2.32	7.82
O60488	ACSL4 Long-chain-fatty-acid--CoA ligase 4	K.GYDAPLC*NLLLFK.K	420	1.42	1.685	1.51	7.35
O60488	ACSL4 Long-chain-fatty-acid--CoA ligase 4	K.TALLDISC*VK.H	221	1.03	1.45	2.53	4.755
O60488	ACSL4 Long-chain-fatty-acid--CoA ligase 4	K.GVEGTWVDIC*NNPAMEAEILK.E	640	1.04	1.09	0.96	3.595
O60488	ACSL4 Long-chain-fatty-acid--CoA ligase 4	R.VGAPLIC*CEIK.L	494	1.015	1.39	1.88	3.225
O60488	ACSL4 Long-chain-fatty-acid--CoA ligase 4	K.NTIAIFC*ETR.A	157	1.2	1.36	1.54	2.75
O60488	ACSL4 Long-chain-fatty-acid--CoA ligase 4	R.AEWMIAAQTC*FK.Y	170				2.1
O60830	TIMM17B Mitochondrial import inner membrane translocase su	R.IVDDC*GGAFTMGVIGGGVFQAIK.G	17	1.03	1.055	1.16	1.25
O75027	ABCB7 ATP-binding cassette sub-family B member 7, mitoch	K.GCGNC*SC.-	750	0.96	1.16	1.305	1.975
O75208	COQ9 Ubiquinone biosynthesis protein COQ9, mitochondria	K.DGSELILHFVTQC*NTR.L	153	0.905	1.05	0.87	1.08
O75306	NDUFS2 NADH dehydrogenase	K.TQPYDVYDQVEFDVPVGSRGDC*YDR.Y	326	0.92	0.94	1.045	1.205
O75306	NDUFS2 NADH dehydrogenase	R.IIAQC*LNK.M	347	0.9	0.96	0.9	0.945
O75306	NDUFS2 NADH dehydrogenase	K.TYLQALPYFDRLDYVSMMC*NEQAYSLAVEK.L	146	0.97	1.24	0.41	0.7
O75323	GBAS Protein NipSnap homolog 2	K.IC*QEVLPK.I	93	0.99	1.045	1.275	1.735
O75380	NDUFS6 NADH dehydrogenase	R.VIAC*DGGGGALGHPK.V	87	0.645	0.575	0.43	0.39
O75380	NDUFS6 NADH dehydrogenase	K.TGTC*GYCGLQFR.Q	112	0.51	0.38	0.29	0.25
O75390	CS Citrate synthase, mitochondrial	R.FRGFSIPEC*QK.L	101	1.145	1.305	1.615	2.19
O75390	CS Citrate synthase, mitochondrial	R.YTC*QREFALK.H	359	1.15	1.28	1.95	2.12
O75390	CS Citrate synthase, mitochondrial	K.LPC*VAAK.I	211	1.115	1.26	1.485	1.86
O75394	MRPL33 39S ribosomal protein L33, mitochondrial	R.MVSEAGTGFC*FNTK.R	29	1.205	1.445	1.325	1.73
O75431	MTX2 Metaxin-2	K.KTLDQVLEDVDQC*C*QALSQR.L	189	1.25	1.215	1.365	1.505
O75431	MTX2 Metaxin-2	K.GEQILLSDNAASLAVQAFLQMC*NLPIK.V	51	0.87	1.015	0.96	1.205
O75431	MTX2 Metaxin-2	K.KTLDQVLEDVDQC*CQALSQR.L	189	0.875	0.83	0.96	1.155
O75431	MTX2 Metaxin-2	K.NYSNLLAFC*R.R	246	0.83	0.83	0.86	0.91

O75439	PMPCB Mitochondrial-processing peptidase subunit beta	R.SNMC*WLRD.-	485		1.76	2.55	4.09
O75439	PMPCB Mitochondrial-processing peptidase subunit beta	K.TNMLLQLDGSTPIC*EDIGR.Q	419	1.21	1.525	2.09	3.34
O75439	PMPCB Mitochondrial-processing peptidase subunit beta	R.IDAVNAETIREVC*TK.Y	454	1.275	1.18	1.885	2.78
O75439	PMPCB Mitochondrial-processing peptidase subunit beta	R.LC*TSVTESEVAR.A	389	0.99	1.275	1.615	2.525
O75439	PMPCB Mitochondrial-processing peptidase subunit beta	R.VTC*LESGLR.V	62	1.2	1.475	1.825	2.515
O75521	ECI2 Enoyl-CoA delta isomerase 2, mitochondrial	K.QATEGPC*NMPKPGVFDLINK.A	77	1.02			
O75521	ECI2 Enoyl-CoA delta isomerase 2, mitochondrial	K.LHAVNAEEC*NVLQGR.W	368	1.265	1.645	2.61	4.59
O75521	ECI2 Enoyl-CoA delta isomerase 2, mitochondrial	K.KLTAGEAC*AQGLVTEVFPDSTFQK.E	312	1.205	1.425	2.04	3.375
O75521	ECI2 Enoyl-CoA delta isomerase 2, mitochondrial	R.WLSDEC*TNAVVNFLSR.K	380	1.27	1.375	2.2	3.065
O75600	GCAT 2-amino-3-ketobutyrate coenzyme A ligase, mitochon	R.LVATDGAFSMDGDIAPLQEIC*CLASR.Y	218	0.92	1.12	1.44	2.98
O75600	GCAT 2-amino-3-ketobutyrate coenzyme A ligase, mitochon	R.FIC*GTQSIHK.N	106	1.03	1.09	1.25	1.255
O75608	LYPLA1 Acyl-protein thioesterase 1	K.LAGVTALSC*WLPLR.A	144	0.79			
O75608	LYPLA1 Acyl-protein thioesterase 1	K.TYEGMMHSSC*QQEMMDVK.Q	211	0.75		0.915	1.44
O75616	ERAL1 GTPase Era, mitochondrial	K.QYLLTQAQPGPWEYHSAVLTSQTPEEIC*ANIIR.E	348	1.17	1.28	1.93	
O75616	ERAL1 GTPase Era, mitochondrial	R.SNGQGSALDHFLGFSQPDSSVTPC*VPAVSMNR.D	86	1.25	1.57		
O75616	ERAL1 GTPase Era, mitochondrial	K.YSQIPSVLVMNKVDC*LK.Q	240	0.84			
O75616	ERAL1 GTPase Era, mitochondrial	R.C*QALGVITEK.E	150	1.075	1.385	2.19	3.61
O75648	TRMU Mitochondrial tRNA-specific 2-thiouridylase 1	K.GRTPNPDIVC*NK.H	101	1.145	1.7	1.965	3.23
O75746	SLC25A12 Calcium-binding mitochondrial carrier protein Aral	K.NSFDC*FK.K	375	1.025	1.07	1.28	1.595
O75746	SLC25A12 Calcium-binding mitochondrial carrier protein Aral	R.AGQTTYSGVIDC*FR.K	563	1.005	1.1	1.305	1.51
O75879	PET112 Glutamyl-tRNA(Gln) amidotransferase subunit B, mit	R.LPIAVNGSLIYGVC*AGK.K	170	1.06			
O75879	PET112 Glutamyl-tRNA(Gln) amidotransferase subunit B, mit	K.LGC*TMSMR.D	322	1.115	1.71	2.08	4.255
O75879	PET112 Glutamyl-tRNA(Gln) amidotransferase subunit B, mit	R.AGVGLLEVVLEPDMSC*GEEAATAVR.E	228	1.23	1.245	2.115	4.185
O75947	ATP5H ATP synthase subunit d, mitochondrial	K.FNALKVPVPEDKYTAQVDAEEKEDVKSC*AEWVSLSK.A	101	0.985	1.015	1.08	1.335
O76031	CLPX ATP-dependent Clp protease ATP-binding subunit clp	K.LLLEPMFEVPNSDIVC*VEVDKEVVEGK.K	586	1.09			
O76031	CLPX ATP-dependent Clp protease ATP-binding subunit clp	R.NAVIPQYQALFSMDKC*ELNVTEDALK.A	538	1.11	1.5	1.89	2.87
O94763	URI1 Unconventional prefoldin RPB5 interactor 1	K.VVTNC*QER.I	44				0.41
O94826	TOMM70A Mitochondrial import receptor subunit TOM70	K.ECLEDVTAVC*ILEGFQNQQSMLLADK.V	214	1.36	1.13	2.53	
O94826	TOMM70A Mitochondrial import receptor subunit TOM70	K.ADEMYDKC*IDLEPDNATTYVHK.G	502	1.225	1.69	3.08	7.28
O94826	TOMM70A Mitochondrial import receptor subunit TOM70	K.AKQYMEEENYDKIISEC*SK.E	317	1.235	1.865	2.98	6.55
O94826	TOMM70A Mitochondrial import receptor subunit TOM70	K.ILLDQVEEAVADFDEC*IR.L	427	1.255	1.71	2.76	6.155
O94826	TOMM70A Mitochondrial import receptor subunit TOM70	K.SEMEMAHLYSLC*DAAHAQTEVAK.K	588	1.25	1.725	2.905	5.785
O94826	TOMM70A Mitochondrial import receptor subunit TOM70	K.EVAQDC*TK.A	176	1.145	1.575	2.585	5.06
O94826	TOMM70A Mitochondrial import receptor subunit TOM70	K.C*FALYR.Q	442	1.24	1.69	2.635	4.97
O94826	TOMM70A Mitochondrial import receptor subunit TOM70	K.AIEIDNKC*DFAYETMGTIEVQR.G	544	1.43	1.6	3	4.15
O94826	TOMM70A Mitochondrial import receptor subunit TOM70	R.C*AEGYALYAQALTDQQQFGK.A	475	0.87	1.595	2.665	4.125
O94826	TOMM70A Mitochondrial import receptor subunit TOM70	K.AGKYEQAIQC*YTEAISLC*PTEK.N	136	0.97	1.405	1.925	4
O94826	TOMM70A Mitochondrial import receptor subunit TOM70	K.AGKYEQAIQC*YTEAISLCPTEK.N	136	1.385	1.55	2.115	3.39
O94903	PROSC Proline synthase co-transcribed bacterial homolog	K.KPTPDKC*AADVK.A	261	0.9	1.19		6.18
O94925	GLS Glutaminase kidney isoform, mitochondrial	K.C*VQSNIVLLTQAFR.R	203	0.965	6.02	2.43	4.23
O94925	GLS Glutaminase kidney isoform, mitochondrial	R.LKEC*MDMLR.L	178	1.085	1.34	1.905	3.365
O95140	MFN2 Mitofusin-2	R.FEEC*ISQSAVK.T	348	1.21	1.705	2.8	10.015
O95182	NDUFA7 NADH dehydrogenase	K.LSNNYYC*TR.D	55	1.185	1.51	2.045	2.95
O95202	LETM1 LETM1 and EF-hand domain-containing protein 1, mit	K.DTAPVLEGLKEEEITKEEIDILSDAC*SK.L	552	0.77	0.85	1.175	2.005
O95202	LETM1 LETM1 and EF-hand domain-containing protein 1, mit	K.ADDKLIAEEGVDSLNVKELQAAC*R.A	379	0.975	1.03	1.11	1.85
O95202	LETM1 LETM1 and EF-hand domain-containing protein 1, mit	K.LFEDELTLDNLTRPQLVALC*K.L	330	0.85	0.875	0.995	1.26
O95299	NDUFA10 NADH dehydrogenase	K.HFPEAGIHYPDSTTGDGKPLATDYNGNC*SLEK.F	112	1.305	1.73	2.72	5.335
O95299	NDUFA10 NADH dehydrogenase	R.SRVITVDGNIC*TGK.G	67	1.25	1.69	2.52	4.495
O95299	NDUFA10 NADH dehydrogenase	K.C*EVLQYSAR.E	253	1.215	1.53	2.105	4.175
O95299	NDUFA10 NADH dehydrogenase	K.QC*VDHYNEVK.S	183	1.145	1.5	2.21	4.06
O95563	MPC2 Mitochondrial pyruvate carrier 2	K.WGLVC*AGLADMAR.P	54	0.885	0.835	0.8	0.85
O95571	ETHE1 Protein ETHE1, mitochondrial	R.TDFQQGC*AK.T	170	0.915	1.045	1.735	3.775
O95571	ETHE1 Protein ETHE1, mitochondrial	R.SLLPGC*QSVISR.L	98	1.61	1.36	1.24	1.59

O95573	ACSL3 Long-chain-fatty-acid--CoA ligase 3	R.VGAPLVC*CEIK.L	503	1.01	1.15		
O95573	ACSL3 Long-chain-fatty-acid--CoA ligase 3	R.SVNSLDGLASVLYPGC*DTLDKVF TYAK.N	85		1.49		
O95573	ACSL3 Long-chain-fatty-acid--CoA ligase 3	R.NTPLC*DSFVFR.K	429	1.24	1.76	2.32	6.58
O95573	ACSL3 Long-chain-fatty-acid--CoA ligase 3	R.LLLC*GGAPLSATTQR.F	450	1.335	1.695	7.31	5.665
O95831	AIFM1 Apoptosis-inducing factor 1, mitochondrial	R.SNIWVAGDAAC*FYDIK.L	441	0.73		0.68	0.525
O95831	AIFM1 Apoptosis-inducing factor 1, mitochondrial	K.C*LIATGGTPR.S	256	0.655	0.585	0.545	0.505
O96000	NDUFB10 NADH dehydrogenase	R.EGQNYQQNC*IK.E	119	1.365	1.59	1.83	
O96000	NDUFB10 NADH dehydrogenase	R.LKAC*QQR.E	107	1.315	2.95		
O96008	TOMM40 Mitochondrial import receptor subunit TOM40 homolo	K.C*KELFPIQMEGVK.L	90	0.88		0.7	
O96008	TOMM40 Mitochondrial import receptor subunit TOM40 homolo	R.TPGAATASASGAAEDGACGC*LP NPGTFEEC*HR.K	76	0.99	2.86		
O96008	TOMM40 Mitochondrial import receptor subunit TOM40 homolo	R.TPGAATASASGAAEDGAC*GCLP NPGTFEEC*HR.K	74	1.01	2.86		
O96008	TOMM40 Mitochondrial import receptor subunit TOM40 homolo	R.TPGAATASASGAAEDGAC*GC*LP NPGTFEECHR.K	74	1.355	2.86		
O96008	TOMM40 Mitochondrial import receptor subunit TOM40 homolo	R.TPGAATASASGAAEDGAC*GCLP NPGTFEECHR.K	74	1.01	0.94	1.09	1.28
O96008	TOMM40 Mitochondrial import receptor subunit TOM40 homolo	K.FQC*GFGLTIG.-	354	0.725	0.675	0.76	0.71
O96011	PEX11B Peroxisomal membrane protein 11B	R.LLMEQESSAC*SR.R	153	0.92		1.34	
P00367	GLUD1 Glutamate dehydrogenase 1, mitochondrial	K.AKPYEGSILEADC*DILIPAASEK.Q	376	1.15	1.45	2.155	3.995
P00367	GLUD1 Glutamate dehydrogenase 1, mitochondrial	K.C*IAVGESDGSIWNPDGIDPK.E	327	1.08	1.35	1.92	3.335
P00367	GLUD1 Glutamate dehydrogenase 1, mitochondrial	K.C*AVVDVPFGGAK.A	172	1.1	1.27	1.78	2.71
P00387	CYB5R3 NADH-cytochrome b5 reductase 3	R.AIMKDPDDHTVC*HLLFANQTEK. D	204	0.94			
P00390	GSR Glutathione reductase, mitochondrial	K.LGGTC*VNVGCVPK.K	102				1.31
P00395	MT-CO1 Cytochrome c oxidase subunit 1	K.VLMVEEPSMNLEWLYGC*PPPYH TFEEPVYMK.S	498	0.6	0.51	0.48	0.465
P00505	GOT2 Aspartate aminotransferase, mitochondrial	K.EYLPIGGLAEFC*K.A	106	0.465	0.335	0.265	0.225
P00505	GOT2 Aspartate aminotransferase, mitochondrial	R.VGAFTMVC*K.D	295	0.425	0.34	0.275	0.2
P00505	GOT2 Aspartate aminotransferase, mitochondrial	K.TC*GFDFTGAVEDISK.I	187				0.2
P03897	MT-ND3 NADH-ubiquinone oxidoreductase chain 3	K.STPYEC*GFDPMSPAR.V	39	1.025	1.255	1.685	2.44
P03928	MT-ATP8 ATP synthase protein 8	K.IC*SLHSLPPQS.-	59	1.005	1.1	1.135	1.415
P04040	CAT Catalase	R.LC*ENIAGHLK.D	460	1.12	1.64	2.825	4.115
P04181	OAT Ornithine aminotransferase, mitochondrial	K.ALSGGLYPVSAVLCDDDIMLTIKP GEHGSTYGGNPLGC*R.V	330	1.12	1.15		
P04181	OAT Ornithine aminotransferase, mitochondrial	K.ALSGGLYPVSAVLC*DDDIMLTIKP GEHGSTYGGNPLGCR.V	306	1.12			
P04181	OAT Ornithine aminotransferase, mitochondrial	K.VLPMNTGVEAGETAC*K.L	150	0.98	1.25	1.815	2.065
P04181	OAT Ornithine aminotransferase, mitochondrial	K.DWDAWKVC*LR.L	394	1.045	1.16	1.535	1.74
P04406	GAPDH Glyceraldehyde-3-phosphate dehydrogenase	K.IISNASC*TTNC*LAPLAK.V	152	1.35			
P04406	GAPDH Glyceraldehyde-3-phosphate dehydrogenase	K.IISNASC*TTNCLAPLAK.V	152	1.565	4.14	3.065	6.7
P04406	GAPDH Glyceraldehyde-3-phosphate dehydrogenase	R.VPTANVSVVDLTC*R.L	247	0.9	0.92	1.015	1.06
P04637	TP53 Cellular tumor antigen p53	K.TC*PVQLWVDSTPPPGTR.V	141	1.17			
P04637	TP53 Cellular tumor antigen p53	R.C*SDSDGLAPPQHLIR.V	182	1.31	1.92	3.2	20
P04637	TP53 Cellular tumor antigen p53	K.SVTC*TYSPALNK.M	124	1.19			3.135
P05091	ALDH2 Aldehyde dehydrogenase, mitochondrial	K.LLC*GGGIAADR.G	386	1.41	1.43	1.845	2.05
P05141	SLC25A5 ADP/ATP translocase 2	K.GTDIMYTGTLDC*WR.K	257	1.07	1.17	1.335	1.67
P05141	SLC25A5 ADP/ATP translocase 2	K.GIIDC*VVR.I	57	0.975	1.02	1.23	1.46
P05141	SLC25A5 ADP/ATP translocase 2	R.EFRGLGDC*LVK.I	160	1.02	1.075	1.195	1.44
P05165	PCCA Propionyl-CoA carboxylase alpha chain, mitochondri	K.MADEAVC*VGPAPTSK.S	111	1.22	1.405	3.025	4.59
P05166	PCCB Propionyl-CoA carboxylase beta chain, mitochondria	K.HLC*GDTNYAWPTAEIAVMGAK. G	448	1.32		1.5	
P05166	PCCB Propionyl-CoA carboxylase beta chain, mitochondria	R.C*ADFGMAADK.N	90	0.95	1.05	1.36	2.655
P05166	PCCB Propionyl-CoA carboxylase beta chain, mitochondria	K.VASGC*LDINSSVK.G	365	1.105	1.305	1.385	1.91
P07203	GPX1 Glutathione peroxidase 1	R.FQTIDIEPDIEALLSQGPSC*A.-	202	1.3	1.66	2.495	5.55
P07237	P4HB Protein disulfide-isomerase	R.ITEFC*HR.F	343	0.58	0.52	0.45	0.435
P07919	UQCRH Cytochrome b-c1 complex subunit 6, mitochondrial	R.DHC*VAHK.L	81	0.57	0.635	0.515	1.365
P07919	UQCRH Cytochrome b-c1 complex subunit 6, mitochondrial	R.ERLELC*DER.V	53	1.475	0.745	0.585	0.815
P07919	UQCRH Cytochrome b-c1 complex subunit 6, mitochondrial	R.SHTEEDC*TEELFDFLHAR.D	67	0.59	0.74	0.705	0.78
P07919	UQCRH Cytochrome b-c1 complex subunit 6, mitochondrial	R.EQCEQLEKC*VK.A	43		0.25	0.42	0.26
P07954	FH Fumarate hydratase, mitochondrial	K.FEALAAHDALVELSGAMNTTAC* SLMK.I	333	1.185	1.35	1.915	
P08559	PDHA1 Pyruvate dehydrogenase E1 component subunit alpha,	R.GFC*HLCDGQEACCVGLEAGINPT DHLITAYR.A	91	1.23	1.465	2.19	
P08559	PDHA1 Pyruvate dehydrogenase E1 component subunit alpha,	K.C*DLHRLEEGPPVTTVLTR.E	41	1.26	1.8		
P08559	PDHA1 Pyruvate dehydrogenase E1 component subunit alpha,	K.NFYGGNGIVGAQVPLGAGIALAC *K.Y	181	1.11	1.59	1.98	4.36

P08559	PDHA1 Pyruvate dehydrogenase E1 component subunit alpha,	K.LPC*IFICENNR.Y	218	1.22	1.33	1.885	3.53
P08559	PDHA1 Pyruvate dehydrogenase E1 component subunit alpha,	R.EATRFAAAYC*R.S	273	1.15	1.435	1.97	3.35
P08559	PDHA1 Pyruvate dehydrogenase E1 component subunit alpha,	R.VDGMDILC*VR.E	261	0.995	1.235	1.73	2.875
P08574	CYC1 Cytochrome c1, heme protein, mitochondrial	R.HGGEDYVFSLLTGYC*EPPTGVSLR.E	219	0.705	0.64	0.57	0.55
P08574	CYC1 Cytochrome c1, heme protein, mitochondrial	K.DVC*TFLR.W	271	0.605	0.525	0.555	0.49
P08574	CYC1 Cytochrome c1, heme protein, mitochondrial	R.HLVGVC*YTEDEAK.E	139	0.755	0.66	0.585	0.415
P09001	MRPL3 39S ribosomal protein L3, mitochondrial	K.YTSKENC*NGK.M	138	1.24	1.575	2.55	5.965
P09110	ACAA1 3-ketoacyl-CoA thiolase, peroxisomal	K.GC*FQAEIVPVTTTVHDDK.G	218	0.94	1.13	0.785	
P09110	ACAA1 3-ketoacyl-CoA thiolase, peroxisomal	K.ARDC*LIPMGITSENVAER.F	177	1.17	1.68		
P09110	ACAA1 3-ketoacyl-CoA thiolase, peroxisomal	R.QC*SSGLQAVASIAGGIR.N	123	1.52			
P09110	ACAA1 3-ketoacyl-CoA thiolase, peroxisomal	K.DVNLRPEQLGDIC*VGNVLQPGAGAIMAR.I	87	1.37	1.375	1.41	2.175
P09417	QDPR Dihydropteridine reductase	K.GAVHQLC*QSLAGK.N	161	0.765			
P09417	QDPR Dihydropteridine reductase	K.NC*DLMWK.Q	104		1.24	1.89	2.12
P09622	DLD Dihydrolipoyl dehydrogenase, mitochondrial	K.NETLGGTC*LNVGCIPSK.A	80	0.925	0.59	0.515	0.5
P09622	DLD Dihydrolipoyl dehydrogenase, mitochondrial	K.TVC*IEKNETLGGTCLNVGCIPSK.A	69				0.295
P0C7P0	CISD3 CDGSH iron-sulfur domain-containing protein 3, mit	K.ATQRPPYC*DGTHR.S	109	1.085	1.31		
P0C7P0	CISD3 CDGSH iron-sulfur domain-containing protein 3, mit	R.MVALC*TCK.A	98	1.26	0.98	1.88	3.29
P10109	FDX1 Adrenodoxin, mitochondrial	R.LGCQIC*LTK.S	155	1.04		0.53	0.405
P10515	DLAT Dihydrolipoyllysine-residue acetyltransferase comp	K.NFSAIINPPQAC*ILAIGASEDK.L	586	1.055	1.165	1.545	2.175
P10515	DLAT Dihydrolipoyllysine-residue acetyltransferase comp	K.ASALAC*LK.V	488	0.91	0.935	1.355	1.925
P10515	DLAT Dihydrolipoyllysine-residue acetyltransferase comp	R.DVPLGTPLC*IIVEK.E	291	0.72	0.675	0.69	0.78
P10620	MGST1 Microsomal glutathione S-transferase 1	K.VFANPEDC*VAFGK.G	50	0.92	0.945	1.02	1.28
P10809	HSPD1 60 kDa heat shock protein, mitochondrial	K.C*EFQDAYVLLSEK.K	237	1.025	1.15	1.38	1.84
P10809	HSPD1 60 kDa heat shock protein, mitochondrial	R.C*IPALDSLTPANEDQK.I	447	1	1.1	1.25	1.545
P10809	HSPD1 60 kDa heat shock protein, mitochondrial	R.AAVEEGIVLGGGC*ALLR.C	442	0.975	1.055	1.19	1.425
P11047	LAMC1 Laminin subunit gamma-1	K.TLPSGC*FNTPSIEKP.-	1600				2.05
P11177	PDHB Pyruvate dehydrogenase E1 component subunit beta,	K.EGVEC*EVINMR.T	263	1.055	1.15	1.46	2.055
P11177	PDHB Pyruvate dehydrogenase E1 component subunit beta,	K.TNHLVTVEGGWPQFGVGAEIC*AR.I	306	1.08	1.16	1.54	1.66
P11177	PDHB Pyruvate dehydrogenase E1 component subunit beta,	R.PVGHC*LEAAAVLSK.E	249	0.71			1.205
P11182	DBT Lipoamide acyltransferase component of branched-ch	K.IPHFGYC*DEIDLTELVK.L	279	1.03	1.03	1.28	1.715
P11182	DBT Lipoamide acyltransferase component of branched-ch	K.AASLGLLQFPILNASVDENC*QNITYK.A	333	0.91	1.01	1.06	1.465
P11310	ACADM Medium-chain specific acyl-CoA dehydrogenase, mito	R.MTEEPLMC*AYC*VTEPGAGSDVAGIK.T	156	1.14		2.04	3.27
P11310	ACADM Medium-chain specific acyl-CoA dehydrogenase, mito	R.MTEEPLMC*AYCVTEPGAGSDVAGIK.T	156	1.07	1.245	1.54	1.96
P11498	PC Pyruvate carboxylase, mitochondrial	R.FLYEC*PWR.R	622		1.22	3.28	
P11498	PC Pyruvate carboxylase, mitochondrial	R.ADFAQAC*QDAGVR.F	131	0.99	1.385	1.76	3.44
P11586	MTHFD1 C-1-tetrahydrofolate synthase, cytoplasmic	K.C*THWAEGGK.G	785	1.475		2.4	10.07
P12235	SLC25A4 ADP/ATP translocase 1	K.GADIMYTGTVDC*WR.K	257	1.115	1.165	1.375	1.75
P12235	SLC25A4 ADP/ATP translocase 1	R.EFHGLGDC*IIK.I	160	1.095	1.095	1.29	1.38
P12235	SLC25A4 ADP/ATP translocase 1	R.YFAGNLASGGAAGATSLC*FVYPLDFAR.T	129	0.99	1.01	1.065	1.23
P12532	CKMT1B Creatine kinase U-type, mitochondrial	R.LGYILTC*PSNLGTGLR.A	316	1.045	1.15	1.3	2.005
P12532	CKMT1B Creatine kinase U-type, mitochondrial	R.GLSLPPAC*TR.A	179	0.71		0.69	0.61
P12532	CKMT1B Creatine kinase U-type, mitochondrial	K.TTPTGWTLDQC*IQTGVDNPGHPFIK.T	89	0.745	0.635	0.58	0.5
P13196	ALAS1 5-aminolevulinate synthase, nonspecific, mitochond	K.NTEVC*DELMSR.H	544	1.59		1.79	
P13804	ETFA Electron transfer flavoprotein subunit alpha, mito	K.QFNYTHIC*AGASAFGK.N	109	1.03	1.12	1.825	
P13804	ETFA Electron transfer flavoprotein subunit alpha, mito	K.C*DKVAQDLC*K.V	68	1.11	1.4	1.41	2.695
P13804	ETFA Electron transfer flavoprotein subunit alpha, mito	R.LGGEVSC*LVAGTK.C	53	1	1.11	1.31	1.54
P13804	ETFA Electron transfer flavoprotein subunit alpha, mito	K.C*DKVAQDLCK.V	60	1.27	1.27	2.71	1.53
P13804	ETFA Electron transfer flavoprotein subunit alpha, mito	R.TIYAGNALC*TVK.C	155	0.885	0.945	1.125	1.35
P13804	ETFA Electron transfer flavoprotein subunit alpha, mito	K.CDKVAQDLC*K.V	68	0.995	0.79	1.44	1.105
P13995	MTHFD2 Bifunctional methylenetetrahydrofolate dehydrogena	R.IC*NAVSPDKDVDGFHVINVGR.M	145	1.155	1.365	1.775	2.795
P14854	COX6B1 Cytochrome c oxidase subunit 6B1	R.NC*WQNYLDFHR.C	30	0.74			
P14854	COX6B1 Cytochrome c oxidase subunit 6B1	R.VYQSLC*PTSWVTDWDEQR.A	65			0.85	0.965
P14854	COX6B1 Cytochrome c oxidase subunit 6B1	K.GGDISVC*EWYQR.V	54	1.13		1.69	0.85
P16219	ACADS Short-chain specific acyl-CoA dehydrogenase, mitoc	K.IGC*FALSEPGNGSDAGAASTTAR.A	151	1.03	1.33	1.21	1.36
P17568	NDUFB7 NADH dehydrogenase	R.HDWDYC*EHR.D	90	1.03			3.83
P17568	NDUFB7 NADH dehydrogenase	R.DSFPNFLAC*K.Q	80	1.61	2.34	2.98	3.69
P19367	HK1 Hexokinase-1	K.LPVGFTFSFPC*QQSK.I	158	1.23	1.86		
P19367	HK1 Hexokinase-1	K.ATDC*VGHDVVTLLR.D	628	1.28	1.83	2.86	5.955

P19367	HK1 Hexokinase-1	R.AILQQLGLNSTC*DDSILVK.T	813	1.21	1.61	2.39	4.675
P19367	HK1 Hexokinase-1	K.C*NVSFLLSEDGSGK.G	886	1.07	1.21	1.35	3.47
P19367	HK1 Hexokinase-1	R.AAQLC*GAGMAAVVDK.I	834	1.34	1.6	2.03	3.18
P19367	HK1 Hexokinase-1	K.TVC*GVVSR.R	823	1.2	1.445	2.135	3.07
P19367	HK1 Hexokinase-1	R.LGVEPSDDDC*VSVQHVCTIVSFR.S	368	1.32			1.295
P19404	NDUFV2 NADH dehydrogenase	K.YHIQVC*TTTPCMLR.N	135		1.15		
P19404	NDUFV2 NADH dehydrogenase	R.FSC*EPAGGLTSLTEPPK.G	225	0.86	0.825	0.86	0.94
P21796	VDAC1 Voltage-dependent anion-selective channel protein	K.YQIDPDAC*FSAK.V	232	0.985	1.06	1.25	1.715
P21796	VDAC1 Voltage-dependent anion-selective channel protein	K.REHINLGC*DMDFDIAGPSIR.G	127	0.875	0.87	0.88	0.835
P21912	SDHB Succinate dehydrogenase	R.EGICGSC*AMNINGGNTLAC*TR.R	101	1.02			1.81
P21912	SDHB Succinate dehydrogenase	R.EGIC*GSCAMNINGGNTLAC*TR.R	98	1.02			1.81
P21912	SDHB Succinate dehydrogenase	R.C*HTIMNCTR.T	243	1.01	1.15	1.32	1.63
P21912	SDHB Succinate dehydrogenase	K.AGDKPHMQTYEVDLNKC*GPMVLDALIK.I	68	0.85	1.025	0.96	1.14
P21912	SDHB Succinate dehydrogenase	R.EGIC*GSCAMNINGGNTLACTR.R	98	1.035	0.95	0.905	1.01
P21953	BCKDHB 2-oxoisovalerate dehydrogenase subunit beta, mitoc	R.SGDLFNC*GSLTIR.S	177	1.145	1.55	2.46	3.435
P21953	BCKDHB 2-oxoisovalerate dehydrogenase subunit beta, mitoc	R.TIIPWDVDTIC*K.S	316	1.37	1.3	2.08	3.36
P21953	BCKDHB 2-oxoisovalerate dehydrogenase subunit beta, mitoc	K.EKLGVSC*EVIDLR.T	299	1.025	1.285	1.81	3.07
P21964	COMT Catechol O-methyltransferase	K.GTVLLADNVIC*PGAPDFLAHVR.G	223	4.99	2.26	2.74	
P21964	COMT Catechol O-methyltransferase	R.YLPDTLLLEEC*GLLR.K	207	1.285	1.395	4.185	9.1
P21964	COMT Catechol O-methyltransferase	R.LITIEINPDC*AAITQR.M	145	1.07	1.28	1.85	3.195
P21964	COMT Catechol O-methyltransferase	K.IVDAVIQEHQPSVLLELGAYC*GYSAVR.M	119	1.055	1.32	2.125	3.03
P22033	MUT Methylmalonyl-CoA mutase, mitochondrial	K.VADPWGGSYMMEC*LTNDVYDAALK.L	433	1.54	1.74	1.965	4.72
P22033	MUT Methylmalonyl-CoA mutase, mitochondrial	K.LRIEEC*AAR.R	471	1.24	1.54	2.385	3.885
P22033	MUT Methylmalonyl-CoA mutase, mitochondrial	R.ARC*TVGEITDALKK.V	560	1.14	1.285	2.3	3.83
P22033	MUT Methylmalonyl-CoA mutase, mitochondrial	R.AHC*QTSGWSLTEQDPYNNIVR.T	351	1.355	1.56	2.905	3.67
P22234	PAICS Multifunctional protein ADE2	R.SNGLGPVMSGNTAYPVISC*PPLTPDWGVQDVWSSLR.L	350		0.75	0.95	
P22234	PAICS Multifunctional protein ADE2	R.VVVLMGSTSDLGHC*EK.I	281		1.13	1.17	1.35
P22307	SCP2 Non-specific lipid-transfer protein	K.ADC*TITMADSDFLALMTGK.M	495			0.9	0.94
P22570	FDXR NADPH:adrenodoxin oxidoreductase, mitochondrial	R.VMDVPGLYC*SGWVK.R	395	1.24	1.93	2.69	
P22570	FDXR NADPH:adrenodoxin oxidoreductase, mitochondrial	R.AVPTGDMEDLPC*GLVLSSIGYK.S	353	0.98	1.625	2.54	8.9
P22570	FDXR NADPH:adrenodoxin oxidoreductase, mitochondrial	R.ALEIPGEELPGVC*SAR.A	152	1.2	1.68		5.395
P22695	UQCRC2 Cytochrome b-c1 complex subunit 2, mitochondrial	R.ENMAYTVEC*LR.G	125	0.74	0.645	0.555	0.49
P22695	UQCRC2 Cytochrome b-c1 complex subunit 2, mitochondrial	R.NALANPLYC*PDYR.I	192	0.86	0.65	0.54	0.45
P22830	FECH Ferrochelatase, mitochondrial	R.AIAFTQYPQYSC*STTGSSLNAIYR.Y	196	0.935	1.045	1.04	1.21
P22830	FECH Ferrochelatase, mitochondrial	R.LEYC*NPYR.L	294	0.895	0.83	0.855	0.83
P23368	ME2 NAD-dependent malic enzyme, mitochondrial	K.YC*TFNDDIQGTAAVALAGLLAAQK.V	274	0.77	0.84	0.74	
P23368	ME2 NAD-dependent malic enzyme, mitochondrial	R.C*LFASGSPFGPVK.L	441	0.975	1.08	1.29	
P23368	ME2 NAD-dependent malic enzyme, mitochondrial	R.AMASINERPVIFALSNPTAQAEC*TAEEAYTLTEGR.C	428	0.84	0.975	0.975	0.98
P23378	GLDC Glycine dehydrogenase	R.IDDIYGDQHLVC*TC*PPMEVYESPFSEQKR.A	1000		1.49	1.56	
P23378	GLDC Glycine dehydrogenase	K.YTGVLTELKLPC*EMDFSGK.D	250			1.72	
P23378	GLDC Glycine dehydrogenase	R.IDDIYGDQHLVCTC*PPMEVYESPFSEQKR.A	1002	0.97	1.39		
P23378	GLDC Glycine dehydrogenase	R.C*HPQTIAVVQTR.A	225		1.49		
P23378	GLDC Glycine dehydrogenase	R.NEDAC*PVGTVSAAPWGSSSILPISWAYIK.M	795	1	1.24	1.62	9.65
P23378	GLDC Glycine dehydrogenase	K.IQCGC*SVK.E	444	0.83	1.26	1.66	2.235
P23378	GLDC Glycine dehydrogenase	K.MEDPVC*ENEILATLHAISSK.N	112	0.98	1.52	1.625	2.045
P23378	GLDC Glycine dehydrogenase	R.SYIGMGYYNC*SVPQTILR.N	141				1.33
P23434	GCSH Glycine cleavage system H protein, mitochondrial	K.HEWVTTENGIGTVGISNFAQEALGDVVYC*SLPEVGTK.L	85			0.29	0.27
P23434	GCSH Glycine cleavage system H protein, mitochondrial	K.SC*YEDGWLIK.M	138	0.445	0.37	0.28	0.255
P23786	CPT2 Carnitine O-palmitoyltransferase 2, mitochondrial	K.RC*SEAFVR.E	512	1.35	1.655	2.345	4.69
P23786	CPT2 Carnitine O-palmitoyltransferase 2, mitochondrial	R.HSAGELQQMMVEC*SK.Y	535	1.295	1.54	2.425	4.515
P23786	CPT2 Carnitine O-palmitoyltransferase 2, mitochondrial	R.QYGQTVATYESC*STAAFK.H	489	1.02	1.495	2.21	4.3
P23786	CPT2 Carnitine O-palmitoyltransferase 2, mitochondrial	K.TLTIDC*VQFQR.G	445	1.14	1.17	1.965	3.36
P23919	DTYMK Thymidylate kinase	K.LVEALC*AAGHR.A	31	1.095	1.24	1.57	2.285
P24752	ACAT1 Acetyl-CoA acetyltransferase, mitochondrial	K.DGLTDVYNKIHMGSC*AENTAK.K	196	1.17	1.425	1.83	2.64
P24752	ACAT1 Acetyl-CoA acetyltransferase, mitochondrial	K.QGEYGLASIC*NGGGGASAMLIQK.L	413	1.14	1.36	1.705	2.425
P24752	ACAT1 Acetyl-CoA acetyltransferase, mitochondrial	R.QAVLGAGLPISTPC*TTINK.V	119	1.11	1.27	1.615	2.225

P24752	ACAT1 Acetyl-CoA acetyltransferase, mitochondrial	K.VC*ASGMK.A	126	1.105	1.335	1.58	2.135
P25325	MPST 3-mercaptopyruvate sulfurtransferase	R.HIPGAAFFDIDQC*SDR.T	65	1.12	1.565	1.825	
P25705	ATP5A1 ATP synthase subunit alpha, mitochondrial	K.YTIVVSATASDAAPLQYLAPYSGC*SMGEYFR.D	294	0.915	0.94	1	1.21
P25705	ATP5A1 ATP synthase subunit alpha, mitochondrial	K.LYC*IYVAIGQK.R	244	0.745	0.65	0.75	0.83
P26440	IVD Isovaleryl-CoA dehydrogenase, mitochondrial	R.ASGAVGLSYGAHSNLC*INQLVR.N	136	1.09			
P26440	IVD Isovaleryl-CoA dehydrogenase, mitochondrial	K.AC*DEGHC*TAK.D	350	1.09	1.86	2.44	5.11
P26440	IVD Isovaleryl-CoA dehydrogenase, mitochondrial	K.AC*DEGHCTAK.D	350	1.06	1.115	1.495	2.26
P26440	IVD Isovaleryl-CoA dehydrogenase, mitochondrial	R.GSNTC*ELIFEDCKIPAANILGHENK.G	254	1.035	0.715	0.985	1.17
P28288	ABCD3 ATP-binding cassette sub-family D member 3	R.SGANVLIC*GPNGCGK.S	472	1.04	1.825	1.62	3.155
P28330	ACADL Long-chain specific acyl-CoA dehydrogenase, mitoch	K.RLDSATAC*MAK.Y	366			0.86	0.7
P28331	NDUFS1 NADH-ubiquinone oxidoreductase 75 kDa subunit, mit	K.DC*FIIYQGHHGDVGAPIADVILPGAAYTEK.S	564	1.02		2.15	
P28331	NDUFS1 NADH-ubiquinone oxidoreductase 75 kDa subunit, mit	R.EGVMEFLLANHPLDCPICDQGGEC*DLQDQSMMFGNDR.S	137			2.4	
P28331	NDUFS1 NADH-ubiquinone oxidoreductase 75 kDa subunit, mit	K.DLLNRVDSDTLC*TEEVFPTAGAGTDLR.S	367	1.27	1.715	2.51	5.39
P28331	NDUFS1 NADH-ubiquinone oxidoreductase 75 kDa subunit, mit	K.VLFLLGADGGC*ITR.Q	554	1.265	1.625	2.625	5.15
P28331	NDUFS1 NADH-ubiquinone oxidoreductase 75 kDa subunit, mit	K.AVTEGAQAVEEPSIC*.-	727	1.14	1.465	2.545	4.12
P28331	NDUFS1 NADH-ubiquinone oxidoreductase 75 kDa subunit, mit	K.VVAAC*AMPVMK.G	92	1.065	1.255	2.145	3.595
P28331	NDUFS1 NADH-ubiquinone oxidoreductase 75 kDa subunit, mit	R.MC*LVEIEK.A	78	0.94	1.35	1.87	3.195
P28331	NDUFS1 NADH-ubiquinone oxidoreductase 75 kDa subunit, mit	R.LSVAGNC*R.M	75	4.72	1.3	1.955	2.93
P28838	LAP3 Cytosol aminopeptidase	K.LNLPINIIGLAPLC*ENMPSGK.A	335	1.24	1.45		
P28838	LAP3 Cytosol aminopeptidase	R.QIQDLELSSVEVDPC*GDAQAAAEGAVLGLYEYDDLKQK.K	145		1.65		
P28838	LAP3 Cytosol aminopeptidase	R.LILADALC*YAHTFNPK.V	376	1.15			
P28838	LAP3 Cytosol aminopeptidase	R.SAGAC*TAAAFLK.E	462	1.215	1.685	2.215	5.03
P28838	LAP3 Cytosol aminopeptidase	R.AAVAAGC*R.Q	129	1.175	1.655	2.42	4.685
P28838	LAP3 Cytosol aminopeptidase	R.QVVDC*QLADVNNIGK.Y	445	1.01	1.555	2.23	4.32
P28838	LAP3 Cytosol aminopeptidase	R.ADMGGAATIC*SAIVSAAK.L	313	1.1	1.45	2.05	3.25
P30038	ALDH4A1 Delta-1-pyrroline-5-carboxylate dehydrogenase, mit	R.LAGEC*GGK.N	315	1.7	2.8	4.64	
P30041	PRDX6 Peroxiredoxin-6	K.DINAYNC*EEPTEK.L	91	1.005	1.38	1.6	3.9
P30041	PRDX6 Peroxiredoxin-6	R.DFTPVC*TTELGR.A	47	1.285	1.605	1.55	3.04
P30044	PRDX5 Peroxiredoxin-5, mitochondrial	K.GVLFGVPGAFTPGC*SK.T	100	1.09	1.345	1.52	
P30044	PRDX5 Peroxiredoxin-5, mitochondrial	K.ALNVEPDGTGLTC*SLAPNIISQL.-	204	1.035	1.165	1.24	1.49
P30048	PRDX3 Thioredoxin-dependent peroxide reductase, mitochon	K.AFQYVETHGEVC*PANWTPDSPTIKPSPAASK.E	229	0.93	1.005	1.09	1.59
P30084	ECHS1 Enoyl-CoA hydratase, mitochondrial	K.AFAAGADIKEMQNLSFQDC*YSSK.F	111	1.26	1.515	2.18	3.97
P30084	ECHS1 Enoyl-CoA hydratase, mitochondrial	K.ALNALC*DGLIDELNQALK.T	62	1.165	1.395	1.84	2.99
P30084	ECHS1 Enoyl-CoA hydratase, mitochondrial	K.IC*PVETLVEEAIQCAEK.I	213	0.965	1.075	1.015	1.275
P30405	PPIF Peptidyl-prolyl cis-trans isomerase F, mitochondri	R.ALC*TGEKGFGYK.G	82	1.12	1.115	2.145	4.64
P30405	PPIF Peptidyl-prolyl cis-trans isomerase F, mitochondri	R.VIPSFMC*QAGDFTNHNGTGGK.S	104	1.285	1.525	2.08	3.025
P30405	PPIF Peptidyl-prolyl cis-trans isomerase F, mitochondri	K.IVITDC*GQLS.-	203	1.19	1.49	1.97	2.93
P30837	ALDH1B1 Aldehyde dehydrogenase X, mitochondrial	K.TIPMDGQHFC*FTR.H	169	1.4	1.46	1.85	2.65
P31040	SDHA Succinate dehydrogenase	R.AGLPC*QDLEFVQFHPTGIYGAGCLITEGCR.G	287	0.7	0.745	0.73	
P31040	SDHA Succinate dehydrogenase	R.AC*ALSIEESCRPGDK.V	467	0.875	0.995	1.38	
P31040	SDHA Succinate dehydrogenase	R.HVNGQDQIVPGLYAC*GEAACASVHGANR.L	438	0.85	0.86		
P31040	SDHA Succinate dehydrogenase	R.AC*ALSIEESC*RPGDK.V	467	1.04			
P31040	SDHA Succinate dehydrogenase	R.VGSVLQEGC*GK.I	536	0.95	0.98	1.09	0.995
P31040	SDHA Succinate dehydrogenase	R.AAFGLSEAGFNTAC*VTK.L	89	1.05	1.075	1.045	0.985
P31040	SDHA Succinate dehydrogenase	K.TLNEADC*ATVPPAIR.S	654		0.9	0.84	0.905
P31040	SDHA Succinate dehydrogenase	R.TYFSC*TSAHTSTGDGTAMITR.A	266	0.83	0.865	0.805	0.72
P31040	SDHA Succinate dehydrogenase	R.C*CCVADR.T	189	0.815	0.76	0.67	0.65
P31040	SDHA Succinate dehydrogenase	R.GVIALC*IEDGSIHR.I	238	0.69		0.72	0.56
P31930	UQCRC1 Cytochrome b-c1 complex subunit 1, mitochondrial	K.HLGGIPWTYAEDAVPTLTPC*R.F	268	0.62			
P31930	UQCRC1 Cytochrome b-c1 complex subunit 1, mitochondrial	K.YIYDQC*PAVAGYGPIEQLPDYNR.I	453	0.715	0.685	0.605	0.59
P31930	UQCRC1 Cytochrome b-c1 complex subunit 1, mitochondrial	K.AVELLGDIVQNC*SLEDSQIEK.E	154	0.715	0.63	0.53	0.445
P31930	UQCRC1 Cytochrome b-c1 complex subunit 1, mitochondrial	R.NALVSHLDGTTPVC*EDIGR.S	410	0.785	0.68	0.54	0.43
P31930	UQCRC1 Cytochrome b-c1 complex subunit 1, mitochondrial	R.LC*TSATESEVAR.G	380	0.745	0.615	0.48	0.375
P31937	HIBADH 3-hydroxyisobutyrate dehydrogenase, mitochondrial	K.HGYPLIIYDVFPDAC*K.E	75				0.29
P31937	HIBADH 3-hydroxyisobutyrate dehydrogenase, mitochondrial	R.C*WSSDTYNPVPGVMDGVPSANNYQGGFGTTLMAK.D	251	0.54		0.27	0.26
P31939	ATIC Bifunctional purine biosynthesis protein PURH	K.YTQSNSVC*YAK.N	434			1.85	2.93

P32119	PRDX2 Peroxiredoxin-2	R.LVQAFQYTDEHGEVC*PAGWKPG SDTIKPNVDDSKEYFSK.H	172	0.91			1.12
P32189	GK Glycerol kinase	R.DC*GIPLSHLQVDGGMTSNK.I	421	0.79		0.73	0.57
P32189	GK Glycerol kinase	K.EVGTSYGC*YFVPAFSGLYAPYWE PSAR.G	364				0.45
P32189	GK Glycerol kinase	K.EILHSVYEC*IEK.T	67			0.55	0.32
P32322	PYCR1 Pyrroline-5-carboxylate reductase 1, mitochondrial	R.C*MTNTPVVVR.E	120	0.87	0.855	1.01	1.025
P33121	ACSL1 Long-chain-fatty-acid--CoA ligase 1	R.NIVSDC*SAFVK.A	297	0.35	1.52	1.33	5.22
P33121	ACSL1 Long-chain-fatty-acid--CoA ligase 1	R.GIQVSNNGPC*LGSR.K	108	1.225	1.915	1.92	3.825
P33121	ACSL1 Long-chain-fatty-acid--CoA ligase 1	K.ATENTVNPC*PDDTLISFLPLAHM FER.V	311			1.55	2.42
P33316	DUT Deoxyuridine 5-triphosphate nucleotidohydrolase,	R.IAQLIC*ER.I	222	0.97	1.07	1.195	1.83
P33316	DUT Deoxyuridine 5-triphosphate nucleotidohydrolase,	K.TDIQIALPSGC*YGR.V	166	0.99	1.195	1.36	1.83
P33897	ABCD1 ATP-binding cassette sub-family D member 1	R.VEEGMHLLITGPNGC*GK.S	511				20
P34897	SHMT2 Serine hydroxymethyltransferase, mitochondrial	K.NTC*PGDR.S	412	0.7	0.64	0.595	0.515
P34897	SHMT2 Serine hydroxymethyltransferase, mitochondrial	K.RYYGGAEVVDEIELLC*QR.R	119	0.62	0.68	0.44	0.435
P34897	SHMT2 Serine hydroxymethyltransferase, mitochondrial	R.GLELIASENFC*SR.A	80	0.67	0.63	0.5	0.39
P34897	SHMT2 Serine hydroxymethyltransferase, mitochondrial	R.AALEALGSC*LNNK.Y	91	0.695	0.595	0.5	0.38
P34897	SHMT2 Serine hydroxymethyltransferase, mitochondrial	R.EVC*DEVK.A	241	0.63	0.505	0.455	0.37
P35232	PHB Prohibitin	K.PIIFDC*R.S	69	1.03	1.245	1.455	1.715
P35270	SPR Sepiapterin reductase	R.AVC*LLTGASR.G	10	1.21			2.94
P35914	HMGCL Hydroxymethylglutaryl-CoA lyase, mitochondrial	K.KNINC*SIEESFQR.F	141	5.58	0.84	1.095	
P35914	HMGCL Hydroxymethylglutaryl-CoA lyase, mitochondrial	K.VAQATC*K.L	323	1.085	1.09	1.385	2.465
P35914	HMGCL Hydroxymethylglutaryl-CoA lyase, mitochondrial	K.LLEAGNFIC*QALNR.K	307	1.3	1.04	1.27	1.445
P36542	ATP5C1 ATP synthase subunit gamma, mitochondrial	R.GLC*GAIHSSIAK.Q	103	0.985	1.035	1.085	1.27
P36551	CPOX Coproporphyrinogen-III oxidase, mitochondrial	K.EGGGGISCVLQDGC*VFEK.A	198	0.655		0.64	0.99
P36551	CPOX Coproporphyrinogen-III oxidase, mitochondrial	K.HC*DDSFTPQEK.L	373	0.72	0.66	0.74	0.7
P36551	CPOX Coproporphyrinogen-III oxidase, mitochondrial	R.C*SSFMAPPVTDLGELR.R	127	0.58	0.58	0.565	0.585
P36551	CPOX Coproporphyrinogen-III oxidase, mitochondrial	K.EAC*DQHGPDLYPK.F	304	0.67	0.82	0.62	0.46
P36776	LONP1 Lon protease homolog, mitochondrial	K.ILC*FYGPPGVGK.T	520	1.02	1.25		
P36776	LONP1 Lon protease homolog, mitochondrial	R.ALC*GLDESK.A	682	1.175	1.35	2.115	3.265
P36776	LONP1 Lon protease homolog, mitochondrial	K.VLFIC*TANVTDTIPEPLR.D	637	1.06	1.245	1.7	2.795
P36776	LONP1 Lon protease homolog, mitochondrial	R.AGVTC*IVLPAENK.K	909	0.97	1.105	1.4	1.895
P36957	DLST Dihydrolipoyllysine-residue succinyltransferase co	K.EAQNTC*AMLTTFNEIDMSNIQE MR.A	245	0.975	0.95	1.395	1.79
P36969	GPX4 Phospholipid hydroperoxide glutathione peroxidase,	R.ILAFPC*NQFGK.Q	102	1.025	1.095		
P36969	GPX4 Phospholipid hydroperoxide glutathione peroxidase,	K.IC*VNGDDAHPLWK.W	134	1.265			
P36969	GPX4 Phospholipid hydroperoxide glutathione peroxidase,	R.YAEC*GLR.I	93	1.635	1.625	1.935	3.055
P36969	GPX4 Phospholipid hydroperoxide glutathione peroxidase,	K.FLIDKNGC*VVK.R	175	1.08	1.09	1.54	1.805
P38117	ETFB Electron transfer flavoprotein subunit beta	K.EVIAVSC*GPAQC*QETIR.T	66	0.91	1.115	1.78	2.08
P38117	ETFB Electron transfer flavoprotein subunit beta	K.EVIAVSC*GPAQCQETIR.T	66	0.93	1.035	1.015	1.955
P38117	ETFB Electron transfer flavoprotein subunit beta	K.HSMNPFC*EIAVEEAVR.L	42	0.985	1.115	1.26	1.65
P38646	HSPA9 Stress-70 protein, mitochondrial	R.RTIAPC*QK.A	366	1.19	1.54	2.35	4.47
P38646	HSPA9 Stress-70 protein, mitochondrial	K.AKC*ELSSSVQTDINLPYLTMDSSG PK.H	317	1.135	1.385	1.98	4.19
P38646	HSPA9 Stress-70 protein, mitochondrial	K.GAVVGIDLGTTNSC*VAVMEGK.Q	66	1.13	1.415	2.17	3.805
P38646	HSPA9 Stress-70 protein, mitochondrial	K.KSQVFSTAADGQTQVEIKVC*QGE R.E	487	0.935	1.31	1.975	3.265
P38646	HSPA9 Stress-70 protein, mitochondrial	K.MEEFKDQLPADEC*NK.L	608	0.56	0.565	0.61	0.72
P40925	MDH1 Malate dehydrogenase, cytoplasmic	K.VIVVGNPANTNC*LTASK.S	137	0.64			0.445
P40925	MDH1 Malate dehydrogenase, cytoplasmic	K.AIC*DHVR.D	251	0.815	1.13	0.83	0.35
P40926	MDH2 Malate dehydrogenase, mitochondrial	K.GYLGPEQLPDC*LK.G	89	0.745	0.72	0.535	0.48
P40926	MDH2 Malate dehydrogenase, mitochondrial	K.GC*DVVVIPAGVPR.K	93	0.77	0.79	0.56	0.47
P40926	MDH2 Malate dehydrogenase, mitochondrial	K.TIIPLISQC*TPK.V	212	0.71	0.555	0.4	0.335
P40926	MDH2 Malate dehydrogenase, mitochondrial	K.SQETEC*TYFSTPLLLGK.K	285	0.515	0.44	0.37	0.31
P40926	MDH2 Malate dehydrogenase, mitochondrial	K.EGVVEC*SFVK.S	275	0.46	0.38	0.32	0.26
P40939	HADHA Trifunctional enzyme subunit alpha, mitochondrial	R.SAVLISSKPGC*FIAGADINMLAAC K.T	97	1.215	1.52	1.92	
P40939	HADHA Trifunctional enzyme subunit alpha, mitochondrial	K.STKPIVAAINGSC*LGGGLEVAISC QYR.I	145	1.47	1.52		
P40939	HADHA Trifunctional enzyme subunit alpha, mitochondrial	K.QFTPC*QLLADHANSPNK.K	747	1.45			
P40939	HADHA Trifunctional enzyme subunit alpha, mitochondrial	K.EVEAVIPDHC*IFASNTSALPISEIA AVSK.R	470	1.335	1.775	3.055	5.89
P40939	HADHA Trifunctional enzyme subunit alpha, mitochondrial	K.TGIEQGSDAGYLC*ESQK.F	322	1.18	1.695	2.625	5.425
P40939	HADHA Trifunctional enzyme subunit alpha, mitochondrial	R.C*LAPMMSEVIR.I	550	1.33	1.65	2.57	5.005
P41250	GARS Glycine--tRNA ligase	K.NGEC*FR.A	211	1.015	1.01	1.09	1.175
P41250	GARS Glycine--tRNA ligase	R.SCYDLSC*HAR.A	471	0.885	0.905	0.84	0.995

P41250	GARS Glycine--tRNA ligase	K.C*SVLPLSQNQEFMPFVK.E	616				0.73
P42126	ECI1 Enoyl-CoA delta isomerase 1, mitochondrial	R.GVILTSDRPGVFSAGLDLTEMC*GR.S	114				0.28
P42704	LRPPRC Leucine-rich PPR motif-containing protein, mitocho	R.AILQENGC*LSDSDMFSQAGLR.S	500	11.195	20	12.305	20
P42704	LRPPRC Leucine-rich PPR motif-containing protein, mitocho	K.AGYPQYVSEILEKVTC*ER.R	330				17.74
P42704	LRPPRC Leucine-rich PPR motif-containing protein, mitocho	K.GDLSTALEVAIDC*YEK.Y	848	1.12	1.27	1.93	9.35
P42704	LRPPRC Leucine-rich PPR motif-containing protein, mitocho	K.DGRYC*QEPR.G	571	1.265	1.785	2.935	6.58
P42704	LRPPRC Leucine-rich PPR motif-containing protein, mitocho	K.LTDYC*KK.L	394	1.51	2.145	2.5	5.19
P42704	LRPPRC Leucine-rich PPR motif-containing protein, mitocho	K.GMQELGVHPDQETYTDYVIPC*FDSVNSAR.A	484	1.155	1.665	2.835	4.78
P42704	LRPPRC Leucine-rich PPR motif-containing protein, mitocho	R.SC*GSLLPELK.L	130	1.195	1.48	2.205	4.64
P42704	LRPPRC Leucine-rich PPR motif-containing protein, mitocho	K.LEDVALQILLAC*PVSK.E	361	1.23	1.46		4.32
P42704	LRPPRC Leucine-rich PPR motif-containing protein, mitocho	R.C*VANNQVETLEK.L	930	1.185	1.45	2.205	4.105
P42704	LRPPRC Leucine-rich PPR motif-containing protein, mitocho	R.LQWFC*DR.C	927	1.17	1.34	1.98	3.595
P42704	LRPPRC Leucine-rich PPR motif-containing protein, mitocho	R.LIASYC*NVGDIEGASK.I	208	1.145	1.375	1.88	3.465
P42704	LRPPRC Leucine-rich PPR motif-containing protein, mitocho	R.IHDVLC*K.L	863	1.045	1.325	1.835	3.37
P42704	LRPPRC Leucine-rich PPR motif-containing protein, mitocho	K.HSLNSSSASTTEPDFQKDILIAC*R.L	1043	1.31	1.325	1.915	2.87
P42704	LRPPRC Leucine-rich PPR motif-containing protein, mitocho	K.EDGPSVFGSFFLQHC*VTMNTPVEK.L	380		0.88	1.88	2.8
P42704	LRPPRC Leucine-rich PPR motif-containing protein, mitocho	K.LFEC*DRDQMYYNLLK.L	952	1.125	1.365	2.025	2.75
P42704	LRPPRC Leucine-rich PPR motif-containing protein, mitocho	K.VFNDTC*R.S	113	1.23	1.485	2.27	2.515
P42704	LRPPRC Leucine-rich PPR motif-containing protein, mitocho	K.QLILVLC*SEENMQK.A	690	1.78	1.265	1.51	2.47
P42765	ACAA2 3-ketoacyl-CoA thiolase, mitochondrial	K.ETPALTINRLC*GSGFQSIVNGCQEICVK.E	92	0.74	0.7	0.61	
P42765	ACAA2 3-ketoacyl-CoA thiolase, mitochondrial	R.IVGYFVSGC*DPSIMGIGPVPAISGALK.K	287	0.605	0.665	0.62	
P42765	ACAA2 3-ketoacyl-CoA thiolase, mitochondrial	K.ISREEC*DKYALQSQQR.W	179	0.595	0.53	0.48	0.455
P43155	CRAT Carnitine O-acetyltransferase	R.IYGQAC*ATYESASLR.M	449	0.92			1.84
P43304	GPD2 Glycerol-3-phosphate dehydrogenase, mitochondrial	R.C*KDVLTGQEFDVR.A	270	0.845	1.61	1.04	
P43304	GPD2 Glycerol-3-phosphate dehydrogenase, mitochondrial	R.NYLSC*DVEVR.R	385	1.07		1.86	2.405
P43304	GPD2 Glycerol-3-phosphate dehydrogenase, mitochondrial	K.AADC*ISEPVNR.E	45	0.925	1.145	1.32	2.225
P43304	GPD2 Glycerol-3-phosphate dehydrogenase, mitochondrial	K.LYDLVAGSNC*LK.S	188	0.71	0.775	0.87	0.94
P43897	TSFM Elongation factor Ts, mitochondrial	R.FEC*GEGEEAAETE.-	315	1.06	1.54	2.01	3.44
P43897	TSFM Elongation factor Ts, mitochondrial	K.YGALVIC*ETSEQK.T	240	1	1.165	1.475	2.615
P43897	TSFM Elongation factor Ts, mitochondrial	K.ALETC*GGDLK.Q	71	0.9	1.155	1.405	2.23
P43897	TSFM Elongation factor Ts, mitochondrial	K.TGYSFVNC*K.K	64	0.795	0.93	1.205	1.85
P45880	VDAC2 Voltage-dependent anion-selective channel protein	R.PMC*IPPSYADLGK.A	13	1.24	1.755	2.345	4.29
P45880	VDAC2 Voltage-dependent anion-selective channel protein	K.WC*EYGLTFTEK.W	76	0.995	1.14	1.5	2.61
P45880	VDAC2 Voltage-dependent anion-selective channel protein	K.VC*EDLDTSVNLAWTSGTNC*TR.F	210	0.95	1.115	1.45	2.415
P45880	VDAC2 Voltage-dependent anion-selective channel protein	K.LDVKTKSC*SGVEFSTSGSSNTDTGK.V	47	1	1.15	1.41	2.045
P45880	VDAC2 Voltage-dependent anion-selective channel protein	K.VC*EDLDTSVNLAWTSGTNCTR.F	210	1.085	1.1	1.23	1.535
P45880	VDAC2 Voltage-dependent anion-selective channel protein	K.WNTDNTLGTEIAIEDQIC*QGLK.L	103	0.84	0.905	0.99	1.185
P45954	ACADSB Short/branched chain specific acyl-CoA dehydrogena	R.ASSTC*PLTFENVK.V	261	1.205	1.49	2.14	3.325
P45954	ACADSB Short/branched chain specific acyl-CoA dehydrogena	K.C*IEWMGGVGYTK.D	385	0.88	1.08	1.54	2.46
P45954	ACADSB Short/branched chain specific acyl-CoA dehydrogena	K.VGSFC*LSEAGAGSDSFALK.T	175	1.155	1.18	1.825	2.455
P48047	ATP5O ATP synthase subunit O, mitochondrial	R.GEVPC*TVTSASPLEEATLSELK.T	141	0.94	0.97	1.095	1.265
P48735	IDH2 Isocitrate dehydrogenase	R.NILGGTVFREPIIC*K.N	154	1.22	1.58		
P48735	IDH2 Isocitrate dehydrogenase	K.DLAGC*IHGLSNVK.L	418	1.145	1.42	2.185	3.97
P48735	IDH2 Isocitrate dehydrogenase	K.SSGGFVWAC*K.N	308	1.055	1.235	1.895	3.495
P48735	IDH2 Isocitrate dehydrogenase	K.NYDGDVQSDILAQGFGSLGLMTSVLVC*PDGK.T	336	1.31	1.325	2.215	3.44
P48735	IDH2 Isocitrate dehydrogenase	K.C*ATITPDEAR.V	113	1.05	1.15	1.51	2.655
P48735	IDH2 Isocitrate dehydrogenase	K.VC*VETVESGAMTK.D	402	0.975	1.17	1.53	2.4
P49189	ALDH9A1 4-trimethylaminobutyraldehyde dehydrogenase	R.VVAELQAGTC*FINNYNVSPVELPFGGYKK.S	443	0.785			
P49189	ALDH9A1 4-trimethylaminobutyraldehyde dehydrogenase	K.GALMANFLTQGQVC*CNGTR.V	288	1.435	1.52	1.84	2.25
P49189	ALDH9A1 4-trimethylaminobutyraldehyde dehydrogenase	K.VLC*GGDIYVPEDPK.L	355	1.24		1.16	1.77
P49189	ALDH9A1 4-trimethylaminobutyraldehyde dehydrogenase	K.SPLIIFSDC*DMNNAVK.G	267	1.165	1.44	1.3	1.28
P49189	ALDH9A1 4-trimethylaminobutyraldehyde dehydrogenase	R.VIATFTC*SGEK.E	45	0.87	1.09	0.98	0.94

P49189	ALDH9A1 4-trimethylaminobutyraldehyde dehydrogenase	K.TVC*VEMGDVESAF.-	484	0.825	0.825	0.84	0.87
P49189	ALDH9A1 4-trimethylaminobutyraldehyde dehydrogenase	R.EDEIATMEC*INNGK.S	96	0.825	0.855	0.74	0.78
P49207	RPL34 60S ribosomal protein L34	K.SAC*GVC*PGR.L	49	0.82	1.02		
P49207	RPL34 60S ribosomal protein L34	R.AYGGSMC*AK.C	83	0.835	0.93	1.185	1.52
P49207	RPL34 60S ribosomal protein L34	K.SACGVC*PGR.L	49	0.86	0.88	0.795	1.095
P49327	FASN Fatty acid synthase	R.LGMLSPEGTC*K.A	212	1.08	1.48	1.665	2.37
P49406	MRPL19 39S ribosomal protein L19, mitochondrial	K.GIRFDLC*LTEQQMK.E	248	0.905	1.015	1.16	1.415
P49406	MRPL19 39S ribosomal protein L19, mitochondrial	K.ISQFLGIC*IQR.S	137	0.83	0.89	0.95	1.285
P49411	TUFM Elongation factor Tu, mitochondrial	R.HYAHTDC*PGHADYVK.N	127	1.045	1.56		
P49411	TUFM Elongation factor Tu, mitochondrial	K.GDEC*ELLGHSK.N	290	1.145	1.455	2.125	4.305
P49411	TUFM Elongation factor Tu, mitochondrial	K.GEETPVIVGSALC*ALEGR.D	222	1.145	1.44	2.145	3.92
P49411	TUFM Elongation factor Tu, mitochondrial	K.NMITGTAPLDGC*ILVVAANDGPMPQTR.E	147	0.97	1.215	1.67	2.69
P49419	ALDH7A1 Alpha-aminoadipic semialdehyde dehydrogenase	K.VLEDNKLPGAIC*SLTCGGADIGTAMAK.D	248	0.9		1.68	
P49419	ALDH7A1 Alpha-aminoadipic semialdehyde dehydrogenase	K.VLEDNKLPGAIC*SLTC*GGADIGTAMAK.D	248	1.23			
P49419	ALDH7A1 Alpha-aminoadipic semialdehyde dehydrogenase	R.RSTC*TINYSK.D	522	1.25	1.935	2.16	4.59
P49419	ALDH7A1 Alpha-aminoadipic semialdehyde dehydrogenase	K.GSDC*GIVNVNIPTSGAEIGGAFGGEK.H	478	1.135	1.22	2.435	3.085
P49419	ALDH7A1 Alpha-aminoadipic semialdehyde dehydrogenase	R.GEVITTYC*PANNEPIAR.V	70	1.16	1.49	1.905	2.795
P49590	HARS2 Probable histidine--tRNA ligase, mitochondrial	R.IGDYVQC*HGGVSLVEQMFQDPR.L	274	0.91		1.895	2.595
P49590	HARS2 Probable histidine--tRNA ligase, mitochondrial	R.AIC*SSIDKLDK.M	236	1.015	1.325	1.73	2.36
P49590	HARS2 Probable histidine--tRNA ligase, mitochondrial	R.IVDGMFAVC*GVPESK.F	225		1.27	3.55	0.2
P49748	ACADVL Very long-chain specific acyl-CoA dehydrogenase, m	K.ELGAFGLQVPSELGGVGLC*NTQYAR.L	156	0.61	0.665	0.4	0.425
P49753	ACOT2 Acyl-coenzyme A thioesterase 2, mitochondrial	R.C*C*WDEPVR.I	75	1.18			
P49753	ACOT2 Acyl-coenzyme A thioesterase 2, mitochondrial	K.SEFYANEAC*KR.L	401	1.195	1.705	2.27	4.41
P49821	NDUFV1 NADH dehydrogenase	K.HESCGQC*TPC*R.E	382	1.05			
P49821	NDUFV1 NADH dehydrogenase	K.HESC*GQCTPC*R.E	379	1.05			
P49821	NDUFV1 NADH dehydrogenase	K.HESC*GQCTPCR.E	379	1.165	1.28	2.53	4.255
P49821	NDUFV1 NADH dehydrogenase	K.YLVVNADEGEPGTC*K.D	125	1.265	1.535	2.03	2.61
P49821	NDUFV1 NADH dehydrogenase	R.GAGAYIC*GEETALIESIEGK.Q	206	1.13	1.265	1.63	2.045
P49821	NDUFV1 NADH dehydrogenase	K.QIEGHTIC*ALGDGAAWPVQGLIR.H	425	1.135	1.375	1.82	2.02
P49821	NDUFV1 NADH dehydrogenase	K.NAC*GSGYDFDVFVVR.G	187	1.135	1.34	1.5	1.79
P49821	NDUFV1 NADH dehydrogenase	K.LLEGC*LVGGR.A	142	1.09	1.305	1.6	1.775
P49916	LIG3 DNA ligase 3	K.AADETLC*QTK.V	929	0.935	1.405	1.56	
P49916	LIG3 DNA ligase 3	R.IFNC*NPDDMAR.D	336			2.91	
P49916	LIG3 DNA ligase 3	K.C*AGGHDDATLAR.L	729		1.93	0.87	1.28
P50213	IDH3A Isocitrate dehydrogenase	K.CREVAESC*K.D	222			1.43	
P50213	IDH3A Isocitrate dehydrogenase	K.C*SDFTEEIC*R.R	351	1.45	2.33	4.06	5.175
P50213	IDH3A Isocitrate dehydrogenase	K.TFDLYANVRPC*VSIEGYK.T	127	1.045	1.165	1.47	1.825
P50213	IDH3A Isocitrate dehydrogenase	K.C*SDFTEEICR.R	351	0.895	0.955	1.11	1.775
P50213	IDH3A Isocitrate dehydrogenase	R.IEAAC*FATIK.D	331	0.875	1.005	1.14	1.395
P50336	PPOX Protoporphyrinogen oxidase	R.SC*FPSLFQAEQTHR.S	183	1.225	1.51		
P50336	PPOX Protoporphyrinogen oxidase	R.LPLTLAGASYEGVAVNDC*IESGR.Q	459	1.115	1.285	1.435	2.505
P50336	PPOX Protoporphyrinogen oxidase	R.GQPVC*GLSLQAEGR.W	258	0.67	1.2		2.27
P50336	PPOX Protoporphyrinogen oxidase	R.LGPEVASLAMDSLC*R.G	167	1.08	1.28	1.445	2
P50416	CPT1A Carnitine O-palmitoyltransferase 1, liver isoform	R.SC*TTESC*DFVR.A	608	1.545	2.13		
P50416	CPT1A Carnitine O-palmitoyltransferase 1, liver isoform	R.TLETANC*MSSQTK.N	96	1.34	1.93	6.67	4.89
P50416	CPT1A Carnitine O-palmitoyltransferase 1, liver isoform	K.FSC*PETDSHR.F	742	1.195	1.485	2.22	3.465
P50416	CPT1A Carnitine O-palmitoyltransferase 1, liver isoform	R.SC*TTESCDFVR.A	608	0.99	1.05	0.68	1.62
P51398	DAP3 28S ribosomal protein S29, mitochondrial	K.NC*RDLLQSSYNK.Q	165	0.96			2.3
P51398	DAP3 28S ribosomal protein S29, mitochondrial	K.TFSEAC*LMVR.K	98	1.01	1.21	1.415	1.99
P51553	IDH3G Isocitrate dehydrogenase	K.LGDGLFLQC*C*R.E	235	0.85	1.33		
P51553	IDH3G Isocitrate dehydrogenase	K.NIANPTATLLASC*MMLDHLK.L	333	0.95			
P51553	IDH3G Isocitrate dehydrogenase	K.LGDGLFLQC*CR.E	235	0.99	1.055	1.28	1.62
P51553	IDH3G Isocitrate dehydrogenase	R.TSLDLYANVIHC*K.S	148	0.97	1.07	1.37	1.55
P51553	IDH3G Isocitrate dehydrogenase	R.HAC*VPVDFEEVHVSSNADEEDIR.N	81	0.875	0.945	1.1	1.31
P51648	ALDH3A2 Fatty aldehyde dehydrogenase	R.EKDILTAIAADLC*K.S	50			1.18	1.6
P51649	ALDH5A1 Succinate-semialdehyde dehydrogenase, mitochondria	R.VAEQLEVGMVGVNEGLISSVEC*PFGGVK.Q	502	1.21	1.33	1.64	
P51649	ALDH5A1 Succinate-semialdehyde dehydrogenase, mitochondria	R.NTGQTC*VC*SNQFLVQR.G	340	1.85	2.035	2.24	
P51649	ALDH5A1 Succinate-semialdehyde dehydrogenase, mitochondria	R.WLPAAATFPVQDPASGAALGMVADC*GVR.E	93	1.03	1.13	4.88	2.66
P51649	ALDH5A1 Succinate-semialdehyde dehydrogenase, mitochondria	K.EVGEAIC*TDPLVSK.I	272	1.2	1.55	1.725	2.29
P51649	ALDH5A1 Succinate-semialdehyde dehydrogenase, mitochondria	R.NTGQTC*VCSNQFLVQR.G	340	0.975	1.04	1.06	1.74
P51649	ALDH5A1 Succinate-semialdehyde dehydrogenase, mitochondria	K.YVC*YGGL.-	531	0.95	1.48	1.24	1.43

P51649	ALDH5A1 Succinate-semialdehyde dehydrogenase, mitochondria	R.AAYEAFC*R.W	110	0.89	0.9	0.805	1.005
P51659	HSD17B4 Peroxisomal multifunctional enzyme type 2	K.C*EAVVADVLDK.G	425	0.945		0.93	
P51659	HSD17B4 Peroxisomal multifunctional enzyme type 2	K.SNIHC*NTIAPNAGSR.M	189	1.24	1.725	3.025	4.175
P51659	HSD17B4 Peroxisomal multifunctional enzyme type 2	K.IC*DFENASKPQSIQESTGSIIEVLSK.I	277	1.11	1.36	1.835	2.9
P51659	HSD17B4 Peroxisomal multifunctional enzyme type 2	K.FIYEGSSDFSC*LPTFGVIIGQK.S	373	1.095	1.195	1.25	1.715
P51970	NDUFA8 NADH dehydrogenase	K.FDEC*VLDK.L	110	2.735	1.425	2.59	3.16
P52789	HK2 Hexokinase-2	K.C*DVSFLQSEDGSGK.G	886	1.58	2.61	4.23	6.4
P53007	SLC25A1 Tricarboxylate transport protein, mitochondrial	R.GLLCGLGAGVAEAVVVVC*PMETIK.V	141	0.72	0.84	0.85	
P53007	SLC25A1 Tricarboxylate transport protein, mitochondrial	R.NTWDC*GLQILK.K	262	1.07	1.155	1.325	1.64
P53007	SLC25A1 Tricarboxylate transport protein, mitochondrial	R.GIGDC*VR.Q	70	1.03	1.125	1.27	1.475
P53396	ACLY ATP-citrate synthase	K.FIC*TTSAIQNR.F	20	1.03	2.86		2.19
P53597	SUCLG1 Succinyl-CoA ligase	K.IIC*QGFTGK.Q	60	1.08	1.225	1.83	2.775
P53597	SUCLG1 Succinyl-CoA ligase	R.LIGPNC*PGVINPGECK.I	172	1.035	1.22	1.57	2.575
P53701	HCCS Cytochrome c-type heme lyase	K.GC*PVNTEPSGPTC*EK.K	35	1.25	1.61	3.21	
P53701	HCCS Cytochrome c-type heme lyase	K.GC*PVNTEPSGPTCEK.K	35	1.065	1.31	1.955	3.48
P53701	HCCS Cytochrome c-type heme lyase	R.AYEYVEC*PIR.G	66	1.075	1.365	1.885	2.74
P53701	HCCS Cytochrome c-type heme lyase	K.WEALHAAECPC*GPSLIR.F	178	1.045	1.155	1.26	1.705
P54098	POLG DNA polymerase subunit gamma-1	R.TPVLGC*CISR.A	1077			1.45	
P54098	POLG DNA polymerase subunit gamma-1	K.LPTGTTLESAGVVC*PYR.A	647	1.24			20
P54136	RARS Arginine--tRNA ligase, cytoplasmic	K.IVFVPGC*SIPLTIVK.S	369	1.175	1.32	2.33	
P54136	RARS Arginine--tRNA ligase, cytoplasmic	K.NC*GCLGASPNLEQLQEENLK.L	32			3.53	
P54136	RARS Arginine--tRNA ligase, cytoplasmic	K.HLPDNEC*IEK.V	150	1.265	1.535		
P54136	RARS Arginine--tRNA ligase, cytoplasmic	K.NC*GC*LGASPNLEQLQEENLK.L	32	1.8			20
P54136	RARS Arginine--tRNA ligase, cytoplasmic	K.FGDYQC*NSAMGISQMLK.T	115	1.04			6.21
P54136	RARS Arginine--tRNA ligase, cytoplasmic	R.MLLC*EAVAAVMAK.G	638				1.23
P54819	AK2 Adenylate kinase 2, mitochondrial	K.NLETPLC*K.N	92	1.205	1.42	1.88	2.945
P54819	AK2 Adenylate kinase 2, mitochondrial	R.LAENFC*VCHLATGDMLR.A	40	0.98	1.08	1.25	1.6
P54886	ALDH18A1 Delta-1-pyrroline-5-carboxylate synthase	K.EAVQLVNTREEVEDLC*R.L	546	1.18	1.54	2.19	4.31
P54886	ALDH18A1 Delta-1-pyrroline-5-carboxylate synthase	K.C*EYPAACNALETLLIHR.D	606	1.05	1.545	2.215	3.85
P54886	ALDH18A1 Delta-1-pyrroline-5-carboxylate synthase	K.LGSAVVTRGDEC*GLALGR.L	88	1.18	1.54	2.255	3.85
P55084	HADHB Trifunctional enzyme subunit beta, mitochondrial	K.FNNWGGSLSLGHPFGATGC*R.L	435	1.2	1.5	1.3	
P55084	HADHB Trifunctional enzyme subunit beta, mitochondrial	K.EGGQYGLVAAC*AAGGQGHAMIVEAYPK.-	458	1.045	1.17	1.395	1.8
P55809	OXCT1 Succinyl-CoA:3-ketoacid coenzyme A transferase 1,	K.STGC*DFAVSPK.L	504	1.25	1.535	2.06	3.47
P55809	OXCT1 Succinyl-CoA:3-ketoacid coenzyme A transferase 1,	R.NFNLPMC*K.A	235	1.155	1.415	1.805	2.765
P55851	UCP2 Mitochondrial uncoupling protein 2	R.ALMAAC*TSR.E	302			1.61	12.46
P56381	ATP5E ATP synthase subunit epsilon, mitochondrial	R.YSQIC*AK.A	19	0.65	0.545	0.465	0.535
P56962	STX17 Syntaxin-17	K.LTSSC*PDLPSQTDKK.C	290	1.16	1.52	2.095	
P57772	EEFSEC Selenocysteine-specific elongation factor	K.AGQATEGHC*PR.Q	406	2.28		0.77	2.71
P58557	YBEY rRNA maturation factor homolog	K.FDLGIIC*VDNK.N	41		0.85		
P62072	TIMM10 Mitochondrial import inner membrane translocase su	R.MTSAC*HR.K	29	0.64	0.76	0.61	0.49
P62244	RPS15A 40S ribosomal protein S15a	K.C*GVISPR.F	72	1.065	1.245	1.51	2.545
P62906	RPL10A 60S ribosomal protein L10a	K.FSVC*VLGDQQHC*DEAK.A	66	1.24	1.68	2.225	4.785
P62906	RPL10A 60S ribosomal protein L10a	K.FSVC*VLGDQQHCDEAK.A	66		1.21	1.525	2.355
P78540	ARG2 Arginase-2, mitochondrial	R.LSSLGC*HLK.D	63	0.9	1.25	1.31	1.28
P82650	MRPS22 28S ribosomal protein S22, mitochondrial	R.HVDVLNLC*FAQFEPDSTEYIK.V	231	0.97	1.515	1.335	1.425
P82663	MRPS25 28S ribosomal protein S25, mitochondrial	R.ECIC*EVEGQVPC*PSLVPLPK.E	141	1.01	1.04	0.99	
P82663	MRPS25 28S ribosomal protein S25, mitochondrial	R.EC*ICEVEGQVPCPSLVPLPK.E	139	0.92	0.88	1.335	1.77
P82673	MRPS35 28S ribosomal protein S35, mitochondrial	K.TDRC*PLR.R	212	1.075	1.47	2.085	3.655
P82675	MRPS5 28S ribosomal protein S5, mitochondrial	R.ERGWSGNSWGGISLGPPDPGPC*GETYEDFDTR.I	211	1.03	1.455	2.16	2.97
P82675	MRPS5 28S ribosomal protein S5, mitochondrial	R.EEC*GPLPIVVASPR.G	377	1.12	1.385	1.82	2.505
P82675	MRPS5 28S ribosomal protein S5, mitochondrial	R.AIITIC*R.L	324	0.955	1.09	1.275	1.85
P82912	MRPS11 28S ribosomal protein S11, mitochondrial	K.ASHNNTQIQVVSASNEPLAFASC*GTEGFR.N	112	1.15	1.38	1.955	3.14
P82921	MRPS21 28S ribosomal protein S21, mitochondrial	R.YYEKPC*R.R	0	1.285	1.6	2.47	4.18
P82921	MRPS21 28S ribosomal protein S21, mitochondrial	K.NRADPWQGC*.-	87	1.175	1.47	2.24	3.75
P82932	MRPS6 28S ribosomal protein S6, mitochondrial	K.EC*EGIVPVPLAEK.L	105	1.07	1.235	1.635	3.385
P82933	MRPS9 28S ribosomal protein S9, mitochondrial	K.HDVTC*TVSGGGR.S	330	1.16	1.31	1.765	2.635
P82933	MRPS9 28S ribosomal protein S9, mitochondrial	K.LLTSQC*GAAEEEFVQR.F	233	1.03	1.155	1.58	2.51
P82933	MRPS9 28S ribosomal protein S9, mitochondrial	K.ALC*SFVTEDEVEWMR.Q	353	0.85	0.845	1.275	1.72
P83111	LACTB Serine beta-lactamase-like protein LACTB, mitochon	R.KQTYGSC*R.K	476	1.34	1.505	2.265	3.805
P83111	LACTB Serine beta-lactamase-like protein LACTB, mitochon	K.EVWSEGLGYADVENRVPC*KPETVMR.I	154	1.2	1.24	1.76	2.57
Q00325	SLC25A3 Phosphate carrier protein, mitochondrial	K.GWAPTFLGYSMQGLC*K.F	136	1.085	1.15	1.29	1.455

Q00325	SLC25A3 Phosphate carrier protein, mitochondrial	K.FAC*FER.T	237	1.01	1.065	1.145	1.32
Q02218	OGDH 2-oxoglutarate dehydrogenase, mitochondrial	K.EVQKYPNAELAWC*QEEHKNQG YYDYVKPR.L	956	1.2			
Q02218	OGDH 2-oxoglutarate dehydrogenase, mitochondrial	R.FLQMC*NDDPDVLPDLK.E	802	1.64			
Q02218	OGDH 2-oxoglutarate dehydrogenase, mitochondrial	K.AEQFYC*GDTEGK.K	395	1.42	2.145	3.06	17.305
Q02218	OGDH 2-oxoglutarate dehydrogenase, mitochondrial	K.RFGLEGC*EVLIPALK.T	283	1.285	1.755	3.005	7.77
Q02218	OGDH 2-oxoglutarate dehydrogenase, mitochondrial	R.VVNAPIFHVNSDDPEAVMYVC*K. V	487	1.1	1.46	2.36	4.225
Q02252	ALDH6A1 Methylmalonate-semialdehyde dehydrogenase	K.ERVC*NLIDSGTK.E	368	1.29	1.55	2.835	4.395
Q02252	ALDH6A1 Methylmalonate-semialdehyde dehydrogenase	K.AEMDAAIASC*K.R	86	1.405	1.565	2.535	3.58
Q02338	BDH1 D-beta-hydroxybutyrate dehydrogenase, mitochondria	K.FGVEAFSDC*LR.Y	221			1.67	3.165
Q02338	BDH1 D-beta-hydroxybutyrate dehydrogenase, mitochondria	K.METYC*SSGSTDTSPVIDAVTHALT ATIPYTR.Y	288		0.76		1.12
Q02978	SLC25A11 Mitochondrial 2-oxoglutarate/malate carrier protei	R.GC*IPTMAR.A	184	1.025	1.065	1.3	1.28
Q07021	C1QBP Complement component 1 Q subcomponent-binding prot	K.ALVLDC*HYPEDEVGQEDEAESDI FSIR.E	186	0.935	1.03	1.19	1.48
Q07812	BAX Apoptosis regulator BAX	K.KLSEC*LKR.I	62		0.97		
Q07812	BAX Apoptosis regulator BAX	K.ALC*TKVPELIR.T	126	1.07			
Q08257	CRYZ Quinone oxidoreductase	K.AGESVLVHGASGGVGLAAC*QIA R.A	166	0.57	0.495	0.36	0.34
Q08257	CRYZ Quinone oxidoreductase	R.ALIHSAC*VK.A	145	0.61			0.32
Q08257	CRYZ Quinone oxidoreductase	K.VHAC*GVNPVETYIR.S	45	0.855	0.8	1.15	0.22
Q08426	EHHADH Peroxisomal bifunctional enzyme	K.AIVIC*GAEGK.F	51	1.08	1.2	1.21	1.43
Q10713	PMPCA Mitochondrial-processing peptidase subunit alpha	R.ENTVGLHRFC*PTENVAK.I	225	1.345	1.53	2.38	3.185
Q10713	PMPCA Mitochondrial-processing peptidase subunit alpha	K.HGGIC*DCQTSR.D	140	1.095	1.395	1.89	2.895
Q12849	GRSF1 G-rich sequence factor 1	R.AQGLPWSC*TMEDVLNFFSDCR.I	161		1.71		
Q12849	GRSF1 G-rich sequence factor 1	R.YIELFLNSC*PK.G	476	0.985	0.985	1.31	1.62
Q12931	TRAP1 Heat shock protein 75 kDa, mitochondrial	K.FEDRSPAAEC*LSEK.E	573	1.025	1.16	1.435	2.39
Q12931	TRAP1 Heat shock protein 75 kDa, mitochondrial	K.SDC*KEFSSEAR.V	261	1.01	1.17	1.455	2.29
Q12931	TRAP1 Heat shock protein 75 kDa, mitochondrial	R.NIYYLC*APNR.H	501	0.97	1.08	1.315	1.965
Q12983	BNIP3 BCL2/adenovirus E1B 19 kDa protein-interacting pro	K.SSHC*DSPPR.S	129	0.885	1.2	1.845	3.16
Q13011	ECH1 Delta(3,5)-Delta(2,4)-dienoyl-CoA isomerase, mitoc	R.YQETFNVIERC*PK.P	159			1.91	2.335
Q13011	ECH1 Delta(3,5)-Delta(2,4)-dienoyl-CoA isomerase, mitoc	R.YC*AQDAFFQVK.E	187	1.025	1.16	1.36	1.97
Q13011	ECH1 Delta(3,5)-Delta(2,4)-dienoyl-CoA isomerase, mitoc	R.EMVEC*FNK.I	92	1.13	1.26	1.46	1.89
Q13011	ECH1 Delta(3,5)-Delta(2,4)-dienoyl-CoA isomerase, mitoc	R.DADC*RAVVISGAGK.M	102	1.06	1.07		1.855
Q13084	MRPL28 39S ribosomal protein L28, mitochondrial	K.TPKEDLC*SK.F	154	1.12	1.375	1.78	2.91
Q13232	NME3 Nucleoside diphosphate kinase 3	R.ADELLC*WEDSAGHWLYE.-	158	1.05		1.73	3.56
Q13423	NNT NAD(P) transhydrogenase, mitochondrial	K.KTC*DALQAK.V	1073	1.13	1.35	1.695	2.5
Q13423	NNT NAD(P) transhydrogenase, mitochondrial	R.EANSIIITPGYGLC*AAK.A	936	1.195	1.195	1.48	1.98
Q13505	MTX1 Metaxin-1	R.EAREC*LTLLSQR.L	326	0.94	0.985	1.01	1.01
Q13686	ALKBH1 Alkylated DNA repair protein alkB homolog 1	K.LYSQKPNVC*NLDK.H	129			7.51	
Q13825	AUH Methylglutaconyl-CoA hydratase, mitochondrial	R.SEVPGIFC*AGADLK.E	138	0.885	1.23	1.61	1.535
Q13907	IDI1 Isopentenyl-diphosphate Delta-isomerase 1	K.KNC*HLNENIEK.G	39	1.265	1.5	2	3.24
Q14197	ICT1 Peptidyl-tRNA hydrolase ICT1, mitochondrial	K.QADSDIPLDRLTISYC*R.S	82	0.96	1.165	1.205	1.65
Q14197	ICT1 Peptidyl-tRNA hydrolase ICT1, mitochondrial	R.NLADC*LQK.I	150	0.985	1.105	1.145	1.4
Q14318	FKBP8 Peptidyl-prolyl cis-trans isomerase FKBP8	K.REC*GNAHYQR.A	227	1.19	1.52	2.755	6.505
Q14318	FKBP8 Peptidyl-prolyl cis-trans isomerase FKBP8	R.SC*SLVLEHQPDNIK.A	295	1.095	1.34	1.815	2.965
Q14318	FKBP8 Peptidyl-prolyl cis-trans isomerase FKBP8	K.C*LNNLAASQLK.L	274	1.025	1.3	1.92	2.94
Q14CZ7	FASTKD3 FAST kinase domain-containing protein 3	K.SFLTPC*C*SLETPVDSQLYR.Y	525	1			
Q14CZ7	FASTKD3 FAST kinase domain-containing protein 3	R.ILQAC*TEKVDEHQTFLNK.I	266	1.68			
Q15031	LARS2 Probable leucine--tRNA ligase, mitochondrial	R.LGLC*FSWDR.E	167			2.35	
Q15031	LARS2 Probable leucine--tRNA ligase, mitochondrial	K.DC*LTPVMAVNMLTQQEVPVVIL AK.A	341	1.18			1.12
Q15046	KARS Lysine--tRNA ligase	K.ILDDIC*VAK.A	427	1.105		2.37	4.61
Q15046	KARS Lysine--tRNA ligase	K.EIC*NAYTELNDPMR.Q	496			1.85	2.84
Q15067	ACOX1 Peroxisomal acyl-coenzyme A oxidase 1	R.ASEAHC*HYVVVK.L	531	1.3		2.065	
Q15067	ACOX1 Peroxisomal acyl-coenzyme A oxidase 1	K.LVC*GMVSYLNDLPSQR.I	449	0.68		0.775	1.11
Q15070	OXA1L Mitochondrial inner membrane protein OXA1L	R.C*LIFPLIVTGQR.E	153		0.87		
Q15118	PDK1	K.HYNTNHEADDWC*VPSREPK.D	421	1.19			
Q15118	PDK1	R.LC*DLYYINSPELELEELNAK.S	240			2.07	4.54
Q15119	PDK2	K.QFLDFGSSNAC*EK.T	45	1.34	3.64		
Q15119	PDK2	K.HIGSIDPNC*NVSEVVK.D	195	1.26		2.86	10.67
Q15119	PDK2	R.HYQTIQEAGDWC*VPSTEPK.N	392	1.175	1.545	1.99	4.285
Q15120	PDK3	K.QFLDFGRDNAC*EK.T	41	1.32	1.34	1.625	3.195

Q15120	PDK3	K.HIGSIDPTC*NVADVVK.D	191	0.875	1.19	1.805	2.96
Q15120	PDK3	K.MLC*EQYYLVAPELEVEEFNAK.A	208	1.23	1.11	1.52	2.85
Q15286	RAB35 Ras-related protein Rab-35	R.WLHEINQNC*DDVC*R.I	110	1.08	0.88	1.43	
Q15286	RAB35 Ras-related protein Rab-35	K.ENVNVEEMFNC*ITELVLR.A	163	0.99	1.13	1.29	1.55
Q15286	RAB35 Ras-related protein Rab-35	R.WLHEINQNC*DDVCR.I	110	0.765	1.085	1.005	1.545
Q15390	MTFR1 Mitochondrial fission regulator 1	K.IC*ALENELAALR.A	145	1.05	1.345	1.95	2.83
Q15390	MTFR1 Mitochondrial fission regulator 1	K.IGTNLSLIQC*PR.V	49	1.14	0.88	1.51	1.885
Q16134	ETFDH Electron transfer flavoprotein-ubiquinone oxidored	K.AAQIGAHTLSGAC*LDPGAFK.E	118	1.09	1.35	1.93	3.005
Q16134	ETFDH Electron transfer flavoprotein-ubiquinone oxidored	R.LQINAQNC*VHCK.T	586	1.18	1.595	1.82	2.955
Q16134	ETFDH Electron transfer flavoprotein-ubiquinone oxidored	R.FC*PAGVYEFVPVEQGDGFR.L	561	1.135	1.42	1.67	2.94
Q16134	ETFDH Electron transfer flavoprotein-ubiquinone oxidored	R.ANC*EPQTYGIGLK.E	266	1.22	1.485	1.96	2.35
Q16611	BAK1 Bcl-2 homologous antagonist/killer	R.QEC*GEPALPSASEEQVAQDTEEVFR.S	14	0.925	1.13	1.51	2.885
Q16698	DECR1 2,4-dienoyl-CoA reductase, mitochondrial	K.ATAEQISSQTGNKVHAIQC*DVRDPDMVQNTVSELIK.V	116	1.08	1.31	2.055	2.755
Q16698	DECR1 2,4-dienoyl-CoA reductase, mitochondrial	K.GMTTLLSSLGAQC*VIASR.K	86	1.115	1.235	1.365	1.84
Q16718	NDUFA5 NADH dehydrogenase	K.TTGLVGLAVC*NTPHER.L	17	0.605	0.62	0.66	0.91
Q16762	TST Thiosulfate sulfurtransferase	R.HVPGASFFDIEEC*R.D	64	1.15	1.38	2.09	
Q16762	TST Thiosulfate sulfurtransferase	K.KVDLSQPLIATC*R.K	248	1.06	1.36	1.82	3.345
Q16775	HAGH Hydroxyacylglutathione hydrolase, mitochondrial	R.VYC*GHEYTINNLK.F	219				1.1
Q16822	PCK2 Phosphoenolpyruvate carboxykinase	R.AVDERFPGC*MQGR.T	151	0.92		0.69	
Q16822	PCK2 Phosphoenolpyruvate carboxykinase	K.VEC*VGDDIAWMR.F	325	1.14	2.65	3.74	
Q16822	PCK2 Phosphoenolpyruvate carboxykinase	R.YVAAAFPSAC*GK.T	306	1.39	2.34	3.42	12.55
Q16822	PCK2 Phosphoenolpyruvate carboxykinase	R.LCQPEGIHIC*DGTEAENTATLTLLEQQGLIR.K	63				10.27
Q16822	PCK2 Phosphoenolpyruvate carboxykinase	K.YNNC*WLAR.T	92	1.435	1.97	3.03	7.255
Q16822	PCK2 Phosphoenolpyruvate carboxykinase	K.CLHSVGQPLTGQGEPVSQWPC*NPEK.T	230	1.02	1.08	1.47	2.04
Q16822	PCK2 Phosphoenolpyruvate carboxykinase	R.QC*PIMDPAWEAPEGVPIDAIIFGGR.R	431	1.67	1.74		1.06
Q16854	DGUOK Deoxyguanosine kinase, mitochondrial	K.AC*TAQSLGNLLDMMYR.E	87	1.23		1.6	1.86
Q16891	IMMT Mitochondrial inner membrane protein	K.ANC*SDNEFTQALTAAIPPESLTR.G	603	0.965	1.105	1.4	2.005
Q16891	IMMT Mitochondrial inner membrane protein	K.LLSYASYC*IEHGDLELAAK.F	697	10.37	20	20	1.205
Q330K2	NDUFAF6 NADH dehydrogenase (ubiquinone) complex I, assembl	K.TVEDIYC*DNPPHQPVAIELWK.A	126	0.94		1.93	
Q3SXM5	HSDL1 Inactive hydroxysteroid dehydrogenase-like protein	K.SITVIC*DFYSLIR.L	42			1.18	
Q3SXM5	HSDL1 Inactive hydroxysteroid dehydrogenase-like protein	K.GAIVTISSGSCC*KPTPQLAAFSASK.A	209		0.82		
Q3SXM5	HSDL1 Inactive hydroxysteroid dehydrogenase-like protein	K.EAISC*TA.-	328		1.25		
Q3SXM5	HSDL1 Inactive hydroxysteroid dehydrogenase-like protein	R.C*SWLVPSPK.V	265	1.1	1.4	1.37	1.76
Q3SY17	SLC25A52 Solute carrier family 25 member 52	K.C*HGIGEYYR.G	166	1.245	1.4	1.63	3.06
Q3SY69	ALDH1L2 Mitochondrial 10-formyltetrahydrofolate dehydrogen	R.SC*DVEPNDTVDALYNR.F	174	1.34	1.635	3.005	6.485
Q3SY69	ALDH1L2 Mitochondrial 10-formyltetrahydrofolate dehydrogen	K.SPLIIFNDC*ELDK.A	707	1.02	1.95	2.58	4.13
Q3SY69	ALDH1L2 Mitochondrial 10-formyltetrahydrofolate dehydrogen	K.LLQYC*ETGVK.E	783	1.18	1.825	2.225	3.155
Q3ZCQ8	TIMM50 Mitochondrial import inner membrane translocase su	R.VVVVDC*KK.E	249	1.11	1.305	1.77	2.74
Q4G0N4	NADKD1 NAD kinase domain-containing protein 1	K.SSGLNLC*TGTGSK.A	311	1.07	1.32	1.605	2.215
Q4G0N4	NADKD1 NAD kinase domain-containing protein 1	R.SEGHLC*LPVR.Y	193	1.07	1.105	1.885	2.15
Q4G176	ACSF3 Acyl-CoA synthetase family member 3, mitochondrial	R.LCGC*VGGDLREER.V	88	0.76	0.61	0.51	1.935
Q4J6C6	PREPL Prolyl endopeptidase-like	K.KLNGLADLEAC*IK.T	538				4.82
Q4VC31	CCDC58 Coiled-coil domain-containing protein 58	K.NC*IAQTSAVVK.N	74		1.93	20	11.21
Q53H12	AGK Acylglycerol kinase, mitochondrial	K.EDFLNIC*IEPDTISK.G	334	1.15	1.38	2.305	3.81
Q53H12	AGK Acylglycerol kinase, mitochondrial	R.AAC*QEAQVFGNQLIPPNAQVK.K	43	1.12	1.34	1.69	2.385
Q53H12	AGK Acylglycerol kinase, mitochondrial	K.HC*DNLLR.R	34	1.08	1.385	1.65	2.335
Q53H12	AGK Acylglycerol kinase, mitochondrial	K.ATVFLNPAAC*K.G	72	1.095	1.31	1.665	2.26
Q53H12	AGK Acylglycerol kinase, mitochondrial	K.LQFFC*DPR.K	408	1.08	1.265	1.46	1.68
Q53H82	LACTB2 Beta-lactamase-like protein 2	R.DHSGGIGDIC*K.S	90	0.815		0.485	0.54
Q53R41	FASTKD1 FAST kinase domain-containing protein 1	R.C*NNVFLSNVDHLDLDSISK.I	252			2.44	
Q53R41	FASTKD1 FAST kinase domain-containing protein 1	R.IEAVLPQC*DLNNLSSFATSVLR.W	446	1.3	1.68	2.62	6.645
Q53S33	BOLA3 BolA-like protein 3	K.VTDISGGC*GAMYEIK.I	59			0.83	0.755
Q567V2	MPV17L2 Mpv17-like protein 2	R.SPVPLTPPGC*VALDTR.A	198	1.11			
Q5HYI7	MTX3 Metaxin-3	R.FC*DDILSSYFR.L	233	0.89			0.58
Q5HYI7	MTX3 Metaxin-3	R.DAKEC*LNLLSNR.L	176	0.645	1.105	0.82	0.53
Q5HYK3	COQ5 2-methoxy-6-polyprenyl-1,4-benzoquinol methylase,	R.FLC*LEFSQVNNPLISR.L	244	1.55			
Q5HYK3	COQ5 2-methoxy-6-polyprenyl-1,4-benzoquinol methylase,	R.VVVC*DINK.E	170	0.92	1.06	1.195	1.415
Q5JPH6	EARS2 Probable glutamate--tRNA ligase, mitochondrial	K.TGAAYPC*FCSPQR.L	140	0.99		2.01	
Q5JRX3	PITRM1 Presequence protease, mitochondrial	R.SQQSKPQDASC*LPALK.V	556	1.065	1.47	2.24	3.45
Q5JRX3	PITRM1 Presequence protease, mitochondrial	K.LGC*GLLDYR.E	627	1.235	1.56	2.16	2.815

Q5JRX3	PITRM1 Presequence protease, mitochondrial	R.C*SVNATPQQMPQTEK.A	780	1.215	1.33		2.275
Q5JRX3	PITRM1 Presequence protease, mitochondrial	R.EFQITC*GPDSFATDPSK.Q	313			1.77	1.845
Q5JRX3	PITRM1 Presequence protease, mitochondrial	R.LLPDHTYSVVSGGDPLC*IPELTWE QLK.Q	241	1.45		1.7	1.55
Q5JRX3	PITRM1 Presequence protease, mitochondrial	K.TGGMSASPHVLPDDSHMDTYEQG VLFSSLC*LDR.N	672				1.33
Q5JRX3	PITRM1 Presequence protease, mitochondrial	K.FRQC*LQENPK.F	477	1.18	1.31	1.7	0.41
Q5JTZ9	AARS2 Alanine--tRNA ligase, mitochondrial	K.HSTYDTDLFSPLLNAIQQGC*R.A	300	1.315	1.92	2.88	
Q5JTZ9	AARS2 Alanine--tRNA ligase, mitochondrial	R.VANSQKC*VR.A	108	1.61	1.75	3.55	7.02
Q5JTZ9	AARS2 Alanine--tRNA ligase, mitochondrial	R.QLC*EQAPSTSVLLLSPQPMGK.V	904	1.17	1.46	1.93	2.39
Q5RI15	COX20 Cytochrome c oxidase protein 20 homolog	K.LLGFLDVENTPC*AR.H	29	1.13	1.1	1.07	1.58
Q5T160	RARS2 Probable arginine--tRNA ligase, mitochondrial	K.LLGITPVC*R.M	576	1.28	1.745	2.23	
Q5T160	RARS2 Probable arginine--tRNA ligase, mitochondrial	R.AIAC*QLSR.V	11	1.31	1.365	1.575	3.195
Q5T2R2	PDSS1 Decaprenyl-diphosphate synthase subunit 1	K.AVSVLGC*PDPVVHEIAYQYGK.N	283			1.35	
Q5T2R2	PDSS1 Decaprenyl-diphosphate synthase subunit 1	K.TASLIANSC*K.A	275	1.045	1.26	1.59	3.095
Q5T440	IBA57 Putative transferase CAF17, mitochondrial	R.VWAVLPSSPEAC*GAASLQER.A	170	1.12	1.645	2.31	3.17
Q5T653	MRPL2 39S ribosomal protein L2, mitochondrial	R.QMQVLETC*VATVGR.V	240	0.975	1.115	1.495	1.975
Q5T653	MRPL2 39S ribosomal protein L2, mitochondrial	R.AAGTC*GVLLR.K	213	1.02	1.185	1.345	1.92
Q5T9A4	ATAD3B ATPase family AAA domain-containing protein 3B	K.FMLVLASNLPEQFDC*AINSR.I	461		1.26	2.02	
Q5T9A4	ATAD3B ATPase family AAA domain-containing protein 3B	R.LHFDNC*VLKPATEGK.R	492	1.21	1.5		
Q5T9A4	ATAD3B ATPase family AAA domain-containing protein 3B	K.DGVLTEAMMDAC*VQDAVQQYR. Q	557	1.145	1.3	1.89	2.95
Q5T9A4	ATAD3B ATPase family AAA domain-containing protein 3B	K.LAQFDYGRKC*SEVAR.L	515	0.85	1.18	1.53	2.85
Q5TC12	ATPAF1 ATP synthase mitochondrial F1 complex assembly fac	K.C*AQNQNK.T	321	0.955	1.075	1.17	1.925
Q5TC12	ATPAF1 ATP synthase mitochondrial F1 complex assembly fac	R.QGDFIKC*VEQK.T	121	0.995	1.03	0.82	1.875
Q5TC12	ATPAF1 ATP synthase mitochondrial F1 complex assembly fac	R.AQSC*PTFLCALPR.R	194	0.755	0.8	0.79	0.76
Q5TEU4	NDUFAF5 NADH dehydrogenase	R.NFPLALDLGC*GR.G	98	1.255	1.09	1.66	1.79
Q5TGZ0	MINOS1 Mitochondrial inner membrane organizing system pro	R.C*LADAVVK.I	13	1.115	1.275	1.46	2.02
Q5U5X0	LYRM7 LYR motif-containing protein 7	R.KDLLVENVPYC*DAPTQK.Q	97	0.95	0.975	1.165	1.61
Q5VT66	MARC1 MOSC domain-containing protein 1, mitochondrial	R.VMAC*SR.C	270	0.835	1.01		
Q5VT66	MARC1 MOSC domain-containing protein 1, mitochondrial	R.C*ILTTVDPDTGVMSR.K	273	1.12		2.7	4.57
Q5VT66	MARC1 MOSC domain-containing protein 1, mitochondrial	K.SYRQC*DPSER.K	300	0.76	0.93	0.1	1.54
Q5VT66	MARC1 MOSC domain-containing protein 1, mitochondrial	K.GVPVSEAEC*TAMGLR.S	79	1.065	0.85	1.2	0.975
Q6IN84	MRM1 rRNA methyltransferase 1, mitochondrial	R.NSC*PLTPVVSK.S	182	0.77	0.95	1.19	1.385
Q6KCM7	SLC25A25 Calcium-binding mitochondrial carrier protein SCaM	R.TC*TAPLDR.L	203	1.2	1.235	2.155	4.025
Q6KCM7	SLC25A25 Calcium-binding mitochondrial carrier protein SCaM	K.TGQYSGMLDC*AR.R	322	0.88	1.05	1.075	2.28
Q6L8Q7	PDE12 2,5-phosphodiesterase 12	R.YIMAGFPVC*PK.L	180	1.5		2.82	
Q6L8Q7	PDE12 2,5-phosphodiesterase 12	R.TVLYPYC*APYALELDYR.Q	321	1.38		4.12	
Q6L8Q7	PDE12 2,5-phosphodiesterase 12	K.LHC*TPGDGQR.F	250	1.485	1.83	2.885	5.965
Q6NUK1	SLC25A24 Calcium-binding mitochondrial carrier protein SCaM	K.TGQYSGIYDC*AK.K	330	1.025	1.115	1.245	1.465
Q6NUK1	SLC25A24 Calcium-binding mitochondrial carrier protein SCaM	K.DSVNPGVMVLLGC*GALSSTCGQ LASYPLALVR.T	391	0.91	0.925	0.96	1.2
Q6NVY1	HIBCH 3-hydroxyisobutyryl-CoA hydrolase, mitochondrial	R.LSQAC*MR.G	336	0.61	1.06	1.95	3.495
Q6NVY1	HIBCH 3-hydroxyisobutyryl-CoA hydrolase, mitochondrial	K.AFC*AGGDIR.V	95	1.22	1.56	2.045	3.185
Q6P087	RPUSD3 RNA pseudouridylate synthase domain-containing pro	R.AQRPTATYC*AVTDGIPAASEGK.I	172	1.365	2.02	3.4	
Q6P087	RPUSD3 RNA pseudouridylate synthase domain-containing pro	K.ESSGLVLLSSC*PQTASR.L	147	1.495	1.75	3.02	4.89
Q6P087	RPUSD3 RNA pseudouridylate synthase domain-containing pro	R.TLQC*LGLR.L	345	1.29	1.565	2.25	3.93
Q6P161	MRPL54 39S ribosomal protein L54, mitochondrial	K.GAVTSEALKDPDVC*TDPVQLTTY AMGVNIYK.E	62	0.865	0.87	0.985	1.415
Q6P1X6	C8orf82 UPF0598 protein C8orf82	R.YEAAFPFLSPC*GR.E	98	0.95	1.06	1.035	1.82
Q6P1X6	C8orf82 UPF0598 protein C8orf82	R.LSYC*GGGEALAVPFEPAR.L	130	1.01			0.94
Q6P4A7	SFXN4 Sideroflexin-4	R.SYTC*KPLER.S	159	0.905	0.98	1.075	1.355
Q6P4A7	SFXN4 Sideroflexin-4	R.QLLC*TNEDVSSPASADQR.I	70	0.775	0.765	0.86	1.01
Q6P4H8	FAM173B Protein FAM173B	K.VC*LPFVPATTK.Q	67	1.1	3.12		
Q6P587	FAHD1 Acylpyruvase FAHD1, mitochondrial	K.SFTASC*PVSAFVPK.E	129	1.32	1.42	1.685	2.46
Q6PI48	DARS2 Aspartate--tRNA ligase, mitochondrial	K.TAELLNAC*K.K	152	1.175	1.58	2.315	4.645
Q6PI48	DARS2 Aspartate--tRNA ligase, mitochondrial	R.C*YRDEGSRPDR.Q	264	1.175	1.475	2.42	4.485
Q6PI48	DARS2 Aspartate--tRNA ligase, mitochondrial	K.AIC*IPEGAK.Y	371	1.205	1.575	2.345	4.46
Q6PI48	DARS2 Aspartate--tRNA ligase, mitochondrial	K.ILC*EAPVESVVQVSGTVISRPAGQ ENPK.M	108	1.125	1.525	2.28	4.42
Q6PI48	DARS2 Aspartate--tRNA ligase, mitochondrial	K.LRLEC*ADLLETR.G	459	1.115	1.44	2.125	3.78
Q6PI48	DARS2 Aspartate--tRNA ligase, mitochondrial	R.TNTC*GELR.S	54	1.29	1.455	2.215	3.31
Q6PI48	DARS2 Aspartate--tRNA ligase, mitochondrial	R.LIC*LVTGSPSIR.D	590	1.035	1.25	1.475	2.16
Q6UB35	MTHFD1L Monofunctional C1-tetrahydrofolate synthase, mitoc	R.GDAHEC*FVSPVAK.A	198	1.21		2.82	
Q6UB35	MTHFD1L Monofunctional C1-tetrahydrofolate synthase, mitoc	R.SSC*SPGGR.T	61	1.33	1.9	3.6	

Q6UB35	MTHFD1L Monofunctional C1-tetrahydrofolate synthase, mitoc	K.VGC*GSPR.I	302	1.34	1.955	3.345	7.74
Q6UB35	MTHFD1L Monofunctional C1-tetrahydrofolate synthase, mitoc	R.AEIDLVC*ELAK.R	814	1.335	1.895	2.405	4.84
Q6UXV4	APOOL Apolipoprotein O-like	R.TATGC*YIGWCK.G	74	1.315	1.52	1.63	1.485
Q6UXV4	APOOL Apolipoprotein O-like	K.ITYPLGLATLGATVC*YPVQSVIIA K.V	152	0.715	0.69	0.615	0.59
Q6YN16	HSDL2 Hydroxysteroid dehydrogenase-like protein 2	K.TAIHTAAMDMLGGPGIESQC*R.K	218	1.11	1.71	1.82	3.66
Q6YN16	HSDL2 Hydroxysteroid dehydrogenase-like protein 2	K.ALPC*IVDVR.D	71	1.145	1.535	1.945	3.105
Q6YN16	HSDL2 Hydroxysteroid dehydrogenase-like protein 2	R.LAGC*TVFITGASR.G	11	0.975	1.11	1.27	1.885
Q6YP21	CCBL2 Kynurenine--oxoglutarate transaminase 3	K.LSAIPVSAFC*NSETK.S	416	1.37			
Q70CQ3	USP30 Ubiquitin carboxyl-terminal hydrolase 30	K.ALSC*QEVTDDEVLDASC*LLDVL R.M	129				19.58
Q70CQ3	USP30 Ubiquitin carboxyl-terminal hydrolase 30	R.MQHQSQEC*K.S	513	1.105	1.53	2.28	4.505
Q7KZF4	SND1 Staphylococcal nuclease domain-containing protein	R.ANNPEQNRLSEC*EEQAK.A	152	1.275	1.61	3.205	6.29
Q7L0Y3	TRMT10C Mitochondrial ribonuclease P protein 1	K.SSVQEEC*VSTISSSK.D	78	1.015	1.385	1.785	3.93
Q7L0Y3	TRMT10C Mitochondrial ribonuclease P protein 1	K.RLNLATEC*LPLDK.Y	335	1.165	1.405	1.85	3.11
Q7L0Y3	TRMT10C Mitochondrial ribonuclease P protein 1	R.NVDPFHIYFC*NLK.I	246	1.04	0.97	1.27	2.34
Q7L0Y3	TRMT10C Mitochondrial ribonuclease P protein 1	K.TLMEC*VSNTAK.K	123	0.96	0.8	0.995	0.985
Q7L2E3	DHX30 Putative ATP-dependent RNA helicase DHX30	K.VSC*LETVWVSR.A	765	1.13			
Q7L2E3	DHX30 Putative ATP-dependent RNA helicase DHX30	R.DTILNAIEQHPVVVISGDTGC*GK. T	461	1.26			
Q7L2E3	DHX30 Putative ATP-dependent RNA helicase DHX30	R.GEPGGILC*FLPGWQEIK.G	673	1.23	1.74	2.12	6.09
Q7L2E3	DHX30 Putative ATP-dependent RNA helicase DHX30	K.AAALAC*K.K	309	1.26	1.695	2.62	4.91
Q7L2E3	DHX30 Putative ATP-dependent RNA helicase DHX30	R.YFGGC*PVIK.V	606	1.28	1.81	2.565	4.655
Q7L2E3	DHX30 Putative ATP-dependent RNA helicase DHX30	R.C*NVIITQPR.R	484	1.155	1.48	2.385	4.415
Q7L2E3	DHX30 Putative ATP-dependent RNA helicase DHX30	R.QAAAAAC*QLFK.G	118	1.055	1.275	1.825	2.55
Q7L2E3	DHX30 Putative ATP-dependent RNA helicase DHX30	R.GPC*GSFDVR.K	1183	0.995	1.445	1.92	2.43
Q7L8L6	FASTKD5 FAST kinase domain-containing protein 5	K.SGAMEMAGLC*PAAC*MQTPR.M	685	0.23			
Q7L8L6	FASTKD5 FAST kinase domain-containing protein 5	K.AAVPLGGFLC*NVADK.S	670	1.04	2.005		7.99
Q7L8L6	FASTKD5 FAST kinase domain-containing protein 5	K.IGDLAC*ANIQHLSSR.S	345	1.305	1.6	2.13	4.39
Q7L8L6	FASTKD5 FAST kinase domain-containing protein 5	R.NQYC*YGSR.D	708	1.255	1.64	2.24	4.135
Q7Z2W9	MRPL21 39S ribosomal protein L21, mitochondrial	R.INSIEIAPC*LL.-	203	1.035	1.14	1.345	1.92
Q7Z2W9	MRPL21 39S ribosomal protein L21, mitochondrial	K.VTSEDLILIGNELDLAC*GER.I	124	1.11	1.215	1.395	1.88
Q7Z4W1	DCXR L-xylulose reductase	R.EC*PGIEPVC*VDLGDWEATER.A	51	1.16	1.73	2.36	4.65
Q7Z4W1	DCXR L-xylulose reductase	R.EC*PGIEPVCVDLGDWEATER.A	51				3.06
Q7Z4W1	DCXR L-xylulose reductase	R.GVPGAIVNVSSQC*SQR.A	138	1.015	1.46	1.94	2.825
Q7Z4W1	DCXR L-xylulose reductase	R.AVTNHSVYC*STK.G	150	1.02	1.27	1.645	2.46
Q7Z4W1	DCXR L-xylulose reductase	R.SGMTTGSTLPVEGGFWAC*.-	244	1.1	1.16	1.875	2.23
Q7Z6M4	MTERFD2 mTERF domain-containing protein 2	R.SNNYVQEPEC*R.R	69	1.405	2	4.12	2.86
Q7Z7H8	MRPL10 39S ribosomal protein L10, mitochondrial	R.MIAVC*QNVALSAEDK.L	99			1.2	
Q7Z7H8	MRPL10 39S ribosomal protein L10, mitochondrial	K.EMVRILRTVPFLPLLGGC*IDDTILS R.Q	180	1.19	1.445	1.965	3.255
Q7Z7K0	CMC1 COX assembly mitochondrial protein homolog	K.ECLTAYYNDPAFYEEC*K.M	77				0.27
Q86SX6	GLRX5 Glutaredoxin-related protein 5, mitochondrial	K.GTPEQPQC*GFSNAVVQILR.L	67	0.815	0.805	0.835	0.915
Q86U28	ISCA2 Iron-sulfur cluster assembly 2 homolog, mitochondr	R.LTDSC*VQR.L	56	0.61	0.57	0.47	0.525
Q86U90	YRDC YrdC domain-containing protein, mitochondrial	R.SEAKPLAVC*LGR.V	121	1.14		2.02	2.47
Q86UT6	NLRX1 NLR family member X1	R.AVLAQLGC*PIK.N	644	1.39	2.12		
Q86UT6	NLRX1 NLR family member X1	R.LNQPYC*GYAVGGSGVSATPAQR. D	331	1.41	1.985	5.44	14.27
Q86UT6	NLRX1 NLR family member X1	K.LGLQLNSLGPEAC*K.D	767		1.28		12.41
Q86UT6	NLRX1 NLR family member X1	R.HALDEVNLASC*QLDPAGLR.T	735	1.3	1.825	2.44	11.34
Q86UT6	NLRX1 NLR family member X1	R.LAGTGLC*SDPEEPQEPAAIIVNLL R.K	259	1.63	1.885		7.44
Q86UT6	NLRX1 NLR family member X1	R.FFLAPC*VEPGR.A	481	1.27		3.88	0.865
Q86UT6	NLRX1 NLR family member X1	R.YGEIC*GFSDTNLQK.L	310	2.03		0.83	0.48
Q86UY8	NT5DC3 5-nucleotidase domain-containing protein 3	K.YIC*YAEQTR.A	276	1.25		1.39	1.395
Q86VU5	COMTD1 Catechol O-methyltransferase domain-containing pro	R.VVTC*EVDAQPPELGRPLWR.Q	133	1.18	1.78	2.57	
Q86VU5	COMTD1 Catechol O-methyltransferase domain-containing pro	K.VLQPPKGDVAAEC*VR.N	231	1.29	1.71	2.68	5.22
Q86VU5	COMTD1 Catechol O-methyltransferase domain-containing pro	R.LLTLEQPQGDSMMTC*EQAQLLA NLAR.L	88	1.295	1.785	2.59	5.005
Q86WA6	BPHL Valacyclovir hydrolase	K.HLPDGNIC*R.H	225	1.13	1.335	1.51	2.645

Q86Y39	NDUFA11 NADH dehydrogenase	R.EKPDDPLNYFLGGC*AGGLTLGAR.T	95	1.21			
Q86Y79	PTRH1 Probable peptidyl-tRNA hydrolase	R.SC*ISCLNSNAMPR.L	147			7.24	
Q86YH6	PDSS2 Decaprenyl-diphosphate synthase subunit 2	K.IAILSGDFLLANAC*NGLALLQNTK.V	200	1.165		2.41	
Q86YH6	PDSS2 Decaprenyl-diphosphate synthase subunit 2	K.AAGPSSVNTSC*QNYDMVSGIYSC*QR.S	132			20	
Q86YH6	PDSS2 Decaprenyl-diphosphate synthase subunit 2	K.SC*QAAMELAK.H	263	1.12	0.98	1.685	2.605
Q86YH6	PDSS2 Decaprenyl-diphosphate synthase subunit 2	K.GVTSAIDLC*R.Y	365		1.25	0.61	0.635
Q8IUX1	TMEM126B Transmembrane protein 126B	K.LFVIDALYSDNISKENC*VFR.S	140	0.61			
Q8IVS2	MCAT Malonyl-CoA-acyl carrier protein transacylase, mit	K.SLGIENPVCEVSNYLFPDC*R.V	235	0.83	1.185	1.16	
Q8IVS2	MCAT Malonyl-CoA-acyl carrier protein transacylase, mit	R.TVHC*QPAIFVASLAAVEK.L	120	1.37	1.34	1.96	
Q8IVS2	MCAT Malonyl-CoA-acyl carrier protein transacylase, mit	K.FNFAC*LEAR.E	208	1.745	1.935	2.805	9.145
Q8IWA4	MFN1 Mitofusin-1	R.LSVLVDEFC*SEFHPNPDVLK.I	428			2.35	
Q8IWA4	MFN1 Mitofusin-1	R.C*LHFLVEELK.V	260	1.06			
Q8IWA4	MFN1 Mitofusin-1	R.MIVSSTSANC*SHQVK.Q	665	1.385	2.32		5.04
Q8IWA4	MFN1 Mitofusin-1	R.LQEFQNFEQIFEEC*ISQSAVK.T	327	1.35	1.63	1.925	3.36
Q8IWA4	MFN1 Mitofusin-1	R.LC*QQVDITQK.Q	681	1.09	1.285	1.665	2.73
Q8IXI1	RHOT2 Mitochondrial Rho GTPase 2	K.SC*FGHPLAPQALEDVK.T	216	1.59	2.09		
Q8IXI1	RHOT2 Mitochondrial Rho GTPase 2	K.ADLPEGVAVSGPSPAEFC*R.K	543	1.35	1.81	2.83	7.565
Q8IXI1	RHOT2 Mitochondrial Rho GTPase 2	K.SFAHC*ASVYK.H	504	1.115	1.12	1.635	3.54
Q8IXI2	RHOT1 Mitochondrial Rho GTPase 1	K.MPPPQAFTC*NTADAPSKDIFVK.L	559	1.22		2.12	
Q8IXI2	RHOT1 Mitochondrial Rho GTPase 1	K.AVLHPTGPLYC*PEEK.E	175	1.19	1.64	2.59	
Q8IXI2	RHOT1 Mitochondrial Rho GTPase 1	K.QEYSISPTDFC*R.K	546				4.58
Q8IXI2	RHOT1 Mitochondrial Rho GTPase 1	R.IPC*LIVAAK.S	522	1.045	1.39	2.035	2.665
Q8IXI2	RHOT1 Mitochondrial Rho GTPase 1	R.IC*FNTPLAPQALEDVK.N	216	1.125	1.12	2.035	2.55
Q8IXI2	RHOT1 Mitochondrial Rho GTPase 1	R.CNVIGVKNC*GK.S	429	0.91	0.65	1.8	1.23
Q8IYB8	SUPV3L1 ATP-dependent RNA helicase SUPV3L1, mitochondrial	K.SNAAGVPC*DLVTGEER.V	251	1.31	1.56	2.74	6.135
Q8IYB8	SUPV3L1 ATP-dependent RNA helicase SUPV3L1, mitochondrial	K.KFNDPNDPC*K.I	418	1.255	1.485	2.05	4.45
Q8IYB8	SUPV3L1 ATP-dependent RNA helicase SUPV3L1, mitochondrial	R.YVFC*TAPINK.K	575	0.94	1.04	1.495	2.34
Q8IYQ7	THNSL1 Threonine synthase-like 1	R.VQDKTC*PVIISSTAHYSK.F	658			1.88	
Q8IYQ7	THNSL1 Threonine synthase-like 1	R.C*IHPADIPAAR.L	299	1.1	1.05		
Q8IYU8	EFHA1 EF-hand domain-containing family member A1	K.DIEDTLSGIQTAGC*GSTFFR.D	144	1.1	1.5	2.12	3.795
Q8IYU8	EFHA1 EF-hand domain-containing family member A1	K.IFDLDGDEC*LSHEEFLGVLK.N	381	0.88	0.935	1.69	1.055
Q8N0V3	RBFA Putative ribosome-binding factor A, mitochondrial	K.ALTDLLC*TPEVSQELYDLNVELSK.V	109			1.47	
Q8N0V3	RBFA Putative ribosome-binding factor A, mitochondrial	R.TEDGHSC*GASRE.-	338	1.03	1.15	4.44	
Q8N0V3	RBFA Putative ribosome-binding factor A, mitochondrial	K.VSLTPDFSAC*R.A	136	1.08	1.11	1.485	2.545
Q8N0Z8	PUSL1 tRNA pseudouridine synthase-like 1	K.SVLYGNLGAASC*TLQGPQFGSHG.-	292	1.065		2.21	
Q8N0Z8	PUSL1 tRNA pseudouridine synthase-like 1	R.LATGC*HR.R	138		1.48	1.12	2.06
Q8N2A8	PLD6 Mitochondrial cardiolipin hydrolase	K.SHGSC*APPVSR.A	226	1.84			
Q8N2F6	ARMC10 Armadillo repeat-containing protein 10	K.SAGALEEGTSEGQLC*GR.S	59	1.12	1.37	2.37	4.45
Q8N442	GUF1 Translation factor GUF1, mitochondrial	K.VFDIPSDEC*IK.I	221	0.99	1.34	2.015	3.74
Q8N442	GUF1 Translation factor GUF1, mitochondrial	K.IMMLC*EAR.R	492	1.13	1.4	1.77	2.75
Q8N4Q0	ZADH2 Zinc-binding alcohol dehydrogenase domain-containi	K.SLGC*DRPINYK.T	218	1.41		2.43	4.94
Q8N4Q0	ZADH2 Zinc-binding alcohol dehydrogenase domain-containi	R.DC*PVPLPGDGDLLVR.N	55	1.105	1.515	2.41	2.64
Q8N4Q0	ZADH2 Zinc-binding alcohol dehydrogenase domain-containi	K.C*HVIGTCSSDEK.S	198	0.995	1.335	1.65	2.53
Q8N4T8	CBR4 Carbonyl reductase family member 4	K.AAAGDLGGDHLAFSC*DVAK.E	55			1.32	
Q8N5K1	CISD2 CDGSH iron-sulfur domain-containing protein 2	K.VVNEINIEDLC*LTK.A	92	0.775	0.93	1.12	1.625
Q8N5M1	ATPAF2 ATP synthase mitochondrial F1 complex assembly fac	K.FLDTDTIC*YR.V	141		0.82	0.56	0.48
Q8N5N7	MRPL50 39S ribosomal protein L50, mitochondrial	K.EKEPVVVETVEEKKEPILVC*PPLR.S	52	0.66	0.62	0.64	
Q8N8R3	SLC25A29 Mitochondrial carnitine/acylcarnitine carrier prot	K.GSLDC*LAQIYGHEGLR.G	137	0.73			
Q8N8R3	SLC25A29 Mitochondrial carnitine/acylcarnitine carrier prot	R.GILDC*VHQSYR.A	234	0.95		1.1	3.04
Q8N983	MRPL43 39S ribosomal protein L43, mitochondrial	R.EESIHC*K.S	91	1.19	1.22	1.67	6.875
Q8NAN2	FAM73A Protein FAM73A	R.AASDKGSSC*SSSR.Q	128	1.045	1.61	2.695	4.11
Q8NAN2	FAM73A Protein FAM73A	R.NRQAEDEAC*GSIK.L	240	1.07		1.72	3.39
Q8NBN7	RDH13 Retinol dehydrogenase 13	R.DMEKC*EAAAK.D	75	1.19	1.93	2.595	4.795
Q8NBN7	RDH13 Retinol dehydrogenase 13	K.DYVTGGAC*PSK.A	30	1.215	1.48	2.055	3.5
Q8NBU5	ATAD1 ATPase family AAA domain-containing protein 1	K.DAAFQNVLTHVC*LD.-	359	1.275	1.405	2.88	5.045
Q8NBU5	ATAD1 ATPase family AAA domain-containing protein 1	K.GVLLYGPPGC*GK.T	137	1.315	1.99	1.77	4.055
Q8NBU5	ATAD1 ATPase family AAA domain-containing protein 1	R.DAALLC*VR.E	310	1.17	1.51	2.1	3.87
Q8NBU5	ATAD1 ATPase family AAA domain-containing protein 1	R.HVDLLEVAQETDGFSGSDLKEMC*R.D	303	1.14	1.51	2.05	3.545
Q8NBX0	SCCPDH Saccharopine dehydrogenase-like oxidoreductase	K.AC*IENGASCIDISGEPQFLELMQLK.Y	113		1.66		

Q8NBX0	SCCPDH Saccharopine dehydrogenase-like oxidoreductase	K.QATVVLNC*VGPYR.F	98	1.17	1.815	2.005	2.47
Q8NBX0	SCCPDH Saccharopine dehydrogenase-like oxidoreductase	R.WPISYC*R.E	238	1.11			2.325
Q8NC60	NOA1 Nitric oxide-associated protein 1	R.LWEDC*AR.A	272	1.38	0.85	1.41	3.91
Q8NC60	NOA1 Nitric oxide-associated protein 1	K.STLFNTLLESDYC*TAK.G	364	0.79	1.73	1.065	1.285
Q8NCN5	PDPR Pyruvate dehydrogenase phosphatase regulatory subu	R.FC*AGILSTAR.H	85	1.17	1.57	1.17	
Q8NCN5	PDPR Pyruvate dehydrogenase phosphatase regulatory subu	K.FFAFWGQDINNLTTPLEC*GR.E	735	1.01			2.6
Q8NCN5	PDPR Pyruvate dehydrogenase phosphatase regulatory subu	K.LVNC*PETFTPDMR.C	357			1.35	2.245
Q8NE62	CHDH Choline dehydrogenase, mitochondrial	K.ADSAYHPSC*TCK.M	514	1.185	2.12	2.615	4.245
Q8NE86	MCU Calcium uniporter protein, mitochondrial	K.TLVQQLYTTLC*IEQHQLNK.E	191	0.85	0.9		
Q8NFF5	FLAD1 FAD synthase	R.LHYGTDPC*TGQPFR.F	236	1.26		1.66	3.16
Q8NFF5	FLAD1 FAD synthase	R.SLGVQVC*R.V	147	1.155	1.34	1.6	2.345
Q8NFF5	FLAD1 FAD synthase	K.LTLDSEEEGPLEEC*LAYLTAR.L	338	1.09	1.265	1.705	2.33
Q8NFF5	FLAD1 FAD synthase	K.GHTQDTNTFFLC*R.T	136	0.88	1.285		2.17
Q8NI60	ADCK3 Chaperone activity of bc1 complex-like, mitochondr	K.AMFEEAYSNYC*K.R	641		1.15		
Q8NI60	ADCK3 Chaperone activity of bc1 complex-like, mitochondr	R.ELALEC*DYQR.E	406	10.62	1.095	0.86	2.92
Q8TAA5	GRPEL2 GrpE protein homolog 2, mitochondrial	R.AIADC*ENIR.R	87	1.305	1.845	3.495	6.135
Q8TAA5	GRPEL2 GrpE protein homolog 2, mitochondrial	K.TTEC*ISEESEPEDQKLTLEK.V	126	1.125	1.525	2.235	3.735
Q8TAA5	GRPEL2 GrpE protein homolog 2, mitochondrial	K.IFGIQSFC*K.D	110	1.23		1.005	1.095
Q8TAE8	GADD45GIP1 Growth arrest and DNA damage-inducible proteins-in	R.EQHIAEC*MAK.M	124	1.075	1.215	1.55	2.37
Q8TBP6	SLC25A40 Solute carrier family 25 member 40	K.LGENETC*IPIVAGIVAR.F	142	1.08	1.36	1.355	1.98
Q8TCS8	PNPT1 Polyribonucleotide nucleotidyltransferase 1, mitoc	R.NVSC*EVDMFK.T	372	1.3	1.175	2.95	
Q8TCS8	PNPT1 Polyribonucleotide nucleotidyltransferase 1, mitoc	R.C*DGRDLTSLR.N	359	1.12	1.48	1.66	2.385
Q8TCS8	PNPT1 Polyribonucleotide nucleotidyltransferase 1, mitoc	K.SQIVMLEASAENILQQDFC*HAIK.V	242	1.23	1.24		1.69
Q8TD30	GPT2 Alanine aminotransferase 2	R.AVQEAKDHC*DPK.V	259	1.13	3.19	3.29	
Q8TD30	GPT2 Alanine aminotransferase 2	K.LFLLADEVYQDNVYSPDC*R.F	311		1.88		
Q8TD30	GPT2 Alanine aminotransferase 2	K.GYMGEC*GYR.G	347	1.45	1.53	3.125	4.515
Q8TD30	GPT2 Alanine aminotransferase 2	R.ILQACGGNSLGSYSASQGVNC*IR.E	158	1.19	1.64	1.97	3.155
Q8TD30	GPT2 Alanine aminotransferase 2	R.QVMALC*TYPNLLDSPSFPEDAK.K	116				1.98
Q8TD30	GPT2 Alanine aminotransferase 2	K.VLC*IINPGNPTGQVQSR.K	265	1.27		0.9	0.97
Q8TDB4	MGARP Protein MGARP	K.EASAC*PGHVEAAPETTAVSAETGPEVTDAAAR.E	139	0.77	0.855	1.07	1.84
Q8WUK0	PTPMT1 Phosphatidylglycerophosphatase and protein-tyrosin	K.YQSLGQC*VYVHCK.A	127	1.17			
Q8WUK0	PTPMT1 Phosphatidylglycerophosphatase and protein-tyrosin	R.FLC*NSSQEWK.R	81	0.72	0.885	0.625	0.77
Q8WV60	PTCD2 Pentatricopeptide repeat-containing protein 2, mit	K.KVAVAC*NLSGTK.E	67	1.13	1.56	1.795	3.19
Q8WV74	NUDT8 Nucleoside diphosphate-linked moiety X motif 8, mi	K.QPLASPC*QASSTPGLNK.G	224	1.415	2.19	3.26	
Q8WV74	NUDT8 Nucleoside diphosphate-linked moiety X motif 8, mi	R.LAGLTC*SGAEGLAR.P	207	1.66	1.95	2.61	9.19
Q8WV74	NUDT8 Nucleoside diphosphate-linked moiety X motif 8, mi	K.C*DPADQDVVHTALR.E	71				3.37
Q8WVC6	DCAKD Dephospho-CoA kinase domain-containing protein	K.HTVVVYC*DR.D	135	0.995	1.185	1.13	
Q8WVM0	TFB1M Dimethyladenosine transferase 1, mitochondrial	K.MC*DEDPQLFAYNFR.E	311	1.24	1.35	11.235	11.8
Q8WVM0	TFB1M Dimethyladenosine transferase 1, mitochondrial	R.LSVMAQYLC*NVR.H	204	1.505	1.11	1.905	5.46
Q8WVM0	TFB1M Dimethyladenosine transferase 1, mitochondrial	K.SLC*DVYR.K	304	1.07	1.44	2.635	3.635
Q8WVM0	TFB1M Dimethyladenosine transferase 1, mitochondrial	K.WLENISC*R.D	160	1.17	1.535	2.165	3.58
Q8WW59	SPRYD4 SPRY domain-containing protein 4	R.DSC*IGVDDR.S	114	0.935	1.035	1.26	1.495
Q8WWV3	RTN4IP1 Reticulon-4-interacting protein 1, mitochondrial	K.VGGLNDKNC*TGK.R	203	1.16	1.395	1.925	3.68
Q8WWV3	RTN4IP1 Reticulon-4-interacting protein 1, mitochondrial	K.AWDAHVTAVC*SQDASELVR.K	236				3.56
Q8WXQ4	ATP5S ATP synthase coupling factor B-like 1	K.CHYIEDDC*LLR.L	113		0.95	1.425	1.59
Q92506	HSD17B8 Estradiol 17-beta-dehydrogenase 8	R.LAGEGATVAAC*DLDR.A	41		0.84	0.97	
Q92552	MRPS27 28S ribosomal protein S27, mitochondrial	R.EKEHYC*LADLASLMDK.T	49	1.125	1.41	2.265	3.99
Q92552	MRPS27 28S ribosomal protein S27, mitochondrial	K.EKLSTC*EAEDIATYEQNLQQWHLDLVQLIQR.E	367	1.055	1.28	1.81	3.43
Q92552	MRPS27 28S ribosomal protein S27, mitochondrial	K.VAASPEDIKLC*R.E	276	1.09	1.285	1.66	2.68
Q92665	MRPS31 28S ribosomal protein S31, mitochondrial	R.HFMELVTC*GLSK.N	356	0.965	0.97		
Q92667	AKAP1 A-kinase anchor protein 1, mitochondrial	R.VC*QASQLQGQKEESCVPVHQK.T	376			1.67	3.68
Q92667	AKAP1 A-kinase anchor protein 1, mitochondrial	K.SIPLEC*PLSSPK.G	147	1.155	1.415	2.07	3.245
Q92667	AKAP1 A-kinase anchor protein 1, mitochondrial	R.ADPAIKEPLPVEDVC*PK.V	64	0.965	1.155	1.56	2.635
Q92947	GCDH Glutaryl-CoA dehydrogenase, mitochondrial	K.GELLGC*FGLTEPNSGSDPSSMETR.A	176	1.31	1.63	2.9	5.67
Q92947	GCDH Glutaryl-CoA dehydrogenase, mitochondrial	R.ASATGMIIMDGVEVPEENVLPGASSLGGPFGC*LNNAR.Y	289	1.345	1.675	2.66	4.555
Q92947	GCDH Glutaryl-CoA dehydrogenase, mitochondrial	R.TYC*QER.L	75	1.39	1.665	2.27	4.13
Q92947	GCDH Glutaryl-CoA dehydrogenase, mitochondrial	K.GYGC*AGVSSVAYGLLAR.E	115	1.12	1.75		3.85

Q969Q5	RAB24 Ras-related protein Rab-24	K.AAIVC*YDLTDSSSFER.A	87				0.695
Q969S9	GFM2 Ribosome-releasing factor 2, mitochondrial	R.LLLAGVEIPEPVFFC*TIEPPSLSK.Q	492	0.89	1.41	1.98	
Q969S9	GFM2 Ribosome-releasing factor 2, mitochondrial	R.VTLAQTAVPVLC*GSALK.N	329	1.15	1.45	2.08	4.01
Q969V5	MUL1 Mitochondrial ubiquitin ligase activator of NFKB 1	R.TTHLWNDC*SK.I	113	0.885	0.9	1.17	1.515
Q969Y2	GTPBP3 tRNA modification GTPase GTPBP3, mitochondrial	K.ELAAVC*GDPSTDPPLLTR.A	419		2.9		
Q969Y2	GTPBP3 tRNA modification GTPase GTPBP3, mitochondrial	R.QLDGELGHLC*R.G	188	1.14		1.79	3.17
Q969Z0	TBRG4 Protein TBRG4	R.LEDKC*LELVEHFGPNELR.K	246	1.015	1.175	1.44	2.19
Q969Z0	TBRG4 Protein TBRG4	R.LATDLLSLMPSLTSGEVAHC*AK.S	335	0.98	1.085	1.64	1.91
Q969Z3	MARC2 MOSC domain-containing protein 2, mitochondrial	K.KVMAC*PR.C	269		1.01	1.21	1.17
Q969Z3	MARC2 MOSC domain-containing protein 2, mitochondrial	K.GRDC*GNEAAK.W	160	0.885	1.01	1.04	1.09
Q969Z3	MARC2 MOSC domain-containing protein 2, mitochondrial	R.C*ILTTVDPDTGVIDR.K	272	1			0.95
Q96A46	SLC25A28 Mitoferrin-2	R.GAGGGEAGAC*RPPVR.Q	49	0.79		1.75	
Q96A46	SLC25A28 Mitoferrin-2	R.VTDC*VR.A	211	1.06	1.46	1.89	2.955
Q96AB3	ISOC2 Isochorismatase domain-containing protein 2, mitoc	K.TC*FSMVPALQQELDSRPQLR.S	84	0.88	1.05	0.94	
Q96AB3	ISOC2 Isochorismatase domain-containing protein 2, mitoc	R.VLPGSSVLFLC*DMQEK.F	21	0.85	0.94	0.85	0.88
Q96AG3	SLC25A46 Solute carrier family 25 member 46	R.DNTGILEC*VK.E	239	1.3	1.93	1.655	
Q96AN5	TMEM143 Transmembrane protein 143	K.SGC*EVTFNGTR.A	408				1.23
Q96AY3	FKBP10 Peptidyl-prolyl cis-trans isomerase FKBP10	K.GMDQGLLGMC*PGER.R	222	1.25	1.6	2.27	3.5
Q96AY3	FKBP10 Peptidyl-prolyl cis-trans isomerase FKBP10	K.VIEGLDTGLQGMC*VGER.R	447	1.2	2.03	3.585	3.22
Q96AY3	FKBP10 Peptidyl-prolyl cis-trans isomerase FKBP10	R.GLMGMC*VNER.R	110	1.09		2.215	2.47
Q96BQ5	CCDC127 Coiled-coil domain-containing protein 127	R.SAYLSC*LQR.E	144	0.785	0.75	0.82	0.955
Q96BW9	TAMM41 Mitochondrial translocator assembly and maintenanc	K.IITSIQNNYGAGVYYNSLIMC*NGR.L	103	0.77	0.75		
Q96BW9	TAMM41 Mitochondrial translocator assembly and maintenanc	K.NRDVEETLFQVAHDPDC*GDVVR.L	285	0.97	1.075	1.37	1.905
Q96C01	FAM136A Protein FAM136A	R.C*SASCCEDSQASMK.Q	35	0.535	0.45	0.4	0.39
Q96CB9	NSUN4 Putative methyltransferase NSUN4	R.VLVDVPC*TTDR.H	258	1.24	1.94	2.22	4.025
Q96CM8	ACSF2 Acyl-CoA synthetase family member 2, mitochondrial	K.TVGQC*LETTAQR.V	77	1.62		4.88	
Q96CM8	ACSF2 Acyl-CoA synthetase family member 2, mitochondrial	K.QIC*PEVENAQPGALK.S	194	1.83			20
Q96CM8	ACSF2 Acyl-CoA synthetase family member 2, mitochondrial	R.MVSTPIGGLSYVQGC*TK.K	64				20
Q96CQ1	SLC25A36 Solute carrier family 25 member 36	K.TC*ATTIAYPHEVVR.T	239	1.165	1.095	1.245	1.34
Q96CQ1	SLC25A36 Solute carrier family 25 member 36	R.MGAFEC*VR.K	163	1.11	0.86	0.84	1.075
Q96CU9	FOXRED1 FAD-dependent oxidoreductase domain-containing pro	K.VQSLGVLFC*QGEVTR.F	239	1.06	1.205	1.345	2.68
Q96D53	ADCK4 Uncharacterized aarF domain-containing protein kin	K.AAADGDRDC*VLQK.S	415	0.98			
Q96D53	ADCK4 Uncharacterized aarF domain-containing protein kin	R.IVQTLC*TVR.G	147	1.16		2.145	3.565
Q96DP5	MTFMT Methionyl-tRNA formyltransferase, mitochondrial	K.NSQAQPSQC*R.F	365	1.12		3.27	5.07
Q96DV4	MRPL38 39S ribosomal protein L38, mitochondrial	K.HQETMTPAGLSFFQC*R.W	321	1.475	1.58	2.305	
Q96DV4	MRPL38 39S ribosomal protein L38, mitochondrial	R.VAEGQVTC*PYLPPFPAR.G	252	1.27	1.59	2.45	4.465
Q96DV4	MRPL38 39S ribosomal protein L38, mitochondrial	K.QDQPIDFSEDARPSPC*YQLAQR.T	290	1.245	1.63	2.155	3.775
Q96E11	MRRF Ribosome-recycling factor, mitochondrial	K.SPQLILVNMASFPEC*TAAAIK.A	154	1.11	1.06	1.145	1.305
Q96E29	MTERFD1 mTERF domain-containing protein 1, mitochondrial	K.LVSIPDEIFC*EEIAK.A	399	1.125	1.02		2.51
Q96EH3	MALSU1 Mitochondrial assembly of ribosomal large subunit	R.SYDDQLAQIAPETVPEDFILGIEDDTSSVTPVELKC*E.-	233	0.89	1.17	1.65	2.57
Q96EH3	MALSU1 Mitochondrial assembly of ribosomal large subunit	R.DIC*VIQVPPEMR.Y	110	1.27	1.05	1.33	1.75
Q96EL2	MRPS24 28S ribosomal protein S24, mitochondrial	K.FMWGTFPGC*LADQLVLK.R	103	1.1		20	
Q96EL2	MRPS24 28S ribosomal protein S24, mitochondrial	R.GNQLEIC*AVVLR.Q	120	0.92	0.83	0.945	2.375
Q96EL3	MRPL53 39S ribosomal protein L53, mitochondrial	R.STNLNC*SVIADVR.H	49	0.885	1.11	1.36	2.06
Q96EL3	MRPL53 39S ribosomal protein L53, mitochondrial	R.VQFC*PFEK.N	21	1.015	1.13	1.435	1.97
Q96EL3	MRPL53 39S ribosomal protein L53, mitochondrial	R.HDGSEPC*VDVLFGDGHR.L	63	0.93	1.09	1.295	1.9
Q96ER9	CCDC51 Coiled-coil domain-containing protein 51	R.QVHSC*LEGLR.E	316	1.04	1.135	1.265	1.825
Q96ER9	CCDC51 Coiled-coil domain-containing protein 51	K.TC*SQMAGVVQLVK.S	331	1.02	0.98	1.2	1.66
Q96EY1	DNAJA3 DnaJ homolog subfamily A member 3, mitochondrial	R.C*NGKGNEPGTK.V	239	1.74	1.34		
Q96EY7	PTCD3 Pentatricopeptide repeat-containing protein 3, mit	K.DPDDDKFFQSAMSIC*SSLR.D	423	1.05	1.555	2.2	11.355
Q96EY7	PTCD3 Pentatricopeptide repeat-containing protein 3, mit	R.DKHPPELQVAFADC*AADIK.S	551	1.105	1.56	2.69	5.435
Q96EY7	PTCD3 Pentatricopeptide repeat-containing protein 3, mit	K.DIAEPHIPC*LMPEYFEPQIK.D	139	1.26	1.59	2.665	4.91

Q96EY7	PTCD3 Pentatricopeptide repeat-containing protein 3, mit	K.NEHSYC*TMIR.G	260	1.25	1.615	2.455	4.29
Q96EY7	PTCD3 Pentatricopeptide repeat-containing protein 3, mit	K.VSNSPSQAIEVVELASAFSLPIC*EG LTQR.V	642	1.215	1.45	1.78	4.19
Q96EY8	MMAB Cob(I)yrinic acid a,c-diamide adenosyltransferase,	K.IQC*TLQDVGSALATPC*SSAR.E	119	1.01	1.23	1.34	
Q96EY8	MMAB Cob(I)yrinic acid a,c-diamide adenosyltransferase,	K.ISSALHFC*R.A	185	0.92	0.81		
Q96EY8	MMAB Cob(I)yrinic acid a,c-diamide adenosyltransferase,	K.IQC*TLQDVGSALATPCSSAR.E	119	1.06	1.155	1.16	1.875
Q96GJ1	TRMT2B tRNA (uracil(54)-C(5))-methyltransferase homolog	R.DGNVVC*VQSNHLK.N	185	1.15	1.11	1.8	
Q96GW9	MARS2 Methionine--tRNA ligase, mitochondrial	R.INPSETYPAFCTTC*FPSEPGLVGPS VR.A	428			1.71	
Q96GW9	MARS2 Methionine--tRNA ligase, mitochondrial	R.VSEQFQQLFQEAGISC*TDFIR.T	132	0.96			0.91
Q96GW9	MARS2 Methionine--tRNA ligase, mitochondrial	K.ALEAVSSC*VR.Q	479	0.73	0.635	0.56	0.615
Q96H55	MYO19 Unconventional myosin-XIX	R.LHPC*TSSGPDSPYPAK.G	678	5.915		4.87	
Q96H55	MYO19 Unconventional myosin-XIX	R.IETALAGSPC*LGHNK.L	515	1.7			
Q96H55	MYO19 Unconventional myosin-XIX	R.YADIC*PEPSPYSITGFNQILLER.H	937	0.76	3.275	0.46	20
Q96HP4	OXNAD1 Oxidoreductase NAD-binding domain-containing prote	K.IAC*SLHVTK.Q	241	1.095	1.6	1.81	
Q96HP4	OXNAD1 Oxidoreductase NAD-binding domain-containing prote	K.VC*GAASESPSVK.S	69	1.265	1.66	2.04	3.64
Q96HS1	PGAM5 Serine/threonine-protein phosphatase PGAM5, mitoch	R.ADARQEEDSYEIFIC*HANVIR.Y	229	0.905	0.965	1.005	1.015
Q96HY7	DHTKD1 Probable 2-oxoglutarate dehydrogenase E1 component	K.LVGC*AIIHVNGDSPEEVVR.A	392		0.86	1.95	
Q96HY7	DHTKD1 Probable 2-oxoglutarate dehydrogenase E1 component	K.TLVFC*SGK.H	808	1.21			3.93
Q96HY7	DHTKD1 Probable 2-oxoglutarate dehydrogenase E1 component	R.SSLYC*SDIGK.L	383	1.33	7.22	1.76	3.25
Q96HY7	DHTKD1 Probable 2-oxoglutarate dehydrogenase E1 component	R.VEELC*PFPLDSLQQEMSK.Y	839	1.115	1.395	2	2.98
Q96I23	PYURF Protein preY, mitochondrial	K.TEEPPRDFDPALLEFLVC*PLSK.K	60		0.68		
Q96I51	WBSCR16 Williams-Beuren syndrome chromosomal region 16 pro	K.ISSAAC*GYGFTLLSSK.T	114	0.96		1.6	
Q96I51	WBSCR16 Williams-Beuren syndrome chromosomal region 16 pro	R.VTMPGEPVDVAC*GVDHMVTLA K.S	451	1.16		1.98	2.98
Q96I51	WBSCR16 Williams-Beuren syndrome chromosomal region 16 pro	R.VLQVSC*GR.A	181	1.1	1.29	1.575	2.28
Q96I59	NARS2 Probable asparagine--tRNA ligase, mitochondrial	R.YLQC*ILGVDNIKDVIPFPR.F	455	1.08			
Q96I59	NARS2 Probable asparagine--tRNA ligase, mitochondrial	K.VIGNC*DAK.D	121	1.175	1.46	1.73	4.555
Q96I99	SUCLG2 Succinyl-CoA ligase	R.SC*NGPVLVGSPQGGVDIEEVAAS NPELIFK.E	162	1.12	1.37	1.765	2.94
Q96I99	SUCLG2 Succinyl-CoA ligase	K.IDATQVEVNPFGETPEGQVVC*FD AK.I	255	1.125	1.245	1.71	2.395
Q96JX3	SERAC1 Protein SERAC1	R.IIAQAC*DPK.T	173	1.15	1.17	1.945	2.535
Q96KR6	FAM210B Protein FAM210B	R.GHQDPSQATGTTGSSVSC*TEEK.K	77	0.94	1.33	1.715	3.485
Q96NB2	SFXN2 Sideroflexin-2	K.C*ELPVSYLEPK.L	290	1.1	1.12	1.74	3.355
Q96Q11	TRNT1 CCA tRNA nucleotidyltransferase 1, mitochondrial	K.YQGEHC*LLK.E	373	0.88			
Q96QE5	TEFM Transcription elongation factor, mitochondrial	K.KITPNVTFC*DENAKEPENALDK.L	50	0.82	1.55	1.72	3.42
Q96QE5	TEFM Transcription elongation factor, mitochondrial	K.STVQVC*NSILCPK.T	130				1.41
Q96RP9	GFM1 Elongation factor G, mitochondrial	K.GFLDAC*EK.G	594	1.005	0.81	1.14	5.855
Q96RP9	GFM1 Elongation factor G, mitochondrial	R.SC*TEGKGEYTMEYSR.Y	706	1.3	1.78	3.56	4.8
Q96RP9	GFM1 Elongation factor G, mitochondrial	R.EYGCPC*ITGKPK.V	516		1.25	2.77	3.71
Q96RP9	GFM1 Elongation factor G, mitochondrial	R.YQPC*LPSTQEDVINK.Y	723	1.19	1.395	1.755	1.24
Q96RP9	GFM1 Elongation factor G, mitochondrial	R.AAATDHRQELIEC*VANSDEQLGE MFLEEK.I	256	0.995	1.19	2.43	0.99
Q96RQ3	MCCC1 Methylcrotonoyl-CoA carboxylase subunit alpha, mit	K.SIMAAAGVPVVEGYHGEDQSDQC *LKEHAR.R	190			10.06	
Q96RR1	PEO1 Twinkle protein, mitochondrial	K.GATTQNSEIC*SGQAPTPDQPDTS KR.S	667	1.1	1.86	2.26	5.7
Q96T52	IMMP2L Mitochondrial inner membrane protease subunit 2	R.VAC*VAR.V	35	1.13	1.41	1.805	1.55
Q96TA2	YME1L1 ATP-dependent zinc metalloprotease YME1L1	K.ANAPC*VIFIDELDSVGGK.R	433	0.91	0.985	0.985	1.225
Q96TC7	FAM82A2 Regulator of microtubule dynamics protein 3	R.DSDKESEDGEDEVSC*ETVK.M	202			1.86	
Q96TC7	FAM82A2 Regulator of microtubule dynamics protein 3	R.C*HMEENQR.V	128	1.51	1.215	1.335	3.465
Q96TC7	FAM82A2 Regulator of microtubule dynamics protein 3	R.AYSDMC*ELTEEVSEK.K	288	0.77	1.125	1.5	2.77
Q99497	PARK7 Protein DJ-1	K.VTVAGLAGKDPVQC*SR.D	46	1.095	1.415	1.84	2.97
Q99536	VAT1 Synaptic vesicle membrane protein VAT-1 homolog	R.AC*GLNFADLMAR.Q	86	0.78	0.695	0.675	0.695
Q99551	MTERF Transcription termination factor, mitochondrial	K.C*HNTDSEPLKNEDLLK.N	62	1.36	1.56	2.745	4.53
Q99595	TIMM17A Mitochondrial import inner membrane translocase su	R.IVDDC*GGAFTMGTIGGGIFQAIK. G	17	1.165	1.09	1.43	1.585
Q99643	SDHC Succinate dehydrogenase cytochrome b560 subunit, m	K.SLC*LGPALIHTAK.F	107	1.005			
Q99714	HSD17B10 3-hydroxyacyl-CoA dehydrogenase type-2	K.KLGNNC*VFAPADVTSEK.D	58	1.19	1.44	1.93	3.125
Q99714	HSD17B10 3-hydroxyacyl-CoA dehydrogenase type-2	K.VC*NFLASQVPFPSR.L	214	1.13	1.27	1.725	2.31
Q99714	HSD17B10 3-hydroxyacyl-CoA dehydrogenase type-2	K.FGRVDVAVNC*AGIAVASK.T	91	0.985	1.085	1.32	1.82

Q99797	MIPEP Mitochondrial intermediate peptidase	R.AVASMVWKEC*FLQDPFNR.A	649	1.42			
Q99797	MIPEP Mitochondrial intermediate peptidase	R.EAAEEAC*R.S	142	1.12	1.41	1.805	2.475
Q99798	ACO2 Aconitate hydratase, mitochondrial	R.DLGGIVLANAC*GPCIGQWDR.K	448	1.17	1.34		
Q99798	ACO2 Aconitate hydratase, mitochondrial	R.DLGGIVLANAC*GPC*IGQWDR.K	448	2.08			
Q99798	ACO2 Aconitate hydratase, mitochondrial	R.VGLIGSC*TNSSYEDMGR.S	385	1.55	1.995	16.34	13.26
Q99798	ACO2 Aconitate hydratase, mitochondrial	K.VAVPSTIHC*DHLIEAQVGGEK.D	126		1.3	1.83	5.41
Q99798	ACO2 Aconitate hydratase, mitochondrial	K.C*TTDHISAAGPWLK.F	592	1.155	1.345	1.95	3.345
Q99807	COQ7 Ubiquinone biosynthesis protein COQ7 homolog	K.SIIQAGC*R.V	207	1.125	0.78	0.655	1.755
Q99832	CCT7 T-complex protein 1 subunit eta	K.C*AMTALSSK.L	158	1.13	1.63	1.91	
Q99832	CCT7 T-complex protein 1 subunit eta	R.TMMAC*GGSIQTSVNALSADVLG R.C	326		0.61		
Q99832	CCT7 T-complex protein 1 subunit eta	K.EGTDSSQGIPQLVSNISAC*QVIAE AVR.T	29		5.07	10.8	20
Q99832	CCT7 T-complex protein 1 subunit eta	R.YNFFTGC*PK.A	364	1.095			3.385
Q99832	CCT7 T-complex protein 1 subunit eta	K.LPIGDVATQYFADRDMFC*AGR.V	310	1.225	1.5	2.05	2.63
Q99832	CCT7 T-complex protein 1 subunit eta	R.QLC*DNAGFDATNILNK.L	450	0.92	1.65	1.77	1.845
Q9BPW8	NIPSNAP1 Protein NipSnap homolog 1	K.LHLDEDYPC*SLVGNWNTWYGEQ DQAVHLWR.F	106	0.97	1.01	1	
Q9BPW8	NIPSNAP1 Protein NipSnap homolog 1	R.FSGGYPALMDC*MNK.L	138	1.005	1.09	1.23	1.53
Q9BPX6	MICU1 Calcium uptake protein 1, mitochondrial	K.SGLC*SALTTYFFGADLK.G	275	1.4	1.36	2.43	
Q9BPX6	MICU1 Calcium uptake protein 1, mitochondrial	R.AHAESPPC*VDNLK.S	62		1.98		20
Q9BPX6	MICU1 Calcium uptake protein 1, mitochondrial	K.NKDEGDVC*NHEK.K	83	1.15		3.58	7.415
Q9BQ52	ELAC2 Zinc phosphodiesterase ELAC protein 2	K.EGPTLSVPMVQGEC*LLK.Y	421	1.04			
Q9BQ52	ELAC2 Zinc phosphodiesterase ELAC protein 2	K.VC*FGDFPTMPK.L	753				0.885
Q9BQ52	ELAC2 Zinc phosphodiesterase ELAC protein 2	R.YLFNC*GEGVQR.L	87	0.93		0.89	0.88
Q9BQ69	MACROD1 O-acetyl-ADP-ribose deacetylase MACROD1	R.EEHYFC*KDFVR.L	116				16.56
Q9BQ69	MACROD1 O-acetyl-ADP-ribose deacetylase MACROD1	R.AAGPLLTDEC*R.T	199	1.24	1.82	3.085	6.96
Q9BQ69	MACROD1 O-acetyl-ADP-ribose deacetylase MACROD1	K.LEVDAIVNAANSSLLGGGGVDGC *IHR.A	186	1.12		2.77	5.71
Q9BQ69	MACROD1 O-acetyl-ADP-ribose deacetylase MACROD1	R.SC*YLSSLDLLLEHR.L	246	2.1	1.585	2.56	4.43
Q9BQP7	C20orf72 Uncharacterized protein C20orf72	R.GVAQTPGSVEEDALLC*GPVSK.H	79	0.985	1.06	1.065	1.21
Q9BQP7	C20orf72 Uncharacterized protein C20orf72	R.ALESAVQHETLNYIGLLDC*VAEY QGK.L	239	1.09		0.83	1.14
Q9BQT8	SLC25A21 Mitochondrial 2-oxodicarboxylate carrier	R.C*ATDPNSYK.S	46		1.17	1.66	2.42
Q9BRJ2	MRPL45 39S ribosomal protein L45, mitochondrial	R.SIHLAC*TAGIFDAYVPPEGDAR.I	80	1.185	1.4	1.875	2.835
Q9BRJ2	MRPL45 39S ribosomal protein L45, mitochondrial	R.C*SSMMNQGNVYGQITVR.M	199	1.07	1.36	1.455	1.815
Q9BRT2	MNF1 Mitochondrial nucleoid factor 1	R.EGENTQVAEPEAC*DQMYESLAR. L	53	0.91	1.54	1.25	
Q9BRT2	MNF1 Mitochondrial nucleoid factor 1	K.LC*EEWPVDETK.R	13	0.8	0.79	0.78	0.78
Q9BSF4	C19orf52 Uncharacterized protein C19orf52	R.DC*DINDDEFLHLPAHLR.V	182	1.135	1.03	10.68	10.925
Q9BSF4	C19orf52 Uncharacterized protein C19orf52	R.ALLRDYAEAC*R.D	46	1.065	1.145	1.37	1.75
Q9BSF4	C19orf52 Uncharacterized protein C19orf52	R.YVNLGLC*SLVYEAPFDAQASLYQ AR.C	130	1.225	0.88		1.05
Q9BSH4	TACO1 Translational activator of cytochrome c oxidase 1	K.LDSLGLC*SVSC*ALEFIPNSK.V	252		1.62		
Q9BSH4	TACO1 Translational activator of cytochrome c oxidase 1	K.EGGPNPEHNSNLANILEVC*R.S	112	1.1	1.37	1.89	2.97
Q9BSH4	TACO1 Translational activator of cytochrome c oxidase 1	K.FIC*DASSLHQVR.K	234	1.1	1.3	1.535	2.005
Q9BSH4	TACO1 Translational activator of cytochrome c oxidase 1	K.LDSLGLC*SVSCALEFIPNSK.V	252			1.72	1.77
Q9BSK2	SLC25A33 Solute carrier family 25 member 33	K.GCASC*IAYPHEVIR.T	249	0.53			
Q9BSK2	SLC25A33 Solute carrier family 25 member 33	R.AVYFAC*YSK.A	111	1.49			1.45
Q9BT30	ALKBH7 Probable alpha-ketoglutarate-dependent dioxygenase	R.ISVIC*R.S	202				2.11
Q9BTZ2	DHRS4 Dehydrogenase/reductase SDR family member 4	R.VNC*LAPGLIK.T	209	1.125	1.32	1.73	2.52
Q9BU61	NDUFAF3 NADH dehydrogenase	R.GIAVEVQDTPNAC*ATFNFLCHEG R.V	150	0.8		0.5	
Q9BUR5	APOO Apolipoprotein O	R.HYC*EPYTTWCQETYSQTKPK.M	71	0.99	1.005	1.08	1.4
Q9BV79	MECR Trans-2-enoyl-CoA reductase, mitochondrial	R.GQLTAPAC*SQVPLQDYQSALEAS MKPFISSK.Q	345	1.33	1.645	2.025	4.13
Q9BV79	MECR Trans-2-enoyl-CoA reductase, mitochondrial	R.LALNC*VGGK.S	263	1.235	1.44	2.055	3.695
Q9BVS5	TRMT61B Potential tRNA (adenine(58)-N(1))-methyltransferas	R.C*GPTHQGSEDPSMLSQAQSATEV EER.H	112	0.975			
Q9BVS5	TRMT61B Potential tRNA (adenine(58)-N(1))-methyltransferas	R.HVSPSC*STSR.E	143	1.115	1.23		3.83
Q9BVV7	TIMM21 Mitochondrial import inner membrane translocase su	K.DGLKHTC*VK.F	192	0.895	1.05	1.19	1.54
Q9BW92	TARS2 Threonine--tRNA ligase, mitochondrial	R.LALSTRPSGFLGDPC*LWDQAEQV LK.Q	506	1.28	1.31	2.42	
Q9BW92	TARS2 Threonine--tRNA ligase, mitochondrial	R.LLGVLAESC*GGK.W	603	1.11		1.78	3.55
Q9BW92	TARS2 Threonine--tRNA ligase, mitochondrial	R.IC*QELTAAAR.P	185	1.13	1.26	1.745	2.445
Q9BWM7	SFXN3 Sideroflexin-3	R.FVPFAAVAAANC*INIPLMR.Q	189		1.295	1.22	0.95
Q9BX68	HINT2 Histidine triad nucleotide-binding protein 2, mito	K.SLPADILYEDQQC*LVFR.D	75			0.54	0.5
Q9BXK5	BCL2L13 Bcl-2-like protein 13	R.HTSPVFSPANPESSMEDC*LAHLG EK.V	103	1.135	1.135	1.195	1.25
Q9BXR0	QTRT1 Queuine tRNA-ribosyltransferase	R.LVAEC*SR.S	23		0.74		
Q9BXW7	CECR5 Cat eye syndrome critical region protein 5	K.AQELSALLGC*EVDADQVILSHSP MK.L	109	1	1.255	1.58	2.56

Q9BYC8	MRPL32 39S ribosomal protein L32, mitochondrial	K.NNIDVC*PEC*GHLK.Q	110	0.75	0.91	1.27	
Q9BYC8	MRPL32 39S ribosomal protein L32, mitochondrial	K.HVLC*AYCYEK.V	123	0.885	0.97	0.895	2.19
Q9BYC8	MRPL32 39S ribosomal protein L32, mitochondrial	K.NNIDVC*PECGHLK.Q	110	1.045	1.355	1.26	2.145
Q9BYD6	MRPL1 39S ribosomal protein L1, mitochondrial	K.IATLDMSSDQIAANLQAVINEVC*R.H	279	0.985	1	1.075	1.295
Q9BYT8	NLN Neurolysin, mitochondrial	R.IVHLQETC*DLGK.I	153	1.095	1.52	1.6	1.97
Q9BZE1	MRPL37 39S ribosomal protein L37, mitochondrial	K.RETYC*PVIVDNLIQLCK.S	177	1.12	2.15	1.02	
Q9BZE1	MRPL37 39S ribosomal protein L37, mitochondrial	R.ETYC*PVIVDNLIQLC*K.S	177	1.18	0.76	2.09	
Q9BZE1	MRPL37 39S ribosomal protein L37, mitochondrial	K.NHVLETFYPISPIIDLHEC*NIYDVK.N	268	1.14	1.38	2.04	3.78
Q9BZE1	MRPL37 39S ribosomal protein L37, mitochondrial	R.NHIENQDEC*VLNVISHAR.L	153	1.14	1.5	1.99	3.775
Q9BZE1	MRPL37 39S ribosomal protein L37, mitochondrial	R.IC*VQNSTFSATWNR.E	203	0.93	1.14	2.445	3.32
Q9GZY8	MFF Mitochondrial fission factor	R.VC*PPHMLPEDGANLSSAR.G	209	1.49	1.36		
Q9H061	TMEM126A Transmembrane protein 126A	R.C*FVSFPLNTGDLDCETC*TITR.S	85			0.72	
Q9H061	TMEM126A Transmembrane protein 126A	R.C*FVSFPLNTGDLDC*ETCTITR.S	85			0.72	
Q9H061	TMEM126A Transmembrane protein 126A	R.C*FVSFPLNTGDLDCETCTITR.S	85	0.84	0.765	0.995	0.755
Q9H078	CLPB Caseinolytic peptidase B protein homolog	K.TIDC*KDAIFIMTSNVASDEIAQHALQLR.Q	486	1.13		1.81	
Q9H078	CLPB Caseinolytic peptidase B protein homolog	R.VVNQLAAAYEQDLLPGGC*TLR.I	647	1.1	1.295	1.65	2.545
Q9H078	CLPB Caseinolytic peptidase B protein homolog	K.GC*TALHYAVLADDYR.T	267	1.08	1.195	1.56	2.485
Q9H0R6	QRSL1 Glutamyl-tRNA(Gln) amidotransferase subunit A, mit	R.C*VDDAAIVLGALAGPDPR.D	236		1.6		
Q9H0R6	QRSL1 Glutamyl-tRNA(Gln) amidotransferase subunit A, mit	K.QVQFPVIQLQELMDDC*SAVLENEK.L	512	1.8	2.01		
Q9H0R6	QRSL1 Glutamyl-tRNA(Gln) amidotransferase subunit A, mit	K.DNFSTSGIETTC*ASNMLK.G	88	1.41	1.775	2.185	12.11
Q9H0R6	QRSL1 Glutamyl-tRNA(Gln) amidotransferase subunit A, mit	K.QGQITPTELC*QK.C	24	1.23	1.565	2.36	5.025
Q9H0R6	QRSL1 Glutamyl-tRNA(Gln) amidotransferase subunit A, mit	R.AFC*DQQLLTVAK.W	483	1.035	2.03	2.635	4.625
Q9H0U6	MRPL18 39S ribosomal protein L18, mitochondrial	R.NVVAC*ESIGR.V	125	1.065	1.155	1.345	1.785
Q9H1K1	ISCU Iron-sulfur cluster assembly enzyme ISCU, mitochon	K.LHC*SMLAEDAIK.A	138	1.165	1.39	3.32	3.245
Q9H2U2	PPA2 Inorganic pyrophosphatase 2, mitochondrial	K.DKSTNC*FGDNDPIDVC*EIGSK.I	161	1.425	1.96	4.575	13.58
Q9H2U2	PPA2 Inorganic pyrophosphatase 2, mitochondrial	R.GQPC*SQNYR.L	44	1.11	1.48	1.945	3.765
Q9H2U2	PPA2 Inorganic pyrophosphatase 2, mitochondrial	K.STHQC*WK.A	274	1.125	1.435	1.78	3.235
Q9H2U2	PPA2 Inorganic pyrophosphatase 2, mitochondrial	K.ILSC*GEVIHVK.I	180	1.165	1.39	1.98	3.055
Q9H2U2	PPA2 Inorganic pyrophosphatase 2, mitochondrial	K.STNC*FGDNDPIDVCEIGSK.I	161	1.09	1.285	1.675	1.5
Q9H300	PARL Presenilins-associated rhomboid-like protein, mito	R.YGPSLGASGAIMTVLAAVC*TK.I	288		0.71		
Q9H4A6	GOLPH3 Golgi phosphoprotein 3	R.LQLEAC*GMR.R	108	1.35	1.04	1.84	3.08
Q9H4B0	OSGEPL1 Probable tRNA threonylcarbamoyladenosine biosynthe	K.HPEC*STMSGGK.A	216	1.48		3.83	
Q9H4B0	OSGEPL1 Probable tRNA threonylcarbamoyladenosine biosynthe	K.C*PLGVDISK.E	390	1.22	1.665		
Q9H4K7	GTPBP5 GTP-binding protein 5	R.APVTC*TPGQPGQQR.V	206	1.17	1.56	2.215	4.055
Q9H5Q4	TFB2M Dimethyladenosine transferase 2, mitochondrial	R.VIHC*DFFK.L	149	1.145	2.11	1.46	
Q9H5Q4	TFB2M Dimethyladenosine transferase 2, mitochondrial	R.SKDC*AYKWLYDETLEDR.-	383		2.57		
Q9H649	NSUN3 Putative methyltransferase NSUN3	K.VLDLC*AAPGGK.S	139	1.075		2.34	3.18
Q9H6K4	OPA3 Optic atrophy 3 protein	R.AQLC*NPGR.S	164	1.575	1.59	2.125	2.985
Q9H7Z7	PTGES2 Prostaglandin E synthase 2	K.TC*PFCSK.V	110	1.19	1.42	1.535	2.16
Q9H845	ACAD9 Acyl-CoA dehydrogenase family member 9, mitochondr	R.GSNTC*EVHFENTK.I	271	1.02	1.16	1.285	1.58
Q9H845	ACAD9 Acyl-CoA dehydrogenase family member 9, mitochondr	R.AYIC*AHPLDR.T	613	1.04	1.14	1.28	1.45
Q9H845	ACAD9 Acyl-CoA dehydrogenase family member 9, mitochondr	K.LASGEHIAAFC*LTEPASGSDAASIR.S	179	0.95	1.025	1.195	1.285
Q9H845	ACAD9 Acyl-CoA dehydrogenase family member 9, mitochondr	R.AYICAHPLDRTC*.-	621	0.77	0.88	0.9	0.99
Q9H857	NT5DC2 5-nucleotidase domain-containing protein 2	R.FSDLYMASLSC*LLNYR.V	475	0.89	0.9		1.3
Q9H936	SLC25A22 Mitochondrial glutamate carrier 1	K.LINGGIAGLIGVTC*VFPIDLAK.T	25	1.04	1.04	1.09	
Q9H936	SLC25A22 Mitochondrial glutamate carrier 1	K.EMLAGC*GAGTC*QVIVTTPMEMLK.I	111	0.925	1.2	1.91	
Q9H936	SLC25A22 Mitochondrial glutamate carrier 1	R.GVNEDTYSGILDC*AR.K	271	1.275	1.335	1.665	2.065
Q9H936	SLC25A22 Mitochondrial glutamate carrier 1	K.EMLAGC*GAGTCQVIVTTPMEMLK.I	111			2.19	1.84
Q9H936	SLC25A22 Mitochondrial glutamate carrier 1	R.VYTSMSDC*LIK.T	52	1.02	1.155	1.36	1.565
Q9H9B4	SFXN1 Sideroflexin-1	R.MSAQVPMNMTITGC*MMTFYR.T	106	0.84	1.045	1.11	
Q9H9J2	MRPL44 39S ribosomal protein L44, mitochondrial	K.NLVDFLTGEEVVC*HVAR.N	167	1.12	1.3	1.94	3.25
Q9H9J2	MRPL44 39S ribosomal protein L44, mitochondrial	K.TAFVNSC*YIK.S	96	1.175	1.355	1.91	3.04
Q9H9J2	MRPL44 39S ribosomal protein L44, mitochondrial	K.SNQELSEQGTSFSQTC*LTQFLEDEYPDMPTEGIK.N	136	1.195	1.42	2	3.04
Q9H9J2	MRPL44 39S ribosomal protein L44, mitochondrial	R.QSGGTTALPLYFVGLYC*DK.K	276	1.045	1.21	1.605	2.15

Q9H9P8	L2HGDH L-2-hydroxyglutarate dehydrogenase, mitochondrial	R.GLMAIDC*PHTGIVDYR.Q	187	1.35	1.59		
Q9H9P8	L2HGDH L-2-hydroxyglutarate dehydrogenase, mitochondrial	R.ISELSGC*TPDPR.I	272	1.16	1.54	2.2	3.2
Q9H9P8	L2HGDH L-2-hydroxyglutarate dehydrogenase, mitochondrial	K.AC*FLGATVK.Y	376	1.125	1.205	1.55	2.17
Q9HA77	CARS2 Probable cysteine--tRNA ligase, mitochondrial	K.GQLAC*GSVR.E	387	1.005	0.99	0.98	1.14
Q9HA92	RSAD1 Radical S-adenosyl methionine domain-containing pr	R.THSAC*DALR.T	175	1.215	1.535	2.245	3.84
Q9HAV7	GRPEL1 GrpE protein homolog 1, mitochondrial	K.ATQC*VPK.E	124	0.99	1.075	1.2	1.44
Q9HAV7	GRPEL1 GrpE protein homolog 1, mitochondrial	K.LYGIQAFC*K.D	108	0.915	0.98	1.005	1.11
Q9HBH1	PDF Peptide deformylase, mitochondrial	R.C*VGLSAPQLGVPR.Q	108	0.49			
Q9HBH1	PDF Peptide deformylase, mitochondrial	R.LVTFPEGCESVAGFLAC*VPR.F	181	0.57	0.59	0.61	0.65
Q9HBH5	RDH14 Retinol dehydrogenase 14	R.LDVLINNAGIFQC*PYMK.T	148	1.165	1.785	12.23	9.34
Q9HBH5	RDH14 Retinol dehydrogenase 14	R.QAAEC*GPEPGVSGVGELIVR.E	97	0.92	1.495	2.5	6.83
Q9HBH5	RDH14 Retinol dehydrogenase 14	R.YFGDC*KEEELLPK.A	306		1.61	2.64	3.54
Q9HBH5	RDH14 Retinol dehydrogenase 14	R.AFC*QEMLQEEPR.L	126		1.555	1.995	2.81
Q9HC21	SLC25A19 Mitochondrial thiamine pyrophosphate carrier	K.KNENLQNLLC*GSGAGVISK.T	222	1.155	1.25	1.605	2.215
Q9HC21	SLC25A19 Mitochondrial thiamine pyrophosphate carrier	K.GLMDC*AK.Q	268	0.925	1.06	1.155	1.52
Q9HC36	RNMTL1 RNA methyltransferase-like protein 1	K.GC*VDAWEPK.V	244	1.155	1.065	0.97	
Q9HC36	RNMTL1 RNA methyltransferase-like protein 1	K.ASDHGWVC*DQR.V	309	1.48	1.62	2.4	4.93
Q9HC36	RNMTL1 RNA methyltransferase-like protein 1	R.SAAGAGC*SK.V	235	1.16	1.38	1.86	2.645
Q9HCC0	MCCC2 Methylcrotonoyl-CoA carboxylase beta chain, mitoch	K.MVAAVAC*AQVPK.I	431	1.035	1.1		
Q9HCC0	MCCC2 Methylcrotonoyl-CoA carboxylase beta chain, mitoch	K.GTHFVQLC*CQR.N	391	0.93	1.21		
Q9HCC0	MCCC2 Methylcrotonoyl-CoA carboxylase beta chain, mitoch	K.AATGEEVSAEDLGGADLHC*R.K	267	1.12	1.495	2.58	5.525
Q9HCC0	MCCC2 Methylcrotonoyl-CoA carboxylase beta chain, mitoch	R.LPC*IYLVDSGGAYLPR.Q	167	1.005	1.11	1.395	2.17
Q9HCC0	MCCC2 Methylcrotonoyl-CoA carboxylase beta chain, mitoch	R.VSGVEC*MIIANDATVK.G	131			1.425	1.52
Q9HD23	MRS2 Magnesium transporter MRS2 homolog, mitochondrial	K.AVITPEC*LLILDYR.N	148		0.49	0.54	0.56
Q9HD33	MRPL47 39S ribosomal protein L47, mitochondrial	K.SGAAWTC*QQLR.N	87	1.08	1.16	1.645	1.98
Q9NNW7	TXNRD2 Thioredoxin reductase 2, mitochondrial	K.ASFVDEHTVC*GVAK.G	168	0.63			1.48
Q9NP81	SARS2 Serine--tRNA ligase, mitochondrial	R.FC*ACPEEAAHALELR.K	64		1.37	3.97	
Q9NP81	SARS2 Serine--tRNA ligase, mitochondrial	R.GAVFEGC*GMTPNANPSQIYNIDPAR.F	272	1.215	1.685	2.175	3.685
Q9NP81	SARS2 Serine--tRNA ligase, mitochondrial	R.FGEVTSASNC*TDFQSR.R	425	1.255	1.51	2.105	3.315
Q9NP81	SARS2 Serine--tRNA ligase, mitochondrial	R.MVCSSTC*YR.A	328	1.265		1.645	1.75
Q9NP92	MRPS30 28S ribosomal protein S30, mitochondrial	K.NIC*WGTQSKPLYETIEDNDVK.G	393	1.23	2.255	4.22	6.69
Q9NP92	MRPS30 28S ribosomal protein S30, mitochondrial	R.QNC*ADQIEVVFR.A	316	1.195	1.78	3.43	5.73
Q9NPL8	TIMMDC1 Translocase of inner mitochondrial membrane domain	R.ISKDLANIC*K.T	78	0.895	0.845	0.915	0.82
Q9NQG6	SMCR7L Mitochondrial dynamic protein MID51	R.ALDQADSGC*R.S	359	1.405	1.76	2.905	4.23
Q9NQH7	XPNPEP3 Probable Xaa-Pro aminopeptidase 3	R.IEDDVVVTQDSPLILSADC*PK.E	492	1.065	1.495	2.74	
Q9NQH7	XPNPEP3 Probable Xaa-Pro aminopeptidase 3	K.FEFEC*R.A	290	1.24	1.44	1.755	2.385
Q9NQZ5	STARD7 StAR-related lipid transfer protein 7, mitochondri	R.KNEGSC*GPAR.I	362	1.045	1.21	1.895	3.475
Q9NRK6	ABCB10 ATP-binding cassette sub-family B member 10, mitoc	K.IGTVSQEPILFSC*SIAENIAYGADDPSSVTAEEIQR.V	582	1.05	1.03	1.015	1.335
Q9NRP4	ACN9 Protein ACN9 homolog, mitochondrial	K.AC*FGTFLPEEK.L	80	1.05	1.09	1.265	1.87
Q9NRY6	PLSCR3 Phospholipid scramblase 3	R.SGAGQPLGQAAEESNCC*AR.L	126			0.76	
Q9NSE4	IARS2 Isoleucine--tRNA ligase, mitochondrial	K.DRLYC*EKENDPK.R	808	0.73		1.21	3.155
Q9NSE4	IARS2 Isoleucine--tRNA ligase, mitochondrial	K.C*GFSELYSWQR.E	91		0.33	1.48	2.765
Q9NSE4	IARS2 Isoleucine--tRNA ligase, mitochondrial	K.KPGLEEAVESAC*AMR.D	883	1.185	1.42	2.255	2.58
Q9NSE4	IARS2 Isoleucine--tRNA ligase, mitochondrial	R.C*AEVVSGK.-	1005	0.735	0.72	1.335	1.885
Q9NSE4	IARS2 Isoleucine--tRNA ligase, mitochondrial	K.YTAESSDTLC*PR.C	1002	0.48	0.76	0.82	1.535
Q9NUJ1	ABHD10 Abhydrolase domain-containing protein 10, mitochon	K.ALAIEEFC*K.S	100	0.81	1.02		0.47
Q9NUL7	DDX28 Probable ATP-dependent RNA helicase DDX28	R.HVVC*AAETGSGK.T	170	1.605	2.04	3.135	4.68
Q9NUQ2	AGPAT5 1-acyl-sn-glycerol-3-phosphate acyltransferase eps	K.ATHVAFDC*MK.N	217	1.025	1.06	1.49	1.8
Q9NUT2	ABCB8 ATP-binding cassette sub-family B member 8, mitoch	R.GAHC*IVVMADGR.V	678	0.67	0.48		
Q9NUT2	ABCB8 ATP-binding cassette sub-family B member 8, mitoch	R.YGAELEAC*R.C	364	1.15	1.25		2.69
Q9NVA1	UQCC Ubiquinol-cytochrome c reductase complex chaperone	R.MYTSC*VEK.T	124	0.925	1.01	1.475	1.52
Q9NVH1	DNAJC11 DnaJ homolog subfamily C member 11	K.AGLPGFYDPC*VGEEK.N	518	1.11	1.23	1.495	2.07
Q9NVH1	DNAJC11 DnaJ homolog subfamily C member 11	R.C*FVTTNCALQFSSR.G	235				1.74
Q9NVH1	DNAJC11 DnaJ homolog subfamily C member 11	K.VIDVTVPLQC*LVK.D	494	0.955	1.055	1.16	1.43
Q9NVH1	DNAJC11 DnaJ homolog subfamily C member 11	R.LC*MLYHPDK.H	38	0.91	1.22	0.925	0.685
Q9NVH6	TMLHE Trimethyllysine dioxygenase, mitochondrial	R.SLDTASVDLC*IKPK.T	103	0.74			
Q9NVH6	TMLHE Trimethyllysine dioxygenase, mitochondrial	R.SASC*YNSK.T	85	0.79			1.81
Q9NVS2	MRPS18A 28S ribosomal protein S18a, mitochondrial	K.ESPNPPNPSGQC*PIC*R.W	70	0.88	1.25		
Q9NVS2	MRPS18A 28S ribosomal protein S18a, mitochondrial	R.DNVC*YSR.T	186	1.215	1.64	2.365	4.285

Q9NVS2	MRPS18A 28S ribosomal protein S18a, mitochondrial	K.ITGLC*QEEHR.K	108	1.17	1.64	2.185	3.385
Q9NVS2	MRPS18A 28S ribosomal protein S18a, mitochondrial	K.ESPNPPNPSGQC*PICR.W	70	1.055	1.03	1.315	1.78
Q9NVV4	MTPAP Poly(A) RNA polymerase, mitochondrial	K.ILSVLGEC*LDHFGPGCVGVQK.I	291	0.94			
Q9NVV4	MTPAP Poly(A) RNA polymerase, mitochondrial	K.TLADAEDKC*VIEGNNC*TFVR.D	412	1.59	2.7	4.19	7.16
Q9NVV4	MTPAP Poly(A) RNA polymerase, mitochondrial	R.FSHQASGFQC*DLTTNNR.I	324	1.26	1.505	2.055	3.135
Q9NW81	ATP5SL ATP synthase subunit s-like protein	R.LYPLADSLQELSLAGC*PR.I	184	1.465	1.525	2.08	3.84
Q9NWR8	CCDC109B Coiled-coil domain-containing protein 109B	K.IAYDVQC*PK.R	147	1.125	1.38	1.665	2.46
Q9NWS8	RMND1 Required for meiotic nuclear division protein 1 ho	K.FAFSNALC*LSVK.L	310	1.365			
Q9NWS8	RMND1 Required for meiotic nuclear division protein 1 ho	K.LQHC*MELTDLMR.N	409	1.26	1.52	1.525	2.065
Q9NWS8	RMND1 Required for meiotic nuclear division protein 1 ho	K.TC*QFLSIGR.R	390	1.19		1.875	1.09
Q9NWU1	OXSM 3-oxoacyl-	K.LPPTLNLDC*SEPEFDLNYVPLK.A	415			0.54	0.33
Q9NWU5	MRPL22 39S ribosomal protein L22, mitochondrial	K.VYC*HYFVK.L	166	0.93	1.27	1.08	1.34
Q9NX14	NDUFB11 NADH dehydrogenase	K.YREANGLPIMESNC*FDPSK.I	141	0.865	0.87	0.995	1.09
Q9NX20	MRPL16 39S ribosomal protein L16, mitochondrial	R.C*EFEEVQGFLDQVAHK.L	167	1.08	1.04		1.7
Q9NX40	OCIAD1 OCIA domain-containing protein 1	R.RVFAEC*NDESFWFR.S	38	1.04	0.885	1.04	1.345
Q9NX40	OCIAD1 OCIA domain-containing protein 1	K.LSYVKTC*QEK.F	98			0.78	0.95
Q9NX47	MARCH5 E3 ubiquitin-protein ligase MARCH5	R.VAC*PQCNAEYLIVFPK.L	65			0.96	0.89
Q9NX63	CHCHD3 Coiled-coil-helix-coiled-coil-helix domain-contain	R.ERIC*SEEER.A	112	1.07	1.13	1.765	3.365
Q9NX63	CHCHD3 Coiled-coil-helix-coiled-coil-helix domain-contain	R.YESHPVC*ADLQAK.I	183	1.035		1.38	2.36
Q9NYK5	MRPL39 39S ribosomal protein L39, mitochondrial	R.APEVPVISGAFC*YDVVLDSK.L	180		1.39		
Q9NYK5	MRPL39 39S ribosomal protein L39, mitochondrial	R.SC*AMMMGCVIER.A	146	1.13		12.205	11.495
Q9NYK5	MRPL39 39S ribosomal protein L39, mitochondrial	K.ATEEC*TST.-	335	1.115	1.415	2.16	8.02
Q9NYK5	MRPL39 39S ribosomal protein L39, mitochondrial	K.DC*DPGEVNK.A	133	1.075	1.345	1.87	3.05
Q9NYY8	FASTKD2 FAST kinase domain-containing protein 2	K.LHTLDTC*LK.L	546	1.175	1.85	2.35	
Q9NYY8	FASTKD2 FAST kinase domain-containing protein 2	K.LSEEC*NSLSDVLDAFSK.A	163		1.65	1.52	13.4
Q9NYY8	FASTKD2 FAST kinase domain-containing protein 2	K.VVLDNIHGC*PLR.I	377	1.155		2.365	4.06
Q9NYY8	FASTKD2 FAST kinase domain-containing protein 2	R.SAYC*LGSSHPR.G	645	1.11	1.43	1.855	3.58
Q9NYY8	FASTKD2 FAST kinase domain-containing protein 2	R.VAVLC*VSR.S	638	1.06	1.08	1.55	2.275
Q9NZ45	CISD1 CDGSH iron-sulfur domain-containing protein 1	K.IVHAFDMEDLGDKAVYC*R.C	72	5.725	0.8	0.78	0.69
Q9NZE8	MRPL35 39S ribosomal protein L35, mitochondrial	R.FLRLHC*GLWVR.R	119	1.085	1.31		
Q9NZE8	MRPL35 39S ribosomal protein L35, mitochondrial	R.EFVFC*NK.T	150	0.68	1.39	1.745	2.805
Q9NZJ6	COQ3 Hexaprenyldihydroxybenzoate methyltransferase, mit	K.GETEELQANAC*TNPAVHEK.L	358	1.195		2.065	
Q9NZJ6	COQ3 Hexaprenyldihydroxybenzoate methyltransferase, mit	K.ILDVGC*GGGLLTEPLGR.L	155	1.205		2.105	3.925
Q9NZJ7	MTCH1 Mitochondrial carrier homolog 1	R.RVSSGSC*FALE.-	385	5.885	10.7	2.15	2.355
Q9NZJ7	MTCH1 Mitochondrial carrier homolog 1	K.ETSYEMMMQC*VSR.M	206	0.86	1.08	1.025	1.2
Q9NZJ7	MTCH1 Mitochondrial carrier homolog 1	R.C*MVQFVGR.E	222	0.915	0.885	0.99	1.17
Q9P032	NDUFAF4 NADH dehydrogenase	K.AAETC*QEPK.E	87	0.885	0.91	1.08	1.58
Q9P0J1	PDP1	R.RSAATC*LQTR.G	132	1.13	1.085	1.455	1.68
Q9P0J6	MRPL36 39S ribosomal protein L36, mitochondrial	R.C*KDCYLVK.R	76	0.765	0.83	0.825	1.08
Q9P0J6	MRPL36 39S ribosomal protein L36, mitochondrial	R.CKDC*YLVK.R	79	0.78	0.83	0.87	1.04
Q9P0M9	MRPL27 39S ribosomal protein L27, mitochondrial	K.C*LYALEEGIVR.Y	88	0.845	0.96	1.105	1.185
Q9P2R7	SUCLA2 Succinyl-CoA ligase	R.IC*NQVLVC*ER.K	152	1.285	1.8	2.38	
Q9P2R7	SUCLA2 Succinyl-CoA ligase	K.ANLNYIGLDGNIGC*LVNGAGLA MATMDIIK.L	320	1.39	1.585	2.01	6.05
Q9P2R7	SUCLA2 Succinyl-CoA ligase	K.YDATMIEINPMVEDSDGAVLC*M DAK.I	270	1.305	1.81	2.015	4.27
Q9P2R7	SUCLA2 Succinyl-CoA ligase	K.ALIADSGLKILAC*DDLDEAAR.M	430	1.31	1.37	2.56	3.775
Q9P2R7	SUCLA2 Succinyl-CoA ligase	R.C*DVIAQGIVMAVK.D	384	1.155	1.325	1.815	2.675
Q9P2R7	SUCLA2 Succinyl-CoA ligase	K.GRIC*NQVLVCER.K	152	1.09	1.335	1.485	2.58
Q9UBQ7	GRHPR Glyoxylate reductase/hydroxypyruvate reductase	R.AADC*EVEQWDSDEPIPAK.E	29		1.57	1.535	2.945
Q9UBQ7	GRHPR Glyoxylate reductase/hydroxypyruvate reductase	R.VGYTPDVLTDTTAELAVSLLLTTC* R.R	123	1.21	1.58	1.72	2.7
Q9UDR5	AASS Alpha-aminoadipic semialdehyde synthase, mitochond	R.FNTDIAPYTTC*LINGIYWEQNTPR. L	305			1.46	
Q9UDR5	AASS Alpha-aminoadipic semialdehyde synthase, mitochond	K.FSPAGVEGC*PALPHK.L	342	1.28	1.93		
Q9UDR5	AASS Alpha-aminoadipic semialdehyde synthase, mitochond	K.GAQAIFNELPC*EYVEPHELK.E	240	1.375	1.15	2.785	12.995
Q9UDR5	AASS Alpha-aminoadipic semialdehyde synthase, mitochond	K.KYNINPVSMDIC*KQEEK.L	534	1.095	1.605	2.42	5.785

Q9UDR5	AASS Alpha-aminoadipic semialdehyde synthase, mitochond	K.AGGILQEDISEAC*LILGVK.R	87				4.52
Q9UDR5	AASS Alpha-aminoadipic semialdehyde synthase, mitochond	K.EVGATIESYISYC*GGLPAPEHSNN PLR.Y	633	1.14	1.71	2.69	4.48
Q9UDR5	AASS Alpha-aminoadipic semialdehyde synthase, mitochond	K.QLLC*DLVGISPSSEHDVLK.E	765	0.96	0.98	1.88	2.69
Q9UG56	PISD Phosphatidylserine decarboxylase proenzyme	R.PVC*GLHSVISPSDGR.I	181		1.81		
Q9UG63	ABCF2 ATP-binding cassette sub-family F member 2	R.LAHEDAEC*EK.L	186	1.13	1.54	2.17	
Q9UGC7	MTRF1L Peptide chain release factor 1-like, mitochondrial	R.IVHLPTGVVSEC*QQER.S	274	1.065	0.92	0.84	1.345
Q9UGM6	WARS2 Tryptophan--tRNA ligase, mitochondrial	K.AKELAYTVC*QEVK.K	350	1.005	1.06	0.955	0.86
Q9UGM6	WARS2 Tryptophan--tRNA ligase, mitochondrial	R.QSILDMTAVLLAC*GINPEK.S	102	0.86		0.76	0.72
Q9UH62	ARMCX3 Armadillo repeat-containing X-linked protein 3	K.MAEGGSGDVDDAGDC*SGAR.Y	52	1.13	1.47	2.325	4.65
Q9UH62	ARMCX3 Armadillo repeat-containing X-linked protein 3	K.VYMNQVC*DDTITSR.L	208	1.135	1.335	2.01	3.665
Q9UI43	FTSJ2 Putative ribosomal RNA methyltransferase 2	R.VLDC*GAAPGAWSQVAVQK.V	79	1.285	1.69	2.28	5.66
Q9UJA2	CRLS1 Cardiolipin synthase	K.YFNPC*YATAR.L	230	1.05	1.285	1.165	1.47
Q9UJS0	SLC25A13 Calcium-binding mitochondrial carrier protein Aral	R.DIPFSAIYFPC*YAHVK.A	503	0.995	1.1	1.18	
Q9UJZ1	STOML2 Stomatin-like protein 2	R.ERESLNASIVDAINQAADC*WGIR. C	167	0.785	0.79	0.825	1.04
Q9UKG9	CROT Peroxisomal carnitine O-octanoyltransferase	K.C*HSEPDGPGIAALTSEER.T	228	1.41		1.94	
Q9UKU7	ACAD8 Isobutyryl-CoA dehydrogenase, mitochondrial	R.KDAVALC*SMAK.L	351	1.45	1.37	1.445	1.405
Q9UKU7	ACAD8 Isobutyryl-CoA dehydrogenase, mitochondrial	K.FASYC*LTEPGSGSDAASLLTSAK.K	159			1.13	1.05
Q9UMS0	NFU1 NFU1 iron-sulfur cluster scaffold homolog, mitocho	K.LQGSC*TSC*PSSIITLK.N	210	1.11	1.6		
Q9UMS0	NFU1 NFU1 iron-sulfur cluster scaffold homolog, mitocho	K.LQGSC*TSCPSSIITLK.N	210		0.69		1.905
Q9UQ90	SPG7 Paraplegin	K.GALLLGPPGC*GK.T	353	1.16	1.49		
Q9UQ90	SPG7 Paraplegin	R.APC*IVYIDEIDAVGK.K	403	0.89			
Q9UQ90	SPG7 Paraplegin	R.LAELTPGFSGADIANIC*NEAALH AAR.E	525				2.72
Q9UQ90	SPG7 Paraplegin	R.MC*MALGGR.A	627	1.025	1.015	1.16	1.78
Q9Y276	BCS1L Mitochondrial chaperone BCS1	R.GYLLYGPPGC*GK.S	234	1.145	1.28	1.63	2.285
Q9Y277	VDAC3 Voltage-dependent anion-selective channel protein	K.YMLDC*R.T	229	1.105	1.33	1.81	3.45
Q9Y277	VDAC3 Voltage-dependent anion-selective channel protein	K.ASGNLETKYKVC*NYGLTFTQK.W	65	1.115	1.34	1.845	2.795
Q9Y277	VDAC3 Voltage-dependent anion-selective channel protein	K.IDLKTKSC*SGVEFSTSGHAYTDTG K.A	36	1.045	1.215	1.545	2.425
Q9Y2Q3	GSTK1 Glutathione S-transferase kappa 1	K.ETTEAAC*R.Y	176	1.08	1.22	1.43	2.13
Q9Y2R9	MRPS7 28S ribosomal protein S7, mitochondrial	K.NC*EPMIGLVPILK.G	152	1.095	1.205	1.38	2.05
Q9Y2R9	MRPS7 28S ribosomal protein S7, mitochondrial	K.WMITEC*R.D	191	1.045	1.19	1.49	1.8
Q9Y2S7	POLDIP2 Polymerase delta-interacting protein 2	R.DC*PHISQR.S	143	1.02	1.11	1.26	1.55
Q9Y2W6	TDRKH Tudor and KH domain-containing protein	K.ITC*DKESEGTLLLSR.L	160	1.345	1.625	2.365	4.085
Q9Y2W6	TDRKH Tudor and KH domain-containing protein	R.SDFLSLPFQAIEC*SLAR.I	419	1.34	1.9	2.36	3.885
Q9Y2W6	TDRKH Tudor and KH domain-containing protein	R.VLLISGFPVQVC*K.A	109	1.31	1.7	2.38	3.405
Q9Y2Z2	MTO1 Protein MTO1 homolog, mitochondrial	R.IC*DQSGVHYK.V	104	1.33		3.365	6.775
Q9Y2Z2	MTO1 Protein MTO1 homolog, mitochondrial	R.GYKDAGC*VSQQR.Y	520	1.83		2.17	6.46
Q9Y2Z4	YARS2 Tyrosine--tRNA ligase, mitochondrial	K.EAPFSEFFLDPGTSVLDTC*R.K	413	1.17	1.495	2.095	3.495
Q9Y305	ACOT9 Acyl-coenzyme A thioesterase 9, mitochondrial	K.SLEIC*HPQER.N	299	1.215	1.335	1.87	3.435
Q9Y375	NDUFAF1 Complex I intermediate-associated protein 30, mito	R.SGYC*AMISR.I	183	0.89	1.035	0.86	1.24
Q9Y399	MRPS2 28S ribosomal protein S2, mitochondrial	K.MNIPTVGIVDTNC*NPCLITYPVPG NDDSPLAVHLYCR.L	227	1.03			
Q9Y399	MRPS2 28S ribosomal protein S2, mitochondrial	R.DC*GEYAHTR.Y	162	1.135	1.335	1.755	2.92
Q9Y3B7	MRPL11 39S ribosomal protein L11, mitochondrial	R.GVSINQFC*K.E	50	1.11	1.175	1.775	1.775
Q9Y3D2	MSRB2 Methionine-R-sulfoxide reductase B2, mitochondrial	K.YC*SGTGWPSFSEAHGTSGSDESH TGILR.R	105			2.7	7.28
Q9Y3D2	MSRB2 Methionine-R-sulfoxide reductase B2, mitochondrial	R.GQAGGGGPGTGPGLGEAGSLATC *ELPLAK.S	45	0.835	0.81	0.945	1.115
Q9Y3D5	MRPS18C 28S ribosomal protein S18c, mitochondrial	K.NVQLLSQFVSPFTGC*IYGR.H	90	0.98	1.165	1.3	
Q9Y3D5	MRPS18C 28S ribosomal protein S18c, mitochondrial	R.HITGLC*GK.K	100	0.99	1.32		4.56
Q9Y3E5	PTRH2 Peptidyl-tRNA hydrolase 2, mitochondrial	K.QWEYC*GQPK.V	111	1.11	1.295	1.565	1.735
Q9Y3E5	PTRH2 Peptidyl-tRNA hydrolase 2, mitochondrial	K.VAAQC*SHAAVSAYK.Q	86	0.91	1.195	1.275	1.67
Q9Y3E5	PTRH2 Peptidyl-tRNA hydrolase 2, mitochondrial	R.VC*FGMLPK.S	36	0.85	0.965	1.02	1.34
Q9Y4W6	AFG3L2 AFG3-like protein 2	K.DVAGC*EEAK.L	313	1.18	1.23	1.735	3.275
Q9Y4W6	AFG3L2 AFG3-like protein 2	K.NAPC*ILFIDEIDAVGR.K	402	0.985	0.99	1.375	2.015
Q9Y4W6	AFG3L2 AFG3-like protein 2	K.LASLTPGFSGADVANVC*NEAALI AAR.H	525	0.955	1.075	1.36	1.98
Q9Y4W6	AFG3L2 AFG3-like protein 2	R.MC*MTLGGR.V	626	1.01	1.085	1.29	1.96
Q9Y512	SAMM50 Sorting and assembly machinery component 50 homolo	R.LELNYC*VPMGVQTGDR.I	445	0.77		0.34	
Q9Y512	SAMM50 Sorting and assembly machinery component 50 homolo	R.IC*DGVQFGAGIR.F	457	0.875	0.805	0.8	0.9

Q9Y512	SAMM50 Sorting and assembly machinery component 50 homolo	K.DDIIIC*EIGDVFK.A	65	0.74	0.72	0.74	0.79
Q9Y512	SAMM50 Sorting and assembly machinery component 50 homolo	R.KLAEC*IR.W	421	0.75	0.68	0.67	0.755
Q9Y584	TIMM22 Mitochondrial import inner membrane translocase su	K.AMESC*AFK.A	69			0.81	1.27
Q9Y584	TIMM22 Mitochondrial import inner membrane translocase su	K.NSVISGC*ITGGAIGFR.A	160				1.24
Q9Y5J9	TIMM8B Mitochondrial import inner membrane translocase su	R.TENC*LSSCVDR.F	55	0.88			
Q9Y5Z9	UBIAD1 UbiA prenyltransferase domain-containing protein 1	K.AGDRDPLGNDC*PEQDRLPQR.S	31	0.95	1.205	1.63	2.35
Q9Y606	PUS1 tRNA pseudouridine synthase A, mitochondrial	R.SGC*IPENHGEDMR.K	125	1.275		2.05	5.58
Q9Y606	PUS1 tRNA pseudouridine synthase A, mitochondrial	K.GPQDPSAC*R.Y	260	1.02	1.02	1.59	2.86
Q9Y619	SLC25A15 Mitochondrial ornithine transporter 1	R.GLTDC*C*LK.T	50	1.14	1.29	1.53	
Q9Y619	SLC25A15 Mitochondrial ornithine transporter 1	R.GLTDC*CLK.T	50	1.15	1.435	1.645	2.72
Q9Y619	SLC25A15 Mitochondrial ornithine transporter 1	K.SNPAIQAAIDLTAGAAGGTAC*VL TGQPFDTMK.V	23	0.89	1.15	1.5	2.06
Q9Y619	SLC25A15 Mitochondrial ornithine transporter 1	K.LSDLQNAAAGSFASAFAALVLC*P TELVK.C	125	0.985	1.18	1.25	1.615
Q9Y676	MRPS18B 28S ribosomal protein S18b, mitochondrial	K.VVGNPC*PICR.D	105	1	1.085	1.36	1.77
Q9Y696	CLIC4 Chloride intracellular channel protein 4	K.AGSDGESIGNC*PFSQR.L	35		1.055	1.58	
Q9Y696	CLIC4 Chloride intracellular channel protein 4	R.DEFTNTC*PSDKEVEIAYSDVAK.R	234		0.86	1.02	1.58
Q9Y697	NFS1 Cysteine desulfurase, mitochondrial	K.DVALSSGSAC*TSASLEPSYVLR.A	381	1.225	1.385	1.82	2.12
Q9Y6C9	MTCH2 Mitochondrial carrier homolog 2	K.TYC*C*DLK.M	296	1.19	1.69	2.745	4.89
Q9Y6C9	MTCH2 Mitochondrial carrier homolog 2	K.YC*GLCDSIITIYR.E	160	1.275	1.435	1.64	2.24
Q9Y6C9	MTCH2 Mitochondrial carrier homolog 2	R.LC*SGVLGTVVHGK.V	79	1.015	1.11	1.745	1.54
Q9Y6C9	MTCH2 Mitochondrial carrier homolog 2	K.TYC*CDLK.M	296	1.055	1	0.865	1.5
Q9Y6C9	MTCH2 Mitochondrial carrier homolog 2	R.QVC*QLPGLFSYAQHIASIDGR.R	49		1.55		0.44
Q9Y6G3	MRPL42 39S ribosomal protein L42, mitochondrial	K.STYSPLPDDYNC*NVELALTSDGR. T	45	1.45			
Q9Y6M9	NDUFB9 NADH dehydrogenase	K.VPEWC*LDDWHPSEK.A	103	0.7	0.94	0.86	1.03
Q9Y6M9	NDUFB9 NADH dehydrogenase	R.HLESWC*VQR.D	31	0.85	0.725	0.72	0.66
Q9Y6M9	NDUFB9 NADH dehydrogenase	R.QHPQPYIFPDSPGGTSYERYDC*YK .V	96	0.695	0.74	0.71	0.57
Q9Y6M9	NDUFB9 NADH dehydrogenase	R.YFAC*LMR.A	42	0.875	0.81	0.705	0.545
Q9Y6N1	COX11 Cytochrome c oxidase assembly protein COX11, mitoc	K.IQC*FC*FEEQR.L	217	1.26			
Q9Y6N1	COX11 Cytochrome c oxidase assembly protein COX11, mitoc	K.IQC*FCFEEQR.L	217	0.99	1.105	1.09	1.255
Q9Y6N1	COX11 Cytochrome c oxidase assembly protein COX11, mitoc	R.LYC*QTTGLGGSAVAGHASDK.I	121	0.8	0.625	0.66	0.67

Table 2A-5. List of average L:H ratios for mitochondrial cysteine containing peptides identified in Mito-P from cells treated with DMSO or AMA. Data was filtered for mitochondrial peptides with ratio values in 2 out of 3 replicates, with a coefficient of variance <50%. Cysteines identified in Mito-P from DMSO- or AMA-treated cells were alkylated by IA-L or IA-H, respectively.

Uniprot ID	Protein Description	Peptide Sequence	Residue	Average L:H	Average log2(L:H)	COV
Q9NYK5	MRPL39 39S ribosomal protein L39, mitochondrial	R.SC*AMMMGCVIER.A	146	19.06	4.25	0.03
P35914	HMGCL Hydroxymethylglutaryl-CoA lyase, mitochondrial	K.LLEAGNFIC*QALNR.K	307	3.46	1.72	0.36
O15270	SPTLC2 Serine palmitoyltransferase 2	K.VLEEYGAGVC*STR.Q	204	3.12	1.63	0.14
Q9Y696	CLIC4 Chloride intracellular channel protein 4	K.AGSDGESIGNC*PFSQR.L	35	2.99	1.57	0.14
Q86YH6	PDSS2 Decaprenyl-diphosphate synthase subunit 2	K.GVTSAIDLC*R.Y	365	2.65	1.40	0.06
Q99832	CCT7 T-complex protein 1 subunit eta	R.YNFFTGC*PK.A	364	2.41	1.25	0.22
P28331	NDUFS1 NADH-ubiquinone oxidoreductase 75 kDa subunit, mit	R.LSVAGNC*R.M	75	2.38	1.24	0.14
Q86UT6	NLRX1 NLR family member X1	R.LNQPYC*GYAVGGSGVSATPAQR.D	331	2.35	1.23	0.11
P49189	ALDH9A1 4-trimethylaminobutyraldehyde dehydrogenase	R.EREDEIATMEC*INNGK.S	96	2.35	1.23	0.10
P49327	FASN Fatty acid synthase	R.LGMLSPEGTC*K.A	212	2.34	1.21	0.24
O00411	POLRMT DNA-directed RNA polymerase, mitochondrial	R.LPEC*GSGDGSLQPPR.K	94	2.33	1.21	0.16
Q96GW9	MARS2 Methionine--tRNA ligase, mitochondrial	K.ALEAVSSC*VR.Q	479	2.33	1.19	0.33
Q96JX3	SERAC1 Protein SERAC1	R.IIAQAC*DPK.T	173	2.32	1.19	0.32
Q9NYY8	FASTKD2 FAST kinase domain-containing protein 2	R.SLILLDEC*SK.V	366	2.30	1.18	0.27
P49327	FASN Fatty acid synthase	K.ADEASELAC*PTPK.E	2202	2.30	1.18	0.26

Q9NYY8	FASTKD2 FAST kinase domain-containing protein 2	K.LSEEC*NSLSDVLDAFSK.A	163	2.18	1.12	0.08
Q9Y5Z9	UBIAD1 UbiA prenyltransferase domain-containing protein 1	K.AGDRDPLGNDC*PEQDRLPQR.S	31	2.18	1.12	0.10
Q8IWA4	MFN1 Mitofusin-1	R.LQEFQNFEQIFEEC*ISQSAVK.T	327	2.19	1.09	0.44
P22234	PAICS Multifunctional protein ADE2	K.ITSC*IFQLLQEAGIK.T	63	2.12	1.08	0.03
Q5T9A4	ATAD3B ATPase family AAA domain-containing protein 3B	K.DGVLTEAMMDAC*VQDAVQQYR.Q	557	2.14	1.08	0.32
Q8TAA5	GRPEL2 GrpE protein homolog 2, mitochondrial	R.AIADC*ENIR.R	87	2.11	1.07	0.04
O95573	ACSL3 Long-chain-fatty-acid--CoA ligase 3	R.NTPLC*DSFVFR.K	429	2.11	1.07	0.13
P53701	HCCS Cytochrome c-type heme lyase	K.GC*PVNTEPSGPTC*EK.K	35	2.11	1.07	0.20
O43169	CYB5B Cytochrome b5 type B	K.DPSKNDTC*K.S	115	2.09	1.07	0.05
P30041	PRDX6 Peroxiredoxin-6	K.DINAYNC*EEPTEK.L	91	2.09	1.05	0.27
Q9H2U2	PPA2 Inorganic pyrophosphatase 2, mitochondrial	K.DKSTNC*FGDNDPIDVC*EIGSK.I	161	2.06	1.04	0.17
P21964	COMT Catechol O-methyltransferase	R.YLPDTLLLEEC*GLLR.K	207	2.05	1.04	0.06
Q9HBH5	RDH14 Retinol dehydrogenase 14	R.AFC*QEMLQEEPR.L	126	2.05	1.04	0.04
Q8N0V3	RBFA Putative ribosome-binding factor A, mitochondrial	R.TEDGHSC*GASR.E	338	2.07	1.03	0.30
O15270	SPTLC2 Serine palmitoyltransferase 2	R.NTGSC*QEAAAK.V	188	2.03	1.02	0.06
P50416	CPT1A Carnitine O-palmitoyltransferase 1, liver isoform	R.TLETANC*MSSQTK.N	96	2.05	1.00	0.43
Q96TC7	FAM82A2 Regulator of microtubule dynamics protein 3	R.C*HMEENQR.V	128	2.02	1.00	0.29
P50213	IDH3A Isocitrate dehydrogenase	K.C*SDFTEEIC*R.R	351	1.99	0.99	0.12
O00411	POLRMT DNA-directed RNA polymerase, mitochondrial	K.DATPVPC*GR.W	119	1.98	0.99	0.01
O75600	GCAT 2-amino-3-ketobutyrate coenzyme A ligase, mitochon	R.FIC*GTQSIHK.N	106	1.99	0.98	0.21
Q92667	AKAP1 A-kinase anchor protein 1, mitochondrial	R.ADPAIKEPLPVEDVC*PK.V	64	1.96	0.97	0.03
Q9HCC0	MCCC2 Methylcrotonoyl-CoA carboxylase beta chain, mitoch	K.AATGEEVSAEDLGGADLHC*R.K	267	1.96	0.97	0.08
Q8TBP6	SLC25A40 Solute carrier family 25 member 40	K.LGENETC*IPIVAGIVAR.F	142	1.96	0.97	0.14
P54136	RARS Arginine--tRNA ligase, cytoplasmic	K.IVFVPGC*SIPLTIVK.S	369	1.98	0.96	0.35
P21964	COMT Catechol O-methyltransferase	R.LITIEINPDC*AAITQR.M	145	1.95	0.96	0.07
Q7L8L6	FASTKD5 FAST kinase domain-containing protein 5	K.IGDLAC*ANIQHLSSR.S	345	1.94	0.96	0.04
P22033	MUT Methylmalonyl-CoA mutase, mitochondrial	K.VADPWGGSYMMEC*LTNDVYDAALK.L	433	1.94	0.96	0.08
P21953	BCKDHB 2-oxoisovalerate dehydrogenase subunit beta, mitoc	R.SGDLFNC*GSLTIR.S	177	1.94	0.95	0.05
P09622	DLD Dihydrolipoyl dehydrogenase, mitochondrial	K.NETLGGTC*LNVGC*IPSK.A	80	1.96	0.95	0.34
Q6P087	RPUSD3 RNA pseudouridylate synthase domain-containing pro	R.AQRPTATYC*AVTDGIPAASEGK.I	172	1.92	0.93	0.20
P49189	ALDH9A1 4-trimethylaminobutyraldehyde dehydrogenase	R.DDMTC*VK.E	387	1.91	0.92	0.23
Q9BYD6	MRPL1 39S ribosomal protein L1, mitochondrial	K.IATLDMSSDQIAANLQAVINEVC*R.H	279	1.92	0.91	0.50
Q969S9	GFM2 Ribosome-releasing factor 2, mitochondrial	R.VTLAQTAVPVLC*GSALK.N	329	1.87	0.90	0.07
Q9NVH1	DNAJC11 DnaJ homolog subfamily C member 11	K.AGLPGFYDPC*VGEEK.N	518	1.87	0.90	0.13
Q9NWU1	OXSM 3-oxoacyl-	K.LPPTLNLDC*SEPEFDLNYVPLK.A	415	1.86	0.89	0.14
O15270	SPTLC2 Serine palmitoyltransferase 2	R.FC*LSAAHTK.E	511	1.86	0.89	0.16
P33316	DUT Deoxyuridine 5-triphosphate nucleotidohydrolase,	K.TDIQIALPSGC*YGR.V	166	1.85	0.89	0.07
P04406	GAPDH Glyceraldehyde-3-phosphate dehydrogenase	R.VPTANVSVVDLTC*R.L	247	1.84	0.88	0.07
P05166	PCCB Propionyl-CoA carboxylase beta chain, mitochondria	K.VASGC*LDINSSVK.G	365	1.85	0.87	0.30
Q9BRJ2	MRPL45 39S ribosomal protein L45, mitochondrial	R.SIHLAC*TAGIFDAYVPPEGDAR.I	80	1.83	0.87	0.04
Q86UT6	NLRX1 NLR family member X1	R.AVLAQLGC*PIK.N	644	1.83	0.87	0.06
Q99798	ACO2 Aconitate hydratase, mitochondrial	K.C*TTDHISAAGPWLK.F	592	1.84	0.87	0.28
O75439	PMPCB Mitochondrial-processing peptidase subunit beta	R.VTC*LESGLR.V	62	1.84	0.86	0.28
Q9BPX6	MICU1 Calcium uptake protein 1, mitochondrial	R.AHAESPPC*VDNLK.S	62	1.86	0.86	0.49
O00411	POLRMT DNA-directed RNA polymerase, mitochondrial	R.VC*VVSVEKPTLPSK.E	413	1.80	0.85	0.11
O95573	ACSL3 Long-chain-fatty-acid--CoA ligase 3	R.LLLC*GGAPLSATTQR.F	450	1.80	0.85	0.10
Q8NBN7	RDH13 Retinol dehydrogenase 13	K.DYVTGGAC*PSK.A	30	1.80	0.84	0.16
Q9Y3E5	PTRH2 Peptidyl-tRNA hydrolase 2, mitochondrial	R.VC*FGMLPK.S	36	1.79	0.84	0.10
E7ERL9	VARS2 Valine--tRNA ligase, mitochondrial	R.LALAAQEC*ER.G	Bad ID	1.79	0.84	0.20
Q9BQ52	ELAC2 Zinc phosphodiesterase ELAC protein 2	R.TC*DLEEFQTC*LVR.H	632	1.79	0.83	0.25
Q9H4K7	GTPBP5 GTP-binding protein 5	R.APVTC*TPGQPGQQR.V	206	1.78	0.83	0.13
Q9BQ52	ELAC2 Zinc phosphodiesterase ELAC protein 2	R.GPSGC*SGGPNTVYLQVVAAGSR.D	51	1.81	0.83	0.47
P30041	PRDX6 Peroxiredoxin-6	R.DFTPVC*TTELGR.A	47	1.78	0.83	0.15
E7ERL9	VARS2 Valine--tRNA ligase, mitochondrial	K.GGEIC*EQLR.A	Bad ID	1.86	0.83	0.63
P36551	CPOX Coproporphyrinogen-III oxidase, mitochondrial	K.EGGGGISC*VLQDGC*VFEK.A	192	1.78	0.82	0.28
P51648	ALDH3A2 Fatty aldehyde dehydrogenase	R.EKDILTAIAADLC*K.S	50	1.80	0.82	0.44
P49419	ALDH7A1 Alpha-aminoadipic semialdehyde dehydrogenase	R.STC*TINYSK.D	522	1.76	0.82	0.14
O94826	TOMM70A Mitochondrial import receptor subunit TOM70	K.YEQAIQC*YTEAISLC*PTEK.N	136	1.77	0.81	0.21
P33316	DUT Deoxyuridine 5-triphosphate nucleotidohydrolase,	R.IAQLIC*ER.I	222	1.76	0.81	0.17
O75431	MTX2 Metaxin-2	K.GEQILLSDNAASLAVQAFLQMC*NLPIK.V	51	1.79	0.80	0.56
P36776	LONP1 Lon protease homolog, mitochondrial	R.ALC*GLDESK.A	682	1.74	0.80	0.05
Q9NVS2	MRPS18A 28S ribosomal protein S18a, mitochondrial	K.ITGLC*QEEHR.K	108	1.78	0.80	0.46
P40925	MDH1 Malate dehydrogenase, cytoplasmic	K.VIVVGNPANTNC*LTASK.S	137	1.74	0.80	0.06
Q6UB35	MTHFD1L Monofunctional C1-tetrahydrofolate synthase, mitoc	K.VGC*GSPR.I	302	1.74	0.80	0.21
O95563	MPC2 Mitochondrial pyruvate carrier 2	K.WGLVC*AGLADMAR.P	54	1.82	0.79	0.69
Q99497	PARK7 Protein DJ-1	R.DVVIC*PDASLEDAKK.E	53	1.81	0.79	0.72
Q9NYK5	MRPL39 39S ribosomal protein L39, mitochondrial	K.DC*DPGEVNK.A	133	1.73	0.79	0.14
P42704	LRPPRC Leucine-rich PPR motif-containing protein, mitocho	K.LTDYC*K.K	394	1.73	0.78	0.18

O94925	GLS Glutaminase kidney isoform, mitochondrial	K.C*VQSNIVLLTQAFR.R	203	1.72	0.78	0.15
O00142	TK2 Thymidine kinase 2, mitochondrial	R.TNPETC*YQR.L	189	1.72	0.78	0.11
P35914	HMGCL Hydroxymethylglutaryl-CoA lyase, mitochondrial	K.VAQATC*K.L	323	1.72	0.78	0.12
Q9H5Q4	TFB2M Dimethyladenosine transferase 2, mitochondrial	R.VIHC*DFFK.L	149	1.72	0.78	0.14
Q7L0Y3	TRMT10C Mitochondrial ribonuclease P protein 1	K.SSVQEEC*VSTISSSK.D	78	1.72	0.78	0.12
Q8WV74	NUDT8 Nucleoside diphosphate-linked moiety X motif 8, mi	R.LAGLTC*SGAEGLARPK.Q	207	1.73	0.78	0.26
P48735	IDH2 Isocitrate dehydrogenase	K.NYDGDVQSDILAQGFGSLGLMTSVLVC*PDGK.T	336	1.72	0.78	0.09
Q16822	PCK2 Phosphoenolpyruvate carboxykinase	K.VEC*VGDDIAWMR.F	325	1.72	0.78	0.18
P42765	ACAA2 3-ketoacyl-CoA thiolase, mitochondrial	K.EAEVVLC*GGTESMSQAPYC*VR.N	116	1.72	0.78	0.19
Q8TD30	GPT2 Alanine aminotransferase 2	K.VLC*IINPGNPTGQVQSR.K	265	1.71	0.78	0.07
Q9NX40	OCIAD1 OCIA domain-containing protein 1	R.VFAEC*NDESFWFR.S	38	1.71	0.78	0.10
Q8IWA4	MFN1 Mitofusin-1	R.LC*QQVDITQK.Q	681	1.71	0.77	0.00
Q5TC12	ATPAF1 ATP synthase mitochondrial F1 complex assembly fac	K.C*AQNQNKT.-	321	1.71	0.77	0.05
Q9NUL7	DDX28 Probable ATP-dependent RNA helicase DDX28	R.HVVC*AAETGSGK.T	170	1.75	0.77	0.58
Q9H9B4	SFXN1 Sideroflexin-1	R.MSAQVPMNMTITGC*MMTFYR.T	106	1.81	0.77	0.91
Q96BR5	SELRC1 Sel1 repeat-containing protein 1	K.DMDLAC*K.Y	172	1.77	0.77	0.62
Q6L8Q7	PDE12 2,5-phosphodiesterase 12	K.LHC*TPGDGQR.F	250	1.71	0.77	0.10
P42765	ACAA2 3-ketoacyl-CoA thiolase, mitochondrial	R.IVGYFVSGC*DPSIMGIGPVPAISGALK.K	287	1.71	0.77	0.19
Q16822	PCK2 Phosphoenolpyruvate carboxykinase	R.FC*APAR.Q	425	1.71	0.77	0.18
O96011	PEX11B Peroxisomal membrane protein 11B	R.LLMEQESSAC*SR.R	153	1.70	0.77	0.06
Q8TAA5	GRPEL2 GrpE protein homolog 2, mitochondrial	K.TTEC*ISEESEPEDQKLTLEK.V	126	1.70	0.77	0.06
Q99832	CCT7 T-complex protein 1 subunit eta	R.C*QVFEETQIGGER.Y	345	1.71	0.77	0.30
O75608	LYPLA1 Acyl-protein thioesterase 1	K.TYEGMMHSSC*QQEMMDVK.Q	211	1.70	0.76	0.13
Q8NFF5	FLAD1 FAD synthase	K.GHTQDTNTFFLC*R.T	136	1.75	0.76	0.67
Q02218	OGDH 2-oxoglutarate dehydrogenase, mitochondrial	R.VVNAPIFHVNSDDPEAVMYVC*K.V	487	1.72	0.76	0.37
P49590	HARS2 Probable histidine--tRNA ligase, mitochondrial	R.IVDGMFAVC*GVPESK.F	225	1.70	0.76	0.20
E7EVK2	MTG1 Mitochondrial GTPase 1	K.NVIFTNC*VKDENVK.Q	113	1.71	0.76	0.36
O60488	ACSL4 Long-chain-fatty-acid--CoA ligase 4	K.TALLDISC*VK.H	221	1.69	0.75	0.11
P49189	ALDH9A1 4-trimethylaminobutyraldehyde dehydrogenase	R.VIATFTC*SGEK.E	45	1.68	0.75	0.02
P50416	CPT1A Carnitine O-palmitoyltransferase 1, liver isoform	R.SC*TTESC*DFVR.A	608	1.68	0.75	0.06
P23368	ME2 NAD-dependent malic enzyme, mitochondrial	R.AMASINERPVIFALSNPTAQAEC*TAEEAYTLTEGR.C	428	1.78	0.75	0.94
Q99497	PARK7 Protein DJ-1	K.DPVQC*SR.D	46	1.68	0.75	0.09
Q96D53	ADCK4 Uncharacterized aarF domain-containing protein kin	R.IVQTLC*TVR.G	147	1.68	0.75	0.10
Q16762	TST Thiosulfate sulfurtransferase	K.KVDLSQPLIATC*R.K	248	1.68	0.74	0.12
Q6YP21	CCBL2 Kynurenine--oxoglutarate transaminase 3	K.LSAIPVSAFC*NSETK.S	416	1.68	0.74	0.09
Q9Y512	SAMM50 Sorting and assembly machinery component 50 homolo	R.IC*DGVQFGAGIR.F	457	1.70	0.74	0.46
P07203	GPX1 Glutathione peroxidase 1	R.FQTIDIEPDIEALLSQGPSC*A.-	202	1.67	0.74	0.13
O75439	PMPCB Mitochondrial-processing peptidase subunit beta	R.LC*TSVTESEVAR.A	389	1.67	0.74	0.05
Q9H0R6	QRSL1 Glutamyl-tRNA(Gln) amidotransferase subunit A, mit	K.QGQITPTELC*QK.C	24	1.71	0.74	0.57
P21964	COMT Catechol O-methyltransferase	K.IVDAVIQEHQPSVLLELGAYC*GYSAVR.M	119	1.67	0.73	0.09
Q9BQ69	MACROD1 O-acetyl-ADP-ribose deacetylase MACROD1	R.SC*YLSSLDLLLEHR.L	246	1.67	0.73	0.22
P51649	ALDH5A1 Succinate-semialdehyde dehydrogenase, mitochondria	K.EVGEAIC*TDPLVSK.I	272	1.66	0.73	0.05
Q92947	GCDH Glutaryl-CoA dehydrogenase, mitochondrial	K.GYGC*AGVSSVAYGLLAR.E	115	1.67	0.73	0.29
Q96CB9	NSUN4 Putative methyltransferase NSUN4	R.VLVDVPC*TTDR.H	258	1.65	0.72	0.14
P35270	SPR Sepiapterin reductase	R.AVC*LLTGASR.G	10	1.66	0.72	0.21
Q5JRX3	PITRM1 Presequence protease, mitochondrial	R.LLPDHTYSVVSGGDPLC*IPELTWEQLK.Q	241	1.65	0.72	0.05
G3V325	PTCD1 Pentatricopeptide repeat-containing protein 1	R.TKPQGDQDTGKEADDGC*ALGGR.-	744	1.65	0.72	0.14
P50213	IDH3A Isocitrate dehydrogenase	R.IEAAC*FATIK.D	331	1.66	0.72	0.27
Q8N442	GUF1 Translation factor GUF1, mitochondrial	K.VFDIPSDEC*IK.I	221	1.65	0.72	0.09
Q9NNW7	TXNRD2 Thioredoxin reductase 2, mitochondrial	R.TVGIHPTC*SEEVVK.L	500	1.67	0.72	0.50
Q8IXI2	RHOT1 Mitochondrial Rho GTPase 1	R.IC*FNTPLAPQALEDVK.N	216	1.65	0.72	0.08
Q9BQ69	MACROD1 O-acetyl-ADP-ribose deacetylase MACROD1	R.AAGPLLTDEC*R.T	199	1.64	0.72	0.03
P49189	ALDH9A1 4-trimethylaminobutyraldehyde dehydrogenase	K.SPLIIFSDC*DMNNAVK.G	267	1.65	0.72	0.17
P31040	SDHA Succinate dehydrogenase	R.AAFGLSEAGFNTAC*VTK.L	89	1.65	0.72	0.28
Q9H2U2	PPA2 Inorganic pyrophosphatase 2, mitochondrial	K.ILSC*GEVIHVK.I	180	1.64	0.71	0.03
P62906	RPL10A 60S ribosomal protein L10a	K.FSVC*VLGDQQHC*DEAK.A	66	1.70	0.71	0.69
Q9NQE9	HINT3 Histidine triad nucleotide-binding protein 3	R.SAGLAPDC*EASATAETTVSSVGTC*EAAGK.S	16	1.64	0.71	0.01
P42704	LRPPRC Leucine-rich PPR motif-containing protein, mitocho	R.AILQENGC*LSDSDMFSQAGLR.S	500	1.63	0.71	0.10
Q709F0	ACAD11 Acyl-CoA dehydrogenase family member 11	R.ALQIMC*ER.A	651	1.64	0.71	0.19
Q16822	PCK2 Phosphoenolpyruvate carboxykinase	R.YVAAAFPSAC*GK.T	306	1.64	0.71	0.20
Q6NVY1	HIBCH 3-hydroxyisobutyryl-CoA hydrolase, mitochondrial	K.AFC*AGGDIR.V	95	1.64	0.70	0.23
Q9H4B0	OSGEPL1 Probable tRNA threonylcarbamoyladenosine biosynthe	K.HPEC*STMSGGK.A	216	1.63	0.70	0.07
Q9Y2W6	TDRKH Tudor and KH domain-containing protein	K.ITC*DKESEGTLLLSR.L	160	1.63	0.70	0.12
Q5JRX3	PITRM1 Presequence protease, mitochondrial	R.SQQSKPQDASC*LPALK.V	556	1.63	0.70	0.05
O15235	MRPS12 28S ribosomal protein S12, mitochondrial	K.GVVLC*TFTR.K	64	1.63	0.70	0.11
P22033	MUT Methylmalonyl-CoA mutase, mitochondrial	R.AHC*QTSGWSLTEQDPYNNIVR.T	351	1.65	0.70	0.46

Q6UB35	MTHFD1L Monofunctional C1-tetrahydrofolate synthase, mitoc	R.SSC*SPGGR.T	61	1.63	0.70	0.13
Q9NVV4	MTPAP Poly(A) RNA polymerase, mitochondrial	R.FSHQASGFQC*DLTTNNR.I	324	1.63	0.70	0.14
Q7L0Y3	TRMT10C Mitochondrial ribonuclease P protein 1	K.TLMEC*VSNTAK.K	123	1.65	0.70	0.44
Q9NQE9	HINT3 Histidine triad nucleotide-binding protein 3	K.DYDSTC*VFC*R.I	48	1.63	0.70	0.22
P36551	CPOX Coproporphyrinogen-III oxidase, mitochondrial	K.EAC*DQHGPDLYPK.F	304	1.62	0.70	0.00
P51659	HSD17B4 Peroxisomal multifunctional enzyme type 2	K.LKC*EAVVADVLDK.G	425	1.62	0.70	0.09
Q9H0R6	QRSL1 Glutamyl-tRNA(Gln) amidotransferase subunit A, mit	R.AFC*DQQLLTVAK.W	483	1.62	0.69	0.12
P36776	LONP1 Lon protease homolog, mitochondrial	R.AGVTC*IVLPAENKK.D	909	1.62	0.69	0.12
Q3SXM5	HSDL1 Inactive hydroxysteroid dehydrogenase-like protein	R.KEALSC*TA.-	328	1.64	0.69	0.42
Q99798	ACO2 Aconitate hydratase, mitochondrial	R.VGLIGSC*TNSSYEDMGR.S	385	1.62	0.69	0.09
P28838	LAP3 Cytosol aminopeptidase	R.SAGAC*TAAAFLK.E	462	1.63	0.69	0.30
Q9Y305	ACOT9 Acyl-coenzyme A thioesterase 9, mitochondrial	K.SLEIC*HPQER.N	299	1.63	0.69	0.34
P05165	PCCA Propionyl-CoA carboxylase alpha chain, mitochondri	K.MADEAVC*VGPAPTSK.S	111	1.62	0.69	0.24
Q9BQP7	C20orf72 Uncharacterized protein C20orf72	R.ALESAVQHETLNYIGLLDC*VAEYQGK.L	239	1.63	0.69	0.42
Q7Z4W1	DCXR L-xylulose reductase	R.EC*PGIEPVC*VDLGDWEATER.A	51	1.62	0.69	0.17
Q9H9P8	L2HGDH L-2-hydroxyglutarate dehydrogenase, mitochondrial	K.AC*FLGATVK.Y	376	1.61	0.69	0.11
P40925	MDH1 Malate dehydrogenase, cytoplasmic	K.ENFSC*LTR.L	154	1.61	0.69	0.20
Q9HC36	RNMTL1 RNA methyltransferase-like protein 1	K.ASDHGWVC*DQR.V	309	1.63	0.69	0.43
Q14197	ICT1 Peptidyl-tRNA hydrolase ICT1, mitochondrial	R.LTISYC*R.S	82	1.62	0.68	0.36
Q96RP9	GFM1 Elongation factor G, mitochondrial	K.GFLDAC*EK.G	594	1.62	0.68	0.39
O15270	SPTLC2 Serine palmitoyltransferase 2	R.ANGC*VANGEVR.N	19	1.61	0.68	0.11
Q5TEU4	NDUFAF5 NADH dehydrogenase	R.NFPLALDLGC*GR.G	98	1.66	0.68	0.75
Q7L2E3	DHX30 Putative ATP-dependent RNA helicase DHX30	R.GEPGGILC*FLPGWQEIK.G	673	1.60	0.68	0.00
Q6P087	RPUSD3 RNA pseudouridylate synthase domain-containing pro	R.TLQC*LGLR.L	345	1.60	0.68	0.15
Q9HCC0	MCCC2 Methylcrotonoyl-CoA carboxylase beta chain, mitoch	R.LPC*IYLVDSGGAYLPR.Q	167	1.60	0.68	0.23
Q96CQ1	SLC25A36 Solute carrier family 25 member 36	K.TC*ATTIAYPHEVVR.T	239	1.61	0.68	0.33
P43304	GPD2 Glycerol-3-phosphate dehydrogenase, mitochondrial	K.AADC*ISEPVNREPPSR.E	45	1.60	0.67	0.18
Q9NSE4	IARS2 Isoleucine--tRNA ligase, mitochondrial	K.C*GFSELYSWQR.E	91	1.60	0.67	0.27
Q13907	IDI1 Isopentenyl-diphosphate Delta-isomerase 1	K.NC*HLNENIEK.G	39	1.60	0.67	0.22
Q92552	MRPS27 28S ribosomal protein S27, mitochondrial	K.EHYC*LADLASLMDK.T	49	1.59	0.67	0.09
O75879	PET112 Glutamyl-tRNA(Gln) amidotransferase subunit B, mit	R.AGVGLLEVVLEPDMSC*GEEAATAVR.E	228	1.59	0.67	0.10
G3V325	PTCD1 Pentatricopeptide repeat-containing protein 1	R.DC*GLGDPQVASELLLKPR.E	381	1.60	0.66	0.36
Q9Y2W6	TDRKH Tudor and KH domain-containing protein	R.SDFLSLPFQAIEC*SLAR.I	419	1.59	0.66	0.29
P10515	DLAT Dihydrolipoyllysine-residue acetyltransferase comp	K.ASALAC*LK.V	488	1.59	0.66	0.24
P45954	ACADSB Short/branched chain specific acyl-CoA dehydrogena	K.VGSFC*LSEAGAGSDSFALK.T	175	1.61	0.66	0.52
Q02252	ALDH6A1 Methylmalonate-semialdehyde dehydrogenase	K.AEMDAAIASC*K.R	86	1.61	0.66	0.48
Q9Y6C9	MTCH2 Mitochondrial carrier homolog 2	K.TYC*C*DLK.M	296	1.58	0.66	0.08
Q16134	ETFDH Electron transfer flavoprotein-ubiquinone oxidored	R.ANC*EPQTYGIGLK.E	266	1.59	0.66	0.31
Q9HA92	RSAD1 Radical S-adenosyl methionine domain-containing pr	R.THSAC*DALR.T	175	1.58	0.66	0.12
O00217	NDUFS8 NADH dehydrogenase	K.LC*EAIC*PAQAITIEAEPR.A	117	1.59	0.66	0.22
Q96AB3	ISOC2 Isochorismatase domain-containing protein 2, mitoc	R.VLPGSSVLFLC*DMQEK.F	21	1.61	0.66	0.50
Q5TGZ0	MINOS1 Mitochondrial inner membrane organizing system pro	R.C*LADAVVK.I	13	1.58	0.66	0.15
Q8WWV3	RTN4IP1 Reticulon-4-interacting protein 1, mitochondrial	K.VGGLNDKNC*TGK.R	203	1.58	0.66	0.13
O75439	PMPCB Mitochondrial-processing peptidase subunit beta	R.SNMC*WLRD.-	485	1.58	0.65	0.23
P32322	PYCR1 Pyrroline-5-carboxylate reductase 1, mitochondrial	R.C*MTNTPVVVR.E	120	1.57	0.65	0.13
Q9HC36	RNMTL1 RNA methyltransferase-like protein 1	R.SAAGAGC*SK.V	235	1.57	0.65	0.09
P23919	DTYMK Thymidylate kinase	K.LVEALC*AAGHR.A	31	1.57	0.65	0.22
Q6P087	RPUSD3 RNA pseudouridylate synthase domain-containing pro	K.ESSGLVLLSSC*PQTASR.L	147	1.57	0.65	0.15
P51649	ALDH5A1 Succinate-semialdehyde dehydrogenase, mitochondria	R.AAYEAFC*R.W	110	1.57	0.65	0.15
P54819	AK2 Adenylate kinase 2, mitochondrial	K.NLETPLC*K.N	92	1.57	0.65	0.16
P49419	ALDH7A1 Alpha-aminoadipic semialdehyde dehydrogenase	K.GSDC*GIVNVNIPTSGAEIGGAFGGEK.H	478	1.57	0.65	0.26
Q9H2U2	PPA2 Inorganic pyrophosphatase 2, mitochondrial	R.C*TQEEAR.S	302	1.57	0.65	0.14
Q9H0R6	QRSL1 Glutamyl-tRNA(Gln) amidotransferase subunit A, mit	K.DNFSTSGIETTC*ASNMLK.G	88	1.57	0.65	0.11
P09110	ACAA1 3-ketoacyl-CoA thiolase, peroxisomal	K.GC*FQAEIVPVTTTVHDDK.G	218	1.57	0.64	0.26
Q6P1X6	C8orf82 UPF0598 protein C8orf82	R.LSYC*GGGEALAVPFEPAR.L	130	1.56	0.64	0.09
P38117	ETFB Electron transfer flavoprotein subunit beta	K.EVIAVSC*GPAQC*QETIR.T	66	1.56	0.64	0.13
P08559	PDHA1 Pyruvate dehydrogenase E1 component subunit alpha,	K.NFYGGNGIVGAQVPLGAGIALAC*K.Y	181	1.57	0.64	0.30
O75431	MTX2 Metaxin-2	K.TLDQVLEDVDQC*C*QALSQR.L	189	1.56	0.64	0.04
P35914	HMGCL Hydroxymethylglutaryl-CoA lyase, mitochondrial	K.KNINC*SIEESFQR.F	141	1.56	0.64	0.16
Q8NBU5	ATAD1 ATPase family AAA domain-containing protein 1	R.HVDLLEVAQETDGFSGSDLKEMC*R.D	303	1.57	0.64	0.40
Q9NNW7	TXNRD2 Thioredoxin reductase 2, mitochondrial	K.C*GASYAQVMR.T	483	1.67	0.64	1.00
Q9H845	ACAD9 Acyl-CoA dehydrogenase family member 9, mitochondr	R.GSNTC*EVHFENTK.I	271	1.57	0.64	0.38

P07237	P4HB Protein disulfide-isomerase	K.KEEC*PAVR.L	312	1.56	0.64	0.22
Q9H845	ACAD9 Acyl-CoA dehydrogenase family member 9, mitochondr	K.LASGEHIAAFC*LTEPASGSDAASIR.S	179	1.56	0.64	0.31
Q02218	OGDH 2-oxoglutarate dehydrogenase, mitochondrial	R.FGLEGC*EVLIPALK.T	283	1.55	0.63	0.08
Q9H9P8	L2HGDH L-2-hydroxyglutarate dehydrogenase, mitochondrial	R.ISELSGC*TPDPR.I	272	1.56	0.63	0.20
Q92947	GCDH Glutaryl-CoA dehydrogenase, mitochondrial	R.ASATGMIIMDGVEVPEENVLPGASSLGG PFGC*LNNAR.Y	289	1.56	0.63	0.30
Q8N4Q0	ZADH2 Zinc-binding alcohol dehydrogenase domain-containi	K.SLGC*DRPINYK.T	218	1.55	0.63	0.03
Q6PI48	DARS2 Aspartate--tRNA ligase, mitochondrial	K.ILC*EAPVESVVQVSGTVISRPAGQENPK. M	108	1.55	0.63	0.05
O94925	GLS Glutaminase kidney isoform, mitochondrial	R.LKEC*MDMLR.L	178	1.55	0.63	0.10
P49189	ALDH9A1 4-trimethylaminobutyraldehyde dehydrogenase	K.VLC*GGDIYVPEDPK.L	355	1.55	0.63	0.19
Q96HP4	OXNAD1 Oxidoreductase NAD-binding domain-containing prote	K.VC*GAASESPSVK.S	69	1.55	0.63	0.19
O94826	TOMM70A Mitochondrial import receptor subunit TOM70	K.SEMEMAHLYSLC*DAAHAQTEVAK.K	588	1.59	0.63	0.63
Q7Z4W1	DCXR L-xylulose reductase	R.GVPGAIVNVSSQC*SQR.A	138	1.55	0.63	0.01
Q7L0Y3	TRMT10C Mitochondrial ribonuclease P protein 1	R.NVDPFHIYFC*NLK.I	246	1.57	0.63	0.46
Q9NZJ6	COQ3 Hexaprenyldihydroxybenzoate methyltransferase, mit	K.ILDVGC*GGGLLTEPLGR.L	155	1.54	0.63	0.04
Q9Y3E5	PTRH2 Peptidyl-tRNA hydrolase 2, mitochondrial	K.VAAQC*SHAAVSAYK.Q	86	1.54	0.63	0.05
P42704	LRPPRC Leucine-rich PPR motif-containing protein, mitocho	R.LIASYC*NVGDIEGASK.I	208	1.54	0.63	0.07
P28331	NDUFS1 NADH-ubiquinone oxidoreductase 75 kDa subunit, mit	K.AVTEGAQAVEEPSIC*.-	727	1.54	0.63	0.10
Q5VT66	MARC1 MOSC domain-containing protein 1, mitochondrial	R.C*ILTTVDPDTGVMSR.K	273	1.55	0.62	0.20
Q9BW92	TARS2 Threonine--tRNA ligase, mitochondrial	R.LLGVLAESC*GGK.W	603	1.54	0.62	0.03
P21953	BCKDHB 2-oxoisovalerate dehydrogenase subunit beta, mitoc	K.EKLGVSC*EVIDLR.T	299	1.54	0.62	0.03
Q9BSH4	TACO1 Translational activator of cytochrome c oxidase 1	K.EGGPNPEHNSNLANILEVC*R.S	112	1.54	0.62	0.11
P43897	TSFM Elongation factor Ts, mitochondrial	K.ALETC*GGDLK.Q	71	1.54	0.62	0.11
Q92947	GCDH Glutaryl-CoA dehydrogenase, mitochondrial	K.GELLGC*FGLTEPNSGSDPSSMETR.A	176	1.54	0.62	0.16
P45880	VDAC2 Voltage-dependent anion-selective channel protein	K.VC*EDLDTSVNLAWTSGTNC*TR.F	210	1.54	0.62	0.05
P82675	MRPS5 28S ribosomal protein S5, mitochondrial	R.AIITIC*R.L	324	1.54	0.62	0.20
P82650	MRPS22 28S ribosomal protein S22, mitochondrial	R.HVDVLNLC*FAQFEPDSTEYIK.V	231	1.54	0.62	0.24
P11182	DBT Lipoamide acyltransferase component of branched-ch	K.IPHFGYC*DEIDLTELVK.L	279	1.55	0.62	0.45
Q9NZJ7	MTCH1 Mitochondrial carrier homolog 1	R.RVSSGSC*FALE.-	385	1.56	0.62	0.47
Q7L8L6	FASTKD5 FAST kinase domain-containing protein 5	R.NQYC*YGSR.D	708	1.54	0.62	0.05
Q3SY17	SLC25A52 Solute carrier family 25 member 52	K.C*HGIGEYYR.G	166	1.54	0.62	0.08
P49753	ACOT2 Acyl-coenzyme A thioesterase 2, mitochondrial	K.SEFYANEAC*K.R	401	1.55	0.62	0.37
Q9NYK5	MRPL39 39S ribosomal protein L39, mitochondrial	K.ATEEC*TST.-	335	1.54	0.62	0.21
P11310	ACADM Medium-chain specific acyl-CoA dehydrogenase, mito	R.MTEEPLMC*AYC*VTEPGAGSDVAGIK.T	156	1.54	0.62	0.21
O15091	KIAA0391 Mitochondrial ribonuclease P protein 3	R.DHKAC*LPDAK.T	507	1.53	0.61	0.16
Q96EY7	PTCD3 Pentatricopeptide repeat-containing protein 3, mit	K.NEHSYC*TMIR.G	260	1.54	0.61	0.31
P23378	GLDC Glycine dehydrogenase	K.MEDPVC*ENEILATLHAISSK.N	112	1.53	0.61	0.11
O75608	LYPLA1 Acyl-protein thioesterase 1	K.LAGVTALSC*WLPLR.A	144	1.53	0.61	0.11
P43897	TSFM Elongation factor Ts, mitochondrial	K.YGALVIC*ETSEQK.T	240	1.53	0.61	0.03
Q5VT66	MARC1 MOSC domain-containing protein 1, mitochondrial	K.GVPVSEAEC*TAMGLR.S	79	1.53	0.61	0.04
Q9Y2W6	TDRKH Tudor and KH domain-containing protein	R.VLLISGFPVQVC*K.A	109	1.53	0.61	0.12
O75394	MRPL33 39S ribosomal protein L33, mitochondrial	R.MVSEAGTGFC*FNTK.R	29	1.53	0.61	0.23
Q8IYB8	SUPV3L1 ATP-dependent RNA helicase SUPV3L1, mitochondrial	K.KFNDPNDPC*K.I	418	1.53	0.61	0.14
Q96T52	IMMP2L Mitochondrial inner membrane protease subunit 2	R.VAC*VAR.V	35	1.53	0.61	0.16
Q70CQ3	USP30 Ubiquitin carboxyl-terminal hydrolase 30	R.MQHQSQEC*K.S	513	1.53	0.61	0.14
Q5T653	MRPL2 39S ribosomal protein L2, mitochondrial	R.QMQVLETC*VATVGR.V	240	1.53	0.61	0.14
O75521	ECI2 Enoyl-CoA delta isomerase 2, mitochondrial	K.LHAVNAEEC*NVLQGR.W	368	1.52	0.61	0.13
O75439	PMPCB Mitochondrial-processing peptidase subunit beta	K.GEIPALPPC*K.F	277	1.53	0.61	0.38
Q92506	HSD17B8 Estradiol 17-beta-dehydrogenase 8	R.C*NSVLPGFIATPMTQK.V	194	1.58	0.60	0.82
P53396	ACLY ATP-citrate synthase	K.FIC*TTSAIQNR.F	20	1.52	0.60	0.02
P43304	GPD2 Glycerol-3-phosphate dehydrogenase, mitochondrial	R.C*KDVLTGQEFDVR.A	270	1.52	0.60	0.13
P09110	ACAA1 3-ketoacyl-CoA thiolase, peroxisomal	K.DVNLRPEQLGDIC*VGNVLQPGAGAIM AR.I	87	1.52	0.60	0.10
Q7L0Y3	TRMT10C Mitochondrial ribonuclease P protein 1	K.RLNLATEC*LPLDK.Y	335	1.52	0.60	0.11
Q9H9P8	L2HGDH L-2-hydroxyglutarate dehydrogenase, mitochondrial	R.GLMAIDC*PHTGIVDYR.Q	187	1.52	0.60	0.18
Q9HC38	GLOD4 Glyoxalase domain-containing protein 4	R.IAFSC*PQK.E	221	1.52	0.60	0.15
Q9BYT8	NLN Neurolysin, mitochondrial	R.IVHLQETC*DLGK.I	153	1.51	0.60	0.03
Q969Z3	MARC2 MOSC domain-containing protein 2, mitochondrial	R.C*ILTTVDPDTGVIDR.K	272	1.52	0.60	0.17
O94826	TOMM70A Mitochondrial import receptor subunit TOM70	K.EVAQDC*TK.A	176	1.51	0.60	0.09
Q96GW9	MARS2 Methionine--tRNA ligase, mitochondrial	R.VSEQFQQLFQEAGISC*TDFIR.T	132	1.55	0.60	0.71
Q9H9J2	MRPL44 39S ribosomal protein L44, mitochondrial	K.TAFVNSC*YIK.S	96	1.51	0.59	0.20
P36776	LONP1 Lon protease homolog, mitochondrial	K.VLFIC*TANVTDTIPEPLR.D	637	1.51	0.59	0.11
O60313	OPA1 Dynamin-like 120 kDa protein, mitochondrial	K.AYMQNPNAIILC*IQDGSVDAER.S	435	1.51	0.59	0.17
P26440	IVD Isovaleryl-CoA dehydrogenase, mitochondrial	K.AC*DEGHC*TAK.D	350	1.51	0.59	0.23

P51649	ALDH5A1 Succinate-semialdehyde dehydrogenase, mitochondria	K.YVC*YGGL.-	531	1.51	0.59	0.09
Q8WV74	NUDT8 Nucleoside diphosphate-linked moiety X motif 8, mi	R.PASAAVLVPLC*SVR.G	39	1.51	0.59	0.01
Q9BQ69	MACROD1 O-acetyl-ADP-ribose deacetylase MACROD1	K.LEVDAIVNAANSSLLGGGGVDGC*IHR.A	186	1.51	0.59	0.08
Q9UI43	FTSJ2 Putative ribosomal RNA methyltransferase 2	R.VLDC*GAAPGAWSQVAVQK.V	79	1.51	0.59	0.10
P04040	CAT Catalase	R.LC*ENIAGHLK.D	460	1.51	0.59	0.18
Q08257	CRYZ Quinone oxidoreductase	K.VHAC*GVNPVETYIR.S	45	1.52	0.59	0.41
Q99797	MIPEP Mitochondrial intermediate peptidase	K.C*LEELLSSR.D	281	1.50	0.59	0.16
P50416	CPT1A Carnitine O-palmitoyltransferase 1, liver isoform	K.FSC*PETDSHR.F	742	1.50	0.59	0.20
Q99714	HSD17B10 3-hydroxyacyl-CoA dehydrogenase type-2	K.FGRVDVAVNC*AGIAVASK.T	91	1.50	0.58	0.10
Q9P2R7	SUCLA2 Succinyl-CoA ligase	K.ILAC*DDLDEAAR.M	430	1.50	0.58	0.13
Q9UBQ7	GRHPR Glyoxylate reductase/hydroxypyruvate reductase	R.AADC*EVEQWDSDEPIPAKELER.G	29	1.51	0.58	0.34
P07237	P4HB Protein disulfide-isomerase	R.ITEFC*HR.F	343	1.50	0.58	0.12
Q6UB35	MTHFD1L Monofunctional C1-tetrahydrofolate synthase, mitoc	K.EYTEENIQLVADGC*C*NLQK.Q	778	1.51	0.58	0.49
Q7Z7H8	MRPL10 39S ribosomal protein L10, mitochondrial	R.TVPFLPLLGGC*IDDTILSR.Q	180	1.50	0.58	0.13
Q9H773	DCTPP1 dCTP pyrophosphatase 1	R.KYTELPHGAISEDQAVGPADIPC*DSTGQTST.-	162	1.50	0.58	0.06
P50213	IDH3A Isocitrate dehydrogenase	K.TFDLYANVRPC*VSIEGYK.T	127	1.50	0.58	0.18
P08559	PDHA1 Pyruvate dehydrogenase E1 component subunit alpha,	R.FAAAYC*R.S	273	1.50	0.58	0.20
Q8NI60	ADCK3 Chaperone activity of bc1 complex-like, mitochondr	R.ELALEC*DYQR.E	406	1.49	0.58	0.10
Q9NYY8	FASTKD2 FAST kinase domain-containing protein 2	R.SAYC*LGSSHPR.G	645	1.50	0.58	0.25
P10515	DLAT Dihydrolipoyllysine-residue acetyltransferase comp	K.NFSAIINPPQAC*ILAIGASEDK.L	586	1.49	0.58	0.18
Q8NFF5	FLAD1 FAD synthase	R.SLGVQVC*R.V	147	1.51	0.58	0.53
Q8TAA5	GRPEL2 GrpE protein homolog 2, mitochondrial	K.IFGIQSFC*K.D	110	1.50	0.57	0.30
Q6PI48	DARS2 Aspartate--tRNA ligase, mitochondrial	R.TNTC*GELR.S	54	1.49	0.57	0.09
Q5JRX3	PITRM1 Presequence protease, mitochondrial	K.LGC*GLLDYR.E	627	1.49	0.57	0.11
Q96GJ1	TRMT2B tRNA (uracil(54)-C(5))-methyltransferase homolog	R.DGNVVC*VQSNHLK.N	185	1.49	0.57	0.14
Q8IXI1	RHOT2 Mitochondrial Rho GTPase 2	K.ADLPEGVAVSGPSPAEFC*R.K	543	1.49	0.57	0.15
Q6YN16	HSDL2 Hydroxysteroid dehydrogenase-like protein 2	R.LAGC*TVFITGASR.G	11	1.49	0.57	0.16
Q9NQZ5	STARD7 StAR-related lipid transfer protein 7, mitochondri	R.KNEGSC*GPAR.I	362	1.49	0.57	0.08
P43897	TSFM Elongation factor Ts, mitochondrial	R.FEC*GEGEEAAETE.-	315	1.49	0.57	0.09
P31930	UQCRC1 Cytochrome b-c1 complex subunit 1, mitochondrial	R.LC*TSATESEVAR.G	380	1.49	0.57	0.09
P22234	PAICS Multifunctional protein ADE2	R.VVVLMGSTSDLGHC*EK.I	281	1.54	0.57	0.92
Q9Y6C9	MTCH2 Mitochondrial carrier homolog 2	R.LC*SGVLGTVVHGK.V	79	1.49	0.57	0.12
Q9BQP7	C20orf72 Uncharacterized protein C20orf72	R.GVAQTPGSVEEDALLC*GPVSK.H	79	1.49	0.57	0.13
Q6UB35	MTHFD1L Monofunctional C1-tetrahydrofolate synthase, mitoc	R.AEIDLVC*ELAK.R	814	1.49	0.57	0.13
Q7L2E3	DHX30 Putative ATP-dependent RNA helicase DHX30	R.YFGGC*PVIK.V	606	1.49	0.57	0.01
P12532	CKMT1B Creatine kinase U-type, mitochondrial	R.GLSLPPAC*TR.A	179	1.49	0.57	0.08
P23786	CPT2 Carnitine O-palmitoyltransferase 2, mitochondrial	R.HSAGELQQMMVEC*SK.Y	535	1.49	0.57	0.11
Q6YN16	HSDL2 Hydroxysteroid dehydrogenase-like protein 2	K.ALPC*IVDVR.D	71	1.49	0.57	0.30
Q7Z4W1	DCXR L-xylulose reductase	R.AVTNHSVYC*STK.G	150	1.48	0.57	0.05
P48735	IDH2 Isocitrate dehydrogenase	K.C*ATITPDEAR.V	113	1.48	0.57	0.05
Q86SX6	GLRX5 Glutaredoxin-related protein 5, mitochondrial	K.GTPEQPQC*GFSNAVVQILR.L	67	1.48	0.57	0.14
P49419	ALDH7A1 Alpha-aminoadipic semialdehyde dehydrogenase	R.GEVITTYC*PANNEPIAR.V	70	1.48	0.57	0.15
Q8IVS2	MCAT Malonyl-CoA-acyl carrier protein transacylase, mit	K.FNFAC*LEAR.E	208	1.48	0.57	0.03
Q14318	FKBP8 Peptidyl-prolyl cis-trans isomerase FKBP8	K.C*LNNLAASQLK.L	274	1.48	0.57	0.05
P04181	OAT Ornithine aminotransferase, mitochondrial	K.DWDAWKVC*LR.L	394	1.48	0.57	0.05
P42765	ACAA2 3-ketoacyl-CoA thiolase, mitochondrial	K.ISREEC*DKYALQSQQR.W	179	1.48	0.56	0.09
P42704	LRPPRC Leucine-rich PPR motif-containing protein, mitocho	R.SC*GSLLPELK.L	130	1.48	0.56	0.13
P28331	NDUFS1 NADH-ubiquinone oxidoreductase 75 kDa subunit, mit	R.VDSDTLC*TEEVFPTAGAGTDLR.S	367	1.48	0.56	0.15
Q9NP81	SARS2 Serine--tRNA ligase, mitochondrial	R.FGEVTSASNC*TDFQSR.R	425	1.50	0.56	0.55
O94826	TOMM70A Mitochondrial import receptor subunit TOM70	K.C*FALYR.Q	442	1.48	0.56	0.16
P31930	UQCRC1 Cytochrome b-c1 complex subunit 1, mitochondrial	R.NALVSHLDGTTPVC*EDIGR.S	410	1.47	0.56	0.04
P53597	SUCLG1 Succinyl-CoA ligase	K.IIC*QGFTGK.Q	60	1.47	0.56	0.14
P51659	HSD17B4 Peroxisomal multifunctional enzyme type 2	K.SNIHC*NTIAPNAGSR.M	189	1.47	0.56	0.18
P16219	ACADS Short-chain specific acyl-CoA dehydrogenase, mitoc	K.IGC*FALSEPGNGSDAGAASTTAR.A	151	1.47	0.56	0.18
Q12849	GRSF1 G-rich sequence factor 1	R.YIELFLNSC*PK.G	476	1.47	0.56	0.18
P42704	LRPPRC Leucine-rich PPR motif-containing protein, mitocho	K.GMQELGVHPDQETYTDYVIPC*FDSVNSAR.A	484	1.47	0.56	0.20
P31939	ATIC Bifunctional purine biosynthesis protein PURH	K.VC*MVYDLYK.T	287	1.47	0.56	0.02
Q8IXI2	RHOT1 Mitochondrial Rho GTPase 1	R.IPC*LIVAAK.S	522	1.47	0.56	0.04
P40926	MDH2 Malate dehydrogenase, mitochondrial	K.SQETEC*TYFSTPLLLGK.K	285	1.47	0.56	0.09
P11498	PC Pyruvate carboxylase, mitochondrial	R.ADFAQAC*QDAGVR.F	131	1.47	0.55	0.17
P49411	TUFM Elongation factor Tu, mitochondrial	K.GDEC*ELLGHSK.N	290	1.47	0.55	0.31
Q96AY3	FKBP10 Peptidyl-prolyl cis-trans isomerase FKBP10	K.GMDQGLLGMC*PGER.R	222	1.47	0.55	0.07
Q9UDR5	AASS Alpha-aminoadipic semialdehyde synthase, mitochond	K.KYNINPVSMDIC*K.Q	534	1.47	0.55	0.28
O75521	ECI2 Enoyl-CoA delta isomerase 2, mitochondrial	K.KLTAGEAC*AQGLVTEVFPDSTFQK.E	312	1.47	0.55	0.11
Q14318	FKBP8 Peptidyl-prolyl cis-trans isomerase FKBP8	R.SC*SLVLEHQPDNIK.A	295	1.47	0.55	0.13

Q96I99	SUCLG2 Succinyl-CoA ligase	K.IDATQVEVNPFGETPEGQVVC*FDAK.I	255	1.47	0.55	0.14
P09622	DLD Dihydrolipoyl dehydrogenase, mitochondrial	K.NETLGGTC*LNVGCIPSK.A	80	1.47	0.55	0.27
Q96EL3	MRPL53 39S ribosomal protein L53, mitochondrial	R.STNLNC*SVIADVR.H	49	1.47	0.55	0.18
P50336	PPOX Protoporphyrinogen oxidase	R.LGPEVASLAMDSLC*R.G	167	1.47	0.55	0.29
Q6PI48	DARS2 Aspartate--tRNA ligase, mitochondrial	K.TAELLNAC*K.K	152	1.46	0.55	0.07
P78540	ARG2 Arginase-2, mitochondrial	R.LSSLGC*HLK.D	63	1.46	0.55	0.17
Q53H82	LACTB2 Beta-lactamase-like protein 2	R.ILIDTGEPAIPEYISC*LK.Q	58	1.47	0.55	0.27
O75521	ECI2 Enoyl-CoA delta isomerase 2, mitochondrial	R.WLSDEC*TNAVVNFLSR.K	380	1.46	0.55	0.17
Q9NRP4	ACN9 Protein ACN9 homolog, mitochondrial	K.AC*FGTFLPEEK.L	80	1.46	0.55	0.00
P51649	ALDH5A1 Succinate-semialdehyde dehydrogenase, mitochondria	R.WLPAAATFPVQDPASGAALGMVADC*GVR.E	93	1.46	0.55	0.08
P28838	LAP3 Cytosol aminopeptidase	R.ADMGGAATIC*SAIVSAAK.L	313	1.46	0.55	0.10
P21953	BCKDHB 2-oxoisovalerate dehydrogenase subunit beta, mitoc	R.TIIPWDVDTIC*K.S	316	1.46	0.55	0.13
P09110	ACAA1 3-ketoacyl-CoA thiolase, peroxisomal	K.ARDC*LIPMGITSENVAER.F	177	1.46	0.54	0.26
Q8IYB8	SUPV3L1 ATP-dependent RNA helicase SUPV3L1, mitochondrial	R.YVFC*TAPINK.K	575	1.46	0.54	0.15
O75439	PMPCB Mitochondrial-processing peptidase subunit beta	K.TNMLLQLDGSTPIC*EDIGR.Q	419	1.47	0.54	0.37
Q8NBU5	ATAD1 ATPase family AAA domain-containing protein 1	K.DAAFQNVLTHVC*LD.-	359	1.46	0.54	0.06
P53701	HCCS Cytochrome c-type heme lyase	R.AYEYVEC*PIR.G	66	1.46	0.54	0.06
P60900	PSMA6 Proteasome subunit alpha type-6	R.GKDC*AVIVTQK.K	47	1.47	0.54	0.45
Q99714	HSD17B10 3-hydroxyacyl-CoA dehydrogenase type-2	K.VC*NFLASQVPFPSR.L	214	1.46	0.54	0.10
P31930	UQCRC1 Cytochrome b-c1 complex subunit 1, mitochondrial	K.AVELLGDIVQNC*SLEDSQIEK.E	154	1.46	0.54	0.11
Q9H9J2	MRPL44 39S ribosomal protein L44, mitochondrial	K.NLVDFLTGEEVVC*HVAR.N	167	1.46	0.54	0.11
Q9Y2Z4	YARS2 Tyrosine--tRNA ligase, mitochondrial	K.EAPFSEFFLDPGTSVLDTC*R.K	413	1.46	0.54	0.12
O94826	TOMM70A Mitochondrial import receptor subunit TOM70	K.ILLDQVEEAVADFDEC*IR.L	427	1.45	0.54	0.04
P31930	UQCRC1 Cytochrome b-c1 complex subunit 1, mitochondrial	K.YIYDQC*PAVAGYGPIEQLPDYNR.I	453	1.45	0.54	0.07
P28838	LAP3 Cytosol aminopeptidase	R.AAVAAGC*R.Q	129	1.45	0.54	0.11
Q92506	HSD17B8 Estradiol 17-beta-dehydrogenase 8	R.LAGEGATVAAC*DLDR.A	41	1.47	0.54	0.52
P82921	MRPS21 28S ribosomal protein S21, mitochondrial	K.NRADPWQGC*.-	87	1.45	0.54	0.17
O15091	KIAA0391 Mitochondrial ribonuclease P protein 3	K.TIESIQLSPEEYEC*LK.G	367	1.46	0.54	0.27
P42704	LRPPRC Leucine-rich PPR motif-containing protein, mitocho	R.C*VANNQVETLEK.L	930	1.45	0.54	0.02
Q12931	TRAP1 Heat shock protein 75 kDa, mitochondrial	R.NIYYLC*APNR.H	501	1.46	0.54	0.32
Q8NBU5	ATAD1 ATPase family AAA domain-containing protein 1	R.DAALLC*VR.E	310	1.45	0.54	0.09
Q9BV79	MECR Trans-2-enoyl-CoA reductase, mitochondrial	R.GQLTAPAC*SQVPLQDYQSALEASMKPFISSK.Q	345	1.46	0.54	0.41
Q15120	PDK3	K.HIGSIDPTC*NVADVVK.D	191	1.45	0.53	0.18
P23378	GLDC Glycine dehydrogenase	R.NEDAC*PVGTVSAAPWGSSSILPISWAYIK.M	795	1.45	0.53	0.22
P42704	LRPPRC Leucine-rich PPR motif-containing protein, mitocho	K.VFNDTC*R.S	113	1.45	0.53	0.01
P13804	ETFA Electron transfer flavoprotein subunit alpha, mito	K.VAQDLC*K.V	68	1.45	0.53	0.05
P40939	HADHA Trifunctional enzyme subunit alpha, mitochondrial	R.C*LAPMMSEVIR.I	550	1.47	0.53	0.60
P30084	ECHS1 Enoyl-CoA hydratase, mitochondrial	K.AFAAGADIKEMQNLSFQDC*YSSK.F	111	1.44	0.53	0.05
Q86UT6	NLRX1 NLR family member X1	R.HALDEVNLASC*QLDPAGLR.T	735	1.44	0.53	0.08
P40926	MDH2 Malate dehydrogenase, mitochondrial	K.EGVVEC*SFVK.S	275	1.44	0.53	0.11
P83111	LACTB Serine beta-lactamase-like protein LACTB, mitochon	K.QTYGSC*R.K	476	1.44	0.52	0.19
P43304	GPD2 Glycerol-3-phosphate dehydrogenase, mitochondrial	K.LYDLVAGSNC*LK.S	188	1.44	0.52	0.07
Q99714	HSD17B10 3-hydroxyacyl-CoA dehydrogenase type-2	K.KLGNNC*VFAPADVTSEK.D	58	1.44	0.52	0.10
Q9HBH1	PDF Peptide deformylase, mitochondrial	R.QVLALELPEALC*R.E	132	1.44	0.52	0.11
Q9UKU7	ACAD8 Isobutyryl-CoA dehydrogenase, mitochondrial	K.FASYC*LTEPGSGSDAASLLTSAK.K	159	1.46	0.52	0.59
Q8NCN5	PDPR Pyruvate dehydrogenase phosphatase regulatory subu	K.LVNC*PETFTPDMR.C	357	1.46	0.52	0.73
P82933	MRPS9 28S ribosomal protein S9, mitochondrial	K.ALC*SFVTEDEVEWMR.Q	353	1.44	0.52	0.22
Q8WVM0	TFB1M Dimethyladenosine transferase 1, mitochondrial	K.WLENISC*R.D	160	1.44	0.52	0.18
P34897	SHMT2 Serine hydroxymethyltransferase, mitochondrial	R.GLELIASENFC*SR.A	80	1.43	0.52	0.01
P08559	PDHA1 Pyruvate dehydrogenase E1 component subunit alpha,	R.VDGMDILC*VR.E	261	1.43	0.52	0.08
Q9H936	SLC25A22 Mitochondrial glutamate carrier 1	R.GVNEDTYSGILDC*AR.K	271	1.43	0.52	0.11
Q96EL3	MRPL53 39S ribosomal protein L53, mitochondrial	R.HDGSEPC*VDVLFGDGHR.L	63	1.43	0.52	0.13
Q99798	ACO2 Aconitate hydratase, mitochondrial	K.VAVPSTIHC*DHLIEAQVGGEK.D	126	1.44	0.52	0.44
P49821	NDUFV1 NADH dehydrogenase	K.YLVVNADEGEPGTC*K.D	125	1.43	0.52	0.07
Q7Z6M4	MTERFD2 mTERF domain-containing protein 2	R.SNNYVQEPEC*R.R	69	1.43	0.52	0.08
Q9UH62	ARMCX3 Armadillo repeat-containing X-linked protein 3	K.MAEGGSGDVDDAGDC*SGAR.Y	52	1.43	0.52	0.09
P10809	HSPD1 60 kDa heat shock protein, mitochondrial	R.C*IPALDSLTPANEDQK.I	447	1.43	0.52	0.11
P13804	ETFA Electron transfer flavoprotein subunit alpha, mito	R.TIYAGNALC*TVK.C	155	1.43	0.52	0.12
P00367	GLUD1 Glutamate dehydrogenase 1, mitochondrial	K.C*AVVDVPFGGAK.A	172	1.43	0.51	0.14
Q9H078	CLPB Caseinolytic peptidase B protein homolog	R.VVNQLAAAYEQDLLPGGC*TLR.I	647	1.43	0.51	0.21
Q8NBX0	SCCPDH Saccharopine dehydrogenase-like oxidoreductase	K.QATVVLNC*VGPYR.F	98	1.44	0.51	0.46
Q7Z4W1	DCXR L-xylulose reductase	R.SGMTTGSTLPVEGGFWAC*.-	244	1.43	0.51	0.22
O75390	CS Citrate synthase, mitochondrial	R.YTC*QREFALK.H	359	1.43	0.51	0.23
B4DLN1	SLC25A10 cDNA FLJ60124, highly similar to Mitochondrial dic	K.GEYQGVFHC*AVETAK.L	395	1.43	0.51	0.05
P30084	ECHS1 Enoyl-CoA hydratase, mitochondrial	K.ALNALC*DGLIDELNQALK.T	62	1.43	0.51	0.06
O95202	LETM1 LETM1 and EF-hand domain-containing protein 1, mit	K.LFEDELTLDNLTRPQLVALC*K.L	330	1.43	0.51	0.15

Q9NWR8	CCDC109B Coiled-coil domain-containing protein 109B	K.IAYDVQC*PK.R	147	1.43	0.51	0.29
Q9UH62	ARMCX3 Armadillo repeat-containing X-linked protein 3	K.VYMNQVC*DDTITSR.L	208	1.43	0.51	0.41
Q6P587	FAHD1 Acylpyruvase FAHD1, mitochondrial	K.SFTASC*PVSAFVPK.E	129	1.42	0.51	0.05
P10515	DLAT Dihydrolipoyllysine-residue acetyltransferase comp	R.DVPLGTPLC*IIVEK.E	291	1.43	0.51	0.25
P54819	AK2 Adenylate kinase 2, mitochondrial	R.LAENFC*VCHLATGDMLR.A	40	1.42	0.51	0.12
Q8N5M1	ATPAF2 ATP synthase mitochondrial F1 complex assembly fac	K.FLDTDTIC*YR.V	141	1.42	0.51	0.13
P00367	GLUD1 Glutamate dehydrogenase 1, mitochondrial	K.C*IAVGESDGSIWNPDGIDPK.E	327	1.43	0.51	0.28
Q9Y512	SAMM50 Sorting and assembly machinery component 50 homolo	R.TKDDIIIC*EIGDVFK.A	65	1.42	0.51	0.16
Q9NSE4	IARS2 Isoleucine--tRNA ligase, mitochondrial	K.KPGLEEAVESAC*AMR.D	883	1.42	0.51	0.11
Q6PI48	DARS2 Aspartate--tRNA ligase, mitochondrial	K.LRLEC*ADLLETR.G	459	1.42	0.50	0.12
O43920	NDUFS5 NADH dehydrogenase	K.IEYDDFVEC*LLR.Q	66	1.42	0.50	0.17
Q00325	SLC25A3 Phosphate carrier protein, mitochondrial	K.FAC*FER.T	237	1.42	0.50	0.07
Q9NUJ1	ABHD10 Abhydrolase domain-containing protein 10, mitochon	K.ALAIEEFC*K.S	100	1.42	0.50	0.07
P04406	GAPDH Glyceraldehyde-3-phosphate dehydrogenase	K.IISNASC*TTNCLAPLAK.V	152	1.42	0.50	0.11
P51553	IDH3G Isocitrate dehydrogenase	R.HAC*VPVDFEEVHVSSNADEEDIR.N	81	1.42	0.50	0.14
Q8N4Q0	ZADH2 Zinc-binding alcohol dehydrogenase domain-containi	R.DC*PVPLPGDGDLLVR.N	55	1.42	0.50	0.18
Q96I99	SUCLG2 Succinyl-CoA ligase	R.SC*NGPVLVGSPQGGVDIEEVAASNPELI FK.E	162	1.42	0.50	0.20
P36542	ATP5C1 ATP synthase subunit gamma, mitochondrial	R.GLC*GAIHSSIAK.Q	103	1.44	0.50	0.70
P51659	HSD17B4 Peroxisomal multifunctional enzyme type 2	K.IC*DFENASKPQSIQESTGSIIEVLSK.I	277	1.42	0.50	0.22
P07203	GPX1 Glutathione peroxidase 1	K.LITWSPVC*R.N	156	1.42	0.50	0.19
P11177	PDHB Pyruvate dehydrogenase E1 component subunit beta,	K.EGVEC*EVINMR.T	263	1.41	0.50	0.02
P13804	ETFA Electron transfer flavoprotein subunit alpha, mito	R.LGGEVSC*LVAGTK.C	53	1.41	0.50	0.02
P49406	MRPL19 39S ribosomal protein L19, mitochondrial	K.ISQFLGIC*IQR.S	137	1.42	0.50	0.35
Q9NP81	SARS2 Serine--tRNA ligase, mitochondrial	R.GAVFEGC*GMTPNANPSQIYNIDPAR.F	272	1.41	0.50	0.09
P34897	SHMT2 Serine hydroxymethyltransferase, mitochondrial	R.AALEALGSC*LNNK.Y	91	1.41	0.50	0.15
P22695	UQCRC2 Cytochrome b-c1 complex subunit 2, mitochondrial	R.NALANPLYC*PDYR.I	192	1.41	0.50	0.21
P30405	PPIF Peptidyl-prolyl cis-trans isomerase F, mitochondri	R.VIPSFMC*QAGDFTNHNGTGGK.S	104	1.41	0.50	0.02
Q7KZF4	SND1 Staphylococcal nuclease domain-containing protein	R.ANNPEQNRLSEC*EEQAK.A	152	1.41	0.50	0.09
P28331	NDUFS1 NADH-ubiquinone oxidoreductase 75 kDa subunit, mit	K.VVAAC*AMPVMK.G	92	1.41	0.50	0.09
Q9Y2Q3	GSTK1 Glutathione S-transferase kappa 1	K.ETTEAAC*R.Y	176	1.41	0.50	0.10
O96000	NDUFB10 NADH dehydrogenase	R.EGQNYQQNC*IK.E	119	1.41	0.49	0.15
P42704	LRPPRC Leucine-rich PPR motif-containing protein, mitocho	R.IHDVLC*K.L	863	1.41	0.49	0.17
P36551	CPOX Coproporphyrinogen-III oxidase, mitochondrial	K.HC*DDSFTPQEK.L	373	1.41	0.49	0.18
P34897	SHMT2 Serine hydroxymethyltransferase, mitochondrial	R.MREVC*DEVK.A	241	1.41	0.49	0.30
Q00325	SLC25A3 Phosphate carrier protein, mitochondrial	K.GWAPTFLGYSMQGLC*K.F	136	1.41	0.49	0.19
Q14318	FKBP8 Peptidyl-prolyl cis-trans isomerase FKBP8	R.EC*GNAHYQR.A	227	1.41	0.49	0.02
Q4G0N4	NADKD1 NAD kinase domain-containing protein 1	K.SSGLNLC*TGTGSK.A	311	1.41	0.49	0.25
P40926	MDH2 Malate dehydrogenase, mitochondrial	K.TIIPLISQC*TPK.V	212	1.41	0.49	0.10
P31937	HIBADH 3-hydroxyisobutyrate dehydrogenase, mitochondrial	R.C*WSSDTYNPVPGVMDGVPSANNYQG GFGTTLMAK.D	251	1.42	0.49	0.49
Q99832	CCT7 T-complex protein 1 subunit eta	K.LPIGDVATQYFADRDMFC*AGR.V	310	1.43	0.49	0.68
P35270	SPR Sepiapterin reductase	R.TVVNISSLC*ALQPFK.G	159	1.41	0.49	0.04
Q6PI48	DARS2 Aspartate--tRNA ligase, mitochondrial	R.LIC*LVTGSPSIR.D	590	1.40	0.49	0.05
P45880	VDAC2 Voltage-dependent anion-selective channel protein	K.WNTDNTLGTEIAIEDQIC*QGLK.L	103	1.40	0.49	0.08
P49411	TUFM Elongation factor Tu, mitochondrial	K.GEETPVIVGSALC*ALEGR.D	222	1.40	0.49	0.09
O15235	MRPS12 28S ribosomal protein S12, mitochondrial	R.EAVC*FIPGEGHTLQEHQIVLVEGGR.T	93	1.40	0.49	0.14
P42704	LRPPRC Leucine-rich PPR motif-containing protein, mitocho	R.YC*QEPR.G	571	1.40	0.49	0.14
P13995	MTHFD2 Bifunctional methylenetetrahydrofolate dehydrogena	R.IC*NAVSPDKDVDGFHVINVGR.M	145	1.40	0.49	0.16
Q96NB2	SFXN2 Sideroflexin-2	K.C*ELPVSYLEPK.L	290	1.41	0.49	0.34
O00330	PDHX Pyruvate dehydrogenase protein X component, mitoch	K.STVPHAYATADC*DLGAVLK.V	307	1.40	0.49	0.06
P45880	VDAC2 Voltage-dependent anion-selective channel protein	R.PMC*IPPSYADLGK.A	13	1.40	0.49	0.06
Q6YN16	HSDL2 Hydroxysteroid dehydrogenase-like protein 2	K.TAIHTAAMDMLGGPGIESQC*R.K	218	1.41	0.48	0.38
P09001	MRPL3 39S ribosomal protein L3, mitochondrial	K.YTSKENC*NGK.M	138	1.40	0.48	0.11
P05141	SLC25A5 ADP/ATP translocase 2	K.GIIDC*VVR.I	57	1.40	0.48	0.15
P05091	ALDH2 Aldehyde dehydrogenase, mitochondrial	K.LLC*GGGIAADR.G	386	1.40	0.48	0.35
Q96DV4	MRPL38 39S ribosomal protein L38, mitochondrial	R.VAEGQVTC*PYLPPFPAR.G	252	1.40	0.48	0.03
O94826	TOMM70A Mitochondrial import receptor subunit TOM70	K.ADEMYDKC*IDLEPDNATTYVHK.G	502	1.40	0.48	0.06
P31040	SDHA Succinate dehydrogenase	R.VGSVLQEGC*GK.I	536	1.40	0.48	0.38
O75616	ERAL1 GTPase Era, mitochondrial	R.C*QALGVITEK.E	150	1.41	0.48	0.47
P48735	IDH2 Isocitrate dehydrogenase	K.DLAGC*IHGLSNVK.L	418	1.39	0.48	0.03
P82675	MRPS5 28S ribosomal protein S5, mitochondrial	R.EEC*GPLPIVVASPR.G	377	1.40	0.48	0.26
P10809	HSPD1 60 kDa heat shock protein, mitochondrial	R.AAVEEGIVLGGGC*ALLR.C	442	1.39	0.48	0.07
P49821	NDUFV1 NADH dehydrogenase	R.GAGAYIC*GEETALIESIEGK.Q	206	1.40	0.48	0.27
P51553	IDH3G Isocitrate dehydrogenase	R.TSLDLYANVIHC*K.S	148	1.40	0.48	0.37
P48735	IDH2 Isocitrate dehydrogenase	K.VC*VETVESGAMTK.D	402	1.39	0.48	0.10
Q9UJA2	CRLS1 Cardiolipin synthase	K.YFNPC*YATAR.L	230	1.39	0.48	0.14
Q14197	ICT1 Peptidyl-tRNA hydrolase ICT1, mitochondrial	R.NLADC*LQK.I	150	1.39	0.48	0.16
Q16698	DECR1 2,4-dienoyl-CoA reductase, mitochondrial	K.GMTTLLSSLGAQC*VIASR.K	86	1.39	0.48	0.24

P42704	LRPPRC Leucine-rich PPR motif-containing protein, mitocho	K.LFEC*DRDQMYYNLLK.L	952	1.39	0.47	0.06
Q9BW92	TARS2 Threonine--tRNA ligase, mitochondrial	R.IC*QELTAAAR.P	185	1.40	0.47	0.41
Q9BZE1	MRPL37 39S ribosomal protein L37, mitochondrial	R.NHIENQDEC*VLNVISHAR.L	153	1.39	0.47	0.06
Q9H2U2	PPA2 Inorganic pyrophosphatase 2, mitochondrial	R.GQPC*SQNYR.L	44	1.39	0.47	0.07
Q9NWU5	MRPL22 39S ribosomal protein L22, mitochondrial	K.VYC*HYFVK.L	166	1.39	0.47	0.14
Q9UGC7	MTRF1L Peptide chain release factor 1-like, mitochondrial	R.IVHLPTGVVSEC*QQER.S	274	1.39	0.47	0.17
Q8NE86	MCU Calcium uniporter protein, mitochondrial	K.TLVQQLYTTLC*IEQHQLNK.E	191	1.40	0.47	0.52
P31040	SDHA Succinate dehydrogenase	K.TLNEADC*ATVPPAIR.S	654	1.39	0.47	0.23
P38646	HSPA9 Stress-70 protein, mitochondrial	K.AKC*ELSSSVQTDINLPYLTMDSSGPK.H	317	1.39	0.47	0.26
Q12931	TRAP1 Heat shock protein 75 kDa, mitochondrial	K.FEDRSPAAEC*LSEK.E	573	1.38	0.47	0.07
Q7L2E3	DHX30 Putative ATP-dependent RNA helicase DHX30	R.C*NVIITQPR.R	484	1.41	0.47	0.77
Q9Y584	TIMM22 Mitochondrial import inner membrane translocase su	K.AMESC*AFK.A	69	1.39	0.47	0.30
P28331	NDUFS1 NADH-ubiquinone oxidoreductase 75 kDa subunit, mit	K.VLFLLGADGGC*ITR.Q	554	1.38	0.47	0.15
O14874	BCKDK	K.LTDFPPIKDQADEAQYC*QLVR.Q	152	1.38	0.47	0.21
P34897	SHMT2 Serine hydroxymethyltransferase, mitochondrial	K.NTC*PGDR.S	412	1.38	0.46	0.05
O60313	OPA1 Dynamin-like 120 kDa protein, mitochondrial	K.C*NEEHPAYLASDEITTVR.K	801	1.38	0.46	0.08
P30044	PRDX5 Peroxiredoxin-5, mitochondrial	K.ALNVEPDGTGLTC*SLAPNIISQL.-	204	1.38	0.46	0.09
P00367	GLUD1 Glutamate dehydrogenase 1, mitochondrial	K.AKPYEGSILEADC*DILIPAASEK.Q	376	1.38	0.46	0.10
O43772	SLC25A20 Mitochondrial carnitine/acylcarnitine carrier prot	K.YTGTLDC*AK.K	155	1.38	0.46	0.10
P40926	MDH2 Malate dehydrogenase, mitochondrial	K.GC*DVVVIPAGVPR.K	93	1.38	0.46	0.12
O00571	DDX3X ATP-dependent RNA helicase DDX3X	K.IGLDFC*K.Y	341	1.38	0.46	0.17
P55809	OXCT1 Succinyl-CoA:3-ketoacid coenzyme A transferase 1,	K.STGC*DFAVSPK.L	504	1.38	0.46	0.18
Q96HY7	DHTKD1 Probable 2-oxoglutarate dehydrogenase E1 component	R.VEELC*PFPLDSLQQEMSK.Y	839	1.39	0.46	0.46
P10809	HSPD1 60 kDa heat shock protein, mitochondrial	K.C*EFQDAYVLLSEK.K	237	1.38	0.46	0.06
Q3ZCQ8	TIMM50 Mitochondrial import inner membrane translocase su	R.VVVVDC*KK.E	249	1.38	0.46	0.06
P49411	TUFM Elongation factor Tu, mitochondrial	K.NMITGTAPLDGC*ILVVAANDGPMPQTR.E	147	1.38	0.46	0.09
Q9Y512	SAMM50 Sorting and assembly machinery component 50 homolo	R.KLAEC*IR.W	421	1.38	0.46	0.12
Q9BQ52	ELAC2 Zinc phosphodiesterase ELAC protein 2	K.VC*FGDFPTMPK.L	753	1.38	0.46	0.16
Q8TAE8	GADD45GIP1 Growth arrest and DNA damage-inducible proteins-in	R.EQHIAEC*MAK.M	124	1.39	0.46	0.63
Q9H9J2	MRPL44 39S ribosomal protein L44, mitochondrial	R.QSGGTTALPLYFVGLYC*DK.K	276	1.38	0.46	0.39
O75746	SLC25A12 Calcium-binding mitochondrial carrier protein Aral	R.AGQTTYSGVIDC*FR.K	563	1.37	0.46	0.12
B4DLN1	SLC25A10 cDNA FLJ60124, highly similar to Mitochondrial dic	R.TDGILALYSGLSASLC*R.Q	224	1.37	0.46	0.15
P42704	LRPPRC Leucine-rich PPR motif-containing protein, mitocho	R.LQWFC*DR.C	927	1.37	0.46	0.17
Q8WVM0	TFB1M Dimethyladenosine transferase 1, mitochondrial	K.SLC*DVYR.K	304	1.38	0.46	0.44
Q6UXV4	APOOL Apolipoprotein O-like	K.ITYPLGLATLGATVC*YPVQSVIIAK.V	152	1.37	0.45	0.25
Q15067	ACOX1 Peroxisomal acyl-coenzyme A oxidase 1	K.LVC*GMVSYLNDLPSQR.I	449	1.37	0.45	0.26
P82933	MRPS9 28S ribosomal protein S9, mitochondrial	K.HDVTC*TVSGGGR.S	330	1.37	0.45	0.27
O75431	MTX2 Metaxin-2	K.NYSNLLAFC*R.R	246	1.37	0.45	0.07
Q9H845	ACAD9 Acyl-CoA dehydrogenase family member 9, mitochondr	R.AYIC*AHPLDR.T	613	1.37	0.45	0.12
Q96BW9	TAMM41 Mitochondrial translocator assembly and maintenanc	K.NRDVEETLFQVAHDPDC*GDVVR.L	285	1.37	0.45	0.34
P31040	SDHA Succinate dehydrogenase	R.TYFSC*TSAHTSTGDGTAMITR.A	266	1.37	0.45	0.08
Q4G0N4	NADKD1 NAD kinase domain-containing protein 1	R.SEGHLC*LPVR.Y	193	1.37	0.45	0.29
Q9P0M9	MRPL27 39S ribosomal protein L27, mitochondrial	K.C*LYALEEGIVR.Y	88	1.38	0.45	0.49
Q13825	AUH Methylglutaconyl-CoA hydratase, mitochondrial	R.SEVPGIFC*AGADLK.E	138	1.37	0.45	0.14
Q86WA6	BPHL Valacyclovir hydrolase	K.HLPDGNIC*R.H	225	1.37	0.45	0.19
Q96RP9	GFM1 Elongation factor G, mitochondrial	R.YQPC*LPSTQEDVINK.Y	723	1.37	0.45	0.37
Q53H82	LACTB2 Beta-lactamase-like protein 2	R.DHSGGIGDIC*K.S	90	1.37	0.45	0.25
P10620	MGST1 Microsomal glutathione S-transferase 1	K.VFANPEDC*VAFGK.G	50	1.36	0.45	0.05
Q8NCN5	PDPR Pyruvate dehydrogenase phosphatase regulatory subu	R.FC*AGILSTAR.H	85	1.38	0.45	0.68
Q6P1X6	C8orf82 UPF0598 protein C8orf82	R.YEAAFPFLSPC*GR.E	98	1.36	0.44	0.24
O96008	TOMM40 Mitochondrial import receptor subunit TOM40 homolo	R.TPGAATASASGAAEDGAC*GCLPNPGTFEECHRK.C	74	1.36	0.44	0.00
Q13011	ECH1 Delta(3,5)-Delta(2,4)-dienoyl-CoA isomerase, mitoc	R.YC*AQDAFFQVK.E	187	1.36	0.44	0.16
Q16822	PCK2 Phosphoenolpyruvate carboxykinase	R.QC*PIMDPAWEAPEGVPIDAIIFGGR.R	431	1.36	0.44	0.20
P82933	MRPS9 28S ribosomal protein S9, mitochondrial	K.LLTSQC*GAAEEEFVQR.F	233	1.36	0.44	0.20
Q16611	BAK1 Bcl-2 homologous antagonist/killer	R.QEC*GEPALPSASEEQVAQDTEEVFR.S	14	1.36	0.44	0.39
Q92552	MRPS27 28S ribosomal protein S27, mitochondrial	K.VAASPEDIKLC*R.E	276	1.36	0.44	0.08
Q53H12	AGK Acylglycerol kinase, mitochondrial	R.AAC*QEAQVFGNQLIPPNAQVK.K	43	1.36	0.44	0.14
P11182	DBT Lipoamide acyltransferase component of branched-ch	K.AASLGLLQFPILNASVDENC*QNITYK.A	333	1.36	0.44	0.15
Q5T160	RARS2 Probable arginine--tRNA ligase, mitochondrial	R.AIAC*QLSR.V	11	1.36	0.44	0.21
P82675	MRPS5 28S ribosomal protein S5, mitochondrial	R.GWSGNSWGGISLGPPDPGPC*GETYEDFDTR.I	211	1.37	0.44	0.63
Q9HC21	SLC25A19 Mitochondrial thiamine pyrophosphate carrier	K.NENLQNLLC*GSGAGVISK.T	222	1.36	0.44	0.31
Q86U28	ISCA2 Iron-sulfur cluster assembly 2 homolog, mitochondr	R.LTDSC*VQR.L	56	1.35	0.44	0.12
P34897	SHMT2 Serine hydroxymethyltransferase, mitochondrial	R.YYGGAEVVDEIELLC*QR.R	119	1.35	0.44	0.12

P22695	UQCRC2 Cytochrome b-c1 complex subunit 2, mitochondrial	R.ENMAYTVEC*LR.G	125	1.35	0.44	0.18
Q9HA77	CARS2 Probable cysteine--tRNA ligase, mitochondrial	K.GQLAC*GSVR.E	387	1.35	0.44	0.18
Q15067	ACOX1 Peroxisomal acyl-coenzyme A oxidase 1	R.ASEAHC*HYVVVK.L	531	1.36	0.43	0.33
Q8N983	MRPL43 39S ribosomal protein L43, mitochondrial	R.EESIHC*K.S	91	1.35	0.43	0.25
Q9HC21	SLC25A19 Mitochondrial thiamine pyrophosphate carrier	K.GLMDC*AK.Q	268	1.35	0.43	0.26
Q8N4Q0	ZADH2 Zinc-binding alcohol dehydrogenase domain-containi	K.C*HVIGTCSSDEK.S	198	1.35	0.43	0.07
P38117	ETFB Electron transfer flavoprotein subunit beta	K.HSMNPFC*EIAVEEAVR.L	42	1.35	0.43	0.07
Q6NUK1	SLC25A24 Calcium-binding mitochondrial carrier protein SCaM	K.TGQYSGIYDC*AK.K	330	1.35	0.43	0.09
P45880	VDAC2 Voltage-dependent anion-selective channel protein	K.SC*SGVEFSTSGSSNTDTGK.V	47	1.35	0.43	0.11
O60313	OPA1 Dynamin-like 120 kDa protein, mitochondrial	K.EGC*TVSPETISLNVK.G	375	1.36	0.43	0.44
P12532	CKMT1B Creatine kinase U-type, mitochondrial	K.TTPTGWTLDQC*IQTGVDNPGHPFIK.T	89	1.35	0.43	0.23
P30405	PPIF Peptidyl-prolyl cis-trans isomerase F, mitochondri	R.ALC*TGEKGFGYK.G	82	1.35	0.43	0.27
P12235	SLC25A4 ADP/ATP translocase 1	R.EFHGLGDC*IIK.I	160	1.35	0.43	0.05
P45880	VDAC2 Voltage-dependent anion-selective channel protein	K.WC*EYGLTFTEK.W	76	1.35	0.43	0.09
P12235	SLC25A4 ADP/ATP translocase 1	R.YFAGNLASGGAAGATSLC*FVYPLDFAR.T	129	1.35	0.43	0.10
Q5T653	MRPL2 39S ribosomal protein L2, mitochondrial	R.AAGTC*GVLLR.K	213	1.35	0.43	0.15
P36551	CPOX Coproporphyrinogen-III oxidase, mitochondrial	R.C*SSFMAPPVTDLGELR.R	127	1.34	0.43	0.01
Q16134	ETFDH Electron transfer flavoprotein-ubiquinone oxidored	K.AAQIGAHTLSGAC*LDPGAFK.E	118	1.34	0.43	0.10
Q9H061	TMEM126A Transmembrane protein 126A	R.C*FVSFPLNTGDLDCETCTITR.S	85	1.35	0.42	0.35
Q96I59	NARS2 Probable asparagine--tRNA ligase, mitochondrial	K.VIGNC*DAK.D	121	1.35	0.42	0.47
Q96I51	WBSCR16 Williams-Beuren syndrome chromosomal region 16 pro	R.VLQVSC*GR.A	181	1.34	0.42	0.28
Q9NVA1	UQCC Ubiquinol-cytochrome c reductase complex chaperone	R.MYTSC*VEK.T	124	1.34	0.42	0.03
Q7Z2W9	MRPL21 39S ribosomal protein L21, mitochondrial	K.VTSEDLILIGNELDLAC*GER.I	124	1.34	0.42	0.07
Q9Y2R9	MRPS7 28S ribosomal protein S7, mitochondrial	K.NC*EPMIGLVPILK.G	152	1.34	0.42	0.12
Q5U5X0	LYRM7 LYR motif-containing protein 7	K.DLLVENVPYC*DAPTQK.Q	97	1.34	0.42	0.19
P21912	SDHB Succinate dehydrogenase	R.EGIC*GSCAMNINGGNTLAC*TR.R	98	1.34	0.42	0.39
P21912	SDHB Succinate dehydrogenase	R.EGICGSC*AMNINGGNTLAC*TR.R	101	1.34	0.42	0.39
Q8IXI1	RHOT2 Mitochondrial Rho GTPase 2	K.SFAHC*ASVYK.H	504	1.34	0.42	0.29
Q9Y6M9	NDUFB9 NADH dehydrogenase	K.VPEWC*LDDWHPSEK.A	103	1.34	0.42	0.31
P56962	STX17 Syntaxin-17	K.LTSSC*PDLPSQTDKK.C	290	1.34	0.42	0.34
O14880	MGST3 Microsomal glutathione S-transferase 3	K.VEYPIMYSTDPENGHIFNC*IQR.A	56	1.34	0.42	0.27
Q9BV79	MECR Trans-2-enoyl-CoA reductase, mitochondrial	R.LALNC*VGGK.S	263	1.33	0.41	0.05
Q9H936	SLC25A22 Mitochondrial glutamate carrier 1	R.VYTSMSDC*LIK.T	52	1.33	0.41	0.13
Q12931	TRAP1 Heat shock protein 75 kDa, mitochondrial	K.SDC*KEFSSEAR.V	261	1.33	0.41	0.17
O95831	AIFM1 Apoptosis-inducing factor 1, mitochondrial	R.SNIWVAGDAAC*FYDIK.L	441	1.34	0.41	0.48
Q16822	PCK2 Phosphoenolpyruvate carboxykinase	K.YNNC*WLAR.T	92	1.33	0.41	0.29
O75306	NDUFS2 NADH dehydrogenase	R.IIAQC*LNK.M	347	1.33	0.41	0.05
P30405	PPIF Peptidyl-prolyl cis-trans isomerase F, mitochondri	K.IVITDC*GQLS.-	203	1.33	0.41	0.07
Q96EL3	MRPL53 39S ribosomal protein L53, mitochondrial	R.VQFC*PFEK.N	21	1.33	0.41	0.16
Q9Y399	MRPS2 28S ribosomal protein S2, mitochondrial	R.DC*GEYAHTR.Y	162	1.33	0.41	0.20
Q86VU5	COMTD1 Catechol O-methyltransferase domain-containing pro	K.VLQPPKGDVAAEC*VR.N	231	1.33	0.41	0.42
Q9H0U6	MRPL18 39S ribosomal protein L18, mitochondrial	R.NVVAC*ESIGR.V	125	1.33	0.41	0.07
Q6P4A7	SFXN4 Sideroflexin-4	R.SYTC*KPLER.S	159	1.33	0.41	0.13
Q8N0V3	RBFA Putative ribosome-binding factor A, mitochondrial	K.VSLTPDFSAC*R.A	136	1.33	0.41	0.16
Q96DV4	MRPL38 39S ribosomal protein L38, mitochondrial	K.QDQPIDFSEDARPSPC*YQLAQR.T	290	1.33	0.41	0.18
Q16134	ETFDH Electron transfer flavoprotein-ubiquinone oxidored	R.LQINAQNC*VHCK.T	586	1.33	0.41	0.19
Q9NVS2	MRPS18A 28S ribosomal protein S18a, mitochondrial	R.DNVC*YSR.T	186	1.33	0.41	0.25
Q330K2	NDUFAF6 NADH dehydrogenase (ubiquinone) complex I, assembl	K.AQGIVTC*LR.A	216	1.32	0.40	0.09
O95299	NDUFA10 NADH dehydrogenase	R.SRVITVDGNIC*TGK.G	67	1.32	0.40	0.14
Q53H12	AGK Acylglycerol kinase, mitochondrial	K.ATVFLNPAAC*K.G	72	1.32	0.40	0.16
P49590	HARS2 Probable histidine--tRNA ligase, mitochondrial	R.IGDYVQC*HGGVSLVEQMFQDPR.L	274	1.33	0.40	0.57
P08574	CYC1 Cytochrome c1, heme protein, mitochondrial	R.HLVGVC*YTEDEAK.E	139	1.32	0.40	0.26
Q7L592	C2orf56 Protein midA homolog, mitochondrial	R.DHVEVC*PDAGVIIEELSQR.I	275	1.33	0.40	0.44
Q9NP81	SARS2 Serine--tRNA ligase, mitochondrial	R.MVC*SSTC*YR.A	324	1.32	0.40	0.35
Q9H1K1	ISCU Iron-sulfur cluster assembly enzyme ISCU, mitochon	K.LHC*SMLAEDAIK.A	138	1.33	0.40	0.66
Q8NI60	ADCK3 Chaperone activity of bc1 complex-like, mitochondr	K.AMFEEAYSNYC*K.R	641	1.32	0.40	0.19
Q8WUK0	PTPMT1 Phosphatidylglycerophosphatase and protein-tyrosin	R.FLC*NSSQEWK.R	81	1.32	0.40	0.43
Q969Z3	MARC2 MOSC domain-containing protein 2, mitochondrial	K.GRDC*GNEAAK.W	160	1.32	0.40	0.29
Q9BRT2	MNF1 Mitochondrial nucleoid factor 1	K.LC*EEWPVDETKR.G	13	1.32	0.40	0.32
P12532	CKMT1B Creatine kinase U-type, mitochondrial	R.LGYILTC*PSNLGTGLR.A	316	1.32	0.40	0.22
Q02252	ALDH6A1 Methylmalonate-semialdehyde dehydrogenase	K.ERVC*NLIDSGTK.E	368	1.32	0.40	0.22
Q9Y2Z2	MTO1 Protein MTO1 homolog, mitochondrial	R.IC*DQSGVHYK.V	104	1.32	0.39	0.47
Q9BPX6	MICU1 Calcium uptake protein 1, mitochondrial	K.SGLC*SALTTYFFGADLK.G	275	1.33	0.39	0.61
P13804	ETFA Electron transfer flavoprotein subunit alpha, mito	K.C*DKVAQDLCK.V	60	1.32	0.39	0.51
Q9Y277	VDAC3 Voltage-dependent anion-selective channel protein	K.ASGNLETKYKVC*NYGLTFTQK.W	65	1.31	0.39	0.14
Q9Y6M9	NDUFB9 NADH dehydrogenase	R.HLESWC*VQR.D	31	1.31	0.39	0.27

P43304	GPD2 Glycerol-3-phosphate dehydrogenase, mitochondrial	R.NYLSC*DVEVR.R	385	1.31	0.39	0.28
P38646	HSPA9 Stress-70 protein, mitochondrial	K.GAVVGIDLGTTNSC*VAVMEGK.Q	66	1.31	0.39	0.30
Q7Z2W9	MRPL21 39S ribosomal protein L21, mitochondrial	R.INSIEIAPC*LL.-	203	1.31	0.39	0.10
Q9HAV7	GRPEL1 GrpE protein homolog 1, mitochondrial	K.ATQC*VPK.E	124	1.31	0.39	0.10
P49821	NDUFV1 NADH dehydrogenase	K.QIEGHTIC*ALGDGAAWPVQGLIR.H	425	1.31	0.39	0.12
Q8NBU5	ATAD1 ATPase family AAA domain-containing protein 1	K.GVLLYGPPGC*GK.T	137	1.31	0.39	0.22
Q53H12	AGK Acylglycerol kinase, mitochondrial	K.EDFLNIC*IEPDTISK.G	334	1.31	0.39	0.42
Q9Y6M9	NDUFB9 NADH dehydrogenase	R.YFAC*LMR.A	42	1.31	0.39	0.03
Q9HAV7	GRPEL1 GrpE protein homolog 1, mitochondrial	K.LYGIQAFC*K.D	108	1.31	0.39	0.14
Q9Y277	VDAC3 Voltage-dependent anion-selective channel protein	K.YMLDC*R.T	229	1.31	0.39	0.14
Q5RI15	COX20 Cytochrome c oxidase protein 20 homolog	K.LLGFLDVENTPC*AR.H	29	1.31	0.38	0.23
Q9NWS8	RMND1 Required for meiotic nuclear division protein 1 ho	K.LQHC*MELTDLMR.N	409	1.31	0.38	0.23
P05141	SLC25A5 ADP/ATP translocase 2	R.EFRGLGDC*LVK.I	160	1.30	0.38	0.13
O95299	NDUFA10 NADH dehydrogenase	K.C*EVLQYSAR.E	253	1.30	0.38	0.15
Q86VU5	COMTD1 Catechol O-methyltransferase domain-containing pro	R.LLTLEQPQGDSMMTC*EQAQLLANLAR.L	88	1.31	0.38	0.44
Q9Y276	BCS1L Mitochondrial chaperone BCS1	R.GYLLYGPPGC*GK.S	234	1.30	0.38	0.36
Q96TC7	FAM82A2 Regulator of microtubule dynamics protein 3	R.AYSDMC*ELTEEVSEK.K	288	1.31	0.38	0.56
P53597	SUCLG1 Succinyl-CoA ligase	R.LIGPNC*PGVINPGECK.I	172	1.30	0.38	0.32
P30837	ALDH1B1 Aldehyde dehydrogenase X, mitochondrial	K.TIPMDGQHFC*FTR.H	169	1.30	0.37	0.09
P22033	MUT Methylmalonyl-CoA mutase, mitochondrial	R.C*TVGEITDALKK.V	560	1.31	0.37	0.60
P21912	SDHB Succinate dehydrogenase	K.C*GPMVLDALIK.I	68	1.30	0.37	0.17
Q7L2E3	DHX30 Putative ATP-dependent RNA helicase DHX30	R.QAAAAAC*QLFK.G	118	1.31	0.37	0.76
Q8IYU8	EFHA1 EF-hand domain-containing family member A1	K.IFDLDGDEC*LSHEEFLGVLK.N	381	1.30	0.37	0.55
Q9Y4W6	AFG3L2 AFG3-like protein 2	K.LASLTPGFSGADVANVC*NEAALIAAR.H	525	1.30	0.37	0.34
Q13423	NNT NAD(P) transhydrogenase, mitochondrial	R.EANSIIITPGYGLC*AAK.A	936	1.29	0.37	0.11
Q99536	VAT1 Synaptic vesicle membrane protein VAT-1 homolog	R.C*LVLTGFGGYDK.V	50	1.30	0.37	0.36
P40939	HADHA Trifunctional enzyme subunit alpha, mitochondrial	K.EVEAVIPDHC*IFASNTSALPISEIAAVSK.R	470	1.29	0.37	0.23
Q567V2	MPV17L2 Mpv17-like protein 2	R.ALLVTNTLGC*GALMAAGDGVR.Q	33	1.30	0.37	0.65
Q9BSH4	TACO1 Translational activator of cytochrome c oxidase 1	K.FIC*DASSLHQVR.K	234	1.30	0.37	0.60
Q9UJZ1	STOML2 Stomatin-like protein 2	R.ERESLNASIVDAINQAADC*WGIR.C	167	1.29	0.37	0.09
Q96BR5	SELRC1 Sel1 repeat-containing protein 1	K.SIAAC*HNVGLLAHDGQVNEDGQPDLGK.A	111	1.29	0.37	0.17
Q9Y2S7	POLDIP2 Polymerase delta-interacting protein 2	R.DC*PHISQR.S	143	1.29	0.37	0.23
O75390	CS Citrate synthase, mitochondrial	R.GFSIPEC*QK.L	101	1.29	0.36	0.04
P04181	OAT Ornithine aminotransferase, mitochondrial	K.VLPMNTGVEAGETAC*K.L	150	1.29	0.36	0.36
O75390	CS Citrate synthase, mitochondrial	K.LPC*VAAK.I	211	1.29	0.36	0.09
P05141	SLC25A5 ADP/ATP translocase 2	K.GTDIMYTGTLDC*WR.K	257	1.29	0.36	0.12
Q9Y277	VDAC3 Voltage-dependent anion-selective channel protein	K.SC*SGVEFSTSGHAYTDTGK.A	36	1.29	0.36	0.14
P23368	ME2 NAD-dependent malic enzyme, mitochondrial	K.YC*TFNDDIQGTAAVALAGLLAAQK.V	274	1.29	0.36	0.19
P42126	ECI1 Enoyl-CoA delta isomerase 1, mitochondrial	R.GVILTSDRPGVFSAGLDLTEMC*GR.S	114	1.29	0.36	0.55
Q9P2R7	SUCLA2 Succinyl-CoA ligase	R.C*DVIAQGIVMAVK.D	384	1.31	0.36	0.91
Q9NVH1	DNAJC11 DnaJ homolog subfamily C member 11	K.VIDVTVPLQC*LVK.D	494	1.28	0.36	0.07
Q7KZF4	SND1 Staphylococcal nuclease domain-containing protein	R.RGEFC*IAK.F	736	1.28	0.36	0.10
Q9NQG6	SMCR7L Mitochondrial dynamic protein MID51	R.ALDQADSGC*R.S	359	1.32	0.36	1.36
Q13505	MTX1 Metaxin-1	R.EC*LTLLSQR.L	326	1.28	0.36	0.27
Q96EY7	PTCD3 Pentatricopeptide repeat-containing protein 3, mit	R.DKHPPELQVAFADC*AADIK.S	551	1.30	0.36	0.98
Q53H12	AGK Acylglycerol kinase, mitochondrial	K.HC*DNLLR.R	34	1.28	0.36	0.18
P24752	ACAT1 Acetyl-CoA acetyltransferase, mitochondrial	K.DGLTDVYNKIHMGSC*AENTAK.K	196	1.28	0.35	0.22
O15235	MRPS12 28S ribosomal protein S12, mitochondrial	K.YDC*GHVQK.K	132	1.29	0.35	0.81
Q53H12	AGK Acylglycerol kinase, mitochondrial	K.LQFFC*DPR.K	408	1.28	0.35	0.11
P53701	HCCS Cytochrome c-type heme lyase	K.WEALHAAECPC*GPSLIR.F	178	1.28	0.35	0.16
P48735	IDH2 Isocitrate dehydrogenase	K.SSGGFVWAC*K.N	308	1.28	0.35	0.26
Q08257	CRYZ Quinone oxidoreductase	K.AGESVLVHGASGGVGLAAC*QIAR.A	166	1.28	0.35	0.34
P40926	MDH2 Malate dehydrogenase, mitochondrial	K.GYLGPEQLPDC*LK.G	89	1.27	0.35	0.08
P53007	SLC25A1 Tricarboxylate transport protein, mitochondrial	R.NTWDC*GLQILK.K	262	1.27	0.35	0.13
P11177	PDHB Pyruvate dehydrogenase E1 component subunit beta,	K.TNHLVTVEGGWPQFGVGAEIC*AR.I	306	1.28	0.35	0.35
P55809	OXCT1 Succinyl-CoA:3-ketoacid coenzyme A transferase 1,	R.NFNLPMC*K.A	235	1.27	0.35	0.22
Q9P032	NDUFAF4 NADH dehydrogenase	K.AAETC*QEPK.E	87	1.27	0.34	0.15
Q9Y2Z4	YARS2 Tyrosine--tRNA ligase, mitochondrial	R.C*TQALYHSSIDALEVMSDQELK.E	369	1.27	0.34	0.19
Q9Y4W6	AFG3L2 AFG3-like protein 2	R.MC*MTLGGR.V	626	1.27	0.34	0.19
P23786	CPT2 Carnitine O-palmitoyltransferase 2, mitochondrial	K.TLTIDC*VQFQR.G	445	1.28	0.34	0.58
P40939	HADHA Trifunctional enzyme subunit alpha, mitochondrial	K.TGIEQGSDAGYLC*ESQK.F	322	1.27	0.34	0.33
P45954	ACADSB Short/branched chain specific acyl-CoA dehydrogena	R.ASSTC*PLTFENVK.V	261	1.27	0.34	0.37
O00483	NDUFA4 NADH dehydrogenase	R.LALFNPDVC*WDR.N	44	1.27	0.34	0.07
P24752	ACAT1 Acetyl-CoA acetyltransferase, mitochondrial	R.QAVLGAGLPISTPC*TTINK.V	119	1.27	0.34	0.13
P12235	SLC25A4 ADP/ATP translocase 1	K.GADIMYTGTVDC*WR.K	257	1.27	0.34	0.22
Q969V5	MUL1 Mitochondrial ubiquitin ligase activator of NFKB 1	R.TTHLWNDC*SK.I	113	1.29	0.34	1.13
Q9HD23	MRS2 Magnesium transporter MRS2 homolog, mitochondrial	K.AVITPEC*LLILDYR.N	148	1.27	0.34	0.63

O75746	SLC25A12 Calcium-binding mitochondrial carrier protein Aral	K.NSFDC*FK.K	375	1.27	0.34	0.51
P24752	ACAT1 Acetyl-CoA acetyltransferase, mitochondrial	K.QGEYGLASIC*NGGGGASAMLIQK.L	413	1.26	0.34	0.17
Q08257	CRYZ Quinone oxidoreductase	R.ALIHSAC*VK.A	145	1.26	0.33	0.16
Q9NYY8	FASTKD2 FAST kinase domain-containing protein 2	R.VAVLC*VSR.S	638	1.27	0.33	0.58
Q96EY7	PTCD3 Pentatricopeptide repeat-containing protein 3, mit	K.VSNSPSQAIEVVELASAFSLPIC*EGLTQR.V	642	1.26	0.33	0.21
Q86YH6	PDSS2 Decaprenyl-diphosphate synthase subunit 2	K.SC*QAAMELAK.H	263	1.27	0.33	0.66
P38646	HSPA9 Stress-70 protein, mitochondrial	K.DQLPADEC*NK.L	608	1.26	0.33	0.21
Q9NVH1	DNAJC11 DnaJ homolog subfamily C member 11	R.LC*MLYHPDK.H	38	1.26	0.33	0.23
Q9NX20	MRPL16 39S ribosomal protein L16, mitochondrial	R.C*EFEEVQGFLDQVAHK.L	167	1.26	0.33	0.27
O60488	ACSL4 Long-chain-fatty-acid--CoA ligase 4	R.VGAPLIC*CEIK.L	494	1.26	0.33	0.35
P49821	NDUFV1 NADH dehydrogenase	K.HESC*GQCTPCR.E	379	1.25	0.33	0.16
P24752	ACAT1 Acetyl-CoA acetyltransferase, mitochondrial	K.VC*ASGMK.A	126	1.25	0.32	0.26
O95140	MFN2 Mitofusin-2	R.RFEEC*ISQSAVK.T	348	1.26	0.32	0.73
P49406	MRPL19 39S ribosomal protein L19, mitochondrial	R.FDLC*LTEQQMK.E	248	1.25	0.32	0.32
P51649	ALDH5A1 Succinate-semialdehyde dehydrogenase, mitochondria	R.VAEQLEVGMVGVNEGLISSVEC*PFGGVK.Q	502	1.25	0.32	0.41
P33897	ABCD1 ATP-binding cassette sub-family D member 1	R.VEEGMHLLITGPNGC*GK.S	511	1.25	0.32	0.52
P00505	GOT2 Aspartate aminotransferase, mitochondrial	K.TC*GFDFTGAVEDISK.I	187	1.26	0.32	0.78
P08574	CYC1 Cytochrome c1, heme protein, mitochondrial	K.DVC*TFLR.W	271	1.24	0.31	0.04
Q13162	PRDX4 Peroxiredoxin-4	R.EEEC*HFYAGGQVYPGEASR.V	51	1.25	0.31	0.39
O95299	NDUFA10 NADH dehydrogenase	R.KQC*VDHYNEVK.S	183	1.24	0.31	0.13
B4DLN1	SLC25A10 cDNA FLJ60124, highly similar to Mitochondrial dic	R.GALVTVGQLSC*YDQAK.Q	336	1.24	0.31	0.52
Q9Y375	NDUFAF1 Complex I intermediate-associated protein 30, mito	R.SGYC*AMISR.I	183	1.24	0.31	0.30
O75521	ECI2 Enoyl-CoA delta isomerase 2, mitochondrial	K.QATEGPC*NMPK.P	77	1.28	0.31	1.63
Q9NX14	NDUFB11 NADH dehydrogenase	K.YREANGLPIMESNC*FDPSK.I	141	1.24	0.31	0.13
I3L0E3	MRPS17 28S ribosomal protein S17, mitochondrial	K.TYFAHDALQQC*TVGDIVLLR.A	153	1.25	0.31	0.96
Q8TDB4	MGARP Protein MGARP	K.EASAC*PGHVEAAPETTAVSAETGPEVTDAAAR.E	139	1.23	0.30	0.10
P22307	SCP2 Non-specific lipid-transfer protein	K.ADC*TITMADSDFLALMTGK.M	495	1.25	0.30	1.05
Q96TA2	YME1L1 ATP-dependent zinc metalloprotease YME1L1	K.ANAPC*VIFIDELDSVGGK.R	433	1.23	0.30	0.42
O95831	AIFM1 Apoptosis-inducing factor 1, mitochondrial	K.C*LIATGGTPR.S	256	1.23	0.30	0.45
Q16891	IMMT Mitochondrial inner membrane protein	K.LLSYASYC*IEHGDLELAAK.F	697	1.23	0.30	0.12
O95299	NDUFA10 NADH dehydrogenase	K.HFPEAGIHYPDSTTGDGKPLATDYNGNC*SLEK.F	112	1.23	0.30	0.21
Q9NZ45	CISD1 CDGSH iron-sulfur domain-containing protein 1	K.IVHAFDMEDLGDKAVYC*R.C	72	1.23	0.30	0.50
P25325	MPST 3-mercaptopyruvate sulfurtransferase	R.HIPGAAFFDIDQC*SDR.T	65	1.27	0.30	1.57
Q7L2E3	DHX30 Putative ATP-dependent RNA helicase DHX30	R.DTILNAIEQHPVVVISGDTGC*GK.T	Bad ID	1.25	0.29	1.35
P08574	CYC1 Cytochrome c1, heme protein, mitochondrial	R.HGGEDYVFSLLTGYC*EPPTGVSLR.E	219	1.23	0.29	0.14
P35232	PHB Prohibitin	K.PIIFDC*R.S	69	1.23	0.29	0.38
Q86VU5	COMTD1 Catechol O-methyltransferase domain-containing pro	R.VVTC*EVDAQPPELGRPLWR.Q	133	1.24	0.29	1.02
P49207	RPL34 60S ribosomal protein L34	R.AYGGSMC*AK.C	83	1.22	0.29	0.30
P04040	CAT Catalase	K.LVNANGEAVYC*K.F	232	1.23	0.29	0.74
P11310	ACADM Medium-chain specific acyl-CoA dehydrogenase, mito	R.MTEEPLMC*AYCVTEPGAGSDVAGIK.T	156	1.24	0.29	1.04
Q16891	IMMT Mitochondrial inner membrane protein	K.ANC*SDNEFTQALTAAIPPESLTR.G	603	1.22	0.29	0.18
P36969	GPX4 Phospholipid hydroperoxide glutathione peroxidase,	K.IC*VNGDDAHPLWK.W	134	1.22	0.28	0.55
Q9Y4W6	AFG3L2 AFG3-like protein 2	K.DVAGC*EEAK.L	313	1.22	0.28	0.79
Q9HD33	MRPL47 39S ribosomal protein L47, mitochondrial	K.SGAAWTC*QQLR.N	87	1.21	0.28	0.02
Q9H078	CLPB Caseinolytic peptidase B protein homolog	K.GC*TALHYAVLADDYR.T	267	1.21	0.28	0.15
Q5HYI7	MTX3 Metaxin-3	R.DAKEC*LNLLSNR.L	176	1.24	0.28	1.31
Q16718	NDUFA5 NADH dehydrogenase	K.TTGLVGLAVC*NTPHER.L	17	1.21	0.27	0.16
P56381	ATP5E ATP synthase subunit epsilon, mitochondrial	R.YSQIC*AK.A	19	1.21	0.27	0.61
Q9NVS2	MRPS18A 28S ribosomal protein S18a, mitochondrial	K.ESPNPPNPSGQC*PICR.W	70	1.21	0.27	0.41
I3L0E3	MRPS17 28S ribosomal protein S17, mitochondrial	K.VIDPVTGKPC*AGTTYLESPLSSETTQLSK.N	195	1.21	0.27	0.11
Q96RQ3	MCCC1 Methylcrotonoyl-CoA carboxylase subunit alpha, mit	K.ESLC*QAALGLILK.E	509	1.21	0.27	0.03
Q9H9J2	MRPL44 39S ribosomal protein L44, mitochondrial	K.SNQELSEQGTSFSQTC*LTQFLEDEYPDMPTEGIK.N	136	1.21	0.27	0.60
P43897	TSFM Elongation factor Ts, mitochondrial	K.TGYSFVNC*K.K	64	1.21	0.27	0.62
Q96HS1	PGAM5 Serine/threonine-protein phosphatase PGAM5, mitoch	R.QEEDSYEIFIC*HANVIR.Y	229	1.22	0.27	1.16
Q12983	BNIP3 BCL2/adenovirus E1B 19 kDa protein-interacting pro	K.SSHC*DSPPR.S	129	1.20	0.26	0.37
P21796	VDAC1 Voltage-dependent anion-selective channel protein	K.YQIDPDAC*FSAK.V	232	1.20	0.26	0.21
Q96E11	MRRF Ribosome-recycling factor, mitochondrial	K.SPQLILVNMASFPEC*TAAAIK.A	154	1.20	0.26	0.33
Q96GW9	MARS2 Methionine--tRNA ligase, mitochondrial	K.IQQAAATAGLAPTELC*DR.V	114	1.20	0.26	0.46
Q02218	OGDH 2-oxoglutarate dehydrogenase, mitochondrial	K.AEQFYC*GDTEGKK.V	395	1.20	0.26	0.50
Q9P2R7	SUCLA2 Succinyl-CoA ligase	K.YDATMIEINPMVEDSDGAVLC*MDAK.I	270	1.22	0.26	1.66
O95182	NDUFA7 NADH dehydrogenase	K.LSNNYYC*TR.D	55	1.19	0.25	0.20
P48047	ATP5O ATP synthase subunit O, mitochondrial	R.GEVPC*TVTSASPLEEATLSELK.T	141	1.19	0.25	0.33
Q6NVY1	HIBCH 3-hydroxyisobutyryl-CoA hydrolase, mitochondrial	R.LSQAC*MR.G	336	1.21	0.25	1.35
Q9H2U2	PPA2 Inorganic pyrophosphatase 2, mitochondrial	K.DKSTNC*FGDNDPIDVCEIGSK.I	161	1.20	0.25	1.01
P21912	SDHB Succinate dehydrogenase	R.CHTIMNC*TR.T	249	1.19	0.24	0.32
Q9UKU7	ACAD8 Isobutyryl-CoA dehydrogenase, mitochondrial	R.KDAVALC*SMAK.L	351	1.19	0.24	0.74
P38117	ETFB Electron transfer flavoprotein subunit beta	K.EVIAVSC*GPAQCQETIR.T	66	1.18	0.24	0.08
Q10713	PMPCA Mitochondrial-processing peptidase subunit alpha	K.HGGIC*DCQTSR.D	140	1.18	0.24	0.37
P21796	VDAC1 Voltage-dependent anion-selective channel protein	R.EHINLGC*DMDFDIAGPSIR.G	127	1.18	0.24	0.31

O14561	NDUFAB1 Acyl carrier protein, mitochondrial	K.LMC*PQEIVDYIADK.K	140	1.18	0.24	0.44
Q92947	GCDH Glutaryl-CoA dehydrogenase, mitochondrial	R.TYC*QER.L	75	1.18	0.24	0.75
P00505	GOT2 Aspartate aminotransferase, mitochondrial	R.VGAFTMVC*K.D	295	1.20	0.24	1.34
P82932	MRPS6 28S ribosomal protein S6, mitochondrial	K.EC*EGIVPVPLAEK.L	105	1.18	0.23	0.11
P00505	GOT2 Aspartate aminotransferase, mitochondrial	K.EYLPIGGLAEFC*K.A	106	1.19	0.23	1.02
Q9Y512	SAMM50 Sorting and assembly machinery component 50 homolo	R.LELNYC*VPMGVQTGDR.I	445	1.18	0.23	0.46
P36969	GPX4 Phospholipid hydroperoxide glutathione peroxidase,	R.YAEC*GLR.I	93	1.17	0.23	0.08
P53007	SLC25A1 Tricarboxylate transport protein, mitochondrial	R.GIGDC*VR.Q	70	1.17	0.23	0.63
Q9Y4W6	AFG3L2 AFG3-like protein 2	K.NAPC*ILFIDEIDAVGR.K	402	1.17	0.23	0.31
P82912	MRPS11 28S ribosomal protein S11, mitochondrial	K.ASHNNTQIQVVSASNEPLAFASC*GTEGFR.N	112	1.17	0.22	0.09
O00217	NDUFS8 NADH dehydrogenase	K.LC*EAICPAQAITIEAEPR.A	117	1.17	0.22	0.21
P53701	HCCS Cytochrome c-type heme lyase	K.GC*PVNTEPSGPTCEK.K	35	1.17	0.22	0.81
Q9NSE4	IARS2 Isoleucine--tRNA ligase, mitochondrial	K.YTAESSDTLC*PR.C	1002	1.18	0.22	1.53
Q96ER9	CCDC51 Coiled-coil domain-containing protein 51	K.TC*SQMAGVVQLVK.S	331	1.16	0.21	0.32
Q96ER9	CCDC51 Coiled-coil domain-containing protein 51	R.QVHSC*LEGLR.E	316	1.16	0.21	0.24
P55084	HADHB Trifunctional enzyme subunit beta, mitochondrial	K.EGGQYGLVAAC*AAGGQGHAMIVEAYPK.-	458	1.16	0.21	0.28
O95831	AIFM1 Apoptosis-inducing factor 1, mitochondrial	K.SITIIGGGFLGSELAC*ALGR.K	317	1.16	0.21	0.13
Q96C01	FAM136A Protein FAM136A	K.QVHQC*IER.C	53	1.15	0.21	0.19
Q8NFF5	FLAD1 FAD synthase	R.LHYGTDPC*TGQPFR.F	236	1.18	0.20	2.40
P36957	DLST Dihydrolipoyllysine-residue succinyltransferase co	K.EAQNTC*AMLTTFNEIDMSNIQEMR.A	245	1.15	0.19	1.07
Q9H2U2	PPA2 Inorganic pyrophosphatase 2, mitochondrial	K.STHQC*WK.A	274	1.18	0.19	2.54
P49821	NDUFV1 NADH dehydrogenase	K.LLEGC*LVGGR.A	142	1.14	0.19	0.37
Q9BPW8	NIPSNAP1 Protein NipSnap homolog 1	R.FSGGYPALMDC*MNK.L	138	1.14	0.18	0.38
P22570	FDXR NADPH:adrenodoxin oxidoreductase, mitochondrial	R.AVPTGDMEDLPC*GLVLSSIGYK.S	353	1.14	0.18	1.19
P45880	VDAC2 Voltage-dependent anion-selective channel protein	K.VC*EDLDTSVNLAWTSGTNCTR.F	210	1.13	0.18	0.48
P30044	PRDX5 Peroxiredoxin-5, mitochondrial	K.GVLFGVPGAFTPGC*SK.T	100	1.14	0.18	1.15
P22830	FECH Ferrochelatase, mitochondrial	R.AIAFTQYPQYSC*STTGSSLNAIYR.Y	196	1.13	0.17	0.15
P22830	FECH Ferrochelatase, mitochondrial	R.LEYC*NPYR.L	294	1.13	0.17	0.57
Q9NX63	CHCHD3 Coiled-coil-helix-coiled-coil-helix domain-contain	R.ERIC*SEEER.A	112	1.14	0.17	1.73
Q7Z7K0	CMC1 COX assembly mitochondrial protein homolog	R.C*SEQVQDFTK.C	31	1.13	0.17	1.23
P03897	MT-ND3 NADH-ubiquinone oxidoreductase chain 3	K.STPYEC*GFDPMSPAR.V	39	1.12	0.16	0.16
P19367	HK1 Hexokinase-1	K.TVC*GVVSR.R	823	1.12	0.16	0.46
Q02252	ALDH6A1 Methylmalonate-semialdehyde dehydrogenase	K.GYENGNFVGPTIISNVKPNMTC*YK.E	413	1.14	0.15	2.96
P49821	NDUFV1 NADH dehydrogenase	K.NAC*GSGYDFDVFVVR.G	187	1.11	0.14	0.32
P19367	HK1 Hexokinase-1	R.AAQLC*GAGMAAVVDK.I	834	1.10	0.14	0.19
P52758	HRSP12 Ribonuclease UK114	K.AAGC*DFTNVVK.T	71	1.11	0.14	1.22
Q9BX68	HINT2 Histidine triad nucleotide-binding protein 2, mito	K.SLPADILYEDQQC*LVFR.D	75	1.10	0.14	0.90
P50213	IDH3A Isocitrate dehydrogenase	K.C*SDFTEEICR.R	351	1.10	0.14	0.27
Q99536	VAT1 Synaptic vesicle membrane protein VAT-1 homolog	R.AC*GLNFADLMAR.Q	86	1.10	0.14	0.58
P03928	MT-ATP8 ATP synthase protein 8	K.IC*SLHSLPPQS.-	59	1.10	0.13	1.12
Q96C01	FAM136A Protein FAM136A	R.C*SASCCEDSQASMK.Q	35	1.10	0.13	0.81
Q6P161	MRPL54 39S ribosomal protein L54, mitochondrial	K.GAVTSEALKDPDVC*TDPVQLTTYAMGVNIYK.E	62	1.10	0.13	1.08
P09001	MRPL3 39S ribosomal protein L3, mitochondrial	K.NLPFPTYFPDGDEEELPEDLYDENVC*QPGAPSITFA.-	338	1.11	0.12	2.77
P07919	UQCRH Cytochrome b-c1 complex subunit 6, mitochondrial	R.EQC*EQLEK.C	37	1.08	0.12	0.37
Q92667	AKAP1 A-kinase anchor protein 1, mitochondrial	R.VC*QASQLQGQK.E	376	1.15	0.11	6.82
P08559	PDHA1 Pyruvate dehydrogenase E1 component subunit alpha,	K.LPCIFIC*ENNR.Y	222	1.08	0.11	0.77
B4DLN1	SLC25A10 cDNA FLJ60124, highly similar to Mitochondrial dic	R.C*EALAGAPLDNAPK.E	45	1.09	0.10	3.16
P49748	ACADVL Very long-chain specific acyl-CoA dehydrogenase, m	K.ELGAFGLQVPSELGGVGLC*NTQYAR.L	156	1.09	0.10	3.62
O60313	OPA1 Dynamin-like 120 kDa protein, mitochondrial	R.TQEQC*VHNETK.N	786	1.09	0.10	3.64
O94826	TOMM70A Mitochondrial import receptor subunit TOM70	R.C*AEGYALYAQALTDQQQFGK.A	475	1.07	0.08	3.46
Q5TC12	ATPAF1 ATP synthase mitochondrial F1 complex assembly fac	R.AQSC*PTFLCALPR.R	194	1.06	0.08	0.93
P25705	ATP5A1 ATP synthase subunit alpha, mitochondrial	K.LYC*IYVAIGQK.R	244	1.14	0.08	9.88
P19367	HK1 Hexokinase-1	K.ATDC*VGHDVVTLLR.D	628	1.05	0.07	0.59
O15382	BCAT2 Branched-chain-amino-acid aminotransferase, mitoch	R.EVFGSGTAC*QVCPVHR.I	342	1.05	0.07	0.55
Q9BXW7	CECR5 Cat eye syndrome critical region protein 5	K.AQELSALLGC*EVDADQVILSHSPMK.L	109	1.13	0.07	10.34
O75947	ATP5H ATP synthase subunit d, mitochondrial	K.SC*AEWVSLSK.A	101	1.05	0.07	0.68
Q07021	C1QBP Complement component 1 Q subcomponent-binding prot	K.ALVLDC*HYPEDEVGQEDEAESDIFSIR.E	186	1.05	0.06	0.97
P30048	PRDX3 Thioredoxin-dependent peroxide reductase, mitochon	K.AFQYVETHGEVC*PANWTPDSPTIKPSPAASK.E	229	1.06	0.06	5.14
P19404	NDUFV2 NADH dehydrogenase	R.FSC*EPAGGLTSLTEPPKGPGFGVQAGL.-	225	1.05	0.05	5.47
Q9NUQ2	AGPAT5 1-acyl-sn-glycerol-3-phosphate acyltransferase eps	K.ATHVAFDC*MK.N	217	1.04	0.05	3.22
Q9Y3D2	MSRB2 Methionine-R-sulfoxide reductase B2, mitochondrial	R.GQAGGGGPGTGPGLGEAGSLATC*ELPLAK.S	45	1.04	0.05	1.82
Q9Y2R9	MRPS7 28S ribosomal protein S7, mitochondrial	K.WMITEC*R.D	191	1.04	0.04	5.60
O43716	GATC Glutamyl-tRNA(Gln) amidotransferase subunit C, mit	R.SDNVVEGNC*ADELLQNSHR.V	99	1.04	0.04	6.70

O75380	NDUFS6 NADH dehydrogenase	K.TGTC*GYCGLQFR.Q	112	1.03	0.04	0.94
P54886	ALDH18A1 Delta-1-pyrroline-5-carboxylate synthase	K.LGSAVVTRGDEC*GLALGR.L	88	1.03	0.04	1.59
Q9NQG6	SMCR7L Mitochondrial dynamic protein MID51	R.C*VVGGYLSPK.T	251	1.04	0.04	8.79
P51553	IDH3G Isocitrate dehydrogenase	K.LGDGLFLQC*CR.E	235	1.04	0.03	9.65
A6NJ78	METTL15 Probable methyltransferase-like protein 15	K.AGVQPGTFDGVLMDLGC*SSMQLDTPER.G	172	1.06	0.02	25.03
Q9Y676	MRPS18B 28S ribosomal protein S18b, mitochondrial	K.VVGNPCPIC*R.D	108	1.01	0.01	13.02
O75380	NDUFS6 NADH dehydrogenase	R.VIAC*DGGGGALGHPK.V	87	1.01	0.01	13.03
P19367	HK1 Hexokinase-1	R.AILQQLGLNSTC*DDSILVK.T	813	1.00	0.00	28.59
P36969	GPX4 Phospholipid hydroperoxide glutathione peroxidase,	R.ILAFPC*NQFGK.Q	102	1.00	-0.01	-12.04
O75431	MTX2 Metaxin-2	K.TLDQVLEDVDQC*CQALSQR.L	189	1.00	-0.01	-14.76
P07919	UQCRH Cytochrome b-c1 complex subunit 6, mitochondrial	R.SHTEEDC*TEELFDFLHAR.D	67	0.99	-0.01	-7.43
P30084	ECHS1 Enoyl-CoA hydratase, mitochondrial	K.IC*PVETLVEEAIQCAEK.I	213	0.98	-0.02	-0.35
P07919	UQCRH Cytochrome b-c1 complex subunit 6, mitochondrial	R.ERLELC*DER.V	53	0.98	-0.03	-4.18
Q9P2R7	SUCLA2 Succinyl-CoA ligase	R.IC*NQVLVCER.K	152	0.99	-0.03	-7.29
P36969	GPX4 Phospholipid hydroperoxide glutathione peroxidase,	K.FLIDKNGC*VVK.R	175	0.98	-0.03	-6.11
P00395	MT-CO1 Cytochrome c oxidase subunit 1	K.VLMVEEPSMNLEWLYGC*PPPYHTFEEPVYMK.S	498	0.98	-0.04	-4.91
Q9Y606	PUS1 tRNA pseudouridine synthase A, mitochondrial	R.SGC*IPENHGEDMR.K	125	0.97	-0.05	-3.78
P28838	LAP3 Cytosol aminopeptidase	R.QVVDC*QLADVNNIGK.Y	445	1.06	-0.07	-13.16
P21912	SDHB Succinate dehydrogenase	R.EGIC*GSCAMNINGGNTLACTR.R	98	0.97	-0.08	-4.52
Q16775	HAGH Hydroxyacylglutathione hydrolase, mitochondrial	R.VYC*GHEYTINNLK.F	219	0.97	-0.08	-5.13
P07919	UQCRH Cytochrome b-c1 complex subunit 6, mitochondrial	R.DHC*VAHK.L	Bad ID	0.94	-0.09	-0.91
P23434	GCSH Glycine cleavage system H protein, mitochondrial	K.SC*YEDGWLIK.M	138	0.93	-0.11	-0.87
Q96BQ5	CCDC127 Coiled-coil domain-containing protein 127	R.SAYLSC*LQR.E	144	0.93	-0.12	-2.68
Q9Y619	SLC25A15 Mitochondrial ornithine transporter 1	K.LSDLQNAAAGSFASAFAALVLC*PTELVK.C	125	0.94	-0.14	-3.58
P07195	LDHB L-lactate dehydrogenase B chain	K.GMYGIENEVFLSLPC*ILNAR.G	294	1.20	-0.16	-10.20
Q9Y6C9	MTCH2 Mitochondrial carrier homolog 2	K.TYC*CDLK.M	296	0.86	-0.22	-0.85
Q9Y3D6	FIS1 Mitochondrial fission 1 protein	K.STQFEYAWC*LVR.S	41	0.82	-0.30	-0.86
Q96LL9	DNAJC30 DnaJ homolog subfamily C member 30	R.QC*FLYHPDR.N	73	0.81	-0.33	-1.02
Q7Z434	MAVS Mitochondrial antiviral-signaling protein	K.QGAESDQAEPIIC*SSGAEAPANSLPSK.V	283	0.40	-1.33	-0.04

Table 2A-6. List of average percent oxidation values for mitochondrial cysteine containing peptides identified in Mito-P from cells treated with DMSO or AMA alkylated by IA-L and IA-H. Data was filtered for mitochondrial peptides with ratio values in 2 out of 3 replicates, with a standard deviation < 20%.

Uniprot ID	Protein Description	Peptide Sequence	Residue	Average % Oxidized DMSO	SEM DMSO	Average % Oxidized AMA	SEM AMA
P82930	MRPS34 28S ribosomal protein S34, mitochondrial	K.SWLWQHDEPC*YWR.L	93	4.76%	0.00%	33.00%	16.30%
P19367	HK1 Hexokinase-1	K.KLPVGFTFSFPC*QQSK.I	158	15.15%	7.49%	24.25%	15.91%
P48735	IDH2 Isocitrate dehydrogenase	K.C*ATITPDEAR.V	113	25.70%	1.81%	41.75%	14.74%
P50213	IDH3A Isocitrate dehydrogenase	K.TFDLYANVRPC*VSIEGYK.T	127	38.33%	13.78%	28.80%	12.45%
P31930	UQCRC1 Cytochrome b-c1 complex subunit 1, mitochondrial	K.HLGGIPWTYAEDAVPTLTPC*R.F	268	33.59%	15.06%	37.15%	12.14%
P14854	COX6B1 Cytochrome c oxidase subunit 6B1	K.GGDISVC*EWYQR.V	54	95.05%	0.13%	77.67%	11.05%
Q15120	PDK3	K.HIGSIDPTC*NVADVVK.D	191	6.01%	0.44%	20.82%	9.79%
P42704	LRPPRC Leucine-rich PPR motif-containing protein, mitocho	K.LFEC*DR.D	952	4.76%	0.00%	16.86%	8.84%
Q9BYD6	MRPL1 39S ribosomal protein L1, mitochondrial	K.IATLDMSSDQIAANLQAVINEVC*R.H	279	4.76%	0.00%	23.13%	8.66%
Q12931	TRAP1 Heat shock protein 75 kDa, mitochondrial	R.NIYYLC*APNR.H	501	9.38%	1.21%	14.20%	8.61%
P51659	HSD17B4 Peroxisomal multifunctional enzyme type 2	K.IC*DFENASKPQSIQESTGSIIEVLSK.I	277	19.23%	3.42%	18.25%	7.79%
Q6UB35	MTHFD1L Monofunctional C1-tetrahydrofolate synthase, mitoc	K.VGC*GSPR.I	302	61.29%	0.16%	48.92%	6.39%

Q7L2E3	DHX30 Putative ATP-dependent RNA helicase DHX30	R.C*NVIITQPR.R	484	7.65%	0.21%	17.99%	5.87%
O94826	TOMM70A Mitochondrial import receptor subunit TOM70	K.ILLDQVEEAVADFDEC*IR.L	427	13.89%	0.43%	14.86%	5.86%
Q9GZT3	SLIRP SRA stem-loop-interacting RNA-binding protein, mit	R.C*ILPFDKETGFHR.G	48	33.70%	8.81%	30.10%	5.85%
Q5VT66	MARC1 MOSC domain-containing protein 1, mitochondrial	K.GVPVSEAEC*TAMGLR.S	79	17.41%	4.34%	16.71%	5.63%
Q9HC21	SLC25A19 Mitochondrial thiamine pyrophosphate carrier	K.NENLQNLLC*GSGAGVISK.T	222	24.33%	4.64%	20.41%	5.30%
P51659	HSD17B4 Peroxisomal multifunctional enzyme type 2	K.FIYEGSSDFSC*LPTFGVIIGQK.S	373	11.38%	1.81%	12.30%	5.15%
Q10713	PMPCA Mitochondrial-processing peptidase subunit alpha	K.FGQFC*TVGILINSGSR.Y	88	4.76%	0.00%	15.61%	5.11%
P48735	IDH2 Isocitrate dehydrogenase	K.DLAGC*IHGLSNVK.L	418	6.83%	1.19%	25.00%	4.91%
Q9BQ69	MACROD1 O-acetyl-ADP-ribose deacetylase MACROD1	R.AAGPLLTDEC*R.T	199	12.20%	0.42%	16.63%	4.71%
Q96I99	SUCLG2 Succinyl-CoA ligase	R.SC*NGPVLVGSPQGGVDIEEVAASNPELIFK.E	162	4.76%	0.00%	29.92%	4.30%
P21796	VDAC1 Voltage-dependent anion-selective channel protein	R.EHINLGC*DMDFDIAGPSIR.G	127	14.83%	4.95%	21.04%	4.26%
Q9H9P8	L2HGDH L-2-hydroxyglutarate dehydrogenase, mitochondrial	R.ISELSGC*TPDPR.I	272	30.46%	5.83%	28.37%	3.94%
Q96I23	PYURF Protein preY, mitochondrial	K.TEEPPRDFDPALLEFLVC*PLSK.K	60	17.33%	3.64%	13.07%	3.92%
Q8N5N7	MRPL50 39S ribosomal protein L50, mitochondrial	R.LHQMC*R.V	121	20.99%	3.83%	29.78%	3.78%
P24752	ACAT1 Acetyl-CoA acetyltransferase, mitochondrial	K.IHMGSC*AENTAK.K	196	19.95%	0.30%	26.30%	3.77%
Q9H078	CLPB Caseinolytic peptidase B protein homolog	K.GC*TALHYAVLADDYR.T	267	19.64%	5.04%	15.94%	3.59%
Q9NSE4	IARS2 Isoleucine--tRNA ligase, mitochondrial	K.YTAESSDTLC*PR.C	1002	31.85%	3.25%	36.24%	3.54%
P48735	IDH2 Isocitrate dehydrogenase	K.SSGGFVWAC*K.N	308	29.58%	0.03%	18.89%	3.15%
Q9NX47	MARCH5 E3 ubiquitin-protein ligase MARCH5	R.VAC*PQC*NAEYLIVFPK.L	65	37.92%	0.15%	30.66%	3.09%
Q9H2W6	MRPL46 39S ribosomal protein L46, mitochondrial	K.FLGNAPC*GHYTFK.F	210	16.53%	2.60%	11.77%	2.86%
Q99798	ACO2 Aconitate hydratase, mitochondrial	K.C*TTDHISAAGPWLK.F	592	19.06%	2.74%	12.04%	2.71%
O00411	POLRMT DNA-directed RNA polymerase, mitochondrial	R.VC*VVSVEKPTLPSK.E	413	26.61%	0.72%	35.53%	2.57%
P19367	HK1 Hexokinase-1	R.AAQLC*GAGMAAVVDK.I	834	16.49%	3.82%	10.88%	2.46%
P12235	SLC25A4 ADP/ATP translocase 1	K.GADIMYTGTVDC*WR.K	257	7.35%	0.83%	9.73%	2.46%
P56381	ATP5E ATP synthase subunit epsilon, mitochondrial	R.YSQIC*AK.A	19	29.79%	1.95%	20.28%	2.33%
P32322	PYCR1 Pyrroline-5-carboxylate reductase 1, mitochondrial	R.C*MTNTPVVVR.E	120	21.09%	3.68%	23.35%	2.24%
P49419	ALDH7A1 Alpha-aminoadipic semialdehyde dehydrogenase	K.GSDC*GIVNVNIPTSGAEIGGAFGGEK.H	478	15.24%	0.03%	9.68%	2.24%
P23368	ME2 NAD-dependent malic enzyme, mitochondrial	R.ILQDDIESLMPIVYTPTVGLAC*SQYGHIFR.R	120	16.83%	0.26%	10.74%	2.11%
Q99714	HSD17B10 3-hydroxyacyl-CoA dehydrogenase type-2	R.VDVAVNC*AGIAVASK.T	91	9.26%	1.05%	9.64%	1.91%
Q9NSE4	IARS2 Isoleucine--tRNA ligase, mitochondrial	R.C*AEVVSGK.-	1005	46.49%	1.54%	40.85%	1.90%
P07237	P4HB Protein disulfide-isomerase	K.KEEC*PAVR.L	312	18.95%	0.87%	11.99%	1.85%
P43897	TSFM Elongation factor Ts, mitochondrial	R.FEC*GEGEEAAETE.-	315	43.37%	0.39%	33.15%	1.84%
P10109	FDX1 Adrenodoxin, mitochondrial	R.LGC*QIC*LTK.S	152	83.05%	0.64%	72.78%	1.84%
P50336	PPOX Protoporphyrinogen oxidase	R.LPLTLAGASYEGVAVNDC*IESGR.Q	459	40.01%	4.47%	23.29%	1.81%
P28331	NDUFS1 NADH-ubiquinone oxidoreductase 75 kDa subunit, mit	K.VVAAC*AMPVMK.G	92	30.04%	7.01%	27.12%	1.80%
Q9NX47	MARCH5 E3 ubiquitin-protein ligase MARCH5	K.LQILNSIFPGIGC*PVPR.I	188	32.67%	4.75%	13.19%	1.79%
Q6P1X6	C8orf82 UPF0598 protein C8orf82	R.YEAAFPFLSPC*GR.E	98	41.94%	0.41%	52.14%	1.70%
Q9BU61	NDUFAF3 NADH dehydrogenase	R.GIAVEVQDTPNAC*ATFNFLC*HEGR.V	150	18.80%	4.96%	15.18%	1.67%
Q8IYB8	SUPV3L1 ATP-dependent RNA helicase SUPV3L1, mitochondrial	K.SNAAGVPC*DLVTGEER.V	251	38.15%	5.19%	52.35%	1.66%
Q13162	PRDX4 Peroxiredoxin-4	R.SINTEVVAC*SVDSQFTHLAWINTPR.R	148	36.24%	0.04%	22.53%	1.63%
Q13084	MRPL28 39S ribosomal protein L28, mitochondrial	K.TPKEDLC*SK.F	154	11.16%	0.15%	9.00%	1.53%
O75439	PMPCB Mitochondrial-processing peptidase subunit beta	R.VTC*LESGLR.V	62	32.57%	1.81%	31.67%	1.51%
O75439	PMPCB Mitochondrial-processing peptidase subunit beta	K.TNMLLQLDGSTPIC*EDIGR.Q	419	59.80%	15.91%	13.64%	1.46%
O75746	SLC25A12 Calcium-binding mitochondrial carrier protein Aral	K.NSFDC*FK.K	375	5.13%	0.17%	6.56%	1.45%

Q5JRX3	PITRM1 Presequence protease, mitochondrial	R.AFSSLNTLPEELRPYVPLFC*SVLTK.L	619	14.82%	0.18%	8.77%	1.42%
Q7Z7H8	MRPL10 39S ribosomal protein L10, mitochondrial	R.TVPFLPLLGGC*IDDTILSR.Q	180	9.26%	1.59%	9.33%	1.40%
P62906	RPL10A 60S ribosomal protein L10a	K.FSVC*VLGDQQHC*DEAK.A	66	40.91%	0.33%	24.00%	1.39%
Q8N5K1	CISD2 CDGSH iron-sulfur domain-containing protein 2	K.VVNEINIEDLC*LTK.A	92	38.13%	1.12%	29.09%	1.39%
Q5RI15	COX20 Cytochrome c oxidase protein 20 homolog	K.LLGFLDVENTPC*AR.H	29	87.89%	0.42%	86.49%	1.37%
P51649	ALDH5A1 Succinate-semialdehyde dehydrogenase, mitochondria	R.AAYEAFC*R.W	110	26.21%	0.90%	22.78%	1.36%
O75380	NDUFS6 NADH dehydrogenase	R.VIAC*DGGGGALGHPK.V	87	28.20%	0.11%	25.19%	1.35%
P43897	TSFM Elongation factor Ts, mitochondrial	K.TGYSFVNC*K.K	64	23.25%	1.92%	18.90%	1.31%
O60313	OPA1 Dynamin-like 120 kDa protein, mitochondrial	K.C*NEEHPAYLASDEITTVR.K	801	41.49%	2.69%	32.59%	1.30%
Q6PI48	DARS2 Aspartate--tRNA ligase, mitochondrial	K.LRLEC*ADLLETR.G	459	23.31%	1.72%	13.46%	1.28%
Q6YN16	HSDL2 Hydroxysteroid dehydrogenase-like protein 2	R.LAGC*TVFITGASR.G	11	13.66%	3.96%	5.97%	1.28%
P33121	ACSL1 Long-chain-fatty-acid--CoA ligase 1	R.NIVSDC*SAFVK.A	297	43.83%	3.91%	26.48%	1.27%
Q99497	PARK7 Protein DJ-1	K.VTVAGLAGKDPVQC*SR.D	46	40.93%	0.16%	35.32%	1.22%
O75323	GBAS Protein NipSnap homolog 2	K.LQFHNVKPEC*LEAYNK.I	85	16.30%	3.03%	8.13%	1.19%
Q5JPH6	EARS2 Probable glutamate--tRNA ligase, mitochondrial	K.TGAAYPC*FC*SPQR.L	140	43.25%	3.42%	27.23%	1.17%
Q53H12	AGK Acylglycerol kinase, mitochondrial	K.EDFLNIC*IEPDTISK.G	334	71.40%	5.44%	47.86%	1.13%
Q9HC36	RNMTL1 RNA methyltransferase-like protein 1	R.SAAGAGC*SK.V	235	20.29%	1.07%	13.34%	1.12%
O95831	AIFM1 Apoptosis-inducing factor 1, mitochondrial	K.SITIIGGGFLGSELAC*ALGR.K	317	24.32%	0.44%	10.61%	1.11%
P13804	ETFA Electron transfer flavoprotein subunit alpha, mito	K.VAQDLC*K.V	68	14.43%	0.05%	12.59%	1.09%
O94826	TOMM70A Mitochondrial import receptor subunit TOM70	R.C*AEGYALYAQALTDQQQFGK.A	475	11.21%	1.67%	7.66%	1.07%
Q13011	ECH1 Delta(3,5)-Delta(2,4)-dienoyl-CoA isomerase, mitoc	R.YC*AQDAFFQVK.E	187	49.47%	8.41%	22.58%	1.03%
P12532	CKMT1B Creatine kinase U-type, mitochondrial	R.LGYILTC*PSNLGTGLR.A	316	14.39%	0.95%	11.80%	1.02%
Q7Z2W9	MRPL21 39S ribosomal protein L21, mitochondrial	R.INSIEIAPC*LL.-	203	25.09%	0.11%	17.07%	1.01%
P49411	TUFM Elongation factor Tu, mitochondrial	K.GEETPVIVGSALC*ALEGRDPELGLK.S	222	45.98%	0.49%	49.18%	0.99%
Q9H845	ACAD9 Acyl-CoA dehydrogenase family member 9, mitochondr	K.LASGEHIAAFC*LTEPASGSDAASIR.S	179	15.37%	0.67%	9.89%	0.98%
Q9H9J2	MRPL44 39S ribosomal protein L44, mitochondrial	K.TAFVNSC*YIK.S	96	12.20%	0.42%	9.55%	0.98%
Q8IXI1	RHOT2 Mitochondrial Rho GTPase 2	K.SC*FGHPLAPQALEDVK.T	216	33.78%	0.32%	30.78%	0.97%
I3L0E3	MRPS17 28S ribosomal protein S17, mitochondrial	K.VIDPVTGKPC*AGTTYLESPLSSETTQLSK.N	195	27.41%	1.00%	20.63%	0.96%
Q9Y5L4	TIMM13 Mitochondrial import inner membrane translocase su	K.C*IGKPGGSLDNSEQK.C	50	95.24%	0.00%	93.89%	0.96%
P10620	MGST1 Microsomal glutathione S-transferase 1	K.VFANPEDC*VAFGK.G	50	7.49%	0.97%	7.10%	0.95%
O14561	NDUFAB1 Acyl carrier protein, mitochondrial	K.LMC*PQEIVDYIADKK.D	140	63.68%	0.55%	49.55%	0.92%
Q9Y277	VDAC3 Voltage-dependent anion-selective channel protein	K.SC*SGVEFSTSGHAYTDTGK.A	36	32.51%	0.19%	28.25%	0.91%
P25705	ATP5A1 ATP synthase subunit alpha, mitochondrial	K.LYC*IYVAIGQK.R	244	8.29%	1.67%	6.76%	0.91%
O94826	TOMM70A Mitochondrial import receptor subunit TOM70	K.EVAQDC*TK.A	176	13.41%	3.64%	6.31%	0.90%
O75431	MTX2 Metaxin-2	K.GEQILLSDNAASLAVQAFLQMC*NLPIK.V	51	21.44%	1.06%	14.37%	0.90%
Q7Z4W1	DCXR L-xylulose reductase	R.GVPGAIVNVSSQC*SQR.A	138	53.50%	1.88%	44.85%	0.89%
P51553	IDH3G Isocitrate dehydrogenase	K.LGDGLFLQC*C*R.E	235	27.39%	1.01%	19.65%	0.88%
Q99714	HSD17B10 3-hydroxyacyl-CoA dehydrogenase type-2	K.VC*NFLASQVPFPSR.L	214	14.21%	0.22%	10.36%	0.87%
P07203	GPX1 Glutathione peroxidase 1	K.LITWSPVC*R.N	156	25.64%	0.37%	24.14%	0.86%
P34897	SHMT2 Serine hydroxymethyltransferase, mitochondrial	K.NTC*PGDR.S	412	27.00%	0.27%	15.78%	0.84%
Q8N5N7	MRPL50 39S ribosomal protein L50, mitochondrial	K.EKEPVVVETVEEKKEPILVC*PPLR.S	52	21.93%	0.55%	10.64%	0.84%
Q96EY1	DNAJA3 DnaJ homolog subfamily A member 3, mitochondrial	R.GSIIISPC*VVC*R.G	289	24.43%	1.54%	23.46%	0.84%
P82933	MRPS9 28S ribosomal protein S9, mitochondrial	K.LLTSQC*GAAEEEFVQR.F	233	10.79%	2.13%	10.50%	0.84%
Q12931	TRAP1 Heat shock protein 75 kDa, mitochondrial	R.SPAAEC*LSEK.E	573	22.52%	0.26%	30.49%	0.81%
P13804	ETFA Electron transfer flavoprotein subunit alpha, mito	R.TIYAGNALC*TVK.C	155	36.65%	0.77%	24.92%	0.81%
B4DLN1	SLC25A10 cDNA FLJ60124, highly similar to Mitochondrial dic	R.TDGILALYSGLSASLC*R.Q	224	16.91%	0.77%	12.88%	0.80%
P52758	HRSP12 Ribonuclease UK114	K.AAGC*DFTNVVK.T	71	15.91%	0.41%	8.98%	0.80%

P19367	HK1 Hexokinase-1	R.AILQQLGLNSTC*DDSILVK.T	813	15.14%	0.16%	7.34%	0.77%
Q9P2R7	SUCLA2 Succinyl-CoA ligase	K.ILAC*DDLDEAAR.M	430	4.76%	0.00%	5.41%	0.76%
Q5TGZ0	MINOS1 Mitochondrial inner membrane organizing system pro	R.C*LADAVVK.I	13	40.78%	0.14%	39.43%	0.74%
P54886	ALDH18A1 Delta-1-pyrroline-5-carboxylate synthase	K.LGSAVVTRGDEC*GLALGR.L	88	43.07%	2.91%	39.62%	0.74%
P30084	ECHS1 Enoyl-CoA hydratase, mitochondrial	K.ALNALC*DGLIDELNQALK.T	62	16.28%	0.42%	21.90%	0.74%
P49411	TUFM Elongation factor Tu, mitochondrial	K.GDEC*ELLGHSK.N	290	30.55%	0.72%	34.82%	0.74%
Q9Y3D5	MRPS18C 28S ribosomal protein S18c, mitochondrial	R.HITGLC*GK.K	100	35.97%	0.39%	25.68%	0.73%
O15270	SPTLC2 Serine palmitoyltransferase 2	R.NTGSC*QEAAAK.V	188	31.60%	0.97%	24.77%	0.72%
P21912	SDHB Succinate dehydrogenase	K.C*GPMVLDALIK.I	68	14.93%	0.53%	10.34%	0.71%
Q13162	PRDX4 Peroxiredoxin-4	R.EEEC*HFYAGGQVYPGEASR.V	51	85.81%	0.12%	76.62%	0.71%
Q9BZE1	MRPL37 39S ribosomal protein L37, mitochondrial	R.NHIENQDEC*VLNVISHAR.L	153	13.23%	0.67%	8.05%	0.70%
P30044	PRDX5 Peroxiredoxin-5, mitochondrial	K.ALNVEPDGTGLTC*SLAPNIISQL.-	204	91.60%	0.20%	92.45%	0.69%
P42704	LRPPRC Leucine-rich PPR motif-containing protein, mitocho	K.VFNDTC*R.S	113	19.11%	0.19%	14.53%	0.69%
Q9HAV7	GRPEL1 GrpE protein homolog 1, mitochondrial	K.ATQC*VPKEEIKDDNPHLK.N	124	25.69%	0.84%	21.44%	0.68%
Q16822	PCK2 Phosphoenolpyruvate carboxykinase	R.YVAAAFPSAC*GK.T	306	22.69%	0.18%	21.00%	0.68%
P35232	PHB Prohibitin	K.PIIFDC*R.S	69	6.73%	0.89%	6.66%	0.68%
O75380	NDUFS6 NADH dehydrogenase	K.TGTC*GYC*GLQFR.Q	112	41.02%	12.37%	23.47%	0.67%
O75390	CS Citrate synthase, mitochondrial	K.LPC*VAAK.I	211	13.82%	0.01%	9.75%	0.67%
Q12849	GRSF1 G-rich sequence factor 1	R.YIELFLNSC*PK.G	476	15.21%	0.31%	38.81%	0.67%
P11177	PDHB Pyruvate dehydrogenase E1 component subunit beta,	K.TNHLVTVEGGWPQFGVGAEIC*AR.I	306	15.57%	0.56%	6.49%	0.66%
P42704	LRPPRC Leucine-rich PPR motif-containing protein, mitocho	R.SC*GSLLPELK.L	130	18.36%	0.32%	12.85%	0.65%
Q9Y2Q3	GSTK1 Glutathione S-transferase kappa 1	K.NQLKETTEAAC*R.Y	176	19.10%	2.23%	13.53%	0.64%
Q9Y4W6	AFG3L2 AFG3-like protein 2	K.LASLTPGFSGADVANVC*NEAALIAAR.H	525	7.42%	0.61%	7.41%	0.64%
P48047	ATP5O ATP synthase subunit O, mitochondrial	R.GEVPC*TVTSASPLEEATLSELK.T	141	13.40%	0.20%	8.46%	0.64%
P49821	NDUFV1 NADH dehydrogenase	R.GAGAYIC*GEETALIESIEGK.Q	206	47.18%	0.39%	34.13%	0.63%
P00367	GLUD1 Glutamate dehydrogenase 1, mitochondrial	K.AKPYEGSILEADC*DILIPAASEK.Q	376	37.48%	0.05%	27.79%	0.63%
O43837	IDH3B Isocitrate dehydrogenase	K.LGDGLFLQC*C*EEVAELYPK.I	232	53.97%	1.41%	32.27%	0.62%
B4DLN1	SLC25A10 cDNA FLJ60124, highly similar to Mitochondrial dic	R.GALVTVGQLSC*YDQAK.Q	336	18.15%	0.99%	12.74%	0.62%
O95299	NDUFA10 NADH dehydrogenase	K.QC*VDHYNEVK.S	183	33.28%	0.05%	24.20%	0.61%
P30405	PPIF Peptidyl-prolyl cis-trans isomerase F, mitochondri	K.IVITDC*GQLS.-	203	39.04%	0.80%	26.84%	0.61%
P42704	LRPPRC Leucine-rich PPR motif-containing protein, mitocho	R.C*VANNQVETLEK.L	930	36.44%	0.37%	22.95%	0.60%
O75431	MTX2 Metaxin-2	K.NYSNLLAFC*R.R	246	5.22%	0.20%	5.17%	0.60%
Q9H0U6	MRPL18 39S ribosomal protein L18, mitochondrial	R.NVVAC*ESIGR.V	125	9.04%	0.44%	5.91%	0.59%
P34897	SHMT2 Serine hydroxymethyltransferase, mitochondrial	R.YYGGAEVVDEIELLC*QR.R	119	20.18%	3.29%	12.58%	0.59%
P04181	OAT Ornithine aminotransferase, mitochondrial	K.VLPMNTGVEAGETAC*K.L	150	8.29%	0.10%	6.42%	0.59%
Q9Y3D5	MRPS18C 28S ribosomal protein S18c, mitochondrial	K.NVQLLSQFVSPFTGC*IYGR.H	90	31.70%	0.29%	22.03%	0.59%
P49821	NDUFV1 NADH dehydrogenase	K.LLEGC*LVGGR.A	142	15.89%	3.46%	9.62%	0.59%
P28331	NDUFS1 NADH-ubiquinone oxidoreductase 75 kDa subunit, mit	K.VLFLLGADGGC*ITR.Q	554	8.75%	0.24%	8.17%	0.58%
P34897	SHMT2 Serine hydroxymethyltransferase, mitochondrial	R.GLELIASENFC*SR.A	80	28.07%	1.25%	17.74%	0.58%
P36969	GPX4 Phospholipid hydroperoxide glutathione peroxidase,	R.YAEC*GLR.I	93	17.41%	0.04%	12.00%	0.57%
Q5XKP0	QIL1 Protein QIL1	K.AGEVVPPAMYQFSQYVC*QQTGLQIPQLPA PPK.I	60	13.46%	0.21%	7.81%	0.57%
P00367	GLUD1 Glutamate dehydrogenase 1, mitochondrial	K.C*AVVDVPFGGAK.A	172	9.56%	0.52%	7.82%	0.57%
P51649	ALDH5A1 Succinate-semialdehyde dehydrogenase, mitochondria	K.YVC*YGGL.-	531	27.94%	1.18%	23.18%	0.57%
P51659	HSD17B4 Peroxisomal multifunctional enzyme type 2	K.SNIHC*NTIAPNAGSR.M	189	16.29%	0.21%	10.97%	0.57%
P13804	ETFA Electron transfer flavoprotein subunit alpha, mito	K.QFNYTHIC*AGASAFGK.N	109	9.18%	1.16%	6.16%	0.56%
Q9NYK5	MRPL39 39S ribosomal protein L39, mitochondrial	K.ATEEC*TST.-	335	57.60%	2.01%	59.43%	0.56%

P23368	ME2 NAD-dependent malic enzyme, mitochondrial	R.C*LFASGSPFGPVK.L	441	10.50%	0.58%	9.07%	0.56%
P11177	PDHB Pyruvate dehydrogenase E1 component subunit beta,	K.EGVEC*EVINMR.T	263	20.49%	0.51%	12.31%	0.56%
Q6PI48	DARS2 Aspartate--tRNA ligase, mitochondrial	R.TNTC*GELR.S	54	17.96%	1.25%	13.50%	0.55%
Q86SX6	GLRX5 Glutaredoxin-related protein 5, mitochondrial	K.GTPEQPQC*GFSNAVVQILR.L	67	15.00%	0.35%	25.29%	0.55%
O75746	SLC25A12 Calcium-binding mitochondrial carrier protein Aral	R.AGQTTYSGVIDC*FR.K	563	4.76%	0.00%	3.83%	0.54%
Q96EY8	MMAB Cob(I)yrinic acid a,c-diamide adenosyltransferase,	K.ISSALHFC*R.A	185	30.29%	0.81%	25.36%	0.52%
P23434	GCSH Glycine cleavage system H protein, mitochondrial	K.SC*YEDGWLIK.M	138	21.76%	0.12%	18.26%	0.51%
Q08257	CRYZ Quinone oxidoreductase	K.VHAC*GVNPVETYIR.S	45	17.54%	2.17%	14.04%	0.51%
Q13423	NNT NAD(P) transhydrogenase, mitochondrial	R.EANSIIITPGYGLC*AAK.A	936	12.24%	0.68%	9.13%	0.51%
Q9NVH1	DNAJC11 DnaJ homolog subfamily C member 11	K.VIDVTVPLQC*LVK.D	494	12.65%	0.16%	7.64%	0.50%
P08574	CYC1 Cytochrome c1, heme protein, mitochondrial	K.DVC*TFLR.W	271	4.54%	0.41%	4.02%	0.50%
P28288	ABCD3 ATP-binding cassette sub-family D member 3	R.SGANVLIC*GPNGC*GK.S	472	41.62%	3.08%	27.06%	0.49%
P34897	SHMT2 Serine hydroxymethyltransferase, mitochondrial	R.AALEALGSC*LNNK.Y	91	7.24%	2.15%	5.05%	0.49%
P21964	COMT Catechol O-methyltransferase	K.GTVLLADNVIC*PGAPDFLAHVR.G	223	10.53%	0.56%	6.89%	0.49%
P38646	HSPA9 Stress-70 protein, mitochondrial	K.GAVVGIDLGTTNSC*VAVMEGK.Q	66	39.39%	0.52%	27.44%	0.49%
O94826	TOMM70A Mitochondrial import receptor subunit TOM70	K.AGKYEQAIQC*YTEAISLC*PTEK.N	136	11.69%	2.45%	10.49%	0.48%
P24752	ACAT1 Acetyl-CoA acetyltransferase, mitochondrial	K.VC*ASGMK.A	126	20.20%	1.01%	17.40%	0.48%
P45880	VDAC2 Voltage-dependent anion-selective channel protein	K.VC*EDLDTSVNLAWTSGTNC*TR.F	210	22.03%	0.48%	16.11%	0.46%
P31930	UQCRC1 Cytochrome b-c1 complex subunit 1, mitochondrial	K.AVELLGDIVQNC*SLEDSQIEK.E	154	9.09%	1.07%	6.15%	0.46%
Q9HCC0	MCCC2 Methylcrotonoyl-CoA carboxylase beta chain, mitoch	R.LPC*IYLVDSGGAYLPR.Q	167	7.65%	0.64%	8.72%	0.46%
Q9BW92	TARS2 Threonine--tRNA ligase, mitochondrial	R.IC*QELTAAAR.P	185	10.41%	0.53%	6.63%	0.46%
O94826	TOMM70A Mitochondrial import receptor subunit TOM70	K.ADEMYDKC*IDLEPDNATTYVHK.G	502	45.35%	0.67%	31.46%	0.45%
P19404	NDUFV2 NADH dehydrogenase	R.FSC*EPAGGLTSLTEPPK.G	225	25.28%	0.30%	18.65%	0.45%
P21953	BCKDHB 2-oxoisovalerate dehydrogenase subunit beta, mitoc	R.SGDLFNC*GSLTIR.S	177	17.71%	0.53%	12.80%	0.45%
O14880	MGST3 Microsomal glutathione S-transferase 3	K.VEYPIMYSTDPENGHIFNC*IQR.A	56	6.60%	0.91%	5.21%	0.45%
Q15286	RAB35 Ras-related protein Rab-35	R.WLHEINQNC*DDVC*R.I	110	29.26%	0.62%	19.97%	0.45%
Q9NNW7	TXNRD2 Thioredoxin reductase 2, mitochondrial	R.TVGIHPTC*SEEVVK.L	500	31.49%	2.63%	33.18%	0.43%
P55809	OXCT1 Succinyl-CoA:3-ketoacid coenzyme A transferase 1,	K.C*TLPLTGK.Q	456	6.07%	0.47%	7.26%	0.42%
Q6UXV4	APOOL Apolipoprotein O-like	K.ITYPLGLATLGATVC*YPVQSVIIAK.V	152	13.30%	2.93%	10.39%	0.42%
P05091	ALDH2 Aldehyde dehydrogenase, mitochondrial	K.LLC*GGGIAADR.G	386	9.79%	0.35%	9.69%	0.42%
Q6PI48	DARS2 Aspartate--tRNA ligase, mitochondrial	R.LIC*LVTGSPSIR.D	590	22.23%	1.62%	17.19%	0.42%
P19367	HK1 Hexokinase-1	K.ATDC*VGHDVVTLLR.D	628	4.76%	0.00%	4.02%	0.41%
O75251	NDUFS7 NADH dehydrogenase	R.IVPVDIYIPGC*PPTAEALLYGILQLQR.K	183	65.19%	0.97%	59.35%	0.40%
P40939	HADHA Trifunctional enzyme subunit alpha, mitochondrial	K.TGIEQGSDAGYLC*ESQK.F	322	18.56%	3.47%	18.34%	0.40%
Q9H2U2	PPA2 Inorganic pyrophosphatase 2, mitochondrial	R.C*TQEEAR.S	302	40.35%	2.05%	35.83%	0.40%
P04406	GAPDH Glyceraldehyde-3-phosphate dehydrogenase	K.IISNASC*TTNC*LAPLAK.V	152	34.88%	0.75%	27.60%	0.39%
Q92552	MRPS27 28S ribosomal protein S27, mitochondrial	K.VAASPEDIKLC*R.E	276	4.81%	0.03%	4.30%	0.38%
P82932	MRPS6 28S ribosomal protein S6, mitochondrial	K.EC*EGIVPVPLAEK.L	105	5.62%	0.36%	6.76%	0.37%
P31930	UQCRC1 Cytochrome b-c1 complex subunit 1, mitochondrial	R.NALVSHLDGTTPVC*EDIGR.S	410	10.63%	0.35%	7.41%	0.37%
Q14197	ICT1 Peptidyl-tRNA hydrolase ICT1, mitochondrial	R.NLADC*LQK.I	150	5.63%	0.38%	3.99%	0.37%
Q9NX40	OCIAD1 OCIA domain-containing protein 1	R.RVFAEC*NDESFWFR.S	38	66.29%	0.64%	63.59%	0.37%
P11177	PDHB Pyruvate dehydrogenase E1 component subunit beta,	R.PVGHC*LEAAAVLSK.E	249	16.28%	0.12%	11.51%	0.36%
P54819	AK2 Adenylate kinase 2, mitochondrial	K.NLETPLC*K.N	92	8.98%	0.06%	8.05%	0.36%
P38646	HSPA9 Stress-70 protein, mitochondrial	R.RTIAPC*QK.A	366	13.14%	0.06%	10.59%	0.36%

Q96RP9	GFM1 Elongation factor G, mitochondrial	R.YQPC*LPSTQEDVINK.Y	723	25.45%	1.75%	13.13%	0.36%
P49207	RPL34 60S ribosomal protein L34	K.SAC*GVC*PGR.L	46	45.18%	0.35%	34.35%	0.35%
Q53H12	AGK Acylglycerol kinase, mitochondrial	R.AAC*QEAQVFGNQLIPPNAQVK.K	43	28.00%	0.35%	18.95%	0.34%
Q9Y277	VDAC3 Voltage-dependent anion-selective channel protein	K.YMLDC*R.T	229	10.13%	0.71%	10.16%	0.34%
Q9Y512	SAMM50 Sorting and assembly machinery component 50 homolo	R.TKDDIIIC*EIGDVFK.A	65	5.10%	0.16%	4.21%	0.34%
P31040	SDHA Succinate dehydrogenase	R.VGSVLQEGC*GK.I	536	6.82%	0.57%	5.23%	0.33%
Q96I59	NARS2 Probable asparagine--tRNA ligase, mitochondrial	R.YLQC*ILGVDNIKDVIPFPR.F	455	12.59%	3.56%	5.81%	0.33%
Q96DV4	MRPL38 39S ribosomal protein L38, mitochondrial	R.VAEGQVTC*PYLPPFPAR.G	252	9.87%	0.61%	6.91%	0.33%
Q8NBU5	ATAD1 ATPase family AAA domain-containing protein 1	R.DAALLC*VR.E	310	37.48%	1.79%	30.06%	0.33%
Q00325	SLC25A3 Phosphate carrier protein, mitochondrial	K.GWAPTFLGYSMQGLC*K.F	136	8.04%	0.64%	6.22%	0.33%
P13804	ETFA Electron transfer flavoprotein subunit alpha, mito	R.LGGEVSC*LVAGTK.C	53	28.97%	0.21%	20.16%	0.32%
Q96EL3	MRPL53 39S ribosomal protein L53, mitochondrial	R.VQFC*PFEK.N	21	12.65%	0.22%	7.65%	0.31%
Q9BWM7	SFXN3 Sideroflexin-3	R.FVPFAAVAAANC*INIPLMR.Q	189	14.04%	0.21%	7.94%	0.31%
Q99536	VAT1 Synaptic vesicle membrane protein VAT-1 homolog	R.AC*GLNFADLMAR.Q	86	6.91%	0.50%	4.15%	0.31%
P10809	HSPD1 60 kDa heat shock protein, mitochondrial	R.C*IPALDSLTPANEDQK.I	447	48.26%	0.16%	42.03%	0.30%
P40939	HADHA Trifunctional enzyme subunit alpha, mitochondrial	R.C*LAPMMSEVIR.I	550	12.22%	0.36%	7.16%	0.30%
Q9NVS2	MRPS18A 28S ribosomal protein S18a, mitochondrial	R.DNVC*YSR.T	186	19.70%	1.03%	19.77%	0.30%
O95299	NDUFA10 NADH dehydrogenase	R.VITVDGNIC*TGK.G	67	14.56%	0.26%	11.38%	0.30%
Q9Y6M9	NDUFB9 NADH dehydrogenase	R.HLESWC*VQR.D	31	12.88%	0.80%	8.54%	0.29%
O94925	GLS Glutaminase kidney isoform, mitochondrial	K.C*VQSNIVLLTQAFR.R	203	19.00%	6.14%	5.97%	0.29%
P24752	ACAT1 Acetyl-CoA acetyltransferase, mitochondrial	R.QAVLGAGLPISTPC*TTINK.V	119	13.65%	0.09%	11.27%	0.29%
P38646	HSPA9 Stress-70 protein, mitochondrial	K.MEEFKDQLPADEC*NK.L	608	13.68%	2.78%	9.06%	0.29%
P43897	TSFM Elongation factor Ts, mitochondrial	K.ALETC*GGDLK.Q	71	19.11%	0.16%	14.64%	0.28%
Q14197	ICT1 Peptidyl-tRNA hydrolase ICT1, mitochondrial	R.LTISYC*R.S	82	16.55%	0.62%	29.55%	0.28%
P00367	GLUD1 Glutamate dehydrogenase 1, mitochondrial	K.C*IAVGESDGSIWNPDGIDPK.E	327	23.16%	0.28%	14.26%	0.28%
Q16891	IMMT Mitochondrial inner membrane protein	K.ANC*SDNEFTQALTAAIPPESLTR.G	603	14.53%	0.30%	11.25%	0.28%
O95202	LETM1 LETM1 and EF-hand domain-containing protein 1, mit	K.LFEDELTLDNLTRPQLVALC*K.L	330	21.17%	0.53%	11.67%	0.28%
P49411	TUFM Elongation factor Tu, mitochondrial	R.HYAHTDC*PGHADYVK.N	127	61.26%	0.61%	70.84%	0.28%
P45880	VDAC2 Voltage-dependent anion-selective channel protein	K.WC*EYGLTFTEK.W	76	11.74%	0.17%	10.03%	0.27%
P40939	HADHA Trifunctional enzyme subunit alpha, mitochondrial	K.ALMGLYHGQVLC*K.K	349	6.41%	0.59%	5.84%	0.27%
P04406	GAPDH Glyceraldehyde-3-phosphate dehydrogenase	R.VPTANVSVVDLTC*R.L	247	9.03%	0.53%	6.41%	0.27%
O75521	ECI2 Enoyl-CoA delta isomerase 2, mitochondrial	R.WLSDEC*TNAVVNFLSR.K	380	6.76%	0.53%	5.59%	0.26%
Q9P032	NDUFAF4 NADH dehydrogenase	K.AAETC*QEPK.E	87	35.87%	0.01%	41.74%	0.26%
P10515	DLAT Dihydrolipoyllysine-residue acetyltransferase comp	K.ASALAC*LK.V	488	7.88%	0.19%	4.87%	0.25%
Q99714	HSD17B10 3-hydroxyacyl-CoA dehydrogenase type-2	K.KLGNNC*VFAPADVTSEK.D	58	10.71%	0.49%	9.00%	0.24%
Q9H2U2	PPA2 Inorganic pyrophosphatase 2, mitochondrial	R.GQPC*SQNYR.L	44	22.77%	0.73%	25.10%	0.24%
P08559	PDHA1 Pyruvate dehydrogenase E1 component subunit alpha,	R.VDGMDILC*VR.E	261	11.94%	0.21%	6.87%	0.24%
Q53H12	AGK Acylglycerol kinase, mitochondrial	K.LQFFC*DPR.K	408	9.11%	0.08%	5.43%	0.24%
Q7L2E3	DHX30 Putative ATP-dependent RNA helicase DHX30	R.QAAAAAC*QLFK.G	118	8.26%	1.15%	37.07%	0.24%
P31040	SDHA Succinate dehydrogenase	R.GVIALC*IEDGSIHR.I	238	13.28%	2.44%	7.71%	0.23%
Q9NX20	MRPL16 39S ribosomal protein L16, mitochondrial	R.C*EFEEVQGFLDQVAHK.L	167	4.87%	0.08%	5.09%	0.23%
Q9BPW8	NIPSNAP1 Protein NipSnap homolog 1	K.LHLDEDYPC*SLVGNWNTWYGEQDQAVH LWR.F	106	9.10%	2.03%	6.31%	0.23%
P53007	SLC25A1 Tricarboxylate transport protein, mitochondrial	R.NTWDC*GLQILK.K	262	6.50%	0.33%	4.45%	0.23%
Q9Y6C9	MTCH2 Mitochondrial carrier homolog 2	R.LC*SGVLGTVVHGK.V	79	5.61%	0.09%	4.54%	0.23%
P50213	IDH3A Isocitrate dehydrogenase	K.C*SDFTEEIC*R.R	351	53.54%	0.38%	36.78%	0.23%

P45880	VDAC2 Voltage-dependent anion-selective channel protein	K.SC*SGVEFSTSGSSNTDTGK.V	47	27.13%	0.23%	22.49%	0.22%
P30044	PRDX5 Peroxiredoxin-5, mitochondrial	K.GVLFGVPGAFTPGC*SK.T	100	57.59%	13.11%	93.72%	0.22%
O75947	ATP5H ATP synthase subunit d, mitochondrial	K.FNALKVPVPEDKYTAQVDAEEKEDVKSC*AEWVSLSK.A	101	9.13%	0.61%	6.93%	0.22%
P45880	VDAC2 Voltage-dependent anion-selective channel protein	R.PMC*IPPSYADLGK.A	13	50.13%	0.53%	45.99%	0.21%
P48735	IDH2 Isocitrate dehydrogenase	R.NILGGTVFREPIIC*K.N	154	15.40%	0.46%	9.93%	0.21%
O95299	NDUFA10 NADH dehydrogenase	K.HFPEAGIHYPDSTTGDGKPLATDYNGNC*SLEK.F	112	41.85%	0.10%	28.80%	0.21%
P40926	MDH2 Malate dehydrogenase, mitochondrial	K.GYLGPEQLPDC*LK.G	89	31.40%	0.08%	20.63%	0.21%
Q00325	SLC25A3 Phosphate carrier protein, mitochondrial	K.FAC*FER.T	237	6.18%	0.17%	4.30%	0.20%
P49821	NDUFV1 NADH dehydrogenase	K.YLVVNADEGEPGTC*K.D	125	44.48%	0.68%	29.24%	0.20%
P40926	MDH2 Malate dehydrogenase, mitochondrial	K.SQETEC*TYFSTPLLLGK.K	285	15.34%	0.62%	9.60%	0.20%
Q6NUK1	SLC25A24 Calcium-binding mitochondrial carrier protein SCaM	K.TGQYSGIYDC*AK.K	330	4.82%	0.04%	4.46%	0.19%
P30048	PRDX3 Thioredoxin-dependent peroxide reductase, mitochon	K.AFQYVETHGEVC*PANWTPDSPTIKPSPAASK.E	229	92.72%	0.60%	89.40%	0.19%
Q16698	DECR1 2,4-dienoyl-CoA reductase, mitochondrial	K.GMTTLLSSLGAQC*VIASR.K	86	6.10%	0.64%	5.29%	0.19%
P12235	SLC25A4 ADP/ATP translocase 1	R.YFAGNLASGGAAGATSLC*FVYPLDFAR.T	129	7.80%	0.22%	5.42%	0.19%
P21796	VDAC1 Voltage-dependent anion-selective channel protein	K.YQIDPDAC*FSAK.V	232	7.91%	0.21%	5.91%	0.19%
O00217	NDUFS8 NADH dehydrogenase	K.LC*EAIC*PAQAITIEAEPR.A	117	93.02%	0.97%	80.88%	0.19%
P09622	DLD Dihydrolipoyl dehydrogenase, mitochondrial	K.NETLGGTC*LNVGC*IPSK.A	80	95.24%	0.00%	95.47%	0.19%
P49406	MRPL19 39S ribosomal protein L19, mitochondrial	K.ISQFLGIC*IQR.S	137	21.62%	3.39%	11.16%	0.19%
P00505	GOT2 Aspartate aminotransferase, mitochondrial	R.VGAFTMVC*K.D	295	20.45%	1.02%	14.31%	0.18%
O75521	ECI2 Enoyl-CoA delta isomerase 2, mitochondrial	K.LHAVNAEEC*NVLQGR.W	368	5.21%	0.18%	4.99%	0.18%
P42704	LRPPRC Leucine-rich PPR motif-containing protein, mitocho	R.LIASYC*NVGDIEGASK.I	208	15.52%	6.61%	6.33%	0.18%
P31930	UQCRC1 Cytochrome b-c1 complex subunit 1, mitochondrial	K.YIYDQC*PAVAGYGPIEQLPDYNR.I	453	19.39%	0.34%	12.56%	0.18%
P50213	IDH3A Isocitrate dehydrogenase	R.IEAAC*FATIK.D	331	4.76%	0.00%	6.01%	0.18%
P07919	UQCRH Cytochrome b-c1 complex subunit 6, mitochondrial	R.DHC*VAHK.L	81	51.68%	0.32%	33.72%	0.18%
Q99798	ACO2 Aconitate hydratase, mitochondrial	R.DLGGIVLANAC*GPC*IGQWDR.K	448	49.83%	1.49%	43.23%	0.18%
Q9NSE4	IARS2 Isoleucine--tRNA ligase, mitochondrial	K.VASVASTLETTFETISTLSGVDLENGTC*SHPLIPDK.A	364	31.06%	0.66%	28.60%	0.18%
P31930	UQCRC1 Cytochrome b-c1 complex subunit 1, mitochondrial	R.LC*TSATESEVAR.G	380	15.78%	0.35%	12.36%	0.18%
O95299	NDUFA10 NADH dehydrogenase	K.C*EVLQYSAR.E	253	21.01%	0.12%	14.08%	0.18%
P78540	ARG2 Arginase-2, mitochondrial	R.LSSLGC*HLK.D	63	10.25%	1.94%	9.44%	0.17%
P10809	HSPD1 60 kDa heat shock protein, mitochondrial	R.AAVEEGIVLGGGC*ALLR.C	442	36.00%	0.11%	34.47%	0.17%
P31040	SDHA Succinate dehydrogenase	K.TLNEADC*ATVPPAIR.S	654	45.91%	0.41%	34.02%	0.17%
Q9UJZ1	STOML2 Stomatin-like protein 2	R.ERESLNASIVDAINQAADC*WGIR.C	167	17.36%	0.35%	13.55%	0.17%
Q99643	SDHC Succinate dehydrogenase cytochrome b560 subunit, m	K.SLC*LGPALIHTAK.F	107	5.62%	0.40%	5.07%	0.17%
P40926	MDH2 Malate dehydrogenase, mitochondrial	K.AAVKGYLGPEQLPDCLKGC*DVVVIPAGVPR.K	93	35.17%	0.10%	22.63%	0.17%
Q9NSE4	IARS2 Isoleucine--tRNA ligase, mitochondrial	K.C*GFSELYSWQR.E	91	23.61%	4.40%	16.88%	0.16%
P10515	DLAT Dihydrolipoyllysine-residue acetyltransferase comp	R.DVPLGTPLC*IIVEK.E	291	27.52%	0.21%	20.29%	0.16%
P42126	ECI1 Enoyl-CoA delta isomerase 1, mitochondrial	R.YC*IGLNETQLGIIAPFWLK.D	173	10.48%	1.33%	5.44%	0.16%
Q7L0Y3	TRMT10C Mitochondrial ribonuclease P protein 1	R.NVDPFHIYFC*NLK.I	246	5.94%	0.25%	4.62%	0.15%
O00483	NDUFA4 NADH dehydrogenase	R.LALFNPDVC*WDR.N	44	16.74%	0.57%	10.36%	0.15%
P82650	MRPS22 28S ribosomal protein S22, mitochondrial	R.HVDVLNLC*FAQFEPDSTEYIK.V	231	8.81%	2.08%	12.65%	0.15%
P31040	SDHA Succinate dehydrogenase	R.TYFSC*TSAHTSTGDGTAMITR.A	266	27.07%	0.24%	20.34%	0.14%
P36542	ATP5C1 ATP synthase subunit gamma, mitochondrial	R.GLC*GAIHSSIAK.Q	103	5.08%	0.14%	5.28%	0.14%
Q8IXI1	RHOT2 Mitochondrial Rho GTPase 2	K.QLRPAC*AQALTR.I	185	11.15%	0.21%	7.94%	0.13%
Q16134	ETFDH Electron transfer flavoprotein-ubiquinone oxidored	K.AAQIGAHTLSGAC*LDPGAFK.E	118	5.75%	0.57%	4.99%	0.13%
Q14318	FKBP8 Peptidyl-prolyl cis-trans isomerase FKBP8	K.REC*GNAHYQR.A	227	29.28%	4.09%	17.60%	0.13%
P00505	GOT2 Aspartate aminotransferase, mitochondrial	K.EYLPIGGLAEFC*K.A	106	13.95%	0.62%	10.08%	0.13%

P08559	PDHA1 Pyruvate dehydrogenase E1 component subunit alpha,	R.FAAAYC*R.S	273	10.34%	0.58%	7.96%	0.13%
P19367	HK1 Hexokinase-1	K.TVC*GVVSR.R	823	29.09%	6.46%	11.07%	0.13%
P05141	SLC25A5 ADP/ATP translocase 2	K.GTDIMYTGTLDC*WR.K	257	8.19%	0.81%	5.50%	0.13%
P82912	MRPS11 28S ribosomal protein S11, mitochondrial	K.ASHNNTQIQVVSASNEPLAFASC*GTEGFR.N	112	24.35%	0.05%	18.38%	0.13%
P13995	MTHFD2 Bifunctional methylenetetrahydrofolate dehydrogena	R.IC*NAVSPDKDVDGFHVINVGR.M	145	9.60%	2.55%	13.68%	0.13%
Q16718	NDUFA5 NADH dehydrogenase	K.TTGLVGLAVC*NTPHER.L	17	10.75%	2.32%	11.80%	0.12%
P45880	VDAC2 Voltage-dependent anion-selective channel protein	K.WNTDNTLGTEIAIEDQIC*QGLK.L	103	18.23%	0.17%	14.81%	0.12%
P40926	MDH2 Malate dehydrogenase, mitochondrial	K.TIIPLISQC*TPK.V	212	15.32%	0.19%	11.23%	0.12%
Q9Y6M9	NDUFB9 NADH dehydrogenase	R.YFAC*LMR.A	42	18.97%	0.50%	11.72%	0.12%
O95831	AIFM1 Apoptosis-inducing factor 1, mitochondrial	K.C*LIATGGTPR.S	256	11.95%	0.38%	7.44%	0.12%
O75306	NDUFS2 NADH dehydrogenase	R.IIAQC*LNK.M	347	17.98%	0.91%	14.04%	0.12%
Q9Y676	MRPS18B 28S ribosomal protein S18b, mitochondrial	K.VVGNPC*PIC*R.D	105	40.53%	2.42%	24.50%	0.12%
P49821	NDUFV1 NADH dehydrogenase	K.NAC*GSGYDFDVFVVR.G	187	21.76%	2.12%	18.90%	0.12%
O75431	MTX2 Metaxin-2	K.KTLDQVLEDVDQC*C*QALSQR.L	189	40.17%	0.38%	27.71%	0.12%
Q5TC12	ATPAF1 ATP synthase mitochondrial F1 complex assembly fac	R.AQSC*PTFLC*ALPR.R	194	57.60%	8.07%	25.68%	0.11%
Q07021	C1QBP Complement component 1 Q subcomponent-binding prot	K.ALVLDC*HYPEDEVGQEDEAESDIFSIR.E	186	42.63%	0.09%	30.66%	0.11%
P53701	HCCS Cytochrome c-type heme lyase	R.AYEYVEC*PIR.G	66	50.93%	0.44%	46.49%	0.11%
P10606	COX5B Cytochrome c oxidase subunit 5B, mitochondrial	R.C*GAHYK.L	116	30.22%	0.11%	29.41%	0.10%
Q9H845	ACAD9 Acyl-CoA dehydrogenase family member 9, mitochondr	R.AYIC*AHPLDR.T	613	29.81%	0.20%	31.83%	0.10%
P31040	SDHA Succinate dehydrogenase	R.AAFGLSEAGFNTAC*VTK.L	89	10.52%	0.25%	7.54%	0.09%
Q15070	OXA1L Mitochondrial inner membrane protein OXA1L	R.C*LIFPLIVTGQR.E	153	28.22%	0.40%	16.70%	0.09%
Q53H12	AGK Acylglycerol kinase, mitochondrial	K.ATVFLNPAAC*K.G	72	6.70%	0.45%	5.52%	0.09%
O95182	NDUFA7 NADH dehydrogenase	K.LSNNYYC*TR.D	55	4.76%	0.00%	4.86%	0.07%
P22695	UQCRC2 Cytochrome b-c1 complex subunit 2, mitochondrial	R.NALANPLYC*PDYR.I	192	21.00%	0.34%	12.24%	0.06%
P40926	MDH2 Malate dehydrogenase, mitochondrial	K.EGVVEC*SFVK.S	275	18.56%	5.69%	8.13%	0.06%
Q9Y277	VDAC3 Voltage-dependent anion-selective channel protein	K.VC*NYGLTFTQK.W	65	16.26%	0.36%	13.78%	0.05%
P08559	PDHA1 Pyruvate dehydrogenase E1 component subunit alpha,	K.NFYGGNGIVGAQVPLGAGIALAC*K.Y	181	13.82%	1.36%	10.63%	0.05%
Q969S9	GFM2 Ribosome-releasing factor 2, mitochondrial	R.VTLAQTAVPVLC*GSALK.N	329	9.89%	0.08%	7.50%	0.05%
Q9Y6C9	MTCH2 Mitochondrial carrier homolog 2	R.QVC*QLPGLFSYAQHIASIDGR.R	49	13.39%	2.85%	8.19%	0.05%
Q9HAV7	GRPEL1 GrpE protein homolog 1, mitochondrial	K.LYGIQAFC*K.D	108	19.23%	9.75%	6.48%	0.04%
P05141	SLC25A5 ADP/ATP translocase 2	R.EFRGLGDC*LVK.I	160	8.47%	1.25%	4.84%	0.04%
P28331	NDUFS1 NADH-ubiquinone oxidoreductase 75 kDa subunit, mit	K.AVTEGAQAVEEPSIC*.-	727	83.46%	0.45%	78.79%	0.03%
Q99798	ACO2 Aconitate hydratase, mitochondrial	K.VAVPSTIHC*DHLIEAQVGGEK.D	126	23.11%	0.43%	16.02%	0.03%
P21964	COMT Catechol O-methyltransferase	R.LITIEINPDC*AAITQR.M	145	20.73%	0.07%	12.34%	0.03%
P10809	HSPD1 60 kDa heat shock protein, mitochondrial	K.C*EFQDAYVLLSEK.K	237	10.27%	0.19%	9.90%	0.02%
P55809	OXCT1 Succinyl-CoA:3-ketoacid coenzyme A transferase 1,	K.STGC*DFAVSPK.L	504	16.87%	2.69%	9.88%	0.02%
Q9BSH4	TACO1 Translational activator of cytochrome c oxidase 1	K.FIC*DASSLHQVR.K	234	4.76%	0.00%	4.78%	0.02%
P51970	NDUFA8 NADH dehydrogenase	K.FDEC*VLDK.L	110	69.02%	9.27%	95.24%	0.00%
P14854	COX6B1 Cytochrome c oxidase subunit 6B1	R.VYQSLC*PTSWVTDWDEQR.A	65	95.24%	0.00%	95.24%	0.00%
P14854	COX6B1 Cytochrome c oxidase subunit 6B1	R.NC*WQNYLDFHR.C	30	95.24%	0.00%	95.24%	0.00%
P40939	HADHA Trifunctional enzyme subunit alpha, mitochondrial	K.EVEAVIPDHC*IFASNTSALPISEIAAVSK.R	470	5.21%	0.21%	4.76%	0.00%
O75390	CS Citrate synthase, mitochondrial	R.FRGFSIPEC*QK.L	101	28.46%	13.68%	4.76%	0.00%
P22033	MUT Methylmalonyl-CoA mutase, mitochondrial	R.C*TVGEITDALKK.V	560	21.61%	3.28%	4.76%	0.00%
Q9NWU5	MRPL22 39S ribosomal protein L22, mitochondrial	K.VYC*HYFVK.L	166	12.67%	2.80%	4.76%	0.00%

P10515	DLAT Dihydrolipoyllysine-residue acetyltransferase comp	K.NFSAIINPPQAC*ILAIGASEDK.L	586	6.38%	0.72%	4.76%	0.00%
P53007	SLC25A1 Tricarboxylate transport protein, mitochondrial	R.GIGDC*VR.Q	70	3.83%	0.66%	0.99%	0.00%
Q96TA2	YME1L1 ATP-dependent zinc metalloprotease YME1L1	K.ANAPC*VIFIDELDSVGGK.R	433	6.00%	0.54%	4.76%	0.00%
P33897	ABCD1 ATP-binding cassette sub-family D member 1	R.LQELC*QILGEAVAPAHVPAPSPQGPGGLQ GAST.-	717	5.42%	0.38%	4.76%	0.00%
P36776	LONP1 Lon protease homolog, mitochondrial	K.ILC*FYGPPGVGK.T	520	4.07%	0.36%	4.76%	0.00%
P33121	ACSL1 Long-chain-fatty-acid--CoA ligase 1	R.GFEGSFEELC*R.N	625	20.11%	0.32%	4.76%	0.00%
Q96EL3	MRPL53 39S ribosomal protein L53, mitochondrial	R.STNLNC*SVIADVR.H	49	5.44%	0.25%	4.76%	0.00%
O95831	AIFM1 Apoptosis-inducing factor 1, mitochondrial	R.SNIWVAGDAAC*FYDIK.L	441	4.76%	0.00%	4.76%	0.00%
Q16891	IMMT Mitochondrial inner membrane protein	K.LLSYASYC*IEHGDLELAAK.F	697	4.76%	0.00%	4.76%	0.00%
Q92552	MRPS27 28S ribosomal protein S27, mitochondrial	K.LSTC*EAEDIATYEQNLQQWHLDLVQLIQR.E	367	4.76%	0.00%	4.76%	0.00%
Q9H9J2	MRPL44 39S ribosomal protein L44, mitochondrial	R.QSGGTTALPLYFVGLYC*DK.K	276	4.76%	0.00%	4.76%	0.00%
P23368	ME2 NAD-dependent malic enzyme, mitochondrial	K.YC*TFNDDIQGTAAVALAGLLAAQK.V	274	4.76%	0.00%	4.76%	0.00%
Q8NE86	MCU Calcium uniporter protein, mitochondrial	R.C*QFTLKPISDSVGVFLR.Q	97	4.76%	0.00%	4.76%	0.00%
P30405	PPIF Peptidyl-prolyl cis-trans isomerase F, mitochondri	R.VIPSFMC*QAGDFTNHNGTGGK.S	104	4.76%	0.00%	4.76%	0.00%
P21964	COMT Catechol O-methyltransferase	R.YLPDTLLLEEC*GLLR.K	207	4.76%	0.00%	4.76%	0.00%
Q5JTJ3	C1orf31 Uncharacterized protein C1orf31	R.SSFESSC*PQQWIK.Y	90	95.24%	0.00%	95.24%	0.00%

Table 2A-7. List of ReDiMe ratios and spectral counts for proteins identified by FLAG immunoprecipitation of overexpressing RARS2-FLAG cell lysates with (light) and without 10 mM peroxide (heavy).

UniProt ID	Gene Symbol	Protein Description	# PSMs	log2 Average Ratio L:H	Average Ratio L:H	SEM
Q5T160	RARS2	probable arginine--tRNA ligase, mitochondrial	1617	1.00	0.00	0.00
P60900	PSMA6	Proteasome subunit alpha type-6	1027	1.29	0.37	0.10
P07437	TUBB	tubulin beta chain	908	0.95	-0.07	0.03
Q9BQE3	TUBA1C	Tubulin alpha-1C chain	843	1.44	0.53	0.41
Q13885	TUBB2A	Tubulin beta-2A chain	769	0.94	-0.08	0.38
P68371	TUBB4B	Tubulin beta-4B chain	704	0.89	-0.17	0.10
Q71U36	TUBA1A	tubulin alpha-1A chain	695	0.96	-0.06	0.08
P68366	TUBA4A	Tubulin alpha-4A chain	669	0.57	-0.80	0.26
P04350	TUBB4A	Tubulin beta-4A chain	624	53.54	5.74	31.51
P07900	HSP90AA1	Heat shock protein HSP 90-alpha	589	1.18	0.24	0.04
P08238	HSP90AB1	Heat shock protein HSP 90-beta	578	1.10	0.14	0.05
P10809	HSPD1	60 kDa heat shock protein, mitochondrial	543	1.35	0.44	0.31
P0DMV8	HSPA1B	heat shock 70 kDa protein 1A	542	1.02	0.03	0.08
P25788-1	PSMA3	Proteasome subunit alpha type-3	366	1.37	0.46	0.08
Q15029	EFTUD2	116 kDa U5 small nuclear ribonucleoprotein component	357	1.29	0.37	0.08
P11142-1	HSPA8	Heat shock cognate 71 kDa protein	344	0.98	-0.03	0.08
P25786-1	PSMA1	Proteasome subunit alpha type-1	337	1.54	0.62	0.10
O75643-1	SNRNP200	U5 small nuclear ribonucleoprotein 200 kDa helicase	334	1.21	0.27	0.10
P28074-1	PSMB5	proteasome subunit beta type-5	332	2.02	1.01	0.30
Q9NYF8-3	BCLAF1	Isoform 3 of Bcl-2-associated transcription factor 1	317	1.61	0.68	0.32
P20618	PSMB1	proteasome subunit beta type-1	284	1.52	0.61	0.07
Q9Y2W1	THRAP3	Thyroid hormone receptor-associated protein 3	281	2.97	1.57	0.89
O14818-1	PSMA7	Proteasome subunit alpha type-7	277	1.47	0.56	0.19
P10644	PRKAR1A	cAMP-dependent protein kinase type I-alpha regulatory subunit	269	0.90	-0.15	0.25
O94776	MTA2	Metastasis-associated protein MTA2	269	0.72	-0.47	0.22
Q13330-1	MTA1	Metastasis-associated protein MTA1	255	0.57	-0.81	0.19
P60709	ACTB	Actin, cytoplasmic 1	249	2.10	1.07	0.42
P28066-1	PSMA5	Proteasome subunit alpha type-5	230	1.56	0.64	0.11
P05141	SLC25A5	ADP/ATP translocase 2	219	0.88	-0.18	0.08
P06576	ATP5B	ATP synthase subunit beta, mitochondrial	217	0.96	-0.06	0.12
P33176	KIF5B	Kinesin-1 heavy chain	212	1.15	0.20	0.07
Q04837	SSBP1	Single-stranded DNA-binding protein, mitochondrial	212	1.35	0.43	0.35
Q04726-4	TLE3	Isoform 4 of Transducin-like enhancer protein 3	207	1.15	0.20	0.25
P52272	HNRNPM	Heterogeneous nuclear ribonucleoprotein M	199	2.00	1.00	0.39
Q8WXI9	GATAD2B	Transcriptional repressor p66-beta	193	0.84	-0.25	0.29
P12270	TPR	Nucleoprotein TPR	190	1.24	0.31	0.17

P62333	PSMC6	26S proteasome regulatory subunit 10B	190	1.01	0.01	0.15
P62195-1	PSMC5	26S proteasome regulatory subunit 8	186	0.94	-0.09	0.14
P29692-3	EEF1D	Isoform 3 of Elongation factor 1-delta	186	56.94	5.83	25.19
Q16576-1	RBBP7	Histone-binding protein RBBP7	184	0.78	-0.36	0.18
P06748	NPM1	Nucleophosmin	181	1.58	0.66	0.16
Q96QK1	VPS35	Vacuolar protein sorting-associated protein 35	180	1.36	0.44	0.16
Q8TAA3-5	PSMA8	Isoform 3 of Proteasome subunit alpha type-7-like	179	0.01	-6.39	0.00
Q14257	RCN2	Reticulocalbin-2	179	0.86	-0.22	0.09
Q04726-2	TLE3	Isoform 2 of Transducin-like enhancer protein 3	178	0.99	-0.01	0.11
Q13200	PSMD2	26S proteasome non-ATPase regulatory subunit 2	175	1.17	0.23	0.09
P43686	PSMC4	26S proteasome regulatory subunit 6B	175	1.07	0.09	0.17
P29692	EEF1D	Elongation factor 1-delta	174	1.62	0.69	0.09
P22626	HNRNPA2B1	heterogeneous nuclear ribonucleoproteins A2/B1	168	2.06	1.04	0.45
P38646	HSPA9	Stress-70 protein, mitochondrial	166	1.32	0.40	0.12
P78371-1	CCT2	T-complex protein 1 subunit beta	162	1.73	0.79	0.14
P28072	PSMB6	Proteasome subunit beta type-6	158	1.41	0.50	0.08
P11021	HSPA5	78 kDa glucose-regulated protein	155	1.06	0.08	0.09
Q99436	PSMB7	Proteasome subunit beta type-7	154	1.27	0.35	0.13
P49720	PSMB3	proteasome subunit beta type-3	154	1.68	0.75	0.29
P49721	PSMB2	proteasome subunit beta type-2	147	1.39	0.47	0.07
Q5JVS0	HABP4	Intracellular hyaluronan-binding protein 4	147	1.40	0.48	0.09
Q5QNW6-1	HIST2H2BF	Histone H2B type 2-F	145	9.54	3.25	5.97
P35998	PSMC2	26S proteasome regulatory subunit 7	138	1.30	0.37	0.11
Q86YP4	GATAD2A	Transcriptional repressor p66-alpha	136	0.95	-0.08	0.28
Q09028	RBBP4	Histone-binding protein RBBP4	135	0.72	-0.48	0.31
P25789	PSMA4	Proteasome subunit alpha type-4	134	1.12	0.16	0.21
Q99460	PSMD1	26S proteasome non-ATPase regulatory subunit 1	131	1.01	0.01	0.04
P08670	VIM	Vimentin	130	6.37	2.67	4.56
Q71DI3	HIST2H3A	histone H3.2	118	16.53	4.05	7.15
Q9NQS1	AVEN	Cell death regulator Aven	115	0.80	-0.31	0.22
P23246-1	SFPQ	splicing factor, proline- and glutamine-rich	114	1.29	0.36	0.10
Q13547	HDAC1	histone deacetylase 1	111	0.81	-0.30	0.25
O95983-1	MBD3	methyl-CpG-binding domain protein 3	111	0.81	-0.31	0.26
P28070	PSMB4	Proteasome subunit beta type-4	109	1.26	0.33	0.15
Q16777	HIST2H2AC	Histone H2A type 2-C	109	23.90	4.58	10.48
P48637	GSS	glutathione synthetase	108	1.47	0.55	0.10
O43852	CALU	Calumenin	106	1.16	0.21	0.11
Q969X5	ERGIC1	Endoplasmic reticulum-Golgi intermediate compartment protein 1	105	1.08	0.12	0.11
Q9Y5U2-1	TSSC4	Protein TSSC4	103	0.98	-0.03	0.17
P13639	EEF2	Elongation factor 2	103	0.49	-1.04	0.09
Q9Y6A5	TACC3	Transforming acidic coiled-coil-containing protein 3	101	1.42	0.51	0.09
P31943	HNRNPH1	Heterogeneous nuclear ribonucleoprotein H	101	1.89	0.92	0.57
Q15233	NONO	Non-POU domain-containing octamer-binding protein	101	1.49	0.57	0.58
Q04727-1	TLE4	Transducin-like enhancer protein 4	100	1.04	0.05	0.18
P62841	RPS15	40S ribosomal protein S15	99	22.50	4.49	20.07
Q16186	ADRM1	Proteasomal ubiquitin receptor ADRM1	98	1.10	0.14	0.08
P17844	DDX5	probable ATP-dependent RNA helicase DDX5	98	1.16	0.21	0.11
Q06830	PRDX1	peroxiredoxin-1	97	0.95	-0.08	0.02
P32322	PYCR1	Pyrroline-5-carboxylate reductase 1, mitochondrial	96	36.59	5.19	22.64
Q12931	TRAP1	heat shock protein 75 kDa, mitochondrial	95	0.86	-0.22	0.11
P19474	TRIM21	E3 ubiquitin-protein ligase TRIM21	94	0.88	-0.19	0.17
P25705-1	ATP5A1	ATP synthase subunit alpha, mitochondrial	93	1.03	0.04	0.02
O43242	PSMD3	26S proteasome non-ATPase regulatory subunit 3	93	1.49	0.58	0.09
Q9Y223-1	GNE	bifunctional UDP-N-acetylglucosamine 2-epimerase/N-acetylmannosamine kinase	93	1.50	0.59	0.17
Q9Y2X7-1	GIT1	ARF GTPase-activating protein GIT1	93	0.87	-0.19	0.18
P48643	CCT5	T-complex protein 1 subunit epsilon	90	1.72	0.79	0.19
Q14203	DCTN1	Dynactin subunit 1	90	1.93	0.95	0.30
P05023	ATP1A1	Sodium/potassium-transporting ATPase subunit alpha-1	90	0.72	-0.47	0.14
Q15293	RCN1	Reticulocalbin-1	89	1.36	0.45	0.13
P26641	EEF1G	elongation factor 1-gamma	88	1.40	0.48	0.14
P09651-1	HNRNPA1	Heterogeneous nuclear ribonucleoprotein A1	87	1.23	0.30	0.07
P62979	RPS27A	Ubiquitin-40S ribosomal protein S27a	86	18.83	4.23	16.02
Q9H0B6	KLC2	Kinesin light chain 2	83	1.25	0.32	0.10
O95400	CD2BP2	CD2 antigen cytoplasmic tail-binding protein 2	80	1.56	0.64	0.28
P38159-1	RBMX	RNA-binding motif protein, X chromosome	80	3.38	1.76	1.31
Q13561-1	DCTN2	dynactin subunit 2	79	1.28	0.36	0.17
P22061	PCMT1	protein-L-isoaspartate(D-aspartate) O-methyltransferase	78	0.77	-0.37	0.20
P62269	RPS18	40S ribosomal protein S18	76	1.51	0.60	0.08
P46782	RPS5	40S ribosomal protein S5	76	1.12	0.16	0.14
P84103	SRSF3	Serine/arginine-rich splicing factor 3	76	0.98	-0.03	0.17
P62191	PSMC1	26S proteasome regulatory subunit 4	76	0.76	-0.40	0.23
P40227-1	CCT6A	T-complex protein 1 subunit zeta	72	1.95	0.96	0.23
Q07955-1	SRSF1	Serine/arginine-rich splicing factor 1	72	0.99	-0.01	0.18
P50402	EMD	Emerin	72	0.96	-0.06	0.17
P19338	NCL	Nucleolin	72	1.47	0.56	0.33
Q07157	TJP1	Tight junction protein ZO-1	72	30.36	4.92	28.77
Q13435	SF3B2	Splicing factor 3b subunit 2	71	0.68	-0.57	0.21
Q9UMS4	PRPF19	Pre-mRNA-processing factor 19	70	1.04	0.06	0.07
A0FGR8-2	ESYT2	Isoform 2 of Extended synaptotagmin-2	69	1.40	0.49	0.16
O43175	PHGDH	D-3-phosphoglycerate dehydrogenase	69	0.77	-0.37	0.14
Q07866-4	KLC1	Isoform J of Kinesin light chain 1	69	0.72	-0.46	0.17
P55884	EIF3B	Eukaryotic translation initiation factor 3 subunit B	67	1.49	0.58	0.09
P43243	MATR3	Matrin-3	67	0.67	-0.59	0.35

O43464	HTRA2	Serine protease HTRA2, mitochondrial	67	48.84	5.61	28.97
Q00325-1	SLC25A3	Phosphate carrier protein, mitochondrial	63	0.81	-0.30	0.07
Q96C36	PYCR2	Pyrroline-5-carboxylate reductase 2	62	1.67	0.74	0.39
O00487	PSMD14	26S proteasome non-ATPase regulatory subunit 14	62	0.81	-0.31	0.28
P62306	SNRPF	Small nuclear ribonucleoprotein F	61	1.29	0.36	0.09
P84090	ERH	Enhancer of rudimentary homolog	61	4.76	2.25	1.60
O14654	IRS4	insulin receptor substrate 4	61	0.45	-1.16	0.17
P61978-2	HNRNPK	Isoform 2 of Heterogeneous nuclear ribonucleoprotein K	60	1.35	0.44	0.11
Q8IX12	CCAR1	Cell division cycle and apoptosis regulator protein 1	58	1.06	0.08	0.26
Q9NW64-1	RBM22	Pre-mRNA-splicing factor RBM22	56	1.99	0.99	0.71
O43719	HTATSF1	HIV Tat-specific factor 1	56	20.56	4.36	19.23
O75956	CDK2AP2	Cyclin-dependent kinase 2-associated protein 2	55	0.73	-0.45	0.19
Q7L014	DDX46	probable ATP-dependent RNA helicase DDX46	54	1.23	0.30	0.04
Q15008	PSMD6	26S proteasome non-ATPase regulatory subunit 6	54	1.44	0.53	0.11
Q9UQ35	SRRM2	serine/arginine repetitive matrix protein 2	53	1.72	0.78	0.29
O14579-1	COPE	coatomer subunit epsilon	53	0.93	-0.10	0.17
P04792	HSPB1	Heat shock protein beta-1	53	0.79	-0.34	0.16
O75436-1	VPS26A	Vacuolar protein sorting-associated protein 26A	53	100.20	6.65	20.36
Q9ULX6	AKAP8L	A-kinase anchor protein 8-like	53	0.84	-0.24	0.18
P23396-1	RPS3	40S ribosomal protein S3	52	1.06	0.09	0.11
Q6P2Q9	PRPF8	Pre-mRNA-processing-splicing factor 8	52	1.87	0.91	0.31
P25787	PSMA2	Proteasome subunit alpha type-2	51	1.31	0.39	0.10
O00148	DDX39A	ATP-dependent RNA helicase DDX39A	51	1.71	0.77	0.22
P62308	SNRPG	Small nuclear ribonucleoprotein G	51	1.47	0.55	0.26
O14545	TRAFD1	TRAF-type zinc finger domain-containing protein 1	50	0.58	-0.80	0.15
Q14152	EIF3A	Eukaryotic translation initiation factor 3 subunit A	49	1.21	0.28	0.05
O95831-1	AIFM1	Apoptosis-inducing factor 1, mitochondrial	49	0.74	-0.44	0.04
Q04724	TLE1	Transducin-like enhancer protein 1	48	0.96	-0.06	0.24
P62753	RPS6	40S RIBOSOMAL PROTEIN S6	47	0.92	-0.12	0.07
Q9NVI7	ATAD3A	ATPase family AAA domain-containing protein 3A	47	1.12	0.16	0.10
Q92841-1	DDX17	Isoform 2 of Probable ATP-dependent RNA helicase DDX17	47	0.80	-0.33	0.12
P17980	PSMC3	26S proteasome regulatory subunit 6A	46	1.08	0.11	0.17
Q56P03	EAPP	e2f-associated phosphoprotein	46	1.15	0.20	0.22
P51114-1	FXR1	Fragile X mental retardation syndrome-related protein 1	46	0.89	-0.17	0.21
Q9UJS0	SLC25A13	Calcium-binding mitochondrial carrier protein Aralar2	46	0.73	-0.46	0.18
Q15365	PCBP1	Poly(RC)-binding protein 1	45	1.29	0.37	0.13
Q13263	TRIM28	Transcription intermediary factor 1-beta	44	1.35	0.43	0.16
Q3ZCQ8	TIMM50	Mitochondrial import inner membrane translocase subunit TIM50	44	1.05	0.07	0.27
P32119	PRDX2	Peroxiredoxin-2	43	1.50	0.59	0.12
Q15393-1	SF3B3	Splicing factor 3B subunit 3	43	21.26	4.41	20.32
Q9NR30-1	DDX21	Nucleolar RNA helicase 2	42	0.85	-0.24	0.11
P68104	EEF1A1	Elongation factor 1-alpha 1	41	0.91	-0.14	0.08
Q02809	PLOD1	Procollagen-lysine,2-oxoglutarate 5-dioxygenase 1	41	0.75	-0.41	0.17
Q06787-7	FMR1	Isoform 7 of Synaptic functional regulator FMR1	41	1.16	0.21	0.28
Q08211	DHX9	Atp-dependent rna helicase a	41	63.16	5.98	28.21
Q13283	G3BP1	Ras GTPase-activating protein-binding protein 1	41	18.22	4.19	16.15
P49959	MRE11A	Double-strand break repair protein MRE11	41	20.38	4.35	19.26
P17987	TCP1	T-complex protein 1 subunit alpha	40	1.38	0.46	0.27
Q99832	CCT7	T-complex protein 1 subunit eta	40	38.94	5.28	24.14
P49368-1	CCT3	T-complex protein 1 subunit gamma	39	1.55	0.63	0.19
Q14974	KPNB1	Importin subunit beta-1	39	1.01	0.01	0.14
Q15181	PPA1	Inorganic pyrophosphatase	39	3.95	1.98	0.87
Q9UBQ0-2	VPS29	Isoform 2 of Vacuolar protein sorting-associated protein 29	39	2.37	1.25	0.60
P27348	YWHAQ	14-3-3 protein theta	38	1.40	0.48	0.11
O00231	PSMD11	26S proteasome non-ATPase regulatory subunit 11	38	0.86	-0.23	0.11
Q16891	IMMT	MICOS complex subunit Mic60	38	0.82	-0.29	0.12
Q9Y230	RUVBL2	RuvB-like 2	38	1.05	0.08	0.17
P51116	FXR2	Fragile X mental retardation syndrome-related protein 2	38	1.02	0.02	0.22
Q9UNE7-1	STUB1	E3 ubiquitin-protein ligase CHIP	38	0.72	-0.47	0.19
P13010	XRCC5	X-ray repair cross-complementing protein 5	38	1.08	0.11	0.29
P31946	YWHAB	14-3-3 protein beta/alpha	38	58.70	5.88	25.69
Q14978-1	NOLC1	nucleolar and coiled-body phosphoprotein 1	38	0.40	-1.30	0.22
O76031	CLPX	ATP-dependent Clp protease ATP-binding subunit clpX-like, mitochondrial	38	0.20	-2.35	0.10
Q14161-1	GIT2	ARF GTPase-activating protein GIT2	38	29.83	4.90	28.95
Q01130	SRSF2	serine/arginine-rich splicing factor 2	37	0.90	-0.15	0.07
P35232	PHB	Prohibitin	37	1.00	0.00	0.14
P26373-1	RPL13	60S ribosomal protein L13	37	0.96	-0.06	0.18
P20700	LMNB1	Lamin-B1	36	119.19	6.90	4.89
P62263	RPS14	40S ribosomal protein S14	36	1.27	0.35	0.32
P04075	ALDOA	fructose-bisphosphate aldolase A	35	1.05	0.07	0.14
O43819	SCO2	Protein SCO2 homolog, mitochondrial	35	0.75	-0.41	0.10
P84098	RPL19	60S ribosomal protein L19	35	1.18	0.24	0.17
P25205	MCM3	DNA replication licensing factor mcm3	35	0.91	-0.13	0.22
O75934	BCAS2	Pre-mRNA-splicing factor spf27	34	1.28	0.35	0.14
Q16555-1	DPYSL2	Dihydropyrimidinase-related protein 2	34	0.98	-0.03	0.12
P62995	TRA2B	transformer-2 protein homolog beta	34	1.20	0.26	0.29
O00217	NDUFS8	NADH dehydrogenase	33	1.01	0.02	0.09
O00165	HAX1	HCLS1-associated protein X-1	33	1.03	0.05	0.21
Q14839	CHD4	Chromodomain-helicase-DNA-binding protein 4	33	0.98	-0.03	0.32
P49411	TUFM	elongation factor Tu, mitochondrial	32	1.43	0.51	0.12
P67809	YBX1	Nuclease-sensitive element-binding protein 1	32	17.22	4.11	16.34
Q8NBH2-2	KY	Isoform 2 of Kyphoscoliosis peptidase	31	120.81	6.92	7.55
Q5VW36	FOCAD	focadhesin	31	0.72	-0.48	0.04

P49419	ALDH7A1	Alpha-aminoadipic semialdehyde dehydrogenase	31	1.02	0.03	0.08
Q13242	SRSF9	serine/arginine-rich splicing factor 9	31	1.21	0.28	0.12
Q16629	SRSF7	serine/arginine-rich splicing factor 7	31	1.12	0.16	0.13
Q9Y383	LUC7L2	Putative RNA-binding protein Luc7-like 2	31	0.86	-0.22	0.18
Q9Y5B9	SUPT16H	FACT complex subunit SPT16	31	1.68	0.74	0.73
P31321	PRKAR1B	cAMP-dependent protein kinase type I-beta regulatory subunit	31	0.83	-0.26	0.40
P62899	RPL31	60S ribosomal protein L31	30	1.18	0.24	0.08
O75494-1	SRSF10	Serine/arginine-rich splicing factor 10	30	1.31	0.39	0.14
Q13247	SRSF6	Serine/arginine-rich splicing factor 6	30	1.02	0.02	0.22
Q96FN9	DTD2	putative D-tyrosyl-tRNA(Tyr) deacylase 2	30	2.48	1.31	0.62
Q9Y678	COPG1	Coatomer subunit gamma-1	30	57.50	5.85	24.95
P23588	EIF4B	eukaryotic translation initiation factor 4B	29	1.11	0.15	0.11
Q68DQ2	CRYBG3	very large A-kinase anchor protein	29	0.95	-0.07	0.26
Q8WVD3-1	RNF138	E3 ubiquitin-protein ligase RNF138	29	0.70	-0.52	0.26
P62917	RPL8	60S ribosomal protein L8	28	1.35	0.44	0.08
Q9UBQ0	VPS29	Vacuolar protein sorting-associated protein 29	28	1.65	0.72	0.22
P23284	PPIB	peptidyl-prolyl cis-trans isomerase B	28	1.23	0.30	0.34
Q71UM5	RPS27L	40S ribosomal protein S27-like	28	0.73	-0.46	0.24
O00303	EIF3F	Eukaryotic translation initiation factor 3 subunit F	28	36.91	5.21	22.54
Q96P70	IPO9	Importin-9	27	1.13	0.18	0.15
P55036-1	PSMD4	26S proteasome non-ATPase regulatory subunit 4	27	0.92	-0.12	0.10
P04843	RPN1	Dolichyl-diphosphooligosaccharide--protein glycosyltransferase subunit 1	27	0.64	-0.63	0.11
Q9UNM6	PSMD13	26S proteasome non-ATPase regulatory subunit 13	27	1.75	0.81	0.33
Q9P0J0	NDUFA13	NADH dehydrogenase	27	0.79	-0.35	0.15
Q9NR50-1	EIF2B3	Translation initiation factor eIF-2B subunit gamma	27	0.09	-3.52	0.04
P33993-1	MCM7	DNA replication licensing factor MCM7	27	43.77	5.45	26.29
P51665	PSMD7	26S proteasome non-ATPase regulatory subunit 7	27	37.76	5.24	23.33
P31689-1	DNAJA1	DnaJ homolog subfamily A member 1	26	1.07	0.10	0.13
P62318	SNRPD3	small nuclear ribonucleoprotein sm d3	26	1.45	0.54	0.29
P62701	RPS4X	40S ribosomal protein S4, X isoform	25	1.34	0.42	0.06
P68400	CSNK2A1	Casein kinase II subunit alpha	25	1.06	0.08	0.11
P35613	BSG	Basigin	25	0.77	-0.38	0.12
O75489	NDUFS3	NADH dehydrogenase	25	1.00	0.00	0.17
P31948	STIP1	stress-induced-phosphoprotein 1	25	0.97	-0.05	0.16
P27635	RPL10	60S ribosomal protein L10	25	36.74	5.20	22.59
Q9NWU1-1	OXSM	3-oxoacyl-	25	23.90	4.58	23.20
P51572	BCAP31	B-cell receptor-associated protein 31	24	1.62	0.70	0.22
Q8N1F7-1	NUP93	Nuclear pore complex protein Nup93	24	2.43	1.28	0.36
Q96A33-1	CCDC47	Coiled-coil domain-containing protein 47	24	0.77	-0.38	0.22
Q06210-1	GFPT1	glutamine--fructose-6-phosphate aminotransferase	24	21.52	4.43	20.27
P50990	CCT8	T-complex protein 1 subunit theta	23	119.19	6.90	4.89
P62851	RPS25	40S ribosomal protein S25	23	1.11	0.15	0.07
Q02978	SLC25A11	Mitochondrial 2-oxoglutarate/malate carrier protein	23	0.86	-0.23	0.16
P12956	XRCC6	X-ray repair cross-complementing protein 6	23	0.94	-0.09	0.36
Q13347	EIF3I	Eukaryotic translation initiation factor 3 subunit I	23	25.28	4.66	24.55
P25398	RPS12	40S ribosomal protein S12	23	21.54	4.43	20.26
Q14498-1	RBM39	RNA-binding protein 39	22	119.19	6.90	4.89
P62249	RPS16	40S ribosomal protein S16	22	1.32	0.40	0.15
P08195	SLC3A2	4F2 cell-surface antigen heavy chain	22	0.89	-0.17	0.13
O95816	BAG2	BAG family molecular chaperone regulator 2	22	0.68	-0.55	0.19
O00571	DDX3X	ATP-dependent RNA helicase DDX3X	22	0.59	-0.77	0.28
Q00839	HNRNPU	Heterogeneous nuclear ribonucleoprotein U	22	36.69	5.20	22.60
Q16740	CLPP	ATP-dependent Clp protease proteolytic subunit, mitochondrial	21	0.82	-0.29	0.10
P22392	NME2	nucleoside diphosphate kinase b	21	1.24	0.31	0.22
Q9BXP5	SRRT	serrate RNA effector molecule homolog	21	1.39	0.48	0.29
O60506	SYNCRIP	Heterogeneous nuclear ribonucleoprotein Q	21	0.95	-0.08	0.22
P60842	EIF4A1	Eukaryotic initiation factor 4A-I	21	1.99	0.99	0.59
P26639-1	TARS	Threonine--tRNA ligase, cytoplasmic	21	57.14	5.84	25.10
O15066	KIF3B	Kinesin-like protein KIF3B	21	20.31	4.34	19.28
Q93008-1	USP9X	Isoform 2 of Probable ubiquitin carboxyl-terminal hydrolase FAF-X	20	1.27	0.34	0.07
O43143	DHX15	Pre-mRNA-splicing factor ATP-dependent RNA helicase DHX15	20	0.96	-0.06	0.28
Q96JN8-1	NEURL4	Neuralized-like protein 4	20	0.88	-0.19	0.27
Q9UL46	PSME2	proteasome activator complex subunit 2	20	17.57	4.13	16.27
Q96PK6-1	RBM14	RNA-binding protein 14	19	119.98	6.91	5.90
P60866	RPS20	40S ribosomal protein S20	19	1.30	0.38	0.13
A2NJV5	IGKV2-29	Immunoglobulin kappa variable 2-29	19	1.51	0.59	0.22
P07197	NEFM	Neurofilament medium polypeptide	19	81.60	6.35	24.33
P15880	RPS2	40S ribosomal protein S2	19	57.20	5.84	25.08
O15160	POLR1C	DNA-directed RNA polymerases I and III subunit RPAC1	19	57.11	5.84	25.12
P62314	SNRPD1	Small nuclear ribonucleoprotein Sm D1	18	123.24	6.95	3.34
P61247	RPS3A	40S ribosomal protein S3a	18	119.19	6.90	4.89
P09874	PARP1	Poly	18	119.19	6.90	4.89
Q676U5	ATG16L1	Autophagy-related protein 16-1	18	1.16	0.21	0.07
Q9H9B4	SFXN1	Sideroflexin-1	18	0.67	-0.58	0.07
Q07666	KHDRBS1	KH domain-containing, RNA-binding, signal transduction-associated protein 1	18	1.77	0.82	0.20
Q9UBB6	NCDN	Neurochondrin	18	1.19	0.26	0.18
P62316	SNRPD2	Small nuclear ribonucleoprotein Sm D2	18	0.39	-1.35	0.07
P33316-3	DUT	Deoxyuridine 5'-triphosphate nucleotidohydrolase, mitochondrial	18	1.43	0.52	0.35
Q9Y6M1	IGF2BP2	Insulin-like growth factor 2 mRNA-binding protein 2	18	0.86	-0.22	0.23
P04637	TP53	Cellular tumor antigen p53	17	1.41	0.50	0.13
Q9BWF3-1	RBM4	RNA-binding protein 4	17	0.86	-0.22	0.15
P07919	UQCRH	Cytochrome b-c1 complex subunit 6, mitochondrial	17	0.89	-0.16	0.18

O76071	CIAO1	Probable cytosolic iron-sulfur protein assembly protein Ciao1	17	1.51	0.60	0.58
Q9H000	MKRN2	Probable E3 ubiquitin-protein ligase makorin-2	17	73.26	6.19	29.55
P11940-1	PABPC1	Polyadenylate-binding protein 1	17	0.85	-0.23	0.38
Q96DI7	SNRNP40	U5 small nuclear ribonucleoprotein 40 kDa protein	17	0.61	-0.72	0.28
Q8IYB3	SRRM1	Serine/arginine repetitive matrix protein 1	17	20.44	4.35	19.25
Q96CT7	CCDC124	Coiled-coil domain-containing protein 124	17	21.47	4.42	20.28
P41223	BUD31	Protein BUD31 homolog	17	20.96	4.39	20.38
P50991	CCT4	T-complex protein 1 subunit delta	16	1.81	0.85	0.40
P62241	RPS8	40S ribosomal protein S8	16	84.61	6.40	28.65
Q9Y265	RUVBL1	RuvB-like 1	16	58.49	5.87	26.00
Q03252	LMNB2	Lamin-B2	16	0.26	-1.94	0.12
Q4G0F5	VPS26B	Vacuolar protein sorting-associated protein 26B	16	20.20	4.34	19.30
Q9UJZ1	STOML2	Stomatin-like protein 2, mitochondrial	15	119.19	6.90	4.89
P04406-1	GAPDH	glyceraldehyde-3-phosphate dehydrogenase	15	117.59	6.88	6.97
P30048	PRDX3	Thioredoxin-dependent peroxide reductase, mitochondrial	15	2.10	1.07	0.24
Q9Y520	PRRC2C	Protein Prrc2c	15	1.71	0.78	0.23
Q9Y3B4	SF3B14	Splicing factor 3B subunit 6	15	1.13	0.18	0.38
P11387	TOP1	DNA topoisomerase 1	15	57.17	5.84	25.09
P16402	HIST1H1D	Histone H1.3	15	40.82	5.35	24.99
P00338-1	LDHA	L-lactate dehydrogenase A chain	15	29.84	4.90	28.46
P48444	ARCN1	Coatomer subunit delta	15	17.42	4.12	16.30
P62857	RPS28	40S ribosomal protein S28	15	17.20	4.10	16.34
Q9NZJ5	EIF2AK3	Eukaryotic translation initiation factor 2-alpha kinase 3	14	0.01	-6.39	0.00
Q76I76	SSH2	Protein phosphatase Slingshot homolog 2	14	0.01	-6.39	0.00
Q5T7W7	TSTD2	Thiosulfate sulfurtransferase/rhodanese-like domain-containing protein 2	14	117.00	6.87	6.57
Q86V81	ALYREF	THO complex subunit 4	14	1.11	0.15	0.08
Q8N357	C2orf18	Solute carrier family 35 member F6	14	0.75	-0.42	0.10
Q5W0B1	RNF219	RING finger protein 219	14	0.78	-0.36	0.17
P53007	SLC25A1	Tricarboxylate transport protein, mitochondrial	14	0.69	-0.54	0.18
Q12906-1	ILF3	Interleukin enhancer-binding factor 3	14	3.44	1.78	1.03
Q9BTZ2	DHRS4	dehydrogenase/reductase sdr family member 4	14	0.68	-0.55	0.28
Q9UDY2	TJP2	Tight junction protein ZO-2	14	57.16	5.84	25.10
P33991	MCM4	DNA replication licensing factor MCM4	14	44.01	5.46	26.19
P14678-1	SNRPB	Small nuclear ribonucleoprotein-associated proteins B and B'	14	22.88	4.52	20.02
P55209	NAP1L1	Nucleosome assembly protein 1-like 1	14	17.52	4.13	16.28
P46100	ATRX	transcriptional regulator ATRX	14	20.45	4.35	19.25
P14625	HSP90B1	Endoplasmin	13	117.59	6.88	6.97
Q96HS1-1	PGAM5	Serine/threonine-protein phosphatase Pgam5, mitochondrial	13	0.67	-0.59	0.12
Q02878	RPL6	60S ribosomal protein L6	13	0.70	-0.52	0.13
P17028-1	ZNF24	zinc finger protein 24	13	0.94	-0.09	0.24
P11908	PRPS2	ribose-phosphate pyrophosphokinase 2	13	0.86	-0.22	0.42
Q6ZNL6-1	FGD5	FYVE, RhoGEF and PH domain-containing protein 5	12	0.01	-6.39	0.00
Q14566	MCM6	DNA replication licensing factor MCM6	12	118.45	6.89	5.92
P61254	RPL26	60S ribosomal protein L26	12	1.52	0.60	0.11
O60841	EIF5B	Eukaryotic translation initiation factor 5B	12	0.93	-0.10	0.08
Q96L92	SNX27	Sorting nexin-27	12	0.84	-0.25	0.08
Q8N490-2	PNKD	Isoform 2 of Probable hydrolase PNKD	12	0.80	-0.32	0.12
Q8TCG1	KIAA1524	Protein CIP2A	12	0.65	-0.62	0.10
P47755	CAPZA2	F-actin-capping protein subunit alpha-2	12	1.18	0.24	0.19
Q9H1A4	ANAPC1	anaphase-promoting complex subunit 1	12	1.16	0.22	0.20
Q15717	ELAVL1	ELAV-like protein 1	12	2.12	1.08	0.49
P18669	PGAM1	Phosphoglycerate mutase 1	12	0.52	-0.93	0.16
O00232-1	PSMD12	26s proteasome non-atpase regulatory subunit 12	12	1.92	0.94	0.87
Q9BUQ8	DDX23	Probable ATP-dependent RNA helicase DDX23	12	40.63	5.34	25.04
O76041	NEBL	Nebulette	12	20.76	4.38	19.19
P61313-1	RPL15	60S ribosomal protein L15	12	21.35	4.42	20.30
P35606	COPB2	Coatomer subunit beta'	11	119.19	6.90	4.89
O60716-1	CTNND1	Catenin delta-1	11	1.02	0.03	0.08
P63244	GNB2L1	Receptor of activated protein C kinase 1	11	1.95	0.97	0.32
Q12874	SF3A3	splicing factor 3a subunit 3	11	99.95	6.64	20.32
Q9H0G5	NSRP1	Nuclear speckle splicing regulatory protein 1	11	57.07	5.83	25.13
Q15459	SF3A1	splicing factor 3A subunit 1	11	57.01	5.83	25.16
P06753-2	TPM3	Isoform 2 of Tropomyosin alpha-3 chain	11	63.22	5.98	27.98
Q9GZV8	PRDM14	PR domain zinc finger protein 14	11	0.06	-3.99	0.05
P78527	PRKDC	DNA-dependent protein kinase catalytic subunit	11	23.46	4.55	23.31
Q05086	UBE3A	Ubiquitin-protein ligase E3A	11	20.49	4.36	19.24
Q9UNX3	RPL26L1	60S ribosomal protein L26-like 1	11	20.90	4.39	20.39
P62854	RPS26	40S ribosomal protein S26	10	1.41	0.50	0.21
Q9NX63	CHCHD3	MICOS complex subunit MIC19	10	0.98	-0.04	0.24
Q13409-1	DYNC1I2	cytoplasmic dynein 1 intermediate chain 2	10	2.49	1.32	0.63
O43491-1	EPB41L2	band 4.1-like protein 2	10	1.01	0.01	0.32
Q15773	MLF2	Myeloid leukemia factor 2	10	0.73	-0.45	0.30
Q9Y5B6	GCFC1	PAX3- and PAX7-binding protein 1	10	57.27	5.84	25.05
O94906-1	PRPF6	Pre-mRNA-processing factor 6	10	57.11	5.84	25.12
P39019	RPS19	40S ribosomal protein S19	10	56.68	5.82	25.31
O15371	EIF3D	Eukaryotic translation initiation factor 3 subunit D	10	48.82	5.61	28.98
Q9H0D6-1	XRN2	5'-3' exoribonuclease 2	10	44.53	5.48	27.35
Q13573	SNW1	SNW domain-containing protein 1	10	36.88	5.20	22.54
Q2TAY7	SMU1	WD40 repeat-containing protein SMU1	10	21.77	4.44	20.22
Q9NVU0	POLR3E	DNA-directed RNA polymerase III subunit RPC5	10	20.46	4.36	19.25
O14828	SCAMP3	Secretory carrier-associated membrane protein 3	10	21.23	4.41	20.32
P53803	POLR2K	DNA-directed RNA polymerases I, II, and III subunit RPABC4	10	16.96	4.08	16.39
Q969V3	NCLN	Nicalin	10	22.34	4.48	21.92

P08243-1	ASNS	Asparagine synthetase	9	113.41	6.83	5.11
B5ME19	EIF3CL	eukaryotic translation initiation factor 3 subunit C-like protein	9	113.41	6.83	5.11
P46087	NOP2	Probable 28S rRNA (cytosine(4447)-C(5))-methyltransferase	9	119.19	6.90	4.89
P05198	EIF2S1	Eukaryotic translation initiation factor 2 subunit 1	9	119.19	6.90	4.89
Q9Y2S7	POLDIP2	Polymerase delta-interacting protein 2	9	119.19	6.90	4.89
Q08945	SSRP1	FACT complex subunit SSRP1	9	119.19	6.90	4.89
O14776-1	TCERG1	Transcription elongation regulator 1	9	119.19	6.90	4.89
P22314	UBA1	Ubiquitin-like modifier-activating enzyme 1	9	117.00	6.87	6.57
P35659-1	DEK	Protein DEK	9	117.00	6.87	6.57
P62910	RPL32	60S ribosomal protein L32	9	1.02	0.03	0.10
O95359	TACC2	Transforming acidic coiled-coil-containing protein 2	9	0.95	-0.07	0.15
Q07020	RPL18	60S ribosomal protein L18	9	2.18	1.13	0.90
O95817	BAG3	BAG family molecular chaperone regulator 3	9	58.06	5.86	24.70
Q2VIQ3	KIF4B	Chromosome-associated kinesin KIF4B	9	57.15	5.84	25.10
Q99567	NUP88	Nuclear pore complex protein Nup88	9	56.88	5.83	25.22
Q9Y508-1	RNF114	E3 ubiquitin-protein ligase RNF114	9	49.03	5.62	30.03
Q9H3K6-1	BOLA2B	bola-like protein 2	9	0.48	-1.05	0.30
Q06323-1	PSME1	Proteasome activator complex subunit 1	9	36.86	5.20	22.55
Q8N163-1	CCAR2	Cell cycle and apoptosis regulator protein 2	9	40.71	5.35	25.01
Q86YZ3	HRNR	Hornerin	9	27.49	4.78	23.81
Q9BQG0	MYBBP1A	Myb-binding protein 1A	9	28.21	4.82	25.34
Q14683	SMC1A	structural maintenance of chromosomes protein 1a	9	17.11	4.10	16.36
Q9Y2Q9	MRPS28	28S ribosomal protein S28, mitochondrial	9	20.15	4.33	19.31
P67870	CSNK2B	Casein kinase II subunit beta	8	1.23	0.30	0.08
P35658-1	NUP214	Nuclear pore complex protein Nup214	8	0.96	-0.07	0.06
Q9UBM7	DHCR7	7-dehydrocholesterol reductase	8	0.81	-0.30	0.13
Q15042-1	RAB3GAP1	Rab3 GTPase-activating protein catalytic subunit	8	1.01	0.02	0.23
Q96J01	THOC3	THO complex subunit 3	8	0.68	-0.57	0.22
Q15149-1	PLEC	plectin	8	0.26	-1.94	0.09
P08865	RPSA	40S ribosomal protein SA	8	64.79	6.02	28.34
Q92598	HSPH1	Heat shock protein 105 kDa	8	57.05	5.83	25.14
Q9UQ80	PA2G4	proliferation-associated protein 2G4	8	55.73	5.80	32.21
Q9BW92	TARS2	Threonine--tRNA ligase, mitochondrial	8	48.22	5.59	29.23
Q9NVM9	ASUN	integrator complex subunit 13	8	40.80	5.35	24.99
O15344-1	MID1	E3 ubiquitin-protein ligase Midline-1	8	27.76	4.79	26.05
P31947-1	SFN	14-3-3 protein sigma	8	18.46	4.21	16.09
O00264	PGRMC1	Membrane-associated progesterone receptor component 1	8	22.53	4.49	21.88
O00567	NOP56	Nucleolar protein 56	7	113.41	6.83	5.11
O14980	XPO1	Exportin-1	7	119.19	6.90	4.89
Q92499	DDX1	ATP-dependent RNA helicase DDX1	7	119.19	6.90	4.89
Q13144	EIF2B5	Translation initiation factor eIF-2B subunit epsilon	7	0.01	-6.38	0.00
Q8N3R9-1	MPP5	MAGUK p55 subfamily member 5	7	0.19	-2.43	0.01
P34932	HSPA4	Heat shock 70 kDa protein 4	7	1.46	0.54	0.18
P19388	POLR2E	DNA-directed RNA polymerases I, II, and III subunit RPABC1	7	1.20	0.27	0.19
P52732	KIF11	Kinesin-like protein KIF11	7	1.48	0.57	0.31
Q5T8P6	RBM26	RNA-binding protein 26	7	0.58	-0.78	0.14
P36957	DLST	Dihydrolipoyllysine-residue succinyltransferase component of 2-oxoglutarate dehydrogenase complex, mitochondrial	7	0.78	-0.36	0.27
Q15070-1	OXA1L	Mitochondrial inner membrane protein OXA1L	7	0.65	-0.62	0.21
O75533-1	SF3B1	splicing factor 3B subunit 1	7	2.30	1.20	0.72
P22234	PAICS	multifunctional protein ADE2	7	0.10	-3.26	0.04
P06312	IGKV4-1	immunoglobulin kappa variable 4-1	7	61.42	5.94	26.88
O75152	ZC3H11A	Zinc finger CCCH domain-containing protein 11A	7	55.79	5.80	24.50
Q9Y608	LRRFIP2	Leucine-rich repeat flightless-interacting protein 2	7	56.89	5.83	25.22
P14868	DARS	Aspartate--tRNA ligase, cytoplasmic	7	53.87	5.75	30.89
Q8NC51-1	SERBP1	Plasminogen activator inhibitor 1 RNA-binding protein	7	36.81	5.20	22.32
Q14676	MDC1	Mediator of DNA damage checkpoint protein 1	7	40.87	5.35	24.96
Q6I9Y2	THOC7	THO complex subunit 7 homolog	7	29.77	4.90	28.97
Q9BQA1	WDR77	Methylosome protein 50	7	17.01	4.09	16.38
P01024	C3	Complement C3	7	21.00	4.39	20.37
O43684	BUB3	Mitotic checkpoint protein BUB3	6	113.41	6.83	5.11
Q16401	PSMD5	26S proteasome non-ATPase regulatory subunit 5	6	116.64	6.87	5.10
P51659-1	HSD17B4	peroxisomal multifunctional enzyme type 2	6	116.64	6.87	5.10
O14974	PPP1R12A	Protein phosphatase 1 regulatory subunit 12A	6	119.19	6.90	4.89
Q96I15-1	SCLY	selenocysteine lyase	6	119.19	6.90	4.89
Q9H2W6	MRPL46	39S ribosomal protein L46, mitochondrial	6	119.19	6.90	4.89
P48047	ATP5O	ATP synthase subunit O, mitochondrial	6	119.19	6.90	4.89
Q9Y5K5-1	UCHL5	Ubiquitin carboxyl-terminal hydrolase isozyme L5	6	119.98	6.91	5.90
Q8WUA2	PPIL4	Peptidyl-prolyl cis-trans isomerase-like 4	6	117.59	6.88	6.97
Q5SW79-1	CEP170	Centrosomal protein of 170 kDa	6	5.77	2.53	1.10
O60313	OPA1	Dynamin-like 120 kDa protein, mitochondrial	6	1.37	0.46	0.28
P57678	GEMIN4	Gem-associated protein 4	6	0.84	-0.25	0.23
Q92609-1	TBC1D5	TBC1 domain family member 5	6	76.11	6.25	23.82
Q96JM7	L3MBTL3	Lethal(3)malignant brain tumor-like protein 3	6	67.69	6.08	27.91
O75746	SLC25A12	Calcium-binding mitochondrial carrier protein Aralar1	6	0.35	-1.51	0.15
Q5GLZ8-1	HERC4	Probable E3 ubiquitin-protein ligase HERC4	6	57.23	5.84	25.07
P48556	PSMD8	26S proteasome non-ATPase regulatory subunit 8	6	57.19	5.84	25.08
P35611-1	ADD1	Alpha-adducin	6	57.11	5.84	25.12
Q15642	TRIP10	Cdc42-interacting protein 4	6	57.02	5.83	25.16
Q8IVS2	MCAT	Malonyl-CoA-acyl carrier protein transacylase, mitochondrial	6	56.96	5.83	25.19
Q8IWX8	CHERP	Calcium homeostasis endoplasmic reticulum protein	6	56.41	5.82	25.43
Q9BWU0	SLC4A1AP	kanadaptin	6	23.21	4.54	18.96
P25490	YY1	Transcriptional repressor protein YY1	6	26.89	4.75	26.26
Q15428	SF3A2	splicing factor 3a subunit 2	6	20.23	4.34	19.29

Q9NS91	RAD18	E3 ubiquitin-protein ligase RAD18	5	123.24	6.95	3.34
Q15014	MORF4L2	Mortality factor 4-like protein 2	5	119.19	6.90	4.89
Q99623	PHB2	Prohibitin-2	5	117.12	6.87	5.42
Q99615-1	DNAJC7	DnaJ homolog subfamily C member 7	5	119.98	6.91	5.90
P41252	IARS	isoleucine--tRNA ligase, cytoplasmic	5	119.98	6.91	5.90
Q9Y312	AAR2	Protein AAR2 homolog	5	117.59	6.88	6.97
P42025	ACTR1B	Beta-centractin	5	1.64	0.71	0.14
P43034	PAFAH1B1	Platelet-activating factor acetylhydrolase IB subunit alpha	5	1.42	0.51	0.14
P39023	RPL3	60S ribosomal protein L3	5	1.79	0.84	0.34
P61289-1	PSME3	Proteasome activator complex subunit 3	5	1.51	0.59	0.33
Q9HB71	CACYBP	Calcyclin-binding protein	5	0.65	-0.62	0.26
P63220	RPS21	40S ribosomal protein S21	5	0.97	-0.04	0.42
Q96H79	ZC3HAV1L	Zinc finger CCCH-type antiviral protein 1-like	5	66.69	6.06	26.43
P02768-1	ALB	Serum albumin	5	0.40	-1.31	0.18
O43896	KIF1C	Kinesin-like protein KIF1C	5	0.19	-2.43	0.09
O14773	TPP1	Tripeptidyl-peptidase 1	5	37.35	5.22	22.40

Table 2A-8. List of ReDiMe ratios and spectral counts for proteins identified by FLAG immunoprecipitation of overexpressing NLRX1WT-FLAG (light) and NLRX1C331S-FLAG (heavy).

UniProt ID	Gene Symbol	Protein Description	# PSMs	log2 Average Ratio L:H	Average RatioL:H	SEM
Q86UT6	NLRX1	NLR family member X1	4439	0.00	1.000	0.000
P60900	PSMA6	Proteasome subunit alpha type-6	2921	-2.08	0.237	0.026
P08238	HSP90AB1	Heat shock protein HSP 90-beta	1047	-1.06	0.480	0.086
P07900	HSP90AA1	Heat shock protein HSP 90-alpha	1021	-1.13	0.458	0.075
P0DMV8	HSPA1B	heat shock 70 kDa protein 1A	643	-1.25	0.421	0.037
P25788-1	PSMA3	Proteasome subunit alpha type-3	608	-1.88	0.272	0.029
P10809	HSPD1	60 kDa heat shock protein, mitochondrial	569	-0.53	0.692	0.086
O94776	MTA2	Metastasis-associated protein MTA2	539	-2.95	0.129	0.020
P60709	ACTB	Actin, cytoplasmic 1	489	-2.02	0.247	0.078
P68363	TUBA1B	Tubulin alpha-1B chain	448	-1.15	0.452	0.071
P25786-1	PSMA1	Proteasome subunit alpha type-1	424	-1.93	0.262	0.046
O75643-1	SNRNP200	U5 small nuclear ribonucleoprotein 200 kDa helicase	423	-1.93	0.263	0.032
P11142-1	HSPA8	Heat shock cognate 71 kDa protein	376	-1.11	0.462	0.059
P10644	PRKAR1A	cAMP-dependent protein kinase type I-alpha regulatory subunit	375	-2.81	0.142	0.023
P07437	TUBB	tubulin beta chain	372	-1.08	0.474	0.051
O14818-1	PSMA7	Proteasome subunit alpha type-7	365	-1.90	0.268	0.042
Q04726-3	TLE3	Isoform 3 of Transducin-like enhancer protein 3	355	-2.64	0.161	0.055
Q04726-2	TLE3	Isoform 2 of Transducin-like enhancer protein 3	340	-2.07	0.238	0.018
Q15029	EFTUD2	116 kDa U5 small nuclear ribonucleoprotein component	339	-1.99	0.251	0.036
Q13330-1	MTA1	Metastasis-associated protein MTA1	333	-2.69	0.155	0.032
P62333	PSMC6	26S proteasome regulatory subunit 10B	327	-1.78	0.292	0.048
P28074-1	PSMB5	proteasome subunit beta type-5	325	-2.09	0.234	0.028
Q04837	SSBP1	Single-stranded DNA-binding protein, mitochondrial	321	-4.56	0.042	0.008
Q8WXI9	GATAD2B	Transcriptional repressor p66-beta	307	-2.66	0.158	0.023
Q15233	NONO	Non-POU domain-containing octamer-binding protein	291	-3.06	0.120	0.044
Q96QK1	VPS35	Vacuolar protein sorting-associated protein 35	285	-1.97	0.256	0.034
Q86YP4	GATAD2A	Transcriptional repressor p66-alpha	283	-2.90	0.134	0.021
P20618	PSMB1	proteasome subunit beta type-1	264	-2.24	0.212	0.030
P23246-1	SFPQ	splicing factor, proline- and glutamine-rich	251	-3.70	0.077	0.013
P49721	PSMB2	proteasome subunit beta type-2	247	-2.17	0.222	0.032
P43686	PSMC4	26S proteasome regulatory subunit 6B	243	-2.13	0.229	0.023
Q9Y2W1	THRAP3	Thyroid hormone receptor-associated protein 3	241	-1.20	0.434	0.109
O95983-1	MBD3	methyl-CpG-binding domain protein 3	239	-3.27	0.104	0.011
Q99436	PSMB7	Proteasome subunit beta type-7	235	-2.30	0.203	0.025
P06748	NPM1	Nucleophosmin	234	-2.38	0.191	0.019
Q9BTC8	MTA3	Metastasis-associated protein MTA3	234	-0.87	0.546	0.186
P28066-1	PSMA5	Proteasome subunit alpha type-5	227	-2.20	0.218	0.031
Q92769	HDAC2	Histone deacetylase 2	221	-2.78	0.146	0.020
Q12931	TRAP1	heat shock protein 75 kDa, mitochondrial	220	-1.93	0.263	0.061
P25789	PSMA4	Proteasome subunit alpha type-4	218	-2.10	0.234	0.032
Q16576-1	RBBP7	Histone-binding protein RBBP7	216	-3.12	0.115	0.017
Q14257	RCN2	Reticulocalbin-2	207	-1.53	0.347	0.045
P62195-1	PSMC5	26S proteasome regulatory subunit 8	202	-1.85	0.278	0.049
Q13200	PSMD2	26S proteasome non-ATPase regulatory subunit 2	201	-2.01	0.248	0.040
P49720	PSMB3	proteasome subunit beta type-3	193	-1.92	0.265	0.045
P33176	KIF5B	Kinesin-1 heavy chain	186	-1.91	0.266	0.040
P06576	ATP5B	ATP synthase subunit beta, mitochondrial	185	-1.85	0.278	0.028
P28072	PSMB6	Proteasome subunit beta type-6	184	-2.35	0.196	0.032

Q04727-1	TLE4	Transducin-like enhancer protein 4	177	-2.24	0.212	0.048
Q5JVS0	HABP4	Intracellular hyaluronan-binding protein 4	173	-1.96	0.257	0.051
Q14839	CHD4	Chromodomain-helicase-DNA-binding protein 4	169	-3.29	0.102	0.025
Q09028	RBBP4	Histone-binding protein RBBP4	167	-4.35	0.049	0.020
P62841	RPS15	40S ribosomal protein S15	166	-4.50	0.044	0.011
P11021	HSPA5	78 kDa glucose-regulated protein	165	-1.91	0.265	0.047
P32322	PYCR1	Pyrroline-5-carboxylate reductase 1, mitochondrial	157	-1.90	0.267	0.034
O43464	HTRA2	Serine protease HTRA2, mitochondrial	149	-1.86	0.275	0.055
O43242	PSMD3	26S proteasome non-ATPase regulatory subunit 3	135	-2.44	0.185	0.016
P35998	PSMC2	26S proteasome regulatory subunit 7	135	-1.84	0.280	0.034
Q9NWU1-1	OXSM	3-oxoacyl-acyl-carrier-protein] synthase, mitochondrial	131	-1.71	0.305	0.048
Q9Y6A5	TACC3	Transforming acidic coiled-coil-containing protein 3	126	-2.52	0.174	0.032
Q9NQS1	AVEN	Cell death regulator Aven	126	-2.06	0.239	0.036
Q13561-1	DCTN2	dynactin subunit 2	126	-1.35	0.391	0.056
P48637	GSS	glutathione synthetase	125	-1.68	0.312	0.050
Q9Y2X7-1	GIT1	ARF GTPase-activating protein GIT1	124	-2.08	0.237	0.040
P38646	HSPA9	Stress-70 protein, mitochondrial	123	-2.14	0.226	0.039
Q8NBH2-2	KY	Isoform 2 of Kyphoscoliosis peptidase	121	-7.09	0.007	0.004
Q14152	EIF3A	Eukaryotic translation initiation factor 3 subunit A	121	-2.43	0.186	0.035
Q6P2Q9	PRPF8	Pre-mRNA-processing-splicing factor 8	118	-2.40	0.189	0.031
P05141	SLC25A5	ADP/ATP translocase 2	117	-1.95	0.258	0.052
O95400	CD2BP2	CD2 antigen cytoplasmic tail-binding protein 2	117	-1.90	0.267	0.049
P29692-3	EEF1D	Isoform 3 of Elongation factor 1-delta	116	-1.70	0.309	0.045
Q9Y223-1	GNE	bifunctional UDP-N-acetylglucosamine 2-epimerase/N-acetylmannosamine kinase	114	-1.77	0.294	0.045
P51114-1	FXR1	Fragile X mental retardation syndrome-related protein 1	109	-2.25	0.210	0.064
P31943	HNRNPH1	Heterogeneous nuclear ribonucleoprotein H	108	-1.65	0.319	0.039
Q9Y5U2-1	TSSC4	Protein TSSC4	107	-2.00	0.250	0.049
Q9H0B6	KLC2	Kinesin light chain 2	105	-1.77	0.293	0.045
P31948	STIP1	stress-induced-phosphoprotein 1	104	-0.19	0.875	0.062
Q99460	PSMD1	26S proteasome non-ATPase regulatory subunit 1	103	-2.23	0.213	0.028
Q9UQ35	SRRM2	serine/arginine repetitive matrix protein 2	101	-2.07	0.239	0.079
P84103	SRSF3	Serine/arginine-rich splicing factor 3	98	-2.53	0.174	0.028
P28070	PSMB4	Proteasome subunit beta type-4	98	-1.85	0.278	0.062
P12270	TPR	Nucleoprotein TPR	96	-2.64	0.161	0.022
Q969X5	ERGIC1	Endoplasmic reticulum-Golgi intermediate compartment protein 1	94	-2.15	0.225	0.049
P62191	PSMC1	26S proteasome regulatory subunit 4	93	-2.27	0.207	0.030
Q06787-7	FMR1	Isoform 7 of Synaptic functional regulator FMR1	92	-4.18	0.055	0.013
P25705-1	ATP5A1	ATP synthase subunit alpha, mitochondrial	92	-1.94	0.260	0.039
P50402	EMD	Emerin	90	-1.53	0.347	0.037
P22626	HNRNPA2B1	heterogeneous nuclear ribonucleoproteins A2/B1	89	-2.43	0.186	0.032
Q7L014	DDX46	probable ATP-dependent RNA helicase DDX46	86	-2.03	0.245	0.047
P62308	SNRPG	Small nuclear ribonucleoprotein G	85	-2.27	0.208	0.031
Q04724	TLE1	Transducin-like enhancer protein 1	83	-2.69	0.155	0.044
Q02809	PLOD1	Procollagen-lysine,2-oxoglutarate 5-dioxygenase 1	83	-2.30	0.203	0.044
P46782	RPS5	40S ribosomal protein S5	83	-2.10	0.233	0.010
O43719	HTATSF1	HIV Tat-specific factor 1	82	-1.98	0.253	0.037
P25787	PSMA2	Proteasome subunit alpha type-2	81	-2.54	0.172	0.021
O43852	CALU	Calumenin	80	-2.02	0.247	0.025
Q07955-1	SRSF1	Serine/arginine-rich splicing factor 1	79	-3.41	0.094	0.026
Q562R1	ACTBL2	Beta-actin-like protein 2	78	-8.55	0.003	0.000
P68400	CSNK2A1	Casein kinase II subunit alpha	78	-2.32	0.200	0.030
Q07157	TJP1	Tight junction protein ZO-1	76	-1.70	0.309	0.062
P78371-1	CCT2	T-complex protein 1 subunit beta	75	-1.18	0.442	0.094
P13639	EEF2	Elongation factor 2	75	-1.09	0.469	0.144
P17844	DDX5	probable ATP-dependent RNA helicase DDX5	72	-2.21	0.216	0.045
Q9UMS4	PRPF19	Pre-mRNA-processing factor 19	65	-1.81	0.284	0.045
O43175	PHGDH	D-3-phosphoglycerate dehydrogenase	65	-1.54	0.344	0.048
P26373-1	RPL13	60S ribosomal protein L13	64	-2.43	0.185	0.031
P48643	CCT5	T-complex protein 1 subunit epsilon	62	-1.00	0.501	0.105
P35232	PHB	Prohibitin	61	-1.91	0.266	0.047
Q14161-1	GIT2	ARF GTPase-activating protein GIT2	61	-1.85	0.278	0.067
P08865	RPSA	40S ribosomal protein SA	61	-1.21	0.432	0.158
Q9UJS0	SLC25A13	Calcium-binding mitochondrial carrier protein Aralar2	60	-0.41	0.752	0.105
Q9UBQ0-2	VPS29	Isoform 2 of Vacuolar protein sorting-associated protein 29	58	-2.26	0.208	0.029
P26641	EEF1G	elongation factor 1-gamma	57	-1.45	0.366	0.055
P51116	FXR2	Fragile X mental retardation syndrome-related protein 2	56	-3.48	0.090	0.011
Q8IX12	CCAR1	Cell division cycle and apoptosis regulator protein 1	56	-1.79	0.289	0.032
O14579-1	COPE	coatomer subunit epsilon	56	-1.54	0.343	0.068
Q9ULX6	AKAP8L	A-kinase anchor protein 8-like	56	-0.38	0.768	0.136
Q9NW64-1	RBM22	Pre-mRNA-splicing factor RBM22	55	-1.97	0.256	0.037
Q06210-1	GFPT1	glutamine--fructose-6-phosphate aminotransferase isomerizing 1	55	-1.31	0.404	0.051
Q05086	UBE3A	Ubiquitin-protein ligase E3A	54	-2.13	0.228	0.033
Q01130	SRSF2	serine/arginine-rich splicing factor 2	54	-1.82	0.283	0.075
Q15293	RCN1	Reticulocalbin-1	53	-2.53	0.173	0.025
P62306	SNRPF	Small nuclear ribonucleoprotein F	52	-2.12	0.231	0.052
P84090	ERH	Enhancer of rudimentary homolog	52	-1.82	0.283	0.040
Q06830	PRDX1	peroxiredoxin-1	52	-1.23	0.427	0.112
P19474	TRIM21	E3 ubiquitin-protein ligase TRIM21	51	-2.53	0.173	0.035
P19338	NCL	Nucleolin	51	-1.80	0.286	0.075
Q15008	PSMD6	26S proteasome non-ATPase regulatory subunit 6	51	-1.65	0.318	0.090
Q9UNE7-1	STUB1	E3 ubiquitin-protein ligase CHIP	51	-0.98	0.508	0.088
P62701	RPS4X	40S ribosomal protein S4, X isoform	48	-2.54	0.172	0.037
P31321	PRKAR1B	cAMP-dependent protein kinase type I-beta regulatory subunit	47	-2.18	0.221	0.059
Q14203	DCTN1	Dynactin subunit 1	47	-1.66	0.317	0.064

O00487	PSMD14	26S proteasome non-ATPase regulatory subunit 14	47	-1.50	0.354	0.083
O75956	CDK2AP2	Cyclin-dependent kinase 2-associated protein 2	46	-4.21	0.054	0.020
O15160	POLR1C	DNA-directed RNA polymerases I and III subunit RPAC1	46	-2.05	0.241	0.039
P62318	SNRPD3	small nuclear ribonucleoprotein sm d3	46	-2.05	0.242	0.039
Q16555-1	DPYSL2	Dihydropyrimidinase-related protein 2	46	-1.76	0.295	0.044
Q14974	KPNB1	Importin subunit beta-1	46	-1.09	0.471	0.091
Q9UBB5-1	MBD2	Methyl-CpG-binding domain protein 2	45	-2.83	0.141	0.032
P49959	MRE11A	Double-strand break repair protein MRE11	45	-2.08	0.237	0.056
Q16777	HIST2H2AC	Histone H2A type 2-C	45	-2.01	0.248	0.049
Q9Y383	LUC7L2	Putative RNA-binding protein Luc7-like 2	44	-1.98	0.254	0.063
P51828	ADCY7	adenylate cyclase type 7	43	-8.48	0.003	0.001
P55884	EIF3B	Eukaryotic translation initiation factor 3 subunit B	43	-2.16	0.224	0.018
Q16629	SRSF7	serine/arginine-rich splicing factor 7	42	-2.64	0.160	0.028
Q96CT7	CCDC124	Coiled-coil domain-containing protein 124	42	-2.41	0.188	0.038
P23284	PPIB	peptidyl-prolyl cis-trans isomerase B	42	-2.41	0.188	0.028
Q9NVI7	ATAD3A	ATPase family AAA domain-containing protein 3A	42	-2.18	0.221	0.048
Q9UBQ0	VPS29	Vacuolar protein sorting-associated protein 29	41	-2.12	0.231	0.028
Q9Y230	RUVBL2	RuvB-like 2	41	-1.75	0.297	0.072
P15880	RPS2	40S ribosomal protein S2	41	-1.30	0.406	0.224
O43819	SCO2	Protein SCO2 homolog, mitochondrial	41	-0.99	0.505	0.095
O00217	NDUFS8	NADH dehydrogenase	40	-1.91	0.266	0.033
Q15393-1	SF3B3	Splicing factor 3B subunit 3	40	-1.79	0.288	0.042
P62995	TRA2B	transformer-2 protein homolog beta	38	-3.08	0.118	0.027
O14519	CDK2AP1	Cyclin-dependent kinase 2-associated protein 1	38	-2.92	0.132	0.029
O00303	EIF3F	Eukaryotic translation initiation factor 3 subunit F	38	-2.08	0.236	0.060
P12956	XRCC6	X-ray repair cross-complementing protein 6	38	-1.99	0.251	0.065
P67809	YBX1	Nuclease-sensitive element-binding protein 1	36	-2.20	0.217	0.037
Q9UNM6	PSMD13	26S proteasome non-ATPase regulatory subunit 13	36	-2.19	0.220	0.046
P33991	MCM4	DNA replication licensing factor MCM4	36	-1.70	0.308	0.064
P40227-1	CCT6A	T-complex protein 1 subunit zeta	34	-1.79	0.290	0.036
P23396-1	RPS3	40S ribosomal protein S3	34	-1.68	0.311	0.062
Q13247	SRSF6	Serine/arginine-rich splicing factor 6	33	-2.52	0.174	0.056
Q9NR30-1	DDX21	Nucleolar RNA helicase 2	33	-2.05	0.241	0.053
Q15365	PCBP1	Poly(RC)-binding protein 1	32	-1.78	0.292	0.020
P09874	PARP1	Poly ADP-ribose polymerase 1	31	-4.39	0.048	0.023
O43390-1	HNRNPR	heterogeneous nuclear ribonucleoprotein r	31	-0.68	0.625	0.137
O75494-1	SRSF10	Serine/arginine-rich splicing factor 10	30	-3.86	0.069	0.021
P62857	RPS28	40S ribosomal protein S28	30	-2.65	0.159	0.051
Q13283	G3BP1	Ras GTPase-activating protein-binding protein 1	30	-2.10	0.233	0.079
Q676U5	ATG16L1	Autophagy-related protein 16-1	30	-1.86	0.275	0.045
Q5VW36	FOCAD	focadhesin	30	-1.82	0.283	0.086
P55209	NAP1L1	Nucleosome assembly protein 1-like 1	29	-3.05	0.120	0.038
Q71UM5	RPS27L	40S ribosomal protein S27-like	29	-1.57	0.337	0.033
Q96FN9	DTD2	putative D-tyrosyl-tRNA(Tyr) deacylase 2	29	-0.79	0.580	0.083
P30048	PRDX3	Thioredoxin-dependent peroxide reductase, mitochondrial	28	-1.33	0.398	0.090
P36578	RPL4	60S ribosomal protein L4	26	-2.63	0.162	0.029
Q9BXP5	SRRT	serrate RNA effector molecule homolog	26	-2.13	0.229	0.058
O15371	EIF3D	Eukaryotic translation initiation factor 3 subunit D	26	-1.94	0.261	0.078
P62851	RPS25	40S ribosomal protein S25	26	-1.72	0.304	0.023
P55036-1	PSMD4	26S proteasome non-ATPase regulatory subunit 4	25	-1.07	0.475	0.115
P60866	RPS20	40S ribosomal protein S20	24	-2.50	0.177	0.041
P49419	ALDH7A1	Alpha-aminoadipic semialdehyde dehydrogenase	24	-1.10	0.466	0.092
Q8N1F7-1	NUP93	Nuclear pore complex protein Nup93	22	-2.62	0.162	0.042
P61978	HNRNPK	Heterogeneous nuclear ribonucleoprotein K	22	-2.18	0.220	0.024
P62979	RPS27A	Ubiquitin-40S ribosomal protein S27a	22	-0.77	0.586	0.207
Q9Y5B9	SUPT16H	FACT complex subunit SPT16	21	-1.69	0.310	0.039
Q92900	UPF1	Regulator of nonsense transcripts 1	21	-1.36	0.388	0.289
P62899	RPL31	60S ribosomal protein L31	21	-1.33	0.398	0.073
P25398	RPS12	40S ribosomal protein S12	20	-4.11	0.058	0.022
Q12874	SF3A3	splicing factor 3a subunit 3	20	-2.09	0.236	0.070
O00264	PGRMC1	Membrane-associated progesterone receptor component 1	20	-1.61	0.327	0.026
P11940-1	PABPC1	Polyadenylate-binding protein 1	20	-1.27	0.414	0.185
P18124	RPL7	60S ribosomal protein L7	19	-4.02	0.061	0.024
P25205	MCM3	DNA replication licensing factor mcm3	19	-2.47	0.181	0.059
Q08211	DHX9	Atp-dependent rna helicase a	19	-2.08	0.236	0.068
P17980	PSMC3	26S proteasome regulatory subunit 6A	19	-1.75	0.298	0.124
Q00839	HNRNPU	Heterogeneous nuclear ribonucleoprotein U	19	-1.63	0.323	0.054
P84098	RPL19	60S ribosomal protein L19	19	-1.53	0.347	0.064
O14773	TPP1	Tripeptidyl-peptidase 1	19	-1.42	0.374	0.080
P11387	TOP1	DNA topoisomerase 1	19	-1.42	0.375	0.115
O60884	DNAJA2	DnaJ homolog subfamily A member 2	19	-1.40	0.378	0.046
P49411	TUFM	elongation factor Tu, mitochondrial	19	-1.33	0.398	0.047
Q9H078-1	CLPB	Caseinolytic peptidase B protein homolog	19	-1.23	0.427	0.108
P15927-1	RPA2	Replication protein A 32 kDa subunit	18	-8.62	0.003	0.001
Q13242	SRSF9	serine/arginine-rich splicing factor 9	18	-3.54	0.086	0.026
Q9H0G5	NSRP1	Nuclear speckle splicing regulatory protein 1	18	-2.17	0.222	0.017
Q9BTZ2	DHRS4	dehydrogenase/reductase sdr family member 4	18	-1.27	0.414	0.033
O00232-1	PSMD12	26s proteasome non-atpase regulatory subunit 12	17	-4.06	0.060	0.039
P52732	KIF11	Kinesin-like protein KIF11	17	-2.64	0.161	0.042
P63220	RPS21	40S ribosomal protein S21	17	-2.42	0.187	0.042
P62910	RPL32	60S ribosomal protein L32	17	-2.40	0.189	0.013
P04637	TP53	Cellular tumor antigen p53	17	-1.89	0.271	0.084
Q96PK6-5	RBM14-RBM4	Isoform 5 of RNA-binding protein 14	17	-1.50	0.353	0.077
O00231	PSMD11	26S proteasome non-ATPase regulatory subunit 11	17	-1.42	0.374	0.070

Q2TAY7	SMU1	WD40 repeat-containing protein SMU1	16	-3.24	0.106	0.036
P51665	PSMD7	26S proteasome non-ATPase regulatory subunit 7	16	-2.81	0.142	0.056
P46778	RPL21	60S ribosomal protein L21	16	-2.61	0.163	0.027
P84243	H3F3A	histone H3.3	16	-2.39	0.191	0.034
P61313-1	RPL15	60S ribosomal protein L15	16	-2.36	0.195	0.045
O43143	DHX15	Pre-mRNA-splicing factor ATP-dependent RNA helicase DHX15	16	-2.30	0.203	0.037
Q14498-2	RBM39	Isoform 2 of RNA-binding protein 39	16	-2.13	0.229	0.073
P62917	RPL8	60S ribosomal protein L8	16	-1.94	0.261	0.026
B5ME19	EIF3CL	eukaryotic translation initiation factor 3 subunit C-like protein	15	-2.68	0.156	0.045
Q14566	MCM6	DNA replication licensing factor MCM6	15	-2.35	0.195	0.049
P62249	RPS16	40S ribosomal protein S16	15	-2.05	0.241	0.075
Q53H80	AKIRIN2	Akirin-2	15	-2.05	0.242	0.088
O75663	TIPRL	TIP41-like protein	15	-1.51	0.350	0.069
Q96BW5-1	PTER	Phosphotriesterase-related protein	15	-1.19	0.439	0.060
P67870	CSNK2B	Casein kinase II subunit beta	15	-0.94	0.520	0.255
Q9Y265	RUVBL1	RuvB-like 1	14	-8.45	0.003	0.000
P19784	CSNK2A2	casein kinase II subunit alpha'	14	-7.35	0.006	0.003
Q9NVM9	ASUN	integrator complex subunit 13	14	-2.87	0.137	0.079
P27635	RPL10	60S ribosomal protein L10	14	-2.63	0.162	0.040
O95831-1	AIFM1	Apoptosis-inducing factor 1, mitochondrial	14	-1.79	0.290	0.074
P14625	HSP90B1	Endoplasmin	14	-1.72	0.304	0.108
P60842	EIF4A1	Eukaryotic initiation factor 4A-I	13	-2.99	0.126	0.048
P35658-1	NUP214	Nuclear pore complex protein Nup214	13	-2.20	0.218	0.032
Q9Y5B6	GCFC1	PAX3- and PAX7-binding protein 1	13	-2.13	0.228	0.070
O75533-1	SF3B1	splicing factor 3B subunit 1	13	-1.69	0.310	0.052
P35613	BSG	Basigin	13	-1.20	0.436	0.043
Q86U06-1	RBM23	probable RNA-binding protein 23	12	-2.14	0.228	0.064
Q9H9B4	SFXN1	Sideroflexin-1	12	-0.76	0.589	0.035
O95714	HERC2	E3 ubiquitin-protein ligase HERC2	12	-0.32	0.802	0.245
Q4G0F5	VPS26B	Vacuolar protein sorting-associated protein 26B	11	-1.82	0.283	0.027
Q96PK6-1	RBM14	RNA-binding protein 14	10	-5.30	0.025	0.021
Q9BVG4	CXorf26	Protein PBDC1	10	-2.09	0.235	0.074
P35606	COPB2	Coatomer subunit beta'	10	-2.06	0.240	0.088
P39019	RPS19	40S ribosomal protein S19	10	-1.71	0.305	0.095
P14678-1	SNRPB	Small nuclear ribonucleoprotein-associated proteins B and B'	9	-1.70	0.307	0.081
P53803	POLR2K	DNA-directed RNA polymerases I, II, and III subunit RPABC4	9	-1.52	0.349	0.096
Q13409-1	DYNC1I2	cytoplasmic dynein 1 intermediate chain 2	9	-1.11	0.462	0.113
Q9BUQ8	DDX23	Probable ATP-dependent RNA helicase DDX23	9	-1.11	0.463	0.106
Q8IZ83	ALDH16A1	Aldehyde dehydrogenase family 16 member A1	8	-8.38	0.003	0.000
P62750	RPL23A	60S ribosomal protein L23a	8	-8.38	0.003	0.000
P01298-2	PPY	Isoform 2 of Pancreatic prohormone	8	-8.18	0.003	0.000
O60841	EIF5B	Eukaryotic translation initiation factor 5B	8	-2.20	0.217	0.056
O95232-1	LUC7L3	Luc7-like protein 3	8	-2.00	0.250	0.052
Q9UII2-1	ATPIF1	ATPase inhibitor, mitochondrial	8	-1.94	0.260	0.030
Q99832	CCT7	T-complex protein 1 subunit eta	8	-1.88	0.271	0.063
P43034	PAFAH1B1	Platelet-activating factor acetylhydrolase IB subunit alpha	8	-1.71	0.306	0.021
P61254	RPL26	60S ribosomal protein L26	8	-1.28	0.413	0.117
Q8WVD3-1	RNF138	E3 ubiquitin-protein ligase RNF138	8	-1.00	0.501	0.077
Q99623	PHB2	Prohibitin-2	7	-8.04	0.004	0.000
Q14978-1	NOLC1	nucleolar and coiled-body phosphoprotein 1	7	-4.53	0.043	0.016
P46779	RPL28	60S ribosomal protein L28	7	-2.23	0.213	0.040
Q92878	RAD50	DNA repair protein Rad50	7	-1.00	0.500	0.087
P62277	RPS13	40S ribosomal protein S13	6	-8.04	0.004	0.000
P53621-1	COPA	coatomer subunit alpha	6	-6.28	0.013	0.009
P11487	FGF3	Fibroblast growth factor 3	6	-6.13	0.014	0.011
Q9Y5K5-1	UCHL5	Ubiquitin carboxyl-terminal hydrolase isozyme L5	6	-5.27	0.026	0.017
P46781	RPS9	40S ribosomal protein S9	6	-2.65	0.159	0.029
P08621-1	SNRNP70	U1 small nuclear ribonucleoprotein 70 kDa	6	-1.92	0.264	0.070
Q9BRP4	PAAF1	Proteasomal ATPase-associated factor 1	6	-1.75	0.298	0.104
O95202-1	LETM1	mitochondrial proton/calcium exchanger protein	6	-0.56	0.676	0.169
Q9NSK0-1	KLC4	Kinesin light chain 4	5	-8.69	0.002	0.000
Q9Y3M2	CBY1	Protein chibby homolog 1	5	-4.37	0.048	0.010
Q14204	DYNC1H1	Cytoplasmic dynein 1 heavy chain 1	5	-2.95	0.129	0.062
Q9Y262	EIF3L	eukaryotic translation initiation factor 3 subunit L	5	-2.89	0.135	0.065
P35268	RPL22	60S ribosomal protein L22	5	-2.61	0.164	0.055
Q9BY77	POLDIP3	Polymerase delta-interacting protein 3	5	-2.47	0.181	0.065
P62854	RPS26	40S ribosomal protein S26	5	-2.19	0.219	0.021
P17480-1	UBTF	Nucleolar transcription factor 1	5	-2.15	0.225	0.017
P48444	ARCN1	Coatomer subunit delta	5	-1.92	0.264	0.028
Q15459	SF3A1	splicing factor 3A subunit 1	5	-1.89	0.270	0.057
P62316	SNRPD2	Small nuclear ribonucleoprotein Sm D2	5	-1.69	0.311	0.135
P61163	ACTR1A	Alpha-centractin	5	-1.53	0.346	0.066
Q15007	WTAP	Pre-mRNA-splicing regulator WTAP	5	-1.53	0.347	0.133
Q12906-1	ILF3	Interleukin enhancer-binding factor 3	5	-1.03	0.489	0.128

Table 2A-9. List of ReDiMe ratios and spectral counts for proteins identified by FLAG immunoprecipitation of overexpressing MAVSWT-FLAG (light) and MAVSC283S-FLAG (heavy).

UniProt ID	Gene Symbol	Description	# PSMs	log2 Average Ratio L:H	Average RatioL:H	SEM
P60900	PSMA6	Proteasome subunit alpha type-6	1314	0.26	1.20	0.08
Q7Z434	MAVS	Mitochondrial antiviral-signaling protein	1202	0.00	1.00	0.00
P07900	HSP90AA1	Heat shock protein HSP 90-alpha	990	0.21	1.16	0.10
P08238	HSP90AB1	Heat shock protein HSP 90-beta	905	0.11	1.08	0.12
O14980	XPO1	Exportin-1	765	-0.08	0.94	0.05
P68363	TUBA1B	Tubulin alpha-1B chain	660	0.34	1.27	0.08
P0DMV8	HSPA1B	heat shock 70 kDa protein 1A	652	-0.07	0.95	0.05
Q14974	KPNB1	Importin subunit beta-1	556	0.42	1.33	0.10
P07437	TUBB	tubulin beta chain	539	0.35	1.27	0.11
P17066	HSPA6	Heat shock 70 kDa protein 6	532	-6.30	0.01	0.00
P35232	PHB	Prohibitin	523	0.07	1.05	0.09
P19474	TRIM21	E3 ubiquitin-protein ligase TRIM21	519	0.10	1.07	0.05
Q9Y2W1	THRAP3	Thyroid hormone receptor-associated protein 3	493	0.43	1.34	0.07
P25788-1	PSMA3	Proteasome subunit alpha type-3	472	-0.07	0.95	0.06
Q92973-1	TNPO1	transportin-1	454	0.15	1.11	0.12
P11142-1	HSPA8	Heat shock cognate 71 kDa protein	404	-0.04	0.97	0.04
P55060-1	CSE1L	Exportin-2	386	0.49	1.40	0.13
Q99623	PHB2	Prohibitin-2	363	0.19	1.14	0.13
P25786-1	PSMA1	Proteasome subunit alpha type-1	362	0.02	1.02	0.06
P05141	SLC25A5	ADP/ATP translocase 2	348	0.46	1.38	0.18
P06576	ATP5B	ATP synthase subunit beta, mitochondrial	332	0.30	1.23	0.10
Q9NYF8-1	BCLAF1	Bcl-2-associated transcription factor 1	326	0.27	1.21	0.05
P28074-1	PSMB5	proteasome subunit beta type-5	322	0.03	1.02	0.09
P11021	HSPA5	78 kDa glucose-regulated protein	318	0.17	1.12	0.05
Q96QK1	VPS35	Vacuolar protein sorting-associated protein 35	310	0.04	1.03	0.08
P28066-1	PSMA5	Proteasome subunit alpha type-5	291	0.30	1.23	0.12
Q12931	TRAP1	heat shock protein 75 kDa, mitochondrial	290	-0.27	0.83	0.07
Q04726-4	TLE3	Isoform 4 of Transducin-like enhancer protein 3	275	0.73	1.66	0.21
P10809	HSPD1	60 kDa heat shock protein, mitochondrial	264	0.17	1.12	0.06
O14818-1	PSMA7	Proteasome subunit alpha type-7	257	0.14	1.10	0.10
Q15029	EFTUD2	116 kDa U5 small nuclear ribonucleoprotein component	250	0.03	1.02	0.07
Q04726-2	TLE3	Isoform 2 of Transducin-like enhancer protein 3	237	0.24	1.18	0.15
P33176	KIF5B	Kinesin-1 heavy chain	234	0.58	1.50	0.15
O75643-1	SNRNP200	U5 small nuclear ribonucleoprotein 200 kDa helicase	230	0.13	1.10	0.05
P20618	PSMB1	proteasome subunit beta type-1	230	0.60	1.52	0.22
P38646	HSPA9	Stress-70 protein, mitochondrial	218	-0.02	0.99	0.10
P25705-1	ATP5A1	ATP synthase subunit alpha, mitochondrial	211	0.50	1.41	0.14
Q99436	PSMB7	Proteasome subunit beta type-7	184	0.46	1.38	0.21
P29692-3	EEF1D	Isoform 3 of Elongation factor 1-delta	184	0.59	1.51	0.17
P49721	PSMB2	proteasome subunit beta type-2	181	-0.54	0.69	0.10
O43464	HTRA2	Serine protease HTRA2, mitochondrial	176	0.36	1.28	0.14
P48637	GSS	glutathione synthetase	172	0.25	1.19	0.06
P05023	ATP1A1	Sodium/potassium-transporting ATPase subunit alpha-1	167	0.45	1.37	0.10
P28072	PSMB6	Proteasome subunit beta type-6	163	-0.04	0.98	0.09
P29692	EEF1D	Elongation factor 1-delta	163	0.28	1.22	0.10
Q8TCG1	KIAA1524	Protein CIP2A	163	1.06	2.08	0.26
Q92616	GCN1L1	eIF-2-alpha kinase activator GCN1	162	0.31	1.24	0.08
Q8NBH2-2	KY	Isoform 2 of Kyphoscoliosis peptidase	161	-4.95	0.03	0.01
P32322	PYCR1	Pyrroline-5-carboxylate reductase 1, mitochondrial	161	-0.25	0.84	0.05
Q16576-1	RBBP7	Histone-binding protein RBBP7	159	-0.08	0.95	0.08
Q9H0B6	KLC2	Kinesin light chain 2	159	0.61	1.52	0.08
Q9Y223-1	GNE	bifunctional UDP-N-acetylglucosamine 2-epimerase/N-acetylmannosamine kinase	158	-0.20	0.87	0.07
Q04727-1	TLE4	Transducin-like enhancer protein 4	156	0.55	1.46	0.20
O94776	MTA2	Metastasis-associated protein MTA2	151	0.32	1.25	0.12
P62333	PSMC6	26S proteasome regulatory subunit 10B	148	0.60	1.51	0.15
Q5JVS0	HABP4	Intracellular hyaluronan-binding protein 4	146	0.11	1.08	0.05
P25789	PSMA4	Proteasome subunit alpha type-4	144	0.16	1.11	0.17
P62195-1	PSMC5	26S proteasome regulatory subunit 8	140	0.21	1.15	0.07
Q96P70	IPO9	Importin-9	139	0.23	1.17	0.14
Q14152	EIF3A	Eukaryotic translation initiation factor 3 subunit A	134	0.37	1.29	0.09
P49720	PSMB3	proteasome subunit beta type-3	130	-0.32	0.80	0.13
Q06830	PRDX1	peroxiredoxin-1	130	0.49	1.41	0.16
P43686	PSMC4	26S proteasome regulatory subunit 6B	127	0.08	1.05	0.12
Q13330-1	MTA1	Metastasis-associated protein MTA1	120	0.05	1.04	0.13
O43175	PHGDH	D-3-phosphoglycerate dehydrogenase	117	0.33	1.26	0.09
P13639	EEF2	Elongation factor 2	115	0.35	1.28	0.13
Q14257	RCN2	Reticulocalbin-2	112	0.26	1.20	0.08
O43852	CALU	Calumenin	111	0.10	1.07	0.12
Q969X5	ERGIC1	Endoplasmic reticulum-Golgi intermediate compartment protein 1	111	0.15	1.11	0.10
P28070	PSMB4	Proteasome subunit beta type-4	109	-0.12	0.92	0.09

Q9Y5U2-1	TSSC4	Protein TSSC4	107	0.64	1.56	0.13
Q13561-1	DCTN2	dynactin subunit 2	105	0.19	1.14	0.10
P50402	EMD	Emerin	105	0.33	1.26	0.13
Q9UBB4-1	ATXN10	Ataxin-10	104	0.26	1.20	0.19
Q07866-4	KLC1	Isoform J of Kinesin light chain 1	104	0.56	1.48	0.06
Q9Y5L0-1	TNPO3	Isoform 1 of Transportin-3	103	-0.23	0.85	0.03
Q9NWU1-1	OXSM	3-oxoacyl-acyl-carrier-protein synthase, mitochondrial	103	-0.01	0.99	0.12
O00264	PGRMC1	Membrane-associated progesterone receptor component 1	103	0.48	1.39	0.16
P06748	NPM1	Nucleophosmin	101	0.47	1.39	0.25
Q86Y56	HEATR2	Dynein assembly factor 5, axonemal	97	0.52	1.43	0.20
O75436-1	VPS26A	Vacuolar protein sorting-associated protein 26A	93	0.38	1.30	0.17
Q13162	PRDX4	Peroxiredoxin-4	92	-1.27	0.41	0.18
P46782	RPS5	40S ribosomal protein S5	91	0.27	1.21	0.15
Q9Y6A5	TACC3	Transforming acidic coiled-coil-containing protein 3	90	-0.06	0.96	0.13
Q9UBB6	NCDN	Neurochondrin	88	0.43	1.35	0.10
Q8WXI9	GATAD2B	Transcriptional repressor p66-beta	86	0.32	1.25	0.05
O95400	CD2BP2	CD2 antigen cytoplasmic tail-binding protein 2	86	0.49	1.41	0.15
P32119	PRDX2	Peroxiredoxin-2	83	-0.10	0.93	0.16
Q00325-1	SLC25A3	Phosphate carrier protein, mitochondrial	80	0.36	1.28	0.10
Q99460	PSMD1	26S proteasome non-ATPase regulatory subunit 1	78	-0.40	0.76	0.10
P78371-1	CCT2	T-complex protein 1 subunit beta	76	0.46	1.38	0.17
Q04837	SSBP1	Single-stranded DNA-binding protein, mitochondrial	74	0.15	1.11	0.11
O14579-1	COPE	coatomer subunit epsilon	73	0.30	1.23	0.15
Q16186	ADRM1	Proteasomal ubiquitin receptor ADRM1	70	0.16	1.12	0.14
A0FGR8-2	ESYT2	Isoform 2 of Extended synaptotagmin-2	69	0.13	1.09	0.05
Q9UMS4	PRPF19	Pre-mRNA-processing factor 19	68	-0.09	0.94	0.12
P19338	NCL	Nucleolin	67	0.52	1.43	0.07
P13637-1	ATP1A3	Sodium/potassium-transporting ATPase subunit alpha-3	66	-6.26	0.01	0.00
P23284	PPIB	peptidyl-prolyl cis-trans isomerase B	65	-0.19	0.88	0.11
P10644	PRKAR1A	cAMP-dependent protein kinase type I-alpha regulatory subunit	64	0.12	1.09	0.08
Q13547	HDAC1	histone deacetylase 1	64	0.43	1.35	0.24
Q7Z4Q2	HEATR3	HEAT repeat-containing protein 3	63	0.26	1.20	0.10
Q9UFG5	C19orf25	UPF0449 protein C19orf25	63	0.59	1.50	0.19
Q8IX12	CCAR1	Cell division cycle and apoptosis regulator protein 1	61	0.40	1.32	0.11
Q16555-1	DPYSL2	Dihydropyrimidinase-related protein 2	61	0.65	1.57	0.13
Q16777	HIST2H2AC	Histone H2A type 2-C	60	0.27	1.20	0.11
O43719	HTATSF1	HIV Tat-specific factor 1	60	0.27	1.21	0.15
Q16891	IMMT	MICOS complex subunit Mic60	60	0.40	1.32	0.09
Q3ZCQ8	TIMM50	Mitochondrial import inner membrane translocase subunit TIM50	60	0.42	1.34	0.14
P62308	SNRPG	Small nuclear ribonucleoprotein G	60	0.46	1.37	0.24
Q9H9B4	SFXN1	Sideroflexin-1	60	0.78	1.72	0.17
Q9UBQ0-2	VPS29	Isoform 2 of Vacuolar protein sorting-associated protein 29	59	-0.47	0.72	0.14
P84090	ERH	Enhancer of rudimentary homolog	59	0.62	1.53	0.24
P35998	PSMC2	26S proteasome regulatory subunit 7	58	-0.15	0.90	0.09
Q7L1Q6-1	BZW1	Basic leucine zipper and W2 domain-containing protein 1	57	-0.63	0.65	0.20
P49959	MRE11A	Double-strand break repair protein MRE11	57	0.02	1.01	0.16
Q14203	DCTN1	Dynactin subunit 1	56	-0.03	0.98	0.14
Q7L014	DDX46	probable ATP-dependent RNA helicase DDX46	56	0.38	1.30	0.08
P04792	HSPB1	Heat shock protein beta-1	56	0.62	1.54	0.16
P48643	CCT5	T-complex protein 1 subunit epsilon	55	0.38	1.30	0.14
O76071	CIAO1	Probable cytosolic iron-sulfur protein assembly protein Ciao1	55	1.00	2.00	0.30
P17844	DDX5	probable ATP-dependent RNA helicase DDX5	53	0.58	1.49	0.14
Q96FN9	DTD2	putative D-tyrosyl-tRNA(Tyr) deacylase 2	53	0.89	1.85	0.21
Q02978	SLC25A11	Mitochondrial 2-oxoglutarate/malate carrier protein	52	-0.03	0.98	0.14
Q01130	SRSF2	serine/arginine-rich splicing factor 2	52	0.29	1.22	0.16
Q9NQS1	AVEN	Cell death regulator Aven	52	0.42	1.33	0.10
O75934	BCAS2	Pre-mRNA-splicing factor spf27	52	0.51	1.42	0.20
P45880	VDAC2	Voltage-dependent anion-selective channel protein 2	51	0.76	1.70	0.19
Q9UNE7-1	STUB1	E3 ubiquitin-protein ligase CHIP	50	0.35	1.28	0.09
Q9HAV4	XPO5	exportin-5	50	0.47	1.38	0.10
Q56P03	EAPP	e2f-associated phosphoprotein	50	0.61	1.52	0.13
Q9NW64-1	RBM22	Pre-mRNA-splicing factor RBM22	48	0.31	1.24	0.09
P22626	HNRNPA2B1	heterogeneous nuclear ribonucleoproteins A2/B1	48	0.32	1.25	0.10
P40227-1	CCT6A	T-complex protein 1 subunit zeta	47	0.04	1.03	0.10
Q29RF7-1	PDS5A	Sister chromatid cohesion protein PDS5 homolog A	46	0.35	1.27	0.26
P62191	PSMC1	26S proteasome regulatory subunit 4	45	0.32	1.24	0.09
Q9Y383	LUC7L2	Putative RNA-binding protein Luc7-like 2	43	0.27	1.20	0.10
O14545	TRAFD1	TRAF-type zinc finger domain-containing protein 1	43	0.47	1.39	0.08
Q9C0E2	XPO4	Exportin-4	42	-0.31	0.81	0.27
Q16778	HIST2H2BE	Histone H2B type 2-E	42	0.35	1.28	0.07
P33991	MCM4	DNA replication licensing factor MCM4	42	0.59	1.50	0.17
P62491-1	RAB11A	Ras-related protein Rab-11A	41	0.41	1.33	0.13
P34932	HSPA4	Heat shock 70 kDa protein 4	40	-0.06	0.96	0.22
Q15365	PCBP1	Poly(RC)-binding protein 1	40	0.31	1.24	0.13
Q9Y678	COPG1	Coatomer subunit gamma-1	39	0.12	1.09	0.16
Q96QU8	XPO6	Exportin-6	39	0.48	1.40	0.22
O43592	XPOT	Exportin-T	39	0.64	1.56	0.19
O43819	SCO2	Protein SCO2 homolog, mitochondrial	38	0.49	1.40	0.11
Q13263	TRIM28	Transcription intermediary factor 1-beta	38	0.52	1.43	0.12
Q8N1F7-1	NUP93	Nuclear pore complex protein Nup93	37	0.21	1.16	0.11
Q9Y6E2	BZW2	Basic leucine zipper and W2 domain-containing protein 2	37	0.32	1.25	0.12
Q676U5	ATG16L1	Autophagy-related protein 16-1	37	0.54	1.45	0.08
Q9NVI7	ATAD3A	ATPase family AAA domain-containing protein 3A	37	0.67	1.60	0.25
P35613	BSG	Basigin	36	0.39	1.31	0.11

P49419	ALDH7A1	Alpha-aminoadipic semialdehyde dehydrogenase	36	0.77	1.71	0.22
Q9Y2X7-1	GIT1	ARF GTPase-activating protein GIT1	35	0.12	1.09	0.14
P68104	EEF1A1	Elongation factor 1-alpha 1	34	-0.38	0.77	0.07
P07919	UQCRH	Cytochrome b-c1 complex subunit 6, mitochondrial	34	0.41	1.33	0.07
O95983-1	MBD3	methyl-CpG-binding domain protein 3	33	-0.72	0.61	0.18
Q9Y230	RUVBL2	RuvB-like 2	33	0.20	1.15	0.11
Q71UM5	RPS27L	40S ribosomal protein S27-like	32	0.51	1.42	0.11
O43242	PSMD3	26S proteasome non-ATPase regulatory subunit 3	32	1.04	2.06	0.29
P31689-1	DNAJA1	DnaJ homolog subfamily A member 1	31	0.24	1.18	0.08
P53007	SLC25A1	Tricarboxylate transport protein, mitochondrial	31	0.34	1.26	0.25
Q15642	TRIP10	Cdc42-interacting protein 4	31	0.43	1.34	0.11
Q4G0F5	VPS26B	Vacuolar protein sorting-associated protein 26B	31	0.57	1.49	0.16
Q13243-1	SRSF5	Serine/arginine-rich splicing factor 5	30	0.08	1.06	0.09
O14828	SCAMP3	Secretory carrier-associated membrane protein 3	30	0.31	1.24	0.12
O00217	NDUFS8	NADH dehydrogenase [ubiquinone] iron-sulfur protein 8, mitochondrial	30	0.46	1.38	0.13
P09651-1	HNRNPA1	Heterogeneous nuclear ribonucleoprotein A1	29	0.26	1.19	0.17
Q96BW5-1	PTER	Phosphotriesterase-related protein	29	0.41	1.32	0.15
Q9Y5B9	SUPT16H	FACT complex subunit SPT16	29	0.50	1.42	0.09
P04075	ALDOA	fructose-bisphosphate aldolase A	28	-0.01	0.99	0.12
P23396-1	RPS3	40S ribosomal protein S3	28	0.17	1.13	0.08
Q9BU61-1	NDUFAF3	NADH dehydrogenase [ubiquinone] 1 alpha subcomplex assembly factor 3	27	-0.38	0.77	0.29
P17987	TCP1	T-complex protein 1 subunit alpha	27	-0.14	0.91	0.08
Q8N3U4-1	STAG2	Cohesin subunit SA-2	27	0.08	1.06	0.07
Q9BWF3-1	RBM4	RNA-binding protein 4	27	0.30	1.23	0.05
Q9UIA9	XPO7	exportin-7	26	-6.26	0.01	0.00
Q8N357	C2orf18	Solute carrier family 35 member F6	26	0.08	1.05	0.06
Q9UBM7	DHCR7	7-dehydrocholesterol reductase	26	0.43	1.35	0.12
Q15070-1	OXA1L	Mitochondrial inner membrane protein OXA1L	26	0.50	1.42	0.11
O43143	DHX15	Pre-mRNA-splicing factor ATP-dependent RNA helicase DHX15	26	0.74	1.67	0.18
P12270	TPR	Nucleoprotein TPR	25	0.21	1.16	0.22
P51648	ALDH3A2	Fatty aldehyde dehydrogenase	25	0.22	1.16	0.18
O94829	IPO13	Importin-13	25	0.27	1.20	0.22
P31943	HNRNPH1	Heterogeneous nuclear ribonucleoprotein H	24	-2.34	0.20	0.10
Q05086	UBE3A	Ubiquitin-protein ligase E3A	24	-0.01	0.99	0.16
P61026	RAB10	ras-related protein rab-10	24	0.37	1.29	0.10
P68400	CSNK2A1	Casein kinase II subunit alpha	23	-0.38	0.77	0.25
P27105	STOM	erythrocyte band 7 integral membrane protein	23	-0.23	0.85	0.10
P23246-1	SFPQ	splicing factor, proline- and glutamine-rich	23	-0.19	0.87	0.19
P62851	RPS25	40S ribosomal protein S25	23	0.12	1.09	0.13
O75155-1	CAND2	Cullin-associated NEDD8-dissociated protein 2	22	0.06	1.04	0.13
Q2TAY7	SMU1	WD40 repeat-containing protein SMU1	22	0.18	1.13	0.16
P84103	SRSF3	Serine/arginine-rich splicing factor 3	21	0.12	1.08	0.11
Q96L92	SNX27	Sorting nexin-27	21	0.30	1.23	0.05
Q99567	NUP88	Nuclear pore complex protein Nup88	21	0.40	1.32	0.23
Q6PJG6-1	BRAT1	BRCA1-associated ATM activator 1	20	-0.52	0.70	0.13
Q14139	UBE4A	ubiquitin conjugation factor e4 a	20	-0.01	1.00	0.29
P60842	EIF4A1	Eukaryotic initiation factor 4A-I	20	0.10	1.07	0.06
Q9Y265	RUVBL1	RuvB-like 1	19	-1.42	0.37	0.16
P60510	PPP4C	Serine/threonine-protein phosphatase 4 catalytic subunit	19	-0.56	0.68	0.17
Q8IYI6	EXOC8	Exocyst complex component 8	19	-0.56	0.68	0.22
P13010	XRCC5	X-ray repair cross-complementing protein 5	19	-0.56	0.68	0.10
Q16695	HIST3H3	histone H3.1t	19	-0.51	0.70	0.06
Q96ER3	SAAL1	protein saal1	19	-0.36	0.78	0.25
P12956	XRCC6	X-ray repair cross-complementing protein 6	19	0.15	1.11	0.22
Q13435	SF3B2	Splicing factor 3b subunit 2	19	0.36	1.28	0.29
Q92598	HSPH1	Heat shock protein 105 kDa	18	-0.60	0.66	0.25
Q8N490-2	PNKD	Isoform 2 of Probable hydrolase PNKD	18	0.00	1.00	0.12
P62249	RPS16	40S ribosomal protein S16	18	0.21	1.16	0.19
O60313	OPA1	Dynamin-like 120 kDa protein, mitochondrial	18	0.42	1.34	0.23
O15160	POLR1C	DNA-directed RNA polymerases I and III subunit RPAC1	17	-2.30	0.20	0.13
P14625	HSP90B1	Endoplasmin	17	-1.84	0.28	0.17
Q06323-1	PSME1	Proteasome activator complex subunit 1	17	-0.83	0.56	0.23
P11908	PRPS2	ribose-phosphate pyrophosphokinase 2	17	-0.22	0.86	0.23
A2NJV5	IGKV2-29	Immunoglobulin kappa variable 2-29	17	0.01	1.01	0.05
O60884	DNAJA2	DnaJ homolog subfamily A member 2	17	0.34	1.26	0.27
P62899	RPL31	60S ribosomal protein L31	17	0.36	1.29	0.11
P09914	IFIT1	interferon-induced protein with tetratricopeptide repeats 1	17	0.39	1.31	0.11
Q5VUJ6	LRCH2	Leucine-rich repeat and calponin homology domain-containing protein 2	17	0.59	1.50	0.11
P62314	SNRPD1	Small nuclear ribonucleoprotein Sm D1	16	-6.35	0.01	0.00
Q9NSK0-1	KLC4	Kinesin light chain 4	16	-1.71	0.31	0.12
P49411	TUFM	elongation factor Tu, mitochondrial	16	-0.74	0.60	0.13
Q9NVU0	POLR3E	DNA-directed RNA polymerase III subunit RPC5	16	-0.01	0.99	0.25
P60866	RPS20	40S ribosomal protein S20	16	0.04	1.03	0.16
Q5BJD5-1	TMEM41B	Transmembrane protein 41B	16	0.52	1.43	0.22
Q9Y6M1	IGF2BP2	Insulin-like growth factor 2 mRNA-binding protein 2	16	1.15	2.22	0.16
O00303	EIF3F	Eukaryotic translation initiation factor 3 subunit F	15	-1.59	0.33	0.21
Q9BVG4	CXorf26	Protein PBDC1	15	-0.91	0.53	0.20
Q9Y4R8	TELO2	telomere length regulation protein TEL2 homolog	15	0.48	1.40	0.22
Q07955-1	SRSF1	Serine/arginine-rich splicing factor 1	15	0.50	1.41	0.12
P47755	CAPZA2	F-actin-capping protein subunit alpha-2	14	-1.24	0.42	0.20
O00487	PSMD14	26S proteasome non-ATPase regulatory subunit 14	14	-1.09	0.47	0.10
P62873	GNB1	Guanine nucleotide-binding protein G(I)/G(S)/G(T) subunit beta-1	14	-0.58	0.67	0.24
P08240-1	SRPR	signal recognition particle receptor subunit alpha	14	-0.37	0.78	0.14
P63220	RPS21	40S ribosomal protein S21	14	-0.19	0.88	0.26

Q15003	NCAPH	Condensin complex subunit 2	14	0.12	1.09	0.05
Q9Y608	LRRFIP2	Leucine-rich repeat flightless-interacting protein 2	14	0.95	1.93	0.19
Q9H0G5	NSRP1	Nuclear speckle splicing regulatory protein 1	13	-6.15	0.01	0.00
Q15181	PPA1	Inorganic pyrophosphatase	13	-1.14	0.45	0.18
Q9UHI6	DDX20	Probable ATP-dependent RNA helicase DDX20	13	-0.71	0.61	0.22
Q9BPU6	DPYSL5	Dihydropyrimidinase-related protein 5	13	0.29	1.22	0.16
Q68DQ2	CRYBG3	very large A-kinase anchor protein	12	-6.26	0.01	0.00
P62995	TRA2B	transformer-2 protein homolog beta	12	-6.26	0.01	0.00
Q92841-1	DDX17	Isoform 2 of Probable ATP-dependent RNA helicase DDX17	12	-1.35	0.39	0.25
O43264	ZW10	Centromere/kinetochore protein zw10 homolog	12	-0.63	0.64	0.23
O95202-1	LETM1	mitochondrial proton/calcium exchanger protein	12	-0.07	0.95	0.17
P57678	GEMIN4	Gem-associated protein 4	12	0.30	1.23	0.13
Q9Y2Q9	MRPS28	28S ribosomal protein S28, mitochondrial	12	0.38	1.30	0.17
Q92747	ARPC1A	Actin-related protein 2/3 complex subunit 1A	12	0.59	1.51	0.25
O95831-1	AIFM1	Apoptosis-inducing factor 1, mitochondrial	12	0.62	1.54	0.28
P52732	KIF11	Kinesin-like protein KIF11	11	0.38	1.30	0.09
P62701	RPS4X	40S ribosomal protein S4, X isoform	11	0.40	1.32	0.24
Q9NX63	CHCHD3	MICOS complex subunit MIC19	11	0.60	1.52	0.22
Q9Y4W6	AFG3L2	AFG3-like protein 2	10	-0.79	0.58	0.21
P35611-1	ADD1	Alpha-adducin	10	0.31	1.24	0.08
Q7RTS9-1	DYM	dymeclin	10	0.49	1.40	0.08
Q8IY26	PPAPDC2	Phospholipid phosphatase 6	10	1.06	2.08	0.30
Q2PPJ7-1	RALGAPA2	Ral GTPase-activating protein subunit alpha-2	10	6.64	100.00	0.00
O14974	PPP1R12A	Protein phosphatase 1 regulatory subunit 12A	9	-6.22	0.01	0.00
Q9H3K6-1	BOLA2B	bola-like protein 2	9	-4.09	0.06	0.05
Q92888-1	ARHGEF1	Rho guanine nucleotide exchange factor 1	9	-2.17	0.22	0.21
P07864	LDHC	L-lactate dehydrogenase C chain	9	-1.96	0.26	0.14
P62857	RPS28	40S ribosomal protein S28	9	0.15	1.11	0.28
P27635	RPL10	60S ribosomal protein L10	9	0.33	1.26	0.11
Q96Q15-1	SMG1	Serine/threonine-protein kinase SMG1	8	-6.22	0.01	0.00
P39656	DDOST	Dolichyl-diphosphooligosaccharide--protein glycosyltransferase 48 kDa subunit	8	-1.86	0.28	0.17
Q96TA2-1	YME1L1	ATP-dependent zinc metalloprotease YME1L1	8	-0.68	0.62	0.18
O75956	CDK2AP2	Cyclin-dependent kinase 2-associated protein 2	8	-0.24	0.85	0.05
P26639-1	TARS	Threonine--tRNA ligase, cytoplasmic	8	-0.05	0.97	0.16
O95359	TACC2	Transforming acidic coiled-coil-containing protein 2	8	-0.03	0.98	0.28
Q14997	PSME4	Proteasome activator complex subunit 4	7	-0.69	0.62	0.23
P17980	PSMC3	26S proteasome regulatory subunit 6A	7	-0.57	0.67	0.20
Q92538	GBF1	Golgi-specific brefeldin A-resistance guanine nucleotide exchange factor 1	7	-0.38	0.77	0.28
Q12933	TRAF2	TNF receptor-associated factor 2	7	-0.10	0.94	0.13
P41223	BUD31	Protein BUD31 homolog	7	0.31	1.24	0.27
O60518	RANBP6	ran-binding protein 6	7	0.40	1.32	0.16
Q9UBE0-1	SAE1	SUMO-activating enzyme subunit 1	7	0.42	1.34	0.17
Q14697-1	GANAB	Neutral alpha-glucosidase AB	7	0.58	1.49	0.20
Q6P597	KLC3	Kinesin light chain 3	6	-6.22	0.01	0.00
P62263	RPS14	40S ribosomal protein S14	6	-2.32	0.20	0.07
Q8IVS2	MCAT	Malonyl-CoA-acyl carrier protein transacylase, mitochondrial	6	-0.76	0.59	0.18
Q15428	SF3A2	splicing factor 3a subunit 2	6	-0.48	0.72	0.27
O60841	EIF5B	Eukaryotic translation initiation factor 5B	6	-0.42	0.75	0.16
Q8NE86	MCU	Calcium uniporter protein, mitochondrial	6	-0.39	0.77	0.18
P28065	PSMB9	Proteasome subunit beta type-9	6	-0.38	0.77	0.13
Q9BS26	ERP44	Endoplasmic reticulum resident protein 44	6	0.02	1.01	0.24
Q9BQE5	APOL2	apolipoprotein L2	6	0.14	1.10	0.13
Q8N4C0	C9orf62	putative uncharacterized protein C9orf62	6	0.29	1.23	0.15
P17028-1	ZNF24	zinc finger protein 24	6	0.39	1.31	0.30
P62917	RPL8	60S ribosomal protein L8	5	-6.26	0.01	0.00
O60469-1	DSCAM	Down syndrome cell adhesion molecule	5	-6.26	0.01	0.00
P16615	ATP2A2	Sarcoplasmic/endoplasmic reticulum calcium ATPase 2	5	-6.25	0.01	0.00
Q04323-1	UBXN1	UBX domain-containing protein 1	5	-6.20	0.01	0.00
P61978	HNRNPK	Heterogeneous nuclear ribonucleoprotein K	5	-4.72	0.04	0.02
P14678-1	SNRPB	Small nuclear ribonucleoprotein-associated proteins B and B'	5	-3.92	0.07	0.05
O95782	AP2A1	AP-2 complex subunit alpha-1	5	-2.69	0.15	0.14
P52272	HNRNPM	Heterogeneous nuclear ribonucleoprotein M	5	-0.84	0.56	0.25
Q9Y3M2	CBY1	Protein chibby homolog 1	5	-0.07	0.95	0.06
Q15005	SPCS2	Signal peptidase complex subunit 2	5	-0.03	0.98	0.25
Q9Y3B4	SF3B14	Splicing factor 3B subunit 6	5	0.21	1.15	0.19
Q96MW5	COG8	Conserved oligomeric Golgi complex subunit 8	5	0.37	1.30	0.12

Table 2A-10. List of ReDiMe ratios and spectral counts for proteins identified by FLAG immunoprecipitation of overexpressing OGDHWT-FLAG (light) and OGDHC395S-FLAG (heavy).

UniProt ID	Gene Symbol	Protein Description	# PSMs	log2 Average Ratio L:H	Average RatioL:H	SEM
Q02218	OGDH	2-oxoglutarate dehydrogenase, mitochondrial	4014	0.00	1.00	0.00
P60900	PSMA6	Proteasome subunit alpha type-6	2247	0.15	1.11	0.16
P08238	HSP90AB1	Heat shock protein HSP 90-beta	755	0.07	1.05	0.09
P07900	HSP90AA1	Heat shock protein HSP 90-alpha	749	0.06	1.04	0.13
P10809	HSPD1	60 kDa heat shock protein, mitochondrial	657	0.19	1.14	0.14
P36957	DLST	Dihydrolipoyllysine-residue succinyltransferase component of 2-oxoglutarate dehydrogenase complex, mitochondrial	626	0.13	1.09	0.22
P60709	ACTB	Actin, cytoplasmic 1	601	0.27	1.20	0.13
P25788-1	PSMA3	Proteasome subunit alpha type-3	483	0.11	1.08	0.15
P09622	DLD	Dihydrolipoyl dehydrogenase, mitochondrial	478	-0.08	0.95	0.09
P68363	TUBA1B	Tubulin alpha-1B chain	434	0.12	1.08	0.04
P0DMV8	HSPA1B	heat shock 70 kDa protein 1A	400	-0.09	0.94	0.06
P17066	HSPA6	Heat shock 70 kDa protein 6	329	6.64	100.00	0.00
P25786-1	PSMA1	Proteasome subunit alpha type-1	321	0.45	1.37	0.19
P07437	TUBB	tubulin beta chain	305	0.20	1.15	0.07
O94776	MTA2	Metastasis-associated protein MTA2	293	0.38	1.30	0.11
P62333	PSMC6	26S proteasome regulatory subunit 10B	244	0.33	1.26	0.15
O14818-1	PSMA7	Proteasome subunit alpha type-7	235	-0.03	0.98	0.13
O75643-1	SNRNP200	U5 small nuclear ribonucleoprotein 200 kDa helicase	230	0.28	1.22	0.12
P49721	PSMB2	proteasome subunit beta type-2	223	-0.21	0.86	0.05
Q04726-3	TLE3	Isoform 3 of Transducin-like enhancer protein 3	223	0.08	1.06	0.08
Q96QK1	VPS35	Vacuolar protein sorting-associated protein 35	210	-0.04	0.98	0.07
Q04726-5	TLE3	Isoform 5 of Transducin-like enhancer protein 3	203	0.24	1.18	0.14
P28074-1	PSMB5	proteasome subunit beta type-5	201	0.08	1.06	0.10
P11142-1	HSPA8	Heat shock cognate 71 kDa protein	199	-0.23	0.85	0.07
Q99436	PSMB7	Proteasome subunit beta type-7	192	0.35	1.27	0.15
P06748	NPM1	Nucleophosmin	189	0.19	1.14	0.20
P48643	CCT5	T-complex protein 1 subunit epsilon	179	0.71	1.63	0.10
P28066-1	PSMA5	Proteasome subunit alpha type-5	176	-0.17	0.89	0.15
Q12931	TRAP1	heat shock protein 75 kDa, mitochondrial	175	0.00	1.00	0.09
P20618	PSMB1	proteasome subunit beta type-1	173	0.00	1.00	0.11
P33176	KIF5B	Kinesin-1 heavy chain	173	0.16	1.11	0.08
P62195-1	PSMC5	26S proteasome regulatory subunit 8	173	0.33	1.26	0.16
P78371-1	CCT2	T-complex protein 1 subunit beta	171	0.40	1.32	0.11
Q13330-1	MTA1	Metastasis-associated protein MTA1	168	0.01	1.01	0.21
P06576	ATP5B	ATP synthase subunit beta, mitochondrial	162	0.10	1.07	0.09
P10644	PRKAR1A	cAMP-dependent protein kinase type I-alpha regulatory subunit	162	0.26	1.20	0.15
P43686	PSMC4	26S proteasome regulatory subunit 6B	157	0.13	1.09	0.14
Q9Y2W1	THRAP3	Thyroid hormone receptor-associated protein 3	149	0.39	1.31	0.19
Q8WXI9	GATAD2B	Transcriptional repressor p66-beta	146	0.44	1.36	0.22
P28072	PSMB6	Proteasome subunit beta type-6	145	0.04	1.03	0.18
Q15029	EFTUD2	116 kDa U5 small nuclear ribonucleoprotein component	143	-0.04	0.97	0.10
Q14257	RCN2	Reticulocalbin-2	130	0.07	1.05	0.10
O95983-1	MBD3	methyl-CpG-binding domain protein 3	122	0.00	1.00	0.08
Q9NYF8-1	BCLAF1	Bcl-2-associated transcription factor 1	121	-0.05	0.97	0.12
P32322	PYCR1	Pyrroline-5-carboxylate reductase 1, mitochondrial	118	-0.07	0.95	0.06
Q16576-1	RBBP7	Histone-binding protein RBBP7	116	-0.26	0.84	0.08
Q04727-1	TLE4	Transducin-like enhancer protein 4	115	-0.40	0.76	0.15
P38646	HSPA9	Stress-70 protein, mitochondrial	114	-0.04	0.97	0.09
P35998	PSMC2	26S proteasome regulatory subunit 7	113	-0.02	0.99	0.12
P25789	PSMA4	Proteasome subunit alpha type-4	113	0.00	1.00	0.20
O43464	HTRA2	Serine protease HTRA2, mitochondrial	110	0.04	1.03	0.09
Q13200	PSMD2	26S proteasome non-ATPase regulatory subunit 2	107	0.28	1.21	0.10
Q13561-1	DCTN2	dynactin subunit 2	107	0.62	1.53	0.19
Q9Y6A5	TACC3	Transforming acidic coiled-coil-containing protein 3	106	-0.37	0.77	0.17
Q5JVS0	HABP4	Intracellular hyaluronan-binding protein 4	99	-0.14	0.91	0.04
P48637	GSS	glutathione synthetase	99	0.20	1.15	0.22
P11021	HSPA5	78 kDa glucose-regulated protein	95	-0.10	0.93	0.04
Q9Y5U2-1	TSSC4	Protein TSSC4	91	-0.09	0.94	0.15
Q04837	SSBP1	Single-stranded DNA-binding protein, mitochondrial	87	0.22	1.16	0.09
Q09028	RBBP4	Histone-binding protein RBBP4	86	-6.47	0.01	0.00
Q9NWU1-1	OXSM	3-oxoacyl-[acyl-carrier-protein] synthase, mitochondrial	83	0.01	1.01	0.06
P29692-3	EEF1D	Isoform 3 of Elongation factor 1-delta	80	0.67	1.59	0.24
O43242	PSMD3	26S proteasome non-ATPase regulatory subunit 3	79	-0.22	0.86	0.09
Q9Y223-1	GNE	bifunctional UDP-N-acetylglucosamine 2-epimerase/N-acetylmannosamine kinase	79	0.00	1.00	0.09
Q7L014	DDX46	probable ATP-dependent RNA helicase DDX46	78	0.22	1.16	0.21
O43719	HTATSF1	HIV Tat-specific factor 1	77	0.41	1.33	0.17

Q92769	HDAC2	Histone deacetylase 2	76	0.68	1.60	0.19
P62841	RPS15	40S ribosomal protein S15	75	-1.73	0.30	0.13
O95400	CD2BP2	CD2 antigen cytoplasmic tail-binding protein 2	72	0.05	1.04	0.13
Q9H0B6	KLC2	Kinesin light chain 2	69	0.21	1.16	0.16
P29692	EEF1D	Elongation factor 1-delta	67	0.16	1.12	0.15
Q86YP4	GATAD2A	Transcriptional repressor p66-alpha	61	-0.11	0.93	0.15
P26641	EEF1G	elongation factor 1-gamma	60	0.13	1.09	0.14
P50402	EMD	Emerin	58	-0.04	0.97	0.12
Q9NQS1	AVEN	Cell death regulator Aven	57	0.04	1.03	0.06
O60282-1	KIF5C	kinesin heavy chain isoform 5C	57	6.64	100.00	0.00
P25705-1	ATP5A1	ATP synthase subunit alpha, mitochondrial	56	0.38	1.30	0.15
Q99460	PSMD1	26S proteasome non-ATPase regulatory subunit 1	55	0.10	1.07	0.13
P40227-1	CCT6A	T-complex protein 1 subunit zeta	53	0.11	1.08	0.18
P84103	SRSF3	Serine/arginine-rich splicing factor 3	53	0.43	1.35	0.13
P19474	TRIM21	E3 ubiquitin-protein ligase TRIM21	51	0.26	1.19	0.19
Q14152	EIF3A	Eukaryotic translation initiation factor 3 subunit A	51	0.47	1.38	0.18
Q9Y2X7-1	GIT1	ARF GTPase-activating protein GIT1	50	0.19	1.14	0.16
P33991	MCM4	DNA replication licensing factor MCM4	50	0.22	1.17	0.17
Q04724	TLE1	Transducin-like enhancer protein 1	49	-0.08	0.95	0.21
P55884	EIF3B	Eukaryotic translation initiation factor 3 subunit B	49	0.18	1.14	0.20
P68400	CSNK2A1	Casein kinase II subunit alpha	49	0.65	1.57	0.14
O75934	BCAS2	Pre-mRNA-splicing factor spf27	48	-0.40	0.76	0.17
P22626	HNRNPA2B1	heterogeneous nuclear ribonucleoproteins A2/B1	48	-0.22	0.86	0.09
P31943	HNRNPH1	Heterogeneous nuclear ribonucleoprotein H	48	-0.19	0.88	0.10
O14579-1	COPE	coatomer subunit epsilon	48	-0.04	0.98	0.08
P05141	SLC25A5	ADP/ATP translocase 2	47	0.24	1.18	0.21
Q06210-1	GFPT1	glutamine--fructose-6-phosphate aminotransferase [isomerizing] 1	44	-0.06	0.96	0.09
P46782	RPS5	40S ribosomal protein S5	44	0.40	1.32	0.28
Q9UNE7-1	STUB1	E3 ubiquitin-protein ligase CHIP	44	0.77	1.70	0.24
Q14839	CHD4	Chromodomain-helicase-DNA-binding protein 4	43	-0.06	0.96	0.29
P62191	PSMC1	26S proteasome regulatory subunit 4	43	0.22	1.16	0.17
Q8IX12	CCAR1	Cell division cycle and apoptosis regulator protein 1	42	0.23	1.17	0.12
O43175	PHGDH	D-3-phosphoglycerate dehydrogenase	42	0.48	1.39	0.16
Q16555-1	DPYSL2	Dihydropyrimidinase-related protein 2	41	-0.30	0.81	0.15
Q9UMS4	PRPF19	Pre-mRNA-processing factor 19	41	-0.12	0.92	0.11
P05023	ATP1A1	Sodium/potassium-transporting ATPase subunit alpha-1	41	0.18	1.14	0.09
P19338	NCL	Nucleolin	41	0.23	1.17	0.21
Q15293	RCN1	Reticulocalbin-1	39	0.11	1.08	0.16
Q15393-1	SF3B3	Splicing factor 3B subunit 3	39	0.54	1.45	0.22
O43852	CALU	Calumenin	38	-0.13	0.91	0.12
Q969X5	ERGIC1	Endoplasmic reticulum-Golgi intermediate compartment protein 1	38	-0.01	1.00	0.11
Q99832	CCT7	T-complex protein 1 subunit eta	38	0.21	1.16	0.23
P82909	MRPS36	28S ribosomal protein S36, mitochondrial	37	-0.56	0.68	0.09
Q9Y5L4	TIMM13	mitochondrial import inner membrane translocase subunit TIM13	37	-0.09	0.94	0.12
P49368-1	CCT3	T-complex protein 1 subunit gamma	37	0.45	1.37	0.08
Q9Y230	RUVBL2	RuvB-like 2	36	-0.15	0.90	0.16
Q15365	PCBP1	Poly(RC)-binding protein 1	36	0.05	1.04	0.08
Q05086	UBE3A	Ubiquitin-protein ligase E3A	36	0.25	1.19	0.16
Q9UBQ0-2	VPS29	Isoform 2 of Vacuolar protein sorting-associated protein 29	35	-0.13	0.92	0.11
O60220	TIMM8A	Mitochondrial import inner membrane translocase subunit Tim8 A	34	-0.50	0.70	0.12
P25787	PSMA2	Proteasome subunit alpha type-2	34	-0.24	0.84	0.10
P62306	SNRPF	Small nuclear ribonucleoprotein F	34	0.31	1.24	0.10
Q9NW64-1	RBM22	Pre-mRNA-splicing factor RBM22	34	0.36	1.28	0.22
Q14974	KPNB1	Importin subunit beta-1	33	0.01	1.01	0.09
P23246-1	SFPQ	splicing factor, proline- and glutamine-rich	32	0.19	1.14	0.12
O00303	EIF3F	Eukaryotic translation initiation factor 3 subunit F	32	0.32	1.25	0.13
O75956	CDK2AP2	Cyclin-dependent kinase 2-associated protein 2	29	-0.01	0.99	0.20
Q15008	PSMD6	26S proteasome non-ATPase regulatory subunit 6	28	0.08	1.06	0.13
A0FGR8-1	ESYT2	Extended synaptotagmin-2	28	0.41	1.33	0.16
P33993-1	MCM7	DNA replication licensing factor MCM7	27	-0.01	0.99	0.11
P04792	HSPB1	Heat shock protein beta-1	26	-0.08	0.94	0.10
P35232	PHB	Prohibitin	26	0.19	1.14	0.22
P25205	MCM3	DNA replication licensing factor mcm3	26	0.30	1.23	0.20
O43819	SCO2	Protein SCO2 homolog, mitochondrial	25	0.49	1.40	0.15
Q676U5	ATG16L1	Autophagy-related protein 16-1	24	0.47	1.39	0.21
P62314	SNRPD1	Small nuclear ribonucleoprotein Sm D1	23	-0.76	0.59	0.27
Q9BTZ2	DHRS4	dehydrogenase/reductase sdr family member 4	23	0.31	1.24	0.11
Q9Y5B9	SUPT16H	FACT complex subunit SPT16	23	0.43	1.35	0.13
P22061	PCMT1	protein-L-isoaspartate(D-aspartate) O-methyltransferase	22	-0.28	0.82	0.23
Q00839	HNRNPU	Heterogeneous nuclear ribonucleoprotein U	20	0.17	1.12	0.18
P51828	ADCY7	adenylate cyclase type 7	18	-6.45	0.01	0.00
P62318	SNRPD3	small nuclear ribonucleoprotein sm d3	18	-0.45	0.73	0.19
Q9BPU6	DPYSL5	Dihydropyrimidinase-related protein 5	18	0.08	1.06	0.18
Q13347	EIF3I	Eukaryotic translation initiation factor 3 subunit I	17	-0.37	0.77	0.11
Q9UL46	PSME2	proteasome activator complex subunit 2	17	0.61	1.53	0.21
Q71UM5	RPS27L	40S ribosomal protein S27-like	17	0.92	1.89	0.17
Q86V81	ALYREF	THO complex subunit 4	16	0.29	1.22	0.16
O14545	TRAFD1	TRAF-type zinc finger domain-containing protein 1	16	0.76	1.70	0.30
Q9Y5J9	TIMM8B	mitochondrial import inner membrane translocase subunit Tim8 B	15	-0.74	0.60	0.26
P62899	RPL31	60S ribosomal protein L31	15	-0.26	0.83	0.22
P05160	F13B	Coagulation factor XIII B chain	14	-5.93	0.02	0.01
O00487	PSMD14	26S proteasome non-ATPase regulatory subunit 14	14	-2.68	0.16	0.10
P04075	ALDOA	fructose-bisphosphate aldolase A	14	-0.61	0.65	0.09
P62851	RPS25	40S ribosomal protein S25	14	0.34	1.27	0.14

Q9H0G5	NSRP1	Nuclear speckle splicing regulatory protein 1	14	0.54	1.45	0.21
Q9NVI7	ATAD3A	ATPase family AAA domain-containing protein 3A	13	-1.24	0.42	0.23
Q13283	G3BP1	Ras GTPase-activating protein-binding protein 1	13	-0.43	0.74	0.15
P84090	ERH	Enhancer of rudimentary homolog	13	0.01	1.01	0.29
P35658-1	NUP214	Nuclear pore complex protein Nup214	13	0.72	1.64	0.27
Q9Y3B4	SF3B14	Splicing factor 3B subunit 6	13	0.89	1.85	0.18
P12956	XRCC6	X-ray repair cross-complementing protein 6	12	-0.39	0.77	0.14
P61978	HNRNPK	Heterogeneous nuclear ribonucleoprotein K	12	0.01	1.01	0.12
Q5VW36	FOCAD	focadhesin	12	0.33	1.26	0.26
Q6ZNL6-1	FGD5	FYVE, RhoGEF and PH domain-containing protein 5	12	6.64	100.00	0.00
P15880	RPS2	40S ribosomal protein S2	11	-6.37	0.01	0.00
P62263	RPS14	40S ribosomal protein S14	11	-1.18	0.44	0.11
Q9BVG4	CXorf26	Protein PBDC1	11	-0.27	0.83	0.13
O75663	TIPRL	TIP41-like protein	11	0.02	1.01	0.23
P30048	PRDX3	Thioredoxin-dependent peroxide reductase, mitochondrial	11	0.43	1.35	0.19
P25398	RPS12	40S ribosomal protein S12	11	0.72	1.65	0.19
Q6P2Q9	PRPF8	Pre-mRNA-processing-splicing factor 8	10	-0.58	0.67	0.14
P52732	KIF11	Kinesin-like protein KIF11	10	0.14	1.10	0.20
O60884	DNAJA2	DnaJ homolog subfamily A member 2	10	0.52	1.43	0.19
Q9NZJ5	EIF2AK3	Eukaryotic translation initiation factor 2-alpha kinase 3	10	6.64	100.00	0.00
P35606	COPB2	Coatomer subunit beta'	9	-0.28	0.82	0.14
Q9UBB6	NCDN	Neurochondrin	9	0.23	1.17	0.20
P67870	CSNK2B	Casein kinase II subunit beta	9	6.64	100.00	0.00
Q8N490-2	PNKD	Isoform 2 of Probable hydrolase PNKD	8	0.08	1.06	0.13
P63220	RPS21	40S ribosomal protein S21	8	0.14	1.10	0.30
P19784	CSNK2A2	casein kinase II subunit alpha'	7	-6.44	0.01	0.00
Q10713	PMPCA	Mitochondrial-processing peptidase subunit alpha	7	-0.84	0.56	0.12
Q9Y312	AAR2	Protein AAR2 homolog	7	-0.43	0.74	0.19
Q9BQ04	RBM4B	RNA-binding protein 4B	7	-0.13	0.91	0.20
Q06323-1	PSME1	Proteasome activator complex subunit 1	7	0.07	1.05	0.26
P27635	RPL10	60S ribosomal protein L10	7	0.41	1.33	0.26
Q5VUJ6	LRCH2	Leucine-rich repeat and calponin homology domain-containing protein 2	7	0.59	1.50	0.19
P35613	BSG	Basigin	7	0.62	1.54	0.14
Q9BUI4	POLR3C	DNA-directed RNA polymerase III subunit RPC3	7	6.64	100.00	0.00
Q96GC6-1	ZNF274	Neurotrophin receptor-interacting factor homolog	6	-6.46	0.01	0.00
P62917	RPL8	60S ribosomal protein L8	6	-6.37	0.01	0.00
P53803	POLR2K	DNA-directed RNA polymerases I, II, and III subunit RPABC4	6	-0.30	0.81	0.23
O95782	AP2A1	AP-2 complex subunit alpha-1	5	-2.22	0.22	0.13
O14773	TPP1	Tripeptidyl-peptidase 1	5	-1.38	0.38	0.11
Q9Y6M1	IGF2BP2	Insulin-like growth factor 2 mRNA-binding protein 2	5	-1.11	0.46	0.21

Table 3A-1. List of all proteins identified in matrix-TID, IMS-TID, and cyto-TID MS analyses. Mitochondrial localization is denoted by "mito", and is derived from uniprot subcellular localization, MitoCarta2.0, and previous studies (mito-APEX, IMS-APEX, and IMSGold+). Protein identifications for matrix-TID and IMS-TID are the average of 3 replicates. Protein identifications for cyto-TID are the average for 2 replicates. All identifications were filtered >10 spectral counts.

UniProt ID	Protein Description	Mitochondrial	IMS-APEX mitochondrial annotation	IMSGold+	mito-APEX mitochondrial annotation	Average Spectral Count Matrix-TID	Average Spectral Count IMS-TID	Average Spectral Count Cyto-TID
Q2M2I8	AAK1 AP2-associated protein kinase 1	-	-	-	-	3	2	10
Q5JTZ9	AARS2 Alanine--tRNA ligase, mitochondrial	Yes	-	-	Yes	29	8	0
Q9NRN7	AASDHPPT L-aminoadipate-semialdehyde dehydrogenase-phosphopantetheinyl transferase	-	-	-	-	7	3	15
Q9UDR5	AASS Alpha-aminoadipic semialdehyde synthase, mitochondrial	Yes	-	-	Yes	22	2	0
P28288	ABCD3 ATP-binding cassette sub-family D member 3	Yes	-	-	-	0	180	0
Q9NUJ1	ABHD10 Abhydrolase domain-containing protein 10, mitochondrial	Yes	Yes	-	Yes	30	6	0

Q13085	ACACA Acetyl-CoA carboxylase 1	Yes	-	-	-	201	395	2
O00763	ACACB Acetyl-CoA carboxylase 2	Yes	-	-	-	31	48	0
Q6JQN1	ACAD10 Acyl-CoA dehydrogenase family member 10	Yes	-	-	Yes	12	3	0
Q9H845	ACAD9 Acyl-CoA dehydrogenase family member 9, mitochondrial	Yes	-	-	Yes	58	19	0
P11310	ACADM Medium-chain specific acyl-CoA dehydrogenase, mitochondrial	Yes	-	-	Yes	14	6	0
P45954	ACADSB Short/branched chain specific acyl-CoA dehydrogenase, mitochondrial	Yes	-	-	Yes	29	3	0
P49748	ACADVL Very long-chain specific acyl-CoA dehydrogenase, mitochondrial	Yes	-	-	Yes	16	14	0
P24752	ACAT1 Acetyl-CoA acetyltransferase, mitochondrial	Yes	-	-	Yes	25	6	2
P12821	ACE Angiotensin-converting enzyme	-	-	-	-	0	16	0
Q9UKV3	ACIN1 Apoptotic chromatin condensation inducer in the nucleus	-	-	-	-	3	2	40
P53396	ACLY ATP-citrate synthase	Yes	-	-	Yes	15	7	10
Q99798	ACO2 Aconitate hydratase, mitochondrial	Yes	-	-	Yes	109	8	4
P49753	ACOT2 Acyl-coenzyme A thioesterase 2, mitochondrial	Yes	-	-	-	134	58	4
Q9Y305	ACOT9 Acyl-coenzyme A thioesterase 9, mitochondrial	Yes	-	-	-	26	9	0
P68133	ACTA1 Actin, alpha skeletal muscle	-	-	-	-	14	14	17
P62736	ACTA2 Actin, aortic smooth muscle	-	-	-	-	14	13	0
P60709	ACTB Actin, cytoplasmic 1	-	-	-	-	33	31	26
O43707	ACTN4 Alpha-actinin-4	-	-	-	-	8	4	10
P55265	ADAR Double-stranded RNA-specific adenosine deaminase	-	-	-	-	3	7	14
Q8NI60	ADCK3 Chaperone activity of bc1 complex-like, mitochondrial	Yes	-	-	Yes	12	3	0
Q9H2P0	ADNP Activity-dependent neuroprotector homeobox protein	-	-	-	-	0	3	26
P25098	ADRBK1 Beta-adrenergic receptor kinase 1	-	-	-	-	0	0	11
P52594	AGFG1 Arf-GAP domain and FG repeat-containing protein 1	-	-	-	-	7	9	11
P23526	AHCY Adenosylhomocysteinase	-	-	-	-	9	8	19
O43865	AHCYL1 Putative adenosylhomocysteinase 2	-	-	-	-	2	3	11
Q09666	AHNAK Neuroblast differentiation-associated protein AHNAK	-	-	-	-	17	8	195
Q8IVF2	AHNAK2 Protein AHNAK2	-	-	-	-	2	0	14
O95433	AHSA1 Activator of 90 kDa heat shock protein ATPase homolog 1	-	-	-	-	3	4	17
Q9UIJ7	AK3 GTP:AMP phosphotransferase, mitochondrial	Yes	-	-	Yes	29	5	0
P27144	AK4 Adenylate kinase isoenzyme 4, mitochondrial	Yes	-	-	Yes	36	8	0
Q92667	AKAP1 A-kinase anchor protein 1, mitochondrial	Yes	Yes	-	-	0	27	8
Q02952	AKAP12 A-kinase anchor protein 12	-	-	-	-	2	3	53
Q12802	AKAP13 A-kinase anchor protein 13	-	-	-	-	0	0	17
Q9Y2D5	AKAP2 A-kinase anchor protein 2	-	-	-	-	0	0	17
P13196	ALAS1 5-aminolevulinate synthase, nonspecific, mitochondrial	Yes	-	-	Yes	12	3	0
P54886	ALDH18A1 Delta-1-pyrroline-5-carboxylate synthase	Yes	-	-	-	270	27	11
P30837	ALDH1B1 Aldehyde dehydrogenase X, mitochondrial	Yes	-	-	Yes	15	3	0
Q3SY69	ALDH1L2 Mitochondrial 10-formyltetrahydrofolate dehydrogenase	Yes	-	-	Yes	54	7	0
P05091	ALDH2 Aldehyde dehydrogenase, mitochondrial	Yes	-	-	Yes	24	7	2
P30038	ALDH4A1 Delta-1-pyrroline-5-carboxylate dehydrogenase, mitochondrial	Yes	-	-	Yes	33	6	0
Q02252	ALDH6A1 Methylmalonate-semialdehyde dehydrogenase	Yes	-	-	Yes	15	5	0
P49419	ALDH7A1 Alpha-aminoadipic semialdehyde dehydrogenase	Yes	-	-	Yes	15	4	3
P04075	ALDOA Fructose-bisphosphate aldolase A	-	-	-	-	15	7	13
Q8TCU4	ALMS1 Alstrom syndrome protein 1	-	-	-	-	2	2	42
Q4VCS5	AMOT Angiomotin	-	-	-	-	39	11	161
Q9H1A4	ANAPC1 Anaphase-promoting complex subunit 1	Yes	Yes	-	Yes	2	13	0
Q8IWZ3	ANKHD1 Ankyrin repeat and KH domain-containing protein 1	-	-	-	-	0	7	11
Q9NQW6	ANLN Actin-binding protein anillin	-	-	-	-	0	2	12
O00203	AP3B1 AP-3 complex subunit beta-1	-	-	-	-	0	3	31
O14617	AP3D1 AP-3 complex subunit delta-1	-	-	-	-	5	12	19
O00213	APBB1 Amyloid beta A4 precursor protein-binding family B member 1	-	-	-	-	3	8	18
Q6UXV4	APOOL Apolipoprotein O-like	Yes	-	-	-	0	11	0
P48444	ARCN1 Coatomer subunit delta	-	-	-	-	4	0	10
Q8N6T3	ARFGAP1 ADP-ribosylation factor GTPase-activating protein 1	-	-	-	-	0	14	12
Q9NRY4	ARHGAP35 Rho GTPase-activating protein 35	-	-	-	-	0	2	30
Q9UH62	ARMCX3 Armadillo repeat-containing X-linked protein 3	Yes	-	-	-	0	11	0
Q8N3C0	ASCC3 Activating signal cointegrator 1 complex subunit 3	-	-	-	-	3	36	10
P08243	ASNS Asparagine synthetase	-	-	-	-	7	2	14
Q9NVI7	ATAD3A ATPase family AAA domain-containing protein 3A	Yes	Yes	Yes	Yes	0	18	0
Q5T9A4	ATAD3B ATPase family AAA domain-containing protein 3B	Yes	Yes	Yes	Yes	0	11	0
Q5T2N8	ATAD3C ATPase family AAA domain-containing protein 3C	-	-	-	-	0	11	0
Q96BY7	ATG2B Autophagy-related protein 2 homolog B	-	-	-	-	0	14	7
P05023	ATP1A1 Sodium/potassium-transporting ATPase subunit alpha-1	-	-	-	-	8	18	3
P25705	ATP5A1 ATP synthase subunit alpha, mitochondrial	Yes	-	-	Yes	19	18	0
P06576	ATP5B ATP synthase subunit beta, mitochondrial	Yes	-	-	Yes	139	53	0
P38606	ATP6V1A V-type proton ATPase catalytic subunit A	-	-	-	-	3	7	22
Q5TC12	ATPAF1 ATP synthase mitochondrial F1 complex assembly factor 1	Yes	-	-	Yes	37	7	0
Q8N5M1	ATPAF2 ATP synthase mitochondrial F1 complex assembly factor 2	Yes	-	-	Yes	11	2	0
Q8WWM7	ATXN2L Ataxin-2-like protein	-	-	-	-	2	4	27
P12694	BCKDHA 2-oxoisovalerate dehydrogenase subunit alpha, mitochondrial	Yes	-	-	Yes	18	3	0
Q9BXK5	BCL2L13 Bcl-2-like protein 13	Yes	Yes	-	-	0	16	0
Q9NYF8	BCLAF1 Bcl-2-associated transcription factor 1	-	-	-	-	4	4	24
Q6W2J9	BCOR BCL-6 corepressor	-	-	-	-	3	7	32
Q9NR09	BIRC6 Baculoviral IAP repeat-containing protein 6	-	-	-	-	5	13	19
Q8NFC6	BOD1L1 Biorientation of chromosomes in cell division protein 1-like 1	-	-	-	-	0	0	19
Q12830	BPTF Nucleosome-remodeling factor subunit BPTF	-	-	-	-	0	0	13
P38398	BRCA1 Breast cancer type 1 susceptibility protein	-	-	-	-	3	7	20
P51587	BRCA2 Breast cancer type 2 susceptibility protein	-	-	-	-	2	5	10
P46736	BRCC3 Lys-63-specific deubiquitinase BRCC36	-	-	-	-	3	3	21
O60885	BRD4 Bromodomain-containing protein 4	-	-	-	-	0	0	18
P43251	BTD Biotinidase	-	-	-	-	13	9	0
O60566	BUB1B Mitotic checkpoint serine/threonine-protein kinase BUB1 beta	-	-	-	-	2	3	14
Q8N6N3	C1orf52 UPF0690 protein C1orf52	-	-	-	-	0	2	13
Q07021	C1QBP Complement component 1 Q subcomponent-binding protein, mitochondrial	Yes	-	-	Yes	21	9	6

Q9BQP7	C20orf72 Uncharacterized protein C20orf72	Yes	-	-	Yes	44	18	0
Q7L592	C2orf56 Protein midA homolog, mitochondrial	Yes	-	-	Yes	45	15	0
Q9HB71	CACYBP Calcyclin-binding protein	-	-	-	-	10	4	13
Q05682	CALD1 Caldesmon	-	-	-	-	0	0	18
Q5T5Y3	CAMSAP1 Calmodulin-regulated spectrin-associated protein 1	-	-	-	-	0	0	19
Q86VP6	CAND1 Cullin-associated NEDD8-dissociated protein 1	-	-	-	-	10	5	4
Q01518	CAP1 Adenylyl cyclase-associated protein 1	-	-	-	-	5	4	12
Q9HA77	CARS2 Probable cysteine--tRNA ligase, mitochondrial	Yes	-	-	Yes	11	4	0
Q8NG31	CASC5 Protein CASC5	-	-	-	-	0	3	13
P20810	CAST Calpastatin	-	-	-	-	0	0	18
P35520	CBS Cystathionine beta-synthase	-	-	-	-	3	0	12
Q96A33	CCDC47 Coiled-coil domain-containing protein 47	-	-	-	-	0	11	0
P78371	CCT2 T-complex protein 1 subunit beta	-	-	-	-	11	6	9
P49368	CCT3 T-complex protein 1 subunit gamma	-	-	-	-	13	6	5
P48643	CCT5 T-complex protein 1 subunit epsilon	-	-	-	-	14	5	16
P40227	CCT6A T-complex protein 1 subunit zeta	-	-	-	-	10	10	10
Q99832	CCT7 T-complex protein 1 subunit eta	-	-	-	-	11	7	7
P50990	CCT8 T-complex protein 1 subunit theta	-	-	-	-	220	275	371
Q9Y5K6	CD2AP CD2-associated protein	-	-	-	-	3	2	73
Q6P1J9	CDC73 Parafibromin	-	-	-	-	0	4	11
Q69YH5	CDCA2 Cell division cycle-associated protein 2	-	-	-	-	0	0	14
Q96SZ6	CDK5RAP1 CDK5 regulatory subunit-associated protein 1	-	-	-	-	13	5	0
Q96SN8	CDK5RAP2 CDK5 regulatory subunit-associated protein 2	-	-	-	-	0	14	0
Q9UKY7	CDV3 Protein CDV3 homolog	-	-	-	-	2	2	10
Q9BXW7	CECR5 Cat eye syndrome critical region protein 5	Yes	-	-	Yes	15	8	0
Q5SW79	CEP170 Centrosomal protein of 170 kDa	-	-	-	-	3	4	26
Q5VT06	CEP350 Centrosome-associated protein 350	-	-	-	-	7	13	13
Q8IW35	CEP97 Centrosomal protein of 97 kDa	-	-	-	-	0	8	11
Q9UEE9	CFDP1 Craniofacial development protein 1	-	-	-	-	0	0	21
P23528	CFL1 Cofilin-1	-	-	-	-	10	3	12
Q96JM3	CHAMP1 Chromosome alignment-maintaining phosphoprotein 1	-	-	-	-	3	5	45
Q12873	CHD3 Chromodomain-helicase-DNA-binding protein 3	-	-	-	-	0	0	13
Q14839	CHD4 Chromodomain-helicase-DNA-binding protein 4	-	-	-	-	2	16	57
Q8TDI0	CHD5 Chromodomain-helicase-DNA-binding protein 5	-	-	-	-	0	3	21
Q9UHD1	CHORDC1 Cysteine and histidine-rich domain-containing protein 1	-	-	-	-	8	4	13
Q6FI81	CIAPIN1 Anamorsin	Yes	-	-	-	3	0	37
P12277	CKB Creatine kinase B-type	-	-	-	-	24	15	18
Q14677	CLINT1 Clathrin interactor 1	-	-	-	-	2	11	7
Q9H078	CLPB Caseinolytic peptidase B protein homolog	Yes	Yes	-	-	3	19	0
O76031	CLPX ATP-dependent Clp protease ATP-binding subunit clpX-like, mitochondrial	Yes	-	-	Yes	36	8	0
Q00610	CLTC Clathrin heavy chain 1	-	-	-	-	19	35	9
Q8N0X4	CLYBL Citrate lyase subunit beta-like protein, mitochondrial	Yes	-	-	Yes	31	3	0
Q8WTW3	COG1 Conserved oligomeric Golgi complex subunit 1	-	-	-	-	0	8	10
P53621	COPA Coatomer subunit alpha	-	-	-	-	4	22	5
Q5HYK3	COQ5 2-methoxy-6-polyprenyl-1,4-benzoquinol methylase, mitochondrial	Yes	-	-	Yes	10	10	0
Q9ULV4	CORO1C Coronin-1C	-	-	-	-	7	7	27
P57737	CORO7 Coronin-7	-	-	-	-	5	11	67
P36551	CPOX Coproporphyrinogen-III oxidase, mitochondrial	Yes	Yes	Yes	Yes	16	4	0
P23786	CPT2 Carnitine O-palmitoyltransferase 2, mitochondrial	Yes	-	-	Yes	28	17	0
O75390	CS Citrate synthase, mitochondrial	Yes	-	-	Yes	22	6	0
O75534	CSDE1 Cold shock domain-containing protein E1	-	-	-	-	3	2	14
P55060	CSE1L Exportin-2	-	-	-	-	7	18	3
P33240	CSTF2 Cleavage stimulation factor subunit 2	-	-	-	-	0	2	10
P35221	CTNNA1 Catenin alpha-1	-	-	-	-	0	0	11
P17812	CTPS1 CTP synthase 1	-	-	-	-	7	4	13
Q14247	CTTN Src substrate cortactin	-	-	-	-	8	8	47
Q13620	CUL4B Cullin-4B	-	-	-	-	4	7	19
P39880	CUX1 Homeobox protein cut-like 1	-	-	-	-	0	0	12
Q6PI48	DARS2 Aspartate--tRNA ligase, mitochondrial	Yes	-	-	Yes	33	11	3
Q16643	DBN1 Drebrin	-	-	-	-	2	0	17
Q9UJU6	DBNL Drebrin-like protein	-	-	-	-	0	0	12
P11182	DBT Lipoamide acyltransferase component of branched-chain alpha-keto acid dehydrogenase complex, mitochondrial	Yes	-	-	Yes	40	15	0
G3V3G9	DCAF8 DDB1- and CUL4-associated factor 8	-	-	-	-	0	19	0
Q9NPI6	DCP1A mRNA-decapping enzyme 1A	-	-	-	-	0	7	25
Q7Z4W1	DCXR L-xylulose reductase	Yes	-	-	Yes	11	2	0
Q16531	DDB1 DNA damage-binding protein 1	-	-	-	-	4	13	4
Q13838	DDX39B Spliceosome RNA helicase DDX39B	-	-	-	-	10	13	13
O00571	DDX3X ATP-dependent RNA helicase DDX3X	Yes	-	-	-	4	21	26
Q86XP3	DDX42 ATP-dependent RNA helicase DDX42	-	-	-	-	0	6	25
Q7L014	DDX46 Probable ATP-dependent RNA helicase DDX46	-	-	-	-	4	10	21
P17844	DDX5 Probable ATP-dependent RNA helicase DDX5	-	-	-	-	5	14	11
Q16698	DECR1 2,4-dienoyl-CoA reductase, mitochondrial	Yes	-	-	Yes	10	2	0
O43143	DHX15 Putative pre-mRNA-splicing factor ATP-dependent RNA helicase DHX15	Yes	-	-	Yes	5	5	19
Q7L2E3	DHX30 Putative ATP-dependent RNA helicase DHX30	Yes	-	-	-	14	33	0
Q08211	DHX9 ATP-dependent RNA helicase A	-	-	-	-	17	32	21
Q9NSV4	DIAPH3 Protein diaphanous homolog 3	-	-	-	-	0	14	2
P10515	DLAT Dihydrolipoyllysine-residue acetyltransferase component of pyruvate dehydrogenase complex, mitochondrial	Yes	-	-	Yes	41	4	0
P09622	DLD Dihydrolipoyl dehydrogenase, mitochondrial	Yes	-	-	Yes	63	30	5
Q9NVR5	DNAAF2 Protein kintoun	-	-	-	-	0	0	10
O00429	DNM1L Dynamin-1-like protein	Yes	-	-	-	2	70	9
Q96N67	DOCK7 Dedicator of cytokinesis protein 7	-	-	-	-	3	12	14
Q16555	DPYSL2 Dihydropyrimidinase-related protein 2	-	-	-	-	3	2	11

Q14195	DPYSL3 Dihydropyrimidinase-related protein 3	-	-	-	-	0	0	12
P33316	DUT Deoxyuridine 5'-triphosphate nucleotidohydrolase, mitochondrial	Yes	-	-	-	11	2	2
O14641	DVL2 Segment polarity protein dishevelled homolog DVL-2	-	-	-	-	3	19	5
O43237	DYNC1LI2 Cytoplasmic dynein 1 light intermediate chain 2	-	-	-	-	0	4	11
Q5JPH6	EARS2 Probable glutamate--tRNA ligase, mitochondrial	Yes	-	-	Yes	12	0	0
Q13011	ECH1 Delta(3,5)-Delta(2,4)-dienoyl-CoA isomerase, mitochondrial	Yes	-	-	Yes	12	4	0
P30084	ECHS1 Enoyl-CoA hydratase, mitochondrial	Yes	-	-	Yes	17	8	3
O75521	ECI2 Enoyl-CoA delta isomerase 2, mitochondrial	Yes	-	-	Yes	20	2	0
Q96F86	EDC3 Enhancer of mRNA-decapping protein 3	-	-	-	-	5	33	61
Q6P2E9	EDC4 Enhancer of mRNA-decapping protein 4	-	-	-	-	0	2	10
P68104	EEF1A1 Elongation factor 1-alpha 1	-	-	-	-	34	36	58
Q05639	EEF1A2 Elongation factor 1-alpha 2	-	-	-	-	21	10	27
P26641	EEF1G Elongation factor 1-gamma	-	-	-	-	10	7	8
P13639	EEF2 Elongation factor 2	-	-	-	-	86	37	71
Q96C19	EFHD2 EF-hand domain-containing protein D2	-	-	-	-	0	0	12
Q15029	EFTUD2 116 kDa U5 small nuclear ribonucleoprotein component	-	-	-	-	6	12	8
Q9H9B1	EHMT1 Histone-lysine N-methyltransferase EHMT1	Yes	-	-	Yes	0	0	10
B5ME19	EIF3CL Eukaryotic translation initiation factor 3 subunit C	-	-	-	-	4	6	10
O00303	EIF3F Eukaryotic translation initiation factor 3 subunit F	-	-	-	-	0	21	5
Q7L2H7	EIF3M Eukaryotic translation initiation factor 3 subunit M	-	-	-	-	0	20	0
P23588	EIF4B Eukaryotic translation initiation factor 4B	-	-	-	-	10	11	85
Q9NRA8	EIF4ENIF1 Eukaryotic translation initiation factor 4E transporter	-	-	-	-	0	11	2
Q04637	EIF4G1 Eukaryotic translation initiation factor 4 gamma 1	-	-	-	-	12	12	65
P78344	EIF4G2 Eukaryotic translation initiation factor 4 gamma 2	-	-	-	-	6	38	23
O43432	EIF4G3 Eukaryotic translation initiation factor 4 gamma 3	-	-	-	-	3	2	15
Q6IS14	EIF5AL1 Eukaryotic translation initiation factor 5A-1-like	-	-	-	-	3	5	10
Q9BQ52	ELAC2 Zinc phosphodiesterase ELAC protein 2	Yes	-	-	Yes	15	8	4
Q9HC35	EML4 Echinoderm microtubule-associated protein-like 4	-	-	-	-	0	0	11
Q8N8S7	ENAH Protein enabled homolog	-	-	-	-	2	0	14
P06733	ENO1 Alpha-enolase	-	-	-	-	32	25	32
O43768	ENSA Alpha-endosulfine	-	-	-	-	2	3	14
O43491	EPB41L2 Band 4.1-like protein 2	-	-	-	-	3	12	38
Q9Y2J2	EPB41L3 Band 4.1-like protein 3	-	-	-	-	3	4	22
P07814	EPRS Bifunctional glutamate/proline--tRNA ligase	-	-	-	-	23	16	48
P42566	EPS15 Epidermal growth factor receptor substrate 15	-	-	-	-	0	0	17
Q9UBC2	EPS15L1 Epidermal growth factor receptor substrate 15-like 1	-	-	-	-	2	0	44
O75616	ERAL1 GTPase Era, mitochondrial	Yes	-	-	Yes	12	4	0
Q2NKX8	ERCC6L DNA excision repair protein ERCC-6-like	-	-	-	-	0	5	19
Q96HE7	ERO1L ERO1-like protein alpha	-	-	-	-	0	17	4
Q9BSJ8	ESYT1 Extended synaptotagmin-1	-	-	-	-	0	16	3
P62495	ETF1 Eukaryotic peptide chain release factor subunit 1	-	-	-	-	0	3	14
P13804	ETFA Electron transfer flavoprotein subunit alpha, mitochondrial	Yes	-	-	Yes	35	10	2
P38117	ETFB Electron transfer flavoprotein subunit beta	Yes	-	-	Yes	12	2	3
Q9NVH0	EXD2 Exonuclease 3'-5' domain-containing protein 2	-	-	-	-	0	27	0
Q96A65	EXOC4 Exocyst complex component 4	-	-	-	-	0	12	6
Q01780	EXOSC10 Exosome component 10	-	-	-	-	0	24	34
P15311	EZR Ezrin	-	-	-	-	7	9	26
Q9NZB2	FAM120A Constitutive coactivator of PPAR-gamma-like protein 1	-	-	-	-	2	3	10
Q96TA1	FAM129B Niban-like protein 1	-	-	-	-	0	0	12
Q5VWN6	FAM208B Protein FAM208B	-	-	-	-	2	3	23
Q641Q2	FAM21A WASH complex subunit FAM21A	-	-	-	-	2	3	66
Q9Y4E1	FAM21C WASH complex subunit FAM21C	-	-	-	-	2	3	58
Q14320	FAM50A Protein FAM50A	-	-	-	-	0	2	28
Q8NAN2	FAM73A Protein FAM73A	Yes	Yes	-	-	0	15	0
Q9NVI1	FANCI Fanconi anemia group I protein	-	-	-	-	2	14	5
P49327	FASN Fatty acid synthase	-	-	-	-	63	19	94
Q9NYY8	FASTKD2 FAST kinase domain-containing protein 2	Yes	-	-	Yes	13	2	0
Q7L8L6	FASTKD5 FAST kinase domain-containing protein 5	Yes	-	-	Yes	47	19	0
P22570	FDXR NADPH:adrenodoxin oxidoreductase, mitochondrial	Yes	-	-	Yes	4	12	0
P16591	FER Tyrosine-protein kinase Fer	-	-	-	-	2	0	15
Q96AC1	FERMT2 Fermitin family homolog 2	-	-	-	-	3	12	13
Q13642	FHL1 Four and a half LIM domains protein 1	-	-	-	-	4	3	19
Q9Y613	FHOD1 FH1/FH2 domain-containing protein 1	-	-	-	-	0	0	15
Q6UN15	FIP1L1 Pre-mRNA 3'-end-processing factor FIP1	-	-	-	-	0	2	23
Q9Y680	FKBP7 Peptidyl-prolyl cis-trans isomerase FKBP7	-	-	-	-	13	7	12
Q14318	FKBP8 Peptidyl-prolyl cis-trans isomerase FKBP8	Yes	-	-	-	0	16	0
P21333	FLNA Filamin-A	-	-	-	-	87	30	327
O75369	FLNB Filamin-B	-	-	-	-	18	6	18
Q14315	FLNC Filamin-C	-	-	-	-	9	0	20
Q13283	G3BP1 Ras GTPase-activating protein-binding protein 1	-	-	-	-	2	4	10
P11413	G6PD Glucose-6-phosphate 1-dehydrogenase	-	-	-	-	4	2	18
Q14697	GANAB Neutral alpha-glucosidase AB	-	-	-	-	12	30	9
P04406	GAPDH Glyceraldehyde-3-phosphate dehydrogenase	-	-	-	-	18	11	12
Q14C86	GAPVD1 GTPase-activating protein and VPS9 domain-containing protein 1	-	-	-	-	0	4	15
P41250	GARS Glycine--tRNA ligase	-	-	-	-	13	7	0
P22102	GART Trifunctional purine biosynthetic protein adenosine-3	-	-	-	-	16	6	12
Q92616	GCN1L1 Translational activator GCN1	-	-	-	-	3	11	7
Q96RP9	GFM1 Elongation factor G, mitochondrial	Yes	-	-	Yes	97	16	0
Q6Y7W6	GIGYF2 PERQ amino acid-rich with GYF domain-containing protein 2	-	-	-	-	7	12	17
Q04760	GLO1 Lactoylglutathione lyase	-	-	-	-	3	3	12
Q86SX6	GLRX5 Glutaredoxin-related protein 5, mitochondrial	Yes	-	-	Yes	11	3	0
O94925	GLS Glutaminase kidney isoform, mitochondrial	Yes	-	-	Yes	143	26	0
P00367	GLUD1 Glutamate dehydrogenase 1, mitochondrial	Yes	-	-	Yes	34	15	4
Q9UKD1	GMEB2 Glucocorticoid modulatory element-binding protein 2	-	-	-	-	0	5	10

Q08378	GOLGA3 Golgin subfamily A member 3	-	-	-	-	0	6	11
P00505	GOT2 Aspartate aminotransferase, mitochondrial	Yes	Yes	-	Yes	17	6	4
Q9BRR8	GPATCH1 G patch domain-containing protein 1	-	-	-	-	3	11	5
P43304	GPD2 Glycerol-3-phosphate dehydrogenase, mitochondrial	Yes	Yes	-	-	0	14	0
Q96D09	GPRASP2 G-protein coupled receptor-associated sorting protein 2	-	-	-	-	0	13	3
Q8TD30	GPT2 Alanine aminotransferase 2	Yes	-	-	Yes	10	0	0
Q12849	GRSF1 G-rich sequence factor 1	Yes	-	-	Yes	118	19	0
P15170	GSPT1 Eukaryotic peptide chain release factor GTP-binding subunit ERF3A	-	-	-	-	21	32	161
Q8IYD1	GSPT2 Eukaryotic peptide chain release factor GTP-binding subunit ERF3B	-	-	-	-	11	20	106
P09211	GSTP1 Glutathione S-transferase P	Yes	-	-	-	8	3	13
P13984	GTF2F2 General transcription factor IIF subunit 2	-	-	-	-	0	0	19
P78347	GTF2I General transcription factor II-I	-	-	-	-	5	11	57
A4D1E9	GTPBP10 GTP-binding protein 10	Yes	-	-	Yes	15	7	0
Q8N442	GUF1 Translation factor GUF1, mitochondrial	Yes	-	-	Yes	11	3	0
P16104	H2AFX Histone H2A.x	-	-	-	-	0	22	0
P40939	HADHA Trifunctional enzyme subunit alpha, mitochondrial	Yes	-	-	Yes	8	13	0
Q7Z4H7	HAUS6 HAUS augmin-like complex subunit 6	-	-	-	-	0	12	12
Q9Y450	HBS1L HBS1-like protein	-	-	-	-	0	3	11
P53701	HCCS Cytochrome c-type heme lyase	Yes	Yes	-	-	0	16	0
P51610	HCFC1 Host cell factor 1	-	-	-	-	10	13	44
P51858	HDGF Hepatoma-derived growth factor	-	-	-	-	0	0	12
Q00341	HDLBP Vigilin	-	-	-	-	3	3	52
Q9NRZ9	HELLS Lymphoid-specific helicase	-	-	-	-	15	52	58
Q6NVY1	HIBCH 3-hydroxyisobutyryl-CoA hydrolase, mitochondrial	Yes	-	-	Yes	38	5	0
Q9BX68	HINT2 Histidine triad nucleotide-binding protein 2, mitochondrial	Yes	-	-	Yes	10	6	0
P16403	HIST1H1C Histone H1.2	-	-	-	-	0	15	0
Q96QV6	HIST1H2AA Histone H2A type 1-A	-	-	-	-	0	22	0
Q99880	HIST1H2BL Histone H2B type 1-L	-	-	-	-	0	96	0
Q99879	HIST1H2BM Histone H2B type 1-M	-	-	-	-	0	96	0
Q16778	HIST2H2BE Histone H2B type 2-E	-	-	-	-	0	92	0
Q5QNW6	HIST2H2BF Histone H2B type 2-F	-	-	-	-	0	74	0
Q8N257	HIST3H2BB Histone H2B type 3-B	-	-	-	-	0	92	0
P62805	HIST4H4 Histone H4	-	-	-	-	3	29	0
P52789	HK2 Hexokinase-2	Yes	-	-	-	0	33	0
O75330	HMMR Hyaluronan mediated motility receptor	Yes	-	-	Yes	0	3	32
Q9UK76	HN1 Hematological and neurological expressed 1 protein	-	-	-	-	0	3	20
Q9H910	HN1L Hematological and neurological expressed 1-like protein	-	-	-	-	3	3	20
P09651	HNRNPA1 Heterogeneous nuclear ribonucleoprotein A1	-	-	-	-	30	141	316
P22626	HNRNPA2B1 Heterogeneous nuclear ribonucleoproteins A2/B1	-	-	-	-	9	33	37
P51991	HNRNPA3 Heterogeneous nuclear ribonucleoprotein A3	-	-	-	-	3	16	19
P52597	HNRNPF Heterogeneous nuclear ribonucleoprotein F	-	-	-	-	5	30	8
P31943	HNRNPH1 Heterogeneous nuclear ribonucleoprotein H	-	-	-	-	7	11	6
P61978	HNRNPK Heterogeneous nuclear ribonucleoprotein K	-	-	-	-	16	45	112
P14866	HNRNPL Heterogeneous nuclear ribonucleoprotein L	-	-	-	-	9	7	10
P52272	HNRNPM Heterogeneous nuclear ribonucleoprotein M	-	-	-	-	3	58	4
O43390	HNRNPR Heterogeneous nuclear ribonucleoprotein R	-	-	-	-	6	7	14
Q00839	HNRNPU Heterogeneous nuclear ribonucleoprotein U	-	-	-	-	21	26	48
Q9BUJ2	HNRNPUL1 Heterogeneous nuclear ribonucleoprotein U-like protein 1	-	-	-	-	0	3	23
Q99714	HSD17B10 3-hydroxyacyl-CoA dehydrogenase type-2	Yes	-	-	Yes	45	14	4
Q6YN16	HSDL2 Hydroxysteroid dehydrogenase-like protein 2	Yes	-	-	Yes	57	5	4
P07900	HSP90AA1 Heat shock protein HSP 90-alpha	-	-	-	-	26	44	35
P08238	HSP90AB1 Heat shock protein HSP 90-beta	-	-	-	-	26	45	36
P14625	HSP90B1 Endoplasmin	-	-	-	-	10	13	6
P08107	HSPA1B Heat shock 70 kDa protein 1A/1B	-	-	-	-	42	44	53
Q53FA3	HSPA1L Heat shock 70kDa protein 1-like variant	-	-	-	-	16	16	14
P54652	HSPA2 Heat shock-related 70 kDa protein 2	-	-	-	-	11	0	0
P34932	HSPA4 Heat shock 70 kDa protein 4	-	-	-	-	11	8	16
O95757	HSPA4L Heat shock 70 kDa protein 4L	-	-	-	-	7	7	10
P17066	HSPA6 Heat shock 70 kDa protein 6	-	-	-	-	14	11	0
P11142	HSPA8 Heat shock cognate 71 kDa protein	-	-	-	-	28	47	27
P38646	HSPA9 Stress-70 protein, mitochondrial	Yes	-	-	Yes	64	45	4
P10809	HSPD1 60 kDa heat shock protein, mitochondrial	Yes	-	-	Yes	240	59	29
P61604	HSPE1 10 kDa heat shock protein, mitochondrial	Yes	Yes	Yes	Yes	174	10	5
Q92598	HSPH1 Heat shock protein 105 kDa	-	-	-	-	10	15	20
O43719	HTATSF1 HIV Tat-specific factor 1	-	-	-	-	0	3	23
Q9NSE4	IARS2 Isoleucine--tRNA ligase, mitochondrial	Yes	-	-	Yes	73	31	8
P48735	IDH2 Isocitrate dehydrogenase	Yes	-	-	Yes	23	4	0
O43837	IDH3B Isocitrate dehydrogenase	Yes	-	-	Yes	17	12	2
Q13123	IK Protein Red	Yes	-	-	Yes	0	4	14
Q12906	ILF3 Interleukin enhancer-binding factor 3	-	-	-	-	5	11	15
Q9H0C8	ILKAP Integrin-linked kinase-associated serine/threonine phosphatase 2C	-	-	-	-	3	2	42
Q16891	IMMT Mitochondrial inner membrane protein	Yes	-	-	-	0	59	0
Q8TEX9	IPO4 Importin-4	-	-	-	-	3	14	2
O00410	IPO5 Importin-5	Yes	-	-	Yes	6	18	0
O95373	IPO7 Importin-7	-	-	-	-	9	31	41
O14654	IRS4 Insulin receptor substrate 4	-	-	-	-	2	23	6
Q9H1K1	ISCU Iron-sulfur cluster assembly enzyme ISCU, mitochondrial	Yes	-	-	Yes	14	3	0
Q14678	KANK1 KN motif and ankyrin repeat domain-containing protein 1	-	-	-	-	4	2	13
Q7LBC6	KDM3B Lysine-specific demethylase 3B	-	-	-	-	2	2	17
Q92945	KHSRP Far upstream element-binding protein 2	-	-	-	-	6	11	10
O15091	KIAA0391 Mitochondrial ribonuclease P protein 3	Yes	-	-	Yes	29	11	0
O75153	KIAA0664 Clustered mitochondria protein homolog	-	-	-	-	3	79	3
Q9BY89	KIAA1671 Uncharacterized protein KIAA1671	-	-	-	-	4	4	13
Q8N163	KIAA1967 DBIRD complex subunit KIAA1967	-	-	-	-	5	34	45

Q96Q89	KIF20B Kinesin-like protein KIF20B	-	-	-	-	0	2	13
P33176	KIF5B Kinesin-1 heavy chain	-	-	-	-	5	0	18
O00505	KPNA3 Importin subunit alpha-3	-	-	-	-	2	3	13
Q14974	KPNB1 Importin subunit beta-1	-	-	-	-	16	31	5
P04264	KRT1 Keratin, type II cytoskeletal 1	-	-	-	-	27	20	6
P13645	KRT10 Keratin, type I cytoskeletal 10	-	-	-	-	29	7	2
P35908	KRT2 Keratin, type II cytoskeletal 2 epidermal	-	-	-	-	23	8	2
P35527	KRT9 Keratin, type I cytoskeletal 9	-	-	-	-	20	5	3
Q86UP2	KTN1 Kinectin	-	-	-	-	0	2	13
Q6PKG0	LARP1 La-related protein 1	-	-	-	-	0	5	14
Q9P2J5	LARS Leucine--tRNA ligase, cytoplasmic	-	-	-	-	9	12	4
Q15031	LARS2 Probable leucine--tRNA ligase, mitochondrial	Yes	-	-	Yes	18	8	0
Q14739	LBR Lamin-B receptor	-	-	-	-	0	36	34
P00338	LDHA L-lactate dehydrogenase A chain	-	-	-	-	13	11	12
P07195	LDHB L-lactate dehydrogenase B chain	Yes	-	-	-	11	11	9
Q9Y2U8	LEMD3 Inner nuclear membrane protein Man1	-	-	-	-	0	23	3
O95202	LETM1 LETM1 and EF-hand domain-containing protein 1, mitochondrial	Yes	Yes	Yes	Yes	9	33	0
Q9UHB6	LIMA1 LIM domain and actin-binding protein 1	-	-	-	-	0	0	18
Q9UPQ0	LIMCH1 LIM and calponin homology domains-containing protein 1	-	-	-	-	0	0	12
Q9UGP4	LIMD1 LIM domain-containing protein 1	-	-	-	-	3	2	11
P36776	LONP1 Lon protease homolog, mitochondrial	Yes	-	-	Yes	16	2	0
P42704	LRPPRC Leucine-rich PPR motif-containing protein, mitochondrial	Yes	-	-	Yes	123	63	2
Q32MZ4	LRRFIP1 Leucine-rich repeat flightless-interacting protein 1	Yes	-	-	Yes	0	0	13
O95372	LYPLA2 Acyl-protein thioesterase 2	-	-	-	-	3	11	26
Q9Y5V3	MAGED1 Melanoma-associated antigen D1	-	-	-	-	2	12	2
P78559	MAP1A Microtubule-associated protein 1A	-	-	-	-	0	0	30
P46821	MAP1B Microtubule-associated protein 1B	-	-	-	-	13	11	114
P27816	MAP4 Microtubule-associated protein 4	-	-	-	-	27	19	312
P56192	MARS Methionine--tRNA ligase, cytoplasmic	-	-	-	-	8	6	13
Q96GW9	MARS2 Methionine--tRNA ligase, mitochondrial	Yes	-	-	Yes	14	2	0
P43243	MATR3 Matrin-3	-	-	-	-	4	24	14
Q7Z434	MAVS Mitochondrial antiviral-signaling protein	Yes	Yes	-	Yes	3	50	7
Q96RQ3	MCCC1 Methylcrotonoyl-CoA carboxylase subunit alpha, mitochondrial	Yes	-	-	-	225	346	7
Q9HCC0	MCCC2 Methylcrotonoyl-CoA carboxylase beta chain, mitochondrial	Yes	-	-	Yes	52	7	0
P33991	MCM4 DNA replication licensing factor MCM4	-	-	-	-	5	7	17
Q14676	MDC1 Mediator of DNA damage checkpoint protein 1	-	-	-	-	2	4	53
P40926	MDH2 Malate dehydrogenase, mitochondrial	Yes	-	-	Yes	73	13	9
P23368	ME2 NAD-dependent malic enzyme, mitochondrial	Yes	-	-	Yes	15	3	0
Q96RN5	MED15 Mediator of RNA polymerase II transcription subunit 15	-	-	-	-	3	11	8
Q9ULK4	MED23 Mediator of RNA polymerase II transcription subunit 23	-	-	-	-	17	18	7
Q8IWI9	MGA MAX gene-associated protein	-	-	-	-	0	7	16
O60502	MGEA5 Bifunctional protein NCOAT	-	-	-	-	0	12	4
Q8N3F8	MICALL1 MICAL-like protein 1	-	-	-	-	0	0	13
Q99797	MIPEP Mitochondrial intermediate peptidase	Yes	-	-	Yes	14	0	0
P46013	MKI67 Antigen KI-67	-	-	-	-	6	5	132
Q03164	MLL Histone-lysine N-methyltransferase MLL	-	-	-	-	0	2	13
O14686	MLL2 Histone-lysine N-methyltransferase MLL2	-	-	-	-	0	2	14
P55196	MLLT4 Afadin	-	-	-	-	4	4	22
Q96EY8	MMAB Cob(I)yrinic acid a,c-diamide adenosyltransferase, mitochondrial	Yes	-	-	Yes	20	0	0
Q00013	MPP1 55 kDa erythrocyte membrane protein	-	-	-	-	2	2	29
P49959	MRE11A Double-strand break repair protein MRE11A	-	-	-	-	14	23	58
Q9BZE1	MRPL37 39S ribosomal protein L37, mitochondrial	Yes	-	-	Yes	10	8	0
Q9H9J2	MRPL44 39S ribosomal protein L44, mitochondrial	Yes	-	-	Yes	11	5	0
I3L0E3	MRPS17 28S ribosomal protein S17, mitochondrial	-	-	-	-	10	5	0
P82650	MRPS22 28S ribosomal protein S22, mitochondrial	Yes	-	-	Yes	17	16	0
Q92665	MRPS31 28S ribosomal protein S31, mitochondrial	Yes	-	-	Yes	59	36	24
P82673	MRPS35 28S ribosomal protein S35, mitochondrial	Yes	-	-	Yes	12	4	0
P82933	MRPS9 28S ribosomal protein S9, mitochondrial	Yes	-	-	Yes	12	8	0
P20585	MSH3 DNA mismatch repair protein Msh3	-	-	-	-	0	0	12
Q9Y3D2	MSRB2 Methionine-R-sulfoxide reductase B2, mitochondrial	Yes	-	-	Yes	17	3	0
Q6UB35	MTHFD1L Monofunctional C1-tetrahydrofolate synthase, mitochondrial	Yes	-	-	Yes	61	14	2
P13995	MTHFD2 Bifunctional methylenetetrahydrofolate dehydrogenase/cyclohydrolase, mitochondrial	Yes	-	-	Yes	13	3	0
P46199	MTIF2 Translation initiation factor IF-2, mitochondrial	Yes	-	-	Yes	17	4	0
Q9Y217	MTMR6 Myotubularin-related protein 6	-	-	-	-	2	4	18
Q99707	MTR Methionine synthase	-	-	-	-	2	24	16
P22033	MUT Methylmalonyl-CoA mutase, mitochondrial	Yes	-	-	Yes	11	3	0
Q9BQG0	MYBBP1A Myb-binding protein 1A	-	-	-	-	0	13	4
P35580	MYH10 Myosin-10	-	-	-	-	5	9	17
P35579	MYH9 Myosin-9	-	-	-	-	20	16	121
Q96H55	MYO19 Unconventional myosin-XIX	Yes	-	-	-	0	17	0
Q9UM54	MYO6 Unconventional myosin-VI	-	-	-	-	9	31	48
Q4G0N4	NADKD1 NAD kinase domain-containing protein 1	Yes	-	-	Yes	44	7	0
P55209	NAP1L1 Nucleosome assembly protein 1-like 1	-	-	-	-	3	12	22
Q99733	NAP1L4 Nucleosome assembly protein 1-like 4	-	-	-	-	3	8	11
P49321	NASP Nuclear autoantigenic sperm protein	Yes	-	-	Yes	3	4	65
Q93015	NAT6 N-acetyltransferase 6	-	-	-	-	0	0	15
Q9BPX3	NCAPG Condensin complex subunit 3	-	-	-	-	2	3	18
P19338	NCL Nucleolin	-	-	-	-	6	18	42
O75376	NCOR1 Nuclear receptor corepressor 1	-	-	-	-	4	7	11
Q9Y618	NCOR2 Nuclear receptor corepressor 2	-	-	-	-	0	0	12
P56556	NDUFA6 NADH dehydrogenase	Yes	-	-	Yes	23	2	0
Q16795	NDUFA9 NADH dehydrogenase	Yes	-	-	Yes	2	11	0
Q9Y6M9	NDUFB9 NADH dehydrogenase	Yes	Yes	-	Yes	12	0	0

P28331	NDUFS1 NADH-ubiquinone oxidoreductase 75 kDa subunit, mitochondrial	Yes	-	-	Yes	66	18	0
O75306	NDUFS2 NADH dehydrogenase	Yes	-	-	Yes	22	16	0
P19404	NDUFV2 NADH dehydrogenase	Yes	-	-	Yes	15	2	0
P07197	NEFM Neurofilament medium polypeptide	-	-	-	-	0	2	66
Q96PY6	NEK1 Serine/threonine-protein kinase Nek1	-	-	-	-	0	3	11
Q8TD19	NEK9 Serine/threonine-protein kinase Nek9	-	-	-	-	2	3	10
Q9Y697	NFS1 Cysteine desulfurase, mitochondrial	Yes	-	-	Yes	18	0	0
Q6KC79	NIPBL Nipped-B-like protein	-	-	-	-	0	3	15
Q9BPW8	NIPSNAP1 Protein NipSnap homolog 1	Yes	-	-	Yes	14	5	0
Q13423	NNT NAD(P) transhydrogenase, mitochondrial	Yes	-	-	Yes	10	8	0
Q15233	NONO Non-POU domain-containing octamer-binding protein	-	-	-	-	3	18	11
Q9Y314	NOSIP Nitric oxide synthase-interacting protein	-	-	-	-	0	0	13
P06748	NPM1 Nucleophosmin	-	-	-	-	7	11	19
Q9H857	NT5DC2 5'-nucleotidase domain-containing protein 2	Yes	-	-	Yes	55	33	0
Q9Y266	NUDC Nuclear migration protein nudC	-	-	-	-	8	4	16
Q8WVJ2	NUDCD2 NudC domain-containing protein 2	-	-	-	-	24	0	5
Q9UKK9	NUDT5 ADP-sugar pyrophosphatase	-	-	-	-	0	0	19
Q9BW91	NUDT9 ADP-ribose pyrophosphatase, mitochondrial	Yes	-	-	Yes	10	3	0
Q14980	NUMA1 Nuclear mitotic apparatus protein 1	-	-	-	-	5	2	70
P57740	NUP107 Nuclear pore complex protein Nup107	-	-	-	-	0	18	2
P49790	NUP153 Nuclear pore complex protein Nup153	-	-	-	-	8	11	77
Q12769	NUP160 Nuclear pore complex protein Nup160	-	-	-	-	0	16	0
P35658	NUP214 Nuclear pore complex protein Nup214	-	-	-	-	5	12	39
Q9UKX7	NUP50 Nuclear pore complex protein Nup50	-	-	-	-	6	3	35
P52948	NUP98 Nuclear pore complex protein Nup98-Nup96	-	-	-	-	2	23	11
P04181	OAT Ornithine aminotransferase, mitochondrial	Yes	-	-	Yes	36	12	5
Q9NX40	OCIAD1 OCIA domain-containing protein 1	Yes	Yes	-	-	0	22	0
Q01968	OCRL Inositol polyphosphate 5-phosphatase OCRL-1	-	-	-	-	3	11	16
Q9UBD5	ORC3 Origin recognition complex subunit 3	-	-	-	-	0	8	17
Q15070	OXA1L Mitochondrial inner membrane protein OXA1L	Yes	-	-	Yes	0	13	0
Q9NWU1	OXSM 3-oxoacyl-[acyl-carrier-protein] synthase, mitochondrial	Yes	-	-	Yes	14	0	0
P07237	P4HB Protein disulfide-isomerase	Yes	Yes	-	-	8	5	10
P11940	PABPC1 Polyadenylate-binding protein 1	-	-	-	-	5	13	11
Q8N7H5	PAF1 RNA polymerase II-associated factor 1 homolog	-	-	-	-	0	3	11
P22234	PAICS Multifunctional protein ADE2	Yes	-	-	Yes	11	6	15
Q13177	PAK2 Serine/threonine-protein kinase PAK 2	-	-	-	-	4	8	27
P09874	PARP1 Poly	-	-	-	-	5	22	29
P11498	PC Pyruvate carboxylase, mitochondrial	Yes	-	-	-	477	477	42
Q15365	PCBP1 Poly(rC)-binding protein 1	-	-	-	-	6	12	22
Q15366	PCBP2 Poly(rC)-binding protein 2	-	-	-	-	5	9	13
P05165	PCCA Propionyl-CoA carboxylase alpha chain, mitochondrial	Yes	-	-	-	222	266	18
P05166	PCCB Propionyl-CoA carboxylase beta chain, mitochondrial	Yes	-	-	-	23	7	0
Q16822	PCK2 Phosphoenolpyruvate carboxykinase	Yes	-	-	Yes	11	3	0
P22061	PCMT1 Protein-L-isoaspartate(D-aspartate) O-methyltransferase	-	-	-	-	14	8	6
Q6L8Q7	PDE12 2',5'-phosphodiesterase 12	Yes	-	-	Yes	11	3	0
P08559	PDHA1 Pyruvate dehydrogenase E1 component subunit alpha, somatic form, mitochondrial	Yes	-	-	Yes	23	7	0
Q15118	PDK1	Yes	-	-	Yes	1175	4	2
Q15119	PDK2	Yes	-	-	Yes	66	3	0
Q15120	PDK3	Yes	-	-	Yes	140	8	0
Q16654	PDK4	Yes	-	-	-	24	0	0
O00151	PDLIM1 PDZ and LIM domain protein 1	-	-	-	-	3	0	20
Q9NR12	PDLIM7 PDZ and LIM domain protein 7	-	-	-	-	0	0	11
Q9P0J1	PDP1	Yes	-	-	Yes	22	7	0
Q8NCN5	PDPR Pyruvate dehydrogenase phosphatase regulatory subunit, mitochondrial	Yes	-	-	Yes	14	4	0
Q6P996	PDXDC1 Pyridoxal-dependent decarboxylase domain-containing protein 1	-	-	-	-	0	2	10
O96011	PEX11B Peroxisomal membrane protein 11B	-	-	-	-	0	26	0
P40855	PEX19 Peroxisomal biogenesis factor 19	-	-	-	-	0	25	0
P56589	PEX3 Peroxisomal biogenesis factor 3	-	-	-	-	0	17	0
O15067	PFAS Phosphoribosylformylglycinamidine synthase	-	-	-	-	12	5	0
P18669	PGAM1 Phosphoglycerate mutase 1	-	-	-	-	11	5	12
P00558	PGK1 Phosphoglycerate kinase 1	-	-	-	-	18	6	8
Q99623	PHB2 Prohibitin-2	Yes	-	-	-	0	24	0
Q92576	PHF3 PHD finger protein 3	Yes	-	-	Yes	0	0	11
O43175	PHGDH D-3-phosphoglycerate dehydrogenase	-	-	-	-	15	8	15
Q9BXM7	PINK1 Serine/threonine-protein kinase PINK1, mitochondrial	Yes	-	-	-	0	12	0
Q5JRX3	PITRM1 Presequence protease, mitochondrial	Yes	-	-	Yes	15	4	3
P14618	PKM Pyruvate kinase isozymes M1/M2	-	-	-	-	58	43	30
Q16512	PKN1 Serine/threonine-protein kinase N1	-	-	-	-	2	5	14
Q16513	PKN2 Serine/threonine-protein kinase N2	-	-	-	-	0	3	10
P13797	PLS3 Plastin-3	-	-	-	-	13	4	10
Q10713	PMPCA Mitochondrial-processing peptidase subunit alpha	Yes	-	-	Yes	11	8	4
O75439	PMPCB Mitochondrial-processing peptidase subunit beta	Yes	-	-	Yes	39	7	2
Q8TCS8	PNPT1 Polyribonucleotide nucleotidyltransferase 1, mitochondrial	Yes	-	-	Yes	31	15	0
Q14181	POLA2 DNA polymerase alpha subunit B	-	-	-	-	2	3	10
Q9Y2S7	POLDIP2 Polymerase delta-interacting protein 2	Yes	-	-	Yes	54	5	0
P54098	POLG DNA polymerase subunit gamma-1	Yes	-	-	Yes	16	3	0
P30876	POLR2B DNA-directed RNA polymerase II subunit RPB2	-	-	-	-	4	20	10
O14802	POLR3A DNA-directed RNA polymerase III subunit RPC1	-	-	-	-	2	11	2
O00411	POLRMT DNA-directed RNA polymerase, mitochondrial	Yes	-	-	Yes	19	9	0
Q6S8J3	POTEE POTE ankyrin domain family member E	-	-	-	-	0	14	0
Q9H2U2	PPA2 Inorganic pyrophosphatase 2, mitochondrial	Yes	-	-	Yes	53	5	3
P62937	PPIA Peptidyl-prolyl cis-trans isomerase A	-	-	-	-	12	7	6
P62136	PPP1CA Serine/threonine-protein phosphatase PP1-alpha catalytic subunit	-	-	-	-	5	0	20

P62140	PPP1CB Serine/threonine-protein phosphatase PP1-beta catalytic subunit	-	-	-	-	3	11	12
P36873	PPP1CC Serine/threonine-protein phosphatase PP1-gamma catalytic subunit	Yes	-	-	-	5	9	19
O14974	PPP1R12A Protein phosphatase 1 regulatory subunit 12A	-	-	-	-	0	2	11
P41236	PPP1R2 Protein phosphatase inhibitor 2	-	-	-	-	2	0	13
Q9UPN7	PPP6R1 Serine/threonine-protein phosphatase 6 regulatory subunit 1	-	-	-	-	0	10	9
Q5H9R7	PPP6R3 Serine/threonine-protein phosphatase 6 regulatory subunit 3	-	-	-	-	3	8	43
Q8NI37	PPTC7 Protein phosphatase PTC7 homolog	Yes	-	-	Yes	11	3	0
Q06830	PRDX1 Peroxiredoxin-1	-	-	-	-	6	2	10
P30048	PRDX3 Thioredoxin-dependent peroxide reductase, mitochondrial	Yes	Yes	-	Yes	30	5	7
P30041	PRDX6 Peroxiredoxin-6	Yes	-	-	-	17	5	10
Q4J6C6	PREPL Prolyl endopeptidase-like	Yes	-	-	Yes	19	5	0
P78527	PRKDC DNA-dependent protein kinase catalytic subunit	-	-	-	-	5	71	5
O43395	PRPF3 U4/U6 small nuclear ribonucleoprotein Prp3	-	-	-	-	5	20	47
Q6P2Q9	PRPF8 Pre-mRNA-processing-splicing factor 8	-	-	-	-	6	48	3
Q9ULL5	PRR12 Proline-rich protein 12	-	-	-	-	0	0	13
P48634	PRRC2A Protein PRRC2A	-	-	-	-	4	7	86
Q5JSZ5	PRRC2B Protein PRRC2B	-	-	-	-	0	2	22
Q9Y520	PRRC2C Protein PRRC2C	-	-	-	-	0	4	78
Q9Y617	PSAT1 Phosphoserine aminotransferase	-	-	-	-	10	3	13
Q99460	PSMD1 26S proteasome non-ATPase regulatory subunit 1	-	-	-	-	2	7	13
P61289	PSME3 Proteasome activator complex subunit 3	-	-	-	-	7	9	20
P26599	PTBP1 Polypyrimidine tract-binding protein 1	-	-	-	-	3	15	13
G3V325	PTCD1 Pentatricopeptide repeat-containing protein 1	Yes	-	-	Yes	15	10	0
Q96EY7	PTCD3 Pentatricopeptide repeat-containing protein 3, mitochondrial	Yes	-	-	Yes	19	21	0
Q9P035	PTPLAD1 3-hydroxyacyl-CoA dehydratase 3	-	-	-	-	0	13	0
Q8WUK0	PTPMT1 Phosphatidylglycerophosphatase and protein-tyrosine phosphatase 1	Yes	-	-	Yes	0	13	0
P18031	PTPN1 Tyrosine-protein phosphatase non-receptor type 1	-	-	-	-	0	13	0
Q9UHX1	PUF60 Poly(U)-binding-splicing factor PUF60	-	-	-	-	2	5	12
Q9Y606	PUS1 tRNA pseudouridine synthase A, mitochondrial	Yes	-	-	Yes	24	5	0
P32322	PYCR1 Pyrroline-5-carboxylate reductase 1, mitochondrial	Yes	-	-	Yes	35	11	0
Q96C36	PYCR2 Pyrroline-5-carboxylate reductase 2	Yes	-	-	Yes	35	16	0
Q9H0R6	QRSL1 Glutamyl-tRNA(Gln) amidotransferase subunit A, mitochondrial	Yes	-	-	Yes	30	5	0
Q6WKZ4	RAB11FIP1 Rab11 family-interacting protein 1	-	-	-	-	0	0	12
Q9BXF6	RAB11FIP5 Rab11 family-interacting protein 5	Yes	-	-	-	0	0	12
Q15042	RAB3GAP1 Rab3 GTPase-activating protein catalytic subunit	-	-	-	-	0	21	3
P62826	RAN GTP-binding nuclear protein Ran	-	-	-	-	8	7	26
P49792	RANBP2 E3 SUMO-protein ligase RanBP2	-	-	-	-	40	53	213
P46060	RANGAP1 Ran GTPase-activating protein 1	-	-	-	-	4	5	57
Q5T160	RARS2 Probable arginine--tRNA ligase, mitochondrial	Yes	-	-	Yes	20	10	0
Q8IY67	RAVER1 Ribonucleoprotein PTB-binding 1	-	-	-	-	2	19	11
Q7Z6E9	RBBP6 E3 ubiquitin-protein ligase RBBP6	-	-	-	-	0	0	13
Q96PK6	RBM14 RNA-binding protein 14	-	-	-	-	6	18	6
Q96D71	REPS1 RalBP1-associated Eps domain-containing protein 1	-	-	-	-	0	0	20
P0DJD1	RGPD2 RANBP2-like and GRIP domain-containing protein 2	-	-	-	-	0	0	18
Q15382	RHEB GTP-binding protein Rheb	-	-	-	-	3	4	19
Q5UIP0	RIF1 Telomere-associated protein RIF1	Yes	-	-	Yes	0	5	30
O15541	RNF113A RING finger protein 113A	-	-	-	-	0	0	10
P27694	RPA1 Replication protein A 70 kDa DNA-binding subunit	-	-	-	-	6	5	29
Q9H6T3	RPAP3 RNA polymerase II-associated protein 3	-	-	-	-	3	3	12
P61313	RPL15 60S ribosomal protein L15	-	-	-	-	0	15	0
P39023	RPL3 60S ribosomal protein L3	-	-	-	-	2	22	4
P36578	RPL4 60S ribosomal protein L4	-	-	-	-	2	13	2
Q02878	RPL6 60S ribosomal protein L6	-	-	-	-	2	15	0
P04843	RPN1 Dolichyl-diphosphooligosaccharide--protein glycosyltransferase subunit 1	-	-	-	-	0	13	0
P04844	RPN2 Dolichyl-diphosphooligosaccharide--protein glycosyltransferase subunit 2	-	-	-	-	0	15	0
Q5VT52	RPRD2 Regulation of nuclear pre-mRNA domain-containing protein 2	-	-	-	-	4	7	29
Q15418	RPS6KA1 Ribosomal protein S6 kinase alpha-1	-	-	-	-	0	3	17
Q9NQC3	RTN4 Reticulon-4	-	-	-	-	0	4	14
Q15424	SAFB Scaffold attachment factor B1	-	-	-	-	6	3	67
Q14151	SAFB2 Scaffold attachment factor B2	-	-	-	-	6	5	56
Q15020	SART3 Squamous cell carcinoma antigen recognized by T-cells 3	-	-	-	-	3	2	12
Q99590	SCAF11 Protein SCAF11	-	-	-	-	3	0	10
Q14160	SCRIB Protein scribble homolog	-	-	-	-	2	4	47
Q96KG9	SCYL1 N-terminal kinase-like protein	-	-	-	-	0	3	15
P31040	SDHA Succinate dehydrogenase	Yes	-	-	Yes	27	26	3
P21912	SDHB Succinate dehydrogenase	Yes	-	-	Yes	10	4	0
O15027	SEC16A Protein transport protein Sec16A	-	-	-	-	7	25	16
Q9UHD8	SEPT9 Septin-9	-	-	-	-	2	3	35
Q8NC51	SERBP1 Plasminogen activator inhibitor 1 RNA-binding protein	-	-	-	-	2	8	51
P50454	SERPINH1 Serpin H1	-	-	-	-	14	7	0
Q9BYW2	SETD2 Histone-lysine N-methyltransferase SETD2	-	-	-	-	0	0	10
Q15637	SF1 Splicing factor 1	-	-	-	-	0	8	10
Q15459	SF3A1 Splicing factor 3A subunit 1	-	-	-	-	0	3	23
O75533	SF3B1 Splicing factor 3B subunit 1	-	-	-	-	3	34	80
Q13435	SF3B2 Splicing factor 3B subunit 2	-	-	-	-	0	7	19
Q15393	SF3B3 Splicing factor 3B subunit 3	-	-	-	-	8	24	23
P23246	SFPQ Splicing factor, proline- and glutamine-rich	-	-	-	-	0	14	3
A1X283	SH3PXD2B SH3 and PX domain-containing protein 2B	-	-	-	-	2	2	17
P29353	SHC1 SHC-transforming protein 1	Yes	-	-	Yes	16	3	3
P34896	SHMT1 Serine hydroxymethyltransferase, cytosolic	-	-	-	-	11	18	0
P34897	SHMT2 Serine hydroxymethyltransferase, mitochondrial	Yes	-	-	Yes	439	155	10
Q00325	SLC25A3 Phosphate carrier protein, mitochondrial	Yes	-	-	-	0	14	0
P12235	SLC25A4 ADP/ATP translocase 1	Yes	-	-	-	0	40	0
P05141	SLC25A5 ADP/ATP translocase 2	Yes	-	-	-	7	99	0

P12236	SLC25A6 ADP/ATP translocase 3	Yes	-	-	-	7	47	0
Q9BWU0	SLC4A1AP Kanadaptin	-	-	-	-	0	0	14
Q9H2G2	SLK STE20-like serine/threonine-protein kinase	-	-	-	-	3	4	33
O60264	SMARCA5 SWI/SNF-related matrix-associated actin-dependent regulator of chromatin subfamily A member 5	-	-	-	-	3	11	11
Q92922	SMARCC1 SWI/SNF complex subunit SMARCC1	-	-	-	-	2	4	25
Q8TAQ2	SMARCC2 SWI/SNF complex subunit SMARCC2	-	-	-	-	0	0	18
Q6STE5	SMARCD3 SWI/SNF-related matrix-associated actin-dependent regulator of chromatin subfamily D member 3	-	-	-	-	12	12	4
Q96C03	SMCR7 Mitochondrial dynamic protein MID49	Yes	-	-	-	0	14	0
Q5SQN1	SNAP47 Synaptosomal-associated protein 47	-	-	-	-	0	15	0
P37840	SNCA Alpha-synuclein	-	-	-	-	4	0	28
Q16143	SNCB Beta-synuclein	-	-	-	-	0	0	13
O75643	SNRNP200 U5 small nuclear ribonucleoprotein 200 kDa helicase	-	-	-	-	7	29	30
P62316	SNRPD2 Small nuclear ribonucleoprotein Sm D2	-	-	-	-	9	7	59
Q13573	SNW1 SNW domain-containing protein 1	-	-	-	-	2	5	21
Q9Y5X1	SNX9 Sorting nexin-9	-	-	-	-	0	4	11
P18583	SON Protein SON	-	-	-	-	0	3	19
O60271	SPAG9 C-Jun-amino-terminal kinase-interacting protein 4	-	-	-	-	5	21	66
Q96T58	SPEN Msx2-interacting protein	-	-	-	-	0	0	16
Q8N0X7	SPG20 Spartin	-	-	-	-	0	6	10
Q8WW59	SPRYD4 SPRY domain-containing protein 4	Yes	-	-	Yes	64	8	0
Q13813	SPTAN1 Spectrin alpha chain, non-erythrocytic 1	-	-	-	-	7	5	48
P61011	SRP54 Signal recognition particle 54 kDa protein	-	-	-	-	0	14	16
Q9UHB9	SRP68 Signal recognition particle 68 kDa protein	-	-	-	-	0	25	12
P08240	SRPR Signal recognition particle receptor subunit alpha	-	-	-	-	0	12	10
Q9UQ35	SRRM2 Serine/arginine repetitive matrix protein 2	-	-	-	-	0	6	20
P05455	SSB Lupus La protein	-	-	-	-	6	4	13
Q04837	SSBP1 Single-stranded DNA-binding protein, mitochondrial	Yes	-	-	Yes	39	9	0
P31948	STIP1 Stress-induced-phosphoprotein 1	-	-	-	-	10	7	10
Q9UJZ1	STOML2 Stomatin-like protein 2	Yes	-	-	Yes	0	25	0
Q96SI9	STRBP Spermatid perinuclear RNA-binding protein	-	-	-	-	0	3	18
O43815	STRN Striatin	-	-	-	-	0	0	18
Q13033	STRN3 Striatin-3	-	-	-	-	0	4	11
Q9P2R7	SUCLA2 Succinyl-CoA ligase	Yes	-	-	Yes	35	11	0
Q96I99	SUCLG2 Succinyl-CoA ligase	Yes	-	-	Yes	12	0	0
Q8IX01	SUGP2 SURP and G-patch domain-containing protein 2	-	-	-	-	5	25	19
Q8IYB8	SUPV3L1 ATP-dependent RNA helicase SUPV3L1, mitochondrial	Yes	-	-	Yes	28	4	0
O15260	SURF4 Surfeit locus protein 4	-	-	-	-	0	13	0
Q9UH65	SWAP70 Switch-associated protein 70	-	-	-	-	0	3	10
Q96A49	SYAP1 Synapse-associated protein 1	-	-	-	-	3	16	41
Q92797	SYMPK Symplekin	-	-	-	-	4	15	68
O60506	SYNCRIP Heterogeneous nuclear ribonucleoprotein Q	-	-	-	-	4	6	10
O15056	SYNJ2 Synaptojanin-2	-	-	-	-	3	2	15
Q9UMZ2	SYNRG Synergin gamma	-	-	-	-	5	8	19
Q15750	TAB1 TGF-beta-activated kinase 1 and MAP3K7-binding protein 1	-	-	-	-	0	0	19
Q9Y6A5	TACC3 Transforming acidic coiled-coil-containing protein 3	-	-	-	-	0	2	13
Q9BSH4	TACO1 Translational activator of cytochrome c oxidase 1	Yes	-	-	Yes	31	7	0
P37802	TAGLN2 Transgelin-2	-	-	-	-	23	57	218
Q13148	TARDBP TAR DNA-binding protein 43	-	-	-	-	0	61	5
P26639	TARS Threonine--tRNA ligase, cytoplasmic	-	-	-	-	8	5	12
Q9BW92	TARS2 Threonine--tRNA ligase, mitochondrial	Yes	-	-	Yes	21	7	0
Q969Z0	TBRG4 Protein TBRG4	Yes	-	-	Yes	11	11	0
Q14241	TCEB3 Transcription elongation factor B polypeptide 3	-	-	-	-	0	0	14
Q9UGU0	TCF20 Transcription factor 20	-	-	-	-	4	2	14
Q13428	TCOF1 Treacle protein	-	-	-	-	5	3	91
P17987	TCP1 T-complex protein 1 subunit alpha	-	-	-	-	18	8	5
Q9Y2W6	TDRKH Tudor and KH domain-containing protein	Yes	-	-	-	0	14	0
Q8IYQ7	THNSL1 Threonine synthase-like 1	Yes	-	-	Yes	20	0	0
Q9Y2W1	THRAP3 Thyroid hormone receptor-associated protein 3	-	-	-	-	0	4	10
O43615	TIMM44 Mitochondrial import inner membrane translocase subunit TIM44	Yes	-	-	Yes	60	50	0
Q07157	TJP1 Tight junction protein ZO-1	-	-	-	-	3	3	24
P29401	TKT Transketolase	-	-	-	-	16	5	9
Q9Y490	TLN1 Talin-1	-	-	-	-	21	6	67
Q9NVH6	TMLHE Trimethyllysine dioxygenase, mitochondrial	Yes	-	-	Yes	11	4	0
Q9NYL9	TMOD3 Tropomodulin-3	-	-	-	-	0	3	12
P42166	TMPO Lamina-associated polypeptide 2, isoform alpha	-	-	-	-	3	58	38
P42167	TMPO Lamina-associated polypeptide 2, isoforms beta/gamma	-	-	-	-	4	95	49
Q6ZXV5	TMTC3 Transmembrane and TPR repeat-containing protein 3	-	-	-	-	0	15	0
Q9C0C2	TNKS1BP1 182 kDa tankyrase-1-binding protein	-	-	-	-	4	3	28
Q92973	TNPO1 Transportin-1	-	-	-	-	2	61	5
O14787	TNPO2 Transportin-2	-	-	-	-	0	16	2
Q9UPQ9	TNRC6B Trinucleotide repeat-containing gene 6B protein	-	-	-	-	2	4	11
Q15388	TOMM20 Mitochondrial import receptor subunit TOM20 homolog	Yes	-	-	-	0	13	0
O94826	TOMM70A Mitochondrial import receptor subunit TOM70	Yes	-	-	-	0	17	0
Q12888	TP53BP1 Tumor suppressor p53-binding protein 1	Yes	-	-	Yes	2	0	27
Q13625	TP53BP2 Apoptosis-stimulating of p53 protein 2	-	-	-	-	0	0	10
P60174	TPI1 Triosephosphate isomerase	-	-	-	-	14	5	9
P12270	TPR Nucleoprotein TPR	Yes	-	-	Yes	3	0	19
Q9ULW0	TPX2 Targeting protein for Xklp2	-	-	-	-	0	2	38
Q12931	TRAP1 Heat shock protein 75 kDa, mitochondrial	Yes	-	-	Yes	829	132	12
Q14258	TRIM25 E3 ubiquitin/ISG15 ligase TRIM25	-	-	-	-	0	8	15
Q13263	TRIM28 Transcription intermediary factor 1-beta	-	-	-	-	14	8	62
Q7L0Y3	TRMT10C Mitochondrial ribonuclease P protein 1	Yes	-	-	Yes	68	20	0

Q96GJ1	TRMT2B tRNA (uracil(54)-C(5))-methyltransferase homolog	Yes	-	-	Yes	11	3	0
Q9BVS5	TRMT61B Potential tRNA (adenine(58)-N(1))-methyltransferase catalytic subunit TRMT61B	Yes	-	-	Yes	17	2	0
P43897	TSFM Elongation factor Ts, mitochondrial	Yes	-	-	Yes	15	0	0
O95801	TTC4 Tetratricopeptide repeat protein 4	-	-	-	-	0	3	12
Q9UNY4	TTF2 Transcription termination factor 2	-	-	-	-	0	13	9
Q71U36	TUBA1A Tubulin alpha-1A chain	-	-	-	-	65	74	121
P68366	TUBA4A Tubulin alpha-4A chain	-	-	-	-	61	77	141
Q9NY65	TUBA8 Tubulin alpha-8 chain	-	-	-	-	42	41	94
P07437	TUBB Tubulin beta chain	-	-	-	-	45	35	54
Q9BVA1	TUBB2B Tubulin beta-2B chain	-	-	-	-	28	25	0
Q13509	TUBB3 Tubulin beta-3 chain	-	-	-	-	0	15	0
P68371	TUBB4B Tubulin beta-4B chain	-	-	-	-	36	28	41
Q9BUF5	TUBB6 Tubulin beta-6 chain	-	-	-	-	11	7	10
P49411	TUFM Elongation factor Tu, mitochondrial	Yes	-	-	Yes	38	7	5
Q6IBS0	TWF2 Twinfilin-2	-	-	-	-	3	2	40
P10599	TXN Thioredoxin	-	-	-	-	4	4	42
Q99757	TXN2 Thioredoxin, mitochondrial	Yes	-	-	Yes	13	0	0
O15042	U2SURP U2 snRNP-associated SURP motif-containing protein	Yes	-	-	Yes	3	18	13
P22314	UBA1 Ubiquitin-like modifier-activating enzyme 1	Yes	-	-	-	33	13	21
Q5T6F2	UBAP2 Ubiquitin-associated protein 2	-	-	-	-	3	0	11
Q14157	UBAP2L Ubiquitin-associated protein 2-like	-	-	-	-	8	11	31
Q9C0C9	UBE2O Ubiquitin-conjugating enzyme E2 O	-	-	-	-	0	2	12
Q9NYU2	UGGT1 UDP-glucose:glycoprotein glucosyltransferase 1	-	-	-	-	0	13	0
F5H5P2	Uncharacterized protein	Yes	-	-	Yes	17	3	0
Q92900	UPF1 Regulator of nonsense transcripts 1	-	-	-	-	9	47	45
P22695	UQCRC2 Cytochrome b-c1 complex subunit 2, mitochondrial	Yes	-	-	Yes	12	6	0
P47985	UQCRFS1 Cytochrome b-c1 complex subunit Rieske, mitochondrial	Yes	-	-	Yes	22	7	0
Q14694	USP10 Ubiquitin carboxyl-terminal hydrolase 10	-	-	-	-	2	4	18
Q9Y4E8	USP15 Ubiquitin carboxyl-terminal hydrolase 15	Yes	-	-	-	5	3	23
Q70CQ3	USP30 Ubiquitin carboxyl-terminal hydrolase 30	Yes	-	-	-	0	31	0
Q70CQ2	USP34 Ubiquitin carboxyl-terminal hydrolase 34	-	-	-	-	0	11	2
P45974	USP5 Ubiquitin carboxyl-terminal hydrolase 5	-	-	-	-	4	6	40
Q93009	USP7 Ubiquitin carboxyl-terminal hydrolase 7	-	-	-	-	4	7	34
B0V043	VARS Valyl-tRNA synthetase	-	-	-	-	6	0	13
E7ERL9	VARS2 Valine--tRNA ligase, mitochondrial	Yes	-	-	Yes	25	6	0
P61758	VBP1 Prefoldin subunit 3	-	-	-	-	2	9	13
P55072	VCP Transitional endoplasmic reticulum ATPase	-	-	-	-	12	8	17
P08670	VIM Vimentin	-	-	-	-	22	58	104
A3KMH1	VWA8 von Willebrand factor A domain-containing protein 8	Yes	-	-	Yes	32	6	0
Q7Z5K2	WAPAL Wings apart-like protein homolog	-	-	-	-	0	3	29
O75717	WDHD1 WD repeat and HMG-box DNA-binding protein 1	-	-	-	-	2	0	15
Q9HCS7	XAB2 Pre-mRNA-splicing factor SYF1	-	-	-	-	13	99	25
Q9NQH7	XPNPEP3 Probable Xaa-Pro aminopeptidase 3	Yes	-	-	Yes	25	4	0
O14980	XPO1 Exportin-1	-	-	-	-	7	20	6
P13010	XRCC5 X-ray repair cross-complementing protein 5	-	-	-	-	7	20	18
P12956	XRCC6 X-ray repair cross-complementing protein 6	-	-	-	-	5	15	6
Q8IZH2	XRN1 5'-3' exoribonuclease 1	-	-	-	-	2	12	8
Q9Y2Z4	YARS2 Tyrosine--tRNA ligase, mitochondrial	Yes	-	-	Yes	28	5	0
P49750	YLPM1 YLP motif-containing protein 1	-	-	-	-	0	4	10
Q6PJT7	ZC3H14 Zinc finger CCCH domain-containing protein 14	-	-	-	-	4	7	14
Q8WU90	ZC3H15 Zinc finger CCCH domain-containing protein 15	-	-	-	-	0	0	15
Q7Z2W4	ZC3HAV1 Zinc finger CCCH-type antiviral protein 1	-	-	-	-	3	25	12
Q7Z3T8	ZFYVE16 Zinc finger FYVE domain-containing protein 16	-	-	-	-	0	4	14
Q96NC0	ZMAT2 Zinc finger matrin-type protein 2	-	-	-	-	0	0	19
Q9UQR1	ZNF148 Zinc finger protein 148	-	-	-	-	0	2	15
P17028	ZNF24 Zinc finger protein 24	-	-	-	-	0	2	10
Q8ND82	ZNF280C Zinc finger protein 280C	-	-	-	-	0	0	11
Q9Y2X9	ZNF281 Zinc finger protein 281	-	-	-	-	5	17	7
Q5VUA4	ZNF318 Zinc finger protein 318	-	-	-	-	2	0	39
Q8TF68	ZNF384 Zinc finger protein 384	-	-	-	-	0	3	13
Q9UEG4	ZNF629 Zinc finger protein 629	-	-	-	-	0	5	24
Q14966	ZNF638 Zinc finger protein 638	-	-	-	-	0	3	32
Q8N1G0	ZNF687 Zinc finger protein 687	-	-	-	-	0	0	13
Q15942	ZYX Zyxin	-	-	-	-	5	5	56

Table 3A-2. Gene ontology (GOrilla) analysis for enrichment of biological processes for proteins identified in matrix-TID analysis.

GO Term	Description	P-value	FDR q-value	Enrichment	N	B	n	b

GO:0044281	small molecule metabolic process	3.50E-04	1.70E-01	1.21	531	196	299	134
GO:0016054	organic acid catabolic process	4.45E-04	1.80E-01	1.47	531	52	299	43
GO:0046395	carboxylic acid catabolic process	4.45E-04	1.66E-01	1.47	531	52	299	43
GO:0000959	mitochondrial RNA metabolic process	3.99E-04	1.76E-01	1.89	531	21	254	19
GO:0043436	oxoacid metabolic process	1.88E-04	1.82E-01	1.4	531	145	207	79
GO:0019752	carboxylic acid metabolic process	1.88E-04	1.52E-01	1.4	531	145	207	79
GO:0006082	organic acid metabolic process	2.80E-04	1.94E-01	1.39	531	146	207	79
GO:0017144	drug metabolic process	1.41E-04	1.71E-01	1.64	531	88	177	48
GO:0006560	proline metabolic process	1.40E-04	2.27E-01	6.99	531	5	76	5
GO:0009084	glutamine family amino acid biosynthetic process	1.37E-04	6.64E-01	6.32	531	7	72	6
GO:0006561	proline biosynthetic process	7.48E-04	2.60E-01	7.59	531	4	70	4
GO:0055129	L-proline biosynthetic process	7.48E-04	2.42E-01	7.59	531	4	70	4
GO:0097411	hypoxia-inducible factor-1alpha signaling pathway	9.38E-04	2.85E-01	44.25	531	2	12	2
GO:0006768	biotin metabolic process	1.37E-04	3.32E-01	33.19	531	6	8	3
GO:0006767	water-soluble vitamin metabolic process	3.21E-04	1.95E-01	16.59	531	16	8	4
GO:0006766	vitamin metabolic process	3.21E-04	1.73E-01	16.59	531	16	8	4

Table 3A-3. Gene ontology (GOrilla) analysis for enrichment of biological processes for proteins identified in IMS-TID analysis.

GO Term	Description	P-value	FDR q-value	Enrichment	N	B	n	b
GO:0017144	drug metabolic process	7.96E-04	2.10E-01	1.26	793	71	575	65
GO:0051240	positive regulation of multicellular organismal process	9.88E-04	2.21E-01	1.48	793	77	363	52
GO:0032481	positive regulation of type I interferon production	8.27E-05	8.00E-02	3.73	793	12	177	10
GO:0032479	regulation of type I interferon production	8.63E-04	2.18E-01	3.2	793	14	177	10
GO:0032647	regulation of interferon-alpha production	9.76E-04	2.36E-01	7.02	793	4	113	4
GO:0032727	positive regulation of interferon-alpha production	9.76E-04	2.27E-01	7.02	793	4	113	4
GO:1990542	mitochondrial transmembrane transport	3.01E-04	1.25E-01	4.93	793	23	63	9
GO:0071310	cellular response to organic substance	2.37E-04	1.25E-01	2.99	793	85	53	17
GO:0010033	response to organic substance	2.43E-04	1.18E-01	2.47	793	133	53	22
GO:1990544	mitochondrial ATP transmembrane transport	4.11E-04	1.59E-01	16.18	793	3	49	3
GO:0140021	mitochondrial ADP transmembrane transport	4.11E-04	1.49E-01	16.18	793	3	49	3
GO:0006839	mitochondrial transport	6.35E-04	2.05E-01	4.7	793	31	49	9
GO:0042026	protein refolding	4.31E-05	6.26E-02	12.31	793	7	46	5
GO:0071219	cellular response to molecule of bacterial origin	2.10E-04	1.53E-01	19.34	793	3	41	3
GO:0071222	cellular response to lipopolysaccharide	2.10E-04	1.36E-01	19.34	793	3	41	3
GO:0006334	nucleosome assembly	2.95E-04	1.32E-01	11.66	793	17	20	5
GO:0006767	water-soluble vitamin metabolic process	4.43E-06	2.57E-02	41.19	793	11	7	4
GO:0006766	vitamin metabolic process	4.43E-06	1.29E-02	41.19	793	11	7	4
GO:0006732	coenzyme metabolic process	2.16E-04	1.25E-01	12.05	793	47	7	5
GO:0051186	cofactor metabolic process	5.77E-04	1.97E-01	10.11	793	56	7	5
GO:0043436	oxoacid metabolic process	6.89E-04	2.10E-01	6.6	793	103	7	6
GO:0006082	organic acid metabolic process	6.89E-04	2.00E-01	6.6	793	103	7	6
GO:0019752	carboxylic acid metabolic process	6.89E-04	1.90E-01	6.6	793	103	7	6
GO:0032787	monocarboxylic acid metabolic process	1.20E-04	9.94E-02	12.71	793	52	6	5
GO:0006768	biotin metabolic process	8.48E-06	1.64E-02	79.3	793	6	5	3
GO:0006790	sulfur compound metabolic process	6.98E-05	8.11E-02	23.5	793	27	5	4

Table 3A-4. Gene ontology (GOrilla) analysis for enrichment of biological processes for proteins identified in cyto-TID analysis.

GO Term	Description	P-value	FDR q-value	Enrichment	N	B	n	b
GO:0043534	blood vessel endothelial cell migration	4.44E-04	5.27E-01	64.54	839	2	13	2
GO:0002576	platelet degranulation	1.79E-04	3.55E-01	35.96	839	7	10	3
GO:0030010	establishment of cell polarity	1.27E-04	7.53E-01	7.15	839	8	88	6
GO:0000226	microtubule cytoskeleton organization	8.27E-04	8.18E-01	6.27	839	52	18	7
GO:0080135	regulation of cellular response to stress	1.95E-04	2.90E-01	2.2	839	66	156	27
GO:0007049	cell cycle	1.58E-04	4.69E-01	2.18	839	58	179	27

Table 3A-5. Sum of all cysteine-containing peptides identified in matrix-TID, IMS-TID, and cyto-TID analyses. Mitochondrial localization is denoted by "mito", and is derived from uniprot subcellular localization, MitoCarta2.0, and previous studies (mito-APEX, IMS-APEX, and IMSGold+). Peptide identifications for matrix-TID and IMS-TID are the sum of 3 replicates. Protein identifications for cyto-TID are the sum of 2 replicates. Data is filtered protein identifications >10 spectral counts.

UniProt ID	Protein Description	Peptide Sequence	Mito	Total Spectral Count Matrix-TID	Total Spectral Count IMS-TID	Total Spectral Count Cyto-TID
P28288	ABCD3 ATP-binding cassette sub-family D member 3	R.TYC*DVWMIQNGTLIESGIIGR.S	Yes	0	16	0
Q13085	ACACA Acetyl-CoA carboxylase 1	R.EC*C*QPVLVYIPPQAELR.G	Yes	12	3	0
Q13085	ACACA Acetyl-CoA carboxylase 1	R.VSALNSVHC*EHVEDEGESR.Y	Yes	11	1	0
Q13085	ACACA Acetyl-CoA carboxylase 1	K.EMAQYASNITSVLC*QFPSQQIANILDSHAATL NR.K	Yes	3	29	1
Q13085	ACACA Acetyl-CoA carboxylase 1	R.MMYGVSPWGDSPIDFEDSAHVPC*PR.G	Yes	3	28	0
Q13085	ACACA Acetyl-CoA carboxylase 1	K.VQAERPDTMLGVVC*GALHVADVSLR.N	Yes	0	26	0
Q13085	ACACA Acetyl-CoA carboxylase 1	K.NLLVTMLIDQLC*GR.D	Yes	0	26	0
Q13085	ACACA Acetyl-CoA carboxylase 1	K.VQAERPDTMLGVVC*GALHVADVSLR.N	Yes	0	18	0
Q13085	ACACA Acetyl-CoA carboxylase 1	K.DNTC*VVEFQFMLPTSHPNR.G	Yes	0	17	0
Q13085	ACACA Acetyl-CoA carboxylase 1	R.TDC*NHIFLNFVPTVIMDPSK.I	Yes	2	15	0
Q13085	ACACA Acetyl-CoA carboxylase 1	K.RPGAALDPGC*VLAK.M	Yes	4	11	1
Q13085	ACACA Acetyl-CoA carboxylase 1	R.MMYGVSPWGDSPIDFEDSAHVPC*PR.G	Yes	1	11	0
Q13085	ACACA Acetyl-CoA carboxylase 1	R.TDC*NHIFLNFVPTVIMDPSKIEESVR.S	Yes	2	10	0
Q9H845	ACAD9 Acyl-CoA dehydrogenase family member 9, mitochondrial	R.AYIC*AHPLDR.T	Yes	12	2	0
P45954	ACADSB Short/branched chain specific acyl-CoA dehydrogenase, mitochondrial	K.VGSFC*LSEAGAGSDSFALK.T	Yes	15	0	0
Q99798	ACO2 Aconitate hydratase, mitochondrial	R.DLGGIVLANAC*GPC*IGQWDR.K	Yes	21	0	0
Q99798	ACO2 Aconitate hydratase, mitochondrial	R.VGLIGSC*TNSSYEDMGR.S	Yes	12	0	0
Q99798	ACO2 Aconitate hydratase, mitochondrial	R.DLGGIVLANAC*GPC*IGQWDR.K	Yes	11	0	0
P49753	ACOT2 Acyl-coenzyme A thioesterase 2, mitochondrial	R.C*C*WDEPVR.I	Yes	54	1	0
Q92667	AKAP1 A-kinase anchor protein 1, mitochondrial	K.LPAEPPALLQTHPPC*R.R	Yes	0	13	0
Q4VCS5	AMOT Angiomotin	K.MQQALVQLQAAC*EK.R	-	7	0	21
Q4VCS5	AMOT Angiomotin	R.QGNC*QPTNVSEYNAAALMELLR.E	-	5	4	17
Q8N3C0	ASCC3 Activating signal cointegrator 1 complex subunit 3	R.VEDLC*C*TLYDMLASIK.S	-	0	27	0
Q5TC12	ATPAF1 ATP synthase mitochondrial F1 complex assembly factor 1	R.AQSC*PTFLC*ALPR.R	Yes	11	1	0
Q07021	C1QBP Complement component 1 Q subcomponent-binding protein, mitochondrial	K.ALVLDC*HYPEDEVGQEDEAESDIFSIR.E	Yes	8	12	1
Q7L592	C2orf56 Protein midA homolog, mitochondrial	R.DHVEVC*PDAGVIIEELSQR.I	Yes	13	10	1
P50990	CCT8 T-complex protein 1 subunit theta	K.AHEILPNLVC*C*SAK.N	-	22	21	8
P50990	CCT8 T-complex protein 1 subunit theta	R.IGLSVSEVIEGYEIAC*R.K	-	19	156	38
P50990	CCT8 T-complex protein 1 subunit theta	K.IAVYSC*PFDGMITETK.G	-	16	19	7
P50990	CCT8 T-complex protein 1 subunit theta	K.QITSYGETC*PGLEQYAIK.K	-	16	19	21
P50990	CCT8 T-complex protein 1 subunit theta	K.LIAQAC*VSIFPDSGHFNVDNIR.V	-	14	9	19
P50990	CCT8 T-complex protein 1 subunit theta	R.LTPPVLEEMGHC*DSVYLSEVGDTQVVVFK.H	-	8	27	71
P50990	CCT8 T-complex protein 1 subunit theta	R.IGLSVSEVIEGYEIAC*R.K	-	1	21	0
P50990	CCT8 T-complex protein 1 subunit theta	K.LIAQAC*VSIFPDSGHFNVDNIR.V	-	0	12	1
P50990	CCT8 T-complex protein 1 subunit theta	R.LTPPVLEEMGHC*DSVYLSEVGDTQVVVFK.H	-	1	4	14
P23786	CPT2 Carnitine O-palmitoyltransferase 2, mitochondrial	R.QYGQTVATYESC*STAAFK.H	Yes	10	0	0
P11182	DBT Lipoamide acyltransferase component of branched-chain alpha-keto acid dehydrogenase complex, mitochondrial	K.AASLGLLQFPILNASVDENC*QNITYK.A	Yes	14	0	0
P10515	DLAT Dihydrolipoyllysine-residue acetyltransferase component of pyruvate dehydrogenase complex, mitochondrial	R.DVPLGTPLC*IIVEK.E	Yes	20	1	0
P10515	DLAT Dihydrolipoyllysine-residue acetyltransferase component of pyruvate dehydrogenase complex, mitochondrial	K.NFSAIINPPQAC*ILAIGASEDK.L	Yes	11	0	0

P09622	DLD Dihydrolipoyl dehydrogenase, mitochondrial	K.NETLGGTC*LNVGC*IPSK.A	Yes	27	3	1
P30084	ECHS1 Enoyl-CoA hydratase, mitochondrial	K.ALNALC*DGLIDELNQALK.T	Yes	16	2	2
P30084	ECHS1 Enoyl-CoA hydratase, mitochondrial	K.IC*PVETLVEEAIQC*AEK.I	Yes	0	10	0
Q96F86	EDC3 Enhancer of mRNA-decapping protein 3	K.DLPTSPVDLVINC*LDC*PENVFLR.D	-	0	20	2
Q96F86	EDC3 Enhancer of mRNA-decapping protein 3	K.ILEIPGPGDNQHFGDLHQTELGPSGAGC*QVGI NQNGTGK.F	-	0	5	13
P68104	EEF1A1 Elongation factor 1-alpha 1	K.DGNASGTTLLEALDC*ILPPTRPTDKPLR.L	-	5	17	12
P68104	EEF1A1 Elongation factor 1-alpha 1	K.SGDAAIVDMVPGKPMC*VESFSDYPPLGR.F	-	2	17	0
P13639	EEF2 Elongation factor 2	R.YVEPIEDVPC*GNIVGLVGVDQFLVK.T	-	17	4	3
P13639	EEF2 Elongation factor 2	R.ETVSEESNVLC*LSK.S	-	16	1	2
P13639	EEF2 Elongation factor 2	R.YVEPIEDVPC*GNIVGLVGVDQFLVK.T	-	10	4	15
P13639	EEF2 Elongation factor 2	R.TFC*QLILDPIFK.V	-	6	20	1
Q04637	EIF4G1 Eukaryotic translation initiation factor 4 gamma 1	R.LQGINC*GPDFTPSFANLGR.T	-	4	3	10
P78344	EIF4G2 Eukaryotic translation initiation factor 4 gamma 2	K.DMGEDLEC*LC*QIMR.T	-	0	23	0
P78344	EIF4G2 Eukaryotic translation initiation factor 4 gamma 2	K.QEGIATSDNFMQAFLNVLDQC*PK.L	-	0	10	4
P09104	ENO2 Gamma-enolase	R.SGETEDTFIADLVVGLC*TGQIK.T	-	4	10	7
P13804	ETFA Electron transfer flavoprotein subunit alpha, mitochondrial	R.LGGEVSC*LVAGTK.C	Yes	17	0	0
Q9NVH0	EXD2 Exonuclease 3'-5' domain-containing protein 2	R.SELEDFPVLGIDC*EWVNLEGK.A	-	0	13	0
Q7L8L6	FASTKD5 FAST kinase domain-containing protein 5	K.ELYTLDGTVGIEC*PDYR.G	Yes	18	0	0
Q7L8L6	FASTKD5 FAST kinase domain-containing protein 5	K.IGDLAC*ANIQHLSSR.S	Yes	12	2	0
Q13642	FHL1 Four and a half LIM domains protein 1	R.FTAVEDQYYC*VDC*YK.N	-	0	1	17
P21333	FLNA Filamin-A	R.ALGALVDSC*APGLC*PDWDSWDASKPVTNAR. E	-	6	2	22
P21333	FLNA Filamin-A	R.YWPQEAGEYAVHVLC*NSEDIR.L	-	3	3	17
P21333	FLNA Filamin-A	R.SPYTVTVGQAC*NPSAC*R.A	-	7	0	12
P21333	FLNA Filamin-A	K.AHVVPC*FDASK.V	-	5	2	10
Q96RP9	GFM1 Elongation factor G, mitochondrial	R.QELIEC*VANSDEQLGEMFLEEK.I	Yes	12	6	0
Q04760	GLO1 Lactoylglutathione lyase	R.GFGHIGIAVPDVYSAC*K.R	-	2	4	11
O94925	GLS Glutaminase kidney isoform, mitochondrial	K.FSPDLWGVSVC*TVDGQR.H	Yes	80	6	0
Q12849	GRSF1 G-rich sequence factor 1	R.YIELFLNSC*PK.G	Yes	32	5	0
P53701	HCCS Cytochrome c-type heme lyase	K.WEALHAAEC*PC*GPSLIR.F	Yes	0	10	0
P52789	HK2 Hexokinase-2	R.SASLC*AATLAAVLQR.I	Yes	0	13	0
Q9H910	HN1L Hematological and neurological expressed 1-like protein	K.DHVFLC*EGEEPK.S	-	1	3	14
P09651	HNRNPA1 Heterogeneous nuclear ribonucleoprotein A1	R.SHFEQWGTLTDC*VVMR.D	-	0	56	13
P09651	HNRNPA1 Heterogeneous nuclear ribonucleoprotein A1	R.SHFEQWGTLTDC*VVMR.D	-	0	29	3
P09651	HNRNPA1 Heterogeneous nuclear ribonucleoprotein A1	K.YHTVNGHNC*EVR.K	-	2	20	6
P52272	HNRNPM Heterogeneous nuclear ribonucleoprotein M	K.DKFNEC*GHVLYADIK.M	-	0	11	2
Q00839	HNRNPU Heterogeneous nuclear ribonucleoprotein U	K.MC*LFAGFQR.K	-	3	16	1
Q99714	HSD17B10 3-hydroxyacyl-CoA dehydrogenase type-2	R.VDVAVNC*AGIAVASK.T	Yes	14	0	0
Q99714	HSD17B10 3-hydroxyacyl-CoA dehydrogenase type-2	K.LGNNC*VFAPADVTSEKDVQTALALAK.G	Yes	10	3	1
Q6YN16	HSDL2 Hydroxysteroid dehydrogenase-like protein 2	R.LAGC*TVFITGASR.G	Yes	13	0	0
P07900	HSP90AA1 Heat shock protein HSP 90-alpha	R.LVTSPC*C*IVTSTYGWTANMER.I	-	0	11	0
P08238	HSP90AB1 Heat shock protein HSP 90-beta	R.GFEVVYMTEPIDEYC*VQQLK.E	-	1	10	0
P08238	HSP90AB1 Heat shock protein HSP 90-beta	R.LVSSPC*C*IVTSTYGWTANMER.I	-	0	10	1
P08107	HSPA1B Heat shock 70 kDa protein 1A/1B	R.ARFEELC*SDLFR.S	-	2	17	4
P38646	HSPA9 Stress-70 protein, mitochondrial	K.MEEFKDQLPADEC*NK.L	Yes	10	2	0
P10809	HSPD1 60 kDa heat shock protein, mitochondrial	R.AAVEEGIVLGGGC*ALLR.C	Yes	62	0	1
P10809	HSPD1 60 kDa heat shock protein, mitochondrial	R.AAVEEGIVLGGGC*ALLR.C	Yes	18	0	0
P10809	HSPD1 60 kDa heat shock protein, mitochondrial	R.C*IPALDSLTPANEDQK.I	Yes	16	1	0
P48735	IDH2 Isocitrate dehydrogenase	K.SSGGFVWAC*K.N	Yes	10	0	0
O43837	IDH3B Isocitrate dehydrogenase	K.LGDGLFLQC*C*EEVAELYPK.I	Yes	4	11	0
Q16891	IMMT Mitochondrial inner membrane protein	K.ANC*SDNEFTQALTAAIPPESLTR.G	Yes	0	10	0
O95373	IPO7 Importin-7	R.GIDQC*IPLFVEAALER.L	-	7	15	1
O75153	KIAA0664 Clustered mitochondria protein homolog	R.TFPPDLNFLPVPGEELPEEC*AR.A	-	0	19	0
Q8N163	KIAA1967 DBIRD complex subunit KIAA1967	R.GEASEDLC*EMALDPELLLLR.D	-	1	15	2
O95202	LETM1 LETM1 and EF-hand domain-containing protein 1, mitochondrial	K.LFEDELTLDNLTRPQLVALC*K.L	Yes	3	11	0
O95202	LETM1 LETM1 and EF-hand domain-containing protein 1, mitochondrial	K.LFEDELTLDNLTRPQLVALC*K.L	Yes	0	11	0
P42704	LRPPRC Leucine-rich PPR motif-containing protein, mitochondrial	R.LIASYC*NVGDIEGASK.I	Yes	22	0	0
P46821	MAP1B Microtubule-associated protein 1B	R.TPQASTYSYETSDLC*YTAEK.K	-	2	0	15
P46821	MAP1B Microtubule-associated protein 1B	R.QDVDLC*LVSSC*EYK.H	-	4	0	12
Q7Z434	MAVS Mitochondrial antiviral-signaling protein	R.GC*ELVDLADEVASVYQSYQPR.T	Yes	0	32	5
Q7Z434	MAVS Mitochondrial antiviral-signaling protein	R.GC*ELVDLADEVASVYQSYQPR.T	Yes	0	18	1
Q96RQ3	MCCC1 Methylcrotonoyl-CoA carboxylase subunit alpha, mitochondrial	K.TFQVLGNLYSEGDC*TYLK.C	Yes	113	90	0
Q96RQ3	MCCC1 Methylcrotonoyl-CoA carboxylase subunit alpha, mitochondrial	K.ESLC*QAALGLILK.E	Yes	23	114	2
Q96RQ3	MCCC1 Methylcrotonoyl-CoA carboxylase subunit alpha, mitochondrial	K.HNFC*FMEMNTR.L	Yes	1	59	0
Q96RQ3	MCCC1 Methylcrotonoyl-CoA carboxylase subunit alpha, mitochondrial	K.TSAAQAIHPGC*GFLSENMEFAELC*K.Q	Yes	0	32	0
Q96RQ3	MCCC1 Methylcrotonoyl-CoA carboxylase subunit alpha, mitochondrial	K.TSAAQAIHPGC*GFLSENMEFAELC*K.Q	Yes	0	12	0
Q96RQ3	MCCC1 Methylcrotonoyl-CoA carboxylase subunit alpha, mitochondrial	K.ESLC*QAALGLILK.E	Yes	0	10	0
Q9HCC0	MCCC2 Methylcrotonoyl-CoA carboxylase beta chain, mitochondrial	R.LPC*IYLVDSGGAYLPR.Q	Yes	14	1	0
P40926	MDH2 Malate dehydrogenase, mitochondrial	K.EGVVEC*SFVK.S	Yes	14	0	0

P40926	MDH2 Malate dehydrogenase, mitochondrial	K.SQETEC*TYFSTPLLLGK.K	Yes	12	3	0
P14174	MIF Macrophage migration inhibitory factor	K.LLC*GLLAER.L	-	10	3	1
P46013	MKI67 Antigen KI-67	K.ELFQTPGHTEESMTDDKITEVSC*K.S	-	1	0	12
Q92665	MRPS31 28S ribosomal protein S31, mitochondrial	R.HFMELVTC*GLSK.N	Yes	4	16	3
Q6UB35	MTHFD1L Monofunctional C1-tetrahydrofolate synthase, mitochondrial	R.AEIDLVC*ELAK.R	Yes	14	0	0
Q4G0N4	NADKD1 NAD kinase domain-containing protein 1	R.SEGHLC*LPVR.Y	Yes	11	3	0
P49321	NASP Nuclear autoantigenic sperm protein	K.YGETANEC*GEAFFFYGK.S	Yes	1	0	19
P49321	NASP Nuclear autoantigenic sperm protein	K.LGEVSVESENYVQAVEEFQSC*LNLQEQYLEAH DR.L	Yes	0	2	11
P49321	NASP Nuclear autoantigenic sperm protein	R.KPTDGASSSNC*VTDISHLVR.K	Yes	3	0	10
P28331	NDUFS1 NADH-ubiquinone oxidoreductase 75 kDa subunit, mitochondrial	K.VLFLLGADGGC*ITR.Q	Yes	11	3	0
Q9H857	NT5DC2 5'-nucleotidase domain-containing protein 2	R.FSDLYMASLSC*LLNYR.V	Yes	0	13	0
Q9UKX7	NUP50 Nuclear pore complex protein Nup50	K.NNVLIVC*VPNPPIDEK.N	-	2	0	12
Q9NX40	OCIAD1 OCIA domain-containing protein 1	R.VFAEC*NDESFWFR.S	Yes	0	41	0
Q15070	OXA1L Mitochondrial inner membrane protein OXA1L	R.C*LIFPLIVTGQR.E	Yes	0	17	0
P11498	PC Pyruvate carboxylase, mitochondrial	R.FLYEC*PWR.R	Yes	36	5	0
P11498	PC Pyruvate carboxylase, mitochondrial	R.ADFAQAC*QDAGVR.F	Yes	18	8	0
P11498	PC Pyruvate carboxylase, mitochondrial	R.AGTHILC*IK.D	Yes	14	7	1
P11498	PC Pyruvate carboxylase, mitochondrial	R.INGC*AIQC*R.V	Yes	14	4	0
P11498	PC Pyruvate carboxylase, mitochondrial	R.GLYAAFDC*TATMK.S	Yes	10	33	0
P11498	PC Pyruvate carboxylase, mitochondrial	K.DMAGLLKPTAC*TMLVSSLR.D	Yes	0	24	0
P11498	PC Pyruvate carboxylase, mitochondrial	K.DMAGLLKPTAC*TMLVSSLR.D	Yes	3	17	5
Q15365	PCBP1 Poly(rC)-binding protein 1	R.C*SDAAGYPHATHDLEGPPLDAYSIQGQHTISPL DLAK.L	-	1	5	12
Q15365	PCBP1 Poly(rC)-binding protein 1	R.C*SDAAGYPHATHDLEGPPLDAYSIQGQHTISPL DLAK.L	-	1	0	11
P05165	PCCA Propionyl-CoA carboxylase alpha chain, mitochondrial	R.C*LAAEDVVFIGPDTHAIQAMGDK.I	Yes	20	14	0
P05165	PCCA Propionyl-CoA carboxylase alpha chain, mitochondrial	R.INGWAVEC*R.V	Yes	16	2	0
P05165	PCCA Propionyl-CoA carboxylase alpha chain, mitochondrial	K.SVHC*QAGDTVGEGDLLVELE.-	Yes	14	86	0
P05165	PCCA Propionyl-CoA carboxylase alpha chain, mitochondrial	R.C*LAAEDVVFIGPDTHAIQAMGDK.I	Yes	11	25	1
P05165	PCCA Propionyl-CoA carboxylase alpha chain, mitochondrial	R.C*LAAEDVVFIGPDTHAIQAMGDKIESK.L	Yes	8	43	0
P05165	PCCA Propionyl-CoA carboxylase alpha chain, mitochondrial	R.LQVEHPVTEC*ITGLDLVQEMIR.V	Yes	5	41	0
P05165	PCCA Propionyl-CoA carboxylase alpha chain, mitochondrial	R.LQVEHPVTEC*ITGLDLVQEMIR.V	Yes	5	38	5
P05165	PCCA Propionyl-CoA carboxylase alpha chain, mitochondrial	K.MADEAVC*VGPAPTSK.S	Yes	2	12	0
P05166	PCCB Propionyl-CoA carboxylase beta chain, mitochondrial	R.IC*C*DLDVLASK.K	Yes	10	0	0
Q15118	PDK1	R.LC*DLYYINSPELELEELNAK.S	Yes	342	0	0
Q15118	PDK1	R.LC*DLYYINSPELELEELNAK.S	Yes	215	0	0
Q15118	PDK1	K.HIGSINPNC*NVLEVIK.D	Yes	102	2	1
Q15118	PDK1	K.QFLDFGSVNAC*EK.T	Yes	61	0	0
Q15118	PDK1	K.HIGSINPNC*NVLEVIK.D	Yes	56	0	0
Q15118	PDK1	K.HYNTNHEADDWC*VPSR.E	Yes	51	0	0
Q15118	PDK1	K.HYNTNHEADDWC*VPSR.E	Yes	30	0	0
Q15118	PDK1	R.RLC*DLYYINSPELELEELNAK.S	Yes	16	0	0
Q15119	PDK2	K.HIGSIDPNC*NVSEVVK.D	Yes	12	0	0
Q15120	PDK3	K.HIGSIDPTC*NVADVVK.D	Yes	38	0	0
O00151	PDLIM1 PDZ and LIM domain protein 1	K.AALANLC*IGDVITAIDGENTSNMTHLEAQNR.I	-	0	0	10
O96011	PEX11B Peroxisomal membrane protein 11B	R.FC*ITVSHLNR.A	-	0	19	0
O96011	PEX11B Peroxisomal membrane protein 11B	R.AAQYAC*SLLGHALQR.H	-	0	14	0
P56589	PEX3 Peroxisomal biogenesis factor 3	R.DMLESPDFSTVLNTC*LNR.G	-	0	10	0
O43175	PHGDH D-3-phosphoglycerate dehydrogenase	K.EELIAELQDC*EGLIVR.S	-	10	5	5
P14618	PKM Pyruvate kinase isozymes M1/M2	R.AEGSDVANAVLDGADC*IMLSGETAK.G	-	11	16	3
P14618	PKM Pyruvate kinase isozymes M1/M2	R.AGKPVIC*ATQMLESMIK.K	-	2	13	3
O43395	PRPF3 U4/U6 small nuclear ribonucleoprotein Prp3	R.VLGFSEPTVVTAALNC*VGK.G	-	3	8	36
P32322	PYCR1 Pyrroline-5-carboxylate reductase 1, mitochondrial	R.SLLINAVEASC*IR.T	Yes	12	0	0
Q9H0R6	QRSL1 Glutamyl-tRNA(Gln) amidotransferase subunit A, mitochondrial	R.C*VDDAAIVLGALAGPDPR.D	Yes	17	1	0
P62826	RAN GTP-binding nuclear protein Ran	R.VC*ENIPIVLC*GNK.V	-	1	3	19
P49792	RANBP2 E3 SUMO-protein ligase RanBP2	K.ETNPVVFFDVC*ADGEPLGR.I	-	4	3	31
P49792	RANBP2 E3 SUMO-protein ligase RanBP2	K.EGQWDC*SAC*LVQNEGSSTK.C	-	5	0	13
P49792	RANBP2 E3 SUMO-protein ligase RanBP2	R.C*VAC*QNPDKPSPSTSVPAPASFK.F	-	4	0	10
P46060	RANGAP1 Ran GTPase-activating protein 1	K.ILAAALTEC*HR.K	-	1	2	10
P35268	RPL22 60S ribosomal protein L22	K.FTLDC*THPVEDGIMDAANFEQFLQER.I	-	0	10	0
P36578	RPL4 60S ribosomal protein L4	R.FC*IWTESAFR.K	-	0	12	0
P46782	RPS5 40S ribosomal protein S5	K.TIAEC*LADELINAAK.G	-	5	17	0
Q15424	SAFB Scaffold attachment factor B1	R.KFDFDAC*NEVPPAPK.E	-	9	0	33
P31040	SDHA Succinate dehydrogenase	R.AAFGLSEAGFNTAC*VTK.L	Yes	10	2	0
P34897	SHMT2 Serine hydroxymethyltransferase, mitochondrial	R.GLELIASENFC*SR.A	Yes	176	33	0
P34897	SHMT2 Serine hydroxymethyltransferase, mitochondrial	R.YYGGAEVVDEIELLC*QR.R	Yes	128	127	2
P34897	SHMT2 Serine hydroxymethyltransferase, mitochondrial	R.YYGGAEVVDEIELLC*QR.R	Yes	71	9	0
P34897	SHMT2 Serine hydroxymethyltransferase, mitochondrial	R.AALEALGSC*LNNK.Y	Yes	20	7	0
P12235	SLC25A4 ADP/ATP translocase 1	R.YFAGNLASGGAAGATSLC*FVYPLDFAR.T	Yes	0	22	0
P12235	SLC25A4 ADP/ATP translocase 1	K.GADIMYTGTVDC*WR.K	Yes	0	12	0

P05141	SLC25A5 ADP/ATP translocase 2	K.GTDIMYTGTLDC*WR.K	Yes	1	113	0
P05141	SLC25A5 ADP/ATP translocase 2	R.KGTDIMYTGTLDC*WR.K	Yes	0	17	0
P62316	SNRPD2 Small nuclear ribonucleoprotein Sm D2	R.HC*NMVLENVK.E	-	9	3	17
P62316	SNRPD2 Small nuclear ribonucleoprotein Sm D2	K.NNTQVLINC*R.N	-	4	1	11
O15260	SURF4 Surfeit locus protein 4	R.LC*LISTFLEDGIR.M	-	0	21	0
Q96A49	SYAP1 Synapse-associated protein 1	K.TQEDEEEISTSPGVSEFVSDAFDAC*NLNQEDLR K.E	-	0	16	1
P37802	TAGLN2 Transgelin-2	K.DGTVLC*ELINALYPEGQAPVKK.I	-	5	28	38
P37802	TAGLN2 Transgelin-2	K.DGTVLC*ELINALYPEGQAPVK.K	-	5	14	12
P37802	TAGLN2 Transgelin-2	K.DGTVLC*ELINALYPEGQAPVKK.I	-	0	13	4
Q13148	TARDBP TAR DNA-binding protein 43	R.VTEDENDEPIEIPSEDDGTVLLSTVTAQFPGAC* GLR.Y	-	0	15	0
Q13148	TARDBP TAR DNA-binding protein 43	R.C*TEDMTEDELREFFSQYGDVMDVFIPKPFR.A	-	0	11	0
Q9Y2W6	TDRKH Tudor and KH domain-containing protein	R.SDFLSLPFQAIEC*SLAR.I	Yes	0	10	0
O43615	TIMM44 Mitochondrial import inner membrane translocase subunit TIM44	K.DWC*YEATYSQLAHPIQQAK.A	Yes	0	12	0
O43615	TIMM44 Mitochondrial import inner membrane translocase subunit TIM44	R.MLYVWALC*R.D	Yes	0	11	0
Q92973	TNPO1 Transportin-1	R.SNILTLMYQC*MQDK.M	-	0	30	0
Q92973	TNPO1 Transportin-1	R.SHAVAC*VNQFIISR.T	-	0	17	1
Q92973	TNPO1 Transportin-1	K.IC*EDSAEILDSDVLDRPLNIMIPK.F	-	0	11	0
O94826	TOMM70A Mitochondrial import receptor subunit TOM70	K.ILLDQVEEAVADFDEC*IR.L	Yes	0	13	0
Q12931	TRAP1 Heat shock protein 75 kDa, mitochondrial	R.NIYYLC*APNR.H	Yes	82	5	1
Q12931	TRAP1 Heat shock protein 75 kDa, mitochondrial	R.SPAAEC*LSEK.E	Yes	22	2	0
Q12931	TRAP1 Heat shock protein 75 kDa, mitochondrial	R.SPAAEC*LSEKETEELMAWMR.N	Yes	7	11	0
Q12931	TRAP1 Heat shock protein 75 kDa, mitochondrial	R.SPAAEC*LSEKETEELMAWMR.N	Yes	6	11	0
Q7L0Y3	TRMT10C Mitochondrial ribonuclease P protein 1	K.SSVQEEC*VSTISSSK.D	Yes	20	0	0
Q7L0Y3	TRMT10C Mitochondrial ribonuclease P protein 1	K.SSVQEEC*VSTISSSKDEDPLAATR.E	Yes	12	0	0
Q71U36	TUBA1A Tubulin alpha-1A chain	K.AYHEQLSVAEITNAC*FEPANQMVK.C	-	4	16	6
Q71U36	TUBA1A Tubulin alpha-1A chain	R.AVC*MLSNTTAIAEAWAR.L	-	6	10	14
Q71U36	TUBA1A Tubulin alpha-1A chain	K.AYHEQLSVAEITNAC*FEPANQMVK.C	-	2	10	9
P68366	TUBA4A Tubulin alpha-4A chain	R.SIQFVDWC*PTGFK.V	-	16	15	20
P68366	TUBA4A Tubulin alpha-4A chain	K.AYHEQLSVAEITNAC*FEPANQMVK.C	-	5	16	6
P68366	TUBA4A Tubulin alpha-4A chain	R.AVC*MLSNTTAIAEAWAR.L	-	6	10	14
P68366	TUBA4A Tubulin alpha-4A chain	K.AYHEQLSVAEITNAC*FEPANQMVK.C	-	2	10	9
P49411	TUFM Elongation factor Tu, mitochondrial	K.GEETPVIVGSALC*ALEGR.D	Yes	10	1	0
J3KR12	Uncharacterized protein	R.SLLINAVEASC*IR.T	-	18	15	0
Q70CQ3	USP30 Ubiquitin carboxyl-terminal hydrolase 30	K.ALSC*QEVTDDEVLDASC*LLDVLR.M	Yes	0	18	0
P08670	VIM Vimentin	R.RQVQSLTC*EVDALK.G	-	0	2	10
Q9HCS7	XAB2 Pre-mRNA-splicing factor SYF1	R.LWLDYC*QFLMDQGR.V	-	0	25	0
Q9HCS7	XAB2 Pre-mRNA-splicing factor SYF1	K.LWC*SLADYYIR.S	-	6	13	0
Q9HCS7	XAB2 Pre-mRNA-splicing factor SYF1	R.AIYSFC*SQIC*DPR.T	-	3	11	2
Q9HCS7	XAB2 Pre-mRNA-splicing factor SYF1	K.SNYQLWHELC*DLISQNPDK.V	-	0	11	2
P62258	YWHAE 14-3-3 protein epsilon	K.LIC*C*DILDVLDK.H	-	1	11	2
P63104	YWHAZ 14-3-3 protein zeta/delta	R.DIC*NDVLSLLEK.F	-	4	10	1

Table 3A-6. Average percent oxidation for mitochondria localized cysteines from matrix-TID analysis. Data was filtered for peptides with ratio values in 2 out of 3 replicates, with a standard deviation <30%.

Uniprot ID	Description	Peptide Sequence	Residue	Average % Oxidation Matrix-TID	Standard Deviation
Q9H857	NT5DC2 5-nucleotidase domain-containing protein 2	R.ELTDLLPPEVC*SLLNPAAIYANNEISLR.D	48	95.24%	0.00%
P54886	ALDH18A1 Delta-1-pyrroline-5-carboxylate synthase	K.GIPVMGHSEGIC*HMYVDSEASVDK.V	584	44.91%	4.01%
P80404	ABAT 4-aminobutyrate aminotransferase, mitochondrial	R.C*LEEVEDLIVK.Y	269	40.99%	20.77%
Q7Z4W1	DCXR L-xylulose reductase	R.GVPGAIVNVSSQC*SQR.A	138	37.19%	24.79%
P22830	FECH Ferrochelatase, mitochondrial	R.LEYC*NPYR.L	294	31.39%	23.06%
Q08257	CRYZ Quinone oxidoreductase	K.VHAC*GVNPVETYIR.S	45	28.35%	20.43%
P42704	LRPPRC Leucine-rich PPR motif-containing protein, mitocho	K.QLILVLC*SEENMQK.A	690	25.86%	29.83%
Q86SX6	GLRX5 Glutaredoxin-related protein 5, mitochondrial	K.GTPEQPQC*GFSNAVVQILR.L	67	25.08%	23.47%
Q8NC60	NOA1 Nitric oxide-associated protein 1	K.STLFNTLLESDYC*TAK.G	364	21.31%	14.33%
Q9BX68	HINT2 Histidine triad nucleotide-binding protein 2, mito	K.SLPADILYEDQQC*LVFR.D	75	21.02%	21.39%
P78540	ARG2 Arginase-2, mitochondrial	R.LSSLGC*HLK.D	63	19.28%	25.14%
P23786	CPT2 Carnitine O-palmitoyltransferase 2, mitochondrial	R.QYGQTVATYESC*STAAFK.H	489	18.04%	19.83%
Q8TAA5	GRPEL2 GrpE protein homolog 2, mitochondrial	K.IFGIQSFC*K.D	110	16.18%	19.78%
Q6PI48	DARS2 Aspartate--tRNA ligase, mitochondrial	K.ILC*EAPVESVVQVSGTVISRPAGQENPK. M	108	15.42%	9.23%
Q07021	C1QBP Complement component 1 Q subcomponent-binding prot	K.ALVLDC*HYPEDEVGQEDEAESDIFSIR.E	186	14.98%	2.21%
Q4G0N4	NADKD1 NAD kinase domain-containing protein 1	R.SEGHLC*LPVR.Y	193	13.52%	9.09%
Q99497	PARK7 Protein DJ-1	R.DVVIC*PDASLEDAKK.E	53	13.31%	3.21%

P43897	TSFM Elongation factor Ts, mitochondrial	K.ALETC*GGDLK.Q	71	12.68%	13.57%
Q99714	HSD17B10 3-hydroxyacyl-CoA dehydrogenase type-2	K.KLGNNC*VFAPADVTSEK.D	58	11.95%	14.46%
Q5T160	RARS2 Probable arginine--tRNA ligase, mitochondrial	R.C*DTVVSEISTGQR.T	74	11.56%	9.61%
P00505	GOT2 Aspartate aminotransferase, mitochondrial	R.VGAFTMVC*K.D	295	11.23%	5.61%
O75521	ECI2 Enoyl-CoA delta isomerase 2, mitochondrial	K.LHAVNAEEC*NVLQGR.W	368	10.40%	9.25%
Q9NSE4	IARS2 Isoleucine--tRNA ligase, mitochondrial	R.C*AEVVSGK.-	1005	9.89%	0.82%
Q9NSE4	IARS2 Isoleucine--tRNA ligase, mitochondrial	K.YTAESSDTLC*PR.C	1002	9.37%	1.11%
Q99832	CCT7 T-complex protein 1 subunit eta	K.EGTDSSQGIPQLVSNISAC*QVIAEAVR.T	29	9.13%	6.18%
Q8TCS8	PNPT1 Polyribonucleotide nucleotidyltransferase 1, mitoc	R.GQTQVLC*TVTFDSLESGIK.S	395	8.89%	7.15%
Q9H1K1	ISCU Iron-sulfur cluster assembly enzyme ISCU, mitochon	K.NVGTGLVGAPAC*GDVMK.L	69	7.65%	2.45%
Q9Y697	NFS1 Cysteine desulfurase, mitochondrial	K.DVALSSGSAC*TSASLEPSYVLR.A	381	7.53%	2.40%
P13804	ETFA Electron transfer flavoprotein subunit alpha, mito	R.TIYAGNALC*TVK.C	155	7.46%	0.19%
P05165	PCCA Propionyl-CoA carboxylase alpha chain, mitochondri	K.MADEAVC*VGPAPTSK.S	111	7.31%	0.71%
Q7Z4W1	DCXR L-xylulose reductase	R.AVTNHSVYC*STK.G	150	7.30%	2.50%
Q99497	PARK7 Protein DJ-1	K.DPVQC*SR.D	46	7.23%	2.40%
Q9P2R7	SUCLA2 Succinyl-CoA ligase	R.IC*NQVLVC*ER.K	152|158	7.06%	2.18%
Q9BVS5	TRMT61B Potential tRNA (adenine(58)-N(1))-methyltransferas	R.C*GPTHQGSEDPSMLSQAQSATEVEER.H	112	6.53%	1.53%
P40926	MDH2 Malate dehydrogenase, mitochondrial	K.GC*DVVVIPAGVPR.K	93	6.44%	1.27%
P40926	MDH2 Malate dehydrogenase, mitochondrial	K.GYLGPEQLPDC*LK.G	89	6.42%	1.54%
Q9Y3D2	MSRB2 Methionine-R-sulfoxide reductase B2, mitochondrial	R.FC*INSVALK.F	169	6.29%	1.19%
Q9UDR5	AASS Alpha-aminoadipic semialdehyde synthase, mitochond	K.EVGATIESYISYC*GGLPAPEHSNNPLR.Y	633	6.26%	2.12%
Q9BVS5	TRMT61B Potential tRNA (adenine(58)-N(1))-methyltransferas	R.HVSPSC*STSR.E	143	6.25%	0.62%
P10109	FDX1 Adrenodoxin, mitochondrial	R.LGC*QIC*LTK.S	152|155	6.04%	1.44%
Q96RQ3	MCCC1 Methylcrotonoyl-CoA carboxylase subunit alpha, mit	K.C*SVNGVASK.A	600	5.97%	0.86%
Q7L8L6	FASTKD5 FAST kinase domain-containing protein 5	K.ELYTLDGTVGIEC*PDYR.G	525	5.78%	1.76%
Q8N0X4	CLYBL Citrate lyase subunit beta-like protein, mitochond	K.IPSLNVDC*AVLDC*EDGVAANK.K	69|74	5.48%	1.24%
P04406	GAPDH Glyceraldehyde-3-phosphate dehydrogenase	K.IISNASC*TTNC*LAPLAK.V	152|156	5.46%	0.86%
Q9H4K7	GTPBP5 GTP-binding protein 5	R.APVTC*TPGQPGQQR.V	206	5.45%	1.20%
P49419	ALDH7A1 Alpha-aminoadipic semialdehyde dehydrogenase	K.VLEDNKLPGAIC*SLTC*GGADIGTAMAK.D	248|252	5.45%	0.97%
P24752	ACAT1 Acetyl-CoA acetyltransferase, mitochondrial	K.IHMGSC*AENTAK.K	196	5.42%	0.58%
P51649	ALDH5A1 Succinate-semialdehyde dehydrogenase, mitochondria	R.NTGQTC*VC*SNQFLVQR.G	340|342	5.41%	0.92%
Q96EY1	DNAJA3 DnaJ homolog subfamily A member 3, mitochondrial	R.GSIIISPC*VVC*R.G	289|292	5.38%	0.54%
Q9NSE4	IARS2 Isoleucine--tRNA ligase, mitochondrial	K.VASVASTLETTFETISTLSGVDLENGTC*SHPLIPDK.A	364	5.25%	0.45%
P42704	LRPPRC Leucine-rich PPR motif-containing protein, mitocho	R.C*VANNQVETLEK.L	930	5.07%	1.47%
P11182	DBT Lipoamide acyltransferase component of branched-ch	K.AASLGLLQFPILNASVDENC*QNITYK.A	333	4.94%	1.06%
Q5JRX3	PITRM1 Presequence protease, mitochondrial	R.SQQSKPQDASC*LPALK.V	556	4.93%	0.24%
Q6PI48	DARS2 Aspartate--tRNA ligase, mitochondrial	K.LRLEC*ADLLETR.G	459	4.88%	3.95%
P49411	TUFM Elongation factor Tu, mitochondrial	K.GEETPVIVGSALC*ALEGR.D	222	4.83%	0.11%
Q99798	ACO2 Aconitate hydratase, mitochondrial	R.DLGGIVLANAC*GPC*IGQWDR.K	448|451	4.79%	1.16%
Q9BQ52	ELAC2 Zinc phosphodiesterase ELAC protein 2	R.FGPDTQHLVLNENC*ASVHNLR.S	374	4.77%	0.02%
Q6YN16	HSDL2 Hydroxysteroid dehydrogenase-like protein 2	R.LAGC*TVFITGASR.G	11	4.76%	0.00%
Q8IYB8	SUPV3L1 ATP-dependent RNA helicase SUPV3L1, mitochondrial	K.KFNDPNDPC*K.I	418	4.76%	0.00%
Q8IYB8	SUPV3L1 ATP-dependent RNA helicase SUPV3L1, mitochondrial	K.QIFPVLDC*K.D	175	4.76%	0.00%
P42704	LRPPRC Leucine-rich PPR motif-containing protein, mitocho	K.LFEC*DR.D	952	4.76%	0.00%
P42704	LRPPRC Leucine-rich PPR motif-containing protein, mitocho	R.IHDVLC*K.L	863	4.76%	0.00%
P42704	LRPPRC Leucine-rich PPR motif-containing protein, mitocho	R.AILQENGC*LSDSDMFSQAGLR.S	500	4.76%	0.00%
P42704	LRPPRC Leucine-rich PPR motif-containing protein, mitocho	K.GMQELGVHPDQETYTDYVIPC*FDSVNSAR.A	484	4.76%	0.00%
P42704	LRPPRC Leucine-rich PPR motif-containing protein, mitocho	R.LIASYC*NVGDIEGASK.I	208	4.76%	0.00%
P43897	TSFM Elongation factor Ts, mitochondrial	K.YGALVIC*ETSEQK.T	240	4.76%	0.00%
P48735	IDH2 Isocitrate dehydrogenase	K.SSGGFVWAC*K.N	308	4.76%	0.00%
Q16822	PCK2 Phosphoenolpyruvate carboxykinase	K.YNNC*WLAR.T	92	4.76%	0.00%
Q02252	ALDH6A1 Methylmalonate-semialdehyde dehydrogenase	K.AEMDAAIASC*K.R	86	4.76%	0.00%
O75616	ERAL1 GTPase Era, mitochondrial	R.C*QALGVITEK.E	150	4.76%	0.00%
P05091	ALDH2 Aldehyde dehydrogenase, mitochondrial	K.LLC*GGGIAADR.G	386	4.76%	0.00%
P22033	MUT Methylmalonyl-CoA mutase, mitochondrial	R.AHC*QTSGWSLTEQDPYNNIVR.T	351	4.76%	0.00%
P11182	DBT Lipoamide acyltransferase component of branched-ch	K.IPHFGYC*DEIDLTELVK.L	279	4.76%	0.00%
P08559	PDHA1 Pyruvate dehydrogenase E1 component subunit alpha,	R.FAAAYC*R.S	273	4.76%	0.00%
P08559	PDHA1 Pyruvate dehydrogenase E1 component subunit alpha,	R.VDGMDILC*VR.E	261	4.76%	0.00%
P11177	PDHB Pyruvate dehydrogenase E1 component subunit beta,	R.PVGHC*LEAAAVLSK.E	249	4.76%	0.00%
P08559	PDHA1 Pyruvate dehydrogenase E1 component subunit alpha,	K.NFYGGNGIVGAQVPLGAGIALAC*K.Y	181	4.76%	0.00%
P10515	DLAT Dihydrolipoyllysine-residue acetyltransferase comp	R.DVPIGAIIC*ITVGKPEDIEAFK.N	164	4.76%	0.00%
P30084	ECHS1 Enoyl-CoA hydratase, mitochondrial	K.EMQNLSFQDC*YSSK.F	111	4.76%	0.00%
P11182	DBT Lipoamide acyltransferase component of branched-ch	K.EGDTVSQFDSIC*EVQSDK.A	99	4.76%	0.00%
Q7L8L6	FASTKD5 FAST kinase domain-containing protein 5	K.AAVPLGGFLC*NVADK.S	670	4.76%	0.00%

Q9NYY8	FASTKD2 FAST kinase domain-containing protein 2	R.SAYC*LGSSHPR.G	645	4.76%	0.00%
Q7L8L6	FASTKD5 FAST kinase domain-containing protein 5	K.IGDLAC*ANIQHLSSR.S	345	4.76%	0.00%
Q7L0Y3	TRMT10C Mitochondrial ribonuclease P protein 1	K.RLNLATEC*LPLDK.Y	335	4.76%	0.00%
Q7L0Y3	TRMT10C Mitochondrial ribonuclease P protein 1	R.NVDPFHIYFC*NLK.I	246	4.76%	0.00%
Q7L8L6	FASTKD5 FAST kinase domain-containing protein 5	R.VNQNNLQAQVIVDYLC*K.L	168	4.76%	0.00%
Q9HCC0	MCCC2 Methylcrotonoyl-CoA carboxylase beta chain, mitoch	R.VSGVEC*MIIANDATVK.G	131	4.76%	0.00%
Q5JRX3	PITRM1 Presequence protease, mitochondrial	R.LLPDHTYSVVSGGDPLC*IPELTWEQLK.Q	241	4.76%	0.00%
Q9NSE4	IARS2 Isoleucine--tRNA ligase, mitochondrial	K.KPGLEEAVESAC*AMR.D	883	4.76%	0.00%
Q5JRX3	PITRM1 Presequence protease, mitochondrial	K.LGC*GLLDYR.E	627	4.76%	0.00%
Q6PI48	DARS2 Aspartate--tRNA ligase, mitochondrial	R.LIC*LVTGSPSIR.D	590	4.76%	0.00%
P36776	LONP1 Lon protease homolog, mitochondrial	K.ILC*FYGPPGVGK.T	520	4.76%	0.00%
Q96I59	NARS2 Probable asparagine--tRNA ligase, mitochondrial	R.YLQC*ILGVDNIK.D	455	4.76%	0.00%
Q02218	OGDH 2-oxoglutarate dehydrogenase, mitochondrial	R.FGLEGC*EVLIPALK.T	283	4.76%	0.00%
Q9P0J1	PDP1	R.VAFSGATAC*VAHVDGVDLHVANTGDSR.A	275	4.76%	0.00%
Q15031	LARS2 Probable leucine--tRNA ligase, mitochondrial	K.EALVNWDPVDQTVLANEQVDEHGC*SWR.S	225	4.76%	0.00%
Q15031	LARS2 Probable leucine--tRNA ligase, mitochondrial	R.LGLC*FSWDR.E	167	4.76%	0.00%
P04181	OAT Ornithine aminotransferase, mitochondrial	K.VLPMNTGVEAGETAC*K.L	150	4.76%	0.00%
Q96GW9	MARS2 Methionine--tRNA ligase, mitochondrial	K.IQQAAATAGLAPTELC*DR.V	114	4.76%	0.00%
P13804	ETFA Electron transfer flavoprotein subunit alpha, mito	K.QFNYTHIC*AGASAFGK.N	109	4.76%	0.00%
Q8NCN5	PDPR Pyruvate dehydrogenase phosphatase regulatory subu	R.FC*AGILSTAR.H	85	4.76%	0.00%
Q9H649	NSUN3 Putative methyltransferase NSUN3	R.EILTSPSC*WQYAVLLNR.F	49	4.76%	0.00%
Q8NI37	PPTC7 Protein phosphatase PTC7 homolog	R.AGGGGGGDYGLVTAGC*GFGK.D	41	4.76%	0.00%
P36551	CPOX Coproporphyrinogen-III oxidase, mitochondrial	K.WC*DDYFFIAHR.G	319	4.76%	0.00%
P36551	CPOX Coproporphyrinogen-III oxidase, mitochondrial	R.C*SSFMAPPVTDLGELR.R	127	4.76%	0.00%
P28331	NDUFS1 NADH-ubiquinone oxidoreductase 75 kDa subunit, mit	K.VLFLLGADGGC*ITR.Q	554	4.76%	0.00%
P28331	NDUFS1 NADH-ubiquinone oxidoreductase 75 kDa subunit, mit	R.VDSDTLC*TEEVFPTAGAGTDLR.S	367	4.76%	0.00%
P12532	CKMT1B Creatine kinase U-type, mitochondrial	R.LGYILTC*PSNLGTGLR.A	316	4.76%	0.00%
O75306	NDUFS2 NADH dehydrogenase	R.IIAQC*LNK.M	347	4.76%	0.00%
Q9H845	ACAD9 Acyl-CoA dehydrogenase family member 9, mitochondr	K.FEENTYC*FGR.T	507	4.76%	0.00%
Q8NC60	NOA1 Nitric oxide-associated protein 1	K.ENC*ILNLLTEK.E	505	4.76%	0.00%
O43615	TIMM44 Mitochondrial import inner membrane translocase su	K.DWC*YEATYSQLAHPIQQAK.A	343	4.76%	0.00%
O95202	LETM1 LETM1 and EF-hand domain-containing protein 1, mit	K.LFEDELTLDNLTRPQLVALC*K.L	330	4.76%	0.00%
P31040	SDHA Succinate dehydrogenase	R.TYFSC*TSAHTSTGDGTAMITR.A	266	4.76%	0.00%
Q5HYK3	COQ5 2-methoxy-6-polyprenyl-1,4-benzoquinol methylase,	R.FLC*LEFSQVNNPLISR.L	244	4.76%	0.00%
Q9H845	ACAD9 Acyl-CoA dehydrogenase family member 9, mitochondr	K.LASGEHIAAFC*LTEPASGSDAASIR.S	179	4.76%	0.00%
Q5TEU4	NDUFAF5 NADH dehydrogenase	R.NFPLALDLGC*GR.G	98	4.76%	0.00%
P31040	SDHA Succinate dehydrogenase	R.AAFGLSEAGFNTAC*VTK.L	89	4.76%	0.00%
O75380	NDUFS6 NADH dehydrogenase	R.VIAC*DGGGGALGHPK.V	87	4.76%	0.00%
Q9Y6M9	NDUFB9 NADH dehydrogenase	R.YFAC*LMR.A	42	4.76%	0.00%
Q9Y6M9	NDUFB9 NADH dehydrogenase	R.HLESWC*VQR.D	31	4.76%	0.00%
Q4G0N4	NADKD1 NAD kinase domain-containing protein 1	K.SSGLNLC*TGTGSK.A	311	4.76%	0.00%
Q7L592	C2orf56 Protein midA homolog, mitochondrial	R.DHVEVC*PDAGVIIEELSQR.I	275	4.76%	0.00%
Q9BQP7	C20orf72 Uncharacterized protein C20orf72	R.ALESAVQHETLNYIGLLDC*VAEYQGK.L	239	4.76%	0.00%
O43766	LIAS Lipoyl synthase, mitochondrial	R.NLNLHTVC*EEAR.C	106	4.76%	0.00%
Q99798	ACO2 Aconitate hydratase, mitochondrial	R.VGLIGSC*TNSSYEDMGR.S	385	4.76%	0.00%
P30048	PRDX3 Thioredoxin-dependent peroxide reductase, mitochon	K.AFQYVETHGEVC*PANWTPDSPTIKPSPAASK.E	229	4.76%	0.00%
Q6UB35	MTHFD1L Monofunctional C1-tetrahydrofolate synthase, mitoc	R.AGAFDAVPC*YHWSVGGK.G	828	4.76%	0.00%
Q6UB35	MTHFD1L Monofunctional C1-tetrahydrofolate synthase, mitoc	R.AEIDLVC*ELAK.R	814	4.76%	0.00%
Q9Y4W6	AFG3L2 AFG3-like protein 2	R.MC*MTLGGR.V	626	4.76%	0.00%
P38646	HSPA9 Stress-70 protein, mitochondrial	K.MEEFKDQLPADEC*NK.L	608	4.76%	0.00%
P31327	CPS1 Carbamoyl-phosphate synthase	R.SAYALGGLGSGIC*PNR.E	600	4.76%	0.00%
Q3SY69	ALDH1L2 Mitochondrial 10-formyltetrahydrofolate dehydrogen	R.YFAGWC*DK.I	558	4.76%	0.00%
P40939	HADHA Trifunctional enzyme subunit alpha, mitochondrial	R.C*LAPMMSEVIR.I	550	4.76%	0.00%
Q9H0R6	QRSL1 Glutamyl-tRNA(Gln) amidotransferase subunit A, mit	K.QVQFPVIQLQELMDDC*SAVLENEK.L	512	4.76%	0.00%
Q9H0R6	QRSL1 Glutamyl-tRNA(Gln) amidotransferase subunit A, mit	R.AFC*DQQLLTVAK.W	483	4.76%	0.00%
Q9P2R7	SUCLA2 Succinyl-CoA ligase	K.ILAC*DDLDEAAR.M	430	4.76%	0.00%
Q96EY7	PTCD3 Pentatricopeptide repeat-containing protein 3, mit	K.DPDDDKFFQSAMSIC*SSLR.D	423	4.76%	0.00%
O00411	POLRMT DNA-directed RNA polymerase, mitochondrial	R.VC*VVSVEKPTLPSK.E	413	4.76%	0.00%
Q9BVS5	TRMT61B Potential tRNA (adenine(58)-N(1))-methyltransferas	R.DWLVC*LAK.Q	396	4.76%	0.00%
Q9P2R7	SUCLA2 Succinyl-CoA ligase	R.C*DVIAQGIVMAVK.D	384	4.76%	0.00%
P82675	MRPS5 28S ribosomal protein S5, mitochondrial	R.EEC*GPLPIVVASPR.G	377	4.76%	0.00%
O15091	KIAA0391 Mitochondrial ribonuclease P protein 3	K.TIESIQLSPEEYEC*LK.G	367	4.76%	0.00%
Q92665	MRPS31 28S ribosomal protein S31, mitochondrial	R.HFMELVTC*GLSK.N	356	4.76%	0.00%
P82933	MRPS9 28S ribosomal protein S9, mitochondrial	K.HDVTC*TVSGGGR.S	330	4.76%	0.00%
Q9Y305	ACOT9 Acyl-coenzyme A thioesterase 9, mitochondrial	K.SLEIC*HPQER.N	299	4.76%	0.00%
P49411	TUFM Elongation factor Tu, mitochondrial	K.KGDEC*ELLGHSK.N	290	4.76%	0.00%
Q9UGC7	MTRF1L Peptide chain release factor 1-like, mitochondrial	R.IVHLPTGVVSEC*QQER.S	274	4.76%	0.00%
Q96I99	SUCLG2 Succinyl-CoA ligase	K.IDATQVEVNPFGETPEGQVVC*FDAK.I	255	4.76%	0.00%
P34897	SHMT2 Serine hydroxymethyltransferase, mitochondrial	R.MREVC*DEVK.A	241	4.76%	0.00%
Q9H0R6	QRSL1 Glutamyl-tRNA(Gln) amidotransferase subunit A, mit	R.C*VDDAAIVLGALAGPDPR.D	236	4.76%	0.00%
P82933	MRPS9 28S ribosomal protein S9, mitochondrial	K.LLTSQC*GAAEEEFVQR.F	233	4.76%	0.00%
Q9BZE1	MRPL37 39S ribosomal protein L37, mitochondrial	R.IC*VQNSTFSATWNR.E	203	4.76%	0.00%
Q6UB35	MTHFD1L Monofunctional C1-tetrahydrofolate synthase, mitoc	R.GDAHEC*FVSPVAK.A	198	4.76%	0.00%
Q7Z7H8	MRPL10 39S ribosomal protein L10, mitochondrial	R.TVPFLPLLGGC*IDDTILSR.Q	180	4.76%	0.00%

Q3SY69	ALDH1L2 Mitochondrial 10-formyltetrahydrofolate dehydrogen	R.SC*DVEPNDTVDALYNR.F	174	4.76%	0.00%
Q9NX20	MRPL16 39S ribosomal protein L16, mitochondrial	R.C*EFEEVQGFLDQVAHK.L	167	4.76%	0.00%
P49411	TUFM Elongation factor Tu, mitochondrial	K.NMITGTAPLDGC*ILVVAANDGPMPQTR.E	147	4.76%	0.00%
O14561	NDUFAB1 Acyl carrier protein, mitochondrial	K.LMC*PQEIVDYIADK.K	140	4.76%	0.00%
Q96EL2	MRPS24 28S ribosomal protein S24, mitochondrial	R.GNQLEIC*AVVLR.Q	120	4.76%	0.00%
P24752	ACAT1 Acetyl-CoA acetyltransferase, mitochondrial	R.QAVLGAGLPISTPC*TTINK.V	119	4.76%	0.00%
Q9BSH4	TACO1 Translational activator of cytochrome c oxidase 1	K.EGGPNPEHNSNLANILEVC*R.S	112	4.76%	0.00%
Q9NUJ1	ABHD10 Abhydrolase domain-containing protein 10, mitochon	K.SLGHAC*IR.F	107	4.76%	0.00%
Q9NUJ1	ABHD10 Abhydrolase domain-containing protein 10, mitochon	K.ALAIEEFC*K.S	100	4.76%	0.00%
Q6NVY1	HIBCH 3-hydroxyisobutyryl-CoA hydrolase, mitochondrial	K.AFC*AGGDIR.V	95	4.76%	0.00%
O75570	MTRF1 Peptide chain release factor 1, mitochondrial	K.EYQTLEQC*LQHIPVNEENRR.S	92	4.76%	0.00%
Q9NWU1	OXSM 3-oxoacyl-	K.SIPC*SVAAYVPR.G	86	4.76%	0.00%
Q13085	ACACA Acetyl-CoA carboxylase 1	K.RVSALNSVHC*EHVEDEGESR.Y	1769	4.76%	0.00%
Q13085	ACACA Acetyl-CoA carboxylase 1	R.NFDLTAIPC*ANHK.M	1396	4.76%	0.00%
Q13085	ACACA Acetyl-CoA carboxylase 1	K.RPGAALDPGC*VLAK.M	813	4.76%	0.00%
Q13085	ACACA Acetyl-CoA carboxylase 1	R.MMYGVSPWGDSPIDFEDSAHVPC*PR.G	500	4.76%	0.00%
Q13085	ACACA Acetyl-CoA carboxylase 1	K.IIEEAPATIATPAVFEHMEQC*AVK.L	407	4.76%	0.00%
Q4J6C6	PREPL Prolyl endopeptidase-like	K.LNGLADLEAC*IK.T	538	4.76%	0.00%
P49327	FASN Fatty acid synthase	R.DGLLENQTPEFFQDVC*KPK.Y	1992	4.76%	0.00%
O94925	GLS Glutaminase kidney isoform, mitochondrial	R.LKEC*MDMLR.L	178	4.76%	0.00%
O75521	ECI2 Enoyl-CoA delta isomerase 2, mitochondrial	R.WLSDEC*TNAVVNFLSR.K	380	4.76%	0.00%
Q9NQH7	XPNPEP3 Probable Xaa-Pro aminopeptidase 3	K.FEFEC*R.A	290	4.76%	0.00%
Q12849	GRSF1 G-rich sequence factor 1	R.GLPYSC*NEK.D	261	4.76%	0.00%
Q9H1K1	ISCU Iron-sulfur cluster assembly enzyme ISCU, mitochon	K.LHC*SMLAEDAIK.A	138	4.76%	0.00%
G3V325	PTCD1 Pentatricopeptide repeat-containing protein 1	R.DC*GLGDPQVASELLLKPR.E	381	4.76%	0.00%
G3V325	PTCD1 Pentatricopeptide repeat-containing protein 1	R.DLEPSDATYTALFNVC*AESPWK.D	267	4.76%	0.00%
Q8TD30	GPT2 Alanine aminotransferase 2	K.LLEETGIC*VVPGSGFGQR.E	477	4.76%	0.00%
Q8TD30	GPT2 Alanine aminotransferase 2	K.LFLLADEVYQDNVYSPDC*R.F	311	4.76%	0.00%
Q96GJ1	TRMT2B tRNA (uracil(54)-C(5))-methyltransferase homolog	R.DGNVVC*VQSNHLK.N	185	4.76%	0.00%
Q9BPW8	NIPSNAP1 Protein NipSnap homolog 1	R.FSGGYPALMDC*MNK.L	138	4.76%	0.00%
Q8WW59	SPRYD4 SPRY domain-containing protein 4	R.DSC*IGVDDR.S	114	4.76%	0.00%
Q8WV74	NUDT8 Nucleoside diphosphate-linked moiety X motif 8, mi	R.PASAAVLVPLC*SVR.G	39	4.76%	0.00%
Q9UBQ7	GRHPR Glyoxylate reductase/hydroxypyruvate reductase	R.AADC*EVEQWDSDEPIPAK.E	29	4.76%	0.00%
I3L0E3	MRPS17 28S ribosomal protein S17, mitochondrial	K.TYFAHDALQQC*TVGDIVLLR.A	153	4.76%	0.00%
Q9UMS0	NFU1 NFU1 iron-sulfur cluster scaffold homolog, mitocho	K.LQGSC*TSC*PSSIITLK.N	210|213	4.76%	0.00%
P26440	IVD Isovaleryl-CoA dehydrogenase, mitochondrial	R.GSNTC*ELIFEDC*K.I	254|261	4.76%	0.00%
P23368	ME2 NAD-dependent malic enzyme, mitochondrial	R.C*LPVC*IDVGTDNIALLK.D	198|202	4.76%	0.00%
P38117	ETFB Electron transfer flavoprotein subunit beta	K.EVIAVSC*GPAQC*QETIR.T	66|71	4.76%	0.00%
P05166	PCCB Propionyl-CoA carboxylase beta chain, mitochondria	R.IC*C*DLDVLASK.K	516|517	4.76%	0.00%
Q9BQ52	ELAC2 Zinc phosphodiesterase ELAC protein 2	R.TC*DLEEFQTC*LVR.H	632|640	4.76%	0.00%
Q96RP9	GFM1 Elongation factor G, mitochondrial	R.EYGC*PC*ITGK.P	514|516	4.76%	0.00%
P54098	POLG DNA polymerase subunit gamma-1	R.TPVLGC*C*ISR.A	1077|1078	4.76%	0.00%
Q7Z4W1	DCXR L-xylulose reductase	R.EC*PGIEPVC*VDLGDWEATER.A	51|58	4.76%	0.00%
Q13085	ACACA Acetyl-CoA carboxylase 1	R.EC*C*QPVLVYIPPQAELR.G	2074|2075	4.76%	0.00%
P31040	SDHA Succinate dehydrogenase	R.C*C*C*VADR.T	189|190|191	4.76%	0.00%
Q7L0Y3	TRMT10C Mitochondrial ribonuclease P protein 1	K.SSVQEEC*VSTISSSK.D	78	4.76%	0.00%
P19404	NDUFV2 NADH dehydrogenase	R.FSC*EPAGGLTSLTEPPK.G	225	4.72%	1.45%
P09622	DLD Dihydrolipoyl dehydrogenase, mitochondrial	K.NETLGGTC*LNVGC*IPSK.A	80|85	4.71%	0.76%
P05165	PCCA Propionyl-CoA carboxylase alpha chain, mitochondri	K.SVHC*QAGDTVGEGDLLVELE.-	712	4.53%	0.46%
P49753	ACOT2 Acyl-coenzyme A thioesterase 2, mitochondrial	R.C*C*WDEPVR.I	75|76	4.53%	0.55%
P13995	MTHFD2 Bifunctional methylenetetrahydrofolate dehydrogena	R.IC*NAVSPDKDVDGFHVINVGR.M	145	4.46%	0.53%
P00505	GOT2 Aspartate aminotransferase, mitochondrial	K.EYLPIGGLAEFC*K.A	106	4.46%	0.53%
Q8N5M1	ATPAF2 ATP synthase mitochondrial F1 complex assembly fac	K.FLDTDTIC*YR.V	141	4.46%	0.53%
P05165	PCCA Propionyl-CoA carboxylase alpha chain, mitochondri	R.INGWAVEC*R.V	398	4.40%	0.50%
P49327	FASN Fatty acid synthase	R.C*VLLSNLSSTSHVPEVDPGSAELQK.V	1471	4.39%	0.83%
P10515	DLAT Dihydrolipoyllysine-residue acetyltransferase comp	K.NFSAIINPPQAC*ILAIGASEDK.L	586	4.30%	0.92%
Q96RQ3	MCCC1 Methylcrotonoyl-CoA carboxylase subunit alpha, mit	K.TFQVLGNLYSEGDC*TYLK.C	595	4.30%	0.92%
Q96RP9	GFM1 Elongation factor G, mitochondrial	R.QELIEC*VANSDEQLGEMFLEEK.I	256	4.30%	0.92%

Q5JPH6	EARS2 Probable glutamate--tRNA ligase, mitochondrial	K.TGAAYPC*FC*SPQR.L	140|142	4.30%	0.92%
P00367	GLUD1 Glutamate dehydrogenase 1, mitochondrial	K.AKPYEGSILEADC*DILIPAASEK.Q	376	4.21%	0.83%
Q9H845	ACAD9 Acyl-CoA dehydrogenase family member 9, mitochondr	R.AYIC*AHPLDR.T	613	4.19%	2.55%
Q6UB35	MTHFD1L Monofunctional C1-tetrahydrofolate synthase, mitoc	K.VGC*GSPR.I	302	4.15%	0.53%
P40926	MDH2 Malate dehydrogenase, mitochondrial	K.TIIPLISQC*TPK.V	212	4.15%	0.75%
Q9H2U2	PPA2 Inorganic pyrophosphatase 2, mitochondrial	R.GQPC*SQNYR.L	44	4.07%	0.88%
Q9HCC0	MCCC2 Methylcrotonoyl-CoA carboxylase beta chain, mitoch	R.LPC*IYLVDSGGAYLPR.Q	167	4.06%	1.40%
P32322	PYCR1 Pyrroline-5-carboxylate reductase 1, mitochondrial	R.C*MTNTPVVVR.E	120	4.06%	1.40%
Q15118	PDK1	K.HYNTNHEADDWC*VPSR.E	421	3.84%	0.92%
P11498	PC Pyruvate carboxylase, mitochondrial	R.INGC*AIQC*R.V	372|376	3.84%	0.92%
P34897	SHMT2 Serine hydroxymethyltransferase, mitochondrial	R.GLELIASENFC*SR.A	80	3.84%	0.92%
Q9NQH7	XPNPEP3 Probable Xaa-Pro aminopeptidase 3	R.IEDDVVVTQDSPLILSADC*PK.E	492	3.83%	1.32%
Q5TC12	ATPAF1 ATP synthase mitochondrial F1 complex assembly fac	R.AQSC*PTFLC*ALPR.R	194|199	3.83%	1.32%
O75390	CS Citrate synthase, mitochondrial	K.LPC*VAAK.I	211	3.83%	1.32%
P40926	MDH2 Malate dehydrogenase, mitochondrial	K.EGVVEC*SFVK.S	275	3.83%	1.32%
P05165	PCCA Propionyl-CoA carboxylase alpha chain, mitochondri	R.C*LAAEDVVFIGPDTHAIQAMGDK.I	155	3.83%	1.32%
Q15119	PDK2	K.QFLDFGSSNAC*EK.T	45	3.83%	1.62%
Q9H845	ACAD9 Acyl-CoA dehydrogenase family member 9, mitochondr	R.GSNTC*EVHFENTK.I	271	3.83%	1.62%
P54886	ALDH18A1 Delta-1-pyrroline-5-carboxylate synthase	R.TEYGDLELC*IEVVDNVQDAIDHIHK.Y	674	3.83%	1.62%
P04406	GAPDH Glyceraldehyde-3-phosphate dehydrogenase	R.VPTANVSVVDLTC*R.L	247	3.83%	1.62%
Q6P1X6	C8orf82 UPF0598 protein C8orf82	R.YEAAFPFLSPC*GR.E	98	3.83%	1.62%
P10809	HSPD1 60 kDa heat shock protein, mitochondrial	R.AAVEEGIVLGGGC*ALLR.C	442	3.82%	1.89%
Q15119	PDK2	K.HIGSIDPNC*NVSEVVK.D	195	3.82%	1.89%
Q7L0Y3	TRMT10C Mitochondrial ribonuclease P protein 1	K.TLMEC*VSNTAK.K	123	3.82%	1.89%
P48735	IDH2 Isocitrate dehydrogenase	K.DLAGC*IHGLSNVK.L	418	3.64%	1.53%
Q15119	PDK2	R.HYQTIQEAGDWC*VPSTEPK.N	392	3.64%	1.53%
P10809	HSPD1 60 kDa heat shock protein, mitochondrial	R.C*IPALDSLTPANEDQK.I	447	3.60%	1.40%
Q9Y2S7	POLDIP2 Polymerase delta-interacting protein 2	R.DC*PHISQR.S	143	3.52%	1.40%
Q15118	PDK1	K.QFLDFGSVNAC*EK.T	71	3.52%	1.40%
Q12849	GRSF1 G-rich sequence factor 1	R.YIELFLNSC*PK.G	476	3.52%	1.40%
P11498	PC Pyruvate carboxylase, mitochondrial	R.AGTHILC*IK.D	739	3.50%	2.18%
P10515	DLAT Dihydrolipoyllysine-residue acetyltransferase comp	K.ASALAC*LK.V	488	3.50%	2.18%
P23368	ME2 NAD-dependent malic enzyme, mitochondrial	R.C*LFASGSPFGPVK.L	441	3.50%	2.18%
P11498	PC Pyruvate carboxylase, mitochondrial	R.AC*TELGIR.T	56	3.50%	2.18%
Q9HCC0	MCCC2 Methylcrotonoyl-CoA carboxylase beta chain, mitoch	K.MVAAVAC*AQVPK.I	431	3.50%	2.18%
P54886	ALDH18A1 Delta-1-pyrroline-5-carboxylate synthase	R.GDEC*GLALGR.L	88	3.50%	2.18%
Q96RP9	GFM1 Elongation factor G, mitochondrial	K.GFLDAC*EK.G	594	3.50%	2.18%
Q9BSH4	TACO1 Translational activator of cytochrome c oxidase 1	K.FIC*DASSLHQVR.K	234	3.50%	2.18%
P10515	DLAT Dihydrolipoyllysine-residue acetyltransferase comp	R.DVPLGTPLC*IIVEK.E	291	3.46%	1.25%
Q9BQP7	C20orf72 Uncharacterized protein C20orf72	R.GVAQTPGSVEEDALLC*GPVSK.H	79	3.46%	1.42%
Q12931	TRAP1 Heat shock protein 75 kDa, mitochondrial	R.SPAAEC*LSEK.E	573	3.36%	1.53%
P30084	ECHS1 Enoyl-CoA hydratase, mitochondrial	K.ALNALC*DGLIDELNQALK.T	62	3.36%	1.80%
O94925	GLS Glutaminase kidney isoform, mitochondrial	K.FSPDLWGVSVC*TVDGQR.H	266	3.27%	1.41%
Q15120	PDK3	K.HIGSIDPTC*NVADVVK.D	191	3.25%	2.07%
Q96RQ3	MCCC1 Methylcrotonoyl-CoA carboxylase subunit alpha, mit	K.ESLC*QAALGLILK.E	509	3.25%	2.07%
P34897	SHMT2 Serine hydroxymethyltransferase, mitochondrial	K.QAC*TPMFR.E	343	3.25%	2.07%
P05165	PCCA Propionyl-CoA carboxylase alpha chain, mitochondri	R.LQVEHPVTEC*ITGLDLVQEMIR.V	363	3.20%	1.75%
P34897	SHMT2 Serine hydroxymethyltransferase, mitochondrial	R.AALEALGSC*LNNK.Y	91	3.12%	1.94%
Q96EY8	MMAB Cob(I)yrinic acid a,c-diamide adenosyltransferase,	K.ISSALHFC*R.A	185	3.08%	1.53%
Q15118	PDK1	R.LC*DLYYINSPELELEELNAK.S	240	3.04%	1.92%
P34897	SHMT2 Serine hydroxymethyltransferase, mitochondrial	R.YYGGAEVVDEIELLC*QR.R	119	3.04%	1.92%
P28331	NDUFS1 NADH-ubiquinone oxidoreductase 75 kDa subunit, mit	R.C*IQC*TR.C	176|179	2.91%	0.94%
P40926	MDH2 Malate dehydrogenase, mitochondrial	K.SQETEC*TYFSTPLLLGK.K	285	2.90%	1.32%
O94925	GLS Glutaminase kidney isoform, mitochondrial	K.VPFC*LQSC*VK.P	283|287	2.89%	1.62%
P49753	ACOT2 Acyl-coenzyme A thioesterase 2, mitochondrial	K.SEFYANEAC*K.R	401	2.89%	1.76%
P11498	PC Pyruvate carboxylase, mitochondrial	R.FLYEC*PWR.R	622	2.88%	2.18%
P11498	PC Pyruvate carboxylase, mitochondrial	R.ADFAQAC*QDAGVR.F	131	2.69%	1.93%
Q96RP9	GFM1 Elongation factor G, mitochondrial	R.YQPC*LPSTQEDVINK.Y	723	2.66%	1.40%
Q9H2U2	PPA2 Inorganic pyrophosphatase 2, mitochondrial	K.STHQC*WK.A	274	2.66%	1.61%
Q15118	PDK1	K.HIGSINPNC*NVLEVIK.D	223	2.52%	2.10%
Q12931	TRAP1 Heat shock protein 75 kDa, mitochondrial	R.NIYYLC*APNR.H	501	2.50%	2.07%
P38646	HSPA9 Stress-70 protein, mitochondrial	R.RTIAPC*QK.A	366	2.44%	0.67%
P54886	ALDH18A1 Delta-1-pyrroline-5-carboxylate synthase	R.EEVEDLC*R.L	546	2.25%	2.18%
Q99798	ACO2 Aconitate hydratase, mitochondrial	K.C*TTDHISAAGPWLK.F	592	1.96%	0.00%

Table 3A-7. Average percent oxidation for mitochondria localized cysteines from IMS-TID analysis. Data was filtered for peptides with ratio values in 2 out of 3 replicates, with a standard deviation <30%.

UniProt ID	Description	Peptide Sequence	Residue	Average % Oxidation IMS-TID Biotin	Average % Standard Deviation IMS-TID Biotin	Average % Oxidation IMS-TID None	Average % Standard Deviation IMS-TID None
Q96BR5	SELRC1 Sel1 repeat-containing protein 1	K.AC*DLGHIWAC*ANASR.M	179 | 187	91.43%	0.75%		
P14854	COX6B1 Cytochrome c oxidase subunit 6B1	R.NC*WQNYLDFHR.C	30	81.80%	2.32%		
P14854	COX6B1 Cytochrome c oxidase subunit 6B1	R.VYQSLC*PTSWVTDWDEQR.A	65	79.01%	0.37%		
Q96C01	FAM136A Protein FAM136A	R.C*HVPLAQAQALVTSELEK.F	57	73.67%	3.88%	71.35%	2.43%
P51970	NDUFA8 NADH dehydrogenase	K.AAAHHYGAQC*DKPNK.E	36	58.55%	4.83%		
Q96BR5	SELRC1 Sel1 repeat-containing protein 1	K.SIAAC*HNVGLLAHDGQVNEDGQP DLGK.A	111	56.96%	3.72%	54.08%	0.89%
P11498	PC Pyruvate carboxylase, mitochondrial	R.INGC*AIQC*R.V	372 | 376	39.05%	20.48 %		
Q9NX40	OCIAD1 OCIA domain-containing protein 1	R.VFAEC*NDESFWFR.S	38	28.79%	0.24%	48.92%	1.30%
Q9Y3D2	MSRB2 Methionine-R-sulfoxide reductase B2, mitochondrial	K.QC*EAHLGHVFPDGPGPNGQR.F	149	25.24%	2.00%		
Q13085	ACACA Acetyl-CoA carboxylase 1	R.MSFSSNLNHYGMTHVASVSDVLLD NSFTPPC*QR.M	1230	19.53%	0.44%		
Q969Z0	TBRG4 Protein TBRG4	R.LATDLLSLMPSLTSGEVAHC*AK.S	335	18.27%	20.22 %		
Q13085	ACACA Acetyl-CoA carboxylase 1	K.RPGAALDPGC*VLAK.M	813	17.76%	4.00%	14.86%	0.46%
Q8IXI1	RHOT2 Mitochondrial Rho GTPase 2	R.SC*LGHLGYLGYPTLC*EQDQAHAIT VTR.E	376 | 389	16.96%	8.95%		
Q9NSE4	IARS2 Isoleucine--tRNA ligase, mitochondrial	K.LASLIDGSSPVSILVWTTQPWTIPANE AVC*YMPESK.Y	311	16.34%	3.76%		
P00395	MT-CO1 Cytochrome c oxidase subunit 1	K.VLMVEEPSMNLEWLYGC*PPPYHTF EEPVYMK.S	498	15.03%	4.09%		
Q13085	ACACA Acetyl-CoA carboxylase 1	R.MMYGVSPWGDSPIDFEDSAHVPC*P R.G	500	14.00%	1.36%	18.54%	3.18%
Q7Z434	MAVS Mitochondrial antiviral-signaling protein	R.PGPPTPAAAHSIPYNSC*R.E	133	13.96%	7.97%		
Q9Y3D2	MSRB2 Methionine-R-sulfoxide reductase B2, mitochondrial	K.YC*SGTGWPSFSEAHGTSGSDESHTG ILR.R	105	13.61%	0.89%		
Q9NZ45	CISD1 CDGSH iron-sulfur domain-containing protein 1	K.FPFC*DGAHTK.H	83	13.40%	0.52%	12.32%	0.54%
O75521	ECI2 Enoyl-CoA delta isomerase 2, mitochondrial	K.LHAVNAEEC*NVLQGR.W	368	13.20%	5.34%		
Q8NBU5	ATAD1 ATPase family AAA domain-containing protein 1	K.SKDAAFQNVLTHVC*LD.-	359	12.71%	11.24 %		
P05165	PCCA Propionyl-CoA carboxylase alpha chain, mitochondri	K.SVHC*QAGDTVGEGDLLVELE.-	712	12.55%	0.72%	13.16%	0.69%
P53701	HCCS Cytochrome c-type heme lyase	K.WEALHAAEC*PC*GPSLIR.F	176 | 178	12.27%	1.38%	25.94%	4.20%
O00429	DNM1L Dynamin-1-like protein	K.YIETSELC*GGAR.I	361	12.22%	4.16%	5.33%	0.80%
P09622	DLD Dihydrolipoyl dehydrogenase, mitochondrial	R.VLGAHILGPGAGEMVNEAALALEY GASC*EDIAR.V	477	11.08%	0.56%		
P09622	DLD Dihydrolipoyl dehydrogenase, mitochondrial	R.VC*HAHPTLSEAFR.E	484	10.21%	0.82%		
O00571	DDX3X ATP-dependent RNA helicase DDX3X	R.GC*HLLVATPGR.L	317	10.21%	1.31%		
Q92667	AKAP1 A-kinase anchor protein 1, mitochondrial	K.LPAEPPALLQTHPPC*R.R	102	9.89%	4.44%	10.99%	1.53%
P11182	DBT Lipoamide acyltransferase component of branched-ch	K.IPHFGYC*DEIDLTELVK.L	279	9.66%	5.66%		
P62263	RPS14 40S ribosomal protein S14	R.C*KELGITALHIK.L	85	9.46%	4.22%	43.69%	20.95 %
O00429	DNM1L Dynamin-1-like protein	R.IIQHC*SNYSTQELLR.F	446	9.28%	7.71%	5.02%	0.86%
Q13085	ACACA Acetyl-CoA carboxylase 1	R.NFDLTAIPC*ANHK.M	1396	9.06%	0.62%	8.79%	0.82%
Q8WUK0	PTPMT1 Phosphatidylglycerophosphatase and protein-tyrosin	K.YQSLGQC*VYVHC*K.A	127 | 132	8.98%	0.17%		
Q9BPW8	NIPSNAP1 Protein NipSnap homolog 1	K.LHLDEDYPC*SLVGNWNTWYGEQD QAVHLWR.F	106	8.79%	1.15%		
P04406	GAPDH Glyceraldehyde-3-phosphate dehydrogenase	K.IISNASC*TTNC*LAPLAK.V	152 | 156	8.78%	3.16%		
Q13085	ACACA Acetyl-CoA carboxylase 1	R.TDC*NHIFLNFVPTVIMDPSK.I	1470	8.73%	1.26%	9.52%	0.39%
Q96H55	MYO19 Unconventional myosin-XIX	R.YADIC*PEPSPYSITGFNQILLER.H	937	8.35%	6.22%		
P54886	ALDH18A1 Delta-1-pyrroline-5-carboxylate synthase	K.C*EYPAAC*NALETLLIHR.D	606 | 612	7.96%	2.39%		
Q5T9A4	ATAD3B ATPase family AAA domain-containing protein 3B	R.LHFDNC*VLKPATEGK.R	492	7.89%	4.43%		
P34897	SHMT2 Serine hydroxymethyltransferase, mitochondrial	R.GLELIASENFC*SR.A	80	7.86%	0.46%		
Q13085	ACACA Acetyl-CoA carboxylase 1	K.EMAQYASNITSVLC*QFPSQQIANIL DSHAATLNR.K	934	7.83%	0.44%	5.20%	0.39%
Q9Y2W6	TDRKH Tudor and KH domain-containing protein	R.SDFLSLPFQAIEC*SLAR.I	419	7.54%	0.22%		
P34897	SHMT2 Serine hydroxymethyltransferase, mitochondrial	K.YSEGYPGKRYYGGAEVVDEIELLC*Q R.R	119	7.42%	0.09%	6.39%	0.69%
Q96RQ3	MCCC1 Methylcrotonoyl-CoA carboxylase subunit alpha, mit	K.SIMAAAGVPVVEGYHGEDQSDQC*L K.E	190	7.32%	0.28%	7.50%	0.24%

P28331	NDUFS1 NADH-ubiquinone oxidoreductase 75 kDa subunit, mit	R.FC*YHER.L	64	7.15%	2.07%		
Q13085	ACACA Acetyl-CoA carboxylase 1	K.VQAERPDTMLGVVC*GALHVADVSLR.N	634	6.80%	0.72%	6.58%	0.87%
P04150	NR3C1 Glucocorticoid receptor	R.AVEGQHNYLC*AGR.N	457	6.63%	2.64%		
Q9NVH0	EXD2 Exonuclease 3-5 domain-containing protein 2	K.SPLYDNC*FLHAPDGQPLC*TC*DR.R	358|369|371	6.44%	2.91%		
P11498	PC Pyruvate carboxylase, mitochondrial	K.DMAGLLKPTAC*TMLVSSLR.D	752	6.44%	0.12%	4.83%	0.60%
Q96RQ3	MCCC1 Methylcrotonoyl-CoA carboxylase subunit alpha, mit	K.TFQVLGNLYSEGDC*TYLK.C	595	6.40%	0.81%	7.68%	0.33%
P09622	DLD Dihydrolipoyl dehydrogenase, mitochondrial	K.NETLGGTC*LNVGC*IPSK.A	80|85	6.30%	2.18%		
Q7L2E3	DHX30 Putative ATP-dependent RNA helicase DHX30	R.RPC*TIQVPEPILR.K	346	6.25%	1.29%		
Q12931	TRAP1 Heat shock protein 75 kDa, mitochondrial	R.SPAAEC*LSEK.E	573	6.25%	1.00%	4.80%	0.06%
Q7L592	C2orf56 Protein midA homolog, mitochondrial	R.DHVEVC*PDAGVIIEELSQR.I	275	6.22%	1.34%		
P13995	MTHFD2 Bifunctional methylenetetrahydrofolate dehydrogena	R.IC*NAVSPDKDVDGFHVINVGR.M	145	6.20%	2.04%		
O94826	TOMM70A Mitochondrial import receptor subunit TOM70	K.ILLDQVEEAVADFDEC*IR.L	427	6.17%	1.57%	4.76%	0.00%
Q07021	C1QBP Complement component 1 Q subcomponent-binding prot	K.ALVLDC*HYPEDEVGQEDEAESDIFSIR.E	186	6.05%	1.49%	4.76%	0.00%
P11498	PC Pyruvate carboxylase, mitochondrial	R.AGTHILC*IK.D	739	5.75%	0.22%	4.66%	1.14%
P05165	PCCA Propionyl-CoA carboxylase alpha chain, mitochondri	R.C*LAAEDVVFIGPDTHAIQAMGDK.I	155	5.71%	1.03%	5.22%	0.39%
Q13085	ACACA Acetyl-CoA carboxylase 1	K.DNTC*VVEFQFMLPTSHPNR.G	1176	5.66%	0.89%	7.02%	1.96%
Q7L2E3	DHX30 Putative ATP-dependent RNA helicase DHX30	R.C*QSGFAYHLFPR.S	786	5.66%	1.56%		
Q9NSE4	IARS2 Isoleucine--tRNA ligase, mitochondrial	R.SC*QTALVEILDVIVR.S	819	5.64%	1.53%	4.76%	0.00%
Q9BXM7	PINK1 Serine/threonine-protein kinase PINK1, mitochondri	R.GGNGC*LMAPEVSTARPGPR.A	412	5.58%	1.16%		
P34897	SHMT2 Serine hydroxymethyltransferase, mitochondrial	R.AALEALGSC*LNNK.Y	91	5.57%	1.09%	5.00%	0.41%
Q9P2R7	SUCLA2 Succinyl-CoA ligase	R.C*DVIAQGIVMAVK.D	384	5.52%	1.07%		
P63167	DYNLL1 Dynein light chain 1, cytoplasmic	K.NADMSEEMQQDSVEC*ATQALEK.Y	24	5.45%	1.19%		
P11498	PC Pyruvate carboxylase, mitochondrial	R.GLYAAFDC*TATMK.S	850	5.34%	0.50%	8.58%	1.77%
P19404	NDUFV2 NADH dehydrogenase	K.YHIQVC*TTTPC*MLR.N	135|140	5.31%	0.78%		
Q7L0Y3	TRMT10C Mitochondrial ribonuclease P protein 1	R.NVDPFHIYFC*NLK.I	246	5.29%	1.05%	25.67%	0.85%
Q7L0Y3	TRMT10C Mitochondrial ribonuclease P protein 1	K.RLNLATEC*LPLDK.Y	335	5.28%	0.90%		
P05165	PCCA Propionyl-CoA carboxylase alpha chain, mitochondri	R.LQVEHPVTEC*ITGLDLVQEMIR.V	363	5.23%	0.40%	4.78%	0.02%
P49748	ACADVL Very long-chain specific acyl-CoA dehydrogenase, m	K.ELGAFGLQVPSELGGVGLC*NTQYAR.L	156	5.16%	0.68%		
Q13085	ACACA Acetyl-CoA carboxylase 1	K.IIEEAPATIATPAVFEHMEQC*AVK.L	407	5.11%	0.39%	4.78%	0.03%
O14880	MGST3 Microsomal glutathione S-transferase 3	K.VEYPIMYSTDPENGHIFNC*IQR.A	56	5.06%	0.42%		
Q9BSH4	TACO1 Translational activator of cytochrome c oxidase 1	K.FIC*DASSLHQVR.K	234	5.04%	0.43%		
O43615	TIMM44 Mitochondrial import inner membrane translocase su	K.QC*ENDIIPNVLEAMISGELDILK.D	319	5.03%	0.90%		
O94925	GLS Glutaminase kidney isoform, mitochondrial	K.VPFC*LQSC*VKPLK.Y	283|287	4.89%	0.23%		
Q9Y606	PUS1 tRNA pseudouridine synthase A, mitochondrial	R.TYC*YLLPTFAFAHK.D	202	4.85%	0.12%		
E7ERL9	VARS2 Valine--tRNA ligase, mitochondrial	R.GLQNHPMVLPIC*SR.S	BAD_ID	4.82%	0.09%		
P11498	PC Pyruvate carboxylase, mitochondrial	R.ADFAQAC*QDAGVR.F	131	4.79%	0.05%	4.76%	0.00%
O43615	TIMM44 Mitochondrial import inner membrane translocase su	K.DWC*YEATYSQLAHPIQQAK.A	343	4.79%	0.05%	4.76%	0.00%
P11498	PC Pyruvate carboxylase, mitochondrial	R.FLYEC*PWR.R	622	4.77%	0.02%	4.53%	0.46%
Q70CQ3	USP30 Ubiquitin carboxyl-terminal hydrolase 30	K.ALSC*QEVTDDEVLDASC*LLDVLR.M	129|142	4.76%	0.00%	4.76%	0.00%
Q70CQ3	USP30 Ubiquitin carboxyl-terminal hydrolase 30	K.LPQC*LC*IHLQR.L	320|322	4.76%	0.00%		
Q96RP9	GFM1 Elongation factor G, mitochondrial	R.QELIEC*VANSDEQLGEMFLEEK.I	256	4.76%	0.00%		
Q12849	GRSF1 G-rich sequence factor 1	R.YIELFLNSC*PK.G	476	4.76%	0.00%		
Q12849	GRSF1 G-rich sequence factor 1	R.AQGLPWSC*TMEDVLNFFSDC*R.I	161|173	4.76%	0.00%		
Q96H55	MYO19 Unconventional myosin-XIX	K.VFMTDSMLELLEC*GR.A	755	4.76%	0.00%	4.76%	0.00%
O95202	LETM1 LETM1 and EF-hand domain-containing protein 1, mit	K.LFEDELTLDNLTRPQLVALC*K.L	330	4.76%	0.00%	4.76%	0.00%
Q15118	PDK1	K.HIGSINPNC*NVLEVIK.D	223	4.76%	0.00%		
P52789	HK2 Hexokinase-2	R.LGLDPTQEDC*VATHR.I	368	4.76%	0.00%		
P52789	HK2 Hexokinase-2	R.SASLC*AATLAAVLQR.I	386	4.76%	0.00%		
Q8TB36	GDAP1 Ganglioside-induced differentiation-associated pro	K.C*EEHDVSLPLSEHNEPWFMR.L	51	4.76%	0.00%		
Q13085	ACACA Acetyl-CoA carboxylase 1	R.EC*C*QPVLVYIPPQAELR.G	2074|2075	4.76%	0.00%	4.76%	0.00%
Q9HCC0	MCCC2 Methylcrotonoyl-CoA carboxylase beta chain, mitoch	K.GTHFVQLC*C*QR.N	391|392	4.76%	0.00%		
Q7Z434	MAVS Mitochondrial antiviral-signaling protein	R.NFSNFC*NVDVVEILPYLPC*LTAR.D	20|33	4.76%	0.00%	4.76%	0.00%
P05165	PCCA Propionyl-CoA carboxylase alpha chain, mitochondri	K.MADEAVC*VGPAPTSK.S	111	4.76%	0.00%	5.76%	0.45%
P28288	ABCD3 ATP-binding cassette sub-family D member 3	R.TYC*DVWMIQNGTLIESGIIGR.S	99	4.76%	0.00%	4.76%	0.00%

Q8N5K1	CISD2 CDGSH iron-sulfur domain-containing protein 2	K.VVNEINIEDLC*LTK.A	92	4.76%	0.00%	4.76%	0.00%
O00429	DNM1L Dynamin-1-like protein	R.C*VELVHEEMQR.I	431	4.76%	0.00%	4.76%	0.00%
O00429	DNM1L Dynamin-1-like protein	R.IC*YIFHETFGR.T	367	4.76%	0.00%		
P04406	GAPDH Glyceraldehyde-3-phosphate dehydrogenase	R.VPTANVSVVDLTC*R.L	247	4.76%	0.00%	4.76%	0.00%
Q9H857	NT5DC2 5-nucleotidase domain-containing protein 2	R.FSDLYMASLSC*LLNYR.V	475	4.76%	0.00%		
P30084	ECHS1 Enoyl-CoA hydratase, mitochondrial	K.IC*PVETLVEEAIQC*AEK.I	213|225	4.76%	0.00%		
P28331	NDUFS1 NADH-ubiquinone oxidoreductase 75 kDa subunit, mit	R.EGVMEFLLANHPLDC*PIC*DQGGEC*DLQDQSMMFGNDR.S	128|131|137	4.76%	0.00%		
Q6YN16	HSDL2 Hydroxysteroid dehydrogenase-like protein 2	K.TAIHTAAMDMLGGPGIESQC*R.K	218	4.76%	0.00%		
P42704	LRPPRC Leucine-rich PPR motif-containing protein, mitocho	R.C*GAIAEQTPILLLFLLR.N	1277	4.76%	0.00%		
P42704	LRPPRC Leucine-rich PPR motif-containing protein, mitocho	R.AILQENGC*LSDSDMFSQAGLR.S	500	4.76%	0.00%		
Q92667	AKAP1 A-kinase anchor protein 1, mitochondrial	R.VC*QASQLQGQKEESC*VPVHQK.T	376|389	4.76%	0.00%		
O94826	TOMM70A Mitochondrial import receptor subunit TOM70	K.YEQAIQC*YTEAISLC*PTEK.N	136|144	4.76%	0.00%		
Q8TB36	GDAP1 Ganglioside-induced differentiation-associated pro	R.ELLDSLPMDAYTHGC*ILHPELTVDSMIPAYATTR.I	140	4.76%	0.00%		
Q9NZJ7	MTCH1 Mitochondrial carrier homolog 1	K.SWIHC*WK.Y	359	4.76%	0.00%		
Q7L8L6	FASTKD5 FAST kinase domain-containing protein 5	R.VNQNNLQAQVIVDYLC*K.L	168	4.76%	0.00%		
Q9NSE4	IARS2 Isoleucine--tRNA ligase, mitochondrial	K.KPGLEEAVESAC*AMR.D	883	4.76%	0.00%	4.76%	0.00%
Q9NSE4	IARS2 Isoleucine--tRNA ligase, mitochondrial	R.RPYWC*ISR.Q	521	4.76%	0.00%		
Q6L8Q7	PDE12 2,5-phosphodiesterase 12	K.SRPNASGGAAC*SGPGPEPAVFC*EPVVK.L	108|119	4.76%	0.00%		
Q9BW92	TARS2 Threonine--tRNA ligase, mitochondrial	K.EQELFFFHELSPGSC*FFLPR.G	322	4.76%	0.00%		
Q10713	PMPCA Mitochondrial-processing peptidase subunit alpha	R.MVLAGVGVEHEHLVDC*AR.K	266	4.76%	0.00%		
Q15031	LARS2 Probable leucine--tRNA ligase, mitochondrial	K.DC*LTPVMAVNMLTQQEVPVVILAK.A	341	4.76%	0.00%		
Q99643	SDHC Succinate dehydrogenase cytochrome b560 subunit, m	K.SLC*LGPALIHTAK.F	107	4.76%	0.00%	4.76%	0.00%
Q00325	SLC25A3 Phosphate carrier protein, mitochondrial	K.GWAPTFLGYSMQGLC*K.F	136	4.76%	0.00%		
Q16891	IMMT Mitochondrial inner membrane protein	K.ANC*SDNEFTQALTAAIPPESLTR.G	603	4.76%	0.00%	4.53%	0.46%
P12235	SLC25A4 ADP/ATP translocase 1	K.GADIMYTGTVDC*WR.K	257	4.76%	0.00%	4.76%	0.00%
Q6UXV4	APOOL Apolipoprotein O-like	K.ITYPLGLATLGATVC*YPVQSVIIAK.V	152	4.76%	0.00%	4.76%	0.00%
P08574	CYC1 Cytochrome c1, heme protein, mitochondrial	R.HGGEDYVFSLLTGYC*EPPTGVSLR.E	219	4.76%	0.00%	4.76%	0.00%
O43615	TIMM44 Mitochondrial import inner membrane translocase su	R.MLYVWALC*R.D	426	4.76%	0.00%	4.76%	0.00%
P12235	SLC25A4 ADP/ATP translocase 1	R.YFAGNLASGGAAGATSLC*FVYPLDFAR.T	129	4.76%	0.00%	4.76%	0.00%
O00483	NDUFA4 NADH dehydrogenase	R.LALFNPDVC*WDR.N	44	4.76%	0.00%	4.76%	0.00%
P05141	SLC25A5 ADP/ATP translocase 2	K.GIIDC*VVR.I	57	4.76%	0.00%	4.76%	0.00%
Q8TBP6	SLC25A40 Solute carrier family 25 member 40	K.LGENETC*IPIVAGIVAR.F	142	4.76%	0.00%		
Q9H3K2	GHITM Growth hormone-inducible transmembrane protein	R.AAWYTAGIVGGLSTVAMC*APSEK.F	235	4.76%	0.00%		
Q9NZJ6	COQ3 Hexaprenyldihydroxybenzoate methyltransferase, mit	K.ILDVGC*GGGLLTEPLGR.L	155	4.76%	0.00%		
Q9Y6C9	MTCH2 Mitochondrial carrier homolog 2	R.LC*SGVLGTVVHGK.V	79	4.76%	0.00%		
P36542	ATP5C1 ATP synthase subunit gamma, mitochondrial	R.GLC*GAIHSSIAK.Q	103	4.76%	0.00%		
Q9Y6N1	COX11 Cytochrome c oxidase assembly protein COX11, mitoc	R.LYC*QTTGLGGSAVAGHASDKIENMVPVK.D	121	4.76%	0.00%		
P28331	NDUFS1 NADH-ubiquinone oxidoreductase 75 kDa subunit, mit	R.VDSDTLC*TEEVFPTAGAGTDLR.S	367	4.76%	0.00%		
Q9H845	ACAD9 Acyl-CoA dehydrogenase family member 9, mitochondr	R.AYIC*AHPLDR.T	613	4.76%	0.00%		
P31040	SDHA Succinate dehydrogenase	R.GVIALC*IEDGSIHR.I	238	4.76%	0.00%		
Q16891	IMMT Mitochondrial inner membrane protein	K.LLSYASYC*IEHGDLELAAK.F	697	4.76%	0.00%		
P22570	FDXR NADPH:adrenodoxin oxidoreductase, mitochondrial	R.AVPTGDMEDLPC*GLVLSSIGYK.S	353	4.76%	0.00%		
Q15070	OXA1L Mitochondrial inner membrane protein OXA1L	R.C*LIFPLIVTGQR.E	153	4.76%	0.00%		
Q14318	FKBP8 Peptidyl-prolyl cis-trans isomerase FKBP8	R.SC*SLVLEHQPDNIK.A	295	4.76%	0.00%		
Q15390	MTFR1 Mitochondrial fission regulator 1	K.IC*ALENELAALR.A	145	4.76%	0.00%	4.76%	0.00%
P49753	ACOT2 Acyl-coenzyme A thioesterase 2, mitochondrial	K.SEFYANEAC*K.R	401	4.76%	0.00%	4.76%	0.00%
P82650	MRPS22 28S ribosomal protein S22, mitochondrial	R.HVDVLNLC*FAQFEPDSTEYIK.V	231	4.76%	0.00%		
Q9NX20	MRPL16 39S ribosomal protein L16, mitochondrial	R.C*EFEEVQGFLDQVAHK.L	167	4.76%	0.00%		
Q96EY7	PTCD3 Pentatricopeptide repeat-containing protein 3, mit	K.DPDDDKFFQSAMSIC*SSLR.D	423	4.76%	0.00%		
Q96EY7	PTCD3 Pentatricopeptide repeat-containing protein 3, mit	R.DKHPPELQVAFADC*AADIK.S	551	4.76%	0.00%		

Q9Y4W6	AFG3L2 AFG3-like protein 2	K.LASLTPGFSGADVANVC*NEAALIAAR.H	525	4.76%	0.00%		
Q99714	HSD17B10 3-hydroxyacyl-CoA dehydrogenase type-2	K.KLGNNC*VFAPADVTSEK.D	58	4.76%	0.00%		
Q9BZE1	MRPL37 39S ribosomal protein L37, mitochondrial	R.NHIENQDEC*VLNVISHAR.L	153	4.76%	0.00%		
Q9HC36	RNMTL1 RNA methyltransferase-like protein 1	K.TQLQHSLPLLLIC*DNLR.D	214	4.76%	0.00%		
Q96EY7	PTCD3 Pentatricopeptide repeat-containing protein 3, mit	K.DIAEPHIPC*LMPEYFEPQIK.D	139	4.76%	0.00%		
Q9NP92	MRPS30 28S ribosomal protein S30, mitochondrial	R.C*PVHFYWVR.G	204	4.76%	0.00%		
P40939	HADHA Trifunctional enzyme subunit alpha, mitochondrial	K.ALMGLYHGQVLC*K.K	349	4.76%	0.00%		
Q9BRJ2	MRPL45 39S ribosomal protein L45, mitochondrial	R.LHTLVTEHC*FPDMTWDIK.Y	168	4.76%	0.00%		
Q3SY69	ALDH1L2 Mitochondrial 10-formyltetrahydrofolate dehydrogen	K.SPLIIFNDC*ELDK.A	707	4.76%	0.00%		
Q7Z7H8	MRPL10 39S ribosomal protein L10, mitochondrial	R.TVPFLPLLGGC*IDDTILSR.Q	180	4.76%	0.00%		
Q9H2W6	MRPL46 39S ribosomal protein L46, mitochondrial	K.FLGNAPC*GHYTFK.F	210	4.76%	0.00%		
Q9BYD6	MRPL1 39S ribosomal protein L1, mitochondrial	K.IATLDMSSDQIAANLQAVINEVC*R.H	279	4.76%	0.00%		
Q12931	TRAP1 Heat shock protein 75 kDa, mitochondrial	R.NIYYLC*APNR.H	501	4.76%	0.00%		
Q9Y2W6	TDRKH Tudor and KH domain-containing protein	R.LTHC*ADWKPLVAK.I	445	4.76%	0.00%	4.76%	0.00%
Q9BXK5	BCL2L13 Bcl-2-like protein 13	R.HTSPVFSPANPESSMEDC*LAHLGEK.V	103	4.76%	0.00%	4.76%	0.00%
O94925	GLS Glutaminase kidney isoform, mitochondrial	K.FSPDLWGVSVC*TVDGQR.H	266	4.76%	0.00%		
O94925	GLS Glutaminase kidney isoform, mitochondrial	K.C*VQSNIVLLTQAFR.R	203	4.76%	0.00%		
I3L0E3	MRPS17 28S ribosomal protein S17, mitochondrial	K.TYFAHDALQQC*TVGDIVLLR.A	153	4.76%	0.00%		
P22234	PAICS Multifunctional protein ADE2	R.VVVLMGSTSDLGHC*EK.I	281	4.76%	0.00%		
O96011	PEX11B Peroxisomal membrane protein 11B	R.AAQYAC*SLLGHALQR.H	25	4.76%	0.00%	7.50%	4.74%
O96011	PEX11B Peroxisomal membrane protein 11B	R.FC*ITVSHLNR.A	85	4.76%	0.00%	4.76%	0.00%
O96011	PEX11B Peroxisomal membrane protein 11B	R.NAC*DLFIPLDK.L	216	4.76%	0.00%	4.76%	0.00%
P33897	ABCD1 ATP-binding cassette sub-family D member 1	R.RLQELC*QILGEAVAPAHVPAPSPQGPGGLQGAST.-	717	4.76%	0.00%		
O96011	PEX11B Peroxisomal membrane protein 11B	R.ALYFAC*DNVLWAGK.S	99	4.76%	0.00%		
O00763	ACACB Acetyl-CoA carboxylase 2	R.TC*MTDFLHSLER.G	790	4.76%	0.00%	4.76%	0.00%
Q13085	ACACA Acetyl-CoA carboxylase 1	R.QSPNSYVVIMNGSC*VEVDVHR.L	701	4.76%	0.00%	4.76%	0.00%
Q13085	ACACA Acetyl-CoA carboxylase 1	K.NLLVTMLIDQLC*GR.D	1049	4.76%	0.00%	4.76%	0.00%
Q9UH62	ARMCX3 Armadillo repeat-containing X-linked protein 3	K.VYMNQVC*DDTITSR.L	208	4.76%	0.00%	4.76%	0.00%
Q9NVH0	EXD2 Exonuclease 3-5 domain-containing protein 2	K.ASPLSLLQMASPSGLC*VLVR.L	133	4.76%	0.00%		
Q8NAN2	FAM73A Protein FAM73A	R.NSLYDLC*C*FFK.N	556 | 557	4.76%	0.00%		
Q4G0N4	NADKD1 NAD kinase domain-containing protein 1	R.SEGHLC*LPVR.Y	193	4.76%	0.00%	4.76%	0.00%
Q5HYI7	MTX3 Metaxin-3	R.FC*DDILSSYFR.L	233	4.76%	0.00%	4.76%	0.00%
Q9BQP7	C20orf72 Uncharacterized protein C20orf72	R.GVAQTPGSVEEDALLC*GPVSK.H	79	4.76%	0.00%		
Q9BQP7	C20orf72 Uncharacterized protein C20orf72	K.DGSPAHPHFMDAELC*SQYWTK.W	314	4.76%	0.00%		
P22314	UBA1 Ubiquitin-like modifier-activating enzyme 1	R.VGEFC*HNR.G	179	4.76%	0.00%		
P36873	PPP1CC Serine/threonine-protein phosphatase PP1-gamma cat	K.TFTDC*FNC*LPIAAIVDEK.I	155 | 158	4.76%	0.00%	7.44%	4.63%
P36873	PPP1CC Serine/threonine-protein phosphatase PP1-gamma cat	K.IFC*C*HGGLSPDLQSMEQIR.R	171 | 172	4.76%	0.00%		
Q9NVH0	EXD2 Exonuclease 3-5 domain-containing protein 2	R.SELEDFPVLGIDC*EWVNLEGK.A	109	4.76%	0.00%	4.76%	0.00%
Q07820	MCL1 Induced myeloid leukemia cell differentiation prot	K.TINQESC*IEPLAESITDVLVR.T	286	4.59%	0.42%	6.26%	2.12%
Q9BQP7	C20orf72 Uncharacterized protein C20orf72	R.ALESAVQHETLNYIGLLDC*VAEYQGK.L	239	4.53%	0.46%		
O00763	ACACB Acetyl-CoA carboxylase 2	K.IVEEAPATIAPLAIFEFMEQC*AIR.L	550	4.46%	0.53%		
Q9UJZ1	STOML2 Stomatin-like protein 2	R.ERESLNASIVDAINQAADC*WGIR.C	167	4.40%	0.50%		
Q7Z434	MAVS Mitochondrial antiviral-signaling protein	R.GC*ELVDLADEVASVYQSYQPR.T	79	4.30%	0.50%	4.76%	0.00%
Q96RQ3	MCCC1 Methylcrotonoyl-CoA carboxylase subunit alpha, mit	K.ESLC*QAALGLILK.E	509	4.30%	0.50%	3.36%	1.62%
Q92665	MRPS31 28S ribosomal protein S31, mitochondrial	R.HFMELVTC*GLSK.N	356	4.30%	0.50%	4.76%	0.00%
Q96RQ3	MCCC1 Methylcrotonoyl-CoA carboxylase subunit alpha, mit	K.TSAAQAIHPGC*GFLSENMEFAELC*K.Q	129 | 142	4.21%	0.83%	4.76%	0.00%
Q96RQ3	MCCC1 Methylcrotonoyl-CoA carboxylase subunit alpha, mit	K.HNFC*FMEMNTR.L	332	4.15%	0.75%	3.65%	1.01%
P05141	SLC25A5 ADP/ATP translocase 2	K.GTDIMYTGTLDC*WR.K	257	4.06%	1.40%	4.76%	0.00%
Q13085	ACACA Acetyl-CoA carboxylase 1	R.VSALNSVHC*EHVEDEGESR.Y	1769			4.76%	0.00%
O00429	DNM1L Dynamin-1-like protein	K.FATEYC*NTIEGTAK.Y	345			4.76%	0.00%
Q13085	ACACA Acetyl-CoA carboxylase 1	K.TDC*DIEDDR.L	1297			14.84%	20.15%

P10809	HSPD1 60 kDa heat shock protein, mitochondrial	K.C*EFQDAYVLLSEK.K	237			4.76%	0.00%
P40926	MDH2 Malate dehydrogenase, mitochondrial	K.GYLGPEQLPDC*LK.G	89			9.01%	1.84%
Q96RQ3	MCCC1 Methylcrotonoyl-CoA carboxylase subunit alpha, mit	K.C*SVNGVASK.A	600			4.76%	0.00%
P40926	MDH2 Malate dehydrogenase, mitochondrial	K.SQETEC*TYFSTPLLLGK.K	285			4.76%	0.00%
Q9H078	CLPB Caseinolytic peptidase B protein homolog	R.VVNQLAAAYEQDLLPGGC*TLR.I	647			6.51%	0.48%
Q9H078	CLPB Caseinolytic peptidase B protein homolog	K.GC*TALHYAVLADDYR.T	267			5.02%	0.37%
Q9H078	CLPB Caseinolytic peptidase B protein homolog	R.INEIVYFLPFC*HSELIQLVNK.E	572			4.76%	0.00%
Q6P4A7	SFXN4 Sideroflexin-4	R.QLLC*TNEDVSSPASADQR.I	70			4.76%	0.00%
O75746	SLC25A12 Calcium-binding mitochondrial carrier protein Aral	R.AGQTTYSGVIDC*FR.K	563			4.76%	0.00%
Q5T9A4	ATAD3B ATPase family AAA domain-containing protein 3B	K.DGVLTEAMMDAC*VQDAVQQYR.Q	557			4.76%	0.00%
Q6KCM7	SLC25A25 Calcium-binding mitochondrial carrier protein SCaM	K.TGQYSGMLDC*AR.R	322			4.76%	0.00%
O00763	ACACB Acetyl-CoA carboxylase 2	R.NFDEVISC*FANVPK.D	1388			4.76%	0.00%
Q13085	ACACA Acetyl-CoA carboxylase 1	R.IFDEVMGC*FSDSPPQSPTFPEAGHTSLYDEDKVPR.D	1255			4.76%	0.00%
Q8NAN2	FAM73A Protein FAM73A	R.TEMLEC*LGDSDFLAK.L	378			43.86%	29.74%

Table 3A-8. Average percent oxidation for localized cysteines from cyto-TID analysis. Data was filtered for peptides with ratio values in 2 out of 3 replicates, with a standard deviation <30%.

UniProt ID	Protein Description	Peptide Sequence	Residue	Average % Oxidation Cyto-TID	% Standard Deviation
P36551	CPOX Coproporphyrinogen-III oxidase, mitochondrial	R.C*SSFMAPPVTDLGELR.R	127	73.39%	5.07%
Q8WU79	SMAP2 Stromal membrane-associated protein 2	R.C*AGIHR.N	51	72.63%	5.55%
Q08211	DHX9 ATP-dependent RNA helicase A	R.AAEC*NIVVTQPR.R	438	60.85%	3.63%
P49411	TUFM Elongation factor Tu, mitochondrial	K.GEETPVIVGSALC*ALEGR.D	222	56.20%	2.55%
P22033	MUT Methylmalonyl-CoA mutase, mitochondrial	R.IEEC*AAR.R	471	54.84%	0.80%
O75380	NDUFS6 NADH dehydrogenase	R.VIAC*DGGGGALGHPK.V	87	54.71%	3.28%
Q9H4A4	RNPEP Aminopeptidase B	R.VGEGPGVC*WLAPEQTAGK.K	151	52.79%	1.89%
Q9BVS5	TRMT61B Potential tRNA (adenine(58)-N(1))-methyltransferas	R.DWLVC*LAK.Q	396	49.68%	2.73%
P42704	LRPPRC Leucine-rich PPR motif-containing protein, mitocho	R.IHDVLC*K.L	863	48.61%	4.15%
Q12923	PTPN13 Tyrosine-protein phosphatase non-receptor type 13	R.SGPIITHC*SAGIGR.S	2408	47.63%	1.58%
J3KR12	Uncharacterized protein	R.SLLINAVEASC*IR.T	188	46.78%	8.45%
Q9NQW6	ANLN Actin-binding protein anillin	R.LWQPDAC*YKPIGKP.-	1117	46.12%	3.62%
P05166	PCCB Propionyl-CoA carboxylase beta chain, mitochondria	K.VASGC*LDINSSVK.G	365	45.81%	6.29%
P31040	SDHA Succinate dehydrogenase	R.VGSVLQEGC*GK.I	536	44.14%	1.05%
P31150	GDI1 Rab GDP dissociation inhibitor alpha	K.QLIC*DPSYIPDR.V	282	42.76%	1.94%
P60174	TPI1 Triosephosphate isomerase	K.VPADTEVVC*APPTAYIDFAR.Q	79	42.68%	2.04%
Q99497	PARK7 Protein DJ-1	K.DPVQC*SR.D	46	41.55%	21.89%
P34897	SHMT2 Serine hydroxymethyltransferase, mitochondrial	R.GLELIASENFC*SR.A	80	39.94%	10.09%
Q9H845	ACAD9 Acyl-CoA dehydrogenase family member 9, mitochondr	R.LIEMTAEYAC*TR.K	327	38.98%	1.73%
Q92547	TOPBP1 DNA topoisomerase 2-binding protein 1	R.IDYC*HLIEK.L	1284	37.98%	28.77%
Q6BDS2	UHRF1BP1 UHRF1-binding protein 1	K.KPSTLLSC*SR.K	494	36.09%	27.13%
Q9GZT9	EGLN1 Egl nine homolog 1	K.AKPPADPAAAASPC*R.A	127	35.92%	26.99%
Q4VCS5	AMOT Angiomotin	K.MQQALVQLQAAC*EK.R	617	33.17%	24.61%
Q7L8L6	FASTKD5 FAST kinase domain-containing protein 5	K.AAVPLGGFLC*NVADK.S	670	32.58%	2.82%
P17844	DDX5 Probable ATP-dependent RNA helicase DDX5	R.RC*DELTR.K	354	32.43%	23.96%
Q96CX2	KCTD12 BTB/POZ domain-containing protein KCTD12	R.C*TVVSVPDSLLWR.M	50	31.68%	1.34%
Q15061	WDR43 WD repeat-containing protein 43	K.KPLTSNC*TIQIATPGK.G	315	30.64%	20.81%
Q6PKG0	LARP1 La-related protein 1	R.EEPEKWPLPPIVDYSQTDFSQLLNC*PEFVPR.Q	502	26.53%	18.85%
Q7Z6E9	RBBP6 E3 ubiquitin-protein ligase RBBP6	R.TALLESDEHTC*PTC*HQNDVSPDALIANK.F	296|299	24.82%	1.31%
Q9BXB4	OSBPL11 Oxysterol-binding protein-related protein 11	R.LQIC*TQHHTEAIGK.N	153	24.24%	1.98%
P55196	MLLT4 Afadin	K.ITSVSTGNLC*TEEQTPPPRPEAYPIPTQTYTR.E	1206	24.07%	16.72%
Q96KR1	ZFR Zinc finger RNA-binding protein	R.NVNLVLLC*SEKPSK.T	812	23.85%	16.53%
Q8N8S7	ENAH Protein enabled homolog	K.IQDHQVVINC*AIPK.G	62	22.83%	27.90%
Q14135	VGLL4 Transcription cofactor vestigial-like protein 4	R.RPPSAATTC*DPVVEEHFR.R	205	22.59%	12.34%

Q8N163	KIAA1967 DBIRD complex subunit KIAA1967	R.PGC*VNLSLHGIVEDR.R	515	22.18%	26.81%
Q9ULH7	MKL2 MKL/myocardin-like protein 2	K.HGSLGSSIKDEASLPDC*SSSR.Q	636	21.57%	25.76%
P62495	ETF1 Eukaryotic peptide chain release factor subunit 1	K.KVNIDFEPFKPINTSLYLC*DNK.F	127	20.85%	25.08%
P55265	ADAR Double-stranded RNA-specific adenosine deaminase	K.SPVTTLLEC*MHK.L	622	19.97%	23.07%
Q9Y490	TLN1 Talin-1	R.VQELGHGC*AALVTK.A	1927	19.16%	21.71%
Q6PJT7	ZC3H14 Zinc finger CCCH domain-containing protein 14	K.PAVAPPAPPSSSQLC*R.Y	682	17.55%	19.01%
P55010	EIF5 Eukaryotic translation initiation factor 5	K.FVLC*PEC*ENPETDLHVNPK.K	99|102	16.45%	0.44%
Q9Y4C1	KDM3A Lysine-specific demethylase 3A	K.KVEPSALAC*R.S	479	15.80%	19.13%
Q13642	FHL1 Four and a half LIM domains protein 1	K.GEDFYC*VTC*HETK.F	150|153	15.12%	0.16%
Q12874	SF3A3 Splicing factor 3A subunit 3	R.YLDLHDC*YLK.Y	145	15.11%	2.59%
P14923	JUP Junction plakoglobin	R.NLALC*PANHAPLQEAAVIPR.L	511	14.40%	8.35%
Q9UEG4	ZNF629 Zinc finger protein 629	R.GERPYIC*ADC*GK.S	432|435	14.23%	0.27%
Q96JM3	CHAMP1 Chromosome alignment-maintaining phosphoprotein 1	R.LEC*DHC*SFR.G	16|19	13.66%	2.53%
P49419	ALDH7A1 Alpha-aminoadipic semialdehyde dehydrogenase	K.VLEDNKLPGAIC*SLTC*GGADIGTAMAK.D	248|252	13.36%	2.34%
Q9Y6A5	TACC3 Transforming acidic coiled-coil-containing protein	R.HGGVC*APAAVATSPPGAIPK.E	242	13.02%	0.15%
P17028	ZNF24 Zinc finger protein 24	R.IHTGEKPYEC*VQC*GK.S	337|340	13.01%	1.86%
P17028	ZNF24 Zinc finger protein 24	R.IHSGEKPYGC*VEC*GK.A	281|284	12.79%	0.94%
Q9UQ35	SRRM2 Serine/arginine repetitive matrix protein 2	K.DSLVQSC*PGSLSLC*AGVK.S	1029|1036	12.49%	6.63%
Q2KHR3	QSER1 Glutamine and serine-rich protein 1	R.NILSNVDDILAATAAAC*GVTPTDFSK.S	862	12.45%	8.05%
Q6KC79	NIPBL Nipped-B-like protein	K.TPITPQDINRPLNAAQC*LSQQEQTAFLPANQVPVLQQNTSVAAK.Q	419	12.28%	10.63%
P62937	PPIA Peptidyl-prolyl cis-trans isomerase A	K.KITIADC*GQLE.-	161	12.25%	3.43%
Q5VZL5	ZMYM4 Zinc finger MYM-type protein 4	K.ATSC*KPHTQNK.E	959	12.11%	1.00%
P49792	RANBP2 E3 SUMO-protein ligase RanBP2	R.C*VAC*QNPDKPSPSTSVPAPASFK.F	1563|1566	12.04%	1.35%
P23528	CFL1 Cofilin-1	K.AVLFC*LSEDKK.N	39	12.03%	10.28%
O43175	PHGDH D-3-phosphoglycerate dehydrogenase	K.VLISDSLDPC*C*R.K	18|19	11.31%	9.26%
Q9UBB4	ATXN10 Ataxin-10	R.DPSQVENLASSLQLITEC*FR.C	84	11.28%	5.64%
Q15365	PCBP1 Poly(rC)-binding protein 1	R.C*SDAAGYPHATHDLEGPPLDAYSIQGQHTISPLDLAK.L	201	11.27%	0.48%
O95218	ZRANB2 Zinc finger Ran-binding domain-containing protein	R.RSEC*NMC*NTPK.Y	85|88	11.11%	1.58%
Q93015	NAT6 N-acetyltransferase 6	K.LPLDSTC*QPEMTFNPGPTELTLDPEHQPEETPAPSLAELTLEPVHR.R	28	11.02%	1.52%
Q13151	HNRNPA0 Heterogeneous nuclear ribonucleoprotein A0	R.C*FGFVTYSNVEEADAAMAASPHAVDGNTVELK.R	49	10.83%	8.58%
Q13642	FHL1 Four and a half LIM domains protein 1	R.FTAVEDQYYC*VDC*YK.N	209|212	10.68%	0.04%
P49792	RANBP2 E3 SUMO-protein ligase RanBP2	K.KC*VSC*QNLNPSNK.E	1372|1375	10.15%	0.48%
P49790	NUP153 Nuclear pore complex protein Nup153	K.C*LAC*ESAKPGTK.S	871|874	10.05%	0.17%
O00221	NFKBIE NF-kappa-B inhibitor epsilon	R.HGDTALHVAC*QR.Q	335	9.72%	7.02%
P68104	EEF1A1 Elongation factor 1-alpha 1	K.SGDAAIVDMVPGKPMC*VESFSDYPPLGR.F	411	9.58%	3.17%
Q6ZWJ1	STXBP4 Syntaxin-binding protein 4	R.NEGPLVYIQEIIPGGDC*YK.D	58	9.40%	5.56%
Q13263	TRIM28 Transcription intermediary factor 1-beta	R.DC*QLNAHK.D	232	9.24%	1.96%
O43175	PHGDH D-3-phosphoglycerate dehydrogenase	R.ALVDHENVISC*PHLGASTK.E	281	9.22%	1.78%
Q53GG5	PDLIM3 PDZ and LIM domain protein 3	K.AAAHQLC*LK.I	77	9.20%	1.22%
Q13642	FHL1 Four and a half LIM domains protein 1	R.FWHDTC*FR.C	65	9.13%	0.04%
P49757	NUMB Protein numb homolog	R.HTEVPTGTC*PVDPFEAQWAALENK.S	611	8.81%	5.09%
Q13642	FHL1 Four and a half LIM domains protein 1	K.C*LHPLANETFVAK.D	71	8.63%	0.35%
P27816	MAP4 Microtubule-associated protein 4	R.KPC*NSQPSELSSETSGIAR.P	654	8.60%	0.45%
Q13642	FHL1 Four and a half LIM domains protein 1	K.FDC*HYC*R.D	7|10	8.51%	0.59%
P50502	ST13 Hsc70-interacting protein	R.LLGHWEEAAHDLALAC*K.L	209	8.31%	2.40%
Q15942	ZYX Zyxin	R.C*SVC*SEPIMPEPGRDETVR.V	504|507	8.26%	0.03%
Q96T51	RUFY1 RUN and FYVE domain-containing protein 1	R.HLSC*TVGDLQTK.I	320	8.21%	2.99%
O43719	HTATSF1 HIV Tat-specific factor 1	K.RGFEGSC*SQK.E	480	7.79%	1.57%
Q8ND82	ZNF280C Zinc finger protein 280C	R.C*RDPPSNPVAASPR.F	94	7.48%	0.87%
Q8N3F8	MICALL1 MICAL-like protein 1	R.C*SSTLLPGAYENGPEEGTFVC*AEHC*AR.L	194|214|218	7.45%	3.80%
P30048	PRDX3 Thioredoxin-dependent peroxide reductase, mitochon	K.AFQYVETHGEVC*PANWTPDSPTIKPSPAASK.E	229	7.45%	3.80%
Q15942	ZYX Zyxin	R.C*HQPLAR.A	387	7.44%	0.05%
P52209	PGD 6-phosphogluconate dehydrogenase, decarboxylating	K.VGTGEPC*C*DWVGDEGAGHFVK.M	170|171	7.43%	1.16%
P14618	PKM Pyruvate kinase isozymes M1/M2	R.AEGSDVANAVLDGADC*IMLSGETAK.G	358	7.36%	3.67%
Q9UGI8	TES Testin	R.HYC*DSEKPR.C	294	7.08%	0.49%
Q0IIM8	TBC1D8B TBC1 domain family member 8B	K.TGSHLEKDPC*SFR.E	1067	7.04%	3.22%
P61289	PSME3 Proteasome activator complex subunit 3	K.RRLDEC*EEAFQGTK.V	92	6.97%	5.77%
Q5VSL9	FAM40A Protein FAM40A	R.AHSNPDFLPVDNC*LQSVLGQR.V	798	6.88%	3.00%
Q12888	TP53BP1 Tumor suppressor p53-binding protein 1	R.EEGGC*SLASTPATTLHLLQLSGQR.S	329	6.71%	1.00%
Q9NW64	RBM22 Pre-mRNA-splicing factor RBM22	K.RGEEC*PYR.H	179	6.66%	0.82%
Q9Y6A5	TACC3 Transforming acidic coiled-coil-containing protein	R.LGQPAAEQLHAGPATEEPGPC*LSQQLHSASAEDTPVVQLAAETPTAESK.E	459	6.63%	1.15%
Q8NFH3	NUP43 Nucleoporin Nup43	R.VPLHC*VDR.H	222	6.63%	2.64%
Q5SW79	CEP170 Centrosomal protein of 170 kDa	K.NHEAGTSGC*GIDAK.Q	212	6.62%	0.90%
Q9NWK9	ZNHIT6 Box C/D snoRNA protein 1	K.VKEEPPINHPVGC*K.R	211	6.58%	1.63%

P49454	CENPF Centromere protein F	K.TKHEC*QNLESEPIR.N	1166	6.57%	2.55%
Q7Z5K2	WAPAL Wings apart-like protein homolog	R.LENLNEAIEEDIVQSVLRPTNC*R.T	293	6.47%	1.04%
Q9Y232	CDYL Chromodomain Y-like protein	R.KLTAQEAC*GK.G	515	6.45%	2.39%
Q99733	NAP1L4 Nucleosome assembly protein 1-like 4	K.SEPDKADPFSFEGPEIVDC*DGC*TIDW K.K	247|250	6.37%	1.77%
Q9Y314	NOSIP Nitric oxide synthase-interacting protein	R.DSLSNATPC*AVLRPSGAVVTLEC*VEK .L	236|250	6.36%	2.26%
P68366	TUBA4A Tubulin alpha-4A chain	K.AYHEQLSVAEITNAC*FEPANQMVK.C	295	6.30%	1.01%
Q96RL1	UIMC1 BRCA1-A complex subunit RAP80	R.C*TGHSAEHTQC*GKPQESTGR.G	220|230	6.24%	1.39%
O75369	FLNB Filamin-B	K.ALGALVDSC*APGLC*PDWESWDPQK PVDNAR.E	178|183	6.23%	2.08%
P62316	SNRPD2 Small nuclear ribonucleoprotein Sm D2	K.NNTQVLINC*R.N	46	6.21%	1.85%
P49792	RANBP2 E3 SUMO-protein ligase RanBP2	K.EGQWDC*SSC*LVR.N	1549|1552	6.20%	2.50%
P21333	FLNA Filamin-A	K.LQVEPAVDTSGVQC*YGPGIEGQGVFR .E	1260	6.19%	2.02%
Q7Z6E9	RBBP6 E3 ubiquitin-protein ligase RBBP6	K.LNYDTVTFDGLHISLC*DLK.K	27	6.15%	1.97%
Q9H9B1	EHMT1 Histone-lysine N-methyltransferase EHMT1	K.APLLVLC*EDHR.G	575	6.10%	1.89%
Q6IS14	EIF5AL1 Eukaryotic translation initiation factor 5A-1-like	K.KYEDIC*PSTHNMDVPNIK.R	73	6.10%	1.89%
P21333	FLNA Filamin-A	K.IVGPSGAAVPC*K.V	1018	6.08%	1.86%
Q14686	NCOA6 Nuclear receptor coactivator 6	R.ATPVQLPSPPC*TSSPVVPSHPPVQQVK .E	1748	6.04%	0.32%
P14618	PKM Pyruvate kinase isozymes M1/M2	R.NTGIIC*TIGPASR.S	49	6.02%	1.78%
P12004	PCNA Proliferating cell nuclear antigen	R.DLSHIGDAVVISC*AK.D	162	6.02%	1.09%
Q14241	TCEB3 Transcription elongation factor B polypeptide 3	K.MMTLHQQC*IR.V	581	6.02%	1.78%
B7ZAP0	RABGAP1L Rab GTPase-activating protein 1-like, isoform 10	K.HC*SDIFSK.E	146	5.94%	1.02%
P46013	MKI67 Antigen KI-67	K.ELFQTPGHTEESMTDDKITEVSC*K.S	1981	5.94%	0.59%
Q9HC35	EML4 Echinoderm microtubule-associated protein-like 4	R.KVIAVADDFC*K.V	811	5.92%	1.64%
Q2VPK5	CTU2 Cytoplasmic tRNA 2-thiolation protein 2	R.TPPGPC*C*SPGVGWAQR.C	433|434	5.91%	1.63%
Q9NZZ3	CHMP5 Charged multivesicular body protein 5	K.APPPSLTDC*IGTVDSR.A	20	5.87%	1.56%
P17098	ZNF8 Zinc finger protein 8	R.THTGEKPYTC*SVC*GK.S	371|374	5.82%	1.50%
Q9UBB4	ATXN10 Ataxin-10	R.HAELIASTFVDQC*K.T	283	5.70%	1.33%
P49792	RANBP2 E3 SUMO-protein ligase RanBP2	K.EGQWDC*SAC*LVQNEGSSTK.C	1485|1488	5.70%	1.07%
Q9ULW0	TPX2 Targeting protein for Xklp2	R.C*ATPVIIDEILPSK.K	145	5.69%	1.32%
Q9UKV3	ACIN1 Apoptotic chromatin condensation inducer in the nu	K.KC*EAEEAEPPAATQPQTSETQTSHLP ESER.I	733	5.69%	0.10%
P35579	MYH9 Myosin-9	R.C*QHLQAEK.K	931	5.66%	0.90%
P49792	RANBP2 E3 SUMO-protein ligase RanBP2	K.LPPTFFC*GVC*SDTDEDNGNGEDFQS ELQK.V	2737|2740	5.56%	0.90%
P49790	NUP153 Nuclear pore complex protein Nup153	K.AGSSWQC*DTC*LLQNK.V	664|667	5.56%	0.35%
P23588	EIF4B Eukaryotic translation initiation factor 4B	K.SLENETLNKEEDC*HSPTSKPPKPDQPL K.V	457	5.46%	0.26%
P62316	SNRPD2 Small nuclear ribonucleoprotein Sm D2	R.HC*NMVLENVK.E	63	5.45%	0.98%
Q9HC35	EML4 Echinoderm microtubule-associated protein-like 4	R.HYLGHTDC*VK.C	311	5.45%	0.61%
Q00610	CLTC Clathrin heavy chain 1	R.IHEGC*EEPATHNALAK.I	870	5.44%	0.96%
Q5VT52	RPRD2 Regulation of nuclear pre-mRNA domain-containing p	K.LPSNSLGFTATHNTSPAAPPTEVTIC*Q SSEVSKPK.L	649	5.44%	0.45%
Q7Z2W4	ZC3HAV1 Zinc finger CCCH-type antiviral protein 1	R.VDDHDSEEIC*LDHLC*K.G	513|518	5.43%	0.24%
Q86XP3	DDX42 ATP-dependent RNA helicase DDX42	R.KSEYTQPTPIQC*QGVPVALSGR.D	281	5.35%	0.83%
P33991	MCM4 DNA replication licensing factor MCM4	R.LGEINVIGEPFLNVNC*EHIK.S	212	5.31%	0.78%
P46060	RANGAP1 Ran GTPase-activating protein 1	K.LDLNGNTLGEEGC*EQLQEVLEGFNM AK.V	338	5.29%	0.75%
P52732	KIF11 Kinesin-like protein KIF11	R.C*RPFNLAER.K	25	5.27%	0.71%
Q9H9J4	USP42 Ubiquitin carboxyl-terminal hydrolase 42	R.SEEPC*EQPLLVHPSGDHAR.D	867	5.21%	0.64%
Q14966	ZNF638 Zinc finger protein 638	K.NSNSLFTLDELIDQDDC*ISHSEPK.D	1654	5.17%	1.14%
Q08211	DHX9 ATP-dependent RNA helicase A	K.LQISHEAAAC*ITGLR.A	1099	5.12%	0.51%
Q8TD19	NEK9 Serine/threonine-protein kinase Nek9	K.EEMEMDPKPDLDSDSWC*LLGTDSC*R PSL.-	968|975	5.09%	0.46%
P49792	RANBP2 E3 SUMO-protein ligase RanBP2	K.EGQWDC*SVC*LVR.N	1612|1615	5.08%	0.99%
P35520	CBS Cystathionine beta-synthase	R.NASNPLAHYDTTADEILQQC*DGK.L	244	5.08%	0.44%
Q6KC79	NIPBL Nipped-B-like protein	K.GSRPPLILQSQSLPC*SSPR.D	304	5.07%	0.42%
O00505	KPNA3 Importin subunit alpha-3	R.AVGNIVTGTDEQTQVVLNC*DVLSHF PNLLSHPK.E	325	5.07%	0.43%
Q92844	TANK TRAF family member-associated NF-kappa-B activator	K.TKPSNLVNTC*IR.T	318	5.00%	0.34%
Q69YH5	CDCA2 Cell division cycle-associated protein 2	R.KEGLSAC*QQSGFPAVLSSK.R	188	4.99%	0.32%
Q8WWM7	ATXN2L Ataxin-2-like protein	K.TESVSDKEDKPPLAPSGGTEGPEQPPP PC*PSQTGSPPVGLIK.G	628	4.96%	0.28%
Q9NRL3	STRN4 Striatin-4	R.IWDPSSSSPAC*LC*TFPTASEHGVPTSV AFTSTEPAHIVASFR.S	580|582	4.95%	0.26%
Q9BXB4	OSBPL11 Oxysterol-binding protein-related protein 11	K.HNITNTVVC*R.V	629	4.94%	0.26%
Q7Z2W4	ZC3HAV1 Zinc finger CCCH-type antiviral protein 1	R.EHGLNPDVVQNIQDIC*NSK.H	219	4.93%	0.24%
Q9NUU7	DDX19A ATP-dependent RNA helicase DDX19A	R.VEPSDRYPQC*LC*LSPTYELALQTGK.V	164|166	4.90%	0.20%
Q9Y490	TLN1 Talin-1	K.APGQLEC*ETAIAALNSC*LR.D	1661|1671	4.90%	0.20%
Q9Y4E8	USP15 Ubiquitin carboxyl-terminal hydrolase 15	R.DKLDTLVDFPINDLDMSEFLINPNAGP C*R.Y	873	4.84%	0.11%
Q9UHD1	CHORDC1 Cysteine and histidine-rich domain-containing prot	R.FDPETNSDDAC*TYHPGVPVFHDALK. G	24	4.84%	0.15%
Q7Z3T8	ZFYVE16 Zinc finger FYVE domain-containing protein 16	K.SNADSLIGLDLSSVSDTPC*VSSTDHDS DTVR.E	174	4.83%	0.10%

Q8TD19	NEK9 Serine/threonine-protein kinase Nek9	R.HC*DSINSDFGSESGGC*GDSSPGPSASQGPR.A	11|25	4.83%	0.09%
P26641	EEF1G Elongation factor 1-gamma	K.AAAPAPEEEMDEC*EQALAAEPK.A	266	4.83%	0.11%
Q6PII3	C3orf19 Uncharacterized protein C3orf19	R.PGPAQSDPGQC*PDQSHGPSPEHTSPTPAPDNPPQAPTVTFK.T	424	4.81%	0.09%
P22314	UBA1 Ubiquitin-like modifier-activating enzyme 1	R.VGEFC*HNR.G	179	4.79%	0.04%
P21333	FLNA Filamin-A	K.VEYTPYEEGLHSVDVTYDGSPVPSSPFQVPVTEGC*DPSR.V	1353	4.77%	0.02%
Q13748	TUBA3D Tubulin alpha-3C/D chain	K.RTIQFVDWC*PTGFK.V	BAD_ID	4.76%	0.00%
O95861	BPNT1 3(2),5-bisphosphate nucleotidase 1	K.KWDTC*APEVILHAVGGK.L	249	4.76%	0.00%
Q92576	PHF3 PHD finger protein 3	K.LSHEDDHILEDAGSSDISSDAAC*TNPNK.T	350	4.76%	0.00%
P11413	G6PD Glucose-6-phosphate 1-dehydrogenase	R.LQFHIDVAGDIFHQQC*K.R	385	4.76%	0.00%
Q04760	GLO1 Lactoylglutathione lyase	R.GFGHIGIAVPDVYSAC*K.R	139	4.76%	0.00%
Q9UHD1	CHORDC1 Cysteine and histidine-rich domain-containing prot	R.TTDFSDFLSIVGC*TK.G	59	4.76%	0.00%
P49643	PRIM2 DNA primase large subunit	K.GTHYQVAC*QK.Y	424	4.76%	0.00%
A6NE09	RPSAP58 Protein RPSAP58	R.ADHQPLTEASYVNLPTIALC*NTDSPLR.Y	BAD_ID	4.76%	0.00%
B4DLE8	CRYBG3 cDNA FLJ60082, weakly similar to Uro-adherence fac	R.HEHLQLPESEC*SDK.Q	474	4.76%	0.00%
O43432	EIF4G3 Eukaryotic translation initiation factor 4 gamma 3	K.MLTEAIMHDC*VVK.L	913	4.76%	0.00%
P08107	HSPA1B Heat shock 70 kDa protein 1A/1B	K.ELEQVC*NPIISGLYQGAGGPGPGGFGAQGPK.G	BAD_ID	4.76%	0.00%
P15170	GSPT1 Eukaryotic peptide chain release factor GTP-bindin	R.TAGTIC*LETFK.D	464	4.76%	0.00%
P22102	GART Trifunctional purine biosynthetic protein adenosin	K.AFTKPEEAC*SFILSADFPALVVK.A	134	4.76%	0.00%
P33981	TTK Dual specificity protein kinase TTK	R.KSEC*INQNPAASSNHWQIPELAR.K	395	4.76%	0.00%
P37802	TAGLN2 Transgelin-2	K.NMAC*VQR.T	124	4.76%	0.00%
P43487	RANBP1 Ran-specific GTPase-activating protein	R.AWVWNTHADFADEC*PKPELLAIR.F	132	4.76%	0.00%
P46109	CRKL Crk-like protein	K.RVPC*AYDK.T	249	4.76%	0.00%
P78344	EIF4G2 Eukaryotic translation initiation factor 4 gamma 2	K.QEGIATSDNFMQAFLNVLDQC*PK.L	629	4.76%	0.00%
Q06323	PSME1 Proteasome activator complex subunit 1	K.KGEDEDKGPPC*GPVNC*NEK.I	101|106	4.76%	0.00%
Q13480	GAB1 GRB2-associated-binding protein 1	R.RPVPVADC*EPPPVDR.N	514	4.76%	0.00%
Q14157	UBAP2L Ubiquitin-associated protein 2-like	K.NQDEC*VIALHDC*NGDVNR.A	68|75	4.76%	0.00%
Q15417	CNN3 Calponin-3	K.DGIILC*ELINK.L	59	4.76%	0.00%
Q15750	TAB1 TGF-beta-activated kinase 1 and MAP3K7-binding pro	R.SENNC*FLYGVFNGYDGNR.V	62	4.76%	0.00%
Q5TGY3	AHDC1 AT-hook DNA-binding motif-containing protein 1	R.GPAAAAAGYGC*PLLSDLTLSPVPR.D	1540	4.76%	0.00%
Q5VWN6	FAM208B Protein FAM208B	R.NLHC*SSELPQNDVLLSK.E	559	4.76%	0.00%
Q5VWN6	FAM208B Protein FAM208B	K.TPLTQGLELC*VQNEQK.K	889	4.76%	0.00%
Q8WZA0	LZIC Protein LZIC	R.LMQQLQDLEEC*REELDTDEYEETKK.E	33	4.76%	0.00%
Q96KB5	PBK Lymphokine-activated killer T-cell-originated prot	K.INPIC*NDHYR.S	70	4.76%	0.00%
Q96QD5	DEPDC7 DEP domain-containing protein 7	K.DKKPTFEDSSC*SLYR.F	129	4.76%	0.00%
Q99460	PSMD1 26S proteasome non-ATPase regulatory subunit 1	R.TPEQC*PSVVSLLSESYNPHVR.Y	633	4.76%	0.00%
Q9BUA3	C11orf84 Uncharacterized protein C11orf84	K.TPPPRPSPLEAGSDGC*EEPK.Q	64	4.76%	0.00%
Q9H0W8	SMG9 Protein SMG9	R.REDFC*PR.K	380	4.76%	0.00%
Q9Y450	HBS1L HBS1-like protein	R.LYSC*LDHMR.E	84	4.76%	0.00%
Q9Y520	PRRC2C Protein PRRC2C	K.EKETNDDNYGPGPSLRPPNVAC*WR.D	177	4.76%	0.00%
Q9Y546	LRRC42 Leucine-rich repeat-containing protein 42	K.APDC*HGPVLK.H	373	4.76%	0.00%
Q9Y546	LRRC42 Leucine-rich repeat-containing protein 42	R.KLNC*LDISGTGLK.D	262	4.76%	0.00%
Q9Y617	PSAT1 Phosphoserine aminotransferase	K.SQTIYEIIDNSQGFYVC*PVEPQNR.S	291	4.76%	0.00%
Q7Z5K2	WAPAL Wings apart-like protein homolog	K.ALQHC*EELIQQYNR.A	891	4.76%	0.00%
O60879	DIAPH2 Protein diaphanous homolog 2	R.LDIDLTHLIDSC*VNK.A	484	4.76%	0.00%
O14929	HAT1 Histone acetyltransferase type B catalytic subunit	K.VDENFDC*VEADDVEGK.I	101	4.76%	0.00%
O94762	RECQL5 ATP-dependent DNA helicase Q5	R.GGEHEPPSRPC*GLLDEDGSEPLPGPR.G	698	4.76%	0.00%
P55196	MLLT4 Afadin	R.NIPNGLQEFLDPLC*QR.G	960	4.76%	0.00%
Q9P266	KIAA1462 Junctional protein associated with coronary artery	R.FRVEEGGGAPFC*SADGSTSAEK.R	946	4.76%	0.00%
P23443	RPS6KB1 Ribosomal protein S6 kinase beta-1	K.IRPEC*FELLR.V	90	4.76%	0.00%
Q4VCS5	AMOT Angiomotin	K.TEQLSC*MRPAK.S	781	4.76%	0.00%
Q00013	MPP1 55 kDa erythrocyte membrane protein	K.KDNLIPC*K.E	179	4.76%	0.00%
Q00013	MPP1 55 kDa erythrocyte membrane protein	K.KLQEAFDQAC*SSPQWVPVSWVY.-	454	4.76%	0.00%
Q14160	SCRIB Protein scribble homolog	R.SLEPSPSPGPQEEDGEVALVLLGRPSPGAVGPEDVALC*SSR.R	1612	4.76%	0.00%
Q14160	SCRIB Protein scribble homolog	R.RSEAC*PC*QPDSGSPLPAEEEKR.L	496|498	4.76%	0.00%
Q2M2I8	AAK1 AP2-associated protein kinase 1	R.GHYVLC*DFGSATNK.F	193	4.76%	0.00%
P46013	MKI67 Antigen KI-67	K.ADVEGELLAC*R.N	1285	4.76%	0.00%
P46013	MKI67 Antigen KI-67	K.ELFQTPIC*TDKPTTHEK.T	2206	4.76%	0.00%
P46013	MKI67 Antigen KI-67	K.SEETNTEIVEC*ILK.R	903	4.76%	0.00%
Q8NFC6	BOD1L1 Biorientation of chromosomes in cell division prot	R.SEEKDEC*AMISTSIGEEFELPISSATTIK.C	2141	4.76%	0.00%
Q8NFC6	BOD1L1 Biorientation of chromosomes in cell division prot	R.SDNFVIC*SVTGAGPR.E	1742	4.76%	0.00%
Q9BY42	C20orf43 UPF0549 protein C20orf43	R.RPIVAC*ELGR.L	51	4.76%	0.00%
P26639	TARS Threonine--tRNA ligase, cytoplasmic	K.VNNVVWDLDRPLEEDC*TLELLK.F	137	4.76%	0.00%
P49327	FASN Fatty acid synthase	K.TGGAYGEDLGADYNLSQVC*DGK.V	2468	4.76%	0.00%
P49327	FASN Fatty acid synthase	K.FC*FTPHTEEGC*LSER.A	1118|1127	4.76%	0.00%
Q09472	EP300 Histone acetyltransferase p300	R.HDC*PVC*LPLK.N	411|414	4.76%	0.00%
A6NHG4	DDTL D-dopachrome decarboxylase-like protein	R.LC*AAAASILGK.P	24	4.76%	0.00%
P36873	PPP1CC Serine/threonine-protein phosphatase PP1-gamma cat	K.IC*GDIHGQYYDLLR.L	62	4.76%	0.00%
P36873	PPP1CC Serine/threonine-protein phosphatase PP1-gamma cat	R.IMRPTDVPDQGLLC*DLLWSDPDKDVLGWGENDR.G	202	4.76%	0.00%

P49321	NASP Nuclear autoantigenic sperm protein	K.KYGETANEC*GEAFFFYGK.S	84	4.76%	0.00%
Q9Y4E8	USP15 Ubiquitin carboxyl-terminal hydrolase 15	K.LKDC*IELFTTK.E	791	4.76%	0.00%
Q9Y4E8	USP15 Ubiquitin carboxyl-terminal hydrolase 15	K.ISTETEETEGSLHC*C*K.D	633|634	4.76%	0.00%
Q9Y4E8	USP15 Ubiquitin carboxyl-terminal hydrolase 15	R.TEDTEHVIIPVC*LR.E	570	4.76%	0.00%
Q9H2G2	SLK STE20-like serine/threonine-protein kinase	K.DVISNTSDVIGTC*EAADVAQK.V	552	4.76%	0.00%
P49588	AARS Alanine--tRNA ligase, cytoplasmic	R.VVSIGVPVSELLDDPSGPAGSLTSVEFC*GGTHLR.N	723	4.76%	0.00%
O14617	AP3D1 AP-3 complex subunit delta-1	K.EKLEDPDPGVQSAAVNVIC*ELAR.R	208	4.76%	0.00%
O15067	PFAS Phosphoribosylformylglycinamidine synthase	R.LGGTALAQC*FSQLGEHPPDLDLPENLVR.A	871	4.76%	0.00%
O43776	NARS Asparagine--tRNA ligase, cytoplasmic	K.YGTC*PHGGYGLGLER.F	511	4.76%	0.00%
O75794	CDC123 Cell division cycle protein 123 homolog	R.DFTQPFIHC*TDDSPDPC*IEYELVLR.K	151|159	4.76%	0.00%
O95757	HSPA4L Heat shock 70 kDa protein 4L	K.ELDNFC*NPIIYKPK.P	782	4.76%	0.00%
O95757	HSPA4L Heat shock 70 kDa protein 4L	R.GC*ALQC*AILSPAFK.V	376|380	4.76%	0.00%
O95757	HSPA4L Heat shock 70 kDa protein 4L	K.KPVADC*VISIPSFFTDAER.R	140	4.76%	0.00%
P08670	VIM Vimentin	R.QVQSLTC*EVDALK.G	328	4.76%	0.00%
P12268	IMPDH2 Inosine-5-monophosphate dehydrogenase 2	R.HGFC*GIPITDTGR.M	140	4.76%	0.00%
P13639	EEF2 Elongation factor 2	K.IWC*FGPDGTGPNILTDITK.G	651	4.76%	0.00%
P13639	EEF2 Elongation factor 2	R.ETVSEESNVLC*LSK.S	591	4.76%	0.00%
P13639	EEF2 Elongation factor 2	R.YVEPIEDVPC*GNIVGLVGVDQFLVK.T	466	4.76%	0.00%
P13639	EEF2 Elongation factor 2	R.C*LYASVLTAQPR.L	728	4.76%	0.00%
P23526	AHCY Adenosylhomocysteinase	K.GETDEEYLWC*IEQTLYFK.D	113	4.76%	0.00%
P23526	AHCY Adenosylhomocysteinase	K.FDNLYGC*R.E	195	4.76%	0.00%
P34932	HSPA4 Heat shock 70 kDa protein 4	K.KPVVDC*VVSVPC*FYTDAER.R	140|146	4.76%	0.00%
P46060	RANGAP1 Ran GTPase-activating protein 1	K.ILAAALTEC*HR.K	169	4.76%	0.00%
P46060	RANGAP1 Ran GTPase-activating protein 1	K.ELNLSFC*EIK.R	303	4.76%	0.00%
P46060	RANGAP1 Ran GTPase-activating protein 1	R.C*HWSDMFTGR.L	82	4.76%	0.00%
P46060	RANGAP1 Ran GTPase-activating protein 1	R.QVEVINFGDC*LVR.S	274	4.76%	0.00%
P48643	CCT5 T-complex protein 1 subunit epsilon	K.ETGANLAIC*QWGFDDEANHLLLQNNLPAVR.W	302	4.76%	0.00%
P48643	CCT5 T-complex protein 1 subunit epsilon	K.IAILTC*PFEPPKPK.T	253	4.76%	0.00%
P50395	GDI2 Rab GDP dissociation inhibitor beta	R.VIC*ILSHPIK.N	302	4.76%	0.00%
P50990	CCT8 T-complex protein 1 subunit theta	R.IGLSVSEVIEGYEIAC*R.K	136	4.76%	0.00%
P51610	HCFC1 Host cell factor 1	R.AGHC*AVAINTR.L	326	4.76%	0.00%
P62195	PSMC5 26S protease regulatory subunit 8	R.AVAHHTDC*TFIR.V	209	4.76%	0.00%
P78347	GTF2I General transcription factor II-I	R.SILSPGGSC*GPIK.V	215	4.76%	0.00%
P78371	CCT2 T-complex protein 1 subunit beta	K.HGINC*FINR.Q	289	4.76%	0.00%
Q08209	PPP3CA Serine/threonine-protein phosphatase 2B catalytic	R.FKEPPAYGPMC*DILWSDPLEDFGNEK.T	228	4.76%	0.00%
Q14258	TRIM25 E3 ubiquitin/ISG15 ligase TRIM25	K.NTVLC*NVVEQFLQADLAR.E	70	4.76%	0.00%
Q14694	USP10 Ubiquitin carboxyl-terminal hydrolase 10	K.VQRPC*TSTPMIDSFVR.L	456	4.76%	0.00%
Q15185	PTGES3 Prostaglandin E synthase 3	K.HLNEIDLFHC*IDPNDSK.H	58	4.76%	0.00%
Q8IWZ3	ANKHD1 Ankyrin repeat and KH domain-containing protein 1	K.SSSLQVADQDLLPSFHPYQPLEC*IVEETEGK.L	777	4.76%	0.00%
Q8N6T3	ARFGAP1 ADP-ribosylation factor GTPase-activating protein	K.FREFLESQEDYDPC*WSLQEK.Y	96	4.76%	0.00%
Q8TD19	NEK9 Serine/threonine-protein kinase Nek9	K.GTPLTPPAC*AC*SSLQVEVER.L	890|892	4.76%	0.00%
Q92598	HSPH1 Heat shock protein 105 kDa	K.KPVTDC*VISVPSFFTDAER.R	140	4.76%	0.00%
Q92598	HSPH1 Heat shock protein 105 kDa	K.IKELNNTC*EPVVTQPKPK.I	796	4.76%	0.00%
Q92598	HSPH1 Heat shock protein 105 kDa	K.LVEHFC*AEFK.T	245	4.76%	0.00%
Q99961	SH3GL1 Endophilin-A2	K.PREPFDLGEPEQSNGGFPC*TTAPK.I	277	4.76%	0.00%
Q99961	SH3GL1 Endophilin-A2	K.QNFIDPLQNLC*EK.D	147	4.76%	0.00%
Q9BPZ3	PAIP2 Polyadenylate-binding protein-interacting protein	R.C*FQEMLEEEEEHEWFIPAR.D	60	4.76%	0.00%
Q9BQG0	MYBBP1A Myb-binding protein 1A	R.HQAC*LLLQK.T	1031	4.76%	0.00%
Q9BYP7	WNK3 Serine/threonine-protein kinase WNK3	R.DTLLTIENNPC*HR.A	927	4.76%	0.00%
Q9C0C9	UBE2O Ubiquitin-conjugating enzyme E2 O	R.LGC*FDHAQR.Q	341	4.76%	0.00%
Q9C0C9	UBE2O Ubiquitin-conjugating enzyme E2 O	K.LYDVC*PHVSDSGLFFDDSYGFYPGQVLIGPAK.I	244	4.76%	0.00%
Q9C0C9	UBE2O Ubiquitin-conjugating enzyme E2 O	R.SNDLFPVHHLDNNEFC*PGDFVVDKR.V	585	4.76%	0.00%
Q9H089	LSG1 Large subunit GTPase 1 homolog	R.DHVPPVSLVC*QNIPR.H	475	4.76%	0.00%
Q9H939	PSTPIP2 Proline-serine-threonine phosphatase-interacting p	R.KKPC*GQSEINTLK.R	65	4.76%	0.00%
Q9NSV4	DIAPH3 Protein diaphanous homolog 3	R.SHYNINC*NSTR.T	1125	4.76%	0.00%
Q9UH65	SWAP70 Switch-associated protein 70	K.VLSHNLC*TVLK.V	40	4.76%	0.00%
Q9UPN7	PPP6R1 Serine/threonine-protein phosphatase 6 regulatory	R.LIEQIHPSKDENQHSNASQSLC*DIIR.L	216	4.76%	0.00%
Q9Y217	MTMR6 Myotubularin-related protein 6	R.C*LEDEHLLQAISK.A	214	4.76%	0.00%
Q9Y2L1	DIS3 Exosome complex exonuclease RRP44	R.RGTTVYLC*EK.R	533	4.76%	0.00%
Q9Y6Q2	STON1 Stonin-1	K.NFPLENQGVC*RPNGLK.L	35	4.76%	0.00%
O60271	SPAG9 C-Jun-amino-terminal kinase-interacting protein 4	K.VDELTC*EKDVLQGELEAVK.Q	443	4.76%	0.00%
O75410	TACC1 Transforming acidic coiled-coil-containing protein	K.KHETQSLALDAC*SR.D	482	4.76%	0.00%
P06733	ENO1 Alpha-enolase	R.SGETEDTFIADLVVGLC*TGQIK.T	389	4.76%	0.00%
P21333	FLNA Filamin-A	K.DNGNGTYSC*SYVPR.K	733	4.76%	0.00%
P21333	FLNA Filamin-A	K.IEC*DDKGDGSC*DVR.Y	623|631	4.76%	0.00%
P21333	FLNA Filamin-A	R.APSVANVGSHC*DLSLK.I	2160	4.76%	0.00%
P21333	FLNA Filamin-A	K.ATC*APQHGAPGPGPADASK.V	2543	4.76%	0.00%
P21333	FLNA Filamin-A	R.VQVQDNEGC*PVEALVK.D	717	4.76%	0.00%
Q02952	AKAP12 A-kinase anchor protein 12	K.SDEVDEQVAC*QEVK.V	1521	4.76%	0.00%
P07437	TUBB Tubulin beta chain	K.VSDTVVEPYNATLSVHQLVENTDETYC*IDNEALYDIC*FR.T	201|211	4.76%	0.00%
O43237	DYNC1LI2 Cytoplasmic dynein 1 light intermediate chain 2	R.C*NVWILDGDLYHK.G	104	4.76%	0.00%
O43491	EPB41L2 Band 4.1-like protein 2	K.VNGEVSHVDIDVLPQIIC*C*SEPPVVK.T	866|867	4.76%	0.00%

P35579	MYH9 Myosin-9	K.KQELEEIC*HDLEAR.V	917	4.76%	0.00%
P35579	MYH9 Myosin-9	R.EDQSILC*TGESGAGK.T	172	4.76%	0.00%
P35579	MYH9 Myosin-9	K.ADFC*IIHYAGK.V	569	4.76%	0.00%
P35579	MYH9 Myosin-9	R.C*IIPNHEK.K	671	4.76%	0.00%
P35579	MYH9 Myosin-9	K.PAGPPGILALLDEEC*WFPK.A	532	4.76%	0.00%
P35579	MYH9 Myosin-9	K.VEDMAELTC*LNEASVLHNLK.E	91	4.76%	0.00%
P49023	PXN Paxillin	R.GSLC*SGC*QKPITGR.C	535|538	4.76%	0.00%
P78559	MAP1A Microtubule-associated protein 1A	R.SSRPDTLLSPEQPVC*PAGGSGGPPSSASPEVEAGPQGC*ATEPR.P	2414|2437	4.76%	0.00%
Q15654	TRIP6 Thyroid receptor-interacting protein 6	R.VNFC*PLPSEQC*YQAPGGPEDR.G	47|54	4.76%	0.00%
Q6IBS0	TWF2 Twinfilin-2	R.AVLPLLDAQQPC*YLLYR.L	67	4.76%	0.00%
Q9HC35	EML4 Echinoderm microtubule-associated protein-like 4	K.VHLFQYPC*SK.A	820	4.76%	0.00%
Q9NYL9	TMOD3 Tropomodulin-3	K.VSLDPELEEALTSASDTELC*DLAAILGMHNLITNTK.F	132	4.76%	0.00%
Q9UHD8	SEPT9 Septin-9	K.LTVIDTPGFGDHINNENC*WQPIMK.F	375	4.76%	0.00%
Q03001	DST Dystonin	R.AAQLQEALLHC*GR.F	5394	4.76%	0.00%
Q12955	ANK3 Ankyrin-3	K.DIEVLEGKPIYVDC*YGNLAPLTK.G	1369	4.76%	0.00%
P46821	MAP1B Microtubule-associated protein 1B	R.TPDTSTYC*YETAEK.I	2041	4.76%	0.00%
P46821	MAP1B Microtubule-associated protein 1B	R.TPQASTYSYETSDLC*YTAEK.K	2065	4.76%	0.00%
Q9NRY4	ARHGAP35 Rho GTPase-activating protein 35	R.FTSIPC*SQPQHK.L	924	4.76%	0.00%
Q96KG9	SCYL1 N-terminal kinase-like protein	K.ILPVLC*GLTVDPEK.S	512	4.76%	0.00%
Q96EA4	CCDC99 Protein Spindly	R.LPPQKEETQSC*PNSLEDNNLQLEK.S	490	4.76%	0.00%
P68366	TUBA4A Tubulin alpha-4A chain	R.AVC*MLSNTTAIAEAWAR.L	376	4.76%	0.00%
Q92797	SYMPK Symplekin	R.C*LHSLTDK.V	859	4.76%	0.00%
Q9Y266	NUDC Nuclear migration protein nudC	R.WTQTLSELDLAVPFC*VNFR.L	188	4.76%	0.00%
P53396	ACLY ATP-citrate synthase	K.GVTIIGPATVGGIKPGC*FK.I	633	4.76%	0.00%
A0JNW5	UHRF1BP1L UHRF1-binding protein 1-like	R.HYLC*NRPVGSDQK.A	1235	4.76%	0.00%
P07814	EPRS Bifunctional glutamate/proline--tRNA ligase	K.ERPTPSLNNNC*TTSEDSLVLYNR.V	744	4.76%	0.00%
P07814	EPRS Bifunctional glutamate/proline--tRNA ligase	K.HEELMLGDPC*LK.D	660	4.76%	0.00%
P07814	EPRS Bifunctional glutamate/proline--tRNA ligase	K.YNVYPTYDFAC*PIVDSIEGVTHALR.T	381	4.76%	0.00%
P17987	TCP1 T-complex protein 1 subunit alpha	R.SLHDALC*VVK.R	397	4.76%	0.00%
P55072	VCP Transitional endoplasmic reticulum ATPase	R.QAAPC*VLFFDELDSIAK.A	572	4.76%	0.00%
P55786	NPEPPS Puromycin-sensitive aminopeptidase	R.LPADVSPINYSLC*LKPDLLDFTFEGK.L	66	4.76%	0.00%
P62318	SNRPD3 Small nuclear ribonucleoprotein Sm D3	K.VLHEAEGHIVTC*ETNTGEVYR.G	20	4.76%	0.00%
Q12802	AKAP13 A-kinase anchor protein 13	R.MFDQQIC*HR.S	1666	4.76%	0.00%
Q12802	AKAP13 A-kinase anchor protein 13	R.QEALGAEHNSSALLPC*LLPDGSDGSDALNC*SQPSPLDVGVK.N	1045|1059	4.76%	0.00%
Q13501	SQSTM1 Sequestosome-1	K.IALESEGRPEEQMESDNC*SGGDDDWTHLSSK.E	331	4.76%	0.00%
Q96TA1	FAM129B Niban-like protein 1	R.HC*NNGIPEDSKVEGPAFTDAIR.M	194	4.76%	0.00%
P04075	ALDOA Fructose-bisphosphate aldolase A	R.YASIC*QQNGIVPIVEPEILPDGDHDLK.R	178	4.76%	0.00%
Q96F86	EDC3 Enhancer of mRNA-decapping protein 3	K.DLPTSPVDLVINC*LDC*PENVFLR.D	410|413	4.76%	0.00%
Q96F86	EDC3 Enhancer of mRNA-decapping protein 3	R.PTVALLC*GPHVK.G	341	4.76%	0.00%
Q9UPQ9	TNRC6B Trinucleotide repeat-containing gene 6B protein	K.GHPLPENQGNAQAPC*WGR.S	557	4.76%	0.00%
Q9UBB4	ATXN10 Ataxin-10	K.SSHAVELAC*R.D	65	4.76%	0.00%
P22061	PCMT1 Protein-L-isoaspartate(D-aspartate) O-methyltransf	K.ALDVGSGSGILTAC*FAR.M	95	4.76%	0.00%
O00273	DFFA DNA fragmentation factor subunit alpha	R.EQHGVAASC*LEDLR.S	38	4.76%	0.00%
O00273	DFFA DNA fragmentation factor subunit alpha	K.KTETVQEAC*ER.E	289	4.76%	0.00%
P12277	CKB Creatine kinase B-type	R.FC*TGLTQIETLFK.S	254	4.76%	0.00%
P13797	PLS3 Plastin-3	K.TISSSLAVVDLIDAIQPGC*INYDLVK.S	566	4.76%	0.00%
P16152	CBR1 Carbonyl reductase	R.DVC*TELLPLIKPQGR.V	122	4.76%	0.00%
P49589	CARS Cysteine--tRNA ligase, cytoplasmic	K.ASKPGEPSWPC*PWGK.G	335	4.76%	0.00%
P42566	EPS15 Epidermal growth factor receptor substrate 15	K.EKDPEIFC*DPFTSATTTTNK.E	824	4.76%	0.00%
Q9UKA4	AKAP11 A-kinase anchor protein 11	R.KPESPYGNLC*DAPDSPRPVK.A	428	4.76%	0.00%
Q9Y613	FHOD1 FH1/FH2 domain-containing protein 1	R.APTC*SLDGALPLGAQIPAVHR.L	43	4.76%	0.00%
Q92900	UPF1 Regulator of nonsense transcripts 1	R.EKDFIILSC*VR.A	852	4.76%	0.00%
P27348	YWHAQ 14-3-3 protein theta	R.SIC*TTVLELLDK.Y	94	4.76%	0.00%
Q86XP3	DDX42 ATP-dependent RNA helicase DDX42	K.ELEPGDGPIAVIVC*PTR.E	333	4.76%	0.00%
Q01780	EXOSC10 Exosome component 10	K.EPQGIIAC*C*NPVPPLVR.Q	554|555	4.76%	0.00%
Q5H9R7	PPP6R3 Serine/threonine-protein phosphatase 6 regulatory	R.HSNASQSLC*EIVR.L	216	4.76%	0.00%
Q5H9R7	PPP6R3 Serine/threonine-protein phosphatase 6 regulatory	R.IANC*IVHSTDK.G	467	4.76%	0.00%
Q5H9R7	PPP6R3 Serine/threonine-protein phosphatase 6 regulatory	R.WETFC*TSSLGETNKR.N	500	4.76%	0.00%
Q9UGP4	LIMD1 LIM domain-containing protein 1	R.LPC*QPLVPGPELRPSAAELK.L	431	4.76%	0.00%
Q12830	BPTF Nucleosome-remodeling factor subunit BPTF	R.EQDVEVLEPLKC*ELVSGESTGNC*EDR.L	1460|1471	4.76%	0.00%
Q12830	BPTF Nucleosome-remodeling factor subunit BPTF	R.KIIC*PIGVPETPK.E	1969	4.76%	0.00%
Q86YS7	KIAA0528 Uncharacterized protein KIAA0528	R.ASTDNEELLQFPLELC*SDSLPSHPFPPAK.A	831	4.76%	0.00%
Q9Y5X1	SNX9 Sorting nexin-9	K.EKIPIIVGDYGPMWVYPTSTFDC*VVADPR.K	252	4.76%	0.00%
Q01968	OCRL Inositol polyphosphate 5-phosphatase OCRL-1	K.GPLREPC*ALTLAQR.N	28	4.76%	0.00%
Q01968	OCRL Inositol polyphosphate 5-phosphatase OCRL-1	K.FQISNNGQVPC*HFSFIPK.L	597	4.76%	0.00%
A4D1P6	WDR91 WD repeat-containing protein 91	K.KPEASGPEAEPC*PELHTEPVEPLTR.A	366	4.76%	0.00%
Q641Q2	FAM21A WASH complex subunit FAM21A	R.HTTQMSDEEEDDDGC*DLFADSEKEEEDIEDIEENTRPK.R	259	4.76%	0.00%
Q641Q2	FAM21A WASH complex subunit FAM21A	K.KQTLC*LQAQR.E	594	4.76%	0.00%
P08240	SRPR Signal recognition particle receptor subunit alpha	K.NVAADIAVQLC*ESVANK.L	363	4.76%	0.00%
Q8WTW3	COG1 Conserved oligomeric Golgi complex subunit 1	K.HIVDC*IR.A	584	4.76%	0.00%
P57737	CORO7 Coronin-7	K.AVEFHEDLFPDTAGC*VPATDPHSWWAGDNQQVQK.V	363	4.76%	0.00%
P57737	CORO7 Coronin-7	R.C*LLVSGFDSQSER.Q	695	4.76%	0.00%
P57737	CORO7 Coronin-7	K.LQGHQDQIFSLAWSPDGQQLATVC*K.D	656	4.76%	0.00%

Q9NR09	BIRC6 Baculoviral IAP repeat-containing protein 6	K.HAQC*LLR.L	4183	4.76%	0.00%
Q9NR09	BIRC6 Baculoviral IAP repeat-containing protein 6	R.RPTLAWLEDSSSC*SDIPK.L	463	4.76%	0.00%
Q9NR09	BIRC6 Baculoviral IAP repeat-containing protein 6	R.YNLAC*HR.L	1932	4.76%	0.00%
Q9UM54	MYO6 Unconventional myosin-VI	R.C*GGIQYLQNAIESR.Q	1265	4.76%	0.00%
Q9UM54	MYO6 Unconventional myosin-VI	K.EGLGVNEVHYVDNQDC*IDLIEAK.L	514	4.76%	0.00%
P86790	CCZ1B Vacuolar fusion protein CCZ1 homolog B	R.NVGLC*EAIVQFTR.T	65	4.76%	0.00%
Q96D71	REPS1 RalBP1-associated Eps domain-containing protein 1	R.AAQLPNDVVLQIMELC*GATR.L	56	4.76%	0.00%
Q96A65	EXOC4 Exocyst complex component 4	R.LKEIIC*EQAAIK.Q	957	4.76%	0.00%
P49411	TUFM Elongation factor Tu, mitochondrial	R.HYAHTDC*PGHADYVK.N	127	4.76%	0.00%
P49411	TUFM Elongation factor Tu, mitochondrial	K.KGDEC*ELLGHSK.N	290	4.76%	0.00%
Q92665	MRPS31 28S ribosomal protein S31, mitochondrial	R.HFMELVTC*GLSK.N	356	4.76%	0.00%
Q9BQ52	ELAC2 Zinc phosphodiesterase ELAC protein 2	R.FGPDTQHLVLNENC*ASVHNLR.S	374	4.76%	0.00%
P05165	PCCA Propionyl-CoA carboxylase alpha chain, mitochondri	R.LQVEHPVTEC*ITGLDLVQEMIR.V	363	4.76%	0.00%
Q96RQ3	MCCC1 Methylcrotonoyl-CoA carboxylase subunit alpha, mit	K.ESLC*QAALGLILK.E	509	4.76%	0.00%
P11498	PC Pyruvate carboxylase, mitochondrial	K.DMAGLLKPTAC*TMLVSSLR.D	752	4.76%	0.00%
Q92667	AKAP1 A-kinase anchor protein 1, mitochondrial	K.LPAEPPALLQTHPPC*R.R	102	4.76%	0.00%
Q7Z434	MAVS Mitochondrial antiviral-signaling protein	R.GC*ELVDLADEVASVYQSYQPR.T	79	4.76%	0.00%
Q9UKK9	NUDT5 ADP-sugar pyrophosphatase	K.QFRPPMGGYC*IEFPAGLIDDGETPEAAALR.E	91	4.76%	0.00%
O43390	HNRNPR Heterogeneous nuclear ribonucleoprotein R	R.GFC*FLEYEDHK.S	292	4.76%	0.00%
Q12888	TP53BP1 Tumor suppressor p53-binding protein 1	K.SATVKPGAVGAGEFVSPC*ESGDNTGEPSALEEQR.G	1703	4.76%	0.00%
Q9ULM3	YEATS2 YEATS domain-containing protein 2	R.C*HGYTPPDPESLR.N	1232	4.76%	0.00%
Q9ULM3	YEATS2 YEATS domain-containing protein 2	R.HSLGEDC*IYPQSSESDISDAPPSLPLTIPAPVK.A	338	4.76%	0.00%
Q9UPN9	TRIM33 E3 ubiquitin-protein ligase TRIM33	R.DIGKPEVEYDC*DNLQHSK.K	943	4.76%	0.00%
Q96J01	THOC3 THO complex subunit 3	K.RPLLAFAC*DDK.D	326	4.76%	0.00%
Q00403	GTF2B Transcription initiation factor IIB	R.VTC*PNHPDAILVEDYR.A	15	4.76%	0.00%
Q9NYP9	MIS18A Protein Mis18-alpha	R.AQLEEEAAAAEERPLVFLC*SGC*R.R	85|88	4.76%	0.00%
O15541	RNF113A RING finger protein 113A	K.RPAC*DPEPGESGSSSDEGC*TVVRPEK.K	36|51	4.76%	0.00%
O43148	RNMT mRNA cap guanine-N7 methyltransferase	K.KGDYPLFGC*K.Y	356	4.76%	0.00%
O43719	HTATSF1 HIV Tat-specific factor 1	R.DPEEADYC*IQTLDGR.W	328	4.76%	0.00%
O75643	SNRNP200 U5 small nuclear ribonucleoprotein 200 kDa helicas	R.DILC*GAADEVLAVLK.N	133	4.76%	0.00%
O95801	TTC4 Tetratricopeptide repeat protein 4	R.LSEAAC*EDEDSASEGLGELFLDGLSTENPHGAR.L	238	4.76%	0.00%
O95801	TTC4 Tetratricopeptide repeat protein 4	R.ENPDLAC*LQSIIFDEER.S	63	4.76%	0.00%
P13010	XRCC5 X-ray repair cross-complementing protein 5	K.ETVYC*LNDDDETEVLKEDIIQGFR.Y	296	4.76%	0.00%
P13010	XRCC5 X-ray repair cross-complementing protein 5	R.LFQC*LLHR.A	493	4.76%	0.00%
P13984	GTF2F2 General transcription factor IIF subunit 2	R.AEC*RPAASENYMR.L	116	4.76%	0.00%
P17028	ZNF24 Zinc finger protein 24	R.HC*DDDGRTENGALAPK.Q	189	4.76%	0.00%
P24928	POLR2A DNA-directed RNA polymerase II subunit RPB1	R.LTHVYDLC*K.G	148	4.76%	0.00%
P27694	RPA1 Replication protein A 70 kDa DNA-binding subunit	K.DSLVDIIGIC*K.S	323	4.76%	0.00%
P30876	POLR2B DNA-directed RNA polymerase II subunit RPB2	R.DC*QIAHGAAQFLR.E	1093	4.76%	0.00%
P49792	RANBP2 E3 SUMO-protein ligase RanBP2	K.TGEEDEEEFFC*NR.A	1196	4.76%	0.00%
P49792	RANBP2 E3 SUMO-protein ligase RanBP2	R.IVKEPTSHDNKDIC*K.S	1335	4.76%	0.00%
P49792	RANBP2 E3 SUMO-protein ligase RanBP2	K.LKEQLLDC*EGEDGWNK.L	141	4.76%	0.00%
P49792	RANBP2 E3 SUMO-protein ligase RanBP2	K.ETNPVVFFDVC*ADGEPLGR.I	3071	4.76%	0.00%
P49792	RANBP2 E3 SUMO-protein ligase RanBP2	R.RITITEC*GQI.-	3221	4.76%	0.00%
P49792	RANBP2 E3 SUMO-protein ligase RanBP2	R.VWLWTAC*DFADGER.K	2407	4.76%	0.00%
P49959	MRE11A Double-strand break repair protein MRE11A	K.TLHTC*LELLR.K	75	4.76%	0.00%
P49959	MRE11A Double-strand break repair protein MRE11A	K.VTQAIQSFC*LEK.I	336	4.76%	0.00%
P55209	NAP1L1 Nucleosome assembly protein 1-like 1	K.RFEIINAIYEPTEEEC*EWKPDEEDEISEELKEK.A	132	4.76%	0.00%
P62258	YWHAE 14-3-3 protein epsilon	K.LIC*C*DILDVLDK.H	97|98	4.76%	0.00%
P62826	RAN GTP-binding nuclear protein Ran	R.VC*ENIPIVLC*GNK.V	112|120	4.76%	0.00%
Q00839	HNRNPU Heterogeneous nuclear ribonucleoprotein U	K.GNFTLPEVAEC*FDEITYVELQK.E	648	4.76%	0.00%
Q13435	SF3B2 Splicing factor 3B subunit 2	K.IPGLNSPIPESC*SFGYHAGGWGKPPVDETGKPLYGDVFGTNAAEFQTK.T	661	4.76%	0.00%
Q14676	MDC1 Mediator of DNA damage checkpoint protein 1	R.DC*GSLNGTQILRPPK.V	92	4.76%	0.00%
Q14676	MDC1 Mediator of DNA damage checkpoint protein 1	R.GDQESPDAC*LPPTVPEAPAPPQKPLNSQSQK.H	1037	4.76%	0.00%
Q14839	CHD4 Chromodomain-helicase-DNA-binding protein 4	R.FAEVEC*LAESHQHLSK.E	1827	4.76%	0.00%
Q14839	CHD4 Chromodomain-helicase-DNA-binding protein 4	R.HLC*EPGADGAETFADGVPR.E	1468	4.76%	0.00%
Q15393	SF3B3 Splicing factor 3B subunit 3	R.SEHPPLC*GR.D	1156	4.76%	0.00%
Q15424	SAFB Scaffold attachment factor B1	R.C*YGFVTMSTAEEATK.C	448	4.76%	0.00%
Q15652	JMJD1C Probable JmjC domain-containing histone demethylat	R.C*SFHPIPTR.S	684	4.76%	0.00%
Q6PCB5	RSBN1L Round spermatid basic protein 1-like protein	K.AVHC*GEWPDQPR.I	595	4.76%	0.00%
Q6VMQ6	ATF7IP Activating transcription factor 7-interacting prot	K.DKEEVNGIEEIC*FDPEGSK.A	78	4.76%	0.00%
Q86WJ1	CHD1L Chromodomain-helicase-DNA-binding protein 1-like	K.YVSGDVTHPQAGAEDALIVHC*VDDSGHWGR.G	739	4.76%	0.00%
Q8IVF2	AHNAK2 Protein AHNAK2	R.LDLTGPHFESSILSPC*EDVTLTK.Y	4787	4.76%	0.00%
Q8IWZ8	SUGP1 SURP and G-patch domain-containing protein 1	K.QNQVASPQPPHPGEITNAHNSSC*ISNK.F	78	4.76%	0.00%
Q8N1G2	FTSJD2 Cap-specific mRNA (nucleoside-2-O-)-methyltransfe	K.DSTFDLPADSIAPFHIC*YYGR.L	794	4.76%	0.00%
Q8N3C0	ASCC3 Activating signal cointegrator 1 complex subunit 3	K.FLNEHLQEAC*TPELKPVEK.T	208	4.76%	0.00%
Q8N3C0	ASCC3 Activating signal cointegrator 1 complex subunit 3	R.LKPEC*STEELLSILSDAEEYTDLPVR.H	1840	4.76%	0.00%
Q8WUA2	PPIL4 Peptidyl-prolyl cis-trans isomerase-like 4	K.YYNYC*LIHNVQR.D	40	4.76%	0.00%
Q8WXE1	ATRIP ATR-interacting protein	R.KNPSVVIKPEAC*SPQFGK.T	238	4.76%	0.00%
Q92922	SMARCC1 SWI/SNF complex subunit SMARCC1	K.TLVQNNC*LTRPNIYLIPDIDLK.L	164	4.76%	0.00%
Q96EI5	TCEAL4 Transcription elongation factor A protein-like 4	R.KPEVTC*TLEDK.K	34	4.76%	0.00%
Q96JM2	ZNF462 Zinc finger protein 462	K.HSFC*DNLPK.F	626	4.76%	0.00%
Q96PY6	NEK1 Serine/threonine-protein kinase Nek1	K.VVHSEHLNLVPQVQSVQC*SPEESFAFR.S	1007	4.76%	0.00%

Q96RL1	UIMC1 BRCA1-A complex subunit RAP80	K.GFGEPVLPRPPSLIQNEC*GQGEQASE K.N	336	4.76%	0.00%
Q96T23	RSF1 Remodeling and spacing factor 1	K.DKRPPILEC*LEK.L	584	4.76%	0.00%
Q99459	CDC5L Cell division cycle 5-like protein	R.TAAQC*LEHYEFLLDK.A	96	4.76%	0.00%
Q99590	SCAF11 Protein SCAF11	K.VYQPVSC*PLSDLSENVESVVNEEK.I	566	4.76%	0.00%
Q9BUJ2	HNRNPUL1 Heterogeneous nuclear ribonucleoprotein U-like pro	R.AEPYC*SVLPGFTFIQHLPLSER.I	391	4.76%	0.00%
Q9BUJ2	HNRNPUL1 Heterogeneous nuclear ribonucleoprotein U-like pro	K.AIVIC*PTDEDLKDR.T	532	4.76%	0.00%
Q9BYW2	SETD2 Histone-lysine N-methyltransferase SETD2	R.NLGWDFSQEKPSTTYQQPDSSYGAC*G GHK.Y	1281	4.76%	0.00%
Q9H410	DSN1 Kinetochore-associated protein DSN1 homolog	K.KGGNC*DLSHQER.L	65	4.76%	0.00%
Q9H6U6	BCAS3 Breast carcinoma-amplified sequence 3	R.GTSHVFPINPYGGQPC*VR.T	442	4.76%	0.00%
Q9HAW4	CLSPN Claspin	K.ESSMGDPMEEALALC*SGSFPTDKEEE DEEEEFGDFR.L	981	4.76%	0.00%
Q9HCS7	XAB2 Pre-mRNA-splicing factor SYF1	R.C*VTDPAYEDVNNC*HER.A	86|98	4.76%	0.00%
Q9NRZ9	HELLS Lymphoid-specific helicase	K.ILENSEDSSPEC*LF.-	836	4.76%	0.00%
Q9NRZ9	HELLS Lymphoid-specific helicase	K.ENEDENSSSTNLC*VEDLQK.N	169	4.76%	0.00%
Q9NRZ9	HELLS Lymphoid-specific helicase	R.DRNALQHC*YWK.Y	346	4.76%	0.00%
Q9NRZ9	HELLS Lymphoid-specific helicase	R.KC*NGQPVPFQQPK.H	205	4.76%	0.00%
Q9NVM9	Asun Protein asunder homolog	R.ISPVDVNSRPSSC*LTNFLLNGR.S	349	4.76%	0.00%
Q9NYP9	MIS18A Protein Mis18-alpha	R.GC*AGGC*EC*GDK.G	13|17 |19	4.76%	0.00%
Q9UEG4	ZNF629 Zinc finger protein 629	R.PAGAEKPYIC*NEC*GK.S	152|1 55	4.76%	0.00%
Q9UK61	FAM208A Protein FAM208A	K.EDPNLISVNNFEDC*SLC*PSVPIEHGFR .R	886|8 89	4.76%	0.00%
Q9UKF6	CPSF3 Cleavage and polyadenylation specificity factor su	R.FC*NTVHDIVNR.G	223	4.76%	0.00%
Q9ULL5	PRR12 Proline-rich protein 12	K.AGAGPPPGPPAYDPYGPYC*PGR.A	994	4.76%	0.00%
Q9ULL5	PRR12 Proline-rich protein 12	R.FVPLTSIC*FPDSLLQDEER.S	933	4.76%	0.00%
Q9ULL5	PRR12 Proline-rich protein 12	R.RLPDLVSSC*R.S	1128	4.76%	0.00%
Q9ULL5	PRR12 Proline-rich protein 12	R.SRPALSPLGDIDFC*PPNPGPDGPR.R	1143	4.76%	0.00%
Q9ULW0	TPX2 Targeting protein for Xklp2	R.TVEIC*PFSFDSR.D	536	4.76%	0.00%
Q14980	NUMA1 Nuclear mitotic apparatus protein 1	K.APVPSTC*SSTFPEELSPPSHQAK.R	160	4.76%	0.00%
Q14980	NUMA1 Nuclear mitotic apparatus protein 1	R.KHPSSPEC*LVSAQK.V	80	4.76%	0.00%
Q14980	NUMA1 Nuclear mitotic apparatus protein 1	K.PQLDLSIDSLDLSC*EEGTPLSITSK.L	1729	4.76%	0.00%
Q14980	NUMA1 Nuclear mitotic apparatus protein 1	R.KVEELQAC*VETAR.Q	658	4.76%	0.00%
P38398	BRCA1 Breast cancer type 1 susceptibility protein	R.HSTVATEC*LSK.N	1251	4.76%	0.00%
P38398	BRCA1 Breast cancer type 1 susceptibility protein	K.YQGSSVSNLHVEPC*GTNTHASSLQHE NSSLLLTK.D	274	4.76%	0.00%
Q03164	MLL Histone-lysine N-methyltransferase MLL	K.SDSDNNNSDDC*GNILPSDIMDFVLK. N	2841	4.76%	0.00%
P09651	HNRNPA1 Heterogeneous nuclear ribonucleoprotein A1	R.SHFEQWGTLTDC*VVMR.D	43	4.76%	0.00%
Q9Y224	C14orf166 UPF0568 protein C14orf166	K.LTALDYHNPAGFNC*K.D	19	4.76%	0.00%
P43243	MATR3 Matrin-3	R.C*RDDSFFGETSHNYHK.F	230	4.76%	0.00%
P18583	SON Protein SON	K.HPVSALMEIC*NK.R	2380	4.76%	0.00%
P23246	SFPQ Splicing factor, proline- and glutamine-rich	R.C*SEGVFLLTTTPRPVIVEPLEQLDDED GLPEK.L	431	4.76%	0.00%
Q92585	MAML1 Mastermind-like protein 1	R.AGLHC*TQAYPVR.T	957	4.76%	0.00%
O00571	DDX3X ATP-dependent RNA helicase DDX3X	K.GADSLEDFLYHEGYAC*TSIHGDR.S	468	4.76%	0.00%
O00571	DDX3X ATP-dependent RNA helicase DDX3X	R.GC*HLLVATPGR.L	317	4.76%	0.00%
O00571	DDX3X ATP-dependent RNA helicase DDX3X	R.VRPC*VVYGGADIGQQIR.D	298	4.76%	0.00%
P49756	RBM25 RNA-binding protein 25	K.AKENDENC*GPTTTVFVGNISEK.A	83	4.76%	0.00%
P37198	NUP62 Nuclear pore glycoprotein p62	K.DIIEHLNTSGAPADTSDPLQQIC*K.I	475	4.76%	0.00%
P35658	NUP214 Nuclear pore complex protein Nup214	R.TSC*KDDEAVVQAPR.H	1003	4.76%	0.00%
Q9UKX7	NUP50 Nuclear pore complex protein Nup50	K.HVNTNPLC*DLTPIFK.D	181	4.76%	0.00%
Q9UKX7	NUP50 Nuclear pore complex protein Nup50	K.NNVLIVC*VPNPPIDEK.N	428	4.76%	0.00%
P17844	DDX5 Probable ATP-dependent RNA helicase DDX5	R.GDGPIC*LVLAPTR.E	170	4.76%	0.00%
Q14692	BMS1 Ribosome biogenesis protein BMS1 homolog	K.HKADSLDC*SR.F	734	4.76%	0.00%
Q9H0D6	XRN2 5-3 exoribonuclease 2	R.KYPSIIVNC*VEEKPK.E	21	4.76%	0.00%
O15084	ANKRD28 Serine/threonine-protein phosphatase 6 regulatory	R.GAVTGHEEC*VDALLQHGAK.C	701	4.76%	0.00%
O15084	ANKRD28 Serine/threonine-protein phosphatase 6 regulatory	K.NTALHLAC*SK.G	898	4.76%	0.00%
Q9H814	PHAX Phosphorylated adapter RNA export protein	R.AFQNTATAC*APVSHYR.A	51	4.76%	0.00%
P17535	JUND Transcription factor jun-D	K.VLSHVNSGC*QLLPQHQVPAY.-	336	4.76%	0.00%
P18858	LIG1 DNA ligase 1	K.NNYHPVEDAC*WKPGQK.V	280	4.76%	0.00%
P26368	U2AF2 Splicing factor U2AF 65 kDa subunit	K.SIEIPRPVDGVEVPGC*GK.I	429	4.76%	0.00%
P51948	MNAT1 CDK-activating kinase assembly factor MAT1	R.AASPQDLAGGYTSSLAC*HR.A	293	4.76%	0.00%
Q09028	RBBP4 Histone-binding protein RBBP4	K.HPSKPDPSGEC*NPDLR.L	167	4.76%	0.00%
Q09666	AHNAK Neuroblast differentiation-associated protein AHNA	K.LEGDLTGPSVDVEVPDVELEC*PDAK.L	2162	4.76%	0.00%
Q09666	AHNAK Neuroblast differentiation-associated protein AHNA	K.GPFVEAEVPDVDLEC*PDAK.L	1833	4.76%	0.00%
Q12824	SMARCB1 SWI/SNF-related matrix-associated actin-dependent	R.NSQWVPTLPNSSHHLDAVPC*STTINR. N	147	4.76%	0.00%
Q68CP9	ARID2 AT-rich interactive domain-containing protein 2	R.KPLVNGIC*DFDK.G	1362	4.76%	0.00%
Q9Y618	NCOR2 Nuclear receptor corepressor 2	K.LPGDPPC*WTSGLPFPVPPR.E	1048	4.76%	0.00%
P49848	TAF6 Transcription initiation factor TFIID subunit 6	K.HC*APVLAK.L	431	4.76%	0.00%
Q9C0C2	TNKS1BP1 182 kDa tankyrase-1-binding protein	R.EHGVGGVSQC*PEPGLR.H	1373	4.76%	0.00%
Q9C0C2	TNKS1BP1 182 kDa tankyrase-1-binding protein	R.C*PARPPPSGSQGLLEEMLAASSSK.A	1443	4.76%	0.00%
Q32MZ4	LRRFIP1 Leucine-rich repeat flightless-interacting protein	K.SEDADRC*TLPEHESPSQDISDAC*EAE STER.C	726|7 42	4.76%	0.00%
Q15418	RPS6KA1 Ribosomal protein S6 kinase alpha-1	R.DLKPSNILYVDESGNPEC*LR.I	552	4.76%	0.00%
Q93052	LPP Lipoma-preferred partner	K.KTYITDPVSAPC*APPLQPK.G	364	4.76%	0.00%
Q9BPX3	NCAPG Condensin complex subunit 3	R.LQDPKDDEC*PVVNAYATLIENDSNPE VR.R	177	4.76%	0.00%
Q15398	DLGAP5 Disks large-associated protein 5	K.LTSHC*FEWDR.K	448	4.76%	0.00%

Q15365	PCBP1 Poly(rC)-binding protein 1	R.LVVPATQC*GSLIGK.G	109	4.76%	0.00%
Q9UKD1	GMEB2 Glucocorticoid modulatory element-binding protein	R.KFVC*PGINVK.C	110	4.76%	0.00%
P49790	NUP153 Nuclear pore complex protein Nup153	K.NEDVC*SC*STDTSEVPR.W	66|68	4.76%	0.00%
Q13838	DDX39B Spliceosome RNA helicase DDX39B	K.HFILDEC*DK.M	198	4.76%	0.00%
O43143	DHX15 Putative pre-mRNA-splicing factor ATP-dependent RN	R.TC*TDIKPEWLVK.I	750	4.76%	0.00%
Q15233	NONO Non-POU domain-containing octamer-binding protein	R.C*SEGSFLLTTFPR.P	208	4.76%	0.00%
P29590	PML Protein PML	R.KC*SQTQC*PR.K	479|484	4.76%	0.00%
Q9BQG2	NUDT12 Peroxisomal NADH pyrophosphatase NUDT12	K.KPWFLTNEVEEC*ENYFSK.T	117	4.76%	0.00%
Q8N3F8	MICALL1 MICAL-like protein 1	R.GSSGPQPAKPC*SGATPTPLLLVGDR.S	597	4.76%	0.00%
Q9Y520	PRRC2C Protein PRRC2C	R.SVEDVRPHHTDANNQSAC*FEAPDQK.T	895	4.76%	0.00%
P21333	FLNA Filamin-A	K.VHSPSGALEEC*YVTEIDQDK.Y	2378	4.76%	0.00%
Q01433	AMPD2 AMP deaminase 2	R.TYEQGPDTPVSADAPVHPPALEQHPYEHC*EPSTMPGDLGLGLR.M	310	4.76%	0.00%
Q14151	SAFB2 Scaffold attachment factor B2	R.KFDFDAC*NEVPPAPK.E	361	4.76%	1.07%
Q96F86	EDC3 Enhancer of mRNA-decapping protein 3	K.ILEIPGPGDNQHFGDLHQTELGPSGAGC*QVGINQNGTGK.F	91	4.59%	0.51%
Q06830	PRDX1 Peroxiredoxin-1	K.HGEVC*PAGWKPGSDTIKPDVQK.S	173	4.53%	0.46%
Q9GZU8	FAM192A Protein FAM192A	R.LKPDPEPDDKNQEPSSC*K.S	187	4.53%	0.46%
P49321	NASP Nuclear autoantigenic sperm protein	K.LGEVSVESENYVQAVEEFQSC*LNLQEQYLEAHDR.L	568	4.46%	0.53%
P13639	EEF2 Elongation factor 2	R.SNTGGQAFPQC*VFDHWQILPGDPFDNSSR.P	812	4.46%	0.53%
Q02952	AKAP12 A-kinase anchor protein 12	K.SSEKNEDFAAHPGEDAVPTGPDC*QAK.S	1479	4.46%	0.53%
P07437	TUBB Tubulin beta chain	K.LTTPTYGDLNHLVSATMSGVTTC*LR.F	239	4.46%	0.53%
P61978	HNRNPK Heterogeneous nuclear ribonucleoprotein K	K.IIPTLEEGLQLPSPTATSQLPLESDAVEC*LNYQHYK.G	132	4.30%	0.53%
Q9H0C8	ILKAP Integrin-linked kinase-associated serine/threonine	R.EEMQDAHVILNDITEEC*RPPSSLITR.V	135	4.30%	0.53%
P56270	MAZ Myc-associated zinc finger protein	K.LSHSDEKPYQC*PVC*QQR.F	309|312	4.30%	0.53%
Q14151	SAFB2 Scaffold attachment factor B2	K.ILDILGETC*K.S	224	4.30%	0.92%
P46013	MKI67 Antigen KI-67	K.ELFQTPVC*TDKPTTHEK.T	1479	4.15%	1.07%
A1X283	SH3PXD2B SH3 and PX domain-containing protein 2B	R.GPQC*EGHESR.A	783	4.15%	1.07%
P08238	HSP90AB1 Heat shock protein HSP 90-beta	K.AKFENLC*K.L	564	4.15%	1.07%
P48634	PRRC2A Protein PRRC2A	R.GGPPC*KPPAPEDEDEAWR.Q	437	4.15%	1.07%
P50990	CCT8 T-complex protein 1 subunit theta	K.IAVYSC*PFDGMITETK.G	244	4.15%	1.07%
P50990	CCT8 T-complex protein 1 subunit theta	R.LTPPVLEEMGHC*DSVYLSEVGDTQVVVFK.H	347	4.15%	1.07%
P49790	NUP153 Nuclear pore complex protein Nup153	K.KTPPEDC*EGPFRPAEILK.E	593	4.15%	1.07%
Q4VCS5	AMOT Angiomotin	R.LSIPSLTC*NPDK.T	1047	4.10%	1.42%
P50990	CCT8 T-complex protein 1 subunit theta	K.AHEILPNLVC*C*SAK.N	148|149	4.07%	0.88%
P61978	HNRNPK Heterogeneous nuclear ribonucleoprotein K	K.LFQEC*C*PHSTDR.V	184|185	4.07%	0.88%
Q14247	CTTN Src substrate cortactin	K.HC*SQVDSVR.G	112	4.07%	0.88%
Q15424	SAFB Scaffold attachment factor B1	K.RDDKC*DR.K	519	4.07%	0.88%
Q9GZU8	FAM192A Protein FAM192A	R.KPEDPEEC*PEEVYDPR.S	44	4.07%	0.88%
Q15750	TAB1 TGF-beta-activated kinase 1 and MAP3K7-binding pro	R.SLLQSEQQPSWTDDLPLC*HLSGVGSASNR.S	24	3.84%	1.07%
P78559	MAP1A Microtubule-associated protein 1A	K.SPC*GLTEQYLHK.D	1174	3.84%	1.31%
Q6IBS0	TWF2 Twinfilin-2	K.HLSSC*AAPAPLTSAER.E	141	3.84%	1.07%
P49327	FASN Fatty acid synthase	R.C*VLLSNLSSTSHVPEVDPGSAELQK.V	1471	3.83%	1.62%
P21333	FLNA Filamin-A	K.THEAEIVEGENHTYC*IR.F	2199	3.83%	1.62%
P21333	FLNA Filamin-A	R.YWPQEAGEYAVHVLC*NSEDIR.L	649	3.83%	1.62%
O75534	CSDE1 Cold shock domain-containing protein E1	K.QRPGQQVATC*VR.L	506	3.83%	1.62%
Q14980	NUMA1 Nuclear mitotic apparatus protein 1	K.HLC*QQLQAEQAAAEK.R	1367	3.83%	1.62%
P43243	MATR3 Matrin-3	K.NTHC*SSLPHYQK.L	821	3.83%	1.62%
P68104	EEF1A1 Elongation factor 1-alpha 1	K.DGNASGTTLLEALDC*ILPPTRPTDK.P	234	3.60%	1.40%
P21333	FLNA Filamin-A	R.ALGALVDSC*APGLC*PDWDSWDASKPVTNAR.E	205|210	3.60%	1.40%
Q00839	HNRNPU Heterogeneous nuclear ribonucleoprotein U	R.KAVVVC*PK.D	607	3.60%	1.40%
O00505	KPNA3 Importin subunit alpha-3	R.KDQVEYLVQQNVIPPFC*NLLSVK.D	417	3.50%	2.18%
P68366	TUBA4A Tubulin alpha-4A chain	K.RSIQFVDWC*PTGFK.V	347	3.50%	2.18%
P15170	GSPT1 Eukaryotic peptide chain release factor GTP-bindin	K.GIEEEEILPGFILC*DPNNLC*HSGR.T	381|387	3.36%	1.62%
P37802	TAGLN2 Transgelin-2	K.DGTVLC*ELINALYPEGQAPVK.K	63	3.36%	1.62%
O75369	FLNB Filamin-B	R.WC*NEHLK.C	26	3.36%	1.62%
P49321	NASP Nuclear autoantigenic sperm protein	R.KPTDGASSSNC*VTDISHLVR.K	708	3.36%	1.62%
O95372	LYPLA2 Acyl-protein thioesterase 2	K.YIC*PHAPR.I	56	3.36%	1.62%
P50990	CCT8 T-complex protein 1 subunit theta	K.QITSYGETC*PGLEQYAIK.K	430	3.36%	1.62%
Q9H910	HN1L Hematological and neurological expressed 1-like pr	K.DHVFLC*EGEEPK.S	118	3.36%	1.62%
P51991	HNRNPA3 Heterogeneous nuclear ribonucleoprotein A3	K.YHTINGHNC*EVK.K	196	3.36%	1.98%
Q13838	DDX39B Spliceosome RNA helicase DDX39B	K.EIRPVC*R.K	239	3.36%	1.98%
Q15020	SART3 Squamous cell carcinoma antigen recognized by T-ce	R.AHGDTQHC*R.K	527	3.21%	1.42%
P21333	FLNA Filamin-A	K.AHVVPC*FDASK.V	1157	3.12%	1.94%
P09651	HNRNPA1 Heterogeneous nuclear ribonucleoprotein A1	K.YHTVNGHNC*EVR.K	175	3.12%	1.94%
P50990	CCT8 T-complex protein 1 subunit theta	K.LIAQAC*VSIFPDSGHFNVDNIR.V	187	2.25%	2.18%
Q14247	CTTN Src substrate cortactin	K.C*ALGWDHQEK.L	246	1.96%	0.00%

Table 4A-1. List of all proteins identified in matrix-APEX analysis. Mitochondrial localization is denoted by "mito", and is derived from uniprot subcellular localization, MitoCarta2.0, and previous studies (mito-APEX, IMS-APEX, and IMSGold+). "DMSO" denotes DMSO treatment for 45 min. "AMA" denotes 100 μM Antimycin A treatment for 45 min. "H2O2" denotes 1 mM H2O2 treatment for 1 min. Protein identifications are the average of 3 replicates for each treatment and > 10 spectral counts.

UniProt ID	Description	Mito	Mito-APEX mito annotation	Average Spectral Count Matrix-APEX DMSO	Average Spectral Count Matrix-APEX2 1mM H2O2	Average Spectral Count Matrix-APEX AMA
Q5JTZ9	AARS2 Alanine--tRNA ligase, mitochondrial	Yes	Yes	0	40	27
Q9UDR5	AASS Alpha-aminoadipic semialdehyde synthase, mitochondrial	Yes	Yes	0	39	53
Q9NUJ1	ABHD10 Abhydrolase domain-containing protein 10, mitochondrial	Yes	Yes	6	68	14
P42765	ACAA2 3-ketoacyl-CoA thiolase, mitochondrial	Yes	Yes	2	19	8
Q13085	ACACA Acetyl-CoA carboxylase 1	Yes		1103	134	464
O00763	ACACB Acetyl-CoA carboxylase 2	Yes		199	23	79
Q9H845	ACAD9 Acyl-CoA dehydrogenase family member 9, mitochondrial	Yes	Yes	0	26	5
P11310	ACADM Medium-chain specific acyl-CoA dehydrogenase, mitochondrial	Yes	Yes	4	22	5
P45954	ACADSB Short/branched chain specific acyl-CoA dehydrogenase, mitochondrial	Yes	Yes	5	26	11
P49748	ACADVL Very long-chain specific acyl-CoA dehydrogenase, mitochondrial	Yes	Yes	0	4	11
P24752	ACAT1 Acetyl-CoA acetyltransferase, mitochondrial	Yes	Yes	15	96	50
P12821	ACE Angiotensin-converting enzyme			12	0	0
P53396	ACLY ATP-citrate synthase	Yes	Yes	16	16	24
Q99798	ACO2 Aconitate hydratase, mitochondrial	Yes	Yes	11	95	99
P49753	ACOT2 Acyl-coenzyme A thioesterase 2, mitochondrial	Yes		2	40	3
Q9Y305	ACOT9 Acyl-coenzyme A thioesterase 9, mitochondrial	Yes		0	29	12
Q9NPH0	ACP6 Lysophosphatidic acid phosphatase type 6	Yes		0	0	10
Q96CM8	ACSF2 Acyl-CoA synthetase family member 2, mitochondrial	Yes	Yes	0	12	11
Q4G176	ACSF3 Acyl-CoA synthetase family member 3, mitochondrial	Yes	Yes	2	29	7
Q9NUB1	ACSS1 Acetyl-coenzyme A synthetase 2-like, mitochondrial	Yes	Yes	0	20	8
Q9H6R3	ACSS3 Acyl-CoA synthetase short-chain family member 3, mitochondrial	Yes		0	11	6
P68133	ACTA1 Actin, alpha skeletal muscle			18	17	34
P60709	ACTB Actin, cytoplasmic 1			31	37	64
Q562R1	ACTBL2 Beta-actin-like protein 2			4	0	12
P12814	ACTN1 Alpha-actinin-1			4	11	0
O43707	ACTN4 Alpha-actinin-4			4	16	2
Q8NI60	ADCK3 Chaperone activity of bc1 complex-like, mitochondrial	Yes	Yes	0	22	0
Q09666	AHNAK Neuroblast differentiation-associated protein AHNAK			3	0	35
P54819	AK2 Adenylate kinase 2, mitochondrial	Yes	Yes	5	3	32
Q9UIJ7	AK3 GTP:AMP phosphotransferase, mitochondrial	Yes	Yes	2	14	0
P27144	AK4 Adenylate kinase isoenzyme 4, mitochondrial	Yes	Yes	3	62	2
Q02952	AKAP12 A-kinase anchor protein 12			0	0	51
P13196	ALAS1 5-aminolevulinate synthase, nonspecific, mitochondrial	Yes	Yes	0	11	3
P02768	ALB Serum albumin			41	4	29
P54886	ALDH18A1 Delta-1-pyrroline-5-carboxylate synthase	Yes		15	283	170
P30837	ALDH1B1 Aldehyde dehydrogenase X, mitochondrial	Yes	Yes	4	54	44
Q3SY69	ALDH1L2 Mitochondrial 10-formyltetrahydrofolate dehydrogenase	Yes	Yes	0	23	36
P05091	ALDH2 Aldehyde dehydrogenase, mitochondrial	Yes	Yes	10	57	54
P51649	ALDH5A1 Succinate-semialdehyde dehydrogenase, mitochondrial	Yes	Yes	0	14	32
Q02252	ALDH6A1 Methylmalonate-semialdehyde dehydrogenase	Yes	Yes	0	10	8
P49419	ALDH7A1 Alpha-aminoadipic semialdehyde dehydrogenase	Yes	Yes	0	23	29
P49189	ALDH9A1 4-trimethylaminobutyraldehyde dehydrogenase	Yes	Yes	2	3	21
P04075	ALDOA Fructose-bisphosphate aldolase A			11	24	16
Q13686	ALKBH1 Alkylated DNA repair protein alkB homolog 1	Yes	Yes	0	11	0
Q4VCS5	AMOT Angiomotin			2	6	22
P07355	ANXA2 Annexin A2			0	0	12
P78540	ARG2 Arginase-2, mitochondrial	Yes	Yes	3	18	5
P08243	ASNS Asparagine synthetase			10	5	9
P05023	ATP1A1 Sodium/potassium-transporting ATPase subunit alpha-1			4	2	18
P25705	ATP5A1 ATP synthase subunit alpha, mitochondrial	Yes	Yes	9	27	8
P06576	ATP5B ATP synthase subunit beta, mitochondrial	Yes	Yes	27	133	44
P24539	ATP5F1 ATP synthase subunit b, mitochondrial	Yes	Yes	0	11	0

P38606	ATP6V1A V-type proton ATPase catalytic subunit A			0	3	45
Q5TC12	ATPAF1 ATP synthase mitochondrial F1 complex assembly factor 1	Yes	Yes	0	28	26
Q8N5M1	ATPAF2 ATP synthase mitochondrial F1 complex assembly factor 2	Yes	Yes	0	14	0
Q9UII2	ATPIF1 ATPase inhibitor, mitochondrial	Yes	Yes	0	16	0
Q8WWM7	ATXN2L Ataxin-2-like protein			0	2	10
O15382	BCAT2 Branched-chain-amino-acid aminotransferase, mitochondrial	Yes	Yes	0	17	3
P12694	BCKDHA 2-oxoisovalerate dehydrogenase subunit alpha, mitochondrial	Yes	Yes	0	31	11
O14874	BCKDK	Yes	Yes	0	16	2
Q86WA6	BPHL Valacyclovir hydrolase	Yes	Yes	0	10	0
P43251	BTD Biotinidase			74	9	56
Q7Z3D6	C14orf159 UPF0317 protein C14orf159, mitochondrial	Yes	Yes	0	10	10
Q07021	C1QBP Complement component 1 Q subcomponent-binding protein, mitochondrial	Yes	Yes	14	46	38
Q9BQP7	C20orf72 Uncharacterized protein C20orf72	Yes	Yes	2	51	9
P30042	C21orf33 ES1 protein homolog, mitochondrial	Yes	Yes	3	55	15
Q7L592	C2orf56 Protein midA homolog, mitochondrial	Yes	Yes	0	24	3
Q6P1X6	C8orf82 UPF0598 protein C8orf82	Yes	Yes	2	17	3
O43852	CALU Calumenin			33	0	26
P17655	CAPN2 Calpain-2 catalytic subunit			0	0	14
P04632	CAPNS1 Calpain small subunit 1			0	0	13
Q6YP21	CCBL2 Kynurenine--oxoglutarate transaminase 3	Yes	Yes	4	20	2
P78371	CCT2 T-complex protein 1 subunit beta			7	6	12
P48643	CCT5 T-complex protein 1 subunit epsilon			8	4	13
P40227	CCT6A T-complex protein 1 subunit zeta			7	3	10
Q96SZ6	CDK5RAP1 CDK5 regulatory subunit-associated protein 1			0	18	0
Q9BXW7	CECR5 Cat eye syndrome critical region protein 5	Yes	Yes	4	57	41
P49454	CENPF Centromere protein F			0	0	48
P23528	CFL1 Cofilin-1			13	4	14
Q9Y6H1	CHCHD2 Coiled-coil-helix-coiled-coil-helix domain-containing protein 2, mitochondrial	Yes		3	10	5
P12277	CKB Creatine kinase B-type			20	40	30
P12532	CKMT1B Creatine kinase U-type, mitochondrial	Yes	Yes	0	2	36
Q16740	CLPP Putative ATP-dependent Clp protease proteolytic subunit, mitochondrial	Yes	Yes	3	17	21
O76031	CLPX ATP-dependent Clp protease ATP-binding subunit clpX-like, mitochondrial	Yes	Yes	0	52	4
Q00610	CLTC Clathrin heavy chain 1			11	10	27
P62633	CNBP Cellular nucleic acid-binding protein			13	2	7
Q13057	COASY Bifunctional coenzyme A synthase	Yes	Yes	0	13	0
O75208	COQ9 Ubiquinone biosynthesis protein COQ9, mitochondrial	Yes	Yes	0	24	0
P20674	COX5A Cytochrome c oxidase subunit 5A, mitochondrial	Yes	Yes	0	31	5
O75131	CPNE3 Copine-3			0	3	10
P36551	CPOX Coproporphyrinogen-III oxidase, mitochondrial	Yes	Yes	0	11	18
P31327	CPS1 Carbamoyl-phosphate synthase	Yes	Yes	0	15	0
P23786	CPT2 Carnitine O-palmitoyltransferase 2, mitochondrial	Yes	Yes	2	49	3
P43155	CRAT Carnitine O-acetyltransferase	Yes	Yes	0	22	3
Q08257	CRYZ Quinone oxidoreductase	Yes	Yes	3	10	6
O75390	CS Citrate synthase, mitochondrial	Yes	Yes	9	79	17
P49711	CTCF Transcriptional repressor CTCF			5	0	10
Q16850	CYP51A1 Lanosterol 14-alpha demethylase			41	0	10
P51398	DAP3 28S ribosomal protein S29, mitochondrial	Yes	Yes	0	11	7
Q6PI48	DARS2 Aspartate--tRNA ligase, mitochondrial	Yes	Yes	4	126	39
Q16643	DBN1 Drebrin			0	5	35
P11182	DBT Lipoamide acyltransferase component of branched-chain alpha-keto acid dehydrogenase complex, mitochondrial	Yes	Yes	0	12	15
Q7Z4W1	DCXR L-xylulose reductase	Yes	Yes	2	5	15
Q13838	DDX39B Spliceosome RNA helicase DDX39B			7	6	11
Q96HY7	DHTKD1 Probable 2-oxoglutarate dehydrogenase E1 component DHKTD1, mitochondrial	Yes	Yes	0	53	24
Q7L2E3	DHX30 Putative ATP-dependent RNA helicase DHX30	Yes		0	39	29
Q08211	DHX9 ATP-dependent RNA helicase A			7	5	23
P10515	DLAT Dihydrolipoyllysine-residue acetyltransferase component of pyruvate dehydrogenase complex, mitochondrial	Yes	Yes	19	67	81
P09622	DLD Dihydrolipoyl dehydrogenase, mitochondrial	Yes	Yes	11	42	17
P36957	DLST Dihydrolipoyllysine-residue succinyltransferase component of 2-oxoglutarate dehydrogenase complex, mitochondrial	Yes	Yes	2	6	17
Q96EY1	DNAJA3 DnaJ homolog subfamily A member 3, mitochondrial	Yes	Yes	0	24	0
Q08554	DSC1 Desmocollin-1			5	0	10
Q02413	DSG1 Desmoglein-1			3	0	15
P15924	DSP Desmoplakin			9	0	17
Q5JPH6	EARS2 Probable glutamate--tRNA ligase, mitochondrial	Yes	Yes	0	22	4
Q13011	ECH1 Delta(3,5)-Delta(2,4)-dienoyl-CoA isomerase, mitochondrial	Yes	Yes	3	49	5
P30084	ECHS1 Enoyl-CoA hydratase, mitochondrial	Yes	Yes	6	54	28
P42126	ECI1 Enoyl-CoA delta isomerase 1, mitochondrial	Yes	Yes	2	26	5
O75521	ECI2 Enoyl-CoA delta isomerase 2, mitochondrial	Yes	Yes	2	20	14
P68104	EEF1A1 Elongation factor 1-alpha 1			42	41	52
Q05639	EEF1A2 Elongation factor 1-alpha 2			27	19	26
P26641	EEF1G Elongation factor 1-gamma			10	12	10
P13639	EEF2 Elongation factor 2			43	49	62
P60842	EIF4A1 Eukaryotic initiation factor 4A-I			14	9	13
Q9BQ52	ELAC2 Zinc phosphodiesterase ELAC protein 2	Yes	Yes	4	46	30
P06733	ENO1 Alpha-enolase			27	15	34
P07814	EPRS Bifunctional glutamate/proline--tRNA ligase			11	3	14
Q9BSJ8	ESYT1 Extended synaptotagmin-1			0	0	11
P13804	ETFA Electron transfer flavoprotein subunit alpha, mitochondrial	Yes	Yes	6	22	14
P38117	ETFB Electron transfer flavoprotein subunit beta	Yes	Yes	5	80	12
O95571	ETHE1 Protein ETHE1, mitochondrial	Yes	Yes	0	20	19
O95864	FADS2 Fatty acid desaturase 2			32	0	5
Q6P587	FAHD1 Acylpyruvase FAHD1, mitochondrial	Yes	Yes	0	40	0

Q6P2I3	FAHD2B Fumarylacetoacetate hydrolase domain-containing protein 2B	Yes	Yes	2	15	7
Q5VSL9	FAM40A Protein FAM40A			0	0	10
O95363	FARS2 Phenylalanine--tRNA ligase, mitochondrial	Yes	Yes	0	15	3
P49327	FASN Fatty acid synthase			55	40	61
Q53R41	FASTKD1 FAST kinase domain-containing protein 1	Yes	Yes	0	13	2
Q9NYY8	FASTKD2 FAST kinase domain-containing protein 2	Yes	Yes	0	30	3
Q7L8L6	FASTKD5 FAST kinase domain-containing protein 5	Yes	Yes	0	25	6
P22570	FDXR NADPH:adrenodoxin oxidoreductase, mitochondrial	Yes	Yes	0	38	3
P22830	FECH Ferrochelatase, mitochondrial	Yes	Yes	0	16	0
P07954	FH Fumarate hydratase, mitochondrial	Yes	Yes	7	37	10
Q8NFF5	FLAD1 FAD synthase	Yes	Yes	0	35	12
P21333	FLNA Filamin-A			16	13	88
O75369	FLNB Filamin-B			5	4	25
Q16658	FSCN1 Fascin			7	2	10
Q14697	GANAB Neutral alpha-glucosidase AB			10	12	25
P04406	GAPDH Glyceraldehyde-3-phosphate dehydrogenase			33	20	44
P41250	GARS Glycine--tRNA ligase			7	38	30
P22102	GART Trifunctional purine biosynthetic protein adenosine-3			5	5	12
O75323	GBAS Protein NipSnap homolog 2	Yes	Yes	0	16	0
O75600	GCAT 2-amino-3-ketobutyrate coenzyme A ligase, mitochondrial	Yes	Yes	0	3	12
Q92947	GCDH Glutaryl-CoA dehydrogenase, mitochondrial	Yes	Yes	0	28	5
P23434	GCSH Glycine cleavage system H protein, mitochondrial	Yes	Yes	3	14	3
P50395	GDI2 Rab GDP dissociation inhibitor beta			6	5	10
Q96RP9	GFM1 Elongation factor G, mitochondrial	Yes	Yes	3	75	36
Q969S9	GFM2 Ribosome-releasing factor 2, mitochondrial	Yes	Yes	0	21	15
P23378	GLDC Glycine dehydrogenase	Yes	Yes	6	81	128
O94925	GLS Glutaminase kidney isoform, mitochondrial	Yes	Yes	6	122	27
P00367	GLUD1 Glutamate dehydrogenase 1, mitochondrial	Yes	Yes	9	110	21
P49448	GLUD2 Glutamate dehydrogenase 2, mitochondrial	Yes	Yes	0	82	0
P63244	GNB2L1 Guanine nucleotide-binding protein subunit beta-2-like 1			7	3	10
Q08379	GOLGA2 Golgin subfamily A member 2			0	0	14
Q08378	GOLGA3 Golgin subfamily A member 3			0	2	21
Q14789	GOLGB1 Golgin subfamily B member 1			0	2	65
P00505	GOT2 Aspartate aminotransferase, mitochondrial	Yes	Yes	29	140	40
Q9UBQ7	GRHPR Glyoxylate reductase/hydroxypyruvate reductase	Yes	Yes	0	12	4
Q9HAV7	GRPEL1 GrpE protein homolog 1, mitochondrial	Yes	Yes	4	74	13
Q12849	GRSF1 G-rich sequence factor 1	Yes	Yes	5	156	64
P00390	GSR Glutathione reductase, mitochondrial	Yes	Yes	4	24	13
P09211	GSTP1 Glutathione S-transferase P	Yes		12	4	10
Q969Y2	GTPBP3 tRNA modification GTPase GTPBP3, mitochondrial	Yes	Yes	0	14	7
Q16836	HADH Hydroxyacyl-coenzyme A dehydrogenase, mitochondrial	Yes	Yes	7	63	16
P40939	HADHA Trifunctional enzyme subunit alpha, mitochondrial	Yes	Yes	0	50	8
Q9BSH5	HDHD3 Haloacid dehalogenase-like hydrolase domain-containing protein 3	Yes	Yes	0	21	9
Q6NVY1	HIBCH 3-hydroxyisobutyryl-CoA hydrolase, mitochondrial	Yes	Yes	2	10	3
Q9BX68	HINT2 Histidine triad nucleotide-binding protein 2, mitochondrial	Yes	Yes	3	10	0
P62805	HIST4H4 Histone H4			10	8	17
P52789	HK2 Hexokinase-2	Yes		0	0	18
P35914	HMGCL Hydroxymethylglutaryl-CoA lyase, mitochondrial	Yes	Yes	3	9	21
P09651	HNRNPA1 Heterogeneous nuclear ribonucleoprotein A1			12	6	16
P22626	HNRNPA2B1 Heterogeneous nuclear ribonucleoproteins A2/B1			10	5	17
P51991	HNRNPA3 Heterogeneous nuclear ribonucleoprotein A3			3	0	10
P61978	HNRNPK Heterogeneous nuclear ribonucleoprotein K			11	6	15
P14866	HNRNPL Heterogeneous nuclear ribonucleoprotein L			7	6	12
O43390	HNRNPR Heterogeneous nuclear ribonucleoprotein R			7	0	11
Q00839	HNRNPU Heterogeneous nuclear ribonucleoprotein U			10	5	13
Q86YZ3	HRNR Hornerin			9	0	20
Q99714	HSD17B10 3-hydroxyacyl-CoA dehydrogenase type-2	Yes	Yes	10	69	146
P51659	HSD17B4 Peroxisomal multifunctional enzyme type 2			3	0	15
Q6YN16	HSDL2 Hydroxysteroid dehydrogenase-like protein 2	Yes	Yes	3	82	46
P07900	HSP90AA1 Heat shock protein HSP 90-alpha			25	35	32
P08238	HSP90AB1 Heat shock protein HSP 90-beta			29	30	36
P14625	HSP90B1 Endoplasmin			8	4	29
P08107	HSPA1B Heat shock 70 kDa protein 1A/1B			21	26	34
Q53FA3	HSPA1L Heat shock 70kDa protein 1-like variant			0	11	18
P34932	HSPA4 Heat shock 70 kDa protein 4			10	3	8
P11021	HSPA5 78 kDa glucose-regulated protein			2	2	25
P11142	HSPA8 Heat shock cognate 71 kDa protein			15	15	20
P38646	HSPA9 Stress-70 protein, mitochondrial	Yes	Yes	27	359	227
P10809	HSPD1 60 kDa heat shock protein, mitochondrial	Yes	Yes	105	931	300
P61604	HSPE1 10 kDa heat shock protein, mitochondrial	Yes	Yes	14	76	20
Q92598	HSPH1 Heat shock protein 105 kDa			3	3	10
Q9NSE4	IARS2 Isoleucine--tRNA ligase, mitochondrial	Yes	Yes	5	136	50
Q5T440	IBA57 Putative transferase CAF17, mitochondrial	Yes	Yes	2	21	12
P48735	IDH2 Isocitrate dehydrogenase	Yes	Yes	13	78	9
P50213	IDH3A Isocitrate dehydrogenase	Yes	Yes	2	32	14
O43837	IDH3B Isocitrate dehydrogenase	Yes	Yes	2	97	7
P51553	IDH3G Isocitrate dehydrogenase	Yes	Yes	0	62	7
Q12906	ILF3 Interleukin enhancer-binding factor 3			4	2	11
Q16891	IMMT Mitochondrial inner membrane protein	Yes		0	12	5
P12268	IMPDH2 Inosine-5'-monophosphate dehydrogenase 2			3	3	21
Q96AB3	ISOC2 Isochorismatase domain-containing protein 2, mitochondrial	Yes	Yes	4	28	11
P26440	IVD Isovaleryl-CoA dehydrogenase, mitochondrial	Yes	Yes	0	14	16
P14923	JUP Junction plakoglobin			6	3	14
Q92945	KHSRP Far upstream element-binding protein 2			6	7	29

O15091	KIAA0391 Mitochondrial ribonuclease P protein 3	Yes	Yes	0	21	0
P33176	KIF5B Kinesin-1 heavy chain			0	0	10
Q14974	KPNB1 Importin subunit beta-1			3	4	10
Q9H9P8	L2HGDH L-2-hydroxyglutarate dehydrogenase, mitochondrial	Yes	Yes	0	15	2
P28838	LAP3 Cytosol aminopeptidase	Yes	Yes	3	19	16
Q15031	LARS2 Probable leucine--tRNA ligase, mitochondrial	Yes	Yes	0	47	39
P00338	LDHA L-lactate dehydrogenase A chain			12	13	13
P07195	LDHB L-lactate dehydrogenase B chain	Yes		14	11	11
O95202	LETM1 LETM1 and EF-hand domain-containing protein 1, mitochondrial	Yes	Yes	0	35	11
Q9UHB6	LIMA1 LIM domain and actin-binding protein 1			0	0	31
P36776	LONP1 Lon protease homolog, mitochondrial	Yes	Yes	6	81	39
P42704	LRPPRC Leucine-rich PPR motif-containing protein, mitochondrial	Yes	Yes	13	310	155
Q5VWZ2	LYPLAL1 Lysophospholipase-like protein 1	Yes	Yes	0	11	2
Q9BQ69	MACROD1 O-acetyl-ADP-ribose deacetylase MACROD1	Yes	Yes	0	18	4
Q96GW9	MARS2 Methionine--tRNA ligase, mitochondrial	Yes	Yes	0	37	13
Q96RQ3	MCCC1 Methylcrotonoyl-CoA carboxylase subunit alpha, mitochondrial	Yes		766	80	697
Q9HCC0	MCCC2 Methylcrotonoyl-CoA carboxylase beta chain, mitochondrial	Yes	Yes	8	123	67
P25205	MCM3 DNA replication licensing factor MCM3			3	2	23
P33992	MCM5 DNA replication licensing factor MCM5			3	3	12
Q14676	MDC1 Mediator of DNA damage checkpoint protein 1			0	0	15
P40926	MDH2 Malate dehydrogenase, mitochondrial	Yes	Yes	21	36	29
P23368	ME2 NAD-dependent malic enzyme, mitochondrial	Yes	Yes	4	121	30
Q9BV79	MECR Trans-2-enoyl-CoA reductase, mitochondrial	Yes	Yes	0	16	0
A6NJ78	METTL15 Probable methyltransferase-like protein 15	Yes	Yes	0	15	0
P14174	MIF Macrophage migration inhibitory factor			11	5	28
Q99797	MIPEP Mitochondrial intermediate peptidase	Yes	Yes	0	60	8
Q96EY8	MMAB Cob(I)yrinic acid a,c-diamide adenosyltransferase, mitochondrial	Yes	Yes	3	16	11
P25325	MPST 3-mercaptopyruvate sulfurtransferase	Yes	Yes	0	18	4
Q9BYD1	MRPL13 39S ribosomal protein L13, mitochondrial	Yes	Yes	0	10	0
Q7Z2W9	MRPL21 39S ribosomal protein L21, mitochondrial	Yes	Yes	2	13	0
Q13084	MRPL28 39S ribosomal protein L28, mitochondrial	Yes	Yes	0	11	0
P09001	MRPL3 39S ribosomal protein L3, mitochondrial	Yes	Yes	0	12	9
Q9BZE1	MRPL37 39S ribosomal protein L37, mitochondrial	Yes	Yes	0	10	3
Q96DV4	MRPL38 39S ribosomal protein L38, mitochondrial	Yes	Yes	0	20	3
Q9NYK5	MRPL39 39S ribosomal protein L39, mitochondrial	Yes	Yes	2	27	15
Q9BYD3	MRPL4 39S ribosomal protein L4, mitochondrial	Yes	Yes	0	27	4
Q9H9J2	MRPL44 39S ribosomal protein L44, mitochondrial	Yes	Yes	0	8	11
Q9BRJ2	MRPL45 39S ribosomal protein L45, mitochondrial	Yes	Yes	0	17	0
Q8N5N7	MRPL50 39S ribosomal protein L50, mitochondrial	Yes	Yes	0	11	5
P82664	MRPS10 28S ribosomal protein S10, mitochondrial	Yes	Yes	0	15	0
Q9Y676	MRPS18B 28S ribosomal protein S18b, mitochondrial	Yes	Yes	3	9	20
P82650	MRPS22 28S ribosomal protein S22, mitochondrial	Yes	Yes	0	20	2
Q9Y3D9	MRPS23 28S ribosomal protein S23, mitochondrial	Yes	Yes	0	10	0
Q92552	MRPS27 28S ribosomal protein S27, mitochondrial	Yes	Yes	0	45	7
Q92665	MRPS31 28S ribosomal protein S31, mitochondrial	Yes	Yes	0	35	0
P82930	MRPS34 28S ribosomal protein S34, mitochondrial	Yes	Yes	0	15	0
P82673	MRPS35 28S ribosomal protein S35, mitochondrial	Yes	Yes	3	27	16
P82675	MRPS5 28S ribosomal protein S5, mitochondrial	Yes	Yes	0	12	5
Q9Y2R9	MRPS7 28S ribosomal protein S7, mitochondrial	Yes	Yes	0	17	2
P82933	MRPS9 28S ribosomal protein S9, mitochondrial	Yes	Yes	0	32	9
Q6UB35	MTHFD1L Monofunctional C1-tetrahydrofolate synthase, mitochondrial	Yes	Yes	7	71	30
P13995	MTHFD2 Bifunctional methylenetetrahydrofolate dehydrogenase/cyclohydrolase, mitochondrial	Yes	Yes	0	43	10
P46199	MTIF2 Translation initiation factor IF-2, mitochondrial	Yes	Yes	0	11	3
Q9Y2Z2	MTO1 Protein MTO1 homolog, mitochondrial	Yes	Yes	0	17	2
Q9NVV4	MTPAP Poly(A) RNA polymerase, mitochondrial	Yes	Yes	0	10	0
Q9UGC7	MTRF1L Peptide chain release factor 1-like, mitochondrial	Yes		0	12	2
P22033	MUT Methylmalonyl-CoA mutase, mitochondrial	Yes	Yes	0	40	10
P35580	MYH10 Myosin-10			3	0	18
P35749	MYH11 Myosin-11			0	0	10
P35579	MYH9 Myosin-9			7	2	85
P60660	MYL6 Myosin light polypeptide 6			0	2	27
Q4G0N4	NADKD1 NAD kinase domain-containing protein 1	Yes	Yes	0	29	19
P19338	NCL Nucleolin			11	2	12
P56556	NDUFA6 NADH dehydrogenase	Yes	Yes	0	10	0
O14561	NDUFAB1 Acyl carrier protein, mitochondrial	Yes	Yes	3	24	5
Q5TEU4	NDUFAF5 NADH dehydrogenase	Yes	Yes	0	11	0
P28331	NDUFS1 NADH-ubiquinone oxidoreductase 75 kDa subunit, mitochondrial	Yes	Yes	3	27	19
O75306	NDUFS2 NADH dehydrogenase	Yes	Yes	0	20	0
O75489	NDUFS3 NADH dehydrogenase	Yes	Yes	0	15	7
P49821	NDUFV1 NADH dehydrogenase	Yes	Yes	0	7	10
Q9Y697	NFS1 Cysteine desulfurase, mitochondrial	Yes	Yes	0	11	8
Q9UMS0	NFU1 NFU1 iron-sulfur cluster scaffold homolog, mitochondrial	Yes	Yes	2	6	12
Q9BPW8	NIPSNAP1 Protein NipSnap homolog 1	Yes	Yes	3	37	2
Q9UFN0	NIPSNAP3A Protein NipSnap homolog 3A	Yes	Yes	2	46	3
Q9BYT8	NLN Neurolysin, mitochondrial	Yes	Yes	0	46	9
P22392	NME2 Nucleoside diphosphate kinase B			9	5	11
Q8NC60	NOA1 Nitric oxide-associated protein 1	Yes	Yes	0	13	4
P55786	NPEPPS Puromycin-sensitive aminopeptidase			3	10	24
Q9H857	NT5DC2 5'-nucleotidase domain-containing protein 2	Yes	Yes	7	58	56
Q86UY8	NT5DC3 5'-nucleotidase domain-containing protein 3	Yes	Yes	0	26	7
A8MXV4	NUDT19 Nucleoside diphosphate-linked moiety X motif 19, mitochondrial	Yes	Yes	0	23	0
Q14980	NUMA1 Nuclear mitotic apparatus protein 1			0	0	34
P49790	NUP153 Nuclear pore complex protein Nup153			0	0	27

P35658	NUP214 Nuclear pore complex protein Nup214			0	0	17
Q9UKX7	NUP50 Nuclear pore complex protein Nup50			2	0	20
P37198	NUP62 Nuclear pore glycoprotein p62			0	0	11
Q9BW27	NUP85 Nuclear pore complex protein Nup85			0	0	21
P04181	OAT Ornithine aminotransferase, mitochondrial	Yes	Yes	15	148	41
Q02218	OGDH 2-oxoglutarate dehydrogenase, mitochondrial	Yes	Yes	3	31	45
O15294	OGT UDP-N-acetylglucosamine--peptide N-acetylglucosaminyltransferase 110 kDa subunit	Yes		2	0	10
P55809	OXCT1 Succinyl-CoA:3-ketoacid coenzyme A transferase 1, mitochondrial	Yes	Yes	0	26	10
Q9NWU1	OXSM 3-oxoacyl-[acyl-carrier-protein] synthase, mitochondrial	Yes	Yes	0	17	0
P07237	P4HB Protein disulfide-isomerase			8	6	19
P11940	PABPC1 Polyadenylate-binding protein 1			5	12	15
Q13310	PABPC4 Polyadenylate-binding protein 4			6	6	12
P22234	PAICS Multifunctional protein ADE2	Yes	Yes	10	5	19
P11498	PC Pyruvate carboxylase, mitochondrial	Yes		1309	185	1097
P05165	PCCA Propionyl-CoA carboxylase alpha chain, mitochondrial	Yes		494	72	474
P05166	PCCB Propionyl-CoA carboxylase beta chain, mitochondrial	Yes		5	8	10
Q16822	PCK2 Phosphoenolpyruvate carboxykinase	Yes	Yes	0	8	23
P22061	PCMT1 Protein-L-isoaspartate(D-aspartate) O-methyltransferase			5	19	10
Q8WUM4	PDCD6IP Programmed cell death 6-interacting protein			0	7	10
Q6L8Q7	PDE12 2',5'-phosphodiesterase 12	Yes	Yes	7	31	9
P08559	PDHA1 Pyruvate dehydrogenase E1 component subunit alpha, somatic form, mitochondrial	Yes	Yes	7	61	50
P11177	PDHB Pyruvate dehydrogenase E1 component subunit beta, mitochondrial	Yes	Yes	2	39	20
O00330	PDHX Pyruvate dehydrogenase protein X component, mitochondrial	Yes	Yes	0	21	17
P30101	PDIA3 Protein disulfide-isomerase A3			8	4	22
P13667	PDIA4 Protein disulfide-isomerase A4			9	4	18
Q15084	PDIA6 Protein disulfide-isomerase A6			11	4	14
Q15118	PDK1	Yes	Yes	129	719	291
Q15119	PDK2	Yes	Yes	6	31	11
Q15120	PDK3	Yes	Yes	5	63	21
Q9P0J1	PDP1	Yes	Yes	0	25	3
Q9P2J9	PDP2	Yes	Yes	0	10	0
Q8NCN5	PDPR Pyruvate dehydrogenase phosphatase regulatory subunit, mitochondrial	Yes	Yes	0	69	5
Q5T2R2	PDSS1 Decaprenyl-diphosphate synthase subunit 1	Yes	Yes	0	13	3
Q86YH6	PDSS2 Decaprenyl-diphosphate synthase subunit 2	Yes	Yes	0	10	2
O75879	PET112 Glutamyl-tRNA(Gln) amidotransferase subunit B, mitochondrial	Yes	Yes	0	14	6
P07737	PFN1 Profilin-1			12	4	15
P00558	PGK1 Phosphoglycerate kinase 1			14	7	15
O43175	PHGDH D-3-phosphoglycerate dehydrogenase			12	6	17
Q5JRX3	PITRM1 Presequence protease, mitochondrial	Yes	Yes	8	110	116
P14618	PKM Pyruvate kinase isozymes M1/M2			47	33	56
Q02809	PLOD1 Procollagen-lysine,2-oxoglutarate 5-dioxygenase 1			10	0	8
P13797	PLS3 Plastin-3			12	11	33
Q10713	PMPCA Mitochondrial-processing peptidase subunit alpha	Yes	Yes	5	147	24
O75439	PMPCB Mitochondrial-processing peptidase subunit beta	Yes	Yes	4	73	77
Q9NVS9	PNPO Pyridoxine-5'-phosphate oxidase	Yes	Yes	0	12	3
Q8TCS8	PNPT1 Polyribonucleotide nucleotidyltransferase 1, mitochondrial	Yes	Yes	2	72	35
Q9Y2S7	POLDIP2 Polymerase delta-interacting protein 2	Yes	Yes	2	40	13
P54098	POLG DNA polymerase subunit gamma-1	Yes	Yes	0	15	5
O00411	POLRMT DNA-directed RNA polymerase, mitochondrial	Yes	Yes	2	28	5
Q6S8J3	POTEE POTE ankyrin domain family member E			0	0	23
Q9H2U2	PPA2 Inorganic pyrophosphatase 2, mitochondrial	Yes	Yes	9	85	75
P62937	PPIA Peptidyl-prolyl cis-trans isomerase A			19	6	16
P30405	PPIF Peptidyl-prolyl cis-trans isomerase F, mitochondrial	Yes	Yes	2	12	3
P50336	PPOX Protoporphyrinogen oxidase	Yes	Yes	0	10	4
P30153	PPP2R1A Serine/threonine-protein phosphatase 2A 65 kDa regulatory subunit A alpha isoform			2	4	17
Q06830	PRDX1 Peroxiredoxin-1			13	14	16
P30048	PRDX3 Thioredoxin-dependent peroxide reductase, mitochondrial	Yes	Yes	17	283	70
Q13162	PRDX4 Peroxiredoxin-4	Yes		10	4	33
P30044	PRDX5 Peroxiredoxin-5, mitochondrial	Yes	Yes	4	19	13
P30041	PRDX6 Peroxiredoxin-6	Yes		11	6	9
Q4J6C6	PREPL Prolyl endopeptidase-like	Yes	Yes	0	42	15
P78527	PRKDC DNA-dependent protein kinase catalytic subunit			5	4	31
P48634	PRRC2A Protein PRRC2A			0	4	10
Q9Y520	PRRC2C Protein PRRC2C			2	4	20
P26599	PTBP1 Polypyrimidine tract-binding protein 1			5	5	16
Q96EY7	PTCD3 Pentatricopeptide repeat-containing protein 3, mitochondrial	Yes	Yes	0	44	11
Q9Y606	PUS1 tRNA pseudouridine synthase A, mitochondrial	Yes	Yes	0	19	2
Q9H0R6	QRSL1 Glutamyl-tRNA(Gln) amidotransferase subunit A, mitochondrial	Yes	Yes	0	15	16
P61106	RAB14 Ras-related protein Rab-14			2	0	13
P62826	RAN GTP-binding nuclear protein Ran			15	9	15
P49792	RANBP2 E3 SUMO-protein ligase RanBP2			3	4	80
P46060	RANGAP1 Ran GTPase-activating protein 1			2	2	17
Q5T160	RARS2 Probable arginine--tRNA ligase, mitochondrial	Yes	Yes	0	18	3
Q15293	RCN1 Reticulocalbin-1			54	3	40
Q5UIP0	RIF1 Telomere-associated protein RIF1	Yes	Yes	0	0	11
Q9HC36	RNMTL1 RNA methyltransferase-like protein 1	Yes	Yes	0	14	0
P46777	RPL5 60S ribosomal protein L5			4	2	10
Q9P2E9	RRBP1 Ribosome-binding protein 1			4	0	14
Q15424	SAFB Scaffold attachment factor B1			0	0	11
Q9NP81	SARS2 Serine--tRNA ligase, mitochondrial	Yes	Yes	0	34	23
P31040	SDHA Succinate dehydrogenase	Yes	Yes	5	124	34
Q9NX18	SDHAF2 Succinate dehydrogenase assembly factor 2, mitochondrial	Yes		0	17	0
O15027	SEC16A Protein transport protein Sec16A			0	3	17
P34896	SHMT1 Serine hydroxymethyltransferase, cytosolic			0	10	4

P34897	SHMT2 Serine hydroxymethyltransferase, mitochondrial	Yes	Yes	18	187	58
Q8WW59	SPRYD4 SPRY domain-containing protein 4	Yes	Yes	0	10	0
Q13813	SPTAN1 Spectrin alpha chain, non-erythrocytic 1			0	5	17
Q9UQ35	SRRM2 Serine/arginine repetitive matrix protein 2			7	3	14
Q04837	SSBP1 Single-stranded DNA-binding protein, mitochondrial	Yes	Yes	9	156	14
Q9P2R7	SUCLA2 Succinyl-CoA ligase	Yes	Yes	0	25	4
P53597	SUCLG1 Succinyl-CoA ligase	Yes	Yes	4	10	5
Q96I99	SUCLG2 Succinyl-CoA ligase	Yes	Yes	0	24	6
Q8IYB8	SUPV3L1 ATP-dependent RNA helicase SUPV3L1, mitochondrial	Yes	Yes	0	31	4
Q9BSH4	TACO1 Translational activator of cytochrome c oxidase 1	Yes	Yes	3	23	3
P37802	TAGLN2 Transgelin-2			5	10	5
Q9BW92	TARS2 Threonine--tRNA ligase, mitochondrial	Yes	Yes	3	52	18
Q969Z0	TBRG4 Protein TBRG4	Yes	Yes	0	47	14
P17987	TCP1 T-complex protein 1 subunit alpha			16	3	20
Q00059	TFAM Transcription factor A, mitochondrial	Yes	Yes	2	25	10
Q8WVM0	TFB1M Dimethyladenosine transferase 1, mitochondrial	Yes	Yes	0	11	0
Q9H5Q4	TFB2M Dimethyladenosine transferase 2, mitochondrial	Yes	Yes	0	21	2
Q8IYQ7	THNSL1 Threonine synthase-like 1	Yes	Yes	2	23	13
O43615	TIMM44 Mitochondrial import inner membrane translocase subunit TIM44	Yes	Yes	0	34	0
P29401	TKT Transketolase			11	4	15
Q9NVH6	TMLHE Trimethyllysine dioxygenase, mitochondrial	Yes	Yes	0	22	9
Q9C0C2	TNKS1BP1 182 kDa tankyrase-1-binding protein			0	0	18
P12270	TPR Nucleoprotein TPR	Yes	Yes	0	0	40
Q12931	TRAP1 Heat shock protein 75 kDa, mitochondrial	Yes	Yes	21	200	153
Q13263	TRIM28 Transcription intermediary factor 1-beta			5	4	10
Q7L0Y3	TRMT10C Mitochondrial ribonuclease P protein 1	Yes	Yes	6	71	14
Q7Z4G4	TRMT11 tRNA (guanine(10)-N2)-methyltransferase homolog	Yes	Yes	0	10	4
Q32P41	TRMT5 tRNA (guanine(37)-N1)-methyltransferase	Yes		0	14	0
O75648	TRMU Mitochondrial tRNA-specific 2-thiouridylase 1	Yes	Yes	0	22	3
P43897	TSFM Elongation factor Ts, mitochondrial	Yes	Yes	2	41	7
Q16762	TST Thiosulfate sulfurtransferase	Yes	Yes	0	12	0
Q71U36	TUBA1A Tubulin alpha-1A chain			35	69	53
P68366	TUBA4A Tubulin alpha-4A chain			32	71	45
Q9NY65	TUBA8 Tubulin alpha-8 chain			22	0	30
P07437	TUBB Tubulin beta chain			31	34	46
Q9BVA1	TUBB2B Tubulin beta-2B chain			0	0	29
Q13509	TUBB3 Tubulin beta-3 chain			16	0	15
P68371	TUBB4B Tubulin beta-4B chain			25	33	35
Q9BUF5	TUBB6 Tubulin beta-6 chain			9	15	9
P49411	TUFM Elongation factor Tu, mitochondrial	Yes	Yes	10	89	52
Q99757	TXN2 Thioredoxin, mitochondrial	Yes	Yes	0	10	4
Q16881	TXNRD1 Thioredoxin reductase 1, cytoplasmic			11	7	12
Q9NNW7	TXNRD2 Thioredoxin reductase 2, mitochondrial	Yes	Yes	4	14	17
P22314	UBA1 Ubiquitin-like modifier-activating enzyme 1	Yes		18	10	30
F5H5P2	Uncharacterized protein	Yes	Yes	0	31	11
H7C455	Uncharacterized protein			0	0	14
P31930	UQCRC1 Cytochrome b-c1 complex subunit 1, mitochondrial	Yes	Yes	3	63	28
P22695	UQCRC2 Cytochrome b-c1 complex subunit 2, mitochondrial	Yes	Yes	2	40	7
P47985	UQCRFS1 Cytochrome b-c1 complex subunit Rieske, mitochondrial	Yes	Yes	0	27	9
E7ERL9	VARS2 Valine--tRNA ligase, mitochondrial	Yes	Yes	0	21	14
P55072	VCP Transitional endoplasmic reticulum ATPase			9	9	16
P45880	VDAC2 Voltage-dependent anion-selective channel protein 2	Yes		2	0	13
P08670	VIM Vimentin			4	7	40
Q96I51	WBSCR16 Williams-Beuren syndrome chromosomal region 16 protein	Yes	Yes	0	17	5
Q9NQH7	XPNPEP3 Probable Xaa-Pro aminopeptidase 3	Yes	Yes	0	16	2
P13010	XRCC5 X-ray repair cross-complementing protein 5			7	4	15
Q9Y2Z4	YARS2 Tyrosine--tRNA ligase, mitochondrial	Yes	Yes	2	48	4
Q8N4Q0	ZADH2 Zinc-binding alcohol dehydrogenase domain-containing protein 2	Yes	Yes	2	19	7

Table 4A-2. Gene ontology (GOrilla) analysis for enrichment of biological processes for proteins identified in matrix-APEX analysis with >5-fold enrichment.

Analysis Type:	PANTHER Overrepresentation Test (Released 20220202)
Annotation Version and Release Date:	PANTHER version 17.0 Released 2022-02-22
Reference List:	Homo sapiens (all genes in database)
Test Type:	FISHER
Correction:	FDR

PANTHER GO-Slim Biological Process	REFLIST	Expected	Fold Enrichment	P-Value	FDR
mitochondrial RNA processing (GO:0000963)	9	0.57	12.18	1.96E-05	2.65E-04
tricarboxylic acid cycle (GO:0006099)	17	1.09	11.05	4.16E-08	1.18E-06
branched-chain amino acid metabolic process (GO:0009081)	10	0.64	10.96	3.15E-05	4.02E-04
mitochondrial RNA metabolic process (GO:0000959)	15	0.96	10.44	8.37E-07	1.82E-05
protein processing involved in protein targeting to mitochondrion (GO:0006627)	6	0.38	10.44	2.03E-03	1.55E-02
mitochondrial gene expression (GO:0140053)	28	1.79	9.51	3.42E-10	1.35E-08
mitochondrial translation (GO:0032543)	14	0.89	8.95	2.47E-05	3.21E-04
glutamate metabolic process (GO:0006536)	7	0.45	8.95	3.03E-03	2.18E-02
ribonucleoside diphosphate metabolic process (GO:0009185)	22	1.41	7.83	1.99E-06	4.08E-05
purine ribonucleoside diphosphate metabolic process (GO:0009179)	22	1.41	7.83	1.99E-06	4.04E-05
purine nucleoside diphosphate metabolic process (GO:0009135)	22	1.41	7.83	1.99E-06	4.01E-05
folic acid-containing compound metabolic process (GO:0006760)	14	0.89	7.83	1.53E-04	1.64E-03
ATP generation from ADP (GO:0006757)	22	1.41	7.83	1.99E-06	3.97E-05
ubiquinone biosynthetic process (GO:0006744)	10	0.64	7.83	1.40E-03	1.12E-02
glycolytic process (GO:0006096)	22	1.41	7.83	1.99E-06	3.94E-05
ADP metabolic process (GO:0046031)	22	1.41	7.83	1.99E-06	3.90E-05
pyrimidine nucleotide biosynthetic process (GO:0006221)	10	0.64	7.83	1.40E-03	1.11E-02
fatty acid beta-oxidation (GO:0006635)	23	1.47	7.49	2.78E-06	5.27E-05
nucleoside diphosphate phosphorylation (GO:0006165)	26	1.66	7.23	1.31E-06	2.80E-05
double-strand break repair via break-induced replication (GO:0000727)	11	0.7	7.12	1.94E-03	1.49E-02
ribosomal subunit export from nucleus (GO:0000054)	11	0.7	7.12	1.94E-03	1.49E-02
nucleotide phosphorylation (GO:0046939)	27	1.72	6.96	1.79E-06	3.75E-05
DNA unwinding involved in DNA replication (GO:0006268)	9	0.57	6.96	5.97E-03	3.91E-02
mitochondrial protein processing (GO:0034982)	9	0.57	6.96	5.97E-03	3.90E-02
ribonucleoside monophosphate metabolic process (GO:0009161)	14	0.89	6.71	8.64E-04	7.41E-03
response to oxidative stress (GO:0006979)	26	1.66	6.62	7.02E-06	1.15E-04
nucleoside monophosphate metabolic process (GO:0009123)	19	1.21	6.59	1.31E-04	1.43E-03
purine ribonucleoside monophosphate metabolic process (GO:0009167)	12	0.77	6.52	2.61E-03	1.92E-02
purine nucleoside monophosphate metabolic process (GO:0009126)	12	0.77	6.52	2.61E-03	1.91E-02
RNA export from nucleus (GO:0006405)	48	3.07	6.52	1.65E-09	5.63E-08
pyrimidine nucleotide metabolic process (GO:0006220)	12	0.77	6.52	2.61E-03	1.90E-02
tRNA metabolic process (GO:0006399)	113	7.22	6.51	1.93E-20	2.52E-18
cellular amino acid metabolic process (GO:0006520)	142	9.07	6.4	1.33E-24	2.68E-22
cellular response to oxidative stress (GO:0034599)	15	0.96	6.26	1.15E-03	9.52E-03
response to toxic substance (GO:0009636)	15	0.96	6.26	1.15E-03	9.48E-03
postreplication repair (GO:0006301)	15	0.96	6.26	1.15E-03	9.45E-03
protein quality control for misfolded or incompletely synthesized proteins (GO:0006515)	10	0.64	6.26	7.96E-03	4.84E-02
RNA transport (GO:0050658)	51	3.26	6.14	3.80E-09	1.24E-07
nucleic acid transport (GO:0050657)	51	3.26	6.14	3.80E-09	1.22E-07
establishment of RNA localization (GO:0051236)	51	3.26	6.14	3.80E-09	1.21E-07
glucose 6-phosphate metabolic process (GO:0051156)	18	1.15	6.09	5.10E-04	4.64E-03
mismatch repair (GO:0006298)	13	0.83	6.02	3.43E-03	2.41E-02
carboxylic acid catabolic process (GO:0046395)	84	5.37	5.96	1.62E-13	1.16E-11
RNA localization (GO:0006403)	56	3.58	5.87	2.97E-09	9.85E-08
cellular response to chemical stress (GO:0062197)	16	1.02	5.87	1.50E-03	1.19E-02
nuclear export (GO:0051168)	67	4.28	5.84	1.03E-10	4.40E-09
organic acid catabolic process (GO:0016054)	86	5.49	5.83	2.72E-13	1.88E-11
fatty acid catabolic process (GO:0009062)	35	2.24	5.82	3.32E-06	6.19E-05
lipid oxidation (GO:0034440)	30	1.92	5.74	2.08E-05	2.80E-04
nucleobase metabolic process (GO:0009112)	22	1.41	5.69	2.94E-04	2.87E-03
mRNA export from nucleus (GO:0006406)	33	2.11	5.69	9.41E-06	1.46E-04
actin filament depolymerization (GO:0030042)	22	1.41	5.69	2.94E-04	2.85E-03
nucleoside diphosphate metabolic process (GO:0009132)	36	2.3	5.65	4.27E-06	7.65E-05
monocarboxylic acid catabolic process (GO:0072329)	39	2.49	5.62	1.94E-06	4.03E-05

mRNA transport (GO:0051028)	34	2.17	5.53	1.20E-05	1.77E-04
nucleobase-containing compound transport (GO:0015931)	64	4.09	5.38	4.68E-09	1.44E-07
carboxylic acid metabolic process (GO:0019752)	314	20.05	5.29	4.71E-38	5.23E-35
heme metabolic process (GO:0042168)	15	0.96	5.22	5.62E-03	3.73E-02
pigment metabolic process (GO:0042440)	27	1.72	5.22	2.12E-04	2.16E-03
glucose metabolic process (GO:0006006)	39	2.49	5.22	8.73E-06	1.39E-04
quinone metabolic process (GO:1901661)	15	0.96	5.22	5.62E-03	3.71E-02
spliceosomal snRNP assembly (GO:0000387)	15	0.96	5.22	5.62E-03	3.70E-02
oxoacid metabolic process (GO:0043436)	318	20.31	5.22	1.19E-37	8.81E-35
import into nucleus (GO:0051170)	58	3.7	5.13	9.74E-08	2.70E-06
protein import into nucleus (GO:0006606)	58	3.7	5.13	9.74E-08	2.67E-06
positive regulation of translation (GO:0045727)	28	1.79	5.03	2.65E-04	2.63E-03
pigment biosynthetic process (GO:0046148)	25	1.6	5.01	5.95E-04	5.37E-03

Table 4A-3. List of all cysteine-containing peptides identified in matrix-APEX analyses. Mitochondrial localization is denoted by "mito", and is derived from uniprot subcellular localization, MitoCarta2.0, and previous studies (mito-APEX, IMS-APEX, and IMSGold+). "DMSO" denotes DMSO treatment for 45 min. "AMA" denotes 100 μM Antimycin A treatment for 45 min. "H2O2" denotes 1 mM H2O2 treatment for 1 min. Peptide identifications are the average of 3 replicates for each treatment and >10 spectral counts.

UniProt ID	Protein Description	Peptide Sequence	Mito	Total Spectral Count Matrix-APEX DMSO	Total Spectral Count Matrix-APEX AMA	Total Spectral Count Matrix-APEX H2O2
Q9UDR5	AASS Alpha-aminoadipic semialdehyde synthase, mitochondrial	K.EVGATIESYISYC*GGLPAPEHSNNPLR.Y	Yes	0	12	1
Q9UDR5	AASS Alpha-aminoadipic semialdehyde synthase, mitochondrial	R.FNTDIAPYTTC*LINGIYWEQNTPR.L	Yes	0	10	4
Q9NUJ1	ABHD10 Abhydrolase domain-containing protein 10, mitochondrial	K.EAEHHC*LLHSPIPVNC*PIR.L	Yes	0	0	14
Q9NUJ1	ABHD10 Abhydrolase domain-containing protein 10, mitochondrial	K.EAEHHC*LLHSPIPVNC*PIR.L	Yes	0	0	11
Q13085	ACACA Acetyl-CoA carboxylase 1	K.EMAQYASNITSVLC*QFPSQQIANILDSHAATLNR.K	Yes	6	11	16
Q13085	ACACA Acetyl-CoA carboxylase 1	K.VQAERPDTMLGVVC*GALHVADVSLR.N	Yes	4	2	12
Q13085	ACACA Acetyl-CoA carboxylase 1	R.VSALNSVHC*EHVEDEGESR.Y	Yes	6	27	2
Q13085	ACACA Acetyl-CoA carboxylase 1	R.VSALNSVHC*EHVEDEGESR.Y	Yes	6	24	4
Q13085	ACACA Acetyl-CoA carboxylase 1	R.EC*C*QPVLVYIPPQAELR.G	Yes	4	24	0
Q13085	ACACA Acetyl-CoA carboxylase 1	R.NFDLTAIPC*ANHK.M	Yes	4	15	3
Q13085	ACACA Acetyl-CoA carboxylase 1	K.RPGAALDPGC*VLAK.M	Yes	6	14	9
P24752	ACAT1 Acetyl-CoA acetyltransferase, mitochondrial	K.IHMGSC*AENTAK.K	Yes	3	5	29
P24752	ACAT1 Acetyl-CoA acetyltransferase, mitochondrial	K.QGEYGLASIC*NGGGGASAMLIQK.L	Yes	0	5	14
P24752	ACAT1 Acetyl-CoA acetyltransferase, mitochondrial	K.AIMMASQSLMC*GHQDVMVAGGMESMSNVPYVMNR.G	Yes	0	0	10
Q99798	ACO2 Aconitate hydratase, mitochondrial	K.C*TTDHISAAGPWLK.F	Yes	0	2	14
Q99798	ACO2 Aconitate hydratase, mitochondrial	K.VAVPSTIHC*DHLIEAQVGGEK.D	Yes	0	10	12
Q99798	ACO2 Aconitate hydratase, mitochondrial	R.VGLIGSC*TNSSYEDMGR.S	Yes	1	18	9
Q99798	ACO2 Aconitate hydratase, mitochondrial	K.VAVPSTIHC*DHLIEAQVGGEK.D	Yes	1	12	4
Q9Y305	ACOT9 Acyl-coenzyme A thioesterase 9, mitochondrial	R.ILEDLDSLGVLIC*YMHNK.I	Yes	0	0	10
P60709	ACTB Actin, cytoplasmic 1	K.LC*YVALDFEQEMATAASSSSLEK.S		0	0	11
P54886	ALDH18A1 Delta-1-pyrroline-5-carboxylate synthase	K.GIPVMGHSEGIC*HMYVDSEASVDK.V	Yes	0	5	19

P54886	ALDH18A1 Delta-1-pyrroline-5-carboxylate synthase	K.C*EYPAAC*NALETLLIHR.D	Yes	0	2	17
P54886	ALDH18A1 Delta-1-pyrroline-5-carboxylate synthase	R.TEYGDLELC*IEVVDNVQDAIDHIHK.Y	Yes	0	2	12
P54886	ALDH18A1 Delta-1-pyrroline-5-carboxylate synthase	R.TEYGDLELC*IEVVDNVQDAIDHIHK.Y	Yes	0	0	12
P54886	ALDH18A1 Delta-1-pyrroline-5-carboxylate synthase	K.GIPVMGHSEGIC*HMYVDSEASVDK.V	Yes	0	0	12
P54886	ALDH18A1 Delta-1-pyrroline-5-carboxylate synthase	R.TEYGDLELC*IEVVDNVQDAIDHIHK.Y	Yes	0	0	11
P05091	ALDH2 Aldehyde dehydrogenase, mitochondrial	R.KTFPTVNPSTGEVIC*QVAEGDKEDVDK.A	Yes	0	12	16
P04075	ALDOA Fructose-bisphosphate aldolase A	R.YASIC*QQNGIVPIVEPEILPDGDHDLKR.C		1	3	10
Q5TC12	ATPAF1 ATP synthase mitochondrial F1 complex assembly factor 1	R.AQSC*PTFLC*ALPR.R	Yes	3	15	6
Q8N5M1	ATPAF2 ATP synthase mitochondrial F1 complex assembly factor 2	R.TAAGTLFIHLC*SESTTVK.H	Yes	0	0	10
O14874	BCKDK	R.MLATHHLALHEDKPDFVGIIC*TR.L	Yes	0	0	10
P43251	BTD Biotinidase	K.DAQEVHC*DEATK.W		6	50	0
Q07021	C1QBP Complement component 1 Q subcomponent-binding protein, mitochondrial	K.ALVLDC*HYPEDEVGQEDEAESDIFSIR.E	Yes	3	14	22
Q07021	C1QBP Complement component 1 Q subcomponent-binding protein, mitochondrial	K.ALVLDC*HYPEDEVGQEDEAESDIFSIR.E	Yes	0	0	15
Q9BQP7	C20orf72 Uncharacterized protein C20orf72	R.ALESAVQHETLNYIGLLDC*VAEYQGK.L	Yes	0	0	14
Q9BQP7	C20orf72 Uncharacterized protein C20orf72	K.DGSPAHPHFMDAELC*SQYWTK.W	Yes	0	0	12
Q6P1X6	C8orf82 UPF0598 protein C8orf82	R.C*EDRPVVFTHLLTADHGPPR.L	Yes	0	1	14
Q6P1X6	C8orf82 UPF0598 protein C8orf82	R.C*EDRPVVFTHLLTADHGPPR.L	Yes	0	0	11
P04632	CAPNS1 Calpain small subunit 1	R.YSDESGNMDFDNFISC*LVR.L		0	14	0
Q9BXW7	CECR5 Cat eye syndrome critical region protein 5	K.AQELSALLGC*EVDADQVILSHSPMK.L	Yes	0	0	10
P12277	CKB Creatine kinase B-type	R.FC*TGLTQIETLFK.S		3	10	4
O76031	CLPX ATP-dependent Clp protease ATP-binding subunit clpX-like, mitochondrial	K.C*HHFFVVLSEADSK.K	Yes	0	0	13
O75208	COQ9 Ubiquinone biosynthesis protein COQ9, mitochondrial	K.DGSELILHFVTQC*NTR.L	Yes	0	0	16
Q6PI48	DARS2 Aspartate--tRNA ligase, mitochondrial	R.SSHLGQEVTLC*GWIQYR.R	Yes	0	0	29
Q6PI48	DARS2 Aspartate--tRNA ligase, mitochondrial	K.ILC*EAPVESVVQVSGTVISR.P	Yes	0	0	17
Q7Z4W1	DCXR L-xylulose reductase	R.EC*PGIEPVC*VDLGDWEATER.A	Yes	0	10	0
P10515	DLAT Dihydrolipoyllysine-residue acetyltransferase component of pyruvate dehydrogenase complex, mitochondrial	R.DVPIGAIIC*ITVGKPEDIEAFK.N	Yes	2	9	27
P10515	DLAT Dihydrolipoyllysine-residue acetyltransferase component of pyruvate dehydrogenase complex, mitochondrial	K.GFDVASMMSVTLSC*DHR.V	Yes	0	0	14
P10515	DLAT Dihydrolipoyllysine-residue acetyltransferase component of pyruvate dehydrogenase complex, mitochondrial	K.NFSAIINPPQAC*ILAIGASEDK.L	Yes	3	21	5
P10515	DLAT Dihydrolipoyllysine-residue acetyltransferase component of pyruvate dehydrogenase complex, mitochondrial	R.DVPLGTPLC*IIVEK.E	Yes	3	18	4
P10515	DLAT Dihydrolipoyllysine-residue acetyltransferase component of pyruvate dehydrogenase complex, mitochondrial	K.NFSAIINPPQAC*ILAIGASEDK.L	Yes	0	14	1
Q13011	ECH1 Delta(3,5)-Delta(2,4)-dienoyl-CoA isomerase, mitochondrial	R.C*PKPVIAAVHGGC*IGGGVDLVTAC*DIR.Y	Yes	0	0	17
P30084	ECHS1 Enoyl-CoA hydratase, mitochondrial	K.IC*PVETLVEEAIQC*AEK.I	Yes	0	0	27
P30084	ECHS1 Enoyl-CoA hydratase, mitochondrial	K.IC*PVETLVEEAIQC*AEK.I	Yes	0	0	15
P30084	ECHS1 Enoyl-CoA hydratase, mitochondrial	K.ALNALC*DGLIDELNQALK.T	Yes	3	14	6
P42126	ECI1 Enoyl-CoA delta isomerase 1, mitochondrial	R.GVILTSDRPGVFSAGLDLTEMC*GR.S	Yes	0	0	15
P42126	ECI1 Enoyl-CoA delta isomerase 1, mitochondrial	R.YC*IGLNETQLGIIAPFWLK.D	Yes	0	2	14
P68104	EEF1A1 Elongation factor 1-alpha 1	K.DGNASGTTLLEALDC*ILPPTRPTDKPLR.L		3	11	5
P13639	EEF2 Elongation factor 2	R.ETVSEESNVLC*LSK.S		3	14	0
P13639	EEF2 Elongation factor 2	R.YVEPIEDVPC*GNIVGLVGVDQFLVK.T		3	13	7
P13639	EEF2 Elongation factor 2	R.YVEPIEDVPC*GNIVGLVGVDQFLVK.T		3	11	0
Q9BQ52	ELAC2 Zinc phosphodiesterase ELAC protein 2	R.TC*DLEEFQTC*LVR.H	Yes	0	10	0
P09104	ENO2 Gamma-enolase	R.SGETEDTFIADLVVGLC*TGQIK.T		3	5	11
P38117	ETFB Electron transfer flavoprotein subunit beta	K.HSMNPFC*EIAVEEAVR.L	Yes	0	3	54
P38117	ETFB Electron transfer flavoprotein subunit beta	K.EVIAVSC*GPAQC*QETIR.T	Yes	2	7	11
P38117	ETFB Electron transfer flavoprotein subunit beta	K.HSMNPFC*EIAVEEAVR.L	Yes	0	0	10
O95571	ETHE1 Protein ETHE1, mitochondrial	R.LTLSC*EEFVK.I	Yes	0	13	0
Q6P587	FAHD1 Acylpyruvase FAHD1, mitochondrial	R.AVPEAAAMDYVGGYALC*LDMTAR.D	Yes	0	0	13
P04406	GAPDH Glyceraldehyde-3-phosphate dehydrogenase	R.VPTANVSVVDLTC*R.L		3	14	5
P23434	GCSH Glycine cleavage system H protein, mitochondrial	K.HEWVTTENGIGTVGISNFAQEALGDVVYC*SLPEVGTK.L	Yes	1	0	10
Q96RP9	GFM1 Elongation factor G, mitochondrial	R.QELIEC*VANSDEQLGEMFLEEK.I	Yes	1	6	14
P23378	GLDC Glycine dehydrogenase	K.TFC*IPHGGGGPGMGPIGVK.K	Yes	0	2	14
P23378	GLDC Glycine dehydrogenase	R.IDDIYGDQHLVC*TC*PPMEVYESPFSEQK.R	Yes	0	13	1
P23378	GLDC Glycine dehydrogenase	K.MEDPVC*ENEILATLHAISSK.N	Yes	1	11	2

O94925	GLS Glutaminase kidney isoform, mitochondrial	K.C*VQSNIVLLTQAFR.R	Yes	0	3	25
O94925	GLS Glutaminase kidney isoform, mitochondrial	K.GIHFC*HDLVSLC*NFHNYDNLR.H	Yes	0	0	14
O94925	GLS Glutaminase kidney isoform, mitochondrial	K.GIHFC*HDLVSLC*NFHNYDNLR.H	Yes	0	0	12
O94925	GLS Glutaminase kidney isoform, mitochondrial	K.FSPDLWGVSVC*TVDGQR.H	Yes	1	21	9
Q14789	GOLGB1 Golgin subfamily B member 1	R.SLLENQSLSSSC*ESLK.L		0	10	0
P00505	GOT2 Aspartate aminotransferase, mitochondrial	R.HFIEQGINVC*LC*QSYAK.N	Yes	0	0	52
P00505	GOT2 Aspartate aminotransferase, mitochondrial	K.EGSTHNWQHITDQIGMFC*FTGLKPEQVER.L	Yes	1	0	25
P00505	GOT2 Aspartate aminotransferase, mitochondrial	K.IPEQSVLLLHAC*AHNPTGVDPRPEQWK.E	Yes	2	1	16
P00505	GOT2 Aspartate aminotransferase, mitochondrial	K.NLDKEYLPIGGLAEFC*K.A	Yes	3	6	12
Q12849	GRSF1 G-rich sequence factor 1	R.AQGLPWSC*TMEDVLNFFSDC*R.I	Yes	0	0	21
Q12849	GRSF1 G-rich sequence factor 1	R.YIELFLNSC*PK.G	Yes	0	4	14
P40939	HADHA Trifunctional enzyme subunit alpha, mitochondrial	K.EVEAVIPDHC*IFASNTSALPISEIAAVSK.R	Yes	0	0	10
Q99714	HSD17B10 3-hydroxyacyl-CoA dehydrogenase type-2	R.VDVAVNC*AGIAVASK.T	Yes	3	89	3
Q99714	HSD17B10 3-hydroxyacyl-CoA dehydrogenase type-2	K.LGNNC*VFAPADVTSEKDVQTALALAK.G	Yes	1	26	6
Q6YN16	HSDL2 Hydroxysteroid dehydrogenase-like protein 2	R.LAGC*TVFITGASR.G	Yes	1	14	17
Q6YN16	HSDL2 Hydroxysteroid dehydrogenase-like protein 2	K.TAIHTAAMDMLGGPGIESQC*R.K	Yes	0	0	15
P38646	HSPA9 Stress-70 protein, mitochondrial	K.GAVVGIDLGTTNSC*VAVMEGK.Q	Yes	1	37	74
P38646	HSPA9 Stress-70 protein, mitochondrial	K.MEEFKDQLPADEC*NK.L	Yes	3	29	14
P38646	HSPA9 Stress-70 protein, mitochondrial	K.C*ELSSSVQTDINLPYLTMDSSGPK.H	Yes	0	4	11
P10809	HSPD1 60 kDa heat shock protein, mitochondrial	R.AAVEEGIVLGGGC*ALLR.C	Yes	6	49	151
P10809	HSPD1 60 kDa heat shock protein, mitochondrial	K.C*EFQDAYVLLSEK.K	Yes	1	7	50
P10809	HSPD1 60 kDa heat shock protein, mitochondrial	R.AAVEEGIVLGGGC*ALLR.C	Yes	1	16	30
P10809	HSPD1 60 kDa heat shock protein, mitochondrial	R.C*IPALDSLTPANEDQK.I	Yes	5	19	25
P10809	HSPD1 60 kDa heat shock protein, mitochondrial	R.AAVEEGIVLGGGC*ALLR.C	Yes	0	0	16
P10809	HSPD1 60 kDa heat shock protein, mitochondrial	K.C*EFQDAYVLLSEK.K	Yes	0	0	15
Q9NSE4	IARS2 Isoleucine--tRNA ligase, mitochondrial	K.KPGLEEAVESAC*AMR.D	Yes	0	4	17
Q9NSE4	IARS2 Isoleucine--tRNA ligase, mitochondrial	R.SC*QTALVEILDVIVR.S	Yes	0	0	16
Q9NSE4	IARS2 Isoleucine--tRNA ligase, mitochondrial	K.TEFC*LHDGPPYANGDPHVGHALNK.I	Yes	0	0	13
Q9NSE4	IARS2 Isoleucine--tRNA ligase, mitochondrial	K.VASVASTLETTFETISTLSGVDLENGTC*SHPLIPDK.A	Yes	1	1	12
Q9NSE4	IARS2 Isoleucine--tRNA ligase, mitochondrial	K.IHFVPGWDC*HGLPIEIK.V	Yes	0	1	10
P48735	IDH2 Isocitrate dehydrogenase	K.DLAGC*IHGLSNVK.L	Yes	2	4	23
O43837	IDH3B Isocitrate dehydrogenase	K.LGDGLFLQC*C*EEVAELYPK.I	Yes	0	1	37
P51553	IDH3G Isocitrate dehydrogenase	R.HAC*VPVDFEEVHVSSNADEEDIR.N	Yes	0	0	15
P51553	IDH3G Isocitrate dehydrogenase	R.HAC*VPVDFEEVHVSSNADEEDIR.N	Yes	0	3	14
P51553	IDH3G Isocitrate dehydrogenase	R.TSLDLYANVIHC*K.S	Yes	0	1	10
P51553	IDH3G Isocitrate dehydrogenase	K.NIANPTATLLASC*MMLDHLK.L	Yes	0	1	10
P12268	IMPDH2 Inosine-5'-monophosphate dehydrogenase 2	R.HGFC*GIPITDTGR.M		3	11	1
Q9H1K1	ISCU Iron-sulfur cluster assembly enzyme ISCU, mitochondrial	K.LHC*SMLAEDAIK.A	Yes	0	3	12
Q96AB3	ISOC2 Isochorismatase domain-containing protein 2, mitochondrial	R.GLQVHVVVDAC*SSR.S	Yes	0	0	10
P26440	IVD Isovaleryl-CoA dehydrogenase, mitochondrial	R.GSNTC*ELIFEDC*K.I	Yes	0	11	0
Q92945	KHSRP Far upstream element-binding protein 2	K.VQQAC*EMVMDILR.E		1	11	0
P00338	LDHA L-lactate dehydrogenase A chain	K.DDVFLSVPC*ILGQNGISDLVK.V		3	11	3
O95202	LETM1 LETM1 and EF-hand domain-containing protein 1, mitochondrial	K.LFEDELTLDNLTRPQLVALC*K.L	Yes	0	1	10
P36776	LONP1 Lon protease homolog, mitochondrial	K.ILC*FYGPPGVGK.T	Yes	3	1	11
P42704	LRPPRC Leucine-rich PPR motif-containing protein, mitochondrial	K.YESDMVTGGYAALINLC*C*R.H	Yes	0	0	37
P42704	LRPPRC Leucine-rich PPR motif-containing protein, mitochondrial	K.QLILVLC*SEENMQK.A	Yes	0	2	27
P42704	LRPPRC Leucine-rich PPR motif-containing protein, mitochondrial	R.AILQENGC*LSDSDMFSQAGLR.S	Yes	1	13	18
P42704	LRPPRC Leucine-rich PPR motif-containing protein, mitochondrial	R.C*GAIAEQTPILLLFLLR.N	Yes	0	0	16
P42704	LRPPRC Leucine-rich PPR motif-containing protein, mitochondrial	R.LIASYC*NVGDIEGASK.I	Yes	3	22	8
Q9BQ69	MACROD1 O-acetyl-ADP-ribose deacetylase MACROD1	R.SC*YLSSLDLLLEHR.L	Yes	0	1	16
Q9BQ69	MACROD1 O-acetyl-ADP-ribose deacetylase MACROD1	R.SC*YLSSLDLLLEHR.L	Yes	0	1	13
Q96GW9	MARS2 Methionine--tRNA ligase, mitochondrial	R.VSEQFQQLFQEAGISC*TDFIR.T	Yes	0	4	11
Q96GW9	MARS2 Methionine--tRNA ligase, mitochondrial	K.GVYEGWYC*ASDEC*FLPEAK.V	Yes	0	0	11

Q96RQ3	MCCC1 Methylcrotonoyl-CoA carboxylase subunit alpha, mitochondrial	K.HNFC*FMEMNTR.L	Yes	4	5	15
Q96RQ3	MCCC1 Methylcrotonoyl-CoA carboxylase subunit alpha, mitochondrial	K.ESLC*QAALGLILK.E	Yes	4	17	13
Q96RQ3	MCCC1 Methylcrotonoyl-CoA carboxylase subunit alpha, mitochondrial	K.TSAAQAIHPGC*GFLSENMEFAELC*K.Q	Yes	3	1	10
Q96RQ3	MCCC1 Methylcrotonoyl-CoA carboxylase subunit alpha, mitochondrial	K.TFQVLGNLYSEGDC*TYLK.C	Yes	6	142	4
Q96RQ3	MCCC1 Methylcrotonoyl-CoA carboxylase subunit alpha, mitochondrial	K.SIMAAAGVPVVEGYHGEDQSDQC*LK.E	Yes	5	15	3
Q9HCC0	MCCC2 Methylcrotonoyl-CoA carboxylase beta chain, mitochondrial	R.VSGVEC*MIIANDATVK.G	Yes	1	19	22
Q9HCC0	MCCC2 Methylcrotonoyl-CoA carboxylase beta chain, mitochondrial	K.ITLIIGGSYGAGNYGMC*GR.A	Yes	0	0	20
Q9HCC0	MCCC2 Methylcrotonoyl-CoA carboxylase beta chain, mitochondrial	R.LPC*IYLVDSGGAYLPR.Q	Yes	3	24	18
Q9HCC0	MCCC2 Methylcrotonoyl-CoA carboxylase beta chain, mitochondrial	K.AATGEEVSAEDLGGADLHC*R.K	Yes	0	7	12
Q9HCC0	MCCC2 Methylcrotonoyl-CoA carboxylase beta chain, mitochondrial	K.GTHFVQLC*C*QR.N	Yes	0	1	12
P23368	ME2 NAD-dependent malic enzyme, mitochondrial	K.YC*TFNDDIQGTAAVALAGLLAAQK.V	Yes	0	0	41
P23368	ME2 NAD-dependent malic enzyme, mitochondrial	R.AMASINERPVIFALSNPTAQAEC*TAEEAYTLTEGR.C	Yes	1	8	23
P23368	ME2 NAD-dependent malic enzyme, mitochondrial	R.C*LFASGSPFGPVK.L	Yes	1	5	18
P23368	ME2 NAD-dependent malic enzyme, mitochondrial	R.ILQDDIESLMPIVYTPTVGLAC*SQYGHIFR.R	Yes	1	0	13
P14174	MIF Macrophage migration inhibitory factor	K.LLC*GLLAER.L		4	34	2
Q99797	MIPEP Mitochondrial intermediate peptidase	R.AC*STPPGPQTVLIFDELSDSLC*R.V	Yes	0	0	14
Q99797	MIPEP Mitochondrial intermediate peptidase	R.ADKPHQDC*HFTIR.G	Yes	0	0	11
Q99797	MIPEP Mitochondrial intermediate peptidase	R.C*PTDFAEVPSILMEYFANDYR.V	Yes	0	0	10
Q9NYK5	MRPL39 39S ribosomal protein L39, mitochondrial	R.TSIC*FQYEVSAVHNLQPTQPSLIR.R	Yes	0	1	12
Q9NYK5	MRPL39 39S ribosomal protein L39, mitochondrial	R.APEVPVISGAFC*YDVVLDSK.L	Yes	0	12	2
Q9Y676	MRPS18B 28S ribosomal protein S18b, mitochondrial	K.VVGNPC*PIC*R.D	Yes	0	11	4
Q92552	MRPS27 28S ribosomal protein S27, mitochondrial	K.LSTC*EAEDIATYEQNLQQWHLDLVQLIQR.E	Yes	0	0	23
P82933	MRPS9 28S ribosomal protein S9, mitochondrial	K.ALC*SFVTEDEVEWMR.Q	Yes	0	0	10
P13995	MTHFD2 Bifunctional methylenetetrahydrofolate dehydrogenase/cyclohydrolase, mitochondrial	R.IC*NAVSPDKDVDGFHVINVGR.M	Yes	0	2	14
P13995	MTHFD2 Bifunctional methylenetetrahydrofolate dehydrogenase/cyclohydrolase, mitochondrial	R.IC*NAVSPDKDVDGFHVINVGR.M	Yes	1	3	10
P22033	MUT Methylmalonyl-CoA mutase, mitochondrial	K.VADPWGGSYMMEC*LTNDVYDAALK.L	Yes	0	0	12
O14561	NDUFAB1 Acyl carrier protein, mitochondrial	K.LMC*PQEIVDYIADKK.D	Yes	2	8	15
O14561	NDUFAB1 Acyl carrier protein, mitochondrial	K.LMC*PQEIVDYIADK.K	Yes	2	3	10
O14561	NDUFAB1 Acyl carrier protein, mitochondrial	K.LMC*PQEIVDYIADKK.D	Yes	0	0	10
Q9BPW8	NIPSNAP1 Protein NipSnap homolog 1	K.LHLDEDYPC*SLVGNWNTWYGEQDQAVHLWR.F	Yes	0	0	13
Q9H857	NT5DC2 5'-nucleotidase domain-containing protein 2	R.TPLQHEAPLWMDQLC*TGC*MK.T	Yes	0	0	10
P04181	OAT Ornithine aminotransferase, mitochondrial	K.YFDFLSSYSAVNQGHC*HPK.I	Yes	1	3	22
P04181	OAT Ornithine aminotransferase, mitochondrial	K.ALSGGLYPVSAVLC*DDDIMLTIKPGEHGSTYGGNPLGC*R.V	Yes	1	0	11
P04181	OAT Ornithine aminotransferase, mitochondrial	K.YFDFLSSYSAVNQGHC*HPK.I	Yes	2	1	10
Q02218	OGDH 2-oxoglutarate dehydrogenase, mitochondrial	R.FGLEGC*EVLIPALK.T	Yes	0	10	0
P11498	PC Pyruvate carboxylase, mitochondrial	R.FLYEC*PWR.R	Yes	6	67	5
P11498	PC Pyruvate carboxylase, mitochondrial	R.INGC*AIQC*R.V	Yes	6	54	3
P11498	PC Pyruvate carboxylase, mitochondrial	R.GLYAAFDC*TATMK.S	Yes	5	45	0
P11498	PC Pyruvate carboxylase, mitochondrial	R.ADFAQAC*QDAGVR.F	Yes	6	26	5
P11498	PC Pyruvate carboxylase, mitochondrial	K.PTAC*TMLVSSLR.D	Yes	3	13	1
P11498	PC Pyruvate carboxylase, mitochondrial	R.AGTHILC*IK.D	Yes	6	11	9
P05165	PCCA Propionyl-CoA carboxylase alpha chain, mitochondrial	R.LQVEHPVTEC*ITGLDLVQEMIR.V	Yes	5	16	12
P05165	PCCA Propionyl-CoA carboxylase alpha chain, mitochondrial	R.C*LAAEDVVFIGPDTHAIQAMGDK.I	Yes	3	51	0
P05165	PCCA Propionyl-CoA carboxylase alpha chain, mitochondrial	R.C*LAAEDVVFIGPDTHAIQAMGDK.I	Yes	3	34	9
P05165	PCCA Propionyl-CoA carboxylase alpha chain, mitochondrial	R.LQVEHPVTEC*ITGLDLVQEMIR.V	Yes	3	31	1
P05165	PCCA Propionyl-CoA carboxylase alpha chain, mitochondrial	K.SVHC*QAGDTVGEGDLLVELE.-	Yes	4	24	5
P05165	PCCA Propionyl-CoA carboxylase alpha chain, mitochondrial	R.C*LAAEDVVFIGPDTHAIQAMGDKIESK.L	Yes	3	20	5
P05165	PCCA Propionyl-CoA carboxylase alpha chain, mitochondrial	K.MADEAVC*VGPAPTSK.S	Yes	6	19	2
P05165	PCCA Propionyl-CoA carboxylase alpha chain, mitochondrial	R.INGWAVEC*R.V	Yes	5	18	0
P05165	PCCA Propionyl-CoA carboxylase alpha chain, mitochondrial	R.C*LAAEDVVFIGPDTHAIQAMGDKIESK.L	Yes	3	12	0

Q6L8Q7	PDE12 2',5'-phosphodiesterase 12	K.LHC*TPGDGQR.F	Yes	1	1	12
P08559	PDHA1 Pyruvate dehydrogenase E1 component subunit alpha, somatic form, mitochondrial	K.NFYGGNGIVGAQVPLGAGIALAC*K.Y	Yes	2	17	13
P08559	PDHA1 Pyruvate dehydrogenase E1 component subunit alpha, somatic form, mitochondrial	R.GFC*HLC*DGQEAC*C*VGLEAGINPTDHLITAYR.A	Yes	0	0	10
P08559	PDHA1 Pyruvate dehydrogenase E1 component subunit alpha, somatic form, mitochondrial	K.YNGKDEVC*LTLYGDGAANQGQIFEAYNMAALWK.L	Yes	0	0	10
P08559	PDHA1 Pyruvate dehydrogenase E1 component subunit alpha, somatic form, mitochondrial	K.NFYGGNGIVGAQVPLGAGIALAC*K.Y	Yes	1	18	0
P11177	PDHB Pyruvate dehydrogenase E1 component subunit beta, mitochondrial	R.GPNGASAGVAAQHSQC*FAAWYGHC*PGLK.V	Yes	0	0	20
P11177	PDHB Pyruvate dehydrogenase E1 component subunit beta, mitochondrial	K.TNHLVTVEGGWPQFGVGAEIC*AR.I	Yes	0	1	13
Q15118	PDK1	R.LC*DLYYINSPELELEELNAK.S	Yes	33	126	166
Q15118	PDK1	K.HIGSINPNC*NVLEVIK.D	Yes	5	25	70
Q15118	PDK1	K.HYNTNHEADDWC*VPSR.E	Yes	6	60	63
Q15118	PDK1	K.HYNTNHEADDWC*VPSR.E	Yes	3	89	41
Q15118	PDK1	R.KHIGSINPNC*NVLEVIK.D	Yes	2	12	23
Q15118	PDK1	K.HIGSINPNC*NVLEVIK.D	Yes	3	10	18
Q15118	PDK1	K.HYNTNHEADDWC*VPSREPK.D	Yes	2	7	16
Q15118	PDK1	R.RLC*DLYYINSPELELEELNAK.S	Yes	3	10	15
Q15118	PDK1	K.QFLDFGSVNAC*EK.T	Yes	6	17	13
Q15118	PDK1	K.HYNTNHEADDWC*VPSREPK.D	Yes	1	0	10
Q15118	PDK1	R.LC*DLYYINSPELELEELNAK.S	Yes	3	33	6
Q8NCN5	PDPR Pyruvate dehydrogenase phosphatase regulatory subunit, mitochondrial	R.HVC*LGFVHNFSEDTGEEQVVTADFINR.G	Yes	0	0	12
Q8NCN5	PDPR Pyruvate dehydrogenase phosphatase regulatory subunit, mitochondrial	K.FFAFWGQDINNLTTPLEC*GR.E	Yes	0	1	10
Q5JRX3	PITRM1 Presequence protease, mitochondrial	R.SQQSKPQDASC*LPALK.V	Yes	2	14	15
Q5JRX3	PITRM1 Presequence protease, mitochondrial	K.TGGMSASPHVLPDDSHMDTYEQGVLFSSLC*LDR.N	Yes	0	5	14
Q5JRX3	PITRM1 Presequence protease, mitochondrial	K.THFLMPFPVNYVGEC*IR.T	Yes	0	1	13
Q5JRX3	PITRM1 Presequence protease, mitochondrial	R.NLPDMMQLWSEIFNNPC*FEEEEHFK.V	Yes	0	0	13
Q5JRX3	PITRM1 Presequence protease, mitochondrial	R.LLPDHTYSVVSGGDPLC*IPELTWEQLK.Q	Yes	1	20	6
Q5JRX3	PITRM1 Presequence protease, mitochondrial	K.LGC*GLLDYR.E	Yes	1	10	2
P14618	PKM Pyruvate kinase isozymes M1/M2	R.AEGSDVANAVLDGADC*IMLSGETAK.G		3	12	4
P14618	PKM Pyruvate kinase isozymes M1/M2	R.NTGIIC*TIGPASR.S		3	10	2
Q10713	PMPCA Mitochondrial-processing peptidase subunit alpha	K.FGQFC*TVGILINSGSR.Y	Yes	0	0	33
Q10713	PMPCA Mitochondrial-processing peptidase subunit alpha	R.MVLAGVGVEHEHLVDC*AR.K	Yes	0	1	30
O75439	PMPCB Mitochondrial-processing peptidase subunit beta	K.TNMLLQLDGSTPIC*EDIGR.Q	Yes	2	10	12
Q8TCS8	PNPT1 Polyribonucleotide nucleotidyltransferase 1, mitochondrial	R.GQTQVLC*TVTFDSLESGIK.S	Yes	0	4	15
Q9H2U2	PPA2 Inorganic pyrophosphatase 2, mitochondrial	K.ILSC*GEVIHVK.I	Yes	3	18	18
P30405	PPIF Peptidyl-prolyl cis-trans isomerase F, mitochondrial	K.HVGPGVLSMANAGPNTNGSQFFIC*TIK.T	Yes	0	0	10
Q06830	PRDX1 Peroxiredoxin-1	K.HGEVC*PAGWKPGSDTIKPDVQK.S		3	18	10
P30048	PRDX3 Thioredoxin-dependent peroxide reductase, mitochondrial	K.ANEFHDVNC*EVVAVSVDSHFSHLAWINTPR.K	Yes	0	0	122
P30048	PRDX3 Thioredoxin-dependent peroxide reductase, mitochondrial	K.ANEFHDVNC*EVVAVSVDSHFSHLAWINTPR.K	Yes	0	0	74
P30048	PRDX3 Thioredoxin-dependent peroxide reductase, mitochondrial	K.AFQYVETHGEVC*PANWTPDSPTIKPSPAASK.E	Yes	4	55	29
P30048	PRDX3 Thioredoxin-dependent peroxide reductase, mitochondrial	K.AFQYVETHGEVC*PANWTPDSPTIKPSPAASK.E	Yes	0	5	11
P30048	PRDX3 Thioredoxin-dependent peroxide reductase, mitochondrial	K.ANEFHDVNC*EVVAVSVDSHFSHLAWINTPR.K	Yes	0	0	10
P30048	PRDX3 Thioredoxin-dependent peroxide reductase, mitochondrial	K.AFQYVETHGEVC*PANWTPDSPTIKPSPAASK.E	Yes	0	11	9
Q13162	PRDX4 Peroxiredoxin-4	K.HGEVC*PAGWKPGSETIIPDPAGK.L	Yes	3	10	1
Q4J6C6	PREPL Prolyl endopeptidase-like	K.NC*PFQLC*SPIRPPK.Y	Yes	0	0	11
P26599	PTBP1 Polypyrimidine tract-binding protein 1	K.LSLDGQNIYNAC*C*TLR.I		3	12	0
P62826	RAN GTP-binding nuclear protein Ran	R.VC*ENIPIVLC*GNK.V		3	15	0
P49792	RANBP2 E3 SUMO-protein ligase RanBP2	K.EGQWDC*SSC*LVR.N		1	20	0
P49792	RANBP2 E3 SUMO-protein ligase RanBP2	K.EGQWDC*SVC*LVR.N		2	14	0
P49792	RANBP2 E3 SUMO-protein ligase RanBP2	K.EGQWDC*SAC*LVQNEGSSTK.C		0	10	0
P46782	RPS5 40S ribosomal protein S5	K.TIAEC*LADELINAAK.G		3	10	0
P31040	SDHA Succinate dehydrogenase	R.HVNGQDQIVPGLYAC*GEAAC*ASVHGANR.L	Yes	0	0	23
P31040	SDHA Succinate dehydrogenase	R.GVIALC*IEDGSIHR.I	Yes	0	4	19
P31040	SDHA Succinate dehydrogenase	R.AGLPC*QDLEFVQFHPTGIYGAGC*LITEGC*R.G	Yes	0	0	15
P31040	SDHA Succinate dehydrogenase	R.AAFGLSEAGFNTAC*VTK.L	Yes	2	12	2
P34897	SHMT2 Serine hydroxymethyltransferase, mitochondrial	R.GLELIASENFC*SR.A	Yes	1	13	41
P34897	SHMT2 Serine hydroxymethyltransferase, mitochondrial	R.YYGGAEVVDEIELLC*QR.R	Yes	3	12	17
P37802	TAGLN2 Transgelin-2	K.QYDADLEQILIQWITTQC*R.K		0	0	10
Q9BW92	TARS2 Threonine--tRNA ligase, mitochondrial	K.EQELFFFHELSPGSC*FFLPR.G	Yes	0	0	12
O43615	TIMM44 Mitochondrial import inner membrane translocase subunit TIM44	K.DWC*YEATYSQLAHPIQQAK.A	Yes	0	0	11
Q12931	TRAP1 Heat shock protein 75 kDa, mitochondrial	R.NIYYLC*APNR.H	Yes	2	16	10

Q7L0Y3	TRMT10C Mitochondrial ribonuclease P protein 1	R.NVDPFHIYFC*NLK.I	Yes	2	2	15
Q71U36	TUBA1A Tubulin alpha-1A chain	R.AVC*MLSNTTAIAEAWAR.L		3	8	13
Q71U36	TUBA1A Tubulin alpha-1A chain	K.AYHEQLSVAEITNAC*FEPANQMVK.C		3	8	11
P68366	TUBA4A Tubulin alpha-4A chain	R.AVC*MLSNTTAIAEAWAR.L		3	9	13
P68366	TUBA4A Tubulin alpha-4A chain	K.AYHEQLSVAEITNAC*FEPANQMVK.C		3	11	11
P68366	TUBA4A Tubulin alpha-4A chain	R.SIQFVDWC*PTGFK.V		3	19	6
P49411	TUFM Elongation factor Tu, mitochondrial	R.HYAHTDC*PGHADYVK.N	Yes	2	6	22
P49411	TUFM Elongation factor Tu, mitochondrial	K.NMITGTAPLDGC*ILVVAANDGPMPQTR.E	Yes	0	2	13
P49411	TUFM Elongation factor Tu, mitochondrial	K.KGDEC*ELLGHSK.N	Yes	1	7	10
P49411	TUFM Elongation factor Tu, mitochondrial	K.GEETPVIVGSALC*ALEGR.D	Yes	2	17	6
P22314	UBA1 Ubiquitin-like modifier-activating enzyme 1	K.VLGPYTFSIC*DTSNFSDYIR.G	Yes	2	10	0
F5H5P2	Uncharacterized protein	R.DYPLELFMAQC*YGNISDLGK.G	Yes	0	2	13
P31930	UQCRC1 Cytochrome b-c1 complex subunit 1, mitochondrial	K.AVELLGDIVQNC*SLEDSQIEK.E	Yes	0	12	9

Table 4A-4. Average percent oxidation for mitochondria localized cysteines from AMA-treated matrix-APEX analysis. Data was filtered for peptides with ratio values in 2 out of 3 replicates, with a standard deviation <30%.

UniProt ID	Protein Description	Peptide Sequence	Residue	Mito	Average % Oxidation Matrix-APEX AMA	% Standard Deviation
P14854	COX6B1 Cytochrome c oxidase subunit 6B1	R.VYQSLC*PTSWVTDWDEQR.A	65	Yes	95.24%	0.00%
Q14061	COX17 Cytochrome c oxidase copper chaperone	K.GEEHC*GHLIEAHK.E	45	Yes	95.24%	0.00%
Q96BR5	SELRC1 Sel1 repeat-containing protein 1	K.SIAAC*HNVGLLAHDGQVNEDGQPDLGK.A	111	Yes	94.04%	1.12%
P54886	ALDH18A1 Delta-1-pyrroline-5-carboxylate synthase	K.C*EYPAAC*NALETLLIHR.D	606|612	Yes	74.53%	0.14%
Q99798	ACO2 Aconitate hydratase, mitochondrial	R.VGLIGSC*TNSSYEDMGR.S	385	Yes	74.23%	0.22%
Q13162	PRDX4 Peroxiredoxin-4	R.TREEEC*HFYAGGQVYPGEASR.V	51	Yes	69.04%	2.78%
P30041	PRDX6 Peroxiredoxin-6	R.DFTPVC*TTELGR.A	47	Yes	68.37%	5.31%
Q9H857	NT5DC2 5-nucleotidase domain-containing protein 2	R.TPLQHEAPLWMDQLC*TGC*MK.T	504|507	Yes	62.86%	0.05%
Q7Z4W1	DCXR L-xylulose reductase	R.GVPGAIVNVSSQC*SQR.A	138	Yes	59.44%	4.72%
Q7Z4W1	DCXR L-xylulose reductase	R.AVTNHSVYC*STK.G	150	Yes	58.58%	1.14%
Q16822	PCK2 Phosphoenolpyruvate carboxykinase	K.VEC*VGDDIAWMR.F	325	Yes	56.20%	5.98%
Q12888	TP53BP1 Tumor suppressor p53-binding protein 1	K.VADPVDSSNLDTC*GSISQVIEQLPQPNR.T	101	Yes	56.04%	5.78%
P53396	ACLY ATP-citrate synthase	K.FIC*TTSAIQNR.F	20	Yes	54.34%	0.01%
Q16822	PCK2 Phosphoenolpyruvate carboxykinase	R.LC*QPEGIHIC*DGTEAENTATLTLLEQQGLIR.K	55|63	Yes	54.32%	2.06%
Q16822	PCK2 Phosphoenolpyruvate carboxykinase	R.QC*PIMDPAWEAPEGVPIDAIIFGGR.R	431	Yes	52.25%	0.14%
P38646	HSPA9 Stress-70 protein, mitochondrial	K.C*ELSSSVQTDINLPYLTMDSSGPK.H	317	Yes	51.12%	1.72%
Q16822	PCK2 Phosphoenolpyruvate carboxykinase	K.YNNC*WLAR.T	92	Yes	48.34%	0.91%
P30048	PRDX3 Thioredoxin-dependent peroxide reductase, mitochon	K.AFQYVETHGEVC*PANWTPDSPTIK.P	229	Yes	47.92%	1.24%
Q9Y3D2	MSRB2 Methionine-R-sulfoxide reductase B2, mitochondrial	R.FC*INSVALK.F	169	Yes	47.60%	1.68%
Q16822	PCK2 Phosphoenolpyruvate carboxykinase	K.C*LHSVGQPLTGQGEPVSQWPC*NPEK.T	210|230	Yes	47.50%	4.63%
Q16822	PCK2 Phosphoenolpyruvate carboxykinase	R.YVAAAFPSAC*GK.T	306	Yes	47.47%	2.43%
P49821	NDUFV1 NADH dehydrogenase	R.GAGAYIC*GEETALIESIEGK.Q	206	Yes	47.29%	5.16%
Q5JRX3	PITRM1 Presequence protease, mitochondrial	K.PQDASC*LPALK.V	556	Yes	46.06%	2.46%
Q6P087	RPUSD3 RNA pseudouridylate synthase domain-containing pro	R.TLQC*LGLR.L	345	Yes	44.65%	0.39%
Q5JRX3	PITRM1 Presequence protease, mitochondrial	R.LLPDHTYSVVSGGDPLC*IPELTWEQLK.Q	241	Yes	43.67%	0.23%
Q8NFF5	FLAD1 FAD synthase	K.C*LSPGGHPTYRPAYLLENEEEER.N	561	Yes	43.49%	0.70%
Q7Z3D6	C14orf159 UPF0317 protein C14orf159, mitochondrial	K.APPGC*LTPER.I	265	Yes	42.52%	3.33%
O94925	GLS Glutaminase kidney isoform, mitochondrial	K.FSPDLWGVSVC*TVDGQR.H	266	Yes	41.63%	1.85%
P49411	TUFM Elongation factor Tu, mitochondrial	K.GEETPVIVGSALC*ALEGR.D	222	Yes	40.55%	4.39%
Q8N4Q0	ZADH2 Zinc-binding alcohol dehydrogenase domain-containi	K.SLGC*DRPINYK.T	218	Yes	39.16%	0.81%
P42704	LRPPRC Leucine-rich PPR motif-containing protein, mitocho	R.YC*QEPR.G	571	Yes	39.02%	1.22%
Q6PI48	DARS2 Aspartate--tRNA ligase, mitochondrial	R.LIC*LVTGSPSIR.D	590	Yes	38.66%	0.37%
P28331	NDUFS1 NADH-ubiquinone oxidoreductase 75 kDa subunit, mit	K.VLFLLGADGGC*ITR.Q	554	Yes	38.61%	0.46%

P42704	LRPPRC Leucine-rich PPR motif-containing protein, mitocho	R.C*VANNQVETLEK.L	930	Yes	38.38%	1.00%
P42704	LRPPRC Leucine-rich PPR motif-containing protein, mitocho	R.LQWFC*DR.C	927	Yes	38.23%	1.30%
Q8IYQ7	THNSL1 Threonine synthase-like 1	R.C*IHPADIPAAR.L	299	Yes	38.15%	28.92%
Q15118	PDK1	K.QFLDFGSVNAC*EK.T	71	Yes	38.11%	0.83%
Q12888	TP53BP1 Tumor suppressor p53-binding protein 1	R.EEGGC*SLASTPATTLHLLQLSGQR.S	329	Yes	37.88%	0.01%
Q6UB35	MTHFD1L Monofunctional C1-tetrahydrofolate synthase, mitoc	K.VGC*GSPR.I	302	Yes	37.52%	0.28%
P49411	TUFM Elongation factor Tu, mitochondrial	R.HYAHTDC*PGHADYVK.N	127	Yes	37.31%	0.28%
Q99798	ACO2 Aconitate hydratase, mitochondrial	R.DLGGIVLANAC*GPC*IGQWDR.K	448|451	Yes	37.13%	2.01%
Q9NP92	MRPS30 28S ribosomal protein S30, mitochondrial	K.NIC*WGTQSKPLYETIEDNDVK.G	393	Yes	37.08%	28.09%
Q6P1X6	C8orf82 UPF0598 protein C8orf82	R.YEAAFPFLSPC*GR.E	98	Yes	35.94%	3.97%
P49411	TUFM Elongation factor Tu, mitochondrial	K.NMITGTAPLDGC*ILVVAANDGPMPQTR.E	147	Yes	35.83%	5.82%
Q9BQ52	ELAC2 Zinc phosphodiesterase ELAC protein 2	K.EGPTLSVPMVQGEC*LLK.Y	421	Yes	34.97%	1.41%
Q8NFF5	FLAD1 FAD synthase	R.LHYGTDPC*TGQPFR.F	236	Yes	34.82%	0.23%
Q7L2E3	DHX30 Putative ATP-dependent RNA helicase DHX30	R.RPC*TIQVPEPILR.K	346	Yes	34.76%	3.03%
P30837	ALDH1B1 Aldehyde dehydrogenase X, mitochondrial	K.TIPMDGQHFC*FTR.H	169	Yes	34.56%	0.11%
Q9H1K1	ISCU Iron-sulfur cluster assembly enzyme ISCU, mitochon	K.TFGC*GSAIASSSLATEWVK.G	95	Yes	33.93%	0.89%
P08559	PDHA1 Pyruvate dehydrogenase E1 component subunit alpha,	K.NFYGGNGIVGAQVPLGAGIALAC*K.Y	181	Yes	33.79%	1.73%
Q16822	PCK2 Phosphoenolpyruvate carboxykinase	R.VLDWIC*R.R	559	Yes	33.31%	1.45%
Q9BQ52	ELAC2 Zinc phosphodiesterase ELAC protein 2	K.C*LQEGAEISSPAVER.L	609	Yes	32.79%	1.02%
P42704	LRPPRC Leucine-rich PPR motif-containing protein, mitocho	K.VFNDTC*R.S	113	Yes	32.49%	13.80%
Q9UDR5	AASS Alpha-aminoadipic semialdehyde synthase, mitochond	K.AGGILQEDISEAC*LILGVK.R	87	Yes	32.04%	2.77%
O75380	NDUFS6 NADH dehydrogenase	R.VIAC*DGGGGALGHPK.V	87	Yes	31.58%	0.10%
P41250	GARS Glycine--tRNA ligase	R.SC*YDLSC*HAR.A	466|471	Yes	31.53%	1.36%
P28331	NDUFS1 NADH-ubiquinone oxidoreductase 75 kDa subunit, mit	K.VVAAC*AMPVMK.G	92	Yes	31.36%	2.16%
P42704	LRPPRC Leucine-rich PPR motif-containing protein, mitocho	R.SC*GSLLPELK.L	130	Yes	31.01%	0.35%
Q4J6C6	PREPL Prolyl endopeptidase-like	R.C*HDVYR.A	227	Yes	30.96%	1.60%
Q9BQ69	MACROD1 O-acetyl-ADP-ribose deacetylase MACROD1	R.SC*YLSSLDLLLEHR.L	246	Yes	30.90%	0.19%
P41250	GARS Glycine--tRNA ligase	K.TSYGWIEIVGC*ADR.S	461	Yes	30.87%	3.23%
Q15118	PDK1	R.LC*DLYYINSPELELEELNAK.S	240	Yes	30.84%	0.47%
Q32MZ4	LRRFIP1 Leucine-rich repeat flightless-interacting protein	R.C*EMSEHPSQTVR.K	750	Yes	30.78%	1.49%
Q4J6C6	PREPL Prolyl endopeptidase-like	K.LDQPFIDC*IR.V	160	Yes	30.67%	0.99%
P30044	PRDX5 Peroxiredoxin-5, mitochondrial	K.GVLFGVPGAFTPGC*SK.T	100	Yes	30.59%	0.89%
P49327	FASN Fatty acid synthase	R.LSIPTYGLQC*TR.A	2273	Yes	30.43%	21.95%
P54886	ALDH18A1 Delta-1-pyrroline-5-carboxylate synthase	R.TEYGDLELC*IEVVDNVQDAIDHIHK.Y	674	Yes	30.38%	13.35%
Q96CM8	ACSF2 Acyl-CoA synthetase family member 2, mitochondrial	K.LNTPGELC*IR.G	462	Yes	30.19%	0.16%
P28331	NDUFS1 NADH-ubiquinone oxidoreductase 75 kDa subunit, mit	R.C*IQC*TR.C	176|179	Yes	30.00%	3.64%
P22314	UBA1 Ubiquitin-like modifier-activating enzyme 1	K.YFLVGAGAIGC*ELLK.N	481	Yes	29.94%	29.22%
Q9NP81	SARS2 Serine--tRNA ligase, mitochondrial	R.FC*AC*PEEAAHALELR.K	64|66	Yes	29.85%	1.38%
P21953	BCKDHB 2-oxoisovalerate dehydrogenase subunit beta, mitoc	R.SGDLFNC*GSLTIR.S	177	Yes	29.35%	0.76%
Q15118	PDK1	K.HIGSINPNC*NVLEVIK.D	223	Yes	28.93%	0.40%
P07203	GPX1 Glutathione peroxidase 1	K.LITWSPVC*R.N	156	Yes	28.43%	8.44%
P30084	ECHS1 Enoyl-CoA hydratase, mitochondrial	K.ALNALC*DGLIDELNQALK.T	62	Yes	28.13%	0.33%
Q9UK39	CCRN4L Nocturnin	R.SAQGC*DLLQNLQNITQGAK.I	302	Yes	28.07%	0.02%
Q9BVS5	TRMT61B Potential tRNA (adenine(58)-N(1))-methyltransferas	R.C*GPTHQGSEDPSMLSQAQSATEVEER.H	112	Yes	28.05%	1.92%
Q5UIP0	RIF1 Telomere-associated protein RIF1	K.TFQTLEC*QHK.R	1718	Yes	27.56%	0.87%
Q9Y3D5	MRPS18C 28S ribosomal protein S18c, mitochondrial	K.NVQLLSQFVSPFTGC*IYGR.H	90	Yes	27.39%	0.58%
P48735	IDH2 Isocitrate dehydrogenase	K.DLAGC*IHGLSNVK.L	418	Yes	26.42%	2.63%
O94925	GLS Glutaminase kidney isoform, mitochondrial	K.C*VQSNIVLLTQAFR.R	203	Yes	25.81%	1.73%
Q96CM8	ACSF2 Acyl-CoA synthetase family member 2, mitochondrial	R.QHLDQLQYNQQFLSC*HDPINIQFTSGTTGSPK.G	254	Yes	25.79%	3.12%
P49411	TUFM Elongation factor Tu, mitochondrial	K.KGDEC*ELLGHSK.N	290	Yes	25.77%	2.52%
P45954	ACADSB Short/branched chain specific acyl-CoA dehydrogena	R.ASSTC*PLTFENVK.V	261	Yes	25.63%	8.36%
O14561	NDUFAB1 Acyl carrier protein, mitochondrial	K.LMC*PQEIVDYIADK.K	140	Yes	25.60%	0.54%
Q5T440	IBA57 Putative transferase CAF17, mitochondrial	R.VWAVLPSSPEAC*GAASLQER.A	170	Yes	25.22%	3.56%
Q9H1K1	ISCU Iron-sulfur cluster assembly enzyme ISCU, mitochon	K.LHC*SMLAEDAIK.A	138	Yes	25.07%	1.21%
Q9Y3D2	MSRB2 Methionine-R-sulfoxide reductase B2, mitochondrial	R.GQAGGGGPGTGPGLGEAGSLATC*ELPLAK.S	45	Yes	24.83%	0.67%

P42126	ECI1 Enoyl-CoA delta isomerase 1, mitochondrial	R.YC*IGLNETQLGIIAPFWLK.D	173	Yes	24.44%	1.63%
P28331	NDUFS1 NADH-ubiquinone oxidoreductase 75 kDa subunit, mit	R.LSVAGNC*R.M	75	Yes	24.30%	2.21%
Q9H1K1	ISCU Iron-sulfur cluster assembly enzyme ISCU, mitochon	K.NVGTGLVGAPAC*GDVMK.L	69	Yes	24.29%	11.72%
Q5UIP0	RIF1 Telomere-associated protein RIF1	R.C*VWSPLASPSTSILK.R	2169	Yes	24.18%	2.05%
P05166	PCCB Propionyl-CoA carboxylase beta chain, mitochondria	R.IC*C*DLDVLASK.K	516|517	Yes	23.68%	1.82%
P38646	HSPA9 Stress-70 protein, mitochondrial	K.DQLPADEC*NK.L	608	Yes	23.45%	0.77%
Q9NP81	SARS2 Serine--tRNA ligase, mitochondrial	R.FGEVTSASNC*TDFQSR.R	425	Yes	23.12%	0.96%
Q9HCC0	MCCC2 Methylcrotonoyl-CoA carboxylase beta chain, mitoch	K.AATGEEVSAEDLGGADLHC*R.K	267	Yes	23.11%	1.68%
Q8N4Q0	ZADH2 Zinc-binding alcohol dehydrogenase domain-containi	R.DC*PVPLPGDGDLLVR.N	55	Yes	22.68%	0.94%
P13804	ETFA Electron transfer flavoprotein subunit alpha, mito	R.TIYAGNALC*TVK.C	155	Yes	22.63%	0.21%
Q96CM8	ACSF2 Acyl-CoA synthetase family member 2, mitochondrial	K.AASGLLSIGLC*K.G	122	Yes	22.43%	0.08%
P09622	DLD Dihydrolipoyl dehydrogenase, mitochondrial	K.NETLGGTC*LNVGC*IPSK.A	80|85	Yes	21.87%	1.03%
P13995	MTHFD2 Bifunctional methylenetetrahydrofolate dehydrogena	R.IC*NAVSPDKDVDGFHVINVGR.M	145	Yes	21.58%	5.01%
Q9H2U2	PPA2 Inorganic pyrophosphatase 2, mitochondrial	K.STHQC*WK.A	274	Yes	21.26%	0.51%
Q8IYQ7	THNSL1 Threonine synthase-like 1	K.LGC*C*VIDVDDDILEK.T	81|82	Yes	21.25%	1.04%
O95571	ETHE1 Protein ETHE1, mitochondrial	R.LTLSC*EEFVK.I	219	Yes	21.08%	1.13%
P45880	VDAC2 Voltage-dependent anion-selective channel protein	K.WNTDNTLGTEIAIEDQIC*QGLK.L	103	Yes	20.33%	3.03%
P53597	SUCLG1 Succinyl-CoA ligase	R.LIGPNC*PGVINPGEC*K.I	172|181	Yes	20.11%	21.54%
Q9UDR5	AASS Alpha-aminoadipic semialdehyde synthase, mitochond	K.EVGATIESYISYC*GGLPAPEHSNNPLR.Y	633	Yes	20.09%	4.01%
Q9Y2S7	POLDIP2 Polymerase delta-interacting protein 2	R.DC*PHISQR.S	143	Yes	20.06%	0.09%
P05091	ALDH2 Aldehyde dehydrogenase, mitochondrial	K.LLC*GGGIAADR.G	386	Yes	19.83%	0.98%
Q5JRX3	PITRM1 Presequence protease, mitochondrial	R.TTPMDSTGVPHILEHTVLC*GSQK.Y	112	Yes	19.13%	1.26%
Q96CM8	ACSF2 Acyl-CoA synthetase family member 2, mitochondrial	K.QIC*PEVENAQPGALK.S	194	Yes	18.89%	1.46%
P23378	GLDC Glycine dehydrogenase	K.TFC*IPHGGGGPGMGPIGVK.K	757	Yes	18.50%	0.97%
P23378	GLDC Glycine dehydrogenase	K.DISLVHSMIPLGSC*TMK.L	558	Yes	18.31%	0.30%
Q15118	PDK1	K.HYNTNHEADDWC*VPSR.E	421	Yes	18.28%	0.97%
Q9H2U2	PPA2 Inorganic pyrophosphatase 2, mitochondrial	R.GQPC*SQNYR.L	44	Yes	17.54%	0.32%
Q92667	AKAP1 A-kinase anchor protein 1, mitochondrial	K.LPAEPPALLQTHPPC*R.R	102	Yes	17.33%	3.05%
Q9NSE4	IARS2 Isoleucine--tRNA ligase, mitochondrial	K.GTGLVHTAPAHGMEDYGVASQHNLPMDC*LVDEDGVFTDVAGPELQNK.A	414	Yes	16.95%	0.32%
O15294	OGT UDP-N-acetylglucosamine--peptide N-acetylglucosami	R.LC*PTHADSLNNLANIK.R	323	Yes	16.18%	1.22%
Q9NP81	SARS2 Serine--tRNA ligase, mitochondrial	R.MVC*SSTC*YR.A	324|328	Yes	15.93%	1.61%
Q6PI48	DARS2 Aspartate--tRNA ligase, mitochondrial	K.ILC*EAPVESVVQVSGTVISR.P	108	Yes	15.93%	5.11%
P42704	LRPPRC Leucine-rich PPR motif-containing protein, mitocho	R.IHDVLC*K.L	863	Yes	15.88%	1.24%
Q16881	TXNRD1 Thioredoxin reductase 1, cytoplasmic	R.WGLGGTC*VNVGC*IPK.K	209|214	Yes	15.51%	0.30%
Q53H82	LACTB2 Beta-lactamase-like protein 2	R.ILIDTGEPAIPEYISC*LK.Q	58	Yes	15.42%	4.45%
Q9NNW7	TXNRD2 Thioredoxin reductase 2, mitochondrial	K.ASFVDEHTVC*GVAK.G	168	Yes	14.92%	0.53%
P05141	SLC25A5 ADP/ATP translocase 2	K.GTDIMYTGTLDC*WR.K	257	Yes	14.67%	10.18%
P23378	GLDC Glycine dehydrogenase	R.IDDIYGDQHLVC*TC*PPMEVYESPFSEQK.R	1000|1002	Yes	14.47%	1.39%
P12532	CKMT1B Creatine kinase U-type, mitochondrial	K.TTPTGWTLDQC*IQTGVDNPGHPFIK.T	89	Yes	14.08%	1.84%
P54886	ALDH18A1 Delta-1-pyrroline-5-carboxylate synthase	R.GDEC*GLALGR.L	88	Yes	13.96%	1.31%
P52789	HK2 Hexokinase-2	K.GAALITAVAC*R.I	909	Yes	13.74%	1.80%
P32322	PYCR1 Pyrroline-5-carboxylate reductase 1, mitochondrial	R.C*MTNTPVVVR.E	120	Yes	13.62%	0.25%
Q6PI48	DARS2 Aspartate--tRNA ligase, mitochondrial	K.TAELLNAC*K.K	152	Yes	13.58%	2.28%
O00763	ACACB Acetyl-CoA carboxylase 2	R.NFDLTAVPC*ANHK.M	1515	Yes	13.18%	2.88%
P04181	OAT Ornithine aminotransferase, mitochondrial	K.YFDFLSSYSAVNQGHC*HPK.I	93	Yes	12.53%	0.56%
Q9H0R6	QRSL1 Glutamyl-tRNA(Gln) amidotransferase subunit A, mit	R.AFC*DQQLLTVAK.W	483	Yes	12.17%	1.76%
Q6P087	RPUSD3 RNA pseudouridylate synthase domain-containing pro	R.AQRPTATYC*AVTDGIPAASEGK.I	172	Yes	11.94%	0.72%
Q12849	GRSF1 G-rich sequence factor 1	R.YIELFLNSC*PK.G	476	Yes	11.74%	4.52%
Q969S9	GFM2 Ribosome-releasing factor 2, mitochondrial	R.IYSGTIKPQLAIHNINGNC*TER.I	406	Yes	11.50%	0.01%
P24752	ACAT1 Acetyl-CoA acetyltransferase, mitochondrial	K.IHMGSC*AENTAK.K	196	Yes	11.47%	0.74%
P10809	HSPD1 60 kDa heat shock protein, mitochondrial	R.AAVEEGIVLGGGC*ALLR.C	442	Yes	11.26%	0.37%
P30084	ECHS1 Enoyl-CoA hydratase, mitochondrial	K.EMQNLSFQDC*YSSK.F	111	Yes	11.19%	0.93%
P42704	LRPPRC Leucine-rich PPR motif-containing protein, mitocho	K.QLILVLC*SEENMQK.A	690	Yes	10.99%	8.80%

Q96I51	WBSCR16 Williams-Beuren syndrome chromosomal region 16 pro	R.VLQVSC*GR.A	181	Yes	10.89%	0.25%
P49207	RPL34 60S ribosomal protein L34	K.SAC*GVC*PGR.L	46|49	Yes	10.78%	1.00%
Q9BQ52	ELAC2 Zinc phosphodiesterase ELAC protein 2	R.FGPDTQHLVLNENC*ASVHNLR.S	374	Yes	10.67%	0.87%
Q96CM8	ACSF2 Acyl-CoA synthetase family member 2, mitochondrial	R.MGEEIC*AC*IR.L	553|555	Yes	10.65%	0.80%
P11177	PDHB Pyruvate dehydrogenase E1 component subunit beta,	K.TNHLVTVEGGWPQFGVGAEIC*AR.I	306	Yes	10.31%	2.93%
P24752	ACAT1 Acetyl-CoA acetyltransferase, mitochondrial	K.QGEYGLASIC*NGGGGASAMLIQK.L	413	Yes	10.30%	3.35%
P00367	GLUD1 Glutamate dehydrogenase 1, mitochondrial	K.C*AVVDVPFGGAK.A	172	Yes	10.15%	1.43%
P51649	ALDH5A1 Succinate-semialdehyde dehydrogenase, mitochondria	R.NTGQTC*VC*SNQFLVQR.G	340|342	Yes	10.07%	1.61%
Q9Y676	MRPS18B 28S ribosomal protein S18b, mitochondrial	K.VVGNPC*PIC*R.D	105|108	Yes	9.88%	0.81%
P09622	DLD Dihydrolipoyl dehydrogenase, mitochondrial	R.VC*HAHPTLSEAFR.E	484	Yes	9.74%	0.84%
O95571	ETHE1 Protein ETHE1, mitochondrial	R.QMFEPVSC*TFTYLLGDR.E	34	Yes	9.65%	0.66%
O75439	PMPCB Mitochondrial-processing peptidase subunit beta	R.SNMC*WLR.D	485	Yes	9.65%	0.85%
Q02218	OGDH 2-oxoglutarate dehydrogenase, mitochondrial	R.FGLEGC*EVLIPALK.T	283	Yes	9.63%	10.57%
P31930	UQCRC1 Cytochrome b-c1 complex subunit 1, mitochondrial	K.YIYDQC*PAVAGYGPIEQLPDYNR.I	453	Yes	9.50%	0.35%
Q8TAA5	GRPEL2 GrpE protein homolog 2, mitochondrial	K.IFGIQSFC*K.D	110	Yes	9.43%	2.11%
Q4G0N4	NADKD1 NAD kinase domain-containing protein 1	K.SSGLNLC*TGTGSK.A	311	Yes	9.33%	5.27%
Q15120	PDK3	K.HIGSIDPTC*NVADVVK.D	191	Yes	9.30%	3.93%
O75521	ECI2 Enoyl-CoA delta isomerase 2, mitochondrial	K.LTAGEAC*AQGLVTEVFPDSTFQK.E	312	Yes	9.17%	3.18%
Q9BSH4	TACO1 Translational activator of cytochrome c oxidase 1	K.FIC*DASSLHQVR.K	234	Yes	9.16%	1.02%
Q7Z7H8	MRPL10 39S ribosomal protein L10, mitochondrial	R.TVPFLPLLGGC*IDDTILSR.Q	180	Yes	9.13%	1.11%
Q07021	C1QBP Complement component 1 Q subcomponent-binding prot	K.ALVLDC*HYPEDEVGQEDEAESDIFSIR.E	186	Yes	9.00%	0.59%
Q96CM8	ACSF2 Acyl-CoA synthetase family member 2, mitochondrial	K.TVGQC*LETTAQR.V	77	Yes	8.98%	2.99%
P35914	HMGCL Hydroxymethylglutaryl-CoA lyase, mitochondrial	K.VAQATC*K.L	323	Yes	8.94%	0.21%
Q96GW9	MARS2 Methionine--tRNA ligase, mitochondrial	R.VSEQFQQLFQEAGISC*TDFIR.T	132	Yes	8.90%	1.40%
P53396	ACLY ATP-citrate synthase	R.KPASFMTSIC*DER.G	845	Yes	8.86%	4.73%
Q6PI48	DARS2 Aspartate--tRNA ligase, mitochondrial	R.TNTC*GELR.S	54	Yes	8.82%	1.75%
P00441	SOD1 Superoxide dismutase	K.DGVADVSIEDSVISLSGDHC*IIGR.T	112	Yes	8.76%	3.17%
Q5JTZ9	AARS2 Alanine--tRNA ligase, mitochondrial	R.C*GLLLDR.T	555	Yes	8.74%	0.55%
Q8NFF5	FLAD1 FAD synthase	R.SLGVQVC*R.V	147	Yes	8.39%	2.90%
O75600	GCAT 2-amino-3-ketobutyrate coenzyme A ligase, mitochon	R.FIC*GTQSIHK.N	106	Yes	8.32%	2.08%
P05165	PCCA Propionyl-CoA carboxylase alpha chain, mitochondri	K.MADEAVC*VGPAPTSK.S	111	Yes	8.31%	0.17%
O75390	CS Citrate synthase, mitochondrial	K.LPC*VAAK.I	211	Yes	8.27%	0.21%
Q9UDR5	AASS Alpha-aminoadipic semialdehyde synthase, mitochond	K.FSPAGVEGC*PALPHK.L	342	Yes	7.98%	1.71%
Q9NNW7	TXNRD2 Thioredoxin reductase 2, mitochondrial	R.TVGIHPTC*SEEVVK.L	500	Yes	7.92%	1.90%
P82933	MRPS9 28S ribosomal protein S9, mitochondrial	K.HDVTC*TVSGGGR.S	330	Yes	7.79%	5.24%
Q7L0Y3	TRMT10C Mitochondrial ribonuclease P protein 1	K.TLMEC*VSNTAK.K	123	Yes	7.76%	0.93%
P31040	SDHA Succinate dehydrogenase	R.C*C*C*VADR.T	189|190|191	Yes	7.74%	1.36%
P31930	UQCRC1 Cytochrome b-c1 complex subunit 1, mitochondrial	K.AVELLGDIVQNC*SLEDSQIEK.E	154	Yes	7.61%	4.27%
Q6UB35	MTHFD1L Monofunctional C1-tetrahydrofolate synthase, mitoc	R.AGAFDAVPC*YHWSVGGK.G	828	Yes	7.47%	0.08%
P63167	DYNLL1 Dynein light chain 1, cytoplasmic	K.NADMSEEMQQDSVEC*ATQALEK.Y	24	Yes	7.46%	1.26%
Q12931	TRAP1 Heat shock protein 75 kDa, mitochondrial	R.SPAAEC*LSEK.E	573	Yes	7.45%	2.78%
P08559	PDHA1 Pyruvate dehydrogenase E1 component subunit alpha,	R.VDGMDILC*VR.E	261	Yes	7.43%	0.64%
P08559	PDHA1 Pyruvate dehydrogenase E1 component subunit alpha,	R.FAAAYC*R.S	273	Yes	7.34%	0.70%
Q9UDR5	AASS Alpha-aminoadipic semialdehyde synthase, mitochond	K.YNINPVSMDIC*K.Q	534	Yes	7.26%	0.95%
Q8NC60	NOA1 Nitric oxide-associated protein 1	K.ENC*ILNLLTEK.E	505	Yes	7.25%	3.52%
P54136	RARS Arginine--tRNA ligase, cytoplasmic	K.VLTAEELNAAQTSVAYGC*IK.Y	502	Yes	7.15%	3.38%
P38117	ETFB Electron transfer flavoprotein subunit beta	K.EVIAVSC*GPAQC*QETIR.T	66|71	Yes	7.07%	0.81%
P22234	PAICS Multifunctional protein ADE2	K.ITSC*IFQLLQEAGIK.T	63	Yes	6.88%	1.47%
P08559	PDHA1 Pyruvate dehydrogenase E1 component subunit alpha,	K.LPC*IFIC*ENNR.Y	218|222	Yes	6.87%	0.81%
P49821	NDUFV1 NADH dehydrogenase	K.YLVVNADEGEPGTC*K.D	125	Yes	6.85%	2.95%
P04181	OAT Ornithine aminotransferase, mitochondrial	K.VLPMNTGVEAGETAC*K.L	150	Yes	6.76%	0.84%
Q6L8Q7	PDE12 2,5-phosphodiesterase 12	K.LHC*TPGDGQR.F	250	Yes	6.75%	0.30%

O75600	GCAT 2-amino-3-ketobutyrate coenzyme A ligase, mitochon	K.MEAAGFTISGASHPIC*PVMLGDAR.L	349	Yes	6.75%	3.44%
Q6UB35	MTHFD1L Monofunctional C1-tetrahydrofolate synthase, mitoc	R.AEIDLVC*ELAK.R	814	Yes	6.71%	1.04%
O75439	PMPCB Mitochondrial-processing peptidase subunit beta	K.FHFGDSLC*THK.G	265	Yes	6.50%	1.07%
Q5UIP0	RIF1 Telomere-associated protein RIF1	K.MELSLENVTVEGNAC*K.V	1904	Yes	6.46%	1.48%
Q15031	LARS2 Probable leucine--tRNA ligase, mitochondrial	R.FFSHFC*HDQK.M	578	Yes	6.46%	2.40%
P50213	IDH3A Isocitrate dehydrogenase	K.C*SDFTEEIC*R.R	351|359	Yes	6.24%	1.20%
P00505	GOT2 Aspartate aminotransferase, mitochondrial	K.TC*GFDFTGAVEDISK.I	187	Yes	6.23%	0.60%
P23378	GLDC Glycine dehydrogenase	R.NEDAC*PVGTVSAAPWGSSSILPISWAYIK.M	795	Yes	6.23%	2.04%
P36551	CPOX Coproporphyrinogen-III oxidase, mitochondrial	K.WC*DDYFFIAHR.G	319	Yes	6.19%	2.01%
P00367	GLUD1 Glutamate dehydrogenase 1, mitochondrial	K.AKPYEGSILEADC*DILIPAASEK.Q	376	Yes	6.11%	0.03%
P23378	GLDC Glycine dehydrogenase	K.MEDPVC*ENEILATLHAISSK.N	112	Yes	6.07%	0.67%
Q15031	LARS2 Probable leucine--tRNA ligase, mitochondrial	R.EITTC*LPDYYK.W	177	Yes	5.97%	1.05%
Q9NSE4	IARS2 Isoleucine--tRNA ligase, mitochondrial	K.KPGLEEAVESAC*AMR.D	883	Yes	5.85%	1.88%
Q4G0N4	NADKD1 NAD kinase domain-containing protein 1	R.SEGHLC*LPVR.Y	193	Yes	5.81%	2.40%
P31040	SDHA Succinate dehydrogenase	R.AAFGLSEAGFNTAC*VTK.L	89	Yes	5.78%	1.41%
P36551	CPOX Coproporphyrinogen-III oxidase, mitochondrial	K.EGGGGISC*VLQDGC*VFEK.A	192|198	Yes	5.76%	4.08%
P54886	ALDH18A1 Delta-1-pyrroline-5-carboxylate synthase	R.EEVEDLC*R.L	546	Yes	5.75%	0.11%
Q96RP9	GFM1 Elongation factor G, mitochondrial	R.QELIEC*VANSDEQLGEMFLEEK.I	256	Yes	5.75%	1.52%
Q99497	PARK7 Protein DJ-1	R.DVVIC*PDASLEDAKK.E	53	Yes	5.75%	1.40%
Q15031	LARS2 Probable leucine--tRNA ligase, mitochondrial	K.GGPPLAMASEWVNC*SC*PR.C	504|506	Yes	5.71%	1.64%
O75390	CS Citrate synthase, mitochondrial	R.FRGFSIPEC*QKLLPK.A	101	Yes	5.66%	0.85%
P31930	UQCRC1 Cytochrome b-c1 complex subunit 1, mitochondrial	R.NALVSHLDGTTPVC*EDIGR.S	410	Yes	5.62%	1.22%
Q5JRX3	PITRM1 Presequence protease, mitochondrial	K.TGGMSASPHVLPDDSHMDTYEQGVLFSSLC*LDR.N	672	Yes	5.59%	0.90%
Q15031	LARS2 Probable leucine--tRNA ligase, mitochondrial	R.LGLC*FSWDR.E	167	Yes	5.58%	0.96%
Q8TCS8	PNPT1 Polyribonucleotide nucleotidyltransferase 1, mitoc	R.GQTQVLC*TVTFDSLESGIK.S	395	Yes	5.58%	1.15%
P42704	LRPPRC Leucine-rich PPR motif-containing protein, mitocho	R.AILQENGC*LSDSDMFSQAGLR.S	500	Yes	5.58%	0.66%
P10809	HSPD1 60 kDa heat shock protein, mitochondrial	R.C*IPALDSLTPANEDQK.I	447	Yes	5.53%	0.90%
Q7L0Y3	TRMT10C Mitochondrial ribonuclease P protein 1	K.RLNLATEC*LPLDK.Y	335	Yes	5.46%	0.82%
P49327	FASN Fatty acid synthase	R.AALQEELQLC*K.G	1141	Yes	5.45%	0.98%
Q96RQ3	MCCC1 Methylcrotonoyl-CoA carboxylase subunit alpha, mit	K.SIMAAAGVPVVEGYHGEDQSDQC*LK.E	190	Yes	5.39%	0.42%
P42704	LRPPRC Leucine-rich PPR motif-containing protein, mitocho	K.GMQELGVHPDQETYTDYVIPC*FDSVNSAR.A	484	Yes	5.37%	0.39%
P24752	ACAT1 Acetyl-CoA acetyltransferase, mitochondrial	R.QAVLGAGLPISTPC*TTINK.V	119	Yes	5.34%	0.37%
Q9NSE4	IARS2 Isoleucine--tRNA ligase, mitochondrial	R.C*AEVVSGK.-	1005	Yes	5.32%	0.86%
P11177	PDHB Pyruvate dehydrogenase E1 component subunit beta,	R.PVGHC*LEAAAVLSK.E	249	Yes	5.24%	0.45%
Q9Y6C9	MTCH2 Mitochondrial carrier homolog 2	R.LC*SGVLGTVVHGK.V	79	Yes	5.23%	0.67%
Q16698	DECR1 2,4-dienoyl-CoA reductase, mitochondrial	K.VHAIQC*DVR.D	116	Yes	5.23%	0.45%
O15294	OGT UDP-N-acetylglucosamine--peptide N-acetylglucosami	R.HGNLC*LDK.I	531	Yes	5.22%	0.37%
Q12849	GRSF1 G-rich sequence factor 1	R.GLPYSC*NEK.D	261	Yes	5.21%	0.37%
P31040	SDHA Succinate dehydrogenase	R.TYFSC*TSAHTSTGDGTAMITR.A	266	Yes	5.19%	0.77%
Q99497	PARK7 Protein DJ-1	K.VTVAGLAGKDPVQC*SR.D	46	Yes	4.99%	0.40%
Q96HY7	DHTKD1 Probable 2-oxoglutarate dehydrogenase E1 component	R.VEELC*PFPLDSLQQEMSK.Y	839	Yes	4.99%	0.45%
Q13085	ACACA Acetyl-CoA carboxylase 1	R.MMYGVSPWGDSPIDFEDSAHVPC*PR.G	500	Yes	4.95%	0.23%
Q13011	ECH1 Delta(3,5)-Delta(2,4)-dienoyl-CoA isomerase, mitoc	R.YC*AQDAFFQVK.E	187	Yes	4.92%	0.22%
P36969	GPX4 Phospholipid hydroperoxide glutathione peroxidase,	R.ILAFPC*NQFGK.Q	102	Yes	4.89%	0.21%
O75521	ECI2 Enoyl-CoA delta isomerase 2, mitochondrial	K.LHAVNAEEC*NVLQGR.W	368	Yes	4.88%	0.19%
Q96RP9	GFM1 Elongation factor G, mitochondrial	R.YQPC*LPSTQEDVINK.Y	723	Yes	4.84%	0.17%
P51649	ALDH5A1 Succinate-semialdehyde dehydrogenase, mitochondria	K.EVGEAIC*TDPLVSK.I	272	Yes	4.84%	0.13%
Q15031	LARS2 Probable leucine--tRNA ligase, mitochondrial	K.EALVNWDPVDQTVLANEQVDEHGC*SWR.S	225	Yes	4.80%	0.06%
P11498	PC Pyruvate carboxylase, mitochondrial	R.GLYAAFDC*TATMK.S	850	Yes	4.78%	3.45%
E7ERL9	VARS2 Valine--tRNA ligase, mitochondrial	R.LALAAQEC*ER.G	BAD_ID	Yes	4.76%	0.00%
E7ERL9	VARS2 Valine--tRNA ligase, mitochondrial	R.PLGPPQVLFSC*ADLGLR.L	BAD_ID	Yes	4.76%	0.00%
O43488	AKR7A2 Aflatoxin B1 aldehyde reductase member 2	R.QVETELFPC*LR.H	214	Yes	4.76%	0.00%
P51649	ALDH5A1 Succinate-semialdehyde dehydrogenase, mitochondria	R.WLPAAATFPVQDPASGAALGMVADC*GVR.E	93	Yes	4.76%	0.00%

Q9HCC0	MCCC2 Methylcrotonoyl-CoA carboxylase beta chain, mitoch	R.VSGVEC*MIIANDATVK.G	131	Yes	4.76%	0.00%
Q13686	ALKBH1 Alkylated DNA repair protein alkB homolog 1	K.LYSQKPNVC*NLDK.H	129	Yes	4.76%	0.00%
Q86SX6	GLRX5 Glutaredoxin-related protein 5, mitochondrial	K.GTPEQPQC*GFSNAVVQILR.L	67	Yes	4.76%	0.00%
P30405	PPIF Peptidyl-prolyl cis-trans isomerase F, mitochondri	R.VIPSFMC*QAGDFTNHNGTGGK.S	104	Yes	4.76%	0.00%
P34897	SHMT2 Serine hydroxymethyltransferase, mitochondrial	R.MREVC*DEVK.A	241	Yes	4.76%	0.00%
Q15119	PDK2	K.HIGSIDPNC*NVSEVVK.D	195	Yes	4.76%	0.00%
Q96I51	WBSCR16 Williams-Beuren syndrome chromosomal region 16 pro	R.C*GLSHFAALTNK.G	401	Yes	4.76%	0.00%
Q92506	HSD17B8 Estradiol 17-beta-dehydrogenase 8	R.C*NSVLPGFIATPMTQK.V	194	Yes	4.76%	0.00%
P42704	LRPPRC Leucine-rich PPR motif-containing protein, mitocho	K.EDGPSVFGSFFLQHC*VTMNTPVEK.L	380	Yes	4.76%	0.00%
Q96GW9	MARS2 Methionine--tRNA ligase, mitochondrial	R.FYGHPC*PFEGR.R	562	Yes	4.76%	0.00%
P09001	MRPL3 39S ribosomal protein L3, mitochondrial	K.HVVTLLQVQDC*HVLK.Y	127	Yes	4.76%	0.00%
Q15119	PDK2	R.HYQTIQEAGDWC*VPSTEPK.N	392	Yes	4.76%	0.00%
O75439	PMPCB Mitochondrial-processing peptidase subunit beta	R.LC*TSVTESEVAR.A	389	Yes	4.76%	0.00%
Q96HY7	DHTKD1 Probable 2-oxoglutarate dehydrogenase E1 component	R.LVTVYC*EHGHK.A	64	Yes	4.76%	0.00%
Q3SY69	ALDH1L2 Mitochondrial 10-formyltetrahydrofolate dehydrogen	R.SC*DVEPNDTVDALYNR.F	174	Yes	4.76%	0.00%
Q9UHN1	POLG2 DNA polymerase subunit gamma-2, mitochondrial	K.SHAELEGNGEHPEAPGSGEGSEALLEIC*QR.R	73	Yes	4.76%	0.00%
P28331	NDUFS1 NADH-ubiquinone oxidoreductase 75 kDa subunit, mit	R.VDSDTLC*TEEVFPTAGAGTDLR.S	367	Yes	4.76%	0.00%
P31040	SDHA Succinate dehydrogenase	R.VGSVLQEGC*GK.I	536	Yes	4.76%	0.00%
Q969S9	GFM2 Ribosome-releasing factor 2, mitochondrial	R.VTLAQTAVPVLC*GSALK.N	329	Yes	4.76%	0.00%
Q02218	OGDH 2-oxoglutarate dehydrogenase, mitochondrial	K.YPNAELAWC*QEEHK.N	956	Yes	4.76%	0.00%
P40926	MDH2 Malate dehydrogenase, mitochondrial	K.EGVVEC*SFVK.S	275	Yes	4.76%	0.00%
Q7L0Y3	TRMT10C Mitochondrial ribonuclease P protein 1	R.NVDPFHIYFC*NLK.I	246	Yes	4.76%	0.00%
Q96HY7	DHTKD1 Probable 2-oxoglutarate dehydrogenase E1 component	K.DVIIDLLC*YR.Q	429	Yes	4.76%	0.00%
P36551	CPOX Coproporphyrinogen-III oxidase, mitochondrial	R.C*SSFMAPPVTDLGELR.R	127	Yes	4.76%	0.00%
Q96I99	SUCLG2 Succinyl-CoA ligase	K.IDATQVEVNPFGETPEGQVVC*FDAK.I	255	Yes	4.76%	0.00%
P52789	HK2 Hexokinase-2	R.LGLDPTQEDC*VATHR.I	368	Yes	4.76%	0.00%
O95202	LETM1 LETM1 and EF-hand domain-containing protein 1, mit	K.LFEDELTLDNLTRPQLVALC*K.L	330	Yes	4.76%	0.00%
P00390	GSR Glutathione reductase, mitochondrial	R.SFDSMISTNC*TEELENAGVEVLK.F	278	Yes	4.76%	0.00%
Q9H9J2	MRPL44 39S ribosomal protein L44, mitochondrial	K.SNQELSEQGTSFSQTC*LTQFLEDEYPDMPTEGIK.N	136	Yes	4.76%	0.00%
Q9H078	CLPB Caseinolytic peptidase B protein homolog	R.VVNQLAAAYEQDLLPGGC*TLR.I	647	Yes	4.76%	0.00%
Q9NYK5	MRPL39 39S ribosomal protein L39, mitochondrial	R.APEVPVISGAFC*YDVVLDSK.L	180	Yes	4.76%	0.00%
P10515	DLAT Dihydrolipoyllysine-residue acetyltransferase comp	K.ATVGFESLEEC*YMAK.I	143	Yes	4.76%	0.00%
Q9BYT8	NLN Neurolysin, mitochondrial	R.C*KEENTIILQQLLPLR.T	272	Yes	4.76%	0.00%
O75600	GCAT 2-amino-3-ketobutyrate coenzyme A ligase, mitochon	R.C*VEAFVEVGR.L	404	Yes	4.76%	0.00%
P12532	CKMT1B Creatine kinase U-type, mitochondrial	R.GLSLPPAC*TR.A	179	Yes	4.76%	0.00%
Q02252	ALDH6A1 Methylmalonate-semialdehyde dehydrogenase	K.LLQDSGAPDGTLNIIHGQHEAVNFIC*DHPDIK.A	249	Yes	4.76%	0.00%
P11182	DBT Lipoamide acyltransferase component of branched-ch	K.NVQIC*SIFDIATELNR.L	365	Yes	4.76%	0.00%
P05166	PCCB Propionyl-CoA carboxylase beta chain, mitochondria	R.AFENDVDALC*NLR.D	269	Yes	4.76%	0.00%
Q9NUJ1	ABHD10 Abhydrolase domain-containing protein 10, mitochon	K.ALAIEEFC*K.S	100	Yes	4.76%	0.00%
O00330	PDHX Pyruvate dehydrogenase protein X component, mitoch	K.STVPHAYATADC*DLGAVLK.V	307	Yes	4.76%	0.00%
Q9BQ52	ELAC2 Zinc phosphodiesterase ELAC protein 2	R.YLFNC*GEGVQR.L	87	Yes	4.76%	0.00%
P36776	LONP1 Lon protease homolog, mitochondrial	K.RAGVTC*IVLPAENKK.D	909	Yes	4.76%	0.00%
P22033	MUT Methylmalonyl-CoA mutase, mitochondrial	R.AHC*QTSGWSLTEQDPYNNIVR.T	351	Yes	4.76%	0.00%
Q02218	OGDH 2-oxoglutarate dehydrogenase, mitochondrial	K.DVVVDLVC*YR.R	507	Yes	4.76%	0.00%
P11177	PDHB Pyruvate dehydrogenase E1 component subunit beta,	K.EGVEC*EVINMR.T	263	Yes	4.76%	0.00%
P49748	ACADVL Very long-chain specific acyl-CoA dehydrogenase, m	K.ELGAFGLQVPSELGGVGLC*NTQYAR.L	156	Yes	4.76%	0.00%
Q96EY7	PTCD3 Pentatricopeptide repeat-containing protein 3, mit	K.DPDDDKFFQSAMSIC*SSLR.D	423	Yes	4.76%	0.00%
Q9BYT8	NLN Neurolysin, mitochondrial	R.IVHLQETC*DLGK.I	153	Yes	4.76%	0.00%
P21953	BCKDHB 2-oxoisovalerate dehydrogenase subunit beta, mitoc	K.LGVSC*EVIDLR.T	299	Yes	4.76%	0.00%
Q9BW92	TARS2 Threonine--tRNA ligase, mitochondrial	R.LLGVLAESC*GGK.W	603	Yes	4.76%	0.00%
P23368	ME2 NAD-dependent malic enzyme, mitochondrial	R.AMASINERPVIFALSNPTAQAEC*TAEEAYTLTEGR.C	428	Yes	4.76%	0.00%
P52789	HK2 Hexokinase-2	R.SASLC*AATLAAVLQR.I	386	Yes	4.76%	0.00%

P23378	GLDC Glycine dehydrogenase	R.SYIGMGYYNC*SVPQTILR.N	141	Yes	4.76%	0.00%
P21953	BCKDHB 2-oxoisovalerate dehydrogenase subunit beta, mitoc	R.TIIPWDVDTIC*K.S	316	Yes	4.76%	0.00%
O75439	PMPCB Mitochondrial-processing peptidase subunit beta	R.VASEDSGLSTC*TVGLWIDAGSR.Y	79	Yes	4.76%	0.00%
P36776	LONP1 Lon protease homolog, mitochondrial	K.VLFIC*TANVTDTIPEPLR.D	637	Yes	4.76%	0.00%
Q02218	OGDH 2-oxoglutarate dehydrogenase, mitochondrial	R.VVNAPIFHVNSDDPEAVMYVC*K.V	487	Yes	4.76%	0.00%
Q3SY69	ALDH1L2 Mitochondrial 10-formyltetrahydrofolate dehydrogen	R.YFAGWC*DK.I	558	Yes	4.76%	0.00%
P00505	GOT2 Aspartate aminotransferase, mitochondrial	K.IPEQSVLLLHAC*AHNPTGVDPR.P	212	Yes	4.76%	0.00%
Q9UDR5	AASS Alpha-aminoadipic semialdehyde synthase, mitochond	R.FNTDIAPYTTC*LINGIYWEQNTPR.L	305	Yes	4.76%	0.00%
P00505	GOT2 Aspartate aminotransferase, mitochondrial	K.EYLPIGGLAEFC*K.A	106	Yes	4.76%	0.00%
P07237	P4HB Protein disulfide-isomerase	K.KEEC*PAVR.L	312	Yes	4.76%	0.00%
P53396	ACLY ATP-citrate synthase	K.GVTIIGPATVGGIKPGC*FK.I	633	Yes	4.76%	0.00%
Q4J6C6	PREPL Prolyl endopeptidase-like	K.LNGLADLEAC*IK.T	538	Yes	4.76%	0.00%
Q6P1X6	C8orf82 UPF0598 protein C8orf82	R.LSYC*GGGEALAVPFEPAR.L	130	Yes	4.76%	0.00%
P53396	ACLY ATP-citrate synthase	R.AVQGMLDFDYVC*SR.D	519	Yes	4.76%	0.00%
Q9UBQ7	GRHPR Glyoxylate reductase/hydroxypyruvate reductase	R.AADC*EVEQWDSDEPIPAK.E	29	Yes	4.76%	0.00%
P28838	LAP3 Cytosol aminopeptidase	R.ADMGGAATIC*SAIVSAAK.L	313	Yes	4.76%	0.00%
Q9BXW7	CECR5 Cat eye syndrome critical region protein 5	K.AQELSALLGC*EVDADQVILSHSPMK.L	109	Yes	4.76%	0.00%
Q7L2E3	DHX30 Putative ATP-dependent RNA helicase DHX30	R.GEPGGILC*FLPGWQEIK.G	673	Yes	4.76%	0.00%
P22234	PAICS Multifunctional protein ADE2	R.VVVLMGSTSDLGHC*EK.I	281	Yes	4.76%	0.00%
Q8TCS8	PNPT1 Polyribonucleotide nucleotidyltransferase 1, mitoc	R.NVSC*EVDMFK.T	372	Yes	4.76%	0.00%
P49189	ALDH9A1 4-trimethylaminobutyraldehyde dehydrogenase	R.VIATFTC*SGEK.E	45	Yes	4.76%	0.00%
Q6YN16	HSDL2 Hydroxysteroid dehydrogenase-like protein 2	R.LAGC*TVFITGASR.G	11	Yes	4.76%	0.00%
P49189	ALDH9A1 4-trimethylaminobutyraldehyde dehydrogenase	R.EREDEIATMEC*INNGK.S	96	Yes	4.76%	0.00%
Q9NQH7	XPNPEP3 Probable Xaa-Pro aminopeptidase 3	R.IEDDVVVTQDSPLILSADC*PK.E	492	Yes	4.76%	0.00%
P28838	LAP3 Cytosol aminopeptidase	K.LNLPINIIGLAPLC*ENMPSGK.A	335	Yes	4.76%	0.00%
P11586	MTHFD1 C-1-tetrahydrofolate synthase, cytoplasmic	R.GDLNDC*FIPC*TPK.G	143|147	Yes	4.76%	0.00%
P00390	GSR Glutathione reductase, mitochondrial	K.LGGTC*VNVGC*VPK.K	102|107	Yes	4.76%	0.00%
P23378	GLDC Glycine dehydrogenase	R.ELEKDLC*ELTGYDQVC*FQPNSGAQGEYAGLATIR.A	603|612	Yes	4.76%	0.00%
P23378	GLDC Glycine dehydrogenase	K.IQC*GC*SVK.E	442|444	Yes	4.76%	0.00%
P23368	ME2 NAD-dependent malic enzyme, mitochondrial	R.C*LPVC*IDVGTDNIALLK.D	198|202	Yes	4.76%	0.00%
P26440	IVD Isovaleryl-CoA dehydrogenase, mitochondrial	R.GSNTC*ELIFEDC*K.I	254|261	Yes	4.76%	0.00%
Q9P2R7	SUCLA2 Succinyl-CoA ligase	R.IC*NQVLVC*ER.K	152|158	Yes	4.76%	0.00%
Q9BQ52	ELAC2 Zinc phosphodiesterase ELAC protein 2	R.TC*DLEEFQTC*LVR.H	632|640	Yes	4.76%	0.00%
Q86X76	NIT1 Nitrilase homolog 1	R.C*SEGPGLC*LAR.I	285|292	Yes	4.76%	0.00%
Q7Z4W1	DCXR L-xylulose reductase	R.EC*PGIEPVC*VDLGDWEATER.A	51|58	Yes	4.76%	0.00%
P49419	ALDH7A1 Alpha-aminoadipic semialdehyde dehydrogenase	K.LPGAIC*SLTC*GGADIGTAMAK.D	248|252	Yes	4.76%	0.00%
Q9BXR0	QTRT1 Queuine tRNA-ribosyltransferase	K.DFGPIDPEC*TC*PTC*QK.H	317|319|322	Yes	4.76%	0.00%
Q9BVL4	SELO Selenoprotein O	R.LMEQC*ASLEELR.L	484	Yes	4.76%	0.00%
P49327	FASN Fatty acid synthase	R.C*VLLSNLSSTSHVPEVDPGSAELQK.V	1471	Yes	4.76%	0.00%
P35270	SPR Sepiapterin reductase	R.AVC*LLTGASR.G	10	Yes	4.76%	0.00%
P51659	HSD17B4 Peroxisomal multifunctional enzyme type 2	K.SNIHC*NTIAPNAGSR.M	189	Yes	4.76%	0.00%
P49327	FASN Fatty acid synthase	K.SFYGSTLFLC*R.R	1403	Yes	4.76%	0.00%
P49327	FASN Fatty acid synthase	R.WVC*SSLR.H	1548	Yes	4.76%	0.00%
P60900	PSMA6 Proteasome subunit alpha type-6	K.YGYEIPVDMLC*K.R	115	Yes	4.76%	0.00%
Q13085	ACACA Acetyl-CoA carboxylase 1	R.IFDEVMGC*FSDSPPQSPTFPEAGHTSLYDEDK.V	1255	Yes	4.76%	0.00%
P49327	FASN Fatty acid synthase	K.TGGAYGEDLGADYNLSQVC*DGK.V	2468	Yes	4.76%	0.00%
P49321	NASP Nuclear autoantigenic sperm protein	R.KPTDGASSSNC*VTDISHLVR.K	708	Yes	4.76%	0.00%
P61221	ABCE1 ATP-binding cassette sub-family E member 1	K.TQAIVC*QQLDLTHLK.E	201	Yes	4.76%	0.00%
P22314	UBA1 Ubiquitin-like modifier-activating enzyme 1	K.DNPGVVTC*LDEAR.H	234	Yes	4.76%	0.00%
P22314	UBA1 Ubiquitin-like modifier-activating enzyme 1	R.VGEFC*HNR.G	179	Yes	4.76%	0.00%
O00410	IPO5 Importin-5	K.ENVNATENC*ISAVGK.I	972	Yes	4.76%	0.00%
P36873	PPP1CC Serine/threonine-protein phosphatase PP1-gamma cat	R.IYGFYDEC*K.R	140	Yes	4.76%	0.00%
P22314	UBA1 Ubiquitin-like modifier-activating enzyme 1	K.VLGPYTFSIC*DTSNFSDYIR.G	278	Yes	4.76%	0.00%
Q6P2I3	FAHD2B Fumarylacetoacetate hydrolase domain-containing pr	K.TFDTFC*PLGPALVTK.D	215	Yes	4.76%	0.00%
Q32MZ4	LRRFIP1 Leucine-rich repeat flightless-interacting protein	R.C*TLPEHESPSQDISDAC*EAESTER.C	726|742	Yes	4.76%	0.00%

Q9H0R6	QRSL1 Glutamyl-tRNA(Gln) amidotransferase subunit A, mit	R.C*VDDAAIVLGALAGPDPR.D	236	Yes	4.72%	0.77%
Q5JRX3	PITRM1 Presequence protease, mitochondrial	R.EFQITC*GPDSFATDPSK.Q	313	Yes	4.64%	0.39%
P42704	LRPPRC Leucine-rich PPR motif-containing protein, mitocho	R.LIASYC*NVGDIEGASK.I	208	Yes	4.63%	0.39%
O75439	PMPCB Mitochondrial-processing peptidase subunit beta	K.TNMLLQLDGSTPIC*EDIGR.Q	419	Yes	4.63%	0.86%
P34897	SHMT2 Serine hydroxymethyltransferase, mitochondrial	R.GLELIASENFC*SR.A	80	Yes	4.61%	0.43%
Q99832	CCT7 T-complex protein 1 subunit eta	R.YNFFTGC*PK.A	364	Yes	4.56%	1.20%
Q9UDR5	AASS Alpha-aminoadipic semialdehyde synthase, mitochond	K.GAQAIFNELPC*EYVEPHELK.E	240	Yes	4.53%	0.46%
O95571	ETHE1 Protein ETHE1, mitochondrial	K.IFTLPGDC*LIYPAHDYHGFTVSTVEEER.T	189	Yes	4.53%	0.46%
P00505	GOT2 Aspartate aminotransferase, mitochondrial	R.VGAFTMVC*K.D	295	Yes	4.51%	2.68%
P05165	PCCA Propionyl-CoA carboxylase alpha chain, mitochondri	R.C*LAAEDVVFIGPDTHAIQAMGDK.I	155	Yes	4.47%	0.49%
Q99798	ACO2 Aconitate hydratase, mitochondrial	K.VAVPSTIHC*DHLIEAQVGGEK.D	126	Yes	4.32%	0.52%
Q9H2U2	PPA2 Inorganic pyrophosphatase 2, mitochondrial	K.ILSC*GEVIHVK.I	180	Yes	4.30%	0.50%
O75439	PMPCB Mitochondrial-processing peptidase subunit beta	R.QMLC*YNR.R	428	Yes	4.30%	0.65%
Q13085	ACACA Acetyl-CoA carboxylase 1	K.RPGAALDPGC*VLAK.M	813	Yes	4.30%	0.50%
P40926	MDH2 Malate dehydrogenase, mitochondrial	K.GYLGPEQLPDC*LK.G	89	Yes	4.30%	0.92%
P35914	HMGCL Hydroxymethylglutaryl-CoA lyase, mitochondrial	K.NINC*SIEESFQR.F	141	Yes	4.30%	0.92%
P49189	ALDH9A1 4-trimethylaminobutyraldehyde dehydrogenase	K.SPLIIFSDC*DMNNAVK.G	267	Yes	4.30%	0.92%
Q10713	PMPCA Mitochondrial-processing peptidase subunit alpha	K.HGGIC*DC*QTSR.D	140|142	Yes	4.30%	0.92%
Q13085	ACACA Acetyl-CoA carboxylase 1	K.TDC*DIEDDR.L	1297	Yes	4.28%	2.36%
P35914	HMGCL Hydroxymethylglutaryl-CoA lyase, mitochondrial	R.GYVSC*ALGC*PYEGK.I	170|174	Yes	4.21%	0.83%
Q9HCC0	MCCC2 Methylcrotonoyl-CoA carboxylase beta chain, mitoch	K.MVAAVAC*AQVPK.I	431	Yes	4.15%	0.75%
O75439	PMPCB Mitochondrial-processing peptidase subunit beta	R.VTC*LESGLR.V	62	Yes	4.15%	0.75%
P38646	HSPA9 Stress-70 protein, mitochondrial	K.GAVVGIDLGTTNSC*VAVMEGK.Q	66	Yes	4.15%	1.07%
O95571	ETHE1 Protein ETHE1, mitochondrial	R.SLLPGC*QSVISR.L	98	Yes	4.15%	1.07%
Q13085	ACACA Acetyl-CoA carboxylase 1	K.VQAERPDTMLGVVC*GALHVADVSLR.N	634	Yes	4.15%	1.07%
Q5JRX3	PITRM1 Presequence protease, mitochondrial	K.LGC*GLLDYR.E	627	Yes	4.03%	0.77%
P23378	GLDC Glycine dehydrogenase	R.FC*DAMISIR.Q	920	Yes	4.02%	1.01%
Q5TC12	ATPAF1 ATP synthase mitochondrial F1 complex assembly fac	R.AQSC*PTFLC*ALPR.R	194|199	Yes	3.99%	0.91%
P34897	SHMT2 Serine hydroxymethyltransferase, mitochondrial	R.YYGGAEVVDEIELLC*QR.R	119	Yes	3.83%	1.32%
Q5JRX3	PITRM1 Presequence protease, mitochondrial	R.AFSSLNTLPEELRPYVPLFC*SVLTK.L	619	Yes	3.83%	1.62%
Q96EY8	MMAB Cob(I)yrinic acid a,c-diamide adenosyltransferase,	K.ISSALHFC*R.A	185	Yes	3.83%	1.62%
Q9Y305	ACOT9 Acyl-coenzyme A thioesterase 9, mitochondrial	K.SLEIC*HPQER.N	299	Yes	3.83%	1.62%
P51553	IDH3G Isocitrate dehydrogenase	K.LGDGLFLQC*C*R.E	235|236	Yes	3.83%	1.62%
Q96RQ3	MCCC1 Methylcrotonoyl-CoA carboxylase subunit alpha, mit	K.HNFC*FMEMNTR.L	332	Yes	3.82%	1.89%
P23368	ME2 NAD-dependent malic enzyme, mitochondrial	R.C*LFASGSPFGPVK.L	441	Yes	3.82%	1.89%
P05165	PCCA Propionyl-CoA carboxylase alpha chain, mitochondri	K.SVHC*QAGDTVGEGDLLVELE.-	712	Yes	3.68%	1.02%
P10515	DLAT Dihydrolipoyllysine-residue acetyltransferase comp	R.DVPLGTPLC*IIVEK.E	291	Yes	3.68%	1.24%
P10515	DLAT Dihydrolipoyllysine-residue acetyltransferase comp	K.NFSAIINPPQAC*ILAIGASEDK.L	586	Yes	3.68%	1.24%
Q13085	ACACA Acetyl-CoA carboxylase 1	R.TDC*NHIFLNFVPTVIMDPSK.I	1470	Yes	3.64%	1.53%
Q13085	ACACA Acetyl-CoA carboxylase 1	K.EMAQYASNITSVLC*QFPSQQIANILDSHAATLNR.K	934	Yes	3.64%	1.53%
Q13085	ACACA Acetyl-CoA carboxylase 1	R.EC*C*QPVLVYIPPQAELR.G	2074|2075	Yes	3.64%	1.53%
P36776	LONP1 Lon protease homolog, mitochondrial	K.ILC*FYGPPGVGK.T	520	Yes	3.62%	1.42%
P10515	DLAT Dihydrolipoyllysine-residue acetyltransferase comp	R.DVPIGAIIC*ITVGKPEDIEAFK.N	164	Yes	3.52%	1.40%
Q13085	ACACA Acetyl-CoA carboxylase 1	K.RVSALNSVHC*EHVEDEGESR.Y	1769	Yes	3.52%	1.40%
Q13085	ACACA Acetyl-CoA carboxylase 1	K.IIEEAPATIATPAVFEHMEQC*AVK.L	407	Yes	3.52%	1.40%
P10515	DLAT Dihydrolipoyllysine-residue acetyltransferase comp	K.ASALAC*LK.V	488	Yes	3.50%	2.18%
P38646	HSPA9 Stress-70 protein, mitochondrial	R.RTIAPC*QK.A	366	Yes	3.37%	0.92%
Q6YN16	HSDL2 Hydroxysteroid dehydrogenase-like protein 2	K.ALPC*IVDVR.D	71	Yes	3.37%	0.92%
P40926	MDH2 Malate dehydrogenase, mitochondrial	K.TIIPLISQC*TPK.V	212	Yes	3.36%	1.98%
P05165	PCCA Propionyl-CoA carboxylase alpha chain, mitochondri	R.LQVEHPVTEC*ITGLDLVQEMIR.V	363	Yes	3.36%	1.53%
Q96RQ3	MCCC1 Methylcrotonoyl-CoA carboxylase subunit alpha, mit	K.TFQVLGNLYSEGDC*TYLK.C	595	Yes	3.36%	1.53%
P23378	GLDC Glycine dehydrogenase	R.C*HPQTIAVVQTR.A	225	Yes	3.36%	1.53%
Q99714	HSD17B10 3-hydroxyacyl-CoA dehydrogenase type-2	K.KLGNNC*VFAPADVTSEK.D	58	Yes	3.36%	1.53%
P34897	SHMT2 Serine hydroxymethyltransferase, mitochondrial	R.AALEALGSC*LNNK.Y	91	Yes	3.36%	1.53%
P04406	GAPDH Glyceraldehyde-3-phosphate dehydrogenase	R.VPTANVSVVDLTC*R.L	247	Yes	3.36%	1.53%
P04406	GAPDH Glyceraldehyde-3-phosphate dehydrogenase	K.IISNASC*TTNC*LAPLAK.V	152|156	Yes	3.36%	1.53%

P23378	GLDC Glycine dehydrogenase	K.LPC*EMDFSGK.D	250	Yes	3.27%	1.41%
Q9HCC0	MCCC2 Methylcrotonoyl-CoA carboxylase beta chain, mitoch	R.LPC*IYLVDSGGAYLPR.Q	167	Yes	3.25%	2.07%
P11498	PC Pyruvate carboxylase, mitochondrial	R.AC*TELGIR.T	56	Yes	3.25%	2.07%
P11498	PC Pyruvate carboxylase, mitochondrial	R.INGC*AIQC*R.V	372|376	Yes	3.20%	1.75%
P05165	PCCA Propionyl-CoA carboxylase alpha chain, mitochondri	R.INGWAVEC*R.V	398	Yes	3.08%	1.53%
P11498	PC Pyruvate carboxylase, mitochondrial	R.ADFAQAC*QDAGVR.F	131	Yes	3.08%	1.53%
P35914	HMGCL Hydroxymethylglutaryl-CoA lyase, mitochondrial	K.LLEAGNFIC*QALNR.K	307	Yes	3.04%	1.92%
Q9H2U2	PPA2 Inorganic pyrophosphatase 2, mitochondrial	K.STNC*FGDNDPIDVC*EIGSK.I	161|171	Yes	2.90%	1.32%
P40926	MDH2 Malate dehydrogenase, mitochondrial	K.SQETEC*TYFSTPLLLGK.K	285	Yes	2.89%	1.76%
P11498	PC Pyruvate carboxylase, mitochondrial	R.AGTHILC*IK.D	739	Yes	2.88%	2.18%
P11498	PC Pyruvate carboxylase, mitochondrial	K.DMAGLLKPTAC*TMLVSSLR.D	752	Yes	2.88%	2.07%
Q96RQ3	MCCC1 Methylcrotonoyl-CoA carboxylase subunit alpha, mit	K.ESLC*QAALGLILK.E	509	Yes	2.88%	2.07%
Q13085	ACACA Acetyl-CoA carboxylase 1	R.NFDLTAIPC*ANHK.M	1396	Yes	2.88%	2.07%
Q12931	TRAP1 Heat shock protein 75 kDa, mitochondrial	R.NIYYLC*APNR.H	501	Yes	2.66%	1.40%
Q99798	ACO2 Aconitate hydratase, mitochondrial	K.C*TTDHISAAGPWLK.F	592	Yes	2.60%	0.55%
P11498	PC Pyruvate carboxylase, mitochondrial	R.FLYEC*PWR.R	622	Yes	2.50%	2.07%
P10809	HSPD1 60 kDa heat shock protein, mitochondrial	K.C*EFQDAYVLLSEK.K	237	Yes	1.96%	0.00%
Q96RQ3	MCCC1 Methylcrotonoyl-CoA carboxylase subunit alpha, mit	K.C*SVNGVASK.A	600	Yes	1.96%	0.00%
P43251	BTD Biotinidase	R.WNPC*LEPHR.F	143		97.12%	2.18%
P43251	BTD Biotinidase	R.LSC*MAIR.G	160		97.11%	1.62%
Q9BS26	ERP44 Endoplasmic reticulum resident protein 44	K.GTINFLHADC*DK.F	301		95.24%	0.00%
Q15043	SLC39A14 Zinc transporter ZIP14	R.IGSSELQEFC*PTILQQLDSR.A	118		95.24%	0.00%
P30101	PDIA3 Protein disulfide-isomerase A3	K.VDC*TANTNTC*NK.Y	85|92		95.24%	0.00%
P06280	GLA Alpha-galactosidase A	K.GVAC*NPAC*FITQLLPVK.R	378|382		95.24%	0.00%
Q9BS26	ERP44 Endoplasmic reticulum resident protein 44	R.VANILHDDC*AFLSAFGDVSKPER.Y	189		95.24%	0.00%
Q14697	GANAB Neutral alpha-glucosidase AB	K.TC*EESSFC*K.R	41|47		95.24%	0.00%
P13674	P4HA1 Prolyl 4-hydroxylase subunit alpha-1	R.HAAC*PVLVGNK.W	503		94.29%	1.34%
P12109	COL6A1 Collagen alpha-1(VI) chain	K.YLIVVTDGHPLEGYKEPC*GGLEDAVNEAK.H	169		93.31%	2.72%
Q96HE7	ERO1L ERO1-like protein alpha	K.YSEEANNLIEEC*EQAER.L	131		76.11%	1.32%
Q8NFQ8	TOR1AIP2 Torsin-1A-interacting protein 2	K.C*LSHHVADAYTSSQK.V	310		74.75%	0.09%
P11142	HSPA8 Heat shock cognate 71 kDa protein	K.GPAVGIDLGTTYSC*VGVFQHGK.V	17		73.28%	3.40%
Q96EI5	TCEAL4 Transcription elongation factor A protein-like 4	R.KPEVTC*TLEDK.K	34		72.19%	2.23%
Q5VSL9	FAM40A Protein FAM40A	R.AHSNPDFLPVDNC*LQSVLGQR.V	798		70.51%	2.71%
Q8NFQ8	TOR1AIP2 Torsin-1A-interacting protein 2	R.ISHLVLPVQPVSSIEEQGC*LF.-	468		69.33%	4.39%
P15924	DSP Desmoplakin	K.NQC*TQVVQER.E	1805		68.95%	0.02%
Q14980	NUMA1 Nuclear mitotic apparatus protein 1	R.KHPSSPEC*LVSAQK.V	80		68.25%	3.00%
Q15365	PCBP1 Poly(rC)-binding protein 1	R.C*SDAAGYPHATHDLEGPPLDAYSIQGQHTISPLDLAK.L	201		66.69%	0.06%
Q4VCS5	AMOT Angiomotin	R.QGNC*QPTNVSEYNAAALMELLR.E	647		65.31%	4.81%
P17025	ZNF182 Zinc finger protein 182	K.C*NECGKAFREK.S	516		62.37%	2.47%
P49454	CENPF Centromere protein F	R.SEC*ITATR.K	1328		62.12%	1.96%
Q9P258	RCC2 Protein RCC2	R.IEYDC*ELVPR.R	305		61.83%	2.40%
P61758	VBP1 Prefoldin subunit 3	R.FLLADNLYC*K.A	113		61.40%	2.54%
Q9BS26	ERP44 Endoplasmic reticulum resident protein 44	K.TPADC*PVIAIDSFR.H	318		60.75%	5.74%
Q14980	NUMA1 Nuclear mitotic apparatus protein 1	R.LDFVC*SFLQK.N	65		60.28%	1.25%
P49454	CENPF Centromere protein F	K.GVEELESLC*EVYR.Q	1556		56.70%	2.47%
P55735	SEC13 Protein SEC13 homolog	R.VFIWTC*DDASSNTWSPK.L	245		53.62%	15.10%
P51610	HCFC1 Host cell factor 1	R.VAGINAC*GR.G	1872		51.16%	1.81%
P49792	RANBP2 E3 SUMO-protein ligase RanBP2	K.LPPTFFC*GVC*SDTDEDNGNGEDFQSELQK.V	2737|2740		48.39%	2.12%
Q9P2E9	RRBP1 Ribosome-binding protein 1	K.HMAAASAEC*QNYAK.E	1216		46.81%	0.65%
Q15334	LLGL1 Lethal(2) giant larvae protein homolog 1	K.LTAHEGC*R.V	855		46.34%	4.36%
Q06830	PRDX1 Peroxiredoxin-1	K.HGEVC*PAGWKPGSDTIKPDVQK.S	173		45.18%	1.42%
P43251	BTD Biotinidase	K.ILSGDPYC*EK.D	371		44.88%	1.01%
Q9UQ35	SRRM2 Serine/arginine repetitive matrix protein 2	K.DSLVQSC*PGSLSLC*AGVK.S	1029|1036		43.68%	5.13%
P33176	KIF5B Kinesin-1 heavy chain	R.FVC*SPDEVMDTIDEGK.S	174		43.29%	1.17%
O60907	TBL1X F-box-like/WD repeat-containing protein TBL1X	K.VGASASDGSVC*VLDLR.K	571		41.85%	0.01%
P49454	CENPF Centromere protein F	R.C*EETGNAYEDLSQK.Y	1029		41.14%	1.19%
P48147	PREP Prolyl endopeptidase	K.ITVPFLEQC*PIR.G	57		40.97%	4.42%
P55786	NPEPPS Puromycin-sensitive aminopeptidase	R.SKDGVC*VR.V	265		40.23%	1.08%
H7BZ11	Uncharacterized protein	R.LEC*VEPNC*R.S	72|77		39.60%	2.07%
P21333	FLNA Filamin-A	K.IEC*DDKGDGSC*DVR.Y	623|631		39.43%	2.10%
Q92769	HDAC2 Histone deacetylase 2	R.LGC*FNLTVK.G	274		38.92%	19.18%
O95218	ZRANB2 Zinc finger Ran-binding domain-containing protein	R.GLFSANDWQC*K.T	71		38.68%	2.40%
P21333	FLNA Filamin-A	R.APSVANVGSHC*DLSLK.I	2160		36.88%	5.08%

P68366	TUBA4A Tubulin alpha-4A chain	K.AYHEQLSVAEITNAC*FEPANQMVK.C	295		36.11%	2.04%
O95218	ZRANB2 Zinc finger Ran-binding domain-containing protein	K.TC*SNVNWAR.R	74		36.10%	0.78%
Q9BTE3	MCMBP Mini-chromosome maintenance complex-binding protei	K.LQHINPLLPAC*LNK.E	325		34.85%	0.30%
Q14789	GOLGB1 Golgin subfamily B member 1	R.ENQQHYGDLLNHC*AVLEK.Q	3090		34.73%	6.47%
Q14126	DSG2 Desmoglein-2	K.TLAEVC*LGQK.I	840		34.60%	1.46%
O14654	IRS4 Insulin receptor substrate 4	R.GSGGGQGSNGQGSSSHSSGGNQC*SGEGQGSR.G	522		33.78%	0.01%
Q14980	NUMA1 Nuclear mitotic apparatus protein 1	R.KVEELQAC*VETAR.Q	658		33.45%	0.16%
Q00839	HNRNPU Heterogeneous nuclear ribonucleoprotein U	R.KAVVVC*PK.D	607		33.28%	0.45%
Q9NZB2	FAM120A Constitutive coactivator of PPAR-gamma-like protei	K.TC*NTNPHLNALSTDSAC*R.R	1088|1103		33.17%	0.33%
P14618	PKM Pyruvate kinase isozymes M1/M2	R.AEGSDVANAVLDGADC*IMLSGETAK.G	358		33.09%	9.21%
P49792	RANBP2 E3 SUMO-protein ligase RanBP2	R.VWLWTAC*DFADGER.K	2407		32.93%	0.51%
P43251	BTD Biotinidase	K.DAQEVHC*DEATK.W	380		32.53%	1.82%
P35579	MYH9 Myosin-9	R.C*QHLQAEK.K	931		32.50%	0.10%
P29590	PML Protein PML	R.TPTLTSIYC*R.G	204		32.35%	0.12%
P48634	PRRC2A Protein PRRC2A	K.NLDSGHC*VPEPSSSGQR.L	1821		31.53%	0.03%
P49454	CENPF Centromere protein F	K.YISGPHELSTSQNDNAHLQC*SLQTTMNK.L	1291		31.37%	0.95%
Q02952	AKAP12 A-kinase anchor protein 12	K.EVSSLEGSPPPC*LGQEEAVC*TK.I	1399|1407		31.23%	0.66%
P49792	RANBP2 E3 SUMO-protein ligase RanBP2	K.EGQWDC*SSC*LVR.N	1549|1552		31.19%	29.31%
Q14566	MCM6 DNA replication licensing factor MCM6	R.NPVC*ANR.R	185		30.57%	0.02%
P07437	TUBB Tubulin beta chain	K.LTTPTYGDLNHLVSATMSGVTTC*LR.F	239		30.31%	2.98%
P49792	RANBP2 E3 SUMO-protein ligase RanBP2	K.C*RPLEENTADNEK.E	2696		30.10%	1.04%
Q13748	TUBA3D Tubulin alpha-3C/D chain	R.TIQFVDWC*PTGFK.V	BAD_ID		29.56%	22.53%
P30153	PPP2R1A Serine/threonine-protein phosphatase 2A 65 kDa reg	R.LNIISNLDC*VNEVIGIR.Q	390		29.53%	1.55%
Q86W42	THOC6 THO complex subunit 6 homolog	R.C*VNQWQLSGELK.A	279		29.43%	0.17%
I3L2F9	Uncharacterized protein	K.NMMAAC*DPR.H	BAD_ID		29.12%	2.17%
Q14789	GOLGB1 Golgin subfamily B member 1	K.ATEQHHTQPVLESNLC*PDWPSHSEDASALQGGTSVAQIK.A	1285		29.12%	0.05%
O15020	SPTBN2 Spectrin beta chain, non-erythrocytic 2	R.SAELGC*TVDEVESLIK.R	2043		29.09%	11.98%
Q9Y2H6	FNDC3A Fibronectin type-III domain-containing protein 3A	K.SNPSEVVEFTTC*PDK.P	560		29.07%	1.68%
Q8NFH5	NUP35 Nucleoporin NUP53	R.IFGESIMIGVKPC*IDK.S	243		28.99%	0.54%
P49790	NUP153 Nuclear pore complex protein Nup153	K.C*LAC*ESAK.P	871|874		28.47%	0.12%
P13639	EEF2 Elongation factor 2	K.IWC*FGPDGTGPNILTDITK.G	651		28.10%	10.72%
P53582	METAP1 Methionine aminopeptidase 1	R.NC*YPSPLNYYNFPK.S	179		27.98%	11.44%
Q9UGP4	LIMD1 LIM domain-containing protein 1	R.LPC*QPLVPGPELRPSAAELK.L	431		27.96%	0.14%
O60343	TBC1D4 TBC1 domain family member 4	R.SQKPEAGGC*GAPAAR.E	74		27.79%	0.38%
P68104	EEF1A1 Elongation factor 1-alpha 1	K.PMC*VESFSDYPPLGR.F	411		27.71%	6.82%
Q96F45	ZNF503 Zinc finger protein 503	R.VPSATC*QPFTPR.T	219		27.58%	4.44%
O00148	DDX39A ATP-dependent RNA helicase DDX39A	K.NC*PHVVVGTPGR.I	164		27.51%	0.61%
P13639	EEF2 Elongation factor 2	K.DLEEDHAC*IPIK.K	567		27.01%	1.18%
P49790	NUP153 Nuclear pore complex protein Nup153	K.TAELSGSSSTLEPIISSSAHHVTTVNSTNC*K.K	585		26.87%	3.66%
Q14980	NUMA1 Nuclear mitotic apparatus protein 1	K.HLC*QQLQAEQAAAEK.R	1367		26.19%	0.25%
P21333	FLNA Filamin-A	K.THEAEIVEGENHTYC*IR.F	2199		25.72%	10.73%
Q8NF37	LPCAT1 Lysophosphatidylcholine acyltransferase 1	R.LPADTC*LLEFAR.L	330		25.27%	5.72%
P46782	RPS5 40S ribosomal protein S5	R.VNQAIWLLC*TGAR.E	155		25.09%	15.83%
H7C455	Uncharacterized protein	K.PIGLC*C*IAPVLAAK.V	BAD_ID		24.99%	2.17%
P21333	FLNA Filamin-A	K.MDC*QEC*PEGYR.V	2476|2479		24.79%	2.77%
Q00839	HNRNPU Heterogeneous nuclear ribonucleoprotein U	K.MC*LFAGFQR.K	594		24.50%	2.09%
P49792	RANBP2 E3 SUMO-protein ligase RanBP2	R.C*VAC*QNPDKPSPSTSVPAPASFK.F	1563|1566		24.14%	0.17%
P49792	RANBP2 E3 SUMO-protein ligase RanBP2	R.RITITEC*GQI.-	3221		23.93%	0.89%
P12268	IMPDH2 Inosine-5-monophosphate dehydrogenase 2	R.HGFC*GIPITDTGR.M	140		23.51%	0.71%
P14923	JUP Junction plakoglobin	R.NLALC*PANHAPLQEAAVIPR.L	511		23.16%	10.66%
Q92841	DDX17 Probable ATP-dependent RNA helicase DDX17	R.GVEIC*IATPGR.L	298		22.96%	15.76%
Q00839	HNRNPU Heterogeneous nuclear ribonucleoprotein U	K.GNFTLPEVAEC*FDEITYVELQK.E	648		22.74%	2.06%
P46777	RPL5 60S ribosomal protein L5	R.IEGDMIVC*AAYAHELPK.Y	76		22.66%	24.84%
P57721	PCBP3 Poly(rC)-binding protein 3	R.LVVPASQC*GSLIGK.G	141		21.95%	0.75%
P04183	TK1 Thymidine kinase, cytosolic	K.ENC*PVPGKPGEAVAAR.K	206		21.88%	0.00%
Q99590	SCAF11 Protein SCAF11	K.VYQPVSC*PLSDLSENVESVVNEEK.I	566		21.84%	1.43%
Q8WUM4	PDCD6IP Programmed cell death 6-interacting protein	R.YYDQIC*SIEPK.F	76		21.79%	24.00%
P21333	FLNA Filamin-A	K.ATC*APQHGAPGPGPADASK.V	2543		21.67%	0.29%
O14686	MLL2 Histone-lysine N-methyltransferase MLL2	R.SVAEQHTPVC*SR.F	369		20.69%	1.16%

Q86YS7	KIAA0528 Uncharacterized protein KIAA0528	K.NFNDLC*ENLLK.S	751		20.68%	18.38%
P68366	TUBA4A Tubulin alpha-4A chain	R.AVC*MLSNTTAIAEAWAR.L	376		20.58%	1.20%
P49454	CENPF Centromere protein F	K.HDVHQIC*DK.D	1694		20.52%	0.16%
P68366	TUBA4A Tubulin alpha-4A chain	R.SIQFVDWC*PTGFK.V	347		20.51%	2.94%
Q14789	GOLGB1 Golgin subfamily B member 1	K.QLQVELC*EMK.Q	1462		20.38%	13.54%
Q01813	PFKP 6-phosphofructokinase type C	K.FTTDDSIC*VLGISK.R	718		20.30%	13.46%
Q8TD19	NEK9 Serine/threonine-protein kinase Nek9	R.LLTFGC*NK.C	623		20.02%	0.03%
Q96HE7	ERO1L ERO1-like protein alpha	K.IWNVIYEENC*FKPQTIK.R	208		19.88%	0.74%
O95613	PCNT Pericentrin	R.EDALLDSVEVGLSC*VGLEEKPEK.G	563		19.26%	2.94%
Q13263	TRIM28 Transcription intermediary factor 1-beta	R.DC*QLNAHK.D	232		19.26%	0.59%
A7E2Y1	MYH7B Myosin-7B	R.C*NGVLEGIR.I	744		18.72%	3.08%
Q9BSJ8	ESYT1 Extended synaptotagmin-1	K.AVYSTNC*PVWEEAFR.F	522		18.60%	1.53%
Q9C0C2	TNKS1BP1 182 kDa tankyrase-1-binding protein	R.EHGVGGVSQC*PEPGLR.H	1373		18.54%	0.22%
P21333	FLNA Filamin-A	K.VHSPSGALEEC*YVTEIDQDK.Y	2378		18.41%	19.30%
P62937	PPIA Peptidyl-prolyl cis-trans isomerase A	R.IIPGFMC*QGGDFTR.H	62		18.30%	28.54%
P25398	RPS12 40S ribosomal protein S12	K.LGEWVGLC*K.I	92		18.22%	0.80%
Q15365	PCBP1 Poly(rC)-binding protein 1	R.LVVPATQC*GSLIGK.G	109		18.17%	0.97%
Q15149	PLEC Plectin	R.C*VEDPETGLC*LLPLTDK.A	3008|3017		18.03%	3.12%
Q99590	SCAF11 Protein SCAF11	R.VGSSSSESC*AQDLPVLVGEEGEVK.K	478		17.87%	9.84%
P14866	HNRNPL Heterogeneous nuclear ribonucleoprotein L	K.QPAIMPGQSYGLEDGSC*SYK.D	472		17.78%	11.27%
P08238	HSP90AB1 Heat shock protein HSP 90-beta	R.GFEVVYMTEPIDEYC*VQQLK.E	521		17.57%	1.89%
I3L420	LSM14A Protein LSM14 homolog A	K.SFFDNISC*DDNR.E	BAD_ID		16.94%	10.55%
Q9BXP5	SRRT Serrate RNA effector molecule homolog	R.C*GIIHVR.G	640		16.68%	0.02%
P57721	PCBP3 Poly(rC)-binding protein 3	R.INISEGNC*PER.I	86		16.48%	0.99%
P62829	RPL23 60S ribosomal protein L23	R.ISLGLPVGAVINC*ADNTGAK.N	28		16.17%	1.93%
O75369	FLNB Filamin-B	R.APSVATVGSIC*DLNLK.I	2115		15.93%	2.42%
P55735	SEC13 Protein SEC13 homolog	R.FASGGC*DNLIK.L	187		15.86%	9.61%
O43175	PHGDH D-3-phosphoglycerate dehydrogenase	R.C*GEEIAVQFVDMVK.G	295		15.76%	2.93%
O43175	PHGDH D-3-phosphoglycerate dehydrogenase	K.NAGNC*LSPAVIVGLLK.E	369		15.43%	0.82%
P21333	FLNA Filamin-A	K.AHVVPC*FDASK.V	1157		15.08%	5.78%
P49454	CENPF Centromere protein F	K.INHLETC*LK.T	650		14.41%	0.82%
Q15365	PCBP1 Poly(rC)-binding protein 1	R.AITIAGVPQSVTEC*VK.Q	158		14.12%	1.34%
P62633	CNBP Cellular nucleic acid-binding protein	R.C*GESGHLAR.E	161		13.85%	0.97%
Q14789	GOLGB1 Golgin subfamily B member 1	R.SLLENQSLSSSC*ESLK.L	1569		13.76%	0.11%
O43390	HNRNPR Heterogeneous nuclear ribonucleoprotein R	K.SAFLC*GVMK.T	99		13.61%	8.41%
Q14151	SAFB2 Scaffold attachment factor B2	R.KFDFDAC*NEVPPAPK.E	361		13.13%	0.12%
P23528	CFL1 Cofilin-1	K.AVLFC*LSEDK.K	39		12.89%	14.08%
F8VP50	Uncharacterized protein	R.KTFPTVNPSTGEVIC*QVAEGDKEDVDK.A	63		12.76%	2.00%
P11908	PRPS2 Ribose-phosphate pyrophosphokinase 2	R.VAILVDDMADTC*GTIC*HAADK.L	226|230		12.73%	4.67%
P14618	PKM Pyruvate kinase isozymes M1/M2	R.NTGIIC*TIGPASR.S	49		12.49%	17.37%
P78527	PRKDC DNA-dependent protein kinase catalytic subunit	R.C*GAALAGHQLIR.G	25		12.42%	1.26%
P78527	PRKDC DNA-dependent protein kinase catalytic subunit	K.GLSSLLC*NFTK.S	232		12.21%	0.10%
P17655	CAPN2 Calpain-2 catalytic subunit	K.LPPGEYILVPSTFEPNKDGDFC*IR.V	498		12.12%	10.12%
P35579	MYH9 Myosin-9	K.KQELEEIC*HDLEAR.V	917		12.10%	1.92%
Q3YEC7	RABL6 Rab-like protein 6	K.VPTHVPVC*VLGNYR.D	172		11.85%	10.02%
Q14789	GOLGB1 Golgin subfamily B member 1	K.LPSTDQQESC*SSTPGLEEPLFK.A	1257		11.81%	1.14%
P26599	PTBP1 Polypyrimidine tract-binding protein 1	K.LSLDGQNIYNAC*C*TLR.I	250|251		11.69%	0.90%
P15880	RPS2 40S ribosomal protein S2	R.C*GSVLVR.L	188		11.67%	11.06%
Q9P2E9	RRBP1 Ribosome-binding protein 1	R.ELC*HTQSSHASLR.A	892		11.36%	0.87%
O43175	PHGDH D-3-phosphoglycerate dehydrogenase	K.VLISDSLDPC*C*R.K	18|19		11.28%	0.43%
P49792	RANBP2 E3 SUMO-protein ligase RanBP2	K.TGEEDEEEFFC*NR.A	1196		10.88%	2.31%
Q9Y520	PRRC2C Protein PRRC2C	R.IAC*GPPQAK.L	223		9.98%	0.82%
P49454	CENPF Centromere protein F	K.ILHDQHC*QMSSK.M	1426		9.88%	0.04%
P61978	HNRNPK Heterogeneous nuclear ribonucleoprotein K	K.IIPTLEEGLQLPSPTATSQLPLESDAVEC*LNYQHYK.G	132		9.82%	0.12%
Q96CX2	KCTD12 BTB/POZ domain-containing protein KCTD12	R.C*TVVSVPDSLLWR.M	50		9.61%	8.40%
Q16658	FSCN1 Fascin	K.VGKDELFALEQSC*AQVVLQAANER.N	260		9.59%	5.71%
P07814	EPRS Bifunctional glutamate/proline--tRNA ligase	K.ERPTPSLNNNC*TTSEDSLVLYNR.V	744		9.52%	1.64%
P04075	ALDOA Fructose-bisphosphate aldolase A	R.YASIC*QQNGIVPIVEPEILPDGDHDLK.R	178		9.47%	7.57%
P49792	RANBP2 E3 SUMO-protein ligase RanBP2	K.C*AAC*QNPR.K	1499|1502		9.35%	0.37%
O43175	PHGDH D-3-phosphoglycerate dehydrogenase	K.EELIAELQDC*EGLIVR.S	48		9.21%	0.33%
P15121	AKR1B1 Aldose reductase	R.HIDC*AHVYQNENEVGVAIQEK.L	45		9.12%	7.54%
P60763	RAC3 Ras-related C3 botulinum toxin substrate 3	R.AVLC*PPPVK.K	178		8.92%	2.46%
P48147	PREP Prolyl endopeptidase	R.LWYC*DLQQESSGIAGILK.W	264		8.75%	5.64%
P55786	NPEPPS Puromycin-sensitive aminopeptidase	R.LPADVSPINYSLC*LKPDLLDFTFEGK.L	66		8.67%	3.34%
P35579	MYH9 Myosin-9	K.KLEEEQIILEDQNC*K.L	988		8.66%	5.66%
P34932	HSPA4 Heat shock 70 kDa protein 4	K.ELTSTC*SPIISK.P	779		8.55%	5.35%

P21333	FLNA Filamin-A	R.TPC*EEILVK.H	2601		8.51%	0.52%
P09132	SRP19 Signal recognition particle 19 kDa protein	K.QEDGSLC*LVQFPSR.K	94		8.31%	0.07%
P17987	TCP1 T-complex protein 1 subunit alpha	R.SLHDALC*VVK.R	397		8.29%	0.99%
Q16643	DBN1 Drebrin	K.VMYGFC*SVK.D	68		8.21%	0.81%
P09132	SRP19 Signal recognition particle 19 kDa protein	R.FIC*IYPAYLNNK.K	17		8.20%	5.31%
P21333	FLNA Filamin-A	K.LQVEPAVDTSGVQC*YGPGIEGQGVFR.E	1260		8.19%	1.22%
Q92945	KHSRP Far upstream element-binding protein 2	K.C*GLVIGR.G	436		8.15%	0.12%
P41252	IARS Isoleucine--tRNA ligase, cytoplasmic	R.NNDLC*YWVPELVR.E	433		8.09%	5.39%
Q9P2E9	RRBP1 Ribosome-binding protein 1	R.SKC*EELSGLHGQLQEAR.A	933		8.03%	4.41%
Q09666	AHNAK Neuroblast differentiation-associated protein AHNA	K.LEGDLTGPSVGVEVPDVELEC*PDAK.L	1900		7.95%	0.85%
Q16643	DBN1 Drebrin	K.APPPVFYNKPPEIDITC*WDADPVPEEEEGFEGGD.-	632		7.79%	0.39%
Q15366	PCBP2 Poly(rC)-binding protein 2	R.AITIAGIPQSIIEC*VK.Q	158		7.49%	0.70%
Q9UBF6	RNF7 RING-box protein 2	R.C*PLC*QQDWVVQR.I	99|102		7.49%	3.86%
P49790	NUP153 Nuclear pore complex protein Nup153	K.AGSSWQC*DTC*LLQNK.V	664|667		7.44%	2.34%
P21333	FLNA Filamin-A	R.VQVQDNEGC*PVEALVK.D	717		7.39%	2.19%
P49792	RANBP2 E3 SUMO-protein ligase RanBP2	K.EGQWDC*SAC*LVQNEGSSTK.C	1485|1488		7.32%	0.68%
P14625	HSP90B1 Endoplasmin	K.GYEVIYLTEPVDEYC*IQALPEFDGK.R	576		7.28%	3.32%
P21283	ATP6V1C1 V-type proton ATPase subunit C 1	R.SSNVLSEDQDSYLC*NVTLFR.K	225		7.26%	3.53%
P14923	JUP Junction plakoglobin	R.AGDKDDITEPAVC*ALR.H	457		7.21%	4.23%
Q86W42	THOC6 THO complex subunit 6 homolog	R.GHTDYIHC*LALR.E	173		7.13%	0.66%
P13639	EEF2 Elongation factor 2	R.YVEPIEDVPC*GNIVGLVGVDQFLVK.T	466		6.92%	0.73%
P60660	MYL6 Myosin light polypeptide 6	K.MTEEEVEMLVAGHEDSNGC*INYEAFVR.H	138		6.75%	2.81%
Q9BTE3	MCMBP Mini-chromosome maintenance complex-binding protei	K.FTVNLSGC*PR.N	396		6.74%	2.79%
Q16643	DBN1 Drebrin	K.EGTQASEGYFSQSQEEEFAQSEELC*AK.A	613		6.70%	0.78%
P15170	GSPT1 Eukaryotic peptide chain release factor GTP-bindin	R.TAGTIC*LETFK.D	464		6.68%	2.71%
P14174	MIF Macrophage migration inhibitory factor	K.LLC*GLLAER.L	81		6.64%	0.12%
O94776	MTA2 Metastasis-associated protein MTA2	K.AMSTLVPQGGPVLC*R.D	261		6.60%	2.60%
P49792	RANBP2 E3 SUMO-protein ligase RanBP2	K.C*IAC*QNPGK.Q	1626|1629		6.56%	0.05%
P18754	RCC1 Regulator of chromosome condensation	K.VASGNDHLVMLTADGDLYTLGC*GEQGQLGR.V	198		6.47%	0.17%
P13010	XRCC5 X-ray repair cross-complementing protein 5	R.LFQC*LLHR.A	493		6.42%	1.44%
P49792	RANBP2 E3 SUMO-protein ligase RanBP2	R.C*IAC*QNTK.S	1435|1438		6.28%	0.55%
P05023	ATP1A1 Sodium/potassium-transporting ATPase subunit alpha	K.NLEAVETLGSTSTIC*SDK.T	374		6.27%	1.71%
P53634	CTSC Dipeptidyl peptidase 1	R.GTDEC*AIESIAVAATPIPK.L	448		6.04%	1.80%
P13010	XRCC5 X-ray repair cross-complementing protein 5	K.ETVYC*LNDDDETEVLK.E	296		5.88%	0.22%
P26641	EEF1G Elongation factor 1-gamma	K.AAAPAPEEEMDEC*EQALAAEPK.A	266		5.79%	1.78%
Q9UHB6	LIMA1 LIM domain and actin-binding protein 1	R.ETC*VEC*QK.T	390|393		5.77%	0.73%
P31943	HNRNPH1 Heterogeneous nuclear ribonucleoprotein H	R.GLPWSC*SADEVQR.F	22		5.71%	1.53%
P78527	PRKDC DNA-dependent protein kinase catalytic subunit	R.VEQLFQVMNGILAQDSAC*SQR.A	3781		5.67%	1.29%
Q9C0C2	TNKS1BP1 182 kDa tankyrase-1-binding protein	R.C*PARPPPSGSQGLLEEMLAASSSK.A	1443		5.66%	1.26%
P33992	MCM5 DNA replication licensing factor MCM5	R.C*SVLAAANSVFGR.W	482		5.61%	0.81%
Q14974	KPNB1 Importin subunit beta-1	R.ESC*LEAYTGIVQGLK.G	765		5.61%	1.47%
P13639	EEF2 Elongation factor 2	R.ETVSEESNVLC*LSK.S	591		5.58%	0.95%
P49454	CENPF Centromere protein F	R.C*YQDLHAEYESLR.D	752		5.57%	1.14%
P08238	HSP90AB1 Heat shock protein HSP 90-beta	R.VFIMDSC*DELIPEYLNFIR.G	366		5.54%	1.09%
P42677	RPS27 40S ribosomal protein S27	R.LTEGC*SFR.R	77		5.32%	0.97%
Q96J01	THOC3 THO complex subunit 3	R.GHGDSVDQLC*WHPSNPDLFVTASGDK.T	106		5.28%	0.74%
O00299	CLIC1 Chloride intracellular channel protein 1	R.EEFASTC*PDDEEIELAYEQVAK.A	223		5.26%	0.70%
O75131	CPNE3 Copine-3	K.NC*LNPQFSK.T	54		5.26%	0.48%
P08514	ITGA2B Integrin alpha-IIb	K.TPVSC*FNIQMC*VGATGHNIPQK.L	515|521		5.25%	0.69%
P09234	SNRPC U1 small nuclear ribonucleoprotein C	K.FYC*DYC*DTYLTHDSPSVR.K	6|9		5.13%	0.45%
J3KR12	Uncharacterized protein	R.SLLINAVEASC*IR.T	188		5.11%	0.43%
P60981	DSTN Destrin	K.HEC*QANGPEDLNR.A	135		5.09%	0.47%
P13489	RNH1 Ribonuclease inhibitor	R.ELDLSNNC*LGDAGILQLVESVR.Q	409		5.04%	0.39%
O43390	HNRNPR Heterogeneous nuclear ribonucleoprotein R	K.KKNRGFC*FLEYEDHKSAAQARRR.L	292		4.98%	0.38%
Q9NQT4	EXOSC5 Exosome complex component RRP46	K.GLYSDTELQQC*LAAAQAASQHVFR.F	209		4.96%	0.34%
P46060	RANGAP1 Ran GTPase-activating protein 1	K.LDLNGNTLGEEGC*EQLQEVLEGFNMAK.V	338		4.95%	0.32%
P62241	RPS8 40S ribosomal protein S8	K.LLAC*IASR.P	174		4.94%	0.22%
P13489	RNH1 Ribonuclease inhibitor	K.LESC*GVTSDNC*R.D	209|216		4.92%	0.23%
P25398	RPS12 40S ribosomal protein S12	K.VVGC*SC*VVVK.D	106|108		4.89%	0.25%
P60174	TPI1 Triosephosphate isomerase	K.VPADTEVVC*APPTAYIDFAR.Q	42		4.88%	0.20%
P55769	NHP2L1 NHP2-like protein 1	K.LLDLVQQSC*NYK.Q	30		4.83%	0.11%

P46060	RANGAP1 Ran GTPase-activating protein 1	R.QVEVINFGDC*LVR.S	274		4.83%	0.11%
P13639	EEF2 Elongation factor 2	R.C*LYASVLTAQPR.L	728		4.81%	0.08%
Q16850	CYP51A1 Lanosterol 14-alpha demethylase	R.C*IGENFAYVQIK.T	449		4.80%	0.05%
P04899	GNAI2 Guanine nucleotide-binding protein G(i) subunit al	K.EIYTHFTC*ATDTK.N	326		4.80%	0.05%
P13639	EEF2 Elongation factor 2	R.C*ELLYEGPPDDEAAMGIK.S	369		4.79%	0.06%
P60709	ACTB Actin, cytoplasmic 1	K.C*DVDIR.K	285		4.77%	0.01%
P17655	CAPN2 Calpain-2 catalytic subunit	R.NEC*LEAGTLFQDPSFPAIPSALGFK.E	39		4.76%	0.00%
P60174	TPI1 Triosephosphate isomerase	R.IIYGGSVTGATC*K.E	218		4.76%	0.00%
P26639	TARS Threonine--tRNA ligase, cytoplasmic	R.C*GPLIDLC*R.G	254|261		4.76%	0.00%
P08107	HSPA1B Heat shock 70 kDa protein 1A/1B	R.ARFEELC*SDLFR.S	BAD_ID		4.76%	0.00%
A6NE09	RPSAP58 Protein RPSAP58	R.ADHQPLTEASYVNLPTIALC*NTDSPLR.Y	BAD_ID		4.76%	0.00%
P49454	CENPF Centromere protein F	R.LMEIC*ESLEK.T	76		4.76%	0.00%
P35520	CBS Cystathionine beta-synthase	R.C*VVILPDSVR.N	370		4.76%	0.00%
Q13838	DDX39B Spliceosome RNA helicase DDX39B	K.HFILDEC*DK.M	198		4.76%	0.00%
Q13526	PIN1 Peptidyl-prolyl cis-trans isomerase NIMA-interacti	K.SGEEDFESLASQFSDC*SSAK.A	113		4.76%	0.00%
Q04760	GLO1 Lactoylglutathione lyase	R.GFGHIGIAVPDVYSAC*K.R	139		4.76%	0.00%
P62273	RPS29 40S ribosomal protein S29	K.YGLNMC*R.Q	39		4.76%	0.00%
Q9UHD1	CHORDC1 Cysteine and histidine-rich domain-containing prot	R.TTDFSDFLSIVGC*TK.G	59		4.76%	0.00%
P37198	NUP62 Nuclear pore glycoprotein p62	K.DIIEHLNTSGAPADTSDPLQQIC*K.I	475		4.76%	0.00%
P22061	PCMT1 Protein-L-isoaspartate(D-aspartate) O-methyltransf	K.ALDVGSGSGILTAC*FAR.M	95		4.76%	0.00%
P25398	RPS12 40S ribosomal protein S12	K.LVEALC*AEHQINLIK.V	69		4.76%	0.00%
P15153	RAC2 Ras-related C3 botulinum toxin substrate 2	K.YLEC*SALTQR.G	157		4.76%	0.00%
P62316	SNRPD2 Small nuclear ribonucleoprotein Sm D2	R.HC*NMVLENVK.E	63		4.76%	0.00%
Q9BWD1	ACAT2 Acetyl-CoA acetyltransferase, cytosolic	K.VNIEGGAIALGHPLGASGC*R.I	360		4.76%	0.00%
P48643	CCT5 T-complex protein 1 subunit epsilon	K.ETGANLAIC*QWGFDDEANHLLLQNNLPAVR.W	302		4.76%	0.00%
P40227	CCT6A T-complex protein 1 subunit zeta	K.NAIDDGC*VVPGAGAVEVAMAEALIK.H	406		4.76%	0.00%
P63244	GNB2L1 Guanine nucleotide-binding protein subunit beta-2-	K.TNHIGHTGYLNTVTVSPDGSLC*ASGGK.D	207		4.76%	0.00%
P49711	CTCF Transcriptional repressor CTCF	R.YHDPNFVPAAFVC*SK.C	557		4.76%	0.00%
P09651	HNRNPA1 Heterogeneous nuclear ribonucleoprotein A1	R.SHFEQWGTLTDC*VVMR.D	43		4.76%	0.00%
P07900	HSP90AA1 Heat shock protein HSP 90-alpha	R.VFIMDNC*EELIPEYLNFIR.G	374		4.76%	0.00%
P09651	HNRNPA1 Heterogeneous nuclear ribonucleoprotein A1	K.YHTVNGHNC*EVR.K	175		4.76%	0.00%
Q96SZ5	ADO 2-aminoethanethiol dioxygenase	R.AEYTEASGPC*ILTPHR.D	183		4.76%	0.00%
P55072	VCP Transitional endoplasmic reticulum ATPase	K.LADDVDLEQVANETHGHVGADLAALC*SEAALQAIR.K	415		4.76%	0.00%
P08670	VIM Vimentin	R.QVQSLTC*EVDALK.G	328		4.76%	0.00%
Q9H3K6	BOLA2B BolA-like protein 2	R.LVNAC*LAEELPHIHAFEQK.T	59		4.76%	0.00%
Q96CS3	FAF2 FAS-associated factor 2	R.NTLC*APEVISLINTR.M	194		4.76%	0.00%
Q9UMS4	PRPF19 Pre-mRNA-processing factor 19	R.IWSVPNASC*VQVVR.A	298		4.76%	0.00%
P35222	CTNNB1 Catenin beta-1	R.NLALC*PANHAPLR.E	520		4.76%	0.00%
P27348	YWHAQ 14-3-3 protein theta	R.YDDMATC*MK.A	25		4.76%	0.00%
Q9UKX7	NUP50 Nuclear pore complex protein Nup50	R.ADTNLGNILLNVLIPPNMPC*TR.T	416		4.76%	0.00%
Q14980	NUMA1 Nuclear mitotic apparatus protein 1	K.APVPSTC*SSTFPEELSPPSHQAK.R	160		4.76%	0.00%
P02545	LMNA Prelamin-A/C	K.AQNTWGC*GNSLR.T	522		4.76%	0.00%
P46060	RANGAP1 Ran GTPase-activating protein 1	R.C*HWSDMFTGR.L	82		4.76%	0.00%
Q16543	CDC37 Hsp90 co-chaperone Cdc37	R.C*IDSGLWVPNSK.A	336		4.76%	0.00%
Q13613	MTMR1 Myotubularin-related protein 1	R.C*SQPLVGPNDKR.C	305		4.76%	0.00%
O95292	VAPB Vesicle-associated membrane protein-associated pro	R.C*VFELPAENDKPHDVEINK.I	121		4.76%	0.00%
Q9BW27	NUP85 Nuclear pore complex protein Nup85	K.EADASPASAGIC*R.I	230		4.76%	0.00%
Q14974	KPNB1 Importin subunit beta-1	K.ESTLEAIGYIC*QDIDPEQLQDK.S	158		4.76%	0.00%
Q9UKF6	CPSF3 Cleavage and polyadenylation specificity factor su	R.FC*NTVHDIVNR.G	223		4.76%	0.00%
O43237	DYNC1LI2 Cytoplasmic dynein 1 light intermediate chain 2	R.GPLTSGSDEENVALPLGDNVLTHNLGIPVLVVC*TK.C	231		4.76%	0.00%
P78527	PRKDC DNA-dependent protein kinase catalytic subunit	R.HEC*MAPLTALVK.H	2093		4.76%	0.00%
Q13613	MTMR1 Myotubularin-related protein 1	K.INSNYEFC*DTYPAIIVVPTSVK.D	258		4.76%	0.00%
Q08378	GOLGA3 Golgin subfamily A member 3	K.IPDC*PVPASLLEELLRPPPAVSK.E	1403		4.76%	0.00%
Q9BXB4	OSBPL11 Oxysterol-binding protein-related protein 11	R.LQIC*TQHHTEAIGK.N	153		4.76%	0.00%
P04899	GNAI2 Guanine nucleotide-binding protein G(i) subunit al	R.LWADHGVQAC*FGR.S	140		4.76%	0.00%
Q02952	AKAP12 A-kinase anchor protein 12	K.NEDFAAHPGEDAVPTGPDC*QAK.S	1479		4.76%	0.00%
Q5VSL9	FAM40A Protein FAM40A	R.NLFSC*INLLR.I	668		4.76%	0.00%
Q9ULV4	CORO1C Coronin-1C	K.NMQEPIALHEMDTSNGVLLPFYDPDTSIIYLC*GK.G	283		4.76%	0.00%
P31150	GDI1 Rab GDP dissociation inhibitor alpha	K.NTNDANSC*QIIIPQNQVNR.K	317		4.76%	0.00%
P15121	AKR1B1 Aldose reductase	K.YKPAVNQIEC*HPYLTQEK.L	187		4.76%	0.00%
Q86WB0	ZC3HC1 Nuclear-interacting partner of ALK	K.WAGKPFELSPLVC*AK.Y	102		4.76%	0.00%
P13639	EEF2 Elongation factor 2	R.SNTGGQAFPQC*VFDHWQILPGDPFDNSSR.P	812		4.76%	0.00%
P49368	CCT3 T-complex protein 1 subunit gamma	R.TLIQNC*GASTIR.L	455		4.76%	0.00%

Q9BW27	NUP85 Nuclear pore complex protein Nup85	K.WQHWHEEC*ER.Y	265		4.76%	0.00%
P17987	TCP1 T-complex protein 1 subunit alpha	K.VLC*ELADLQDK.E	76		4.76%	0.00%
Q14103	HNRNPD Heterogeneous nuclear ribonucleoprotein D0	R.GFC*FITFK.E	226		4.76%	0.00%
P62306	SNRPF Small nuclear ribonucleoprotein F	R.C*NNVLYIR.G	66		4.76%	0.00%
Q9P258	RCC2 Protein RCC2	R.LIEGLSHEVIVSAAC*GR.N	209		4.76%	0.00%
P26641	EEF1G Elongation factor 1-gamma	R.WFLTC*INQPQFR.A	194		4.76%	0.00%
Q92841	DDX17 Probable ATP-dependent RNA helicase DDX17	R.C*TYLVLDEADR.M	319		4.76%	0.00%
P78527	PRKDC DNA-dependent protein kinase catalytic subunit	K.ITAQSIEELC*AVNLYGPDAQVDR.S	1432		4.76%	0.00%
P17655	CAPN2 Calpain-2 catalytic subunit	K.LEEEDEDEEDGESGC*TFLVGLIQK.H	405		4.76%	0.00%
O15067	PFAS Phosphoribosylformylglycinamidine synthase	R.LGGTALAQC*FSQLGEHPPDLDLPENLVR.A	871		4.76%	0.00%
Q13867	BLMH Bleomycin hydrolase	K.LNSDPQFVLAQNVGTTHDLLDIC*LK.R	40		4.76%	0.00%
P78527	PRKDC DNA-dependent protein kinase catalytic subunit	K.LPVLAGC*LK.G	223		4.76%	0.00%
O95757	HSPA4L Heat shock 70 kDa protein 4L	R.NFDEALVDYFC*DEFK.T	245		4.76%	0.00%
P30153	PPP2R1A Serine/threonine-protein phosphatase 2A 65 kDa reg	R.NLC*SDDTPMVR.R	174		4.76%	0.00%
P23921	RRM1 Ribonucleoside-diphosphate reductase large subunit	K.NQIIAC*NGSIQSIPEIPDDLK.Q	662		4.76%	0.00%
P55072	VCP Transitional endoplasmic reticulum ATPase	R.QAAPC*VLFFDELDSIAK.A	572		4.76%	0.00%
O75131	CPNE3 Copine-3	K.VALNVSC*ANLLDK.D	15		4.76%	0.00%
P12081	HARS Histidine--tRNA ligase, cytoplasmic	K.VPC*VGLSIGVER.I	379		4.76%	0.00%
Q8NFH3	NUP43 Nucleoporin Nup43	R.VPLHC*VDR.H	222		4.76%	0.00%
P48739	PITPNB Phosphatidylinositol transfer protein beta isoform	R.VVLPC*SVQEYQVGQLYSVAEASK.N	13		4.76%	0.00%
P38606	ATP6V1A V-type proton ATPase catalytic subunit A	K.YSNSDVIIYVGC*GER.G	277		4.76%	0.00%
P50991	CCT4 T-complex protein 1 subunit delta	K.AQDIEAGDGTTSVVIIAGSLLDSC*TK.L	120		4.76%	0.00%
P13639	EEF2 Elongation factor 2	K.EGALC*EENMR.G	693		4.76%	0.00%
P61081	UBE2M NEDD8-conjugating enzyme Ubc12	K.LVIC*PDEGFYK.S	65		4.76%	0.00%
Q9H4A4	RNPEP Aminopeptidase B	R.AFFPC*FDTPAVK.Y	181		4.76%	0.00%
O95757	HSPA4L Heat shock 70 kDa protein 4L	R.AQFEQLC*ASLLAR.V	310		4.76%	0.00%
P62316	SNRPD2 Small nuclear ribonucleoprotein Sm D2	K.NNTQVLINC*R.N	46		4.76%	0.00%
O60361	NME2P1 Putative nucleoside diphosphate kinase	R.GDFC*IQVGR.N	94		4.76%	0.00%
Q9Y617	PSAT1 Phosphoserine aminotransferase	R.C*ADYVVTGAWSAK.A	98		4.76%	0.00%
P21333	FLNA Filamin-A	K.IVGPSGAAVPC*K.V	1018		4.76%	0.00%
P11940	PABPC1 Polyadenylate-binding protein 1	K.ALYDTFSAFGNILSC*K.V	128		4.76%	0.00%
P50991	CCT4 T-complex protein 1 subunit delta	K.IGLIQFC*LSAPK.T	252		4.76%	0.00%
P49458	SRP9 Signal recognition particle 9 kDa protein	K.VTDDLVC*LVYK.T	48		4.76%	0.00%
P51991	HNRNPA3 Heterogeneous nuclear ribonucleoprotein A3	K.YHTINGHNC*EVK.K	196		4.76%	0.00%
P33992	MCM5 DNA replication licensing factor MCM5	K.AIAC*LLFGGSR.K	355		4.76%	0.00%
P13797	PLS3 Plastin-3	K.AVGDGIVLC*K.M	167		4.76%	0.00%
Q14697	GANAB Neutral alpha-glucosidase AB	R.DEADVLEVDQGFDDHNLPC*DVIWLDIEHADGK.R	423		4.76%	0.00%
P27694	RPA1 Replication protein A 70 kDa DNA-binding subunit	K.DSLVDIIGIC*K.S	323		4.76%	0.00%
O75643	SNRNP200 U5 small nuclear ribonucleoprotein 200 kDa helicas	R.LTAIDILTTC*AADIQR.Q	1580		4.76%	0.00%
P48643	CCT5 T-complex protein 1 subunit epsilon	K.MLVIEQC*K.N	377		4.76%	0.00%
Q9UKX7	NUP50 Nuclear pore complex protein Nup50	K.NNVLIVC*VPNPPIDEK.N	428		4.76%	0.00%
Q99961	SH3GL1 Endophilin-A2	K.QNFIDPLQNLC*EK.D	147		4.76%	0.00%
Q9Y6Y8	SEC23IP SEC23-interacting protein	R.SIIEC*VDDFR.V	467		4.76%	0.00%
Q9UGP4	LIMD1 LIM domain-containing protein 1	R.TPSVSAPLALSC*PR.Q	305		4.76%	0.00%
P11413	G6PD Glucose-6-phosphate 1-dehydrogenase	R.TQVC*GILR.E	13		4.76%	0.00%
P60953	CDC42 Cell division control protein 42 homolog	K.YVEC*SALTQK.G	157		4.76%	0.00%
Q86X55	CARM1 Histone-arginine methyltransferase CARM1	R.C*LFQSPLFAK.A	420		4.76%	0.00%
Q16850	CYP51A1 Lanosterol 14-alpha demethylase	R.TPQTVAGYTIPPGHQVC*VSPTVNQR.L	402		4.76%	0.00%
P00338	LDHA L-lactate dehydrogenase A chain	R.VIGSGC*NLDSAR.F	163		4.76%	0.00%
P30086	PEBP1 Phosphatidylethanolamine-binding protein 1	R.APVAGTC*YQAEWDDYVPK.L	168		4.76%	0.00%
P00338	LDHA L-lactate dehydrogenase A chain	K.DDVFLSVPC*ILGQNGISDLVK.V	293		4.76%	0.00%
P12277	CKB Creatine kinase B-type	R.FC*TGLTQIETLFK.S	254		4.76%	0.00%
P23528	CFL1 Cofilin-1	K.HELQANC*YEEVK.D	139		4.76%	0.00%
P17987	TCP1 T-complex protein 1 subunit alpha	K.ILATGANVILTTGGIDDMC*LK.Y	296		4.76%	0.00%
P49368	CCT3 T-complex protein 1 subunit gamma	K.IPGGIIEDSC*VLR.G	213		4.76%	0.00%
P12004	PCNA Proliferating cell nuclear antigen	K.LMDLDVEQLGIPEQEYSC*VVK.M	135		4.76%	0.00%
P14618	PKM Pyruvate kinase isozymes M1/M2	K.PVIC*ATQMLESMIK.K	326		4.76%	0.00%
P06733	ENO1 Alpha-enolase	R.SGETEDTFIADLVVGLC*TGQIK.T	389		4.76%	0.00%
P39687	ANP32A Acidic leucine-rich nuclear phosphoprotein 32 fami	K.SLDLFNC*EVTNLNDYR.E	123		4.76%	0.00%
P46782	RPS5 40S ribosomal protein S5	K.TIAEC*LADELINAAK.G	172		4.76%	0.00%
Q15370	TCEB2 Transcription elongation factor B polypeptide 2	K.TLGEC*GFTSQTAR.P	60		4.76%	0.00%
P47756	CAPZB F-actin-capping protein subunit beta	K.DYLLC*DYNR.D	62		4.76%	0.00%

Q92598	HSPH1 Heat shock protein 105 kDa	R.SVLDAAQIVGLNC*LR.L	167		4.76%	0.00%
P50395	GDI2 Rab GDP dissociation inhibitor beta	R.VIC*ILSHPIK.N	302		4.76%	0.00%
Q15185	PTGES3 Prostaglandin E synthase 3	K.HLNEIDLFHC*IDPNDSK.H	58		4.76%	0.00%
P63244	GNB2L1 Guanine nucleotide-binding protein subunit beta-2-	K.LWNTLGVC*K.Y	138		4.76%	0.00%
P63244	GNB2L1 Guanine nucleotide-binding protein subunit beta-2-	R.YWLC*AATGPSIK.I	249		4.76%	0.00%
P50990	CCT8 T-complex protein 1 subunit theta	K.IAVYSC*PFDGMITETK.G	244		4.76%	0.00%
P27348	YWHAQ 14-3-3 protein theta	R.SIC*TTVLELLDK.Y	94		4.76%	0.00%
Q92945	KHSRP Far upstream element-binding protein 2	K.VQQAC*EMVMDILR.E	296		4.76%	0.00%
Q9GZZ1	NAA50 N-alpha-acetyltransferase 50	K.MLNHVLNIC*EK.D	100		4.76%	0.00%
P37802	TAGLN2 Transgelin-2	K.DGTVLC*ELINALYPEGQAPVK.K	63		4.76%	0.00%
P61978	HNRNPK Heterogeneous nuclear ribonucleoprotein K	K.GSDFDC*ELR.L	145		4.76%	0.00%
P17987	TCP1 T-complex protein 1 subunit alpha	K.IAC*LDFSLQK.T	236		4.76%	0.00%
P17987	TCP1 T-complex protein 1 subunit alpha	R.IC*DDELILIK.N	357		4.76%	0.00%
Q08211	DHX9 ATP-dependent RNA helicase A	K.LAAQSC*ALSLVR.Q	242		4.76%	0.00%
P14625	HSP90B1 Endoplasmin	R.LTESPC*ALVASQYGWSGNMER.I	645		4.76%	0.00%
Q9NZL4	HSPBP1 Hsp70-binding protein 1	R.AAQLIGTC*SQNVAAIQEQVLGLGALR.K	172		4.76%	0.00%
Q9BW27	NUP85 Nuclear pore complex protein Nup85	R.AC*MEEMHQVAIAAK.D	112		4.76%	0.00%
P09132	SRP19 Signal recognition particle 19 kDa protein	K.AVENPTATEIQDVC*SAVGLNVFLEK.N	53		4.76%	0.00%
Q15417	CNN3 Calponin-3	K.DGIILC*ELINK.L	59		4.76%	0.00%
O75643	SNRNP200 U5 small nuclear ribonucleoprotein 200 kDa helicas	R.DILC*GAADEVLAVLK.N	133		4.76%	0.00%
P55735	SEC13 Protein SEC13 homolog	R.DVAWAPSIGLPTSTIASC*SQDGR.V	234		4.76%	0.00%
Q04917	YWHAH 14-3-3 protein eta	K.ELETVC*NDVLSLLDK.F	97		4.76%	0.00%
P30153	PPP2R1A Serine/threonine-protein phosphatase 2A 65 kDa reg	R.ENVIMSQILPC*IK.E	329		4.76%	0.00%
Q9H0D6	XRN2 5-3 exoribonuclease 2	R.FDSNC*ITPGTEFMDNLAK.C	159		4.76%	0.00%
Q13185	CBX3 Chromobox protein homolog 3	K.GFTDADNTWEPEENLDC*PELIEAFLNSQK.A	69		4.76%	0.00%
Q9UL25	RAB21 Ras-related protein Rab-21	K.GIEELFLDLC*K.R	177		4.76%	0.00%
P07355	ANXA2 Annexin A2	K.GLGTDEDSLIEIIC*SR.T	133		4.76%	0.00%
Q09666	AHNAK Neuroblast differentiation-associated protein AHNA	K.GPFVEAEVPDVDLEC*PDAK.L	1833		4.76%	0.00%
P21283	ATP6V1C1 V-type proton ATPase subunit C 1	K.IDC*NLLEFK.-	376		4.76%	0.00%
Q09666	AHNAK Neuroblast differentiation-associated protein AHNA	K.LEGDLTGPSVDVEVPDVELEC*PDAK.L	2162		4.76%	0.00%
Q9BW27	NUP85 Nuclear pore complex protein Nup85	K.SEMVPSC*PFIYIIR.K	51		4.76%	0.00%
P04632	CAPNS1 Calpain small subunit 1	K.TDGFGIDTC*R.S	144		4.76%	0.00%
Q5RKV6	EXOSC6 Exosome complex component MTR3	K.VLC*AVSGPR.Q	64		4.76%	0.00%
P04632	CAPNS1 Calpain small subunit 1	R.YSDESGNMDFDNFISC*LVR.L	232		4.76%	0.00%
Q7RTV0	PHF5A PHD finger-like domain-containing protein 5A	R.IC*DEC*NYGSYQGR.C	46|49		4.76%	0.00%
P38606	ATP6V1A V-type proton ATPase catalytic subunit A	R.VLDALFPC*VQGGTTAIPGAFGC*GK.T	240|254		4.76%	0.00%
P21333	FLNA Filamin-A	R.ALGALVDSC*APGLC*PDWDSWDASKPVTNAR.E	205|210		4.76%	0.00%
P10768	ESD S-formylglutathione hydrolase	K.SVSAFAPIC*NPVLC*PWGK.K	176|181		4.76%	0.00%
P56270	MAZ Myc-associated zinc finger protein	K.NHAC*EMC*GK.A	281|284		4.76%	0.00%
P56270	MAZ Myc-associated zinc finger protein	K.LSHSDEKPYQC*PVC*QQR.F	309|312		4.76%	0.00%
P34932	HSPA4 Heat shock 70 kDa protein 4	R.C*TPAC*ISFGPK.N	34|38		4.76%	0.00%
P62241	RPS8 40S ribosomal protein S8	R.LDVGNFSWGSEC*C*TR.K	71|72		4.76%	0.00%
P30153	PPP2R1A Serine/threonine-protein phosphatase 2A 65 kDa reg	R.TSAC*GLFSVC*YPR.V	148|154		4.76%	0.00%
P56270	MAZ Myc-associated zinc finger protein	K.GPYIC*ALC*AK.E	192|195		4.76%	0.00%
P62826	RAN GTP-binding nuclear protein Ran	R.VC*ENIPIVLC*GNK.V	112|120		4.76%	0.00%
P52209	PGD 6-phosphogluconate dehydrogenase, decarboxylating	K.VGTGEPC*C*DWVGDEGAGHFVK.M	170|171		4.76%	0.00%
P55072	VCP Transitional endoplasmic reticulum ATPase	R.EAVC*IVLSDDTC*SDEK.I	69|77		4.76%	0.00%
P30153	PPP2R1A Serine/threonine-protein phosphatase 2A 65 kDa reg	K.EFC*ENLSADC*R.E	310|317		4.76%	0.00%
P68104	EEF1A1 Elongation factor 1-alpha 1	K.DGNASGTTLLEALDC*ILPPTRPTDK.P	234		4.63%	0.92%
Q99873	PRMT1 Protein arginine N-methyltransferase 1	K.VEDLTFTSPFC*LQVK.R	272		4.53%	0.46%
Q13642	FHL1 Four and a half LIM domains protein 1	R.FWHDTC*FR.C	65		4.53%	0.46%
P35579	MYH9 Myosin-9	K.VEDMAELTC*LNEASVLHNLK.E	91		4.53%	0.46%
Q14151	SAFB2 Scaffold attachment factor B2	K.ILDILGETC*K.S	224		4.46%	0.53%
P62937	PPIA Peptidyl-prolyl cis-trans isomerase A	K.KITIADC*GQLE.-	161		4.30%	0.92%
P49792	RANBP2 E3 SUMO-protein ligase RanBP2	K.EGQWDC*SVC*LVR.N	1612|1615		4.30%	0.92%
P46060	RANGAP1 Ran GTPase-activating protein 1	K.ILAAALTEC*HR.K	169		4.15%	1.07%
P62937	PPIA Peptidyl-prolyl cis-trans isomerase A	K.HTGPGILSMANAGPNTNGSQFFIC*TAK.T	115		4.15%	1.07%
P13797	PLS3 Plastin-3	K.TISSSLAVVDLIDAIQPGC*INYDLVK.S	566		4.06%	1.40%
P60660	MYL6 Myosin light polypeptide 6	K.ILYSQC*GDVMR.A	32		3.84%	1.01%
Q9P258	RCC2 Protein RCC2	K.AVQDLC*GWR.I	428		3.83%	1.62%

P05023	ATP1A1 Sodium/potassium-transporting ATPase subunit alpha	K.AC*VVHGSDLK.D	663		3.38%	0.66%
Q15185	PTGES3 Prostaglandin E synthase 3	R.SILC*C*LR.K	75|76		3.12%	1.94%
P13639	EEF2 Elongation factor 2	R.TFC*QLILDPIFK.V	290		2.88%	2.18%
P62937	PPIA Peptidyl-prolyl cis-trans isomerase A	K.GSC*FHR.I	52		2.66%	1.40%

Table 4A-5. Average percent oxidation for mitochondria localized cysteines from 1 mM H_2O_2-treated matrix-APEX analysis. Data was filtered for peptides with ratio values in 2 out of 3 replicates, with a standard deviation <30%.

UniProt ID	Description	Peptide Sequence	Residue	Mito	Average % Oxidation Matrix-APEX H2O2	% Standard Deviation
P00441	SOD1 Superoxide dismutase	K.GLTEGLHGFHVHEFGDNTAGC*TSAGPHFNPLS R.K	58	X	95.24%	0.00%
P00390	GSR Glutathione reductase, mitochondrial	K.VMWNTAVHSEFMHDHADYGFPSC*EGK.F	134	X	72.05%	0.29%
P43251	BTD Biotinidase	K.ILSGDPYC*EK.D	371		63.30%	0.96%
P21953	BCKDHB 2-oxoisovalerate dehydrogenase subunit beta, mitoc	K.NPC*IFFEPK.I	235	X	62.69%	3.56%
Q7Z7B0	FILIP1 Filamin-A-interacting protein 1	R.DKIAKGEC*GNSSLMAEVENLRKR.V	371		57.08%	1.47%
Q9NWU5	MRPL22 39S ribosomal protein L22, mitochondrial	R.RPAEIYHC*R.R	70	X	55.00%	1.75%
Q96PZ2	FAM111A Protein FAM111A	K.SKQKEDNHIFGRQDKASTEC*VK.F	181		54.70%	3.60%
Q13085	ACACA Acetyl-CoA carboxylase 1	R.TDC*NHIFLNFVPTVIMDPSK.I	1470	X	53.95%	4.85%
P62826	RAN GTP-binding nuclear protein Ran	R.VC*ENIPIVLC*GNK.V	112|120		53.45%	2.54%
Q9UGI8	TES Testin	K.MGLGHEQGFGAPC*LK.C	22		48.94%	2.38%
Q16762	TST Thiosulfate sulfurtransferase	K.KVDLSQPLIATC*R.K	248	X	46.69%	1.11%
O15091	KIAA0391 Mitochondrial ribonuclease P protein 3	K.TSFESWIISQMAGC*HSSIDVAK.S	151	X	46.15%	10.87%
P43897	TSFM Elongation factor Ts, mitochondrial	K.TGYSFVNC*K.K	64	X	39.17%	23.73%
Q8IYB8	SUPV3L1 ATP-dependent RNA helicase SUPV3L1, mitochondrial	R.YVFC*TAPINK.K	575	X	38.05%	28.83%
P07737	PFN1 Profilin-1	K.C*YEMASHLR.R	128		37.74%	28.30%
P05455	SSB Lupus La protein	K.IC*HQIEYYFGDFNLPR.D	18		29.02%	17.23%
P11177	PDHB Pyruvate dehydrogenase E1 component subunit beta,	R.PVGHC*LEAAAVLSK.E	249	X	27.49%	29.45%
Q7L2E3	DHX30 Putative ATP-dependent RNA helicase DHX30	R.C*QSGFAYHLFPR.S	786	X	27.28%	13.98%
P00390	GSR Glutathione reductase, mitochondrial	R.SFDSMISTNC*TEELENAGVEVLK.F	278	X	26.77%	1.21%
Q6UB35	MTHFD1L Monofunctional C1-tetrahydrofolate synthase, mitoc	K.RAGAFDAVPC*YHWSVGGK.G	828	X	26.38%	24.96%
Q9NWU1	OXSM 3-oxoacyl-	K.GPNHAVSTAC*TTGAHAVGDSFR.F	209	X	24.53%	1.31%
Q5JRX3	PITRM1 Presequence protease, mitochondrial	R.LLPDHTYSVVSGGDPLC*IPELTWEQLK.Q	241	X	23.10%	0.51%
Q99797	MIPEP Mitochondrial intermediate peptidase	K.VC*AAADMQLQVFYATLDQIYHGK.H	568	X	22.22%	24.69%
Q6PI48	DARS2 Aspartate--tRNA ligase, mitochondrial	R.SSHLGQEVTLC*GWIQYR.R	69	X	22.16%	23.33%
Q9H845	ACAD9 Acyl-CoA dehydrogenase family member 9, mitochondr	R.TVDLGLTGNHGVVHPSLADSANKFEENTYC*FG R.T	507	X	21.77%	0.71%
Q9BQ52	ELAC2 Zinc phosphodiesterase ELAC protein 2	R.YLFNC*GEGVQR.L	87	X	21.18%	15.96%
Q6PI48	DARS2 Aspartate--tRNA ligase, mitochondrial	K.ILC*EAPVESVVQVSGTVISR.P	108	X	21.11%	21.52%
Q9Y305	ACOT9 Acyl-coenzyme A thioesterase 9, mitochondrial	K.MQMFQLHGDEFC*PVLDATFVMVAR.D	194	X	18.99%	4.14%
P42704	LRPPRC Leucine-rich PPR motif-containing protein, mitocho	R.IHDVLC*K.L	863	X	18.87%	26.34%
P38117	ETFB Electron transfer flavoprotein subunit beta	K.EVIAVSC*GPAQC*QETIR.T	66|71	X	18.69%	27.86%
P34897	SHMT2 Serine hydroxymethyltransferase, mitochondrial	R.YYGGAEVVDEIELLC*QR.R	119	X	18.48%	14.26%
Q9H2U2	PPA2 Inorganic pyrophosphatase 2, mitochondrial	K.ILSC*GEVIHVK.I	180	X	17.61%	25.69%
Q96RQ3	MCCC1 Methylcrotonoyl-CoA carboxylase subunit alpha, mit	K.SIMAAAGVPVVEGYHGEDQSDQC*LK.E	190	X	16.45%	1.76%
O75323	GBAS Protein NipSnap homolog 2	K.LQFHNVKPEC*LEAYNK.I	85	X	15.94%	1.56%
Q6L8Q7	PDE12 2,5-phosphodiesterase 12	R.YIMAGFPVC*PK.L	180	X	15.77%	9.53%
Q9P2R7	SUCLA2 Succinyl-CoA ligase	R.C*DVIAQGIVMAVK.D	384	X	15.36%	16.70%
Q13085	ACACA Acetyl-CoA carboxylase 1	K.IIEEAPATIATPAVFEHMEQC*AVK.L	407	X	15.29%	12.16%
Q8NFF5	FLAD1 FAD synthase	R.LHYGTDPC*TGQPFR.F	236	X	15.14%	0.30%

O43615	TIMM44 Mitochondrial import inner membrane translocase su	K.QC*ENDIIPNVLEAMISGELDILK.D	319	X	13.99%	8.00%
O15067	PFAS Phosphoribosylformylglycinamidine synthase	R.LGGTALAQC*FSQLGEHPPDLDLPENLVR.A	871		13.70%	7.74%
P42126	ECI1 Enoyl-CoA delta isomerase 1, mitochondrial	R.YC*IGLNETQLGIIAPFWLK.D	173	X	13.33%	3.26%
Q99797	MIPEP Mitochondrial intermediate peptidase	R.ADKPHQDC*HFTIR.G	448	X	13.31%	0.42%
O75208	COQ9 Ubiquinone biosynthesis protein COQ9, mitochondria	K.DGSELILHFVTQC*NTR.L	153	X	13.21%	14.64%
Q8TCS8	PNPT1 Polyribonucleotide nucleotidyltransferase 1, mitoc	R.GQTQVLC*TVTFDSLESGIK.S	395	X	12.94%	7.70%
Q99714	HSD17B10 3-hydroxyacyl-CoA dehydrogenase type-2	K.KLGNNC*VFAPADVTSEK.D	58	X	12.88%	18.15%
O75390	CS Citrate synthase, mitochondrial	R.GFSIPEC*QK.L	101	X	12.75%	6.91%
Q8N4Q0	ZADH2 Zinc-binding alcohol dehydrogenase domain-containi	R.DC*PVPLPGDGDLLVR.N	55	X	12.57%	0.36%
Q6UB35	MTHFD1L Monofunctional C1-tetrahydrofolate synthase, mitoc	R.ASIGAGFIYPLVGTMSTMPGLPTRPC*FYDIDLDT ETEQVK.G	961	X	12.56%	0.48%
P00367	GLUD1 Glutamate dehydrogenase 1, mitochondrial	K.C*IAVGESDGSIWNPDGIDPK.E	327	X	12.13%	10.42%
P05165	PCCA Propionyl-CoA carboxylase alpha chain, mitochondri	K.MADEAVC*VGPAPTSK.S	111	X	11.86%	6.15%
Q99798	ACO2 Aconitate hydratase, mitochondrial	K.DHLVPDPGC*HYDQLIEINLSELKPHINGPFTPD LAHPVAEVGK.V	332	X	11.66%	0.42%
Q9HCC0	MCCC2 Methylcrotonoyl-CoA carboxylase beta chain, mitoch	K.AATGEEVSAEDLGGADLHC*R.K	267	X	11.65%	0.65%
Q7L2E3	DHX30 Putative ATP-dependent RNA helicase DHX30	R.RPC*TIQVPEPILR.K	346	X	11.48%	3.97%
P31040	SDHA Succinate dehydrogenase	R.GC*GPEKDHVYLQLHHLPPEQLATR.L	357	X	11.25%	5.62%
Q99798	ACO2 Aconitate hydratase, mitochondrial	R.VGLIGSC*TNSSYEDMGR.S	385	X	11.25%	2.16%
P23368	ME2 NAD-dependent malic enzyme, mitochondrial	R.C*LFASGSPFGPVK.L	441	X	11.16%	10.68%
O95571	ETHE1 Protein ETHE1, mitochondrial	R.QMFEPVSC*TFTYLLGDR.E	34	X	11.11%	0.34%
P00367	GLUD1 Glutamate dehydrogenase 1, mitochondrial	K.AKPYEGSILEADC*DILIPAASEK.Q	376	X	11.06%	10.91%
Q8TCS8	PNPT1 Polyribonucleotide nucleotidyltransferase 1, mitoc	K.SQIVMLEASAENILQQDFC*HAIK.V	242	X	10.94%	2.17%
Q9Y2S7	POLDIP2 Polymerase delta-interacting protein 2	R.DC*PHISQR.S	143	X	10.72%	0.79%
Q96AB3	ISOC2 Isochorismatase domain-containing protein 2, mitoc	K.TC*FSMVPALQQELDSRPQLR.S	84	X	10.69%	1.64%
Q5JRX3	PITRM1 Presequence protease, mitochondrial	K.PQDASC*LPALK.V	556	X	10.68%	3.32%
Q96RP9	GFM1 Elongation factor G, mitochondrial	R.YQPC*LPSTQEDVINK.Y	723	X	10.68%	0.84%
P21333	FLNA Filamin-A	K.AHVVPC*FDASK.V	1157		10.62%	8.28%
Q9NSE4	IARS2 Isoleucine--tRNA ligase, mitochondrial	K.GTGLVHTAPAHGMEDYGVASQHNLPMDC*LV DEDGVFTDVAGPELQNK.A	414	X	10.48%	1.10%
Q9NVH6	TMLHE Trimethyllysine dioxygenase, mitochondrial	K.HEYIEDVGEC*HNHMIGIGPVLNIYPWNK.E	308	X	10.17%	4.68%
P07954	FH Fumarate hydratase, mitochondrial	K.FEALAAHDALVELSGAMNTTAC*SLMK.I	333	X	10.09%	1.32%
P40926	MDH2 Malate dehydrogenase, mitochondrial	K.SQETEC*TYFSTPLLLGK.K	285	X	9.76%	7.06%
P28331	NDUFS1 NADH-ubiquinone oxidoreductase 75 kDa subunit, mit	K.DC*FIIYQGHHGDVGAPIADVILPGAAYTEK.S	564	X	9.71%	6.47%
Q6PI48	DARS2 Aspartate--tRNA ligase, mitochondrial	K.TAELLNAC*K.K	152	X	9.70%	10.50%
P23378	GLDC Glycine dehydrogenase	R.NEDAC*PVGTVSAAPWGSSSILPISWAYIK.M	795	X	9.57%	2.78%
Q9BSH5	HDHD3 Haloacid dehalogenase-like hydrolase domain-contai	R.LAHMEPVVAAHVGDNYLC*DYQGPR.A	196	X	9.41%	2.24%
Q6P2I3	FAHD2B Fumarylacetoacetate hydrolase domain-containing pr	K.TFDTFC*PLGPALVTK.D	215	X	9.39%	5.13%
O43837	IDH3B Isocitrate dehydrogenase	K.LGDGLFLQC*C*EEVAELYPK.I	232|233	X	9.37%	7.98%
P13639	EEF2 Elongation factor 2	R.SNTGGQAFPQC*VFDHWQILPGDPFDNSSRPSQ VVAETR.K	812		9.36%	6.51%
P30837	ALDH1B1 Aldehyde dehydrogenase X, mitochondrial	R.HEPVGVC*GQIIPWNFPLVMQGWK.L	179	X	9.34%	1.12%
Q86WA6	BPHL Valacyclovir hydrolase	R.VQC*PALIVHGEK.D	234	X	9.30%	7.26%
Q15031	LARS2 Probable leucine--tRNA ligase, mitochondrial	R.YWGTPIPIVHC*PVC*GPTPVPLEDLPVTLPNIASF TGK.G	464|467	X	9.12%	3.82%
P30084	ECHS1 Enoyl-CoA hydratase, mitochondrial	K.ALNALC*DGLIDELNQALK.T	62	X	8.99%	0.79%
O14561	NDUFAB1 Acyl carrier protein, mitochondrial	K.LMC*PQEIVDYIADK.K	140	X	8.99%	0.56%
Q96I99	SUCLG2 Succinyl-CoA ligase	R.SC*NGPVLVGSPQGGVDIEEVAASNPELIFK.E	162	X	8.96%	2.87%
Q9UGC7	MTRF1L Peptide chain release factor 1-like, mitochondrial	R.IVHLPTGVVSEC*QQER.S	274	X	8.84%	7.07%
P05165	PCCA Propionyl-CoA carboxylase alpha chain, mitochondri	R.C*LAAEDVVFIGPDTHAIQAMGDK.I	155	X	8.61%	2.35%
P07203	GPX1 Glutathione peroxidase 1	R.GLVVLGFPC*NQFGHQENAK.N	78	X	8.60%	3.33%
Q9BQ52	ELAC2 Zinc phosphodiesterase ELAC protein 2	R.DAIITC*NPEEFIVEALQLPNFQQSVQEYR.R	441	X	8.53%	1.20%
Q96GW9	MARS2 Methionine--tRNA ligase, mitochondrial	R.INPSETYPAFC*TTC*FPSEPGLVGPSVR.A	425|428	X	8.30%	2.88%
P54886	ALDH18A1 Delta-1-pyrroline-5-carboxylate synthase	K.C*EYPAAC*NALETLLIHR.D	606|612	X	8.29%	0.21%
Q9NUJ1	ABHD10 Abhydrolase domain-containing protein 10, mitochon	K.ALAIEEFC*K.S	100	X	8.27%	3.04%
Q8NFF5	FLAD1 FAD synthase	K.C*LSPGGHPTYRPAYLLENEEEER.N	561	X	8.26%	4.29%

Q9BQ69	MACROD1 O-acetyl-ADP-ribose deacetylase MACROD1	K.LEVDAIVNAANSSLLGGGGVDGC*IHR.A	186	X	8.17%	2.16%
Q96AB3	ISOC2 Isochorismatase domain-containing protein 2, mitoc	R.VLPGSSVLFLC*DMQEK.F	21	X	8.14%	2.00%
P11177	PDHB Pyruvate dehydrogenase E1 component subunit beta,	K.TNHLVTVEGGWPQFGVGAEIC*AR.I	306	X	8.12%	4.59%
Q6UB35	MTHFD1L Monofunctional C1-tetrahydrofolate synthase, mitoc	K.LHEADIVVLGSPKPEEIPLTWIQPGTTVLNC*SHDFLSGK.V	291	X	8.09%	1.04%
Q15118	PDK1	K.QFLDFGSVNAC*EK.T	71	X	7.87%	0.36%
Q9BYT8	NLN Neurolysin, mitochondrial	K.YNHAAC*FGLQPGC*LLPDGSR.M	451|458	X	7.70%	5.08%
Q9NSE4	IARS2 Isoleucine--tRNA ligase, mitochondrial	K.LASLIDGSSPVSILVWTTQPWTIPANEAVC*YMPESK.Y	311	X	7.69%	0.38%
P38646	HSPA9 Stress-70 protein, mitochondrial	K.DQLPADEC*NK.L	608	X	7.67%	0.39%
Q9Y6M9	NDUFB9 NADH dehydrogenase	R.HLESWC*VQR.D	31	X	7.61%	0.54%
P04179	SOD2 Superoxide dismutase	R.GHLQIAAC*PNQDPLQGTTGLIPLLGIDVWEHAYYLQYK.N	164	X	7.57%	4.87%
Q9H1K1	ISCU Iron-sulfur cluster assembly enzyme ISCU, mitochon	K.NVGTGLVGAPAC*GDVMK.L	69	X	7.50%	0.00%
Q15120	PDK3	K.HIGSIDPTC*NVADVVK.D	191	X	7.44%	2.42%
Q96CM8	ACSF2 Acyl-CoA synthetase family member 2, mitochondrial	K.AASGLLSIGLC*K.G	122	X	7.38%	3.70%
O75380	NDUFS6 NADH dehydrogenase	R.VIAC*DGGGGALGHPK.V	87	X	7.22%	1.03%
P63000	RAC1 Ras-related C3 botulinum toxin substrate 1	R.HHC*PNTPIILVGTK.L	105		7.03%	3.21%
P30048	PRDX3 Thioredoxin-dependent peroxide reductase, mitochon	K.AFQYVETHGEVC*PANWTPDSPTIK.P	229	X	7.00%	0.56%
Q9Y3D3	MRPS16 28S ribosomal protein S16, mitochondrial	R.HWIGC*GAHLSK.P	79	X	6.98%	3.13%
Q9NSE4	IARS2 Isoleucine--tRNA ligase, mitochondrial	K.VASVASTLETTFETISTLSGVDLENGTC*SHPLIPDK.A	364	X	6.94%	0.56%
Q96HY7	DHTKD1 Probable 2-oxoglutarate dehydrogenase E1 component	K.LVGC*AIIHVNGDSPEEVVR.A	392	X	6.85%	2.96%
Q9Y6G3	MRPL42 39S ribosomal protein L42, mitochondrial	R.TIVC*YHPSVDIPYEHTKPIPR.P	60	X	6.66%	2.61%
P13995	MTHFD2 Bifunctional methylenetetrahydrofolate dehydrogena	R.IC*NAVSPDKDVDGFHVINVGR.M	145	X	6.62%	0.84%
Q9H2U2	PPA2 Inorganic pyrophosphatase 2, mitochondrial	K.STHQC*WK.A	274	X	6.59%	1.59%
Q9H857	NT5DC2 5-nucleotidase domain-containing protein 2	R.FSDLYMASLSC*LLNYR.V	475	X	6.56%	2.55%
Q9BXW7	CECR5 Cat eye syndrome critical region protein 5	R.DLC*FSPGLMEASHVVNDVNEAVQLVFR.K	392	X	6.53%	2.50%
Q9Y676	MRPS18B 28S ribosomal protein S18b, mitochondrial	K.VVGNPC*PIC*R.D	105|108	X	6.50%	2.46%
P30042	C21orf33 ES1 protein homolog, mitochondrial	K.VVTTPAFMC*ETALHYIHDGIGAMVR.K	BAD_ID	X	6.46%	0.95%
P42765	ACAA2 3-ketoacyl-CoA thiolase, mitochondrial	R.IVGYFVSGC*DPSIMGIGPVPAISGALK.K	287	X	6.45%	0.30%
Q9BQP7	C20orf72 Uncharacterized protein C20orf72	R.GVAQTPGSVEEDALLC*GPVSK.H	79	X	6.40%	1.43%
J3KR12	Uncharacterized protein	K.DNVC*SPGGATIHALHFLESGGFR.S	158		6.37%	2.27%
O00330	PDHX Pyruvate dehydrogenase protein X component, mitoch	K.STVPHAYATADC*DLGAVLK.V	307	X	6.30%	2.17%
P14618	PKM Pyruvate kinase isozymes M1/M2	R.GIFPVLC*KDPVQEAWAEDVDLR.V	474		6.28%	2.15%
P36873	PPP1CC Serine/threonine-protein phosphatase PP1-gamma cat	K.IFC*C*HGGLSPDLQSMEQIR.R	171|172	X	6.24%	1.36%
P21953	BCKDHB 2-oxoisovalerate dehydrogenase subunit beta, mitoc	R.VC*GYDTPFPHIFEPFYIPDK.W	361	X	6.16%	1.98%
Q15118	PDK1	K.HYNTNHEADDWC*VPSR.E	421	X	6.12%	0.51%
O75521	ECI2 Enoyl-CoA delta isomerase 2, mitochondrial	R.ATFHTPFSHLGQSPEGC*SSYTFPK.I	282	X	6.10%	1.10%
P40939	HADHA Trifunctional enzyme subunit alpha, mitochondrial	K.EVEAVIPDHC*IFASNTSALPISEIAAVSK.R	470	X	6.08%	1.38%
Q12931	TRAP1 Heat shock protein 75 kDa, mitochondrial	R.SPAAEC*LSEK.E	573	X	5.91%	0.75%
P49411	TUFM Elongation factor Tu, mitochondrial	K.NMITGTAPLDGC*ILVVAANDGPMPQTR.E	147	X	5.84%	0.95%
Q07021	C1QBP Complement component 1 Q subcomponent-binding prot	K.ALVLDC*HYPEDEVGQEDEAESDIFSIR.E	186	X	5.76%	0.66%
P05165	PCCA Propionyl-CoA carboxylase alpha chain, mitochondri	R.LQVEHPVTEC*ITGLDLVQEMIR.V	363	X	5.75%	0.88%
P00505	GOT2 Aspartate aminotransferase, mitochondrial	K.IPEQSVLLLHAC*AHNPTGVDPR.P	212	X	5.75%	1.05%
Q9Y3D2	MSRB2 Methionine-R-sulfoxide reductase B2, mitochondrial	R.GQAGGGGPGTGPGLGEAGSLATC*ELPLAK.S	45	X	5.75%	0.89%
Q13085	ACACA Acetyl-CoA carboxylase 1	R.MMYGVSPWGDSPIDFEDSAHVPC*PR.G	500	X	5.72%	0.79%
P68104	EEF1A1 Elongation factor 1-alpha 1	K.SGDAAIVDMVPGKPMC*VESFSDYPPLGR.F	411		5.69%	0.79%
P23919	DTYMK Thymidylate kinase	K.LVEALC*AAGHR.A	31	X	5.69%	1.25%
Q9BPW8	NIPSNAP1 Protein NipSnap homolog 1	K.LHLDEDYPC*SLVGNWNTWYGEQDQAVHLWR.F	106	X	5.68%	0.27%
P31930	UQCRC1 Cytochrome b-c1 complex subunit 1, mitochondrial	K.YIYDQC*PAVAGYGPIEQLPDYNR.I	453	X	5.66%	0.89%
Q9BW92	TARS2 Threonine--tRNA ligase, mitochondrial	R.LALSTRPSGFLGDPC*LWDQAEQVLK.Q	506	X	5.65%	1.55%
P33991	MCM4 DNA replication licensing factor MCM4	R.C*HTTHSMALIHNR.S	331		5.64%	1.25%
O43175	PHGDH D-3-phosphoglycerate dehydrogenase	R.ALVDHENVISC*PHLGASTK.E	281		5.62%	0.57%
Q7Z7H8	MRPL10 39S ribosomal protein L10, mitochondrial	K.LMAVTEYIPPKPAIHPSC*LPSPPSPPQEEIGLIR.L	64	X	5.60%	1.19%

Q9BSH5	HDHD3 Haloacid dehalogenase-like hydrolase domain-contai	K.EHILPSLAHLLPALDC*LEGSTPGL.-	243	X	5.60%	0.89%
O75323	GBAS Protein NipSnap homolog 2	K.HYPC*TLVGTWNTWYGEQDQAVHLWR.Y	108	X	5.59%	0.74%
Q969Z0	TBRG4 Protein TBRG4	K.C*LELVEHFGPNELR.K	246	X	5.59%	1.44%
P42704	LRPPRC Leucine-rich PPR motif-containing protein, mitocho	K.QLILVLC*SEENMQK.A	690	X	5.54%	1.34%
Q8N5M1	ATPAF2 ATP synthase mitochondrial F1 complex assembly fac	R.TAAGTLFIHLC*SESTTVK.H	276	X	5.48%	1.01%
Q9BZE1	MRPL37 39S ribosomal protein L37, mitochondrial	K.DQAC*YIFHHR.C	104	X	5.43%	0.59%
Q9H6R3	ACSS3 Acyl-CoA synthetase short-chain family member 3, m	R.VPVLDHWWQTETGSPITASC*VGLGNSK.T	461	X	5.43%	0.94%
P43487	RANBP1 Ran-specific GTPase-activating protein	K.IC*ANHYITPMMELKPNAGSDR.A	99		5.43%	0.59%
Q02252	ALDH6A1 Methylmalonate-semialdehyde dehydrogenase	K.LLQDSGAPDGTLNIIHGQHEAVNFIC*DHPDIK.A	249	X	5.35%	0.84%
O75879	PET112 Glutamyl-tRNA(Gln) amidotransferase subunit B, mit	R.AGVGLLEVVLEPDMSC*GEEAATAVR.E	228	X	5.35%	0.83%
Q6PI48	DARS2 Aspartate--tRNA ligase, mitochondrial	R.LIC*LVTGSPSIR.D	590	X	5.34%	0.82%
P00338	LDHA L-lactate dehydrogenase A chain	R.LGVHPLSC*HGWVLGEHGDSSVPVWSGMNVAGVSLK.T	185		5.33%	0.38%
Q8IVS2	MCAT Malonyl-CoA-acyl carrier protein transacylase, mit	R.TVHC*QPAIFVASLAAVEK.L	120	X	5.33%	0.99%
O00411	POLRMT DNA-directed RNA polymerase, mitochondrial	K.AAEPTLTFEAVDVPMLC*PPLPWTSPHSGAFLLSPTK.L	650	X	5.32%	0.96%
Q9Y3B8	REXO2 Oligoribonuclease, mitochondrial	R.QQTPPGLC*PLAGNSVHEDKK.F	137	X	5.29%	0.47%
Q06830	PRDX1 Peroxiredoxin-1	K.HGEVC*PAGWKPGSDTIKPDVQK.S	173		5.28%	1.70%
P23378	GLDC Glycine dehydrogenase	K.TFC*IPHGGGGPGMGPIGVK.K	757	X	5.26%	0.44%
P54886	ALDH18A1 Delta-1-pyrroline-5-carboxylate synthase	R.TEYGDLELC*IEVVDNVQDAIDHIHK.Y	674	X	5.25%	0.45%
Q5JPH6	EARS2 Probable glutamate--tRNA ligase, mitochondrial	K.SDGFPTYHLAC*VVDDHHMGISHVLR.G	232	X	5.25%	0.57%
F8VP50	Uncharacterized protein	R.KTFPTVNPSTGEVIC*QVAEGDKEDVDK.A	63		5.23%	0.37%
O00411	POLRMT DNA-directed RNA polymerase, mitochondrial	R.VC*VVSVEKPTLPSK.E	413	X	5.21%	0.39%
Q10713	PMPCA Mitochondrial-processing peptidase subunit alpha	K.LPHELC*TLIR.N	466	X	5.21%	0.49%
P42704	LRPPRC Leucine-rich PPR motif-containing protein, mitocho	K.GMQELGVHPDQETYTDYVIPC*FDSVNSAR.A	484	X	5.19%	0.41%
P31040	SDHA Succinate dehydrogenase	R.GVIALC*IEDGSIHR.I	238	X	5.15%	0.55%
P23368	ME2 NAD-dependent malic enzyme, mitochondrial	R.AMASINERPVIFALSNPTAQAEC*TAEEAYTLTEGR.C	428	X	5.12%	0.49%
P12277	CKB Creatine kinase B-type	K.DYEFMWNPHLGYILTC*PSNLGTGLR.A	283		5.12%	0.50%
P07900	HSP90AA1 Heat shock protein HSP 90-alpha	K.C*LELFTELAEDKENYK.K	420		5.11%	0.61%
Q9UGM6	WARS2 Tryptophan--tRNA ligase, mitochondrial	R.QSILDMTAVLLAC*GINPEK.S	102	X	5.09%	0.47%
Q99497	PARK7 Protein DJ-1	K.VTVAGLAGKDPVQC*SR.D	46	X	5.09%	0.57%
P23368	ME2 NAD-dependent malic enzyme, mitochondrial	R.ILQDDIESLMPIVYTPTVGLAC*SQYGHIFR.R	120	X	5.06%	0.41%
Q8TAA5	GRPEL2 GrpE protein homolog 2, mitochondrial	K.LTPIGDKYDPHEHELIC*HVPAGVGVQPGTVALVR.Q	182	X	5.03%	0.37%
P41250	GARS Glycine--tRNA ligase	R.SC*YDLSC*HAR.A	466|471	X	5.03%	0.46%
Q969S9	GFM2 Ribosome-releasing factor 2, mitochondrial	R.IYSGTIKPQLAIHNINGNC*TER.I	406	X	5.00%	0.67%
Q96RQ3	MCCC1 Methylcrotonoyl-CoA carboxylase subunit alpha, mit	K.TSAAQAIHPGC*GFLSENMEFAELC*K.Q	129|142	X	5.00%	0.41%
P04075	ALDOA Fructose-bisphosphate aldolase A	R.YASIC*QQNGIVPIVEPEILPDGDHDLK.R	178		5.00%	0.41%
P28331	NDUFS1 NADH-ubiquinone oxidoreductase 75 kDa subunit, mit	R.FC*YHER.L	64	X	4.98%	0.76%
Q7L592	C2orf56 Protein midA homolog, mitochondrial	R.DHVEVC*PDAGVIIEELSQR.I	275	X	4.98%	0.37%
P00505	GOT2 Aspartate aminotransferase, mitochondrial	K.EGSTHNWQHITDQIGMFC*FTGLKPEQVER.L	382	X	4.97%	0.42%
Q99797	MIPEP Mitochondrial intermediate peptidase	R.C*PTDFAEVPSILMEYFANDYR.V	518	X	4.93%	0.30%
Q8NCN5	PDPR Pyruvate dehydrogenase phosphatase regulatory subu	R.AVDVLSELSYAPMTPDHFPSLFC*K.E	653	X	4.90%	0.23%
Q5JPH6	EARS2 Probable glutamate--tRNA ligase, mitochondrial	R.TLPELITQFNLTQVTC*HSALLDLEK.L	341	X	4.89%	0.19%
Q7L0Y3	TRMT10C Mitochondrial ribonuclease P protein 1	K.SSVQEEC*VSTISSSK.D	78	X	4.88%	0.16%
Q5JRX3	PITRM1 Presequence protease, mitochondrial	R.TTPMDSTGVPHILEHTVLC*GSQK.Y	112	X	4.86%	0.68%
P24752	ACAT1 Acetyl-CoA acetyltransferase, mitochondrial	K.IHMGSC*AENTAK.K	196	X	4.85%	0.60%
O00411	POLRMT DNA-directed RNA polymerase, mitochondrial	K.DAGLTPDLLSYAAALQC*MGR.Q	305	X	4.84%	0.14%
P08238	HSP90AB1 Heat shock protein HSP 90-beta	R.GFEVVYMTEPIDEYC*VQQLK.E	521		4.83%	0.13%
Q9BRJ2	MRPL45 39S ribosomal protein L45, mitochondrial	R.SIHLAC*TAGIFDAYVPPEGDAR.I	80	X	4.83%	0.12%
Q9H1K1	ISCU Iron-sulfur cluster assembly enzyme ISCU, mitochon	K.LHC*SMLAEDAIK.A	138	X	4.83%	0.09%
P31930	UQCRC1 Cytochrome b-c1 complex subunit 1, mitochondrial	K.HLGGIPWTYAEDAVPTLTPC*R.F	268	X	4.82%	0.10%
P24752	ACAT1 Acetyl-CoA acetyltransferase, mitochondrial	R.QAVLGAGLPISTPC*TTINK.V	119	X	4.82%	0.11%
P09622	DLD Dihydrolipoyl dehydrogenase, mitochondrial	R.VC*HAHPTLSEAFR.E	484	X	4.81%	0.59%

P62937	PPIA Peptidyl-prolyl cis-trans isomerase A	K.HTGPGILSMANAGPNTNGSQFFIC*TAK.T	115		4.81%	0.06%
E7ERL9	VARS2 Valine--tRNA ligase, mitochondrial	R.GLQNHPMVLPIC*SR.S	BAD_ID	X	4.81%	0.08%
Q6YN16	HSDL2 Hydroxysteroid dehydrogenase-like protein 2	R.LAGC*TVFITGASR.G	11	X	4.80%	0.05%
Q5JRX3	PITRM1 Presequence protease, mitochondrial	K.TGGMSASPHVLPDDSHMDTYEQGVLFSSLC*LDR.N	672	X	4.80%	0.07%
P07437	TUBB Tubulin beta chain	K.LTTPTYGDLNHLVSATMSGVTTC*LR.F	239		4.80%	0.06%
Q6P1X6	C8orf82 UPF0598 protein C8orf82	R.C*EDRPVVFTHLLTADHGPPR.L	107	X	4.77%	0.77%
Q9BSH4	TACO1 Translational activator of cytochrome c oxidase 1	K.FIC*DASSLHQVR.K	234	X	4.77%	0.01%
Q6JQN1	ACAD10 Acyl-CoA dehydrogenase family member 10	K.LC*LEQLGLQPSESIFLDDLGTNLK.E	197	X	4.76%	0.00%
Q8WV74	NUDT8 Nucleoside diphosphate-linked moiety X motif 8, mi	R.ARPASAAVLVPLC*SVR.G	39	X	4.76%	0.00%
Q8WV74	NUDT8 Nucleoside diphosphate-linked moiety X motif 8, mi	K.C*DPADQDVVHTALR.E	71	X	4.76%	0.00%
E7ERL9	VARS2 Valine--tRNA ligase, mitochondrial	R.LPQATGETFSMC*IPPPNVTGSLHIGHALTVAIQDALVR.W	BAD_ID	X	4.76%	0.00%
P09417	QDPR Dihydropteridine reductase	K.GAVHQLC*QSLAGK.N	161	X	4.76%	0.00%
P22234	PAICS Multifunctional protein ADE2	R.LPSGLGC*STVLSPEGSAQFAAQIFGLSNHLVWSK.L	374	X	4.76%	0.00%
Q6YP21	CCBL2 Kynurenine--oxoglutarate transaminase 3	K.KLSAIPVSAFC*NSETK.S	416	X	4.76%	0.00%
Q86Y79	PTRH1 Probable peptidyl-tRNA hydrolase	R.HC*AADLALAPLGDAQLVLLRPR.R	72	X	4.76%	0.00%
Q9BPW8	NIPSNAP1 Protein NipSnap homolog 1	R.FSGGYPALMDC*MNK.L	138	X	4.76%	0.00%
Q9BSH5	HDHD3 Haloacid dehalogenase-like hydrolase domain-contai	K.DFSHPC*TWQVLDGAEDTLR.E	109	X	4.76%	0.00%
Q6YP21	CCBL2 Kynurenine--oxoglutarate transaminase 3	K.RMDDPEC*YFNSLPK.E	337	X	4.76%	0.00%
Q7Z4G4	TRMT11 tRNA (guanine(10)-N2)-methyltransferase homolog	K.KPQHVFSVLEDYGLDPNC*IPENPHNIYFGR.W	161	X	4.76%	0.00%
Q8IYQ7	THNSL1 Threonine synthase-like 1	K.FIC*ASNQNHVLTDFIK.T	532	X	4.76%	0.00%
Q8N0U4	FAM185A Protein FAM185A	R.LPC*HLAVRPLDPLTYPDGDR.V	83	X	4.76%	0.00%
Q96GJ1	TRMT2B tRNA (uracil(54)-C(5))-methyltransferase homolog	R.LSC*LLHPIIPSPVINGYR.N	138	X	4.76%	0.00%
Q8IYQ7	THNSL1 Threonine synthase-like 1	R.C*IHPADIPAAR.L	299	X	4.76%	0.00%
Q9BXW7	CECR5 Cat eye syndrome critical region protein 5	R.QQQPSASQSC*ISILVC*TGVYNPR.N	356|362	X	4.76%	0.00%
Q9H857	NT5DC2 5-nucleotidase domain-containing protein 2	R.TPLQHEAPLWMDQLC*TGC*MK.T	504|507	X	4.76%	0.00%
Q8IWL3	HSCB Iron-sulfur cluster co-chaperone protein HscB, mit	R.C*WNC*GGPWGPGR.E	41|44	X	4.76%	0.00%
Q8IWL3	HSCB Iron-sulfur cluster co-chaperone protein HscB, mit	R.DYFSLMDC*NR.S	79	X	4.76%	0.00%
Q12849	GRSF1 G-rich sequence factor 1	R.AQGLPWSC*TMEDVLNFFSDC*R.I	161|173	X	4.76%	0.00%
Q05932	FPGS Folylpolyglutamate synthase, mitochondrial	R.SNAALALQLAHC*WLQR.Q	315	X	4.76%	0.00%
Q8NFF5	FLAD1 FAD synthase	K.LTLDSEEEGPLEEC*LAYLTAR.L	338	X	4.76%	0.00%
Q05932	FPGS Folylpolyglutamate synthase, mitochondrial	R.KPVVC*GVSSLGIDHTSLLGDTVEK.I	219	X	4.76%	0.00%
Q8NFF5	FLAD1 FAD synthase	K.GHTQDTNTFFLC*R.T	136	X	4.76%	0.00%
Q9BV79	MECR Trans-2-enoyl-CoA reductase, mitochondrial	R.GQLTAPAC*SQVPLQDYQSALEASMKPFISSK.Q	345	X	4.76%	0.00%
Q9Y606	PUS1 tRNA pseudouridine synthase A, mitochondrial	R.SGC*IPENHGEDMR.K	125	X	4.76%	0.00%
Q9Y606	PUS1 tRNA pseudouridine synthase A, mitochondrial	R.TYC*YLLPTFAFAHK.D	202	X	4.76%	0.00%
O75521	ECI2 Enoyl-CoA delta isomerase 2, mitochondrial	R.WLSDEC*TNAVVNFLSR.K	380	X	4.76%	0.00%
O75521	ECI2 Enoyl-CoA delta isomerase 2, mitochondrial	K.LHAVNAEEC*NVLQGR.W	368	X	4.76%	0.00%
Q9NQH7	XPNPEP3 Probable Xaa-Pro aminopeptidase 3	R.IEDDVVVTQDSPLILSADC*PK.E	492	X	4.76%	0.00%
Q05932	FPGS Folylpolyglutamate synthase, mitochondrial	R.AQQISC*PLYLC*PMLEALEEGGPPLTLGLEGEHQR.S	275|280	X	4.76%	0.00%
O94925	GLS Glutaminase kidney isoform, mitochondrial	K.EC*MDMLR.L	178	X	4.76%	0.00%
O94925	GLS Glutaminase kidney isoform, mitochondrial	R.NTLSLMHSC*GMYDFSGQFAFHVGLPAK.S	463	X	4.76%	0.00%
O94925	GLS Glutaminase kidney isoform, mitochondrial	K.FSPDLWGVSVC*TVDGQR.H	266	X	4.76%	0.00%
O94925	GLS Glutaminase kidney isoform, mitochondrial	K.C*VQSNIVLLTQAFR.R	203	X	4.76%	0.00%
O94925	GLS Glutaminase kidney isoform, mitochondrial	K.VPFC*LQSC*VKPLK.Y	283|287	X	4.76%	0.00%
O94925	GLS Glutaminase kidney isoform, mitochondrial	K.GIHFC*HDLVSLC*NFHNYDNLR.H	518|525	X	4.76%	0.00%
Q86X76	NIT1 Nitrilase homolog 1	K.IYNC*HVLLNSK.G	145	X	4.76%	0.00%
Q86X76	NIT1 Nitrilase homolog 1	R.LGAC*LAFLPEAFDFIAR.D	80	X	4.76%	0.00%
O15382	BCAT2 Branched-chain-amino-acid aminotransferase, mitoch	R.LC*LPSFDKLELLEC*IR.R	135|147	X	4.76%	0.00%
P00390	GSR Glutathione reductase, mitochondrial	K.VVGIHMQGLGC*DEMLQGFAVAVK.M	484	X	4.76%	0.00%
Q5T1C6	THEM4 Thioesterase superfamily member 4	R.KFFVSC*NVQSVDEK.T	212	X	4.76%	0.00%
Q9UJZ1	STOML2 Stomatin-like protein 2	R.ESLNASIVDAINQAADC*WGIR.C	167	X	4.76%	0.00%
Q7L2E3	DHX30 Putative ATP-dependent RNA helicase DHX30	R.DTILNAIEQHPVVVISGDTGC*GK.T	461	X	4.76%	0.00%

P25325	MPST 3-mercaptopyruvate sulfurtransferase	R.HIPGAAFFDIDQC*SDR.T	65	X	4.76%	0.00%
Q7L2E3	DHX30 Putative ATP-dependent RNA helicase DHX30	R.GEPGGILC*FLPGWQEIK.G	673	X	4.76%	0.00%
O43708	GSTZ1 Maleylacetoacetate isomerase	R.LLVLEAFQVSHPC*R.Q	205	X	4.76%	0.00%
O95571	ETHE1 Protein ETHE1, mitochondrial	R.ASPGHTPGC*VTFVLNDHSMAFTGDALLIR.G	139	X	4.76%	0.00%
O95571	ETHE1 Protein ETHE1, mitochondrial	R.LLYAVNTHC*HADHITGSGLLR.S	80	X	4.76%	0.00%
Q08257	CRYZ Quinone oxidoreductase	K.VHAC*GVNPVETYIR.S	45	X	4.76%	0.00%
Q9NVV4	MTPAP Poly(A) RNA polymerase, mitochondrial	R.FSHQASGFQC*DLTTNNR.I	324	X	4.76%	0.00%
P28838	LAP3 Cytosol aminopeptidase	R.LILADALC*YAHTFNPK.V	376	X	4.76%	0.00%
Q92552	MRPS27 28S ribosomal protein S27, mitochondrial	R.HSPNC*WYLR.N	101	X	4.76%	0.00%
Q96AB3	ISOC2 Isochorismatase domain-containing protein 2, mitoc	R.GLQVHVVVDAC*SSR.S	136	X	4.76%	0.00%
Q8TCS8	PNPT1 Polyribonucleotide nucleotidyltransferase 1, mitoc	R.NVSC*EVDMFK.T	372	X	4.76%	0.00%
Q9NVV4	MTPAP Poly(A) RNA polymerase, mitochondrial	R.YLTC*SLIEDMAAAYFPDC*IVRPFGSSVNTFGK.L	211|225	X	4.76%	0.00%
Q9NVV4	MTPAP Poly(A) RNA polymerase, mitochondrial	K.ILSVLGEC*LDHFGPGC*VGVQK.I	291|299	X	4.76%	0.00%
Q4J6C6	PREPL Prolyl endopeptidase-like	K.DHC*VLFLK.H	359	X	4.76%	0.00%
Q4J6C6	PREPL Prolyl endopeptidase-like	K.KLNGLADLEAC*IK.T	538	X	4.76%	0.00%
P53396	ACLY ATP-citrate synthase	K.GVTIIGPATVGGIKPGC*FK.I	633	X	4.76%	0.00%
Q4J6C6	PREPL Prolyl endopeptidase-like	K.NC*PFQLC*SPIRPPK.Y	404|409	X	4.76%	0.00%
P07203	GPX1 Glutathione peroxidase 1	R.RFQTIDIEPDIEALLSQGPSC*A.-	202	X	4.76%	0.00%
O43488	AKR7A2 Aflatoxin B1 aldehyde reductase member 2	R.LQC*PQVDLFYLHAPDHGTPVEETLHAC*QR.L	132|156	X	4.76%	0.00%
P31327	CPS1 Carbamoyl-phosphate synthase	R.MC*HPSIEGFTPR.L	816	X	4.76%	0.00%
O43766	LIAS Lipoyl synthase, mitochondrial	R.NLNLHTVC*EEAR.C	106	X	4.76%	0.00%
Q99798	ACO2 Aconitate hydratase, mitochondrial	R.DLGGIVLANAC*GPC*IGQWDR.K	448|451	X	4.76%	0.00%
Q969Y2	GTPBP3 tRNA modification GTPase GTPBP3, mitochondrial	K.SDLLSPEGPGPGPDLPPHLLLSC*LTGEGLDGLLEALR.K	398	X	4.76%	0.00%
P49411	TUFM Elongation factor Tu, mitochondrial	K.GEETPVIVGSALC*ALEGR.D	222	X	4.76%	0.00%
Q96RP9	GFM1 Elongation factor G, mitochondrial	R.QELIEC*VANSDEQLGEMFLEEK.I	256	X	4.76%	0.00%
Q9NYK5	MRPL39 39S ribosomal protein L39, mitochondrial	K.NISTPYSC*AMHLSEWYC*R.K	91|100	X	4.76%	0.00%
O43766	LIAS Lipoyl synthase, mitochondrial	K.ILVEC*LTPDFR.G	211	X	4.76%	0.00%
O15091	KIAA0391 Mitochondrial ribonuclease P protein 3	K.QASC*FFADDISEDDPFLLYATLHSGNHC*R.F	469|493	X	4.76%	0.00%
Q9Y3D2	MSRB2 Methionine-R-sulfoxide reductase B2, mitochondrial	K.YC*SGTGWPSFSEAHGTSGSDESHTGILR.R	105	X	4.76%	0.00%
P23434	GCSH Glycine cleavage system H protein, mitochondrial	K.HEWVTTENGIGTVGISNFAQEALGDVVYC*SLPEVGTK.L	85	X	4.76%	0.00%
Q9Y305	ACOT9 Acyl-coenzyme A thioesterase 9, mitochondrial	K.SLEIC*HPQER.N	299	X	4.76%	0.00%
Q9Y305	ACOT9 Acyl-coenzyme A thioesterase 9, mitochondrial	K.MSPLSIVTALVDKIDMC*K.K	155	X	4.76%	0.00%
Q9Y305	ACOT9 Acyl-coenzyme A thioesterase 9, mitochondrial	R.ILEDLDSLGVLIC*YMHNK.I	128	X	4.76%	0.00%
Q8N465	D2HGDH D-2-hydroxyglutarate dehydrogenase, mitochondrial	K.GSC*HIGGNVATNAGGLR.F	198	X	4.76%	0.00%
Q9H9J2	MRPL44 39S ribosomal protein L44, mitochondrial	R.QSGGTTALPLYFVGLYC*DK.K	276	X	4.76%	0.00%
Q9P2R7	SUCLA2 Succinyl-CoA ligase	K.YDATMIEINPMVEDSDGAVLC*MDAK.I	270	X	4.76%	0.00%
Q96I99	SUCLG2 Succinyl-CoA ligase	K.IDATQVEVNPFGETPEGQVVC*FDAK.I	255	X	4.76%	0.00%
O75648	TRMU Mitochondrial tRNA-specific 2-thiouridylase 1	R.VC*QILDIPFHQVSYVK.E	61	X	4.76%	0.00%
P40939	HADHA Trifunctional enzyme subunit alpha, mitochondrial	K.ALMGLYHGQVLC*K.K	349	X	4.76%	0.00%
P51553	IDH3G Isocitrate dehydrogenase	R.TSLDLYANVIHC*K.S	148	X	4.76%	0.00%
P51553	IDH3G Isocitrate dehydrogenase	K.NIANPTATLLASC*MMLDHLK.L	333	X	4.76%	0.00%
P55084	HADHB Trifunctional enzyme subunit beta, mitochondrial	K.FNNWGGSLSLGHPFGATGC*R.L	435	X	4.76%	0.00%
P78540	ARG2 Arginase-2, mitochondrial	R.AVSDGYSC*VTLGGDHSLAIGTISGHAR.H	113	X	4.76%	0.00%
P82930	MRPS34 28S ribosomal protein S34, mitochondrial	K.SWLWQHDEPC*YWR.L	93	X	4.76%	0.00%
P82933	MRPS9 28S ribosomal protein S9, mitochondrial	K.ALC*SFVTEDEVEWMR.Q	353	X	4.76%	0.00%
Q3SY69	ALDH1L2 Mitochondrial 10-formyltetrahydrofolate dehydrogen	K.SAAC*LAAGNTLVLKPAQVTPLTALK.F	608	X	4.76%	0.00%
Q5JTZ9	AARS2 Alanine--tRNA ligase, mitochondrial	K.HSTYDTDLFSPLLNAIQQGC*R.A	300	X	4.76%	0.00%
Q5T2R2	PDSS1 Decaprenyl-diphosphate synthase subunit 1	K.LGLATGPVLFAC*QQFPEMNAMIMR.R	340	X	4.76%	0.00%
Q6P587	FAHD1 Acylpyruvase FAHD1, mitochondrial	R.AVPEAAAMDYVGGYALC*LDMTAR.D	100	X	4.76%	0.00%
Q8TAE8	GADD45GIP1 Growth arrest and DNA damage-inducible proteins-in	R.EREQHIAEC*MAK.M	124	X	4.76%	0.00%
Q92665	MRPS31 28S ribosomal protein S31, mitochondrial	R.HFMELVTC*GLSK.N	356	X	4.76%	0.00%
Q969Y2	GTPBP3 tRNA modification GTPase GTPBP3, mitochondrial	R.LTGGGGTEEILDIIFQDFC*VGK.-	489	X	4.76%	0.00%
Q96DV4	MRPL38 39S ribosomal protein L38, mitochondrial	K.HQETMTPAGLSFFQC*R.W	321	X	4.76%	0.00%
Q96EY7	PTCD3 Pentatricopeptide repeat-containing protein 3, mit	K.HPPELQVAFADC*AADIK.S	551	X	4.76%	0.00%
Q9BQ52	ELAC2 Zinc phosphodiesterase ELAC protein 2	K.AWLQQYHNQC*QEVLHHISMIPAK.C	595	X	4.76%	0.00%

Q9BQ52	ELAC2 Zinc phosphodiesterase ELAC protein 2	K.HAFGC*ALVHTSGWK.V	651	X	4.76%	0.00%
Q9BRJ2	MRPL45 39S ribosomal protein L45, mitochondrial	R.LHTLVTEHC*FPDMTWDIK.Y	168	X	4.76%	0.00%
Q9BYD6	MRPL1 39S ribosomal protein L1, mitochondrial	K.IATLDMSSDQIAANLQAVINEVC*R.H	279	X	4.76%	0.00%
Q9H0R6	QRSL1 Glutamyl-tRNA(Gln) amidotransferase subunit A, mit	R.NPAAHC*GLVGFK.P	203	X	4.76%	0.00%
Q9H2W6	MRPL46 39S ribosomal protein L46, mitochondrial	R.LLGALC*LQRPPVVSK.P	52	X	4.76%	0.00%
Q9HC36	RNMTL1 RNA methyltransferase-like protein 1	K.TQLQHSLPLLLIC*DNLR.D	214	X	4.76%	0.00%
Q9NP92	MRPS30 28S ribosomal protein S30, mitochondrial	R.C*PVHFYWVR.G	204	X	4.76%	0.00%
Q9NP92	MRPS30 28S ribosomal protein S30, mitochondrial	R.KNIC*WGTQSKPLYETIEDNDVK.G	393	X	4.76%	0.00%
Q9NWU1	OXSM 3-oxoacyl-	K.LPPTLNLDC*SEPEFDLNYVPLK.A	415	X	4.76%	0.00%
Q9NYK5	MRPL39 39S ribosomal protein L39, mitochondrial	R.TSIC*FQYEVSAVHNLQPTQPSLIR.R	275	X	4.76%	0.00%
Q9P2R7	SUCLA2 Succinyl-CoA ligase	K.ILAC*DDLDEAAR.M	430	X	4.76%	0.00%
Q9UDR5	AASS Alpha-aminoadipic semialdehyde synthase, mitochond	K.QLLC*DLVGISPSSEHDVLK.E	765	X	4.76%	0.00%
Q9Y2R9	MRPS7 28S ribosomal protein S7, mitochondrial	K.WMITEC*R.D	191	X	4.76%	0.00%
O75648	TRMU Mitochondrial tRNA-specific 2-thiouridylase 1	K.MMEC*HFR.F	329	X	4.76%	0.00%
P24752	ACAT1 Acetyl-CoA acetyltransferase, mitochondrial	K.AIMMASQSLMC*GHQDVMVAGGMESMSNVPY VMNR.G	142	X	4.76%	0.00%
P40939	HADHA Trifunctional enzyme subunit alpha, mitochondrial	K.QFTPC*QLLADHANSPNK.K	747	X	4.76%	0.00%
P82650	MRPS22 28S ribosomal protein S22, mitochondrial	R.HVDVLNLC*FAQFEPDSTEYIK.V	231	X	4.76%	0.00%
Q16854	DGUOK Deoxyguanosine kinase, mitochondrial	K.AC*TAQSLGNLLDMMYR.E	87	X	4.76%	0.00%
Q3SY69	ALDH1L2 Mitochondrial 10-formyltetrahydrofolate dehydrogen	K.SPLIIFNDC*ELDK.A	707	X	4.76%	0.00%
Q5T2R2	PDSS1 Decaprenyl-diphosphate synthase subunit 1	R.AC*NIHHNNSR.H	148	X	4.76%	0.00%
Q6NVY1	HIBCH 3-hydroxyisobutyryl-CoA hydrolase, mitochondrial	K.C*LFAMPETAIGLFPDVGGGYFLPR.L	163	X	4.76%	0.00%
Q8N5N7	MRPL50 39S ribosomal protein L50, mitochondrial	K.KEPILVC*PPLR.S	52	X	4.76%	0.00%
Q969S9	GFM2 Ribosome-releasing factor 2, mitochondrial	R.LLLAGVEIPEPVFFC*TIEPPSLSK.Q	492	X	4.76%	0.00%
Q96EL2	MRPS24 28S ribosomal protein S24, mitochondrial	K.FMWGTFPGC*LADQLVLK.R	103	X	4.76%	0.00%
Q96EY7	PTCD3 Pentatricopeptide repeat-containing protein 3, mit	R.QTAQDWPATSLNC*IAILFLR.A	578	X	4.76%	0.00%
Q96RP9	GFM1 Elongation factor G, mitochondrial	K.GFLDAC*EK.G	594	X	4.76%	0.00%
Q9BSH4	TACO1 Translational activator of cytochrome c oxidase 1	K.EGGPNPEHNSNLANILEVC*R.S	112	X	4.76%	0.00%
Q5JTZ9	AARS2 Alanine--tRNA ligase, mitochondrial	K.EEAC*NMAWELLTQVYGIPEER.L	149	X	4.76%	0.00%
Q5JTZ9	AARS2 Alanine--tRNA ligase, mitochondrial	R.QLC*EQAPSTSVLLLSPQPMGK.V	904	X	4.76%	0.00%
Q8NI60	ADCK3 Chaperone activity of bc1 complex-like, mitochondr	K.MGGSFLIC*SK.L	620	X	4.76%	0.00%
Q9H9P8	L2HGDH L-2-hydroxyglutarate dehydrogenase, mitochondrial	R.GLMAIDC*PHTGIVDYR.Q	187	X	4.76%	0.00%
Q9Y2R9	MRPS7 28S ribosomal protein S7, mitochondrial	K.NC*EPMIGLVPILK.G	152	X	4.76%	0.00%
P38646	HSPA9 Stress-70 protein, mitochondrial	K.C*ELSSSVQTDINLPYLTMDSSGPK.H	317	X	4.76%	0.00%
Q5T440	IBA57 Putative transferase CAF17, mitochondrial	R.VWAVLPSSPEAC*GAASLQER.A	170	X	4.76%	0.00%
P23378	GLDC Glycine dehydrogenase	K.DISLVHSMIPLGSC*TMK.L	558	X	4.76%	0.00%
Q9BQ52	ELAC2 Zinc phosphodiesterase ELAC protein 2	R.FGPDTQHLVLNENC*ASVHNLR.S	374	X	4.76%	0.00%
Q9UDR5	AASS Alpha-aminoadipic semialdehyde synthase, mitochond	K.FSPAGVEGC*PALPHK.L	342	X	4.76%	0.00%
P82933	MRPS9 28S ribosomal protein S9, mitochondrial	K.HDVTC*TVSGGGR.S	330	X	4.76%	0.00%
Q6UB35	MTHFD1L Monofunctional C1-tetrahydrofolate synthase, mitoc	R.AEIDLVC*ELAK.R	814	X	4.76%	0.00%
P23378	GLDC Glycine dehydrogenase	K.MEDPVC*ENEILATLHAISSK.N	112	X	4.76%	0.00%
Q96HY7	DHTKD1 Probable 2-oxoglutarate dehydrogenase E1 component	R.VEELC*PFPLDSLQQEMSK.Y	839	X	4.76%	0.00%
Q13011	ECH1 Delta(3,5)-Delta(2,4)-dienoyl-CoA isomerase, mitoc	R.YC*AQDAFFQVK.E	187	X	4.76%	0.00%
P23378	GLDC Glycine dehydrogenase	R.SYIGMGYYNC*SVPQTILR.N	141	X	4.76%	0.00%
P34897	SHMT2 Serine hydroxymethyltransferase, mitochondrial	R.MREVC*DEVK.A	241	X	4.76%	0.00%
Q96EY7	PTCD3 Pentatricopeptide repeat-containing protein 3, mit	K.DPDDDKFFQSAMSIC*SSLR.D	423	X	4.76%	0.00%
Q96HY7	DHTKD1 Probable 2-oxoglutarate dehydrogenase E1 component	K.DVIIDLLC*YR.Q	429	X	4.76%	0.00%
Q96HY7	DHTKD1 Probable 2-oxoglutarate dehydrogenase E1 component	R.LVTVYC*EHGHK.A	64	X	4.76%	0.00%
P09001	MRPL3 39S ribosomal protein L3, mitochondrial	K.HVVTLLQVQDC*HVLK.Y	127	X	4.76%	0.00%

P34897	SHMT2 Serine hydroxymethyltransferase, mitochondrial	R.GLELIASENFC*SR.A	80	X	4.76%	0.00%
Q9UDR5	AASS Alpha-aminoadipic semialdehyde synthase, mitochond	K.GAQAIFNELPC*EYVEPHELK.E	240	X	4.76%	0.00%
Q96EY8	MMAB Cob(I)yrinic acid a,c-diamide adenosyltransferase,	K.ISSALHFC*R.A	185	X	4.76%	0.00%
P23378	GLDC Glycine dehydrogenase	R.C*HPQTIAVVQTR.A	225	X	4.76%	0.00%
P23378	GLDC Glycine dehydrogenase	K.LPC*EMDFSGK.D	250	X	4.76%	0.00%
Q99798	ACO2 Aconitate hydratase, mitochondrial	K.C*TTDHISAAGPWLK.F	592	X	4.76%	0.00%
O00411	POLRMT DNA-directed RNA polymerase, mitochondrial	R.TVEGATQHQELLETC*PPTALHGALDALTQLGN C*AWR.V	687|705	X	4.76%	0.00%
P49753	ACOT2 Acyl-coenzyme A thioesterase 2, mitochondrial	R.KPQIIC*YPETGHYIEPPYFPLC*R.A	416|432	X	4.76%	0.00%
Q96RP9	GFM1 Elongation factor G, mitochondrial	R.EYGC*PC*ITGKPK.V	514|516	X	4.76%	0.00%
Q9BQ52	ELAC2 Zinc phosphodiesterase ELAC protein 2	R.NVSATLVNISPDTSLLLDC*GEGTFGQLC*R.H	516|525	X	4.76%	0.00%
Q9H2U2	PPA2 Inorganic pyrophosphatase 2, mitochondrial	K.DKSTNC*FGDNDPIDVC*EIGSK.I	161|171	X	4.76%	0.00%
Q9NUJ1	ABHD10 Abhydrolase domain-containing protein 10, mitochon	K.EAEHHC*LLHSPIPVNC*PIR.L	229|239	X	4.76%	0.00%
P40939	HADHA Trifunctional enzyme subunit alpha, mitochondrial	R.SAVLISSKPGC*FIAGADINMLAAC*K.T	97|110	X	4.76%	0.00%
P82673	MRPS35 28S ribosomal protein S35, mitochondrial	K.DFC*TEWPAALDSDEKC*EK.H	130|143	X	4.76%	0.00%
P51553	IDH3G Isocitrate dehydrogenase	K.LGDGLFLQC*C*R.E	235|236	X	4.76%	0.00%
Q13011	ECH1 Delta(3,5)-Delta(2,4)-dienoyl-CoA isomerase, mitoc	R.C*PKPVIAAVHGGC*IGGGVDLVTAC*DIR.Y	159|171|182	X	4.76%	0.00%
P28331	NDUFS1 NADH-ubiquinone oxidoreductase 75 kDa subunit, mit	R.EGVMEFLLANHPLDC*PIC*DQGGEC*DLQDQS MMFGNDR.S	128|131|137	X	4.76%	0.00%
O95202	LETM1 LETM1 and EF-hand domain-containing protein 1, mit	K.LFEDELTLDNLTRPQLVALC*K.L	330	X	4.76%	0.00%
O43615	TIMM44 Mitochondrial import inner membrane translocase su	K.DWC*YEATYSQLAHPIQQAK.A	343	X	4.76%	0.00%
O43615	TIMM44 Mitochondrial import inner membrane translocase su	R.MLYVWALC*R.D	426	X	4.76%	0.00%
P22570	FDXR NADPH:adrenodoxin oxidoreductase, mitochondrial	R.AVPTGDMEDLPC*GLVLSSIGYK.S	353	X	4.76%	0.00%
P22695	UQCRC2 Cytochrome b-c1 complex subunit 2, mitochondrial	R.NALANPLYC*PDYR.I	192	X	4.76%	0.00%
P22695	UQCRC2 Cytochrome b-c1 complex subunit 2, mitochondrial	R.ENMAYTVEC*LR.G	125	X	4.76%	0.00%
Q5TEU4	NDUFAF5 NADH dehydrogenase	R.NFPLALDLGC*GR.G	98	X	4.76%	0.00%
Q8NC60	NOA1 Nitric oxide-associated protein 1	R.C*WLLSHHR.R	182	X	4.76%	0.00%
Q96CU9	FOXRED1 FAD-dependent oxidoreductase domain-containing pro	R.YVYVWHC*PQGPGLETPLVADTSGAYFR.R	331	X	4.76%	0.00%
Q9H845	ACAD9 Acyl-CoA dehydrogenase family member 9, mitochondr	R.AYIC*AHPLDR.T	613	X	4.76%	0.00%
P31930	UQCRC1 Cytochrome b-c1 complex subunit 1, mitochondrial	R.LC*TSATESEVAR.G	380	X	4.76%	0.00%
P50336	PPOX Protoporphyrinogen oxidase	R.LGPEVASLAMDSLC*R.G	167	X	4.76%	0.00%
P50336	PPOX Protoporphyrinogen oxidase	K.NC*IPQYTLGHWQK.L	418	X	4.76%	0.00%
P50336	PPOX Protoporphyrinogen oxidase	R.SC*FPSLFQAEQTHR.S	183	X	4.76%	0.00%
P54886	ALDH18A1 Delta-1-pyrroline-5-carboxylate synthase	K.YGSSHTDVIVTEDENTAEFFLQHVDSAC*VFWN ASTR.F	718	X	4.76%	0.00%
P54886	ALDH18A1 Delta-1-pyrroline-5-carboxylate synthase	R.GDEC*GLALGR.L	88	X	4.76%	0.00%
P31930	UQCRC1 Cytochrome b-c1 complex subunit 1, mitochondrial	K.AVELLGDIVQNC*SLEDSQIEK.E	154	X	4.76%	0.00%
P31040	SDHA Succinate dehydrogenase	R.AC*ALSIEESC*RPGDK.V	467|475	X	4.76%	0.00%
P31040	SDHA Succinate dehydrogenase	R.HVNGQDQIVPGLYAC*GEAAC*ASVHGANR.L	438|443	X	4.76%	0.00%
P31040	SDHA Succinate dehydrogenase	R.AGLPC*QDLEFVQFHPTGIYGAGC*LITEGC*R.G	287|305|311	X	4.76%	0.00%
P22830	FECH Ferrochelatase, mitochondrial	K.ALADLVHSHIQSNELC*SK.Q	395	X	4.76%	0.00%
P21912	SDHB Succinate dehydrogenase	R.C*HTIMNC*TR.T	243|249	X	4.76%	0.00%
P23786	CPT2 Carnitine O-palmitoyltransferase 2, mitochondrial	R.HSAGELQQMMVEC*SK.Y	535	X	4.76%	0.00%
P23786	CPT2 Carnitine O-palmitoyltransferase 2, mitochondrial	K.TLTIDC*VQFQR.G	445	X	4.76%	0.00%
P23786	CPT2 Carnitine O-palmitoyltransferase 2, mitochondrial	R.QYGQTVATYESC*STAAFK.H	489	X	4.76%	0.00%
P49821	NDUFV1 NADH dehydrogenase	K.LFNISGHVNHPC*TVEEEMSVPLK.E	286	X	4.76%	0.00%
P19404	NDUFV2 NADH dehydrogenase	K.YHIQVC*TTTPC*MLR.N	135|140	X	4.76%	0.00%
P19404	NDUFV2 NADH dehydrogenase	R.FSC*EPAGGLTSLTEPPKGPGFGVQAGL.-	225	X	4.76%	0.00%
Q9BYT8	NLN Neurolysin, mitochondrial	R.MSELC*IDFNK.N	199	X	4.76%	0.00%
Q9BYT8	NLN Neurolysin, mitochondrial	R.TYFHEFGHVMHQIC*AQTDFAR.F	507	X	4.76%	0.00%
Q9BYT8	NLN Neurolysin, mitochondrial	R.IVHLQETC*DLGK.I	153	X	4.76%	0.00%
Q9BYT8	NLN Neurolysin, mitochondrial	R.C*KEENTIILQQLLPLR.T	272	X	4.76%	0.00%
P36551	CPOX Coproporphyrinogen-III oxidase, mitochondrial	K.WC*DDYFFIAHR.G	319	X	4.76%	0.00%
Q9HCC0	MCCC2 Methylcrotonoyl-CoA carboxylase beta chain, mitoch	R.VSGVEC*MIIANDATVK.G	131	X	4.76%	0.00%
Q5JRX3	PITRM1 Presequence protease, mitochondrial	R.EFQITC*GPDSFATDPSK.Q	313	X	4.76%	0.00%
P11310	ACADM Medium-chain specific acyl-CoA dehydrogenase, mito	R.MTEEPLMC*AYC*VTEPGAGSDVAGIK.T	156|159	X	4.76%	0.00%
Q9P0J1	PDP1	R.VAFSGATAC*VAHVDGVDLHVANTGDSR.A	275	X	4.76%	0.00%
Q9P2J9	PDP2	R.LLGVLIPC*R.A	345	X	4.76%	0.00%

P30405	PPIF Peptidyl-prolyl cis-trans isomerase F, mitochondri	R.VIPSFMC*QAGDFTNHNGTGGK.S	104	X	4.76%	0.00%
P36776	LONP1 Lon protease homolog, mitochondrial	K.RAGVTC*IVLPAENK.K	909	X	4.76%	0.00%
P36776	LONP1 Lon protease homolog, mitochondrial	K.DGPSAGC*TIVTALLSLAMGR.P	858	X	4.76%	0.00%
P05166	PCCB Propionyl-CoA carboxylase beta chain, mitochondria	K.HLC*GDTNYAWPTAEIAVMGAK.G	448	X	4.76%	0.00%
Q9HCC0	MCCC2 Methylcrotonoyl-CoA carboxylase beta chain, mitoch	K.GTHFVQLC*C*QR.N	391|392	X	4.76%	0.00%
Q96RQ3	MCCC1 Methylcrotonoyl-CoA carboxylase subunit alpha, mit	K.HNFC*FMEMNTR.L	332	X	4.76%	0.00%
A6NJ78	METTL15 Probable methyltransferase-like protein 15	K.LHIPVMVDEVVHC*LSPQK.G	83	X	4.76%	0.00%
P04181	OAT Ornithine aminotransferase, mitochondrial	K.PGEHGSTYGGNPLGC*R.V	330	X	4.76%	0.00%
P09622	DLD Dihydrolipoyl dehydrogenase, mitochondrial	R.VLGAHILGPGAGEMVNEAALALEYGASC*EDIA R.V	477	X	4.76%	0.00%
P22033	MUT Methylmalonyl-CoA mutase, mitochondrial	K.VADPWGGSYMMEC*LTNDVYDAALK.L	433	X	4.76%	0.00%
Q02218	OGDH 2-oxoglutarate dehydrogenase, mitochondrial	R.SMSC*PSTGLTEDILTHIGNVASSVPVENFTIHGG LSR.I	604	X	4.76%	0.00%
Q10713	PMPCA Mitochondrial-processing peptidase subunit alpha	R.MVLAGVGVEHEHLVDC*AR.K	266	X	4.76%	0.00%
Q10713	PMPCA Mitochondrial-processing peptidase subunit alpha	K.FGQFC*TVGILINSGSR.Y	88	X	4.76%	0.00%
Q5T160	RARS2 Probable arginine--tRNA ligase, mitochondrial	R.C*QHVPFGVVQGMK.T	372	X	4.76%	0.00%
Q6L8Q7	PDE12 2,5-phosphodiesterase 12	R.IC*VANTHLYWHPK.G	451	X	4.76%	0.00%
Q6L8Q7	PDE12 2,5-phosphodiesterase 12	R.C*NMSLTHFFK.L	530	X	4.76%	0.00%
Q8NCN5	PDPR Pyruvate dehydrogenase phosphatase regulatory subu	R.HVC*LGFVHNFSEDTGEEQVVTADFINR.G	813	X	4.76%	0.00%
Q8NCN5	PDPR Pyruvate dehydrogenase phosphatase regulatory subu	R.SFFMISPTDQQVHC*WAWLK.K	598	X	4.76%	0.00%
Q969Z0	TBRG4 Protein TBRG4	R.AQDITLPHLC*SVLLAFAR.L	370	X	4.76%	0.00%
Q969Z0	TBRG4 Protein TBRG4	K.HLAFLAESC*ATLSQEQHSQELLAELLTHLER.R	191	X	4.76%	0.00%
Q969Z0	TBRG4 Protein TBRG4	R.LATDLLSLMPSLTSGEVAHC*AK.S	335	X	4.76%	0.00%
Q9NUB1	ACSS1 Acetyl-coenzyme A synthetase 2-like, mitochondrial	R.DTLVWDTPYHTVWDC*DFSTGK.I	93	X	4.76%	0.00%
Q9NUB1	ACSS1 Acetyl-coenzyme A synthetase 2-like, mitochondrial	R.VAIYMPVSPLAVAAMLAC*AR.I	185	X	4.76%	0.00%
Q9Y2Z4	YARS2 Tyrosine--tRNA ligase, mitochondrial	R.C*TQALYHSSIDALEVMSDQELK.E	369	X	4.76%	0.00%
P13804	ETFA Electron transfer flavoprotein subunit alpha, mito	K.QFNYTHIC*AGASAFGK.N	109	X	4.76%	0.00%
P22033	MUT Methylmalonyl-CoA mutase, mitochondrial	K.LRIEEC*AAR.R	471	X	4.76%	0.00%
Q5JPH6	EARS2 Probable glutamate--tRNA ligase, mitochondrial	R.QGDVFLEHFAADGFLPDSLLDIITNC*GSGFAEN QMGR.T	314	X	4.76%	0.00%
Q6PI48	DARS2 Aspartate--tRNA ligase, mitochondrial	R.EYLC*NLHGFVDIETPTLFK.R	202	X	4.76%	0.00%
Q9NP81	SARS2 Serine--tRNA ligase, mitochondrial	R.LHIMFQTEAGELQFAHTVNATAC*AVPR.L	455	X	4.76%	0.00%
Q9NSE4	IARS2 Isoleucine--tRNA ligase, mitochondrial	R.WGIMADWNNC*YYTFDGK.Y	211	X	4.76%	0.00%
P26440	IVD Isovaleryl-CoA dehydrogenase, mitochondrial	R.ASGAVGLSYGAHSNLC*INQLVR.N	136	X	4.76%	0.00%
Q02218	OGDH 2-oxoglutarate dehydrogenase, mitochondrial	R.FLQMC*NDDPDVLPDLK.E	802	X	4.76%	0.00%
Q6PI48	DARS2 Aspartate--tRNA ligase, mitochondrial	K.LRLEC*ADLLETR.G	459	X	4.76%	0.00%
Q8NCN5	PDPR Pyruvate dehydrogenase phosphatase regulatory subu	K.FFAFWGQDINNLTTPLEC*GR.E	735	X	4.76%	0.00%
Q8NCN5	PDPR Pyruvate dehydrogenase phosphatase regulatory subu	R.FC*AGILSTAR.H	85	X	4.76%	0.00%
Q8NCN5	PDPR Pyruvate dehydrogenase phosphatase regulatory subu	K.EAVC*VIDMSSFTK.F	522	X	4.76%	0.00%
Q96GW9	MARS2 Methionine--tRNA ligase, mitochondrial	K.IQQAAATAGLAPTELC*DR.V	114	X	4.76%	0.00%
Q9NSE4	IARS2 Isoleucine--tRNA ligase, mitochondrial	K.C*GFSELYSWQR.E	91	X	4.76%	0.00%
Q9NVH6	TMLHE Trimethyllysine dioxygenase, mitochondrial	K.SLTC*AWQQHEDHFELK.Y	51	X	4.76%	0.00%
Q9NP81	SARS2 Serine--tRNA ligase, mitochondrial	R.FGEVTSASNC*TDFQSR.R	425	X	4.76%	0.00%
O75439	PMPCB Mitochondrial-processing peptidase subunit beta	R.SNMC*WLR.D	485	X	4.76%	0.00%
Q96GW9	MARS2 Methionine--tRNA ligase, mitochondrial	R.VSEQFQQLFQEAGISC*TDFIR.T	132	X	4.76%	0.00%
Q6PI48	DARS2 Aspartate--tRNA ligase, mitochondrial	R.TNTC*GELR.S	54	X	4.76%	0.00%
Q6L8Q7	PDE12 2,5-phosphodiesterase 12	K.LHC*TPGDGQR.F	250	X	4.76%	0.00%
Q15031	LARS2 Probable leucine--tRNA ligase, mitochondrial	R.LGLC*FSWDR.E	167	X	4.76%	0.00%
Q15031	LARS2 Probable leucine--tRNA ligase, mitochondrial	K.EALVNWDPVDQTVLANEQVDEHGC*SWR.S	225	X	4.76%	0.00%
O75439	PMPCB Mitochondrial-processing peptidase subunit beta	R.LC*TSVTESEVAR.A	389	X	4.76%	0.00%
P00505	GOT2 Aspartate aminotransferase, mitochondrial	K.EYLPIGGLAEFC*K.A	106	X	4.76%	0.00%
Q96GW9	MARS2 Methionine--tRNA ligase, mitochondrial	R.FYGHPC*PFEGR.R	562	X	4.76%	0.00%

Q9BW92	TARS2 Threonine--tRNA ligase, mitochondrial	R.LLGVLAESC*GGK.W	603	X	4.76%	0.00%
P40926	MDH2 Malate dehydrogenase, mitochondrial	K.EGVVEC*SFVK.S	275	X	4.76%	0.00%
P36776	LONP1 Lon protease homolog, mitochondrial	K.VLFIC*TANVTDTIPEPLR.D	637	X	4.76%	0.00%
P36776	LONP1 Lon protease homolog, mitochondrial	K.ILC*FYGPPGVGK.T	520	X	4.76%	0.00%
P40926	MDH2 Malate dehydrogenase, mitochondrial	K.TIIPLISQC*TPK.V	212	X	4.76%	0.00%
P35914	HMGCL Hydroxymethylglutaryl-CoA lyase, mitochondrial	K.LLEAGNFIC*QALNR.K	307	X	4.76%	0.00%
Q96RQ3	MCCC1 Methylcrotonoyl-CoA carboxylase subunit alpha, mit	K.ESLC*QAALGLILK.E	509	X	4.76%	0.00%
P00505	GOT2 Aspartate aminotransferase, mitochondrial	R.HFIEQGINVC*LC*QSYAK.N	272|274	X	4.76%	0.00%
P04181	OAT Ornithine aminotransferase, mitochondrial	K.ALSGGLYPVSAVLC*DDDIMLTIKPGEHGSTYGG NPLGC*R.V	306|330	X	4.76%	0.00%
Q9BW92	TARS2 Threonine--tRNA ligase, mitochondrial	K.VTGPTATVYGC*GTLVDLC*QGPHLR.H	233|240	X	4.76%	0.00%
Q9NVH6	TMLHE Trimethyllysine dioxygenase, mitochondrial	R.HTDTTYFQEPC*GIQVFHC*LK.H	252|259	X	4.76%	0.00%
P22033	MUT Methylmalonyl-CoA mutase, mitochondrial	R.C*LAALTEC*AASGDGNILALAVDASR.A	533|540	X	4.76%	0.00%
Q5T160	RARS2 Probable arginine--tRNA ligase, mitochondrial	R.LHSLEETFGC*GYLNDFNTAC*LQEPQSVSILQHL LR.F	479|489	X	4.76%	0.00%
Q6L8Q7	PDE12 2,5-phosphodiesterase 12	K.SRPNASGGAAC*SGPGPEPAVFC*EPVVK.L	108|119	X	4.76%	0.00%
Q96GW9	MARS2 Methionine--tRNA ligase, mitochondrial	K.GVYEGWYC*ASDEC*FLPEAK.V	170|175	X	4.76%	0.00%
Q96GW9	MARS2 Methionine--tRNA ligase, mitochondrial	R.IC*VHSHWTVC*GQK.M	336|344	X	4.76%	0.00%
Q9NP81	SARS2 Serine--tRNA ligase, mitochondrial	R.FC*AC*PEEAAHALELR.K	64|66	X	4.76%	0.00%
Q15031	LARS2 Probable leucine--tRNA ligase, mitochondrial	K.GGPPLAMASEWVNC*SC*PR.C	504|506	X	4.76%	0.00%
Q10713	PMPCA Mitochondrial-processing peptidase subunit alpha	K.HGGIC*DC*QTSR.D	140|142	X	4.76%	0.00%
Q7L0Y3	TRMT10C Mitochondrial ribonuclease P protein 1	K.RLNLATEC*LPLDK.Y	335	X	4.76%	0.00%
Q9NYY8	FASTKD2 FAST kinase domain-containing protein 2	R.SAYC*LGSSHPR.G	645	X	4.76%	0.00%
Q9NYY8	FASTKD2 FAST kinase domain-containing protein 2	R.LMFSHPAFNQLC*EHMMR.E	217	X	4.76%	0.00%
Q9NYY8	FASTKD2 FAST kinase domain-containing protein 2	K.LSEEC*NSLSDVLDAFSK.A	163	X	4.76%	0.00%
Q7L8L6	FASTKD5 FAST kinase domain-containing protein 5	K.IGDLAC*ANIQHLSSR.S	345	X	4.76%	0.00%
Q9NYY8	FASTKD2 FAST kinase domain-containing protein 2	K.VVLDNIHGC*PLR.I	377	X	4.76%	0.00%
Q9NYY8	FASTKD2 FAST kinase domain-containing protein 2	K.LHTLDTC*LK.L	546	X	4.76%	0.00%
P30837	ALDH1B1 Aldehyde dehydrogenase X, mitochondrial	K.SPSIVLADADMEHAVEQC*HEALFFNMGQC*C* C*AGSR.T	307|318 |319|32 0	X	4.76%	0.00%
P30084	ECHS1 Enoyl-CoA hydratase, mitochondrial	K.IC*PVETLVEEAIQC*AEK.I	213|225	X	4.76%	0.00%
Q16762	TST Thiosulfate sulfurtransferase	R.HVPGASFFDIEEC*R.D	64	X	4.76%	0.00%
P11498	PC Pyruvate carboxylase, mitochondrial	R.FLYEC*PWR.R	622	X	4.76%	0.00%
Q15119	PDK2	K.HIGSIDPNC*NVSEVVK.D	195	X	4.76%	0.00%
P11498	PC Pyruvate carboxylase, mitochondrial	R.INGC*AIQC*R.V	372|376	X	4.76%	0.00%
P05091	ALDH2 Aldehyde dehydrogenase, mitochondrial	K.ANYLSQALQAGTVWVNC*YDVFGAQSPFGGYK .M	472	X	4.76%	0.00%
P10515	DLAT Dihydrolipoyllysine-residue acetyltransferase comp	K.GFDVASMMSVTLSC*DHR.V	618	X	4.76%	0.00%
P13196	ALAS1 5-aminolevulinate synthase, nonspecific, mitochond	R.QMLMDAGLPVVHC*PSHIIPVR.V	525	X	4.76%	0.00%
P23368	ME2 NAD-dependent malic enzyme, mitochondrial	R.VFTPGQGNNVYIFPGVALAVILC*NTR.H	481	X	4.76%	0.00%
P11182	DBT Lipoamide acyltransferase component of branched-ch	K.IPHFGYC*DEIDLTELVK.L	279	X	4.76%	0.00%
P30837	ALDH1B1 Aldehyde dehydrogenase X, mitochondrial	K.TIPMDGQHFC*FTR.H	169	X	4.76%	0.00%
P30084	ECHS1 Enoyl-CoA hydratase, mitochondrial	K.EMQNLSFQDC*YSSK.F	111	X	4.76%	0.00%
P08559	PDHA1 Pyruvate dehydrogenase E1 component subunit alpha,	R.VDGMDILC*VR.E	261	X	4.76%	0.00%
Q15119	PDK2	R.HYQTIQEAGDWC*VPSTEPK.N	392	X	4.76%	0.00%
P11177	PDHB Pyruvate dehydrogenase E1 component subunit beta,	K.EGVEC*EVINMR.T	263	X	4.76%	0.00%
P10515	DLAT Dihydrolipoyllysine-residue acetyltransferase comp	K.ASALAC*LK.V	488	X	4.76%	0.00%
P11177	PDHB Pyruvate dehydrogenase E1 component subunit beta,	R.GPNGASAGVAAQHSQC*FAAWYGHC*PGLK.V	161|169	X	4.76%	0.00%
P21953	BCKDHB 2-oxoisovalerate dehydrogenase subunit beta, mitoc	K.GLLLSC*IEDKNPC*IFFEPK.I	228|235	X	4.76%	0.00%
P08559	PDHA1 Pyruvate dehydrogenase E1 component subunit alpha,	K.LPC*IFIC*ENNR.Y	218|222	X	4.76%	0.00%
P23368	ME2 NAD-dependent malic enzyme, mitochondrial	R.C*LPVC*IDVGTDNIALLK.D	198|202	X	4.76%	0.00%
P08559	PDHA1 Pyruvate dehydrogenase E1 component subunit alpha,	R.GFC*HLC*DGQEAC*C*VGLEAGINPTDHLITAYR .A	91|94|1 00|101	X	4.76%	0.00%

Q96EY1	DNAJA3 DnaJ homolog subfamily A member 3, mitochondrial	K.VQHC*HYC*GGSGMETINTGPFVMR.S	253|256	X	4.76%	0.00%
O14874	BCKDK	R.MLATHHLALHEDKPDFVGIIC*TR.L	222	X	4.76%	0.00%
Q96I51	WBSCR16 Williams-Beuren syndrome chromosomal region 16 pro	R.C*LHFSGVGK.V	329	X	4.76%	0.00%
Q96I51	WBSCR16 Williams-Beuren syndrome chromosomal region 16 pro	R.VTMPGEPVDVAC*GVDHMVTLAK.S	451	X	4.76%	0.00%
Q96I51	WBSCR16 Williams-Beuren syndrome chromosomal region 16 pro	R.EGVFSMGNNSYGQC*GR.K	206	X	4.76%	0.00%
P43897	TSFM Elongation factor Ts, mitochondrial	K.YGALVIC*ETSEQK.T	240	X	4.76%	0.00%
P51649	ALDH5A1 Succinate-semialdehyde dehydrogenase, mitochondria	R.WLPAAATFPVQDPASGAALGMVADC*GVR.E	93	X	4.76%	0.00%
P13995	MTHFD2 Bifunctional methylenetetrahydrofolate dehydrogena	R.MC*LDQYSMLPATPWGVWEIIK.R	166	X	4.76%	0.00%
P48735	IDH2 Isocitrate dehydrogenase	K.NYDGDVQSDILAQGFGSLGLMTSVLVC*PDGK.T	336	X	4.76%	0.00%
P48735	IDH2 Isocitrate dehydrogenase	K.SSGGFVWAC*K.N	308	X	4.76%	0.00%
P48735	IDH2 Isocitrate dehydrogenase	R.NILGGTVFREPIIC*K.N	154	X	4.76%	0.00%
P48735	IDH2 Isocitrate dehydrogenase	K.VC*VETVESGAMTK.D	402	X	4.76%	0.00%
Q9UHN1	POLG2 DNA polymerase subunit gamma-2, mitochondrial	R.DSLLSGC*HPGFGPLGVELR.K	95	X	4.76%	0.00%
P48735	IDH2 Isocitrate dehydrogenase	K.DLAGC*IHGLSNVK.L	418	X	4.76%	0.00%
P51649	ALDH5A1 Succinate-semialdehyde dehydrogenase, mitochondria	K.NFFEPTLLC*NVTQDMLC*THEETFGPLAPVIK.F	426|434	X	4.76%	0.00%
P50213	IDH3A Isocitrate dehydrogenase	K.C*REVAESC*K.D	215|222	X	4.76%	0.00%
O76031	CLPX ATP-dependent Clp protease ATP-binding subunit clp	K.C*HHFFVVLSEADSK.K	130	X	4.76%	0.00%
O76031	CLPX ATP-dependent Clp protease ATP-binding subunit clp	K.C*ELNVTEDALK.A	538	X	4.76%	0.00%
P42704	LRPPRC Leucine-rich PPR motif-containing protein, mitocho	K.EVQMHSFPLQFTLHC*ALLANK.T	413	X	4.76%	0.00%
P42704	LRPPRC Leucine-rich PPR motif-containing protein, mitocho	K.GDLSTALEVAIDC*YEK.Y	848	X	4.76%	0.00%
P42704	LRPPRC Leucine-rich PPR motif-containing protein, mitocho	K.LFEC*DRDQMYYNLLK.L	952	X	4.76%	0.00%
P42704	LRPPRC Leucine-rich PPR motif-containing protein, mitocho	R.C*VANNQVETLEK.L	930	X	4.76%	0.00%
P42704	LRPPRC Leucine-rich PPR motif-containing protein, mitocho	R.LQWFC*DR.C	927	X	4.76%	0.00%
P42704	LRPPRC Leucine-rich PPR motif-containing protein, mitocho	R.SC*GSLLPELK.L	130	X	4.76%	0.00%
P42704	LRPPRC Leucine-rich PPR motif-containing protein, mitocho	R.AILQENGC*LSDSDMFSQAGLR.S	500	X	4.76%	0.00%
P42704	LRPPRC Leucine-rich PPR motif-containing protein, mitocho	K.EDGPSVFGSFFLQHC*VTMNTPVEK.L	380	X	4.76%	0.00%
P42704	LRPPRC Leucine-rich PPR motif-containing protein, mitocho	R.LIASYC*NVGDIEGASK.I	208	X	4.76%	0.00%
P42704	LRPPRC Leucine-rich PPR motif-containing protein, mitocho	K.AKYESDMVTGGYAALINLC*C*R.H	721|722	X	4.76%	0.00%
Q13686	ALKBH1 Alkylated DNA repair protein alkB homolog 1	R.VLPNPEGEGLPHC*LEAPLPAVLPR.D	304	X	4.76%	0.00%
Q8IYB8	SUPV3L1 ATP-dependent RNA helicase SUPV3L1, mitochondrial	R.LTPISVLDHALESLDNLRPGDC*IVC*FSK.N	369|372	X	4.76%	0.00%
Q9BQ69	MACROD1 O-acetyl-ADP-ribose deacetylase MACROD1	R.EEHYFC*K.D	116	X	4.76%	0.00%
Q9BU61	NDUFAF3 NADH dehydrogenase	R.GIAVEVQDTPNAC*ATFNFLC*HEGR.V	150|157	X	4.76%	0.00%
Q6YN16	HSDL2 Hydroxysteroid dehydrogenase-like protein 2	K.ALPC*IVDVR.D	71	X	4.76%	0.00%
O75608	LYPLA1 Acyl-protein thioesterase 1	K.LAGVTALSC*WLPLR.A	144	X	4.76%	0.00%
P49327	FASN Fatty acid synthase	K.C*TVFHGAQVEDAFR.Y	1828	X	4.76%	0.00%
P41250	GARS Glycine--tRNA ligase	K.TSYGWIEIVGC*ADR.S	461	X	4.76%	0.00%
P41250	GARS Glycine--tRNA ligase	R.QHMENEMAHYAC*DC*WDAESK.T	442|444	X	4.76%	0.00%
P04406	GAPDH Glyceraldehyde-3-phosphate dehydrogenase	R.VPTANVSVVDLTC*R.L	247	X	4.76%	0.00%
Q13085	ACACA Acetyl-CoA carboxylase 1	K.RVSALNSVHC*EHVEDEGESR.Y	1769	X	4.76%	0.00%
Q13085	ACACA Acetyl-CoA carboxylase 1	K.RPGAALDPGC*VLAK.M	813	X	4.76%	0.00%
Q13085	ACACA Acetyl-CoA carboxylase 1	K.DNTC*VVEFQFMLPTSHPNR.G	1176	X	4.76%	0.00%
Q13085	ACACA Acetyl-CoA carboxylase 1	R.VFHYVLDNLVNVMNGYC*LPDPFFSSK.V	868	X	4.76%	0.00%
Q13085	ACACA Acetyl-CoA carboxylase 1	K.VQAERPDTMLGVVC*GALHVADVSLR.N	634	X	4.76%	0.00%
P07195	LDHB L-lactate dehydrogenase B chain	K.GMYGIENEVFLSLPC*ILNAR.G	294	X	4.76%	0.00%
Q9H6R3	ACSS3 Acyl-CoA synthetase short-chain family member 3, m	K.GHVPLALC*VLR.K	602	X	4.76%	0.00%
Q8N4Q0	ZADH2 Zinc-binding alcohol dehydrogenase domain-containi	K.C*HVIGTC*SSDEK.S	198|204	X	4.76%	0.00%
Q8N3Z3	GTPBP8 GTP-binding protein 8	K.TQGC*FPQLFPVSAVTFSGIHLLR.C	254	X	4.76%	0.00%
Q8N3Z3	GTPBP8 GTP-binding protein 8	R.IDHAPDLPRPEVC*FIGR.S	114	X	4.76%	0.00%
Q6P2I3	FAHD2B Fumarylacetoacetate hydrolase domain-containing pr	K.KGDEVQC*EIEELGVIINK.V	301	X	4.76%	0.00%
Q6P2I3	FAHD2B Fumarylacetoacetate hydrolase domain-containing pr	K.VVC*VGMNYVDHC*K.E	110|119	X	4.76%	0.00%
P63167	DYNLL1 Dynein light chain 1, cytoplasmic	K.NADMSEEMQQDSVEC*ATQALEK.Y	24	X	4.76%	0.00%
Q9BQP7	C20orf72 Uncharacterized protein C20orf72	K.DGSPAHPHFMDAELC*SQYWTK.W	314	X	4.76%	0.00%
Q7L592	C2orf56 Protein midA homolog, mitochondrial	K.NC*DISVHLVEVSQK.L	148	X	4.76%	0.00%
Q4G0N4	NADKD1 NAD kinase domain-containing protein 1	K.SSGLNLC*TGTGSK.A	311	X	4.76%	0.00%
Q96RR1	PEO1 Twinkle protein, mitochondrial	R.GHGIPFQDGHSC*LR.A	77	X	4.76%	0.00%

Q9NXH9	TRMT1 tRNA (guanine(26)-N(2))-dimethyltransferase	R.TAAVGEIC*EEGLHVLEGLAASGLR.S	150		4.76%	0.00%
P49773	HINT1 Histidine triad nucleotide-binding protein 1	R.C*LAFHDISPQAPTHFLVIPK.K	38		4.76%	0.00%
Q04760	GLO1 Lactoylglutathione lyase	R.GFGHIGIAVPDVYSAC*K.R	139		4.76%	0.00%
P26641	EEF1G Elongation factor 1-gamma	R.WFLTC*INQPQFR.A	194		4.76%	0.00%
E7EMT2	Uncharacterized protein	R.FPEELTQTFMSC*NLITGMFQR.L	BAD_ID		4.76%	0.00%
P08107	HSPA1B Heat shock 70 kDa protein 1A/1B	K.ELEQVC*NPIISGLYQGAGGPGPGGFGAQGPK.G	BAD_ID		4.76%	0.00%
F5H5T6	Uncharacterized protein	R.GMLENC*ILLSLFAK.E	83		4.76%	0.00%
P20073	ANXA7 Annexin A7	K.TILQC*ALNRPAFFAER.L	413		4.76%	0.00%
P37802	TAGLN2 Transgelin-2	K.DGTVLC*ELINALYPEGQAPVK.K	63		4.76%	0.00%
Q9BSD7	NTPCR Cancer-related nucleoside-triphosphatase	R.NHLLPDIVTC*VQSSR.K	184		4.76%	0.00%
P37802	TAGLN2 Transgelin-2	K.QYDADLEQILIQWITTQC*R.K	38		4.76%	0.00%
Q13642	FHL1 Four and a half LIM domains protein 1	R.FWHDTC*FR.C	65		4.76%	0.00%
P14923	JUP Junction plakoglobin	R.C*TTSILHNLSHHR.E	204		4.76%	0.00%
P08134	RHOC Rho-related GTP-binding protein RhoC	K.HFC*PNVPIILVGNK.K	107		4.76%	0.00%
P63244	GNB2L1 Guanine nucleotide-binding protein subunit beta-2-	K.TNHIGHTGYLNTVTVSPDGSLC*ASGGK.D	207		4.76%	0.00%
P63244	GNB2L1 Guanine nucleotide-binding protein subunit beta-2-	K.HLYTLDGGDIINALC*FSPNR.Y	240		4.76%	0.00%
P08238	HSP90AB1 Heat shock protein HSP 90-beta	R.LVSSPC*C*IVTSTYGWTANMER.I	589|590		4.76%	0.00%
P13639	EEF2 Elongation factor 2	R.TFC*QLILDPIFK.V	290		4.76%	0.00%
Q06830	PRDX1 Peroxiredoxin-1	K.LNC*QVIGASVDSHFC*HLAWVNTPK.K	71|83		4.76%	0.00%
P61978	HNRNPK Heterogeneous nuclear ribonucleoprotein K	K.LFQEC*C*PHSTDR.V	184|185		4.76%	0.00%
Q15185	PTGES3 Prostaglandin E synthase 3	K.HLNEIDLFHC*IDPNDSK.H	58		4.76%	0.00%
P08238	HSP90AB1 Heat shock protein HSP 90-beta	R.VFIMDSC*DELIPEYLNFIR.G	366		4.76%	0.00%
P13639	EEF2 Elongation factor 2	R.YVEPIEDVPC*GNIVGLVGVDQFLVK.T	466		4.76%	0.00%
P14618	PKM Pyruvate kinase isozymes M1/M2	R.AGKPVIC*ATQMLESMIK.K	326		4.76%	0.00%
P30153	PPP2R1A Serine/threonine-protein phosphatase 2A 65 kDa reg	K.DNTIEHLLPLFLAQLKDEC*PEVR.L	377		4.76%	0.00%
P08238	HSP90AB1 Heat shock protein HSP 90-beta	K.C*LELFSELAEDKENYK.K	412		4.76%	0.00%
P23526	AHCY Adenosylhomocysteinase	K.SKFDNLYGC*R.E	195		4.76%	0.00%
P62140	PPP1CB Serine/threonine-protein phosphatase PP1-beta cata	R.HDLDLIC*R.A	244		4.76%	0.00%
P63104	YWHAZ 14-3-3 protein zeta/delta	R.DIC*NDVLSLLEK.F	94		4.76%	0.00%
P78371	CCT2 T-complex protein 1 subunit beta	R.SLHDALC*VLAQTVK.D	395		4.76%	0.00%
Q13347	EIF3I Eukaryotic translation initiation factor 3 subunit	K.HVLTGSADNSC*R.L	76		4.76%	0.00%
P13639	EEF2 Elongation factor 2	K.IWC*FGPDGTGPNILTDITK.G	651		4.76%	0.00%
P14618	PKM Pyruvate kinase isozymes M1/M2	R.AEGSDVANAVLDGADC*IMLSGETAK.G	358		4.76%	0.00%
Q6IS14	EIF5AL1 Eukaryotic translation initiation factor 5A-1-like	K.KYEDIC*PSTHNMDVPNIK.R	73		4.76%	0.00%
Q9H3K6	BOLA2B BolA-like protein 2	R.LVNAC*LAEELPHIHAFEQK.T	59		4.76%	0.00%
P68104	EEF1A1 Elongation factor 1-alpha 1	K.NDPPMEAAGFTAQVIILNHPGQISAGYAPVLDC*HTAHIAC*K.F	363|370		4.76%	0.00%
P62633	CNBP Cellular nucleic acid-binding protein	R.EQC*C*YNC*GKPGHLAR.D	97|98|101		4.76%	0.00%
P06733	ENO1 Alpha-enolase	R.SGETEDTFIADLVVGLC*TGQIK.T	389		4.76%	0.00%
P60709	ACTB Actin, cytoplasmic 1	K.LC*YVALDFEQEMATAASSSSLEK.S	217		4.76%	0.00%
P60709	ACTB Actin, cytoplasmic 1	R.C*PEALFQPSFLGMESC*GIHETTFNSIMK.C	257|272		4.76%	0.00%
P68366	TUBA4A Tubulin alpha-4A chain	R.SIQFVDWC*PTGFK.V	347		4.76%	0.00%
P68366	TUBA4A Tubulin alpha-4A chain	K.AYHEQLSVAEITNAC*FEPANQMVK.C	295		4.76%	0.00%
Q71U36	TUBA1A Tubulin alpha-1A chain	K.LADQC*TGLQGFLVFHSFGGGTGSGFTSLLMER.L	129		4.76%	0.00%
P68366	TUBA4A Tubulin alpha-4A chain	R.AVC*MLSNTTAIAEAWAR.L	376		4.76%	0.00%
P68366	TUBA4A Tubulin alpha-4A chain	K.YMAC*C*LLYR.G	315|316		4.76%	0.00%
Q71U36	TUBA1A Tubulin alpha-1A chain	R.EC*ISIHVGQAGVQIGNAC*WELYC*LEHGIQPDGQMPSDK.T	4|20|25		4.76%	0.00%
Q13155	AIMP2 Aminoacyl tRNA synthase complex-interacting multif	R.LLC*EHFR.V	143		4.76%	0.00%
P04075	ALDOA Fructose-bisphosphate aldolase A	R.VNPC*IGGVILFHETLYQK.A	73		4.76%	0.00%
P00492	HPRT1 Hypoxanthine-guanine phosphoribosyltransferase	R.SPGVVISDDEPGYDLDLFC*IPNHYAEDLER.V	23		4.76%	0.00%
P22061	PCMT1 Protein-L-isoaspartate(D-aspartate) O-methyltransf	K.ALDVGSGSGILTAC*FAR.M	95		4.76%	0.00%
P12277	CKB Creatine kinase B-type	R.GFC*LPPHC*SR.G	141|146		4.76%	0.00%
P13489	RNH1 Ribonuclease inhibitor	R.ELDLSNNC*LGDAGILQLVESVR.Q	409		4.76%	0.00%
P15121	AKR1B1 Aldose reductase	R.HIDC*AHVYQNENEVGVAIQEK.L	45		4.76%	0.00%
P00338	LDHA L-lactate dehydrogenase A chain	K.DDVFLSVPC*ILGQNGISDLVK.V	293		4.76%	0.00%
P48147	PREP Prolyl endopeptidase	K.FSC*MAWTHDGK.G	175		4.76%	0.00%
P27348	YWHAQ 14-3-3 protein theta	R.SIC*TTVLELLDK.Y	94		4.76%	0.00%
O43707	ACTN4 Alpha-actinin-4	K.TFTAWC*NSHLR.K	60		4.76%	0.00%
P07900	HSP90AA1 Heat shock protein HSP 90-alpha	K.HGLEVIYMIEPIDEYC*VQQLK.E	529		4.76%	0.00%
P07900	HSP90AA1 Heat shock protein HSP 90-alpha	R.VFIMDNC*EELIPEYLNFIR.G	374		4.76%	0.00%
P55209	NAP1L1 Nucleosome assembly protein 1-like 1	R.FEIINAIYEPTEEEC*EWKPDEEDEISEELKEK.A	132		4.76%	0.00%

P09651	HNRNPA1 Heterogeneous nuclear ribonucleoprotein A1	K.YHTVNGHNC*EVR.K	175		4.76%	0.00%
Q08J23	NSUN2 tRNA (cytosine(34)-C(5))-methyltransferase	R.LSSPC*IMVVNHDASSIPR.L	235		4.76%	0.00%
P31943	HNRNPH1 Heterogeneous nuclear ribonucleoprotein H	R.YGDGGSTFQSTTGHC*VHMR.G	290		4.76%	0.00%
P84243	H3F3B Histone H3.3	R.FQSAAIGALQEASEAYLVGLFEDTNLC*AIHAK.R	111		4.76%	0.00%
Q13838	DDX39B Spliceosome RNA helicase DDX39B	K.HFILDEC*DK.M	198		4.76%	0.00%
Q13838	DDX39B Spliceosome RNA helicase DDX39B	R.C*IALAQLLVEQNFPAIAIHR.G	300		4.76%	0.00%
P14174	MIF Macrophage migration inhibitory factor	K.LLC*GLLAER.L	81		4.76%	0.00%
Q96EY7	PTCD3 Pentatricopeptide repeat-containing protein 3, mit	K.NEHSYC*TMIR.G	260	X	4.76%	0.00%
Q99714	HSD17B10 3-hydroxyacyl-CoA dehydrogenase type-2	K.VC*NFLASQVPFPSR.L	214	X	4.76%	0.00%
P42126	ECI1 Enoyl-CoA delta isomerase 1, mitochondrial	R.GVILTSDRPGVFSAGLDLTEMC*GR.S	114	X	4.76%	0.00%
Q9BW92	TARS2 Threonine--tRNA ligase, mitochondrial	K.EQELFFFHELSPGSC*FFLPR.G	322	X	4.76%	0.00%
P10515	DLAT Dihydrolipoyllysine-residue acetyltransferase comp	K.NFSAIINPPQAC*ILAIGASEDK.L	586	X	4.76%	0.00%
Q5TC12	ATPAF1 ATP synthase mitochondrial F1 complex assembly fac	R.AQSC*PTFLC*ALPR.R	194|199	X	4.76%	0.00%
O76031	CLPX ATP-dependent Clp protease ATP-binding subunit clp	K.LLLEPMFEVPNSDIVC*VEVDK.E	586	X	4.76%	0.00%
Q15118	PDK1	R.LC*DLYYINSPELELEELNAK.S	240	X	4.63%	0.38%
Q92552	MRPS27 28S ribosomal protein S27, mitochondrial	K.EKLSTC*EAEDIATYEQNLQQWHLDLVQLIQR.E	367	X	4.61%	0.37%
P54886	ALDH18A1 Delta-1-pyrroline-5-carboxylate synthase	K.GIPVMGHSEGIC*HMYVDSEASVDK.V	584	X	4.59%	0.42%
Q9NSE4	IARS2 Isoleucine--tRNA ligase, mitochondrial	K.TEFC*LHDGPPYANGDPHVGHALNK.I	110	X	4.58%	0.41%
Q9Y2Z4	YARS2 Tyrosine--tRNA ligase, mitochondrial	K.EAPFSEFFLDPGTSVLDTC*R.K	413	X	4.58%	0.41%
H7C455	Uncharacterized protein	K.EFHQAGKPIGLC*C*IAPVLAAK.V	BAD_ID		4.58%	0.41%
Q9BYD1	MRPL13 39S ribosomal protein L13, mitochondrial	R.LQGLHKPVYHALSDC*GDHVVIMNTR.H	53	X	4.53%	0.46%
P31040	SDHA Succinate dehydrogenase	R.TYFSC*TSAHTSTGDGTAMITR.A	266	X	4.53%	0.46%
P30405	PPIF Peptidyl-prolyl cis-trans isomerase F, mitochondri	K.HVGPGVLSMANAGPNTNGSQFFIC*TIK.T	157	X	4.53%	0.46%
P10809	HSPD1 60 kDa heat shock protein, mitochondrial	R.C*IPALDSLTPANEDQK.I	447	X	4.53%	0.46%
Q9BQP7	C20orf72 Uncharacterized protein C20orf72	R.ALESAVQHETLNYIGLLDC*VAEYQGK.L	239	X	4.53%	0.46%
P23368	ME2 NAD-dependent malic enzyme, mitochondrial	K.YC*TFNDDIQGTAAVALAGLLAAQK.V	274	X	4.51%	1.89%
Q92552	MRPS27 28S ribosomal protein S27, mitochondrial	R.EKEHYC*LADLASLMDK.T	49	X	4.47%	0.54%
Q9Y3D2	MSRB2 Methionine-R-sulfoxide reductase B2, mitochondrial	K.QC*EAHLGHVFPDGPGPNGQR.F	149	X	4.46%	0.53%
P40926	MDH2 Malate dehydrogenase, mitochondrial	K.GC*DVVVIPAGVPR.K	93	X	4.46%	0.53%
Q5JRX3	PITRM1 Presequence protease, mitochondrial	K.LGC*GLLDYR.E	627	X	4.46%	0.53%
Q9H5Q4	TFB2M Dimethyladenosine transferase 2, mitochondrial	K.PSRPPHLLLEC*NPGPGILTQALLEAGAK.V	102	X	4.42%	0.85%
Q5JRX3	PITRM1 Presequence protease, mitochondrial	R.AFSSLNTLPEELRPYVPLFC*SVLTK.L	619	X	4.40%	0.50%
P10515	DLAT Dihydrolipoyllysine-residue acetyltransferase comp	R.DVPLGTPLC*IIVEK.E	291	X	4.40%	0.50%
P23434	GCSH Glycine cleavage system H protein, mitochondrial	K.SC*YEDGWLIK.M	138	X	4.39%	0.83%
Q9NSE4	IARS2 Isoleucine--tRNA ligase, mitochondrial	K.IHFVPGWDC*HGLPIEIK.V	155	X	4.30%	0.50%
Q6YN16	HSDL2 Hydroxysteroid dehydrogenase-like protein 2	K.TAIHTAAMDMLGGPGIESQC*R.K	218	X	4.30%	0.50%
P68104	EEF1A1 Elongation factor 1-alpha 1	K.DGNASGTTLLEALDC*ILPPTRPTDK.P	234		4.30%	0.50%
Q9NSE4	IARS2 Isoleucine--tRNA ligase, mitochondrial	R.RPYWC*ISR.Q	521	X	4.30%	0.77%
Q12849	GRSF1 G-rich sequence factor 1	R.YIELFLNSC*PK.G	476	X	4.30%	0.92%
P49411	TUFM Elongation factor Tu, mitochondrial	K.GDEC*ELLGHSK.N	290	X	4.30%	0.92%
P34897	SHMT2 Serine hydroxymethyltransferase, mitochondrial	R.AALEALGSC*LNNK.Y	91	X	4.30%	0.92%
P04181	OAT Ornithine aminotransferase, mitochondrial	K.VLPMNTGVEAGETAC*K.L	150	X	4.30%	0.92%
P10515	DLAT Dihydrolipoyllysine-residue acetyltransferase comp	R.DVPIGAIIC*ITVGKPEDIEAFK.N	164	X	4.30%	0.92%
P11498	PC Pyruvate carboxylase, mitochondrial	R.ADFAQAC*QDAGVR.F	131	X	4.30%	0.92%
Q9BQ69	MACROD1 O-acetyl-ADP-ribose deacetylase MACROD1	R.SC*YLSSLDLLLEHR.L	246	X	4.23%	0.85%
P51553	IDH3G Isocitrate dehydrogenase	R.HAC*VPVDFEEVHVSSNADEEDIR.N	81	X	4.21%	0.83%
O75439	PMPCB Mitochondrial-processing peptidase subunit beta	K.TNMLLQLDGSTPIC*EDIGR.Q	419	X	4.21%	0.83%
P13639	EEF2 Elongation factor 2	R.LMEPIYLVEIQC*PEQVVGGIYGVLNR.K	751		4.20%	1.23%
P30048	PRDX3 Thioredoxin-dependent peroxide reductase, mitochon	K.ANEFHDVNC*EVVAVSVDSHFSHLAWINTPR.K	127	X	4.15%	0.75%

Q9NSE4	IARS2 Isoleucine--tRNA ligase, mitochondrial	K.KPGLEEAVESAC*AMR.D	883	X	4.15%	0.75%
P22033	MUT Methylmalonyl-CoA mutase, mitochondrial	R.AHC*QTSGWSLTEQDPYNNIVR.T	351	X	4.15%	0.75%
Q7L0Y3	TRMT10C Mitochondrial ribonuclease P protein 1	K.TLMEC*VSNTAK.K	123	X	4.15%	1.07%
P43897	TSFM Elongation factor Ts, mitochondrial	K.FQLLVQQVALGTMMHC*QTLK.D	149	X	4.15%	1.07%
Q7Z7H8	MRPL10 39S ribosomal protein L10, mitochondrial	R.TVPFLPLLGGC*IDDTILSR.Q	180	X	4.06%	1.40%
P31930	UQCRC1 Cytochrome b-c1 complex subunit 1, mitochondrial	R.NALVSHLDGTTPVC*EDIGR.S	410	X	4.06%	1.40%
Q9HCC0	MCCC2 Methylcrotonoyl-CoA carboxylase beta chain, mitoch	R.LPC*IYLVDSGGAYLPR.Q	167	X	4.06%	1.40%
Q7L0Y3	TRMT10C Mitochondrial ribonuclease P protein 1	R.NVDPFHIYFC*NLK.I	246	X	4.06%	1.40%
P10809	HSPD1 60 kDa heat shock protein, mitochondrial	K.C*EFQDAYVLLSEK.K	237	X	4.06%	1.40%
Q8N4Q0	ZADH2 Zinc-binding alcohol dehydrogenase domain-containi	K.SLGC*DRPINYK.T	218	X	4.06%	1.40%
Q99798	ACO2 Aconitate hydratase, mitochondrial	K.VAVPSTIHC*DHLIEAQVGGEK.D	126	X	3.99%	0.91%
Q15118	PDK1	K.HIGSINPNC*NVLEVIK.D	223	X	3.99%	1.09%
P08559	PDHA1 Pyruvate dehydrogenase E1 component subunit alpha,	K.NFYGGNGIVGAQVPLGAGIALAC*K.Y	181	X	3.84%	1.07%
O75439	PMPCB Mitochondrial-processing peptidase subunit beta	K.FHFGDSLC*THK.G	265	X	3.84%	1.01%
P00367	GLUD1 Glutamate dehydrogenase 1, mitochondrial	K.PC*NHVLSLSFPIR.R	112	X	3.83%	1.18%
P38646	HSPA9 Stress-70 protein, mitochondrial	R.RTIAPC*QK.A	366	X	3.83%	1.62%
P42704	LRPPRC Leucine-rich PPR motif-containing protein, mitocho	R.C*GAIAEQTPILLLFLLR.N	1277	X	3.82%	1.89%
P04181	OAT Ornithine aminotransferase, mitochondrial	K.YFDFLSSYSAVNQGHC*HPK.I	93	X	3.68%	1.24%
Q5JRX3	PITRM1 Presequence protease, mitochondrial	K.THFLMPFPVNYVGEC*IR.T	869	X	3.68%	1.24%
P10809	HSPD1 60 kDa heat shock protein, mitochondrial	R.AAVEEGIVLGGGC*ALLR.C	442	X	3.68%	1.24%
Q12931	TRAP1 Heat shock protein 75 kDa, mitochondrial	R.NIYYLC*APNR.H	501	X	3.64%	1.53%
P38117	ETFB Electron transfer flavoprotein subunit beta	K.HSMNPFC*EIAVEEAVR.L	42	X	3.64%	1.53%
P00505	GOT2 Aspartate aminotransferase, mitochondrial	R.VGAFTMVC*K.D	295	X	3.60%	1.40%
Q9NSE4	IARS2 Isoleucine--tRNA ligase, mitochondrial	R.SC*QTALVEILDVIVR.S	819	X	3.52%	1.40%
Q15031	LARS2 Probable leucine--tRNA ligase, mitochondrial	R.FFSHFC*HDQK.M	578	X	3.36%	1.62%
Q9BQ52	ELAC2 Zinc phosphodiesterase ELAC protein 2	K.VVYSGDTMPC*EALVR.M	670	X	2.44%	0.67%

Table 4A-6. Average percent oxidation for mitochondria localized cysteines from 100 μM peroxide-treated matrix-APEX analysis. Data was filtered for peptides with ratio values in 2 out of 3 replicates, with a standard deviation <30%.

UniProt ID	Description	Peptide Sequence	Residue	Mito	Average % Oxidation Matrix-APEX 100 μM H2O2	% Standard Deviation
E7ERL9	VARS2 Valine--tRNA ligase, mitochondrial	R.NHQLVNWSC*ALR.S	BAD_ID	Yes	73.79%	8.25%
P08133	ANXA6 Annexin A6	R.LIVGLMRPPAYC*DAK.E	96		69.31%	5.30%
Q5JRX3	PITRM1 Presequence protease, mitochondrial	R.TTPMDSTGVPHILEHTVLC*GSQK.Y	112	Yes	43.32%	0.60%
P07203	GPX1 Glutathione peroxidase 1	R.GLVVLGFPC*NQFGHQENAK.N	78	Yes	43.01%	3.15%
Q16822	PCK2 Phosphoenolpyruvate carboxykinase	R.QC*PIMDPAWEAPEGVPIDAIIFGGR.R	431	Yes	36.74%	5.01%
Q53R41	FASTKD1 FAST kinase domain-containing protein 1	R.IEAVLPQC*DLNNLSSFATSVLR.W	446	Yes	34.61%	2.11%
Q15365	PCBP1 Poly(rC)-binding protein 1	R.VMTIPYQPMPASSPVIC*AGGQDR.C	194		32.45%	0.02%
Q7Z4W1	DCXR L-xylulose reductase	R.AVTNHSVYC*STK.G	150	Yes	31.05%	0.50%
P00505	GOT2 Aspartate aminotransferase, mitochondrial	K.TC*GFDFTGAVEDISK.I	187	Yes	30.38%	1.38%
P13639	EEF2 Elongation factor 2	K.STLTDSLVC*K.A	41		29.49%	21.41 %

Q6P2I3	FAHD2B Fumarylacetoacetate hydrolase domain-containing pr	K.TFDTFC*PLGPALVTK.D	215		29.13%	2.32%
Q9NUB1	ACSS1 Acetyl-coenzyme A synthetase 2-like, mitochondrial	R.TLGSVGEPINC*EAWEWLHR.V	422	Yes	29.11%	10.52 %
P11177	PDHB Pyruvate dehydrogenase E1 component subunit beta,	R.PVGHC*LEAAAVLSK.E	249	Yes	28.39%	29.67 %
Q9NWU5	MRPL22 39S ribosomal protein L22, mitochondrial	R.RPAEIYHC*R.R	70	Yes	27.22%	0.25%
Q8IYQ7	THNSL1 Threonine synthase-like 1	R.C*IHPADIPAAR.L	299	Yes	26.60%	9.67%
Q99714	HSD17B10 3-hydroxyacyl-CoA dehydrogenase type-2	R.VDVAVNC*AGIAVASK.T	91	Yes	24.37%	16.98 %
O60888	CUTA Protein CutA	R.LAAC*VNLIPQITSIYEWK.G	96		23.65%	1.94%
O76031	CLPX ATP-dependent Clp protease ATP-binding subunit clp	K.C*HHFFVVLSEADSK.K	130	Yes	22.78%	7.54%
Q9Y3D2	MSRB2 Methionine-R-sulfoxide reductase B2, mitochondrial	K.QC*EAHLGHVFPDGPGPNGQR.F	149	Yes	22.71%	3.75%
Q9NWU1	OXSM 3-oxoacyl-	K.GPNHAVSTAC*TTGAHAVGDSFR.F	209	Yes	22.03%	6.46%
P54886	ALDH18A1 Delta-1-pyrroline-5-carboxylate synthase	K.C*EYPAAC*NALETLLIHR.D	606|612	Yes	21.88%	0.50%
P31930	UQCRC1 Cytochrome b-c1 complex subunit 1, mitochondrial	K.AVELLGDIVQNC*SLEDSQIEK.E	154	Yes	20.67%	29.14 %
Q9H1K1	ISCU Iron-sulfur cluster assembly enzyme ISCU, mitochon	K.NVGTGLVGAPAC*GDVMK.L	69	Yes	20.39%	2.35%
P22061	PCMT1 Protein-L-isoaspartate(D-aspartate) O-methyltransf	K.ALDVGSGSGILTAC*FAR.M	95		20.21%	20.08 %
Q8NFF5	FLAD1 FAD synthase	K.GHTQDTNTFFLC*R.T	136	Yes	19.29%	7.03%
Q96AB3	ISOC2 Isochorismatase domain-containing protein 2, mitoc	K.TC*FSMVPALQQELDSRPQLR.S	84	Yes	19.12%	1.29%
P13995	MTHFD2 Bifunctional methylenetetrahydrofolate dehydrogena	R.IC*NAVSPDKDVDGFHVINVGR.M	145	Yes	18.64%	1.93%
Q5JRX3	PITRM1 Presequence protease, mitochondrial	R.LLPDHTYSVVSGGDPLC*IPELTWEQLK.Q	241	Yes	18.55%	0.51%
Q9NSE4	IARS2 Isoleucine--tRNA ligase, mitochondrial	K.LASLIDGSSPVSILVWTTQPWTIPANEAVC*YMPESK.Y	311	Yes	18.44%	0.83%
Q8NC60	NOA1 Nitric oxide-associated protein 1	R.C*WLLSHHR.R	182	Yes	18.35%	0.42%
Q9BSH5	HDHD3 Haloacid dehalogenase-like hydrolase domain-contai	R.LAHMEPVVAAHVGDNYLC*DYQGPR.A	196	Yes	18.27%	19.33 %
Q9H0R6	QRSL1 Glutamyl-tRNA(Gln) amidotransferase subunit A, mit	R.NPAAHC*GLVGFK.P	203	Yes	18.06%	0.11%
P22830	FECH Ferrochelatase, mitochondrial	K.ALADLVHSHIQSNELC*SK.Q	395	Yes	17.75%	6.69%
P07737	PFN1 Profilin-1	K.C*YEMASHLR.R	128		17.61%	16.40 %
P30042	C21orf33 ES1 protein homolog, mitochondrial	K.VVTTPAFMC*ETALHYIHDGIGAMVR.K	BAD_ID	Yes	17.57%	0.67%
Q9Y606	PUS1 tRNA pseudouridine synthase A, mitochondrial	R.TYC*YLLPTFAFAHK.D	202	Yes	17.07%	10.66 %
P22570	FDXR NADPH:adrenodoxin oxidoreductase, mitochondrial	R.VMDVPGLYC*SGWVK.R	395	Yes	16.92%	17.19 %
Q9Y3D5	MRPS18C 28S ribosomal protein S18c, mitochondrial	R.HITGLC*GK.K	100	Yes	16.77%	0.46%
Q99797	MIPEP Mitochondrial intermediate peptidase	R.C*PTDFAEVPSILMEYFANDYR.V	518	Yes	16.74%	4.49%
P34897	SHMT2 Serine hydroxymethyltransferase, mitochondrial	R.GLELIASENFC*SR.A	80	Yes	16.61%	0.96%
Q9BXW7	CECR5 Cat eye syndrome critical region protein 5	R.DLC*FSPGLMEASHVVNDVNEAVQLVFR.K	392	Yes	16.40%	1.07%
Q6PI48	DARS2 Aspartate--tRNA ligase, mitochondrial	K.ILC*EAPVESVVQVSGTVISR.P	108	Yes	16.37%	4.43%
Q6UB35	MTHFD1L Monofunctional C1-tetrahydrofolate synthase, mitoc	R.ASIGAGFIYPLVGTMSTMPGLPTRPC*FYDIDLDTETEQVK.G	961	Yes	16.34%	0.43%
P34897	SHMT2 Serine hydroxymethyltransferase, mitochondrial	K.YSEGYPGKRYYGGAEVVDEIELLC*QR.R	119	Yes	16.00%	15.90 %
Q5JRX3	PITRM1 Presequence protease, mitochondrial	R.NLPDMMQLWSEIFNNPC*FEEEEHFK.V	692	Yes	15.99%	1.12%
Q86SX6	GLRX5 Glutaredoxin-related protein 5, mitochondrial	K.GTPEQPQC*GFSNAVVQILR.L	67	Yes	15.91%	0.91%
O75323	GBAS Protein NipSnap homolog 2	K.LQFHNVKPEC*LEAYNK.I	85	Yes	15.89%	2.29%
Q9BQ52	ELAC2 Zinc phosphodiesterase ELAC protein 2	K.VC*FGDFPTMPK.L	753	Yes	15.74%	9.50%
P04075	ALDOA Fructose-bisphosphate aldolase A	K.ALSDHHIYLEGTLLKPNMVTPGHAC*TQK.F	240		15.73%	1.14%
P23378	GLDC Glycine dehydrogenase	K.TFC*IPHGGGGPGMGPIGVK.K	757	Yes	15.63%	0.77%
Q99797	MIPEP Mitochondrial intermediate peptidase	R.ADKPHQDC*HFTIR.G	448	Yes	15.63%	0.47%
Q6L8Q7	PDE12 2,5-phosphodiesterase 12	K.LHC*TPGDGQR.F	250	Yes	15.57%	4.46%
Q13642	FHL1 Four and a half LIM domains protein 1	R.FWHDTC*FR.C	65		15.44%	2.72%
Q6P1X6	C8orf82 UPF0598 protein C8orf82	R.C*EDRPVVFTHLLTADHGPPR.L	107	Yes	15.41%	0.96%
P14174	MIF Macrophage migration inhibitory factor	R.ASVPDGFLSELTQQLAQATGKPPQYIAVHVVPDQLMAFGGSSEPC*ALC*SLHSIGK.I	57|60		15.15%	2.37%
Q6P1X6	C8orf82 UPF0598 protein C8orf82	R.YEAAFPFLSPC*GR.E	98	Yes	15.09%	0.93%
Q9BQ69	MACROD1 O-acetyl-ADP-ribose deacetylase MACROD1	R.SC*YLSSLDLLLEHR.L	246	Yes	14.94%	0.98%
Q99798	ACO2 Aconitate hydratase, mitochondrial	R.VGLIGSC*TNSSYEDMGR.S	385	Yes	14.92%	0.34%
P13995	MTHFD2 Bifunctional methylenetetrahydrofolate dehydrogena	R.MC*LDQYSMLPATPWGVWEIIK.R	166	Yes	14.85%	1.39%
P30837	ALDH1B1 Aldehyde dehydrogenase X, mitochondrial	R.HEPVGVC*GQIIPWNFPLVMQGWK.L	179	Yes	14.73%	0.94%
P00505	GOT2 Aspartate aminotransferase, mitochondrial	K.IPEQSVLLLHAC*AHNPTGVDPR.P	212	Yes	14.43%	0.61%
Q9BQP7	C20orf72 Uncharacterized protein C20orf72	R.GVAQTPGSVEEDALLC*GPVSK.H	79	Yes	14.23%	0.32%
Q08257	CRYZ Quinone oxidoreductase	R.ALIHSAC*VK.A	145	Yes	14.21%	0.33%
Q6UB35	MTHFD1L Monofunctional C1-tetrahydrofolate synthase, mitoc	K.LHEADIVVLGSPKPEEIPLTWIQPGTTVLNC*SHDFLSGK.V	291	Yes	14.19%	0.69%
Q9Y6G3	MRPL42 39S ribosomal protein L42, mitochondrial	R.TIVC*YHPSVDIPYEHTKPIPR.P	60	Yes	14.13%	3.83%
P42126	ECI1 Enoyl-CoA delta isomerase 1, mitochondrial	R.YC*IGLNETQLGIIAPFWLK.D	173	Yes	14.10%	2.08%

P49411	TUFM Elongation factor Tu, mitochondrial	K.GEETPVIVGSALC*ALEGR.D	222	Yes	13.87%	16.21 %
Q9HCC0	MCCC2 Methylcrotonoyl-CoA carboxylase beta chain, mitoch	K.AATGEEVSAEDLGGADLHC*R.K	267	Yes	13.73%	0.80%
O76031	CLPX ATP-dependent Clp protease ATP-binding subunit clp	K.LLLEPMFEVPNSDIVC*VEVDK.E	586	Yes	13.70%	0.27%
Q9BPW8	NIPSNAP1 Protein NipSnap homolog 1	K.LHLDEDYPC*SLVGNWNTWYGEQDQ AVHLWR.F	106	Yes	13.67%	0.65%
P34897	SHMT2 Serine hydroxymethyltransferase, mitochondrial	R.AALEALGSC*LNNK.Y	91	Yes	13.65%	0.95%
O75521	ECI2 Enoyl-CoA delta isomerase 2, mitochondrial	R.ATFHTPFSHLGQSPEGC*SSYTFPK.I	282	Yes	13.65%	0.24%
P38646	HSPA9 Stress-70 protein, mitochondrial	K.DQLPADEC*NK.L	608	Yes	13.65%	0.33%
P54886	ALDH18A1 Delta-1-pyrroline-5-carboxylate synthase	R.TEYGDLELC*IEVVDNVQDAIDHIHK.Y	674	Yes	13.56%	0.41%
P54886	ALDH18A1 Delta-1-pyrroline-5-carboxylate synthase	K.GIPVMGHSEGIC*HMYVDSEASVDK.V	584	Yes	13.50%	1.18%
J3KR12	Uncharacterized protein	K.DNVC*SPGGATIHALHFLESGGFR.S	158		13.41%	1.74%
Q9Y2S7	POLDIP2 Polymerase delta-interacting protein 2	R.DC*PHISQR.S	143	Yes	13.38%	0.68%
Q15118	PDK1	K.QFLDFGSVNAC*EK.T	71	Yes	13.08%	0.80%
Q9BZE1	MRPL37 39S ribosomal protein L37, mitochondrial	K.DQAC*YIFHHR.C	104	Yes	12.99%	0.69%
P24752	ACAT1 Acetyl-CoA acetyltransferase, mitochondrial	K.AIMMASQSLMC*GHQDVMVAGGMES MSNVPYVMNR.G	142	Yes	12.82%	1.09%
Q96DV4	MRPL38 39S ribosomal protein L38, mitochondrial	R.VAEGQVTC*PYLPPFPAR.G	252	Yes	12.58%	4.55%
H7C455	Uncharacterized protein	K.EFHQAGKPIGLC*C*IAPVLAAK.V	BAD_ID		12.57%	0.77%
P49411	TUFM Elongation factor Tu, mitochondrial	K.NMITGTAPLDGC*ILVVAANDGPMPQ TR.E	147	Yes	12.49%	1.29%
P36776	LONP1 Lon protease homolog, mitochondrial	K.ILC*FYGPPGVGK.T	520	Yes	12.47%	7.37%
Q9NSE4	IARS2 Isoleucine--tRNA ligase, mitochondrial	K.VASVASTLETTFETISTLSGVDLENGTC* SHPLIPDK.A	364	Yes	12.39%	0.75%
P11177	PDHB Pyruvate dehydrogenase E1 component subunit beta,	K.EGVEC*EVINMR.T	263	Yes	12.07%	4.29%
O75439	PMPCB Mitochondrial-processing peptidase subunit beta	K.FHFGDSLC*THK.G	265	Yes	11.86%	0.82%
P09001	MRPL3 39S ribosomal protein L3, mitochondrial	K.LC*PLKDEPWPIHPWEPGSFR.V	78	Yes	11.84%	1.55%
O95571	ETHE1 Protein ETHE1, mitochondrial	R.QMFEPVSC*TFTYLLGDR.E	34	Yes	11.81%	4.53%
P42704	LRPPRC Leucine-rich PPR motif-containing protein, mitocho	K.GMQELGVHPDQETYTDYVIPC*FDSVN SAR.A	484	Yes	11.78%	0.53%
P09622	DLD Dihydrolipoyl dehydrogenase, mitochondrial	R.VC*HAHPTLSEAFR.E	484	Yes	11.77%	0.54%
P23528	CFL1 Cofilin-1	K.AVLFC*LSEDKK.N	39		11.70%	9.46%
Q9UFN0	NIPSNAP3A Protein NipSnap homolog 3A	K.DKEWQEQFLIPNLALIDKQESEITYLVP WC*K.L	135	Yes	11.62%	2.41%
Q9P2R7	SUCLA2 Succinyl-CoA ligase	R.C*DVIAQGIVMAVK.D	384	Yes	11.49%	11.65 %
Q6PI48	DARS2 Aspartate--tRNA ligase, mitochondrial	R.LIC*LVTGSPSIR.D	590	Yes	11.43%	1.22%
Q5VWZ 2	LYPLAL1 Lysophospholipase-like protein 1	K.ITNDC*PEHLESIDVMC*QVLTDLIDEE VK.S	87|98		11.35%	5.71%
P62937	PPIA Peptidyl-prolyl cis-trans isomerase A	R.IIPGFMC*QGGDFTR.H	62		11.33%	0.39%
O75390	CS Citrate synthase, mitochondrial	K.LPC*VAAK.I	211	Yes	11.16%	0.84%
Q86WA6	BPHL Valacyclovir hydrolase	R.VQC*PALIVHGEK.D	234	Yes	11.15%	2.77%
J3KR12	Uncharacterized protein	R.SLLINAVEASC*IR.T	188		11.11%	11.00 %
P23378	GLDC Glycine dehydrogenase	K.DISLVHSMIPLGSC*TMK.L	558	Yes	11.10%	0.50%
P49773	HINT1 Histidine triad nucleotide-binding protein 1	R.C*LAFHDISPQAPTHFLVIPK.K	38		11.07%	10.93 %
Q9BZE1	MRPL37 39S ribosomal protein L37, mitochondrial	R.NHIENQDEC*VLNVISHAR.L	153	Yes	11.05%	1.11%
O43175	PHGDH D-3-phosphoglycerate dehydrogenase	R.ALVDHENVISC*PHLGASTK.E	281		11.04%	3.27%
P31040	SDHA Succinate dehydrogenase	R.HVNGQDQIVPGLYAC*GEAAC*ASVH GANR.L	438|443	Yes	11.02%	2.75%
Q06830	PRDX1 Peroxiredoxin-1	K.HGEVC*PAGWKPGSDTIKPDVQK.S	173		10.94%	2.29%
Q6P4F2	FDX1L Adrenodoxin-like protein, mitochondrial	R.LGC*QIVLTPELEGAEFTLPK.I	154	Yes	10.90%	3.52%
P68104	EEF1A1 Elongation factor 1-alpha 1	K.PMC*VESFSDYPPLGR.F	411		10.72%	0.78%
P22033	MUT Methylmalonyl-CoA mutase, mitochondrial	K.VADPWGGSYMMEC*LTNDVYDAALK. L	433	Yes	10.69%	3.01%
Q9NSE4	IARS2 Isoleucine--tRNA ligase, mitochondrial	K.TEFC*LHDGPPYANGDPHVGHALNK.I	110	Yes	10.66%	0.08%
F8VP50	Uncharacterized protein	R.KTFPTVNPSTGEVIC*QVAEGDKEDVD K.A	63		10.64%	3.38%
O75439	PMPCB Mitochondrial-processing peptidase subunit beta	K.TNMLLQLDGSTPIC*EDIGR.Q	419	Yes	10.63%	1.68%
Q9H857	NT5DC2 5-nucleotidase domain-containing protein 2	R.TPLQHEAPLWMDQLC*TGC*MK.T	504|507	Yes	10.59%	8.24%
P09622	DLD Dihydrolipoyl dehydrogenase, mitochondrial	R.VLGAHILGPGAGEMVNEAALALEYGA SC*EDIAR.V	477	Yes	10.56%	1.09%
F5H5P2	Uncharacterized protein	R.DYPLELFMAQC*YGNISDLGK.G	212		10.50%	0.66%
Q8TAA5	GRPEL2 GrpE protein homolog 2, mitochondrial	K.LTPIGDKYDPHEHELIC*HVPAGVGVQ PGTVALVR.Q	182	Yes	10.47%	1.64%
Q99798	ACO2 Aconitate hydratase, mitochondrial	R.DLGGIVLANAC*GPC*IGQWDR.K	448|451	Yes	10.36%	0.36%
Q5JPH6	EARS2 Probable glutamate--tRNA ligase, mitochondrial	K.SDGFPTYHLAC*VVDDHHMGISHVLR. G	232	Yes	10.36%	0.55%
P30837	ALDH1B1 Aldehyde dehydrogenase X, mitochondrial	K.TIPMDGQHFC*FTR.H	169	Yes	10.34%	1.08%
P24752	ACAT1 Acetyl-CoA acetyltransferase, mitochondrial	R.QAVLGAGLPISTPC*TTINK.V	119	Yes	10.34%	0.56%
P07954	FH Fumarate hydratase, mitochondrial	K.FEALAAHDALVELSGAMNTTAC*SLM K.I	333	Yes	10.28%	1.27%
P23378	GLDC Glycine dehydrogenase	K.RNEDAC*PVGTVSAAPWGSSSILPISWA YIK.M	795	Yes	10.20%	0.87%
O75648	TRMU Mitochondrial tRNA-specific 2-thiouridylase 1	R.VC*QILDIPFHQVSYVK.E	61	Yes	10.10%	3.39%
Q6QEF8	CORO6 Coronin-6	R.KC*EPIIMTVPR.K	344		10.02%	4.37%
Q8TCS8	PNPT1 Polyribonucleotide nucleotidyltransferase 1, mitoc	K.SQIVMLEASAENILQQDFC*HAIK.V	242	Yes	9.93%	1.08%
P51649	ALDH5A1 Succinate-semialdehyde dehydrogenase, mitochondria	R.WLPAAATFPVQDPASGAALGMVADC *GVR.E	93	Yes	9.86%	1.84%

P00338	LDHA L-lactate dehydrogenase A chain	R.LGVHPLSC*HGWVLGEHGDSSVPVWSGMNVAGVSLK.T	185		9.86%	0.24%
Q6NVY1	HIBCH 3-hydroxyisobutyryl-CoA hydrolase, mitochondrial	K.INSC*FSANTVEEIIENLQQDGSSFALEQLK.V	271	Yes	9.79%	1.66%
P13639	EEF2 Elongation factor 2	K.DLEEDHAC*IPIK.K	567		9.71%	1.82%
P62937	PPIA Peptidyl-prolyl cis-trans isomerase A	K.HTGPGILSMANAGPNTNGSQFFIC*TAK.T	115		9.69%	0.72%
P24752	ACAT1 Acetyl-CoA acetyltransferase, mitochondrial	K.IHMGSC*AENTAK.K	196	Yes	9.61%	0.33%
Q9H2U2	PPA2 Inorganic pyrophosphatase 2, mitochondrial	K.STHQC*WK.A	274	Yes	9.60%	0.51%
P55809	OXCT1 Succinyl-CoA:3-ketoacid coenzyme A transferase 1,	K.STGC*DFAVSPK.L	504	Yes	9.56%	2.56%
O14561	NDUFAB1 Acyl carrier protein, mitochondrial	K.LMC*PQEIVDYIADK.K	140	Yes	9.56%	0.54%
Q08257	CRYZ Quinone oxidoreductase	K.VHAC*GVNPVETYIR.S	45	Yes	9.55%	4.36%
Q9NSE4	IARS2 Isoleucine--tRNA ligase, mitochondrial	K.GTGLVHTAPAHGMEDYGVASQHNLPMDC*LVDEDGVFTDVAGPELQNK.A	414	Yes	9.54%	3.08%
P49821	NDUFV1 NADH dehydrogenase	K.LFNISGHVNHPC*TVEEEMSVPLK.E	286	Yes	9.37%	2.67%
Q9Y2Z4	YARS2 Tyrosine--tRNA ligase, mitochondrial	K.EAPFSEFFLDPGTSVLDTC*R.K	413	Yes	9.35%	1.60%
P40926	MDH2 Malate dehydrogenase, mitochondrial	K.GYLGPEQLPDC*LK.G	89	Yes	9.22%	3.02%
Q12931	TRAP1 Heat shock protein 75 kDa, mitochondrial	R.SPAAEC*LSEK.E	573	Yes	9.18%	2.70%
Q96GW9	MARS2 Methionine--tRNA ligase, mitochondrial	R.FYGHPC*PFEGR.R	562	Yes	9.16%	0.10%
Q9NWU5	MRPL22 39S ribosomal protein L22, mitochondrial	K.VYC*HYFVK.L	166	Yes	9.06%	2.08%
Q13085	ACACA Acetyl-CoA carboxylase 1	R.MMYGVSPWGDSPIDFEDSAHVPC*PR.G	500	Yes	9.00%	1.69%
P08559	PDHA1 Pyruvate dehydrogenase E1 component subunit alpha,	K.NFYGGNGIVGAQVPLGAGIALAC*K.Y	181	Yes	9.00%	0.76%
P40939	HADHA Trifunctional enzyme subunit alpha, mitochondrial	K.EVEAVIPDHC*IFASNTSALPISEIAAVSK.R	470	Yes	8.98%	1.02%
Q9H6R3	ACSS3 Acyl-CoA synthetase short-chain family member 3, m	R.VPVLDHWWQTETGSPITASC*VGLGNSK.T	461	Yes	8.82%	5.09%
Q15118	PDK1	K.HYNTNHEADDWC*VPSR.E	421	Yes	8.82%	0.99%
Q99714	HSD17B10 3-hydroxyacyl-CoA dehydrogenase type-2	K.KLGNNC*VFAPADVTSEK.D	58	Yes	8.81%	3.93%
O94925	GLS Glutaminase kidney isoform, mitochondrial	K.FSPDLWGVSVC*TVDGQR.H	266	Yes	8.77%	0.57%
Q96EY7	PTCD3 Pentatricopeptide repeat-containing protein 3, mit	K.NEHSYC*TMIR.G	260	Yes	8.77%	2.09%
P13639	EEF2 Elongation factor 2	R.SNTGGQAFPQC*VFDHWQILPGDPFDNSSRPSQVVAETR.K	812		8.72%	1.53%
P08559	PDHA1 Pyruvate dehydrogenase E1 component subunit alpha,	K.KC*DLHR.L	41	Yes	8.72%	2.36%
O43615	TIMM44 Mitochondrial import inner membrane translocase su	K.DWC*YEATYSQLAHPIQQAK.A	343	Yes	8.65%	5.50%
P31040	SDHA Succinate dehydrogenase	R.TYFSC*TSAHTSTGDGTAMITR.A	266	Yes	8.63%	1.10%
Q9BQ52	ELAC2 Zinc phosphodiesterase ELAC protein 2	R.FGPDTQHLVLNENC*ASVHNLR.S	374	Yes	8.61%	0.50%
Q92552	MRPS27 28S ribosomal protein S27, mitochondrial	K.EHYC*LADLASLMDK.T	49	Yes	8.61%	2.23%
Q15118	PDK1	R.LC*DLYYINSPELELEELNAK.S	240	Yes	8.59%	1.40%
Q96HY7	DHTKD1 Probable 2-oxoglutarate dehydrogenase E1 component	R.FLQMC*DSAEEGVDGDTVNMFVVHPTTPAQYFHLLR.R	720	Yes	8.56%	3.45%
Q9UMS0	NFU1 NFU1 iron-sulfur cluster scaffold homolog, mitocho	K.LQGSC*TSC*PSSIITLK.N	210|213	Yes	8.55%	5.36%
P55084	HADHB Trifunctional enzyme subunit beta, mitochondrial	K.FNNWGGSLSLGHPFGATGC*R.L	435	Yes	8.54%	1.95%
Q9NSE4	IARS2 Isoleucine--tRNA ligase, mitochondrial	R.SC*QTALVEILDVIVR.S	819	Yes	8.53%	0.56%
Q6YN16	HSDL2 Hydroxysteroid dehydrogenase-like protein 2	K.TAIHTAAMDMLGGPGIESQC*R.K	218	Yes	8.36%	0.81%
Q9H845	ACAD9 Acyl-CoA dehydrogenase family member 9, mitochondr	R.AYIC*AHPLDR.T	613	Yes	8.31%	1.73%
P78540	ARG2 Arginase-2, mitochondrial	R.LSSLGC*HLK.D	63	Yes	8.30%	3.07%
Q8TD30	GPT2 Alanine aminotransferase 2	K.LTEDLFNQVPGIHC*NPLQGAMYAFPR.I	432	Yes	8.30%	0.70%
Q13011	ECH1 Delta(3,5)-Delta(2,4)-dienoyl-CoA isomerase, mitoc	R.YC*AQDAFFQVK.E	187	Yes	8.28%	1.23%
Q00610	CLTC Clathrin heavy chain 1	R.HSSLAGC*QIINYR.T	151		8.26%	4.95%
P22570	FDXR NADPH:adrenodoxin oxidoreductase, mitochondrial	K.TPQIC*VVGSGPAGFYTAQHLLK.H	42	Yes	8.25%	2.50%
Q9P2R7	SUCLA2 Succinyl-CoA ligase	K.ILAC*DDLDEAAR.M	430	Yes	8.23%	0.98%
P15927	RPA2 Replication protein A 32 kDa subunit	K.AC*PRPEGLNFQDLK.N	219		8.17%	5.91%
P49411	TUFM Elongation factor Tu, mitochondrial	R.HYAHTDC*PGHADYVK.N	127	Yes	8.14%	2.74%
Q12931	TRAP1 Heat shock protein 75 kDa, mitochondrial	R.NIYYLC*APNR.H	501	Yes	8.11%	0.68%
Q07021	C1QBP Complement component 1 Q subcomponent-binding prot	K.ALVLDC*HYPEDEVGQEDEAESDIFSIR.E	186	Yes	8.09%	0.66%
O14874	BCKDK	R.MLATHHLALHEDKPDFVGIIC*TR.L	222	Yes	8.08%	1.98%
P40939	HADHA Trifunctional enzyme subunit alpha, mitochondrial	K.QFTPC*QLLADHANSPNK.K	747	Yes	8.08%	2.96%
P42126	ECI1 Enoyl-CoA delta isomerase 1, mitochondrial	R.GVILTSDRPGVFSAGLDLTEMC*GR.S	114	Yes	8.07%	0.94%
Q92552	MRPS27 28S ribosomal protein S27, mitochondrial	K.EKLSTC*EAEDIATYEQNLQQWHLDLVQLIQR.E	367	Yes	8.05%	0.63%
P40926	MDH2 Malate dehydrogenase, mitochondrial	K.EGVVEC*SFVK.S	275	Yes	8.00%	1.60%
Q15118	PDK1	K.HIGSINPNC*NVLEVIK.D	223	Yes	7.98%	0.41%
P10809	HSPD1 60 kDa heat shock protein, mitochondrial	R.AAVEEGIVLGGGC*ALLR.C	442	Yes	7.96%	0.39%
P30405	PPIF Peptidyl-prolyl cis-trans isomerase F, mitochondri	K.HVGPGVLSMANAGPNTNGSQFFIC*TIK.T	157	Yes	7.90%	1.20%
Q02218	OGDH 2-oxoglutarate dehydrogenase, mitochondrial	K.AEQFYC*GDTEGKK.V	395	Yes	7.81%	3.00%
Q9H2U2	PPA2 Inorganic pyrophosphatase 2, mitochondrial	K.ILSC*GEVIHVK.I	180	Yes	7.80%	0.88%
P21333	FLNA Filamin-A	K.ATC*APQHGAPGPGPADASK.V	2543		7.79%	2.27%
Q5JRX3	PITRM1 Presequence protease, mitochondrial	K.THFLMPFPVNYVGEC*IR.T	869	Yes	7.76%	1.17%
Q13642	FHL1 Four and a half LIM domains protein 1	K.C*LHPLANETFVAK.D	71		7.73%	4.20%
P42704	LRPPRC Leucine-rich PPR motif-containing protein, mitocho	R.AILQENGC*LSDSDMFSQAGLR.S	500	Yes	7.60%	2.46%

Q8WV74	NUDT8 Nucleoside diphosphate-linked moiety X motif 8, mi	R.ARPASAAVLVPLC*SVR.G	39	Yes	7.60%	1.52%
Q9NSE4	IARS2 Isoleucine--tRNA ligase, mitochondrial	K.IHFVPGWDC*HGLPIEIK.V	155	Yes	7.59%	1.58%
P38646	HSPA9 Stress-70 protein, mitochondrial	K.C*ELSSSVQTDINLPYLTMDSSGPK.H	317	Yes	7.51%	2.08%
Q8NCN5	PDPR Pyruvate dehydrogenase phosphatase regulatory subu	K.FFAFWGQDINNLTTPLEC*GR.E	735	Yes	7.49%	3.86%
Q96I99	SUCLG2 Succinyl-CoA ligase	R.SC*NGPVLVGSPQGGVDIEEVAASNPE LIFK.E	162	Yes	7.48%	2.01%
P23368	ME2 NAD-dependent malic enzyme, mitochondrial	R.AMASINERPVIFALSNPTAQAEC*TAEE AYTLTEGR.C	428	Yes	7.46%	2.33%
P68366	TUBA4A Tubulin alpha-4A chain	K.AYHEQLSVAEITNAC*FEPANQMVK.C	295		7.43%	0.14%
P23434	GCSH Glycine cleavage system H protein, mitochondrial	K.SC*YEDGWLIK.M	138	Yes	7.37%	0.06%
Q96I51	WBSCR16 Williams-Beuren syndrome chromosomal region 16 pro	R.C*GLSHFAALTNK.G	401	Yes	7.33%	3.63%
Q969S9	GFM2 Ribosome-releasing factor 2, mitochondrial	R.IYSGTIKPQLAIHNINGNC*TER.I	406	Yes	7.33%	2.97%
Q92552	MRPS27 28S ribosomal protein S27, mitochondrial	R.HSPNC*WYLR.N	101	Yes	7.29%	0.87%
P10515	DLAT Dihydrolipoyllysine-residue acetyltransferase comp	R.DVPLGTPLC*IIVEK.E	291	Yes	7.25%	0.87%
Q7L0Y3	TRMT10C Mitochondrial ribonuclease P protein 1	K.TLMEC*VSNTAK.K	123	Yes	7.20%	2.22%
Q02218	OGDH 2-oxoglutarate dehydrogenase, mitochondrial	R.VVNAPIFHVNSDDPEAVMYVC*K.V	487	Yes	7.17%	1.47%
Q9NSE4	IARS2 Isoleucine--tRNA ligase, mitochondrial	K.KPGLEEAVESAC*AMR.D	883	Yes	7.17%	1.38%
P42704	LRPPRC Leucine-rich PPR motif-containing protein, mitocho	R.C*VANNQVETLEK.L	930	Yes	7.17%	2.09%
P40926	MDH2 Malate dehydrogenase, mitochondrial	K.GC*DVVVIPAGVPR.K	93	Yes	7.11%	0.34%
Q53H96	PYCRL Pyrroline-5-carboxylate reductase 3	R.HVGSSETNLLQHLLEAC*GR.C	RESIDUE_NOT_FOUND		7.11%	3.32%
P10809	HSPD1 60 kDa heat shock protein, mitochondrial	R.C*IPALDSLTPANEDQK.I	447	Yes	7.08%	0.40%
Q9UGC7	MTRF1L Peptide chain release factor 1-like, mitochondrial	R.IVHLPTGVVSEC*QQER.S	274	Yes	7.02%	2.12%
O43708	GSTZ1 Maleylacetoacetate isomerase	R.LLVLEAFQVSHPC*R.Q	205	Yes	6.99%	1.94%
Q9NSE4	IARS2 Isoleucine--tRNA ligase, mitochondrial	R.RPYWC*ISR.Q	521	Yes	6.97%	0.63%
P23368	ME2 NAD-dependent malic enzyme, mitochondrial	R.ILQDDIESLMPIVYTPTVGLAC*SQYGHI FR.R	120	Yes	6.97%	0.78%
Q9BW92	TARS2 Threonine--tRNA ligase, mitochondrial	K.EQELFFFHELSPGSC*FFLPR.G	322	Yes	6.97%	1.24%
Q5JRX3	PITRM1 Presequence protease, mitochondrial	K.TGGMSASPHVLPDDSHMDTYEQGVLF SSLC*LDR.N	672	Yes	6.95%	1.97%
O00411	POLRMT DNA-directed RNA polymerase, mitochondrial	R.TVEGATQHQELLETC*PPTALHGALDA LTQLGNC*AWR.V	687|705	Yes	6.95%	3.09%
Q9BPW8	NIPSNAP1 Protein NipSnap homolog 1	R.FSGGYPALMDC*MNK.L	138	Yes	6.86%	0.43%
Q15120	PDK3	K.HIGSIDPTC*NVADVVK.D	191	Yes	6.85%	2.96%
Q6YN16	HSDL2 Hydroxysteroid dehydrogenase-like protein 2	R.LAGC*TVFITGASR.G	11	Yes	6.83%	2.33%
P42704	LRPPRC Leucine-rich PPR motif-containing protein, mitocho	R.SC*GSLLPELK.L	130	Yes	6.79%	0.53%
P30084	ECHS1 Enoyl-CoA hydratase, mitochondrial	K.ALNALC*DGLIDELNQALK.T	62	Yes	6.76%	0.42%
P51553	IDH3G Isocitrate dehydrogenase	R.HAC*VPVDFEEVHVSSNADEEDIR.N	81	Yes	6.76%	1.21%
P22234	PAICS Multifunctional protein ADE2	R.VVVLMGSTSDLGHC*EK.I	281	Yes	6.69%	0.13%
P12277	CKB Creatine kinase B-type	K.DYEFMWNPHLGYILTC*PSNLGTGLR. A	283		6.69%	2.20%
P00367	GLUD1 Glutamate dehydrogenase 1, mitochondrial	K.PC*NHVLSLSFPIR.R	112	Yes	6.68%	1.17%
P31930	UQCRC1 Cytochrome b-c1 complex subunit 1, mitochondrial	R.LC*TSATESEVAR.G	380	Yes	6.65%	1.64%
P24752	ACAT1 Acetyl-CoA acetyltransferase, mitochondrial	K.QGEYGLASIC*NGGGGASAMLIQK.L	413	Yes	6.57%	1.57%
P22695	UQCRC2 Cytochrome b-c1 complex subunit 2, mitochondrial	R.NALANPLYC*PDYR.I	192	Yes	6.56%	1.30%
P30084	ECHS1 Enoyl-CoA hydratase, mitochondrial	K.EMQNLSFQDC*YSSK.F	111	Yes	6.56%	0.66%
P22033	MUT Methylmalonyl-CoA mutase, mitochondrial	R.AHC*QTSGWSLTEQDPYNNIVR.T	351	Yes	6.54%	0.93%
Q99798	ACO2 Aconitate hydratase, mitochondrial	K.VAVPSTIHC*DHLIEAQVGGEK.D	126	Yes	6.52%	0.58%
Q5T440	IBA57 Putative transferase CAF17, mitochondrial	R.VWAVLPSSPEAC*GAASLQER.A	170	Yes	6.49%	2.45%
P22102	GART Trifunctional purine biosynthetic protein adenosin	R.FGDPEC*QVILPLLK.S	298		6.41%	2.33%
P00505	GOT2 Aspartate aminotransferase, mitochondrial	R.VGAFTMVC*K.D	295	Yes	6.34%	0.42%
P51553	IDH3G Isocitrate dehydrogenase	K.NIANPTATLLASC*MMLDHLK.L	333	Yes	6.34%	1.46%
P04181	OAT Ornithine aminotransferase, mitochondrial	K.VLPMNTGVEAGETAC*K.L	150	Yes	6.32%	1.46%
P28838	LAP3 Cytosol aminopeptidase	K.LNLPINIIGLAPLC*ENMPSGK.A	335	Yes	6.29%	0.82%
P04075	ALDOA Fructose-bisphosphate aldolase A	R.YASIC*QQNGIVPIVEPEILPDGDHDLK. R	178		6.22%	1.34%
Q9H1K1	ISCU Iron-sulfur cluster assembly enzyme ISCU, mitochon	K.LHC*SMLAEDAIK.A	138	Yes	6.17%	2.45%
O76031	CLPX ATP-dependent Clp protease ATP-binding subunit clp	K.C*GDLC*THVETFVSSTR.F	108|112	Yes	6.16%	0.29%
Q92665	MRPS31 28S ribosomal protein S31, mitochondrial	R.HFMELVTC*GLSK.N	356	Yes	6.15%	2.95%
Q9H2W6	MRPL46 39S ribosomal protein L46, mitochondrial	K.FLGNAPC*GHYTFK.F	210	Yes	6.13%	0.79%
P30626	SRI Sorcin	R.DTAQQGVVNFPYDDFIQC*VMSV.-	194		6.12%	1.57%
Q9UBQ7	GRHPR Glyoxylate reductase/hydroxypyruvate reductase	R.GVAGAHGLLC*LLSDHVDK.R	57	Yes	6.09%	2.30%
P10515	DLAT Dihydrolipoyllysine-residue acetyltransferase comp	K.NFSAIINPPQAC*ILAIGASEDK.L	586	Yes	6.09%	1.17%
Q9BQP7	C20orf72 Uncharacterized protein C20orf72	R.ALESAVQHETLNYIGLLDC*VAEYQGK. L	239	Yes	6.07%	0.70%
P04181	OAT Ornithine aminotransferase, mitochondrial	K.YFDFLSSYSAVNQGHC*HPK.I	93	Yes	6.07%	0.75%
P41250	GARS Glycine--tRNA ligase	K.C*SVLPLSQNQEFMPFVK.E	616	Yes	6.05%	1.82%
Q96J01	THOC3 THO complex subunit 3	K.RPLLAFAC*DDKDGK.Y	326		6.03%	1.79%
Q969Z0	TBRG4 Protein TBRG4	R.LATDLLSLMPSLTSGEVAHC*AK.S	335	Yes	6.03%	0.57%
Q9NWU1	OXSM 3-oxoacyl-	K.LPPTLNLDC*SEPEFDLNYVPLK.A	415	Yes	6.02%	1.10%
Q9P2R7	SUCLA2 Succinyl-CoA ligase	K.YDATMIEINPMVEDSDGAVLC*MDAK. I	270	Yes	5.99%	2.13%

Q6UB35	MTHFD1L Monofunctional C1-tetrahydrofolate synthase, mitoc	K.RAGAFDAVPC*YHWSVGGK.G	828	Yes	5.96%	1.09%
O00330	PDHX Pyruvate dehydrogenase protein X component, mitoch	K.STVPHAYATADC*DLGAVLK.V	307	Yes	5.95%	1.68%
Q9BYT8	NLN Neurolysin, mitochondrial	R.C*KEENTIILQQLLPLR.T	272	Yes	5.94%	2.04%
P54886	ALDH18A1 Delta-1-pyrroline-5-carboxylate synthase	R.EEVEDLC*R.L	546	Yes	5.90%	0.99%
O75439	PMPCB Mitochondrial-processing peptidase subunit beta	R.LC*TSVTESEVAR.A	389	Yes	5.90%	0.99%
Q9Y3C8	UFC1 Ubiquitin-fold modifier-conjugating enzyme 1	K.IC*LTDHFKPLWAR.N	116		5.87%	1.56%
P10515	DLAT Dihydrolipoyllysine-residue acetyltransferase comp	R.DVPIGAIIC*ITVGKPEDIEAFK.N	164	Yes	5.86%	1.90%
P22314	UBA1 Ubiquitin-like modifier-activating enzyme 1	R.VGEFC*HNR.G	179		5.85%	0.75%
Q9BQ52	ELAC2 Zinc phosphodiesterase ELAC protein 2	K.AWLQQYHNQC*QEVLHHISMIPAK.C	595	Yes	5.82%	0.93%
P13639	EEF2 Elongation factor 2	R.YVEPIEDVPC*GNIVGLVGVDQFLVK.T	466		5.77%	0.78%
Q99798	ACO2 Aconitate hydratase, mitochondrial	K.C*TTDHISAAGPWLK.F	592	Yes	5.76%	0.54%
Q10713	PMPCA Mitochondrial-processing peptidase subunit alpha	K.LPHELC*TLIR.N	466	Yes	5.76%	0.76%
P50502	ST13 Hsc70-interacting protein	R.LLGHWEEAAHDLALAC*K.L	209		5.74%	1.35%
P68104	EEF1A1 Elongation factor 1-alpha 1	K.DGNASGTTLLEALDC*ILPPTRPTDKPLR.L	234		5.68%	0.14%
P08238	HSP90AB1 Heat shock protein HSP 90-beta	R.GFEVVYMTEPIDEYC*VQQLK.E	521		5.66%	1.55%
P13804	ETFA Electron transfer flavoprotein subunit alpha, mito	K.QFNYTHIC*AGASAFGK.N	109	Yes	5.64%	1.76%
P30048	PRDX3 Thioredoxin-dependent peroxide reductase, mitochon	K.ANEFHDVNC*EVVAVSVDSHFSHLAWINTPR.K	127	Yes	5.62%	0.89%
P49411	TUFM Elongation factor Tu, mitochondrial	K.GDEC*ELLGHSK.N	290	Yes	5.62%	0.26%
Q8IVS2	MCAT Malonyl-CoA-acyl carrier protein transacylase, mit	R.MPGQC*SVLLFPGQGSQVVGMGR.G	62	Yes	5.58%	0.24%
Q9BSH5	HDHD3 Haloacid dehalogenase-like hydrolase domain-contai	K.DFSHPC*TWQVLDGAEDTLR.E	109	Yes	5.56%	1.13%
P14174	MIF Macrophage migration inhibitory factor	K.LLC*GLLAER.L	81		5.56%	0.12%
Q8TD19	NEK9 Serine/threonine-protein kinase Nek9	R.PIFGSLHHVPDLSC*R.G	715		5.54%	1.10%
O75600	GCAT 2-amino-3-ketobutyrate coenzyme A ligase, mitochon	R.ARPYLFSNSLPPAVVGC*ASK.A	305	Yes	5.51%	1.06%
Q8NCW5	APOA1BP NAD(P)H-hydrate epimerase	R.SPPTVLVIC*GPGNNGGDGLVC*AR.H	115|127	Yes	5.50%	1.05%
P08238	HSP90AB1 Heat shock protein HSP 90-beta	K.C*LELFSELAEDKENYK.K	412		5.50%	1.04%
Q71U36	TUBA1A Tubulin alpha-1A chain	K.RTIQFVDWC*PTGFK.V	347		5.45%	0.85%
Q5JRX3	PITRM1 Presequence protease, mitochondrial	R.AFSSLNTLPEELRPYVPLFC*SVLTK.L	619	Yes	5.43%	0.26%
P40926	MDH2 Malate dehydrogenase, mitochondrial	K.SQETEC*TYFSTPLLLGK.K	285	Yes	5.42%	0.39%
P10809	HSPD1 60 kDa heat shock protein, mitochondrial	K.C*EFQDAYVLLSEK.K	237	Yes	5.40%	0.69%
Q4G0N4	NADKD1 NAD kinase domain-containing protein 1	R.SEGHLC*LPVR.Y	193	Yes	5.39%	0.89%
P55809	OXCT1 Succinyl-CoA:3-ketoacid coenzyme A transferase 1,	K.DIPDGATVLVGGFGLC*GIPENLIDALLK.T	67	Yes	5.37%	0.86%
Q9UJZ1	STOML2 Stomatin-like protein 2	R.ESLNASIVDAINQAADC*WGIR.C	167	Yes	5.37%	0.52%
Q9BYD1	MRPL13 39S ribosomal protein L13, mitochondrial	K.PVYHALSDC*GDHVVIMNTR.H	53	Yes	5.36%	1.03%
Q8TAE8	GADD45GIP1 Growth arrest and DNA damage-inducible proteins-in	R.EREQHIAEC*MAK.M	124	Yes	5.35%	0.51%
P22570	FDXR NADPH:adrenodoxin oxidoreductase, mitochondrial	R.AVPTGDMEDLPC*GLVLSSIGYK.S	353	Yes	5.35%	0.51%
P07437	TUBB Tubulin beta chain	K.LTTPTYGDLNHLVSATMSGVTTC*LR.F	239		5.34%	0.38%
P14618	PKM Pyruvate kinase isozymes M1/M2	R.AEGSDVANAVLDGADC*IMLSGETAK.G	358		5.32%	0.79%
O75131	CPNE3 Copine-3	K.EALAQC*VLAEIPQQVVGYFNTYK.L	506		5.31%	0.78%
Q14166	TTLL12 Tubulin--tyrosine ligase-like protein 12	K.LSQERPGVLLNQFPC*ENLLTVK.D	361		5.31%	0.78%
P07900	HSP90AA1 Heat shock protein HSP 90-alpha	K.C*LELFTELAEDKENYK.K	420		5.29%	0.91%
P30405	PPIF Peptidyl-prolyl cis-trans isomerase F, mitochondri	R.VIPSFMC*QAGDFTNHNGTGGK.S	104	Yes	5.28%	0.61%
P30626	SRI Sorcin	R.C*LTQSGIAGGYKPFNLETC*R.L	57|75		5.28%	0.89%
P26641	EEF1G Elongation factor 1-gamma	R.WFLTC*INQPQFR.A	194		5.27%	0.88%
P36776	LONP1 Lon protease homolog, mitochondrial	K.VLFIC*TANVTDTIPEPLR.D	637	Yes	5.27%	0.59%
Q86Y79	PTRH1 Probable peptidyl-tRNA hydrolase	R.HC*AADLALAPLGDAQLVLLRPR.R	72	Yes	5.23%	0.66%
P60709	ACTB Actin, cytoplasmic 1	R.C*PEALFQPSFLGMESC*GIHETTFNSIMK.C	257|272		5.21%	0.78%
Q6IS14	EIF5AL1 Eukaryotic translation initiation factor 5A-1-like	K.KYEDIC*PSTHNMDVPNIK.R	73		5.16%	0.56%
Q9BXR0	QTRT1 Queuine tRNA-ribosyltransferase	R.C*IAAHQRPDK.Q	185	Yes	5.10%	0.58%
O94925	GLS Glutaminase kidney isoform, mitochondrial	K.VPFC*LQSC*VKPLK.Y	283|287	Yes	5.10%	0.43%
P08134	RHOC Rho-related GTP-binding protein RhoC	K.HFC*PNVPIILVGNK.K	107		5.09%	0.57%
Q86X76	NIT1 Nitrilase homolog 1	K.IYNC*HVLLNSK.G	145	Yes	5.08%	0.45%
P00338	LDHA L-lactate dehydrogenase A chain	K.DDVFLSVPC*ILGQNGISDLVK.V	293		5.05%	0.42%
P48735	IDH2 Isocitrate dehydrogenase	R.NILGGTVFREPIIC*K.N	154	Yes	5.04%	0.41%
Q9BSD7	NTPCR Cancer-related nucleoside-triphosphatase	R.NHLLPDIVTC*VQSSR.K	184		5.03%	0.38%
Q13085	ACACA Acetyl-CoA carboxylase 1	K.RPGAALDPGC*VLAK.M	813	Yes	5.03%	0.47%
P08559	PDHA1 Pyruvate dehydrogenase E1 component subunit alpha,	K.LPC*IFIC*ENNR.Y	218|222	Yes	5.00%	0.40%
P37802	TAGLN2 Transgelin-2	K.DGTVLC*ELINALYPEGQAPVK.K	63		4.99%	0.39%
P08559	PDHA1 Pyruvate dehydrogenase E1 component subunit alpha,	R.FAAAYC*R.S	273	Yes	4.94%	0.83%
Q99714	HSD17B10 3-hydroxyacyl-CoA dehydrogenase type-2	K.VC*NFLASQVPFPSR.L	214	Yes	4.94%	0.71%
Q9NVH6	TMLHE Trimethyllysine dioxygenase, mitochondrial	K.SLTC*AWQQHEDHFELK.Y	51	Yes	4.91%	0.21%
P31040	SDHA Succinate dehydrogenase	R.GC*GPEKDHVYLQLHHLPPEQLATR.L	357	Yes	4.90%	0.20%
P36776	LONP1 Lon protease homolog, mitochondrial	K.DGPSAGC*TIVTALLSLAMGR.P	858	Yes	4.90%	0.79%
Q9UBQ7	GRHPR Glyoxylate reductase/hydroxypyruvate reductase	R.AADC*EVEQWDSDEPIPAK.E	29	Yes	4.89%	0.18%
P50990	CCT8 T-complex protein 1 subunit theta	K.AHEILPNLVC*C*SAK.N	148|149		4.87%	0.16%

Q96RQ3	MCCC1 Methylcrotonoyl-CoA carboxylase subunit alpha, mit	K.TSAAQAIHPGC*GFLSENMEFAELC*K.Q	129|142	Yes	4.84%	0.13%
E7EVK2	MTG1 Mitochondrial GTPase 1	R.FGYVQHYGLGSAC*DNVER.V	211	Yes	4.83%	0.10%
Q9BTE3	MCMBP Mini-chromosome maintenance complex-binding protei	K.LQHINPLLPAC*LNK.E	325		4.83%	0.11%
Q96I51	WBSCR16 Williams-Beuren syndrome chromosomal region 16 pro	R.VTMPGEPVDVAC*GVDHMVTLAK.S	451	Yes	4.82%	0.09%
P00505	GOT2 Aspartate aminotransferase, mitochondrial	K.EGSTHNWQHITDQIGMFC*FTGLKPEQVER.L	382	Yes	4.82%	0.11%
P11498	PC Pyruvate carboxylase, mitochondrial	R.ADFAQAC*QDAGVR.F	131	Yes	4.82%	0.12%
P08559	PDHA1 Pyruvate dehydrogenase E1 component subunit alpha,	R.VDGMDILC*VR.E	261	Yes	4.81%	0.08%
P22234	PAICS Multifunctional protein ADE2	R.LPSGLGC*STVLSPEGSAQFAAQIFGLSNHLVWSK.L	374	Yes	4.79%	0.04%
P30153	PPP2R1A Serine/threonine-protein phosphatase 2A 65 kDa reg	K.DNTIEHLLPLFLAQLKDEC*PEVR.L	377		4.78%	0.04%
P43897	TSFM Elongation factor Ts, mitochondrial	K.YGALVIC*ETSEQK.T	240	Yes	4.76%	0.00%
P31040	SDHA Succinate dehydrogenase	R.AC*ALSIEESC*RPGDK.V	467|475	Yes	4.76%	0.00%
Q9UDR5	AASS Alpha-aminoadipic semialdehyde synthase, mitochond	K.AGGILQEDISEAC*LILGVK.R	87	Yes	4.76%	0.00%
P31040	SDHA Succinate dehydrogenase	R.AGLPC*QDLEFVQFHPTGIYGAGC*LITEGC*R.G	287|305|311	Yes	4.76%	0.00%
Q969Z0	TBRG4 Protein TBRG4	R.AQDITLPHLC*SVLLAFAR.L	370	Yes	4.76%	0.00%
P23368	ME2 NAD-dependent malic enzyme, mitochondrial	R.C*LPVC*IDVGTDNIALLK.D	198|202	Yes	4.76%	0.00%
P00367	GLUD1 Glutamate dehydrogenase 1, mitochondrial	K.C*AVVDVPFGGAK.A	172	Yes	4.76%	0.00%
Q969Z0	TBRG4 Protein TBRG4	K.C*LELVEHFGPNELR.K	246	Yes	4.76%	0.00%
Q96RQ3	MCCC1 Methylcrotonoyl-CoA carboxylase subunit alpha, mit	K.ESLC*QAALGLILK.E	509	Yes	4.76%	0.00%
P38117	ETFB Electron transfer flavoprotein subunit beta	K.EKKLVKEVIAVSC*GPAQC*QETIR.T	66|71	Yes	4.76%	0.00%
Q96EY7	PTCD3 Pentatricopeptide repeat-containing protein 3, mit	K.DPDDDKFFQSAMSIC*SSLR.D	423	Yes	4.76%	0.00%
Q10713	PMPCA Mitochondrial-processing peptidase subunit alpha	K.FGQFC*TVGILINSGSR.Y	88	Yes	4.76%	0.00%
Q9UDR5	AASS Alpha-aminoadipic semialdehyde synthase, mitochond	R.FNTDIAPYTTC*LINGIYWEQNTPR.L	305	Yes	4.76%	0.00%
P08559	PDHA1 Pyruvate dehydrogenase E1 component subunit alpha,	R.GFC*HLC*DGQEAC*C*VGLEAGINPTDHLITAYR.A	91|94|100|101	Yes	4.76%	0.00%
Q15031	LARS2 Probable leucine--tRNA ligase, mitochondrial	K.GGPPLAMASEWVNC*SC*PR.C	504|506	Yes	4.76%	0.00%
P21953	BCKDHB 2-oxoisovalerate dehydrogenase subunit beta, mitoc	K.GLLLSC*IEDKNPC*IFFEPK.I	228|235	Yes	4.76%	0.00%
P11177	PDHB Pyruvate dehydrogenase E1 component subunit beta,	R.GPNGASAGVAAQHSQC*FAAWYGHC*PGLK.V	161|169	Yes	4.76%	0.00%
P00505	GOT2 Aspartate aminotransferase, mitochondrial	R.HFIEQGINVC*LC*QSYAK.N	272|274	Yes	4.76%	0.00%
Q96DV4	MRPL38 39S ribosomal protein L38, mitochondrial	K.HQETMTPAGLSFFQC*R.W	321	Yes	4.76%	0.00%
P82650	MRPS22 28S ribosomal protein S22, mitochondrial	R.HVDVLNLC*FAQFEPDSTEYIK.V	231	Yes	4.76%	0.00%
P49406	MRPL19 39S ribosomal protein L19, mitochondrial	K.ISQFLGIC*IQR.S	137	Yes	4.76%	0.00%
P42704	LRPPRC Leucine-rich PPR motif-containing protein, mitocho	K.LFEC*DRDQMYYNLLK.L	952	Yes	4.76%	0.00%
P51553	IDH3G Isocitrate dehydrogenase	K.LGDGLFLQC*C*R.E	235|236	Yes	4.76%	0.00%
Q9BRJ2	MRPL45 39S ribosomal protein L45, mitochondrial	R.LHTLVTEHC*FPDMTWDIK.Y	168	Yes	4.76%	0.00%
P35914	HMGCL Hydroxymethylglutaryl-CoA lyase, mitochondrial	K.LLEAGNFIC*QALNR.K	307	Yes	4.76%	0.00%
P23378	GLDC Glycine dehydrogenase	K.MEDPVC*ENEILATLHAISSK.N	112	Yes	4.76%	0.00%
Q9Y305	ACOT9 Acyl-coenzyme A thioesterase 9, mitochondrial	K.MQMFQLHGDEFC*PVLDATFVMVAR.D	194	Yes	4.76%	0.00%
Q9BQ52	ELAC2 Zinc phosphodiesterase ELAC protein 2	R.NVSATLVNISPDTSLLLDC*GEGTFGQLC*R.H	516|525	Yes	4.76%	0.00%
P50213	IDH3A Isocitrate dehydrogenase	K.TFDLYANVRPC*VSIEGYK.T	127	Yes	4.76%	0.00%
P00367	GLUD1 Glutamate dehydrogenase 1, mitochondrial	K.AKPYEGSILEADC*DILIPAASEK.Q	376	Yes	4.76%	0.00%
Q9UDR5	AASS Alpha-aminoadipic semialdehyde synthase, mitochond	K.QLLC*DLVGISPSSEHDVLK.E	765	Yes	4.76%	0.00%
Q9UGM6	WARS2 Tryptophan--tRNA ligase, mitochondrial	R.QSILDMTAVLLAC*GINPEK.S	102	Yes	4.76%	0.00%
Q9H0R6	QRSL1 Glutamyl-tRNA(Gln) amidotransferase subunit A, mit	K.QVQFPVIQLQELMDDC*SAVLENEK.L	512	Yes	4.76%	0.00%
P48735	IDH2 Isocitrate dehydrogenase	K.SSGGFVWAC*K.N	308	Yes	4.76%	0.00%
Q3SY69	ALDH1L2 Mitochondrial 10-formyltetrahydrofolate dehydrogen	R.SVGAELNVLPFC*TQFIPMDIIDSPK.H	108	Yes	4.76%	0.00%
P23378	GLDC Glycine dehydrogenase	R.SYIGMGYYNC*SVPQTILR.N	141	Yes	4.76%	0.00%
P11177	PDHB Pyruvate dehydrogenase E1 component subunit beta,	K.TNHLVTVEGGWPQFGVGAEIC*AR.I	306	Yes	4.76%	0.00%
P51553	IDH3G Isocitrate dehydrogenase	R.TSLDLYANVIHC*K.S	148	Yes	4.76%	0.00%
Q16718	NDUFA5 NADH dehydrogenase	K.TTGLVGLAVC*NTPHER.L	17	Yes	4.76%	0.00%
Q6L8Q7	PDE12 2,5-phosphodiesterase 12	R.TVLYPYC*APYALELDYR.Q	321	Yes	4.76%	0.00%
P48735	IDH2 Isocitrate dehydrogenase	K.VC*VETVESGAMTK.D	402	Yes	4.76%	0.00%
Q96GW9	MARS2 Methionine--tRNA ligase, mitochondrial	R.VSEQFQQLFQEAGISC*TDFIR.T	132	Yes	4.76%	0.00%
Q96EY7	PTCD3 Pentatricopeptide repeat-containing protein 3, mit	K.VSNSPSQAIEVVELASAFSLPIC*EGLTQR.V	642	Yes	4.76%	0.00%
P42704	LRPPRC Leucine-rich PPR motif-containing protein, mitocho	K.YESDMVTGGYAALINLC*C*R.H	721|722	Yes	4.76%	0.00%
P23378	GLDC Glycine dehydrogenase	R.C*HPQTIAVVQTR.A	225	Yes	4.76%	0.00%
P23368	ME2 NAD-dependent malic enzyme, mitochondrial	R.C*LFASGSPFGPVK.L	441	Yes	4.76%	0.00%
Q9NP92	MRPS30 28S ribosomal protein S30, mitochondrial	R.C*PVHFYWVR.G	204	Yes	4.76%	0.00%
Q6PI48	DARS2 Aspartate--tRNA ligase, mitochondrial	R.EYLC*NLHGFVDIETPTLFK.R	202	Yes	4.76%	0.00%
Q9H845	ACAD9 Acyl-CoA dehydrogenase family member 9, mitochondr	R.TVDLGLTGNHGVVHPSLADSANKFEENTYC*FGR.T	507	Yes	4.76%	0.00%
Q02218	OGDH 2-oxoglutarate dehydrogenase, mitochondrial	R.FLQMC*NDDPDVLPDLK.E	802	Yes	4.76%	0.00%
Q92947	GCDH Glutaryl-CoA dehydrogenase, mitochondrial	K.GELLGC*FGLTEPNSGSDPSSMETR.A	176	Yes	4.76%	0.00%
Q10713	PMPCA Mitochondrial-processing peptidase subunit alpha	K.HGGIC*DC*QTSR.D	140|142	Yes	4.76%	0.00%

Q9NVH6	TMLHE Trimethyllysine dioxygenase, mitochondrial	R.HTDTTYFQEPC*GIQVFHC*LK.H	252|259	Yes	4.76%	0.00%
P42765	ACAA2 3-ketoacyl-CoA thiolase, mitochondrial	R.IVGYFVSGC*DPSIMGIGPVPAISGALK.K	287	Yes	4.76%	0.00%
Q9NYY8	FASTKD2 FAST kinase domain-containing protein 2	K.LSEEC*NSLSDVLDAFSK.A	163	Yes	4.76%	0.00%
Q9Y2R9	MRPS7 28S ribosomal protein S7, mitochondrial	K.NC*EPMIGLVPILK.G	152	Yes	4.76%	0.00%
Q6L8Q7	PDE12 2,5-phosphodiesterase 12	K.SRPNASGGAAC*SGPGPEPAVFC*EPVVK.L	108|119	Yes	4.76%	0.00%
P11498	PC Pyruvate carboxylase, mitochondrial	K.DMAGLLKPTAC*TMLVSSLR.D	752	Yes	4.76%	0.00%
Q96RP9	GFM1 Elongation factor G, mitochondrial	R.QELIEC*VANSDEQLGEMFLEEK.I	256	Yes	4.76%	0.00%
Q96EY7	PTCD3 Pentatricopeptide repeat-containing protein 3, mit	R.QTAQDWPATSLNC*IAILFLR.A	578	Yes	4.76%	0.00%
P50336	PPOX Protoporphyrinogen oxidase	R.SC*FPSLFQAEQTHR.S	183	Yes	4.76%	0.00%
Q9Y305	ACOT9 Acyl-coenzyme A thioesterase 9, mitochondrial	K.SLEIC*HPQER.N	299	Yes	4.76%	0.00%
Q9NUB1	ACSS1 Acetyl-coenzyme A synthetase 2-like, mitochondrial	R.VAIYMPVSPLAVAAMLAC*AR.I	185	Yes	4.76%	0.00%
P45954	ACADSB Short/branched chain specific acyl-CoA dehydrogena	K.VDASVAVFC*EIQNTLINTLIR.K	139	Yes	4.76%	0.00%
P23368	ME2 NAD-dependent malic enzyme, mitochondrial	R.VFTPGQGNNVYIFPGVALAVILC*NTR.H	481	Yes	4.76%	0.00%
Q5T2R2	PDSS1 Decaprenyl-diphosphate synthase subunit 1	R.AC*NIHHNNSR.H	148	Yes	4.76%	0.00%
P82933	MRPS9 28S ribosomal protein S9, mitochondrial	K.ALC*SFVTEDEVEWMR.Q	353	Yes	4.76%	0.00%
P05091	ALDH2 Aldehyde dehydrogenase, mitochondrial	K.ANYLSQALQAGTVWVNC*YDVFGAQSPFGGYK.M	472	Yes	4.76%	0.00%
P00367	GLUD1 Glutamate dehydrogenase 1, mitochondrial	K.C*IAVGESDGSIWNPDGIDPK.E	327	Yes	4.76%	0.00%
Q6L8Q7	PDE12 2,5-phosphodiesterase 12	R.C*NMSLTHFFK.L	530	Yes	4.76%	0.00%
Q8IWL3	HSCB Iron-sulfur cluster co-chaperone protein HscB, mit	R.DYFSLMDC*NR.S	79	Yes	4.76%	0.00%
P22695	UQCRC2 Cytochrome b-c1 complex subunit 2, mitochondrial	R.ENMAYTVEC*LR.G	125	Yes	4.76%	0.00%
Q8N5M1	ATPAF2 ATP synthase mitochondrial F1 complex assembly fac	K.FLDTDTIC*YR.V	141	Yes	4.76%	0.00%
Q96RP9	GFM1 Elongation factor G, mitochondrial	K.GFLDAC*EK.G	594	Yes	4.76%	0.00%
Q9Y3D2	MSRB2 Methionine-R-sulfoxide reductase B2, mitochondrial	R.GQAGGGGPGTGPGLGEAGSLATC*ELPLAK.S	45	Yes	4.76%	0.00%
P23786	CPT2 Carnitine O-palmitoyltransferase 2, mitochondrial	R.HSAGELQQMMVEC*SK.Y	535	Yes	4.76%	0.00%
Q8NCN5	PDPR Pyruvate dehydrogenase phosphatase regulatory subu	R.HVC*LGFVHNFSEDTGEEQVVTADFINR.G	813	Yes	4.76%	0.00%
Q7L8L6	FASTKD5 FAST kinase domain-containing protein 5	K.IGDLAC*ANIQHLSSR.S	345	Yes	4.76%	0.00%
P21953	BCKDHB 2-oxoisovalerate dehydrogenase subunit beta, mitoc	K.LGVSC*EVIDLR.T	299	Yes	4.76%	0.00%
Q9BW92	TARS2 Threonine--tRNA ligase, mitochondrial	R.LLGVLAESC*GGK.W	603	Yes	4.76%	0.00%
P05165	PCCA Propionyl-CoA carboxylase alpha chain, mitochondri	R.LQVEHPVTEC*ITGLDLVQEMIR.V	363	Yes	4.76%	0.00%
Q8WVM0	TFB1M Dimethyladenosine transferase 1, mitochondrial	K.MC*DEDPQLFAYNFR.E	311	Yes	4.76%	0.00%
Q9HCC0	MCCC2 Methylcrotonoyl-CoA carboxylase beta chain, mitoch	K.MVAAVAC*AQVPK.I	431	Yes	4.76%	0.00%
P51649	ALDH5A1 Succinate-semialdehyde dehydrogenase, mitochondria	K.NFFEPTLLC*NVTQDMLC*THEETFGPLAPVIK.F	426|434	Yes	4.76%	0.00%
P04181	OAT Ornithine aminotransferase, mitochondrial	K.PGEHGSTYGGNPLGC*R.V	330	Yes	4.76%	0.00%
Q9NYK5	MRPL39 39S ribosomal protein L39, mitochondrial	R.SC*AMMMGC*VIER.A	146|152	Yes	4.76%	0.00%
Q9H2U2	PPA2 Inorganic pyrophosphatase 2, mitochondrial	K.STNC*FGDNDPIDVC*EIGSK.I	161|171	Yes	4.76%	0.00%
P31930	UQCRC1 Cytochrome b-c1 complex subunit 1, mitochondrial	K.YIYDQC*PAVAGYGPIEQLPDYNR.I	453	Yes	4.76%	0.00%
Q96CU9	FOXRED1 FAD-dependent oxidoreductase domain-containing pro	R.YVYVWHC*PQGPGLETPLVADTSGAYFR.R	331	Yes	4.76%	0.00%
P30048	PRDX3 Thioredoxin-dependent peroxide reductase, mitochon	K.AFQYVETHGEVC*PANWTPDSPTIKPSPAASK.E	229	Yes	4.76%	0.00%
P26440	IVD Isovaleryl-CoA dehydrogenase, mitochondrial	R.ASGAVGLSYGAHSNLC*INQLVR.N	136	Yes	4.76%	0.00%
Q13011	ECH1 Delta(3,5)-Delta(2,4)-dienoyl-CoA isomerase, mitoc	R.C*PKPVIAAVHGGC*IGGGVDLVTAC*DIR.Y	159|171|182	Yes	4.76%	0.00%
Q9GZT3	SLIRP SRA stem-loop-interacting RNA-binding protein, mit	R.C*ILPFDKETGFHR.G	48	Yes	4.76%	0.00%
Q5T160	RARS2 Probable arginine--tRNA ligase, mitochondrial	R.C*QHVPFGVVQGMK.T	372	Yes	4.76%	0.00%
Q5HYK3	COQ5 2-methoxy-6-polyprenyl-1,4-benzoquinol methylase,	R.FLC*LEFSQVNNPLISR.L	244	Yes	4.76%	0.00%
O94925	GLS Glutaminase kidney isoform, mitochondrial	K.GIHFC*HDLVSLC*NFHNYDNLR.H	518|525	Yes	4.76%	0.00%
P31937	HIBADH 3-hydroxyisobutyrate dehydrogenase, mitochondrial	K.HGYPLIIYDVFPDAC*K.E	75	Yes	4.76%	0.00%
Q969Z0	TBRG4 Protein TBRG4	K.HLAFLAESC*ATLSQEQHSQELLAELLTHLER.R	191	Yes	4.76%	0.00%
Q96RQ3	MCCC1 Methylcrotonoyl-CoA carboxylase subunit alpha, mit	K.HNFC*FMEMNTR.L	332	Yes	4.76%	0.00%
Q5JTZ9	AARS2 Alanine--tRNA ligase, mitochondrial	K.HSTYDTDLFSPLLNAIQQGC*R.A	300	Yes	4.76%	0.00%
P09001	MRPL3 39S ribosomal protein L3, mitochondrial	K.HVVTLLQVQDC*HVLK.Y	127	Yes	4.76%	0.00%
Q96I99	SUCLG2 Succinyl-CoA ligase	K.IDATQVEVNPFGETPEGQVVC*FDAK.I	255	Yes	4.76%	0.00%
Q96EY8	MMAB Cob(I)yrinic acid a,c-diamide adenosyltransferase,	K.ISSALHFC*R.A	185	Yes	4.76%	0.00%
Q6PI48	DARS2 Aspartate--tRNA ligase, mitochondrial	K.LRLEC*ADLLETR.G	459	Yes	4.76%	0.00%
Q5T2R2	PDSS1 Decaprenyl-diphosphate synthase subunit 1	K.LGLATGPVLFAC*QQFPEMNAMIMR.R	340	Yes	4.76%	0.00%
Q9NYY8	FASTKD2 FAST kinase domain-containing protein 2	R.LMFSHPAFNQLC*EHMMR.E	217	Yes	4.76%	0.00%
Q969Y2	GTPBP3 tRNA modification GTPase GTPBP3, mitochondrial	R.LTGGGGTEEILDIIFQDFC*VGK.-	489	Yes	4.76%	0.00%
P31327	CPS1 Carbamoyl-phosphate synthase	R.MC*HPSIEGFTPR.L	816	Yes	4.76%	0.00%
O43615	TIMM44 Mitochondrial import inner membrane translocase su	R.MLYVWALC*R.D	426	Yes	4.76%	0.00%

Q9Y399	MRPS2 28S ribosomal protein S2, mitochondrial	K.MNIPTVGIVDTNC*NPC*LITYPVPGNDDSPLAVHLYC*R.L	227|230|250	Yes	4.76%	0.00%
P42704	LRPPRC Leucine-rich PPR motif-containing protein, mitocho	K.QLILVLC*SEENMQK.A	690	Yes	4.76%	0.00%
P00390	GSR Glutathione reductase, mitochondrial	R.SFDSMISTNC*TEELENAGVEVLK.F	278	Yes	4.76%	0.00%
Q6PI48	DARS2 Aspartate--tRNA ligase, mitochondrial	R.SSHLGQEVTLC*GWIQYR.R	69	Yes	4.76%	0.00%
P82930	MRPS34 28S ribosomal protein S34, mitochondrial	K.SWLWQHDEPC*YWR.L	93	Yes	4.76%	0.00%
Q8N5M1	ATPAF2 ATP synthase mitochondrial F1 complex assembly fac	R.TAAGTLFIHLC*SESTTVK.H	276	Yes	4.76%	0.00%
Q9HC36	RNMTL1 RNA methyltransferase-like protein 1	K.TQLQHSLPLLLIC*DNLR.D	214	Yes	4.76%	0.00%
Q8IVS2	MCAT Malonyl-CoA-acyl carrier protein transacylase, mit	R.TVHC*QPAIFVASLAAVEK.L	120	Yes	4.76%	0.00%
Q02218	OGDH 2-oxoglutarate dehydrogenase, mitochondrial	K.YPNAELAWC*QEEHK.N	956	Yes	4.76%	0.00%
Q12849	GRSF1 G-rich sequence factor 1	R.AQGLPWSC*TMEDVLNFFSDC*R.I	161|173	Yes	4.76%	0.00%
Q8IYQ7	THNSL1 Threonine synthase-like 1	K.FIC*ASNQNHVLTDFIK.T	532	Yes	4.76%	0.00%
Q8TCS8	PNPT1 Polyribonucleotide nucleotidyltransferase 1, mitoc	R.GQTQVLC*TVTFDSLESGIK.S	395	Yes	4.76%	0.00%
O15382	BCAT2 Branched-chain-amino-acid aminotransferase, mitoch	R.LC*LPSFDKLELLEC*IR.R	135|147	Yes	4.76%	0.00%
O75521	ECI2 Enoyl-CoA delta isomerase 2, mitochondrial	K.LHAVNAEEC*NVLQGR.W	368	Yes	4.76%	0.00%
P49419	ALDH7A1 Alpha-aminoadipic semialdehyde dehydrogenase	K.LPGAIC*SLTC*GGADIGTAMAK.D	248|252	Yes	4.76%	0.00%
O43488	AKR7A2 Aflatoxin B1 aldehyde reductase member 2	R.LQC*PQVDLFYLHAPDHGTPVEETLHAC*QR.L	132|156	Yes	4.76%	0.00%
P54136	RARS Arginine--tRNA ligase, cytoplasmic	R.MLLC*EAVAAVMAK.G	638	Yes	4.76%	0.00%
Q9NQH7	XPNPEP3 Probable Xaa-Pro aminopeptidase 3	R.IEDDVVVTQDSPLILSADC*PK.E	492	Yes	4.76%	0.00%
O75521	ECI2 Enoyl-CoA delta isomerase 2, mitochondrial	R.WLSDEC*TNAVVNFLSR.K	380	Yes	4.76%	0.00%
Q9BSH5	HDHD3 Haloacid dehalogenase-like hydrolase domain-contai	K.EHILPSLAHLLPALDC*LEGSTPGL.-	243	Yes	4.76%	0.00%
Q8NFF5	FLAD1 FAD synthase	K.LTLDSEEEGPLEEC*LAYLTAR.L	338	Yes	4.76%	0.00%
Q8TCS8	PNPT1 Polyribonucleotide nucleotidyltransferase 1, mitoc	R.NVSC*EVDMFK.T	372	Yes	4.76%	0.00%
Q08257	CRYZ Quinone oxidoreductase	K.AGESVLVHGASGGVGLAAC*QIAR.A	166	Yes	4.76%	0.00%
Q6YN16	HSDL2 Hydroxysteroid dehydrogenase-like protein 2	K.ALPC*IVDVR.D	71	Yes	4.76%	0.00%
Q8NFF5	FLAD1 FAD synthase	K.DC*TALLHLFHAAVQR.K	409	Yes	4.76%	0.00%
Q5T1C6	THEM4 Thioesterase superfamily member 4	R.KFFVSC*NVQSVDEK.T	212	Yes	4.76%	0.00%
Q9H857	NT5DC2 5-nucleotidase domain-containing protein 2	R.FSDLYMASLSC*LLNYR.V	475	Yes	4.76%	0.00%
Q96GJ1	TRMT2B tRNA (uracil(54)-C(5))-methyltransferase homolog	R.LSC*LLHPIIPSPVINGYR.N	138	Yes	4.76%	0.00%
Q9UBQ7	GRHPR Glyoxylate reductase/hydroxypyruvate reductase	K.NC*VILPHIGSATHR.T	288	Yes	4.76%	0.00%
P53396	ACLY ATP-citrate synthase	R.KPASFMTSIC*DER.G	845	Yes	4.76%	0.00%
Q5T1C6	THEM4 Thioesterase superfamily member 4	K.RPIPLC*SVVMINSQLDKVEGR.K	191	Yes	4.76%	0.00%
Q05932	FPGS Folylpolyglutamate synthase, mitochondrial	R.SNAALALQLAHC*WLQR.Q	315	Yes	4.76%	0.00%
Q13085	ACACA Acetyl-CoA carboxylase 1	K.VQAERPDTMLGVVC*GALHVADVSLR.N	634	Yes	4.76%	0.00%
P04406	GAPDH Glyceraldehyde-3-phosphate dehydrogenase	R.VPTANVSVVDLTC*R.L	247	Yes	4.76%	0.00%
Q9NQR4	NIT2 Omega-amidase NIT2	R.GC*QLLVYPGAFNLTTGPAHWELLQR.S	170	Yes	4.76%	0.00%
P49327	FASN Fatty acid synthase	R.DGLLENQTPEFFQDVC*KPK.Y	1992	Yes	4.76%	0.00%
Q9BQP7	C20orf72 Uncharacterized protein C20orf72	K.DGSPAHPHFMDAELC*SQYWTK.W	314	Yes	4.76%	0.00%
Q32P41	TRMT5 tRNA (guanine(37)-N1)-methyltransferase	K.KNC*TVFANDLNPESHK.W	321	Yes	4.76%	0.00%
P60174	TPI1 Triosephosphate isomerase	K.VPADTEVVC*APPTAYIDFAR.Q	42		4.76%	0.00%
P26639	TARS Threonine--tRNA ligase, cytoplasmic	R.DQELYFFHELSPGSC*FFLPK.G	343		4.76%	0.00%
P68366	TUBA4A Tubulin alpha-4A chain	R.AVC*MLSNTTAIAEAWAR.L	376		4.76%	0.00%
P11172	UMPS Uridine 5-monophosphate synthase	K.C*HEFLIFEDR.K	304		4.76%	0.00%
P63104	YWHAZ 14-3-3 protein zeta/delta	R.DIC*NDVLSLLEK.F	94		4.76%	0.00%
P13489	RNH1 Ribonuclease inhibitor	R.ELDLSNNC*LGDAGILQLVESVR.Q	409		4.76%	0.00%
P62633	CNBP Cellular nucleic acid-binding protein	R.EQC*C*YNC*GKPGHLAR.D	97|98|101		4.76%	0.00%
P23526	AHCY Adenosylhomocysteinase	K.SKFDNLYGC*R.E	195		4.76%	0.00%
P08107	HSPA1B Heat shock 70 kDa protein 1A/1B	R.ARFEELC*SDLFR.S	BAD_ID		4.76%	0.00%
Q04760	GLO1 Lactoylglutathione lyase	R.GFGHIGIAVPDVYSAC*K.R	139		4.76%	0.00%
P14618	PKM Pyruvate kinase isozymes M1/M2	R.GIFPVLC*KDPVQEAWAEDVDLR.V	474		4.76%	0.00%
P62316	SNRPD2 Small nuclear ribonucleoprotein Sm D2	R.HC*NMVLENVK.E	63		4.76%	0.00%
P12268	IMPDH2 Inosine-5-monophosphate dehydrogenase 2	R.HGFC*GIPITDTGR.M	140		4.76%	0.00%
Q15185	PTGES3 Prostaglandin E synthase 3	K.HLNEIDLFHC*IDPNDSK.H	58		4.76%	0.00%
P62258	YWHAE 14-3-3 protein epsilon	K.LIC*C*DILDVLDK.H	97|98		4.76%	0.00%
P13639	EEF2 Elongation factor 2	R.LMEPIYLVEIQC*PEQVVGGIYGVLNR.K	751		4.76%	0.00%
P11413	G6PD Glucose-6-phosphate 1-dehydrogenase	R.LQFHDVAGDIFHQQC*K.R	385		4.76%	0.00%
Q9H3K6	BOLA2B BolA-like protein 2	R.LVNAC*LAEELPHIHAFEQK.T	59		4.76%	0.00%
P08238	HSP90AB1 Heat shock protein HSP 90-beta	R.LVSSPC*C*IVTSTYGWTANMER.I	589|590		4.76%	0.00%
P14618	PKM Pyruvate kinase isozymes M1/M2	R.AGKPVIC*ATQMLESMIK.K	326		4.76%	0.00%
P68366	TUBA4A Tubulin alpha-4A chain	R.SIQFVDWC*PTGFK.V	347		4.76%	0.00%
O43707	ACTN4 Alpha-actinin-4	K.TFTAWC*NSHLR.K	60		4.76%	0.00%
P20073	ANXA7 Annexin A7	R.VLIEILC*TR.T	285		4.76%	0.00%
Q9BWD1	ACAT2 Acetyl-CoA acetyltransferase, cytosolic	K.VNIEGGAIALGHPLGASGC*R.I	360		4.76%	0.00%
P04075	ALDOA Fructose-bisphosphate aldolase A	R.VNPC*IGGVILFHETLYQK.A	73		4.76%	0.00%
P68366	TUBA4A Tubulin alpha-4A chain	K.YMAC*C*LLYR.G	315|316		4.76%	0.00%
P04075	ALDOA Fructose-bisphosphate aldolase A	K.C*PLLKPWALTFSYGR.A	290		4.76%	0.00%
P34932	HSPA4 Heat shock 70 kDa protein 4	K.FLEMC*NDLLAR.V	310		4.76%	0.00%
P26641	EEF1G Elongation factor 1-gamma	R.FPEELTQTFMSC*NLITGMFQR.L	339		4.76%	0.00%
P07741	APRT Adenine phosphoribosyltransferase	R.GFLFGPSLAQELGLGC*VLIR.K	83		4.76%	0.00%
O95373	IPO7 Importin-7	R.GIDQC*IPLFVEAALER.L	757		4.76%	0.00%

Q71U36	TUBA1A Tubulin alpha-1A chain	K.LADQC*TGLQGFLVFHSFGGGTGSGFTSLLMER.L	129		4.76%	0.00%
P17812	CTPS1 CTP synthase 1	K.LC*SAHGVLVPGGFGVR.G	362		4.76%	0.00%
P60709	ACTB Actin, cytoplasmic 1	K.LC*YVALDFEQEMATAASSSSLEK.S	217		4.76%	0.00%
P13639	EEF2 Elongation factor 2	R.TFC*QLILDPIFK.V	290		4.76%	0.00%
P52292	KPNA2 Importin subunit alpha-2	K.YGAVDPLLALLAVPDMSSLAC*GYLR.N	223		4.76%	0.00%
Q9BXJ9	NAA15 N-alpha-acetyltransferase 15, NatA auxiliary subun	R.AFAIDSSHPWLHEC*MIR.L	711		4.76%	0.00%
P31948	STIP1 Stress-induced-phosphoprotein 1	K.ALSVGNIDDALQC*YSEAIK.L	26		4.76%	0.00%
Q8WUM4	PDCD6IP Programmed cell death 6-interacting protein	R.DTIVLLC*KPEPELNAAIPSANPAK.T	524		4.76%	0.00%
Q9NX46	ADPRHL2 Poly(ADP-ribose) glycohydrolase ARH3	R.EEVVSELGNGIAAFESVPTAIYC*FLR.C	283		4.76%	0.00%
Q9H074	PAIP1 Polyadenylate-binding protein-interacting protein	R.ELLNALFSNPMDDNLIC*AVK.L	318		4.76%	0.00%
Q9BY32	ITPA Inosine triphosphate pyrophosphatase	K.KLEEVVQILGDKFPC*TLVAQK.I	33		4.76%	0.00%
P07900	HSP90AA1 Heat shock protein HSP 90-alpha	K.HGLEVIYMIEPIDEYC*VQQLK.E	529		4.76%	0.00%
P15121	AKR1B1 Aldose reductase	R.HIDC*AHVYQNENEVGVAIQEK.L	45		4.76%	0.00%
P48643	CCT5 T-complex protein 1 subunit epsilon	K.IAILTC*PFEPPKPK.T	253		4.76%	0.00%
P31946	YWHAB 14-3-3 protein beta/alpha	K.IEAELQDIC*NDVLELLDK.Y	96		4.76%	0.00%
Q13155	AIMP2 Aminoacyl tRNA synthase complex-interacting multif	R.LLC*EHFR.V	143		4.76%	0.00%
P62714	PPP2CB Serine/threonine-protein phosphatase 2A catalytic	R.LQEVPHEGPMC*DLLWSDPDDR.G	196		4.76%	0.00%
P17812	CTPS1 CTP synthase 1	K.SC*GLHVTSIK.I	30		4.76%	0.00%
P27348	YWHAQ 14-3-3 protein theta	R.SIC*TTVLELLDK.Y	94		4.76%	0.00%
Q13283	G3BP1 Ras GTPase-activating protein-binding protein 1	K.VMSQNFTNC*HTK.I	73		4.76%	0.00%
P62714	PPP2CB Serine/threonine-protein phosphatase 2A catalytic	R.AHQLVMEGYNWC*HDR.N	251		4.76%	0.00%
P15927	RPA2 Replication protein A 32 kDa subunit	R.AQHIVPC*TISQLLSATLVDEVFR.I	49		4.76%	0.00%
Q13838	DDX39B Spliceosome RNA helicase DDX39B	R.C*IALAQLLVEQNFPAIAIHR.G	300		4.76%	0.00%
P39687	ANP32A Acidic leucine-rich nuclear phosphoprotein 32 fami	K.C*PNLTHLNLSGNK.I	87		4.76%	0.00%
P14923	JUP Junction plakoglobin	R.C*TTSILHNLSHHR.E	204		4.76%	0.00%
P10768	ESD S-formylglutathione hydrolase	K.SYPGSQLDILIDQGKDDQFLLDGQLLPDNFIAAC*TEK.K	243		4.76%	0.00%
P15170	GSPT1 Eukaryotic peptide chain release factor GTP-bindin	K.EQSDFC*PWYIGLPFIPYLDNLPNFNR.S	276		4.76%	0.00%
Q9NTK5	OLA1 Obg-like ATPase 1	R.FDFLC*QYHKPASK.I	75		4.76%	0.00%
Q9UHD1	CHORDC1 Cysteine and histidine-rich domain-containing prot	R.FDPETNSDDAC*TYHPGVPVFHDALK.G	24		4.76%	0.00%
O75832	PSMD10 26S proteasome non-ATPase regulatory subunit 10	K.GAQVNAVNQNGC*TPLHYAASK.N	107		4.76%	0.00%
O14979	HNRPDL Heterogeneous nuclear ribonucleoprotein D-like	R.GFC*FITYTDEEPVKK.L	277		4.76%	0.00%
O43390	HNRNPR Heterogeneous nuclear ribonucleoprotein R	R.GFC*FLEYEDHK.S	292		4.76%	0.00%
P61978	HNRNPK Heterogeneous nuclear ribonucleoprotein K	K.GSDFDC*ELR.L	145		4.76%	0.00%
P21266	GSTM3 Glutathione S-transferase Mu 3	R.KHNMC*GETEEEK.I	91		4.76%	0.00%
P30876	POLR2B DNA-directed RNA polymerase II subunit RPB2	R.IC*RPLLIVEK.Q	622		4.76%	0.00%
P36873	PPP1CC Serine/threonine-protein phosphatase PP1-gamma cat	K.IFC*C*HGGLSPDLQSMEQIR.R	171|172		4.76%	0.00%
P26038	MSN Moesin	R.ILALC*MGNHELYMR.R	284		4.76%	0.00%
Q96H79	ZC3HAV1L Zinc finger CCCH-type antiviral protein 1-like	R.ILLLQNDPC*LLPEVC*LLYNK.G	163|169		4.76%	0.00%
P15311	EZR Ezrin	R.ILQLC*MGNHELYMR.R	284		4.76%	0.00%
Q9UHB6	LIMA1 LIM domain and actin-binding protein 1	R.IYC*KPHFNQLFK.S	438		4.76%	0.00%
P13010	XRCC5 X-ray repair cross-complementing protein 5	R.LFQC*LLHR.A	493		4.76%	0.00%
P41743	PRKCI Protein kinase C iota type	R.LGC*HPQTGFADIQGHPFFR.N	507		4.76%	0.00%
Q12904	AIMP1 Aminoacyl tRNA synthase complex-interacting multif	R.MVILLC*NLKPAK.M	211		4.76%	0.00%
Q14566	MCM6 DNA replication licensing factor MCM6	K.NLYHNLC*TSLFPTIHGNDEVKR.G	351		4.76%	0.00%
P49321	NASP Nuclear autoantigenic sperm protein	R.KPTDGASSSNC*VTDISHLVR.K	708		4.76%	0.00%
P23526	AHCY Adenosylhomocysteinase	K.QAQYLGMSC*DGPFKPDHYR.Y	421		4.76%	0.00%
Q9UMS4	PRPF19 Pre-mRNA-processing factor 19	R.QELSHALYQHDAAC*R.V	114		4.76%	0.00%
P06733	ENO1 Alpha-enolase	R.SGETEDTFIADLVVGLC*TGQIK.T	389		4.76%	0.00%
P78371	CCT2 T-complex protein 1 subunit beta	R.SLHDALC*VLAQTVK.D	395		4.76%	0.00%
P17987	TCP1 T-complex protein 1 subunit alpha	R.SLHDALC*VVK.R	397		4.76%	0.00%
Q96J01	THOC3 THO complex subunit 3	K.VHSVAWSC*DGR.R	65		4.76%	0.00%
Q14166	TTLL12 Tubulin--tyrosine ligase-like protein 12	R.WGEDNHWIC*KPWNLAR.S	418		4.76%	0.00%
P52597	HNRNPF Heterogeneous nuclear ribonucleoprotein F	R.YGDSEFTVQSTTGHC*VHMR.G	290		4.76%	0.00%
P09651	HNRNPA1 Heterogeneous nuclear ribonucleoprotein A1	K.YHTVNGHNC*EVR.K	175		4.76%	0.00%
Q86X76	NIT1 Nitrilase homolog 1	R.LGAC*LAFLPEAFDFIAR.D	80	Yes	4.76%	0.00%
P23919	DTYMK Thymidylate kinase	K.LVEALC*AAGHR.A	31	Yes	4.76%	0.00%
Q9BYT8	NLN Neurolysin, mitochondrial	R.TYFHEFGHVMHQIC*AQTDFAR.F	507	Yes	4.76%	0.00%
P36776	LONP1 Lon protease homolog, mitochondrial	K.RAGVTC*IVLPAENK.K	909	Yes	4.76%	0.00%
P53396	ACLY ATP-citrate synthase	K.GVTIIGPATVGGIKPGC*FK.I	633	Yes	4.76%	0.00%
P13639	EEF2 Elongation factor 2	K.IWC*FGPDGTGPNILTDITK.G	651		4.76%	0.00%
P08238	HSP90AB1 Heat shock protein HSP 90-beta	R.VFIMDSC*DELIPEYLNFIR.G	366		4.76%	0.00%
Q7Z7H8	MRPL10 39S ribosomal protein L10, mitochondrial	R.TVPFLPLLGGC*IDDTILSR.Q	180	Yes	4.70%	0.47%
Q7L0Y3	TRMT10C Mitochondrial ribonuclease P protein 1	K.RLNLATEC*LPLDK.Y	335	Yes	4.61%	0.70%
P12277	CKB Creatine kinase B-type	R.GFC*LPPHC*SR.G	141|146		4.61%	0.37%
P15121	AKR1B1 Aldose reductase	K.YKPAVNQIEC*HPYLTQEK.L	187		4.60%	0.42%
P23368	ME2 NAD-dependent malic enzyme, mitochondrial	K.YC*TFNDDIQGTAAVALAGLLAAQK.V	274	Yes	4.56%	0.48%

P48735	IDH2 Isocitrate dehydrogenase	K.DLAGC*IHGLSNVK.L	418	Yes	4.53%	0.46%
Q969Y2	GTPBP3 tRNA modification GTPase GTPBP3, mitochondrial	K.SDLLSPEGPGPGPDLPPHLLLSC*LTGE GLDGLLEALR.K	398	Yes	4.53%	0.46%
Q6PI48	DARS2 Aspartate--tRNA ligase, mitochondrial	K.TAELLNAC*K.K	152	Yes	4.53%	0.46%
P40926	MDH2 Malate dehydrogenase, mitochondrial	K.TIIPLISQC*TPK.V	212	Yes	4.53%	0.46%
P42704	LRPPRC Leucine-rich PPR motif-containing protein, mitocho	R.LIASYC*NVGDIEGASK.I	208	Yes	4.53%	0.46%
P38117	ETFB Electron transfer flavoprotein subunit beta	K.HSMNPFC*EIAVEEAVR.L	42	Yes	4.31%	0.78%
H0YN64	MRPL46 39S ribosomal protein L46, mitochondrial	R.LLGALC*LQRPPVVSK.P	52	Yes	4.30%	0.50%
O95202	LETM1 LETM1 and EF-hand domain-containing protein 1, mit	K.LFEDELTLDNLTRPQLVALC*K.L	330	Yes	4.30%	0.92%
Q7L0Y3	TRMT10C Mitochondrial ribonuclease P protein 1	R.NVDPFHIYFC*NLK.I	246	Yes	4.21%	0.83%
P09417	QDPR Dihydropteridine reductase	K.GAVHQLC*QSLAGK.N	161	Yes	4.21%	0.83%
P00505	GOT2 Aspartate aminotransferase, mitochondrial	K.EYLPIGGLAEFC*K.A	106	Yes	4.15%	0.75%
Q9NUJ1	ABHD10 Abhydrolase domain-containing protein 10, mitochon	K.ALAIEEFC*K.S	100	Yes	4.15%	1.07%
P07900	HSP90AA1 Heat shock protein HSP 90-alpha	R.VFIMDNC*EELIPEYLNFIR.G	374		4.07%	0.88%
Q9BYD6	MRPL1 39S ribosomal protein L1, mitochondrial	K.IATLDMSSDQIAANLQAVINEVC*R.H	279	Yes	4.02%	1.01%
Q9HCC0	MCCC2 Methylcrotonoyl-CoA carboxylase beta chain, mitoch	K.GTHFVQLC*C*QR.N	391|392	Yes	3.96%	1.74%
Q10713	PMPCA Mitochondrial-processing peptidase subunit alpha	R.MVLAGVGVEHEHLVDC*AR.K	266	Yes	3.84%	1.01%
O43837	IDH3B Isocitrate dehydrogenase	K.LGDGLFLQC*C*EEVAELYPK.I	232|233	Yes	3.83%	1.32%
P42704	LRPPRC Leucine-rich PPR motif-containing protein, mitocho	R.IHDVLC*K.L	863	Yes	3.83%	1.32%
P30084	ECHS1 Enoyl-CoA hydratase, mitochondrial	K.IC*PVETLVEEAIQC*AEK.I	213|225	Yes	3.82%	1.89%
P04181	OAT Ornithine aminotransferase, mitochondrial	K.ALSGGLYPVSAVLC*DDDIMLTIKPGE HGSTYGGNPLGC*R.V	306|330	Yes	3.64%	1.53%
P34897	SHMT2 Serine hydroxymethyltransferase, mitochondrial	R.MREVC*DEVK.A	241	Yes	3.53%	1.07%
P42704	LRPPRC Leucine-rich PPR motif-containing protein, mitocho	R.C*GAIAEQTPILLLFLLR.N	1277	Yes	3.52%	1.40%

Table 4A-7. List of all proteins identified in cyto-APEX analysis. "LPS" denotes 1 μg/mL LPS. "none" denotes no treatment. Protein identifications are the average of 4 replicates (2 technical replicates from 2 biological replicates).

UniProt ID	Protein Description	Cytoplasm/ Cell Membrane	Average Spectral Count cyto-APEX LPS	Average Spectral Count cyto-APEX None
Q8BGQ7	Aars Alanine--tRNA ligase, cytoplasmic	YES	11	0
Q99LR1	Abhd12 Monoacylglycerol lipase ABHD12	YES	16	0
Q921H8	Acaa1a 3-ketoacyl-CoA thiolase A, peroxisomal	-	63	6
Q5SWU9	Acaca Acetyl-CoA carboxylase 1	YES	298	447
Q91V92	Acly ATP-citrate synthase	YES	11	0
Q99KI0	Aco2 Aconitate hydratase, mitochondrial	YES	21	5
Q9EPL9	Acox3 Peroxisomal acyl-coenzyme A oxidase 3	-	21	2
P68134	Acta1 Actin, alpha skeletal muscle	YES	26	7
P62737	Acta2 Actin, aortic smooth muscle	YES	20	7
P60710	Actb Actin, cytoplasmic 1	YES	131	16
P57780	Actn4 Alpha-actinin-4	YES	12	3
Q99JY9	Actr3 Actin-related protein 3	YES	14	0
Q8C0I1	Agps Alkyldihydroxyacetonephosphate synthase, peroxisomal	-	41	2
Q9Z110	Aldh18a1 Delta-1-pyrroline-5-carboxylate synthase	-	12	3
P47738	Aldh2 Aldehyde dehydrogenase, mitochondrial	-	11	11
P05064	Aldoa Fructose-bisphosphate aldolase A	YES	32	5
A6ZI46	Aldoart1 Fructose-bisphosphate aldolase	YES	15	2
P10107	Anxa1 Annexin A1	YES	39	3
P07356	Anxa2 Annexin A2	YES	43	4
P97429	Anxa4 Annexin A4	YES	18	2
P48036	Anxa5 Annexin A5	YES	14	3
P14824	Anxa6 Annexin A6	YES	12	0
P84078	Arf1 ADP-ribosylation factor 1	YES	12	3
P61205	Arf3 ADP-ribosylation factor 3	YES	12	3
P84084	Arf5 ADP-ribosylation factor 5	YES	11	0
Q8BSY0	Asph Aspartyl/asparaginyl beta-hydroxylase	YES	63	2
Q9CWJ9	Atic Bifunctional purine biosynthesis protein PURH	YES	11	2
Q8VDN2	Atp1a1 Sodium/potassium-transporting ATPase subunit alpha-1	YES	34	6
Q6PIE5	Atp1a2 Sodium/potassium-transporting ATPase subunit alpha-2	YES	16	0
Q6PIC6	Atp1a3 Sodium/potassium-transporting ATPase subunit alpha-3	YES	14	0
O55143	Atp2a2 Sarcoplasmic/endoplasmic reticulum calcium ATPase 2	YES	26	2
G5E829	Atp2b1 MCG13663, isoform CRA_a	YES	11	0
Q03265	Atp5a1 ATP synthase subunit alpha, mitochondrial	YES	16	7

P56480	Atp5b ATP synthase subunit beta, mitochondrial	YES	17	7
P50516	Atp6v1a V-type proton ATPase catalytic subunit A	YES	22	4
P62814	Atp6v1b2 V-type proton ATPase subunit B, brain isoform	YES	19	0
Q8CIF4	Btd Biotinidase	-	0	13
B2RQC6	Cad Carbamoyl-phosphate synthetase 2, aspartate transcarbamylase, and dihydroorotase, isoform CRA_c	YES	12	2
P14211	Calr Calreticulin	YES	196	2
O35887	Calu Calumenin	-	20	0
P35564	Canx Calnexin	YES	111	3
P40124	Cap1 Adenylyl cyclase-associated protein 1	YES	26	3
P24270	Cat Catalase	YES	29	3
Q9D024	Ccdc47 Coiled-coil domain-containing protein 47	-	15	0
P80314	Cct2 T-complex protein 1 subunit beta	YES	25	2
P80318	Cct3 T-complex protein 1 subunit gamma	YES	15	0
P80315	Cct4 T-complex protein 1 subunit delta	YES	12	2
P80316	Cct5 T-complex protein 1 subunit epsilon	YES	20	0
P80313	Cct7 T-complex protein 1 subunit eta	YES	16	2
P60766	Cdc42 Cell division control protein 42 homolog	YES	17	2
Q924Z4	Cers2 Ceramide synthase 2	-	16	0
P18760	Cfl1 Cofilin-1	YES	20	0
Q8BMK4	Ckap4 Cytoskeleton-associated protein 4	YES	14	0
Q04447	Ckb Creatine kinase B-type	YES	13	0
Q99LI2	Clcc1 Chloride channel CLIC-like protein 1	YES	19	0
Q8VBZ3	Clptm1 Cleft lip and palate transmembrane protein 1 homolog	YES	11	0
Q68FD5	Cltc Clathrin heavy chain 1	YES	95	5
Q8CIE6	Copa Coatomer subunit alpha	YES	19	0
Q9JIF7	Copb1 Coatomer subunit beta	YES	13	0
Q9QZE5	Copg1 Coatomer subunit gamma-1	YES	19	0
O89053	Coro1a Coronin-1A	YES	11	2
Q9ERK4	Cse1l Exportin-2	YES	10	0
P10605	Ctsb Cathepsin B	YES	14	2
Q61093	Cybb Cytochrome b-245 heavy chain	YES	43	4
Q7TMB8	Cyfip1 Cytoplasmic FMR1-interacting protein 1	YES	14	2
P16381	D1Pas1 Putative ATP-dependent RNA helicase Pl10	YES	19	3
O54734	Ddost Dolichyl-diphosphooligosaccharide--protein glycosyltransferase 48 kDa subunit	-	26	2
Q62167	Ddx3x ATP-dependent RNA helicase DDX3X	YES	20	3
Q62095	Ddx3y ATP-dependent RNA helicase DDX3Y	YES	15	2
O70133	Dhx9 ATP-dependent RNA helicase A	YES	10	2
Q9DC23	Dnajc10 DnaJ homolog subfamily C member 10	-	16	0
Q91YW3	Dnajc3 DnaJ homolog subfamily C member 3	YES	27	0
Q9JHU4	Dync1h1 Cytoplasmic dynein 1 heavy chain 1	YES	35	0
P10126	Eef1a1 Elongation factor 1-alpha 1	YES	87	12
Q9D8N0	Eef1g Elongation factor 1-gamma	YES	22	2
P58252	Eef2 Elongation factor 2	YES	89	6
P23116	Eif3a Eukaryotic translation initiation factor 3 subunit A	YES	15	0
Q8JZQ9	Eif3b Eukaryotic translation initiation factor 3 subunit B	YES	11	0
P60843	Eif4a1 Eukaryotic initiation factor 4A-I	YES	27	5
P10630	Eif4a2 Eukaryotic initiation factor 4A-II	YES	14	5
P63242	Eif5a Eukaryotic translation initiation factor 5A-1	YES	28	0
P17182	Eno1 Alpha-enolase	YES	131	11
P17183	Eno2 Gamma-enolase	YES	21	0
P21550	Eno3 Beta-enolase	YES	20	0
Q8CGC7	Eprs Bifunctional glutamate/proline--tRNA ligase	YES	16	3
Q9EQH2	Erap1 Endoplasmic reticulum aminopeptidase 1	YES	16	0
Q8R180	Ero1l ERO1-like protein alpha	-	23	0
P57759	Erp29 Endoplasmic reticulum resident protein 29	-	43	2
Q9D1Q6	Erp44 Endoplasmic reticulum resident protein 44	-	36	2
Q9R0P3	Esd S-formylglutathione hydrolase	YES	12	0
Q9Z0R9	Fads2 Fatty acid desaturase 2	-	3	12
Q8R1F1	Fam129b Niban-like protein 1	YES	17	0
P19096	Fasn Fatty acid synthase	YES	45	0
Q8K1B8	Fermt3 Fermitin family homolog 3	-	13	2
Q8BTM8	Flna Filamin-A	YES	26	2
Q80X90	Flnb Filamin-B	YES	10	0
Q80VA0	Galnt7 N-acetylgalactosaminyltransferase 7	-	37	0
Q8BHN3	Ganab Neutral alpha-glucosidase AB	-	98	3
P16858	Gapdh Glyceraldehyde-3-phosphate dehydrogenase	YES	106	19
Q9CZD3	Gars Glycine--tRNA ligase	YES	11	0
E9PVA8	Gcn1l1 Protein Gcn1l1	YES	19	0
Q61598	Gdi2 Rab GDP dissociation inhibitor beta	YES	25	2
Q61543	Glg1 Golgi apparatus protein 1	YES	24	0
Q8K297	Glt25d1 Procollagen galactosyltransferase 1	-	33	0
E9Q3T0	Gm10073 Uncharacterized protein	-	10	0
F6QXU4	Gm4795 Glyceraldehyde-3-phosphate dehydrogenase	-	13	0
E9Q7H5	Gm8991 Uncharacterized protein	-	14	3
P08752	Gnai2 Guanine nucleotide-binding protein G(i) subunit alpha-2	YES	16	3
P06745	Gpi Glucose-6-phosphate isomerase	YES	32	3
P12265	Gusb Beta-glucuronidase	-	10	0
P01899	H2-D1 H-2 class I histocompatibility antigen, D-B alpha chain	YES	11	2
P01897	H2-L H-2 class I histocompatibility antigen, L-D alpha chain	YES	20	2
Q8R1M2	H2afj Histone H2A.J	-	19	6
P27661	H2afx Histone H2A.x	-	11	4
Q8BMS1	Hadha Trifunctional enzyme subunit alpha, mitochondrial	-	15	4
Q8CGP4	Hist1h2aa Histone H2A	-	19	6

Q64475	Hist1h2bb Histone H2B type 1-B	YES	41	5
Q8CGP1	Hist1h2bk Histone H2B type 1-K	YES	41	5
P10854	Hist1h2bm Histone H2B type 1-M	YES	41	5
Q8CGP2	Hist1h2bp Histone H2B type 1-P	YES	41	5
Q64525	Hist2h2bb Histone H2B type 2-B	YES	41	5
Q8BFU2	Hist3h2a Histone H2A type 3	-	19	6
P62806	Hist4h4 Histone H4	-	16	8
P38060	Hmgcl Hydroxymethylglutaryl-CoA lyase, mitochondrial	-	11	2
Q8BG05	Hnrnpa3 Heterogeneous nuclear ribonucleoprotein A3	YES	14	3
Q99020	Hnrnpab Heterogeneous nuclear ribonucleoprotein A/B	YES	11	3
Q9Z2X1	Hnrnpf Heterogeneous nuclear ribonucleoprotein F	YES	15	2
O35737	Hnrnph1 Heterogeneous nuclear ribonucleoprotein H	YES	10	2
P61979	Hnrnpk Heterogeneous nuclear ribonucleoprotein K	YES	13	3
P51660	Hsd17b4 Peroxisomal multifunctional enzyme type 2	-	22	0
P07901	Hsp90aa1 Heat shock protein HSP 90-alpha	YES	29	5
P11499	Hsp90ab1 Heat shock protein HSP 90-beta	YES	49	4
P08113	Hsp90b1 Endoplasmin	YES	245	9
P17156	Hspa2 Heat shock-related 70 kDa protein 2	YES	19	0
P20029	Hspa5 78 kDa glucose-regulated protein	YES	135	9
P63017	Hspa8 Heat shock cognate 71 kDa protein	YES	51	10
P38647	Hspa9 Stress-70 protein, mitochondrial	YES	19	6
P63038	Hspd1 60 kDa heat shock protein, mitochondrial	YES	37	8
Q9JKR6	Hyou1 Hypoxia up-regulated protein 1	-	95	4
Q8BU30	Iars Isoleucine--tRNA ligase, cytoplasmic	YES	10	0
O88844	Idh1 Isocitrate dehydrogenase	YES	15	0
Q9D6R2	Idh3a Isocitrate dehydrogenase	-	16	4
Q64282	Ifit1 Interferon-induced protein with tetratricopeptide repeats 1	YES	15	0
Q8BKC5	Ipo5 Importin-5	YES	22	3
Q9EPL8	Ipo7 Importin-7	YES	11	0
Q9JKF1	Iqgap1 Ras GTPase-activating-like protein IQGAP1	YES	50	7
P54987	Irg1 Immune-responsive gene 1 protein	-	29	0
Q60766	Irgm1 Immunity-related GTPase family M protein 1	YES	11	0
P11835	Itgb2 Integrin beta-2	YES	13	0
P70168	Kpnb1 Importin subunit beta-1	YES	22	0
Q8BMJ2	Lars Leucine--tRNA ligase, cytoplasmic	YES	25	0
Q3U9G9	Lbr Lamin-B receptor	YES	19	2
Q61233	Lcp1 Plastin-2	YES	43	13
P06151	Ldha L-lactate dehydrogenase A chain	YES	17	5
P16110	Lgals3 Galectin-3	YES	18	7
Q07797	Lgals3bp Galectin-3-binding protein	-	18	0
Q9D0F3	Lman1 Protein ERGIC-53	-	25	0
Q9DBH5	Lman2 Vesicular integral-membrane protein VIP36	YES	19	0
Q8CGK3	Lonp1 Lon protease homolog, mitochondrial	YES	16	5
P11152	Lpl Lipoprotein lipase	YES	13	0
Q91ZX7	Lrp1 Prolow-density lipoprotein receptor-related protein 1	YES	24	0
P55302	Lrpap1 Alpha-2-macroglobulin receptor-associated protein	YES	11	0
Q6PB66	Lrpprc Leucine-rich PPR motif-containing protein, mitochondrial	YES	11	3
Q68FL6	Mars Methionine--tRNA ligase, cytoplasmic	YES	11	0
Q99MR8	Mccc1 Methylcrotonoyl-CoA carboxylase subunit alpha, mitochondrial	-	146	548
P08249	Mdh2 Malate dehydrogenase, mitochondrial	YES	16	5
P34884	Mif Macrophage migration inhibitory factor	YES	43	9
Q6ZQI3	Mlec Malectin	-	10	0
Q80UM7	Mogs Mannosyl-oligosaccharide glucosidase	-	40	0
P26041	Msn Moesin	YES	13	3
Q8VDD5	Myh9 Myosin-9	YES	29	2
Q8BP47	Nars Asparagine--tRNA ligase, cytoplasmic	YES	17	3
Q8BLF1	Nceh1 Neutral cholesterol ester hydrolase 1	YES	18	0
Q8VCM8	Ncln Nicalin	-	13	0
Q6GQT9	Nomo1 Nodal modulator 1	-	45	0
P29477	Nos2 Nitric oxide synthase, inducible	YES	52	0
Q02819	Nucb1 Nucleobindin-1	YES	11	0
P81117	Nucb2 Nucleobindin-2	YES	12	0
Q9QY81	Nup210 Nuclear pore membrane glycoprotein 210	-	14	0
P11928	Oas1a 2'-5'-oligoadenylate synthase 1A	YES	12	0
Q8VI93	Oas3 2'-5'-oligoadenylate synthase 3	YES	12	0
Q8VI94	Oasl1 2'-5'-oligoadenylate synthase-like protein 1	YES	14	0
Q60597	Ogdh 2-oxoglutarate dehydrogenase, mitochondrial	-	14	0
Q60715	P4ha1 Prolyl 4-hydroxylase subunit alpha-1	-	59	0
P09103	P4hb Protein disulfide-isomerase	YES	129	0
P50580	Pa2g4 Proliferation-associated protein 2G4	YES	10	0
Q05920	Pc Pyruvate carboxylase, mitochondrial	YES	211	417
Q91ZA3	Pcca Propionyl-CoA carboxylase alpha chain, mitochondrial	-	299	787
Q99MN9	Pccb Propionyl-CoA carboxylase beta chain, mitochondrial	-	20	59
P27773	Pdia3 Protein disulfide-isomerase A3	YES	279	7
P08003	Pdia4 Protein disulfide-isomerase A4	-	50	0
Q921X9	Pdia5 Protein disulfide-isomerase A5	-	11	0
Q922R8	Pdia6 Protein disulfide-isomerase A6	YES	66	4
P12382	Pfkl 6-phosphofructokinase, liver type	YES	18	2
Q9WUA3	Pfkp 6-phosphofructokinase type C	YES	18	2
P62962	Pfn1 Profilin-1	YES	46	10
Q9DBJ1	Pgam1 Phosphoglycerate mutase 1	YES	26	4
Q9DCD0	Pgd 6-phosphogluconate dehydrogenase, decarboxylating	YES	25	2
P09411	Pgk1 Phosphoglycerate kinase 1	YES	57	5
P09041	Pgk2 Phosphoglycerate kinase 2	YES	10	0

Q9CQ60	Pgls 6-phosphogluconolactonase	YES	11	0
Q9CXY9	Pigk GPI-anchor transamidase	-	18	0
Q6PD26	Pigs GPI transamidase component PIG-S	-	15	0
P52480	Pkm Pyruvate kinase isozymes M1/M2	YES	257	26
Q9QXS1	Plec Plectin	YES	17	0
Q9R0E2	Plod1 Procollagen-lysine,2-oxoglutarate 5-dioxygenase 1	-	20	0
Q9R0E1	Plod3 Procollagen-lysine,2-oxoglutarate 5-dioxygenase 3	-	57	0
Q91ZW2	Pofut1 GDP-fucose protein O-fucosyltransferase 1	-	16	0
Q8VHI3	Pofut2 GDP-fucose protein O-fucosyltransferase 2	-	10	0
P37040	Por NADPH--cytochrome P450 reductase	YES	10	0
P17742	Ppia Peptidyl-prolyl cis-trans isomerase A	YES	30	10
Q76MZ3	Ppp2r1a Serine/threonine-protein phosphatase 2A 65 kDa regulatory subunit A alpha isoform	YES	15	0
P35700	Prdx1 Peroxiredoxin-1	YES	20	3
O08807	Prdx4 Peroxiredoxin-4	YES	20	2
Q9QUR6	Prep Prolyl endopeptidase	YES	17	0
O08795	Prkcsh Glucosidase 2 subunit beta	-	12	0
Q9Z1R9	Prss1 Protease, serine, 1 (Trypsin 1)	-	44	98
Q8VDM4	Psmd2 26S proteasome non-ATPase regulatory subunit 2	-	12	0
P97371	Psme1 Proteasome activator complex subunit 1	YES	13	0
P97372	Psme2 Proteasome activator complex subunit 2	YES	12	0
P22437	Ptgs1 Prostaglandin G/H synthase 1	YES	17	0
Q05769	Ptgs2 Prostaglandin G/H synthase 2	YES	565	8
P29351	Ptpn6 Tyrosine-protein phosphatase non-receptor type 6	YES	14	3
P06800	Ptprc Receptor-type tyrosine-protein phosphatase C	YES	10	0
P62821	Rab1A Ras-related protein Rab-1A	YES	11	2
P51150	Rab7a Ras-related protein Rab-7a	YES	10	3
Q99JI6	Rap1b Ras-related protein Rap-1b	YES	20	0
Q9D0I9	Rars Arginine--tRNA ligase, cytoplasmic	YES	16	0
Q8BP92	Rcn2 Reticulocalbin-2	-	31	0
Q62159	Rhoc Rho-related GTP-binding protein RhoC	YES	10	3
E9Q555	Rnf213 E3 ubiquitin-protein ligase RNF213	YES	48	0
Q91VI7	Rnh1 Ribonuclease inhibitor	YES	16	2
Q9CZM2	Rpl15 60S ribosomal protein L15	YES	10	5
P35980	Rpl18 60S ribosomal protein L18	YES	4	10
P27659	Rpl3 60S ribosomal protein L3	YES	19	5
Q9D8E6	Rpl4 60S ribosomal protein L4	YES	11	11
P47911	Rpl6 60S ribosomal protein L6	YES	16	7
Q91YQ5	Rpn1 Dolichyl-diphosphooligosaccharide--protein glycosyltransferase subunit 1	YES	54	2
Q9DBG6	Rpn2 Dolichyl-diphosphooligosaccharide--protein glycosyltransferase subunit 2	-	57	0
P62908	Rps3 40S ribosomal protein S3	YES	12	3
P50543	S100a11 Protein S100-A11	YES	11	0
P26638	Sars Serine--tRNA ligase, cytoplasmic	YES	18	0
Q8K2B3	Sdha Succinate dehydrogenase	-	14	3
Q9Z2G6	Sel1l Protein sel-1 homolog 1	-	12	0
Q8R0X7	Sgpl1 Sphingosine-1-phosphate lyase 1	YES	19	0
Q9CZN7	Shmt2 Protein Shmt2	YES	21	7
Q8VEM8	Slc25a3 Phosphate carrier protein, mitochondrial	-	17	4
P48962	Slc25a4 ADP/ATP translocase 1	-	13	5
P51881	Slc25a5 ADP/ATP translocase 2	-	27	8
Q78PY7	Snd1 Staphylococcal nuclease domain-containing protein 1	YES	20	0
Q61263	Soat1 Sterol O-acyltransferase 1	-	19	0
P46978	Stt3a Dolichyl-diphosphooligosaccharide--protein glycosyltransferase subunit STT3A	-	20	0
Q9D666	Sun1 SUN domain-containing protein 1	YES	10	0
Q64310	Surf4 Surfeit locus protein 4	-	21	2
Q7TMK9	Syncrip Heterogeneous nuclear ribonucleoprotein Q	YES	10	0
Q9R233	Tapbp Tapasin	YES	35	0
Q9D0R2	Tars Threonine--tRNA ligase, cytoplasmic	YES	13	2
P11983	Tcp1 T-complex protein 1 subunit alpha	YES	12	2
P40142	Tkt Transketolase	-	23	2
P26039	Tln1 Talin-1	YES	82	4
Q9QUN7	Tlr2 Toll-like receptor 2	YES	10	0
Q9ET30	Tm9sf3 Transmembrane 9 superfamily member 3	-	10	2
Q9D1D4	Tmed10 Transmembrane emp24 domain-containing protein 10	YES	11	2
D3YZZ5	Tmed7 Protein Tmed7	-	12	0
Q8BXZ1	Tmx3 Protein disulfide-isomerase TMX3	-	14	0
Q9ER39	Tor1a Torsin-1A	YES	11	0
Q921T2	Tor1aip1 Torsin-1A-interacting protein 1	-	20	0
Q9ER41	Tor1b Torsin-1B	YES	12	0
Q9ER38	Tor3a Torsin-3A	YES	16	0
P17751	Tpi1 Triosephosphate isomerase	YES	16	7
P68369	Tuba1a Tubulin alpha-1A chain	YES	80	12
P68368	Tuba4a Tubulin alpha-4A chain	YES	76	7
Q9JJZ2	Tuba8 Tubulin alpha-8 chain	YES	48	5
Q7TMM9	Tubb2a Tubulin beta-2A chain	YES	72	0
Q9ERD7	Tubb3 Tubulin beta-3 chain	YES	57	13
P68372	Tubb4b Tubulin beta-4B chain	YES	88	16
P99024	Tubb5 Tubulin beta-5 chain	YES	104	16
Q922F4	Tubb6 Tubulin beta-6 chain	YES	59	8
Q91W90	Txndc5 Thioredoxin domain-containing protein 5	-	35	0
Q02053	Uba1 Ubiquitin-like modifier-activating enzyme 1	YES	40	3
Q6P5E4	Uggt1 UDP-glucose:glycoprotein glucosyltransferase 1	-	60	0
Q6ZQM8	Ugt1a7c UDP-glucuronosyltransferase 1-7C	-	21	2
Q9Z1Q9	Vars Valine--tRNA ligase	YES	32	0
Q01853	Vcp Transitional endoplasmic reticulum ATPase	YES	26	3

P20152	Vim Vimentin	YES	14	5
Q8BX70	Vps13c Vacuolar protein sorting-associated protein 13C	YES	11	0
O88342	Wdr1 WD repeat-containing protein 1	YES	12	0
Q6P5F9	Xpo1 Exportin-1	YES	10	0
P61982	Ywhag 14-3-3 protein gamma	YES	11	3
P63101	Ywhaz 14-3-3 protein zeta/delta	YES	22	3

Table 4A-8. Gene ontology (GOrilla) analysis for enrichment of biological processes for proteins identified in cyto-APEX analysis with >5-fold enrichment.

Analysis Type: PANTHER Overrepresentation Test (Released 20220202)
Annotation Version and Release Date: PANTHER version 17.0 Released 2022-02-22

Reference List: Mus musculus (all genes in database)
Test Type: FISHER
Correction: FDR

PANTHER GO-Slim Biological Process	REFLIST	Sample (1563)	Expected	Fold Enrichment	P-Value	FDR
positive regulation of type I interferon production (GO:0032481)	4	3	0.28	10.56	8.33E-03	4.88E-02
purine ribonucleoside monophosphate metabolic process (GO:0009167)	11	8	0.78	10.24	1.44E-05	1.90E-04
purine nucleoside monophosphate metabolic process (GO:0009126)	11	8	0.78	10.24	1.44E-05	1.89E-04
IMP metabolic process (GO:0046040)	7	5	0.5	10.05	6.82E-04	5.91E-03
ribonucleoside diphosphate metabolic process (GO:0009185)	24	17	1.71	9.97	2.82E-10	8.68E-09
purine ribonucleoside diphosphate metabolic process (GO:0009179)	24	17	1.71	9.97	2.82E-10	8.56E-09
purine nucleoside diphosphate metabolic process (GO:0009135)	24	17	1.71	9.97	2.82E-10	8.45E-09
ATP generation from ADP (GO:0006757)	24	17	1.71	9.97	2.82E-10	8.33E-09
glycolytic process (GO:0006096)	24	17	1.71	9.97	2.82E-10	8.23E-09
ADP metabolic process (GO:0046031)	24	17	1.71	9.97	2.82E-10	8.12E-09
ribonucleoside monophosphate metabolic process (GO:0009161)	13	9	0.92	9.74	5.48E-06	7.91E-05
cytoplasmic translational initiation (GO:0002183)	14	9	0.99	9.05	8.48E-06	1.17E-04
tricarboxylic acid cycle (GO:0006099)	19	12	1.35	8.89	3.01E-07	5.17E-06
AMP metabolic process (GO:0046033)	8	5	0.57	8.8	1.05E-03	8.42E-03
protein N-linked glycosylation via asparagine (GO:0018279)	8	5	0.57	8.8	1.05E-03	8.39E-03
nucleoside diphosphate phosphorylation (GO:0006165)	29	18	2.06	8.74	4.03E-10	1.12E-08
nucleotide phosphorylation (GO:0046939)	30	18	2.13	8.44	6.05E-10	1.60E-08
nucleoside monophosphate metabolic process (GO:0009123)	17	10	1.21	8.28	4.76E-06	6.96E-05
COPII-coated vesicle budding (GO:0090114)	12	7	0.85	8.21	1.38E-04	1.52E-03
C4-dicarboxylate transport (GO:0015740)	8	4	0.57	7.04	6.21E-03	3.72E-02
nuclear envelope organization (GO:0006998)	14	7	0.99	7.04	2.84E-04	2.79E-03
nucleoside diphosphate metabolic process (GO:0009132)	39	19	2.77	6.86	2.88E-09	6.95E-08
ribosomal subunit export from nucleus (GO:0000054)	13	6	0.92	6.5	1.08E-03	8.63E-03
cellular glucose homeostasis (GO:0001678)	9	4	0.64	6.25	8.50E-03	4.96E-02
prostaglandin metabolic process (GO:0006693)	9	4	0.64	6.25	8.50E-03	4.95E-02
pyrimidine nucleotide biosynthetic process (GO:0006221)	9	4	0.64	6.25	8.50E-03	4.94E-02
carbohydrate catabolic process (GO:0016052)	46	20	3.27	6.12	5.14E-09	1.21E-07
response to oxidative stress (GO:0006979)	28	12	1.99	6.03	6.80E-06	9.50E-05
cytoplasmic translation (GO:0002181)	49	20	3.48	5.74	1.21E-08	2.63E-07
protein folding (GO:0006457)	100	40	7.11	5.63	1.21E-15	6.22E-14
ATP metabolic process (GO:0046034)	68	27	4.83	5.59	5.79E-11	1.95E-09
actin filament depolymerization (GO:0030042)	23	9	1.63	5.51	1.69E-04	1.81E-03
glucose 6-phosphate metabolic process (GO:0051156)	18	7	1.28	5.47	9.28E-04	7.69E-03
chromosome condensation (GO:0030261)	18	7	1.28	5.47	9.28E-04	7.66E-03
hexose biosynthetic process (GO:0019319)	16	6	1.14	5.28	2.50E-03	1.73E-02
generation of precursor metabolites and energy (GO:0006091)	121	45	8.6	5.23	1.82E-16	1.06E-14
'de novo' protein folding (GO:0006458)	19	7	1.35	5.19	1.20E-03	9.50E-03
protein N-linked glycosylation (GO:0006487)	36	13	2.56	5.08	1.26E-05	1.68E-04
nucleus organization (GO:0006997)	25	9	1.78	5.07	2.80E-04	2.76E-03

Table 4A-9. List of all cysteine-containing peptides identified in cyto-APEX analyses. "LPS" denotes 1 μg/mL LPS. "none" denotes no treatment. Peptide identifications are the average of 4 replicates (2 technical replicates from 2 biological replicates) and filtered for >10 spectral counts.

UniProt ID	Protein Description	Peptide Sequence	Cytosol/Cell Membrane	Total Spectral Count cyto-APEX LPS	Total Spectral Count cyto-APEX None
Q921H8	Acaa1a 3-ketoacyl-CoA thiolase A, peroxisomal	K.VNPLGGAIALGHPLGC*TGAR.Q	-	17	1
Q921H8	Acaa1a 3-ketoacyl-CoA thiolase A, peroxisomal	R.DC*LTPMGMTSENVAER.F	-	13	0
Q921H8	Acaa1a 3-ketoacyl-CoA thiolase A, peroxisomal	R.QC*SSGLQAVANIAGGIR.N	-	11	0
Q5SWU9	Acaca Acetyl-CoA carboxylase 1	K.VQAERPDTMLGVVC*GALHVADVSLR.N	YES	32	40
Q5SWU9	Acaca Acetyl-CoA carboxylase 1	R.MMYGVSPWGDAPIDFENSAHVPC*PR.G	YES	16	89
Q5SWU9	Acaca Acetyl-CoA carboxylase 1	K.EMAQYASNITSVLC*QFPSQQIANILDSHAATLNR.K	YES	16	14
Q5SWU9	Acaca Acetyl-CoA carboxylase 1	R.TDC*NHIFLNFVPTVIMDPSKIEESVR.S	YES	15	3
Q5SWU9	Acaca Acetyl-CoA carboxylase 1	K.RPGAALDPGC*VIAK.M	YES	14	39
Q5SWU9	Acaca Acetyl-CoA carboxylase 1	K.VQAERPDTMLGVVC*GALHVADVSLR.N	YES	14	4
Q5SWU9	Acaca Acetyl-CoA carboxylase 1	R.TDC*NHIFLNFVPTVIMDPSK.I	YES	14	1
Q5SWU9	Acaca Acetyl-CoA carboxylase 1	K.IIEEAPAAIATPAVFEHMEQC*AVK.L	YES	11	21
Q5SWU9	Acaca Acetyl-CoA carboxylase 1	K.NLLVTMLIDQLC*GR.D	YES	10	2
Q5SWU9	Acaca Acetyl-CoA carboxylase 1	K.IIEEAPAAIATPAVFEHMEQC*AVK.L	YES	6	23
Q5SWU9	Acaca Acetyl-CoA carboxylase 1	R.NFDLTAIPC*ANHK.M	YES	8	14
Q5SWU9	Acaca Acetyl-CoA carboxylase 1	K.DNTC*VVEFQFMLPTSHPNR.G	YES	5	12
P60710	Actb Actin, cytoplasmic 1	K.LC*YVALDFEQEMATAASSSSLEK.S	YES	103	5
P60710	Actb Actin, cytoplasmic 1	K.LC*YVALDFEQEMATAASSSSLEK.S	YES	39	0
P60710	Actb Actin, cytoplasmic 1	R.C*PEALFQPSFLGMESC*GIHETTFNSIMK.C	YES	21	1
P05064	Aldoa Fructose-bisphosphate aldolase A	R.YASIC*QQNGIVPIVEPEILPDGDHDLKR.C	YES	20	0
P07356	Anxa2 Annexin A2	K.GLGTDEDSLIEIIC*SR.T	YES	82	8
P97429	Anxa4 Annexin A4	K.GAGTDEGC*LIEILASR.T	YES	20	4
P97429	Anxa4 Annexin A4	R.SLEEDIC*SDTSFMFQR.V	YES	11	0
Q8VDN2	Atp1a1 Sodium/potassium-transporting ATPase subunit alpha-1	R.NIAFFSTNC*VEGTAR.G	YES	12	2
Q8VDN2	Atp1a1 Sodium/potassium-transporting ATPase subunit alpha-1	K.AC*VVHGSDLK.D	YES	11	0
O55143	Atp2a2 Sarcoplasmic/endoplasmic reticulum calcium ATPase 2	R.C*LALATHDNPLKR.E	YES	11	0
O55143	Atp2a2 Sarcoplasmic/endoplasmic reticulum calcium ATPase 2	K.VGEATETALTC*LVEK.M	YES	10	0
Q8R5M8	Cadm1 Cell adhesion molecule 1	R.EGDAFELTC*EAIGKPQPVMVTWVR.V	YES	11	0
P14211	Calr Calreticulin	R.C*KDDEFTHLYTLIVRPDNTYEVK.I	YES	115	0
P14211	Calr Calreticulin	R.C*KDDEFTHLYTLIVRPDNTYEVK.I	YES	67	0
P14211	Calr Calreticulin	R.C*KDDEFTHLYTLIVRPDNTYEVK.I	YES	38	0
P14211	Calr Calreticulin	K.DMHGDSEYNIMFGPDIC*GPGTK.K	YES	38	0
P14211	Calr Calreticulin	K.HEQNIDC*GGGYVK.L	YES	24	0
P14211	Calr Calreticulin	K.DMHGDSEYNIMFGPDIC*GPGTK.K	YES	22	0
P35564	Canx Calnexin	K.C*ESAPGC*GVWQRPMIDNPNYK.G	YES	11	0
Q8C172	Cers6 Ceramide synthase 6	R.VGTLVLC*LHDSADALLEAAK.M	-	18	0
Q8C172	Cers6 Ceramide synthase 6	R.VGTLVLC*LHDSADALLEAAK.M	-	10	0
P18760	Cfl1 Cofilin-1	K.HELQANC*YEEVKDR.C	YES	13	0
Q9QYB1	Clic4 Chloride intracellular channel protein 4	R.FLDGDEMTLADC*NLLPK.L	YES	12	0
Q8VBZ3	Clptm1 Cleft lip and palate transmembrane protein 1 homolog	R.VSFC*PLSLWR.W	YES	10	0
Q68FD5	Cltc Clathrin heavy chain 1	R.GQC*DLELINVC*NENSLFK.S	YES	16	0
P53996	Cnbp Cellular nucleic acid-binding protein	R.GFQFVSSSLPDIC*YR.C	YES	16	0
Q9QXT0	Cnpy2 Protein canopy homolog 2	R.SEAHLTELLEEVC*DR.M	-	11	0
Q9QZE5	Copg1 Coatomer subunit gamma-1	R.DSPLFDFIESC*LR.N	YES	15	0
Q9CYA0	Creld2 Cysteine-rich with EGF-like domain protein 2	K.GPLC*IDC*TDGFFSLQR.N	-	12	0
P10605	Ctsb Cathepsin B	R.DQGSC*GSC*WAFGAVEAISDR.T	YES	11	0
Q61093	Cybb Cytochrome b-245 heavy chain	R.GQTAESLEEHNLDIC*ADKIEEWGK.I	YES	24	0
Q61093	Cybb Cytochrome b-245 heavy chain	K.TIASEHPNTTIGVFLC*GPEALAETLSK.Q	YES	22	0
Q61093	Cybb Cytochrome b-245 heavy chain	K.WIVGPMFLYLC*ER.L	YES	14	0
Q61093	Cybb Cytochrome b-245 heavy chain	R.IVGDWTEGLFNAC*GC*DK.Q	YES	10	1
Q61093	Cybb Cytochrome b-245 heavy chain	R.IVGDWTEGLFNAC*GC*DKQEFQDAWK.L	YES	10	0
P10126	Eef1a1 Elongation factor 1-alpha 1	K.DGSASGTTLLEALDC*ILPPTRPTDKPLR.L	YES	51	2
P10126	Eef1a1 Elongation factor 1-alpha 1	K.SGDAAIVDMVPGKPMC*VESFSDYPPLGR.F	YES	41	0
P10126	Eef1a1 Elongation factor 1-alpha 1	R.KDGSASGTTLLEALDC*ILPPTRPTDKPLR.L	YES	20	0
P10126	Eef1a1 Elongation factor 1-alpha 1	K.SGDAAIVDMVPGKPMC*VESFSDYPPLGR.F	YES	10	0
Q9D8N0	Eef1g Elongation factor 1-gamma	R.WFLTC*INQPQFR.A	YES	35	0
P58252	Eef2 Elongation factor 2	R.TFC*QLILDPIFK.V	YES	44	0
P58252	Eef2 Elongation factor 2	K.IWC*FGPDGTGPNILTDITK.G	YES	22	3

P58252	Eef2 Elongation factor 2	R.YVEPIEDVPC*GNIVGLVGVDQFLVK.T	YES	18	1
P58252	Eef2 Elongation factor 2	R.LMEPIYLVEIQC*PEQVVGGIYGVLNR.K	YES	17	0
P58252	Eef2 Elongation factor 2	R.KIWC*FGPDGTGPNILTDITK.G	YES	14	0
P58252	Eef2 Elongation factor 2	R.KIWC*FGPDGTGPNILTDITK.G	YES	11	0
P58252	Eef2 Elongation factor 2	R.YVEPIEDVPC*GNIVGLVGVDQFLVK.T	YES	10	0
O70194	Eif3d Eukaryotic translation initiation factor 3 subunit D	K.TQGNVFATDAILATLMSC*TR.S	YES	13	0
P17182	Eno1 Alpha-enolase	R.SGETEDTFIADLVVGLC*TGQIK.T	YES	46	0
P17183	Eno2 Gamma-enolase	R.SGETEDTFIADLVVGLC*TGQIK.T	YES	15	1
Q8R180	Ero1l ERO1-like protein alpha	K.HDDSSDSFC*EIDDIQSPDAEYVDLLLNPER.Y	-	22	0
Q8R180	Ero1l ERO1-like protein alpha	K.ENTFYNWLEGLC*VEK.R	-	16	0
P57759	Erp29 Endoplasmic reticulum resident protein 29	K.GQGVYLGMPGC*LPAYDALAGEFIK.A	-	62	0
Q9D1Q6	Erp44 Endoplasmic reticulum resident protein 44	R.VASILHDDC*AFLSAFGDLSKPER.Y	-	22	0
Q9D1Q6	Erp44 Endoplasmic reticulum resident protein 44	K.TPADC*PVIAIDSFR.H	-	19	1
Q9R059	Fhl3 Four and a half LIM domains protein 3	R.DDDPYC*VAC*FGELFAPK.C	YES	14	0
Q80VA0	Galnt7 N-acetylgalactosaminyltransferase 7	R.SEVLHQVFISTC*DSSK.M	-	11	0
Q8BHN3	Ganab Neutral alpha-glucosidase AB	R.DGSDYEGWC*WPGSASYPDFTNPR.M	-	28	0
P16858	Gapdh Glyceraldehyde-3-phosphate dehydrogenase	R.VPTPNVSVVDLTC*R.L	YES	9	22
P16858	Gapdh Glyceraldehyde-3-phosphate dehydrogenase	K.IVSNASC*TTNC*LAPLAK.V	YES	3	10
Q61598	Gdi2 Rab GDP dissociation inhibitor beta	R.VIC*ILSHPIK.N	YES	11	0
Q61543	Glg1 Golgi apparatus protein 1	K.TETGQELEC*LQDHLDDLAVEC*R.D	YES	14	0
Q61543	Glg1 Golgi apparatus protein 1	R.AC*EPIIQNFC*HDVADNQIDSGDLMEC*LIQNK.H	YES	12	0
Q8K297	Glt25d1 Procollagen galactosyltransferase 1	R.ALHEQEIDC*QLVEAVDGK.A	-	12	0
D3Z5M2	Gm10110 Protein Gm10110	K.ALYDTFSAFGNILSC*K.V	-	16	0
A2AD25	Gm4987 Novel protein silmilar to ribosomal protein L32	K.SYC*AEIAHNVSSK.N	-	6	13
P08752	Gnai2 Guanine nucleotide-binding protein G(i) subunit alpha-2	R.LWADHGVQAC*FGR.S	YES	14	1
P62874	Gnb1 Guanine nucleotide-binding protein G(I)/G(S)/G(T) subunit beta-1	R.VSC*LGVTDDGMAVATGSWDSFLK.I	YES	20	0
P62880	Gnb2 Guanine nucleotide-binding protein G(I)/G(S)/G(T) subunit beta-2	R.VSC*LGVTDDGMAVATGSWDSFLK.I	YES	24	0
P01897	H2-L H-2 class I histocompatibility antigen, L-D alpha chain	R.GYEQFAYDGC*DYIALNEDLK.T	YES	22	0
P01897	H2-L H-2 class I histocompatibility antigen, L-D alpha chain	R.AYLEGEC*VEWLHR.Y	YES	10	0
P70349	Hint1 Histidine triad nucleotide-binding protein 1	R.C*LAFHDISPQAPTHFLVIPK.K	YES	11	0
P07901	Hsp90aa1 Heat shock protein HSP 90-alpha	R.LVTSPC*C*IVTSTYGWTANMER.I	YES	12	0
P11499	Hsp90ab1 Heat shock protein HSP 90-beta	R.LVSSPC*C*IVTSTYGWTANMER.I	YES	39	0
P11499	Hsp90ab1 Heat shock protein HSP 90-beta	R.GFEVVYMTEPIDEYC*VQQLK.E	YES	38	1
P11499	Hsp90ab1 Heat shock protein HSP 90-beta	R.VFIMDSC*DELIPEYLNFIR.G	YES	17	0
P11499	Hsp90ab1 Heat shock protein HSP 90-beta	K.C*LELFSELAEDKENYKK.F	YES	12	0
P11499	Hsp90ab1 Heat shock protein HSP 90-beta	K.C*LELFSELAEDKENYK.K	YES	11	2
P11499	Hsp90ab1 Heat shock protein HSP 90-beta	R.LVSSPC*C*IVTSTYGWTANMER.I	YES	10	0
P08113	Hsp90b1 Endoplasmin	R.LTESPC*ALVASQYGWSGNMER.I	YES	95	0
P08113	Hsp90b1 Endoplasmin	K.KGYEVIYLTEPVDEYC*IQALPEFDGKR.F	YES	42	0
P08113	Hsp90b1 Endoplasmin	K.GYEVIYLTEPVDEYC*IQALPEFDGKR.F	YES	24	0
P08113	Hsp90b1 Endoplasmin	K.GYEVIYLTEPVDEYC*IQALPEFDGK.R	YES	22	0
P08113	Hsp90b1 Endoplasmin	K.GYEVIYLTEPVDEYC*IQALPEFDGKR.F	YES	12	0
Q9JKR6	Hyou1 Hypoxia up-regulated protein 1	R.VEFEELC*ADLFDR.V	-	29	0
P11835	Itgb2 Integrin beta-2	K.VMASEC*IQEQSFVIR.A	YES	10	0
P70168	Kpnb1 Importin subunit beta-1	K.ESTLEAIGYIC*QDIDPEQLQDK.S	YES	13	0
Q61233	Lcp1 Plastin-2	K.VDTDGNGYISC*NELNDLFK.A	YES	16	2
Q61233	Lcp1 Plastin-2	R.HVIPMNPNTDDLFNAVGDGIVLC*K.M	YES	12	0
Q61233	Lcp1 Plastin-2	R.WANYHLENAGC*TK.I	YES	10	0
Q07797	Lgals3bp Galectin-3-binding protein	K.TPSLFPC*ASGAFSSFR.V	-	11	0
Q99MR8	Mccc1 Methylcrotonoyl-CoA carboxylase subunit alpha, mitochondrial	K.ESVC*QAALGLILK.E	-	83	108
Q99MR8	Mccc1 Methylcrotonoyl-CoA carboxylase subunit alpha, mitochondrial	R.YC*LHQYNIVGLR.S	-	26	83
Q99MR8	Mccc1 Methylcrotonoyl-CoA carboxylase subunit alpha, mitochondrial	R.YC*LHQYNIVGLR.S	-	12	12
Q99MR8	Mccc1 Methylcrotonoyl-CoA carboxylase subunit alpha, mitochondrial	R.VLGDLSSEDGC*TYLK.S	-	10	26
Q99MR8	Mccc1 Methylcrotonoyl-CoA carboxylase subunit alpha, mitochondrial	K.SSAAQAIHPGYGFLSENMEFAELC*K.Q	-	7	120
P34884	Mif Macrophage migration inhibitory factor	K.LLC*GLLSDR.L	YES	52	16
Q6ZQI3	Mlec Malectin	K.VC*ALYILAGTVDDVPK.L	-	13	0
P10404	MLV-related proviral Env polyprotein	K.LYFDLC*DLIGDDWDETGLGC*R.T	YES	59	0
P10404	MLV-related proviral Env polyprotein	R.C*NPLVLEFTDAGKK.A	YES	20	2
P10404	MLV-related proviral Env polyprotein	K.LTLSEVTGQGLC*VGAVPK.T	YES	12	0
Q6GQT9	Nomo1 Nodal modulator 1	K.VSC*LDTC*GDLLVTLQSLSR.Q	-	13	0
Q78XF5	Ostc Oligosaccharyltransferase complex subunit OSTC	R.VPFLVLEC*PNLK.L	-	13	7
Q60715	P4ha1 Prolyl 4-hydroxylase subunit alpha-1	K.SFLTAEDC*FELGK.V	-	12	0
Q05920	Pc Pyruvate carboxylase, mitochondrial	K.DMAGLLKPAAC*TMLVSSLR.D	YES	11	16
Q05920	Pc Pyruvate carboxylase, mitochondrial	R.FLYEC*PWR.R	YES	5	37
Q05920	Pc Pyruvate carboxylase, mitochondrial	R.ADFAQAC*QDAGVR.F	YES	0	26
Q05920	Pc Pyruvate carboxylase, mitochondrial	R.INGC*AIQC*R.V	YES	2	21
Q05920	Pc Pyruvate carboxylase, mitochondrial	K.DMAGLLKPAAC*TMLVSSLR.D	YES	6	16
Q05920	Pc Pyruvate carboxylase, mitochondrial	R.GLYAAFDC*TATMK.S	YES	4	16
Q05920	Pc Pyruvate carboxylase, mitochondrial	K.PAAC*TMLVSSLR.D	YES	1	13
Q05920	Pc Pyruvate carboxylase, mitochondrial	R.AGTHILC*IK.D	YES	3	12
Q91ZA3	Pcca Propionyl-CoA carboxylase alpha chain, mitochondrial	R.HKQEDIPISGWAVEC*R.V	-	31	334
Q91ZA3	Pcca Propionyl-CoA carboxylase alpha chain, mitochondrial	R.HKQEDIPISGWAVEC*R.V	-	30	280
Q91ZA3	Pcca Propionyl-CoA carboxylase alpha chain, mitochondrial	R.LQVEHPVTEC*ITGLDLVQEMILVAK.G	-	17	45

Q91ZA3	Pcca Propionyl-CoA carboxylase alpha chain, mitochondrial	K.QEDIPISGWAVEC*R.V	-	13	92
Q91ZA3	Pcca Propionyl-CoA carboxylase alpha chain, mitochondrial	R.LQVEHPVTEC*ITGLDLVQEMILVAK.G	-	12	12
Q91ZA3	Pcca Propionyl-CoA carboxylase alpha chain, mitochondrial	K.MADEAVC*VGPAPTSK.S	-	6	15
Q99MN9	Pccb Propionyl-CoA carboxylase beta chain, mitochondrial	R.AFDNDVDALC*NLR.E	-	5	20
Q99MN9	Pccb Propionyl-CoA carboxylase beta chain, mitochondrial	R.IC*C*DLEVLASK.K	-	0	12
P27773	Pdia3 Protein disulfide-isomerase A3	K.FIQDSIFGLC*PHMTEDNKDLIQGK.D	YES	25	0
P27773	Pdia3 Protein disulfide-isomerase A3	K.FIQDSIFGLC*PHMTEDNKDLIQGK.D	YES	12	0
Q922R8	Pdia6 Protein disulfide-isomerase A6	K.TC*EEHQLC*VVAVLPHILDTGAAGR.N	YES	12	0
P09411	Pgk1 Phosphoglycerate kinase 1	K.DC*VGPEVENAC*ANPAAGTVILLENLR.F	YES	16	0
Q9CQ60	Pgls 6-phosphogluconolactonase	R.TGALC*WFLDEAAAR.L	YES	10	0
Q61753	Phgdh D-3-phosphoglycerate dehydrogenase	K.NAGTC*LSPAVIVGLLR.E	-	15	1
Q61753	Phgdh D-3-phosphoglycerate dehydrogenase	K.EELIAELQDC*EGLIVR.S	-	13	3
P52480	Pkm Pyruvate kinase isozymes M1/M2	R.AEGSDVANAVLDGADC*IMLSGETAK.G	YES	80	10
P52480	Pkm Pyruvate kinase isozymes M1/M2	R.AEGSDVANAVLDGADC*IMLSGETAK.G	YES	42	2
P52480	Pkm Pyruvate kinase isozymes M1/M2	R.AGKPVIC*ATQMLESMIK.K	YES	38	0
P52480	Pkm Pyruvate kinase isozymes M1/M2	R.AEGSDVANAVLDGADC*IMLSGETAKGDYPLEAVR.M	YES	36	0
P52480	Pkm Pyruvate kinase isozymes M1/M2	K.C*DENILWLDYK.N	YES	23	7
P52480	Pkm Pyruvate kinase isozymes M1/M2	R.AGKPVIC*ATQMLESMIK.K	YES	20	0
P52480	Pkm Pyruvate kinase isozymes M1/M2	R.NTGIIC*TIGPASR.S	YES	9	12
Q9R0E2	Plod1 Procollagen-lysine,2-oxoglutarate 5-dioxygenase 1	R.FWTFETGC*TVC*DEGLR.S	-	13	0
P17742	Ppia Peptidyl-prolyl cis-trans isomerase A	K.HTGPGILSMANAGPNTNGSQFFIC*TAK.T	YES	12	7
P62141	Ppp1cb Serine/threonine-protein phosphatase PP1-beta catalytic subunit	K.TFTDC*FNC*LPIAAIVDEK.I	YES	10	0
P63330	Ppp2ca Serine/threonine-protein phosphatase 2A catalytic subunit alpha isoform	R.LQEVPHEGPMC*DLLWSDPDDR.G	YES	10	0
Q05769	Ptgs2 Prostaglandin G/H synthase 2	K.IINTASIQSLIC*NNVK.G	YES	170	0
Q05769	Ptgs2 Prostaglandin G/H synthase 2	R.VC*DILKQEHPEWGDEQLFQTSR.L	YES	60	0
Q05769	Ptgs2 Prostaglandin G/H synthase 2	K.GLMGNPIC*SPQYWKPSTFGGEVGFK.I	YES	41	0
Q05769	Ptgs2 Prostaglandin G/H synthase 2	K.GC*PFTSFNVQDPQPTK.T	YES	38	2
Q05769	Ptgs2 Prostaglandin G/H synthase 2	K.IINTASIQSLIC*NNVK.G	YES	26	0
Q05769	Ptgs2 Prostaglandin G/H synthase 2	R.ALPPVADDC*PTPMGVK.G	YES	24	0
Q05769	Ptgs2 Prostaglandin G/H synthase 2	K.GLMGNPIC*SPQYWKPSTFGGEVGFK.I	YES	18	0
Q05769	Ptgs2 Prostaglandin G/H synthase 2	K.GLMGNPIC*SPQYWK.P	YES	14	0
Q05769	Ptgs2 Prostaglandin G/H synthase 2	R.VC*DILKQEHPEWGDEQLFQTSR.L	YES	13	0
Q05769	Ptgs2 Prostaglandin G/H synthase 2	R.GEC*MSTGFDQYK.C	YES	11	1
Q91VI7	Rnh1 Ribonuclease inhibitor	R.ELDLSNNC*MGGPGVLQLLESLK.Q	YES	14	0
Q91VI7	Rnh1 Ribonuclease inhibitor	K.LGNAGIAALC*PGLLLPSC*K.L	YES	14	0
Q91VI7	Rnh1 Ribonuclease inhibitor	R.TNELGDGGVGLVLQGLQNPTC*K.I	YES	10	0
Q91VI7	Rnh1 Ribonuclease inhibitor	R.SLLELQMSSNPLGDEGVQELC*K.A	YES	10	0
Q91VI7	Rnh1 Ribonuclease inhibitor	R.LLC*ESLLEPGC*QLESLWIK.T	YES	10	0
Q91VI7	Rnh1 Ribonuclease inhibitor	R.ELWLGDC*DVTNSGC*SSLANVLLANR.S	YES	10	0
P62889	Rpl30 60S ribosomal protein L30	R.VC*TLAIIDPGDSDIIR.S	YES	8	10
P97351	Rps3a 40S ribosomal protein S3a	K.NC*LTNFHGMDLTR.D	YES	11	6
P62702	Rps4x 40S ribosomal protein S4, X isoform	R.EC*LPLIIFLR.N	YES	25	0
P97461	Rps5 40S ribosomal protein S5	R.VNQAIWLLC*TGAR.E	YES	12	6
P50543	S100a11 Protein S100-A11	R.C*IESLIAVFQK.Y	YES	15	0
Q9CZN7	Shmt2 Protein Shmt2	R.YYGGAEVVDEIELLC*QR.R	YES	23	3
Q9CZN7	Shmt2 Protein Shmt2	R.YYGGAEVVDEIELLC*QR.R	YES	10	0
P51912	Slc1a5 Neutral amino acid transporter B(0)	R.SC*TVLNVEGDAFGAGLLQSYVDR.T	YES	23	0
P51881	Slc25a5 ADP/ATP translocase 2	K.GTDIMYTGTLDC*WR.K	-	16	5
Q64310	Surf4 Surfeit locus protein 4	R.LC*LISTFLEDGIR.M	-	40	2
P26039	Tln1 Talin-1	K.AQEAC*GPLEMDSALSVVQNLEK.D	YES	16	0
Q8BH24	Tm9sf4 Transmembrane 9 superfamily member 4	R.TQLPYEYYSLPFC*QPIK.I	-	12	0
D3YZZ5	Tmed7 Protein Tmed7	K.FC*FSNEFSTFTHK.T	-	16	0
D3YZZ5	Tmed7 Protein Tmed7	R.VSALTQMESAC*VSIHEALK.S	-	10	0
Q99KF1	Tmed9 Transmembrane emp24 domain-containing protein 9	R.C*FIEEIPDETMVIGNYR.T	-	11	0
Q8VBT0	Tmx1 Thioredoxin-related transmembrane protein 1	R.FIITALPSIYHC*K.D	-	10	0
P17751	Tpi1 Triosephosphate isomerase	K.VSHALAEGLGVIAC*IGEK.L	YES	12	2
Q61510	Trim25 E3 ubiquitin/ISG15 ligase TRIM25	K.NTVMC*AVVEQFLQAEQAR.T	YES	10	0
P68369	Tuba1a Tubulin alpha-1A chain	R.AVC*MLSNTTAIAEAWAR.L	YES	23	0
P68369	Tuba1a Tubulin alpha-1A chain	R.TIQFVDWC*PTGFK.V	YES	20	7
P68369	Tuba1a Tubulin alpha-1A chain	K.YMAC*C*LLYR.G	YES	10	0
P68369	Tuba1a Tubulin alpha-1A chain	R.AVC*MLSNTTAIAEAWAR.L	YES	10	0
P68368	Tuba4a Tubulin alpha-4A chain	R.SIQFVDWC*PTGFK.V	YES	67	9
P68368	Tuba4a Tubulin alpha-4A chain	R.AVC*MLSNTTAIAEAWAR.L	YES	34	0
P68368	Tuba4a Tubulin alpha-4A chain	R.AVC*MLSNTTAIAEAWAR.L	YES	13	0
P68368	Tuba4a Tubulin alpha-4A chain	K.YMAC*C*LLYR.G	YES	10	0
P99024	Tubb5 Tubulin beta-5 chain	K.EAESC*DC*LQGFQLTHSLGGGTGSGMGTLLISK.I	YES	13	0
Q91W90	Txndc5 Thioredoxin domain-containing protein 5	K.EFPGLSDVTIAEVDC*TAER.N	-	28	0
Q91W90	Txndc5 Thioredoxin domain-containing protein 5	K.VDC*TQHYAVC*SEHQVR.G	-	10	0
Q6P5E4	Uggt1 UDP-glucose:glycoprotein glucosyltransferase 1	K.SLPQEWLWC*ETWC*DDASK.K	-	20	0
Q6ZQM8	Ugt1a7c UDP-glucuronosyltransferase 1-7C	K.QTSFDAVFLDPFDVC*GLTVAK.Y	-	16	0
P62259	Ywhae 14-3-3 protein epsilon	K.LIC*C*DILDVLDK.H	YES	18	0
P68510	Ywhah 14-3-3 protein eta	K.ELETVC*NDVLALLDK.F	YES	16	0
P63101	Ywhaz 14-3-3 protein zeta/delta	R.DIC*NDVLSLLEK.F	YES	42	0

Table 4A-10. Average percent oxidation for cysteines from cyto-APEX analysis. Data was filtered for peptides with ratio values in 2 out of 4 replicates, with a standard deviation <30%.

UniProt ID	Protein Description	Peptide Sequence	Average % oxidation Cyto-APEX none	Average % standard deviation Cyto-APEX none	Average % oxidation Cyto-APEX LPS	Average % standard deviation Cyto-APEX LPS
Q6ZWV3	Rpl10 60S ribosomal protein L10	K.AKVDEFPLC*GHMVSDEYEQLSSEALEAAR.I			74.70%	29.74%
Q61635	Ifi47 Interferon gamma inducible protein 47, isoform CRA	K.DNSIIAQATSAAEAFC*AVK.G			65.64%	27.78%
Q9D6K9	Cers5 Ceramide synthase 5	R.VGALIFC*LHDFADPLLEAAK.M			36.26%	27.27%
P68372	Tubb4b Tubulin beta-4B chain	K.LTTPTYGDLNHLVSATMSGVTTC*LR.F			69.22%	25.45%
Q8BYB9	Poglut1 Protein O-glucosyltransferase 1	R.C*SGVEHFILEVIHR.L			76.32%	24.16%
P06800	Ptprc Receptor-type tyrosine-protein phosphatase C	K.FSLHDC*TPK.E			38.28%	23.17%
P61161	Actr2 Actin-related protein 2	K.C*GYAGSNFPEHIFPALVGR.P			73.38%	22.53%
P97351	Rps3a 40S ribosomal protein S3a	K.AC*QSIYPLHDVFVR.K	4.76%	0.00%	51.58%	21.22%
P60710	Actb Actin, cytoplasmic 1	K.C*DVDIRK.D			69.00%	19.77%
Q9DB29	Iah1 Isoamyl acetate-hydrolyzing esterase 1 homolog	R.DC*GTDVLDLWTLMQK.D			71.64%	17.93%
O55143	Atp2a2 Sarcoplasmic/endoplasmic reticulum calcium ATPase	R.C*LALATHDNPLK.R			69.93%	17.18%
Q9D1Q6	Erp44 Endoplasmic reticulum resident protein 44	K.GTINFLHADC*DK.F			80.94%	16.93%
Q61879	Myh10 Myosin-10	K.VEDMAELTC*LNEASVLHNLK.D			79.52%	16.25%
D3YZZ5	Tmed7 Protein Tmed7	R.VSALTQMESAC*VSIHEALK.S			38.89%	15.70%
Q6GQT9	Nomo1 Nodal modulator 1	R.FC*LSKPGVYK.V			74.42%	15.55%
Q61792	Lasp1 LIM and SH3 domain protein 1	K.KPYC*NAHYPK.Q			55.69%	15.46%
P62702	Rps4x 40S ribosomal protein S4, X isoform	K.FDTGNLC*MVTGGANLGR.I	12.58%	4.76%	82.18%	15.06%
Q61543	Glg1 Golgi apparatus protein 1	K.C*AIGVTHFQLVQMK.D			86.75%	14.69%
B2RQC6	Cad Carbamoyl-phosphate synthetase 2, aspartate transc	R.GHNQPC*LLVGTGR.C			78.32%	14.65%
Q8BKC5	Ipo5 Importin-5	K.HFADLLPGFLQAVNDSC*YQNDDSVLK.S			64.54%	14.63%
Q3UY34	Uncharacterized protein C12orf43 homolog	K.EASPRPC*R.K			17.42%	14.58%
P26041	Msn Moesin	R.ILALC*MGNHELYMR.R			22.25%	13.97%
Q99LX0	Park7 Protein DJ-1	K.VTVAGLAGKDPVQC*SR.D			86.86%	13.59%
Q9QZE5	Copg1 Coatomer subunit gamma-1	R.DSPLFDFIESC*LR.N			35.90%	12.98%
Q8R1V4	Tmed4 Transmembrane emp24 domain-containing protein 4	R.C*FIEEIPDETMVIGNYR.T			79.68%	12.90%
Q9QXS1	Plec Plectin	R.GHVPLIAVC*DYK.Q			57.00%	12.81%
Q9D1M7	Fkbp11 Peptidyl-prolyl cis-trans isomerase FKBP11	K.QVIPGLEQSLLDMC*VGEK.R			69.75%	12.68%
Q9D0F3	Lman1 Protein ERGIC-53	K.TLTVMINNGFTPDKNDYEFC*AK.V			75.71%	12.63%
Q61233	Lcp1 Plastin-2	R.HVIPMNPNTDDLFNAVGDGIVLC*K.M			56.40%	12.35%
Q61598	Gdi2 Rab GDP dissociation inhibitor beta	R.VIC*ILSHPIK.N			34.16%	12.21%
Q921H8	Acaa1a 3-ketoacyl-CoA thiolase A, peroxisomal	R.QC*SSGLQAVANIAGGIR.N	54.98%	7.15%	62.63%	12.07%
Q01853	Vcp Transitional endoplasmic reticulum ATPase	K.LADDVDLEQVANETHGHVGADLAALC*SEAALQAIR.K			23.21%	11.76%
P97461	Rps5 40S ribosomal protein S5	R.VNQAIWLLC*TGAR.E			46.73%	11.56%
Q07076	Anxa7 Annexin A7	R.LGTDESC*FNMILATR.S			57.14%	11.53%
Q91VI7	Rnh1 Ribonuclease inhibitor	R.TNELGDGGVGLVLQGLQNPTC*K.I			82.63%	11.18%
P97372	Psme2 Proteasome activator complex subunit 2	R.QNLFQEADDFLC*TFLPR.K			75.77%	10.92%
P26151	Fcgr1 High affinity immunoglobulin gamma Fc receptor I	R.C*QIGSSMPSDPVQLQIHNDWLLLQASR.R			85.83%	10.86%
Q99KI0	Aco2 Aconitate hydratase, mitochondrial	K.VAVPSTIHC*DHLIEAQVGGEK.D			67.60%	10.65%
O08807	Prdx4 Peroxiredoxin-4	K.SINTEVVAC*SVDSQFTHLAWINTPR.R			52.08%	10.62%
Q05920	Pc Pyruvate carboxylase, mitochondrial	K.DMAGLLKPAAC*TMLVSSLR.D	5.08%	0.69%	37.98%	10.57%
Q78XF5	Ostc Oligosaccharyltransferase complex subunit OSTC	R.VPFLVLEC*PNLK.L	4.76%	0.00%	35.03%	10.17%
Q07113	Igf2r Cation-independent mannose-6-phosphate receptor	R.VTGPPIFNPVANEVYLNFESSTHC*LADR.Y			79.27%	9.95%
Q8BKC5	Ipo5 Importin-5	R.MLVQC*MQDQEHPSIR.T			53.45%	9.92%
O70194	Eif3d Eukaryotic translation initiation factor 3 subunit	K.TQGNVFATDAILATLMSC*TR.S			63.64%	9.70%
Q3U5Q7	Cmpk2 UMP-CMP kinase 2, mitochondrial	K.AVLLQSPPPC*ISQWR.K			79.70%	9.62%
P05214	Tuba3b Tubulin alpha-3 chain	R.TIQFVDWC*PTGFK.V	33.53%	8.37%	84.29%	9.59%
Q8R5M8	Cadm1 Cell adhesion molecule 1	R.EGDAFELTC*EAIGKPQPVMVTWVR.V			67.59%	9.59%
P68510	Ywhah 14-3-3 protein eta	K.ELETVC*NDVLALLDK.F			25.01%	9.54%
P63017	Hspa8 Heat shock cognate 71 kDa protein	K.C*NEIISWLDK.N			20.60%	9.27%
P63017	Hspa8 Heat shock cognate 71 kDa protein	K.GPAVGIDLGTTYSC*VGVFQHGK.V			61.62%	8.90%

O55143	Atp2a2 Sarcoplasmic/endoplasmic reticulum calcium ATPase	R.SLPSVETLGC*TSVIC*SDK.T			88.97%	8.87%
Q6P5E4	Uggt1 UDP-glucose:glycoprotein glucosyltransferase 1	R.MDFILSHALYC*R.D			11.35%	8.69%
P62874	Gnb1 Guanine nucleotide-binding protein G(I)/G(S)/G(T)	K.AC*ADATLSQITNNIDPVGR.I			68.01%	8.68%
P63038	Hspd1 60 kDa heat shock protein, mitochondrial	R.C*IPALDSLKPANEDQK.I			54.34%	8.39%
Q61543	Glg1 Golgi apparatus protein 1	R.LSYLLMC*LESAVHR.G			80.63%	8.23%
P68040	Gnb2l1 Guanine nucleotide-binding protein subunit beta-2-	K.HLYTLDGGDIINALC*FSPNR.Y			71.77%	7.89%
P09411	Pgk1 Phosphoglycerate kinase 1	K.TGQATVASGIPAGWMGLDC*GTESSK.K			81.04%	7.85%
P62281	Rps11 40S ribosomal protein S11	R.DVQIGDIVTVGEC*RPLSK.T	60.75 %	0.70%	89.78%	7.72%
Q61263	Soat1 Sterol O-acyltransferase 1	K.SASLDNGGC*ALTTFSILEEMK.K			82.56%	7.46%
P07901	Hsp90aa1 Heat shock protein HSP 90-alpha	R.VFIMDNC*EELIPEYLNFIR.G			53.64%	7.36%
O88342	Wdr1 WD repeat-containing protein 1	R.MTVNESEQLVSC*SMDDTVR.Y			90.05%	7.33%
Q61233	Lcp1 Plastin-2	K.VDTDGNGYISC*NELNDLFK.A			67.03%	7.19%
Q9QUJ7	Acsl4 Long-chain-fatty-acid--CoA ligase 4	K.GVEGSWVDIC*NNPAMEAEILK.E			80.49%	7.07%
O88342	Wdr1 WD repeat-containing protein 1	K.SIQC*LTVHR.N			76.44%	7.06%
Q8CIE6	Copa Coatomer subunit alpha	K.LGEVALLQGNHQIVEMC*YQR.T			63.93%	6.95%
P18760	Cfl1 Cofilin-1	K.AVLFC*LSEDK.K			81.07%	6.93%
Q61233	Lcp1 Plastin-2	R.WANYHLENAGC*TK.I			62.17%	6.87%
Q61543	Glg1 Golgi apparatus protein 1	R.SGDPMILSC*LMEHLYTEK.M			91.32%	6.78%
Q99JI0	Ctu1 Cytoplasmic tRNA 2-thiolation protein 1	R.LALAPAAKPPPPGTC*SR.C			72.17%	6.70%
P07356	Anxa2 Annexin A2	K.ALLYLC*GGDD.-			29.13%	6.52%
Q80VA0	Galnt7 N-acetylgalactosaminyltransferase 7	R.GLETAYC*IDSMGK.T			90.64%	6.51%
Q99MR8	Mccc1 Methylcrotonoyl-CoA carboxylase subunit alpha, mit	K.SSAAQAIHPGYGFLSENMEFAELC*K.Q	8.73%	2.12%	66.45%	6.47%
P11835	Itgb2 Integrin beta-2	K.SRGDC*DGVQINNPVTFQVK.V			91.55%	6.39%
Q64737	Gart Trifunctional purine biosynthetic protein adenosin	R.AFTNPEDAC*SFITSANFPALVVK.A			88.31%	6.23%
P80316	Cct5 T-complex protein 1 subunit epsilon	K.IAILTC*PFEPPKPK.T			80.40%	6.16%
Q91YQ5	Rpn1 Dolichyl-diphosphooligosaccharide--protein glycosy	K.DPAAEARMKVAC*ITEQVLTLVNKR.L			66.75%	6.08%
Q8C172	Cers6 Ceramide synthase 6	R.VGTLVLC*LHDSADALLEAAK.M			14.90%	6.05%
P11499	Hsp90ab1 Heat shock protein HSP 90-beta	K.C*LELFSELAEDKENYK.K			35.90%	6.03%
Q3TRM8	Hk3 Hexokinase-3	K.LFDHIVDC*IVDFQK.R			32.75%	6.01%
P70404	Idh3g Isocitrate dehydrogenase	R.HAC*VPVDFEEVHVSSNADEEDIR.N			68.04%	5.97%
Q8C3J5	Dock2 Dedicator of cytokinesis protein 2	K.IFLIC*QIVR.I			22.62%	5.95%
Q9D0R2	Tars Threonine--tRNA ligase, cytoplasmic	K.VVWDLDRPLETDC*TLELLK.F			88.13%	5.94%
Q01853	Vcp Transitional endoplasmic reticulum ATPase	R.LGDVISIQPC*PDVK.Y			38.47%	5.80%
Q501J6	Ddx17 Probable ATP-dependent RNA helicase DDX17	R.GDGPIC*LVLAPTR.E			72.93%	5.77%
P58252	Eef2 Elongation factor 2	K.DLEEDHAC*IPIK.K			91.03%	5.76%
Q6GQT9	Nomo1 Nodal modulator 1	K.ELLFYPPSMEATVSGESC*PGK.L			91.18%	5.73%
Q8C0I1	Agps Alkyldihydroxyacetonephosphate synthase, peroxisom	R.IPDIVVWPTC*HDDVVK.I			67.89%	5.66%
Q9D8N0	Eef1g Elongation factor 1-gamma	K.AAAPAPEEEMDEC*EQALAAEPK.A			84.75%	5.63%
Q8C0I1	Agps Alkyldihydroxyacetonephosphate synthase, peroxisom	K.ESGYC*TGHEPDSLEFSTVGGWISTR.A			88.57%	5.52%
Q8K297	Glt25d1 Procollagen galactosyltransferase 1	R.ALHEQEIDC*QLVEAVDGK.A			81.81%	5.50%
P16110	Lgals3 Galectin-3	R.RVIVC*NTK.Q			61.52%	5.49%
Q61598	Gdi2 Rab GDP dissociation inhibitor beta	R.TDDYLDQPC*C*ETINR.I			88.38%	5.43%
Q64337	Sqstm1 Sequestosome-1	K.IALESVGQPEEQMESGNC*SGGDDDWTHLSSK.E			83.11%	5.35%
P26039	Tln1 Talin-1	R.VQELGHGC*SALVTK.A			70.28%	5.31%
P09055	Itgb1 Integrin beta-1	K.LPQPVQVDPVTHC*K.E			89.63%	5.20%
P05063	Aldoc Fructose-bisphosphate aldolase C	R.YASIC*QQNGIVPIVEPEILPDGDHDLK.R			42.67%	5.11%
Q61233	Lcp1 Plastin-2	K.KLENC*NYAVDLGK.N			27.04%	5.11%
A6ZI46	Aldoart1 Fructose-bisphosphate aldolase	R.ALANSLAC*QGK.Y			64.90%	5.10%
P11983	Tcp1 T-complex protein 1 subunit alpha	R.IC*DDELILIK.N			81.91%	5.06%
Q8VCH0	Acaa1b 3-ketoacyl-CoA thiolase B, peroxisomal	K.VNPLGGAIALGHPLGC*TGAR.Q			83.92%	4.97%
P29477	Nos2 Nitric oxide synthase, inducible	R.YAVFGLGSSMYPQFC*AFAHDIDQK.L			67.80%	4.90%
Q9DBJ1	Pgam1 Phosphoglycerate mutase 1	R.YADLTEDQLPSC*ESLK.D			78.12%	4.76%
P07901	Hsp90aa1 Heat shock protein HSP 90-alpha	K.C*LELFTELAEDKENYK.K			8.61%	4.76%
O55143	Atp2a2 Sarcoplasmic/endoplasmic reticulum calcium ATPase	K.VGEATETALTC*LVEK.M	44.71 %	10.66%	65.52%	4.66%
Q61599	Arhgdib Rho GDP-dissociation inhibitor 2	R.LSLVC*DSAPGPITMDLTGDLEALKK.D			50.15%	4.66%
P58252	Eef2 Elongation factor 2	R.C*ELLYEGPPDDEAAMGIK.S			89.99%	4.65%
Q9WUM4	Coro1c Coronin-1C	R.KC*EPIIMTVPR.K			92.01%	4.57%
Q9D0I9	Rars Arginine--tRNA ligase, cytoplasmic	R.MLLC*EAVAAVMAK.G			55.82%	4.57%
P51912	Slc1a5 Neutral amino acid transporter B(0)	R.SC*TVLNVEGDAFGAGLLQSYVDR.T			25.57%	4.54%
P08249	Mdh2 Malate dehydrogenase, mitochondrial	K.GYLGPEQLPDC*LK.G			77.75%	4.54%
E9PWZ3	Rpl3l Protein Rpl3l	K.VAC*IGAWHPAR.V			78.06%	4.53%
Q9EPL8	Ipo7 Importin-7	R.GIDQC*IPLFVEAALER.L			51.60%	4.45%
Q9ESP1	Sdf2l1 Stromal cell-derived factor 2-like protein 1	K.ASAGLVTC*GSVLK.L			80.99%	4.37%
P16381	D1Pas1 Putative ATP-dependent RNA helicase Pl10	R.GC*HLLVATPGR.L			79.90%	4.36%
P26039	Tln1 Talin-1	R.ELLENPVQPINDMSYFGC*LDSVMENSK.V			69.97%	4.35%
P17742	Ppia Peptidyl-prolyl cis-trans isomerase A	K.KITISDC*GQL.-			86.52%	4.35%
P05214	Tuba3b Tubulin alpha-3 chain	K.AYHEQLSVAEITNAC*FEPANQMVK.C			90.00%	4.30%
Q9ER38	Tor3a Torsin-3A	R.LFSSQGC*K.S			92.25%	4.22%

Q8QZT1	Acat1 Acetyl-CoA acetyltransferase, mitochondrial	K.IHMGNC*AENTAK.K			63.25%	4.14%
P60766	Cdc42 Cell division control protein 42 homolog	K.YVEC*SALTQK.G			53.33%	4.03%
Q68FD5	Cltc Clathrin heavy chain 1	K.RDPHLAC*VAYER.G			79.19%	4.01%
Q05769	Ptgs2 Prostaglandin G/H synthase 2	K.GC*PFTSFNVQDPQPTK.T			86.28%	3.95%
Q5SWU9	Acaca Acetyl-CoA carboxylase 1	K.IIEEAPAAIATPAVFEHMEQC*AVK.L	4.87%	0.51%	51.62%	3.92%
P09103	P4hb Protein disulfide-isomerase	K.ITEFC*HR.F			38.57%	3.91%
Q9JMA1	Usp14 Ubiquitin carboxyl-terminal hydrolase 14	K.FPLMLDVYELC*TPELQEK.M			44.86%	3.81%
P63017	Hspa8 Heat shock cognate 71 kDa protein	K.VC*NPIITK.L			37.93%	3.80%
P26039	Tln1 Talin-1	K.AQEAC*GPLEMDSALSVVQNLEK.D			53.14%	3.78%
P17751	Tpi1 Triosephosphate isomerase	K.VSHALAEGLGVIAC*IGEK.L			62.95%	3.78%
Q9JKR6	Hyou1 Hypoxia up-regulated protein 1	R.VEFEELC*ADLFDR.V			55.59%	3.75%
Q64310	Surf4 Surfeit locus protein 4	R.LC*LISTFLEDGIR.M			22.97%	3.74%
P70349	Hint1 Histidine triad nucleotide-binding protein 1	R.C*LAFHDISPQAPTHFLVIPK.K			69.50%	3.74%
P62192	Psmc1 26S protease regulatory subunit 4	K.LPLVTPHTQC*R.L			54.95%	3.72%
Q9D8E6	Rpl4 60S ribosomal protein L4	R.SGQGAFGNMC*R.G	7.63%	1.94%	80.10%	3.71%
P57759	Erp29 Endoplasmic reticulum resident protein 29	K.GQGVYLGMPGC*LPAYDALAGEFIK.A			55.39%	3.67%
P52480	Pkm Pyruvate kinase isozymes M1/M2	K.C*DENILWLDYK.N			75.87%	3.66%
P50516	Atp6v1a V-type proton ATPase catalytic subunit A	R.VLDALFPC*VQGGTTAIPGAFGC*GK.T			69.17%	3.65%
Q8BP47	Nars Asparagine--tRNA ligase, cytoplasmic	K.YGTC*PHGGYGLGLER.F			81.17%	3.59%
P27773	Pdia3 Protein disulfide-isomerase A3	K.FIQDSIFGLC*PHMTEDNK.D			70.25%	3.59%
Q5SWU9	Acaca Acetyl-CoA carboxylase 1	R.TDC*NHIFLNFVPTVIMDPSK.I	14.20%	2.22%	68.64%	3.57%
Q9CQ60	Pgls 6-phosphogluconolactonase	R.TGALC*WFLDEAAAR.L			61.46%	3.56%
P62962	Pfn1 Profilin-1	K.C*YEMASHLR.R			71.45%	3.55%
Q99MR8	Mccc1 Methylcrotonoyl-CoA carboxylase subunit alpha, mit	K.ESVC*QAALGLILK.E	5.01%	0.58%	56.86%	3.48%
P58252	Eef2 Elongation factor 2	K.IWC*FGPDGTGPNILTDITK.G	4.76%	0.00%	30.73%	3.47%
Q8VDN2	Atp1a1 Sodium/potassium-transporting ATPase subunit alpha	R.NIAFFSTNC*VEGTAR.G			34.54%	3.47%
Q8R2E9	Ero1lb ERO1-like protein beta	R.GEDDGESFYTWLEGLC*LEK.R			91.90%	3.41%
P10404	MLV-related proviral Env polyprotein	K.EGGLC*AALK.E			80.46%	3.37%
Q6P5F9	Xpo1 Exportin-1	K.LDINLLDNVVNC*LYHGEGAQQR.M			63.73%	3.36%
P08113	Hsp90b1 Endoplasmin	R.LTESPC*ALVASQYGWSGNMER.I			67.81%	3.36%
P51881	Slc25a5 ADP/ATP translocase 2	R.YFAGNLASGGAAGATSLC*FVYPLDFAR.T			28.92%	3.32%
Q3U5Q7	Cmpk2 UMP-CMP kinase 2, mitochondrial	R.FTVELPDC*SLTHFVLGDATDHR.D			80.09%	3.26%
E9Q7H5	Gm8991 Uncharacterized protein	K.YHTINGHNC*EVK.K			68.56%	3.25%
P35123	Usp4 Ubiquitin carboxyl-terminal hydrolase 4	R.VTVPLMGAISDLC*EALSK.L			48.64%	3.24%
P60766	Cdc42 Cell division control protein 42 homolog	K.WVPEITHHC*PK.T			60.91%	3.18%
Q9ER38	Tor3a Torsin-3A	R.C*HQSTFVFDEAEK.L			93.00%	3.17%
O89053	Coro1a Coronin-1A	R.KC*EPIAMTVPR.K			87.82%	3.16%
Q6PHZ2	Camk2d Calcium/calmodulin-dependent protein kinase type I	K.IC*DPGLTAFEPEALGNLVEGMDFHR.F			39.81%	3.16%
O08807	Prdx4 Peroxiredoxin-4	K.HGEVC*PAGWKPGSETIIPDPAGK.L			65.45%	3.10%
P01897	H2-L H-2 class I histocompatibility antigen, L-D alpha	R.AYLEGEC*VEWLHR.Y			68.90%	3.09%
P08249	Mdh2 Malate dehydrogenase, mitochondrial	K.ETEC*TYFSTPLLLGK.K	9.98%	2.64%	64.46%	3.08%
P58252	Eef2 Elongation factor 2	K.STLTDSLVC*K.A			76.34%	3.07%
O08795	Prkcsh Glucosidase 2 subunit beta	K.YEQGTGC*WQGPNR.S			91.54%	3.02%
Q01853	Vcp Transitional endoplasmic reticulum ATPase	R.QAAPC*VLFFDELDSIAK.A			29.29%	3.00%
Q9D8N0	Eef1g Elongation factor 1-gamma	R.FPEELTQTFMSC*NLITGMFQR.L			61.28%	2.99%
Q9D0R2	Tars Threonine--tRNA ligase, cytoplasmic	R.FQQDDAHIFC*AMEQIEDEIK.G			66.41%	2.99%
P18760	Cfl1 Cofilin-1	K.MLPDKDC*R.Y			80.43%	2.99%
D3YZZ5	Tmed7 Protein Tmed7	K.FC*FSNEFSTFTHK.T			38.79%	2.98%
P08113	Hsp90b1 Endoplasmin	K.GYEVIYLTEPVDEYC*IQALPEFDGK.R			74.70%	2.97%
Q9R1W5	Calcrl Calcitonin gene-related peptide type 1 receptor	K.IC*DQDGHWFR.H			92.87%	2.92%
P58252	Eef2 Elongation factor 2	R.TFC*QLILDPIFK.V			45.62%	2.92%
P11835	Itgb2 Integrin beta-2	K.VMASEC*IQEQSFVIR.A			93.18%	2.91%
Q91VI7	Rnh1 Ribonuclease inhibitor	K.LGNAGIAALC*PGLLLPSC*K.L			93.79%	2.90%
Q99MR8	Mccc1 Methylcrotonoyl-CoA carboxylase subunit alpha, mit	K.DQSDQC*LR.E	13.25%	2.24%	82.34%	2.90%
P09103	P4hb Protein disulfide-isomerase	K.KEEC*PAVR.L			55.99%	2.89%
Q62167	Ddx3x ATP-dependent RNA helicase DDX3X	R.VRPC*VVYGGAEIGQQIR.D			64.00%	2.84%
Q60715	P4ha1 Prolyl 4-hydroxylase subunit alpha-1	R.HAAC*PVLVGNK.W			85.25%	2.83%
P52480	Pkm Pyruvate kinase isozymes M1/M2	R.AEGSDVANAVLDGADC*IMLSGETAK.G	11.79%	0.71%	71.15%	2.82%
P58252	Eef2 Elongation factor 2	R.SNTGGQAFPQC*VFDHWQILPGDPFDNSSRPSQVVAETR.K			56.52%	2.82%
P19096	Fasn Fatty acid synthase	K.FVFTPHMEAEC*LSESTALQK.E			57.08%	2.81%
P16858	Gapdh Glyceraldehyde-3-phosphate dehydrogenase	R.AAIC*SGK.V			61.55%	2.81%
Q99JW4	Lims1 LIM and senescent cell antigen-like-containing dom	K.C*HAIIDEQPLIFK.N			79.36%	2.80%
P46978	Stt3a Dolichyl-diphosphooligosaccharide--protein glycosy	R.EGSPVLLNC*LMYK.M			75.00%	2.80%
Q8CIE6	Copa Coatomer subunit alpha	R.C*LFTLLGHLDYIR.T			22.29%	2.78%
P05214	Tuba3b Tubulin alpha-3 chain	R.AVC*MLSNTTAIAEAWAR.L			72.09%	2.76%
Q61263	Soat1 Sterol O-acyltransferase 1	K.EVGC*HFDDFVTNLIEK.S			71.33%	2.75%

Q60715	P4ha1 Prolyl 4-hydroxylase subunit alpha-1	K.SFLTAEDC*FELGK.V			62.88%	2.73%
D3Z5M2	Gm10110 Protein Gm10110	K.ALYDTFSAFGNILSC*K.V			83.96%	2.73%
P62715	Ppp2cb Serine/threonine-protein phosphatase 2A catalytic	R.LQEVPHEGPMC*DLLWSDPDDR.G			69.79%	2.72%
P16045	Lgals1 Galectin-1	K.DSNNLC*LHFNPR.F			89.61%	2.71%
Q9D8E6	Rpl4 60S ribosomal protein L4	R.GPC*IIYNEDNGIIK.A	5.27%	0.87%	75.02%	2.69%
Q99JY9	Actr3 Actin-related protein 3	R.TLTGTVIDSGDGVTHVIPVAEGYVIGSC*IK.H			56.16%	2.69%
P62702	Rps4x 40S ribosomal protein S4, X isoform	R.EC*LPLIIFLR.N			73.07%	2.67%
Q61093	Cybb Cytochrome b-245 heavy chain	K.TIASEHPNTTIGVFLC*GPEALAETLSK.Q			65.58%	2.67%
Q8VBT0	Tmx1 Thioredoxin-related transmembrane protein 1	R.FIITALPSIYHC*K.D			58.32%	2.65%
P52480	Pkm Pyruvate kinase isozymes M1/M2	R.GIFPVLC*K.D	9.41%	3.23%	60.57%	2.65%
Q8BU30	Iars Isoleucine--tRNA ligase, cytoplasmic	K.NNDLC*YWVPEFVR.E			68.64%	2.63%
P80314	Cct2 T-complex protein 1 subunit beta	K.HGINC*FINR.Q			37.80%	2.61%
P60710	Actb Actin, cytoplasmic 1	K.LC*YVALDFEQEMATAASSSSLEK.S	14.61%	5.03%	62.13%	2.61%
Q64345	Ifit3 Interferon-induced protein with tetratricopeptide	K.C*HFTWNLFR.E			83.12%	2.61%
P80313	Cct7 T-complex protein 1 subunit eta	R.INALTAASEAAC*LIVSVDETIK.N			55.25%	2.60%
P51881	Slc25a5 ADP/ATP translocase 2	K.GTDIMYTGTLDC*WR.K	4.76%	0.00%	32.91%	2.59%
Q99JY9	Actr3 Actin-related protein 3	K.LGYAGNTEPQFIIPSC*IAIK.E			58.85%	2.57%
Q68FD5	Cltc Clathrin heavy chain 1	R.GQC*DLELINVC*NENSLFK.S			83.52%	2.56%
Q8BU30	Iars Isoleucine--tRNA ligase, cytoplasmic	K.HNC*FQEC*LK.Q			93.76%	2.55%
P10126	Eef1a1 Elongation factor 1-alpha 1	K.DGSASGTTLLEALDC*ILPPTRPTDK.P	17.77%	6.17%	62.33%	2.54%
P68372	Tubb4b Tubulin beta-4B chain	K.NMMAAC*DPR.H			81.91%	2.53%
Q61543	Glg1 Golgi apparatus protein 1	K.FC*HGILTK.A			93.13%	2.53%
Q05920	Pc Pyruvate carboxylase, mitochondrial	R.FLYEC*PWR.R	4.61%	0.37%	34.57%	2.51%
Q61093	Cybb Cytochrome b-245 heavy chain	R.GQTAESLEEHNLDIC*ADK.I			90.19%	2.51%
P35979	Rpl12 60S ribosomal protein L12	R.HPHDIIDDINSGAVEC*PAS.-			68.94%	2.50%
Q80UM7	Mogs Mannosyl-oligosaccharide glucosidase	R.HTC*EQGDGVGPYGWEFHDGR.T			75.05%	2.49%
Q8R0X7	Sgpl1 Sphingosine-1-phosphate lyase 1	R.NTAMLVC*STPQFPHGVMDPVPEVAK.L			73.11%	2.47%
P52480	Pkm Pyruvate kinase isozymes M1/M2	K.PVIC*ATQMLESMIK.K			77.85%	2.47%
P62889	Rpl30 60S ribosomal protein L30	R.VC*TLAIIDPGDSDIIR.S	10.22%	3.17%	60.34%	2.44%
P68368	Tuba4a Tubulin alpha-4A chain	K.RSIQFVDWC*PTGFK.V	27.21%	4.71%	74.79%	2.40%
Q8C0I1	Agps Alkyldihydroxyacetonephosphate synthase, peroxisom	K.YGSVAFPNFEQGVAC*LR.E			57.37%	2.39%
Q9QYB1	Clic4 Chloride intracellular channel protein 4	K.TDVNKIEEFLEEVLC*PPK.Y			79.60%	2.37%
Q64345	Ifit3 Interferon-induced protein with tetratricopeptide	K.ALEEKPKDPEC*SSGMAIAMFR.L	3.28%	1.54%	93.60%	2.32%
Q9QYB1	Clic4 Chloride intracellular channel protein 4	R.FLDGDEMTLADC*NLLPK.L			75.15%	2.31%
P62830	Rpl23 60S ribosomal protein L23	R.ISLGLPVGAVINC*ADNTGAK.N	7.86%	0.55%	74.44%	2.31%
Q5SWU9	Acaca Acetyl-CoA carboxylase 1	R.NFDLTAIPC*ANHK.M	13.82%	1.72%	72.12%	2.30%
P07901	Hsp90aa1 Heat shock protein HSP 90-alpha	K.HGLEVIYMIEPIDEYC*VQQLK.E			59.76%	2.30%
Q9D1Q6	Erp44 Endoplasmic reticulum resident protein 44	K.TPADC*PVIAIDSFR.H			93.50%	2.29%
Q9QXK3	Copg2 Coatomer subunit gamma-2	R.ELAPAVSVLQLFC*SSPK.P			48.39%	2.29%
P16045	Lgals1 Galectin-1	R.FNAHGDANTIVC*NTK.E			87.18%	2.29%
Q6ZQI3	Mlec Malectin	K.VC*ALYILAGTVDDVPK.L			67.00%	2.27%
P58252	Eef2 Elongation factor 2	R.ETVSEESNVLC*LSK.S	11.30%	5.67%	72.04%	2.26%
P11983	Tcp1 T-complex protein 1 subunit alpha	R.SLHDALC*VVK.R			68.60%	2.26%
Q9QUN7	Tlr2 Toll-like receptor 2	K.VFLVPC*SFSQHLK.S			93.65%	2.25%
Q99JW4	Lims1 LIM and senescent cell antigen-like-containing dom	K.AMNNSWHPEC*FR.C			66.91%	2.24%
P54987	Irg1 Immune-responsive gene 1 protein	K.LEDLEDC*SVLTR.L			53.43%	2.23%
Q64282	Ifit1 Interferon-induced protein with tetratricopeptide	R.VC*QNVHLVESTSLLGLVYK.L			67.50%	2.22%
P08249	Mdh2 Malate dehydrogenase, mitochondrial	K.TIIPLISQC*TPK.V			57.77%	2.22%
F8VPN3	Gm5160 Peptidyl-prolyl cis-trans isomerase	R.IIPGFMC*QGGDFTR.H	17.53%	2.72%	78.31%	2.21%
O35598	Adam10 Disintegrin and metalloproteinase domain-containin	R.DFDDGVLGLAWVGAPSGSSGGIC*EK.S			73.39%	2.20%
P10126	Eef1a1 Elongation factor 1-alpha 1	K.PMC*VESFSDYPPLGR.F			77.99%	2.19%
Q9D1Q6	Erp44 Endoplasmic reticulum resident protein 44	R.VASILHDDC*AFLSAFGDLSKPER.Y			82.29%	2.19%
P52480	Pkm Pyruvate kinase isozymes M1/M2	R.NTGIIC*TIGPASR.S	11.20%	3.32%	70.02%	2.18%
Q8VEK3	Hnrnpu Heterogeneous nuclear ribonucleoprotein U	K.GNFTLPEVAEC*FDEITYVELQK.E			65.05%	2.17%
Q60864	Stip1 Stress-induced-phosphoprotein 1	K.ALSAGNIDDALQC*YSEAIK.L			65.15%	2.14%
P14211	Calr Calreticulin	R.C*KDDEFTHLYTLIVRPDNTYEVK.I			85.89%	2.12%
Q02053	Uba1 Ubiquitin-like modifier-activating enzyme 1	R.VGEFC*HSR.G			56.64%	2.11%
Q8VBZ3	Clptm1 Cleft lip and palate transmembrane protein 1 homol	R.VSFC*PLSLWR.W			74.42%	2.10%
Q8VEM8	Slc25a3 Phosphate carrier protein, mitochondrial	K.GWAPTLIGYSMQGLC*K.F			22.42%	2.09%
Q04447	Ckb Creatine kinase B-type	R.FC*TGLTQIETLFK.S			49.94%	2.09%
Q9R233	Tapbp Tapasin	R.VSLTPAPVVWAAPGEAPPELLC*LASHFFPAEGLEVK.W			87.44%	2.09%
P40124	Cap1 Adenylyl cyclase-associated protein 1	R.ALLATASQC*QQPAGNK.L	4.90%	0.19%	77.07%	2.07%
Q6P5E4	Uggt1 UDP-glucose:glycoprotein glucosyltransferase 1	R.DFNLDGAPYGYTPFC*DSR.R			89.41%	2.07%

P51660	Hsd17b4 Peroxisomal multifunctional enzyme type 2	K.NNIHC*NTIAPNAGSR.M			61.45%	2.07%
P45878	Fkbp2 Peptidyl-prolyl cis-trans isomerase FKBP2	K.GWDQGLLGMC*EGEK.R			80.39%	2.02%
Q8BYB9	Poglut1 Protein O-glucosyltransferase 1	R.GSQFIINHLQMDDITC*YWENLLTDYSK.F			76.17%	2.01%
Q61753	Phgdh D-3-phosphoglycerate dehydrogenase	K.NAGTC*LSPAVIVGLLR.E			87.88%	2.00%
P68254	Ywhaq 14-3-3 protein theta	R.SIC*TTVLELLDK.Y			21.62%	1.99%
P63242	Eif5a Eukaryotic translation initiation factor 5A-1	K.KYEDIC*PSTHNMDVPNIK.R			83.71%	1.97%
Q05769	Ptgs2 Prostaglandin G/H synthase 2	K.GLMGNPIC*SPQYWK.P			29.05%	1.95%
Q9EPL9	Acox3 Peroxisomal acyl-coenzyme A oxidase 3	R.EAC*GGHGYLAMNR.F			90.06%	1.94%
P40142	Tkt Transketolase	R.TVPFC*STFAAFFTR.A			72.17%	1.94%
A2AD25	Gm4987 Novel protein silmilar to ribosomal protein L32	K.SYC*AEIAHNVSSK.N	9.79%	5.13%	93.56%	1.94%
P11835	Itgb2 Integrin beta-2	K.AC*QPPFAFR.H			93.87%	1.94%
Q9JKR6	Hyou1 Hypoxia up-regulated protein 1	K.LC*QGLFFR.V			15.23%	1.92%
Q8VEH8	Erlec1 Endoplasmic reticulum lectin 1	R.ASPVNDIFC*QSLPGSPFKPLTLR.Q			93.88%	1.92%
Q922R8	Pdia6 Protein disulfide-isomerase A6	K.KTC*EEHQLC*VVAVLPHILDTGAAGR.N			94.13%	1.91%
Q61753	Phgdh D-3-phosphoglycerate dehydrogenase	K.EELIAELQDC*EGLIVR.S			75.19%	1.90%
Q921F2	Tardbp TAR DNA-binding protein 43	R.VTEDENDEPIEIPSEDDGTVLLSTVTAQFP GAC*GLR.Y			87.86%	1.88%
Q99MR8	Mccc1 Methylcrotonoyl-CoA carboxylase subunit alpha, mit	R.YC*LHQYNIVGLR.S	3.37%	1.51%	30.37%	1.88%
Q8CIE6	Copa Coatomer subunit alpha	K.HAIVIC*NR.K			48.38%	1.87%
P62281	Rps11 40S ribosomal protein S11	K.NMSVHLSPC*FR.D	18.76 %	2.24%	89.27%	1.86%
Q91VI7	Rnh1 Ribonuclease inhibitor	K.LQLEYC*NLTATSC*EPLASVLR.V			93.93%	1.85%
Q64112	Ifit2 Interferon-induced protein with tetratricopeptide	R.NYC*IDSLEQAIQLSPDNTYVK.V			92.01%	1.83%
Q07797	Lgals3bp Galectin-3-binding protein	K.TPSLFPC*ASGAFSSFR.V			92.12%	1.81%
P68368	Tuba4a Tubulin alpha-4A chain	K.TIGGGDDSFTTFFC*ETGAGK.H			93.96%	1.81%
P05064	Aldoa Fructose-bisphosphate aldolase A	R.VNPC*IGGVILFHETLYQK.A			53.30%	1.80%
P11499	Hsp90ab1 Heat shock protein HSP 90-beta	R.GFEVVYMTEPIDEYC*VQQLK.E			72.22%	1.76%
P50580	Pa2g4 Proliferation-associated protein 2G4	K.VAHSFNC*TPIEGMLSHQLK.Q			85.99%	1.76%
P62874	Gnb1 Guanine nucleotide-binding protein G(I)/G(S)/G(T)	R.VSC*LGVTDDGMAVATGSWDSFLK.I			83.36%	1.75%
Q61543	Glg1 Golgi apparatus protein 1	R.GEIEHHC*SGLHR.K			93.78%	1.75%
Q61510	Trim25 E3 ubiquitin/ISG15 ligase TRIM25	K.NTVMC*AVVEQFLQAEQAR.T			66.07%	1.75%
Q8VDN2	Atp1a1 Sodium/potassium-transporting ATPase subunit alpha	K.AC*VVHGSDLK.D			52.86%	1.72%
P11499	Hsp90ab1 Heat shock protein HSP 90-beta	R.VFIMDSC*DELIPEYLNFIR.G			59.55%	1.71%
Q5SWU9	Acaca Acetyl-CoA carboxylase 1	R.VSALNSVHC*EHVEDEGESR.Y			76.87%	1.70%
Q9R0E1	Plod3 Procollagen-lysine,2-oxoglutarate 5-dioxygenase 3	K.EVFSSSDTDPDMAFC*K.S			86.40%	1.70%
Q64737	Gart Trifunctional purine biosynthetic protein adenosin	R.C*FGPTAQAAQLESSKK.F			60.31%	1.70%
Q9DCD0	Pgd 6-phosphogluconate dehydrogenase, decarboxylating	K.VGTGEPC*C*DWVGDEGAGHFVK.M			93.87%	1.70%
Q9CZN7	Shmt2 Protein Shmt2	R.YYGGAEVVDEIELLC*QR.R			83.85%	1.68%
Q9D024	Ccdc47 Coiled-coil domain-containing protein 47	K.LNQENEHIYNLWC*SGR.V			49.43%	1.66%
O55143	Atp2a2 Sarcoplasmic/endoplasmic reticulum calcium ATPase	K.SMSVYC*TPNKPSR.T			84.77%	1.66%
P70168	Kpnb1 Importin subunit beta-1	K.ESTLEAIGYIC*QDIDPEQLQDK.S			50.93%	1.66%
Q9R0P3	Esd S-formylglutathione hydrolase	K.AYSGSQIDILIDQGKDDEFLSNGQLLPDN FIAAC*TEK.K			86.08%	1.65%
P17742	Ppia Peptidyl-prolyl cis-trans isomerase A	K.HTGPGILSMANAGPNTNGSQFFIC*TAK. T			73.05%	1.62%
Q9WUA3	Pfkp 6-phosphofructokinase type C	R.NESC*SVNYTTDFIYQLYSEEGK.G			94.12%	1.58%
P68040	Gnb2l1 Guanine nucleotide-binding protein subunit beta-2-	K.TNHIGHTGYLNTVTVSPDGSLC*ASGGK. D			71.55%	1.57%
Q9JLJ2	Aldh9a1 4-trimethylaminobutyraldehyde dehydrogenase	K.SPLIIFSDC*NMENAVK.G			66.59%	1.57%
P62889	Rpl30 60S ribosomal protein L30	K.TGVHHYSGNNIELGTAC*GK.Y			53.59%	1.56%
Q9CXY9	Pigk GPI-anchor transamidase	R.LGIPDSHIVLMLADDMAC*NAR.N			86.08%	1.56%
Q8CGK3	Lonp1 Lon protease homolog, mitochondrial	K.ILC*FHGPPGVGK.T			68.52%	1.51%
Q5SWU9	Acaca Acetyl-CoA carboxylase 1	K.KNLLVTMLIDQLC*GR.D			51.25%	1.48%
Q8BHN3	Ganab Neutral alpha-glucosidase AB	K.TRDGSDYEGWC*WPGSASYPDFTNPR.M			73.58%	1.47%
Q80VA0	Galnt7 N-acetylgalactosaminyltransferase 7	K.TNGGFVELGPC*HR.M			94.14%	1.46%
P34884	Mif Macrophage migration inhibitory factor	K.PAQYIAVHVVPDQLMTFSGTNDPC*ALC *SLHSIGK.I			76.47%	1.46%
Q68FL6	Mars Methionine--tRNA ligase, cytoplasmic	K.DNVPFHGLVFPC*SVLGAEDNYTLVK.H			78.46%	1.44%
Q9QY81	Nup210 Nuclear pore membrane glycoprotein 210	R.LTLMPVYALPQLDLSC*PLLQQNK.Q			94.23%	1.43%
P58252	Eef2 Elongation factor 2	R.YVEPIEDVPC*GNIVGLVGVDQFLVK.T			67.36%	1.43%
Q5SWU9	Acaca Acetyl-CoA carboxylase 1	R.EC*SQPVMVYIPPQAELR.G	4.76%	0.00%	68.41%	1.42%
Q5SWU9	Acaca Acetyl-CoA carboxylase 1	K.RPGAALDPGC*VIAK.M	17.21 %	1.47%	83.66%	1.42%
P11680	Cfp Properdin	R.LC*TPLLPK.Y			83.95%	1.40%
Q61543	Glg1 Golgi apparatus protein 1	K.GNLGMNC*QQALQTLIQETDPGADYR.I			94.43%	1.40%
Q05920	Pc Pyruvate carboxylase, mitochondrial	R.AGTHILC*IK.D	6.11%	0.96%	44.10%	1.39%
P62814	Atp6v1b2 V-type proton ATPase subunit B, brain isoform	K.IPIFSAAGLPHNEIAAQIC*R.Q			34.89%	1.39%
P29477	Nos2 Nitric oxide synthase, inducible	R.DGQGPLHHGVC*STWIR.N			76.42%	1.39%

Q8VEK3	Hnrnpu Heterogeneous nuclear ribonucleoprotein U	K.EKPYFPIPEDC*TFIQNVPLEDR.V			71.79%	1.38%
Q9R0Q7	Ptges3 Prostaglandin E synthase 3	K.HLNEIDLFHC*IDPNDSK.H			94.27%	1.37%
P45376	Akr1b1 Aldose reductase	K.YKPAVNQIEC*HPYLTQEK.L			84.88%	1.37%
Q5SWU9	Acaca Acetyl-CoA carboxylase 1	R.MMYGVSPWGDAPIDFENSAHVPC*PR.G	13.95%	1.21%	83.92%	1.34%
P14211	Calr Calreticulin	K.DMHGDSEYNIMFGPDIC*GPGTK.K			93.37%	1.34%
Q9R233	Tapbp Tapasin	R.RYPAGASAPHC*EMSR.F			91.87%	1.32%
P14211	Calr Calreticulin	K.HEQNIDC*GGGYVK.L			87.12%	1.29%
Q8VI93	Oas3 2-5-oligoadenylate synthase 3	K.TC*HSETLGAMR.M			84.42%	1.28%
Q4KN81	H2-Q2 Histocompatibility 2, Q region locus 2	R.YTC*HVEHEGLPEPLTLR.W			94.50%	1.27%
O08807	Prdx4 Peroxiredoxin-4	R.ENEC*HFYAGGQVYPGEASR.V			83.01%	1.25%
P24547	Impdh2 Inosine-5-monophosphate dehydrogenase 2	R.HGFC*GIPITDTGR.M			65.79%	1.24%
P11680	Cfp Properdin	R.HGGPFC*AGDATR.N			95.57%	1.24%
P28867	Prkcd Protein kinase C delta type	R.ASTFC*GTPDYIAPEILQGLK.Y			90.75%	1.23%
P24270	Cat Catalase	R.LC*ENIAGHILK.D			30.14%	1.23%
P34884	Mif Macrophage migration inhibitory factor	K.LLC*GLLSDR.L	4.76%	0.00%	29.46%	1.22%
Q3TRM8	Hk3 Hexokinase-3	R.TQLQQIQASLLC*SMEQALK.G			76.47%	1.21%
Q9D0I9	Rars Arginine--tRNA ligase, cytoplasmic	K.IVFVPGC*SVPLTIVK.S			74.12%	1.21%
P17182	Eno1 Alpha-enolase	R.SGETEDTFIADLVVGLC*TGQIK.T			85.32%	1.21%
P58252	Eef2 Elongation factor 2	R.LMEPIYLVEIQC*PEQVVGGIYGVLNR.K			49.26%	1.19%
Q921H8	Acaa1a 3-ketoacyl-CoA thiolase A, peroxisomal	R.DC*LTPMGMTSENVAER.F			82.37%	1.18%
Q5SWU9	Acaca Acetyl-CoA carboxylase 1	K.VQAERPDTMLGVVC*GALHVADVSLR.N	23.30%	13.35%	69.93%	1.18%
Q8R180	Ero1l ERO1-like protein alpha	K.HDDSSDSFC*EIDDIQSPDAEYVDLLLNPER.Y			54.06%	1.17%
P51670	Ccl9 C-C motif chemokine 9	K.RGFQVC*ANPSDR.R			94.57%	1.16%
P07901	Hsp90aa1 Heat shock protein HSP 90-alpha	R.LVTSPC*C*IVTSTYGWTANMER.I			94.57%	1.16%
P97429	Anxa4 Annexin A4	R.SLEEDIC*SDTSFMFQR.V			32.39%	1.13%
Q61543	Glg1 Golgi apparatus protein 1	R.HLYFAC*R.D			94.28%	1.11%
O88844	Idh1 Isocitrate dehydrogenase	K.SEGGFIWAC*K.N			94.45%	1.11%
Q05769	Ptgs2 Prostaglandin G/H synthase 2	R.VC*DILKQEHPEWGDEQLFQTSR.L			22.32%	1.11%
P09411	Pgk1 Phosphoglycerate kinase 1	K.DC*VGPEVENAC*ANPAAGTVILLENLR.F	19.41%	4.99%	95.92%	1.10%
Q9Z2L6	Minpp1 Multiple inositol polyphosphate phosphatase 1	R.RDPELLAGTC*TPVQLVALIR.H			94.69%	1.09%
Q05769	Ptgs2 Prostaglandin G/H synthase 2	K.IINTASIQSLIC*NNVK.G			95.17%	1.07%
Q07113	Igf2r Cation-independent mannose-6-phosphate receptor	R.ATLITFLC*DR.D			94.37%	1.06%
P62137	Ppp1ca Serine/threonine-protein phosphatase PP1-alpha cat	K.TFTDC*FNC*LPIAAIVDEK.I			90.63%	1.06%
P16858	Gapdh Glyceraldehyde-3-phosphate dehydrogenase	R.VPTPNVSVVDLTC*R.L	18.44%	6.36%	74.44%	1.05%
Q05769	Ptgs2 Prostaglandin G/H synthase 2	R.GEC*MSTGFDQYK.C			95.24%	1.01%
Q9Z1Q5	Clic1 Chloride intracellular channel protein 1	K.LHIVQVVC*K.K			44.53%	1.01%
P62259	Ywhae 14-3-3 protein epsilon	K.LIC*C*DILDVLDK.H			80.37%	1.01%
P17751	Tpi1 Triosephosphate isomerase	K.IAVAAQNC*YK.V	5.16%	0.56%	72.07%	1.01%
Q78PY7	Snd1 Staphylococcal nuclease domain-containing protein	R.RGEFC*IAK.F			63.72%	1.00%
Q05920	Pc Pyruvate carboxylase, mitochondrial	R.ADFAQAC*QDAGVR.F	8.38%	2.16%	57.97%	1.00%
P46061	Rangap1 Ran GTPase-activating protein 1	K.ILAAALTEC*HR.K			67.34%	0.97%
Q91ZA3	Pcca Propionyl-CoA carboxylase alpha chain, mitochondri	K.QEDIPISGWAVEC*R.V	8.11%	0.61%	42.58%	0.97%
P80318	Cct3 T-complex protein 1 subunit gamma	K.IPGGIIEDSC*VLR.G			56.38%	0.95%
Q5SWU9	Acaca Acetyl-CoA carboxylase 1	K.EMAQYASNITSVLC*QFPSQQIANILDSHAATLNR.K	7.67%	1.61%	60.99%	0.91%
P10404	MLV-related proviral Env polyprotein	K.LTLSEVTGQGLC*VGAVPK.T			94.82%	0.91%
P97429	Anxa4 Annexin A4	K.GAGTDEGC*LIEILASR.T	4.76%	0.00%	22.41%	0.86%
Q61990	Pcbp2 Poly(rC)-binding protein 2	R.AITIAGIPQSIIEC*VK.Q			44.44%	0.85%
Q8CIE6	Copa Coatomer subunit alpha	K.IQVPNC*DEIFYAGTGNLLLR.D			59.12%	0.84%
P19096	Fasn Fatty acid synthase	K.GHALGETLAC*LPSEVQPAPSLLSQEEWESLFSR.K			76.03%	0.83%
Q8R180	Ero1l ERO1-like protein alpha	K.KPC*PFWNDINQC*GR.R			94.82%	0.83%
Q68FD5	Cltc Clathrin heavy chain 1	R.AHIAQLC*EK.A			34.82%	0.83%
Q9D1M0	Sec13 Protein SEC13 homolog	R.DVAWAPSIGLPTSTIASC*SQDGR.V			57.49%	0.81%
Q62159	Rhoc Rho-related GTP-binding protein RhoC	K.HFC*PNVPIILVGNK.K			77.99%	0.80%
Q91VI7	Rnh1 Ribonuclease inhibitor	R.ELDLSNNC*MGGPGVLQLLESLK.Q			84.63%	0.80%
Q80VA0	Galnt7 N-acetylgalactosaminyltransferase 7	R.SEVLHQVFISTC*DSSK.M			94.00%	0.77%
Q91VI7	Rnh1 Ribonuclease inhibitor	R.SLLELQMSSNPLGDEGVQELC*K.A			85.63%	0.77%
P60710	Actb Actin, cytoplasmic 1	R.C*PEALFQPSFLGMESC*GIHETTFNSIMK.C			94.86%	0.74%
Q6ZQM8	Ugt1a7c UDP-glucuronosyltransferase 1-7C	K.QTSFDAVFLDPFDVC*GLTVAK.Y			91.27%	0.73%
Q91ZA3	Pcca Propionyl-CoA carboxylase alpha chain, mitochondri	K.MADEAVC*VGPAPTSK.S	14.57%	3.38%	66.19%	0.72%
P35564	Canx Calnexin	K.C*GEDYKLHFIFR.H			94.43%	0.71%
Q9D662	Sec23b Protein transport protein Sec23B	R.MVVPLAC*LLTPLK.E			76.29%	0.70%
Q05769	Ptgs2 Prostaglandin G/H synthase 2	R.ALPPVADDC*PTPMGVK.G			95.70%	0.70%
Q9D8N0	Eef1g Elongation factor 1-gamma	R.WFLTC*INQPQFR.A			34.73%	0.68%
P50543	S100a11 Protein S100-A11	R.C*IESLIAVFQK.Y			24.34%	0.67%
Q64345	Ifit3 Interferon-induced protein with tetratricopeptide	R.YC*NLQEYHR.K			89.03%	0.62%
Q9Z1Q5	Clic1 Chloride intracellular channel protein 1	R.EEFASTC*PDDEEIELAYEQVAR.A			76.18%	0.62%
Q9WV32	Arpc1b Actin-related protein 2/3 complex subunit 1B	R.VAWVSHDSTVC*LVDADKK.M			68.55%	0.62%

Q91ZW2	Pofut1 GDP-fucose protein O-fucosyltransferase 1	R.STATPLTMTMC*LPDLK.E			94.89%	0.60%
P17182	Eno1 Alpha-enolase	K.SC*NC*LLLK.V			94.90%	0.58%
P27512	Cd40 Tumor necrosis factor receptor superfamily member	R.LTSHC*TALEK.T			94.91%	0.57%
Q6PIC6	Atp1a3 Sodium/potassium-transporting ATPase subunit alpha	K.NLEAVETLGSTSTIC*SDK.T	8.01%	0.52%	60.31%	0.54%
Q921T2	Tor1aip1 Torsin-1A-interacting protein 1	R.GLPHNQDFPAHENQPLLTSGC*QENPQ EWVDR.A			86.50%	0.51%
P07356	Anxa2 Annexin A2	K.GDLENAFLNLVQC*IQNKPLYFADR.L			11.70%	0.51%
Q9CXY9	Pigk GPI-anchor transamidase	K.SLC*VSTPGHR.T			94.41%	0.50%
P18760	Cfl1 Cofilin-1	K.HELQANC*YEEVK.D			94.90%	0.47%
Q9D071	Mms19 MMS19 nucleotide excision repair protein homolog	R.ADAEDLLGSFLSNILQDC*R.H			94.98%	0.44%
O89053	Coro1a Coronin-1A	K.HLEEPLSLQELDTSSGVLLPFFDPDTNIVY LC*GK.G			82.44%	0.39%
P07356	Anxa2 Annexin A2	K.GLGTDEDSLIEIIC*SR.T	4.76%	0.00%	15.66%	0.38%
Q8VIB3	St3gal6 Type 2 lactosamine alpha-2,3-sialyltransferase	R.FPQLYPFLC*R.A			94.97%	0.38%
Q8K297	Glt25d1 Procollagen galactosyltransferase 1	K.GELGC*FLSHYNIWK.E			76.42%	0.34%
P17918	Pcna Proliferating cell nuclear antigen	K.LMDLDVEQLGIPEQEYSC*VIK.M			95.00%	0.34%
P17751	Tpi1 Triosephosphate isomerase	R.IIYGGSVTGATC*K.E	10.84%	1.44%	75.36%	0.33%
Q99MR8	Mccc1 Methylcrotonoyl-CoA carboxylase subunit alpha, mit	R.VLGDLSSEDGC*TYLK.S	7.79%	1.03%	69.71%	0.33%
Q01853	Vcp Transitional endoplasmic reticulum ATPase	K.MTNGFSGADLTEIC*QR.A			30.36%	0.29%
Q9QUR6	Prep Prolyl endopeptidase	K.VLVPEHEKDVLEWVAC*VR.S			32.56%	0.28%
P02463	Col4a1 Collagen alpha-1(IV) chain	R.AHGQDLGTAGSC*LR.K			89.90%	0.27%
E9Q7H5	Gm8991 Uncharacterized protein	K.WGTLTDC*VVMR.D			63.90%	0.27%
A6H5X4	Phf11l PHD finger protein 11-like	R.LVDETASESDYEGIETLLFDC*GLFK.D			74.94%	0.26%
Q8K2B3	Sdha Succinate dehydrogenase	R.GVIALC*IEDGSIHR.I			60.32%	0.22%
Q05144	Rac2 Ras-related C3 botulinum toxin substrate 2	R.HHC*PSTPIILVGTK.L			79.52%	0.22%
Q91ZA3	Pcca Propionyl-CoA carboxylase alpha chain, mitochondri	R.LQVEHPVTEC*ITGLDLVQEMILVAK.G	7.09%	1.04%	39.29%	0.22%
Q64345	Ifit3 Interferon-induced protein with tetratricopeptide	R.STVNNSPLYSLVMC*R.Y			76.78%	0.20%
P68372	Tubb4b Tubulin beta-4B chain	K.EAESC*DC*LQGFQLTHSLGGGTGSGMG TLLISK.I			95.14%	0.20%
P29477	Nos2 Nitric oxide synthase, inducible	R.LEALC*QPSEYNDWK.F			83.47%	0.19%
Q8CIH9	Ppat Amidophosphoribosyltransferase	R.YC*HEVKPGEIVEISR.H			56.51%	0.19%
Q9DCL9	Paics Multifunctional protein ADE2	R.VVVLMGSTSDLGHC*EK.I			73.40%	0.19%
Q7TMB8	Cyfip1 Cytoplasmic FMR1-interacting protein 1	R.NFVGPPHFQVIC*R.L			24.38%	0.19%
Q9WV32	Arpc1b Actin-related protein 2/3 complex subunit 1B	R.TQIAIC*PNNHEVHIYEK.S			75.89%	0.18%
P63101	Ywhaz 14-3-3 protein zeta/delta	R.DIC*NDVLSLLEK.F			9.07%	0.18%
Q9D8E6	Rpl4 60S ribosomal protein L4	R.FC*IWTESAFR.K	5.54%	1.34%	70.80%	0.18%
Q9ET30	Tm9sf3 Transmembrane 9 superfamily member 3	K.YFSLPFC*VGSK.K			91.87%	0.17%
O89053	Coro1a Coronin-1A	R.VSQTTWDSGFC*AVNPK.F			86.13%	0.17%
P11680	Cfp Properdin	R.TC*DHPAPR.H			95.14%	0.17%
Q9Z1N5	Ddx39b Spliceosome RNA helicase Ddx39b	R.C*IALAQLLVEQNFPAIAIHR.G			17.24%	0.16%
P36371	Tap2 Antigen peptide transporter 2	R.VLILDEATSALDAQC*EQALQNWR.S			68.14%	0.16%
Q91WJ8	Fubp1 Far upstream element-binding protein 1	R.C*QHAAEIITDLLR.S			20.52%	0.16%
Q9EPR4	Slc23a2 Solute carrier family 23 member 2	R.LSC*APPPPIHAINR.G			81.82%	0.16%
Q68FD5	Cltc Clathrin heavy chain 1	R.IHEGC*EEPATHNALAK.I			66.33%	0.15%
P62245	Rps15a 40S ribosomal protein S15a	R.QVLIRPC*SK.V			72.57%	0.15%
Q9D1A2	Cndp2 Cytosolic non-specific dipeptidase	R.FC*LEGMEESGSEGLDELIFAQK.D			67.22%	0.15%
Q9JII6	Akr1a1 Alcohol dehydrogenase	R.HIDC*ASVYGNETEIGEALK.E			64.00%	0.14%
P67984	Rpl22 60S ribosomal protein L22	K.FTLDC*THPVEDGIMDAANFEQFLQER.I			47.27%	0.14%
P62274	Rps29 40S ribosomal protein S29	K.YGLNMC*R.Q	6.80%	2.88%	80.74%	0.14%
Q9JIF0	Prmt1 Protein arginine N-methyltransferase 1	K.IHWWENVYGFDMSC*IK.D			34.11%	0.14%
P62874	Gnb1 Guanine nucleotide-binding protein G(I)/G(S)/G(T)	R.ELAGHTGYLSC*C*R.F			95.14%	0.14%
O35598	Adam10 Disintegrin and metalloproteinase domain-containin	R.NTC*QLYIQTDHLFFK.Y			24.91%	0.13%
Q9CR67	Tmem33 Transmembrane protein 33	R.LC*LQSIAFISR.L			37.41%	0.13%
Q01853	Vcp Transitional endoplasmic reticulum ATPase	K.AIANEC*QANFISIK.G			29.67%	0.13%
Q9DCE9	Igtp Interferon gamma induced GTPase	R.DPPLFLISC*FSPSFHDFPELR.N			70.33%	0.13%
Q91YW3	Dnajc3 DnaJ homolog subfamily C member 3	K.ILEVC*VWDAELR.E			67.94%	0.13%
Q99MN9	Pccb Propionyl-CoA carboxylase beta chain, mitochondria	R.IC*C*DLEVLASK.K	6.67%	0.01%	23.17%	0.13%
Q8VI94	Oasl1 2-5-oligoadenylate synthase-like protein 1	R.MYYC*QELMDLGLSNLSVTNR.V			57.72%	0.12%
P97855	G3bp1 Ras GTPase-activating protein-binding protein 1	K.VMSQNFTNC*HTK.I			67.65%	0.12%
Q8BHN3	Ganab Neutral alpha-glucosidase AB	R.SSDC*MKDDPITLFVALSPQGTAQGELFL DDGHTFNYQTR.H			67.65%	0.12%
Q8VDN2	Atp1a1 Sodium/potassium-transporting ATPase subunit alpha	R.IISANGC*K.V			51.37%	0.12%
Q99N69	Lpxn Leupaxin	K.GYC*ASC*QKPIAGK.V			87.81%	0.12%
P62814	Atp6v1b2 V-type proton ATPase subunit B, brain isoform	R.GPVVLAEDFLDIMGQPINPQC*R.I			69.52%	0.11%
P70168	Kpnb1 Importin subunit beta-1	R.ESC*LEAYTGIVQGLK.G			34.56%	0.11%
Q9Z1N5	Ddx39b Spliceosome RNA helicase Ddx39b	K.NC*PHIVVGTPGR.I			75.68%	0.10%
P14206	Rpsa 40S ribosomal protein SA	R.ADHQPLTEASYVNLPTIALC*NTDSPLR.Y			64.86%	0.10%

Q60597	Ogdh 2-oxoglutarate dehydrogenase, mitochondrial	R.VVNAPIFHVNSDDPEAVMYVC*K.V			58.41%	0.10%
P34022	Ranbp1 Ran-specific GTPase-activating protein	K.IC*ANHYITPMMELKPNAGSDR.A			67.50%	0.10%
P19096	Fasn Fatty acid synthase	K.AC*VDTALENLSTLK.M			25.44%	0.10%
Q8VI94	Oasl1 2-5-oligoadenylate synthase-like protein 1	K.HYTLQHPVIEAC*VR.R			68.09%	0.09%
Q9EQK5	Mvp Major vault protein	R.HYC*IVANPVSR.D			26.94%	0.09%
P26039	Tln1 Talin-1	K.ALC*GFTEAAAQAAYLVGVSDPNSQAG QQGLVEPTQFAR.A			76.86%	0.09%
Q99KP6	Prpf19 Pre-mRNA-processing factor 19	R.IWSVPNTSC*VQVVR.A			57.20%	0.09%
Q3UPL0	Sec31a Protein transport protein Sec31A	K.SC*ATFSSSHR.Y			69.38%	0.08%
P59511	Adamts20 A disintegrin and metalloproteinase with thrombosp	R.TC*GGGIKSTARLCDRPEPR.N			25.98%	0.08%
Q8VDN2	Atp1a1 Sodium/potassium-transporting ATPase subunit alpha	R.C*SSILLHGK.E			14.54%	0.08%
P05202	Got2 Aspartate aminotransferase, mitochondrial	R.VGAFTVVC*K.D			48.13%	0.08%
Q8CIE6	Copa Coatomer subunit alpha	R.KLDALC*NIHENIR.V			55.30%	0.08%
P19096	Fasn Fatty acid synthase	R.C*LAQHGR.F			61.78%	0.07%
Q9Z1Q9	Vars Valine--tRNA ligase	K.C*VVHPFLSR.S			78.07%	0.07%
Q61753	Phgdh D-3-phosphoglycerate dehydrogenase	R.ALQSGQC*AGAALDVFTEEPPR.D			90.86%	0.07%
Q8QZY1	Eif3l Eukaryotic translation initiation factor 3 subunit	K.GDPQVYEELFSYAC*PK.F			54.60%	0.07%
P62715	Ppp2cb Serine/threonine-protein phosphatase 2A catalytic	R.AHQLVMEGYNWC*HDR.N			54.60%	0.07%
Q8VI93	Oas3 2-5-oligoadenylate synthase 3	R.WDVLAQEAESSFSQQC*FK.Q			88.41%	0.07%
Q921T2	Tor1aip1 Torsin-1A-interacting protein 1	K.YC*DHENAAFK.D			75.71%	0.06%
P51410	Rpl9 60S ribosomal protein L9	R.TIC*SHVQNMIK.G			71.39%	0.06%
Q99NB5	Gsdmc Gasdermin-C	K.FC*LFNILQETSSRLALK.T			39.80%	0.06%
Q9CQC6	Bzw1 Basic leucine zipper and W2 domain-containing prot	R.FDPTQFQDC*IIQGLTETGTDLEAVAK.F			71.47%	0.06%
Q3UGY8	Arfgef3 Brefeldin A-inhibited guanine nucleotide-exchange	R.LDDSTVAGVAFARYILVGC*WK.N			34.17%	0.06%
P29477	Nos2 Nitric oxide synthase, inducible	K.KTPC*AVLSPTIQDDPK.S			86.92%	0.06%
P51863	Atp6v0d1 V-type proton ATPase subunit d 1	R.NIVWIAEC*IAQR.H			32.01%	0.06%
Q3TXS7	Psmd1 26S proteasome non-ATPase regulatory subunit 1	R.TPEQC*PSVVSLLSESYNPHVR.Y			43.14%	0.06%
Q3U5Q7	Cmpk2 UMP-CMP kinase 2, mitochondrial	R.MENPSC*HLVDASPSR.E			81.34%	0.05%
Q9R1W5	Calcrl Calcitonin gene-related peptide type 1 receptor	R.SASYTVSTISDMQGYSHDC*PTEHLNGK.S			70.88%	0.05%
Q61699	Hsph1 Heat shock protein 105 kDa	K.LMSSNSTDLPLNIEC*FMNDKDVSGK.M			87.75%	0.05%
Q8CGC7	Eprs Bifunctional glutamate/proline--tRNA ligase	K.YNVYPTYDFAC*PIVDSIEGVTHALR.T			67.60%	0.05%
Q8R2E9	Ero1lb ERO1-like protein beta	R.YDDSQDHFC*ELDDERSPAAQYVDLLLN PER.Y			52.12%	0.05%
Q63ZW6	Col4a5 Procollagen type IV alpha 5	R.HSQTTEAPQC*PR.G			53.73%	0.04%
Q61510	Trim25 E3 ubiquitin/ISG15 ligase TRIM25	R.NPNSWC*VEWFNNK.I			53.73%	0.04%
P08752	Gnai2 Guanine nucleotide-binding protein G(i) subunit al	R.LWADHGVQAC*FGR.S			75.22%	0.04%
P48722	Hspa4l Heat shock 70 kDa protein 4L	R.GC*ALQC*AILSPAFK.V			14.50%	0.04%
Q61753	Phgdh D-3-phosphoglycerate dehydrogenase	R.ALVDHENVISC*PHLGASTK.E			84.77%	0.04%
P97429	Anxa4 Annexin A4	K.VLLVLC*GGDD.-			15.23%	0.04%
Q9DBK7	Uba7 Ubiquitin-activating enzyme E1-like	R.C*QNYGILPVNHAR.I			13.02%	0.04%
Q68FD5	Cltc Clathrin heavy chain 1	R.HSSLAGC*QIINYR.T			35.87%	0.04%
Q80X90	Flnb Filamin-B	R.C*VYKPVQPGPHVVK.V			78.10%	0.04%
Q9JM76	Arpc3 Actin-related protein 2/3 complex subunit 3	K.WWTC*FVK.R			69.90%	0.04%
Q9D1P4	Chordc1 Cysteine and histidine-rich domain-containing prot	R.TTDFSDFLSIVGC*TK.G			65.77%	0.03%
Q921F2	Tardbp TAR DNA-binding protein 43	R.YRNPVSQC*MR.G			82.63%	0.03%
P10605	Ctsb Cathepsin B	R.TC*IHTNGR.V			87.70%	0.02%
P51670	Ccl9 C-C motif chemokine 9	R.FIGYFPTSGGC*TR.P			95.22%	0.02%
Q3TDQ1	Stt3b Dolichyl-diphosphooligosaccharide--protein glycosy	K.AGSPTLLNC*LMYK.M			47.38%	0.02%
P58252	Eef2 Elongation factor 2	R.C*LYASVLTAQPR.L			47.63%	0.02%
Q68FD5	Cltc Clathrin heavy chain 1	K.YESLELC*RPVLQQGR.K			42.54%	0.02%
Q99JB8	Pacsin3 Protein kinase C and casein kinase II substrate pr	K.LQERVGRC*TKEAEK.M			58.84%	0.02%
A2AE21	Zfp300 Zinc finger protein 300	K.C*SRAFREKSK.L			68.04%	0.02%
Q9EPE9	Atp13a1 Probable cation-transporting ATPase 13A1	R.SPQENLVPC*DVLLLR.G			76.35%	0.02%
Q791V5	Mtch2 Mitochondrial carrier homolog 2	R.LC*SGVLGTVVHGK.V			50.75%	0.02%
Q9QZE5	Copg1 Coatomer subunit gamma-1	K.FLGMHPC*ER.S			72.98%	0.01%
P26039	Tln1 Talin-1	K.AVEGC*VSASQAATEDGQLLR.G			41.85%	0.01%
P10404	MLV-related proviral Env polyprotein	R.C*NPLVLEFTDAGK.K			95.23%	0.01%
Q9CR57	Rpl14 60S ribosomal protein L14	R.ALVDGPC*TR.V			53.48%	0.01%
P26443	Glud1 Glutamate dehydrogenase 1, mitochondrial	K.VYEGSILEADC*DILIPAASEK.Q			53.48%	0.01%
Q6PB66	Lrpprc Leucine-rich PPR motif-containing protein, mitocho	R.SC*GSLLPELSLAER.T			27.54%	0.01%
P45376	Akr1b1 Aldose reductase	R.HIDC*AQVYQNEK.E			29.07%	0.01%
P63005	Pafah1b1 Platelet-activating factor acetylhydrolase IB subu	K.LWDFQGFEC*IR.T			74.62%	0.01%
Q921H8	Acaa1a 3-ketoacyl-CoA thiolase A, peroxisomal	K.AGLTVNDIDIFEINEAFASQAVYC*VEK.L			74.62%	0.01%
Q9ET30	Tm9sf3 Transmembrane 9 superfamily member 3	R.NLSGQPNFPC*R.V			49.75%	0.00%
Q9CWJ9	Atic Bifunctional purine biosynthesis protein PURH	R.VTVVC*EPEDYAGVAAEMHGSDSK.D			57.80%	0.00%

D3YU05	Gm6316 Glyceraldehyde-3-phosphate dehydrogenase	K.IVSNASC*TTNC*LAPLAK.V			95.24%	0.00%
P02468	Lamc1 Laminin subunit gamma-1	R.STGHGGHC*TNC*R.D			95.24%	0.00%
Q07797	Lgals3bp Galectin-3-binding protein	K.GPIMLDEVEC*TGTESSLASC*R.S			95.24%	0.00%
P11680	Cfp Properdin	R.VEDC*C*LNAAYAFQEHDGGLC*QAC*R.S			95.24%	0.00%
P53996	Cnbp Cellular nucleic acid-binding protein	R.GFQFVSSSLPDIC*YR.C			95.24%	0.00%
P53996	Cnbp Cellular nucleic acid-binding protein	R.EQC*C*YNC*GKPGHLAR.D			95.24%	0.00%
Q99KI0	Aco2 Aconitate hydratase, mitochondrial	R.DVGGIVLANAC*GPC*IGQWDR.K			95.24%	0.00%
P18242	Ctsd Cathepsin D	K.GGC*EAIVDTGTSLLVGPVEEVK.E			95.24%	0.00%
P10605	Ctsb Cathepsin B	R.DQGSC*GSC*WAFGAVEAISDR.T			95.24%	0.00%
Q9Z2G6	Sel1l Protein sel-1 homolog 1	R.SC*HTAVELFK.N			95.24%	0.00%
Q9CYA0	Creld2 Cysteine-rich with EGF-like domain protein 2	K.ESGQC*TDIDEC*SLEEK.A			95.24%	0.00%
Q8BHN3	Ganab Neutral alpha-glucosidase AB	K.TC*DESSFC*K.R			95.24%	0.00%
P27773	Pdia3 Protein disulfide-isomerase A3	K.VDC*TANTNTC*NK.Y			95.24%	0.00%
Q64337	Sqstm1 Sequestosome-1	R.NMVHPNVIC*DGC*NGPVVGTR.Y			95.24%	0.00%
P68372	Tubb4b Tubulin beta-4B chain	K.VSDTVVEPYNATLSVHQLVENTDETYC*IDNEALYDIC*FR.T			95.24%	0.00%
Q76MZ3	Ppp2r1a Serine/threonine-protein phosphatase 2A 65 kDa reg	R.TSAC*GLFSVC*YPR.V			95.24%	0.00%
P61979	Hnrnpk Heterogeneous nuclear ribonucleoprotein K	K.LFQEC*C*PHSTDR.V			95.24%	0.00%
Q9CZD3	Gars Glycine--tRNA ligase	K.TSYGWIEIVGC*ADR.S			95.24%	0.00%
Q91VI7	Rnh1 Ribonuclease inhibitor	R.ELWLGDC*DVTNSGC*SSLANVLLANR.S			95.24%	0.00%
Q61543	Glg1 Golgi apparatus protein 1	K.HTWSNNLAVLEC*LQDVR.E			95.24%	0.00%
Q61543	Glg1 Golgi apparatus protein 1	R.AC*EPIIQNFC*HDVADNQIDSGDLMEC*LIQNK.H			95.24%	0.00%
P11835	Itgb2 Integrin beta-2	R.DSEGC*WITYTLQQK.D			95.24%	0.00%
Q91ZX7	Lrp1 Prolow-density lipoprotein receptor-related protei	R.LDGLC*IPLR.W			95.24%	0.00%
Q91ZX7	Lrp1 Prolow-density lipoprotein receptor-related protei	R.GC*HVNEC*LSR.K			95.24%	0.00%
P18572	Bsg Basigin	R.SGEYSC*IFLPEPVGR.S			95.24%	0.00%
Q9D8E6	Rpl4 60S ribosomal protein L4	R.YAIC*SALAASALPALVMSK.G			95.24%	0.00%
E9PZM5	Gm2075 Uncharacterized protein	K.GGKNRC*RGKNENESEKR.E			4.76%	0.00%
P08905	Lyz2 Lysozyme C-2	R.AVNAC*GINC*SALLQDDITAAIQC*AK.R			95.24%	0.00%
P28798	Grn Granulins	K.GVSC*GDGYHC*C*PQGFHC*SADGK.S			95.24%	0.00%
Q9CXI5	Manf Mesencephalic astrocyte-derived neurotrophic facto	K.ILDDWGEMC*K.G			95.24%	0.00%
B8JJN0	Gm20547 Complement component 2 (Within H-2S)	K.YGQTLRPIC*LPC*TEGTTR.A			95.24%	0.00%
Q07797	Lgals3bp Galectin-3-binding protein	R.WGTVC*DNLWNLLDAHVVC*R.A			95.24%	0.00%
P11680	Cfp Properdin	R.MSINC*EGTPGQQSR.S			95.24%	0.00%
P11680	Cfp Properdin	R.SC*LHVPVC*K.D			95.24%	0.00%
P11680	Cfp Properdin	K.C*GGHC*PGEAQQSQAC*DTQK.T			95.24%	0.00%
Q9R0E2	Plod1 Procollagen-lysine,2-oxoglutarate 5-dioxygenase 1	R.FWTFETGC*TVC*DEGLR.S			95.24%	0.00%
Q9R059	Fhl3 Four and a half LIM domains protein 3	K.TPLAGQQFTSRDDDPYC*VAC*FGELFAPK.C			95.24%	0.00%
Q9R059	Fhl3 Four and a half LIM domains protein 3	K.GAHYC*VPC*YENK.F			95.24%	0.00%
Q00PI9	Hnrnpul2 Heterogeneous nuclear ribonucleoprotein U-like pro	R.ALLPHVLC*K.N			95.24%	0.00%
P22893	Zfp36 Tristetraprolin	R.C*HFIHNPTEDLALPGQPHVLR.Q			95.24%	0.00%
Q61656	Ddx5 Probable ATP-dependent RNA helicase DDX5	R.ELAQQVQQVAAEYC*R.A			95.24%	0.00%
P60335	Pcbp1 Poly(rC)-binding protein 1	R.VMTIPYQPMPASSPVIC*AGGQDR.C			95.24%	0.00%
Q6PB66	Lrpprc Leucine-rich PPR motif-containing protein, mitocho	K.VGVDPDQETYINYVFPC*FDSAQSVR.A			95.24%	0.00%
Q05769	Ptgs2 Prostaglandin G/H synthase 2	R.TGFYGENC*TTPEFLTR.I			95.24%	0.00%
P13597	Icam1 Intercellular adhesion molecule 1	K.LFC*SLEGLFPASEAR.I			95.24%	0.00%
Q9ET30	Tm9sf3 Transmembrane 9 superfamily member 3	K.FKDDVMPGTYC*EIDLDK.E			95.24%	0.00%
Q07113	Igf2r Cation-independent mannose-6-phosphate receptor	K.ETSDC*SYMFEWR.T			95.24%	0.00%
Q80VA0	Galnt7 N-acetylgalactosaminyltransferase 7	R.INEANQLMQYDQC*LTK.G			95.24%	0.00%
Q80VA0	Galnt7 N-acetylgalactosaminyltransferase 7	K.VMITHC*NLNEFK.E			95.24%	0.00%
P58021	Tm9sf2 Transmembrane 9 superfamily member 2	R.LDSVESVLPYEYTAFDFC*QASEGK.R			95.24%	0.00%
Q8BXQ2	Pigt GPI transamidase component PIG-T	R.NAHC*TSISWELR.Q			95.24%	0.00%
P35564	Canx Calnexin	K.C*ESAPGC*GVWQR.P			95.24%	0.00%
Q6ZQM8	Ugt1a7c UDP-glucuronosyltransferase 1-7C	R.GIFC*HYLEDAAQC*PSPPSYIPR.M			95.24%	0.00%
Q6GQT9	Nomo1 Nodal modulator 1	K.VSC*LDTC*GDLLVTLQSLSR.Q			95.24%	0.00%
Q8R180	Ero1l ERO1-like protein alpha	K.ENTFYNWLEGLC*VEK.R			95.24%	0.00%
Q8R180	Ero1l ERO1-like protein alpha	R.C*FC*QVSGYLDDC*TC*DVETIDKFNNYR.L			95.24%	0.00%
Q8BM55	Tmem214 Transmembrane protein 214	K.KGSGGSEHVLTC*DTAC*K.G			95.24%	0.00%
Q91W90	Txndc5 Thioredoxin domain-containing protein 5	K.VDC*TQHYAVC*SEHQVR.G			95.24%	0.00%
Q91W90	Txndc5 Thioredoxin domain-containing protein 5	K.VDC*TADSDVC*SAQGVR.G			95.24%	0.00%
Q6P5E4	Uggt1 UDP-glucose:glycoprotein glucosyltransferase 1	K.SLPQEWLWC*ETWC*DDASK.K			95.24%	0.00%
Q9DAU1	Cnpy3 Protein canopy homolog 3	R.NHQEEDLTEFLC*ANHVLK.G			95.24%	0.00%
Q9QXT0	Cnpy2 Protein canopy homolog 2	R.SQDLHC*GAC*R.A			95.24%	0.00%
Q9CYA0	Creld2 Cysteine-rich with EGF-like domain protein 2	K.GPLC*IDC*TDGFFSLQR.N			95.24%	0.00%

Q9CYA0	Creld2 Cysteine-rich with EGF-like domain protein 2	K.DC*IQC*EVGWAR.V			95.24%	0.00%
Q9EQP2	Ehd4 EH domain-containing protein 4	K.LADC*DC*DGMLDEEEFALAK.H			95.24%	0.00%
Q9R0P3	Esd S-formylglutathione hydrolase	R.SVSAFAPIC*NPVLC*SWGK.K			95.24%	0.00%
Q9QUR6	Prep Prolyl endopeptidase	K.QNC*FDDFQC*AAEYLIK.E			95.24%	0.00%
P62880	Gnb2 Guanine nucleotide-binding protein G(I)/G(S)/G(T)	R.ELPGHTGYLSC*C*R.F			95.24%	0.00%
P68368	Tuba4a Tubulin alpha-4A chain	K.YMAC*C*LLYR.G			95.24%	0.00%
Q61792	Lasp1 LIM and SH3 domain protein 1	K.AC*FHC*ETC*K.M			95.24%	0.00%
P11499	Hsp90ab1 Heat shock protein HSP 90-beta	R.LVSSPC*C*IVTSTYGWTANMER.I			95.24%	0.00%
O70194	Eif3d Eukaryotic translation initiation factor 3 subunit	R.YLEVSEPQDIEC*C*GALEYYDK.A			95.24%	0.00%
Q80X95	Rraga Ras-related GTP-binding protein A	R.LSRPLEC*AC*FR.T			95.24%	0.00%
P42932	Cct8 T-complex protein 1 subunit theta	K.AHEILPELVC*C*SAK.N			95.24%	0.00%
Q02053	Uba1 Ubiquitin-like modifier-activating enzyme 1	K.VLGPYTFSIC*DTSNFSDYIR.G			95.24%	0.00%
Q99N69	Lpxn Leupaxin	R.GTLC*HDC*GQPITGR.C			95.24%	0.00%
Q91VI7	Rnh1 Ribonuclease inhibitor	R.C*KDISSAVQANPALTELSLR.T			95.24%	0.00%
Q91VI7	Rnh1 Ribonuclease inhibitor	K.LLC*EGLQDPQC*R.L			95.24%	0.00%
Q91VI7	Rnh1 Ribonuclease inhibitor	K.LSLQNC*GLTEAGC*GILPGMLR.S			95.24%	0.00%
Q91VI7	Rnh1 Ribonuclease inhibitor	R.LLC*ESLLEPGC*QLESLWIK.T			95.24%	0.00%
Q91VI7	Rnh1 Ribonuclease inhibitor	K.TC*SLTAASC*PYFC*SVLTK.S			95.24%	0.00%
Q61093	Cybb Cytochrome b-245 heavy chain	R.IVGDWTEGLFNAC*GC*DK.Q			95.24%	0.00%
Q61543	Glg1 Golgi apparatus protein 1	K.GYMVSC*LVDHR.G			95.24%	0.00%
Q61543	Glg1 Golgi apparatus protein 1	K.ADIFVDPVLHTAC*ALDIK.H			95.24%	0.00%
Q61543	Glg1 Golgi apparatus protein 1	K.TETGQELEC*LQDHLDDLAVEC*R.D			95.24%	0.00%
Q61543	Glg1 Golgi apparatus protein 1	R.LIC*GFMDDC*KNDINLLK.C			95.24%	0.00%
Q8R5M8	Cadm1 Cell adhesion molecule 1	K.VHKEDDGVPVIC*QVEHPAVTGNLQTQ R.Y			95.24%	0.00%
P68040	Gnb2l1 Guanine nucleotide-binding protein subunit beta-2-	R.YWLC*AATGPSIK.I			99.01%	0.00%
Q99JW4	Lims1 LIM and senescent cell antigen-like-containing dom	K.NDPYHPDHFNC*ANC*GK.E			95.24%	0.00%
P10404	MLV-related proviral Env polyprotein	K.LYFDLC*DLIGDDWDETGLGC*R.T			95.24%	0.00%
P10404	MLV-related proviral Env polyprotein	K.WGC*ETTGQAYWKPSSSWDLISLK.R			95.24%	0.00%
O35516	Notch2 Neurogenic locus notch homolog protein 2	K.IGGFTC*LC*MPGFK.G			95.24%	0.00%
Q91ZX7	Lrp1 Prolow-density lipoprotein receptor-related protei	R.SGFHTVPGQPGC*QDINEC*LR.F			95.24%	0.00%
P27512	Cd40 Tumor necrosis factor receptor superfamily member	K.TQC*HPC*DSGEFSAQWNR.E			95.24%	0.00%
Q61753	Phgdh D-3-phosphoglycerate dehydrogenase	R.C*GEEIAVQFVDMVK.G			95.24%	0.00%
Q61753	Phgdh D-3-phosphoglycerate dehydrogenase	K.VLISDSLDPC*C*R.K			95.24%	0.00%
B2RQY6	BC035947 BC035947 protein	K.EEC*C*FYADHTGIVR.D			95.24%	0.00%
D3Z6F0	Gm14446 RIKEN cDNA 2010002M12	R.LEC*AEMDC*EEGWALLK.C			95.24%	0.00%
G3UW78	Cyp4f17 Protein Cyp4f17	R.C*RQEVQELLR.G	5.44%	0.97%		
P62242	Rps8 40S ribosomal protein S8	K.NC*IVLIDSTPYR.Q	15.37 %	11.65%		
Q99MN9	Pccb Propionyl-CoA carboxylase beta chain, mitochondria	R.AFDNDVDALC*NLR.E	4.30%	0.77%		
P08249	Mdh2 Malate dehydrogenase, mitochondrial	K.GC*DVVVIPAGVPR.K	4.76%	0.00%		
Q5SWU 9	Acaca Acetyl-CoA carboxylase 1	K.TC*VFEKENDPSVMR.S	10.36 %	4.85%		
P62889	Rpl30 60S ribosomal protein L30	K.LVILANNC*PALR.K	4.76%	0.00%		
Q05920	Pc Pyruvate carboxylase, mitochondrial	R.AC*TELGIR.T	4.83%	0.11%		
Q99MN9	Pccb Propionyl-CoA carboxylase beta chain, mitochondria	R.TVGIVGNQPNVASGC*LDINSSVK.G	8.48%	2.08%		
P00342	Ldhc L-lactate dehydrogenase C chain	R.VIGSGC*NLDSAR.F	12.12 %	0.22%		
P47962	Rpl5 60S ribosomal protein L5	R.DIIC*QIAYAR.I	9.29%	6.40%		
P84096	Rhog Rho-related GTP-binding protein RhoG	R.YLEC*SALQQDGVK.E	61.25 %	3.51%		
Q80VA0	Galnt7 N-acetylgalactosaminyltransferase 7	K.LLFVPC*SR.V	61.60 %	1.66%		
Q61093	Cybb Cytochrome b-245 heavy chain	K.WIVGPMFLYLC*ER.L	64.37 %	3.11%		
Q8CIF4	Btd Biotinidase	K.QPC*LSSDPGC*PQDGR.Y	95.24 %	0.00%		
P08905	Lyz2 Lysozyme C-2	R.YWC*NDGK.T	90.37 %	6.84%		
Q8BKC5	Ipo5 Importin-5	R.VQAHAAAALINFTEDC*PK.S	73.31 %	2.06%		
O70370	Ctss Cathepsin S	K.LISLSAQNLVDC*SNEEK.Y	72.14 %	5.46%		
Q8VEK3	Hnrnpu Heterogeneous nuclear ribonucleoprotein U	R.KAVVVC*PK.D	64.04 %	0.54%		
Q62159	Rhoc Rho-related GTP-binding protein RhoC	K.LVIVGDGAC*GK.T	53.95 %	7.68%		
P62242	Rps8 40S ribosomal protein S8	R.LDVGNFSWGSEC*C*TR.K	35.31 %	14.78%		
Q8VEK3	Hnrnpu Heterogeneous nuclear ribonucleoprotein U	K.MC*LFAGFQR.K	23.66 %	3.14%		
Q5SWU 9	Acaca Acetyl-CoA carboxylase 1	R.MSFASNLNHYGMTHVASVSDVLLDNAF TPPC*QR.M	19.56 %	0.40%		
Q5SWU 9	Acaca Acetyl-CoA carboxylase 1	K.DNTC*VVEFQFMLPTSHPNR.G	11.15 %	4.71%		
Q05920	Pc Pyruvate carboxylase, mitochondrial	R.GLYAAFDC*TATMK.S	10.85 %	5.28%		
P62281	Rps11 40S ribosomal protein S11	K.C*PFTGNVSIR.G	4.76%	0.00%		

Table 5A-1. List of proteins enriched in cells treated with either DMSO or 500 nM PJDU-112, PJDU-156, and PDJU-229. Data is filtered for > 20 spectral counts.

		Average Spectral Counts			
UniProt ID	Protein Description	DMSO	PJDU-112	PDJU-156	PJDU-216
Q04695	KRT17 , type I cytoskeletal 17	3	663	583.5	261
P07237	P4HB Protein disulfide-isomerase	0	456.5	16	335
P60709	ACTB Actin, cytoplasmic 1	109.5	444.5	504.5	321
P02538	KRT6A , type II cytoskeletal 6A	7.5	409	312.5	242
P13647	KRT5 , type II cytoskeletal 5	7	243.5	209.5	156
P08729	KRT7 , type II cytoskeletal 7	4.5	196.5	65	72
A8MW45	KRT17P1 Protein KRT17P1	0	194	127	73
P30519	HMOX2 Heme oxygenase 2	0	163	13	50
Q9H7Z7	PTGES2 Prostaglandin E synthase 2	0	149	32	55
P02533	KRT14 , type I cytoskeletal 14	0	146.5	160.5	72
P19012	KRT15 , type I cytoskeletal 15	3	141.5	100.5	63
O95678	KRT75 , type II cytoskeletal 75	0	130.5	104	83
Q15149	PLEC Plectin	10.5	115.5	123.5	117
P10809	HSPD1 60 kDa heat shock protein, mitochondrial	8	104.5	23.5	26
P45880	VDAC2 Voltage-dependent anion-selective channel protein 2	8	100	119.5	135
P11498	PC Pyruvate carboxylase, mitochondrial	143.5	97	75.5	89
P68133	ACTA1 Actin, alpha skeletal muscle	40	97	70.5	51
P35908	KRT2 , type II cytoskeletal 2 epidermal	6.5	91	0	0
Q5XKE5	KRT79 , type II cytoskeletal 79	5	86	88.5	0
P08779	KRT16 , type I cytoskeletal 16	0	83.5	68	28.5
P16615	ATP2A2 Sarcoplasmic/endoplasmic reticulum calcium ATPase 2	3	79.5	29	168
Q9NQC3	RTN4 Reticulon-4	0	78	7	59
P12821	ACE Angiotensin-converting enzyme	0	75	83	87
P30101	PDIA3 Protein disulfide-isomerase A3	0	57.5	9.5	71.5
P07355	ANXA2 Annexin A2	22.5	54.5	180.5	68
P0C0S8	HIST1H2AM Histone H2A type 1	13	54.5	3	9
Q16777	HIST2H2AC Histone H2A type 2-C	13	54.5	3	9
Q9BTM1	H2AFJ Histone H2A.J	13	54.5	3	9
P19338	NCL Nucleolin	5.5	54	6	9.5
P16104	H2AFX Histone H2A.x	0	53.5	5	9
Q96QV6	HIST1H2AA Histone H2A type 1-A	0	53.5	5	9
Q7L7L0	HIST3H2A Histone H2A type 3	5	52	0	6
P08727	KRT19 , type I cytoskeletal 19	0	51.5	14.5	0
P11021	HSPA5 78 kDa glucose-regulated protein	5.5	51	11.5	10.5
P09651	HNRNPA1 Heterogeneous nuclear ribonucleoprotein A1	3	50	12.5	10.5
Q96RQ3	MCCC1 Methylcrotonoyl-CoA carboxylase subunit alpha, mitochondrial	72.5	47	27.5	38
P38646	HSPA9 Stress-70 protein, mitochondrial	5	47	15.5	15.5
Q16881	TXNRD1 Thioredoxin reductase 1, cytoplasmic	2	46.5	67	246.5
P12035	KRT3 , type II cytoskeletal 3	0	46	77	48
O43169	CYB5B Cytochrome b5 type B	0	45	23	64.5
P05787	KRT8 , type II cytoskeletal 8	0	43.5	16	21
Q08211	DHX9 ATP-dependent RNA helicase A	4	42	29	19.5
P06748	NPM1 Nucleophosmin	3	42	17	11.5
Q00839	HNRNPU Heterogeneous nuclear ribonucleoprotein U	2.5	41	37.5	28
O75369	FLNB Filamin-B	38	40.5	374	270.5
P02545	LMNA Prelamin-A/C	0	40.5	23.5	9
Q14534	SQLE Squalene monooxygenase	0	39.5	16.5	46
P22626	HNRNPA2B1 Heterogeneous nuclear ribonucleoproteins A2/B1	0	39	7	6
Q8IUE6	HIST2H2AB Histone H2A type 2-B	0	37	7	9
Q562R1	ACTBL2 Beta-actin-like protein 2	0	36.5	39	17
P13667	PDIA4 Protein disulfide-isomerase A4	0	36.5	3	52.5
P04264	KRT1 , type II cytoskeletal 1	12	35.5	16	23
P42704	LRPPRC Leucine-rich PPR motif-containing protein, mitochondrial	3.5	35	30	49
P05023	ATP1A1 Sodium/potassium-transporting ATPase subunit alpha-1	0	35	13.5	10.5
P14625	HSP90B1 Endoplasmin	6.5	34	16.5	9
Q6PIU2	NCEH1 Neutral cholesterol ester hydrolase 1	0	33	3.5	37
P68104	EEF1A1 Elongation factor 1-alpha 1	54.5	32.5	218	116.5
P37268	FDFT1 Squalene synthase	3	32.5	14	23.5
P08195	SLC3A2 4F2 cell-surface antigen heavy chain	4.5	32.5	13.5	16.5
P04843	RPN1 Dolichyl-diphosphooligosaccharide--protein glycosyltransferase subunit 1	3	32	40	28.5
P31930	UQCRC1 Cytochrome b-c1 complex subunit 1, mitochondrial	2	32	12	95.5
P31943	HNRNPH1 Heterogeneous nuclear ribonucleoprotein H	0	31.5	53.5	21
P05141	SLC25A5 ADP/ATP translocase 2	2	31.5	21.5	13
P07900	HSP90AA1 Heat shock protein HSP 90-alpha	18.5	31	120.5	124.5
O43707	ACTN4 Alpha-actinin-4	12.5	31	65	59.5
P08670	VIM Vimentin	3	30	16.5	8.5
P62805	HIST4H4 Histone H4	3.5	29.5	6.5	10
Q15084	PDIA6 Protein disulfide-isomerase A6	0	29.5	5.5	33.5
Q5T9A4	ATAD3B ATPase family AAA domain-containing protein 3B	0	29	23	55
P52597	HNRNPF Heterogeneous nuclear ribonucleoprotein F	3	28.5	67.5	24.5
P27824	CANX Calnexin	0	28.5	13.5	27.5

P52272	HNRNPM Heterogeneous nuclear ribonucleoprotein M	3	28.5	8	6.5
Q14697	GANAB Neutral alpha-glucosidase AB	3	28	18.5	14
P19013	KRT4 , type II cytoskeletal 4	0	27.5	0	0
Q56VL3	OCIAD2 OCIA domain-containing protein 2	0	27	10	35.5
P25705	ATP5A1 ATP synthase subunit alpha, mitochondrial	5	26.5	7	4
O75367	H2AFY Core histone macro-H2A.1	4	26.5	6	6
P21796	VDAC1 Voltage-dependent anion-selective channel protein 1	2	26.5	4.5	7
P34897	SHMT2 Serine hydroxymethyltransferase, mitochondrial	0	26	6.5	7.5
P08238	HSP90AB1 Heat shock protein HSP 90-beta	13	25.5	116.5	119.5
P35221	CTNNA1 Catenin alpha-1	0	25.5	4.5	3
P07437	TUBB Tubulin beta chain	24	25	162	135.5
Q9Y277	VDAC3 Voltage-dependent anion-selective channel protein 3	0	25	61.5	43.5
P16144	ITGB4 Integrin beta-4	3	25	16.5	27
P12814	ACTN1 Alpha-actinin-1	21	24.5	77.5	70.5
P12236	SLC25A6 ADP/ATP translocase 3	0	24.5	11	8
P05783	KRT18 , type I cytoskeletal 18	2	24	10.5	7
Q96AG4	LRRC59 Leucine-rich repeat-containing protein 59	0	24	6	6.5
P68371	TUBB4B Tubulin beta-4B chain	29	23	158.5	133
Q14CN4	KRT72 , type II cytoskeletal 72	0	23	9	0
Q07065	CKAP4 Cytoskeleton-associated protein 4	0	23	0	14
Q7RTS7	KRT74 , type II cytoskeletal 74	0	23	0	0
Q86Y46	KRT73 , type II cytoskeletal 73	0	23	0	0
Q9NR30	DDX21 Nucleolar RNA helicase 2	2.5	22.5	11.5	9.5
P14618	PKM Pyruvate kinase isozymes M1/M2	14.5	22	96	106.5
P26599	PTBP1 Polypyrimidine tract-binding protein 1	2	22	45	16
P54886	ALDH18A1 Delta-1-pyrroline-5-carboxylate synthase	0	22	17	23.5
Q9NVI7	ATAD3A ATPase family AAA domain-containing protein 3A	0	22	16.5	32
Q15233	NONO Non-POU domain-containing octamer-binding protein	0	22	7.5	9
P51991	HNRNPA3 Heterogeneous nuclear ribonucleoprotein A3	0	21.5	4.5	10.5
P22695	UQCRC2 Cytochrome b-c1 complex subunit 2, mitochondrial	6	21	13	9
Q5QNW6	HIST2H2BF Histone H2B type 2-F	11	21	6	8
Q99879	HIST1H2BM Histone H2B type 1-M	11	21	6	8
Q99880	HIST1H2BL Histone H2B type 1-L	11	21	6	8
P49327	FASN Fatty acid synthase	42	20.5	430.5	438
P68366	TUBA4A Tubulin alpha-4A chain	45	20.5	130.5	116
P40939	HADHA Trifunctional enzyme subunit alpha, mitochondrial	4	20	19	16
Q02878	RPL6 60S ribosomal protein L6	12.5	20	9	14.5
P40429	RPL13A 60S ribosomal protein L13a	8	20	5.5	14.5
P06576	ATP5B ATP synthase subunit beta, mitochondrial	2.5	20	0	3.5
P11216	PYGB Glycogen phosphorylase, brain form	3	9.5	171	81.5
P35579	MYH9 Myosin-9	30.5	9.5	141.5	127.5
P53396	ACLY ATP-citrate synthase	11	3	132.5	105
Q71U36	TUBA1A Tubulin alpha-1A chain	60	0	129.5	111.5
Q00610	CLTC Clathrin heavy chain 1	12	16	112	104
P04083	ANXA1 Annexin A1	14.5	8	105.5	50.5
P29034	S100A2 Protein S100-A2	3	6	105	25
Q9BVA1	TUBB2B Tubulin beta-2B chain	29	0	102	119.5
P15121	AKR1B1 Aldose reductase	0	0	80	4
P78527	PRKDC DNA-dependent protein kinase catalytic subunit	4.5	9	77.5	102.5
Q9BUF5	TUBB6 Tubulin beta-6 chain	13.5	6.5	73	92
P62736	ACTA2 Actin, aortic smooth muscle	40	0	73	0
O43143	DHX15 Putative pre-mRNA-splicing factor ATP-dependent RNA helicase DHX15	0	17	68	31.5
P13639	EEF2 Elongation factor 2	18.5	15	68	44.5
P31947	SFN 14-3-3 protein sigma	3	15.5	56.5	90.5
Q14204	DYNC1H1 Cytoplasmic dynein 1 heavy chain 1	6.5	0	54	89.5
P07814	EPRS Bifunctional glutamate/proline--tRNA ligase	5.5	3	53.5	51
Q9NY65	TUBA8 Tubulin alpha-8 chain	0	0	52	64
Q13085	ACACA Acetyl-CoA carboxylase 1	154.5	2	51.5	127
Q13509	TUBB3 Tubulin beta-3 chain	18	0	51	45
P61978	HNRNPK Heterogeneous nuclear ribonucleoprotein K	4	12	49	14
P22314	UBA1 Ubiquitin-like modifier-activating enzyme 1	8.5	0	47	28
P11217	PYGM Glycogen phosphorylase, muscle form	0	0	46	0
P06733	ENO1 Alpha-enolase	9	18	45	25
P27708	CAD CAD protein	2	0	43.5	88
P22102	GART Trifunctional purine biosynthetic protein adenosine-3	4.5	0	43.5	24
P09382	LGALS1 Galectin-1	2	4.5	40	4
Q01813	PFKP 6-phosphofructokinase type C	0	0	40	16.5
P54136	RARS Arginine--tRNA ligase, cytoplasmic	0	0	39.5	28.5
P63244	GNB2L1 Guanine nucleotide-binding protein subunit beta-2-like 1	9	7	39	23.5
P49915	GMPS GMP synthase	2.5	0	38.5	20
Q01581	HMGCS1 Hydroxymethylglutaryl-CoA synthase, cytoplasmic	0	2	38	31
P13646	KRT13 , type I cytoskeletal 13	0	0	38	0
P15924	DSP Desmoplakin	2	7.5	37.5	42
P11142	HSPA8 Heat shock cognate 71 kDa protein	7.5	15.5	37	16.5
Q9ULV4	CORO1C Coronin-1C	3	10	37	13.5
P26641	EEF1G Elongation factor 1-gamma	3.5	4.5	36	18.5
Q99873	PRMT1 Protein arginine N-methyltransferase 1	0	6.5	35.5	17.5
Q16658	FSCN1 Fascin	6.5	5	35.5	22.5
Q92598	HSPH1 Heat shock protein 105 kDa	0	2	35.5	19
P34932	HSPA4 Heat shock 70 kDa protein 4	2	2.5	35	18.5
P09211	GSTP1 Glutathione S-transferase P	0	3	34.5	22.5
P46940	IQGAP1 Ras GTPase-activating-like protein IQGAP1	2	2	34.5	22
Q9NQ88	TIGAR Fructose-2,6-bisphosphatase TIGAR	0	0	34	8.5
P00558	PGK1 Phosphoglycerate kinase 1	11	2.5	33.5	20.5

P55060	CSE1L Exportin-2	3	0	33.5	24.5
P12268	IMPDH2 Inosine-5'-monophosphate dehydrogenase 2	3	4	33	35
P14866	HNRNPL Heterogeneous nuclear ribonucleoprotein L	0	18.5	32.5	20
Q96FQ6	S100A16 Protein S100-A16	0	15.5	32.5	10
Q5TFE4	NT5DC1 5'-nucleotidase domain-containing protein 1	0	6	32.5	34
O00410	IPO5 Importin-5	0	0	32.5	59.5
P13010	XRCC5 X-ray repair cross-complementing protein 5	2.5	6	31.5	16.5
Q92616	GCN1L1 Translational activator GCN1	3	0	31.5	42.5
P60842	EIF4A1 Eukaryotic initiation factor 4A-I	10	5	31	20
Q15021	NCAPD2 Condensin complex subunit 1	0	0	30	22.5
Q9P258	RCC2 Protein RCC2	0	0	30	19.5
Q99575	POP1 Ribonucleases P/MRP protein subunit POP1	3	12	29	19.5
P62937	PPIA Peptidyl-prolyl cis-trans isomerase A	8	6	29	18
Q9P2J5	LARS Leucine--tRNA ligase, cytoplasmic	2	2.5	29	42
P06737	PYGL Glycogen phosphorylase, liver form	0	0	29	14.5
Q6IS14	EIF5AL1 Eukaryotic translation initiation factor 5A-1-like	0	0	29	13.5
P55795	HNRNPH2 Heterogeneous nuclear ribonucleoprotein H2	0	0	28.5	11
P78371	CCT2 T-complex protein 1 subunit beta	2	5	28	10
P17655	CAPN2 Calpain-2 catalytic subunit	3	2	28	41
P53602	MVD Diphosphomevalonate decarboxylase	0	2	28	12
P53621	COPA Coatomer subunit alpha	2	2	27	30
P11413	G6PD Glucose-6-phosphate 1-dehydrogenase	4	2	26	10
O00571	DDX3X ATP-dependent RNA helicase DDX3X	7	9	25.5	21.5
P23528	CFL1 Cofilin-1	0	3	25.5	13.5
P36578	RPL4 60S ribosomal protein L4	3	16.5	25	19
P55072	VCP Transitional endoplasmic reticulum ATPase	6	10	25	16
O00154	ACOT7 Cytosolic acyl coenzyme A thioester hydrolase	0	7.5	25	25
P25398	RPS12 40S ribosomal protein S12	4	2.5	25	13.5
Q9UL46	PSME2 Proteasome activator complex subunit 2	2	2	25	19
O60610	DIAPH1 Protein diaphanous homolog 1	0	0	25	13
Q14974	KPNB1 Importin subunit beta-1	2	4.5	24.5	25
Q9BQA1	WDR77 Methylosome protein 50	0	2	24.5	8
Q9BSJ8	ESYT1 Extended synaptotagmin-1	0	13.5	24	10.5
P36952	SERPINB5 Serpin B5	3	2	24	16
O00429	DNM1L Dynamin-1-like protein	0	0	24	22
P12081	HARS Histidine--tRNA ligase, cytoplasmic	0	0	24	6.5
O95373	IPO7 Importin-7	0	0	23.5	19.5
Q09666	AHNAK Neuroblast differentiation-associated protein AHNAK	0	4	23	5
Q8TEQ6	GEMIN5 Gem-associated protein 5	0	0	23	33.5
Q9NSD9	FARSB Phenylalanine--tRNA ligase beta subunit	0	0	23	6.5
P35580	MYH10 Myosin-10	0	0	22.5	21
P60981	DSTN Destrin	0	0	22.5	4.5
Q13200	PSMD2 26S proteasome non-ATPase regulatory subunit 2	3	4.5	22	21.5
P04035	HMGCR 3-hydroxy-3-methylglutaryl-coenzyme A reductase	0	3	22	13
P11940	PABPC1 Polyadenylate-binding protein 1	4	11	21.5	10
P15170	GSPT1 Eukaryotic peptide chain release factor GTP-binding subunit ERF3A	3	2	21.5	8
B0V043	VARS Valyl-tRNA synthetase	2	0	21.5	19
Q9Y678	COPG1 Coatomer subunit gamma-1	3	3	21	27.5
Q9Y490	TLN1 Talin-1	0	2	21	19
P0CG39	POTEJ POTE ankyrin domain family member J	0	0	21	0
A0AVT1	UBA6 Ubiquitin-like modifier-activating enzyme 6	0	0	20.5	23
P50395	GDI2 Rab GDP dissociation inhibitor beta	5	4.5	20	13.5
O14980	XPO1 Exportin-1	2	2	20	22
Q7Z6Z7	HUWE1 E3 ubiquitin-protein ligase HUWE1	0	0	20	16.5
P78417	GSTO1 Glutathione S-transferase omega-1	0	4	6.5	144
P10599	TXN Thioredoxin	0	0	7.5	125.5
P52209	PGD 6-phosphogluconate dehydrogenase, decarboxylating	3	2	13	57
P38606	ATP6V1A V-type proton ATPase catalytic subunit A	2	4.5	12	56.5
O75153	KIAA0664 Clustered mitochondria protein homolog	0	0	16.5	43
Q8IZL8	PELP1 Proline-, glutamic acid- and leucine-rich protein 1	0	19	6.5	38
O14744	PRMT5 Protein arginine N-methyltransferase 5	0	0	8	32
P35573	AGL Glycogen debranching enzyme	0	0	11	31.5
P42765	ACAA2 3-ketoacyl-CoA thiolase, mitochondrial	0	10	0	31
P53675	CLTCL1 Clathrin heavy chain 2	0	0	0	31
P12532	CKMT1B Creatine kinase U-type, mitochondrial	0	3	0	30
Q5JRX3	PITRM1 Presequence protease, mitochondrial	0	14.5	15.5	27.5
Q5T4S7	UBR4 E3 ubiquitin-protein ligase UBR4	0	0	14.5	26.5
P50416	CPT1A Carnitine O-palmitoyltransferase 1, liver isoform	4	14.5	7	26.5
P45974	USP5 Ubiquitin carboxyl-terminal hydrolase 5	0	3	14	25.5
P41252	IARS Isoleucine--tRNA ligase, cytoplasmic	2	0	16.5	25
O95573	ACSL3 Long-chain-fatty-acid--CoA ligase 3	0	19	14	24.5
Q02218	OGDH 2-oxoglutarate dehydrogenase, mitochondrial	3	19	14	24
P53618	COPB1 Coatomer subunit beta	3	0	17	23
Q13751	LAMB3 Laminin subunit beta-3	0	19.5	16	22.5
Q00796	SORD Sorbitol dehydrogenase	0	0	5	22.5
P28062	PSMB8 Proteasome subunit beta type-8	0	5	3	22.5
Q8WTS1	ABHD5 1-acylglycerol-3-phosphate O-acyltransferase ABHD5	0	5	3	22.5
Q9UGP8	SEC63 Translocation protein SEC63 homolog	0	13	13	21.5
O95336	PGLS 6-phosphogluconolactonase	0	0	5	21.5
Q13045	FLII Protein flightless-1 homolog	0	0	16.5	21
P55786	NPEPPS Puromycin-sensitive aminopeptidase	0	0	14	20.5
O14880	MGST3 Microsomal glutathione S-transferase 3	0	13.5	13	20.5
Q14997	PSME4 Proteasome activator complex subunit 4	0	0	6	20.5
Q9HCC0	MCCC2 Methylcrotonoyl-CoA carboxylase beta chain, mitochondrial	0	7.5	4.5	20.5

Q9NZB2	FAM120A Constitutive coactivator of PPAR-gamma-like protein 1	0	0	15.5	20
Q9NQR4	NIT2 Omega-amidase NIT2	0	3.5	3	20

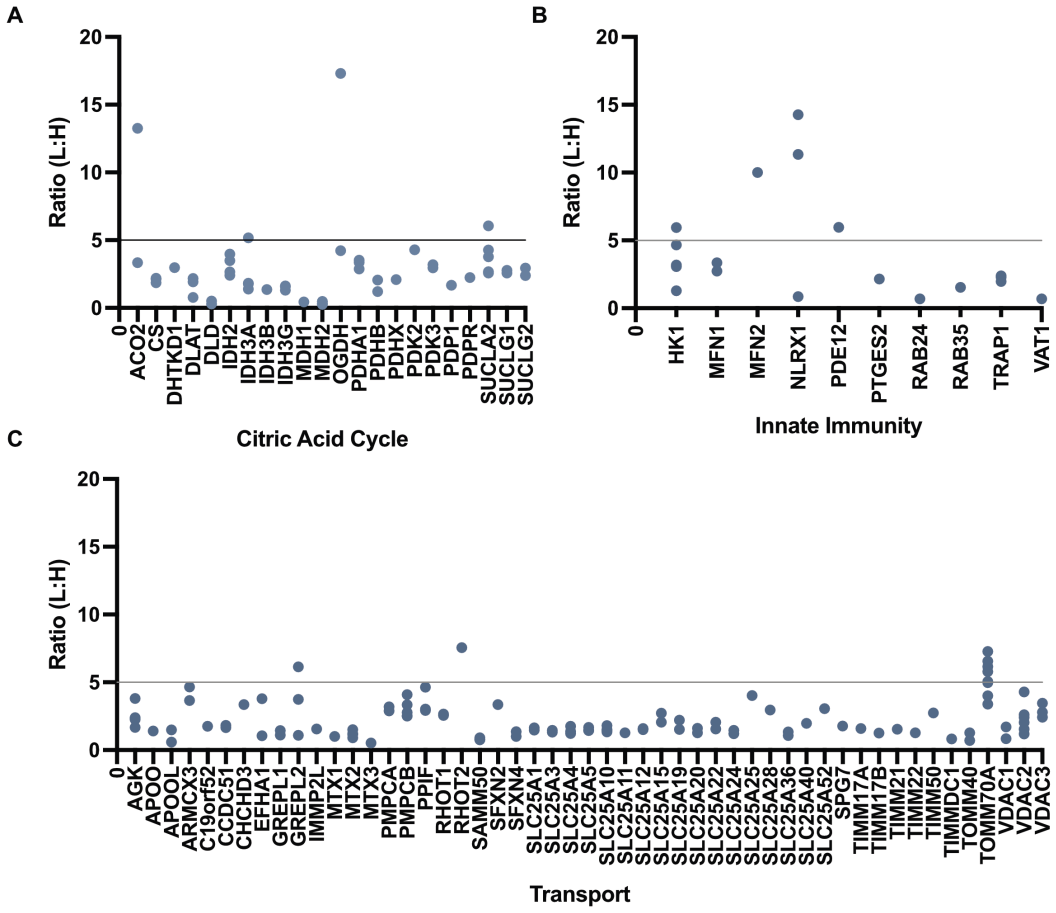
Table 5A-2. List of spectral counts and L:H ratios of ReDiMe labeled proteins enriched in cells treated with either 500 nM PJDU-112 (heavy) or 500 nM VPDU-229 (light).

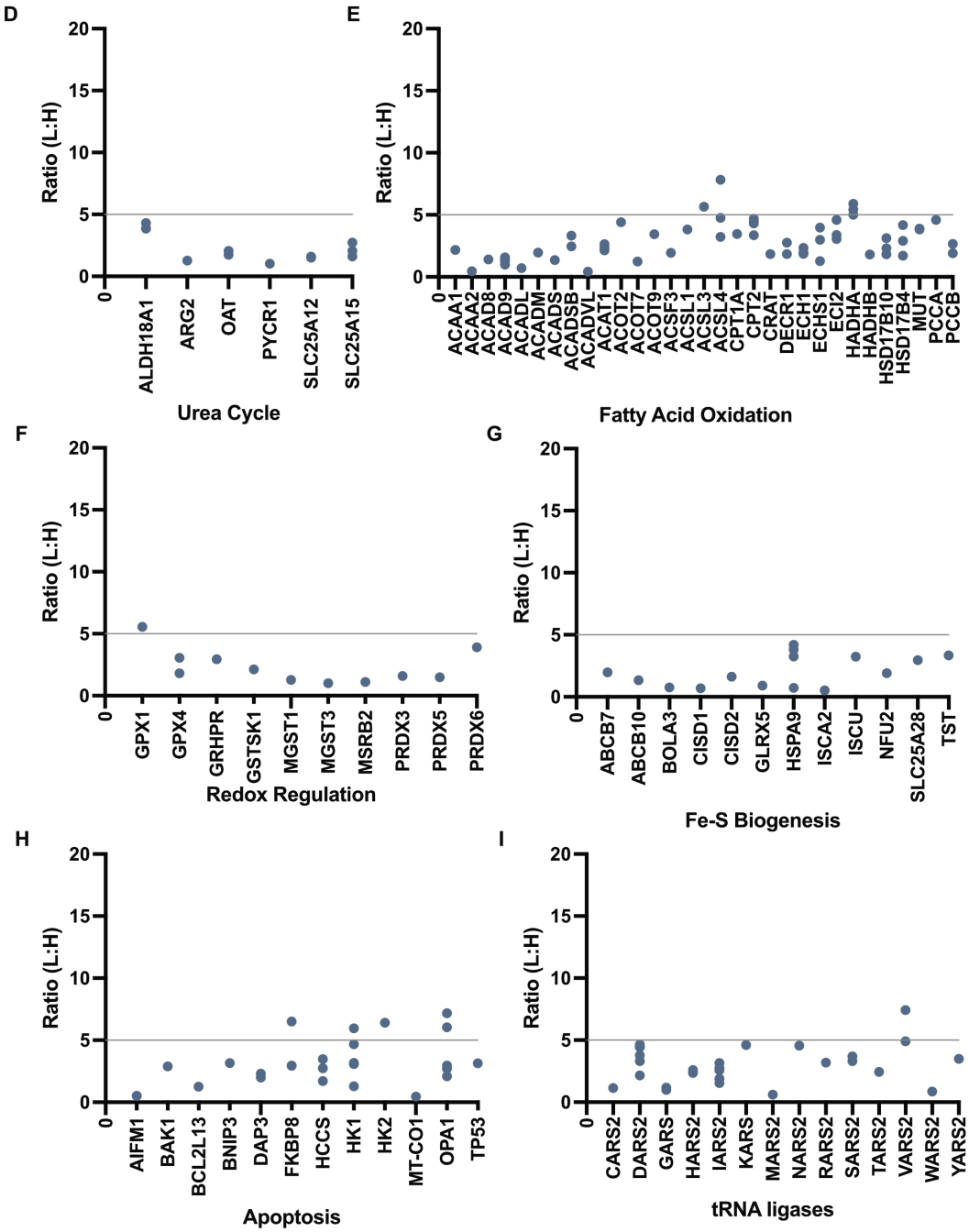
Protein Identification		Average Spectral Counts		Average ReDiMe PJDU-112:VPDU-229
UniProt ID	Description	PJDU-112	VPDU-229	Ratio H:L
P07237	P4HB Protein disulfide-isomerase	478	1.5	20
P49327	FASN Fatty acid synthase	116	40	3.495
Q16881	TXNRD1 Thioredoxin reductase 1, cytoplasmic	81.5	0	20
O75369	FLNB Filamin-B	67.5	34	2.05
P60709	ACTB Actin, cytoplasmic 1	58.5	24.5	2.405
P13639	EEF2 Elongation factor 2	55	27	2.22
P35579	MYH9 Myosin-9	49	18	1.91
P06733	ENO1 Alpha-enolase	49	19.5	2.305
P68371	TUBB4B Tubulin beta-4B chain	48.5	26	1.815
P07437	TUBB Tubulin beta chain	47.5	26	2.015
Q5TFE4	NT5DC1 5'-nucleotidase domain-containing protein 1	44.5	7.5	7.375
P78417	GSTO1 Glutathione S-transferase omega-1	43.5	0	20
P68366	TUBA4A Tubulin alpha-4A chain	43.5	22.5	1.67
Q9H7Z7	PTGES2 Prostaglandin E synthase 2	40.5	0	20
Q71U36	TUBA1A Tubulin alpha-1A chain	39.5	20.5	1.645
P08238	HSP90AB1 Heat shock protein HSP 90-beta	35	18	2.84
P16615	ATP2A2 Sarcoplasmic/endoplasmic reticulum calcium ATPase 2	33.5	7.5	5.195
P14618	PKM Pyruvate kinase isozymes M1/M2	30.5	12.5	2.515
Q13509	TUBB3 Tubulin beta-3 chain	30.5	14	1.775
P07900	HSP90AA1 Heat shock protein HSP 90-alpha	29.5	14.5	2.68
P53396	ACLY ATP-citrate synthase	26.5	8	2.74
P30519	HMOX2 Heme oxygenase 2	25.5	0	18.035
P68104	EEF1A1 Elongation factor 1-alpha 1	21.5	8.5	2.215
P07355	ANXA2 Annexin A2	19.5	9	2.91
P31947	SFN 14-3-3 protein sigma	18	2.5	7.605
P10809	HSPD1 60 kDa heat shock protein, mitochondrial	18	9	2.58
P78371	CCT2 T-complex protein 1 subunit beta	17	5.5	3.3
P11142	HSPA8 Heat shock cognate 71 kDa protein	17	8.5	2.605
P04075	ALDOA Fructose-bisphosphate aldolase A	17	10.5	2.055
Q9BVL4	SELO Selenoprotein O	16.5	0	20
O00410	IPO5 Importin-5	16	1	9.79
Q9BUF5	TUBB6 Tubulin beta-6 chain	16	6.5	1.81
P30101	PDIA3 Protein disulfide-isomerase A3	15.5	1	18.165
P11021	HSPA5 78 kDa glucose-regulated protein	14.5	3.5	3.04
P29401	TKT Transketolase	14.5	4.5	2.355
P37802	TAGLN2 Transgelin-2	13.5	2	2.4
P19338	NCL Nucleolin	13.5	3.5	2.57
Q92696	RABGGTA Geranylgeranyl transferase type-2 subunit alpha	12.5	0	20
P78527	PRKDC DNA-dependent protein kinase catalytic subunit	12.5	0	5.19
P55072	VCP Transitional endoplasmic reticulum ATPase	12.5	2	2.285
O75153	KIAA0664 Clustered mitochondria protein homolog	12	0	20
P34932	HSPA4 Heat shock 70 kDa protein 4	12	0	1.97
Q15084	PDIA6 Protein disulfide-isomerase A6	12	0	20
Q01581	HMGCS1 Hydroxymethylglutaryl-CoA synthase, cytoplasmic	12	4	3.17
P12814	ACTN1 Alpha-actinin-1	11.5	1.5	2.56
P04083	ANXA1 Annexin A1	11.5	6.5	2.6
P49356	FNTB Protein farnesyltransferase subunit beta	11	0	20
P14625	HSP90B1 Endoplasmin	11	4	3.53
P22314	UBA1 Ubiquitin-like modifier-activating enzyme 1	11	5.5	2.595
Q92598	HSPH1 Heat shock protein 105 kDa	10.5	2.5	2.72
Q16658	FSCN1 Fascin	10.5	3.5	2.405
P50990	CCT8 T-complex protein 1 subunit theta	10	1	2.635
P36969	GPX4 Phospholipid hydroperoxide glutathione peroxidase, mitochondrial	10	0	20
P07195	LDHB L-lactate dehydrogenase B chain	10	2	3.28
P29034	S100A2 Protein S100-A2	10	2	3.11
Q01813	PFKP 6-phosphofructokinase type C	10	2.5	2.49
P11216	PYGB Glycogen phosphorylase, brain form	10	4.5	2.715

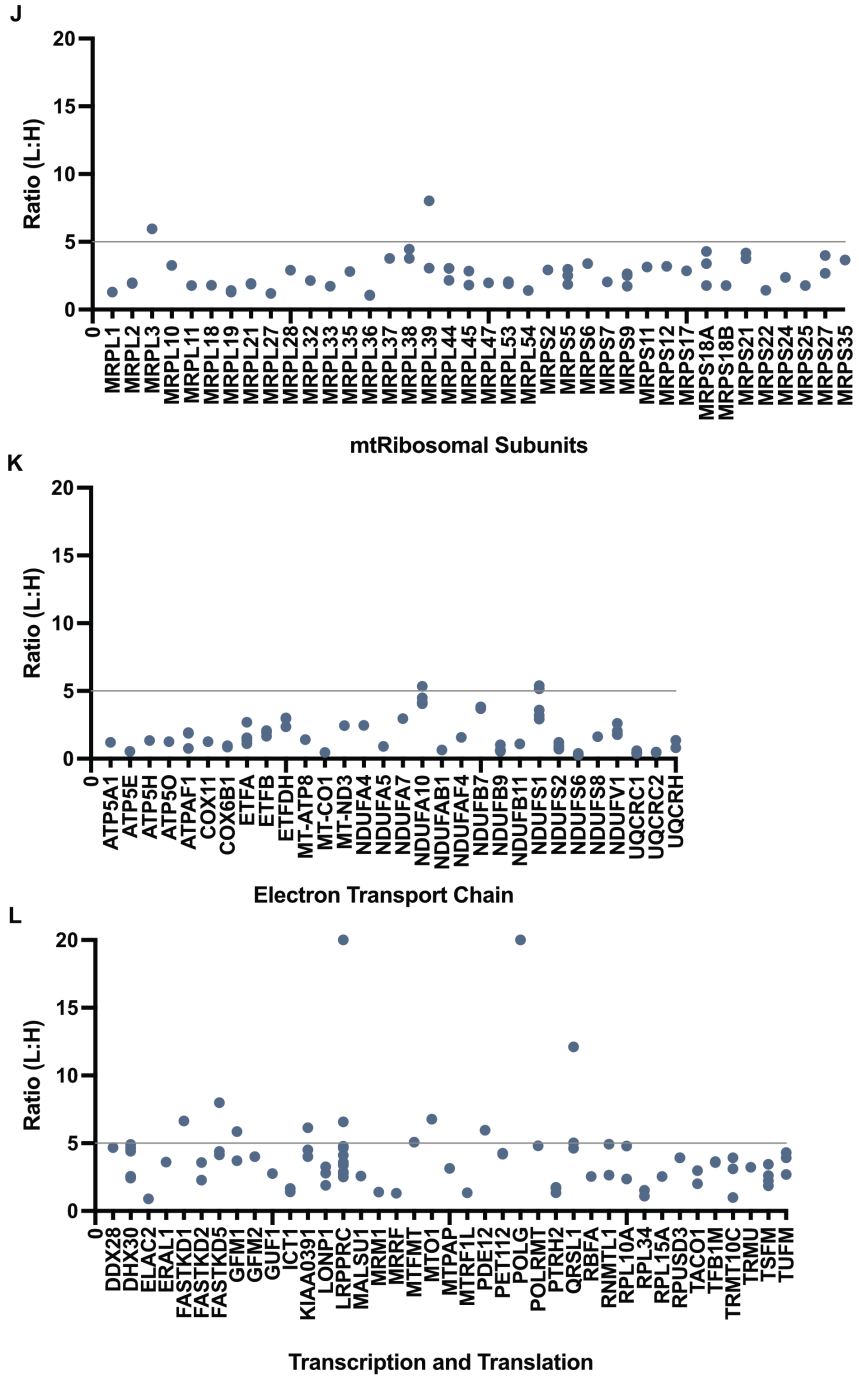
Appendix II

Supplemental Figures

Supplemental Figure 2-1. L:H ratios plotted for 10 mM peroxide treated Mito-P isoTOP-ABPP sample. Cysteines are plotted for proteins belonging to mitochondrial biological pathways and categories including the (A) citric acid cycle, (B) innate immunity, (C) transport, (D) urea cycle, (E) fatty acid oxidation, (F) redox regulation, (G) Fe-S biogenesis, (H) apoptosis, (I) tRNA ligases, (J) mitochondrial (mt)-ribosomal subunits, (K) electron transport chain, (L) transcription and translation.




D
E
Ratio (L:H)
0
5
10
15
20
ALDH18A1
ARG2
OAT
PYCR1
SLC25A12
SLC25A15
Urea Cycle
ACAA1
ACAA2
ACAD8
ACAD9
ACADL
ACADM
ACADS
ACADSB
ACADVL
ACAT1
ACOT2
ACOT7
ACOT9
ACSF3
ACSL1
ACSL3
ACSL4
CPT1A
CPT2
CRAT
DECR1
ECH1
ECHS1
ECI2
HADHA
HADHB
HSD17B10
HSD17B4
MUT
PCCA
PCCB
Fatty Acid Oxidation
F
G
GPX1
GPX4
GRHPR
GSTSK1
MGST1
MGST3
MSRB2
PRDX3
PRDX5
PRDX6
Redox Regulation
ABCB7
ABCB10
BOLA3
CISD1
CISD2
GLRX5
HSPA9
ISCA2
ISCU
NFU2
SLC25A28
TST
Fe-S Biogenesis
H
I
AIFM1
BAK1
BCL2L13
BNIP3
DAP3
FKBP8
HCCS
HK1
HK2
MT-CO1
OPA1
TP53
Apoptosis
CARS2
DARS2
GARS
HARS2
IARS2
KARS
MARS2
NARS2
RARS2
SARS2
TARS2
VARS2
WARS2
YARS2
tRNA ligases


J
Ratio (L:H)
20
15
10
5
0
0
MRPL1
MRPL2
MRPL3
MRPL10
MRPL11
MRPL18
MRPL19
MRPL21
MRPL27
MRPL28
MRPL32
MRPL33
MRPL35
MRPL36
MRPL37
MRPL38
MRPL39
MRPL44
MRPL45
MRPL47
MRPL53
MRPL54
MRPS2
MRPS5
MRPS6
MRPS7
MRPS9
MRPS11
MRPS12
MRPS17
MRPS18A
MRPS18B
MRPS21
MRPS22
MRPS24
MRPS25
MRPS27
MRPS35
mtRibosomal Subunits
K
Ratio (L:H)
20
15
10
5
0
0
ATP5A1
ATP5E
ATP5H
ATP5O
ATPAF1
COX11
COX6B1
ETFA
ETFB
ETFDH
MT-ATP8
MT-CO1
MT-ND3
NDUFA4
NDUFA5
NDUFA7
NDUFA10
NDUFAB1
NDUFAF4
NDUFB7
NDUFB9
NDUFB11
NDUFS1
NDUFS2
NDUFS6
NDUFS8
NDUFV1
UQCRC1
UQCRC2
UQCRH
Electron Transport Chain
L
Ratio (L:H)
20
15
10
5
0
0
DDX28
DHX30
ELAC2
ERAL1
FASTKD1
FASTKD2
FASTKD5
GFM1
GFM2
GUF1
ICT1
KIAA0391
LONP1
LRPPRC
MALSU1
MRM1
MRRF
MTFMT
MTO1
MTPAP
MTRF1L
PDE12
PET112
POLG
POLRMT
PTRH2
QRSL1
RBFA
RNMTL1
RPL10A
RPL34
RPL15A
RPUSD3
TACO1
TFB1M
TRMT10C
TRMU
TSFM
TUFM
Transcription and Translation